AMAP

UN environment

Technical Background Report to the Global Mercury Assessment 2018

UN environment

AMAP

Technical Background Report to the Global Mercury Assessment 2018

Technical Background Report to the Global Mercury Assessment 2018

Production

MIX
Paper from responsible sources
FSC
www.fsc.org
FSC™ C010651

Acknowledgements

Contents

Preface

This report details the technical background to the *Global Mercury Assessment 2018* that has been developed in response to a decision at the twenty-seventh session of the Governing Council of the United Nations Environment Programme (Decision 27/12 (III.21)) that requested the Executive Director "to provide an update *[to the GMA 2013 report]* within six years". The *Global Mercury Assessment 2018* (summary for policy-makers) was delivered to the fourth session of the UN Environment Assembly (UNEA4) in March 2019.

This technical background report has been developed in collaboration with the Arctic Monitoring and Assessment Programme (AMAP). As such, this report also constitutes a contribution to the work of AMAP and the Arctic Council.

Chapter 2 (Recent advances in understanding global mercury cycling), Chapter 3 (Global emissions of mercury to the atmosphere from anthropogenic sources) and Chapter 8 (Relationships between trends in atmospheric mercury and mercury in aquatic biota) of this report were developed by a joint UN Environment/AMAP Expert Group, building on the competence established during the AMAP/UN Environment collaboration that resulted in the Technical Background Report to the 2013 Global Mercury Assessment report. Chapters 2 and 8 were prepared under the leadership of experts from the Geological Survey of Canada and University of Manitoba (Canada), and work on Chapter 3 was coordinated by experts from AMAP Secretariat and Swedish Environmental Research Institute (IVL).

Chapter 4 of this report (Levels of mercury in Air) and Chapter 7 (Mercury concentrations in biota) were prepared under the leadership of experts from the UN Environment Mercury Air Transport and Fate Research Partnership Area.

Chapter 5 (Atmospheric pathways, transport and fate) was prepared by a UN Environment/AMAP expert group under the leadership of experts from the Meteorological Synthesising Centre East (Russia).

Chapters 6 (Releases of mercury to the aquatic environment from anthropogenic sources) was prepared by a UN Environment/AMAP expert group under the leadership of experts from the Institute Jožef Stefan (Slovenia).

 Chapter 9 (Mercury levels and trends in human populations worldwide) was prepared by a UN Environment/AMAP expert group in collaboration with experts from the World Health Organization.

The work on Chapters 6, 7 and 8, addressing mercury in aquatic systems, and Chapter 9, addressing mercury exposure in human populations represent significant extensions to the subject matter considered in the 2013 Global Mercury Assessment.

In producing, in particular Chapters 3 and 6 of the report, and the associated 2015 global inventories of emissions of mercury to air and releases to aquatic systems from anthropogenic sources, efforts were made to engage a wide participation of national experts from regions around the globe. Thanks to funding provided by Canada, Denmark, Japan, Sweden, Norway, the Nordic Council of Ministers, and the EU, experts from Argentina, Australia, Brazil, China, Denmark,, Egypt, India, Indonesia, Japan, Malaysia, Mexico, Norway, Republic of Korea, Russia, Slovenia, South Africa, Sweden, Vietnam and the USA actively participated in the work to develop Chapters 3 and 6 of this report. Experts from the cement and oil and gas industrial sectors also contributed to this work, together with experts from UN bodies coordinating inventory work under the Minamata Convention and under the UN ECE Convention on Long-range Transboundary Air Pollution. Expertise and information made available through the UN Environment Partnership area on Mercury Control from Coal Combustion Information was used, as were data acquired during the preparation of the UN Environment report on Global Mercury Supply, Trade and Demand). The sections concerning artisanal and small-scale gold mining were developed through cooperation with experts from the UN Environment Partnership on Reducing Mercury in Artisanal and Small-scale Gold Mining and from the Artisanal Gold Council (AGC). The contributions made by all of these experts were much appreciated.

1. Introduction

Authors: Simon Wilson, John Munthe, Eisaku Toda

1.1 Background and mandate

This report constitutes the Technical Background to the Global Mercury Assessment (GMA) 2018. The GMA2018 is a response to a request, in 2013, from the Governing Council of UN Environment (the UN Environment Assembly – UNEA)[1] which called for an updated Global Mercury Assessment for delivery no later than 2019.

The GMA2018 is the fourth such assessment undertaken by the United Nations Environment Programme (UN Environment) (UNEP, 2002; UNEP, 2008; UNEP, 2013) and is the second assessment produced by UN Environment in collaboration with the Arctic Monitoring and Assessment Programme (AMAP) (AMAP/UNEP, 2013).

The Technical Background to the Global Mercury Assessment 2018 forms the basis for the statements made in the GMA2018 Report (UN Environment, 2019); it is fully referenced and peer-reviewed according to standard scientific practice. As such, it is the single reference for the (policy-makers summary) GMA2018 report (UN Environment, 2019).

The first three Global Mercury Assessments (UNEP, 2002; UNEP, 2008; UNEP, 2013) provided scientific information that contributed to the negotiations that resulted in the Minamata Convention on Mercury (UN Environment, 2017), which was adopted in October 2013 and entered into force in August 2017.

Although the work to produce the GMA2018 was not formally connected with activities that were taking place in parallel to implement the Minamata Convention (work is conducted under the auspices of the Minamata Convention Conference of Parties; COP), it was recognized that parts of the GMA2018 would be of interest to the Minamata process. For example, the Minamata process includes new work to develop national inventories of emissions to air and releases to land and water through Minamata Initial Assessments (MIAs) and emissions inventory work under the GMA provided comparative information that was used to provide feedback to those initiatives, as described in Chapter 3. Selected results of the GMA2018 were presented at the Minamata Convention COP2 in Geneva in November 2018.

The GMA2018 Technical Background report is prepared by an international group of experts identified by UN Environment and AMAP. It includes contributions from the UN Environment's Mercury Partnership, in particular its partnership areas on mercury in artisanal and small-scale gold mining, and mercury air transport and fate; the AMAP mercury expert group; experts working with the UN Economic Commission for Europe Convention on Long-range Transboundary Air Pollution; World Health Organization; industry; and nongovernmental organizations. Each chapter was prepared by an expert author group and was subject to a comprehensive international peer-review process to ensure its scientific accuracy.

1.2 Scope and coverage

In updating the GMA2013 (UNEP, 2013), the GMA2018 provides the most recent information available for the worldwide emissions to air, releases to water, transport of mercury in atmospheric and aquatic environments, and levels in air and biota. The GMA2018 complements previous GMAs (UNEP, 2002; UNEP, 2008; UNEP, 2013) and intentionally avoids repetition of information contained in those assessments. The GMA2018 Technical Background report reflects progress made by the scientific community, national authorities and organizations, and reviews and summarizes information from the recently published scientific literature (in the period 2013–2018), supplemented where necessary by other sources. The GMA2018 is intended to provide a basis for decision making; therefore, emphasis is given to anthropogenic emissions (mercury entering the atmosphere) and releases (to water) associated with human activities.

The evaluation of information on mercury levels in humans is a new component of GMA2018 and benefits from contributions from experts from the World Health Organization. Other new components introduced in the GMA2018 include a (first) global inventory of mercury releases to aquatic environments from anthropogenic sources, and a review of mercury levels in biota.

The report is structured according to four main subject areas:

- Understanding global mercury cycling (Chapter 2)

- *Air*: anthropogenic mercury emissions to air (Chapter 3), mercury levels in air (Chapter 4), atmospheric transport and fate (Chapter 5)

- *Water*: releases to water (Chapter 6), the cycling and methylation of mercury in the aquatic environment, and relationship between trends in atmospheric mercury and mercury in aquatic biota (Chapter 8);

- *Biota and Humans*: observed levels of mercury in biota (Chapter 7), and observed levels and trends of mercury exposure in humans (Chapter 9).

Chapters 6, 7, 8 and 9 in particular constitute new additions to the GMA and are subjects that were not addressed in the GMA2013 (AMAP/UNEP, 2013; UNEP, 2013).

Global inventories for mercury emissions to air from anthropogenic sources have been produced at about five-year intervals since 1990 by scientific groups associated with assessments of mercury in the Arctic prepared by AMAP. Cooperation with AMAP therefore focused on chapters concerned with global mercury cycling, emissions to air from anthropogenic sources, and cycling and methylation of mercury in the aquatic environment. Cooperation with the World Health Organization was sought during the

---

[1] Twenty-seventh session of the UNEP Governing Council/Global Ministerial Environment Forum, Nairobi, 18–22 February 2013. UNEP Governing Council Decision 27/12 (III.21) "Acknowledges the 2013 update of the 2008 report from the Executive Director: 'Global Atmospheric Mercury Assessment: Sources, Emissions and Transport' and requests the Executive Director to provide a further update within six years".

preparation of Chapter 9 on mercury exposure in humans, and this part of the GMA work was co-sponsored by the World Health Organization.

It should also be recognized that the GMA2018 is not a complete review of all aspects of global mercury cycling. Specifically, it does not address mercury releases to land (other than combined releases to land and water associated with artisanal and small-scale mining). It should also be noted that in the GMA2018, 'mercury' refers to the chemical element in all forms, in contrast to the Minamata Convention, which distinguishes 'mercury' from 'mercury compounds'.

The chapters on emissions to air and releases to water use both national and independently compiled global data on activity levels to derive estimates of emissions and releases using a standardized methodology. As such, the resulting estimates are not official national estimates.

The Global Mercury Assessment is based on improved information for estimating emissions and releases and improved understanding of the mercury cycle in the environment. Information about mercury exposure in animals and humans reflects increased recent availability of results from mercury research and monitoring around the world.

Further improvements in our understanding of mercury can further refine the ability to identify efficient actions to reduce mercury pollution and its effects. Such improvements include basic research on aspects of the mercury cycle as well as systematic monitoring methods to expand the geographic coverage of measurements of mercury pollution. As a chemical element, mercury cannot be destroyed. Mercury removed from fuels and raw materials in order to reduce emissions will result in mercury-contaminated waste, which in turn can be a source of releases. Mercury removed from emissions and from releases must still be managed responsibly to avoid it becoming a waste management problem or a secondary source. Understanding how mercury removed from current uses and sources is currently managed and how it can be safely managed and stored in the future will help account for the full life-cycle of mercury that is mobilized through human activity, safeguarding the environment and humans when it is removed.

2. Recent advances in understanding of global mercury cycling

Authors: Peter Outridge, Robert Mason, Feiyue Wang, Lars-Eric Heimbürger-Boavida, Xinbin Feng

Key messages

- *Considerable work has been published in the world literature concerning global mercury (Hg) cycling and budgets, since the last Global Mercury Assessment in 2013. A major point of recent debate has been the impact of historical atmospheric emissions, mainly from silver and gold mining and amalgamation in the 16th to late 19th centuries, on current Hg levels in the environment, especially the oceans.*

- *Based on an evaluation of historic information, and of atmospheric Hg fluxes recorded in lake sediment, peat bog and glacier ice archives, the weight of evidence at present strongly supports a 'low mining emission' scenario.*

- *Building on a global model using the low emission scenario, this assessment estimates human activities to have increased total atmospheric Hg concentrations by about 450% above natural levels (i.e., those before 1450 AD). The anthropogenic effect represents an increase in mass of 3600 t above the natural value of 800 t for a current total of 4400 t. This increase includes the impact of revolatilization from soils and oceans of the 'legacy' Hg emitted from natural and human sources in the past but which is still circulating in the biosphere.*

- *Current anthropogenic emissions to air are estimated at 2500±500 t/y, which is the sum of the documented emission inventory presented later in this Assessment (2220 t/y) and undocumented releases from likely important sources such as agricultural waste burning, and municipal and industrial waste.*

- *Bearing in mind the uncertainties in natural and anthropogenic emission estimates, and the many deficiencies in our understanding of the processes and flux rates governing Hg transport and fate between the air, soil and ocean compartments, the best information currently available suggests that the increase in atmospheric Hg concentrations has driven a ~310% increase in average deposition rates to the Earth's surface in*

recent decades. This is the largest source (~90%) of Hg in the surface ocean; rivers are minor contributors.*

- *Surface marine waters have shown a 230% increase in Hg concentrations above natural levels. The increase in surface soils (~15%) has been an order of magnitude lower due to the large mass of natural Hg present in soils from rock weathering. Evasion of dissolved gaseous Hg from the ocean's surface back to the atmosphere has increased 250%. Deeper marine waters show increases of only 12–25% above natural levels owing to the slow rate of penetration of anthropogenic Hg and the large volume of mid- and deep-ocean waters.*

- *Even using the low mining emission scenario, the cumulative effect on today's oceanic Hg cycle of several centuries of emissions has been dramatic, with about two-thirds of the overall increase in marine Hg concentrations occurring before 1920 (mainly due to precious metal mining and associated cinnabar refining). About 20% of the overall increase is due to coal combustion since 1920, and another ~10% is due to other industrial activities.*

- *Marine Hg concentrations are expected to show a slow recovery following regulatory reductions in global Hg emissions (on the order of decades to centuries depending on the ocean basin and the trajectory of reductions). Mercury has a relatively long half-life in surface soils and marine waters, because of its recycling between the surface environment and atmosphere and between surface and intermediate ocean waters. Permanent removal of anthropogenic Hg from the biologically-active part of the environment will only occur once it is buried in deep ocean sediments and in mineral soils.*

- *Recommendations to improve the scientific knowledge base underpinning global models and budgets of Hg fall into two general areas: better understanding of natural inputs and processes, and more accurate and complete anthropogenic emissions inventories.*

2.1 General overview

An improved understanding of the global mercury (Hg) cycle is important for our capacity to predict how regulatory efforts to reduce current emissions to air, water and land will affect Hg concentrations in environmental compartments, biota and humans. The aim of this chapter is to provide a broad perspective for all subsequent chapters by describing the sources, transport and fate of Hg, especially anthropogenic Hg, in the global environment. Owing to its scale and chemical complexity, and the lack of detailed information for many aspects of it, the planetary Hg cycle is best described and communicated in a quantitative manner by using the budgets derived from global-scale models. This chapter presents a synthesis of recent advances in knowledge of the global Hg cycle, including the influence of historic emissions on current anthropogenic Hg

levels in the environment, and provides updated global and oceanic total Hg budgets.

Mercury is released into the environment through human activities, as well as from natural sources and processes such as volcanoes and rock weathering. Following its release, Hg is transported and recycled between the major environmental compartments – air, soils and waters – until it is eventually removed from the system through burial in coastal and deep ocean sediments, lake sediments, and subsurface soils (Amos et al., 2014; Fitzgerald and Lamborg, 2014). Only a very small fraction of the Hg present in the environment is monomethylmercury – the only Hg form that biomagnifies in food chains. Hereafter, for the sake of simplicity, monomethylmercury is referred to by its generic name, methylmercury (MeHg). Methylmercury is produced from inorganic Hg mainly in aquatic ecosystems through biochemical processes mediated by naturally-occurring microorganisms.

Table 2.1 Recent estimates of total, anthropogenic and natural[a] Hg masses in global air, soils and oceans (data in kilotonnes).

	Mason et al. (2012); AMAP/UNEP (2013)	Amos et al. (2013)	Zhang et al. (2014b)	Lamborg et al. (2014)	Present report[b]
Atmospheric Hg					
Total	5.1	5.3	4.4	n/a	4.4
Anthropogenic	3.4–4.1	4.6	3.6	n/a	3.6
Natural	1.0–1.7	0.7	0.8	n/a	0.8
Soil Hg (organic layers)					
Total	201	271	n/a	n/a	150
Anthropogenic	40	89	92	n/a	20
Natural	161	182	n/a	n/a	130
Oceanic Hg					
Total	358	343	257	316	313
Anthropogenic	53	222	66 (38–106)[c]	58±16[d]	55
Natural	305	122	191	258[e]	258

[a]The time point for designation of the 'natural' Hg state, and thus the quantification of 'natural' and 'anthropogenic' Hg masses, differed between studies: 2000 BC in the 'pre-anthropogenic period' by Amos et al. (2013), prior to 1450 AD by Zhang et al. (2014b) which preceded New World gold, silver and cinnabar mining, and about 1840 AD by Lamborg et al. (2014) which was prior to the North American Gold Rush and the expansion of coal-fired combustion sources. The anthropogenic Hg values from Mason et al. (2012) and Lamborg et al. (2014) are based on increases over the past ~100 to 150 years, and thus their 'natural' Hg masses may be over-estimated and the anthropogenic masses under-estimated compared with the other studies; [b]estimates modified from Zhang et al.'s (2014b) model (see Section 2.3), and thus the anthropogenic values represent the impact of human activities since before 1450 AD; [c]uncertainty range shown in brackets; [d]based on an oceanic anthropogenic Hg:anthropogenic CO_2 ratio for 1994; a more recent (higher) oceanic CO_2 estimate gave an Hg_{ant} estimate of 76 kt Hg (Lamborg et al., 2014); [e]calculated by subtraction.

Recent findings on the methylation/demethylation part of the aquatic Hg cycle are presented in Chapter 8, Section 8.2; many of these processes are only partly understood, which contributes to the difficulties in predicting the direct positive effects of regulatory action on biological Hg concentrations and human exposure.

In the 2013 technical background report to the Global Mercury Assessment (AMAP/UNEP, 2013), based on a global model and budget developed by Mason et al. (2012), it was estimated that human activities cumulatively had increased atmospheric Hg concentrations by 300–500% over the past century, whereas Hg in surface ocean waters less than 200 m deep had increased on average by ~200%. Deeper waters exhibited smaller increases (11–25%) because of limited exposure to atmospheric and riverine anthropogenic Hg inputs, and the century- to millennium-scale residence times of these slowly overturning, isolated water masses. Owing to the naturally large Hg mass present in soils, the average Hg increase was only ~20% in surface organic soils and was negligible in mineral soils. The revolatilization of 'legacy Hg' (i.e., the Hg that was emitted and deposited historically) from soils and oceans, and its long residence time in those compartments, act to maintain atmospheric Hg concentrations and deposition rates at higher levels than are supported by current primary emissions (Fitzgerald and Lamborg, 2014).

It is increasingly recognized, as a result of recent studies of Hg consumption and production in New World precious metal and cinnabar mining from the 16th century onwards (Guerrero, 2016, 2017), and re-examination of the atmospheric Hg flux rates recorded in long lake sediment and peat bog cores (Amos et al., 2015), that significant amounts of Hg were emitted by human activities during the 'pre-industrial period' (variably defined but generally accepted as ending about 1850) and that some fraction of this Hg is still circulating in the environment (Streets et al., 2011, 2017; Amos et al., 2013, 2015). Overall, studies since about 2012 indicate that the last few centuries

of the 'pre-industrial period' are not a suitable reference point from which to gauge the full impact of human activities on the current global Hg cycle. However, there are different definitions of a time period that truly represents natural or 'pre-anthropogenic' conditions: for example, 2000 BC (Amos et al., 2013); 3000 BC to 1550 AD (Amos et al., 2015); or prior to 1450 AD (Zhang et al., 2014a).

Nonetheless, two new estimates generally agree that human activities have increased atmospheric Hg concentrations by 450% (Zhang et al., 2014b) to 660% (Amos et al., 2013), such that total atmospheric Hg concentrations today are 5.5-fold to 7.6-fold higher, respectively, than pre-anthropogenic 'natural' values (Table 2.1). These estimates include revolatilized legacy Hg. Zhang et al. (2014b) further calculated that the increased atmospheric concentrations had resulted in a 4.8-fold increase in average Hg deposition to oceans and a 7.8-fold increase in deposition to land above natural levels. However, Amos et al. (2015), based on a re-evaluation of long peat and lake sediment cores, proposed that substantially higher increases had occurred in deposition rates. Median increases in Hg accumulation rates between the pre-anthropogenic period – defined by Amos et al. (2015) as up to 1550 AD – and the 20th century peak were a factor of ~26 in peat bogs and ~14 in lake sediments, with both archive types showing increases of about 5-fold between the pre-anthropogenic and pre-industrial (1760–1880) periods. These total increases are several times higher than previous reviews of the sediment-based Hg literature indicated, of a ~3-fold increase since the pre-anthropogenic or 'pre-human' period (Fitzgerald et al., 1998; Engstrom et al., 2014; Fitzgerald and Lamborg, 2014). Amos et al. (2015) attributed the latter, lower value to an erroneous selection of 'natural' deposition values that were too high, based on 18th and early 19th century sediment samples that were already contaminated with mining-emitted Hg. Thus, recent studies since 2012 indicate that the true impact of anthropogenic emissions on atmospheric Hg, based on a comparison to pre-anthropogenic

Global anthropogenic Hg emission to air, t/y
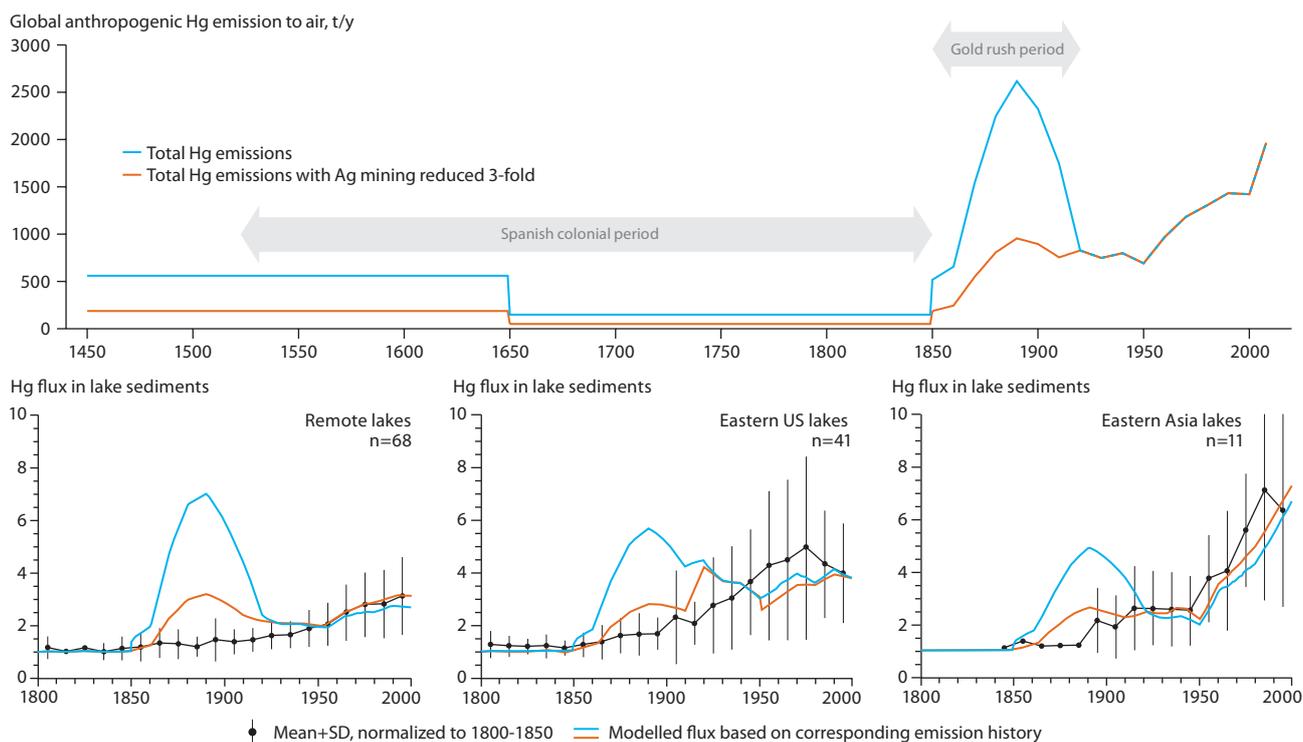
Figure 2.1. Two contrasting views of global anthropogenic Hg emissions to air through history, compared to Hg fluxes to lake sediments. The upper plot compares combined anthropogenic Hg emissions after 1450 from Streets et al. (2011) and the same emission inventory but with Ag mining emissions reduced three-fold (Zhang et al., 2014b). The lower plots show Hg fluxes in lake sediments after 1800 from remote lakes, lakes in the eastern USA and lakes in eastern Asia.

values, is greater than previous comparisons to the 19th century had suggested. But there is considerable variation in the estimates of the degree of that impact.

As with almost all modelled global budgets of elements and other chemical substances, large uncertainties exist regarding the amounts of Hg 'stored' in different environmental compartments, the fluxes of Hg between them, and the rates of removal of Hg from the biosphere (AMAP/UNEP, 2013). These uncertainties limit confidence in our understanding of the Hg cycle and in our ability to predict the responses of ecosystem Hg concentrations to changes in emissions due to international regulatory actions. Therefore, major ongoing efforts have been mounted to reduce these uncertainties and derive a more robust, accurate global budget. Since 2012, additional measurements of Hg concentrations and fluxes in oceans, the atmosphere and soils have led to suggested refinements of global budgets and models by several research groups. Nevertheless major uncertainties persist, especially in oceanic budgets.

The new estimates of the amounts of natural and anthropogenic Hg in the atmosphere by Amos et al. (2013) and Zhang et al. (2014b) agree to within about 30% of the estimates in the AMAP/UNEP (2013) budget (see Table 2.1). In the terrestrial system, both Amos et al. (2013) and Zhang et al. (2014b) suggested that soils globally contain more anthropogenic Hg than was stated in AMAP/UNEP (2013). This revision is supported by new modelling of the transport and fate of atmospheric Hg (Song et al., 2015). However, the balance of anthropogenic Hg distribution between global soils and oceans differs between models, with oceans holding either about as much anthropogenic Hg mass as soils (AMAP/UNEP, 2013; Zhang et al., 2014b) or substantially less (Amos et al., 2013). Again, the difference between model outcomes may be partly due to our lack of understanding of some of the basic processes governing Hg transport and fate. For example, recent studies

on atmospheric Hg dynamics under a range of different plant communities – from tundra plants to forests – have indicated that the direct uptake of gaseous elemental Hg (Hg^0; GEM) through the stomata of plant leaves is more significant than previously thought (Enrico et al., 2016; Fu et al., 2016b; Wang et al., 2016a; Obrist et al., 2017, 2018; Risch et al., 2017). Risch et al. (2017) reported that at 27 forest sites across the eastern United States, litterfall Hg deposition equaled or exceeded the precipitation Hg flux in 70% of cases, and was on average 20% higher than in precipitation across all sites. Also, MeHg constituted ~0.5% of total Hg in litterfall, significantly higher than in precipitation (Risch et al., 2017). Thus, the litterfall total Hg flux was previously under-estimated, and litterfall MeHg could be a contributor to the terrestrially-sourced MeHg that is assimilated by some freshwater biota, especially in headwater streams (Tsui et al., 2014). Globally, GEM-containing litterfall and throughfall, and not wet and dry deposition of oxidized Hg species, may thus represent the largest net flux of atmospheric Hg to terrestrial ecosystems, at 1930 t/y (Fu et al., 2016b).

With respect to the world's oceans, there are significant differences between the new models concerning the quantity of anthropogenic Hg presently circulating in seawater (cf. Amos et al., 2013, 2015; Lamborg et al., 2014; Zhang et al., 2014b; see Table 2.1). Because much of the current risk from Hg to humans and wildlife originates in marine food webs, how much anthropogenic Hg is present in the oceans, its distribution, and its likely rate of clearance from seawater following emission reductions, are of fundamental importance.

Until 2012, published estimates of oceanic anthropogenic Hg exhibited more than an order of magnitude range, from 7.2 to 263 kt (Mason et al., 1994; Lamborg et al., 2002a; Sunderland and Mason, 2007; Selin et al., 2008; Soerensen et al., 2010b; Strode et al., 2010; Streets et al., 2011; Mason et al., 2012). Since then, another estimate (222 kt) near the upper end of this range

was derived by Amos et al. (2013) based on the putative inventory of all-time anthropogenic emissions by Streets et al. (2011), which indicated large releases from historic silver (Ag) mining activities (see also Streets et al., 2017). Zhang et al. (2014b) subsequently revised the historic mining emissions downward by 3-fold to make the trends in global Hg emissions more compatible with the Hg deposition histories recorded in 120 lake sediments world-wide (Figure 2.1), but retained all other elements of the Streets et al. (2011) inventory. Lake sediments and other natural archives of atmospheric deposition such as peat bogs and glacial ice are widely employed to reconstruct historic patterns of deposition flux, and the reconstructed fluxes are assumed to apply equally to deposition over both oceans and land.

The differences between the two most recent global budgets (i.e., Amos et al., 2013 and Zhang et al., 2014b) are primarily due to varying estimates of the amount and environmental fate of atmospheric emissions from historic Ag and gold (Au) mining in the Americas between the 16th and late-19th centuries, and to differences in the estimated amount of natural Hg originally present in the oceans. Overall, the different chemical rate constants used for modelling circulation processes within and between oceanic, atmospheric and terrestrial compartments are a secondary factor in uncertainty. Significant Hg releases to land, freshwaters and air occurred from the mining and amalgamation of Ag (and Au) in South/Central America during the Spanish colonial period (about 1520–1850 AD), and later from North American artisanal and small-scale mining during the 'Gold Rush' era (about 1850–1920) (Nriagu, 1993, 1994; Strode et al., 2009). Based on the relative importance of Spanish colonial Ag production for the three centuries after 1520 (~69% of total world Ag; TePaske and Brown, 2010), and the use of Hg amalgamation to process some of the Spanish New World Ag (and all of the Au) ores, Hg losses to the local environment from these operations must have been substantial (Guerrero, 2016, 2017). In terms of the global environment, it is generally agreed that some fraction of the Hg from both historic periods is still circulating within the biosphere, and that this has had an effect on present-day environmental Hg levels. But quantification of that effect is uncertain. Thus, before considering the question of how much anthropogenic Hg is in the biosphere, evidence for the impact of historic mining on the global environment and its relative importance in different models must be evaluated.

2.2 Influence of historic Ag mining on anthropogenic Hg emission inventories

The total amount of Hg currently in the environment reflects a mixture of sources: historic anthropogenic releases to air, land and oceans; historic natural inputs; and present-day anthropogenic and natural releases. Global models need to estimate these quantities and how the historic emissions have been remobilized, transported and transformed over long (decadal to century) timescales. The influence of historic Ag mining on the oceanic Hg budget is particularly important (Zhang et al., 2014b).

A historical analysis of elemental Hg importation and consumption in the 16th to 19th centuries, in what is today Mexico, Peru and Bolivia, indicated that large quantities of liquid Hg were consumed during Spanish colonial Ag production (TePaske and Brown, 2010). Mercury was also refined from cinnabar at two major sites in the Spanish New World, as well as in California, and at Idrija and Almaden in Europe (Guerrero, 2016, 2018). During the 250 years after ~1560, records indicate that over 120 kt of liquid Hg (average of at least 0.48 kt/y) were imported from Europe or produced in the region, and virtually all of this was lost to the regional environment (TePaske and Brown, 2010). Given the likely large scale of contraband Hg involved in mining, this amount may be considerably underestimated. Given the importance of legacy Hg in the modern environment, a correct interpretation of the impact of historic Ag mining emissions on the current global and oceanic Hg budgets is particularly critical (Zhang et al., 2014a; Amos et al., 2015).

Streets et al.'s (2011, 2017) inventories assumed emission factors of 52% and 40%, respectively, to calculate atmospheric Hg emissions from historic Ag mining, based on Ag metal production figures. These factors were adapted from Nriagu (1993, 1994), based on artisanal Au mining which commonly used direct amalgamation of Au with elemental Hg (a physical process), which was then heated to recover the Au. In contrast, the nature of Ag ore geochemistry, and different Ag production practices, meant atmospheric Hg emissions were much lower per unit of historic Ag metal production than from artisanal Au (Guerrero, 2012, 2016, 2018). Unlike Au, the Ag in economic ores is not present in its elemental form. Smelting (without any Hg involvement) was applied to Ag-rich galena (PbS) or copper ores, producing about half of all global Ag production up to 1900 (Director of U.S. Mint, 1945; Guerrero, 2018). Thus, Hg emissions from this industry must have come only from the non-smelted half, using other ore types. Many Ag-rich ore bodies, including predominantly those in the New World, contain silver chloride and sulfide compounds in varying proportions (Guerrero, 2012, 2017). Historic refining of these ores used Hg, and involved two distinct but concurrent chemical reactions: an oxidative chloride leach to convert silver sulfide to silver chloride, and a redox reaction with Hg to produce metallic silver from silver chloride, followed by amalgamation of the Ag with excess Hg (Guerrero, 2017). The AgHg amalgam was then heated to remove the Hg. These Spanish colonial practices were later employed during the 19th century North American Gold Rush, except that iron was added to the chemical slurry to reduce Hg loss to insoluble calomel (Hg_2Cl_2; Guerrero, 2018). In the refining process, the major cause of Hg loss was calomel formation, with minimal volatile emissions even during the heating stage (Guerrero, 2017, 2018). Mercury was carefully controlled during these reactions and during heating, and was recycled as much as possible because Hg was expensive relative to Ag, unlike the current situation where Hg is cheap relative to Au. The calomel reaction in the Hg treatment of Ag ores has been confirmed by laboratory experiments (Johnson and Whittle, 1999). The waste rock tailings were typically disposed of with the calomel, thereby burying it in soils and sediments, although its long-term fate in the environment has not yet been studied.

In contrast to the application by Streets et al. (2011, 2017) of constant emission factors to Ag production figures to estimate Hg releases, Guerrero (2012) used importation statistics and consumption records on Hg itself, from Spanish colonial government and independant observers. These calculations suggested that no more than 7–34% of the Hg used during Ag production was physically lost through volatilization, ground spills and in waste water, with 66–93% of the consumed Hg chemically transformed into calomel. Volatilization was thus

a small fraction (<34%) of total Hg consumption. During the 19th century, numerous sources reported Hg losses to air of less than 1% of the Hg consumed by refining (Guerrero, 2016, 2017, 2018), owing to improvements in the equipment used to recapture and condense gaseous Hg after amalgamation and heating. Thus, the putative 40–52% emission factors for Ag mining, adopted from Au, appear to be inconsistent with the available historical and chemical information. Recognition of the importance of history and chemistry in resolving the role of Ag mining is an important recent advance, and represents a fundamental difference between the low and high mining emission scenarios discussed in this chapter.

The AMAP/UNEP (2013) report used an emission factor of 45% for Hg emissions from artisanal and small-scale gold mining (ASGM) in the present-day. That estimate is not affected by the new evidence concerning lower Hg losses from Ag mining. The Au amalgamation process with Hg does not involve calomel formation, and thus historic Hg losses from Ag mining are not representative of those from ASGM (Guerrero, 2017), which are likely to be higher.

These historical studies of the fate of Hg used in Ag mining represent an important advance in understanding the global Hg cycle because they concern a potentially major anthropogenic source. Streets et al. (2017) calculated that Ag production was the largest single atmospheric source of anthropogenic Hg throughout history, contributing several-times more Hg to air (146 kt, 31% of total atmospheric emissions) than combined large-scale Au production and ASGM (55.4 kt), and coal combustion (26.4 kt). Mercury production, much of which was destined for use in Ag and Au amalgamation, contributed the second highest amount, 91.7 kt.

Zhang et al. (2014b) adopted a median volatilization rate of 17% of Hg during historic Ag mining (based on Guerrero, 2012) and assumed that the same rate applied to 19th century Gold Rush Au and Ag mining. The resulting tally of cumulative atmospheric anthropogenic emissions was just over half that of Streets et al. (2011) (totals of 190 kt versus 351 kt, respectively), with markedly lower emissions during the Spanish colonial and Gold Rush mining periods (see Figure 2.1). Using their revised inventory, Zhang et al. (2014b) found a 3-fold lower current oceanic anthropogenic Hg mass compared to that derived by Amos et al. (2013), who incorporated Streets et al.'s (2011) larger mining estimate in their model (see Table 2.1).

Corroborative data supporting the lower New World mining emissions used by Zhang et al. (2014b) came from an independent analysis by Engstrom et al. (2014) of another large global set of lake sediment Hg profiles. Atmospheric Hg deposition was substantially increased during the Spanish colonial period in one South American lake (Laguna Negrilla) near the major cinnabar mining and Hg production site of Huancavelica, Peru, with less impact in another lake (El Junco, Galápagos Islands) further away from Ag and Hg mining and amalgamation operations. But little evidence of increased deposition at this time was found in sediment cores from many remote North American, Arctic or African lakes, suggesting that most of the contamination from Spanish colonial mining operations was limited to surrounding terrestrial, freshwater and coastal marine ecosystems in western South/Central America (Engstrom et al., 2014). Thus, the world-wide lake sediment record appears to suggest a negligible global impact from Ag and Au production during the 16th to 19th centuries.

Similarly, there is little evidence in natural archives to support a dominant impact on the global atmosphere from late 19th-century North American Au and Ag mining, as suggested by Streets et al. (2011, 2017). Streets et al. (2017) proposed a bimodal pattern of anthropogenic Hg emissions from 1850 onwards, with values in the late 1890s that were as high or higher than in the mid- to late-20th century, due to a 450% increase in primary emissions between 1850 and 1890 (from 0.58 to 3.2 kt/y) mostly from the North American Gold Rush. Although increases in Hg accumulation occurred in remote lake sediments at this time, they were small relative to those observed later in the 20th century in the same core profiles (Strode et al., 2009; Engstrom et al., 2014; Zhang et al., 2014b). Coincident increases in emissions from other sources such as coal combustion and industrial Hg production and use (Streets et al., 2017, 2018) may have contributed to the elevated Hg deposition that was observed world-wide during the late 19th century. Commercial Hg-containing products have also been suggested to be significant contributors to global Hg releases to air, soil and water from the late 1800s onwards (Horowitz et al., 2014).

Amos et al. (2015) discounted this evidence by arguing that lake sediments in general respond relatively slowly and insensitively to changes in atmospheric Hg deposition compared with peat bogs. Amos et al. (2015) also proposed that the Guerrero (2012) volatilization estimate was unrealistically low because it omitted Hg losses during reprocessing of Hg-containing Ag and Au products, and revolatilization from solid mining wastes. There is some evidence that calomel may dissociate to GEM and gaseous mercuric chloride ($HgCl_2$) under ambient environmental temperatures and sunlight (Copan et al., 2015), but this has not been demonstrated under realistic controlled conditions. Evaluation of alternative global model scenarios by Amos et al. (2015) suggested that the 'mining reduced 3x' history of Zhang et al. (2014b) was inconsistent with Hg measurements in present-day environmental matrices, as well as with the magnitude of Hg enrichment in peat and some lake sediment archives. However, close examination of the published outputs shows that the 'mining reduced 3x' scenario gave better agreement with observed upper ocean total Hg concentrations and net oceanic evasion rates than the larger mining emission inventory of Streets et al. (2011), with similar estimates for present-day soil Hg concentrations and net terrestrial flux (see Amos et al., 2015: their figs. 3d, 3g, 3f and 3h, respectively). Furthermore, the sediment-based interpretations of Strode et al. (2009), Engstrom et al. (2014) and Zhang et al. (2014b) agreed with earlier peat bog Hg studies from the Faroe Islands (Shotyk et al., 2005), Maine, USA (Roos-Barraclough et al., 2006), and Swiss Jura Mountains (Roos-Barraclough and Shotyk, 2003) that also showed relatively muted Hg increases prior to 1900, and with 20th-century accumulation rates substantially higher than in the late 19th century.

Independent evidence supporting the lower Zhang et al. (2014b) emission history, and the lake sediment and peat bog patterns, was provided by three recent studies of glacier ice cores (Figure 2.2). In contrast to the 450% increase in global primary Hg emissions between 1850 and 1890 estimated by Streets et al. (2017), two Arctic or subarctic glacier records – Mount Logan, Yukon (Beal et al., 2015) and the North Greenland Eemian Ice Drilling (NEEM) site (Zheng, 2015) – showed increases in average Hg accumulation of only 150% and 40%, respectively, between 1840–1860 and 1880–1900, while an ice core from the Tibetan Plateau in central Asia (Mount Geladaindong, Kang et al., 2016) displayed a 140% increase. All three studies showed that Hg
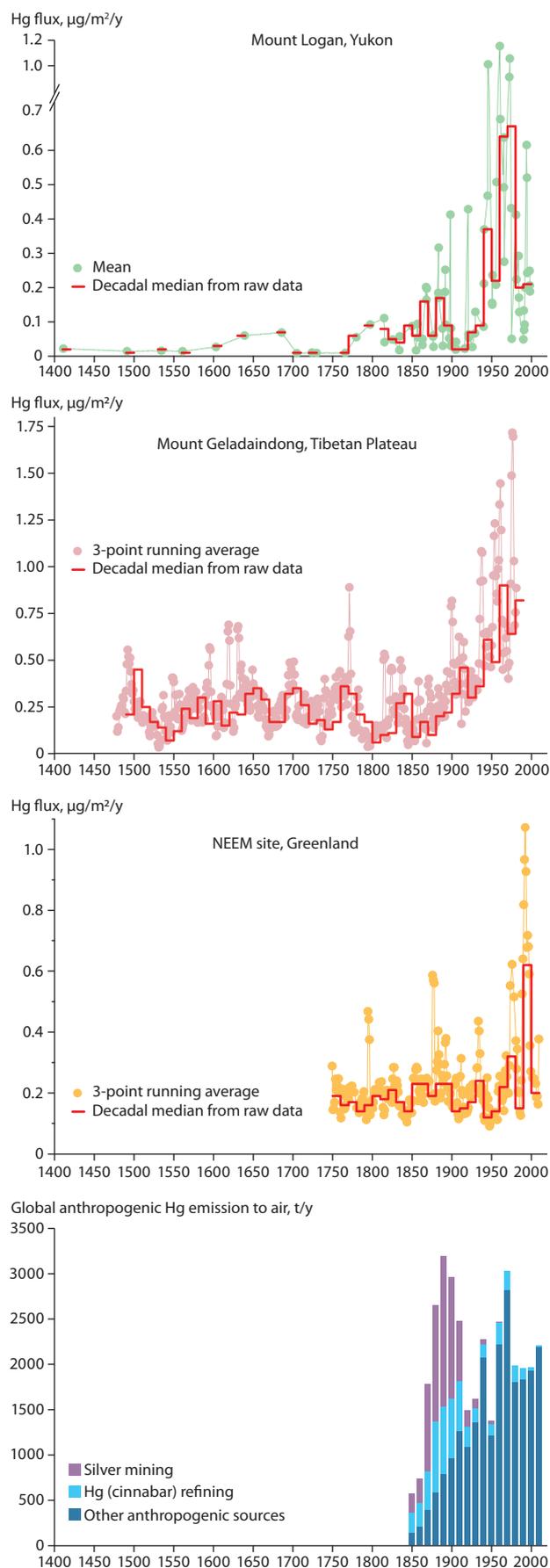
Figure 2.2. Glacial ice core records of atmospheric Hg deposition from Mount Logan, Yukon (Beal et al., 2015), Mount Geladaindong, Tibetan Plateau, China (Kang et al., 2016), and the NEEM site, Greenland (Zheng, 2015), compared with the global atmospheric emission history since 1850 AD (Streets et al., 2017).

accumulation rates were substantially greater after 1950 than in the late 1800s, in contrast to Streets et al.'s (2011, 2017) inventory (see Figure 2.2). Furthermore, during the 16th to mid-19th centuries neither the Mount Logan core (which extended back to ~1400 AD) or the Mount Geladaindong core (which extended back to 1477 AD) revealed consistent or large increases in Hg fluxes that could represent a major atmospheric impact from the Spanish New World mining operations (compare Figure 2.1: upper plot, blue line, with Figure 2.2: upper three plots). Small increases in Hg accumulation were noted during the period 1600–1700 and again in the late 18th century at Mount Logan which could be a Spanish New World signal, but overall the peak periods of Spanish colonial mining (1600–1850) and the North American Gold Rush (1850–1900) represented only 8% and 14%, respectively, of total anthropogenic Hg deposition in the Mount Logan ice core, with 78% occurring during the 20th century (Beal et al., 2015).

Thus, the weight of evidence at present supports the Zhang et al. (2014b) emission history, and suggests that the atmospheric Hg emissions produced by historic precious metal and cinnabar mining and refining techniques were not globally or hemispherically distributed to a significant degree. That these historic emissions had effects on Hg levels in some areas around mining operations is not in dispute. Other studies have shown marked contamination of lake sediments and glacial ice by nearby historic Ag/Au mining (e.g., Cooke et al., 2013; Correla et al., 2017), although these regional effects are not seen everywhere. For example, reassessment of a glacier ice core Hg record from the western United States revealed no evidence of elevated Hg deposition from late 19th century Gold Rush mining operations (Chellman et al., 2017). To summarize, current evidence supports the interpretation that historic mining had much less impact on globally-distributed atmospheric emissions and deposition than coal combustion and other industrial sources had in the 20th century. A possible explanation for this finding is that modern high-temperature Hg sources, such as coal-fired power generators or cement kilns, which emit Hg tens to hundreds of meters above the ground, may have different Hg speciation and distribution profiles to historic mining sources, which were typically relatively low temperature emissions at ground level (Guerrero, 2016, 2017). High temperature sources emitting a larger fraction of GEM above the ground boundary layer would likely distribute more of that Hg further than historic mining sources.

2.3 Revised global and oceanic total Hg budgets

Even with the lower mining emissions inventory, Zhang et al.'s (2014b) modelling indicated that the cumulative impact of those emissions over four centuries on the current levels of oceanic anthropogenic Hg has been substantial, with 67% of the increase in oceanic Hg mass above natural levels occurring prior to 1920 mainly due to precious metal mining. A further 21% of the increase was from coal combustion and 11% from other industrial activities after 1920. The total anthropogenic mass in today's oceans (66 kt) estimated by Zhang et al. (2014b) is in good agreement with another recent estimate of oceanic anthropogenic Hg (58±16 kt; Lamborg et al., 2014) derived using a different methodology based on seawater Hg
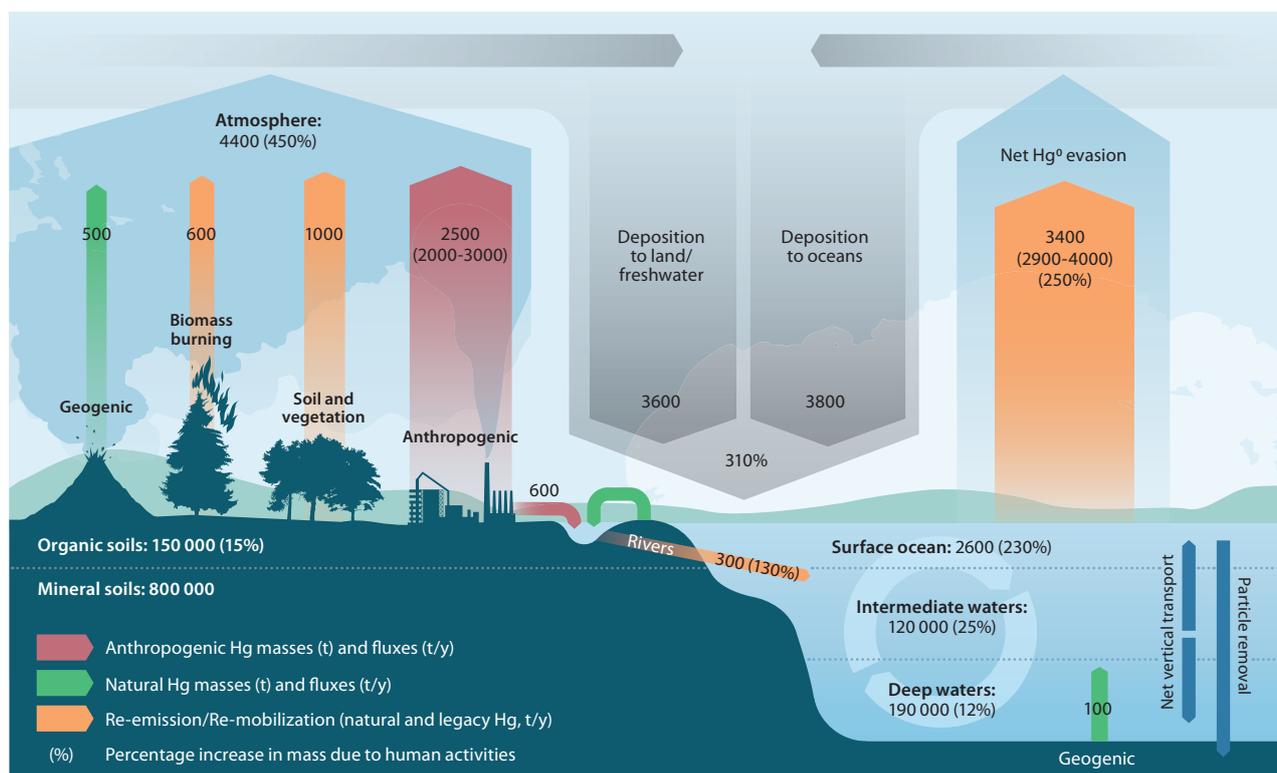
Figure 2.3 Updated global Hg budget showing the anthropogenic impact on the Hg cycle since the pre-anthropogenic period (prior to 1450 AD) (see text for explanation of its derivation). Ranges are given in brackets after the best estimate values; percentages in brackets represent the estimated increase in mass or flux due to human activities since the pre-anthropogenic period (i.e., pre-1450 AD).

concentration profiles combined with anthropogenic carbon dioxide (CO_2) and remineralized phosphate as proxies for oceanic Hg distribution. That the two studies, using different approaches, arrived at similar estimates increases confidence in the robustness of their conclusions. Both of these recent estimates fall within the lower half of the previous range of values and are close to the Mason et al. (2012) estimate of 53 kt used in AMAP/UNEP (2013) (see Table 2.1).

From these observations, a revised global total Hg budget (Figure 2.3) was constructed updating the previous version in AMAP/UNEP (2013; Mason et al. 2012). Changes in reservoirs and fluxes are based primarily on the discussion in Section 2.2 concerning more recent modeling efforts and budgets. Information and estimates from Lamborg et al. (2014) and Zhang et al. (2014b) were considered, and the revised ocean inventories are an average of the values in these two papers and the previous assessment. The new terrestrial reservoir and flux estimates are based largely on Driscoll et al. (2013) and Amos et al. (2015). Fluxes were also modified based on Pacyna et al. (2016) and Cohen et al. (2016), who advocated for specific values for the terrestrial fluxes from biomass burning, soil and vegetation emissions, and geogenic sources. These were adopted in the revised budget. The revised soil plus vegetation emissions are lower than the previous average, but for most of the remaining fluxes, the changes are relatively small (<30%) compared to the previous estimates.

Fluxes between terrestrial and oceanic reservoirs and the atmosphere were changed in accordance with the current best estimate for global atmospheric anthropogenic emissions (2500 t/y, which is 25% higher than in the previous assessment (AMAP/UNEP, 2013). This revised value reflects the fact that the current documented global inventory presented in this report (2220 t/y, range 2000–2820 for 2015; see Chapter 3)

does not include emissions for several sectors that cannot yet be reliably quantified. Provisionally, these sectors, which include agricultural waste burning and municipal and industrial waste disposal (see Chapter 3) can be expected to contribute tens to hundreds of additional tonnes of atmospheric Hg. The 2500 t/y value adopted here is therefore considered to be a reasonable estimate for use in a contemporary global budget calculation. This estimate contains several acknowledged uncertainties (especially for emissions from ASGM, and waste combustion) and so a relatively wide range of ±500 t/y is included. Similarly, there is a large range in estimates for ocean evasion. A new estimate for anthropogenic release to freshwaters, of ~0.6 kt/y, is taken from Chapter 6; an estimate from that chapter for oil and gas releases to marine systems (~0.015 kt/y) is insignificant compared with the other fluxes and so is not included in Figure 2.3. Fluxes in the budget should each be regarded as spanning a range of at least ±20%, and subject to future revision. The mass budget is balanced to within 5%.

Based on this revised global budget, the Hg budget in the world's oceans, as presented in the Zhang et al. (2014b) paper, was updated in light of the mass balance fluxes and reservoirs in Figure 2.3, and is presented in Figure 2.4. The ratios of natural to anthropogenic Hg as reported by Zhang et al. (2014b) were retained for most of the reservoirs and fluxes, although the relative increase in oceanic Hg mass due to anthropogenic inputs reported by Zhang et al. (2014b) is higher than in other publications. This difference was taken into account in updating and revising their budget for this report. The graphic breaks down each reservoir and flux in terms of how much Hg is natural, and how much is anthropogenic. The graphic also shows the cycling of Hg in the ocean through uptake onto particulate organic matter, which is a major mechanism for transport of Hg between surface
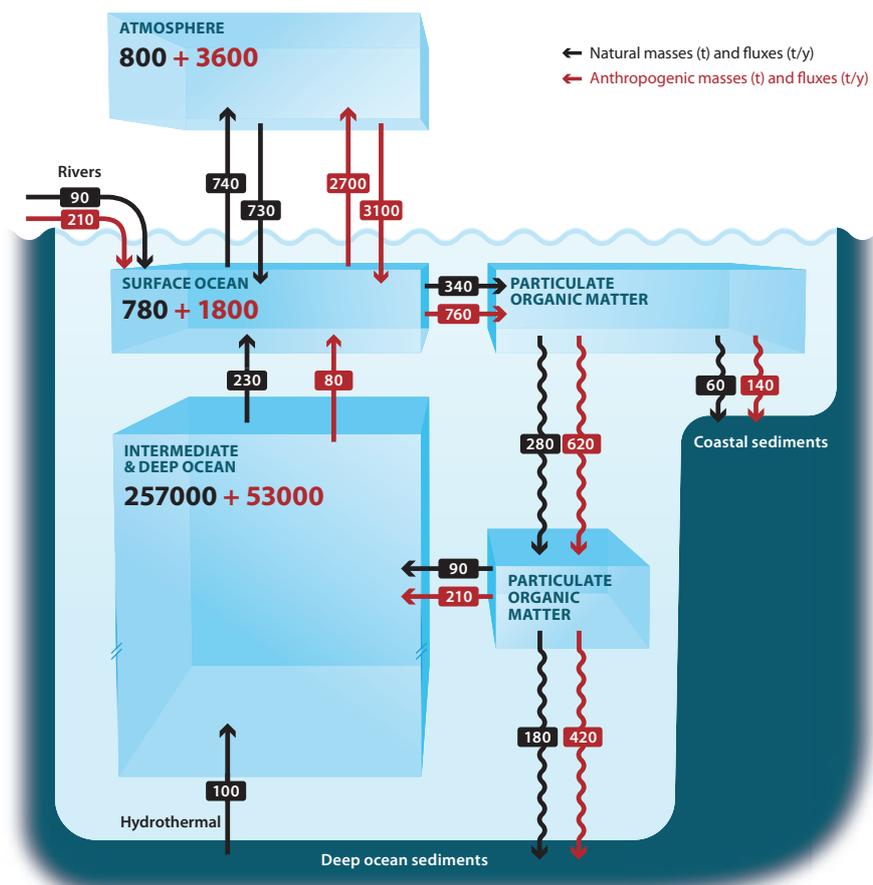
Figure 2.4. Natural and anthropogenic Hg fluxes and masses in the world's oceans. Data adapted and revised from Zhang et al. (2014b), based on the revised global budget shown in Figure 2.3.

waters and deep ocean. In this graphic, the intermediate and deep waters are combined, whereas they are treated separately in the global budget (see Figure 2.3).

Inconsistencies remain in the evidence pertaining to the actual rates of atmospheric historic mining emissions that impacted the global environment, and thus, the evidence supporting these revised estimates of oceanic and global Hg cycling. Although the 3-fold reduction in mining emissions by Zhang et al. (2014b) brought their modelled emission history during the late 19th and early 20th centuries closer to the global lake sediment pattern, compared with the Streets et al. (2011) inventory, the modelled emissions remained relatively elevated compared to lake sediment Hg accumulation during the same period (see Figure 2.1). It may be that a further reduction in the assumed proportion of volatilized Hg from historic mining/amalgamation, which would not be inconsistent with the evidence discussed above, would bring the Zhang et al. (2014b) emission history, and the remote lake sediment, peat and ice core records, into even closer agreement. There is recent evidence that further reductions may be justified. Guerrero's (2018) analysis of reports from all global Ag mining jurisdictions between 1590 and 1895 suggested a total global Hg release to air from Ag mining of just 6 kt. By comparison, Zhang et al. (2014a) and Streets et al. (2017) estimated 48 kt and 146 kt (most before 1920), respectively. These new estimates urgently need further investigation as they have significant potential implications for our understanding of the anthropogenic component of the modern global Hg cycle and budget. If implemented in future models, the additional reduction would reduce the relative amount of anthropogenic Hg in modern oceans and soils.

2.4 Distribution of anthropogenic Hg in the environment, especially the oceans

The Zhang et al. (2014b) global model projected that in the current global environment, 2% (3.6 kt) of the all-time cumulative anthropogenic emissions remains in the atmosphere, 48% (92 kt) is held in soils, and 50% (94 kt) in the oceans – 35% (66 kt) in seawater, and 15% (28 kt) buried in ocean sediments. For the oceans, atmospheric deposition from current primary emissions as well as revolatilization of legacy emissions contributes over 90% of the total (atmosphere + rivers) Hg inputs (4.0 out of 4.3 kt/y; Figure 2.3), with riverine inputs that reach the open ocean comprising a minor fraction (6%, 0.3 kt/y). Amos et al. (2014) estimated a substantially higher riverine contribution (1.5±0.8 kt/y; 30% of total 5.2 kt/y inputs) to the open ocean based on an observational database of riverwater Hg concentrations and consideration of river-offshore transport efficiencies for different estuary types. Most (72%) of the riverine Hg entering estuaries was scavenged and deposited in coastal marine sediments (Amos et al., 2014). By comparison, Mason et al. (2012) arrived at an estimate of 0.38 kt/y from rivers, which comprised ~10% of total ocean inputs. Recent data from Chinese rivers (Liu et al., 2016) support the lower estimates of Mason et al. (2012) and Zhang et al. (2014b), and so the revised oceanic budget proposes a total riverine input of 0.3 kt/y into oceans (see Figure 2.4).

Significant differences exist between recent models in their portrayal of the vertical distribution of oceanic anthropogenic Hg owing to the above-mentioned variance in historic emission estimates and different assumptions about the penetration

rate of anthropogenic Hg into deep ocean waters. Zhang et al. (2014b) and Lamborg et al. (2014) largely agreed in their relative distribution, except that the deep ocean (below 1000 m depth) contained proportionally more anthropogenic Hg in Zhang et al.'s (2014b) simulation; 45% of total oceanic anthropogenic Hg vs 35% in the simulation by Lamborg et al. (2014). Compared to Zhang et al. (2014b), Streets et al. (2011) and Amos et al. (2013) calculated similar increases in the anthropogenic Hg content of the surface ocean (4.4 times natural concentrations vs. 3.6–5.9 times, respectively), but larger increases in the thermocline/intermediate depths (1.2 times vs 2.7–5.3 times) and deep ocean (1.2 times vs. 1.5–2.1 times). In addition to their use of larger historic mining emission estimates, Streets et al. (2011) and Amos et al. (2013) assumed faster vertical mixing rates compared with the other two studies.

Large inter-basin differences in the distribution of anthropogenic Hg were also apparent in intermediate and deep ocean waters, but were relatively uniform in surface waters, in the modelling of Zhang et al. (2014b). Vertical and horizontal advection of Hg inputs to the ocean which reflect ocean currents and areas of deep water formation, and high biological productivity and rapid particle scavenging of dissolved Hg in some tropical seas, account for the inter-basin patterns.

2.5 Rate of clearance of anthropogenic Hg from the world's oceans

The differences between models and their underpinning historic mining emission estimates are associated with significant differences in the implied response times of the oceans to emission reduction scenarios. All global ocean-atmosphere models predict that Hg clearance rates from most ocean basins will be slow relative to the rate of anthropogenic emission reductions in future, such that removal of anthropogenic Hg from the world's oceans will take many decades to centuries depending on the specific ocean basin and depth interval of the water mass in question, as well as the trajectory of emission controls (Mason et al., 2012; Lamborg et al., 2014; Zhang et al., 2014b; Amos et al., 2015). But according to Selin (2014) and Engstrom et al. (2014), the 'high emission' scenario of Streets et al. (2011; also 2017) and modelling by Amos et al. (2013, 2015) suggests much slower and delayed reductions in environmental Hg levels following emission curbs than the low emissions scenario by Zhang et al. (2014b), especially for the oceans. Even at current global emission levels, there is a general scientific consensus that seawater and marine foodchain Hg levels are likely to substantially increase over time, because of the slow clearance rate of legacy Hg from the world's oceans coupled with additional legacy anthropogenic Hg released from soil profiles into rivers and revolatilized into the air (Sunderland and Selin, 2013).

Until significant deficiencies in our current understanding of marine Hg cycling, and the rates of transformation between species that influence the major sinks for ocean Hg (evasion to the atmosphere and burial in sediments) are resolved, and greater consistency is achieved in the interpretation of natural archives of Hg deposition from the atmosphere, the prediction of the timeline and effects of global emission reductions will remain uncertain. It is clear, however, that irrespective of these scientific uncertainties, emissions reductions are required to reverse the trend in oceanic anthropogenic Hg back towards natural levels, owing to the long response time of the ocean to changes in inputs (Sunderland and Selin, 2013; Engstrom et al., 2014; Selin, 2014).

2.6 Main uncertainties in global Hg models and budgets

This section summarizes the knowledge gaps and recommendations for further research stated in or developed from recent papers (Amos et al., 2013; Engstrom et al., 2014; Lamborg et al., 2014, 2016; Zhang et al., 2014b, 2016c; Song et al., 2015; Kwon and Selin, 2016). Recommendations were selected on the basis of their relevance to global or oceanic models and budgets. Scientific uncertainties can be grouped under two headings: natural inputs and processes, and anthropogenic emissions.

2.6.1 Uncertainties in natural inputs and processes

Net removal rates of anthropogenic Hg from the surface ocean are the result of competition between three simultaneously occurring natural processes: the particulate flux from the surface to the deep ocean (the 'biological pump', involving particle scavenging, remineralization and settling); the mixing of surface and deep-ocean waters; and the reduction of inorganic Hg^{II} and subsequent evasion of Hg^0 back into the atmosphere. Some of the evaded Hg^0 is rapidly photo-oxidized in the lower troposphere and re-deposited to the ocean surface. Additional coupled ocean-atmosphere measurement studies are needed to comprehensively measure the concentrations of various Hg species spatially and temporally, and to better understand the transport and transformation rates of these co-occurring processes. The need is particularly acute in the Southern Hemisphere open oceans, as well as in regions where elevated anthropogenic Hg concentrations can be expected, such as the eastern equatorial Atlantic Ocean, eastern equatorial and high latitude Pacific Ocean, and northern Indian Ocean.

Uncertainties in the robustness of measurements of atmospheric and seawater Hg concentrations are exacerbated by relatively large inter-laboratory comparison errors, and so there is a particular need to improve the overall reliability of atmospheric and seawater Hg concentration and speciation measurements. Few inter-comparison efforts have been mounted (but see Gustin et al., 2015 for a review of atmospheric Hg determinations). Past intercalibration exercises for seawater have only addressed total Hg, and the results have indicated significant discrepancies among the participating laboratories (Lamborg et al., 2012). Future intercalibration exercises should continue the effort of attaining reliable data, and should be extended to include all Hg species, even unstable species such as dimethyl Hg and dissolved Hg^0. The development of suitable seawater reference materials is encouraged.

The role of natural inputs in the global Hg budget is poorly constrained but potentially of major importance. If the actual rate of emissions from natural sources such as volcanoes and marine hydrothermal vents is markedly higher or lower than currently thought, this would affect assumptions about the absolute amounts of, and relative balance between, natural and anthropogenic sources which are fundamental to modelling efforts and to our

understanding of the global Hg cycle. Present estimates of global volcanic Hg emissions to air range over three orders of magnitude (0.1–1000 t/y) (Nriagu, 1989; Ferrara et al., 2000; Pyle and Mather, 2003; Nriagu and Becker, 2003; Bagnato et al., 2014). For oceans, the AMAP/UNEP (2013) report assigned a value of <600 t/y total Hg input from hydrothermal vents, which was based on few data and no systematic studies. Two recent GEOTRACES cruises sampled waters around hydrothermal vents in the North Atlantic and equatorial Pacific Oceans (Bowman et al., 2015, 2016). In the North Atlantic, elevated Hg concentrations were detected near the Mid-Atlantic Ridge (Bowman et al., 2015). In contrast, there was little evidence for hydrothermal Hg inputs over the East Pacific Rise in the equatorial Pacific (Bowman et al., 2016). These results suggest substantial variation in the extent of Hg inputs from different hydrothermal sources, as was found for other metals. Overall, there is insufficient new information to update the estimate of hydrothermal inputs made in 2013. In order to make direct estimations for global hydrothermal Hg fluxes, more observations of focused and diffuse-flow vent fluids and hydrothermal plumes are needed to better constrain the Hg flux, and its contribution to the global Hg cycle (German et al., 2016). In addition, analysis of sediments in regions close to hydrothermal sources relative to remote locations would help establish whether there is a strong hydrothermal signal. Submarine groundwater discharges are also likely to bring important amounts of Hg into the ocean, for which global models do not yet account. Several papers indicate that Hg inputs via submarine groundwater may be locally as important as atmospheric inputs, at least in coastal environments (Bone et al., 2007; Laurier et al., 2007; Black et al., 2009; Lee et al., 2011; Ganguli et al., 2012).

Given the importance of terrestrial soils as possibly the largest reservoir of natural and legacy anthropogenic Hg, global budget calculations will benefit from a better understanding of terrestrial Hg cycling. The lack of knowledge on the actual reservoir size that may be interacting with other parts of the biosphere has been highlighted by Schuster et al. (2018), who suggest that Arctic permafrost soils up to 300 cm deep are an unrecognized, globally significant repository of Hg. Currently, most models include only the shallow surface layer (10 cm active layer) of global soils in model parameterization and budgets. Although this permafrost Hg is mainly natural in origin, having been accumulated mostly during the early to mid-Holocene, it could represent an important potential source of Hg to the biosphere in future. There is little understanding of precisely how large and how rapidly releases from this source may develop with future climate warming, but they are expected to grow as permafrost thaws and releases its stored Hg and organic matter, both of which could lead to greater MeHg production in northern aquatic ecosystems (Stern et al., 2012). Other research priorities in this area include more measurements of the evasion rates of Hg from soils and the release rates of Hg to water following degradation of soil organic matter, as well as incorporation of the foliar uptake Hg^0 pathway into global models.

2.6.2 Uncertainties in anthropogenic emissions

The absolute amounts in historic emission inventories, and especially the role of precious metal mining, have been questioned in recent work comparing model outputs with past Hg deposition rates as reconstructed from natural archives of atmospheric deposition (see Section 2.2). Some of the uncertainty lies with the natural archives. For example, a recent paper has shown that the Hg accumulation rates in a Tibetan Plateau glacier ice core were one to two orders of magnitude lower than in a nearby lake sediment, yet both archives yielded remarkably similar trends (Kang et al., 2016). Similarly, the sediment, peat and ice core literature reviewed in Section 2.2 displays similar Hg deposition trends over time, but different absolute values, with ice cores exhibiting the lowest values of all. While the agreement in trends between archives is encouraging, the difference in absolute values begs the question of what is the most reliable quantitative estimate of past atmospheric deposition. Given the apparent importance of historic deposition to current world Hg budgets and to future emission reduction scenarios, a concerted effort to understand the reasons for the different findings from peat, lake sediment and glacial ice archives is called for that would build upon earlier work (e.g., Lamborg et al., 2002b; Biester et al., 2007; Outridge et al., 2011; Amos et al., 2015). Arriving at an agreed historic emission amount from precious metal mining would eliminate much of the uncertainty surrounding current anthropogenic Hg inventories in soils and the oceans.

The accuracy of the recent atmospheric emission inventories, including that of AMAP/UNEP (2013), has also been questioned, in part due to the inconsistency between the recent trends in primary industrial emissions, which are flat or rising, and the large (~30–40%) decreases in atmospheric GEM concentrations and wet deposition at background Northern Hemisphere monitoring stations since 1990 (see Engstrom et al., 2014; Zhang et al., 2016c). Zhang et al. (2016c) found that primary industrial emissions and GEM trends could be brought into closer agreement by accounting for the decline in Hg release from commercial products over this period, by reducing the atmospheric revolatilization rate of Hg from present-day ASGM, and by accounting for the shift in Hg^0/Hg^{II} speciation of emissions from coal-fired utilities after implementation of gaseous pollutant control measures. Because the emission inventories are the basis of global modelling efforts, resolving this discrepancy should improve the accuracy of global budgets and future trend scenarios. ASGM emissions were the largest single anthropogenic source of atmospheric Hg in the AMAP/UNEP (2013) report, but this finding has been disputed (Engstrom et al., 2014; Zhang et al., 2016c). Verifiable and higher quality emission data from ASGM operations are therefore a priority need. Studies of the speciation and distribution of the Hg released into air, land and waters from present-day ASGM operations are also called for, given the evidence reviewed in Section 2.2 suggesting that historic emissions from Ag and Au mining were geographically restricted.

The identified uncertainties and knowledge gaps described above should not be construed as undermining the rationale for the Minamata Convention on Mercury. All models are based on field measurements and are in agreement that current levels of anthropogenic Hg emissions are likely to lead to increased environmental exposure of wildlife and humans (albeit of varying magnitude), and that reducing these emissions is essential for reducing their negative environmental and health impacts. The uncertainties and knowledge gaps mainly affect our capability to predict where and when, rather than if, the environment will respond to reduced emissions.

3. Global emissions of mercury to the atmosphere from anthropogenic sources

Authors: Simon Wilson, Karin Kindbom, Katarina Yaramenka, John Munthe

Contributing authors: Jennifer O'Neill, Rasmus Parsmo, Frits Steenhuisen, Kevin Telmer

Contributors: Abdouraman Bary, Rob Cox, Kenneth Davis, Kanina Dewi, Kexiong Du, Rico Euripidou, Dave Evers, Christian Lange Fogh, Gunnar Futsaeter, Arturo Gavilan, Volker Hoenig, Young-Hee Kim, Hoang Ngoc Luu, Jacob Maag, Peter Maxson, Gabriela Medina, Jackie Mercer, James Mulolo, Peter Nelson, Ole-Kenneth Nielsen, Adel Shafei Mohamed Osman, Diego Pereira, Asif Qureshi, Alexander Romanov, Juha Ronkainen, Young-Chil Seo, Madeleine Strum, Noriyuki Suzuki, Zuraini Ahmad Tajudin, Kanduc Tjasa, Melanie Tista, Shuxiao Wang

Key messages

- A new global inventory of mercury (Hg) emissions to air from anthropogenic sources in 2015 estimates emissions from 17 key sectors at ~2220 t (2000–2820 t). Additional emissions of the order of tens to hundreds of tonnes per year may arise from (generally smaller) anthropogenic sources not currently detailed in the global inventory work, bringing a total estimate up to ~2500 t/y.

- Anthropogenic emissions of Hg to the atmosphere account for ~30% of Hg emitted annually to the atmosphere, the remainder coming from environmental processes (60%) that result in re-emission of Hg previously deposited to soils and water (much of which is itself derived from earlier anthropogenic emissions and releases), and natural sources (~10%).

- Regional and sectoral attribution of the 2015 global emissions inventory indicates that emissions patterns in 2015 are very similar to those in 2010. The majority of the 2015 emissions occur in Asia (49%; primarily East and South-east Asia) followed by South America (18%) and Sub-Saharan Africa (16%). In the latter two regions, emissions associated with artisanal and small-scale gold mining (ASGM) account for ~70–85% of the emissions. ASGM-related emissions constitute almost 38% of the global total and also account for a significant proportion of emissions in Central America and the Caribbean (31%) and East and South-east Asia (25%). In other regions (e.g., Europe and North America), emissions associated with energy production and industrial emissions predominate.

- Stationary combustion of fossil fuels and biomass is responsible for ~24% of the estimated global emissions, with coal burning accounting for 21%. Emissions from combustion of biomass for energy production are quantified for the first time in the 2015 inventory work and comprise ~2.3% of the global inventory.

- The principal industrial sectors remain non-ferrous metal production (15% of the global inventory), cement production (10%) and ferrous metal production (2%). Emissions from wastes from Hg-added products comprise ~7.3% of the global inventory estimate in 2015. With a Hg consumption in 2015 estimated at more than 1500 t, the chemicals industry is also identified as a significant emitter of Hg. The vinyl chloride monomer (VCM) and chlor-alkali chemical industries alone are estimated to be responsible for 3.3% of global emissions to air in 2015.

- Inventory methodologies are constantly improved as new information and data become available. Changes in emissions estimates for different periods therefore reflect both real-world trends and artefacts of improvements in inventory methods and data availability. Simple comparisons between the new inventory and previous inventories can result in misinterpretation and should therefore be avoided. Based on comparisons between the 2015 inventory and an updated inventory for 2010, estimated global emissions of Hg to the atmosphere in 2015 are ~20% higher than in 2010. However, different sectors contribute in different ways to this apparent overall increase.

- Estimated emissions from ASGM are almost 160 t higher in 2015 than in 2010 (accounting for about 45% of the overall increase); however, this is mainly a result of improved information rather than a real trend of increased ASGM-associated emissions over the five years between 2010 and 2015. Significant increases in emissions estimates for South America in particular are attributable mainly to the improved ASGM estimates.

- If increases due to ASGM (as well as the VCM sector, which was not quantified for 2010) are discounted, the percentage increase is reduced to ~17% (equivalent to ~195 t of emissions). Around 75% of this increase is associated with emissions from industrial sectors, 15% to stationary combustion, and 13% to (non-ASGM) intentional use sectors. Industrial emissions increased in Asia in particular, indicating that increased economic activity has more than offset any efforts to reduce emissions. In other regions, economic recovery following the financial crisis in 2008 (that may have influenced global emissions in 2010) may also have influenced observed trends in estimated emissions. Changes in fuel use and continuing action to reduce emissions resulted in modest decreases in emissions in North America and the EU (~11 t in each region), and essentially unchanged emissions in the Australia, New Zealand and Oceania and the South America regions. In all other regions, however, emissions increased, by 26% and 30%, respectively, in South Asia and East and Southeast Asia, and by 10–20% in other regions.

- Comparison between the 2015 global inventory estimates and other national and regional inventories is complicated by use of different sectoral breakdown and methods of quantification (including sources of information used,

application of emission reporting thresholds, etc.). In general, however, GMA inventory estimates were in reasonable agreement with nationally compiled inventory estimates for most sectors, taking uncertainties into account. Additional comparisons with inventories compiled as part of Minamata Initial Assessments (MIAs) and National Action Plans (NAPs – specific to the ASGM sector) could, in most cases, only be made on the basis of preliminary MIAs and NAPs. The preliminary comparisons yielded a number of issues warranting follow-up when final MIAs and NAPs are available.

- *Comparing emissions estimates produced using different methodologies and procedures (including both mass-balance and measurement-based estimates) provides important insights into limitations of reporting procedures, availability of key information and uncertainties associated with emissions quantification. Multiple approaches are essential for verifying emissions and release estimates and validating national reporting. Although challenging, harmonization of sector definitions between different reporting and inventory systems applied in different regions/countries, is an important consideration in relation to eventual Minamata emissions and release reporting requirements.*

3.1 Introduction: sources of anthropogenic Hg emissions to the atmosphere

Previous assessments (e.g., AMAP/UNEP, 2008, 2013) have described how industrial activities to generate energy, and produce metals, cement and other commodities, together with a range of intentional uses of mercury (Hg) in processes and products, result in anthropogenic emissions of Hg to the atmosphere. Present-day anthropogenic emissions are estimated at more than 2200 t/y (in 2015), accounting for about 30% of Hg emitted annually to the atmosphere; the remainder coming from environmental processes (60%) that result in re-emission of Hg previously deposited to soils and water (much of which is itself derived from earlier anthropogenic emissions and releases), and natural sources such as volcanoes (~10%).

Mercury emissions to air are associated with a number of anthropogenic activities that can be broadly characterized into 'by-product' and 'intentional-use' sectors (AMAP/UNEP, 2013). Stationary combustion of fossil fuels (coal in particular), and high temperature processes involved in industrial activities such as primary metal smelting and cement production give rise to 'unintentional' Hg emissions (i.e., the Hg emissions are a by-product of their presence in trace quantities in fuels and raw materials). Intentional-use sectors include the use of Hg-added products (e.g., lamps, batteries, instrumentation) and Hg use in dentistry (dental amalgam), where much of the Hg emissions to air (and releases to water) are associated with waste disposal. A further intentional use of Hg is in artisanal and small-scale gold mining (ASGM) where Hg is used to extract gold from gold-bearing sediments and rocks. Of these sources, stationary combustion of coal (for power, industry and domestic/residential heating) and ASGM were estimated to be responsible for over 60% of emissions to air in 2010 (UNEP, 2013a).

Mercury emissions to air have changed over time. Historically gold and silver mining have been major sources of Hg emissions and releases. These emissions/releases have had local and regional impacts that can be traced today in sedimentary records (see Chapter 2). With the advent of the industrial revolution (~1850s) and the subsequent rise of fossil fuel economies, Hg emissions increased and are believed to have peaked around the start of the 20th century. Emissions have since declined but remain high, estimated at around 2000–2500 t/y during the first decades of the 21st century. These emissions give rise to global pollution; including long-range

transport to remote regions (see Chapter 5), with associated concerns for impacts on wildlife and human health (see Chapters 8 and 9).

The GMA2013 (AMAP/UNEP, 2013; UNEP, 2013a) included a first global inventory of anthropogenic Hg emissions to air for 2010 prepared according to an updated core methodology, an extension of methods employed to produce earlier global inventories for the years 1995–2005 (Pacyna and Pacyna, 2002; Pacyna et al., 2003, 2006, 2010).

As part of the work to update the GMA2013, a new global inventory of anthropogenic Hg emissions to air has been produced, for the target year 2015. The 2015 GMA inventory, presented in this report, addresses emissions from the following key emission sectors:

- Artisanal and small-scale gold mining
- Biomass burning (domestic, industrial and power plant energy production)
- Cement production (raw materials and fuel, excluding coal)
- Cremation emissions
- Chlor-alkali production (mercury process)
- Large-scale gold production
- Mercury production
- Oil refining
- Non-ferrous metal production (primary aluminum, copper, lead, zinc)
- Pig iron and steel production (primary)
- Secondary steel production
- Stationary combustion of coal, gas and oil (domestic/residential, transportation)
- Stationary combustion of coal, gas and oil (industrial)
- Stationary combustion of coal, gas and oil (power plants)
- Vinyl-chloride monomer (mercury catalyst)
- Waste (other waste)
- Waste incineration (controlled burning, including waste to energy).

These source sectors and related (sub)activities (identified in Table 3.1) include three new sectors not previously quantified, namely biomass combustion (for energy production), secondary steel production and Hg emitted during the production of vinyl chloride monomer (VCM), a raw material for plastics including polymer polyvinyl chloride (PVC).

For the above-listed sectors it is possible to derive reasonably robust estimates of emissions at the regional and global scale that can also be assigned at a national level with some degree of confidence.

It is important, however, to recognize that the inventory estimates reported here are not fully complete. Although the inventory includes the main anthropogenic emission sectors, there remain sectors for which it is not yet possible to reliably quantify emissions, even at the global scale. These include sectors where information is currently inadequate to reliably quantify the scale of the activity or to define appropriate emission factors, such as agricultural burning and incineration of certain types of wastes including industrial waste and sewage sludge. Table 3.4 identifies additional sectors not yet fully quantified in global emission inventory work. Where possible, available information (e.g., national estimates for some countries) is used to provide some insight into the level of emissions that may be expected from sectors not included in the robust global inventory, but these values should be considered speculative at best.

3.2 Estimating 2015 global anthropogenic Hg emissions to air: General methodology and important considerations

3.2.1 General methodology

The methodology employed to produce the 2015 global inventory of anthropogenic emissions to air is essentially the same as that applied in developing the 2010 GMA inventory reported in the GMA2013 (AMAP/UNEP, 2013). The methodology applies a mass-balance approach (see Figure 3.1 and E-Annex 3, Section A3.1) to derive emissions estimates that considers: the amounts of fuels and raw materials used, or commodities produced (activity data); the associated Hg content of fuels and raw materials and the types of process involved (reflected in 'unabated' emissions factors); and technology applied to reduce (abate) emissions to air (through technology profiles that reflect the degree of application and the degree of effectiveness of air pollution controls).

The ASGM and Hg-added product sectors employ a similar approach with some variations, combining activity data with emission factors and other factors that reflect distribution pathways to different environmental media and/or waste endpoints (see E-Annex 3, Sections A3.2 to A3.4).

The general methodological approach and its development from earlier methods that were used to produce the original (1995, 2000, 2005) global inventories of emissions to air is described in the GMA2013 report (AMAP/UNEP, 2013: section 2.2) and is not repeated here. However, in order that the GMA inventory process remains transparent, the documentation in this report includes a discussion of some of the more significant changes that have been applied in the methods and/or to key parameters that influence calculated emissions estimates for particular sectors (E-Annex 3, Section A3.5). Generally, this reflects improvements in available information. The current report therefore also includes comprehensive documentation collated in an electronic annex (E-Annex 3) that presents the (updated) factors and assumptions applied in calculating the 2015 emissions estimates (E-Annex 3, Section A3.6) and uncertainties (E-Annex 3, Section A3.7), together with the activity data used (E-Annex 3, Section A3.8) and the resulting emission estimates on a country/sector basis (E-Annex 3, Section A3.9).

The methods employed to geospatially distribute national emissions estimates are as described by Wilson et al. (2006), Pacyna et al. (2010) and Steenhuisen and Wilson (2019). In addition to improving the methods used to estimate global emissions by incorporating new information, the methodology used to geospatially distribute the global inventory has also been upgraded as part of the GMA2018 work (see Section 3.2.4).

3.2.1.1 Activity data

Information on amounts of fuel or raw materials used in different applications or amounts of products or commodities produced is one of the primary inputs for estimating emissions of Hg to air. Activity data are available from various sources, such as national statistics agencies, international organizations and industry associations. Activity data compiled in a consistent manner for all countries that have a significant activity in a given sector are essential for the development of global inventories (and their temporal comparability). For this reason, the GMA inventory depends heavily on data compiled by the International Energy Agency (IEA) and sources such as the U.S. Geological Survey (Minerals Yearbook). National data made available by some countries were also incorporated.
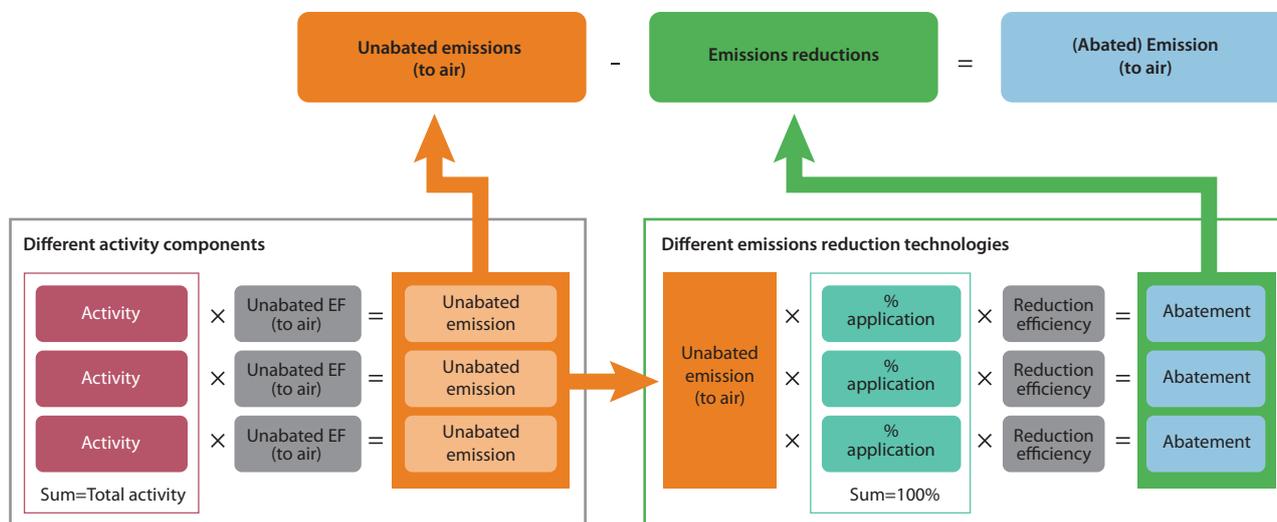
Figure 3.1 General methodology employed to produce the 2015 global inventory of anthropogenic emissions to air.

Table 3.1 Sectors/codes for which emissions have been estimated and sources of activity data used.

Sector code	Sector description	Activity code	Activity description	Sources of activity data	Year of activity data
Artisanal and small-scale gold mining					
ASGM	Artisanal and small-scale gold mining	ASGM	Artisanal and small-scale gold mining	Telmer and O'Neill (AGC) pers. comm., 2017; UN Environment, 2017a	2012+ for >80% of estimated emissions
Combustion of fuels for energy and in industry and domestic/residential uses					
BIO	Biomass burning (domestic, industrial and power plant)	PSB – DR	domestic residential burning	IEA, 2017	2015
		PSB – IND	industry	IEA, 2017	2015
		PSB – PP	power plants	IEA, 2017	2015
SC-DR-coal	Stationary combustion of coal (domestic/residential, transportation)	BC-DR	brown coal	IEA, 2017	2015
		HC-DR	hard coal	IEA, 2017	2015
SC-DR-gas	Stationary combustion of gas (domestic/residential, transportation)	NG-DR	natural gas	IEA, 2017	2015
SC-DR-oil	Stationary combustion of oil (domestic/residential, transportation)	CO-HF-IND	heavy fuel oil	IEA, 2017	2015
		CO-IND	crude oil	IEA, 2017	2015
		CO-LF-IND	light fuel oil	IEA, 2017	2015
SC-IND-coal	Stationary combustion of coal (industrial)	BC-IND-CEM	brown coal (cement industry)	IEA, 2017	2015
		BC-IND-NFM	brown coal (NFM industry)		2015
		BC-IND-OTH	brown coal (other industry)		2015
		BC-IND-PIP	brown coal (ferrous metal industry)		2015
		HC-IND-CEM	hard coal (cement industry)	IEA, 2017	2015
		HC-IND-NFM	hard coal (NFM industry)		2015
		HC-IND-OTH	hard coal (other industry)		2015
		HC-IND-PIP	hard coal (ferrous metal industry)[a]		2015
SC-IND-gas	Stationary combustion of gas (industrial)	NG-IND	natural gas	IEA, 2017	2015
SC-IND-oil	Stationary combustion of oil (industrial)	CO-HF-IND	heavy fuel oil	IEA, 2017	2015
		CO-IND	crude oil	IEA, 2017	2015
		CO-LF-IND	light fuel oil	IEA, 2017	2015
SC-PP-coal	Stationary combustion of coal (power plants)	BC-L-PP	brown coal (lignite)	IEA, 2017	2015
		BC-S-PP	brown coal (sub-bituminous)	IEA, 2017	2015
		HC-A-PP	hard coal (anthracite)	IEA, 2017	2015
		HC-B-PP	hard coal (bituminous)	IEA, 2017	2015
SC-PP-gas	Stationary combustion of gas (power plants)	NG-PP	natural gas	IEA, 2017	2015
SC-PP-oil	Stationary combustion of oil (power plants)	CO-HF-PP	heavy fuel oil	IEA, 2017	2015
Industry sectors					
CEM	Cement production (raw materials and fuel, excluding coal)	CEM	cement (fuels excl.)	USGS, 2016	2014
		PC-CEM	pet coke	IEA, 2017	2015
			See also BC–IND-CEM and HC-IND-CEM		

Sector code	Sector description	Activity code	Activity description	Sources of activity data	Year of activity data
NFMP	Non-ferrous metal production (primary Al, Cu, Pb, Zn)	AL-P	aluminum (primary production)	USGS, 2017	2015
		CU-P	copper (primary production)	USGS, 2017	2015
		CU-T	copper (total production)[b]	USGS, 2017	2015
		PB-P	lead (primary production)	USGS, 2017	2015
		PB-T	lead (total production)[b]	USGS, 2017	2015
		ZN-P	zinc (primary production)	USGS, 2017	2015
		ZN-T	zinc (total production)[b]	USGS, 2017	2015
			See also BC–IND-NFM and HC-IND-NFM		
NFMP-AU	Large-scale gold production	GP-L	gold production	USGS, 2017	2015
NFMP-HG	Mercury production	HG-P	mercury production	USGS, 2016	2013/2014
				UN Environment, 2017a	2015
OR	Oil refining	CO-OR	oil refining	IEA, 2017	2015
PISP	Pig iron and steel production (primary)	PIP	iron and steel (primary production)	USGS, 2016	2014
SSC	Secondary steel production	SP-S	secondary steel production	World Steel Association, 2015	2014
Intentional uses (other than ASGM)					
CREM	Cremation emissions	CREM	Cremation emissions	National reports and International Cremation Statistics	2014
CSP	Chlor-alkali production (mercury process)	CSP-C	capacity based	UNEP, 2013b	2012
		CSP-P	production based	UNEP, 2013b; OSPAR, 2016; EuroChlor, 2017	2012-2015
			See also BC–IND-PIP and HC-IND-PIP		
		CO-LF-PP	light fuel oil	IEA, 2017	2015
		CO-PP	crude oil	IEA, 2017	2015
VCM	Vinyl-chloride monomer (mercury catalyst)	VCM	Vinyl-chloride monomer	National and literature information on VCM production, Hg consumption and emissions	2015
WASOTH	Waste (other waste)	WASOTH	other waste	Estimated consumption of Hg in Hg-added products in 2015 by world region (UN Environment, 2017a)	2015
WI	Waste incineration (controlled burning)	WI	waste incineration	Estimated consumption of Hg in Hg-added products in 2015 by world region (UN Environment, 2017a)	2015

[a]HC-IND-PIP: does not include 'non-energy coke' (see E-Annex 3, Section A3.5); [b]PB-T, CU-T, ZN-T: total (primary+secondary) production used as activity for countries where activity data for primary production alone were not available.

Sectors and sources of activity data used in preparing the 2015 global estimates are presented in Table 3.1. Sectors are grouped according to four main categories: combustion of fuels; industrial sectors; artisanal and small-scale gold mining; and (non-ASGM) intentional use sectors. These main groups are also reflected in subsequent presentations of results. Activity data used to develop the 2015 GMA national emission estimates are presented in E-Annex 3, Section A3.8.

Whenever available, statistics for the target year 2015 have been used for this emission inventory. In some cases, data for 2015 were not available at the time of preparing the inventory; in such cases, data from 2014 (and in a few cases earlier) were used.

Lack of globally consistent activity data is one of the major obstacles to the inclusion (at the present time) of some additional sectors that are implicated in Hg emissions to the atmosphere in the global inventory. Some of these sectors are identified in Table 3.4.

3.2.1.2 Emission factors and technology profiles

Information on (unabated and abated) emissions factors and technology profiles – reflecting the degree of application and effectiveness of air pollution control (APC) technologies to reduce emissions of Hg; see AMAP/UNEP (2013) – are detailed in E-Annex 3, Section A3.6. These factors are defined for individual countries where data are available. Where national data are lacking, default factors are applied to groups of countries based on assumptions regarding their level of technological development. For ASGM-associated emissions a similar but more specific approach is employed (see E-Annex 3, Section A3.2). The assignment of (emission and APC technology) factors for particular countries/sectors builds on work described in the GMA2013 report, and utilizes a considerable amount of new information that has since become available from published literature, especially concerning China, as well as information from national experts from more than 25 countries from all world regions during inventory workshops and meetings organized as part of the 2015 inventory compilation activity.

Updates to applied emission factors and assumptions regarding application and effectiveness of APC technologies can significantly affect derived (national-sector) emission estimates; some revisions reflect developments (such as in applied APC measures, or changes in sources of fuels or raw materials used nationally) since 2010; others reflect improved information on, for example, the Hg content of fuels and raw materials that would also apply in relation to revised 2010 emissions estimates. Revisions to factors applied in the 2015 inventory work are – for the most part – not yet reflected in the UNEP Toolkits that are being used as the basis for most national Minamata Initial Assessments; see Section 3.3.3 (ii). The next section and E-Annex 3, Section A3.5 discuss some of the more significant changes introduced for individual sectors.

3.2.2 Sector specific methodologies – significant changes and improvements

For the sectors: Stationary combustion – oil burning, Stationary combustion – gas burning, Primary production of non-ferrous metals – Hg from cinnabar ore, and Chlor-alkali production, methods employed are essentially identical to those applied in the GMA2013 (AMAP/UNEP, 2013). Updated information on the basis for calculations applied in the 2015 inventory can be found in E-Annex 3, Section A3.6.

For several other sectors, methods have been updated. E-Annex 3, Section A3.5 details substantive methodological changes that have been introduced in relation to specific sectors. These changes can have implications for calculated estimates that need to be appreciated when comparing 2015 inventory estimates with previous estimates (including 2010 inventory estimates presented in the GMA2013 report). For a more detailed discussion of the results regarding emission estimates for selected emission source sectors see Section 3.4.3.

3.2.3 Uncertainties

Estimating the uncertainties associated with Hg emissions is not a simple task: the nature of the data means that there will never be a single 'good' answer, only answers that are based on

sensible approaches and that can be considered 'reasonable' in relation to the context in which they are presented.

In the GMA2013 (AMAP/UNEP, 2013), a simplistic approach was applied to calculate uncertainties associated with the 2010 inventory estimates. Essentially, this involved calculating high- and low-range estimates for individual country-sector emissions based on assumptions regarding reliability of activity data and (unabated) emission factors and aggregating these to produce 'extreme' range values. Uncertainties associated with assumptions about applied technologies were ignored. It was noted that, since over- and under-estimation will to some extent cancel out in aggregated estimates, this approach would result in 'overstating' uncertainties associated with aggregated emissions estimates such as regional, sectoral or global totals. However, the method did promote awareness that inventory estimates – whatever their source or basis – have large associated uncertainties and need to be regarded in this light.

In the 2015 inventory work, a more detailed evaluation of uncertainties has been applied considering three different approaches: (i) calculating uncertainties using the approach applied in the GMA2013; (ii) applying a modification of this whereby uncertainties associated with technology assumptions were also introduced for most sectors, and (iii) employing the propagation of errors method (Frey et al., 2006) to evaluate uncertainties associated with aggregated estimates. The latter method was adapted to apply a cut-off in extreme situations, for example, so that abatement efficiency could not exceed 100%. Further assumptions were applied in relation to other factors; for example, unabated emissions factors used in range estimates were based on assumptions regarding skewed (log-normal) distribution of Hg-content of fuels and raw materials.

In the case of ASGM, the situation is somewhat different in that the main source of uncertainty in relation to emissions is considered to be associated with level of activity rather than the (unabated) emission factor. The emission factor from amalgam is effectively 100% of the Hg contained in the amalgam, and the quantity of amalgam is directly proportional to the amount of gold produced. This does not account for the use of retorts (Hg recycling); however, their use is small to negligible globally. Therefore, with respect to emissions of Hg to the atmosphere, the uncertainty in the estimate is largely equivalent to the uncertainty in the amount of gold produced. As a further consequence, if emissions to air are over-estimated, releases to land/water will be under-estimated, and vice versa.

Further details of the three approaches considered in evaluating uncertainty are described in E-Annex 3, Section A3.7. Results of the modified approach (approach 'ii') are reflected in the values for individual country-sector estimates tabulated in E-Annex 3, Section A3.9 and Table 3.5.

The 'propagation of errors' approach was considered to best represent the scale of the uncertainties for aggregated inventory estimates compared with those achieved by simply summing uncertainties for individual (country-sector) emission estimates. This is therefore the basis for uncertainty estimates associated with aggregated emission estimates presented in Section 3.3.

At the global level, uncertainties calculated using approach (i) are -55% to +157%, using method (ii) -64% to +213%, and using method (iii) -10% to +27%.

3.2.4 Spatial distribution

The process of (geo-)spatially distributing national/sectoral emission estimates to reflect patterns of emission intensity across the globe is a prerequisite to many approaches to model atmospheric transport and deposition (see Chapter 5). Methods previously applied (Wilson et al., 2006; Pacyna et al., 2010; Steenhuisen and Wilson, 2015) have been updated and improved (Steenhuisen and Wilson, 2019).

Major new developments in the spatial distribution methodology include:

• Compilation of new information on point sources from available public domain resources (including geographical location, reported emissions where available from national inventories and pollution transfer and release inventories – for Europe, USA, Canada, Australia).

• Updated modelling of emissions from point sources that lack plant specific emissions estimates, using information on, for example, plant capacity in combination with the national emissions totals for the sector concerned, and setting maximum values based on available information on emissions from relevant large facilities to avoid extreme emission values.

• Introduction of new procedures to allow national estimates to be mapped (gridded) at a finer resolution, such as for use in modelling work with flexibility to define different output resolutions.

• Introduction of new procedures to make it easier to incorporate and select proxy 'distribution masks' for application to different emission sectors and update proxy data for individual countries as opposed to global level only.

• Development of new distribution masks for 'population' and 'urban population'; and for ASGM using new information to better define relevant areas of countries concerned, including information for African countries from experts engaged in the preparation of regional NAPs.

• Implementation of new options to allow more flexible introduction of alternative speciation schemes and emission height classification schemes for emissions from different sectors according to country groupings.

• Options to allow future applications to take advantage of improved information on individual plants (e.g., plant specific speciation schemes, emission stack heights, etc.).

Results of the spatial distribution of the GMA global inventory estimates of anthropogenic emissions to air in 2015 are presented in Section 3.5 (Figure 3.9); related datasets are available (https://www.amap.no/documents/doc/global-mercury-emissions-2015/1816) and were employed in modelling work reported in Chapter 5. The work undertaken to improve the spatial distribution procedures illustrates the importance of compiling better information on emissions at individual point source facilities, including the location of the facilities, associated (quantified) Hg emissions, and characteristics of the plants in relation to applied technology, fuels, and installed emission controls. Such data also need to be compiled in a manner that can track temporal changes in point-source emissions, to complement the development of temporally-consistent emission

inventories. Facility-level reporting systems are only available for a limited number of countries, and some employ thresholds for mandatory reporting that may result in under-estimation of total national emissions. Better information is also needed to improve 'proxy' data that are applied for distribution of non-point source emissions; for sectors, such as ASGM in particular, where information on the (spatial) extent of the activity is difficult to determine from easily-accessible sources.

New information is also becoming available on speciation of emissions from point sources, in particular from China (e.g., Zhang et al., 2008, 2016d; Chen et al., 2013a; Liu et al., 2018b) that needs to be evaluated as a basis for improving speciation schemes that are applied in connection with the spatial distribution work. Changes in APCD implemented in different countries over time influences the associated sectoral emission speciation of Hg. This is illustrated in recent work considering the impact on speciation of changes in (APC) technology at the national level (e.g., Wu et al., 2016b). Speciation changes have not yet been adequately addressed in global inventories and failure to track the changes of Hg speciation can compromise assessment of air transport and deposition as well as environmental impact assessment of Hg emissions; see also discussions in Chapter 5 (Section 5.2.1). Notwithstanding these observations, the results of the spatial distribution work, and basic speciation scheme applied in this work provide an important additional perspective on global emissions from anthropogenic sources, and are critical to the validity of work to investigate air transport and deposition and source-receptor relationships (see Chapter 5).

3.3 Estimating 2015 global anthropogenic Hg emissions to air: Results

Results for the 2015 global inventory estimates are reviewed below from the perspective of regional- and sectoral-based summaries, followed by commentaries on comparisons with national inventories and air emissions on a sector by sector basis, and an evaluation of apparent trends in emissions between 2010 and 2015.

The global inventory of Hg emissions to the atmosphere in 2015 from the 17 major anthropogenic source sectors quantitatively evaluated in this work is estimated at 2220 t (range 2000–2820 t).

This global inventory total for 2015 does not include sectors that are not yet addressed discretely in the inventory work; that is, sectors that lack information required for detailed estimation at the regional level, such as 'contaminated sites' (e.g., old mines / mine tailings and decommissioned industrial facilities). Emissions to air from 'contaminated sites' in 2010 were estimated at ~80 t in the GMA2013 work, and can be assumed to be similar in 2015. Sources not fully addressed in the quantitative inventory are discussed in Section 3.3.2.1 and Table 3.4. Some key observations are as follows:

• The 2015 global inventory estimate of Hg emissions to air from anthropogenic sources of 2220 t aligns with the GMA2013 statement that global emissions to air in the first decades of the 21st century from the main anthropogenic sectors are of the order of 2000 t/y.

- Uncertainties associated with the current air inventory estimate of 2220 t are of the order of -10% to +30% (i.e., an approximate range of 2000–2820 t).

- Estimated global Hg emissions to air from anthropogenic sources in 2015 are ~17% higher than the inventory for 2010, when 2010 estimates are retrospectively updated for comparable methodology and sectors not addressed in the original 2010 inventory are excluded. Different sectors contribute to the increase to a different extent. High apparent increases in emissions from ASGM (almost 160 t) are most likely to be associated primarily with improvements in the information upon which these estimates are based. The second major contributor to the increase is industrial sectors (142 t) where increased economic activity in certain regions is reflected in activity data for production and use of raw materials. Changes in estimated emissions between 2010 and 2015 are discussed in more detail in Sections 3.3.3 and 3.4.

- Sectors not yet quantified in the national inventory estimates may contribute additional emissions to air of the order of tens to hundreds of tonnes per year globally. These include, for example, about 70–95 t of emissions from contaminated sites (see Section 3.3.2.1).

3.3.1 Summary of results by region

The regional (sub-continental) contributions to the global inventory in 2015 are illustrated in Figure 3.2. The pattern of emissions is very similar to that in 2010, with the majority of the emissions occurring in Asia (49%, of which 39% are in East and South-east Asia, compared with about 48% in 2010) followed by South America (18%) and Sub-Saharan Africa (16%) (see

- East and Southeast Asia
- South America
- Sub-Saharan Africa
- South Asia
- CIS & other European countries
- EU28
- Middle Eastern States
- Central America and the Caribbean
- North America
- North Africa
- Australia, New Zealand & Oceania
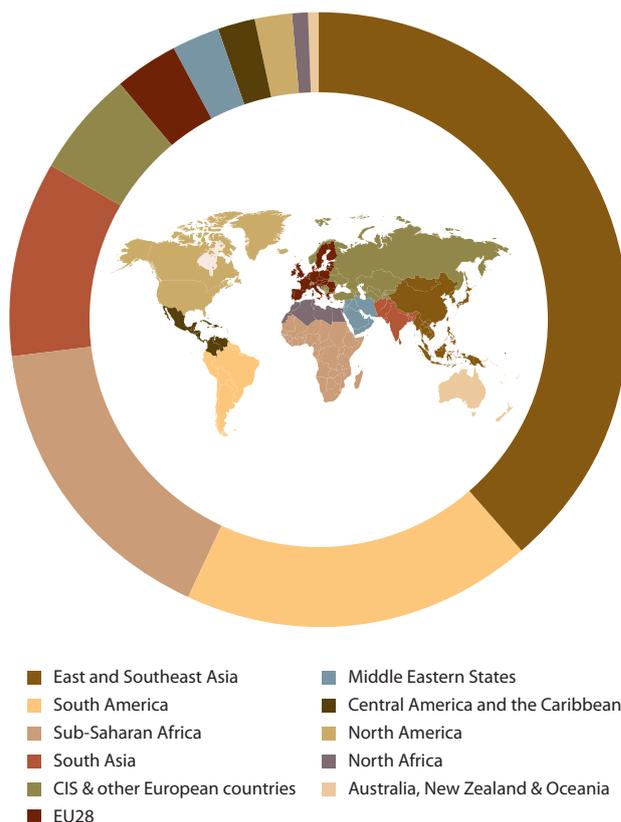
Figure 3.2 Regional breakdown of global emissions of Hg to air from anthropogenic sources in 2015.

also Table 3.2). The consistency in the regional distribution of emissions between the 2010, 2010-updated, and 2015 GMA datasets discussed in this report (illustrated in Figure 3.6 in

Table 3.2 Regional breakdown of global emissions of Hg to air from anthropogenic sources in 2015. Data shown to three significant figures.

	Sector group[a], tonnes				Regional total (and range)[b], tonnes	% of global total
	Fuel combustion	Industry sectors	Intentional-use (including product waste)	ASGM		
Australia, New Zealand and Oceania	3.57	4.07	1.15	0	8.79 (6.93–13.7)	0.4
Central America and the Caribbean	5.69	19.1	6.71	14.3	45.8 (37.2–61.4)	2.1
CIS and other European countries	26.4	64.7	20.7	12.7	124 (105–170)	5.6
East and Southeast Asia	229	307	109	214	859 (685–1430)	38.6
EU28	46.5	22.0	8.64	0	77.2 (67.2–107)	3.5
Middle Eastern States	11.4	29.0	12.1	0.225	52.8 (40.7–93.8)	2.4
North Africa	1.36	12.6	6.89	0	20.9 (13.5–45.8)	0.9
North America	27.0	7.63	5.77	0	40.4 (33.8–59.6)	1.8
South America	8.25	47.3	13.5	340	409 (308–522)	18.4
South Asia	125	59.1	37.2	4.50	225 (190–296)	10.1
Sub-Saharan Africa	48.9	41.9	17.1	252	360 (276–445)	16.2
Global inventory	533	614	239	838	2220 (2000–2820)	100

[a]See Table 3.1 for a definition of the sectors comprising each group; [b]uncertainty ranges calculated using error propagation method (see Section 3.2.3).

Australia, New Zealand
& Oceania

Central America and
the Caribbean

CIS & other
European countries

East and
Southeast Asia

EU28

Middle Eastern States

North Africa

North America

South America

South Asia

Sub-Saharan Africa

■ Stationary Combustion ■ Industry ■ Intentional Use ■ ASGM
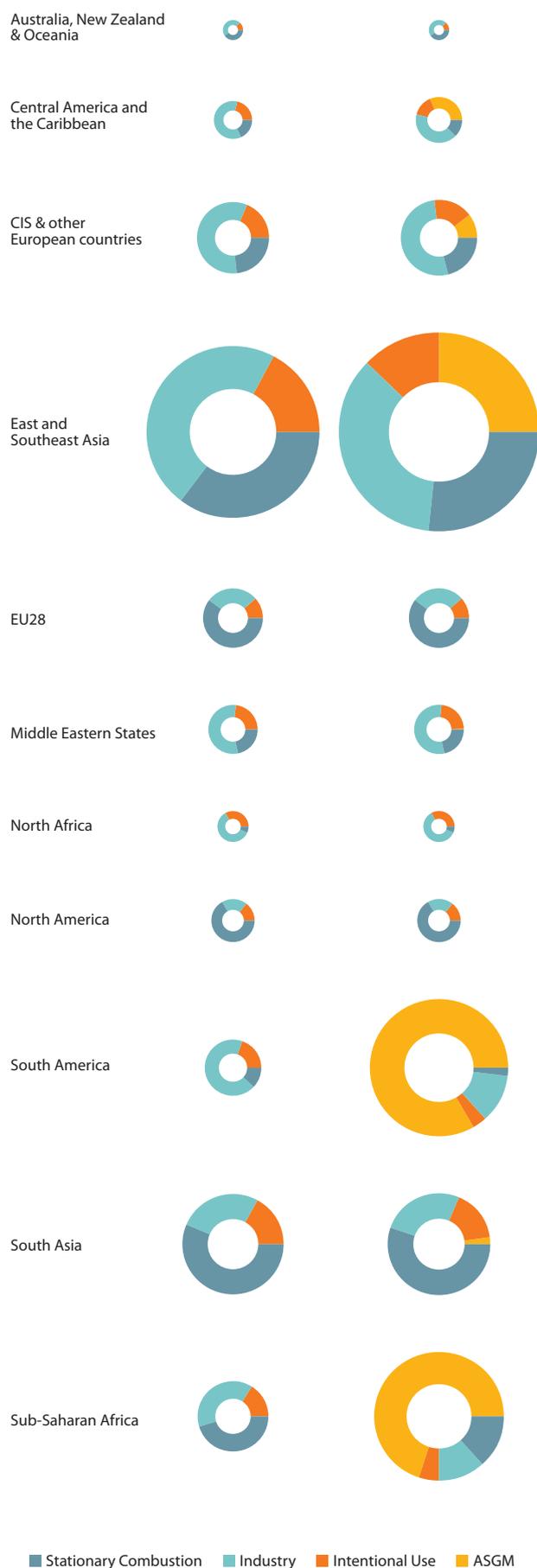
Figure 3.3 Contributions of the main groups of sectors to total emissions in different sub-regions in 2015 including ASGM (graphs, right column) and with ASGM emissions excluded (graphs, left column).

Section 3.4.2) indicates that these patterns are robust and not influenced to any undue extent by artefacts resulting from changes in methodology and additional sectors introduced since the GMA2013 work.

The relative pattern of contributions of the regions to the inventory total is heavily influenced by emissions from ASGM. ASGM-associated emissions account for about 70–75% of the emissions that occur in South America and Sub-Saharan Africa (see Figure 3.3; graphs, right column). If ASGM-associated emissions are omitted (see Figure 3.3; graphs, left column), then the East and South-east Asian region remains the region responsible for the majority of emissions (47% on the non-ASGM total), with South Asia responsible for a further 16%. The non-ferrous metals industry is the main source of emissions in Sub-Saharan Africa and the 'CIS and other European countries' region; thus these two regions, between them, contribute a further 16% of the total non-ASGM emissions. In the remaining regions, coal combustion still accounts for the major part of the emissions in North America (almost 60%), the EU (about 54%) and Australia, New Zealand and Oceania (37%). In the Middle Eastern States and North Africa, the cement industry is the main source of emissions (43% and 52% of the regional totals, respectively). Sources associated with wastes from Hg-added products account for approximately 10–20% of emissions in most regions, somewhat higher in North Africa (27%) and lower in the EU and East and South-east Asian regions.

All percentage contributions need to be considered in relation to the total (absolute) amounts of Hg emitted in each sub-region. The sector-based emission discussion (Section 3.3.3) provides additional insights into the relative amounts of emissions from different source sectors.

3.3.2 Summary of results by sector

As with the regional breakdown, the relative breakdown of anthropogenic Hg emissions in 2015 between sectors is, in most respects, very similar to that in 2010. The predominant source sector is ASGM (~33.8%) followed by stationary combustion of coal (~22.4%; of which 13.9%, 6% and 2.6% are from, respectively, power plants, industrial uses and domestic/residential burning). These are followed by emissions from non-ferrous metal production (~15.1%, of which 3.8% is from large-scale gold production and 1% from production of Hg), and cement production (~10.8%). Emissions associated with disposal of Hg-added product waste (7.6%), ferrous-metal production (3.4%, of which 0.5% is from secondary steel production), stationary combustion of other fuels (3%, from combustion of oil, gas and biomass – the latter a newly included component contributing 2.6%) and other (2.9%, with another newly included sector – VCM – responsible for 2.3%) make up the rest. See Figure 3.4 and Table 3.3.

More detailed discussions for individual sectors, also considering changes from 2010 to 2015 are presented in Section 3.4.

Table 3.3 Global emissions of Hg to air from different anthropogenic source sectors in 2015. The color code reflects the four main sector groupings represented in Figure 3.3 and elsewhere, see Table 3.1. Data shown to three significant figures.

Sector code	Description	Activity code	Description	Emission 2015[a], tonnes	Sector emission (range)[b], tonnes	Sector % of total
ASGM	Artisanal and small-scale gold mining	ASGM	Artisanal and small-scale gold mining	838	838 (675–1000)	37.7
BIO	Biomass burning (domestic, industrial and power plant)	PSB – DR	domestic residential burning	38.3	51.9 (44.3–62.1)	2.33
		PSB – IND	industry	7.92		
		PSB – PP	power plants	5.68		
CEM	Cement production (raw materials and fuel, excluding coal)	CEM	cement (fuels excl.)	232	233 (117–782)	10.5
		PC-CEM	pet coke	1.14		
			See also BC–IND-CEM and HC-IND-CEM			
CREM	Cremation emissions	CREM	Cremation emissions	3.77	3.77 (3.51–4.02)	0.17
CSP	Chlor-alkali production (mercury process)	CSP-C	capacity based	13.5	15.1 (12.2–18.3)	0.68
		CSP-P	production based	1.61		
NFMP	Non-ferrous metal production (primary Al, Cu, Pb, Zn)	AL-P	aluminum (primary production)	6.61	228 (154–338)	10.3
		CU-P	copper (primary production)	48.4		
		CU-T	copper (total production)	0.424		
		PB-P	lead (primary production)	28.6		
		PB-T	lead (total production)	2.92		
		ZN-P	zinc (primary production)	17.5		
		ZN-T	zinc (total production)	124		
			See also BC–IND-NFM and HC-IND-NFM			
NFMP-AU	Large-scale gold production)	GP-L	gold production	84.5	84.5 (72.3–97.4)	3.8
NFMP-HG	Mercury production)	HG-P	mercury production	13.8	13.8 (7.9–19.7)	0.62
OR	Oil refining	CO-OR	oil refining	14.4	14.4 (11.5–17.2)	0.65
PISP	Pig iron and steel production (primary)	PIP	iron and steel (primary production)	29.8	29.8 (19.1–76.0)	1.34
			See also BC–IND-PIP and HC-IND-PIP			
SC-DR-coal	Stationary combustion of coal (domestic/residential, transportation)	BC-DR	brown coal	1.77	55.8 (36.7–69.4)	2.51
		HC-DR	hard coal	54.0		
SC-DR-gas	Stationary combustion of gas (domestic/residential, transportation)	NG-DR	natural gas	0.165	0.165 (0.13–0.22)	0.01
SC-DR-oil	Stationary combustion of oil (domestic/residential, transportation)	CO-DR	crude oil	0.001	2.70 (2.33–3.21)	0.12
		CO-HF-DR	heavy fuel oil	0.524		
		CO-LF-DR	light fuel oil	2.18		
SC-IND-coal	Stationary combustion of coal (industrial)	BC-IND-CEM	brown coal (cement industry)	2.15	126 (106–146)	5.67
		BC-IND-NFM	brown coal (NFM industry)	0.413		
		BC-IND-OTH	brown coal (other industry)	4.81		
		BC-IND-PIP	brown coal (ferrous metal industry)	0.151		
		HC-IND-CEM	hard coal (cement industry)	41.6		
		HC-IND-NFM	hard coal (NFM industry)	3.32		
		HC-IND-OTH	hard coal (other industry)	43.7		
		HC-IND-PIP	hard coal (ferrous metal industry)	30.1		
SC-IND-gas	Stationary combustion of gas (industrial)	NG-IND	natural gas	0.123	0.123 (0.10–0.15)	0.01
SC-IND-oil	Stationary combustion of oil (industrial)	CO-HF-IND	heavy fuel oil	1.11	1.40 (1.18–1.69)	0.06
		CO-IND	crude oil	0.085		
		CO-LF-IND	light fuel oil	0.206		

Sector code	Description	Activity code	Description	Emission 2015[a], tonnes	Sector emission (range)[b], tonnes	Sector % of total
SC-PP-coal	Stationary combustion of coal (power plants)	BC-L-PP	brown coal (lignite)	59.3	292 (255–346)	13.1
		BC-S-PP	brown coal (sub-bituminous)	37.2		
		HC-A-PP	hard coal (anthracite)	3.14		
		HC-B-PP	hard coal (bituminous)	192		
SC-PP-gas	Stationary combustion of gas (power plants)	NG-PP	natural gas	0.349	0.349 (0.285–0.435)	0.02
SC-PP-oil	Stationary combustion of oil (power plants)	CO-HF-PP	heavy fuel oil	1.96	2.45 (2.17–2.84)	0.11
		CO-LF-PP	light fuel oil	0.164		
		CO-PP	crude oil	0.322		
SSC	Secondary steel production	SP-S	secondary steel production	10.1	10.1 (7.65–18.1)	0.46
VCM	Vinyl-chloride monomer (mercury catalyst)	VCM-P	Vinyl-chloride monomer production	12.3	58.2 (28.0–88.8)	2.6
		VCM-R	Vinyl-chloride monomer recycling	45.9		
WASOTH	Waste (other waste)	WASOTH	other waste	147	147 (120–223)	6.6
WI	Waste incineration (controlled burning)	WI	waste incineration	15.0	15.0 (8.9–32.3)	0.67
Total				2220	2220 (2000–2820)	100

[a]The indicated uncertainties are based on the propagation of errors approach; for by-product sectors, individual country-sector estimates were assigned uncertainties based on the modified GMA2013 approach (including uncertainties associated with APC technology); for ASGM and sectors concerning waste from Hg-added products, the basic GMA2013 approach was used for country-estimates; [b]uncertainty ranges calculated using error propagation method (see Section 3.2.3).
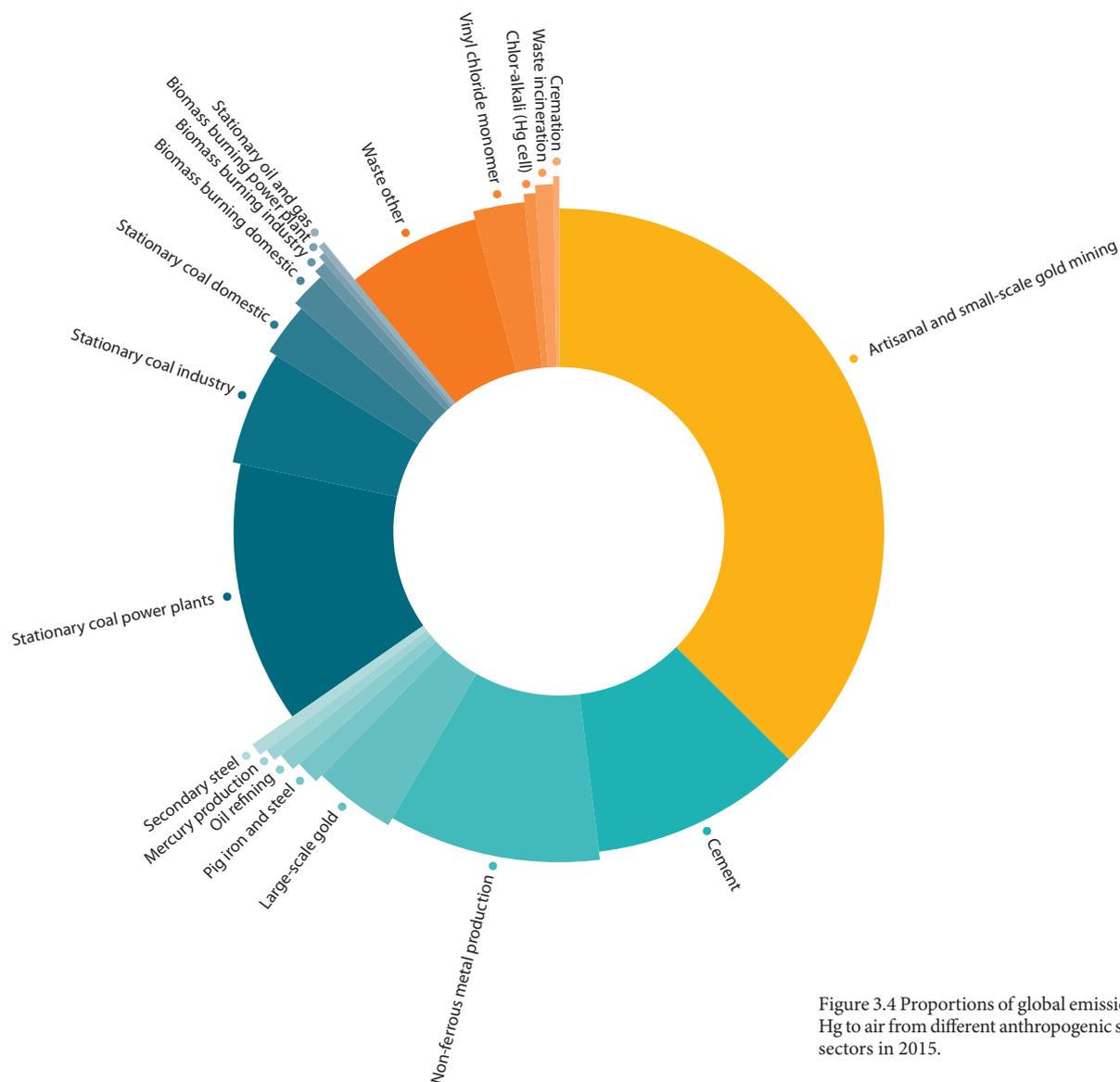
Figure 3.4 Proportions of global emissions of Hg to air from different anthropogenic source sectors in 2015.

Table 3.4 Anthropogenic source sectors for which emissions cannot yet be reliably estimated.

Other potential emissions (sectors quantified only as global totals)	Issues
Contaminated sites	Mercury-contaminated sites (e.g., former mining waste disposal sites) may contribute significant emissions to air on a local to regional scale. Emission rate is likely to depend on Hg-content as well as local soil conditions and climate etc. which makes global estimates difficult
Agricultural burning	Agricultural burning, including burning to clear land for agricultural use (as well as biomass burning) is a potentially important source and probably also linked to climate change and natural disasters
	Information is lacking on global amounts incinerated and Hg content of materials burned which makes global estimates uncertain
Incineration of industrial and sewage sludge and some hazardous wastes	Information on total amounts of industrial waste and sewage sludge incinerated is not available. Some hazardous waste (Hg-added products) is covered in the inventory
	Hg contents of industrial wastes and sewage sludge are highly variable, no generally applicable information is available
	Some nationally compiled inventories include estimates of emissions from incineration of industrial waste and sewage sludge
Oil and gas extraction (upstream of refineries and unaccounted)	Extraction and processing of oil may release Hg to water, soil and air. Hg content of crude oil is highly variable and there is a general lack of information needed to quantify these emissions on a global scale
	Natural gas can contain variable concentrations of Hg, depending on the geological properties of the surrounding minerals. Hg vapor is often removed from natural gas prior to processing and distribution due to risk of damage to metal pipes and processing equipment
	General lack of knowledge on Hg contents, removal efficiency and leakage risks
Gas flaring	
Geothermal power plant emissions	Geothermal power plants can result in Hg emissions to air if located in an area with significant geological mercury contents in the bedrock. Sufficient information to provide global estimates is not available
Dental use (amalgam fillings)	Emissions associated with dental applications are not fully included in the inventory; emissions of Hg present in amalgam are included only as associated with human cremation. Emissions during the preparation of amalgams and their subsequent removal and disposal in wastes are not included
Other potential sources	Varying amounts of Hg are likely to be emitted from other industrial sources including pulp and paper manufacture, secondary non-ferrous metals, food industry, chemical industry, production of bricks, ceramics, lime, coke, charcoal, fertilizers, and combustion of peat. Global statistics and/or national inventories are lacking. Emissions from some of these sources may be included in national inventories under reported categories such as energy, industrial or 'other'
Informal/unorganized activities associated with a diverse range of industrial processes in developing countries (e.g., waste recycling); from small-scale to very large operations in some countries	No reliable statistics available
Speculative additional total global emissions	

3.3.2.1 Anthropogenic sources not fully quantified in the inventory

The robust global inventory presented in Table 3.3 includes the source sectors that are responsible for the majority of anthropogenic emissions of Hg to air. There are, however, additional sources that cannot yet be reliably quantified at the regional and global scale. Table 3.4 lists a number of these sectors and summarizes the state of available information and in some cases presents an indicative (often incomplete) estimate of possible emissions. These are only intended to provide an indication of the order of magnitude of emissions that may not yet be included in the quantified global inventory. Although it is not anticipated that sectors not currently included would significantly alter the total estimate of global anthropogenic emissions, they may be regionally and locally important.

3.3.3 Comparing GMA global inventory estimates with national inventories

The target for the GMA2018 air emissions inventory activity remains the production of a robust global inventory for the target year of 2015, for a defined set of sectors for which reliable global estimates can be produced. Although it presents emission estimates broken down by sector for each of some 200 countries, the applied methodology is directed at global/regional rather than national level application.

All methods and approaches associated with the generation of emissions estimates (whether produced by measurements or theoretical calculations) have (often large) associated uncertainties. It should therefore not be expected that estimates produced using different approaches (global vs national, etc.) will necessarily be identical. Estimates may differ for several reasons including:

Available information	Best estimate (contemporary emissions), tonnes
Kocman et al. (2013) estimated global emissions from contaminated sites to air and water at 198 t/y, of which 82 t were emitted to air	82 (70–95)
Emissions from China: ~1 t (average for 2000–2010) from waste burning of crop residue (with an additional 2.3 t from burning of crop residue as fuel); 70% emitted as Hg^0 For comparison 2.15 t from fuelwood burning and 0.79 t from grassland and forest fires (Chen et al., 2013b). Crop residue and wood burning for fuel should be covered under biomass burning for energy	1 (China)
IEA data include information on industrial waste incinerated for energy production (801,025 TJ-net, globally in 2014). But there is no information on amounts of other industrial waste burning (without energy recovery) Hg-added products in municipal solid waste are accounted for in the inventory estimates	No estimate available
Informal estimates published in Petro Industry News (2015) indicate that total environmental emissions and releases of Hg from the oil and gas industry can be in the range 80–400 t, with an (unknown) fraction released to air. Identified (unaccounted) emissions and releases include those associated with the molecular sieve regeneration cycle; gas flaring; CO_2 and N_2 removal technology; pipework and equipment decommissioning; and inappropriate treatment and disposal of effluent water The global inventory includes estimates of emissions from oil refineries only and these differ significantly from lower estimates produced by the IPIECA (see Section 3.4.3.8)	No comprehensive estimate available
NOAA/World Bank Gas Flaring Project 2015 (estimate of amount of gas flared globally) + UNEP Toolkit (emission factor); no corresponding estimate for emissions from venting	0.15 (from flaring, global)
Mercury emissions from geothermal power plants have been studied in Tuscany, Italy (Bravi and Basosi, 2014). They estimate a total emission of 1.2 t for Italy based on a (conservative) emission factor of 0.2 g/MWh	1.2 (Italy)
Mercury emissions to air from dental use in the EU ~2010 (including cremation emissions) estimated at 52 t/y with dental amalgam contributing ~21–32% to overall EU Hg emissions to air and up to 9–13% to overall EU Hg emissions to surface water (BIO IS, 2012)	~50 t/y (EU region)
Residual totals from national emissions inventories covering primarily North America, Europe, Australia and some countries in Asia	(see Table 3.5)
	?
	10s to 100s t/y

- use of activity data corresponding to different years or different sources
- differences in reporting/sector attribution
- differences in applied EFs (amount and quality of measurement data used to derive emissions factors; high variability of Hg content in some raw materials and fuels)
- assumptions applied in deriving annual emissions estimates from measurements
- assumptions regarding efficiency and degree of application of APC equipment (and variability and uncertainty associated with APC efficiency).

Comparimg estimates for 2015 made for the global inventory presented in this report (E-Annex 3, Section A3.9) with national emission estimates from other sources is an important part of verification of the global inventory estimates. Where differences occur, these can often be explained, and even when this is not the case the discrepancies can reveal methodological or data issues that need further investigation and guide future work.

A major development since the GMA2013 work is that a large number of countries are now engaged in preparing new national inventories or national emission/release estimates. Many of these are associated with the Minamata Initial Assessments (MIAs) or Minamata National Action Plans (NAPs). This will provide increased possibilities for comparing the global and nationally derived emissions estimates.

When considering estimates compiled as part of the MIA process, most of the MIAs use an approach based on the UNEP Toolkit. The Toolkit was updated in 2013 to reflect new information compiled when developing the 2010 global inventory, and other updates of the Toolkit were made in 2015 and 2017. In general, however, new refinements introduced in the work to produce the 2015 global inventory will not yet be reflected in the UNEP Toolkit.

Comparisons between the GMA2018 inventory estimates for the nominal year 2015 and national estimates are collated in Table 3.5.

Table 3.5 Comparison between national inventory results and GMA2018 estimates for 2015 (units: emissions to air in 2015, kg). GMA values >1 are rounded to avoid decimal numbers. Uncertainties for individual country-sector GMA estimates reflect a maximum uncertainty range (see E-Annex 3, Section A3.7; method 2)

Sector	Australia[a]		Canada	
	National (2015)	GMA2018 (2015)	NPRI (2015)[c]	GMA2018 (2015)
Stationary combustion in power plants				
– coal	2657	2878 (1210-4340)	790	1836 (897-3140)
– oil	1	8 (1-17)		11 (2-24)
– gas	7	4 (0.6-8)		11 (2-20)
Stationary combustion in industry				
– coal	?	141 (69-244)	238	119 (52-333)
– oil	?	10 (1-20)	48.6	17 (2-33)
– gas	?	2 (0.3-3)	0	3 (0.5-6)
Stationary combustion (domestic/ residential/other)				
– coal	?	1 (0.3-1)	264	3 (0.9-6)
– oil	?	32 (5-59)		67 (10-123)
– gas	?	1 (0.2-2)		7 (1-13)
Biomass burning	?	178 (27-391)	0	485 (80-1050)
Ferrous metal production				
– primary pig iron and steel	165	5 (0.1-52)	630	200 (57-1360)
– secondary steel	21	24 (7-146)	0	117 (32-708)
Non-ferrous metal production				
– primary copper/lead/zinc	611	803 (47-15500)	173[d]	44 (12-9100)
– primary aluminum	1635	41 (21-71)	19.8	36 (10-82)
– large-scale gold	3871	1833 (525-4230)	0	353 (3-1510)
– mercury production	0	0	0	0
Other industry				
– cement	96	796 (211-5220)	262	128 (38-3070)
– oil refining	23	27 (8-43)		71 (20-112)
Intentional use				
Chlor-alkali industry	0	0	8.88	0
VCM	0	0		0
Waste				
– controlled incineration	0	235 (71-705)	673	117 (35-352)
– other (landfill, etc.)	1	581 (174-1740)	141	307 (92-921)
Cremation	29	70 (63-84)		89 (74-102)
ASGM	0	0		0
Other	1074[b]		1128[e]	
Total	10191	*7672 (2440-32900)*	4377	*4021 (1420-22100)*

[a] Australia: EPA 2015, sector attribution based on GMA author interpretation of EPA records.

[b] Australia: Other includes mining and processing of coal, iron and non-ferrous metals (873), timber/pulp and paper (20), oil and gas production (28), lime production (42), chemical industry (26), brick manufacture (21), food industry (15).

[c] Accessed 21 May 2018. Canada also reports emissions (totalling 4387 kg) under the CLRTAP reporting system.

[d] Amount reported under metal production (other).

[e] Canada: Other includes: pulp and paper = 39.6; municipal waste incineration = 673; solid waste disposal on land = 141.

China (and Hong Kong)		Japan		Republic of Korea	
National (2014/2015)	GMA2018 (2015)	National (2015)	GMA2018 (2015)	National (2014)	GMA2018 (2015)
75900	81805 (41400-140200)	1300	1297 (703-2100)	1167	1710 (820-3740)
_[f]	89	13	134 (25-295)	5[i]	33 (6-73)
	13	2	18 (3-33)	0	4 (0.6-8)
80400	63363	240	304 (152-519)	1433[i]	203 (103-343)
_[f]	126	2	51 (7-99)	51[i]	26 (4-51)
	9	1	3 (0.4-5)	4	2 (0.3-3)
27700[g]	37803	0	0.1 (0.03-0.12)	0	0
800	427	0	103 (15-189)	72[i]	49 (7-91)
	13	0	4 (0.6-8)	1[i]	3 (0.4-6)
4100[g]	5119 (684-10000)	0	373 (66-843)	0[i]	86 (13-177)
32730	8566 (2190-493000)	2000	2219 (1200-5320)	1337	687 (378-1090)
	1023 (268-2490)	540	599 (163-3630)	407	340 (94-647)
68900	126220 (25800-422000)	260	1562 (67-47500)	16	296 (63-31900)
6500[g]	3121 (869-10000)	0	0.4 (0.1-0.9)	0	0
3400	202 (4-1530)	0	18 (0.2-76)	0	1 (0.01-3)
13300[g]	8100 (1580-17600)	0	0	0	0
127700	106283 (29300-1240000)	5500	3474 (861-8860)	2795	1258 (357-2590)
	2695 (728-4450)	120	1138 (324-1790)	6	968 (203-1890)
560	405 (113-948)	0	0	0	0
	57808 (12100-113000)	0	0	0	0
[h]					
	8649 (2590-25900)	1500	1210 (363-3630)	1366	570 (171-1710)
	19101 (5730-57300)	3850	2399 (720-7200)	0	671 (201-2010)
4500[g]	553 (503-614)	69	101 (92-112)	5	41 (37-45)
7700	33750 (8440-59000)	0	0	0	0
		1351		519[j]	
468600 530000[g]	**565244 (174000-2770000)**	**16747**	**15007 (4760-82200)**	**9186**	**6948 (2460-46400)**

[f] Included in domestic residential oil

[g] 2014

[h] China: Municipal solid waste incineration 11800; hazardous waste incineration 2500; production of mercury-added products (lamps, batteries, thermometers, sphygmomanometers) 100;

[i] Republic of Korea: Estimated using UNEP emission factor.

[j] Republic of Korea: Other: Haz. waste (283.4) Sew sludge (32.99) Pulp-paper (177.82) On road (25.12)

Table 3.5 continued

Sector	Malaysia		Mexico	
	National (MIA version 12/5/17)	GMA2018 (2015)	National (MIA)	GMA2018 (2015)
Stationary combustion in power plants				
– coal	2667	2389 (1290-5690)	2121	2913 (1890-4470)
– oil	0	4 (0.8-7)		115 (27-212)
– gas	0	6 (1-11)	786	11 (2.6-21)
Stationary combustion in industry				
– coal	387	238 (129-567)	763	719 (477-990)
– oil	6	12 (3-23)		13 (3-24)
– gas	3	1 (0.3-2)	–[l]	3 (1-5)
Stationary combustion (domestic/ residential/other)				
– coal	0	0		0
– oil	0	20 (5-38)		35 (8-64)
– gas	0	0.1 (0.02-0.13)	–[l]	0.3 (0-0.5)
Biomass burning	0	41 (9-80)	974	435 (103-800)
Ferrous metal production				
– primary pig iron and steel	0	0	218	285 (98-1510)
– secondary steel	21	101 (38-480)		336 (125-1600)
Non-ferrous metal production				
– primary copper/lead/zinc	0	0	2090	5872 (2115-21150)
– primary aluminum	0	68 (24-133)		0
– large-scale gold	0	128 (45-250)	200	5336 (1870-10400)
– mercury production	0	0	767	2025 (710-3950)
Other industry				
– cement	3502	1655 (585-8720)	6281	1241 (470-9390)
– oil refining	22	224 (100-370)	47	54 (25-84)
Intentional use				
Chlor-alkali industry	0		1808	600 (210-1170)
VCM	0			0
Waste				
– controlled incineration	0	49 (15-148)		24 (7-71)
– other (landfill, etc.)	0	1694 (510-5080)	2870	3462 (1040-10400)
Cremation	0	5 (4-6)	328	35 (28-42)
ASGM	0	1663 (415-2910)	28072	3563 (890-6230)
Other	1643[k]		–[m]	
Total	8251	8296 (3170-24500)	47325 (19253 excl ASGM)	27075 (10100-73600)

[k] Malaysia: Other includes 1410 kg from extraction, refining and use of natural gas and mineral oils and 51 kg from incineration of hazardous waste.

[l] Mexico: Included in domestic residential gas.

[m] Mexico: Other – extraction of petroleum products 361 (oil) 1372; pulp and paper 3.6; lime production 670; use/disposal of thermometers 881; switches 881; lamps 749; batteries 359; use of mercury catalysts 358.

Russia		USA		Vietnam	
National (2015)	GMA2018 (2015)	National (2014)[o]	GMA2018 (2015)	National (MIA)	GMA2018 (2015)
10130	5782 (2500-10900)	20795	19145 (10100-37400)	4898	2652 (1430-10930)
277	171 (23-330)	39	37 (7-84)		4 (1-9)
1290	51 (7-97)	822	70 (10-128)		3 (0.4-4)
15700	186 (68-309)	1078	2257 (949-6490)		2447 (1320-5833)
2	15 (2-29)	668[p]	46 (6-88)		8 (2-16)
	8 (1-16)	1150	27 (4-50)		0.35 (0-0.7)
	661 (250-945)	0.8	168 (54-415)		401 (217-957)
229	60 (8-116)	1529	367 (52-675)		13 (3-24)
25	17 (2-33)	58	47 (7-86)		0
81.7	145 (20-280)	853	2231 (368-4870)	1168	736 (165-1420)
				561	
1910	4843 (1070-10000)	1551	513 (145-3410)		
0	638 (135-3290)	4597	1288 (350-7810)		128 (48-610)
11460	12890 (2700-77000)	162	110 (20-15430)		249 (89-960)
133	1094 (230-2130)	362	123 (34-288)		150 (53-293)
32500	12474 (2430-27000)	521	494 (4-2110)		0
0	0	0	0		0
4120	2339 (877-4280)	2874	3120 (786-29500)	5840	5770 (2040-30400)
226	201 (54-332)	338	1034 (295-1630)		121 (54-200)
360	3790 (796-7390)	82	183 (51-427)		
124	310 (65-604)	0	0		
287	31 (9-93)	1640	1253 (376-3760)		5 (2-16)
759	9896 (2970-29700)	3249	3298 (989-9890)	1958	1741 (520-5220)
335	122 (89-163)	1388	523 (438-600)	92	61 (55-67)
0	5225 (1310-9140)	0	0	97	3562 (890-6230)
8211[n]		3245[p]		13230[q]	
88164	*60949 (15600-184000)*	*47004*	*36332 (15000-125000)*	*27844*	*18050 (6890-63200)*

[n] Russia: Other – pulp and paper = 671; other NFM = 202; extraction/refining of gas = 443; combustion of peat/oil shale = 178; municipal waste incineration = 287; sewage sludge incineration = 670; medical waste incineration = 1090; Hg-added consumer products = 4774.

[o] The United States reported their NEI 2014 v1 inventory to LRTAP; the data entered here are from the US NEI 2014 v2 inventory (updated January 2018).

[p] USA: Other – brick (34), chemical manufacturing (838), gypsum (141), lime manufacture (160), manufacture of mercury relays (38), mineral products (152), other (381), pulp and paper (164), recycling of EAF dust from steel manufacture (421), secondary metals and metal waste/non-ferrous (342), utility MACT pet coke (31), dental amalgam (419).

[q] Vietnam: Other includes natural gas extraction, refining and use = 159 kg; incineration of municipal/hazardous and medical waste = 11880; consumer products = 1236; dental amalgam product use = 12.4.
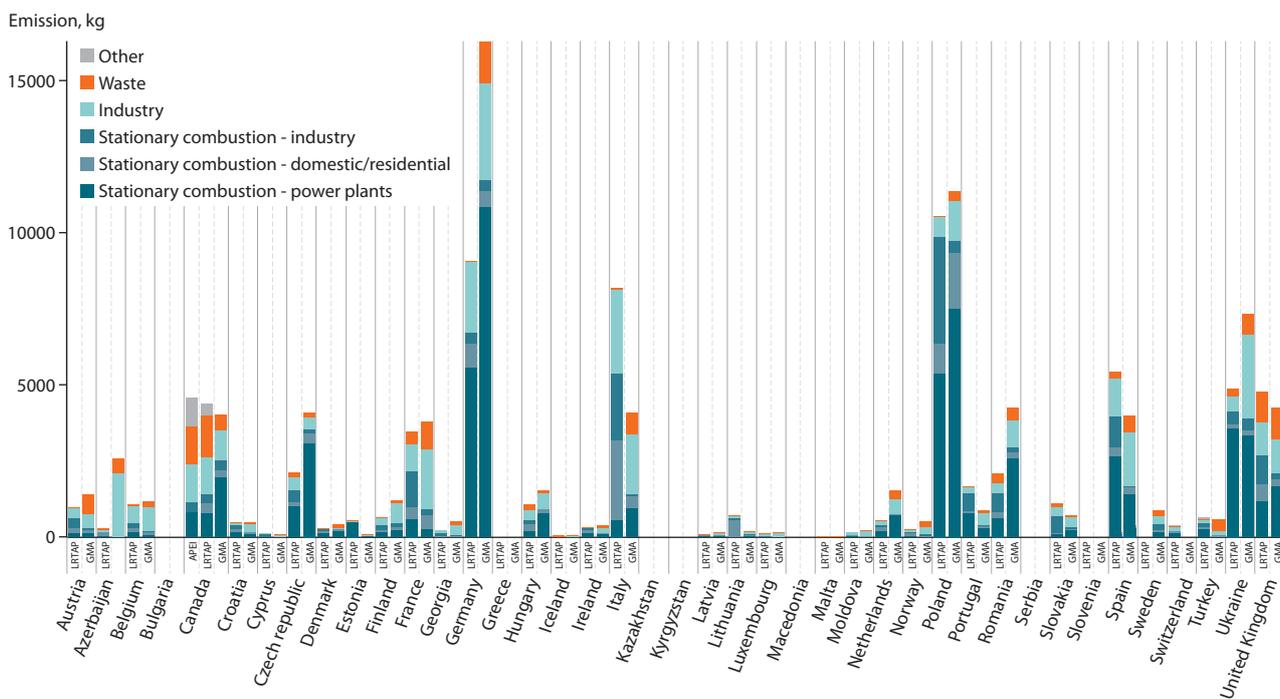
Figure 3.5 Comparisons of emission estimates reported to CLRTAP and GMA inventory estimates for 2015; also including emission estimates for Canada derived from the Canadian national pollution release inventory (NPRI, 2016).

Information compiled as part of the GMA2018 work, including information exchanged at international meetings organized as part of the inventory work, identified over 70 national inventories that may be suitable for comparison with the 2015 inventory estimates. These include:

i. Inventories prepared under the auspices of the UNECE Convention on Long-range Transboundary Air Pollution (CLRTAP) reporting for 2015: covering 39 countries primarily in the EU and CIS and Other European countries regions, but also including Canada.

An initial evaluation, based on total national Hg emission estimates for these countries indicated that GMA inventory estimates are generally higher than CLRTAP reported emissions, but comparable if uncertainties and sector-matching issues are taken into account. For some countries (Azerbaijan, Bulgaria, Kazakhstan, Kyrgyzstan, Macedonia, Serbia) differences between GMA estimates and CLRTAP reported emissions are substantial and need further investigation. Comparing estimates for the remaining 33 countries, total estimated emissions to air were 67.5 t in CLRTAP reporting vs. 86.7 t in the GMA inventory. For 22 countries, national CLRTAP inventories were lower than the GMA estimates, and for 11 countries higher; GMA inventory estimates were on average about 36% greater than emissions reported to CLRTAP. It is possible that there are gaps in CLRTAP national Hg inventories; in recent years efforts to improve CLRTAP reporting have largely been directed at greenhouse gas emissions, while Hg and some other air pollutants have received low priority.

Figure 3.5 presents comparisons between emission estimates reported to CLRTAP and GMA inventory estimates for 2015. Difficulties in precisely matching sectors defined under the CLRTAP reporting system and those applied in the GMA work are apparent. Harmonization of sector definitions between

different reporting and inventory systems applied in different regions/countries will be a challenge and an important consideration in relation to eventual Minamata emissions and release reporting requirements.

ii. Inventories currently being compiled as part of MIAs for about 30 countries from the Sub-Saharan Africa, East and South-east Asia, South Asia, South America and Central America and the Caribbean regions. At the time of preparing the GMA2018, the majority of MIA inventories were preliminary, and not all were available for (provisional) comparison with GMA inventory estimates. Therefore only provisional conclusions can be drawn based on comparisons of results from some countries, and discussions with MIA national and regional coordinators. MIA inventory estimates for Malaysia and Vietnam are included in Table 3.5.

Comparisons between GMA inventory results and results presented in (preliminary) MIA inventories gave rise to the following general observations:

• With few exceptions, MIAs are being prepared using the UNEP Toolkit which is available in two versions: Level 1 and Level 2. The Level 1 approach is designed to be employed for producing first rough estimates of Hg emissions and releases. Level 2 is designed to represent national circumstances at a more detailed level, supported by available national data. There can be very substantial differences between emissions/release estimates for individual countries produced using the UNEP Toolkit Level 1 and Toolkit Level 2 (UN Environment, 2017b,c). For this reason, comparisons made between GMA inventory and MIA results focus on MIAs produced using Toolkit Level 2.

• In general, estimates of national emissions totals agree fairly well, but there can be significant differences at the sector level. These differences may be due to methodological differences in the MIA and GMA approaches, or use of

different years of (activity) data. They can also be due to errors in national data collection for the MIAs; or in the case of GMA estimates, application of default emission factors or technology profiles that are not sufficiently representative for the country concerned.

- The GMA inventory is based on activity data for a single year – nominally 2015. Most MIAs use this approach with a predefined base year (not always 2015), but when data from that year are not available, they use the most recent available data, and sometimes the exact year of activity data concerned is not defined. Activity data are a major factor determining estimated emissions using the GMA and Toolkit approaches, and consequently lack of consistency in this respect is a possible explanation for substantial differences that can exist between GMA and MIA inventory estimates.

- Other reasons identified on the basis of preliminary comparisons that may explain differences between the GMA estimates and the MIAs are:

  ○ MIA estimates associated with oil and gas extraction – a component currently not included in the GMA inventory.

  ○ MIA estimates associated with waste categories such as industrial waste and wastewaters, currently not included in the GMA inventory.

  ○ Estimates of emissions from large-scale gold mining, where the default factor in the Toolkit is three-fold higher than that applied in the GMA inventory methodology; data necessary to improve quantification of emissions from this sector are largely lacking.

  ○ For copper production, the GMA approach may over-estimate the degree of application and effectiveness of abatement, at least for some African countries.

  ○ For cement production there are differences in assumptions applied in calculating emission estimates.

  ○ Some differences in ASGM/large-scale gold sector emissions estimates exist. The Toolkit default factors and methodology were revised in 2017; however many MIAs are still using earlier Toolkit versions.

  ○ Caution should be applied to avoid double counting in totals for inputs to waste and releases to some pathways from products in MIA results, as prescribed in the Toolkit.

  ○ A major source of differences between GMA inventory estimates and preliminary MIA estimates can be traced to differences in estimates associated with use and disposal of waste (especially waste burning) from Hg-added products. The methodology applied in the GMA work and the Toolkit approaches are very different. GMA emissions from waste are based on estimates of the amount of Hg in Hg-added products that are consumed in the country, while MIAs (using the UNEP Toolkit approach) calculate emissions using generic numbers for Hg-content of burned waste.

  ○ Discrepancies exist between estimates of amounts of Hg reported in MIAs for Hg-added products and regional consumption estimates presented in the UNEP Trade and Supply report (UN Environment, 2017a) that was used

as the basis for GMA estimates. In some MIAs, problems have been identified with data collection, especially for Hg-added products, including differentiation of, for example, consumption of Hg-containing batteries and thermometers and Hg-free batteries and thermometers. Similar difficulties exist for other products, such as paints and skin-lightening creams, where Hg-free product variants are predominant on the national market but it is difficult for countries to establish nationally if Hg is present in the products imported and/or consumed. Countries have used different assumptions in this regard, resulting in quite different results. Generally, countries have substantial data gaps for products. These problems may be exacerbated by insufficiently detailed customs statistics and lack of resources to contact producers and importers for supplementary information. Consequently, there are indications that the default factors for Hg content in general waste burnt (applied in many of the MIAs) may be too high.

iii. National inventories provided by Australia, Canada, Japan, Republic of Korea, Russia and USA. National estimates for China from published sources.

Detailed comparisons between GMA estimates and national inventories provided by these countries are presented in Table 3.5. From this table it is apparent that estimates match to differing degrees for different sectors, and that this also varies between countries. However, in these example comparisons, the degree of consistency between national inventory estimates and the GMA estimates for this group of countries is generally good, and (with some exceptions) well within the bounds of associated uncertainties. As with the CLRTAP data comparisons (see 'i'), part of the differences can be explained by difference in the way emissions are assigned between sectors. This is particularly the case for some of the stationary combustion sectors and differentiation of power, industrial and domestic/residential burning sources, and whether or not fuels are included under stationary combustion or individual industrial sectors. One potential inconsistency identified is that activity data from the IEA (used in the GMA2018) do not always match with nationally reported activity data; for example, for fuel consumption reported by Canada, where differences have been attributed to dataset timing (monthly and annual, provisional and revised) and possible use of different factors for conversions from physical fuel units to energy units.

Some national inventories include additional emissions that are not yet quantified in the GMA inventory. 'Other' sources include emissions from activities such as other chemical manufacturing processes; other mineral products (e.g., lime manufacturing), secondary non-ferrous metal production, oil and gas extraction, pulp and paper industry, and food industry. These emission sources are currently difficult to quantify at the global scale – largely due to a lack of comprehensive activity data as well as a lack of emission factors for highly variable process technologies. However, for the few (generally developed) countries reporting emissions from 'other' sources the contribution is roughly 5–20% of the national inventory totals, which extrapolated globally (on non-ASGM emissions totals) could represent additional emissions of the order of 100 to 200 tonnes.

3.4 Comparing 2010 and 2015 global inventory estimates

3.4.1 Cautionary notes

Inventory methodologies are constantly improved as new information and data become available. With each new round of inventory development, methods are improved, both with respect to understanding of important factors/ parameters and availability, and the quality of essential data. This has implications for consistency over time. Changes in emissions estimates for different periods reflect both real-world trends and artefacts of improvements in inventory methods and data availability. Over-simplistic comparisons between the new inventory and previous inventories can result in misinterpretation and should therefore be avoided.

The increased focus on Hg emissions resulting from the adoption of the Minamata Convention has also led to new research activities, national efforts and industrial focus related to Hg emissions. These efforts all contribute to providing more accurate and complete information on Hg emissions but unavoidably also introduce changes to both current and previous emission inventories.

It is inevitable that comparisons will be made between results presented in the GMA2013 (AMAP/UNEP, 2013) and the results in this update GMA – including comparing individual country sector-based estimates in the 2010 and 2015 inventories. If the implications of methodological refinements, addition of new sectors, and improved quality of base information, among others, are not properly appreciated, such comparisons can result in inappropriate and misleading conclusions. *It is strongly recommended that any such comparisons therefore refer to the information presented in this report only.*

3.4.2 Observations on changes between 2010 and 2015

As a first step in trying to address some of these issues and gain a reliable insight into whether apparent changes in emissions patterns between 2010 and 2015 represent real changes in emissions or are artefacts of improved information and methodologies, an updated 2010 inventory was prepared in addition to the 2015 inventory. This updated 2010 inventory incorporated various 'improvements' including new (relevant) information on emission factors and application of APC technology, as well as updated activity data[2]. It also included a retrospective calculation of 2010 emissions for some sectors newly introduced in the 2015 inventory. Table 3.6 shows the estimated emissions for the main sector groups in the (updated) 2010 and 2015 inventories.

Figures 3.6 and 3.7 compare (in absolute and relative terms, respectively) the pattern of regional emissions in 2010 (GMA2013) with the updated-2010 inventory and the 2015 (GMA2018) inventory. The updated estimate of total emissions to air for 2010 is very similar (at the global level) to the original global estimate for 2010 published in the GMA2013 report (AMAP/UNEP, 2013). This consistency is also apparent when
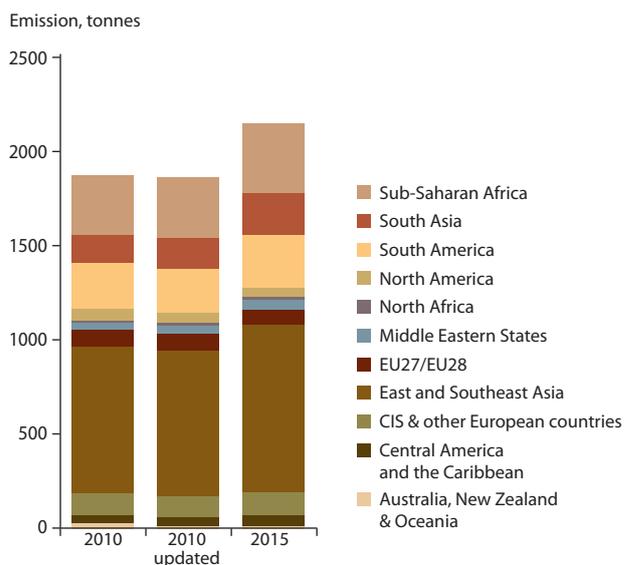
Figure 3.6 Regional breakdown of global emissions of Hg to air from anthropogenic sources (results for 2015 compared with original and updated inventory for 2010).
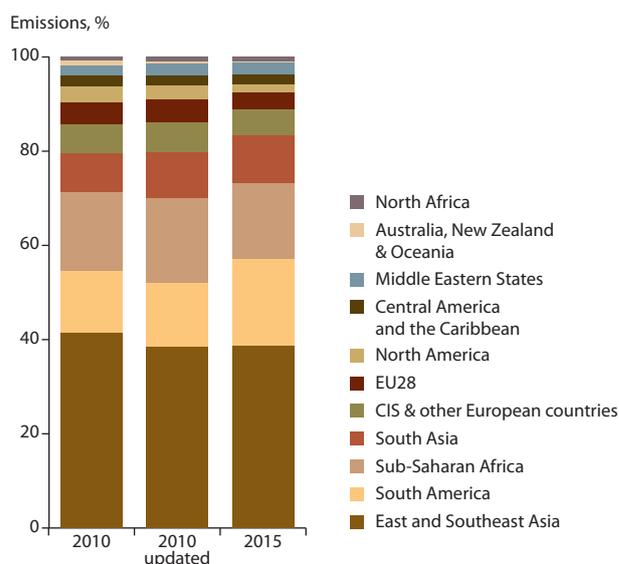
Figure 3.7 Proportion of global emissions of Hg to air from anthropogenic sources in different regions (results for 2015 compared with original and updated inventory for 2010).

considering aggregated emissions for (most) regions and sector groupings. The fact that changes in methods introduced for estimating emissions from specific sectors or country groups, the use of more representative 2010 activity data, and other 'artefacts' (including the introduction of at least one sector in 2015 not represented in the updated 2010 inventory) do not appear to have unduly influenced global or regional inventory results is considered a validation of the general approach employed for deriving global inventory estimates. At the same time, however, it should be noted that values for individual country-sector estimates have in some cases changed

---

[2] In the 2010 inventory presented in the GMA2013 much of the activity data used were preliminary, corresponding to the period for which latest-data were available (typically 2008 or 2009). The updated 2010 inventory values presented in this report include a number that have been revised for 'final' 2010 activity data. The 2015 inventory presented in this report is based on latest available activity data (see Table 3.1).

Table 3.6 Global emissions of Hg to air from different anthropogenic source sectors in 2015 and 2010 (updated). Data shown to three significant figures.

Sector code	Description	Estimated emissions 2010 (updated), tonnes	Estimated emissions 2015, tonnes
ASGM	Artisanal and small-scale gold mining	679	838
BIO	Biomass burning (domestic, industrial and power plant)	49.5	51.9
CEM	Cement production (raw materials and fuel, excluding coal)[a]	187	233
CREM	Cremation emissions	4.91	3.77
CSP	Chlor-alkali production (mercury process)	21.0	15.2
NFMP	Non-ferrous metal production (primary Al, Cu, Pb, Zn)[a]	151	228
NFMP-AU	Large-scale gold production)	73.1	84.5
NFMP-HG	Mercury production)	12.2	13.8
OR	Oil refining	13.1	14.4
PISP	Pig iron and steel production (primary)[a]	26.7	29.8
SC-DR-coal	Stationary combustion of coal (domestic/residential, transportation)	54.4	55.8
SC-DR-gas	Stationary combustion of gas (domestic/residential, transportation)	0.162	0.165
SC-DR-oil	Stationary combustion of oil (domestic/residential, transportation)	2.63	2.70
SC-IND-coal	Stationary combustion of coal (industrial)	123	126
SC-IND-gas	Stationary combustion of gas (industrial)	0.115	0.123
SC-IND-oil	Stationary combustion of oil (industrial)	3.05	1.40
SC-PP-coal	Stationary combustion of coal (power plants)	268	292
SC-PP-gas	Stationary combustion of gas (power plants)	0.319	0.349
SC-PP-oil	Stationary combustion of oil (power plants)	2.58	2.44
SSC	Secondary steel production	9.69	10.1
VCM	Vinyl-chloride monomer (mercury catalyst)	[b]	58.3
WASOTH	Waste (other waste)[c]	115	147
WI	Waste incineration (controlled burning)[c]	15.4	15.0
Total		1810	2220

[a]Emissions from associated combustion of coal are counted under SC-IND-coal; [b]not estimated in original 2010 inventory (AMAP/UNEP, 2013) and lacking information for retrospective emissions estimates for 2010; [c]in the original 2010, ~30% of Hg consumed in products was allocated as 'remaining in society'; in the 2015 (and revised 2010) values this amount is incorporated in the waste-stream estimates.

significantly. Where possible, discussions in Section 3.4.3 attempt to address the issue of whether apparent trends (between 2010 and 2015 estimates) reflect genuine changes in emissions over time or are artefacts related to improved information, etc. On the basis of this evaluation of apparent changes, some observations are made:

- The GMA inventory estimates of global emissions of Hg to the atmosphere in 2015 are roughly 20% higher than they were in 2010; however, different sectors contribute to this overall increase in different ways. An overview of the scale of changes in estimated emissions in different regions for the main sectors addressed in the 2015 global emissions inventory is presented in Table 3.7 and Figure 3.8.

- The increase in estimated emissions from ASGM (160 t more in 2015 than in 2010) account for about 45% of the overall increase in inventory estimates from 2010 to 2015,

with significant increases in estimated ASGM emissions for, in particular, South America. As previously noted, changes in estimated emissions may be associated with both real world changes and changes in the underlying information or methods that are the basis for the estimates. In the case of ASGM, it is not a simple matter to distinguish between these two components. The judgment of those working in the area of ASGM is that the apparent increases in estimates from 2010 to 2015 are largely associated with improved information rather than a significant increase in real world emissions from ASGM in this five-year period.

- For other groups of sectors, estimates are based on more (temporally and methodologically) consistent sources of, for example, activity data. This and knowledge of applied changes in calculation methods and assumptions makes it easier to draw general conclusions about factors that may be responsible for trends in emissions.

Table 3.7 Percentage changes in emissions of Hg to air in different regions from different anthropogenic source sectors from 2010 (updated estimates) to 2015.

	Australia, New Zealand & Oceania	Central America and the Caribbean	CIS & other European countries	East and Southeast Asia	EU28	Middle Eastern States	North Africa	North America	South America	South Asia	Sub-Saharan Africa	Grand Total
ASGM	0.0	18.4	5.6	-12.4	0.0	0.0	0.0	0.0	91.6	300.0	8.6	23.4
BIO	1.6	11.0	14.1	-5.5	6.2	-33.3	-2.7	-1.4	6.1	9.5	10.1	4.8
CEM	7.4	9.3	27.8	32.2	-14.0	13.9	4.8	23.0	19.8	24.3	62.0	24.9
CREM	-16.5	-70.2	40.9	-33.2	-37.6	-20.5	-19.0	-5.2	-69.5	46.1	-9.3	-23.3
CSP	0.0	0.0	-3.9	0.0	-66.2	0.0	0.0	-83.3	5.1	-74.0	0.0	-28.0
NFMP	-1.9	-22.1	6.1	158.0	-15.6	2.9	-53.4	-8.6	-5.0	12.7	-32.4	51.7
NFMP-AU	1.3	100.1	33.7	-28.5	76.8	47.8	316.2	9.9	7.9	-30.9	11.0	15.6
NFMP-HG	0.0	1900.0	-57.3	3.1	0.0	0.0	-50.0	0.0	0.0	0.0	0.0	13.0
OR	-13.8	1.0	5.8	9.7	-3.3	14.2	-14.2	6.2	-2.0	18.3	-11.6	9.4
PISP	-10.4	8.7	2.4	17.4	2.7	19.3	-29.4	2.5	-8.4	38.5	-13.6	11.5
SC-DR-coal	-25.2	0.0	-22.8	9.2	-20.5	-27.9	0.0	-51.5	69.1	-8.8	58.5	2.5
SC-DR-gas	13.1	6.3	-7.6	44.3	-17.9	26.6	56.9	1.6	10.7	15.9	400.0	1.8
SC-DR-oil	16.3	-1.0	-6.7	5.2	-6.7	40.6	-0.6	-4.8	5.0	5.0	26.5	2.9
SC-IND-coal	4.2	438.6	-28.7	-5.5	-8.6	-19.5	-15.2	-19.0	11.8	25.4	6.9	2.6
SC-IND-gas	7.3	8.5	-1.4	33.6	-4.6	16.4	-13.9	7.8	-11.2	-30.6	129.0	6.9
SC-IND-oil	-38.8	-47.0	-26.1	-80.0	-36.8	1.3	-31.5	-57.5	-40.8	-13.9	0.0	-54.1
SC-PP-coal	-10.9	-19.1	-3.0	22.1	-2.9	4.9	59.8	-23.0	66.5	38.0	-13.9	9.0
SC-PP-gas	11.0	6.2	-4.8	23.6	-31.0	26.8	19.2	27.0	27.5	-23.3	40.2	9.4
SC-PP-oil	13.8	-4.6	-15.2	-18.5	-46.2	1.6	22.5	-15.0	21.4	3.9	12.3	-5.3
SSC	-11.2	12.9	18.8	-10.3	-7.2	36.9	-4.1	9.7	0.8	27.0	-12.3	4.7
WASOTH	46.2	20.0	42.6	11.2	-33.0	51.4	66.7	-44.7	1.5	47.6	164.3	27.8
WI	46.2	20.0	42.6	11.2	-33.0	51.4	66.7	-44.7	1.5	47.6	164.3	-2.9
Grand Total	0.2	18.6	10.2	23.4	-12.5	14.5	15.8	-21.8	67.6	28.0	9.1	22.8

If increases due to ASGM (as well as emissions from the VCM sector, which are not quantified for 2010) are discounted, the percentage increase in the estimated global inventory from 2010 to 2015 is about 17% (equivalent to ~195 t of emissions). This increase is mainly (~75%) associated with emissions from industrial sectors, 15% with stationary combustion, and 13% with (non-ASGM) intentional use sectors.

Estimated Hg emissions to air decreased between 2010 and 2015 in two of the 11 world regions, namely North America and the EU region, by ~11 t in each of these regions. Emissions over this period were relatively unchanged in Australia, New Zealand and Oceania, and (if ASGM is discounted) in South America. In the case of North America in particular, shifts in fuel use (from coal to oil/gas) in the energy sector, combined with the introduction of highly efficient APCD at major point sources appears to be a major factor in the changes observed. In both Canada and Australia, closure or major changes in applied technology (including APC technology) at a few significant point sources associated with non-ferrous metal and large-scale gold production may have resulted in decreasing national emissions.

In all other regions, however, the estimated emissions to air increased, by approximately 10–20% in most other regions and

up to 26% and 30% in South Asia and East and Southeast Asia, respectively (see Table 3.7).

Emissions associated with industrial sectors increased, in Asia in particular, indicating that economic growth and increased industrial activity have more than offset any efforts to reduce emissions. Globally, cement production, ferrous (primary iron- and steel) and non-ferrous (primary aluminum, copper, lead, zinc) metal production, and large-scale gold and Hg production all had associated increases in emissions in 2015 compared with updated estimates for 2010. Estimated emissions from waste (from Hg-added products) also increased, but were slightly lower from controlled waste burning. Estimated emissions from chlor-alkali production, however, decreased between 2010 and 2015. Other source sectors responsible for, at the global scale, relatively minor contributions to overall emissions were largely similar in 2010 and 2015 (see Table 3.7). Estimated emissions from coal combustion in power plants in 2015 are about 9% higher in 2015 than 2010.

In some regions, economic recovery following the financial crisis of 2008 (that may have influenced global emissions in 2010) may also have influenced observed trends in estimated emissions.
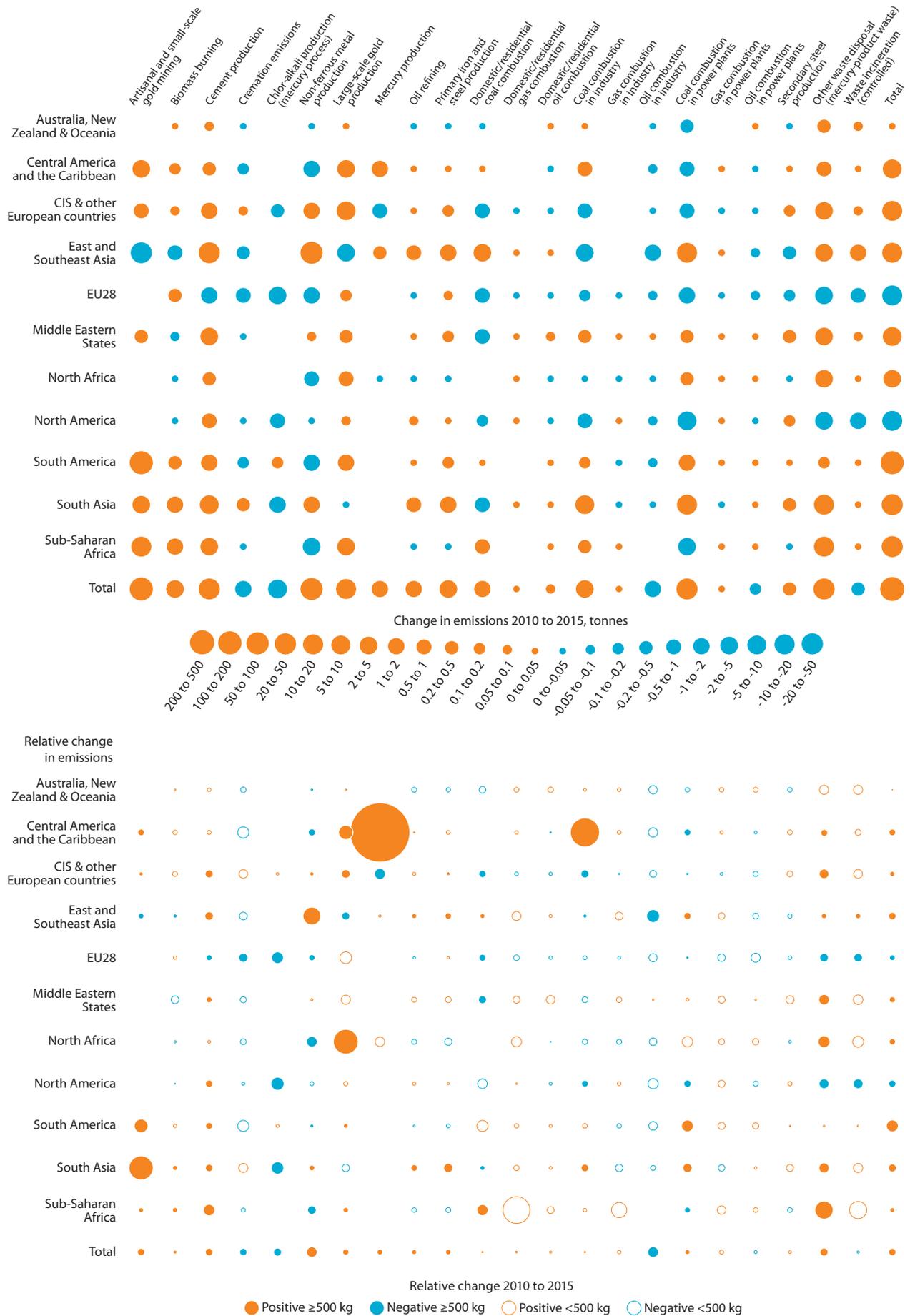
Figure 3.8 Changes in emissions of Hg to air in different regions from different anthropogenic source sectors from 2010 (updated estimates) to 2015 in absolute terms (upper) and relative terms (lower). Orange colour indicates increased emissions and blue decreased emissions.

3.4.3 Sector-based observations

The observations presented in this section include comparisons between 2015 inventory estimates and updated 2010 inventory estimates.

3.4.3.1 Stationary combustion – coal, oil and gas burning

Stationary combustion of fossil and biomass fuels for energy (see Section 3.4.3.2) are estimated to account for about 535 t of Hg emitted to air in 2015. Of the emissions from combustion of fossil fuels, coal-burning is responsible for by far the largest amount (~475 t) followed by oil (7 t) and gas (1 t). Of these emissions, about 295 t are associated with burning of fossil fuels in power plants, 128 t in industrial uses and the remaining 60 t in other, primarily domestic and residential uses. Coal burning is thus the second largest contributor to global Hg emissions after ASGM.

The 2015 inventory estimate (based on IEA activity data) includes 292 t (255–346 t) from coal burning in power plants (an increase of 9% on the updated revised estimate for 2010) and 126 t (106–146 t) in industry (close to the updated estimate for 2010). Mercury emissions from coal burning in other (mainly domestic and residential) uses are also relatively stable between 2010 and 2015 at around 56 t (37–69 t).

Considering the increase in emissions from coal burning in power plants in more detail, these are almost entirely due to increased emissions in the East and South-east Asian and South Asia regions. Increased Hg emissions of about 19 and 17 t, respectively in these two regions, constitute a rise of ~21% in East and South-east Asia and 38% in South Asia. Decreasing Hg emissions from coal burning in power plants in Australia, New Zealand and Oceania (-11%), Central America and the Caribbean (-19%), CIS and other European countries (-3%), the EU region (-3%), North America (-23%) and Sub-Saharan Africa (-14%) amount to a cumulative reduction of about 14 t of Hg emitted in these regions.

A new feature of the 2015 inventory is the differentiation of emissions from coal burning in industry between some major component activities. Of the total emissions from coal burning in industry of 126 t, about 44 t were associated with the cement industry; 30 t with ferrous metal production (not including 'non-energy coke'); 3.7 t with non-ferrous metal production; and 48 t with other industrial uses. These emissions are counted in the 2015 inventory under coal combustion but may also be taken into account as additional emissions when considering the cement, ferrous and non-ferrous metal sectors (see following sections).

3.4.3.2 Stationary combustion – biomass burning

Biomass burning constitutes a new sector introduced in the 2015 inventory. Estimated emissions are based on IEA activity data and concern only biomass burning of primary solid biofuels for energy production (in power, industrial, and domestic/residential situations). Thus, they do not include biomass burning from, for example, the agricultural burning or land clearance practices that take place in many countries.

The estimated Hg emissions from primary solid biofuel burning in 2015 are 52 t (44–62 t; ~2.3% of the global

inventory). A comparable value of about 49 t was calculated retrospectively for 2010.

The main emissions from biomass burning are associated with Sub-Saharan Africa, South Asia and East and Southeast Asia (about 28%, 25% and 21% of the biomass emissions total, respectively).

3.4.3.3 Cement production

Estimated total global Hg emissions to air from the cement sector are 233 t (117–782 t) in 2015. However, the updated methodology allows an improved differentiation of the contribution to Hg emissions associated with fuels burned in cement-clinker production and the non-fuel raw materials. In the 2015 inventory, therefore, a part of the emissions counted under 'industrial coal combustion' are identified with the use of coal as fuel in the cement industry. If this additional 44 t of emissions is counted under cement production, the contribution of the cement sector in the global inventory rises from ~10.5% to ~12.5% making the cement sector the third largest contributor after ASGM and coal burning.

The total Hg emissions in 2015 directly associated with the cement sector (233 t) is considerably higher than the ~187 t associated with this sector in 2010 (updated), an increase of 25%. Only in the EU region do the estimated emissions from the cement sector decrease between 2010 and 2015 (by ~14%); in all other regions increases are observed, ranging from ~7% in the Australia, New Zealand, Oceania region, up to 62% in Sub-Saharan Africa. These emission trends closely mirror the trends in cement production in the different regions, that is, the primary activity data used in calculating emissions for the cement sector (see Figure 3.9).
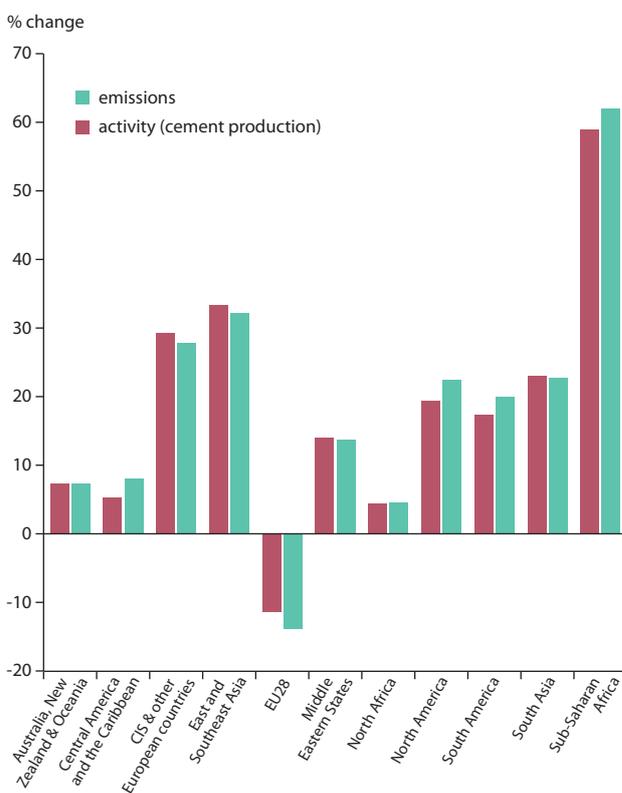
Figure 3.9 Relative changes between 2010 and 2015 in activity data (cement production) and Hg emissions associated with cement production in different regions.

3.4.3.4 Ferrous metal production (pig iron and steel and secondary steel)

Mercury emissions from primary ferrous metal (pig iron and steel) production are estimated at about 30 t in 2015, with a relatively large uncertainty range (19–76 t) which is higher than the updated 2010 estimate of 27 t).

Of the increase in Hg emissions between 2010 (updated) and 2015, 1.8 t is from increased emissions in East and Southeast Asia and 1.1 t from increased emissions in South Asia. These two regions are responsible for, respectively 40% and 13.5% of emissions in 2015 from primary non-ferrous metal production. The other main region contributing to emissions from this sector is the CIS and other European countries region (responsible for ~22% of the sector emissions).

Secondary steel production was not included in the GMA2013 but has been added in this work.

The estimated emissions from secondary steel production in 2015 are 10 t (7.6–18 t) of Hg (~0.5% of the global inventory), compared to a retrospectively calculated estimate of 9.7 t for 2010. These totals are higher than might be expected for a process based on electric arc furnaces if relatively uncontaminated scrap metal is used and imply that significant amounts of Hg are present in the recycled scrap used in secondary steel production; assumptions applied in calculating the estimated emissions are given in E-Annex 3, Sections A3.5 and A3.6.

3.4.3.5 (Primary) non-ferrous metal production (Al, Cu, Pb, Zn)

Primary production of aluminum, copper, lead and zinc were together estimated to be responsible for 228 t of Hg emissions in 2015, significantly more than the ~150 t in a revised estimate for 2010. It should be noted that the estimated emissions from this sector have relatively large uncertainties (154–338 t in 2015).

Aluminum production makes a modest contribution (6.6 t) to the total estimated emissions for the primary non-ferrous metals sector, with decreased emissions in several regions totaling about 0.5 t offset by increases of 2.3 t (about 85% of which occur in East and Southeast Asia).

Primary production of copper, lead and zinc make a significantly greater contribution to global Hg emissions, at 222 t in 2015 (from 146 t in 2010). Again, increased estimated emissions in Asia (almost 85 t, or 98% of the total increase), together with increased emissions in the CIS and other European countries region (1.7 t) offset decreases in emissions (totaling about 9 t) in other regions.

Secondary production of non-ferrous metals is not yet addressed as a separate activity in the global emissions inventory activity (see Section 3.3.2).

3.4.3.6 (Primary) non-ferrous metal production (Hg)

Estimated Hg emissions to air associated with the production of Hg increased between 2010 (12.2 t) and 2015 (13.8 t). With modest decreases in estimated emissions from Hg production in the CIS and other European countries region and North Africa, the increase is almost entirely associated with emissions in Indonesia (estimated at 3 t in 2015 with no emissions

documented for 2010) and Central America and the Caribbean region (where estimated emissions from Hg production in Mexico increased from 0.1 t in 2010 to 2 t in 2015). In absolute terms, China (8.1 t in 2015) remains the main contributor to emissions from Hg production worldwide.

3.4.3.7 (Primary) non-ferrous metal production (large scale-gold production)

Mercury emissions from large-scale gold production in 2015 are estimated at about 84 t (72–97 t), 11 t more than the revised 2010 estimate. In the Asian region, estimated emissions decreased by about 2.8 t, partly explained by revisions in both activity data and emission factors to better reflect the current situation in, for example, East and South-east Asia. In other regions, in particular the CIS and other European countries region, Central America and the Caribbean, Sub-Saharan Africa and South America emissions increased, by an estimated total of 13 t in these four regions in the period 2010 to 2015. Again, it is important to remember the large uncertainties associated with these emission estimates.

3.4.3.8 Oil and gas production and refining

Mercury is a trace contaminant present in varying concentrations in produced oil and gas. Mercury emissions associated with oil and gas production arise during different phases of operations. Emissions associated with the production (well-head) activities (including emissions from flaring) are currently not quantified in the global emission inventory due to lack of relevant information. Globally, the quantity of Hg in produced gas is greater than in produced oil; however, the Hg content varies greatly between regions and between gas fields depending on local geology.

A study by the US NOAA in 2015 (Elvidge et al., 2015) estimated the total flared gas volume at 143 billion m^3 (about 3.5% of global gas production), with about 90% of the flaring occurring in upstream production areas and 8% at refineries. Using the Level 2 Toolkit default factor for Hg content of raw gas of 100 $\mu g/m^3$ (UN Environment, 2017b) this would yield a potential Hg emission to air of ~0.15 t/y from flaring.

Mercury is removed from oil and gas prior to its transport, in particular by pipeline, to avoid corrosion and damage to distribution systems. A significant part of the removal is achieved in connection with oil refining operations. By-product Hg recovery (or 'production') from oil and gas processing and non-ferrous mining operations constitutes one of the five main sources of Hg supply with an estimated 30–100 t of Hg captured from gas processing globally in 2015 (UN Environment, 2017a).

GMA inventory estimates for emissions to air from oil refineries in 2010 (updated) and 2015 are 13.1 and 14.4 t, respectively. In a commentary on the 2010 estimates presented in the GMA2013 report (AMAP/UNEP, 2013), the International Petroleum Industry Environmental Conservation Association (IPIECA) presented their view that the GMA estimates for emissions to air were significantly over-estimated; they estimated emissions to air (in 2012) at about 1.35 t (IPIECA, 2014). Total inputs (i.e., amounts of oil refined multiplied by Hg content of the oil) associated with the refinery sector do not differ greatly between the approaches employed in the GMA and the IPIECA calculations. The main differences between the GMA and IPIECA estimates for emissions to air (and releases to water) appear to

be associated with the assumptions regarding the fate of Hg at refineries. In the IPIECA approach, ~5% of emissions to air are assumed, based on studies at US refineries (WSPA, 2009) (with the major part of the Hg – 87% – associated with solid waste). The GMA (and UNEP Toolkit) methodology assumes higher emissions to air (~25%) based on other industry reported studies (e.g., IKIMP, 2012 and references therein), with less of the Hg input being distributed to other media. No new information was identified that allowed this discrepancy regarding the fate of Hg from oil refineries to be resolved, thus the GMA estimates of refinery emissions to air continue to differ from industry estimates by a factor of 10. Notwithstanding this degree of uncertainty, Hg emissions associated with oil and gas refining currently appear to constitute less than 1% of the total global anthropogenic emission to air.

3.4.3.9 Chlor-alkali production

Emissions from intentional use of Hg in the chlor-alkali industry have been decreasing for some time in most areas of the world. In part this is due to increased attention to best practices to reduce emissions, but is primarily due to the shift from production based on the Hg-process to membrane production technology. The Hg cell process currently accounts for about 8% of the global chlorine production capacity of around 60 million tonnes, at about 75 plants worldwide (UN Environment, 2017a).

GMA estimated emissions for this sector decreased from ~21 t in 2010 to ~15 t in 2015. It should also be noted that, depending on available information, emissions from some countries are based on caustic soda production statistics, and in other countries on plant production capacity.

For many parts of the world, updated activity data relevant to the 2015 inventory period are lacking; consequently, emission trends can only be described in relation to the EU, North America and South Asia regions, where emissions reportedly decreased by about 3 t (66%), 0.9 t (83%) and 1.9 t (74%) between 2010 and 2015, respectively. In the case of South Asia, the reductions are largely associated with the phase-out of Hg-process chlor-alkali production in India where the last Hg-cell facility closed at the end of 2015. Within the EU, Hg-cell production was due to be phased out by the end of 2017, and as of 2015 only two Hg-cell facilities exist in the USA with both scheduled to convert to membrane cell technology (UN Environment, 2017a).

The overall decrease in Hg emissions from the chlor-alkali industry would appear to be consistent with a reported 20% decrease in consumption of Hg in the chlor-alkali sector between 2010 and 2015; however, this is not entirely the case because much of the capacity that closed during that period involved the (relatively cleaner) plants in the EU and so it would not be expected that global emissions would have declined at the same rate as Hg consumption in this sector.

Although a relatively small component in the total global inventory, the continuing decrease in global Hg emissions from the chlor-alkali sector between 2010 and 2015 is a positive development, unrelated to changes in inventory methodology. However, with a total inventory of about 10,000 t of Hg in use in the industry globally (UN Environment, 2017a), the fate of Hg recovered from phased-out Hg-cell production plants is an ongoing concern.

3.4.3.10 Waste and waste incineration

Mercury emissions to air from disposal of waste from Hg-added products are estimated at 162 t in 2015; 147 t (120–223 t) from uncontrolled burning and landfill, and 15 t (8.9–32.3 t) from controlled incineration.

The 2015 estimated emissions from these sectors are considerably higher than the estimate of 96 t in the original 2010 inventory (AMAP/UNEP, 2013). This is largely due to a change in methodology where previously about 30% of Hg in Hg-added products was assumed to be 'retained in society'. In the 2015 updated methodology, this amount is now counted as part of the waste-stream and the updated 2010 emissions estimate of 130 t reflects this methodological change.

Based on updated 2010 estimates, emissions from waste sectors declined in the EU and North America regions (by 33% and 45%, respectively; equivalent to 3–4 t of Hg emitted in these regions). In all other regions, waste-associated Hg emissions increased, by more than 10 t in South Asia and Sub-Saharan Africa, and around 3–5 t in the Middle East, CIS and other European countries and East and South-east Asia. Emissions in Australia, New Zealand and Oceania and South America regions were relatively unchanged from 2010 to 2015.

Emissions from the waste sector have large associated uncertainties; quoted ranges are conservative and primarily reflect uncertainties attributed to activity data (i.e., estimates of regional consumption of Hg in Hg-added products).

In general, the estimates addressed in the global inventory do not include industrial wastes and only partially include waste that may be classified as hazardous or medical waste, some of which may also be incorporated in fuels used in, for example, the cement industry.

Emissions associated with waste from Hg-added products is also an area where large discrepancies were identified between estimates made in the GMA inventory and those included in some national inventories produced as part of (preliminary) Minamata Initial Assessments (see Section 3.3.4).

3.4.3.11 Crematoria emissions

Human cremation represents a relatively small but important source of emissions associated with intentional use of Hg – specifically Hg use in dental amalgam fillings. Estimated global Hg emissions to air from cremation are highly uncertain, but estimated to be less than 5 t/y (in 2015 and 2010) (~0.25% of the global inventory). The proportion of regional emissions associated with cremation is slightly greater (around 1%) in the Australia, New Zealand and Oceania region and the EU and North America, probably reflecting comprehensive access to dental care that – in past decades at least – included widespread use of Hg amalgam fillings. With increasing use of alternatives to Hg amalgam fillings in many of these countries but greater access to dental care (including use of amalgam fillings) in developing countries, emission patterns from cremation can be expected to change in the future. Cultural and religious practices associated with burial and cremation also play a role in determining whether cremation emissions are a significant part of the national air emission profile.

For some countries, emissions from cremation may be (significantly) over-estimated as available information is currently insufficient (see E-Annex 3, Section A3.4) to allow

account to be taken of APCDs (including activated carbon systems) that are being introduced at crematoria.

Cremation emissions are only part of the emissions associated with use of Hg in dental applications. The 2015 global inventory does not yet quantify other emissions that can occur during preparation and routine disposal of Hg fillings. In the clinic these may occur during the collection and storage of biomedical and other solid dental wastes, during maintenance of amalgam separators, and during dental procedures, etc. Outside the clinic they may occur during waste collection and management, including waste recycling and treatment and disposal of hazardous waste, municipal waste treatment, wastewater treatment, and wastewater sludge incineration, etc. Other work has estimated emissions to air from these activities in the European Union region at ~50 t/y (AMAP/UNEP, 2013); they are also reported to contribute significantly to Hg releases to waste waters in many countries.

3.4.3.12 Artisanal and small-scale gold production

Intentional use of Hg in ASGM is the predominant source of Hg emissions to air at the global level in the 2015 inventory, as was also the case in 2010. There remain, however, large uncertainties associated with emissions from ASGM.

ASGM activities take place in seven of the 11 sub-regions considered in the current work. Of the estimated total global emissions from ASGM of about 835 t in 2015, around 41% is from South America, 30% from Sub-Saharan Africa and 26% from East and South-east Asia. Mercury emissions from ASGM activities in Central America and the Caribbean, the CIS region and South Asia are considerably lower (4.5–15 t in 2015) with a very minor contribution from Middle Eastern States.

ASGM-associated emissions are thus the predominant source of Hg emissions in some regions, accounting for more than 80% of the estimated emissions in South America, 70% of emissions in Sub-Saharan Africa, 30% of emissions in Central America and the Caribbean and about 25% of emissions in East and South-east Asia.

The estimated emissions from ASGM in 2015 (835 t) are significantly higher than the value reported for 2010 in the GMA2013. A recalculation of the 2010 emissions using the improved information base on ASGM-related activities, and revised emission factor assumptions results in an estimated Hg emission from ASGM of about 680 t in 2010. This would imply that ASGM emissions increased by ~23% between 2010 and 2015. There are, however, large differences in apparent trends in emissions between 2010 and 2015 in different regions. The most significant increases are for South America (Hg emissions increasing from about 177 t in 2010 to 340 t in 2015) and Sub-Saharan Africa (from about 230 to 250 t); conversely, ASGM emissions from East and South-east Asia declined from an estimated 245 t in 2010 to 214 t in 2015. In the latter region, estimates of ASGM emissions in China sharply declined (attributable to banning of Hg use in ASGM, but also uncertainty regarding the validity of high estimates for earlier years) but this was largely offset by increases in emission estimates for other countries in the region, Indonesia in particular. In South America and Sub-Saharan Africa the apparent trends may be influenced to a substantial extent by new information that has become available for these regions

as a result of Minamata Initial Assessments and related work on National Action Plans for ASGM. This may also be the case for South-east Asia where, for example, Myanmar has recently been identified as having significant ASGM emissions according to preliminary information from its MIA and NAP work. Consequently, the apparent increase in emissions from ASGM between 2010 and 2015 is considered to be more a reflection of improved information used in developing 2015 estimates than a 25% change in actual ASGM.

3.5 Conclusions

Quantified descriptions of regional emission patterns and sector contributions to global emissions, as well as trends in emissions from 2010 to 2015 are presented in the 'Key messages' at the start of the chapter and detailed in previous sections. To avoid repetition, findings and numerical results are only summarized briefly here, or referred to within the context of a more general discussion of the air emissions inventory results.

The GMA2018 inventory of global emissions of Hg to air from anthropogenic sources in 2015 is the second inventory produced using the consistent and transparent 'GMA methodology' originally documented in the GMA2013 report (AMAP/UNEP, 2013).

The inventory produces an estimate of total emissions to air in 2015 of 2220 t (2000–2820 t) and is presented in terms of regional and sectoral summaries (Section 3.3), as well as national-sector based estimates for 17 key emission sectors (E-Annex 3, Section A3.9). Regional emissions patterns and sector contributions were generally similar to those in 2010 reported in the GMA2013 (AMAP/UNEP, 2013). Approximately 50% of estimated emissions to air occur in Asia, in particular the East and Southeast Asia region, followed by South America and Sub-Saharan Africa, with ASGM emissions dominating in the latter two regions. ASGM activities and stationary combustion of fossil fuels (primarily coal burning) account for more than 60% of the estimated global emissions from anthropogenic sources in 2015 (38% and 24%, respectively), with the major industrial sectors (non-ferrous metals, cement and ferrous metals) responsible for a further 27%. Emissions from Hg-added product waste and intentional-use in the chemical industry contribute a further 7.3% and 3.3%, respectively. Additional sectors for which it is not yet possible to prepare reliable global emission estimates are identified; the current evaluation, however, is that potential emissions from these sources are not expected to substantially increase the global emissions total or alter conclusions regarding, for example, regional emission patterns; they may however be of local or national significance in certain countries.

Geospatial distribution of the resulting inventory yields the pattern of Hg emissions shown in Figure 3.10. This illustrates the concentration of emissions sources in Asia (especially East and South-east Asia) associated with energy production and industry, and in some countries ASGM. It also shows the significant contribution to emissions in South America, Sub-Saharan Africa and Central America and the Caribbean associated with ASGM activities. In the industrialized population centers of Europe and North America, emissions associated with energy production and industrial sources predominate. Increased use of information on point sources

All sectors (excluding ASGM)

Industry

Power generation

HgT g/km²

0–0.001
0.001–0.005
0.005–0.01
0.01–0.05
0.05–0.1
0.1–0.5
0.5–1
1–5
5–10
10–100
100–500
500–1000
1000–5000
5000–10000

Intentional use and waste

ASGM

All sectors (including ASGM)
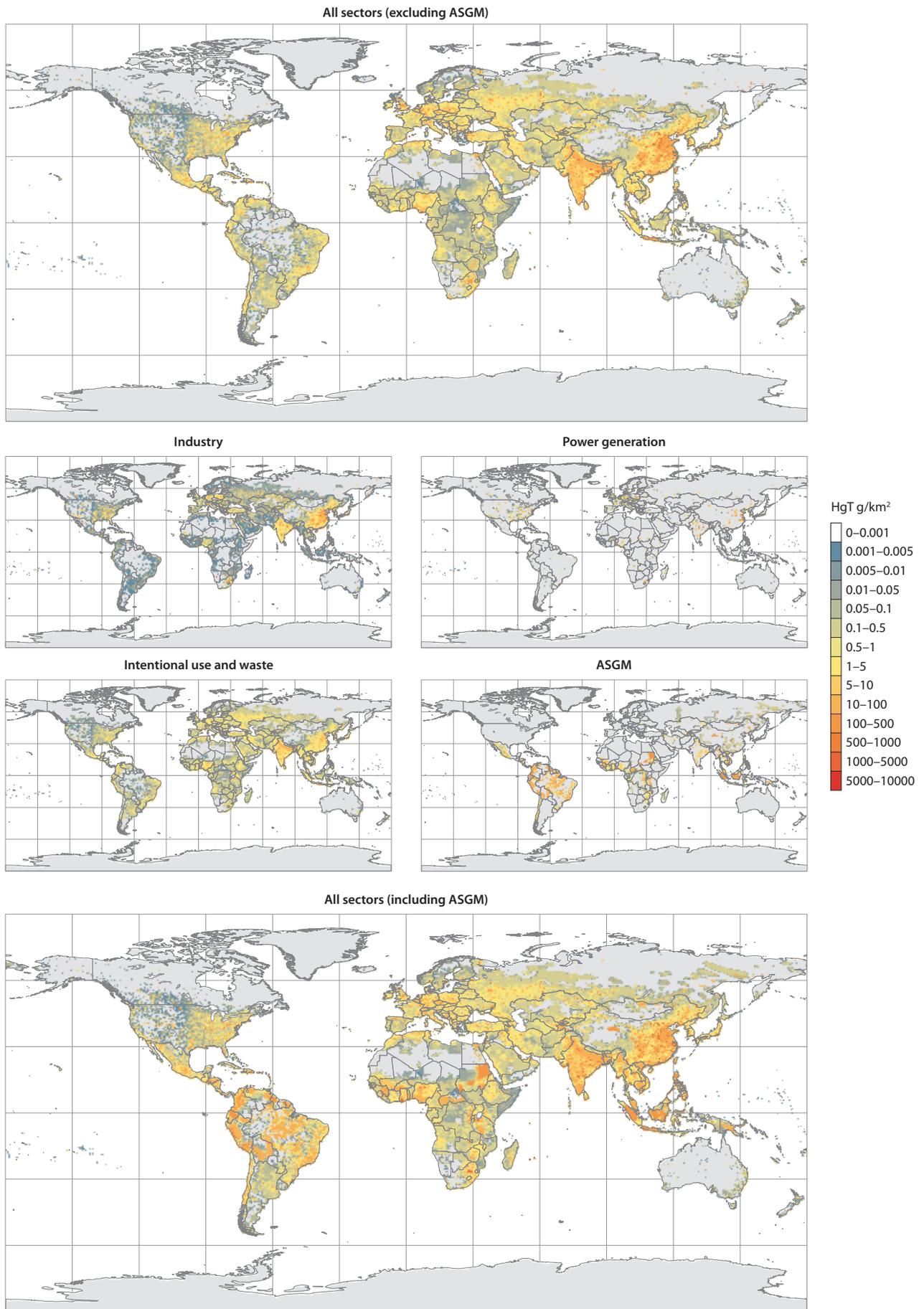
Figure 3.10 Geospatially distributed (total) Hg emissions to air from anthropogenic sources in 2015.

in the geospatial distribution procedure has resulted in more precise location of emissions – reflected by individual grid cells with high emission rates coincident with power plants and industrial facilities such as cement plants and non-ferrous metal smelters. The lower emission rates observed over wider areas are associated in some countries with activities such as ASGM (that are generally difficult to locate to specific areas at present), and in particular Hg emissions arising from disposal of waste from societal use of Hg-added products. Emissions from waste are assumed to be greatest in areas of high population and/or countries where consumption of Hg-added products is greatest.

The *Global Mercury Supply, Trade and Demand* report (UN Environment, 2017a) summarizes the regional consumption of Hg in a range of applications including consumption in Hg-added products that are the source of much of the Hg emitted to air following waste disposal, as well as ASGM and chemical industry uses. E-Annex 3, Section A3.3 includes a summary of estimated Hg consumption by world region and product group in 2015 based on this report (see Table A3.3.1).

Improvement in available information is identified as a reason for the increase in estimates of emissions from ASGM in 2015 relative to those in 2010. This is consistent with data indicating that consumption of Hg in ASGM was relatively stable between 2010 (range 912–2305 t) and 2015 (range 872–2598 t); this followed a large increase between 2005 (range 650–1000 t) and 2010 (UN Environment, 2017a).

Estimated emissions to air from sources other than ASGM increased by about 17% (~195 t) from 2010 to 2015, the majority of this increase being associated with industrial sources. In the chemicals industry, a decrease in consumption of Hg in the chlor-alkali industry (of about 75 t between 2010 and 2015; UN Environment, 2017a) is reflected in decreasing emissions, from an estimated 21 t in 2010 to 15 t in 2015. However, over the same period, consumption in VCM production increased by around 280 t, with emissions from this sector in 2015 estimated at about 60 t. The majority of the VCM production is in China.

In industrial sectors where Hg emissions are a 'by-product' of the presence of Hg in fuels and raw materials, the regional trends in emission observed between 2010 and 2015 are determined largely by trends in 'activity' data. In the case of the cement industry, for example, estimated emissions increased in all regions except the EU28, the only region where cement production also declined between 2010 and 2015 (Figure 3.11). Steel production on the other hand declined between 2010 and 2015 in six of the nine regions considered, but increased significantly in East and Southeast Asia, South Asia and the Middle East (by about 20%, 30% and 47%, respectively). Production volumes in the Middle East are far lower than in the Asian regions. Estimated emissions from pig iron and steel manufacture correspondingly increased (by 17%, 38% and 19%) in these three regions, and 11% globally, and decreased (or were relatively unchanged) in six regions. At present, therefore, indications are that mitigation of emissions by implementing control technology is unable to offset increases due to increased activity in several industrial sectors in several regions; decreasing emissions are therefore primarily associated with decreasing activity or changes in fuel mix (reduced use of coal) in the energy sector.
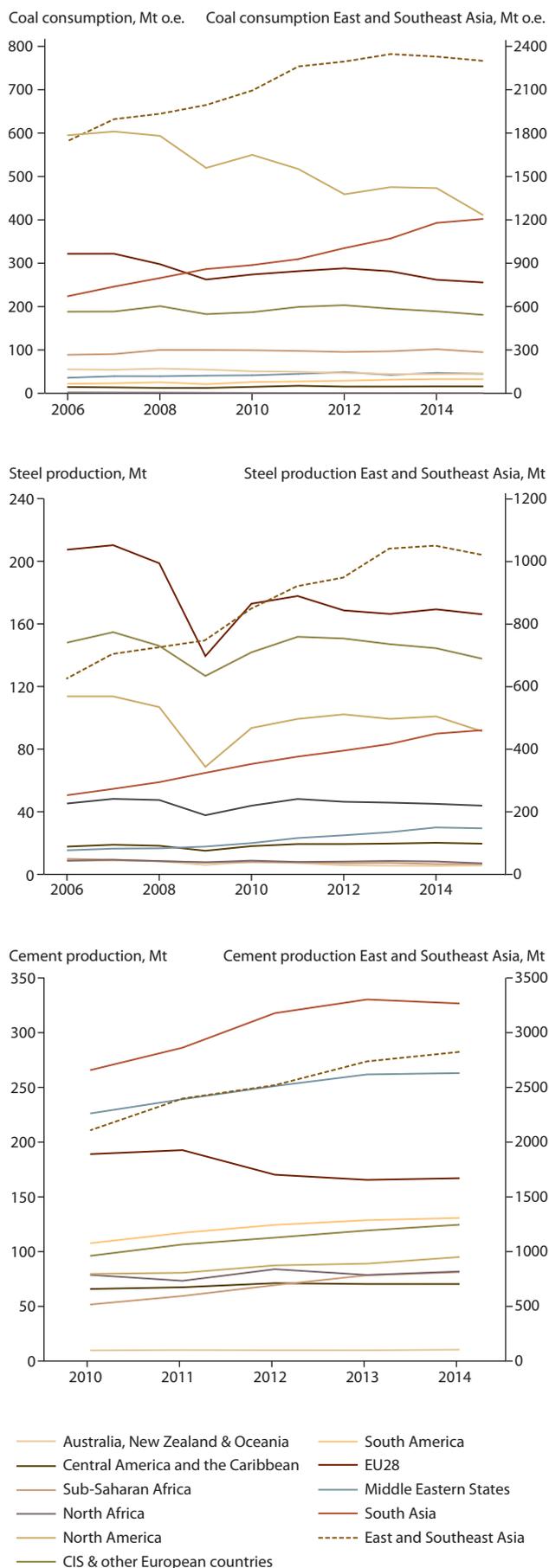
Figure 3.11 Trends in consumption of coal (BP, 2017), and production of steel and cement (USGS, 2017b) in different regions. Note different scale for East and Southeast Asia.

Table 3.8 Mercury consumption[a] in Hg-added products for the period 2005–2015 (UN Environment, 2017a)

Sector mercury consumption (tonnes)	2005	2010	2015
Batteries	300–600	230–350	159–304
Dental applications	240–300	270–341	226–322
Measuring and control devices	150–350	219–280	267–392
Lamps	100–150	105–135	112–173
Electrical and electronic devices	150–350	140–170	109–185
Other (paints, laboratory, pharmaceutical, cultural/traditional uses, etc.)	30–60	222–389	215–492

[a] 'consumption' is defined in terms of the end-use of Hg-added products (i.e., place of consumption), as opposed to regional 'demand' for Hg; tabulated values are means of wider ranges of estimates representing various levels of uncertainty (see UN Environment, 2017a).

Estimated emissions from disposal of (Hg-added product) waste increased substantially (in percentage terms) in all regions – up to 165% in Sub-Saharan Africa and 28% globally – apart from the EU28 and North America, where emissions declined by 33% and 45%, respectively. Global consumption of Hg in Hg-added products (batteries in particular) declined or was relatively stable between 2010 and 2015 (Table 3.8); however, regional patterns appear to be changing due to increased use and disposal of these products in some regions, and decreased use combined with more efficient recycling in others.

Possibilities to compare emissions (in 2015) estimated as part of the GMA2018 work are limited. No other global inventory produced using a consistent methodology is available; therefore, comparisons can only be made with estimates compiled at the regional or national level.

Comparisons between GMA inventory estimates and those prepared under other initiatives (including pollutant release and transfer inventories compiled by some countries) are not simple. In part this is due to differences in the categories covered, but the major obstacle that remains is differences in how emissions are characterized and reported under different activity or sector categories. Additional factors that need to be accounted for include reporting thresholds, that is, the emissions level or alternative criteria above which (facility level) reporting becomes mandatory. Also, whether estimates based on measurements intended to document that air concentrations are below some regulatory limit are appropriate for the purpose of establishing (annual) emissions estimates. Notwithstanding these issues, in many cases GMA and nationally-reported emissions estimates agree reasonably well (if uncertainties are taken into consideration), especially in terms of national totals. Where differences exist, these can often be explained and attributed to the factors mentioned above, especially to differences in source categorization.

Reporting systems currently in use are often adapted from systems not originally developed for reporting Hg emissions, and so may not be ideally suited for this purpose; the CLRTAP reporting mechanism is an example. Emissions estimates compiled using the UN-Toolkit (employed in compiling the majority of MIAs), should be generally compatible with the GMA approach. Preliminary comparisons with MIAs, however, indicate that there are areas of inconsistency, especially where the Toolkit Level 1 has been employed or where countries have (uncritically) adopted default factors or employed inappropriate activity data (typically to fill gaps where appropriate data are not available).

In all such comparisons, it is important to note that there is no 'correct estimate' (all are based on some underlying and often very uncertain assumptions). For regulatory reasons, 'official' emissions estimates often lack any quantification of uncertainty, but this does not mean that the values are assured. The value of comparing emissions estimates from different sources, especially if derived using different methods, lies primarily in the possibilities that this gives for implying confidence in estimates or identifying areas where knowledge gaps exist. Streamlining and improvement of emissions estimation and reporting systems, including attention to underlying data used to calculate estimates, remains an important objective for future work. Efforts to harmonize reporting and inventory estimate systems will improve the ability to confidently measure the success of the Minamata Convention.

Chapter 3 E-Annex: Methodology for estimating mercury emissions to air and results of the 2015 global emissions inventory

A3.1 Main 'by-product' emission sectors and the chlor-alkali industry

A3.1.1 Description of methodology

The 2015 inventory estimates for most sectors are based on a three step approach.

Step 1: Compiling *activity data* – statistical data concerning the consumption of fuels and raw materials and the production of products that are relevant to calculation of mercury (Hg) emissions from energy/industrial sectors; and data on Hg consumption in intentional use sectors and in Hg-added products that allows estimates to be made of Hg emissions from waste streams, etc.

Step 2: Compiling 'emission factors' that can be applied to the activity data to derive estimates of *unabated/uncontrolled emissions to air* – a typical example might be the fraction of Hg in coal that is released to the atmosphere when the coal is burned (prior to any technological measures to reduce emissions of air pollutants). It should be noted that these are *unabated emission factors (UEFs)* and therefore differ from the *(abated) emission factors (AEFs)* that are commonly reported/used to produce end-of-pipe emissions estimates. These UEFs can be considered as being similar to the *input factors* applied in the UNEP Toolkit approach (UN Environment, 2017b), but differ in that – in most cases – they relate to the emissions/inputs only to air as opposed to the total release of Hg to all media that are obtained from the UNEP Toolkit input factors. To take this comparison a stage further, the UEFs employed in this work are <u>approximately</u> comparable to the UNEP Toolkit input factors multiplied by their respective *distribution factor (DF)* for the proportion of the input released to air; however, it should be noted that UNEP Toolkit factors were not always adopted, and that information developed during the current work is being used in updating of the UNEP Toolkit factors. The UEFs, when applied to the activity data from 'Step 1' yield estimates of unabated (uncontrolled) emissions to air from the activity concerned.

Step 3: Attempting to represent the 'technology' that is applied in the respective sectors in different countries to control (reduce) Hg emissions to the air – typically through the application of *air pollution control devices (APCDs)*. These technologies are characterized by their effectiveness (Hg emissions reduction efficiency) and their degree of application. In 'Step 3' it is necessary to recognize that available information – based on a relatively few (but increasing numbers of) measurements made at individual plants in certain (mainly developed) countries – demonstrates that effectiveness of APCDs is very variable and depends on plant operating conditions, and specific characteristics of fuel and raw materials, etc. In addition, the general scarcity of relevant information on both the effectiveness of APCDs and their degree of application in various sectors/countries means that assumptions need to be made. First, on the basis of available information, technologies have been grouped according to their general degree of effectiveness at reducing Hg emissions; and according to their degree of use (e.g., commonly applied APCD configurations). Second, countries have been assigned – on the basis of an assumed general level of technological implementation of APCDs – into five groupings (see Section 3.2.1.2 and this E-Annex, Section A3.9). Information on the effectiveness and degree of implementation of APCDs in those countries for which information is available (derived from published literature, grey literature and application of the UNEP Toolkit, etc.) has then been used to characterize the *technological profile* for the country-group to which the country belongs. The resulting technology profile – or a specific national profile for countries where such detailed data are available – has been applied to the unabated/uncontrolled emissions estimates resulting from 'Step 2' to produce abated (controlled) emission estimates for all countries/sectors for which activity data are available from 'Step 1'. These estimates constitute the global inventory of Hg emissions to air from the represented anthropogenic sectors.

As described, the applied methodology relies on statistical data and assumptions concerning emission factors and technological profiles, etc., that are based on often very limited available information. However, this methodology is designed to derive global emissions inventories and to compile relevant statistics and other information in a manner that allows it to be transparent, readily updatable as new information becomes available, and potentially useful for other purposes (such as emission scenario development).

A full description of the emission factors and technology profiles applied in this work is given in this E-Annex, Section A3.6, which also contains extensive notes explaining their basis, and comparisons with emission factors used in other studies, including the UNEP Toolkit (UN Environment, 2017b), the GMA2013 (AMAP/UNEP, 2013) and the 2005 inventory (AMAP/UNEP, 2008).

The documentation procedures described above and transparency regarding assumptions made are intended to allow for future updates of the inventory for individual countries and sectors as more detailed information becomes available.

A3.1.2 Example calculation

This example shows the calculations applied to estimate Hg emissions from cement production in China. Under the regionalization approach described in Section 3.2.1.2, China is in the Group 3 countries with respect to characterization of applied technology.

According to the US Geological Survey, China produced 2 492 000 kt of cement in 2014 (see this E-Annex, Section A3.8).

The (country-specific) UEF applied to cement production in China is 0.071 g/t cement produced (see this E-Annex,

Section A3.6). About 80% of cement production in China is based on coal; emissions from coal used in cement production are separately accounted under the SC-IND – stationary fossil fuel combustion in industrial uses – sector. The UEF applied to cement production in China is a nationally-specific UEF for cement production resulting from Hg in raw materials (limestone) with assumed 6% co-incineration of waste. The resulting unabated emission estimate for this sector in China is therefore 176.932 t (= 2 492 000 000 × 0.071 grams).

In Group 3 countries, the technology profile applied for cement production (see this E-Annex, Section A3.6) would imply that ~20% of the emissions from cement production in China are not subject to any emission control, and that 80% are subject to (basic particulate matter) emission controls that reduce Hg emissions by about 25%. On the basis of these assumptions, the associated (abated) Hg emissions would be reduced from around 177 t to around 142 t, with some 35.4 t (= 176.932 × 0.8 × 0.25) of Hg being captured by the APCDs.

However, national information provided by China indicated that a more accurate representation of the abatement technology applied in the Chinese cement sector is that all Chinese cement plants are fitted with dust removal systems (about 80% equipped with fabric filters and about 20–40% with electrostatic precipitators) with an effective Hg capture of 40%. Applying this new profile, about 56.7 t (= 176.932 × 1 × 0.4) of Hg are removed by the APCDs, resulting in an estimated emission to air from the cement sector in China of some 106 t.

To estimate an uncertainty range for this estimate, these calculations were repeated using low and high values of 1 744 400 kt and 3 239 600 kt, respectively for the activity data, that is ±30% applied to activity data from sources other than the International Energy Agency or official national data (see AMAP/UNEP, 2013: their Table 2.3). In addition, for the low range estimate the UEF was reduced from 0.071 to 0.042 g/t (= 0.071 minus half the difference between this value and the tabulated low UEF of 0.013 g/t); and for the high range estimate a UEF of 0.478 g/t was applied (= 0.071 plus half the difference between this value and the tabulated high UEF of 0.885 g/t) (see this E-Annex, Section A3.6). Finally, to account for uncertainties in the applied technology profile, a high and low range TF (technology factor) was applied. A TF of 0.6 (1 minus the 40% reduction due to abatement) was applied in calculating the 'mid-range' estimate. In calculating the high- and low-range estimates, TFs of 0.8 and 0.4, corresponding to lower- and higher-levels of abatement, respectively, were applied. The resulting range of (abated) estimates is therefore 29 t (= 1 744 400 000 × 0.042 × 0.000001 × 0.4) to 1239 t (= 3 239 600 000 × 0.478 × 0.000001 × 0.8), where the first term is the activity in tonnes, the second term is the UEF in grams per tonne, the third term is the factor to convert the emission estimate from grams to tonnes, and the fourth term is 1 minus the reduction due to abatement. In this example, the uncertainty range is primarily associated with the UEF applied in the high range estimate; in other cases the activity data may be the larger source of uncertainty.

On the basis of similar calculations, stationary combustion of coal in the cement industry was estimated to result in a further 26.6 t (11.2–50.7 t) of cement industry related Hg emissions to air from China in 2015.

A3.2 Artisanal and small-scale gold mining

A3.2.1 Description of methodology

The 2015 inventory estimate of Hg emissions from artisanal and small-scale gold mining (ASGM) is based on an understanding of ASGM based on direct field evidence and a wide variety of secondary information sources (including analysis of official trade data, and extrapolation of these data to regional and national scales). The quality of (purpose-specific) direct field evidence has improved significantly for a number of countries, mainly due to the implementation of Minamata National Action Plan (NAP) projects.

The general approach to estimate 2015 emissions from ASGM is the same as that applied in deriving the 2010 estimate (AMAP/UNEP, 2013). Reasonably good information exists about where ASGM is occurring (documented now for 81 countries compared to 70 in 2013) – this mainly reflects new data acquisition rather than new ASGM activity. Main information sources used include: decades of archives from the Northern Miner (a mining trade magazine that regularly reports the 'presence of artisanals'); reports and conference materials from the World Bank; information under work programs of the United Nations Development Programme, UN Environment and the United Nations Industrial Development Organization; reports from other intervention programs such as the Swiss Agency for Development and Cooperation, Global Affairs Canada, the United States Agency for International Development, the German Gesellschaft für Internationale Zusammenarbeit, the World Wildlife Fund, and Conservation International etc.; reports and abstracts from the International Conferences on Mercury as a Global Pollutant up to 2017 (13 congresses); follow-up on older reports, such as those of the Mining, Minerals and Sustainable Development (MMSD) articles published in the peer-reviewed literature; and new field reports from field programs and intervention programs such as the Minamata NAPs that are directly engaged with government ministries and individuals working in the ASGM sector, including miners and gold and Hg traders.

The information base that underpins the assumptions regarding use of Hg in ASGM has been significantly updated and improved for a number of countries since 2013. Improved knowledge has resulted in an adjustment of the factors applied in assigning ASGM emissions associated with whole ore amalgamation and concentrate amalgamation. This results in a 5% decrease in the estimate of emissions to air per unit Hg consumed in ASGM relative to the estimates reported for 2010 by AMAP/UNEP (2013).

Knowledge concerning ASGM practices has improved with continued social, environmental, and financial development efforts in the sector worldwide, particularly through on-the-ground observations and interviews with ASGM miners and stakeholders. Physical measurements of Hg use over a cross-section of ore processing techniques and operators has led to a better understanding of the amount of Hg used in producing gold in ASGM and its variations. The new knowledge has also led to adjustments in the distribution factors that apportion Hg losses into emissions (to air) and releases (to land and water) for the GMA2018. While concentrate amalgamation

distribution remains unchanged from the GMA2013 (at 75% emission and 25% release), the distribution for whole-ore amalgamation (WOA) has changed to 20% emission and 80% release (from 25% and 75%, respectively). This reflects a change in the understanding of the global mercury:gold (Hg:Au) ratio for WOA; from 4:1 to 5:1.

The distribution of Hg consumed in ASGM between emissions and releases is derived from global statistics and the assumptions applied must capture the large variation of Hg:Au ratios across the global ASGM sector. The Hg:Au ratio varies widely due to metallurgy and practices. For example, when ore is relatively free of other metals and the gold is coarse, the WOA ratio tends to be low (at around 4:1). However, for other ores with fine-grained gold that contain silver, ratios of up to 60:1 can be observed. Other important factors are: variability in practices (methods employed in crushing, milling, and concentrating); whether Hg is being captured and recycled; the grade of the ore, with high grade ore using less Hg; the socio-economic circumstances of the miners; and other factors (Lacerda, 2003; Telmer and Veiga, 2009). Direct measurement of WOA ratios around the world have yielded ratios of 2:1, 8:1, and 11:1 in Nicaragua (AGC, 2016), and as high as 15:1 in Antioquia, Colombia (Cordy et al., 2011), 12:1 in Ecuador (Velasquez-Lopez et al., 2010), a range of 4–11:1 in China (Gunson, 2004), and a range of 40–60:1 in Indonesia (Pereira Filho et al., 2004). The adjustment of the global WOA ratio from 4:1 to 5:1 accommodates the occurrence of very high ratios in some countries (e.g., Indonesia), but remains conservative.

Based on information on practices used in different countries, it is estimated that, on average 40% of Hg used in ASGM is emitted to the atmosphere with the remainder released to land and water. In regions where concentrate amalgamation is practiced, while the absolute amount of Hg used is lower than for whole ore amalgamation, 75% of the Hg used is emitted to the atmosphere. In regions where whole ore amalgamation is practiced, more Hg is consumed per unit of gold produced, but here a much larger proportion of the Hg is released to aquatic and terrestrial systems than is emitted to air; some of the Hg released to aquatic and terrestrial systems is subsequently re-emitted to the atmosphere. Estimates from Australia and Canada (Winch et al., 2008; Parsons et al., 2011) suggest that a large proportion of the Hg used in historical gold mining operations in the 1800s has been remobilized. New work has identified that some historical practices used in silver mining in Latin America resulted in less (re)emission of Hg to the atmosphere than previously assumed (see Chapter 2).

The amount of Hg used in ASGM (see Table A3.2.1) can be estimated using four main approaches: (1) direct measurements – using a balance to directly weigh amounts of Hg used; (2) applying a Hg:Au ratio to the quantity of gold produced based on the type of process used (whole ore amalgamation, concentrate amalgamation, also taking account of the use of emission controls such as retorts, etc.); (3) interviewing miners and gold merchants who buy or sell Hg; (4) using official trade data. The first three approaches involve working directly with miners and gold merchants. This information can then be used to constrain other estimates, through triangulation, to produce

Table A3.2.1. Mercury consumption in artisanal and small-scale gold mining and calculation of associated emissions (Telmer, K. and J. O'Neill (AGC) pers. comm., 2017).

Best estimate for ASGM Hg use and air emissions until August 2012						Percentage of total Hg applied in concentrate amalgamation, %CA	Percentage of total Hg applied in whole ore amalgamation, %WOA	Emission Factor, EF $EF_{CA}=75\%$ $(1/1.3)$ $EF_{WOA}=$ 20% $(1/5)$	Year of most recent data	Mean air emission, t	Release to water and land, t
Country, count = 81	Quality of data[a]	± error, %	ASGM Hg use, t					$(\%CA \times EF_{CA})$ $+ (\%WOA \times$ $EF_{WOA})$		(Hg use) × (EF)	(Hg use) – (air emission)
			min	mean	max						
Total		74	985.9	2058.9	3131.9					837.7	1221.2
Bolivia	4	30	84.0	120.0	156.0	25.0	75.0	0.34	2012	40.5	79.5
Guinea	4	30	13.4	19.1	24.8	100.0	0.0	0.75	2017	14.3	4.8
Nicaragua	4	30	2.5	3.5	4.6	0.0	100.0	0.20	1999	0.7	2.8
Peru	4	50	163.5	327.0	490.5	25.0	75.0	0.34	2017	110.4	216.6
Senegal	4	30	2.1	3.0	3.9	100.0	0.0	0.75	2015	2.3	0.8
Suriname	4	30	44.1	63.0	81.9	5.0	95.0	0.23	2016	14.3	48.7
Brazil	3	50	52.5	105.0	157.5	50.0	50.0	0.48	2015	49.9	55.1
Burkina Faso	3	50	17.6	35.1	52.7	100.0	0.0	0.75	2011	26.3	8.8
Cambodia	3	50	3.8	7.5	11.3	50.0	50.0	0.48	2006	3.6	3.9
Colombia	3	50	87.5	175.0	262.5	16.7	83.3	0.29	2014	51.0	124.0
Ecuador	3	50	42.5	85.0	127.5	20.0	80.0	0.31	2014	26.4	58.7
French Guiana	3	50	3.8	7.5	11.3	100.0	0.0	0.75	2008	5.6	1.9
Ghana	3	50	27.5	55.0	82.5	100.0	0.0	0.75	2016	41.3	13.8
Guyana	3	50	7.5	15.0	22.5	100.0	0.0	0.75	2008	11.3	3.8
Honduras	3	50	2.5	5.0	7.5	50.0	50.0	0.48	1999	2.4	2.6
India	3	50	3.0	6.0	9.0	100.0	0.0	0.75	2013	4.5	1.5
Indonesia	3	50	213.5	427.0	640.5	16.7	83.3	0.29	2014	124.5	302.5
Lao Peoples Democratic Republic	3	50	1.5	3.0	4.5	100.0	0.0	0.75	2007	2.3	0.8
Mali	3	50	6.3	12.5	18.8	100.0	0.0	0.75	2016	9.4	3.1
Mongolia	3	50	5.8	11.5	17.3	50.0	50.0	0.48	2007	5.5	6.0
Mozambique	3	50	2.0	4.0	6.0	100.0	0.0	0.75	2009	3.0	1.0
Nigeria	3	50	10.0	20.0	30.0	100.0	0.0	0.75	2011	15.0	5.0
Philippines	3	50	35.0	70.0	105.0	25.0	75.0	0.34	2010	23.6	46.4
Sierra Leone	3	50	5.5	11.0	16.5	100.0	0.0	0.75	2004	8.3	2.8
Venezuela	3	50	51.0	102.0	153.0	25.0	75.0	0.34	2017	34.4	67.6
Zimbabwe	3	50	12.5	25.0	37.5	20.0	80.0	0.31	2016	7.8	17.3
Botswana	2	75	0.2	0.8	1.4	50.0	50.0	0.48	2016	0.4	0.4
Cameroon	2	75	0.4	1.5	2.6	100.0	0.0	0.75	2011	1.1	0.4
Central African Republic	2	75	2.0	8.0	14.0	100.0	0.0	0.75	2016	6.0	2.0
Chile	2	75	1.0	4.0	7.0	50.0	50.0	0.48	2009	1.9	2.1
China	2	75	25.0	100.0	175.0	25.0	75.0	0.34	2015	33.8	66.3
Congo	2	75	0.4	1.5	2.6	100.0	0.0	0.75	2010	1.1	0.4
DRC	2	75	3.8	15.0	26.3	100.0	0.0	0.75	2010	11.3	3.8
Guatemala	2	75	0.4	1.5	2.6	50.0	50.0	0.48	2005	0.7	0.8
Kenya	2	75	0.9	3.5	6.1	100.0	0.0	0.75	2016	2.6	0.9
Kyrgyzstan	2	75	1.9	7.5	13.1	50.0	50.0	0.48	2004	3.6	3.9
Madagascar	2	75	0.4	1.5	2.6	100.0	0.0	0.75	2003	1.1	0.4
Malaysia	2	75	0.9	3.5	6.1	50.0	50.0	0.48	1992	1.7	1.8
Mexico	2	75	1.9	7.5	13.1	50.0	50.0	0.48	2003	3.6	3.9
Myanmar	2	75	3.8	15.0	26.3	100.0	0.0	0.75	2016	11.3	3.8
Panama	2	75	0.4	1.5	2.6	50.0	50.0	0.48	1999	0.7	0.8

Best estimate for ASGM Hg use and air emissions until August 2012						Percentage of total Hg applied in concentrate amalgamation, %CA	Percentage of total Hg applied in whole ore amalgamation, %WOA	Emission Factor, EF $EF_{CA}=75\%$ $(1/1.3)$ $EF_{WOA}=$ 20% $(1/5)$	Year of most recent data	Mean air emission, t	Release to water and land, t
Country, count = 81	Quality of data[a]	± error, %	ASGM Hg use, t					$(\%CA \times EF_{CA})$ $+ (\%WOA \times EF_{WOA})$		(Hg use) × (EF)	(Hg use) − (air emission)
			min	mean	max						
Papua New Guinea	2	75	1.8	7.0	12.3	50.0	50.0	0.48	2010	3.3	3.7
Russia	2	75	2.8	11.0	19.3	50.0	50.0	0.48	2001	5.2	5.8
South Africa	2	75	0.9	3.5	6.1	50.0	50.0	0.48	2016	1.7	1.8
South Sudan	2	75	0.0	0.0	0.0	0.0	0.0	0.00	2016	0.0	0.0
Sudan	2	75	20.8	83.0	145.3	100.0	0.0	0.75	2015	62.3	20.8
Tajikistan	2	75	1.0	4.0	7.0	100.0	0.0	0.75	1996	3.0	1.0
Tanzania	2	75	8.8	35.0	61.3	100.0	0.0	0.75	2015	26.3	8.8
Thailand	2	75	0.4	1.5	2.6	100.0	0.0	0.75	2007	1.1	0.4
Togo	2	75	1.0	4.0	7.0	100.0	0.0	0.75	2002	3.0	1.0
Uganda	2	75	1.0	4.0	7.0	100.0	0.0	0.75	2016	3.0	1.0
Vietnam	2	75	1.9	7.5	13.1	50.0	50.0	0.48	2001	3.6	3.9
Angola	1	100	0.1	0.3	0.5	100.0	0.0	0.75	2014	0.2	0.1
Azerbaijan	1	100	0.1	0.3	0.5	100.0	0.0	0.75	2010	0.2	0.1
Benin	1	100	0.1	0.3	0.5	100.0	0.0	0.75	2010	0.2	0.1
Burundi	1	100	0.1	0.3	0.5	100.0	0.0	0.75	2010	0.2	0.1
Chad	1	100	0.1	0.3	0.5	100.0	0.0	0.75	2010	0.2	0.1
Costa Rica	1	100	0.1	0.3	0.5	50.0	50.0	0.48	1998	0.1	0.2
Cote d'Ivoire	1	100	0.1	0.3	0.5	100.0	0.0	0.75	2012	0.2	0.1
Dominican Rep.	1	100	0.1	0.3	0.5	100.0	0.0	0.75	1997	0.2	0.1
El Salvador	1	100	0.1	0.3	0.5	100.0	0.0	0.75	2010	0.2	0.1
Equitorial Guinea	1	100	0.1	0.3	0.5	100.0	0.0	0.75	2010	0.2	0.1
Eritrea	1	100	0.1	0.3	0.5	100.0	0.0	0.75	2017	0.2	0.1
Ethiopia	1	100	0.1	0.3	0.5	100.0	0.0	0.75	2010	0.2	0.1
Gabon	1	100	0.1	0.3	0.5	100.0	0.0	0.75	2010	0.2	0.1
Gambia	1	100	0.1	0.3	0.5	100.0	0.0	0.75	1996	0.2	0.1
Guinea-Bissau	1	100	0.1	0.3	0.5	100.0	0.0	0.75	2002	0.2	0.1
Iran	1	100	0.1	0.3	0.5	100.0	0.0	0.75		0.2	0.1
Kazakhstan	1	100	0.1	0.3	0.5	100.0	0.0	0.75		0.2	0.1
Lesotho	1	100	0.1	0.3	0.5	100.0	0.0	0.75	2016	0.2	0.1
Liberia	1	100	0.1	0.3	0.5	100.0	0.0	0.75	2003	0.2	0.1
Malawi	1	100	0.1	0.3	0.5	100.0	0.0	0.75	2001	0.2	0.1
Mauritania	1	100	0.1	0.3	0.5	100.0	0.0	0.75	2004	0.2	0.1
Niger	1	100	0.1	0.3	0.5	100.0	0.0	0.75	2000	0.2	0.1
Paraguay	1	100	0.1	0.3	0.5	100.0	0.0	0.75	2012	0.2	0.1
Rwanda	1	100	0.1	0.3	0.5	100.0	0.0	0.75	1992	0.2	0.1
Swaziland	1	100	0.1	0.3	0.5	100.0	0.0	0.75	2017	0.2	0.1
Ukraine	1	100	0.1	0.3	0.5	100.0	0.0	0.75		0.2	0.1
Uzbekistan	1	100	0.1	0.3	0.5	100.0	0.0	0.75	2001	0.2	0.1
Zambia	1	100	0.1	0.3	0.5	100.0	0.0	0.75	2008	0.2	0.1
Zambia	1	100	0.1	0.3	0.5	100	0	0.75	2008	0.2	0.1

[a] Class 4: recent quantitative data, error ±30% (5); Class 3: quantitative data but significantly updated within the past 5 years, error ±50% (20 countries); Class 2: some indication of quantity of Hg used, estimated average error ±75% (27 countries); Class 1: presence/absence, no quantitative information, error can be greater than ±100% (29 countries).

a more robust estimate of the amount of Hg used and thereafter emitted to the atmosphere or released to the terrestrial/aquatic environment.

The most reliable results are grounded in fieldwork and relationships established with stakeholder communities. In order to achieve this, personnel involved in collecting information and preparing estimates must be capable of understanding mining practices and the (local) gold trade. Mercury use practices and gold production are key items of necessary information. Determining these requires combining information from field data, miners, mining communities, buyers, traders, geological surveys, ministries responsible for mining, mining commissions, the private sector, exploration company press releases, industry magazines, environmental ministries, and others. This information must be analyzed to understand what is reasonable based on expert knowledge of geology, mining, ASGM practices, mining communities, and socio-economics. The results of the analysis should be discussed with stakeholders, such as miners, concession holders, local governments, and national governments to obtain their input and help constrain the analysis. A robust and comprehensive tool for making such estimates, that includes extensive background, examples, data entry forms and worksheets is now available (O'Neil and Telmer, 2017).

The fundamental questions to be answered in order to make an annual estimate of Hg use and emissions are:

1. What are the practices in use? (whole ore amalgamation; concentrate amalgamation; Hg recycling – retorts)

2. How much Hg is used per unit gold produced? (the Hg:Au ratio; grams of Hg lost per gram of gold produced); Do miners discard used Hg or recycle Hg?

3. How much gold do miners produce per year? It is important to evaluate the value of the gold and consider whether that value makes sense.

4. What is the total number of miners involved in this production?

Questions 3 and 4 are key to extrapolating to larger scales. For an elaboration of many important considerations and approaches in obtaining high quality information, see O'Neil and Telmer (2017).

The quality of estimates varies across countries and is grouped according to four main classes: Class 1 (presence/absence of ASGM activity, no quantitative information, uncertainties can be more than ±100%); Class 2 (some indication of the quantity of Hg used, estimated average uncertainty ±75%); Class 3 (quantitative data but not significantly updated within the past five years, uncertainty ±50%); Class 4 (recent quantitative data; uncertainty ±30%).

A3.2.2 **Example calculation**[3]

This example describes the method used to make a Class 4 estimate of Hg use from ASGM in Burkina Faso over a two-year period (2011–2012).

The Director of the Ministry of Mines, Geology, and Quarries estimates that 600 000 adults are living on 221 ASGM sites in Burkina Faso that are registered for ASGM exploitation permits and plotted on a cadastral map. About the same number operate on unregistered land informally or illegally. Meetings were held before and again after field visits with miners, government agencies, miners associations (formal + informal), gold traders and Hg traders. The results are as follows: All ASGM activities use Hg. The practice used by miners is exclusively concentrate amalgamation; whole ore amalgamation is not practiced. Mercury recycling is not practiced – amalgam is burned using an open flame. Miners do not throw away used ('dirty') Hg. The amount of Hg used per unit gold produced is on average 1.3 parts mercury to 1 part gold (i.e., a Hg:Au ratio of 1.3:1). This accounts for the Hg that ends up in the amalgam (1 part) and the Hg that is lost during processing to the tailings (0.3 parts). All Hg used is released to the environment, with 75% (that in the amalgam) directly emitted to the atmosphere during amalgam burning and the residual (0.3 parts) lost to the tailings. In Burkina Faso, it is likely that the amount lost to the tailings is re-emitted to the atmosphere on a relatively short timescale of one to several years as the tailings are accumulated in above ground piles and often later reprocessed.

A third of the 600 000 government reported ASGM population are estimated to be active miners. They produce 20 to 30 t of gold per year (~25). This is reasonable considering the known geology (abundance of gold-bearing formations of sufficient grade throughout the country), a processing lens (gold production per miner using the observed processing techniques), and a socio-economic lens based on the cost of living at ASGM localities. This estimate was discussed with the gold buyers and site owners and the Ministry of Mines and was found to be reasonable by these groups. The amount of Hg used and emitted to the atmosphere is thereby determined as follows: 25 t of gold are produced annually; all of which is amalgamated using 32.5 t of Hg per annum. All amalgam is burned openly thereby emitting 25 t of Hg directly to the atmosphere with the remaining 7.5 t being released to the land and water in the waste stream (tailings). The Hg contained in tailings is likely to also be emitted to the atmosphere within a decade.

It may be helpful to describe briefly some of the other supporting information that is typically used in determining the annual gold production and Hg use. In Burkina Faso, ASGM miners typically operate in five- to ten-person partnerships comprising diggers, haulers, crushers, millers, and amalgamators. Women also work in groups, but typically only haul, crush and process tailings. Relatively small amounts of Hg are used (1.3 units Hg for 1 unit gold). Awareness of the dangers of Hg is low and so health impacts are not minimized. Ore grades are high (often 10–50 g/t) but traditional mining is inefficient (15–50% recovery). On average, miners yield half a gram per day for about 270 days per year, equating to about 135 g/miner/y. They receive 70–80% of the international price when selling to the local buyer who has a relationship to the land holder of the site. Using 80% of a gold price of USD 1300/oz (USD 42/g), each miner makes about USD 4500/y. This income is expended on processing (milling and Hg), food, shelter, transport, and remittances to family, including off-site family.

This example estimate for Burkina Faso illustrates some useful points for emissions estimations in general. A 2005 emission estimate for Burkina Faso was about 3 t Hg/y based

---

[3] For further example calculations, see O'Neil and Telmer (2017).

on MMSD (Mining, Minerals and Sustainable Development) work in 2001. The current estimate of 32.5 t Hg/y represents a ten-fold increase. This increase is almost certainly not a result of increased use or more ASGM, but rather of better information drawn from purpose-specific studies. This example suggests that other countries with weak information on ASGM that are currently categorized as Class 1 (presence/absence with no quantitative data and assigned a conservative minimum Hg use of 0.3 t/y) are likely to report higher Hg use in the future as better data become available through better inventory work.

In conclusion, robust estimates of Hg emissions from ASGM remain sparse and the global estimate needs significant further work. The current estimate of roughly 1700 t total Hg use per year ±50% remains a conservative minimum by assigning small numbers and large errors to countries where little information exists. The estimate has risen since the 2010 estimate primarily due to improved information rather than increased use, although there have probably also been increased levels of ASGM activity as the global population grows. The price of gold remains high, and ASGM remains an important source of income for the rural poor. The estimation of Hg use in ASGM requires trained experts that can reliably assess the informal gold economy and its Hg use, as well as reliably upscale field observations to national levels. Aside from technical geo-scientific expertise, this frequently requires establishing adequate relationships with the many stakeholders. Significant knowledge gaps about Hg use in ASGM remain and the global community must continue to fill the gaps in order to reliably measure the rate of success of the Minamata Convention.

A3.3 Wastes associated with mercury-added products

A3.3.1 Description of methodology

Estimates of mercury (Hg) emission to air from Hg-added products (see text on sectors/activities below) are calculated using a slightly different but comparable methodology to that applied to calculate emissions from unintentional emission sectors (see this E-Annex, Section A3.1). Use is made of available data on regional patterns of consumption of Hg and Hg-containing products, since national consumption data are unavailable in most cases. Mercury releases at various points in the life-cycle of these products are calculated using assumptions regarding rates of breakage, waste handling, and factors for emissions to air, etc.

The method applied is the same as in the 2010 inventory (AMAP/UNEP, 2013) and a variation on the method used in the 2005 inventory (AMAP/UNEP, 2008) where product-related Hg emissions were estimated for 11 world regions. The methodology allows for a consistent and transparent treatment and calculation of product-related Hg emissions for each individual country, also taking country-specific information into account, where available. The method is illustrated schematically in Figure A3.3.1.

The input data comprise estimated Hg consumption in one year (2015) covering the product groups: batteries, measuring and control devices, lamps, electrical and electronic devices, and other use (Table A3.3.1).

Consumption is estimated for each product group for 11 world regions; East and Southeast Asia, South Asia, European Union, CIS and other European countries, Middle Eastern States, North Africa, Sub-Saharan Africa, North America, Central America and the Caribbean, South America, Australia New Zealand and Oceania. Consumption in this context refers

to the region where the product is used and thus subsequently ends up in the waste stream, and not the region where it was produced.

To estimate consumption in each country of the world, the consumption figures (for batteries, measuring and control devices, lamps, electrical and electronic devices and other uses – see Table A3.3.1) as developed by the UN Environment (2017a) for each region were distributed among the countries in that region based on gross domestic product (GDP) at purchasing power parity (PPP). GDP-PPP data for individual countries were obtained from the data catalog at the World Bank (World Bank, 2016, 2017) and where countries were not available in the list from the World Bank, from the World Factbook by the U.S. Central Intelligence Agency (CIA, 2016, 2017). In the model the estimated amount of Hg in products consumed in a country is distributed to three initial pathways (Figure A3.3.1) using distribution factors. The main initial paths of the products containing Hg are collection for safe storage (no emissions assumed), breakage and release of Hg during use, and paths to the waste stream (with further differentiation of waste pathways). In the inventory for 2010 there was an additional pathway for products remaining 'in use' in society. This pathway, amounting to 30% of Hg consumed, did not contribute any emissions in those calculations since emissions were considered to be delayed. That way of thinking is more in line with reality, but only takes 70% of the Hg contained in products into account. To simulate emissions to air from one year's consumption of Hg, this pathway was removed in the 2015 inventory. It should be noted that only one years' consumption is taken into account, while any Hg emissions from stocks remaining in society from consumption of Hg-added products in previous years are not included in the estimates. This remaining Hg will be distributed
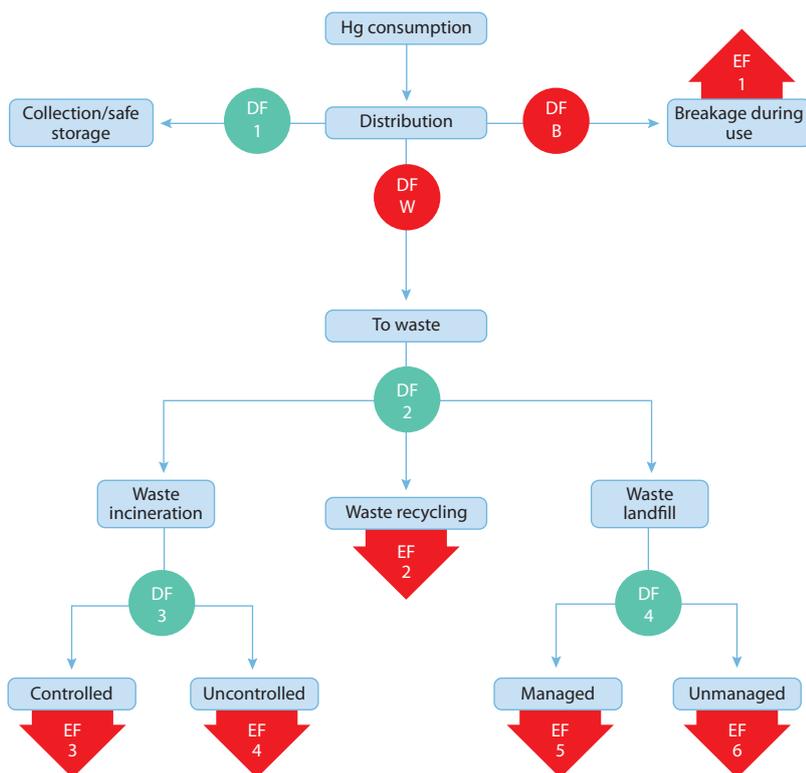
Figure A3.3.1 Schematic representation of the model used to estimate Hg emissions from waste streams associated with Hg-added products.

Table A3.3.1 Estimated Hg consumption[a] by world region and product group, 2015 (UN Environment, 2017a).

	Average, t						
	Batteries	Measuring and control devices	Lamps	Electrical and electronic devices	Other use[b]	Dental applications[c]	Sum
East and Southeast Asia	95	208	69	52	62	52	538
South Asia	33	39	12	12	59	72	227
European Union (28 countries)	8	3	13	1	84	56	165
CIS and other European countries	13	12	7	7	37	19	95
Middle Eastern States	13	18	7	9	9	13	69
North Africa	8	6	4	2	5	4	29
Sub-Saharan Africa	24	11	5	19	15	7	81
North America	9	2	8	19	61	32	131
Central America and the Caribbean	9	9	4	6	8	6	42
South America	18	20	9	8	13	12	80
Australia New Zealand and Oceania	1	1	3	13	1	3	22
Total	231	330	142	147	354	274	1478

	Minimum–Maximum, t						
	Batteries	Measuring and control devices	Lamps	Electrical and electronic devices	Other use[b]	Dental applications[c]	Sum
East and Southeast Asia	72–119	177–239	55–83	42–62	44–81	47–57	437–641
South Asia	23–43	32–47	10–14	10–14	30–89	61–83	166–290
European Union (28 countries)	6–9	2–3	11–15	0–1	59–110	44–67	122–205
CIS and other European countries	9–17	9–16	5–10	5–10	19–56	13–24	60–133
Middle Eastern States	9–17	13–24	5–9	6–11	4–13	10–16	47–90
North Africa	5–10	4–8	3–5	2–3	3–8	3–5	20–39
Sub-Saharan Africa	7–40	8–14	4–7	9–28	4–25	5–9	37–123
North America	7–10	2–2	7–9	16–21	42–79	27–37	101–158
Central America and the Caribbean	6–12	8–11	4–5	4–8	4–12	5–7	31–55
South America	13–	14–25	6–12	5–10	7–20	8–15	53–105
Australia New Zealand and Oceania	1–1	1–1	2–4	9–17	0–1	3–4	16–28
Total	159–304	267–392	112–173	109–185	215–492	226–322	1090–1867

[a] 'Consumption' is defined in terms of the end-use of Hg-added products (i.e., place of consumption), as opposed to regional 'demand' for Hg; tabulated values are means of wider ranges of estimates representing various levels of uncertainty (see source report); [b] the 'other use' category includes, for example, pesticides, fungicides, laboratory chemicals, chemical intermediates, pharmaceuticals, preservative in paints, traditional medicines, cultural and ritual uses, cosmetics – especially skin-lightening creams, etc.; [c] consumption in dental applications is not included in the calculations described in this section; the methodology employed to calculate emissions from dental amalgam use associated with human cremation are described in E-Annex 3, Section A3.4.

to one of the endpoints as the product reaches its end of life. This also implies that trends in consumption in recent years, and similar delayed trends in disposed Hg amounts, are not captured in the method used.

The share of Hg in products entering the waste stream is distributed between waste recycling, waste incineration and waste landfill. The amounts of Hg going to waste incineration and waste landfill are further distributed between two types of waste management: controlled incineration and uncontrolled waste burning, and managed and unmanaged waste landfill. Controlled incineration in this context represents waste incineration with efficient air pollution abatement installed. Uncontrolled waste burning includes, for example, open burning with no or poor abatement of air emissions. Managed landfill implies relatively low expected emissions of Hg. Unmanaged landfills (or waste dumps) are landfills such as those where a higher frequency of unintentional fires could be expected, resulting in higher Hg emissions to air.

To take into account varying waste management practices, five different 'profiles' of distribution factors and emissions factors were assumed. Each country has been assigned one of these five generic profiles based on assumptions (and available information) regarding national/regional waste handling practices, including discussions with regional representatives (see Section 3.2.1.2 and this E-Annex, Section A3.9). Four profiles were included in the inventory for 2010, while a fifth, representing least developed waste handling technologies was added in the 2015 inventory. Profile 1 represents the most technically advanced waste management practices while Profile 5 represents the least advanced.

In the model, several assumptions regarding distribution factors and emission factors have been made. Discussions have been held with representatives from all of the world's regions and assumptions have been adjusted accordingly. Rough generalizations are more or less inevitable, however, in order to achieve harmonized and transparent calculations for all individual countries, since country-specific information in most cases is still scarce or non-existent.

The initial distribution factors determine the amount distributed to the waste stream. Table A3.3.2 presents the general distribution factors used for the five profiles. The distribution for breakage and release during use is the same for all profiles, while the share collected for safe storage varies.

Table A3.3.2 Initial distribution factors for Hg-containing products.

Profile	Collection for safe storage, %	Breakage during use, %	To the waste stream, %	Total, %
1	15	3.5	81.5	100
2	5	3.5	91.5	100
3	1	3.5	95.5	100
4	1	3.5	95.5	100
5	1	3.5	95.5	100

The waste stream distribution pathways, given as distribution factors, are presented in Table A3.3.3. There are different assumptions regarding the share of Hg contained in products which is recycled, as well as on the shares going to waste incineration and landfill. For Profiles 3 and 4 the distributions between recycling, incineration and landfill are the same. A differentiation is introduced in the specific distribution factors for the share of the incinerated and landfilled waste that is treated under controlled/managed or uncontrolled/unmanaged conditions.

At this stage in the model calculations, the initial amount of Hg in products in a specific country has been distributed to all endpoints in the model (Figure A3.3.1) where emissions to air

Table A3.3.3 Waste distribution factors and specific distribution factors for controlled/uncontrolled waste incineration and managed/unmanaged waste landfill.

Waste distribution pathways			
Profile	Waste recycling, %	Waste incineration, %	Waste landfill, %
1	17	18	65
2	4	12	84
3	2	5	93
4	2	5	93
5	2	5	93

Specific distribution factors for incineration and landfill				
		Incineration		Landfill
Profile		Controlled, %	Uncontrolled burning, %	Managed, %	Unmanaged, %
1		100	0	60	40
2		40	60	30	70
3		20	80	30	70
4		15	85	10	90
5		1	99	1	99

Table A3.3.4 Emission factors (fraction emitted) applied to distributed amounts of Hg in products.

Profile	Breakage/release during use	Waste recycling	Waste incineration, controlled	Waste incineration, uncontrolled	Landfill, managed	Landfill, unmanaged
1	0.1	0.03	0.1	0.9	0.05	0.07
2	0.1	0.03	0.1	0.9	0.05	0.14
3	0.1	0.03	0.1	0.9	0.05	0.14
4	0.1	0.03	0.1	0.9	0.05	0.23
5	0.1	0.03	0.1	0.9	0.05	0.23

can occur. Emissions are calculated by applying emission factors (EFs) according to Table A3.3.4 to the distributed individual amounts of Hg. For all endpoints, except for unmanaged landfill, the EFs are the same for all assigned generic profiles of waste management. The expected releases of Hg from unmanaged landfills are highly dependent on the frequency and duration of landfill fires. The more landfills under fire, the more Hg will be released. Rough assumptions and simplifications, largely based on Maxson (2009) and Wiedinmyer et al. (2014), have been applied for developing profile EFs for unmanaged landfills, taking landfill fires into account.

It should be noted that where relevant national information was available, factors applied to specific countries were adjusted accordingly, such was the case for the distribution factors applied in the case of Japan, Republic of Korea, China, Egypt, Tunisia and for countries in South America.

In the 2015 inventory, emissions using the above methodology are quantified under two main categories: emissions associated with controlled incineration (WI) and all other (waste) components (WASOTH). The WI component is assumed to be associated with incineration at (large incineration) facilities with applied air pollution control technology. The amount of Hg calculated as emitted from waste incineration in this exercise only includes the Hg-added product groups concerned in Section A3.3 (i.e. excluding dental). Additional emissions of Hg could arise from incineration of other types of Hg-containing waste, such as sewage sludge and industrial wastes.

A3.3.2 Example calculation

This example shows the calculation scheme applied to estimate product waste emissions for Mexico. Mexico belongs to the Central America and the Caribbean region, which has an estimated consumption of Hg in intentional use products (batteries, measuring control devices/lighting, electronic devices and other – with dental uses excluded) of 36 t (see Table A3.3.1). Based on GDP-PPP, 25.1 t of this Hg consumption is attributed to Mexico.

Under the regionalization approach described in Section 3.2.1.2, it is concluded that Mexico's general waste stream characterization and waste management practices are best described by Profile 3 (see Tables A3.3.2 to A3.3.4). Figure A3.3.2 illustrates how, on this basis, Hg emission estimates to air totaling about 3.5 t are calculated; of which about 0.024 t are estimated to be emitted from controlled waste incineration.
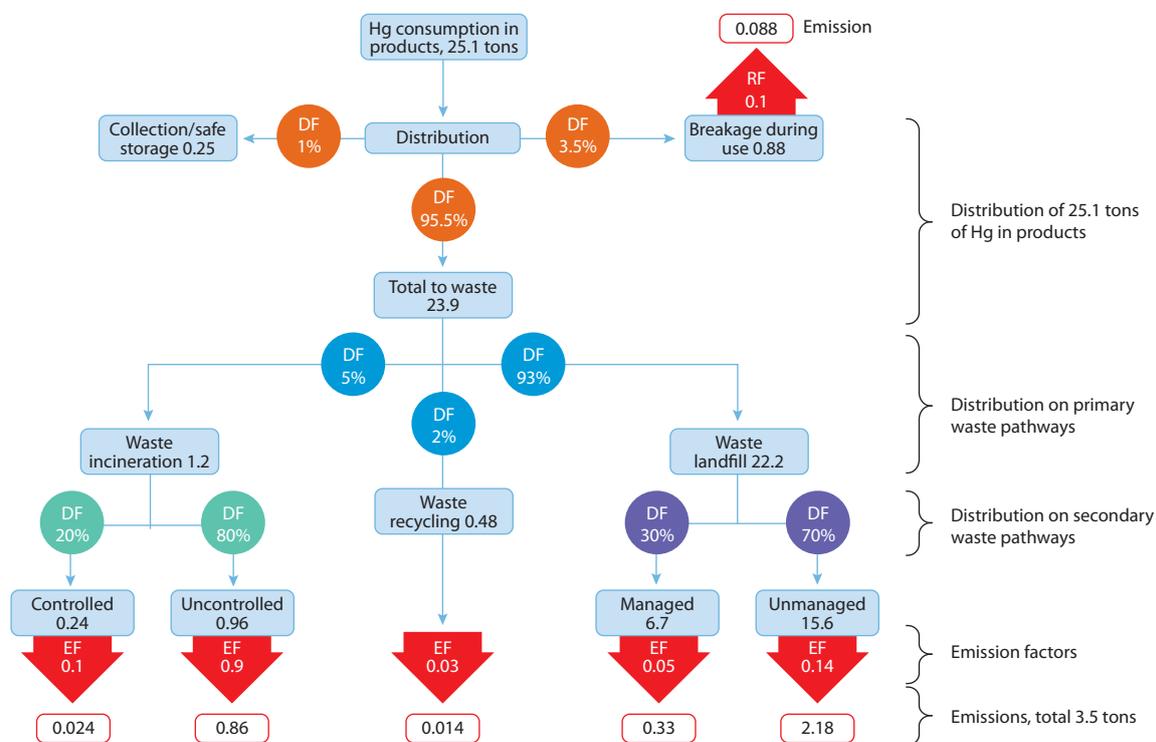
Figure A3.3.2 Example calculation of Hg emissions from waste streams associated with Hg-added products. The example is for Mexico.

A3.4 Dental amalgam and human cremation

Emissions from use of mercury (Hg) in dental amalgam fillings can occur during the preparation of the amalgams and their subsequent removal and disposal in wastes. Emissions can also occur when human remains with amalgam fillings are cremated.

Emissions associated with cremation sources were estimated using a similar approach to that employed for estimating emissions associated with other intentional-use sectors. That is to say, Hg consumption in dentistry (see this E-Annex, Section A3.3, Table A3.3.1) was combined with assumptions regarding its use and fate. Dental amalgam fillings comprise an alloy with a Hg content of about 50% by weight. Emissions were calculated based on an emission factor of 0.04 g per g Hg consumption – derived using the UNEP Toolkit default factor of 2.5 g per cremation (UNEP, 2011b) and an average per capita (dental) consumption based on the European average, which may result in an overestimation of emissions for countries where the average number of amalgams per person is lower than the European average.

Mercury amounts associated with fillings in cremated human remains were allocated to countries based on regional consumption statistics and population distributions, also taking into account factors such as religious practices and regulations in some countries concerning human cremation. It is recognized that the approach does not account for the time lag between the placing of dental fillings and the death of individuals with Hg amalgam fillings, or the changes in regional patterns that have occurred over recent decades. In some regions (such as Scandinavian countries) cremation emissions are associated with dental use of Hg that was common in past decades but is now being phased-out; in other (developing) regions increased access to health care and the relatively low cost of amalgam fillings compared with Hg-free alternatives means that Hg fillings introduced now are likely to result in emissions from cremation several decades from now.

Some countries in the EU28 region and Asia (Japan, Republic of Korea) have informed that air pollution control devices (including activated carbon systems) are increasingly being introduced at crematoria. At present the degree of implementation and effectiveness of these controls are not well documented and therefore estimated emissions do not yet take account of these developments.

A significant amount of the amalgam prepared when placing a filling remains unused and enters the waste stream (recycled, going to solid waste, or wastewater). It has been estimated that 30–40% of the amalgam material prepared for a filling typically ends up as waste (EEB, 2007; UNEP, 2015). Emissions to air associated with the preparation of dental amalgam and subsequent loss and disposal of unused amalgam are not included in emissions calculated for crematoria.

A3.5 Methodology update: principal changes in methodologies applied to specific sectors

A3.5.1 Methodology update: Stationary combustion – coal burning

The methods are essentially the same as those applied in the GMA2013 (AMAP/UNEP, 2013).

For stationary combustion of coal in power plants (SC-PP-coal) and industry (SC-IND-coal) technology profiles for several countries have been updated. The updates are based on new information concerning the application of advanced air pollution control devices in some countries, and better information regarding their effectiveness at reducing emissions of mercury (Hg) to the atmosphere.

For hard coal (HC) and brown coal (BC) combustion, activity data for coal used in industry are now separated between cement (-CEM), iron and steel (-PIP), non-ferrous metal (-NFM), and other industrial uses (-OTH). This allows attribution of industrial coal burning emissions to specific industrial sectors. Unabated emission factors (UEFs) applied are equivalent to those defined for the IND-coal activities in the GMA2013. For more details see this E-Annex, Section A3.6.

A3.5.2 Methodology: Stationary combustion – biomass burning

Mercury is a trace contaminant present in varying concentrations in biomass fuel. Mercury emissions to air arise when biomass is combusted in power plants, in industry and in domestic/residential use. This source was not addressed in the 2010 global emission inventory.

Emission estimates for 2015 have been developed following the general inventory methodology and using activity data from the International Energy Agency (IEA) on amounts of biomass combusted as fuel in power plants, industry, and domestic/residential use. IEA data only cover solid biomass used as fuel for energy production, therefore the 2015 emission estimates presented do not include wildfires (a natural source) or agricultural burning, the latter an anthropogenic (or at least anthropogenically enhanced) source that can be a significant activity in some countries. Emission factors were derived using the heat value for air dried wood of 16 MJ/kg (OECD/IEA, 2005) and literature discussing the Hg content of biomass. Detailed information on the factors used in estimating emissions from biomass burning is presented in this E-Annex, Section A3.6.

A3.5.3 Methodology update: Cement production

Mercury emissions associated with cement production originate from the use of Hg-containing fuels (including conventional, mainly fossil fuels and co-incinerated wastes) and raw materials (limestone, iron oxides, fly ash, clay, silica). The majority of the emissions occur during clinker production (calcination) in high temperature kilns – they include contributions from both fuels and raw materials (further mixed and going through the same flue gas cleaning equipment). Emissions can also occur during drying and preheating processes, but are assumed to be much lower than from calcination. Very small amounts of Hg are bound in the clinker itself, therefore subsequent stages of cement production (blending clinker with other materials, such as gypsum to form cement) are assumed to be a negligible source of Hg emission (UNEP, 2015).

The main conventional fuels used in the cement industry are coal and petroleum coke. Allocation of Hg emissions from these fuels in emission inventories and studies can vary – they are often aggregated with other fossil fuel combustion or included in the emission factors for cement production. For example, coal combustion in the cement industry was included under the category 'stationary combustion of fuel in industry' in the 2010 inventory.

A new development in the methodology applied to prepare the 2015 inventory estimates is the way in which emissions associated with fuels and raw materials used in the cement industry are derived. In the 2015 global inventory (i.e., the work reported here), emissions associated with (conventional) fuel combustion in the cement sector are now allocated to new (sub-)activities under the sectors concerned with stationary combustion of coal, and in the case of petroleum coke a sub-activity under cement itself. This E-annex to Chapter 3 of the report therefore separately presents information on emission factors, activity data and Hg emissions for coal and petroleum coke combusted in the cement industry. This modification to the methodology also allows separate assignment of technology profiles for this sector and enables comparison of emission estimates and emission factors with data sources where emission contributions from fuels and raw materials are separated. For certain data sources (e.g., stack measurements results) a comparison would not be that straightforward, although still possible to make – by first applying assumptions on amounts of fuel per tonne produced clinker/cement, and then summarizing fuel-related and raw material-related emission inputs.

These changes have been implemented to allow better attribution of emissions between contributions from fuel and cement raw materials. This is done for all fuels, except co-incinerated waste. The contribution from alternative fuels (mainly comprising waste) varies considerably between countries and is considered in the emission factors applied in the current inventory (see this E-Annex, Section A3.6).

Key modifications to cement sector emission factors and technology profiles

The methodology used to estimate cement sector emissions is similar to that applied in the GMA2013, but with the following changes:

- Unabated emission factors (UEFs) are first calculated per tonne clinker and then adjusted with respect to country- or region-specific clinker/cement ratios.

- Conventional fuels (mainly petroleum coke and coal) are allocated to separate (sub-) sectors and not included in the emission factors for cement production. Region-specific default UEFs are developed for all countries based on data on clinker/cement ratios, energy demand and co-incineration

of waste as alternative fuel obtained from the GNR database (GNR, 2014). This means that a global-average default UEF is no longer applied for cement emission calculations, only country-specific or region-specific UEFs.

- Values of Hg content in raw materials and co-incinerated waste are adjusted in accordance with data presented in recent articles and reports and provided by national experts. The default Hg content of total raw mix is estimated assuming variable additions of Hg-rich materials such as fly ash and iron oxides and is thus higher than the Hg content of limestone alone.

- A distribution factor to air of 0.95 is used (as opposed to a value of 0.8 based on the default UNEP 2011 value that was applied in the 2010 global inventory calculations). This revision is based on information in UNEP (2016) and Wang et al. (2014a) indicating that only about 1–5% of the total Hg input is bound in clinker.

- All technology profiles associated with the cement sector (cement production and related fuel combustion) have been harmonized because process-related emissions (originating in raw materials) and energy-related emissions (originating in fuels) are usually treated in the same abatement system at cement facilities.

For further details see this E-Annex, Section A3.6.

A3.5.4 Methodology update: Primary iron and steel production

Primary pig iron and steel is typically produced at integrated facilities where raw materials (iron ore, limestone, lime, dolomite, metal scrap) undergo several processes. Emissions originate from Hg in these raw materials and fuels used (mainly coal/coke). Virtually all Hg emissions occur during thermal processes – sintering/pelletizing, pig iron production in blast furnaces, and steel-making in basic oxygen furnaces (UNEP, 2015).

Key modifications to pig iron and steel sector emission factors and technology profiles

The methodology used to estimate pig iron and steel sector emissions is similar to that applied in the GMA2013, but with the following changes:

- The steel-making stage in basic oxygen furnaces is included

- The Hg input from dolomite is included

- Values of Hg content in raw materials are adjusted with respect to data presented in recent articles and reports and provided by national experts.

Combustion of coal and other fuels in the production of pig iron and steel is now identified as a separate (sub-) activity under 'industrial stationary combustion emissions'. For further details see this E-Annex, Section A3.6.

A3.5.5 Methodology: Secondary steel production

Most secondary steel production is based on an electric arc furnace (EAF) process using steel scrap as the input material. Mercury may be present as a contaminant in the scrap steel, in amounts that are highly variable depending on the type of scrap. In some countries, Hg-containing scrap may be sorted and removed before the scrap enters the EAF. Mercury contained in scrap that is not removed in this way is released during the EAF smelting process. This source was not addressed in the 2010 global emission inventory.

Emission estimates for 2015 have been developed following the general inventory methodology using activity data on annual steel production by EAF from the World Steel Association. Default UEFs were derived from Roseborough and Linbad (2008), Kim et al. (2010a), Ocio et al. (2012), Burger Chakraborty et al. (2013), Remus et al. (2013) and Wang et al. (2016d) and a default technology profile was developed based mainly on national information by Kim et al. (2010a) and Roseborough and Lindblad (2008). For further details see this E-Annex, Section A3.6.

A3.5.6 Methodology update: Primary production of non-ferrous metals (copper, lead and zinc)

Primary production of the non-ferrous metals copper, lead and zinc is a significant source of Hg emissions and releases, originating from raw materials (metal ores) and fuels used in the process. Metal ores are mined and concentrated; concentrates are further pre-treated, roasted, smelted and refined. Most of the Hg present in metal concentrates evaporates during high-temperature roasting (or sintering) and smelting stages (UN Environment, 2017b). Releases from ore mining operations are not included in the scope of this inventory.

Most large smelters include acid plants that remove a substantial proportion of the Hg emitted from the off-gas during the smelting stage. This Hg is either treated as waste, sold as a commodity (if removed prior to acid production) or contained in the acid (UNEP, 2016). In the latter case, some of the Hg may subsequently be emitted during the use of the acid. Acid plants are considered a form of (air) pollution control device in the applied methodology.

Key modifications to primary non-ferrous (copper, lead, zinc) sector emission factors and technology profiles

The methodology used to estimate Hg emissions from the (copper, lead, zinc) non-ferrous metals sector is similar to that applied in the GMA2013, but with the following changes:

- Concentrate/metal ratios and values of Hg content in concentrates have been adjusted to reflect new information and data presented in recent articles and reports and provided by national experts. Assumptions concerning the metal content of concentrates are also revised based on concentrate/metal ratios provided in recent literature.

- A distribution factor to air of 1 was applied in the 2010 global inventory based on the default UNEP Toolkit value (UNEP, 2011). This value has now been adjusted to take account of information by Hui et al. (2017) indicating that about 3–10% of the total Hg input is bound in smelting slag. The proportion of Hg bound in smelting slag is assumed to be 0.9 for zinc (a weighted average over two main production processes, assuming that the hydrometallurgical process is used more widely than the pyrometallurgical process), 0.96 for copper and 0.97 for lead.

- Default technology profiles of country groups 1 and 2 are revised and imply higher abatement levels in the current inventory than in 2010.

- 'and other fuels' in production of non-ferrous metals is now identified as a separate (sub-) activity under 'industrial stationary combustion emissions'.

For further details see this E-Annex, Section A3.6.

A3.5.7 Methodology update: Primary production of non-ferrous metals – aluminum

The methodology used to estimate NFM-aluminum production sector emissions is similar to that applied in the GMA2013, but with a small adjustment to the applied bauxite/alumina ratio based on BREF data (JRC, 2014). For a group of countries producing alumina for export only, a new emission factor has been developed, see details this E-Annex, Section A3.6.

A3.5.8 Methodology update: Primary production of non-ferrous metals – large-scale gold production

The methodology used to estimate NFM-large-scale gold production sector emissions is similar to that applied in the GMA2013; however, the default technology profile for Group 1 countries has been revised and implies higher abatement levels in the current inventory than in the 2010 inventory. See this E-Annex, Section A3.6.

Activity data on large-scale gold production from the United States Geological Survey includes a number of footnotes concerning difficulties distinguishing artisanal and small-scale gold mining (ASGM) and large-scale gold production in some countries. Where possible, these footnotes have been considered in the light of other published information and or discussions with national experts to correctly characterize gold production; however, the possibility that (some) ASGM produced gold is included in activity data for large-scale gold production remains for some countries.

A3.5.9 Methodology update: Oil refining

The methodology used to estimate emissions from oil refineries is similar to that applied in the GMA2013; with some minor adjustments to the assumptions (weighting) applied when calculating the Hg content of oils refined in different countries. These adjustments result in a small decrease in total emissions from this sector if 2010 calculations are repeated, but may significantly influence estimates for individual countries. Industry sources have delivered some new information on the Hg content of oil from different regions (IPIECA, 2012), but for reasons of commercial confidentiality they are unable to specify the exact sources of these oils (i.e., the countries/fields of origin). Lack of detailed information on the Hg-content of refined oils therefore remains a limitation in estimating emissions and releases from oil refineries at a national level. Other knowledge gaps include information to resolve different assumptions regarding the fate of Hg emitted/released during refinery operations (see Section 3.4.3.8). See also this E-Annex, Section A3.6.

A3.5.10 Methodology: Vinyl chloride monomer production with mercury-dichloride (HgCl$_2$) as catalyst

Two processes are used in the manufacture of vinyl chloride monomer (VCM): the acetylene process that uses mercuric chloride on carbon pellets as a catalyst, and a process based on the oxychlorination of ethylene that does not use Hg. Production of VCM with Hg-containing catalyst occurs only in a few countries (China, India, Russian Federation). Mercury can be emitted during the production of VCM but a large proportion of the Hg remains in the used catalyst. Recycling of used catalyst is, however, an additional substantial source of Hg emissions. The 2015 estimates of Hg emissions to air from VCM production and from recycling of Hg-containing catalyst are based on national information, in combination with literature information. For further information see this E-Annex, Section A3.6.

This source was not addressed in the 2010 global emission inventory.

A3.5.11 Methodology update: Waste and waste incineration

Mercury emissions from waste originating from Hg-added products (lamps, batteries, measuring and control devices, electric and electronic devices, and other applications) have been estimated based on assumptions regarding their entry into different waste streams. The majority of wastes associated with Hg-added products end up in landfill or are incinerated or burnt. Mercury 'consumption' in these Hg-added products is defined in terms of final regional consumption of Hg products to reflect that, for example, although most measuring and control devices are produced in China, many of them are exported, 'consumed' and disposed of in other countries (UN Environment, 2017a).

It is important to recognize that estimates for Hg emitted from the waste sector do not currently include emissions due to incineration of industrial waste and sewage sludge, or (in most cases) hazardous waste. This is because it is not currently possible to obtain reliable information on the amounts of such wastes incinerated, and more importantly the Hg content of such wastes, which can be highly variable. This subject is further discussed below in relation to national comparisons, Section 3.3.3.

Key modifications to (mercury-added product) waste and waste incineration sector emission factors and technology profiles

The basic methodology applied to estimate Hg emissions from waste originating from Hg-added products is the same as that applied for the 2010 inventory, but with the following changes:

- In the 2010 global inventory (i.e., GMA2013) about 30% of the Hg was assumed to remain in products in society and not be emitted until later. In the 2015 global inventory this component is set to zero, to (some extent) take account of the continuous release of materials in societal use. Consequently, all Hg consumed in one year (2015) is now distributed on pathways of safe storage, breakage or flow into the waste stream.

- Mercury consumed in Hg-added products is distributed on different pathways using distribution factors with emission factors applied to estimate emissions; some distribution factors have been revised based on information from national experts.

- A new technology group was added, covering the least developed level of technology for waste handling. Most countries in Sub-Saharan Africa were assigned to this technology level based on information from experts responsible for coordinating regional Minamata Initial Assessments (MIAs); some additional reclassifications of countries between technology groups, relative to assignments used in the 2010 global inventory, were also applied.

For further details see this E-Annex, Section A3.3.

A3.5.12 Methodology update: Crematoria emissions

Methods employed were essentially identical to those applied in the GMA 2013. Updated information on regional Hg consumption in dental uses in 2015 was obtained from UN Environment (2017a) and, where available, cremation statistics were updated based on national information and data from the Cremation Society of Great Britain (CSGB, 2017). The methodology is considered sub-optimal in that it does not take account of, for example, the relationship between time of application of amalgam fillings and life-expectancy, and other factors that will determine cremation emissions following use of Hg in dental amalgam. However, it does provide a first-level estimate of emissions from this use of Hg that can be compared with other such estimates (e.g., those derived in national inventories or MIAs, see Section 3.3.3). See also this E-Annex, Section A3.4.

A3.5.13 Methodology update: Artisanal and small-scale gold production

The information base that underpins the assumptions applied regarding use of Hg in ASGM has been significantly updated and improved for several countries. Improved knowledge has also resulted in an adjustment to the factors applied in assigning ASGM emissions associated with the use of whole ore amalgamation and concentrate amalgamation. One result is a small decrease in the estimate of emissions to air per unit Hg consumed in ASGM that is reflected in both retrospectively updated (national) estimates for 2010, as well as for 2015. See Section 3.4 and this E-Annex, Section A3.2.

A3.6 Emission factors and technology profiles used in the calculation of Hg emission estimates

During the compilation of country-specific unabated emission factors (UEFs), an effort was made to use as much national data as possible.

In many of the literature sources, only abated country-specific EFs were reported, often with no specification on the abatement technologies and their implementation rates. Considering the methodology used in the current inventory, these abated emission factors (AEFs) were not directly applicable in the calculations. They were, however, used as benchmarks when calculating country-specific UEFs and generic UEFs. Where possible, information relating to abatement technologies was extracted and used in developing technology profiles.

The default technology profiles reflect assumptions based on available national information for countries in the respective groups regarding mercury (Hg) reduction efficiencies associated with typically employed air pollution control device (APCD) configurations and their degree of application (including the application of integrated acid plants in the case of copper, lead and zinc smelters). In particular, use was made of available information from European countries, the Republic of Korea, Japan and the USA (Group 1); Australia and China (for coal burning in power plants) (Group 2); South Africa and China (Group 3); Russia (Group 4); and India (Group 5). These profiles represent a starting point for further refinement as additional (national) information becomes available.

Section A3.6 provides detailed information for the following sectors:

A3.6.1 Coal combustion, hard coal (anthracite and bituminous coal)

A3.6.2 Coal combustion, brown coal (sub-bituminous coal and lignite)

A3.6.3 Oil combustion

A3.6.4 Natural gas combustion

A3.6.5 Biomass combustion

A3.6.6 Pig iron and steel production

A3.6.7 Secondary steel production (electric arc furnace, EAF)

A3.6.8 Non-ferrous metal production: copper (Cu)

A3.6.9 Non-ferrous metal production: lead (Pb)

A3.6.10 Non-ferrous metal production: zinc (Zn)

A3.6.11 Non-ferrous metal production: mercury (Hg) dedicated production from cinnabar ore

A3.6.12 Non-ferrous metal production: aluminum (Al) and alumina production from bauxite ore

A3.6.13 Large-scale gold production

A3.6.14 Cement production

A3.6.14a Fossil fuel combustion in cement production

A3.6.15 Oil refining

A3.6.16 Chlor-alkali industry

A3.6.17 Vinyl chloride monomer (VCM) production and recycling of mercury catalyst

A3.6.1 Coal combustion, hard coal (anthracite and bituminous coal)

Basis for 2015 emission estimates: UEFs and technology employed to reduce emissions from this sector, applied to activity data concerning combustion of hard coal (anthracite and bituminous coals).

Applied UEFs: These are shown in Table A3.6.1.

Comparative EFs: These are shown in Table A3.6.2.

Discussion of EFs: The generic default UEFs derived in this work are the result of expert evaluation and are intended to represent a reasonable general default factor, based on consideration of a wide range of literature, including the UNEP Toolkit (UNEP, 2011b; UN Environment, 2017b), Paragraph-29 (UNEP, 2010a) study data, recent UNEP reports on coal combustion in power plants in China, Russia and India, peer-reviewed journal articles and other literature, including country-specific data and national reports.

Basic assumptions during calculations of UEF: For hard coal combustion, the UEFs represent the Hg content of coal, which is generally reported on a dry weight basis.

Applied technology profile: This is shown in Table A3.6.3. Hg-specific abatement could, for example, be activated carbon injection, and/or additives to remove Hg.

Discussion of technology profile: In addition to discussions with representatives from different countries, the following references were important sources of information when deriving the technology profiles used in this work: EC (2006), Srivastava et al. (2006), Nelson et al. (2009), Pudasainee et al. (2009b, 2010), Kim et al. (2010a,b), Pavlish et al. (2010), UNEP (2010b: tables 1+4, 2011c,d, 2014), UNEP/CIMFR-CSIR (2012), Garnham and Langerman (2016), Wu et al. (2016b), US EPA (NEEDS v.5.15 Database).

Comparison with UNEP Toolkit factors: The default UEF has been updated in the UNEP toolkit (UN Environment, 2017b) to correspond to the default factor of 0.15 g/t applied in this work, both in the 2010 inventory and retained in this 2015 inventory.

Comparison with 2005 inventory factors: The default factor applied when calculating emissions in 2005 (0.2 g Hg/t coal) is a global average abated factor. The default factors used in the current inventory are unabated and differentiated by coal type.

Gaps/needs to improve factors and profiles: Information base for assumptions regarding technology profiles.

Table A3.6.1 Unabated emission factors applied for coal combustion, hard coal (anthracite and bituminous coal).

	Unabated emission factor (UEF)				Source	Notes/adjustments to reported data
	Low	Intermediate	High	Units		
Generic default						
Anthracite – PP		0.15		g/t		Expert evaluation of reasonable general default factor based on the UNEP Toolkit (UNEP, 2011b), other literature, country-specific data
Bituminous – PP		0.15		g/t		
Hard coal – IND		0.15		g/t		
Hard coal – DR		0.15		g/t		
Country-specific						
Australia						
PP anthracite		0.068		g/t		P. Nelson (pers. comm.)
PP bituminous		0.068		g/t		P. Nelson (pers. comm.)
IND hard coal		0.042		g/t		
DR hard coal		0.068		g/t		
Canada						
PP bituminous		0.070		g/t	Mazzi et al. (2006: in figure 1)	Average of data in figure 1
China						
PP bituminous		0.17		g/t	Wang et al. (2012a), Zhang et al. (2015b)	
IND hard coal		0.17		g/t		
DR hard coal		0.19		g/t	Sloss (2008), UNEP (2011c)	
India						
PP bituminous		0.14		g/t	UNEP/CIMFR-CSIR (2012), UNEP (2014)	Average of coals burned in PPs in India
IND hard coal		0.292		g/t	Mukherjee et al. (2008)	
DR hard coal		0.292		g/t		
Japan						
PP bituminous		0.0454		g/t		National information
IND hard coal		0.0454		g/t		National information
DR hard coal		0.0454		g/t		
Republic of Korea						
PP anthracite		0.082		g/t	Kim et al. (2010a: table 3)	Table 3
PP bituminous		0.046		g/t	Kim et al. (2010a,b)	Mixed coals
IND hard coal		0.069		g/t	Kim et al. (2010a)	Average of 0.082 and 0.046
DR hard coal		0.046		g/t	Kim et al. (2010b)	Mixed coals
Russian Federation						
PP bituminous		0.063		g/t	UNEP (2011d)	Weighted average Hg content of coals consumed in Russia
IND hard coal		0.1		g/t		
DR hard coal		0.1		g/t		
South Africa						
PP bituminous		0.28		g/t	Garnham and Langerman (2016)	Weighted average
IND hard coal		0.28		g/t		
DR hard coal		0.28		g/t		
USA						
PP bituminous		0.1		g/t	Sloss (2008)	Srivastava et al. (2006)

Table A3.6.2 Comparative emission factors for coal combustion, hard coal (anthracite and bituminous coal).

	Emission factor (EF)				Source	Notes/adjustments to reported data
	Low	Intermediate	High	Units		
Unabated EF						
All coals	0.05	0.15	0.50	g/t	UN Environment (2017b)	UNEP Toolkit default input factor same as this work
Abated EF						
2005 inventory All coals – power plants		0.2		g/t	AMAP/UNEP (2008)	
2005 inventory All coals – residential and commercial boilers		0.3		g/t	AMAP/UNEP (2008)	

Table A3.6.3 Technology profile applied for coal combustion, hard coal (anthracite and bituminous coal).

Abbreviations. ACI: activated carbon injection; B: bag filter; CYC: cyclone; (c/w) ESP (C/H): (cold-side=dry / hot-side=wet) electrostatic precipitator; FF: fabric filter; (SDA/ w) FGD: (spray drier absorber/ wet) flue gas desulfurization; IDRD: integrated dust removal; low NO$_X$: low NO$_X$ burners; mod NO$_X$: modified combustion; PM: particulate matter control; PS: particle scrubber; SCR: selective catalytic reduction; SNCR: selective non-catalytic reduction; WET: wet scrubber; WS: wet scrubber.

Technology profile	Reduction efficiency, %			Degree of application, % Country group					Source
	Low	Intermediate	High	1	2	3	4	5	
Default									
PP anthracite									
Level 0: None		0							See Section A3.6.1
Level 1: Particulate matter simple APC: ESP/PS/CYC		25		30	65	70	100	100	
Level 2: Particulate matter (FF)		50		5	30	30			
Level 3: Efficient APC: PM+SDA/wFGD		65		20					
Level 4: Very efficient APC: PM+FGD+SCR		70		40	5				
Level 5: Mercury-specific		97		5					
PP bituminous									
Level 0: None		0							See Section A3.6.1
Level 1: Particulate matter simple APC: ESP/PS/CYC	15	25	60	30	65	70	100	100	
Level 2: Particulate matter (FF)	40	50	93	5	30	30			
Level 3: Efficient APC: PM+SDA/wFGD	35	65	99	20					
Level 4: Very efficient APC: PM+FGD+SCR	90	90	99	40	5				
Level 5: Mercury-specific	95	97	99	5					
IND hard coal									
Level 0: None		0				25	50	75	See Section A3.6.1
Level 1: Particulate matter simple APC: ESP/PS/CYC		25		25	25	50	50	25	
Level 2: Particulate matter (FF)		50		25	50	25			
Level 3: Efficient APC: PM+SDA/wFGD		50		25	25				
Level 4: Very efficient APC: PM+FGD+SCR		90		25					
Level 5: Mercury-specific		97							

Table A3.6.3 continued

Technology profile	Reduction efficiency, %			Degree of application, % Country group					Source
	Low	Intermediate	High	1	2	3	4	5	
DR hard coal									
Level 0: None		0		50	50	100	100	100	See Section A3.6.1
Level 1: Particulate matter simple APC: ESP/PS/CYC		25		50	50				
Country-specific									
Australia									
PP bituminous									
ESP		46.5			75				Nelson et al. (2009: Table 44)
FF		83.1			19				
ESP/FF		90.0			6				
Brazil									
PP coal not defined									
ESP+PS					100				This work
China and Hong Kong[a]									
PP all coals									
ESP+wFGD		60			13.9				Wu et al. (2016b)
FF+wFGD		86			0.2				
ESP-FF+wFGD		95			1.4				
SCR+ESP+wFGD		70			63.5				
SCR+FF+wFGD		88			4				
SCR+ESP+wFGD+wESP		94			2.5				
SCR+ESP-FF+wFGD		97			14.6				
IND all coals									
WET		23			47				
IDRD		38			41				
FF+(w)FGD		86			11				
ESP-FF+(w)FGD		95			1				
Europe (EU28+Norway)									
PP bituminous									
FF		40		40					EC (2006)
ESP/FF+FGD		75		30					
ESP/FF+FGD+high dust SCR		90		30					
India									
PP bituminous									
Mostly ESP (some PPs other APC and coal washing)		42						100	Average value in UNEP (2014)
Japan									
PP bituminous & IND bituminous									
APCD		72.9		100					Generic APCD for power plants and industry
Republic of Korea									
PP bituminous									
SCR+cESP+wFGD		75		100					National information

Table A3.6.3 continued

Technology profile	Reduction efficiency, %			Degree of application, % Country group					Source
	Low	Intermediate	High	1	2	3	4	5	
PP anthracite									
ESP		78		28					National information
cESP+wFGD		83		38					
SCR+cESP+wFGD		77		34					
Mexico									
PP coal not defined									
lowNO$_X$						35.6			This work
modNO$_X$						7.8			
ESP						5.2			
SCR						1.7			
Russian Federation									
PP bituminous									
Level 1: Particulate matter simple APC: ESP/PS/CYC		25					43		National information
Level 2: Particulate matter (FF)		50					53		
Level 3: Efficient APC: PM+SDA/wFGD		65					4		
IND bituminous									
Level 1: Particulate matter simple APC: ESP/PS/CYC		25					100		
South Africa									
PP coal not defined									
ESP		25				67			Garnham and Langerman (2016) (reduction efficiency generic)
FF		50				24			
ESP+FF		50				9			
Sweden									
PP bituminous									
Particulate matter (FF)		50		20					National comments
ESP/FF+FGD+high dust SCR		90		80					
USA									
PP bituminous									
No control		0		0.1					Derived from NEEDS v.5.15 Database (XLSX) Accessed 2017-03-02
ESPH		10		1.0					
ESPC		36		23.0					
ESPH+WS		42		1.4					
ESPC+WS+ SNCR (not all)		66		4.0					
ESPC+B+WS+SNCR		70		2.0					
ESPC+B		80		1.6					
B		89		2.3					
ACI+APC combination		90		58.5					
APC combinations 1		93		0.8					
APC combinations 2		95		4.6					
APC combinations 3		97		0.6					

[a] China – assigned to Group 2 for coal burning in power stations (in Group 3 for other sectors).

A3.6.2 Coal combustion, brown coal (sub-bituminous coal and lignite)

Basis for 2015 emission estimates: UEFs and technology employed to reduce emissions from this sector, applied to activity data concerning combustion of brown coal (sub-bituminous coal and lignite).

Applied UEFs: These are shown in Table A3.6.4.

Comparative EFs: These are shown in Table A3.6.5.

Discussion of EFs: The generic default UEFs are derived in this work as expert evaluation of a reasonable level of a general default factor, based on a literature survey including the UNEP Toolkit (UNEP, 2011b; UN Environment, 2017b) and other literature, including country-specific data.

During compilation of country-specific UEFs, an effort was made to use as much national data as possible. One issue that arose during this work was that some lignite and sub-bituminous coals have a very high moisture content (up to 50% in some coals burned in power plants in Australia; P. Nelson pers. comm.). If high moisture content coals are burned (without drying), then there is potential for over-estimating EFs if these are derived from coal Hg content values on a dry weight basis without adjusting for the moisture content.

Basic assumptions during calculations of UEF: For brown coal combustion, the UEFs represent the Hg content of coal as burned.

Applied technology profile: This is shown in Table A3.6.6.

Discussion of technology profile: In addition to discussions with representatives from different countries, the following references were important sources of information when deriving the technology profiles used in this work: EC (2006), Srivastava et al. (2006), Nelson et al. (2009), Pudasainee et al. (2009b, 2010), Kim et al. (2010a,b), Pavlish et al. (2010), UNEP (2010b: tables 1+4, 2011c,d), UNEP/CIMFR-CSIR (2012), US EPA (NEEDS v.5.15 Database).

Comparison with UNEP Toolkit factors: The default UEF has been updated in the UNEP toolkit (UN Environment, 2017b) to correspond to the default factors of 0.1 and 0.15 g/t applied in this work, both in the 2010 inventory and retained in this 2015 inventory.

Comparison with 2005 inventory factors: The default factor applied when calculating emissions in 2005 (0.2 g Hg/t coal) is a global average <u>abated</u> factor. The default factors used in the current inventory are <u>unabated</u> and differentiated by coal type.

Gaps/needs to improve factors and profiles: Information base for assumptions regarding technology profiles. Moisture content of lignite and sub-bituminous coals burned in different countries and the implications of high moisture content for emission factors that are normally derived from coal Hg content expressed on a dry weight basis.

Table A3.6.4 Unabated emission factors applied for coal combustion, brown coal (sub-bituminous coal and lignite).

	Unabated emission factor (UEF)				Source	Notes/adjustments to reported data
	Low	Intermediate	High	Units		
Generic default						
Sub-bituminous - PP		0.15		g/t		Expert evaluation of reasonable general default factor based on the UNEP Toolkit (UNEP, 2011b), other literature, country-specific data
Lignite – PP		0.10		g/t		
Brown coal – IND		0.15		g/t		
Brown coal – DR		0.15		g/t		
Country-specific						
Australia						
PP lignite		0.032		g/t	P. Nelson (pers. comm.)	UEF takes into account high moisture content of coal
PP sub-bituminous		0.032		g/t	P. Nelson (pers. comm.)	UEF takes into account high moisture content of coal
IND brown coal		0.068		g/t		
DR brown coal		0.032		g/t		
Canada						
PP sub-bituminous/ lignite		0.07		g/t	Mazzi et al. (2006: figure 1)	Average of data in figure 1
Germany						
PP lignite		0.063		g/t		UEF takes into account high moisture content of coal

Table A3.6.4 continued

	Unabated emission factor (UEF)				Source	Notes/adjustments to reported data
	Low	Intermediate	High	Units		
India						
PP lignite		0.140		g/t	UNEP/CIMFR-CSIR (2012)	Average of Indian coals burned in PPs
IND brown coal		0.292		g/t	Mukherjee et al. (2008)	
Mexico						
PP sub-bituminous		0.293		g/t	This work	Non-washed coal, Maíz (2008)
IND brown coal		0.293		g/t		
Russia						
PP lignite		0.063		g/t	UNEP (2011d)	Weighted average Hg content of coals consumed in Russia
IND brown coal		0.1		g/t	UNEP (2011d)	
DR brown coal		0.1		g/t	UNEP (2011d)	
USA						
PP sub-bituminous		0.055		g/t	UNEP (2010a), This work	UEF takes into account high moisture content of coal

Table A3.6.5 Comparative emission factors for coal combustion, brown coal (sub-bituminous coal and lignite).

	Emission factor (EF)				Source	Notes/adjustments to reported data
	Low	Intermediate	High	Units		
Unabated EF						
Sub-bituminous/ lignite	0.05	0.15/0.1	0.50	g/t	UN Environment (2017b)	UNEP Toolkit default input factor same as this work
Abated EF						
2005 inventory All coals – power plants		0.2			AMAP/UNEP (2008)	
2005 inventory All coals – residential and commercial boilers		0.3			AMAP/UNEP (2008)	

Table A3.6.6 Technology profile applied for coal combustion, brown coal (sub-bituminous coal and lignite).

Abbreviations. ACI: activated carbon injection; B: bag filter; CYC: cyclone; ESP(C/H): (cold-side / hot-side) electrostatic precipitator; FF: fabric filter; (SDA/ w) FGD: (spray drier absorber/ wet) flue gas desulfurization; PM: particulate matter control; PS: particle scrubber; SCR: selective catalytic reduction; SNCR: selective non-catalytic reduction; WS: wet scrubber.

Technology profile	Reduction efficiency, %			Degree of application, % Country group					Source
	Low	Intermediate	High	1	2	3	4	5	
Default									
PP sub-bituminous									
Level 0: None		0							See Section A3.6.2
Level 1: Particulate matter simple APC: ESP/PS/CYC	0	10	25	30	65	70	100	100	
Level 2: Particulate matter (FF)	20	50	85	5	30	30			
Level 3: Efficient APC: PM+SDA/wFGD	0	40	75	20					
Level 4: Very efficient APC: PM+FGD+SCR	0	25	47	40	5				
Level 5: Mercury-specific	50	75	95	5					

Table A3.6.6 continued

Technology profile	Reduction efficiency, %			Degree of application, % Country group					Source
	Low	Intermediate	High	1	2	3	4	5	
PP lignite									
Level 0: None		0							See Section A3.6.2
Level 1: Particulate matter simple APC: ESP/PS/CYC	0	2	10	30	65	70	100	100	
Level 2: Particulate matter (FF)	0	5	10	5	30	30			
Level 3: Efficient APC: PM+SDA/wFGD	0	20	55	20					
Level 4: Very efficient APC: PM+FGD+SCR	0	20	96	40	5				
Level 5: Mercury-specific	50	75	95	5					
IND brown coal									
Level 0: None		0				25	50	75	See Section A3.6.2
Level 1: Particulate matter simple APC: ESP/PS/CYC		5		25	25	50	50	25	
Level 2: Particulate matter (FF)		50		25	50	25			
Level 3: Efficient APC: PM+SDA/wFGD		30		25	25				
Level 4: Very efficient APC: PM+FGD+SCR		20		25					
Level 5: Mercury-specific		75							
DR brown coal									
Level 0: None		0		50	50	100	100	100	See Section A3.6.2
Level 1: Particulate matter simple APC: ESP/PS/CYC		5		50	50				
Country-specific									
Australia									
PP sub-bituminous									
ESP		46.5			100				Nelson et al. (2009: table 43)
Russian Federation									
PP sub-bituminous									
Level 1: Particulate matter simple APC: ESP/PS/CYC		10					43		National information
Level 2: Particulate matter (FF)		50					53		
Level 3: Efficient APC: PM+SDA/wFGD		40					4		
IND sub-bituminous									
Level 1: Particulate matter simple APC: ESP/PS/CYC		5					100		
USA									
PP sub-bituminous									
No control		0		0.04					Derived from NEEDS v.5.15 Database (XLSX) Accessed 2017-03-02
ESPC		3		21					
ESPH		6		0.1					
ESPC+WS+SCR		16		19					
ESPH+WS		20		2					
ESPC+B		25		6.5					
ESPC+		35		0.1					
B+SNCR		57		0.1					
ESPC+B+WS		70		0.6					
B		73		16					
ACI+APC		90		34					
PP lignite									
No control		0		15					
ESPC+CYC		38		0.4					
ESPC WS		44		41					
B		57		2.5					
ACI+APC comb		90		41					

A3.6.3 Oil combustion

Basis for 2015 emission estimates: UEFs and technology employed to reduce emissions from this sector, applied to activity data concerning combustion of crude oil, heavy fuel oil and light fuel oil.

Applied UEFs: These are shown in Table A3.6.7.

Comparative EFs: These are shown in Table A3.6.8.

Discussion of EFs: -

Basic assumptions during calculations of UEF: Default UEFs used in this work were based on the lower range default input factors employed in the UNEP Toolkit (UNEP, 2011b), using twice these values. This choice was based on comparison of the UNEP Toolkit defaults and available information on the Hg content of crude and refined oil.

Applied technology profile: This is shown in Table A3.6.9.

Discussion of technology profile: It was assumed that only major point sources in Group 1 to 3 countries will employ APCDs that reduce Hg emissions from oil combustion, and the reported effectiveness of such devices for reducing Hg emissions from oil combustion is generally low. For sources other than power plants and industrial facilities it was assumed that no emission abatement is applied.

Comparison with UNEP Toolkit factors: The UNEP Toolkit default input factors of 0.055 g/t for crude and heavy fuel oil and 0.006 g/t for light fuel oil are somewhat higher than the values selected for use in this work, which were based on the lower range UNEP default factors.

Comparison with 2005 inventory factors: An abated EF of 0.001 g/t was applied in the 2005 inventory calculations, comparable to that for light fuel oil burning in the 2010 inventory, but relatively low compared with the UEFs applied to crude oil and heavy fuel oil combustion in 2010.

Gaps/needs to improve factors and profiles: Information base for assumptions regarding technology profiles.

Table A3.6.7 Unabated emission factors applied for oil combustion.

	Unabated emission factor (UEF)				Source	Notes/adjustments to reported data
	Low	Intermediate	High	Units		
Generic default						
Crude oil – PP		0.01		g/t	UNEP (2011b)	Twice the UNEP Toolkit default minimum value, see discussion
Heavy fuel oil – PP		0.02		g/t		
Light fuel oil – PP		0.002		g/t		
Crude oil – IND		0.01		g/t		
Heavy fuel oil – IND		0.02		g/t		
Light fuel oil – IND		0.002		g/t		
Crude oil – DR		0.01		g/t		
Heavy fuel oil – DR		0.02		g/t		
Light fuel oil – DR		0.002		g/t		
Country-specific						
Republic of Korea						
PP crude oil		0.027		g/t	Kim et al. (2010a)	

Table A3.6.8 Comparative emission factors for oil combustion.

	Emission factor (EF)				Source	Notes/adjustments to reported data
	Low	Intermediate	High	Units		
Unabated EF						
Crude oil	0.005	0.055	0.300	g/t	UNEP (2011b)	
Heavy fuel oil	0.010	0.055	0.100			
Light fuel oil	0.001	0.006	0.010			
Abated EF						
2005 inventory		0.001			AMAP/UNEP (2008)	

Table A3.6.9 Technology profile applied for oil combustion.

Abbreviations. cESP: cold-side electrostatic precipitator; FGD: flue gas desulfurization; PM: particulate matter control

Technology profile	Reduction efficiency, %			Degree of application, % Country group					Source
	Low	Intermediate	High	1	2	3	4	5	
Default									
PP crude oil									
Level 0: None		0				50	100	100	
Level 1: PM+FGD (cESP, scrubbers+FGD)		50		100	100	50			
PP heavy fuel oil									
Level 0: None		0				50	100	100	
Level 1: PM+FGD (cESP, scrubbers+FGD)		50		100	100	50			
PP light fuel oil									
Level 0: None		0		50	50	50	100	100	
Level 1: PM+FGD (cESP, scrubbers+FGD)		50		50	50	50			
IND crude oil									
Level 0: None		0		50	50	50	100	100	
Level 1: PM (cESP, scrubbers)		10		50	50	50			
IND heavy fuel oil									
Level 0: None		0		50	50	50	100	100	
Level 1: PM (cESP, scrubbers)		10		50	50	50			
IND light fuel oil									
Level 0: None		0		50	50	50	100	100	
Level 1: PM (cESP, scrubbers)		10		50	50	50			
DR crude oil									
Level 0: None		0		100	100	100	100	100	
DR heavy fuel oil									
Level 0: None		0		100	100	100	100	100	
DR light fuel oil									
Level 0: None		0		100	100	100	100	100	

A3.6.4 Natural gas combustion

Basis for 2015 emission estimates: UEFs and technology employed to reduce emissions from this sector, applied to activity data concerning combustion of natural gas (activity data in TJ, gross calorific value).

Applied UEFs: These are shown in Table A3.6.10.

Comparative EFs: These are shown in Table A3.6.11.

Discussion of EFs: -

Basic assumptions during calculations of UEF: Calorific values of natural gas vary (e.g., North Sea natural gas 39 MJ/m³, NPL, 2012; generic value 43 MJ/m³, Engineering Toolbox, 2012); a value of 40 MJ/m³ has been assumed for the purposes of developing a UEF in this work. The UNEP Toolkit emission factors (0.2 and 100 μg/m³, for pipeline and raw/untreated gas respectively) used as a basis for suggested generic UEF values are derived based on analysis of Hg concentrations in natural gas. Emissions estimates assume combustion of pipeline/consumer gas (with low Hg content); if raw/untreated gas is burned at installations the emissions would be considerably higher (by a factor of 500).

Applied technology profile: This is shown in Table A3.6.12.

Discussion of technology profile: It was assumed that APCDs are either absent at sites where natural gas is burned, or are inefficient at reducing Hg emissions to air from this source.

Comparison with UNEP Toolkit factors: The UNEP Toolkit (UN Environment, 2017b) input factors are used as the basis for the UEFs.

Comparison with 2005 inventory factors: Emissions from natural gas combustion were not included in the 2005 inventory.

Gaps/needs to improve factors and profiles: Information base for assumptions regarding technology profiles and type of gas burned.

Table A3.6.10 Unabated emission factors applied for natural gas combustion.

	Unabated emission factor (UEF)				Source	Notes/adjustments to reported data
	Low	Intermediate	High	Units		
Generic default		0.005		g/TJ	UNEP (2011b)	Pipeline/consumer quality gas; UEF g/TJ based on UNEP (2011b) value of 0.2 μg/m³
		2.5				Raw/pre-cleaned gas; UEF g/TJ based on UNEP (2011b) value of 100 μg/m³

Table A3.6.11 Comparative emission factors for natural gas combustion.

	Emission factor (EF)				Source	Notes/adjustments to reported data
	Low	Intermediate	High	Units		
Unabated EF						
Natural gas		0.2		μg/m³	UNEP (2011b)	Pipeline/consumer quality gas; DF=1
		100				Raw/pre-cleaned gas; DF=1

Table A3.6.12 Technology profile applied for natural gas combustion.

Technology profile	Reduction efficiency, %			Degree of application, % Country group					Source
	Low	Intermediate	High	1	2	3	4	5	
Default									
None		0		100	100	100	100	100	

A3.6.5 **Biomass combustion**

Basis for 2015 emission estimates: UEFs and technology employed to reduce emissions from this sector, applied to activity data concerning combustion of primary solid biomass (IEA, 2016, 2017).

Applied UEFs: These are shown in Table A3.6.13.

Comparative EFs: These are shown in Table A3.6.14.

Discussion of EFs: The generic default UEFs are derived in this work as expert evaluation of a reasonable level of a general default factor, based on a literature survey including the UNEP Toolkit (UN Environment, 2017b) and other general or country-specific literature, such as Kindbom and Munthe (1998), Friedli et al. (2009), Pirrone et al. (2010), Huang et al. (2011), Obrist et al. (2011), Zhang et al. (2013a) and literature cited in those papers.

Basic assumptions during calculations of UEF: For biomass combustion, the UEFs represent the Hg content of biomass as burned. A conversion of data on the Hg content of biomass in mg/t to mg/GJ was made using a heating value of 16 MJ/kg for air dried wood, moisture content 10–20% (OECD/IEA, 2005).

Applied technology profile: This is shown in Table A3.6.15.

Discussion of technology profile: The removal efficiencies of abatement technologies were adopted from the combustion of brown coal. The application rates of air pollutant abatement technologies for the technology groups were developed based on very limited national information and complemented with assumptions.

Comparison with UNEP Toolkit factors: In the UNEP toolkit (UN Environment, 2017b) the default UEF is 0.03 (0.007–0.07) g Hg/t (dry weight), which corresponds to 1.67 mg/GJ (using a heating value of 18 MJ/kg for oven dried wood (OECD/IEA, 2005). All of the Hg in biomass is assumed to be emitted to air (output distribution factor = 1).

Comparison with 2010 inventory factors: Biomass combustion was not included in the 2010 inventory.

Gaps/needs to improve factors and profiles: Technology profiles and removal efficiencies. National data on Hg content in biomass.

Table A3.6.13 Unabated emission factors applied for biomass combustion.

	Unabated emission factor (UEF)				Source	Notes/adjustments to reported data
	Low	Intermediate	High	Units		
Generic default						
Biomass* (unit mg/GJ)		1.25		mg/GJ		Expert evaluation of reasonable general default factor based on UNEP Toolkit (UN Environment, 2017b) and other literature. NB. Note that the data have different units.
Biomass (unit mg/t)	5	20	50	mg/t		

*Conversion using heating value of 16 MJ/kg (air dried wood, moisture content 10–20%) (OECD/IEA, 2005).

Table A3.6.14 Comparative emission factors for biomass combustion.

	Emission factor (EF)				Source	Notes/adjustments to reported data
	Low	Intermediate	High	Units		
Unabated EF						
Biomass	7	30	70	mg/t (dw)	UN Environment (2017b)	UNEP Toolkit default input factor

Table A3.6.15 Technology profile applied for biomass combustion.

Abbreviations. CYC: cyclone; ESP: electrostatic precipitator; FF: fabric filter; (SDA/ w) FGD: (spray drier absorber/ wet) flue gas desulfurization; PM: particulate matter control; PS: particle scrubber; SCR: selective catalytic reduction

Technology profile	Reduction efficiency, %			Degree of application, % Country group					Source
	Low	Intermediate	High	1	2	3	4	5	
Default									
PP biomass									
Level 0: None		0		15	30	60	100	100	Sub-bituminous coal
Level 1: Particulate matter simple APC: ESP/PS/CYC	0	10	25	60	50	30			reduction efficiencies (Table A3.6.6) assumed
Level 2: Particulate matter (FF)	20	50	85	20	20	10			
Level 3: Efficient APC: PM+SDA/wFGD	0	40	75	5					
IND biomass									
Level 0: None		0			25	50	75		Sub-bituminous coal
Level 1: Particulate matter simple APC: ESP/PS/CYC		5		25	25	50	50	25	reduction efficiencies (Table A3.6.6) assumed
Level 2: Particulate matter (FF)		50		25	50	25			
Level 3: Efficient APC: PM+SDA/wFGD		30		25	25				
Level 4: Very efficient APC: PM+FGD+SCR		20		25					
DR biomass									
Level 0: None		0		50	50	100	100	100	Sub-bituminous coal
Level 1: Particulate matter simple APC: ESP/PS/CYC		5		50	50				reduction efficiencies (Table A3.6.6) assumed

A3.6.6 **Pig iron and steel production**

Basis for 2015 emission estimates: UEFs and technology employed to reduce emissions from this sector, applied to activity data concerning primary production of pig iron. Note: Emission estimates associated with secondary steel production are accounted for separately.

Applied UEFs: These are shown in Table A3.6.16.

Comparative EFs: These are shown in Table A3.6.17.

Discussion of EFs: During compilation of country-specific UEFs, an effort was made to use as much national data as possible. Most countries do not have complete mass balances but national data on material consumption and/or Hg content was used instead of generic values wherever possible.

The following literature sources were studied: Kim et al. (2010a), Mlakar et al. (2010), Fukuda et al. (2011), Won and Lee (2012), Remus et al. (2013), Burger Chakraborty et al. (2013), Wang et al. (2014a, 2016d), LKAB (2015), SSAB (2015), Zhang et al. (2015b), Hui et al. (2017), UN Environment (2017b), COWI, and national information provided by China, Republic of Korea, Japan and USA.

Basic assumptions during calculations of UEF: (1) Production processes included are pellet plant, sinter plant, blast furnace and basic oxygen steelmaking. (2) Materials included in the UEF are iron ore, lime/limestone and dolomite. Fuels – both combusted and injected in the process as reduction agents – are excluded. (3) Import/export of sinter pellets is not considered. (4) Hg content of products (pig iron, steel) is zero, almost all Hg is volatized during thermal processes, especially sintering and pelletizing. (5) Recycling of filter materials on-site is not considered for UEF since recycling is only possible if abatement is present. (6) Energy re-use (further combustion of off-gases) is not considered.

Raw material consumption per 1 t of pig iron, according to the BREF-based mass balance:

- Iron ore: 0.09–2.97 t, intermediate value – 1.42 t (Remus et al., 2013; SSAB 2015)

- Limestone/lime: 0.04–0.40 t, intermediate value – 0.23 t (Remus et al., 2013; SSAB 2015)

- Dolomite: 0–0.05 t, intermediate value – 0.02 t (Remus et al., 2013; SSAB 2015)

Range of Hg content of materials:

- Iron ore: 0.001–0.097 g/t, intermediate value – 0.04 g/t (Fukuda et al., 2011; Burger Chakraborty et al., 2013; Wang et al., 2016d; Hui et al., 2017; UN Environment, 2017b; national information provided by Republic of Korea)

- Limestone/lime: 0.001–0.39 g/t, intermediate value – 0.04 g/t (Mlakar et al., 2010; Fukuda et al., 2011; Won and Lee, 2012; Burger Chakraborty et al., 2013; Wang et al., 2014a; Zhang et al., 2015b; UN Environment, 2017b; national information provided by Republic of Korea, Japan and China)

- Dolomite: 0.04–0.07 g/t, intermediate value – 0.06 g/t (Wang et al., 2016d)

The ratio hot metal : liquid steel is 0.74–0.98 t/t, intermediate value – 0.94 t/t (Fukuda et al., 2011; Remus et al., 2013; SSAB 2015).

For all UEFs, <u>distribution factor</u> = 1. Other pathways (sector-specific treatment/disposal) are assumed to refer to treatment of residues from abatement equipment (UN Environment, 2017b).

Applied technology profile: This is shown in Table A3.6.18.

Discussion of technology profile: Steel-making facilities are usually complex systems including several processes at different sites, all of which are usually equipped with separate APCDs. In the technology profiles in Table A3.6.18 it is APCDs installed at sinter plants that are mainly considered because, according to available information (UN Environment 2017b, country inventories, reports, etc.), their contribution to Hg emissions is the most significant.

The following literature sources were studied: Nelson et al. (2009), Fukuda et al. (2011), Remus et al. (2013), UNEP (2015), UN Environment (2017b), and national information provided by Brazil, China, Republic of Korea and Mexico.

Comparison with UNEP Toolkit factors: The default UEF used in this inventory (0.063 g Hg/t pig iron production) is ~26% higher than the UNEP Toolkit default factor (0.05 g Hg/t pig iron production).

Potential for double counting: Generic EFs for primary pig iron production compiled by the Swedish Environmental Institute (IVL) based on BREF mass-balance exclude use of fuels: oil, gas, coke (produced from coal) and coal (added as pulverized coal and used for coke production). Emissions from fuel combustion are accounted for in the sector Stationary combustion of coal and oil in industry of this inventory, so there should be no double counting. Emissions from non-energy use of fuels, especially from use of injected coal and metallurgical coke as reducing agents and use of coking coal to produce metallurgical coke, are not accounted for under the pig iron and steel production sector. Neither are they accounted for under stationary combustion. Available activity data indicate that non-energy use of coal constitutes a very small component of the total use of coal. The contribution of non-energy use of coal and coke to total coal-associated emissions is therefore considered insignificant.

Country-specific emission factors are derived using the same principle.

Comparison with 2010 inventory factors: The default emission factor used in the current inventory (0.063 g Hg/t pig iron production) is 26% higher than the default emission factor applied when calculating emissions in 2010 (0.05 g Hg/t pig iron production – same as in the UNEP Toolkit). Hg contents of iron ore and limestone have been revised based on the latest available data in the literature; the intermediate values are now higher than those used in 2010. In addition, the current emission factor takes into account basic oxygen steelmaking, which was not considered in the 2010 inventory. It also includes the use of dolomite in the production process, which was excluded in 2010.

Gaps/needs to improve factors and profiles: Information base for assumptions regarding technology profiles.

Table A3.6.16 Unabated emission factors applied for pig iron and steel production.

	Unabated emission factor (UEF)				Source	Notes/adjustments to reported data
	Low	Intermediate	High	Units		
Generic default	0.0001	0.063	0.450	g/t (primary) pig-iron production		Expert evaluation based on Remus et al. (2013), UN Environment (2017b) and country-specific data
Country-specific						
Australia	0.003	0.054	0.253	g/t (primary) pig-iron production	Fukuda et al. (2011), Remus et al. (2013), UN Environment (2017b)	National data: 0.031 g Hg/t iron ore
Belarus	0.0002	0.074	0.360		Remus et al. (2013), UN Environment (2017b)	National data: 0.088 g Hg/t limestone
Brazil	0.003	0.054	0.253		Fukuda et al. (2011), Remus et al. (2013), UN Environment (2017b)	National data: 0.031 g Hg/t iron ore
Canada	0.0001	0.058	0.450		Remus et al. (2013), UN Environment (2017b)	National data: 0.017 g Hg/t limestone/lime
China	0.0001	0.033	2.247		Remus et al. (2013), Wu et al. (2017)	National data: 0.02 g Hg/t iron ore, 0.018 g Hg/t limestone, 0.009 g Hg/t dolomite, 0.22 t limestone/t pig iron, 0.04 t dolomite /t pig iron
Chile	0.050	0.525	1.000		COWI	National data: total Hg input 0.05–1 g Hg/t pig iron
Denmark	0.0004	0.056	0.296		Remus et al. (2013), UN Environment (2017b)	National data: 0.01 g Hg/t limestone/lime
Germany	0.0002	0.061	0.344		Remus et al. (2013), UN Environment (2017b)	National data: 0.03 g Hg/t limestone/lime
India	0.004	0.073	0.187		Remus et al. (2013), Burger Chakraborty et al. (2013), UN Environment (2017b)	National data: 0.065 g Hg/t limestone/lime, 0.04 g Hg/t iron ore
Japan	0.052	0.055	0.113		Fukuda et al. (2011)	National data: 0.02 g Hg/t limestone/lime, 0.031 g Hg/t iron ore; 0.29 t limestone/t pig iron; 1.59 t iron ore /t pig iron
Republic of Korea	0.028	0.029	0.030		Kim et al. (2010a)	UEFs reported by Kim et al. (2010a)
Russia	0.008	0.098	0.202		Remus et al. (2013), UN Environment (2017b)	National data: 0.06 g Hg/t iron ore, 0.05 g Hg/t limestone
Slovenia	0.0003	0.055	0.295		Mlakar et al. (2010), Remus et al. (2013), UN Environment (2017b)	National data: 0.008 g Hg/t limestone/lime
Sweden	0.001	0.048	0.146		LKAB (2015), SSAB (2015), UN Environment (2017b)	National data: 0.03 t limestone/t pig iron, 1.23 t iron ore /t pig iron, 0.02 t dolomite /t pig iron
Switzerland	0.001	0.059	0.304		Remus et al. (2013), UN Environment (2017b)	National data: 0.025 g Hg/t limestone/lime
USA	0.0001	0.034	0.257		Remus et al. (2013), UN Environment (2017b), national information	National data: 0.016 g Hg/t iron ore, 0.045 g Hg/t limestone/lime

Table A3.6.17 Comparative emission factors for pig iron and steel production.

	Emission factor (EF)				Source	Notes/adjustments to reported data
	Low	Intermediate	High	Units		
Unabated EF						
UNEP Toolkit-based unabated input to air		0.05		g/t (primary) pig-iron production	UNEP (2015)	Default input factor 0.05 g/t; DF=1 if no abatement assumed. Fuels are excluded
2010 inventory		0.05		g/t (primary) pig-iron production	AMAP/UNEP (2013)	Default input factor 0.05 g/t; DF=1. Fuels are excluded
EMEP/EEA	0.02	0.1	0.5	g/t (primary) steel production	EMEP/EEA (2016)	Numbers in g/t steel adjusted with the ratio 0.74–0.98 t pig iron/ t steel
	0.020	0.106	0.676	g/t (primary) pig-iron production		
	0.016	0.049	0.15	g/ t sinter		Numbers in g/t sinter adjusted with the ratio 0.116–1.621 t sinter/t pig iron (BREF)
	0.002	0.053	0.24	g/t (primary) pig-iron production		
Abated EF						
UNEP Toolkit abated input to air		0.048		g/t (primary) pig-iron production	UNEP (2015)	Default input factor 0.05 g/t; DF=0.95 assuming abatement (wet scrubber or similar)
EEA/EMEP	0.012	0.018	0.036	g/ t sinter	EMEP/EEA (2016)	Wet gas desulfurization
	0.006	0.009	0.018			Dry electrostatic precipitator
	0.004	0.006	0.012			Activated carbon injection + fabric filter
	0.001	0.020	0.058	g/t (primary) pig-iron production		Numbers in g/t sinter adjusted with the ratio 0.116–1.621 t sinter/t pig iron (BREF). Same abatement implied
	0.0007	0.010	0.029			
	0.0005	0.007	0.019			

Table A3.6.18 Technology profile applied for pig iron and steel production.

Abbreviations. ACT: activated carbon tower; AIRFINE: high-efficiency scrubber (trademark); CYC: cyclone; ESP: electrostatic precipitator; FF: fabric filter; (W/D) FGD: (wet/dry) flue gas desulfurization; RAC: regenerative activated carbon process; WS: wet scrubber

Technology profile	Reduction efficiency, %			Degree of application, % Country group					Source
	Low	Intermediate	High	1	2	3	4	5	
Default									
Level 0: None		0					20	100	Fukuda et al. (2011), Remus et al. (2013), UNEP (2015)
Level 1: Basic APC: WS(+FF) (sinter plant)		5			20	50	80		
Level 2: Standard APC: ESP/CYC/FGD (sinter plant)		20		30	80	50			
Level 3: Efficient APC: ESP+FGD/ACT/ ESP+ACT (sinter plant)	40	55	75	60					
Level 4: Very efficient APC: ESP+ACT/RAC (sinter plant)	95	97	99	10					
Country-specific									
Australia									
Sinter plant: Regenerative activated carbon process + Pelletising plant: AIRFINE = ESP/ CYC + quench. scrubber + fine WS	95	97	99		100				Nelson et al. (2009), Remus et al. (2013)
Brazil									
Level 1		5				33			National information
Level 2		20				67			
China									
WS		38				2.5			Wang, S., pers. comm.
Cooler		79				16.8			
Cooler +WS		95				16.8			
ESP		29				10.3			
WS+ESP		45				18.3			
FF		67				11.3			
ESP+WFGD		57				20			
ESP+DFGD+FF		72				4			
Japan									
Sinter plant ESP + Blast furnace FF/ESP		26		30					Fukuda et al. (2011)
Sinter plant ESP+FGD + Blast furnace FF/ESP		47		30					
Sinter plant ESP+ACT + Blast furnace FF/ESP		75		40					
Mexico									
Direct Flame Afterburner with Heat Exchanger / ESP / Wet cyclonic separator/ Gravity collector; venturi scrubbers; cyclones; mat or panel filter		20				51			National information
FF		5				30			
None		0				19			
Republic of Korea									
ESP+SCR+FGD		50		100					National information

A3.6.7 Secondary steel production (electric arc furnace, EAF)

Basis for 2015 emission estimates: UEFs and technology employed to reduce emissions from this sector, applied to activity data concerning secondary steel production with Electric Arc Furnace (World Steel Association, 2015).

Applied UEFs: These are shown in Table A3.6.19.

Comparative EFs: These are shown in Table A3.6.20.

Discussion of EFs: During compilation of country-specific UEFs, an effort was made to use as much national information as possible. National information was used instead of generic values wherever possible.

The following literature sources were studied: Roseborough and Lindblad (2008), Kim et al. (2010a), Ocio et al. (2012), Burger Chakrabortry (2013), Wang et al. (2016d), Remus et al. (2013: table 8.1).

Basic assumptions during calculations of UEF: The national literature emission factors are given as abated emission factors. These were transformed into UEFs assuming reduction efficiencies according to the technology profile.

Applied technology profile: This is shown in Table A3.6.21.

Discussion of technology profile: A technology profile was developed based on UN Environment (2017b) and national information by Kim et al. (2010a) and Roseborough and Lindblad (2008).

Comparison with UNEP Toolkit factors: The default UEF used in this inventory (0.032 g Hg/t EAF steel produced) is not directly comparable to the UNEP Toolkit default factor, which is based on the number of recycled vehicles (0.2–2 g Hg/vehicle).

Potential for double counting: No potential for double counting.

Comparison with 2010 inventory factors: Secondary steel production was not included in the 2010 inventory.

Gaps/needs to improve factors and profiles: Information base for assumptions regarding emission factors and technology profiles.

Table A3.6.19 Unabated emission factors applied for secondary steel production in Electric Arc Furnace.

	Unabated emission factor (UEF)				Source	Notes/adjustments to reported data
	Low	Intermediate	High	Units		
Generic default	0.002	0.032	0.200	g/t secondary steel produced (EAF)		Expert evaluation based on Remus et al. (2013: table 8.1 and country-specific data.
Country-specific						
China		0.026		g/t secondary steel produced (EAF)	Wang et al. (2016d)	Abated EF from source is 0.021
Republic of Korea		0.019			Kim et al. (2010a)	Abated EF from source is 0.009
Turkey		0.017			Ocio et al. (2012)	Abated EF from source is 0.014

Table A3.6.20 Comparative emission factors for secondary steel production.

	Emission factor (EF)				Source	Notes/adjustments to reported data
	Low	Intermediate	High	Units		
UNEP Toolkit-based unabated input to air	0.2		2	g/vehicle	UNEP (2015)	Unit for EF not comparable.

Table A3.6.21 Technology profile applied for secondary steel production.

Abbreviations. CYC: cyclone; ESP: electrostatic precipitator; FF: fabric filter; PS: particle scrubber.

Technology profile	Reduction efficiency, %			Degree of application, % Country group					Source
	Low	Intermediate	High	1	2	3	4	5	
Default									
Level 0: None		0					25	50	Roseborough and Lindblad (2008), Kim et al. (2010a)
Level 1: Particulate matter (ESP/PS/CYC)		10		20	20	50	75	50	
Level 2: Particulate matter (FF)		30		80	80	50			
Level 3: Particulate matter plus other abatement		50							
Level 4: Advanced abatement		80							

A3.6.8 Non-ferrous metal production: copper (Cu)

Basis for 2015 emission estimates: UEFs and technology employed to reduce emissions from this sector, applied to activity data concerning primary copper production (and in some cases total copper production where primary production is not separately distinguished).

Applied UEFs: These are shown in Table A3.6.22.

Comparative EFs: These are shown in Table A3.6.23.

Discussion of EFs: Information on mass balances for non-ferrous metal production and Hg content of ores and concentrates produced and used in different countries is sparse. National data on consumption of raw materials and/or Hg content was used instead of generic values where available.

The following literature sources were studied: Hylander and Herbert (2008), Nelson et al. (2009), BREF NF (2009), Kribek et al. (2010), Kumari (2011), Zhang et al. (2012a), Joint Research Centre (2014), Wu (2012, 2016a), Boliden (2015), EMEP/EEA (2016), Hui et al. (2017), UN Environment (2017b), OUTOTEC, Hylander, pers. comm.; Maag, pers. comm.

Basic assumptions during calculations of UEF: (1) Initial oxidation stage (roasting or sintering of concentrate) is considered to be major source of Hg emissions. (2) Mining and concentrating processes are not considered due to lack of data. Inputs from these processes are considered as insignificant because they do not involve thermal processes. (3) Fuels can be a source of minor Hg inputs (UN Environment, 2017b) but these inputs are considered insignificant compared to inputs from metal ores. Eventual Hg emissions from fuels in the non-ferrous metals production are allocated to a separate activity under 'industrial stationary combustion emissions'. (4) An integrated acid plant is considered as a part of applied technology profile, see discussion of technology profile.

Metal contents, recovery rates, concentrate/metal ratios:

- Copper content of concentrates: 15–51%, intermediate value 28% (Kribek et al., 2010; Joint Research Centre, 2014; Boliden, 2015; EMEP/EEA, 2016; UN Environment, 2017b; OUTOTEC)

- Mercury content of concentrates: 1–100 g/t, intermediate value 26 g/t (Hylander and Herbert, 2008; Kribek et al., 2010; Kumari, 2011; Wu, 2012, 2016a; Zhang et al., 2012a; Boliden, 2015; UN Environment, 2017b)

- Rate of copper recovery from concentrates: 85–97%, intermediate value 93% (Boliden, 2015; UN Environment, 2017b)

- Concentrate/copper ratios: 2.0–7.8, intermediate value 3.8 (BREF, 2009; Zhang et al., 2012a; Boliden, 2015; OUTOTEC).

For all UEFs, <u>distribution factor</u> = 0.96. 4% of the total Hg input is assumed to be bound in smelting slag (Hui et al., 2017). Other pathways are assumed to refer to the treatment of residues from abatement equipment (UN Environment, 2017b; Maag, pers. comm.).

Applied technology profile: This is shown in Table A3.6.24.

Discussion of technology profile: Particular attention should be given to the comments in table note 'b'. When considering Hg reduction efficiencies for combinations of acid plant removal (assumed 90%) and APCDs, the AP reduction efficiency applies to the remaining Hg that is not removed by the APCDs. Therefore the removal efficiency of an efficient basic particle matter + wet gas control configuration in combination with an acid plant is 50% plus 90% of the remaining 50% = effective 95% reduction; similarly the removal efficiency of an efficient particle matter + wet gas control + Hg-specific control configuration in combination with an acid plant is 98% plus 90% of the remaining 2% = effective 99.8% reduction.

The following literature sources were studied: Hylander and Herbert (2008), BREF (2009), Kim et al. (2010a), Li et al. (2010), Boliden (2015), UNEP (2015), Wu (2016a), BAT/BEP (2017), UN Environment 2017b), national information provided by South Africa, Botswana, Namibia, Zambia, Australia, and Republic of Korea; Maag, pers. comm.; Wang, pers. comm., Euripidou, pers. comm.

Comparison with UNEP Toolkit factors: The default factor used (96.0 g/t Cu produced) is 11% lower than the default factor in the UNEP Toolkit (107.5 g/t Cu produced).

Potential for double counting: UNEP Toolkit EFs are derived based on analysis of Hg concentrations in ores, metal concentrates and reject materials. Country-specific EFs are derived based on the same principle. Fuels are not included so there should be no double counting.

Emissions estimates are calculated separately for each (non-ferrous) metal. In cases where large parts of the production are associated with co-production of several metals from the same concentrate/ore, there may be an over-estimation of the summed emissions for the non-ferrous metal sector.

Comparison with 2010 inventory factors: The default unabated EF applied in calculations for 2010 (107 g Hg/t Cu produced) is higher than the default unabated EF used in the current inventory (96 g/t Cu produced). This is due to the updates in Hg content of the concentrates and distribution factor (both are lower in this inventory than in calculations for 2010), based on the latest available national data as well as information in the literature.

Acid plants decrease Hg emissions significantly, and are often combined with Hg-specific abatement measures that decrease Hg emissions even more. Applying abatement technology (especially acid plants) to the UEF of 96 g/t would correspond to an abated EF of around 1–10 g/t; however under the current work this assumption is not applied to all production in all countries as some countries still have artisanal production where abatement factors are considerably lower.

Gaps/needs to improve factors and profiles: (1) Information on the Hg and metal content of concentrates processed in different countries, including details of co-production of non-ferrous metals. (2) Information base for assumptions regarding technology profiles, especially detailed information on the amount of production in different countries that is associated with facilities with integrated acid plants as opposed to artisanal production or production at larger facilities with no integrated acid plant.

Table A3.6.22 Unabated emission factors applied for non-ferrous metal production: copper.

	Unabated emission factor (UEF)				Source	Notes/adjustments to reported data
	Low	Intermediate	High	Units		
Generic default	1.9	96.1	748	g/t Cu produced (primary production)	Hylander and Herbert (2008), BREF (2009), UN Environment (2017b), OUTOTEC, country-specific data	Expert evaluation; intermediate based on 26 g/t in concentrate (low/high based on 1 and 100 g/t in concentrate, respectively)
Country-specific						
Australia	2.0	71.6	449	g/t Cu produced (primary production)	Hylander and Herbert (2008), BREF (2009), Nelson et al. (2009)	National data: 38% copper in concentrate
Canada	4.5	8.5	17.2		BREF (2009), UN Environment (2017b), OUTOTEC	National data: 2.3 Hg/t concentrate
China	6.4	16.1	245		Wu (2012, 2016a), Zhang et al. (2012a)	National data: 3.7 Hg/t concentrate, concentrate/copper ratio of 4.6
India	4.5	8.5	17.2		BREF (2009), Kumari (2011), OUTOTEC	National data: 2.3 Hg/t concentrate
Sweden	4.5	116.8	449		Boliden (2015), UN Environment (2017b)	National data: 24% copper in concentrate, 91% recovery rate, concentrate/copper ratio of 4.7
Zambia	4.5	5.2	6.2		BREF (2009), Kribek et al. (2010)	National data: 1.13 g Hg/t concentrate, 23% copper in concentrate

Table A3.6.23 Comparative emission factors for non-ferrous metal production: copper.

	Emission factor (EF)				Source	Notes/adjustments to reported data
	Low	Intermediate	High	Units		
Unabated EF						
UNEP Toolkit-based unabated input to air	1	30	300	g/t concentrate used	UN Environment (2017b)	Default input factor (Hg content of concentrate) 1–100 g/t; DF=1
	2.1	107.5	716.8	g/t Cu produced	UN Environment (2017b)	Default input factor (Hg content of concentrate) 1–100 g/t; DF=1
2010 inventory	2	107	717	g/t Cu produced	AMAP/UNEP (2013)	Default input factor (Hg content of concentrate) 1–100 g/t; concentrate/Cu ratio 2.8–3.3; DF=1.
Abated EF						
EMEP/EEA	0.021	0.031	0.052	g/t Cu produced	EMEP/EEA (2016)	Abatement not specified
UNEP Toolkit abated input to air	1.9	96.8	645.1	g/t Cu produced	UN Environment (2017b)	Default input factor 2.1–716.8 g/t. No filters or only coarse, dry PM retention. DF=0.9
	1.0	52.7	351.2	g/t Cu produced	UN Environment (2017b)	Default input factor 2.1–716.8 g/t. Wet gas cleaning. DF=0.49
	0.2	10.8	71.7	g/t Cu produced	UN Environment (2017b)	Default input factor 2.1–716.8 g/t. Wet gas cleaning and acid plant. DF=0.1
	0.04	2.2	14.3	g/t Cu produced	UN Environment (2017b)	Default input factor 2.1–716.8 g/t. Wet gas cleaning, acid plant and Hg specific filter. DF=0.02

Table A3.6.24 Technology profile applied for non-ferrous metal production: copper.

Abbreviations. AP: acid plant; DC: dust collector; DCDA: double contact and double absorption tower; ESD: electrostatic demister; ESP: electrostatic precipitator; (W/D) FGD: (wet/dry) flue gas desulfurization; FGS: flue gas scrubber; HgX: Hg-specific abatement technologies; WGC: wet gas cleaning.

Technology profile	Reduction efficiency, %			Degree of application, % Country group					Source
	Low	Intermediate	High	1	2	3	4	5	
Default									
Level 0: None or simple particle filters		0				2.5	5	10	Hylander and Herbert (2008), BREF (2009), Kim et al. (2010a), Li et al. (2010), UNEP (2015)
Level 1: Simple APC: particle control[a] only		10							
Level 2: Basic APC: particle control + WGC[a]		50				2.5	5		
Level 3: Efficient APC: particle control + WGC + AP[b]		95			20	95	90	90	
Level 4: Very efficient APC: particle control + WGC + HgX[c] + AP		99.8		100	80				
Country-specific									
Australia									
Level 4		99.8			100				National information
Botswana									
Simple APC – particle control only		10					100		Euripidou, pers. comm
China									
DC+FGS+ESD+DCDA		97				52.5			Wu (2016a), Wang, pers. comm.
DC+FGS+ESD+DCDA+DFGD		98.5				28.5			
DC+FGS+ESD+DCDA+WFGD		99.0				19.0			
Namibia, South Africa									
Level 1: Simple APC: particle control only		10				15			Euripidou, pers. comm
Level 2: Basic APC: particle control + WGC		50				25			
Level 3: Efficient APC: particle control + WGC + AP[b]		95				60			
Republic of Korea									
ESP-Venturi Scrubber-ESP-Boliden Norzink-DCDA		99.9		100					Kim et al. (2010a), and national information
Sweden									
ESP + scrubber + Boliden/Norzink + DCDA		99.7		100					Boliden (2015), BAT/BEP (2017)
Zambia									
Level 1: Simple APC: particle control only		10				15			Euripidou, pers. comm
Level 2: Basic APC: particle control + WGC		50				25			
Level 3: Efficient APC: particle control + WGC + AP[b]		95				60			

[a] Particle control = cyclones and ESP, [b] integrated acid plant (AP) downstream of APCDs is assumed to remove 90% of the remaining Hg from gas flow; [c] Hg-specific abatement technologies (HgX) can be the following processes and equipment types: Boliden/Norzink process, Outokumpu process, Bolchem, Sodium thiocyanate process, activated carbon filter/Lurgi process, Tinfos/Miltec process, selenium scrubber or filter, lead sulfide process, Hg reclaiming tower. Average removal efficiency of Hg-specific abatement technologies is assumed to be 98%.

A3.6.9 Non-ferrous metal production: lead (Pb)

Basis for 2015 emission estimates: UEFs and technology employed to reduce emissions from this sector, applied to activity data concerning primary lead production (and in some cases total lead production where primary production is not separately distinguished).

Applied UEFs: These are shown in Table A3.6.25.

Comparative EFs: These are shown in Table A3.6.26.

Discussion of EFs: Information on mass balances for non-ferrous metal production and Hg content of ores and concentrates produced and used in different countries is sparse. National data on consumption of raw materials and/or Hg content was used instead of generic values where available.

The following literature sources were studied: Hylander and Herbert (2008), BREF (2009), Kumari (2011), Wu (2012, 2016a), Zhang et al. (2012a), Joint Research Centre (2014), EMEP/EEA (2016), Hui et al. (2017), UN Environment (2017b), COWI, OUTOTEC, national information provided by Brazil; Hylander, pers. comm.; Maag, pers. comm.

Basic assumptions during calculations of UEF: (1) Initial oxidation stage (roasting or sintering of concentrate) is considered to be a major source of Hg emissions. (2) Mining and concentrating processes are not considered due to lack of data. Inputs from these processes are considered as insignificant because they do not involve thermal processes. (3) Fuels can be a source of minor Hg inputs (UN Environment, 2017b) but these inputs are considered insignificant compared to inputs from metal ores. Eventual Hg emissions from fuels in the non-ferrous metals production are allocated to a separate activity under 'industrial stationary combustion emissions'. (4) An integrated acid plant is considered as a part of an applied technology profile.

Metal contents, recovery rates, concentrate/metal ratios:

- Lead content of concentrates: 35–90%, intermediate value 50% (BREF, 2009)

- Mercury content of concentrates: 2–62.2 g/t, intermediate value 30 g/t (Hylander and Herbert, 2008; Kumari, 2011; Wu, 2012, 2016a; Zhang et al., 2012a; UN Environment, 2017b)

- Rate of lead recovery from concentrates: 80% (Paragraph 29 study (UNEP, 2010a) response from Brazil)

- Concentrate/lead ratios: 1.4-3.6, intermediate value 2.5 (COWI, OUTOTEC, Zhang et al., 2012a).

For all UEFs, <u>distribution factor</u> = 0.97. 3% of the total Hg input is assumed to be bound in smelting slag (Hui et al., 2017). Other pathways are assumed to refer to treatment of residues from abatement equipment (UN Environment, 2017b; Maag, pers. comm.).

Applied technology profile: This is shown in Table A3.6.27.

Discussion of technology profile: Particular attention should be given to the comments in table note 'b'. When considering Hg reduction efficiencies for combinations of acid plant removal (assumed 90%) and APCDs, the AP reduction efficiency applies to the remaining Hg that is not removed by the APCDs. Therefore the removal efficiency of an efficient basic particle matter + wet gas control configuration in combination with an acid plant is 50% plus 90% of the remaining 50% = effective 95% reduction; similarly the removal efficiency of an efficient particle matter + wet gas control + Hg-specific control configuration in combination with an acid plant is 98% plus 90% of the remaining 2% = effective 99.8% reduction.

The following literature sources were studied: Hylander and Herbert (2008), BREF (2009), Kim et al. (2010a); Li et al. (2010), Boliden (2015), UNEP (2015), Wu (2016a), BAT/BEP (2017), UN Environment (2017b), national information provided by Republic of Korea; Maag, pers. comm.; Wang, pers. comm., Seo, pers. comm.

Comparison with UNEP Toolkit factors: The default factor used (73.1 g/t Pb produced) is slightly lower than the default factor in the UNEP Toolkit (75 g/t Pb produced).

Potential for double counting: The UNEP Toolkit EFs are derived based on analysis of Hg concentrations in ores, metal concentrates and reject materials. Country-specific EFs are derived based on the same principle. Fuels are not included so there should be no double counting.

Emissions estimates are calculated separately for each (non-ferrous) metal. In cases where large parts of the production are associated with co-production of several metals from the same concentrate/ore, there may be an over-estimation of the summed emissions for the non-ferrous metal sector.

Comparison with 2010 inventory factors: The default unabated EF applied in calculations for 2010 (75 g Hg/t Pb produced) is slightly lower than the default unabated EF used in the current inventory (73.1 g/t Pb produced). This is due to the updated distribution factor (lower in this inventory than in calculations for 2010).

Acid plants decrease Hg emissions significantly, and are often combined with Hg-specific abatement measures that decrease Hg emissions even more. Applying abatement technology (especially acid plants) to the UEF of 73.1 g/t would correspond to an abated EF of around 1–7 g/t; however under the current work this assumption is not applied to all production in all countries because some countries still have artisanal production where abatement factors are considerably lower.

Gaps/needs to improve factors and profiles: (1) Information on the Hg and metal content of concentrates processed in different countries, including details of co-production of non-ferrous metals. (2) Information base for assumptions regarding technology profiles, especially detailed information on the amount of production in different countries that is associated with facilities with integrated acid plants as opposed to artisanal production or production at larger facilities with no integrated acid plant.

Table A3.6.25 Unabated emission factors applied for non-ferrous metal production: lead.

	Unabated emission factor (UEF)				Source	Notes/adjustments to reported data
	Low	Intermediate	High	Units		
Generic default	2.7	73.1	216	g/t Pb produced (primary production)	Hylander and Herbert (2008), BREF (2009), UN Environment (2017b), OUTOTEC; country-specific data	Expert evaluation; intermediate based on 30 g/t in concentrate (low/high based on 2 and 62 g/t in concentrate, respectively)
Bulgaria, Dem. Rep. Korea, Romania, Morocco, Myanmar, Russia, Serbia and Montenegro	10.1	18.3	26.1			Based on 7.5 g/t in concentrate
Argentina, Bolivia, Iran, Mexico, Peru	8.4	15.1	21.6			Based on 6.2 g/t in concentrate
Belgium, Italy, France, Germany, Japan, Republic of Korea, Poland, Sweden, United Kingdom, United States	6.8	12.2	17.4			Based on 5 g/t in concentrate
Country-specific						
Australia	4.3	7.7	11.0		BREF (2009), Wu et al. (2012), OUTOTEC	National data: 3.2 Hg/t concentrate
Canada	3.7	6.6	9.4		BREF (2009), UN Environment (2017b), OUTOTEC	National data: 2.7 Hg/t concentrate
China	8.3	44.3	102		Wu et al. (2012, 2016a), Zhang et al. (2012a)	National data: 27.1 Hg/t concentrate, concentrate/lead ratio of 1.7
India	2.7	10.8	21.6		BREF (2009), Kumari (2011), OUTOTEC	National data: 4.5 Hg/t concentrate
Kazakhstan	4.3	7.7	11.0		BREF (2009), Wu et al. (2012), OUTOTEC	National data: 3.2 Hg/t concentrate

Table A3.6.26 Comparative emission factors for non-ferrous metal production: lead.

	Emission factor (EF)				Source	Notes/adjustments to reported data
	Low	Intermediate	High	Units		
Unabated EF						
UNEP Toolkit-based unabated input to air	2	30	60	g/t concentrate used	UN Environment (2017b)	Default input factor (Hg content of concentrate) 2–60 g/t; DF=1
	2.8	75	214.3	g/t Pb produced	UN Environment (2017b)	Default input factor (Hg content of concentrate) 2–60 g/t; DF=1.
2010 inventory	3	75	214	g/t Pb produced	AMAP/UNEP (2013)	Default input factor (Hg content of concentrate) 2–60 g/t; concentrate/Pb ratio 2.5–3.3; DF=1.
EMEP/EEA	0.8	1	1.2	g/t Pb produced	EMEP/EEA (2016)	
Abated EF						
EMEP/EEA	0.2	0.3	0.4	g/t Pb produced	EMEP/EEA (2016)	2015 technology level
UNEP Toolkit abated input to air	2.52	67.5	192.9	g/t Pb produced	UN Environment (2017b)	Default input factor 2.8–214.3 g/t. No filters or only coarse, dry PM retention. DF= 0.9
	1.37	36.8	105	g/t Pb produced	UN Environment (2017b)	Default input factor 2.8–214.3 g/t. Wet gas cleaning. DF= 0.49
	0.28	7.5	21.4	g/t Pb produced	UN Environment (2017b)	Default input factor 2.8–214.3 g/t. Wet gas cleaning and acid plant. DF=0.1
	0.06	1.5	4.3	g/t Pb produced	UN Environment (2017b)	Default input factor 2.8–214.3 g/t. Wet gas cleaning, acid plant and Hg specific filter. DF=0.02

Table A3.6.27 Technology profile applied for non-ferrous metal production: lead.

Abbreviations. AP: acid plant; DC: dust collector; DCDA: double contact and double absorption tower; DOWA filter: lead[II] sulfide process, a dry media technique; ESD: electrostatic demister; ESP: electrostatic precipitator; FGS: flue gas scrubber; HgX: Hg-specific abatement technologies; SCSA: single contact and single absorption tower; WGC: wet gas cleaning.

Technology profile	Reduction efficiency, %			Degree of application, % Country group					Source
	Low	Intermediate	High	1	2	3	4	5	
Default									
Level 0: None or simple particle filters		0				2.5	5	10	Hylander and Herbert (2008), BREF (2009), Kim et al. (2010a), Li et al. (2010), UNEP, (2015)
Level 1: Simple APC: particle control[a] only		10							
Level 2: Basic APC: particle control + WGC		50				2.5	5		
Level 3: Efficient APC: particle control + WGC + AP[b]		95			20	95	90	90	
Level 4: Very efficient APC: particle control + WGC + HgX[c] + AP		99.8		100	80				
Country-specific									
China									
None		0				5.7			Wu et al. (2016a), Wang, pers. comm.
DC		12				6.2			
DC+FGS		41				12.6			
DC+FGS+ESD+SCSA		87				16.1			
DC+FGS+ESD+DCDA		97				59.4			
Republic of Korea									
ESP-Venturi Scrubber-ESP-Boliden Norzink-DCDA		99.9		100					Seo, pers. comm.
Sweden									
ESP + DOWA filter + DCDA		99.7		100					Boliden (2015), BAT/BEP (2017)

[a] Particle control = cyclones and ESP, [b] integrated acid plant (AP) downstream of APCDs is assumed to remove 90% of the remaining Hg from gas flow; [c] Hg-specific abatement technologies (HgX) can be the following processes and equipment types: Boliden/Norzink process, Outokumpu process, Bolchem, sodium thiocyanate process, activated carbon filter/Lurgi process, Tinfos/Miltec process, selenium scrubber or filter, lead sulfide process, Hg reclaiming tower. Average removal efficiency of Hg-specific abatement technologies is assumed to be 98%.

A3.6.10 Non-ferrous metal production: zinc (Zn)

Basis for 2015 emission estimates: UEFs and technology employed to reduce emissions from this sector, applied to activity data concerning primary zinc production (and in some cases total production where primary production is not separately distinguished).

Applied UEFs: These are shown in Table A3.6.28.

Comparative EFs: These are shown in Table A3.6.29.

Discussion of EFs: Information on mass balances for non-ferrous metal production and Hg content of ores and concentrates produced and used in different countries is sparse. National data on consumption of raw materials and/or Hg content was used instead of generic values where available.

The following literature sources were studied: Hylander and Herbert (2008), BREF (2009), Kim et al. (2010a), Li et al. (2010), Wang et al. (2010a), Kumari (2011), Wu et al. (2012, 2016a), Zhang et al. (2012a), Joint Research Centre (2014), EMEP/EEA (2016), Hui et al. (2017), UN Environment, 2017b, OUTOTEC, Paragraph 29 study (UNEP, 2010a) answer from Brazil, Hylander, pers. comm.; Maag, pers. comm.

Basic assumptions during calculations of UEF: (1) Initial oxidation stage (roasting or sintering of concentrate) is considered to be a major source of Hg emissions. (2) Mining and concentrating processes are not considered due to lack of data. Inputs from these processes are considered as insignificant because they do not involve thermal processes. (3) Fuels can be a source of minor Hg inputs (UN Environment, 2017b) but these inputs are considered insignificant compared to inputs from metal ores. Eventual Hg emissions from fuels in non-ferrous metals production are allocated to a separate activity under 'industrial stationary combustion emissions'. (4) An integrated acid plant is considered as a part of the applied technology profile.

Metal contents, recovery rates, concentrate/metal ratios:

- Zinc content of concentrates: 33–60%, intermediate value 46% (Paragraph 29 study (UNEP, 2010a) answer from Brazil; BREF, 2009; Li et al., 2010)

- Mercury content of concentrates: 1–147 g/t, intermediate value 64 g/t (Hylander and Herbert, 2008; Kumari, 2011; Wu et al., 2012, 2016a; Zhang et al., 2012a; UN Environment, 2017b)

- Rate of Zn recovery from concentrates: 95–97% (Li et al., 2010)

- Concentrate/zinc ratios: 1.7–3.2, intermediate value 2.3 (Wang et al., 2010a; Zhang et al., 2012a; OUTOTEC).

For all UEFs, <u>distribution factor</u> = 0.9. 1–17% of the total Hg input is assumed to be bound in smelting slag (Hui et al., 2017) – the current work uses 10% as a weighted average over the two main processes – hydrometallurgical (more widely used, with an estimated share of Hg input bound in slag of 17%) and pyrometallurgical (share of Hg input bound in slag of 0.5–2.3%). Other pathways are assumed to refer to treatment of residues from abatement equipment (UN Environment, 2017b; Maag, pers. comm.).

Applied technology profile: This is shown in Table A3.6.30.

Discussion of technology profile: Particular attention should be given to the comments in table note 'b'. When considering Hg reduction efficiencies for combinations of acid plant removal (assumed 90%) and APCDs, the AP reduction efficiency applies to the remaining Hg that is not removed by the APCDs. Therefore the removal efficiency of an efficient basic particle matter + wet gas control configuration in combination with an acid plant is 50% plus 90% of the remaining 50% = effective 95% reduction; similarly the removal efficiency of an efficient particle matter + wet gas control + Hg-specific control configuration in combination with an acid plant is 98% plus 90% of the remaining 2% = effective 99.8% reduction.

The following literature sources were studied: Hylander and Herbert (2008), BREF (2009), Kim et al. (2010a), Li et al. (2010), UNEP (2015), UN Environment (2017b), Wu et al. (2016a), Maag, pers. comm.; Wang, pers. comm.; Euripidou, pers. comm.

Comparison with UNEP Toolkit factors: The default factor used (130.8 g/t Zn produced) is 6% higher than the default factor in the UNEP Toolkit (123.3 g/t Zn produced).

Potential for double counting: The UNEP Toolkit EFs are derived based on analysis of Hg concentrations in ores, metal concentrates and reject materials. Country-specific EFs are derived based on the same principle. Fuels are not included so there should be no double counting.

Emissions estimates are calculated separately for each (non-ferrous) metal. In cases where large parts of the production are associated with co-production of several metals from the same concentrate/ore, there may be an over-estimation of the summed emissions for the non-ferrous metal sector.

Comparison with 2010 inventory factors: The default unabated EF applied in calculations for 2010 (123 g/t Zn produced) is lower than the default unabated EF used in the current inventory (130.8 g/t Zn produced). This is due to the updated metal content of the concentrates which is lower in this inventory than in calculations for 2010 (46% and 55%, respectively).

Acid plants decrease Hg emissions significantly, and are often combined with Hg-specific abatement measures that decrease Hg emissions even more. Applying abatement technology (especially acid plants) to the UEF of 130.8 g/t would correspond to an abated EF of around 1–13 g/t; however, under the current work this assumption is not applied to all production in all countries because some countries still have artisanal production where abatement factors are considerably lower.

Gaps/needs to improve factors and profiles: (1) Information on the Hg and metal content of concentrates processed in different countries, including details of co-production of non-ferrous metals. (2) Information base for assumptions regarding technology profiles, especially detailed information on the amount of production in different countries that is associated with facilities with integrated acid plants as opposed to artisanal production or production at larger facilities with no integrated acid plant.

Table A3.6.28 Unabated emission factors applied for non-ferrous metal production: zinc.

	Unabated emission factor (UEF)				Source	Notes/adjustments to reported data
	Low	Intermediate	High	Units		
Generic default	1.6	130.8	422	g/t Zn produced (primary production)	Hylander and Herbert (2008), BREF (2009), UN Environment (2017b), OUTOTEC; country-specific data	Expert evaluation; intermediate based on 64 g/t in concentrate (low/high based on 1 and 147 g/t in concentrate, respectively)
Country-specific						
Australia	74.5	127.3	256	g/t Zn produced (primary production)	BREF (2009), UN Environment (2017b), OUTOTEC	National data: 62.3 Hg/t concentrate
Brazil	2.3	146.6	340		BREF (2009), Paragraph 29 study (UNEP, 2010a) answer from Brazil, UN Environment (2017b)	National data: 41% zinc in concentrate
Canada	17.1	27.6	353		BREF (2009), UN Environment (2017b), OUTOTEC	National data: 13.5 Hg/t concentrate
China	1.8	159.7	737		Wang et al. (2010a) Wu et al. (2012, 2016a), Zhang et al. (2012a), Hui et al. (2017)	National data: 77.5 Hg/t concentrate, concentrate/zinc ratio of 2.4, DF=0.86
Germany	9.3	299.1	422		BREF (2009), UN Environment (2017b), OUTOTEC	National data: 146.4 Hg/t concentrate
India	17.1	51.2	422		BREF (2009), Kumari (2011), OUTOTEC	National data: 25 Hg/t concentrate
Namibia	1.7	110.2	253		BREF (2009), UN Environment (2017b), NAM Zn,	National data: 55% zinc in concentrate; 95% recovery rate
Norway	1.6	122.6	422		BREF (2009), UN Environment (2017b), OUTOTEC	National data: 60 Hg/t concentrate
Peru	1.6	74.8	422		BREF (2009), UN Environment (2017b), OUTOTEC	National data: 37 Hg/t concentrate
Russia	1.6	155.3	353		BREF (2009), UN Environment (2017b), OUTOTEC	National data: 76 Hg/t concentrate
Spain	66.7	162.4	422		BREF (2009), UN Environment (2017b), OUTOTEC	National data: 79.5 Hg/t concentrate
USA	1.6	33.9	60.3		BREF (2009), UN Environment (2017b), OUTOTEC	National data: 17 Hg/t concentrate

Table A3.6.29 Comparative emission factors for non-ferrous metal production: zinc.

	Emission factor (EF)				Source	Notes/adjustments to reported data
	Low	Intermediate	High	Units		
Unabated EF						
UNEP Toolkit-based unabated input to air	5	65	130	g/t concentrate used	UN Environment (2017b)	Default input factor (Hg content of concentrate) 5–130 g/t; DF=1.
	8.6	123.3	342.1	g/t Zn produced	UN Environment (2017b)	Default input factor (Hg content of concentrate) 5–130 g/t; DF=1.
2010 inventory	9	123	342	g/t Zn produced	AMAP/UNEP (2013)	Default input factor (Hg content of concentrate) 5–130 g/t; concentrate/Zn ratio 2.0–2.2; DF=1.
EMEP/EEA	2	5	8	g/t Zn produced	EMEP/EEA (2016)	
Abated EF						
EMEP/EEA	20.1	50.6	81.5	g/t Zn produced	EMEP/EEA (2016)	Abatement not specified
UNEP Toolkit abated input to air	7.7	111.0	307.9	g/t Zn produced	UN Environment (2017b)	Default input factor 8.6–342.1 g/t. No filters or only coarse, dry PM retention. DF=0.9
	4.2	60.4	167.6	g/t Zn produced	UN Environment (2017b)	Default input factor 8.6–342.1 g/t. Wet gas cleaning. DF=0.49
	0.9	12.3	34.2	g/t Zn produced	UN Environment (2017b)	Default input factor 8.6–342.1 g/t. Wet gas cleaning and acid plant. DF=0.1
	0.2	2.5	6.8	g/t Zn produced	UN Environment (2017b)	Default input 8.6–342.1 g/t. Wet gas cleaning, acid plant and Hg specific filter. DF=0.02

Table A3.6.30 Technology profile applied for non-ferrous metal production: zinc.

Abbreviations. AP: acid plant; DC: dust collector; DCDA: double contact and double absorption tower; ESD: electrostatic demister; ESP: electrostatic precipitator; (D/W) FGD: (dry/wet) flue gas desulfurization; FGS: flue gas scrubber; HgX: Hg-specific abatement technologies; SCSA: single contact and single absorption tower; WGC: wet gas cleaning.

Technology profile	Reduction efficiency, %			Degree of application, % Country group					Source
	Low	Intermediate	High	1	2	3	4	5	
Default									
Level 0: None or simple particle filters		0				2.5	5	10	Hylander and Herbert (2008), BREF (2009), Kim et al. (2010a), Li et al. (2010), UNEP (2015)
Level 1: Simple APC: particle control[a] only		10							
Level 2: Basic APC: particle control + WGC		50				2.5	5		
Level 3: Efficient APC: particle control + WGC + AP[b]		95			20	95	90	90	
Level 4: Very efficient APC: particle control + WGC + HgX[c] + AP		99.8		100	80				
Country-specific									
Algeria									
Level 1: Simple APC: particle control only		10						15	Euripidou, pers. comm.
Level 2: Basic APC: particle control + WGC		50						25	
Level 3: Efficient APC: particle control + WGC + AP[b]		95						60	
China									
DC+FGS		41				0.2			Wu et al. (2016a), Wang, pers. comm.
DC+FGS+ESD+SCSA		87				0.2			
DC+FGS+ESD+DCDA		97.4				49.5			
DC+FGS+ESD+DCDA+DFGD		98.5				20			
DC+FGS+ESD+DCDA+WFGD		99.0				20			
DC+FGS+ESD+SMR+DCDA		99.2				10.1			
Namibia									
Level 1: Simple APC: particle control only		10						15	Euripidou, pers. comm.
Level 2: Basic APC: particle control + WGC		50						25	
Level 3: Efficient APC: particle control + WGC + AP[b]		95						60	
Republic of Korea									
ESP-Venturi Scrubber-ESP-Boliden/ Norzink-DCDA		99.9		100					Kim et al. (2010a), national information

[a] Particle control = cyclones and ESP, [b] integrated acid plant (AP) downstream of APCDs is assumed to remove 90% of the remaining Hg from gas flow; [c] Hg-specific abatement technologies (HgX) can be the following processes and equipment types: Boliden/Norzink process, Outokumpu process, Bolchem, sodium thiocyanate process, activated carbon filter/Lurgi process, Tinfos/Miltec process, selenium scrubber or filter, lead sulfide process, Hg reclaiming tower. Average removal efficiency of Hg-specific abatement technologies is assumed to be 98%.

A3.6.11 Non-ferrous metal production: mercury (Hg) dedicated production from cinnabar ore

Basis for 2015 emission estimates: UEFs and technology employed to reduce emissions from this sector, applied to activity data concerning primary Hg production from cinnabar ore; restricted to countries with primary mine production.

Applied UEFs: These are shown in Table A3.6.31.

Comparative EFs: These are shown in Table A3.6.32.

Discussion of EFs: In the absence of any additional/new national information, the UNEP Toolkit factors were adopted in this work.

The following literature sources were studied: BREF (2009) Joint Research Centre (2014), UN Environment (2017b), national information provided by Mexico.

Basic assumptions during calculations of UEF: (1) Mining and concentrating processes are not considered due to lack of data. (2) Eventual Hg emissions from fuels in the non-ferrous metals production are allocated to a separate activity under 'industrial stationary combustion emissions' (see E-Annex, Section A3.5.6).

For all EFs, <u>distribution factor</u> = 0.25 (as in the UNEP Toolkit, applied to total Hg release during the process).

Applied technology profile: This is shown in Table A3.6.33.

Discussion of technology profile: Minimal abatement in the form of basic particle matter control was assumed; production occurs in Group 3, 4 and 5 countries only.

Comparison with UNEP Toolkit factors: The default factor used (7500 g/t Hg produced) is the same as the factor in the UNEP Toolkit.

Potential for double counting: The UNEP Toolkit EF, used as a generic value also in this work, is derived based on analysis of Hg concentrations in ore, concentrates and reject materials. The same principle was applied to country-specific EFs. Fuels are not included so there is no risk of double counting.

Comparison with 2010 inventory factors: The same unabated emission factor is used as in the calculations for 2010.

Gaps/needs to improve factors and profiles: Information base for assumptions regarding technology profiles.

Table A3.6.31 Unabated emission factors applied for non-ferrous metal production: mercury (dedicated production from cinnabar ore).

	Unabated emission factor (UEF)				Source	Notes/adjustments to reported data
	Low	Intermediate	High	Units		
Generic default		7500		g/t Hg produced	UN Environment (2017b)	The UNEP Toolkit factor has been adopted

Table A3.6.32 Comparative emission factors for non-ferrous metal production: mercury (dedicated production from cinnabar ore).

	Emission factor (EF)				Source	Notes/adjustments to reported data
	Low	Intermediate	High	Units		
Unabated EF						
UNEP Toolkit unabated input to air	5000	7500	10000	g/t Hg produced	UN Environment (2017b)	DF=0.25, total Hg released = 20–40 kg/t Hg produced. DF applies here to Hg releases, not total Hg input (1020–1040 kg/t Hg produced). Since no information on control systems is found, the UNEP Toolkit EF is considered as unabated.
2010 inventory		7500		g/t Hg produced	AMAP/UNEP (2013)	The UNEP Toolkit factor has been adopted

Table A3.6.33 Technology profile applied for non-ferrous metal production: mercury (dedicated production from cinnabar ore).

Technology profile	Reduction efficiency, %			Degree of application, % Country group					Source
	Low	Intermediate	High	1	2	3	4	5	
Default									
Level 1: None or simple particle filters	10	10				100	100	100	Expert estimate
Country-specific									
Mexico									
Particle control only		40				100			National information

A3.6.12 Non-ferrous metal production: aluminum (Al) and alumina production from bauxite ore

Basis for 2015 emission estimates: UEFs and technology employed to reduce emissions from this sector, applied to activity data concerning primary Al and alumina production from bauxite.

Applied EFs: These are shown in Table A3.6.34.

Comparative EFs: These are shown in Table A3.6.35.

Discussion of EFs: National data on material consumption and/or Hg contents was used instead of generic values wherever possible.

The following literature sources were studied: BREF (2009), Joint Research Centre (2014), Nelson et al. (2009), UN Environment (2017b), national comments from China.

Basic assumptions during calculations of UEF:

- Emissions from Al production assume: (1) production of alumina from bauxite, (2) production of aluminum from locally produced alumina, and (3) production of aluminum from imported alumina

- Digestion of bauxite is considered to be a major source of Hg emissions

- Fuels can be a source of significant Hg inputs but these inputs are not included in the EFs. Eventual Hg emissions from fuels in the non-ferrous metals production are allocated to a separate activity under 'industrial stationary combustion emissions'.

- Metal contents and ratios: Bauxite/alumina ratio – 2.0–2.5, intermediate value 2.3 (Nelson et al., 2009; BREF, 2009); Alumina/aluminum ratio – 1.6–2.5, intermediate value 1.9 (BREF, 2009); Mercury content of bauxite – 0.07–1.00 g/t, intermediate value 0.49 g/t (UN Environment, 2017b).

Distribution factor = 0.15 (as in the UNEP Toolkit, applied to total Hg release during the process).

Since Al is produced from alumina, which is traded internationally, three different emission factors have been developed:

- The EF for production of Al from bauxite – applied to major bauxite-producing countries that also produce aluminum

- The EF for production of Al from alumina – applied to major aluminum-producing countries that are not bauxite-producers (production from imported alumina)

- The EF for production of alumina for export – applied to major bauxite-producing countries that also produce alumina but not aluminum.

Applied technology profile. This is shown in Table A3.6.36.

Discussion of technology profile: The following literature sources were studied: BREF (2009), Nelson et al. (2009), UNEP (2011b, 2015), national information provided by China.

Comparison with UNEP Toolkit factors: The default factor used (0.31 g/t Al produced) is a (rounded) equivalent to the default factors from the UNEP Toolkit (with adjustment for the application to Al production activity data rather than bauxite ore used).

Potential for double counting: The UNEP Toolkit EFs are derived based on analysis of Hg concentrations in bauxite ore. Country-specific EFs are derived based on the same principle. Fuels are not included so there should be no potential for double counting.

Comparison with 2010 inventory factors: The default unabated EF applied in calculations for 2010 (0.32 g Hg/t Al produced) is slightly higher than the default unabated EF used in the current inventory (0.31 g/t Cu produced). This is due to the update in bauxite/alumina ratio, based on the latest available information in the literature.

Gaps/needs to improve factors and profiles: (1) Information on the basis for national production of Al (alumina vs. bauxite). (2) Information base for assumptions regarding technology profiles.

Table A3.6.34 Unabated emission factors applied for non-ferrous metal production: aluminum and alumina production from bauxite ore.

	Unabated emission factor (UEF)				Source	Notes/adjustments to reported data
	Low	Intermediate	High	Units		
Generic default						
Applied to major bauxite-producing countries	0.03	0.31	0.9	g/t Al produced		Expert evaluation based on BREF (2009), Nelson et al. (2009), UNEP (2015), and country-specific data
Applied to Al-producing countries without major bauxite production		0.05				
Applied to major bauxite-producing countries without Al-production (alumina for export)		0.26		g/t Al produced		
		0.14		g/t alumina produced		
Country-specific						
Australia	0.04	0.05	0.06		BREF (2009), Nelson (2009), UN Environment (2017b)	National data: 0.07 g Hg/t bauxite, 2.5 t bauxite/ t alumina
China	0.03	0.28	0.8		UN Environment (2017b), national information	National data: 2.0 t bauxite/ t alumina
Sub-Saharan African countries	0.10	0.13	0.2		BREF (2009), UN Environment (2017b)	National data: 0.2 g Hg/t bauxite

Table A3.6.35 Comparative emission factors for non-ferrous metal production: aluminum and alumina production from bauxite ore.

	Emission factor (EF)				Source	Notes/adjustments to reported data
	Low	Intermediate	High	Units		
Unabated EF						
	0.01	0.08	0.15	g/t bauxite used	UN Environment (2017b)	Default input factor (Hg content of bauxite) 0.07–1 g/t; DF to air = 0.15.
	0.04	0.32	0.70	g/t Al produced	BREF (2009), Nelson et al. (2009), UN Environment (2017b), and country-specific data	UNEP TK numbers are adjusted using bauxite/aluminum ratio ~3.8–4.7 (2–2.46 t bauxite/t alumina) × 1.9 t alumina/t Al

Table A3.6.36 Technology profile applied for non-ferrous metal production: aluminum and alumina production from bauxite ore.

Abbreviations. ESP: electrostatic precipitator; FF: fabric filter; WS: wet scrubber.

Technology profile	Reduction efficiency, %			Degree of application, % Country group					Source
	Low	Intermediate	High	1	2	3	4	5	
Default									
Level 0: None		0					100	100	Nelson et al. (2009), UNEP (2011b)
Level 1: Particle control (cyclones+ ESP/FF) + WS		50			100	100			
Level 2: particle control (cyclones+ ESP/FF) + WS + Hg collection/reduction		75		100					
Country-specific									
China									
Cyclone + ESP/FF		60				10			Wang, pers. comm.
Particle control + Desulfurization towers		65				90			

A3.6.13 Large-scale gold production

Basis for 2015 emission estimates: UEFs applied to activity data concerning mine production of gold in tonnes. Activity is the production of gold from large-scale mine production (and does not include ASGM production).

Applied EFs: These are shown in Table A3.6.37.

Comparative EFs: These are shown in Table A3.6.38.

Discussion of EFs: -

The following literature sources were studied: Hui et al. (2017), Yang et al. (2016), UNEP (2010a), BAT/BEP (2017), UN Environment (2017b), Nelson, pers. comm.

Basic assumptions during calculations of UEF:

The UEF depends on:

- Amount of Au in ore (which determines the ratio of tonnes of ore needed to produce a tonne of gold)

- Mercury content of ores

- Distribution factor to air (proportion of Hg that is released to air).

The first two at least are likely to vary considerably from mine to mine; however, as it was not possible in this work to consider emissions estimates on a mine-by-mine basis, a generic average UEF was applied with the following assumptions:

Amount of gold in ore = a (generic) value of 4 g Au/t ore was assumed, yielding a ratio of 250,000 tonnes ore for one tonne of gold. Figure A3.6.1 illustrates the development of exploited Au-ore grade in previous years, which in itself can be expected to have resulted in considerable changes in factors applicable to Hg releases from large-scale gold production. Generally, Hg releases would be expected to increase if the Au-content decreases and the Hg-content of the ore remains the same – which is not necessarily the case – due to the increased amount of ore mined for a given production of gold.

Mercury content of ore: 5.5 g Hg/t Au ore was used in the current global inventory calculations. For comparison, the UNEP Toolkit quotes a range of 10–100 g/t ore; UNEP Paragraph-29 (UNEP, 2010a) reported values of 0.1–100 g/t ore, and US Paragraph-29 sources (UNEP, 2010a) reported values of 0.1–30 g/t ore.

Distribution factor to air = 0.04 was used, adopted from the UNEP Toolkit (UN Environment, 2017b). A major part of the total Hg input (over 90%) is often released to land on-site, presumably without entering the roasting stage. On this basis, the (unabated) EF is = 5.5 × 250,000 × 0.04 = 55,000 g Hg emitted/tonne gold produced.

Applied technology profile: This is shown in Table A3.6.39.

Discussion of technology profile: According to BAT/BEP (2017) and information obtained from Australia (Nelson, pers. comm.) and China (Hui et al., 2017; Yang et al., 2016), it is not unusual to use highly efficient APCDs in large-scale gold production. BAT/BEP (2017) reports that removal

efficiency of APCDs on roasters – including acid plants and upstream abatement such as a sulfur-impregnated activate carbon filter (the most common and proven technology in this sector) – can be higher than 99%. The Jerritt process used at some facilities in North America has a removal efficiency of 99.97% (BAT/BEP, 2017). According to Hui et al. (2017), all large-scale gold production in China is covered by APCDs that remove 97–99% of Hg from the flue gas. In Australia, the new production technology launched in 2015 is claimed to reduce Hg emissions from large-scale gold production by 90% (Nelson, pers. comm.) In the current inventory, it has been assumed that the most efficient APCDs, applied mainly in technology Group 1 countries, remove 99% of Hg. These can include a sulfur-impregnated activated carbon filter, Boliden/Norzink process or Jerritt process with an acid plant downstream. Australia and China are assigned country-specific technology profiles.

Comparison with UNEP Toolkit factors: The UEF used in this work is about three-fold lower than the UNEP Toolkit default factor – 150 kg Hg/t gold (assuming 3750 kg/gold produced and DF = 0.04). In the current inventory, the Hg content of ore is assumed to be 5.5 g/t while in the UNEP Toolkit a value of 15 g Hg/t ore is used.

Potential for double counting: UEFs are derived from the Hg and gold content of ores. Fuels consumed at gold production plants are not included so there is no risk of double counting.

Comparison with 2010 inventory factors: The default factor used in the current inventory is the same as used in calculations for 2010.

Gaps/needs to improve factors and profiles: (1) Relevant information on Hg and Au content of ores and concentrates processed in different countries, including the distribution of these factors for individual mines/processing facilities. (2) Information on APCDs employed at large-scale gold production facilities.
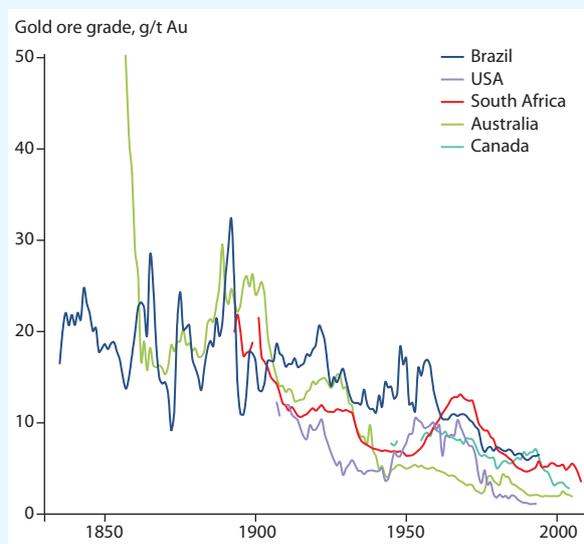
Figure A3.6.1. Changes in gold ore grade over time in different countries. Source: after Giurco et al., 2010.

Table A3.6.37 Emission factors applied for large-scale gold production.

	Unabated emission factor (UEF)				Source	Notes/adjustments to reported data
	Low	Intermediate	High	Units		
Generic default		55,000		g/t (mine) Au produced	UN Environment (2017b)	4 g Au/t ore; 5.5 g Hg/tonne Au ore; DF=0.04 (applied to Hg in ores)
Country-specific						
Australia		12,000		g/t (mine) Au produced	Nelson, pers. comm.	Expert estimate based on national data: 1.24 g Hg/t Au ore
China		26,000		g/t (mine) Au produced	Yang et al. (2016)	National data: 0.73 g Hg/t Au concentrate, 0.004% Au in Au concentrate, 70% recovery rate, DF=0.89 (applied to Hg in concentrated Au, including roasting and cyanidation stages)

Table A3.6.38 Comparative emission factors (EFs) for large-scale gold production.

	Emission factor				Source	Notes/adjustments to reported data
	Low	Intermediate	High	Units		
Unabated EF						
UNEP Toolkit input to air	10	150	300	g/t ore used (extracted)	UN Environment (2017b)	Default input factor 15 (1–30) g/t ore used, or 3750 (250–7500) kg/t gold produced; DF to air = 0.04.
2010 inventory		55000		g/t (mine) Au produced	AMAP/UNEP (2013)	

Table A3.6.39 Technology profile applied for large-scale gold production.

Abbreviations. AP: acid plant; HgX: Hg-specific abatement technologies; WGC: wet gas cleaning.

Technology profile	Reduction efficiency, %			Degree of application, % Country group					Source
	Low	Intermediate	High	1	2	3	4	5	
Default									
Level 0: None or simple particle filters		0						100	Expert estimate based on Hui et al. (2017), Yang et al. (2016), BAT/BEP (2017), Nelson, pers. comm.
Level 1: Simple APC: particle control[a] only		10					100		
Level 2: Basic APC: simple particle control + WGC		25				80			
Level 3: Medium-efficiency APC: more efficient particle control + WGC		40			80	20			
Level 4: Efficient APC: particle control + WGC + less efficient HgX + AP[b]		95		80	20				
Level 5: Very efficient APC: particle control + WGC + more efficient HgX + AP		99		20					
Country-specific									
Australia									
No control		0			50				Nelson, pers. comm.
Ultra-fine grinding mill		90			50				
China									
Single-phase roasting +APC		97				30			Hui et al. (2017), Yang et al. (2016)
Dual-phase roasting +APC		98				13			
Production with cyanidation+ APC		99				57			

[a] Particle control = cyclones and ESP; [b] Hg-specific abatement technologies (HgX) can be the following processes and equipment types: Boliden/Norzink process, sulfur-impregnated active carbon filter, Jerritt process. Average removal efficiency of Hg-specific abatement technologies combined with an integrated acid plant (AP) downstream of APCDs is assumed to be 95% for less efficient technologies and 99% for more efficient technologies.

A3.6.14 Cement production

Basis for 2015 emission estimates: UEFs and technology employed to reduce emissions from this sector, applied to activity data concerning production of cement.

Applied UEFs: These are shown in Table A3.6.40.

Comparative EFs: These are shown in Table A3.6.41.

Discussion of EFs: During compilation of unabated country-specific EFs, an effort was made to use as much national data as possible. Most of the countries do not have complete mass balances but national data on material consumption and/or Hg contents was used instead of generic values wherever possible.

The following literature sources were studied: CSI (2005), CEMBUREAU (2010), Mlakar et al. (2010), UNEP (2010a: report and answers to the questionnaire by Barbados, Brazil, Cyprus, Iceland, USA; 2017), Fukuda et al. (2011), Won and Lee (2012), Burger Chakraborty et al. (2013), Schorcht et al. (2013), GNR (2014), Wang et al. (2014a, 2016d), Cementa (2015), VDZ (2015), Zhang et al. (2015b), BAT/BEP (2017), national comments and personal communication (Maioli, Seo, Solórzano, Suzuki).

Basic assumptions during calculations of UEF: (1) Only the clinker formation stage is considered; subsequent mixing stage is assumed to make insignificant input to Hg emissions compared to the thermal processes according to UN Environment (2017b), with the exception of fly ash addition during mixing which is not accounted for. (2) Clinker is assumed to be produced within a country; eventual import-export of clinker is not accounted for, which might result in over- or underestimations of country-specific emissions from cement production. (3) Recycling of filter materials on-site is not considered for the UEF since recycling is only possible if abatement is present.

Raw materials – input to the raw mill – are assumed to be a mixture of limestone with other, often more Hg-rich materials (clay, shale, fly ash, iron oxide). Significant amount of raw materials other than limestone can result in different input and emission factors. For countries that provided data on country-specific raw material consumption, these data were used in calculations.

Range of Hg content of raw materials:

- Total raw mix: 001–0.46 g/t, intermediate value – 0.09 g/t (CSI, 2005; Mlakar et al., 2010; UNEP, 2010a 2017; Fukuda et al., 2011; Won and Lee, 2012; Burger Chakraborty et al., 2013; Schorcht et al., 2013; Wang et al., 2014a, 2016d; Cementa, 2015; Zhang et al., 2015b, Seo, pers. comm., Suzuki, pers. comm.)

- Limestone: 0.001–0.46 g/t, intermediate value – 0.04 g/t (CSI, 2005; Mlakar et al., 2010; UNEP, 2010a, 2017; Fukuda et al., 2011; Won and Lee, 2012; Burger Chakraborty et al., 2013; Schorcht et al., 2013; Wang et al., 2014a, 2016d; Zhang et al., 2015b; Seo, pers. comm., Suzuki, pers. comm.)

- Clay: 0.001–0.45 g/t, intermediate value 0.08 g/t (CEMBUREAU, 2010; Won and Lee, 2012; Schorcht et al., 2013; Wang et al. 2014a; UN Environment, 2017b; Suzuki, pers. comm.)

- Shale: 0.002–0.44 g/t, intermediate value 0.05 g/t (CEMBUREAU, 2010; Wang et al., 2014a; UN Environment, 2017b)

- Iron oxide: 0–0.68 g/t, intermediate value 0.24 g/t (CEMBUREAU, 2010; Wang et al., 2014a)

- Fly ash: 0.03–0.39 g/t, intermediate value 0.14 g/t (Won and Lee, 2012).

Fuel combustion in the cement industry is accounted for in Section A3.6.14a, except for co-incinerated waste. Fossil fuels are therefore excluded from the UEF. Characteristics of co-incinerated waste (also called alternative fuels when referring to co-incineration in cement kilns):

- Calorific value – 22.9 MJ/kg, which is calculated as a weighted average over most widespread alternative fuels in Europe (according to Schorcht et al., 2013).

- Mercury content: 0.006–0.57 g/t, intermediate value – 0.24 g/t (CEMBUREAU, 2010; Mlakar et al., 2010; Won and Lee, 2012; Schorcht et al., 2013; Cementa, 2015).

Instead of using one world-wide UEF default, in this work either country-specific UEFs or regional UEF defaults were applied based on specific values of parameters as summarized in Table A3.6.42.

For all EFs, distribution factor = 0.95 (BAT/BEP, 2017); 5% of the Hg input is assumed to be bound in clinker.

Applied technology profile: This is shown in Table A3.6.43.

Discussion of technology profile: For countries with data on dust recycling back to the cement kiln, removal efficiencies are assumed to be 50% lower than generic or country-specific values for the same types of technologies based on APC outlet/inlet ratios of Hg concentrations or flows. This is because dust recycling results in an increased part of the Hg ultimately emitted to the air (BAT/BEP, 2017; UN Environment, 2017b) even though in this case removal efficiency cannot be defined as outlet to inlet ratio. The value 50% is based on distribution factors presented in the UNEP Toolkit for cases with and without dust recycling (particle control only).

The following literature sources were studied: Theloke et al. (2008), US EPA (2008), Nelson et al. (2009), Pudasainee et al. (2009a), BREF (2010), CEMBUREAU (2010), NESHAP (2010), Senior (2010), UNEP (2010a: report and answers to the questionnaire, 2011b), Schorcht et al. (2013); UN Environment (2017b), national comments and pers. comms. (Hagström, Maioli, Solórzano, Suzuki, Seo, Hoenig, Euripidou).

Comparison with UNEP Toolkit factors: The range of (central) regional default factors used in this inventory is 0.092–0.113 g Hg/t cement. This is higher than the UNEP Toolkit default unabated factor for cement production without waste co-incineration (0.088 g Hg/t cement) and lower than the UNEP Toolkit default unabated factor for production facilities with waste co-incineration (0.120 g Hg/t cement).

Potential for double counting: Generic EFs for cement production include waste co-incineration but not coal, petroleum coke or oil, which are accounted for in a separate sector, such that there should be no double counting. Country-specific EFs are derived using the same principle. However, in cases when the reported data are used, these can include use of coal and oil so there is a possibility of double counting for these countries.

Comparison with 2010 inventory factors: The default unabated factors applied when calculating emissions in 2010 are 0.087 g Hg/t cement without waste co-incineration and 0.118 g/t cement with waste co-incineration (assuming 12% thermal substitution by waste). In the current inventory, no single world-average emission factor was derived but several regional emission factors were derived instead, varying from 0.092 g Hg/t cement to 0.113 g Hg/t cement. All such emission factors include waste co-incineration – from 1% in CIS countries to 27% in the EU-27. The default values are lower than those used for 2010 mainly due to the revised Hg contents of raw materials and especially waste (0.32 g Hg/t waste is used for 2010, which is 33% higher than 0.24 g/t waste used now), calorific value of waste, and clinker/cement ratios.

Gaps/needs to improve factors and profiles: Information base for assumptions regarding technology profiles.

Table A3.6.40 Unabated emission factors applied for cement production.

	Unabated emission factor (UEF)				Source	Notes/adjustments to reported data
	Low	Intermediate	High	Units		
Generic default						
North America	0.001	0.111	0.855	g/t cement		Based on Schorcht et al. 2013, GNR 2014, UN Environment (2017b), and country-specific data. Waste co-incineration is included
Central America	0.001	0.106	0.789			
South America	0.001	0.092	0.659			
Oceania	0.001	0.109	0.775			
Middle East	0.001	0.113	0.788			
CIS	0.001	0.112	0.762			
Asia	0.001	0.109	0.775			
Africa	0.001	0.105	0.733			
EU-27	0.001	0.110	0.921			
Country-specific						
Algeria	0.001	0.099	0.688	g/t cement	Schorcht et al. (2013), GNR (2014), UN Environment (2017b)	National data: 3.52 MJ/kg clinker, 3% waste, CC ratio = 0.70
Australia	0.001	0.110	0.783		CSI (2005), Schorcht et al. (2013), GNR (2014), UN Environment (2017b)	National data: 6% waste
Austria	0.001	0.114	1.178		Schorcht et al. (2013), GNR (2014), UN Environment (2017b)	National data: 3.72 MJ/kg clinker, 63% waste, CC ratio = 0.70
Barbados	0.002	0.071	0.813		UNEP (2010a) Schorcht et al. (2013), GNR (2014), UN Environment (2017b)	1.81 t limestone + 0.43 t shale /t clinker
Belarus	0.006	0.109	0.285		Schorcht et al. (2013), GNR (2014), UN Environment (2017b)	National data: 0.088 g Hg/t raw mix
Belgium	0.001	0.112	0.989		Schorcht et al. (2013), GNR (2014), UN Environment (2017b)	National data: 35% waste
Brazil	0.027	0.029	0.105		UNEP (2010a), Schorcht et al. (2013), GNR (2014), UN Environment (2017b), Maioli, pers. comm.	2.09 t raw mix (0.02 g Hg/t) /t clinker
Canada	0.001	0.023	0.700		Schorcht et al. (2013), GNR (2014), UN Environment (2017b)	National data: 3.81 MJ/kg clinker, 10% waste, CC ratio = 0.77, 0.02 g Hg/t raw mix
China	0.013	0.071	0.885		Schorcht et al. (2013), GNR (2014), Wang et al. (2014a), Zhang et al. (2015b), UN Environment (2017b)	1.5 t limestone + 1.2 t iron oxide/t clinker
Cyprus	0.001	0.071	0.602		UNEP (2010a), Schorcht et al. (2013), GNR (2014), UN Environment (2017b)	1.4 t limestone + 0.44 t clay + 0.01 t iron oxide + 0.02 t waste/t clinker
Czech Republic	0.001	0.117	1.061		Schorcht et al. (2013), GNR (2014), UN Environment (2017b)	National data: 3.72 MJ/kg clinker, 39% waste, CC ratio = 0.76
Denmark	0.011	0.024	0.419		Schorcht et al. (2013), GNR (2014), UN Environment (2017b)	National data: 47% waste, 0.01 g Hg/t raw mix
Egypt	0.001	0.122	0.848		Schorcht et al. (2013), GNR (2014), UN Environment (2017b)	National data: 4.00 MJ/kg clinker, 3% waste, CC ratio = 0.87

Table A3.6.40 continued

	Unabated emission factor (UEF)				Source	Notes/adjustments to reported data
	Low	Intermediate	High	Units		
Estonia	0.001	0.111	0.955		Schorcht et al. (2013), GNR (2014), UN Environment (2017b)	National data: 31% waste
Finland	0.001	0.115	1.093		Schorcht et al. (2013), GNR (2014), UN Environment (2017b)	National data: 47% waste
France	0.001	0.109	0.890		Schorcht et al. (2013), GNR (2014), UN Environment (2017b)	National data: 3.95 MJ/kg clinker, 24% waste, CC ratio = 0.73
Germany	0.006	0.052	0.222		Schorcht et al. (2013), GNR (2014), VDZ (2015), UN Environment (2017b)	3.78 MJ/kg clinker, 45% waste, CC ratio = 0.70; 1.59 t limestone (0.03 g Hg/t) + 0.05 t clay (0.08 g Hg/t) + 0.05 t fly ash (0.08 g Hg/t) + 0.01 t iron ore (0.04 g Hg/t) /t clinker
Greece	0.001	0.103	0.714		Schorcht et al. (2013), GNR (2014), UN Environment (2017b)	National data: 3% waste
Greenland	0.001	0.111	0.855		Schorcht et al. (2013), GNR (2014), UN Environment (2017b)	National data: 3.81 MJ/kg clinker, 15% waste, CC ratio = 0.77
Hungary	0.001	0.111	0.955		Schorcht et al. (2013), GNR (2014), UN Environment (2017b)	National data: 31% waste
Iceland	0.001	0.114	0.778		UNEP (2010a), Schorcht et al. (2013), GNR (2014), UN Environment (2017b)	National data: 3.75 MJ/kg clinker, 27% waste, CC ratio = 0.73, 1.7 t raw mix/ t clinker
India	0.048	0.124	0.200		Burger Chakraborty et al. (2013), GNR (2014), UN Environment (2017b)	National data: total input 0.187 g Hg/t clinker, CC ratio = 0.70
Ireland	0.001	0.115	1.093		Schorcht et al. (2013), GNR (2014), UN Environment (2017b)	National data: 47% waste
Italy	0.001	0.108	0.817		Schorcht et al. (2013), GNR (2014), UN Environment (2017b)	National data: 3.58 MJ/kg clinker, 12% waste, CC ratio = 0.75
Japan	0.088	0.088	0.088		GNR (2014), Suzuki, pers. comm.	Country-specific mix and Hg content. Fossil fuels excluded. CC ratio = 0.76
Latvia	0.001	0.111	0.955		Schorcht et al. (2013), GNR (2014), UN Environment (2017b)	National data: 3.75 MJ/kg clinker, 31% waste, CC ratio = 0.73
Luxemburg	0.001	0.112	0.989		Schorcht et al. (2013), GNR (2014), UN Environment (2017b)	National data: 35% waste
Mexico	0.001	0.040	0.440		Schorcht et al. (2013), GNR (2014), UN Environment (2017b), Solórzano, pers. comm.	1.29 t limestone + 0.002 t waste/t clinker
Morocco	0.001	0.099	0.688		Schorcht et al. (2013), GNR (2014), UN Environment (2017b)	National data: 3.52 MJ/kg clinker, 3% waste, CC ratio = 0.70
Netherlands	0.001	0.112	0.989		Schorcht et al. (2013), GNR (2014), UN Environment (2017b)	National data: 35% waste
Norway	0.001	0.115	1.093		Schorcht et al. (2013), GNR (2014), UN Environment (2017b)	National data: 47% waste
Philippines	0.001	0.112	0.834		Schorcht et al. (2013), GNR (2014), UN Environment (2017b)	National data: 3.53 MJ/kg clinker, 10% waste, CC ratio = 0.79
Poland	0.001	0.114	1.003		Schorcht et al. (2013), GNR (2014), UN Environment (2017b)	National data: 3.82 MJ/kg clinker, 35% waste, CC ratio = 0.74
Portugal	0.001	0.103	0.714		Schorcht et al. (2013), GNR (2014), UN Environment (2017b)	National data: 3% waste
Republic of Korea	0.006	0.071	0.108		Won and Lee (2012); GNR (2014), Seo, pers. comm.	1.43 t limestone (0.06 g Hg/t) + 0.08 t clay (0.01 g Hg/t) + 0.04 t fly ash (0.14 g Hg/t) + 0.04 t silica stone (0.01 g Hg/t) /t clinker; CC ratio = 0.76
Romania	0.001	0.103	0.714		Schorcht et al. (2013), GNR (2014), UN Environment (2017b)	National data: 3% waste
Russia	0.038	0.039	0.057		Schorcht et al. (2013), GNR (2014), UN Environment (2017b)	National data: 4.59 MJ/kg clinker, 1% waste, CC ratio = 0.81, 0.03 g Hg/t raw mix
Slovenia	0.018	0.022	0.043		Mlakar et al. (2010), Schorcht et al. (2013), GNR (2014), UN Environment (2017b)	National data: 0.02 g Hg/t raw mix, 0.13 g Hg/t waste, 3% waste
Spain	0.001	0.110	0.852		Schorcht et al. (2013), GNR (2014), UN Environment (2017b)	National data: 3.70 MJ/kg clinker, 15% waste, CC ratio = 0.76
Sweden	0.002	0.052	0.096		Schorcht et al. (2013), GNR (2014), Cementa (2015), UN Environment (2017b)	National data: 3.75 MJ/kg clinker, CC ratio = 0.92; 1.64 t raw mix (0.03 g Hg/t) + 0.09 t waste (0.12 g Hg/t) /t clinker

Table A3.6.40 continued

	Unabated emission factor (UEF)				Source	Notes/adjustments to reported data
	Low	Intermediate	High	Units		
Switzerland	0.023	0.041	0.456		Schorcht et al. (2013), GNR (2014), UN Environment (2017b)	National data: 48% waste, 0.03 g Hg/t raw mix
Thailand	0.001	0.115	0.810		Schorcht et al. (2013), GNR (2014), UN Environment (2017b)	National data: 3.30 MJ/kg clinker, 5% waste, CC ratio = 0.81
Tunisia	0.001	0.099	0.688		Schorcht et al. (2013), GNR (2014), UN Environment (2017b)	National data: 3.52 MJ/kg clinker, 3% waste, CC ratio = 0.70
Turkey	0.001	0.119	0.829		Schorcht et al. (2013), GNR (2014), UN Environment (2017b)	National data: 3.43 MJ/kg clinker, 3% waste, CC ratio = 0.85
UK	0.001	0.105	0.878		Schorcht et al. (2013), GNR (2014), UN Environment (2017b)	National data: 3.83 MJ/kg clinker, 26% waste, CC ratio = 0.70
USA	0.001	0.055	0.564		UNEP (2010a), Schorcht et al. (2013), GNR (2014), UN Environment (2017b)	3.87 MJ/kg clinker, 12% waste, CC ratio = 0.84, 1.42 t limestone (0.04 g Hg/t) /t clinker

Table A3.6.41 Comparative emission factors for cement production.

	Emission factor (EF)				Source	Notes/adjustments to reported data
	Low	Intermediate	High	Units		
Unabated EF						
UNEP Toolkit unabated input to air, no waste co-incineration	0.003	0.088	0.4	g/t cement	UN Environment (2017b)	Default input factor 0.004–0.5 g/t; DF to air = 0.8
UNEP Toolkit unabated input to air, waste co-incineration	0.048	0.12	0.8		UN Environment (2017b)	Default input factor 0.06–1 g/t; DF to air = 0.8. Percentage of co-incinerated waste not specified
2010 inventory, no waste co-incineration	0.003	0.087	0.4		AMAP/UNEP (2013)	BREF-based mass-balance and expert evaluations with consideration to national data; DF to air = 0.8
2010 inventory, waste co-incineration	0.05	0.118	0.8		AMAP/UNEP (2013)	BREF-based mass-balance and expert evaluations with consideration to national data; DF to air = 0.8. Percentage of co-incinerated waste – 12%
Abated EF						
UNEP Toolkit abated input to air, with waste co-incineration and no filter dust recycling	0.029	0.072	0.48	g/t cement	UN Environment (2017b)	Default input factor 0.08–0.8 g/t. Simple particle control (ESP/PS/FF). DF=0.6
	0.019	0.048	0.32			Default input factor 0.08–0.8 g/t. Optimized particle control (FF-SNCR /FF+WS /ESP+GFD /optimized FF). DF=0.4
	0.010	0.024	0.16			Default input factor 0.08–0.8 g/t. Efficient Hg pollution control (FF+DS / ESP+DS / ESP+WS / ESP+SNCR). DF=0.2
	0.002	0.005	0.03			Default input factor 0.08–0.8 g/t. Very efficient Hg pollution control (wet FGD +ACI / FF +scrubber +SNCR). DF=0.04
UNEP Toolkit abated input to air, with waste co-incineration and filter dust recycling	0.034	0.084	0.56		UN Environment (2017b)	Default input factor 0.08–0.8 g/t. Simple particle control (ESP/PS/FF). DF=0.7
	0.029	0.072	0.48			Default input factor 0.08–0.8 g/t. Optimized particle control (FF-SNCR /FF+WS /ESP+GFD /optimized FF). DF=0.6
	0.024	0.060	0.40			Default input factor 0.08–0.8 g/t. Efficient Hg pollution control (FF+DS / ESP+DS / ESP+WS / ESP+SNCR). DF=0.5
	0.002	0.005	0.03			Default input factor 0.08–0.8 g/t. Very efficient Hg pollution control (wet FGD +ACI / FF +scrubber +SNCR). DF=0.04
CEMBUREAU		0.035			CEMBUREAU (2010)	

Table A3.6.42 Parameters for calculation of regional UEF for cement production (GNR, 2014).

Region	Thermal energy demand, MJ/kg clinker	Fuel substitution by waste, % of thermal energy	Clinker/cement ratio (CC ratio), t/t
North America	3.81	15	0.77
Central America	3.67	11	0.74
South America	3.65	6	0.65
Oceania	3.36	5	0.78
Middle East	3.43	3	0.81
CIS	4.59	1	0.81
Asia	3.36	5	0.78
Africa	3.78	3	0.75
EU-27	3.75	27	0.73

Table A3.6.43 Technology profile applied for cement production.

Abbreviations. ACI: activated carbon injection; DS: dry scrubber; ESP: electrostatic precipitator; (D/W) FGD: (dry/wet) flue gas desulfurization; FF: fabric filter; PS: particle scrubber; SNCR: selective non-catalytic reduction; WS: wet scrubber.

Technology profile	Reduction efficiency, %			Degree of application, % Country group					Source
	Low	Intermediate	High	1	2	3	4	5	
Default									
Level 0: None		0				20	50	100	US EPA (2008), Theloke et al. (2008), Pudasainee et al. (2009a), BREF (2010), CEMBUREAU (2010), NESHAP (2010); Senior (2010), UNEP (2010a, 2011b)
Level 1: Particulate matter simple APC: FF/ESP/PS		25		80	80	80	50		
Level 2: Particulate matter optimized/ combination APC: FF+SNCR/FF+WS/ ESP+FGD/optimized FF		55		15	20				
Level 3: Efficient APC: FF+DS/ESP+DS/ESP+WS/ESP+SNCR		75		4					
Level 4: Very efficient APC: WFGD + /ACI / FF + scrubber+ SNCR		95		1					
Country-specific									
Australia									
ESP		5			50				Nelson et al. (2009)
FF		78			50				
Brazil									
PM: ESP or PS		25				50			Maioli, pers. comm.
PM: FF or other efficient particle control		25				50			
Canada									
Level 1: Particulate matter simple APC: FF/ESP/PS		25		10					UNEP (2010a)
Level 2: Particulate matter optimized/ combination APC: FF+SNCR/FF+WS/ ESP+FGD/optimized FF		55		70					
Level 3: Efficient APC: FF+DS/ESP+DS/ESP+WS/ESP+SNCR		75		20					
China, Hong Kong									
Dust removal – FF/ESP		40				100			UNEP (2010a)

Table A3.6.43 continued

Technology profile	Reduction efficiency, %			Degree of application, % Country group					Source
	Low	Intermediate	High	1	2	3	4	5	
EU28 (if not separately listed) + Norway, Iceland and Switzerland									
Level 1: Particulate matter simple APC: FF/ESP/PS		25		39					Group 1 default adjusted to reflect increased controls due to regulation associated with increased use of co-incineration of waste
Level 2: Particulate matter optimized/ combination APC: FF+SNCR/FF+WS/ ESP+FGD/optimized FF		55		30					
Level 3: Efficient APC: FF+DS/ESP+DS/ ESP+WS/ESP+SNCR		75		30					
Level 4: Very efficient APC: WFGD + /ACI / FF + scrubber+ SNCR		95		1					
Germany									
Level 2: Particulate matter optimized/ combination APC: FF+SNCR/FF+WS/ ESP+FGD/optimized FF		55		75					Hoenig, pers. comm.
Level 3: Efficient APC: FF+DS/ESP+DS/ ESP+WS/ESP+SNCR		75		25					
India									
Uncontrolled		0						1	UNEP (2010a)
ESP		25						99	
Japan									
Particulate matter simple APC: FF/ESP/PS		25		80					Suzuki, pers. comm.
Particulate matter optimized/ combination APC: FF+SNCR/FF+WS/ESP+FGD/ optimized FF		55		15					
Efficient APC: FF+DS/ESP+DS/ESP+WS/ ESP+SNCR		75		4					
Very efficient APC: WFGD + /ACI / FF + scrubber+ SNCR		95		1					
Republic of Korea									
Spray tower + particle control (FF)		60.5		100					Seo, pers comm.
Mexico									
Particle control: FF, ESP, cyclones		25				100			Solórzano, pers. comm.
South Africa									
FF + ESP		30				100			Euripidou, pers. comm.
Sweden									
FF + SNCR		55		28					Hagström, pers. comm.
FF + scrubber+ SNCR		75		72					
UK									
Particulate matter control		25		26					UNEP (2010a)
FF + SNCR		50		27					
ESP + WS		55		8					
ESP + DS		73		39					

A3.6.14a Fossil fuel combustion in cement production

Basis for 2015 emission estimates: UEFs and technology employed to reduce emissions from this sector, applied to activity data concerning amount of hard coal, brown coal and petroleum coke combustion in the cement sector.

Applied EFs: EFs for petroleum coke are shown in Table A3.6.44. EFs for hard coal are shown in Table A3.6.1 and for brown coal in Table A3.6.4.

Comparative EFs: For hard coal and brown coal, the same emission factors are used as in the more general coal combustion sector (see Sections A3.6.1 and A3.6.2). For petroleum coke combustion, comparative EFs are shown in Table A3.6.45. DF to air is assumed to be 1 for unabated emissions.

Discussion of EFs: During the compilation of unabated country-specific EFs, an effort was made to use as much national data as possible.

The following literature sources were studied: CEMBUREAU (2010), Mlakar et al. (2010), Fukuda et al. (2011), Schorcht et al. (2013), Cementa (2015), UN Environment (2017b).

Basic assumptions during calculations of UEF: Same as for UEF in the more general coal combustion sector (see Sections A3.6.1 and A3.6.2).

Applied technology profile: Default and country-specific technology profiles are harmonized with the technology profiles in the cement production sector (Section A3.6.14).

Discussion of technology profile: Process-related emissions (originating in raw materials) and energy-related emissions (originating in fuels) are usually treated in the same abatement system at cement facilities.

Comparison with UNEP Toolkit factors: The default input factor for unspecified petroleum coke combustion in the UNEP Toolkit (0.02 g Hg/t oil product) is about half the emission factors used in this work.

Potential for double counting: UEFs are derived from analysis of Hg concentration of coal and petroleum coke combusted at cement producing facilities. Combustion in cement production is intentionally separated from other fuel combustion and is not accounted for in other sectors so there is no risk of double counting.

Comparison with 2010 inventory factors: Emissions from coal combustion in cement production were allocated to the coal combustion sector in the 2010 inventory. Emissions from petroleum coke combustion were included in the emission factors for cement production in the 2010 inventory.

Gaps/needs to improve factors and profiles: Additional information on Hg content of hard coal, brown coal and petroleum coke in different countries.

Table A3.6.44 Unabated emission factors applied for petroleum coke combustion in cement production.

	Unabated emission factor (UEF)				Source	Notes/adjustments to reported data
	Low	Intermediate	High	Units		
Generic default	0.010	0.040	0.370	g/t petroleum coke	CEMBUREAU (2010), Fukuda et al. (2011), Schorcht et al. (2013), Cementa (2015), UN Environment (2017b)	Expert estimate based on available data. Default input factor 0.01–0.37 g/t. DF=1
Country-specific						
Slovenia	0.058	0.214	0.370		CEMBUREAU (2010), Mlakar et al. (2010), Schorcht et al. (2013), UN Environment (2017b)	National data: 0.214 g Hg/t petroleum coke
USA	0.010	0.050	0.250		CEMBUREAU (2010), Schorcht et al. (2013), UN Environment (2017b)	National data: 0.05 g Hg/t petroleum coke

Table A3.6.45 Comparative emission factors for petroleum coke combustion.

	Emission factor (EF)				Source	Notes/adjustments to reported data
	Low	Intermediate	High	Units		
Unabated EF						
UNEP Toolkit-based unabated input to air	0.01	0.02	0.1	g/t petroleum coke	UN Environment (2017b)	Default input factor (Hg content of petroleum coke) 0.01–0.1 g/t; DF=1
Abated EF						
EMEP/EEA	0.01	0.049	0.24	g/t clinker	EMEP/EEA (2016)	Industrial combustion. Abatement not specified

A3.6.15 Oil refining

Basis for 2015 emission estimates: UEFs and technology employed to reduce emissions from this sector, applied to activity data concerning amount of crude oil refined.

Applied EFs: These are shown in Table A3.6.46.

Comparative EFs. These are shown in Table A3.6.47.

Discussion of EFs: Regional and global UEFs are based on weighted averages derived from national UEFs. The values used for regional/global Hg content of crude oils are generally similar to those suggested by IPIECA (2012). The 2015 inventory continues to use a value of 25% as the factor for emissions to air is higher than that suggested by IPIECA (8%, based on studies at five San Francisco Bay refineries, McGuire et al., 2009) but consistent with values given by UNEP (2011b; provided by Petroleum Association of Japan for Japanese refineries, and reported by US-EPA (Wilhelm, 2001) cited by IKIMP (2012)).

The application of the 25% value is one of the main factors in discrepancies between current GMA estimates and estimates made by IPIECA in comments to the GMA 2013 and information conveyed by R. Cox (pers. comm.) during preparation of the 2015 inventory. Lack of new measurement data from a more representative range of refineries continues to be an obstacle to resolving this question.

The following literature sources were studied: Wilhelm et al. (2007), EMEP/EEA (2009), UNEP (2011b), BREF (2012), IKIMP (2012), IPIECA (2012), Petroleum Association of Japan, pers. comm.

Basic assumptions during calculations of UEF: (1) UEFs are based on information concerning Hg content of crude oils produced in different countries (mainly from Wilhelm et al., 2007 and Petroleum Association of Japan, pers. comm.;

and assume that 25% of the Hg in refined oil is emitted to air (UNEP, 20011b; IKIMP, 2012) (2) Where a country's production exceeds its consumption, it is assumed that the refined oil is from national sources. Where national consumption exceeds production (or there is no national production) assumptions are made regarding the proportions of the refined oil that are obtained from different (national, regional and global) sources, and use is made of national, regional and global UEFs accordingly (3) The oil extraction stage and transport prior to refining is not included although these activities can potentially give rise to significant releases of Hg (UNEP, 2011b) (4) Combustion of fuels in oil refineries is accounted for separately as stationary combustion.

Applied technology profile: This is shown in Table A3.6.48.

Discussion of technology profile: It was assumed that APCDs are either absent at oil refineries, or are inefficient at reducing Hg emissions to air from this source.

Comparison with UNEP Toolkit factors: The default factor used (0.0034 g/t crude oil refined) is significantly lower than the UNEP Toolkit default factor of 0.038 g/t crude oil refined.

Potential for double counting: UEFs are derived from analysis of Hg concentration of (refined) crude oil. Fuels consumed at oil refineries are not included so there is no risk of double counting.

Comparison with 2005 inventory factors: Emissions from oil refining were not included in the 2005 inventory.

Gaps/needs to improve factors and profiles: Additional information on Hg content of oil from different sources (countries and fields), and on the volumes, sources and Hg content of the oil refined in different countries/refineries.

Table A3.6.46 Unabated emission factors (UEFs) applied for oil refining.

	Unabated emission factor				Source/Notes (adjustments to reported data)
	Low	Intermediate	High	Units	
Generic default factor		Not used		g/t crude oil refined	Weighted average of national estimates and their proportional contribution to global supply.
Algeria		0.003325		g/t crude oil refined	Wilhelm et al., 2007; Petroleum Association of Japan, pers. comm., UNEP, 2011b; IKIMP, 2012; Cox, pers. comm.
Angola		0.0004			
Argentina		0.004025			
Australia		0.001191			
Austria		0.001806			
Azerbaijan		0.00025			
Bahrain		0.000368			
Bangladesh		0.001806			
Belarus		0.001131			
Belgium		0.001806			
Brazil		0.000966			
Brunei Darussalam		0.00065			
Bulgaria		0.001806			
Canada		0.001081			
Chile		0.000966			
China		0.005066			
Columbia		0.00085			

Table A3.6.46 continued

	Unabated emission factor				Source/Notes (adjustments to reported data)
	Low	Intermediate	High	Units	
Congo		0.000843			
Croatia		0.001131			
Cuba		0.000835		g/t crude oil refined	
Czech Republic		0.001806			
Denmark		0.000437			
Dominican Republic		0.000835			
Ecuador		0.000966			
Egypt		0.001928			
Finland		0.001806			
France		0.001806			
Gabon		0.00025			
Germany		0.001806			
Ghana		0.000843			
Greece		0.001806			
Hungary		0.001806			
India		0.014716			
Indonesia		0.012973			
Iran		0.000525			
Iraq		0.000175			
Ireland		0.001806			
Israel		0.000368			
Italy		0.001806			
Ivory Coast		0.000075			
Jamaica		0.000835			
Japan		0.00739			
Jordan		0.000368			
Kazakhstan		0.001131			
Kenya		0.000843			
Korea- Rep. of		0.00739			
Kuwait		0.00025			
Kyrgystan		0.001131			
Libya		0.001928			
Malaysia		0.009425			
Mexico		0.0009			
Morocco		0.001928			
Myanmar		0.012973			
Netherlands		0.001806			
New Zealand		0.000521			
Nicaragua		0.000835			
Nigeria		0.00075			
Norway		0.004875			
Oman		0.000375			
Pakistan		0.001806			
Peru		0.000966			
Philippines		0.012973			
Poland		0.001806			
Portugal		0.001806			
Qatar		0.0005			
Romania		0.001806			
Russia		0.000775			
Saudi Arabia		0.000375			
Senegal		0.000843			

Table A3.6.46 continued

	Unabated emission factor				Source/Notes (adjustments to reported data)
	Low	Intermediate	High	Units	
Singapore		0.012973			
Slovakia		0.001806			
South Korea		0.012973		g/t crude oil refined	
Spain		0.001806			
Sri Lanka		0.001806			
Sudan		0.0085			
Sweden		0.001806			
Switzerland		0.001131			
Syrian Arab Rep.		0.000368			
Taiwan		0.012973			
Tajikistan		0.001131			
Thailand		0.012973			
Trinidad and Tobago		0.000835			
Tunisia		0.001928			
Turkey		0.000368			
Turkmenistan		0.001131			
Ukraine		0.001131			
United Arab Emirates		0.000425			
United Kingdom		0.001806			
United States		0.001294			
Uruguay		0.000966			
Uzbekistan		0.001131			
Venezuela		0.00105			
Vietnam		0.016625			
Yemen		0.000368			
Central America and the Caribbean		0.000845		g/t crude oil refined	Weighted average based on national estimates and their proportional contribution to global supply for countries within region.
East and Southeast Asia		0.013			
Europe		0.00113			
South America		0.000966			
South Asia		0.0276			
Sub-Saharan Africa		0.000843			

Table A3.6.47 Comparative emission factors for oil refining.

	Emission factor (EF)				Source	Notes/adjustments to reported data
	Low	Intermediate	High	Units		
Unabated EF						
UNEP Toolkit input to air	0.001	0.038	0.075	g/t crude oil refined	UNEP (2011b)	Default input factor (Hg content of crude oil) 5–300 mg/t (mean value 55 mg/t); DF to air = 0.25
UEF based on BREF Hg concentrations	0.008	0.016	0.025	g/t crude oil refined	UNEP (2011b), BREF (2012b)	Input factor (Hg content of crude oil) 30–100 mg/t (BREF, range); DF to air = 0.25 (UNEP, 2011b)
Abated EF						
EMEP/EEA	0.002	0.0051	0.015	g/t crude oil refined	EMEP/EEA (2009)	Abatement not specified

Table A3.6.48 Technology profile applied for oil refining.

Technology profile	Reduction efficiency, %			Degree of application, % Country group					Source
	Low	Intermediate	High	1	2	3	4	5	
Default									
None		0		100	100	100	100	100	

A3.6.16 Chlor-alkali industry

Basis for 2015 emission estimates: UEFs and technology employed to reduce emissions from this sector, applied to activity data concerning chlorine (Cl$_2$) production capacity (or production where available) using Hg-cell technology are the same as in the GMA 2013 (AMAP/UNEP, 2013).

Activity data have been updated where available, in particular for European countries based on 2015 data from OSPAR (2015, 2016) and Euro Chlor (2017) sources, and for some other countries including India from national reports on the closure or conversion of production plants using mercury-cell technology. For a number of other countries, however, updated activity data are lacking and older data were applied.

Applied UEFs: These are shown in Table A3.6.49.

Comparative EFs: These are shown in Table A3.6.50.

Discussion of EFs: The following sources were studied: OSPAR (2011), UNEP (2011b), national information received from: Argentina, Brazil, India (Corporate Responsibility for Environmental Protection (CREP) Charter); Romania, and LRTAP sources.

OSPAR (2015) reported ranges of Hg emissions in 2014 of 0.125–1.15 g/t Cl$_2$. Approximately 10 plants reporting emissions to OSPAR in 2010 were shut-down or converted (or partially converted) to membrane technology production. Of the 19 plants still reporting mercury emissions, only two still report emissions >1 g/t (compared to five plants in 2007 and 17 plants in 2005) and most plants emitting around 0.5 g/t.

Applied technology profile: This is shown in Table A3.6.51.

Discussion of technology profile: The EC Reference Document on Best Available Techniques in the Chlor-alkali Industry identifies the Hg-free membrane process as BAT. In as far as chlor-alkali production based on Hg-cell technology is concerned; much of the abatement potential lies in applying best practices and good management of operations. As such, technological abatement is represented as BAP in the technology profile, with reduction effectiveness based on reported national data largely for the OSPAR region. For India, information was used describing application within the chlor-alkali industry in India of the CREP Charter which incorporates: complete recycling of Hg-bearing effluent; treatment of cell-room ventilation gas; reduction of Hg in hydrogen gas; installation of a salt washery unit; installation of Hg distillation units; brine sludge treatment and disposal in secured landfill.

Comparison with UNEP Toolkit factors: In this work, the applied UEFs were based on the low-intermediate ranges of the UNEP Toolkit (UNEP, 2011b) default factors reflecting trends in reductions in Hg consumption in the chlor-alkali industry in recent years; this also converged estimates towards recently reported national emissions estimates for some countries. Recent research, however, indicates that commonly applied emission estimation approaches do not always include (potentially significant) fugitive emissions.

Potential for double counting: There is no identified potential double counting associated with estimates for the chlor-alkali sector.

Gaps/needs to improve factors and profiles: Information on potential Hg releases associated with non-standard operating conditions (accidental releases) in developed countries, and improvements in applied technology and BAP in other countries.

Table A3.6.49 Unabated emission factors applied for the chlor-alkali industry.

	Unabated emission factor (UEF)				Source	Notes/adjustments to reported data
	Low	Intermediate	High	Units		
Generic default		20		g/t Cl_2 capacity	UNEP (2011b)	UNEP Toolkit low–intermediate (unaccounted consumption considered released)
Country-specific						
Argentina	3.75	10	21.6	g/t Cl_2 production		National comments (5.8 g/t): Intermediate: 57.88 g/t Cl_2 produced (DF=0.1); 15% of production; High: 215.97 g/t Cl_2 produced (DF=0.1); 3.3 % of production; Low: 15.34 g/t Cl_2 produced (DF=0.245); 82% of production
Brazil		10				
Italy		20		g/t Cl_2 capacity	OSPAR (2011)	Based on OSPAR (2011)
Sweden		0.5			OSPAR (2011)	Based on OSPAR (2011)
OSPAR countries (Belgium, Finland, France, Germany, Spain, Switzerland) excluding the UK		2.5			OSPAR (2011)	Based on OSPAR (2011) and UNEP Toolkit (with assumed on-/off-site storage/recycling/ dumping)
Other Group 1 and 2 countries		5			UNEP (2011b)	UNEP Toolkit low (with assumed on-/off-site storage/recycling/ dumping)
Group 3 countries		10			UNEP (2011b)	UNEP Toolkit low–intermediate (with assumed on-/off-site storage/ recycling/ dumping)

Table A3.6.50 Comparative emission factors for the chlor-alkali industry.

	Emission factor (EF)				Source	Notes/adjustments to reported data
	Low	Intermediate	High	Units		
Unabated EF						
	5	42	80	g/t Cl_2 produced	UNEP (2011b)	For production using Hg-cell technology; 0.2 of total release is to air (unaccounted consumption considered released)
	2.5	21	40	g/t Cl_2 produced	UNEP (2011b)	For production using Hg-cell technology; 0.1 of total release is to air (with assumed on-/off-site storage/recycling/ dumping)
	2.2	18.6	35.5	g/t NaOH produced	UNEP (2011b)	For production using Hg-cell technology (with assumed on-/off-site storage/recycling/ dumping). For conversion between a Cl_2-basis and an NaOH basis, the following factor can be used: g/t NaOH = g/t Cl_2/1.128 (based on European Commission, 2001b cited in UNEP, 2011b)

Table A3.6.51 Technology profile applied for the chlor-alkali industry.

Abbreviation. BEP: best environmental practices.

Technology profile	Reduction efficiency, %			Degree of application, % Country group					Source
	Low	Intermediate	High	1	2	3	4	5	
Default									
Level 0: None		0					100	100	
Level 1: advanced BEP		50		100	100	100			
Country-specific									
India		50						100	

A3.6.17 Vinyl chloride monomer (VCM) production and recycling of mercury catalyst

Basis for 2015 emission estimates: National information and information from literature, in combination with Hg consumption data for vinyl chloride monomer (VCM) production by world region from UN Environment (2017b).

Applied UEFs: These are shown in Table A3.6.52.

Comparative EFs: These are shown in Table A3.6.53.

Discussion of EFs: The EFs used are country-specific.

Applied output distribution factors: These are shown in Table A3.6.54.

Discussion of output distribution factors: The distribution factors to air from VCM production as well as the fractions of catalyst Hg that goes to recycling are based on country-specific data. The distribution factor for Hg to air from recycling of spent catalyst is based on Lin et al. (2016), and applied to all countries.

Comparison with UNEP Toolkit factors: In the UNEP Toolkit (UN Environment, 2017b) the default factor is 120 (100–140) g Hg/t VCM produced. The default output distribution factor to air is 0.02 from VCM production and 0.6 to 'sector specific treatment'.

Gaps/needs to improve factors and profiles: Up to date national information in general, but especially regarding recycling practices, and the extent of the use of low-Hg catalyst in Chinese industry. According to current estimates recycling of the Hg chloride catalyst contributes more to air emissions than the actual VCM production.

Table A3.6.52 Unabated emission factors applied for VCM production

	Unabated emission factor (UEF)				Source	Notes/adjustments to reported data
	Low	Average	High	Unit		
VCM production						
Country-specific						
China	49	86.9	97	g Hg/t VCM produced	Lin et al. (2016), UNIDO (2016)	Average from UNIDO (2016), low and high values from Lin et al. (2016)
India*		n.a.				
Russian Federation		96.07			National information	

*Emission estimate for India based on estimated consumption of Hg in catalyst in South Asia region from UN Environment (2017a).

Table A3.6.53 Comparative emission factors for VCM production.

	Unabated emission factor (UEF)				Source	Notes/adjustments to reported data
	Low	Intermediate	High	Units		
VCM production	100	120	140	g Hg/t VCM produced	UN Environment (2017b)	UN Environment (2017b) Toolkit default input factor

Table A3.6.54 Applied output distribution factors.

	Hg output distribution factors		Source	Notes/adjustments to reported data
		Units		
Factor to air from VCM production				
China	0.01	Fraction of catalyst Hg	Wang[a], pers. comm.	
India	0.005		Burger Chakraborty et al. (2013)	
Russian Federation	0.02		National information	
To recycling of catalyst				
China	0.75	Fraction of catalyst Hg to recycling	Lin et al. (2016)	Russia: assumption that amount to sector specific treatment = recycling
India	0.5		Burger Chakraborty et al. (2013)	
Russian Federation	0.6		National information	
Factor to air from recycling				
Default	0.05		Lin et al. (2016)	

* Information based on: Mercury Emission and Release Inventory of Chinese Key Mercury-Involved Industries in 2014 from the preliminary assessment project of the Minamata Convention in China (unpublished).

A3.7 Methodology for calculating uncertainty ranges

For the majority of the estimates presented in this report, country-sector emission estimates were derived using the general equation:

$$Emission = Activity \times UEF \times (1 - Abatement)$$

where *Activity* represents the amount of, for example, product produced or fuel/raw material consumed, *UEF* is the associated (unabated) emission factor, and *Abatement* represents the proportion of the emission that is avoided, for example by the application of air pollution control devices.

Each of the three terms *Activity*, *UEF* and *Abatement* have associated uncertainties (represented in the current work by high and low bound values for the factor concerned), which combine to generate an overall (uncertainty) range for the estimated emission value.

In general, uncertainties associated with *UEFs* and *Abatement* are likely to contribute more to uncertainty in the overall emission estimates than those associated with *Activity* data. This is particularly the case for sectors such as non-ferrous metal production where the metal and mercury (Hg) content of ores can vary widely but information on these values for different countries and regions is very limited compared with production statistics. The EMEP/EEA (2009) air pollutant emission inventory guidebook assigns uncertainties associated with activity data (not specific to Hg) of the order of ±5–10%.

Evaluation of uncertainties associated with (emission factor-based) estimates depends on the procedures involved. For estimates based on a small number of measurements at representative facilities or engineering calculations based on assumptions alone – which between them cover most Hg emissions estimates – the uncertainties are typically considered to be of the order of ±50% to ± an order of magnitude.

Three approaches to calculating, and combining, the uncertainties associated with country-sector based emission estimates were compared:

(i) Approach applied in the GMA 2013

A relatively crude (and intentionally conservative) approach was adopted to provide some quantification of the scale of uncertainties in the estimates presented in the GMA 2013 (see Table A3.7.1).

Of the three major components contributing to the uncertainties associated with the emission estimates, only those associated with *Activity* data and *UEFs* were addressed, by introducing into the emission calculations, respectively, the 'high' and 'low' bound values for each of these factors. The high and low bound values were established as described in Table A3.7.1. Uncertainties associated with *Abatement* were not considered.

For emissions based on Hg consumption in intentional use sectors, and associated waste handling, upper and lower range estimates were produced using the respective upper and lower ranges of the Hg consumption data. These however do not reflect the considerable uncertainties associated with the assumptions made regarding Hg flow in waste streams and associated emission factors. Consequently, uncertainties in estimates associated with these sectors were assigned at ± a factor of 3. Uncertainties associated with the assumptions regarding assignment of countries to particular 'country groupings' for applied technology or waste handling procedures were not taken into account.

Uncertainty ranges for combined country-sector estimates (e.g., global, regional or sectoral totals) were established by simply summing high/low range values to obtain a maximum and minimum range value for the aggregated emissions.

(ii) Introducing uncertainty associated with air pollution control technology assumptions

In a modified version of the GMA 2013 approach, an attempt was made to introduce uncertainties associated with *Abatement*. High range emissions estimates were established using the high *Activity* and *UEF* bounds (as described in '(i)') together with a low bound for *Abatement*; and conversely for the low bound emission estimate.

The high and low bounds for *Abatement* were established by considering 'average reduction efficiency' under various technology profiles, defined as the sum of the (weighted) abatement. The calculation of the average reduction efficiency for iron and steel production in country group 1 (48.7%) is illustrated in Table A3.7.2. The average reduction efficiency may also be derived by dividing the emission estimate by the activity data set and the unabated emission factor.

Uncertainty associated with the removal efficiency was then categorized into four different profiles, based on the average removal efficiency for that particular activity, see Table A3.7.3. It should be noted that this approach was only applied for 'by-product' sectors; no uncertainty on the removal efficiency was applied in the case of estimated emissions from ASGM or intentional-use waste streams.

As with approach '(i)', uncertainty ranges for combined country-sector estimates (e.g., global, regional or sectoral totals) were established by summing high/low range values to obtain a maximum and minimum range value for the aggregated emissions.

(iii) Employing the propagation of errors method to evaluate uncertainties associated with aggregated estimates

Error propagation is a method for combining uncertainties associated with individual estimates when these are aggregated. In the current assessment, an approach based on the procedure recommended in the IPCC guidelines for calculating the uncertainty for greenhouse gas emissions (Frey et al., 2006) was used to determine uncertainty ranges associated with aggregated inventory emissions estimates (i.e., regional, sectoral and global emission totals).

The combined uncertainty for one activity (i.e., a national-sector/activity emission estimate) is calculated according the following equation:

$$U_{combined} = \sqrt{U_{AD}^2 + U_{TF}^2 + U_{UEF}^2}$$

where:

U_{AD}: Uncertainty associated with the activity data, see Table A3.7.1

U_{UEF}: Uncertainty associated with the unabated emissions factor, see Table A3.7.1

U_{TF}: Uncertainty associated with the average reduction efficiency, see Table A3.7.3

Table A3.7.1 Procedures adopted for calculating low/high range emissions estimates.

		Lower range estimate	Upper range estimate	Source
Activity data derived from IEA/official national sources	OECD countries	0.95 × Activity data	1.05 × Activity data	Modified after EMEP/EEA, 2009
	Non-OECD countries	0.90 × Activity data	1.10 × Activity data	Modified after EMEP/EEA, 2009
Activity data derived from other sources		0.70 × Activity data	1.30 × Activity data	Based on AMAP/UNEP 2008
Unabated EFs	All countries	0.7 × UEF[a] for coal sectors; 0.5 × UEF[a] or 0.25 × UEF for all other sectors	1.3 × UEF[a] for coal sectors; 1.5 × UEF[a] or 1.75 × UEF for all other sectors	Assumptions applied in the GMA 2013
Emissions estimates for intentional-use waste stream emissions and emissions from cremations		0.3 × mid-range estimate	3 × mid-range estimate	
Emissions estimates for ASGM		Mid-range estimate minus 15–100% depending on country	Mid-range estimate plus 15–100% depending on country	

[a] UEF – as tabulated in this E-Annex, Section A3.6.

Table A3.7.2 Default technology profile applied for pig iron and steel production for country group 1.

Technology	Emission reduction efficiency, %	Degree of application, %	Weighted reduction efficiency, %
Standard APC: ESP/CYC/FGD (sinter plant)	20	30	6
Efficient APC: ESP+FGD/ACT/ESP+ACT (sinter plant)	55	60	33
Very efficient APC: ESP+ACT/RAC (sinter plant)	97	10	9.7
		Average reduction efficiency	48.7

Abbreviations. ACP: air pollution control; ACT: activated carbon tower; CYC: cyclone; ESP: electrostatic precipitator; FGD: flue gas desulfurization; RAC: regenerative activated carbon process.

Table A3.7.3 Procedures adopted for calculating low/high range technology profiles.

Abatement profile	Average reduction efficiency range, %	Upper range estimate	Lower range estimate	Source
Low	0–30	0 reduction	1.4 × Average reduction efficiency	Assumptions applied in this work
Medium	30–50	0.8 × Average reduction efficiency	1.2 × Average reduction efficiency	Assumptions applied in this work
High	50–85	0.9 × Average reduction efficiency	1.1 × Average reduction efficiency	Assumptions applied in this work
Very high	85–100	0.95 × Average reduction efficiency	1.05 × Average reduction efficiency (with a maximum bound of 99.99%)	Assumptions applied in this work

The maximum (i.e., quantitatively largest) uncertainty derived using the assumptions quantified in Tables A3.7.2 and A3.7.3 were employed. Uncertainties associated with *Activity* data and *Abatement* (technology profiles) were assumed to be symmetrically distributed around the mean. However, this was not always the case for *Abatement,* as cut-offs were applied to the bound values for technology profiles to eliminate cases where the (average) Hg removal efficiency would exceed 100% or be lower than 0%.

Since the unabated emission factor is dependent on the Hg content of the fuel/raw material, *UEFs* were assumed to be log-normally distributed. This reflects common properties of such materials; see for example Wu et al. (2010) for the Hg content of coal, Hylander and Herbert (2008) for the Hg content of non-ferrous metal ores, and Section A3.6.15 for the Hg content of crude oils. The uncertainty around the *UEF* was thus assigned to a high and a low range uncertainty using the geometric mean and geometric standard deviation. Although this is different

to the assumptions made in approaches '(i)' and '(ii)', the low and high bounds in Table A3.7.1 are still used to derive an asymmetric distribution with 'comparable spread'.

The geometric mean is calculated by the following equation:

$$\mu_g = e^{\ln(\mu) - \frac{\ln\left(1 + \left(\frac{U_{UEF}}{200}\right)^2\right)}{2}}$$

where:

μ_g: Geometric mean

μ: Arithmetic mean, the unabated emission factor used in this study

U_{UEF}:   The maximal uncertainty for the unabated emission factor

The geometric standard deviation is calculated by the following equation:

$$\sigma_g = e^{\sqrt{\ln\left(1 + \left(\frac{U_{UEF}}{200}\right)^2\right)}}$$

where:

σ_g Geometric standard deviation

The high and low uncertainty for the unabated emission factor is derived using two logarithmic transformations:

$$U_{UEF,low} = \frac{e^{\ln(\mu_g) - 1.96 \cdot \ln(\sigma_g)} - \mu}{\mu} \cdot 100$$

$$U_{UEF,high} = \frac{e^{\ln(\mu_g) + 1.96 \cdot \ln(\sigma_g)} - \mu}{\mu} \cdot 100$$

The following equation is used for combining the uncertainty:

$$U_{total} = \sqrt{\left(\frac{ee_1 \cdot U_{combined,1}}{EE}\right)^2 + \left(\frac{ee_2 \cdot U_{combined,2}}{EE}\right)^2 + \cdots + \left(\frac{ee_n \cdot U_{combined,n}}{EE}\right)^2}$$

where:

ee: Emission estimate for one activity in one country

EE: Emission estimate for the combined inventory. In this study the combined inventory is calculated at a global, sector and subcontinent level

The IPCC guidelines are primarily developed for calculating uncertainties associated with greenhouse gas emission estimates. Uncertainties associated with, for example, anthropogenic carbon dioxide emission factors are relatively small compared with those for Hg. The results of applying the error propagation method to Hg emissions may therefore be weak in some cases. Underestimation or overestimation of the uncertainties may also be a consequence where: (1) distributions are not distributed symmetrically around the mean or (2) correlations exist between the activity data, the technology profiles and the unabated emission factor.

Notwithstanding these limitations, the uncertainty estimates obtained using the propagation of errors approach are considered to better represent the scale of the uncertainties for aggregated inventory estimates than those achieved by simply summing uncertainties for individual (country-sector) emission estimates.

A3.8 Activity data and sources used to prepare estimates of 2015 mercury emissions to air

Country code	Country name	Sector code	Activity code	Activity amount	Units	Year	Source
AFG	Afghanistan	BIO	PSB – DR	106086.7325	TJ	2015	IEA (2017)#
		BIO	PSB – IND	4618.211542	TJ	2015	IEA (2017)#
		CEM	CEM	102	kt	2014	USGS (2017a)
		NFMP-AU	GP-L	40	kg	2015	USGS (2017b)
		OR	CO-OR	468.7363233	kt	2015	IEA (2017)#
		SC-DR-gas	NG-DR	2356.390576	TJ	2015	IEA (2017)#
		SC-DR-oil	CO-HF-DR	29.15584786	kt	2015	IEA (2017)#
		SC-DR-oil	CO-LF-DR	746.4644638	kt	2015	IEA (2017)#
		SC-IND-coal	BC-IND-OTH	8.971030111	kt	2015	IEA (2017)#
		SC-IND-coal	HC-IND-OTH	630.5886582	kt	2015	IEA (2017)#
		SC-IND-oil	CO-HF-IND	63.91858954	kt	2015	IEA (2017)#
		SC-IND-oil	CO-LF-IND	69.89927628	kt	2015	IEA (2017)#
		SC-PP-coal	HC-B-PP	165.964057	kt	2015	IEA (2017)#
		SC-PP-gas	NG-PP	2572.442884	TJ	2015	IEA (2017)#
		SC-PP-oil	CO-HF-PP	329.3115636	kt	2015	IEA (2017)#
		SC-PP-oil	CO-LF-PP	430.6094453	kt	2015	IEA (2017)#
ALB	Albania	BIO	PSB – DR	8136	TJ	2015	IEA (2017)
		BIO	PSB – IND	419	TJ	2015	IEA (2017)
		CEM	CEM	2200	kt	2014	USGS (2017a)
		CEM	PC-CEM	47	kt	2015	IEA (2017)
		OR	CO-OR	276	kt	2015	IEA (2017)
		SC-DR-coal	HC-DR	5	kt	2015	IEA (2017)
		SC-DR-oil	CO-LF-DR	737	kt	2015	IEA (2017)
		SC-IND-coal	HC-IND-CEM	196	kt	2015	IEA (2017)
		SC-IND-gas	NG-IND	519	TJ	2015	IEA (2017)
		SC-IND-oil	CO-HF-IND	1	kt	2015	IEA (2017)
		SC-IND-oil	CO-LF-IND	7	kt	2015	IEA (2017)
		SC-PP-gas	NG-PP	754	TJ	2015	IEA (2017)
		SSC	SP-S	560	kt	2014	World Steel Association (2015)
DZA	Algeria	BIO	PSB – DR	84	TJ	2015	IEA (2017)
		BIO	PSB – IND	167	TJ	2015	IEA (2017)
		CEM	CEM	21000	kt	2014	USGS (2017a)
		CSP	CSP-C	14	kt	2010	UNEP (2011e)
		NFMP	ZN-P	15000	t	2015	USGS (2017b)
		NFMP-AU	GP-L	200	kg	2015	USGS (2017b)
		OR	CO-OR	25106	kt	2015	IEA (2017)
		PISP	PIP	360	kt	2014	USGS (2017a)
		SC-DR-gas	NG-DR	380873	TJ	2015	IEA (2017)
		SC-DR-oil	CO-DR	6	kt	2015	IEA (2017)
		SC-DR-oil	CO-LF-DR	9525	kt	2015	IEA (2017)
		SC-IND-gas	NG-IND	159685	TJ	2015	IEA (2017)
		SC-IND-oil	CO-LF-IND	672	kt	2015	IEA (2017)
		SC-PP-gas	NG-PP	897524	TJ	2015	IEA (2017)
		SC-PP-oil	CO-LF-PP	421	kt	2015	IEA (2017)
		SC-PP-oil	CO-PP	608	kt	2015	IEA (2017)

Country code	Country name	Sector code	Activity code	Activity amount	Units	Year	Source
AGO	Angola	BIO	PSB – DR	185757	TJ	2015	IEA (2017)
		BIO	PSB – IND	5395	TJ	2015	IEA (2017)
		CEM	CEM	2500	kt	2014	USGS (2017a)
		CSP	CSP-C	10	kt	2010	UNEP (2011e)
		OR	CO-OR	2647	kt	2015	IEA (2017)
		SC-DR-oil	CO-LF-DR	2825	kt	2015	IEA (2017)
		SC-IND-gas	NG-IND	29260	TJ	2015	IEA (2017)
		SC-IND-oil	CO-HF-IND	39	kt	2015	IEA (2017)
		SC-IND-oil	CO-LF-IND	136	kt	2015	IEA (2017)
		SC-PP-oil	CO-HF-PP	42	kt	2015	IEA (2017)
		SC-PP-oil	CO-LF-PP	1136	kt	2015	IEA (2017)
ATG	Antigua	BIO	PSB – DR	96.11011345	TJ	2015	IEA (2017)[#]
		BIO	PSB – IND	386.7109149	TJ	2015	IEA (2017)[#]
		BIO	PSB – PP	126.9070198	TJ	2015	IEA (2017)[#]
		OR	CO-OR	47.13967581	kt	2015	IEA (2017)[#]
		SC-DR-coal	HC-DR	9.885696476	kt	2015	IEA (2017)[#]
		SC-DR-gas	NG-DR	23.47244188	TJ	2015	IEA (2017)[#]
		SC-DR-oil	CO-HF-DR	2.094014525	kt	2015	IEA (2017)[#]
		SC-DR-oil	CO-LF-DR	50.20765058	kt	2015	IEA (2017)[#]
		SC-IND-gas	NG-IND	1.071356268	TJ	2015	IEA (2017)[#]
		SC-IND-oil	CO-HF-IND	6.330741586	kt	2015	IEA (2017)[#]
		SC-IND-oil	CO-LF-IND	3.603652903	kt	2015	IEA (2017)[#]
		SC-PP-gas	NG-PP	1498.778721	TJ	2015	IEA (2017)[#]
		SC-PP-oil	CO-HF-PP	76.50457717	kt	2015	IEA (2017)[#]
		SC-PP-oil	CO-LF-PP	56.2949021	kt	2015	IEA (2017)[#]
ARG	Argentina	BIO	PSB – DR	10561	TJ	2015	IEA (2017)
		BIO	PSB – IND	34928	TJ	2015	IEA (2017)
		BIO	PSB – PP	30121	TJ	2015	IEA (2017)
		CEM	CEM	11408	kt	2014	USGS (2017a)
		CSP	CSP-P	100	kt	2015	UNEP (2013)
		NFMP	AL-P	440	kt	2015	USGS (2017b)
		NFMP	PB-P	8000	t	2015	USGS (2017b)
		NFMP	ZN-P	30000	t	2015	USGS (2017b)
		NFMP-AU	GP-L	64000	kg	2015	USGS (2017b)
		NFMP-HG	HG-P	25	t	2015	USGS (2017b)
		OR	CO-OR	26695	kt	2015	IEA (2017)
		PISP	PIP	2766	kt	2014	USGS (2017a)
		SC-DR-gas	NG-DR	615023	TJ	2015	IEA (2017)
		SC-DR-oil	CO-HF-DR	241	kt	2015	IEA (2017)
		SC-DR-oil	CO-LF-DR	10009	kt	2015	IEA (2017)
		SC-IND-coal	HC-IND-OTH	7	kt	2015	IEA (2017)
		SC-IND-gas	NG-IND	336216	TJ	2015	IEA (2017)
		SC-IND-oil	CO-HF-IND	177	kt	2015	IEA (2017)
		SC-IND-oil	CO-LF-IND	111	kt	2015	IEA (2017)
		SC-PP-coal	HC-B-PP	908	kt	2015	IEA (2017)
		SC-PP-gas	NG-PP	986403	TJ	2015	IEA (2017)
		SC-PP-oil	CO-HF-PP	3435	kt	2015	IEA (2017)
		SC-PP-oil	CO-LF-PP	1952	kt	2015	IEA (2017)
		SC-PP-oil	CO-PP	91	kt	2015	IEA (2017)
		SSC	SP-S	2740	kt	2014	World Steel Association (2015)

Country code	Country name	Sector code	Activity code	Activity amount	Units	Year	Source
ARM	Armenia	BIO	PSB – DR	7965	TJ	2015	IEA (2017)
		BIO	PSB – IND	1	TJ	2015	IEA (2017)
		CEM	CEM	427	kt	2014	USGS (2017a)
		NFMP	CU-P	11600	t	2015	USGS (2017b)
		NFMP-AU	GP-L	5500	kg	2015	USGS (2017b)
		SC-DR-gas	NG-DR	43451	TJ	2015	IEA (2017)
		SC-DR-oil	CO-LF-DR	128	kt	2015	IEA (2017)
		SC-IND-gas	NG-IND	7995	TJ	2015	IEA (2017)
		SC-IND-oil	CO-LF-IND	1	kt	2015	IEA (2017)
		SC-PP-gas	NG-PP	25295	TJ	2015	IEA (2017)
ABW	Aruba	BIO	PSB – DR	116.6201755	TJ	2015	IEA (2017)[#]
		BIO	PSB – IND	503.0365589	TJ	2015	IEA (2017)[#]
		BIO	PSB – PP	165.0816361	TJ	2015	IEA (2017)[#]
		OR	CO-OR	61.3196561	kt	2015	IEA (2017)[#]
		SC-DR-coal	HC-DR	12.85939069	kt	2015	IEA (2017)[#]
		SC-DR-gas	NG-DR	30.53313454	TJ	2015	IEA (2017)[#]
		SC-DR-oil	CO-HF-DR	2.723910343	kt	2015	IEA (2017)[#]
		SC-DR-oil	CO-LF-DR	65.31050148	kt	2015	IEA (2017)[#]
		SC-IND-gas	NG-IND	1.393628548	TJ	2015	IEA (2017)[#]
		SC-IND-oil	CO-HF-IND	8.235077781	kt	2015	IEA (2017)[#]
		SC-IND-oil	CO-LF-IND	4.68765966	kt	2015	IEA (2017)[#]
		SC-PP-gas	NG-PP	1949.622991	TJ	2015	IEA (2017)[#]
		SC-PP-oil	CO-HF-PP	99.51774765	kt	2015	IEA (2017)[#]
		SC-PP-oil	CO-LF-PP	73.2288455	kt	2015	IEA (2017)[#]
AUS	Australia (and Christmas Is.)	BIO	PSB – DR	50117	TJ	2015	IEA (2017)
		BIO	PSB – IND	115318	TJ	2015	IEA (2017)
		BIO	PSB – PP	20555	TJ	2015	IEA (2017)
		CEM	CEM	9000	kt	2014	USGS (2017a)
		NFMP	AL-P	1645	kt	2015	USGS (2017b)
		NFMP	CU-P	442000	t	2015	USGS (2017b)
		NFMP	PB-P	182000	t	2015	USGS (2017b)
		NFMP	ZN-P	489594	t	2015	USGS (2017b)
		NFMP-AU	GP-L	277800	kg	2015	USGS (2017b)
		OR	CO-OR	22850	kt	2015	IEA (2017)
		PISP	PIP	3282	kt	2014	USGS (2017a)
		SC-DR-coal	BC-DR	14	kt	2015	IEA (2017)
		SC-DR-coal	HC-DR	5	kt	2015	IEA (2017)
		SC-DR-gas	NG-DR	232516	TJ	2015	IEA (2017)
		SC-DR-oil	CO-HF-DR	58	kt	2015	IEA (2017)
		SC-DR-oil	CO-LF-DR	15378	kt	2015	IEA (2017)
		SC-IND-coal	BC-IND-CEM	414	kt	2015	IEA (2017)
		SC-IND-coal	BC-IND-NFM	1615	kt	2015	IEA (2017)
		SC-IND-coal	BC-IND-OTH	202	kt	2015	IEA (2017)
		SC-IND-coal	HC-IND-CEM	337	kt	2015	IEA (2017)
		SC-IND-coal	HC-IND-NFM	432	kt	2015	IEA (2017)
		SC-IND-coal	HC-IND-OTH	595	kt	2015	IEA (2017)
		SC-IND-coal	HC-IND-PIP	51	kt	2015	IEA (2017)
		SC-IND-gas	NG-IND	358622	TJ	2015	IEA (2017)
		SC-IND-oil	CO-HF-IND	242	kt	2015	IEA (2017)
		SC-IND-oil	CO-IND	15	kt	2015	IEA (2017)
		SC-IND-oil	CO-LF-IND	2945	kt	2015	IEA (2017)

Country code	Country name	Sector code	Activity code	Activity amount	Units	Year	Source
		SC-PP-coal	BC-L-PP	64847	kt	2015	IEA (2017)
		SC-PP-coal	BC-S-PP	20531	kt	2015	IEA (2017)
		SC-PP-coal	HC-B-PP	23625	kt	2015	IEA (2017)
		SC-PP-gas	NG-PP	887922	TJ	2015	IEA (2017)
		SC-PP-oil	CO-HF-PP	224	kt	2015	IEA (2017)
		SC-PP-oil	CO-LF-PP	3387	kt	2015	IEA (2017)
		SC-PP-oil	CO-PP	53	kt	2015	IEA (2017)
		SSC	SP-S	1034	kt	2014	World Steel Association (2015)
AUT	Austria	BIO	PSB – DR	76425	TJ	2015	IEA (2017)
		BIO	PSB – IND	45057	TJ	2015	IEA (2017)
		BIO	PSB – PP	69890	TJ	2015	IEA (2017)
		CEM	CEM	4400	kt	2014	USGS (2017a)
		CEM	PC-CEM	48	kt	2015	IEA (2017)
		OR	CO-OR	8881	kt	2015	IEA (2017)
		PISP	PIP	6029	kt	2014	USGS (2017a)
		SC-DR-coal	BC-DR	2	kt	2015	IEA (2017)
		SC-DR-coal	HC-DR	7	kt	2015	IEA (2017)
		SC-DR-gas	NG-DR	85850	TJ	2015	IEA (2017)
		SC-DR-oil	CO-HF-DR	30	kt	2015	IEA (2017)
		SC-DR-oil	CO-LF-DR	6797	kt	2015	IEA (2017)
		SC-IND-coal	BC-IND-CEM	91	kt	2015	IEA (2017)
		SC-IND-coal	HC-IND-CEM	29	kt	2015	IEA (2017)
		SC-IND-coal	HC-IND-OTH	130	kt	2015	IEA (2017)
		SC-IND-gas	NG-IND	116443	TJ	2015	IEA (2017)
		SC-IND-oil	CO-HF-IND	123	kt	2015	IEA (2017)
		SC-IND-oil	CO-LF-IND	358	kt	2015	IEA (2017)
		SC-PP-coal	HC-B-PP	966	kt	2015	IEA (2017)
		SC-PP-gas	NG-PP	100856	TJ	2015	IEA (2017)
		SC-PP-oil	CO-HF-PP	288	kt	2015	IEA (2017)
		SC-PP-oil	CO-LF-PP	4	kt	2015	IEA (2017)
		SSC	SP-S	691	kt	2014	World Steel Association (2015)
AZE	Azerbaijan	BIO	PSB – DR	3020	TJ	2015	IEA (2017)
		BIO	PSB – IND	11	TJ	2015	IEA (2017)
		CEM	CEM	2867	kt	2014	USGS (2017a)
		CSP	CSP-C	145	kt	2010	UNEP (2011e)
		NFMP	AL-P	50	kt	2015	USGS (2017b)
		NFMP-AU	GP-L	2229	kg	2015	USGS (2017b)
		OR	CO-OR	6215	kt	2015	IEA (2017)
		SC-DR-gas	NG-DR	118375	TJ	2015	IEA (2017)
		SC-DR-oil	CO-HF-DR	3	kt	2015	IEA (2017)
		SC-DR-oil	CO-LF-DR	1082	kt	2015	IEA (2017)
		SC-IND-gas	NG-IND	42204	TJ	2015	IEA (2017)
		SC-IND-oil	CO-HF-IND	13	kt	2015	IEA (2017)
		SC-IND-oil	CO-LF-IND	50	kt	2015	IEA (2017)
		SC-PP-gas	NG-PP	239641	TJ	2015	IEA (2017)
		SC-PP-oil	CO-HF-PP	389	kt	2015	IEA (2017)
		SC-PP-oil	CO-LF-PP	5	kt	2015	IEA (2017)
		SSC	SP-S	180	kt	2014	World Steel Association (2015)

Country code	Country name	Sector code	Activity code	Activity amount	Units	Year	Source
BHS	Bahamas	BIO	PSB – DR	337.4989668	TJ	2015	IEA (2017)#
		BIO	PSB – IND	1450.034468	TJ	2015	IEA (2017)#
		BIO	PSB – PP	475.858182	TJ	2015	IEA (2017)#
		OR	CO-OR	176.7577591	kt	2015	IEA (2017)#
		SC-DR-coal	HC-DR	37.06800113	kt	2015	IEA (2017)#
		SC-DR-gas	NG-DR	88.01367757	TJ	2015	IEA (2017)#
		SC-DR-oil	CO-HF-DR	7.851842604	kt	2015	IEA (2017)#
		SC-DR-oil	CO-LF-DR	188.2616215	kt	2015	IEA (2017)#
		SC-IND-gas	NG-IND	4.017221798	TJ	2015	IEA (2017)#
		SC-IND-oil	CO-HF-IND	23.7381288	kt	2015	IEA (2017)#
		SC-IND-oil	CO-LF-IND	13.51247332	kt	2015	IEA (2017)#
		SC-PP-gas	NG-PP	5619.910694	TJ	2015	IEA (2017)#
		SC-PP-oil	CO-HF-PP	286.8661565	kt	2015	IEA (2017)#
		SC-PP-oil	CO-LF-PP	211.0867454	kt	2015	IEA (2017)#
BHR	Bahrain	CEM	CEM	1500	kt	2014	USGS (2017a)
		NFMP	AL-P	960.643	kt	2015	USGS (2017b)
		OR	CO-OR	13356	kt	2015	IEA (2017)
		SC-DR-oil	CO-LF-DR	322	kt	2015	IEA (2017)
		SC-IND-gas	NG-IND	41447	TJ	2015	IEA (2017)
		SC-PP-gas	NG-PP	467228	TJ	2015	IEA (2017)
		SC-PP-oil	CO-HF-PP	4	kt	2015	IEA (2017)
BGD	Bangladesh	BIO	PSB – DR	380136	TJ	2015	IEA (2017)
		CEM	CEM	17000	kt	2014	USGS (2017a)
		OR	CO-OR	1209	kt	2015	IEA (2017)
		SC-DR-gas	NG-DR	187182	TJ	2015	IEA (2017)
		SC-DR-oil	CO-LF-DR	2759	kt	2015	IEA (2017)
		SC-IND-coal	BC-IND-OTH	32	kt	2015	IEA (2017)
		SC-IND-coal	HC-IND-CEM	3978	kt	2015	IEA (2017)
		SC-IND-gas	NG-IND	162597	TJ	2015	IEA (2017)
		SC-IND-oil	CO-HF-IND	13	kt	2015	IEA (2017)
		SC-IND-oil	CO-LF-IND	199	kt	2015	IEA (2017)
		SC-PP-coal	HC-B-PP	546	kt	2015	IEA (2017)
		SC-PP-gas	NG-PP	556783	TJ	2015	IEA (2017)
		SC-PP-oil	CO-HF-PP	923	kt	2015	IEA (2017)
		SC-PP-oil	CO-LF-PP	470	kt	2015	IEA (2017)
		SSC	SP-S	90	kt	2014	World Steel Association (2015)
BRB	Barbados	BIO	PSB – DR	302.1548251	TJ	2015	IEA (2017)#
		BIO	PSB – IND	855.1512978	TJ	2015	IEA (2017)#
		BIO	PSB – PP	280.63522	TJ	2015	IEA (2017)#
		CEM	CEM	160	kt	2014	USGS (2017a)
		OR	CO-OR	104.2420925	kt	2015	IEA (2017)#
		SC-DR-coal	HC-DR	21.86068675	kt	2015	IEA (2017)#
		SC-DR-gas	NG-DR	51.90567001	TJ	2015	IEA (2017)#
		SC-DR-oil	CO-HF-DR	4.630588818	kt	2015	IEA (2017)#
		SC-DR-oil	CO-LF-DR	111.0264435	kt	2015	IEA (2017)#
		SC-IND-gas	NG-IND	2.369138465	TJ	2015	IEA (2017)#
		SC-IND-oil	CO-HF-IND	13.99945457	kt	2015	IEA (2017)#
		SC-IND-oil	CO-LF-IND	7.968920292	kt	2015	IEA (2017)#
		SC-PP-gas	NG-PP	3314.317025	TJ	2015	IEA (2017)#
		SC-PP-oil	CO-HF-PP	169.178024	kt	2015	IEA (2017)#
		SC-PP-oil	CO-LF-PP	124.4874575	kt	2015	IEA (2017)#

Country code	Country name	Sector code	Activity code	Activity amount	Units	Year	Source
BLR	Belarus	BIO	PSB – DR	23529	TJ	2015	IEA (2017)
		BIO	PSB – IND	2136	TJ	2015	IEA (2017)
		BIO	PSB – PP	29984	TJ	2015	IEA (2017)
		CEM	CEM	5618	kt	2014	USGS (2017a)
		OR	CO-OR	23003	kt	2015	IEA (2017)
		SC-DR-coal	HC-DR	11	kt	2015	IEA (2017)
		SC-DR-gas	NG-DR	95481	TJ	2015	IEA (2017)
		SC-DR-oil	CO-HF-DR	10	kt	2015	IEA (2017)
		SC-DR-oil	CO-LF-DR	2584	kt	2015	IEA (2017)
		SC-IND-coal	HC-IND-CEM	633	kt	2015	IEA (2017)
		SC-IND-gas	NG-IND	43299	TJ	2015	IEA (2017)
		SC-IND-oil	CO-HF-IND	22	kt	2015	IEA (2017)
		SC-IND-oil	CO-LF-IND	118	kt	2015	IEA (2017)
		SC-PP-coal	HC-B-PP	2	kt	2015	IEA (2017)
		SC-PP-gas	NG-PP	530949	TJ	2015	IEA (2017)
		SC-PP-oil	CO-HF-PP	490	kt	2015	IEA (2017)
		SC-PP-oil	CO-LF-PP	17	kt	2015	IEA (2017)
		SSC	SP-S	2513	kt	2014	World Steel Association (2015)
BEL	Belgium	BIO	PSB – DR	22916	TJ	2015	IEA (2017)
		BIO	PSB – IND	26672	TJ	2015	IEA (2017)
		BIO	PSB – PP	31708	TJ	2015	IEA (2017)
		CEM	CEM	6100	kt	2014	USGS (2017a)
		CEM	PC-CEM	25	kt	2015	IEA (2017)
		CSP	CSP-C	315	kt	2015	OSPAR (2016)
		NFMP	ZN-P	260000	t	2015	USGS (2017b)
		OR	CO-OR	32051	kt	2015	IEA (2017)
		PISP	PIP	4388	kt	2014	USGS (2017a)
		SC-DR-coal	HC-DR	120	kt	2015	IEA (2017)
		SC-DR-gas	NG-DR	239014	TJ	2015	IEA (2017)
		SC-DR-oil	CO-HF-DR	1	kt	2015	IEA (2017)
		SC-DR-oil	CO-LF-DR	10638	kt	2015	IEA (2017)
		SC-IND-coal	HC-IND-CEM	235	kt	2015	IEA (2017)
		SC-IND-coal	HC-IND-OTH	70	kt	2015	IEA (2017)
		SC-IND-coal	HC-IND-PIP	77	kt	2015	IEA (2017)
		SC-IND-gas	NG-IND	173874	TJ	2015	IEA (2017)
		SC-IND-oil	CO-HF-IND	56	kt	2015	IEA (2017)
		SC-IND-oil	CO-LF-IND	241	kt	2015	IEA (2017)
		SC-PP-coal	HC-B-PP	775	kt	2015	IEA (2017)
		SC-PP-gas	NG-PP	186523	TJ	2015	IEA (2017)
		SC-PP-oil	CO-HF-PP	32	kt	2015	IEA (2017)
		SC-PP-oil	CO-LF-PP	6	kt	2015	IEA (2017)
		SSC	SP-S	2379	kt	2014	World Steel Association (2015)
BLZ	Belize	BIO	PSB – DR	361.1761002	TJ	2015	IEA (2017)[#]
		BIO	PSB – IND	517.253726	TJ	2015	IEA (2017)[#]
		BIO	PSB – PP	169.7472875	TJ	2015	IEA (2017)[#]
		OR	CO-OR	63.05271462	kt	2015	IEA (2017)[#]
		SC-DR-coal	HC-DR	13.22283168	kt	2015	IEA (2017)[#]
		SC-DR-gas	NG-DR	31.3960831	TJ	2015	IEA (2017)[#]
		SC-DR-oil	CO-HF-DR	2.800895381	kt	2015	IEA (2017)[#]
		SC-DR-oil	CO-LF-DR	67.15635203	kt	2015	IEA (2017)[#]
		SC-IND-gas	NG-IND	1.433016241	TJ	2015	IEA (2017)[#]
		SC-IND-oil	CO-HF-IND	8.467823244	kt	2015	IEA (2017)[#]
		SC-IND-oil	CO-LF-IND	4.820145539	kt	2015	IEA (2017)[#]
		SC-PP-gas	NG-PP	2004.724584	TJ	2015	IEA (2017)[#]
		SC-PP-oil	CO-HF-PP	102.330387	kt	2015	IEA (2017)[#]
		SC-PP-oil	CO-LF-PP	75.29848977	kt	2015	IEA (2017)[#]

Country code	Country name	Sector code	Activity code	Activity amount	Units	Year	Source
BEN	Benin	BIO	PSB – DR	60207	TJ	2015	IEA (2017)
		BIO	PSB – IND	377	TJ	2015	IEA (2017)
		CEM	CEM	1396	kt	2014	USGS (2017a)
		SC-DR-oil	CO-LF-DR	669	kt	2015	IEA (2017)
		SC-IND-coal	HC-IND-OTH	41	kt	2015	IEA (2017)
		SC-IND-oil	CO-HF-IND	25	kt	2015	IEA (2017)
		SC-IND-oil	CO-LF-IND	41	kt	2015	IEA (2017)
		SC-PP-oil	CO-LF-PP	72	kt	2015	IEA (2017)
BMU	Bermuda	BIO	PSB – DR	72.98612579	TJ	2015	IEA (2017)[#]
		BIO	PSB – IND	1066.415553	TJ	2015	IEA (2017)[#]
		BIO	PSB – PP	349.9658648	TJ	2015	IEA (2017)[#]
		OR	CO-OR	129.994995	kt	2015	IEA (2017)[#]
		SC-DR-coal	HC-DR	27.2613471	kt	2015	IEA (2017)[#]
		SC-DR-gas	NG-DR	64.72891282	TJ	2015	IEA (2017)[#]
		SC-DR-oil	CO-HF-DR	5.774571061	kt	2015	IEA (2017)[#]
		SC-DR-oil	CO-LF-DR	138.4554131	kt	2015	IEA (2017)[#]
		SC-IND-gas	NG-IND	2.954431706	TJ	2015	IEA (2017)[#]
		SC-IND-oil	CO-HF-IND	17.45800553	kt	2015	IEA (2017)[#]
		SC-IND-oil	CO-LF-IND	9.937633919	kt	2015	IEA (2017)[#]
		SC-PP-gas	NG-PP	4133.115664	TJ	2015	IEA (2017)[#]
		SC-PP-oil	CO-HF-PP	210.9732822	kt	2015	IEA (2017)[#]
		SC-PP-oil	CO-LF-PP	155.2419569	kt	2015	IEA (2017)[#]
BTN	Bhutan	BIO	PSB – DR	2416.992257	TJ	2015	IEA (2017)[#]
		BIO	PSB – IND	454.0966101	TJ	2015	IEA (2017)[#]
		CEM	CEM	690	kt	2014	USGS (2017a)
		OR	CO-OR	46.08961142	kt	2015	IEA (2017)[#]
		SC-DR-gas	NG-DR	231.6976957	TJ	2015	IEA (2017)[#]
		SC-DR-oil	CO-HF-DR	2.866817935	kt	2015	IEA (2017)[#]
		SC-DR-oil	CO-LF-DR	73.39788995	kt	2015	IEA (2017)[#]
		SC-IND-coal	BC-IND-OTH	0.882097826	kt	2015	IEA (2017)[#]
		SC-IND-coal	HC-IND-OTH	62.00412636	kt	2015	IEA (2017)[#]
		SC-IND-oil	CO-HF-IND	6.284947011	kt	2015	IEA (2017)[#]
		SC-IND-oil	CO-LF-IND	6.873012229	kt	2015	IEA (2017)[#]
		SC-PP-coal	HC-B-PP	16.31880978	kt	2015	IEA (2017)[#]
		SC-PP-gas	NG-PP	252.9415516	TJ	2015	IEA (2017)[#]
		SC-PP-oil	CO-HF-PP	32.38034103	kt	2015	IEA (2017)[#]
		SC-PP-oil	CO-LF-PP	42.34069566	kt	2015	IEA (2017)[#]
BOL	Bolivia	BIO	PSB – DR	18647	TJ	2015	IEA (2017)
		BIO	PSB – IND	20567	TJ	2015	IEA (2017)
		BIO	PSB – PP	4611	TJ	2015	IEA (2017)
		CEM	CEM	3500	kt	2014	USGS (2017a)
		NFMP-AU	GP-L	12170	kg	2015	USGS (2017b)
		OR	CO-OR	2943	kt	2015	IEA (2017)
		SC-DR-gas	NG-DR	30086	TJ	2015	IEA (2017)
		SC-DR-oil	CO-LF-DR	1425	kt	2015	IEA (2017)
		SC-IND-gas	NG-IND	31751	TJ	2015	IEA (2017)
		SC-IND-oil	CO-LF-IND	88	kt	2015	IEA (2017)
		SC-PP-gas	NG-PP	74155	TJ	2015	IEA (2017)
		SC-PP-oil	CO-LF-PP	57	kt	2015	IEA (2017)

Country code	Country name	Sector code	Activity code	Activity amount	Units	Year	Source
BIH	Bosnia-Herzegovina	BIO	PSB – DR	56406	TJ	2015	IEA (2017)
		BIO	PSB – IND	1532	TJ	2015	IEA (2017)
		BIO	PSB – PP	128	TJ	2015	IEA (2017)
		CEM	CEM	840	kt	2014	USGS (2017a)
		CEM	PC-CEM	3	kt	2015	IEA (2017)
		NFMP	AL-P	100	kt	2015	USGS (2017b)
		OR	CO-OR	926	kt	2015	IEA (2017)
		PISP	PIP	860	kt	2014	USGS (2017a)
		SC-DR-coal	BC-DR	641	kt	2015	IEA (2017)
		SC-DR-gas	NG-DR	2754	TJ	2015	IEA (2017)
		SC-DR-oil	CO-HF-DR	3	kt	2015	IEA (2017)
		SC-DR-oil	CO-LF-DR	873	kt	2015	IEA (2017)
		SC-IND-coal	BC-IND-CEM	68	kt	2015	IEA (2017)
		SC-IND-coal	BC-IND-NFM	163	kt	2015	IEA (2017)
		SC-IND-coal	BC-IND-OTH	36	kt	2015	IEA (2017)
		SC-IND-gas	NG-IND	3378	TJ	2015	IEA (2017)
		SC-IND-oil	CO-HF-IND	20	kt	2015	IEA (2017)
		SC-IND-oil	CO-LF-IND	65	kt	2015	IEA (2017)
		SC-PP-coal	BC-L-PP	5151	kt	2015	IEA (2017)
		SC-PP-coal	BC-S-PP	5759	kt	2015	IEA (2017)
		SC-PP-gas	NG-PP	2056	TJ	2015	IEA (2017)
		SC-PP-oil	CO-HF-PP	114	kt	2015	IEA (2017)
		SC-PP-oil	CO-LF-PP	48	kt	2015	IEA (2017)
BWA	Botswana	BIO	PSB – DR	23156	TJ	2015	IEA (2017)
		CEM	CEM	370	kt	2014	USGS (2017a)
		NFMP	CU-P	13900	t	2015	USGS (2017b)
		NFMP-AU	GP-L	756	kg	2015	USGS (2017b)
		SC-DR-coal	HC-DR	7	kt	2015	IEA (2017)
		SC-DR-oil	CO-LF-DR	367	kt	2015	IEA (2017)
		SC-IND-coal	HC-IND-OTH	75	kt	2015	IEA (2017)
		SC-IND-oil	CO-HF-IND	11	kt	2015	IEA (2017)
		SC-IND-oil	CO-LF-IND	158	kt	2015	IEA (2017)
		SC-PP-coal	HC-B-PP	1657	kt	2015	IEA (2017)
		SC-PP-oil	CO-LF-PP	36	kt	2015	IEA (2017)
BRA	Brazil	BIO	PSB – DR	386923	TJ	2015	IEA (2017)
		BIO	PSB – IND	1242148	TJ	2015	IEA (2017)
		BIO	PSB – PP	913298	TJ	2015	IEA (2017)
		CEM	CEM	71254	kt	2015	National information
		CEM	PC-CEM	4366	kt	2015	IEA (2017)
		CSP	CSP-P	221.3	kt	2015	National information
		NFMP	AL-P	772.2	kt	2015	USGS (2017b)
		NFMP	CU-P	156000	t	2015	USGS (2017b)
		NFMP	ZN-P	230000	t	2015	USGS (2017b)
		NFMP-AU	GP-L	73.09	t	2015	National information
		OR	CO-OR	98480.796	kt	2015	National information
		PISP	PIP	27803.302	kt	2015	National information
		SC-DR-gas	NG-DR	123097	TJ	2015	IEA (2017)
		SC-DR-oil	CO-HF-DR	809	kt	2015	IEA (2017)
		SC-DR-oil	CO-LF-DR	41833	kt	2015	IEA (2017)
		SC-IND-coal	BC-IND-CEM	156	kt	2015	IEA (2017)
		SC-IND-coal	BC-IND-OTH	1483	kt	2015	IEA (2017)

Country code	Country name	Sector code	Activity code	Activity amount	Units	Year	Source
		SC-IND-coal	HC-IND-CEM	114	kt	2015	IEA (2017)
		SC-IND-coal	HC-IND-NFM	1209	kt	2015	IEA (2017)
		SC-IND-coal	HC-IND-OTH	398	kt	2015	IEA (2017)
		SC-IND-coal	HC-IND-PIP	3727	kt	2015	IEA (2017)
		SC-IND-gas	NG-IND	438042	TJ	2015	IEA (2017)
		SC-IND-oil	CO-HF-IND	2304	kt	2015	IEA (2017)
		SC-IND-oil	CO-LF-IND	1108	kt	2015	IEA (2017)
		SC-PP-coal	BC-L-PP	2700	kt	2015	IEA (2017)
		SC-PP-coal	BC-S-PP	3081	kt	2015	IEA (2017)
		SC-PP-coal	HC-B-PP	4131	kt	2015	IEA (2017)
		SC-PP-gas	NG-PP	957940	TJ	2015	IEA (2017)
		SC-PP-oil	CO-HF-PP	3716	kt	2015	IEA (2017)
		SC-PP-oil	CO-LF-PP	3733	kt	2015	IEA (2017)
		SSC	SP-S	7877	kt	2014	World Steel Association (2015)
VGB	British Virgin Islands	BIO	PSB – DR	34.78371776	TJ	2015	IEA (2017)[#]
		BIO	PSB – IND	250.8543886	TJ	2015	IEA (2017)[#]
		BIO	PSB – PP	82.32294883	TJ	2015	IEA (2017)[#]
		OR	CO-OR	30.57890041	kt	2015	IEA (2017)[#]
		SC-DR-coal	HC-DR	6.41272395	kt	2015	IEA (2017)[#]
		SC-DR-gas	NG-DR	15.22627066	TJ	2015	IEA (2017)[#]
		SC-DR-oil	CO-HF-DR	1.358360245	kt	2015	IEA (2017)[#]
		SC-DR-oil	CO-LF-DR	32.56905612	kt	2015	IEA (2017)[#]
		SC-IND-gas	NG-IND	0.694975009	TJ	2015	IEA (2017)[#]
		SC-IND-oil	CO-HF-IND	4.10667051	kt	2015	IEA (2017)[#]
		SC-IND-oil	CO-LF-IND	2.337643213	kt	2015	IEA (2017)[#]
		SC-PP-gas	NG-PP	972.2384483	TJ	2015	IEA (2017)[#]
		SC-PP-oil	CO-HF-PP	49.62753362	kt	2015	IEA (2017)[#]
		SC-PP-oil	CO-LF-PP	36.51777776	kt	2015	IEA (2017)[#]
BRN	Brunei Darussalam	CEM	CEM	350	kt	2014	USGS (2017a)
		OR	CO-OR	348	kt	2015	IEA (2017)
		SC-DR-gas	NG-DR	736	TJ	2015	IEA (2017)
		SC-DR-oil	CO-LF-DR	164	kt	2015	IEA (2017)
		SC-IND-oil	CO-LF-IND	119	kt	2015	IEA (2017)
		SC-PP-gas	NG-PP	79669	TJ	2015	IEA (2017)
		SC-PP-oil	CO-LF-PP	11	kt	2015	IEA (2017)
BGR	Bulgaria	BIO	PSB – DR	30961	TJ	2015	IEA (2017)
		BIO	PSB – IND	10572	TJ	2015	IEA (2017)
		BIO	PSB – PP	1603	TJ	2015	IEA (2017)
		CEM	CEM	1850	kt	2014	USGS (2017a)
		CEM	PC-CEM	112	kt	2015	IEA (2017)
		NFMP	CU-P	302000	t	2015	USGS (2017b)
		NFMP	PB-T	90000	t	2015	USGS (2017b)
		NFMP	ZN-P	75100	t	2015	USGS (2017b)
		NFMP-AU	GP-L	7300	kg	2015	USGS (2017b)
		OR	CO-OR	6037	kt	2015	IEA (2017)
		SC-DR-coal	BC-DR	93	kt	2015	IEA (2017)
		SC-DR-coal	HC-DR	155	kt	2015	IEA (2017)
		SC-DR-gas	NG-DR	18365	TJ	2015	IEA (2017)
		SC-DR-oil	CO-HF-DR	20	kt	2015	IEA (2017)
		SC-DR-oil	CO-LF-DR	1937	kt	2015	IEA (2017)
		SC-IND-coal	BC-IND-CEM	12	kt	2015	IEA (2017)

Country code	Country name	Sector code	Activity code	Activity amount	Units	Year	Source
		SC-IND-coal	BC-IND-OTH	3	kt	2015	IEA (2017)
		SC-IND-coal	HC-IND-CEM	103	kt	2015	IEA (2017)
		SC-IND-coal	HC-IND-OTH	150	kt	2015	IEA (2017)
		SC-IND-gas	NG-IND	42746	TJ	2015	IEA (2017)
		SC-IND-oil	CO-HF-IND	29	kt	2015	IEA (2017)
		SC-IND-oil	CO-LF-IND	45	kt	2015	IEA (2017)
		SC-PP-coal	BC-L-PP	33410	kt	2015	IEA (2017)
		SC-PP-coal	HC-A-PP	50	kt	2015	IEA (2017)
		SC-PP-coal	HC-B-PP	595	kt	2015	IEA (2017)
		SC-PP-gas	NG-PP	40675	TJ	2015	IEA (2017)
		SC-PP-oil	CO-HF-PP	39	kt	2015	IEA (2017)
		SC-PP-oil	CO-LF-PP	2	kt	2015	IEA (2017)
		SSC	SP-S	612	kt	2014	World Steel Association (2015)
BFA	Burkina Faso	BIO	PSB – DR	172942.8463	TJ	2015	IEA (2017)#
		BIO	PSB – IND	4460.436244	TJ	2015	IEA (2017)#
		BIO	PSB – PP	1595.745004	TJ	2015	IEA (2017)#
		CEM	CEM	403	kt	2014	USGS (2017a)
		NFMP-AU	GP-L	36210	kg	2015	USGS (2017b)
		SC-DR-coal	HC-DR	7.252601469	kt	2015	IEA (2017)#
		SC-DR-oil	CO-LF-DR	243.3075112	kt	2015	IEA (2017)#
		SC-IND-coal	HC-IND-OTH	7.51162295	kt	2015	IEA (2017)#
		SC-IND-gas	NG-IND	2.417533823	TJ	2015	IEA (2017)#
		SC-IND-oil	CO-HF-IND	44.29267325	kt	2015	IEA (2017)#
		SC-IND-oil	CO-IND	12.17400961	kt	2015	IEA (2017)#
		SC-IND-oil	CO-LF-IND	42.39318239	kt	2015	IEA (2017)#
		SC-PP-coal	HC-B-PP	63.54660334	kt	2015	IEA (2017)#
		SC-PP-gas	NG-PP	1672.847065	TJ	2015	IEA (2017)#
		SC-PP-oil	CO-HF-PP	57.58910928	kt	2015	IEA (2017)#
		SC-PP-oil	CO-LF-PP	119.1498813	kt	2015	IEA (2017)#
BDI	Burundi	BIO	PSB – DR	98131.76638	TJ	2015	IEA (2017)#
		BIO	PSB – IND	1191.037445	TJ	2015	IEA (2017)#
		BIO	PSB – PP	426.1000379	TJ	2015	IEA (2017)#
		CEM	CEM	70	kt	2014	USGS (2017a)
		NFMP-AU	GP-L	500	kg	2015	USGS (2017b)
		SC-DR-coal	HC-DR	1.936608764	kt	2015	IEA (2017)#
		SC-DR-oil	CO-LF-DR	64.96861307	kt	2015	IEA (2017)#
		SC-IND-coal	HC-IND-OTH	2.005773363	kt	2015	IEA (2017)#
		SC-IND-gas	NG-IND	0.645536255	TJ	2015	IEA (2017)#
		SC-IND-oil	CO-HF-IND	11.82714638	kt	2015	IEA (2017)#
		SC-IND-oil	CO-IND	3.25073614	kt	2015	IEA (2017)#
		SC-IND-oil	CO-LF-IND	11.31993933	kt	2015	IEA (2017)#
		SC-PP-coal	HC-B-PP	16.96838155	kt	2015	IEA (2017)#
		SC-PP-gas	NG-PP	446.6880335	TJ	2015	IEA (2017)#
		SC-PP-oil	CO-HF-PP	15.37759578	kt	2015	IEA (2017)#
		SC-PP-oil	CO-LF-PP	31.81571541	kt	2015	IEA (2017)#
KHM	Cambodia	BIO	PSB – DR	88123	TJ	2015	IEA (2017)
		BIO	PSB – IND	37089	TJ	2015	IEA (2017)
		BIO	PSB – PP	545	TJ	2015	IEA (2017)
		CEM	CEM	1400	kt	2014	USGS (2017a)
		SC-DR-oil	CO-LF-DR	1029	kt	2015	IEA (2017)

Country code	Country name	Sector code	Activity code	Activity amount	Units	Year	Source
		SC-IND-coal	BC-IND-CEM	27	kt	2015	IEA (2017)
		SC-IND-oil	CO-HF-IND	26	kt	2015	IEA (2017)
		SC-IND-oil	CO-LF-IND	29	kt	2015	IEA (2017)
		SC-PP-coal	BC-S-PP	1208	kt	2015	IEA (2017)
		SC-PP-oil	CO-HF-PP	45	kt	2015	IEA (2017)
		SC-PP-oil	CO-LF-PP	15	kt	2015	IEA (2017)
CMR	Cameroon	BIO	PSB – DR	197640	TJ	2015	IEA (2017)
		BIO	PSB – PP	717	TJ	2015	IEA (2017)
		CEM	CEM	1300	kt	2014	USGS (2017a)
		NFMP	AL-P	90	kt	2015	USGS (2017b)
		NFMP-AU	GP-L	1500	kg	2015	USGS (2017b)
		OR	CO-OR	1793	kt	2015	IEA (2017)
		SC-DR-oil	CO-LF-DR	630	kt	2015	IEA (2017)
		SC-IND-oil	CO-HF-IND	113	kt	2015	IEA (2017)
		SC-IND-oil	CO-LF-IND	8	kt	2015	IEA (2017)
		SC-PP-gas	NG-PP	10984	TJ	2015	IEA (2017)
		SC-PP-oil	CO-HF-PP	94	kt	2015	IEA (2017)
		SC-PP-oil	CO-LF-PP	210	kt	2015	IEA (2017)
CAN	Canada	BIO	PSB – DR	125680	TJ	2015	IEA (2017)
		BIO	PSB – IND	236905	TJ	2015	IEA (2017)
		BIO	PSB – PP	110778	TJ	2015	IEA (2017)
		CEM	CEM	11879	kt	2014	USGS (2017a)
		CEM	PC-CEM	452	kt	2015	IEA (2017)
		NFMP	AL-P	2880.035	kt	2015	USGS (2017b)
		NFMP	CU-P	280000	t	2015	USGS (2017b)
		NFMP	PB-P	128000	t	2015	USGS (2017b)
		NFMP	ZN-P	683118	t	2015	USGS (2017b)
		NFMP-AU	GP-L	152747	kg	2015	USGS (2017b)
		OR	CO-OR	65871	kt	2015	IEA (2017)
		PISP	PIP	6728	kt	2014	USGS (2017a)
		SC-DR-coal	BC-DR	19	kt	2015	IEA (2017)
		SC-DR-gas	NG-DR	1403184	TJ	2015	IEA (2017)
		SC-DR-oil	CO-HF-DR	1001	kt	2015	IEA (2017)
		SC-DR-oil	CO-LF-DR	23337	kt	2015	IEA (2017)
		SC-IND-coal	BC-IND-CEM	413	kt	2015	IEA (2017)
		SC-IND-coal	BC-IND-OTH	217	kt	2015	IEA (2017)
		SC-IND-coal	HC-IND-CEM	413	kt	2015	IEA (2017)
		SC-IND-coal	HC-IND-NFM	298	kt	2015	IEA (2017)
		SC-IND-coal	HC-IND-OTH	279	kt	2015	IEA (2017)
		SC-IND-gas	NG-IND	661611	TJ	2015	IEA (2017)
		SC-IND-oil	CO-HF-IND	614	kt	2015	IEA (2017)
		SC-IND-oil	CO-LF-IND	2811	kt	2015	IEA (2017)
		SC-PP-coal	BC-L-PP	8847	kt	2015	IEA (2017)
		SC-PP-coal	BC-S-PP	24479	kt	2015	IEA (2017)
		SC-PP-coal	HC-B-PP	2899	kt	2015	IEA (2017)
		SC-PP-gas	NG-PP	2136026	TJ	2015	IEA (2017)
		SC-PP-oil	CO-HF-PP	800	kt	2015	IEA (2017)
		SC-PP-oil	CO-LF-PP	1948	kt	2015	IEA (2017)
		SSC	SP-S	5007	kt	2014	World Steel Association (2015)

Country code	Country name	Sector code	Activity code	Activity amount	Units	Year	Source
CPV	Cape Verde	BIO	PSB – DR	4987.7007	TJ	2015	IEA (2017)#
		BIO	PSB – IND	491.8577893	TJ	2015	IEA (2017)#
		BIO	PSB – PP	175.9647638	TJ	2015	IEA (2017)#
		SC-DR-coal	HC-DR	0.799753282	kt	2015	IEA (2017)#
		SC-DR-oil	CO-LF-DR	26.82981843	kt	2015	IEA (2017)#
		SC-IND-coal	HC-IND-OTH	0.828315899	kt	2015	IEA (2017)#
		SC-IND-gas	NG-IND	0.266584427	TJ	2015	IEA (2017)#
		SC-IND-oil	CO-HF-IND	4.884207543	kt	2015	IEA (2017)#
		SC-IND-oil	CO-IND	1.342443009	kt	2015	IEA (2017)#
		SC-IND-oil	CO-LF-IND	4.67474835	kt	2015	IEA (2017)#
		SC-PP-coal	HC-B-PP	7.007362089	kt	2015	IEA (2017)#
		SC-PP-gas	NG-PP	184.4669028	TJ	2015	IEA (2017)#
		SC-PP-oil	CO-HF-PP	6.350421893	kt	2015	IEA (2017)#
		SC-PP-oil	CO-LF-PP	13.13880392	kt	2015	IEA (2017)#
CYM	Cayman Islands	BIO	PSB – DR	58.32152499	TJ	2015	IEA (2017)#
		BIO	PSB – IND	435.5202162	TJ	2015	IEA (2017)#
		BIO	PSB – PP	142.9247807	TJ	2015	IEA (2017)#
		OR	CO-OR	53.08948109	kt	2015	IEA (2017)#
		SC-DR-coal	HC-DR	11.13343457	kt	2015	IEA (2017)#
		SC-DR-gas	NG-DR	26.43505153	TJ	2015	IEA (2017)#
		SC-DR-oil	CO-HF-DR	2.358313726	kt	2015	IEA (2017)#
		SC-DR-oil	CO-LF-DR	56.54468492	kt	2015	IEA (2017)#
		SC-IND-gas	NG-IND	1.206579116	TJ	2015	IEA (2017)#
		SC-IND-oil	CO-HF-IND	7.129785683	kt	2015	IEA (2017)#
		SC-IND-oil	CO-LF-IND	4.058493389	kt	2015	IEA (2017)#
		SC-PP-gas	NG-PP	1687.949338	TJ	2015	IEA (2017)#
		SC-PP-oil	CO-HF-PP	86.16071776	kt	2015	IEA (2017)#
		SC-PP-oil	CO-LF-PP	63.40024808	kt	2015	IEA (2017)#
CAF	Central African Republic	BIO	PSB – DR	49252.24837	TJ	2015	IEA (2017)#
		BIO	PSB – IND	448.3354948	TJ	2015	IEA (2017)#
		BIO	PSB – PP	160.3944294	TJ	2015	IEA (2017)#
		SC-DR-coal	HC-DR	0.728986693	kt	2015	IEA (2017)#
		SC-DR-oil	CO-LF-DR	24.45576788	kt	2015	IEA (2017)#
		SC-IND-coal	HC-IND-OTH	0.755021932	kt	2015	IEA (2017)#
		SC-IND-gas	NG-IND	0.242995564	TJ	2015	IEA (2017)#
		SC-IND-oil	CO-HF-IND	4.452025877	kt	2015	IEA (2017)#
		SC-IND-oil	CO-IND	1.223656235	kt	2015	IEA (2017)#
		SC-IND-oil	CO-LF-IND	4.261100791	kt	2015	IEA (2017)#
		SC-PP-coal	HC-B-PP	6.38731198	kt	2015	IEA (2017)#
		SC-PP-gas	NG-PP	168.1442522	TJ	2015	IEA (2017)#
		SC-PP-oil	CO-HF-PP	5.788501482	kt	2015	IEA (2017)#
		SC-PP-oil	CO-LF-PP	11.97620996	kt	2015	IEA (2017)#
TCD	Chad	BIO	PSB – DR	106254.5147	TJ	2015	IEA (2017)#
		BIO	PSB – IND	4191.278814	TJ	2015	IEA (2017)#
		BIO	PSB – PP	1499.452489	TJ	2015	IEA (2017)#
		CEM	CEM	200	kt	2014	USGS (2017a)
		SC-DR-coal	HC-DR	6.814955583	kt	2015	IEA (2017)#
		SC-DR-oil	CO-LF-DR	228.6255337	kt	2015	IEA (2017)#
		SC-IND-coal	HC-IND-OTH	7.058346854	kt	2015	IEA (2017)#
		SC-IND-gas	NG-IND	2.271651861	TJ	2015	IEA (2017)#
		SC-IND-oil	CO-HF-IND	41.61990731	kt	2015	IEA (2017)#
		SC-IND-oil	CO-IND	11.43938973	kt	2015	IEA (2017)#

Country code	Country name	Sector code	Activity code	Activity amount	Units	Year	Source
		SC-IND-oil	CO-LF-IND	39.83503799	kt	2015	IEA (2017)#
		SC-PP-coal	HC-B-PP	59.71199178	kt	2015	IEA (2017)#
		SC-PP-gas	NG-PP	1571.901957	TJ	2015	IEA (2017)#
		SC-PP-oil	CO-HF-PP	54.11399255	kt	2015	IEA (2017)#
		SC-PP-oil	CO-LF-PP	111.9599846	kt	2015	IEA (2017)#
CHL	Chile	BIO	PSB – DR	69396	TJ	2015	IEA (2017)
		BIO	PSB – IND	81345	TJ	2015	IEA (2017)
		BIO	PSB – PP	149448	TJ	2015	IEA (2017)
		CEM	CEM	5000	kt	2014	USGS (2017a)
		CEM	PC-CEM	288	kt	2015	IEA (2017)
		NFMP	CU-P	1496200	t	2015	USGS (2017b)
		NFMP-AU	GP-L	42501	kg	2015	USGS (2017b)
		OR	CO-OR	8502	kt	2015	IEA (2017)
		PISP	PIP	584	kt	2014	USGS (2017a)
		SC-DR-coal	HC-DR	5	kt	2015	IEA (2017)
		SC-DR-gas	NG-DR	28187	TJ	2015	IEA (2017)
		SC-DR-oil	CO-HF-DR	275	kt	2015	IEA (2017)
		SC-DR-oil	CO-LF-DR	4536	kt	2015	IEA (2017)
		SC-IND-coal	HC-IND-CEM	1	kt	2015	IEA (2017)
		SC-IND-coal	HC-IND-OTH	393	kt	2015	IEA (2017)
		SC-IND-gas	NG-IND	35858	TJ	2015	IEA (2017)
		SC-IND-oil	CO-HF-IND	486	kt	2015	IEA (2017)
		SC-IND-oil	CO-LF-IND	2772	kt	2015	IEA (2017)
		SC-PP-coal	HC-B-PP	11179	kt	2015	IEA (2017)
		SC-PP-gas	NG-PP	100203	TJ	2015	IEA (2017)
		SC-PP-oil	CO-HF-PP	153	kt	2015	IEA (2017)
		SC-PP-oil	CO-LF-PP	502	kt	2015	IEA (2017)
		SSC	SP-S	382	kt	2014	World Steel Association (2015)
CHN	China (and Hong Kong if not separately reported)	BIO	PSB – DR	3377056	TJ	2015	IEA (2017)
		BIO	PSB – PP	777971	TJ	2015	IEA (2017)
		CEM	CEM	2492000	kt	2014	USGS (2017a)
		CSP	CSP-C	81	kt	2010	UNEP (2011e)
		NFMP	AL-P	31400	kt	2015	USGS (2017b)
		NFMP	CU-P	5500000	t	2015	USGS (2017b)
		NFMP	PB-P	2850000	t	2015	USGS (2017b)
		NFMP	ZN-T	6100000	t	2015	USGS (2017b)
		NFMP-AU	GP-L	450000	kg	2015	USGS (2017b)
		NFMP-HG	HG-P	1200	t	2015	National information
		OR	CO-OR	531992	kt	2015	IEA (2017)
		PISP	PIP	711600	kt	2014	USGS (2017a)
		SC-DR-coal	HC-DR	198964	kt	2015	IEA (2017)
		SC-DR-gas	NG-DR	2649321	TJ	2015	IEA (2017)
		SC-DR-oil	CO-HF-DR	5978	kt	2015	IEA (2017)
		SC-DR-oil	CO-LF-DR	152155	kt	2015	IEA (2017)
		SC-IND-coal	HC-IND-CEM	297537	kt	2015	IEA (2017)
		SC-IND-coal	HC-IND-NFM	19701	kt	2015	IEA (2017)
		SC-IND-coal	HC-IND-OTH	262489	kt	2015	IEA (2017)
		SC-IND-coal	HC-IND-PIP	102091	kt	2015	IEA (2017)
		SC-IND-gas	NG-IND	1791798	TJ	2015	IEA (2017)
		SC-IND-oil	CO-HF-IND	3808	kt	2015	IEA (2017)
		SC-IND-oil	CO-IND	2066	kt	2015	IEA (2017)
		SC-IND-oil	CO-LF-IND	17239	kt	2015	IEA (2017)

Country code	Country name	Sector code	Activity code	Activity amount	Units	Year	Source
		SC-PP-coal	HC-B-PP	2118802	kt	2015	IEA (2017)
		SC-PP-gas	NG-PP	2468684	TJ	2015	IEA (2017)
		SC-PP-oil	CO-HF-PP	3318	kt	2015	IEA (2017)
		SC-PP-oil	CO-LF-PP	2967	kt	2015	IEA (2017)
		SC-PP-oil	CO-PP	4596	kt	2015	IEA (2017)
		SSC	SP-S	49938	kt	2014	World Steel Association (2015)
		VCM	VCM-P	1217000	kg	2015	National information
		VCM	VCM-R	912750	kg	2015	Lin et al. (2016)
COL	Colombia	BIO	PSB – DR	84450	TJ	2015	IEA (2017)
		BIO	PSB – IND	30874	TJ	2015	IEA (2017)
		BIO	PSB – PP	23179	TJ	2015	IEA (2017)
		CEM	CEM	12384	kt	2014	USGS (2017a)
		CSP	CSP-C	22	kt	2010	UNEP (2011e)
		NFMP-AU	GP-L	59202	kg	2015	USGS (2017b)
		OR	CO-OR	14038	kt	2015	IEA (2017)
		PISP	PIP	234	kt	2014	USGS (2017a)
		SC-DR-coal	HC-DR	114	kt	2015	IEA (2017)
		SC-DR-gas	NG-DR	86364	TJ	2015	IEA (2017)
		SC-DR-oil	CO-HF-DR	18	kt	2015	IEA (2017)
		SC-DR-oil	CO-LF-DR	5967	kt	2015	IEA (2017)
		SC-IND-coal	HC-IND-CEM	563	kt	2015	IEA (2017)
		SC-IND-coal	HC-IND-OTH	608	kt	2015	IEA (2017)
		SC-IND-coal	HC-IND-PIP	259	kt	2015	IEA (2017)
		SC-IND-gas	NG-IND	113481	TJ	2015	IEA (2017)
		SC-IND-oil	CO-HF-IND	63	kt	2015	IEA (2017)
		SC-IND-oil	CO-LF-IND	226	kt	2015	IEA (2017)
		SC-PP-coal	HC-B-PP	2994	kt	2015	IEA (2017)
		SC-PP-gas	NG-PP	180586	TJ	2015	IEA (2017)
		SC-PP-oil	CO-HF-PP	44	kt	2015	IEA (2017)
		SC-PP-oil	CO-LF-PP	67	kt	2015	IEA (2017)
		SC-PP-oil	CO-PP	228	kt	2015	IEA (2017)
		SSC	SP-S	910	kt	2014	World Steel Association (2015)
COM	Comoros	BIO	PSB – DR	7134.248247	TJ	2015	IEA (2017)[#]
		BIO	PSB – IND	162.3548581	TJ	2015	IEA (2017)[#]
		BIO	PSB – PP	58.0833218	TJ	2015	IEA (2017)[#]
		SC-DR-coal	HC-DR	0.263986529	kt	2015	IEA (2017)[#]
		SC-DR-oil	CO-LF-DR	8.856119513	kt	2015	IEA (2017)[#]
		SC-IND-coal	HC-IND-OTH	0.273414619	kt	2015	IEA (2017)[#]
		SC-IND-gas	NG-IND	8.80E-02	TJ	2015	IEA (2017)[#]
		SC-IND-oil	CO-HF-IND	1.612203446	kt	2015	IEA (2017)[#]
		SC-IND-oil	CO-IND	0.443120245	kt	2015	IEA (2017)[#]
		SC-IND-oil	CO-LF-IND	1.543064117	kt	2015	IEA (2017)[#]
		SC-PP-coal	HC-B-PP	2.313024827	kt	2015	IEA (2017)[#]
		SC-PP-gas	NG-PP	60.88975002	TJ	2015	IEA (2017)[#]
		SC-PP-oil	CO-HF-PP	2.096178749	kt	2015	IEA (2017)[#]
		SC-PP-oil	CO-LF-PP	4.33692155	kt	2015	IEA (2017)[#]
COG	Congo	BIO	PSB – DR	45126	TJ	2015	IEA (2017)
		CEM	CEM	460	kt	2014	USGS (2017a)
		NFMP-AU	GP-L	150	kg	2015	USGS (2017b)
		OR	CO-OR	804	kt	2015	IEA (2017)
		SC-DR-oil	CO-LF-DR	454	kt	2015	IEA (2017)
		SC-IND-oil	CO-LF-IND	24	kt	2015	IEA (2017)
		SC-PP-gas	NG-PP	9410	TJ	2015	IEA (2017)

Country code	Country name	Sector code	Activity code	Activity amount	Units	Year	Source
COK	Cook Islands	BIO	PSB – DR	32.04981922	TJ	2015	IEA (2017)
		BIO	PSB – IND	9.032123015	TJ	2015	IEA (2017)
		OR	CO-OR	0.916736727	kt	2015	IEA (2017)
		SC-DR-gas	NG-DR	4.608539335	TJ	2015	IEA (2017)
		SC-DR-oil	CO-HF-DR	5.70E-02	kt	2015	IEA (2017)
		SC-DR-oil	CO-LF-DR	1.459906893	kt	2015	IEA (2017)
		SC-IND-coal	BC-IND-OTH	0.017545201	kt	2015	IEA (2017)
		SC-IND-coal	HC-IND-OTH	1.233281386	kt	2015	IEA (2017)
		SC-IND-oil	CO-HF-IND	0.125009554	kt	2015	IEA (2017)
		SC-IND-oil	CO-LF-IND	0.136706354	kt	2015	IEA (2017)
		SC-PP-coal	HC-B-PP	0.32458621	kt	2015	IEA (2017)
		SC-PP-gas	NG-PP	5.031086248	TJ	2015	IEA (2017)
		SC-PP-oil	CO-HF-PP	0.644055069	kt	2015	IEA (2017)
		SC-PP-oil	CO-LF-PP	0.842169625	kt	2015	IEA (2017)
CRI	Costa Rica	BIO	PSB – DR	6233	TJ	2015	IEA (2017)
		BIO	PSB – IND	18870	TJ	2015	IEA (2017)
		BIO	PSB – PP	1314	TJ	2015	IEA (2017)
		CEM	CEM	1500	kt	2014	USGS (2017a)
		NFMP-AU	GP-L	400	kg	2015	USGS (2017b)
		SC-DR-oil	CO-HF-DR	5	kt	2015	IEA (2017)
		SC-DR-oil	CO-LF-DR	896	kt	2015	IEA (2017)
		SC-IND-coal	HC-IND-CEM	1	kt	2015	IEA (2017)
		SC-IND-oil	CO-HF-IND	99	kt	2015	IEA (2017)
		SC-IND-oil	CO-LF-IND	59	kt	2015	IEA (2017)
		SC-PP-oil	CO-HF-PP	32	kt	2015	IEA (2017)
		SC-PP-oil	CO-LF-PP	1	kt	2015	IEA (2017)
HRV	Croatia	BIO	PSB – DR	48644	TJ	2015	IEA (2017)
		BIO	PSB – IND	1272	TJ	2015	IEA (2017)
		BIO	PSB – PP	2189	TJ	2015	IEA (2017)
		CEM	CEM	2345	kt	2014	USGS (2017a)
		CEM	PC-CEM	167	kt	2015	IEA (2017)
		OR	CO-OR	2863	kt	2015	IEA (2017)
		SC-DR-coal	BC-DR	8	kt	2015	IEA (2017)
		SC-DR-gas	NG-DR	29610	TJ	2015	IEA (2017)
		SC-DR-oil	CO-HF-DR	9	kt	2015	IEA (2017)
		SC-DR-oil	CO-LF-DR	1590	kt	2015	IEA (2017)
		SC-IND-coal	BC-IND-CEM	3	kt	2015	IEA (2017)
		SC-IND-coal	BC-IND-OTH	26	kt	2015	IEA (2017)
		SC-IND-coal	HC-IND-CEM	75	kt	2015	IEA (2017)
		SC-IND-coal	HC-IND-PIP	3	kt	2015	IEA (2017)
		SC-IND-gas	NG-IND	15851	TJ	2015	IEA (2017)
		SC-IND-oil	CO-HF-IND	23	kt	2015	IEA (2017)
		SC-IND-oil	CO-LF-IND	113	kt	2015	IEA (2017)
		SC-PP-coal	BC-L-PP	8	kt	2015	IEA (2017)
		SC-PP-coal	HC-B-PP	873	kt	2015	IEA (2017)
		SC-PP-gas	NG-PP	27706	TJ	2015	IEA (2017)
		SC-PP-oil	CO-HF-PP	185	kt	2015	IEA (2017)
		SC-PP-oil	CO-LF-PP	6	kt	2015	IEA (2017)
		SSC	SP-S	167	kt	2014	World Steel Association (2015)

Country code	Country name	Sector code	Activity code	Activity amount	Units	Year	Source
CUB	Cuba	BIO	PSB – DR	2426	TJ	2015	IEA (2017)
		BIO	PSB – IND	42083	TJ	2015	IEA (2017)
		BIO	PSB – PP	13051	TJ	2015	IEA (2017)
		CEM	CEM	1580	kt	2014	USGS (2017a)
		CSP	CSP-C	7	kt	2010	UNEP (2011e)
		OR	CO-OR	5239	kt	2015	IEA (2017)
		SC-DR-gas	NG-DR	2437	TJ	2015	IEA (2017)
		SC-DR-oil	CO-HF-DR	562	kt	2015	IEA (2017)
		SC-DR-oil	CO-LF-DR	632	kt	2015	IEA (2017)
		SC-IND-coal	HC-IND-OTH	3	kt	2015	IEA (2017)
		SC-IND-gas	NG-IND	14730	TJ	2015	IEA (2017)
		SC-IND-oil	CO-HF-IND	1199	kt	2015	IEA (2017)
		SC-IND-oil	CO-IND	851	kt	2015	IEA (2017)
		SC-IND-oil	CO-LF-IND	401	kt	2015	IEA (2017)
		SC-PP-gas	NG-PP	29500	TJ	2015	IEA (2017)
		SC-PP-oil	CO-HF-PP	1608	kt	2015	IEA (2017)
		SC-PP-oil	CO-LF-PP	463	kt	2015	IEA (2017)
		SC-PP-oil	CO-PP	2440	kt	2015	IEA (2017)
		SSC	SP-S	256	kt	2014	World Steel Association (2015)
CUW	Curaçao	OR	CO-OR	9232	kt	2015	IEA (2017)
		SC-DR-oil	CO-LF-DR	272	kt	2015	IEA (2017)
		SC-IND-oil	CO-HF-IND	127	kt	2015	IEA (2017)
		SC-PP-oil	CO-HF-PP	277	kt	2015	IEA (2017)
		SC-PP-oil	CO-LF-PP	16	kt	2015	IEA (2017)
CYP	Cyprus	BIO	PSB – DR	161	TJ	2015	IEA (2017)
		BIO	PSB – IND	154	TJ	2015	IEA (2017)
		CEM	CEM	735	kt	2014	USGS (2017a)
		CEM	PC-CEM	128	kt	2015	IEA (2017)
		SC-DR-oil	CO-HF-DR	3	kt	2015	IEA (2017)
		SC-DR-oil	CO-LF-DR	355	kt	2015	IEA (2017)
		SC-IND-coal	HC-IND-CEM	6	kt	2015	IEA (2017)
		SC-IND-oil	CO-HF-IND	22	kt	2015	IEA (2017)
		SC-IND-oil	CO-LF-IND	10	kt	2015	IEA (2017)
		SC-PP-oil	CO-HF-PP	858	kt	2015	IEA (2017)
		SC-PP-oil	CO-LF-PP	91	kt	2015	IEA (2017)
CZE	Czech Republic	BIO	PSB – DR	74423	TJ	2015	IEA (2017)
		BIO	PSB – IND	19831	TJ	2015	IEA (2017)
		BIO	PSB – PP	26065	TJ	2015	IEA (2017)
		CEM	CEM	3691	kt	2014	USGS (2017a)
		OR	CO-OR	7223	kt	2015	IEA (2017)
		PISP	PIP	4152	kt	2014	USGS (2017a)
		SC-DR-coal	BC-DR	1483	kt	2015	IEA (2017)
		SC-DR-coal	HC-DR	349	kt	2015	IEA (2017)
		SC-DR-gas	NG-DR	137047	TJ	2015	IEA (2017)
		SC-DR-oil	CO-HF-DR	12	kt	2015	IEA (2017)
		SC-DR-oil	CO-LF-DR	4222	kt	2015	IEA (2017)
		SC-IND-coal	BC-IND-CEM	14	kt	2015	IEA (2017)
		SC-IND-coal	BC-IND-OTH	746	kt	2015	IEA (2017)
		SC-IND-coal	BC-IND-PIP	16	kt	2015	IEA (2017)
		SC-IND-coal	HC-IND-CEM	164	kt	2015	IEA (2017)
		SC-IND-coal	HC-IND-OTH	69	kt	2015	IEA (2017)
		SC-IND-coal	HC-IND-PIP	60	kt	2015	IEA (2017)
		SC-IND-gas	NG-IND	96678	TJ	2015	IEA (2017)

Country code	Country name	Sector code	Activity code	Activity amount	Units	Year	Source
		SC-IND-oil	CO-HF-IND	17	kt	2015	IEA (2017)
		SC-IND-oil	CO-LF-IND	58	kt	2015	IEA (2017)
		SC-PP-coal	BC-L-PP	34218	kt	2015	IEA (2017)
		SC-PP-coal	HC-B-PP	3612	kt	2015	IEA (2017)
		SC-PP-gas	NG-PP	58020	TJ	2015	IEA (2017)
		SC-PP-oil	CO-HF-PP	23	kt	2015	IEA (2017)
		SC-PP-oil	CO-LF-PP	20	kt	2015	IEA (2017)
		SSC	SP-S	354	kt	2014	World Steel Association (2015)
COD	Dem. Rep. of Congo (Zaire)	BIO	PSB – DR	587094	TJ	2015	IEA (2017)
		BIO	PSB – IND	128213	TJ	2015	IEA (2017)
		BIO	PSB – PP	3014	TJ	2015	IEA (2017)
		CEM	CEM	330	kt	2014	USGS (2017a)
		NFMP-AU	GP-L	37000	kg	2015	USGS (2017b)
		SC-DR-oil	CO-LF-DR	538	kt	2015	IEA (2017)
		SC-IND-oil	CO-HF-IND	16	kt	2015	IEA (2017)
		SC-PP-gas	NG-PP	46	TJ	2015	IEA (2017)
		SC-PP-oil	CO-LF-PP	3	kt	2015	IEA (2017)
		SSC	SP-S	30	kt	2014	World Steel Association (2015)
DNK	Denmark	BIO	PSB – DR	43549	TJ	2015	IEA (2017)
		BIO	PSB – IND	4553	TJ	2015	IEA (2017)
		BIO	PSB – PP	57903	TJ	2015	IEA (2017)
		CEM	CEM	1876	kt	2014	USGS (2017a)
		CEM	PC-CEM	209	kt	2015	IEA (2017)
		OR	CO-OR	7336	kt	2015	IEA (2017)
		SC-DR-coal	HC-DR	31	kt	2015	IEA (2017)
		SC-DR-gas	NG-DR	37308	TJ	2015	IEA (2017)
		SC-DR-oil	CO-HF-DR	5	kt	2015	IEA (2017)
		SC-DR-oil	CO-LF-DR	3076	kt	2015	IEA (2017)
		SC-IND-coal	HC-IND-CEM	81	kt	2015	IEA (2017)
		SC-IND-coal	HC-IND-OTH	69	kt	2015	IEA (2017)
		SC-IND-gas	NG-IND	30298	TJ	2015	IEA (2017)
		SC-IND-oil	CO-HF-IND	43	kt	2015	IEA (2017)
		SC-IND-oil	CO-LF-IND	169	kt	2015	IEA (2017)
		SC-PP-coal	HC-B-PP	2966	kt	2015	IEA (2017)
		SC-PP-gas	NG-PP	65015	TJ	2015	IEA (2017)
		SC-PP-oil	CO-HF-PP	56	kt	2015	IEA (2017)
		SC-PP-oil	CO-LF-PP	23	kt	2015	IEA (2017)
DJI	Djibouti	BIO	PSB – DR	7566.822641	TJ	2015	IEA (2017)[#]
		BIO	PSB – IND	367.3578674	TJ	2015	IEA (2017)[#]
		BIO	PSB – PP	131.4242486	TJ	2015	IEA (2017)[#]
		CEM	CEM	350	kt	2014	USGS (2017a)
		SC-DR-coal	HC-DR	0.597318303	kt	2015	IEA (2017)[#]
		SC-DR-oil	CO-LF-DR	20.03860689	kt	2015	IEA (2017)[#]
		SC-IND-coal	HC-IND-OTH	0.6186511	kt	2015	IEA (2017)[#]
		SC-IND-gas	NG-IND	0.199106101	TJ	2015	IEA (2017)[#]
		SC-IND-oil	CO-HF-IND	3.647908209	kt	2015	IEA (2017)[#]
		SC-IND-oil	CO-IND	1.002641437	kt	2015	IEA (2017)[#]
		SC-IND-oil	CO-LF-IND	3.491467701	kt	2015	IEA (2017)[#]
		SC-PP-coal	HC-B-PP	5.233646085	kt	2015	IEA (2017)[#]
		SC-PP-gas	NG-PP	137.774311	TJ	2015	IEA (2017)[#]
		SC-PP-oil	CO-HF-PP	4.742991765	kt	2015	IEA (2017)[#]
		SC-PP-oil	CO-LF-PP	9.813086409	kt	2015	IEA (2017)[#]

Country code	Country name	Sector code	Activity code	Activity amount	Units	Year	Source
DMA	Dominica	BIO	PSB – DR	76.53270501	TJ	2015	IEA (2017)#
		BIO	PSB – IND	139.6163174	TJ	2015	IEA (2017)#
		BIO	PSB – PP	45.81792256	TJ	2015	IEA (2017)#
		OR	CO-OR	17.01909019	kt	2015	IEA (2017)#
		SC-DR-coal	HC-DR	3.569086063	kt	2015	IEA (2017)#
		SC-DR-gas	NG-DR	8.474381686	TJ	2015	IEA (2017)#
		SC-DR-oil	CO-HF-DR	0.756013304	kt	2015	IEA (2017)#
		SC-DR-oil	CO-LF-DR	18.12673759	kt	2015	IEA (2017)#
		SC-IND-gas	NG-IND	0.386797504	TJ	2015	IEA (2017)#
		SC-IND-oil	CO-HF-IND	2.285621617	kt	2015	IEA (2017)#
		SC-IND-oil	CO-LF-IND	1.301046151	kt	2015	IEA (2017)#
		SC-PP-gas	NG-PP	541.1121269	TJ	2015	IEA (2017)#
		SC-PP-oil	CO-HF-PP	27.62085815	kt	2015	IEA (2017)#
		SC-PP-oil	CO-LF-PP	20.32445068	kt	2015	IEA (2017)#
DOM	Dominican Republic	BIO	PSB – DR	17567	TJ	2015	IEA (2017)
		BIO	PSB – IND	9727	TJ	2015	IEA (2017)
		BIO	PSB – PP	650	TJ	2015	IEA (2017)
		CEM	CEM	4800	kt	2014	USGS (2017a)
		NFMP-AU	GP-L	30816	kg	2015	USGS (2017b)
		OR	CO-OR	841	kt	2015	IEA (2017)
		SC-DR-gas	NG-DR	933	TJ	2015	IEA (2017)
		SC-DR-oil	CO-LF-DR	627	kt	2015	IEA (2017)
		SC-IND-coal	HC-IND-CEM	108	kt	2015	IEA (2017)
		SC-IND-coal	HC-IND-OTH	3	kt	2015	IEA (2017)
		SC-IND-gas	NG-IND	3819	TJ	2015	IEA (2017)
		SC-IND-oil	CO-HF-IND	107	kt	2015	IEA (2017)
		SC-IND-oil	CO-LF-IND	99	kt	2015	IEA (2017)
		SC-PP-coal	HC-B-PP	946	kt	2015	IEA (2017)
		SC-PP-gas	NG-PP	36589	TJ	2015	IEA (2017)
		SC-PP-oil	CO-HF-PP	1585	kt	2015	IEA (2017)
		SC-PP-oil	CO-LF-PP	624	kt	2015	IEA (2017)
ECU	Ecuador	BIO	PSB – DR	8913	TJ	2015	IEA (2017)
		BIO	PSB – IND	15300	TJ	2015	IEA (2017)
		BIO	PSB – PP	11464	TJ	2015	IEA (2017)
		CEM	CEM	6600	kt	2014	USGS (2017a)
		NFMP-AU	GP-L	7112	kg	2015	USGS (2017b)
		OR	CO-OR	6742	kt	2015	IEA (2017)
		SC-DR-gas	NG-DR	13	TJ	2015	IEA (2017)
		SC-DR-oil	CO-HF-DR	30	kt	2015	IEA (2017)
		SC-DR-oil	CO-LF-DR	3147	kt	2015	IEA (2017)
		SC-IND-gas	NG-IND	575	TJ	2015	IEA (2017)
		SC-IND-oil	CO-HF-IND	267	kt	2015	IEA (2017)
		SC-IND-oil	CO-LF-IND	917	kt	2015	IEA (2017)
		SC-PP-gas	NG-PP	25310	TJ	2015	IEA (2017)
		SC-PP-oil	CO-HF-PP	1579	kt	2015	IEA (2017)
		SC-PP-oil	CO-LF-PP	826	kt	2015	IEA (2017)
		SC-PP-oil	CO-PP	353	kt	2015	IEA (2017)
		SSC	SP-S	667	kt	2014	World Steel Association (2015)

Country code	Country name	Sector code	Activity code	Activity amount	Units	Year	Source
EGY	Egypt	BIO	PSB – DR	73259	TJ	2015	IEA (2017)
		CEM	CEM	49000	kt	2014	USGS (2017a)
		NFMP	AL-P	300	kt	2015	USGS (2017b)
		NFMP-AU	GP-L	13700	kg	2015	USGS (2017b)
		OR	CO-OR	26087	kt	2015	IEA (2017)
		PISP	PIP	550	kt	2014	USGS (2017a)
		SC-DR-gas	NG-DR	86491	TJ	2015	IEA (2017)
		SC-DR-oil	CO-HF-DR	340	kt	2015	IEA (2017)
		SC-DR-oil	CO-LF-DR	9939	kt	2015	IEA (2017)
		SC-IND-gas	NG-IND	198522	TJ	2015	IEA (2017)
		SC-IND-oil	CO-HF-IND	2100	kt	2015	IEA (2017)
		SC-IND-oil	CO-LF-IND	2584	kt	2015	IEA (2017)
		SC-PP-gas	NG-PP	1243874	TJ	2015	IEA (2017)
		SC-PP-oil	CO-HF-PP	9079	kt	2015	IEA (2017)
		SC-PP-oil	CO-LF-PP	1818	kt	2015	IEA (2017)
		SSC	SP-S	5970	kt	2014	World Steel Association (2015)
SLV	El Salvador	BIO	PSB – DR	11133	TJ	2015	IEA (2017)
		BIO	PSB – IND	933	TJ	2015	IEA (2017)
		BIO	PSB – PP	11522	TJ	2015	IEA (2017)
		CEM	CEM	1000	kt	2014	USGS (2017a)
		SC-DR-oil	CO-HF-DR	28	kt	2015	IEA (2017)
		SC-DR-oil	CO-LF-DR	508	kt	2015	IEA (2017)
		SC-IND-oil	CO-HF-IND	22	kt	2015	IEA (2017)
		SC-IND-oil	CO-LF-IND	156	kt	2015	IEA (2017)
		SC-PP-oil	CO-HF-PP	511	kt	2015	IEA (2017)
		SSC	SP-S	121	kt	2014	World Steel Association (2015)
GNQ	Equatorial Guinea	BIO	PSB – DR	6766.761441	TJ	2015	IEA (2017)[#]
		BIO	PSB – IND	3264.628729	TJ	2015	IEA (2017)[#]
		BIO	PSB – PP	1167.938448	TJ	2015	IEA (2017)[#]
		SC-DR-coal	HC-DR	5.308236643	kt	2015	IEA (2017)[#]
		SC-DR-oil	CO-LF-DR	178.0787007	kt	2015	IEA (2017)[#]
		SC-IND-coal	HC-IND-OTH	5.497816523	kt	2015	IEA (2017)[#]
		SC-IND-gas	NG-IND	1.769412214	TJ	2015	IEA (2017)[#]
		SC-IND-oil	CO-HF-IND	32.4181595	kt	2015	IEA (2017)[#]
		SC-IND-oil	CO-IND	8.910254365	kt	2015	IEA (2017)[#]
		SC-IND-oil	CO-LF-IND	31.02790704	kt	2015	IEA (2017)[#]
		SC-PP-coal	HC-B-PP	46.51026392	kt	2015	IEA (2017)[#]
		SC-PP-gas	NG-PP	1224.370059	TJ	2015	IEA (2017)[#]
		SC-PP-oil	CO-HF-PP	42.14992668	kt	2015	IEA (2017)[#]
		SC-PP-oil	CO-LF-PP	87.20674485	kt	2015	IEA (2017)[#]
ERI	Eritrea	BIO	PSB – DR	14091	TJ	2015	IEA (2017)
		CEM	CEM	300	kt	2014	USGS (2017a)
		NFMP-AU	GP-L	1390	kg	2015	USGS (2017b)
		SC-DR-oil	CO-HF-DR	1	kt	2015	IEA (2017)
		SC-DR-oil	CO-LF-DR	47	kt	2015	IEA (2017)
		SC-IND-oil	CO-HF-IND	5	kt	2015	IEA (2017)
		SC-IND-oil	CO-LF-IND	1	kt	2015	IEA (2017)
		SC-PP-oil	CO-HF-PP	73	kt	2015	IEA (2017)
		SC-PP-oil	CO-LF-PP	38	kt	2015	IEA (2017)

Country code	Country name	Sector code	Activity code	Activity amount	Units	Year	Source
EST	Estonia	BIO	PSB – DR	15703	TJ	2015	IEA (2017)
		BIO	PSB – IND	4260	TJ	2015	IEA (2017)
		BIO	PSB – PP	14594	TJ	2015	IEA (2017)
		CEM	CEM	447	kt	2014	USGS (2017a)
		SC-DR-coal	HC-DR	4	kt	2015	IEA (2017)
		SC-DR-gas	NG-DR	5960	TJ	2015	IEA (2017)
		SC-DR-oil	CO-HF-DR	7	kt	2015	IEA (2017)
		SC-DR-oil	CO-LF-DR	632	kt	2015	IEA (2017)
		SC-IND-coal	HC-IND-CEM	22	kt	2015	IEA (2017)
		SC-IND-gas	NG-IND	4387	TJ	2015	IEA (2017)
		SC-IND-oil	CO-HF-IND	13	kt	2015	IEA (2017)
		SC-IND-oil	CO-LF-IND	50	kt	2015	IEA (2017)
		SC-PP-coal	HC-B-PP	3	kt	2015	IEA (2017)
		SC-PP-gas	NG-PP	7817	TJ	2015	IEA (2017)
		SC-PP-oil	CO-HF-PP	41	kt	2015	IEA (2017)
		SC-PP-oil	CO-LF-PP	15	kt	2015	IEA (2017)
ETH	Ethiopia	BIO	PSB – DR	1351776	TJ	2015	IEA (2017)
		CEM	CEM	5400	kt	2014	USGS (2017a)
		CEM	PC-CEM	211	kt	2015	IEA (2017)
		NFMP-AU	GP-L	9200	kg	2015	USGS (2017b)
		SC-DR-oil	CO-LF-DR	1466	kt	2015	IEA (2017)
		SC-IND-coal	HC-IND-CEM	411	kt	2015	IEA (2017)
		SC-IND-oil	CO-HF-IND	67	kt	2015	IEA (2017)
		SC-IND-oil	CO-LF-IND	454	kt	2015	IEA (2017)
		SC-PP-oil	CO-LF-PP	1	kt	2015	IEA (2017)
FLK	Falkland Is. (Malvinas)	BIO	PSB – DR	3.49459184	TJ	2015	IEA (2017)[#]
		BIO	PSB – IND	33.00741857	TJ	2015	IEA (2017)[#]
		BIO	PSB – PP	10.83205299	TJ	2015	IEA (2017)[#]
		OR	CO-OR	4.023571486	kt	2015	IEA (2017)[#]
		SC-DR-coal	HC-DR	0.843786169	kt	2015	IEA (2017)[#]
		SC-DR-gas	NG-DR	2.003472579	TJ	2015	IEA (2017)[#]
		SC-DR-oil	CO-HF-DR	0.178733031	kt	2015	IEA (2017)[#]
		SC-DR-oil	CO-LF-DR	4.285436159	kt	2015	IEA (2017)[#]
		SC-IND-gas	NG-IND	9.14E-02	TJ	2015	IEA (2017)[#]
		SC-IND-oil	CO-HF-IND	0.540355675	kt	2015	IEA (2017)[#]
		SC-IND-oil	CO-LF-IND	0.307587076	kt	2015	IEA (2017)[#]
		SC-PP-gas	NG-PP	127.9271277	TJ	2015	IEA (2017)[#]
		SC-PP-oil	CO-HF-PP	6.529990501	kt	2015	IEA (2017)[#]
		SC-PP-oil	CO-LF-PP	4.805008923	kt	2015	IEA (2017)[#]
FJI	Fiji	BIO	PSB – DR	2962.568922	TJ	2015	IEA (2017)[#]
		BIO	PSB – IND	610.8999933	TJ	2015	IEA (2017)[#]
		CEM	CEM	190	kt	2014	USGS (2017a)
		NFMP-AU	GP-L	1360	kg	2015	USGS (2017b)
		OR	CO-OR	62.00474234	kt	2015	IEA (2017)[#]
		SC-DR-gas	NG-DR	311.704861	TJ	2015	IEA (2017)[#]
		SC-DR-oil	CO-HF-DR	3.856754308	kt	2015	IEA (2017)[#]
		SC-DR-oil	CO-LF-DR	98.7427994	kt	2015	IEA (2017)[#]
		SC-IND-coal	BC-IND-OTH	1.186693633	kt	2015	IEA (2017)[#]
		SC-IND-coal	HC-IND-OTH	83.4146733	kt	2015	IEA (2017)[#]
		SC-IND-oil	CO-HF-IND	8.455192137	kt	2015	IEA (2017)[#]
		SC-IND-oil	CO-LF-IND	9.246321226	kt	2015	IEA (2017)[#]
		SC-PP-coal	HC-B-PP	21.95383222	kt	2015	IEA (2017)[#]
		SC-PP-gas	NG-PP	340.2843993	TJ	2015	IEA (2017)[#]
		SC-PP-oil	CO-HF-PP	43.56154545	kt	2015	IEA (2017)[#]
		SC-PP-oil	CO-LF-PP	56.9612944	kt	2015	IEA (2017)[#]

Country code	Country name	Sector code	Activity code	Activity amount	Units	Year	Source
FIN	Finland	BIO	PSB – DR	59248	TJ	2015	IEA (2017)
		BIO	PSB – IND	142825	TJ	2015	IEA (2017)
		BIO	PSB – PP	129806	TJ	2015	IEA (2017)
		CEM	CEM	1250	kt	2014	USGS (2017a)
		CEM	PC-CEM	52	kt	2015	IEA (2017)
		NFMP	CU-P	175000	t	2015	USGS (2017b)
		NFMP	ZN-P	305717	t	2015	USGS (2017b)
		NFMP-AU	GP-L	9300	kg	2015	USGS (2017b)
		OR	CO-OR	9809	kt	2015	IEA (2017)
		PISP	PIP	12000	kt	2014	USGS (2017a)
		SC-DR-coal	HC-DR	4	kt	2015	IEA (2017)
		SC-DR-gas	NG-DR	2877	TJ	2015	IEA (2017)
		SC-DR-oil	CO-HF-DR	60	kt	2015	IEA (2017)
		SC-DR-oil	CO-LF-DR	3058	kt	2015	IEA (2017)
		SC-IND-coal	HC-IND-CEM	52	kt	2015	IEA (2017)
		SC-IND-coal	HC-IND-OTH	68	kt	2015	IEA (2017)
		SC-IND-coal	HC-IND-PIP	6	kt	2015	IEA (2017)
		SC-IND-gas	NG-IND	25726	TJ	2015	IEA (2017)
		SC-IND-oil	CO-HF-IND	183	kt	2015	IEA (2017)
		SC-IND-oil	CO-LF-IND	461	kt	2015	IEA (2017)
		SC-PP-coal	HC-B-PP	2394	kt	2015	IEA (2017)
		SC-PP-gas	NG-PP	63193	TJ	2015	IEA (2017)
		SC-PP-oil	CO-HF-PP	254	kt	2015	IEA (2017)
		SC-PP-oil	CO-LF-PP	23	kt	2015	IEA (2017)
		SSC	SP-S	1265	kt	2014	World Steel Association (2015)
FRA	France	BIO	PSB – DR	289123	TJ	2015	IEA (2017)
		BIO	PSB – IND	54784	TJ	2015	IEA (2017)
		BIO	PSB – PP	60585	TJ	2015	IEA (2017)
		CEM	CEM	17000	kt	2014	USGS (2017a)
		CEM	PC-CEM	599	kt	2015	IEA (2017)
		CSP	CSP-C	278.54	kt	2015	OSPAR (2016)
		NFMP	AL-P	420	kt	2015	USGS (2017b)
		NFMP	ZN-P	169000	t	2015	USGS (2017b)
		OR	CO-OR	57342	kt	2015	IEA (2017)
		PISP	PIP	10866	kt	2014	USGS (2017a)
		SC-DR-coal	HC-DR	92	kt	2015	IEA (2017)
		SC-DR-gas	NG-DR	773999	TJ	2015	IEA (2017)
		SC-DR-oil	CO-HF-DR	80	kt	2015	IEA (2017)
		SC-DR-oil	CO-LF-DR	41923	kt	2015	IEA (2017)
		SC-IND-coal	BC-IND-CEM	26	kt	2015	IEA (2017)
		SC-IND-coal	BC-IND-OTH	95	kt	2015	IEA (2017)
		SC-IND-coal	BC-IND-PIP	2	kt	2015	IEA (2017)
		SC-IND-coal	HC-IND-CEM	336	kt	2015	IEA (2017)
		SC-IND-coal	HC-IND-OTH	886	kt	2015	IEA (2017)
		SC-IND-coal	HC-IND-PIP	889	kt	2015	IEA (2017)
		SC-IND-gas	NG-IND	478575	TJ	2015	IEA (2017)
		SC-IND-oil	CO-HF-IND	514	kt	2015	IEA (2017)
		SC-IND-oil	CO-LF-IND	918	kt	2015	IEA (2017)
		SC-PP-coal	HC-B-PP	3946	kt	2015	IEA (2017)
		SC-PP-gas	NG-PP	288458	TJ	2015	IEA (2017)
		SC-PP-oil	CO-HF-PP	390	kt	2015	IEA (2017)
		SC-PP-oil	CO-LF-PP	90	kt	2015	IEA (2017)
		SSC	SP-S	5498	kt	2014	World Steel Association (2015)

Country code	Country name	Sector code	Activity code	Activity amount	Units	Year	Source
GUF	French Guiana	BIO	PSB – DR	260.0502441	TJ	2015	IEA (2017)[#]
		CEM	CEM	86	kt	2014	USGS (2017a)
		NFMP-AU	GP-L	1200	kg	2015	USGS (2017b)
PYF	French Polynesia	BIO	PSB – DR	920.9778454	TJ	2015	IEA (2017)[#]
		BIO	PSB – IND	550.7428134	TJ	2015	IEA (2017)[#]
		OR	CO-OR	55.89894682	kt	2015	IEA (2017)[#]
		SC-DR-gas	NG-DR	281.0103355	TJ	2015	IEA (2017)[#]
		SC-DR-oil	CO-HF-DR	3.476967984	kt	2015	IEA (2017)[#]
		SC-DR-oil	CO-LF-DR	89.0192957	kt	2015	IEA (2017)[#]
		SC-IND-coal	BC-IND-OTH	1.069836303	kt	2015	IEA (2017)[#]
		SC-IND-coal	HC-IND-OTH	75.20057679	kt	2015	IEA (2017)[#]
		SC-IND-oil	CO-HF-IND	7.622583658	kt	2015	IEA (2017)[#]
		SC-IND-oil	CO-LF-IND	8.335807859	kt	2015	IEA (2017)[#]
		SC-PP-coal	HC-B-PP	19.7919716	kt	2015	IEA (2017)[#]
		SC-PP-gas	NG-PP	306.7755598	TJ	2015	IEA (2017)[#]
		SC-PP-oil	CO-HF-PP	39.27190762	kt	2015	IEA (2017)[#]
		SC-PP-oil	CO-LF-PP	51.35214254	kt	2015	IEA (2017)[#]
GAB	Gabon	BIO	PSB – DR	43468	TJ	2015	IEA (2017)
		BIO	PSB – IND	115821	TJ	2015	IEA (2017)
		BIO	PSB – PP	306	TJ	2015	IEA (2017)
		CEM	CEM	170	kt	2014	USGS (2017a)
		OR	CO-OR	802	kt	2015	IEA (2017)
		SC-DR-oil	CO-LF-DR	228	kt	2015	IEA (2017)
		SC-IND-gas	NG-IND	114	TJ	2015	IEA (2017)
		SC-IND-oil	CO-HF-IND	67	kt	2015	IEA (2017)
		SC-IND-oil	CO-LF-IND	284	kt	2015	IEA (2017)
		SC-PP-gas	NG-PP	14154	TJ	2015	IEA (2017)
		SC-PP-oil	CO-LF-PP	64	kt	2015	IEA (2017)
GMB	Gambia	BIO	PSB – DR	17975.21865	TJ	2015	IEA (2017)[#]
		BIO	PSB – IND	436.3349256	TJ	2015	IEA (2017)[#]
		BIO	PSB – PP	156.1011613	TJ	2015	IEA (2017)[#]
		SC-DR-coal	HC-DR	0.70947395	kt	2015	IEA (2017)[#]
		SC-DR-oil	CO-LF-DR	23.80116181	kt	2015	IEA (2017)[#]
		SC-IND-coal	HC-IND-OTH	0.734812306	kt	2015	IEA (2017)[#]
		SC-IND-gas	NG-IND	0.236491317	TJ	2015	IEA (2017)[#]
		SC-IND-oil	CO-HF-IND	4.332858769	kt	2015	IEA (2017)[#]
		SC-IND-oil	CO-IND	1.190902703	kt	2015	IEA (2017)[#]
		SC-IND-oil	CO-LF-IND	4.147044163	kt	2015	IEA (2017)[#]
		SC-PP-coal	HC-B-PP	6.216343185	kt	2015	IEA (2017)[#]
		SC-PP-gas	NG-PP	163.6435451	TJ	2015	IEA (2017)[#]
		SC-PP-oil	CO-HF-PP	5.633561011	kt	2015	IEA (2017)[#]
		SC-PP-oil	CO-LF-PP	11.65564347	kt	2015	IEA (2017)[#]
GEO	Georgia	BIO	PSB – DR	16637	TJ	2015	IEA (2017)
		BIO	PSB – IND	35	TJ	2015	IEA (2017)
		CEM	CEM	1626	kt	2014	USGS (2017a)
		NFMP-AU	GP-L	3600	kg	2015	USGS (2017b)
		OR	CO-OR	14	kt	2015	IEA (2017)
		SC-DR-coal	BC-DR	3	kt	2015	IEA (2017)
		SC-DR-coal	HC-DR	1	kt	2015	IEA (2017)
		SC-DR-gas	NG-DR	48414	TJ	2015	IEA (2017)
		SC-DR-oil	CO-HF-DR	1	kt	2015	IEA (2017)

Country code	Country name	Sector code	Activity code	Activity amount	Units	Year	Source
		SC-DR-oil	CO-LF-DR	526	kt	2015	IEA (2017)
		SC-IND-coal	BC-IND-CEM	300	kt	2015	IEA (2017)
		SC-IND-coal	HC-IND-CEM	117	kt	2015	IEA (2017)
		SC-IND-coal	HC-IND-OTH	3	kt	2015	IEA (2017)
		SC-IND-gas	NG-IND	4464	TJ	2015	IEA (2017)
		SC-IND-oil	CO-LF-IND	79	kt	2015	IEA (2017)
		SC-PP-coal	BC-L-PP	1	kt	2015	IEA (2017)
		SC-PP-gas	NG-PP	25252	TJ	2015	IEA (2017)
DEU	Germany	BIO	PSB – DR	272666	TJ	2015	IEA (2017)
		BIO	PSB – IND	90388	TJ	2015	IEA (2017)
		BIO	PSB – PP	141939	TJ	2015	IEA (2017)
		CEM	CEM	32099	kt	2014	USGS (2017a)
		CEM	PC-CEM	102	kt	2015	IEA (2017)
		CSP	CSP-C	484.543	kt	2015	OSPAR (2016)
		NFMP	AL-P	530	kt	2015	USGS (2017b)
		NFMP	CU-P	338300	t	2015	USGS (2017b)
		NFMP	PB-P	130000	t	2015	USGS (2017b)
		NFMP	ZN-T	169000	t	2015	USGS (2017b)
		OR	CO-OR	93344	kt	2015	IEA (2017)
		PISP	PIP	27379	kt	2014	USGS (2017a)
		SC-DR-coal	HC-DR	472	kt	2015	IEA (2017)
		SC-DR-gas	NG-DR	1423599	TJ	2015	IEA (2017)
		SC-DR-oil	CO-LF-DR	49464	kt	2015	IEA (2017)
		SC-IND-coal	BC-IND-OTH	526	kt	2015	IEA (2017)
		SC-IND-coal	HC-IND-CEM	437	kt	2015	IEA (2017)
		SC-IND-coal	HC-IND-NFM	27	kt	2015	IEA (2017)
		SC-IND-coal	HC-IND-OTH	1451	kt	2015	IEA (2017)
		SC-IND-coal	HC-IND-PIP	1083	kt	2015	IEA (2017)
		SC-IND-gas	NG-IND	869941	TJ	2015	IEA (2017)
		SC-IND-oil	CO-HF-IND	1471	kt	2015	IEA (2017)
		SC-IND-oil	CO-LF-IND	734	kt	2015	IEA (2017)
		SC-PP-coal	BC-L-PP	162623	kt	2015	IEA (2017)
		SC-PP-coal	HC-A-PP	2287	kt	2015	IEA (2017)
		SC-PP-coal	HC-B-PP	39167	kt	2015	IEA (2017)
		SC-PP-gas	NG-PP	720716	TJ	2015	IEA (2017)
		SC-PP-oil	CO-HF-PP	1020	kt	2015	IEA (2017)
		SC-PP-oil	CO-LF-PP	307	kt	2015	IEA (2017)
		SSC	SP-S	13062	kt	2014	World Steel Association (2015)
GHA	Ghana	BIO	PSB – DR	48995	TJ	2015	IEA (2017)
		BIO	PSB – IND	16947	TJ	2015	IEA (2017)
		CEM	CEM	3000	kt	2014	USGS (2017a)
		NFMP	AL-P	40	kt	2015	USGS (2017b)
		NFMP-AU	GP-L	88000	kg	2015	USGS (2017b)
		OR	CO-OR	110	kt	2015	IEA (2017)
		SC-DR-oil	CO-LF-DR	1397	kt	2015	IEA (2017)
		SC-IND-oil	CO-HF-IND	13	kt	2015	IEA (2017)
		SC-IND-oil	CO-LF-IND	506	kt	2015	IEA (2017)
		SC-PP-gas	NG-PP	49495	TJ	2015	IEA (2017)
		SC-PP-oil	CO-HF-PP	2	kt	2015	IEA (2017)
		SC-PP-oil	CO-PP	249	kt	2015	IEA (2017)
		SSC	SP-S	25	kt	2014	World Steel Association (2015)

Country code	Country name	Sector code	Activity code	Activity amount	Units	Year	Source
GIB	Gibraltar	SC-DR-oil	CO-LF-DR	99	kt	2015	IEA (2017)
		SC-PP-oil	CO-HF-PP	51	kt	2015	IEA (2017)
GRC	Greece	BIO	PSB – DR	34751	TJ	2015	IEA (2017)
		BIO	PSB – IND	7551	TJ	2015	IEA (2017)
		BIO	PSB – PP	4	TJ	2015	IEA (2017)
		CEM	CEM	5128	kt	2014	USGS (2017a)
		CEM	PC-CEM	731	kt	2015	IEA (2017)
		NFMP	AL-P	170	kt	2015	USGS (2017b)
		NFMP-AU	GP-L	500	kg	2015	USGS (2017b)
		OR	CO-OR	21695	kt	2015	IEA (2017)
		SC-DR-coal	BC-DR	51	kt	2015	IEA (2017)
		SC-DR-gas	NG-DR	25003	TJ	2015	IEA (2017)
		SC-DR-oil	CO-HF-DR	331	kt	2015	IEA (2017)
		SC-DR-oil	CO-LF-DR	3745	kt	2015	IEA (2017)
		SC-IND-coal	BC-IND-NFM	193	kt	2015	IEA (2017)
		SC-IND-coal	HC-IND-CEM	81	kt	2015	IEA (2017)
		SC-IND-coal	HC-IND-NFM	200	kt	2015	IEA (2017)
		SC-IND-gas	NG-IND	20068	TJ	2015	IEA (2017)
		SC-IND-oil	CO-HF-IND	193	kt	2015	IEA (2017)
		SC-IND-oil	CO-LF-IND	207	kt	2015	IEA (2017)
		SC-PP-coal	BC-L-PP	44023	kt	2015	IEA (2017)
		SC-PP-gas	NG-PP	61818	TJ	2015	IEA (2017)
		SC-PP-oil	CO-HF-PP	1405	kt	2015	IEA (2017)
		SC-PP-oil	CO-LF-PP	259	kt	2015	IEA (2017)
		SSC	SP-S	1022	kt	2014	World Steel Association (2015)
GRD	Grenada	BIO	PSB – DR	115.093826	TJ	2015	IEA (2017)#
		BIO	PSB – IND	257.0565415	TJ	2015	IEA (2017)#
		BIO	PSB – PP	84.35831094	TJ	2015	IEA (2017)#
		OR	CO-OR	31.33493668	kt	2015	IEA (2017)#
		SC-DR-coal	HC-DR	6.571272879	kt	2015	IEA (2017)#
		SC-DR-gas	NG-DR	15.60272674	TJ	2015	IEA (2017)#
		SC-DR-oil	CO-HF-DR	1.391944501	kt	2015	IEA (2017)#
		SC-DR-oil	CO-LF-DR	33.37429723	kt	2015	IEA (2017)#
		SC-IND-gas	NG-IND	0.712157652	TJ	2015	IEA (2017)#
		SC-IND-oil	CO-HF-IND	4.208204307	kt	2015	IEA (2017)#
		SC-IND-oil	CO-LF-IND	2.395439374	kt	2015	IEA (2017)#
		SC-PP-gas	NG-PP	996.2761842	TJ	2015	IEA (2017)#
		SC-PP-oil	CO-HF-PP	50.8545305	kt	2015	IEA (2017)#
		SC-PP-oil	CO-LF-PP	37.42064753	kt	2015	IEA (2017)#
GLP	Guadeloupe	BIO	PSB – DR	418.1022838	TJ	2015	IEA (2017)#
		CEM	CEM	300	kt	2014	USGS (2017a)
GTM	Guatemala	BIO	PSB – DR	251501	TJ	2015	IEA (2017)
		BIO	PSB – PP	55237	TJ	2015	IEA (2017)
		CEM	CEM	3500	kt	2014	USGS (2017a)
		NFMP-AU	GP-L	5600	kg	2015	USGS (2017b)
		OR	CO-OR	63	kt	2015	IEA (2017)
		SC-DR-oil	CO-LF-DR	1056	kt	2015	IEA (2017)
		SC-IND-oil	CO-HF-IND	228	kt	2015	IEA (2017)
		SC-IND-oil	CO-LF-IND	121	kt	2015	IEA (2017)
		SC-PP-coal	HC-B-PP	1528	kt	2015	IEA (2017)
		SC-PP-oil	CO-HF-PP	311	kt	2015	IEA (2017)
		SC-PP-oil	CO-LF-PP	41	kt	2015	IEA (2017)
		SSC	SP-S	395	kt	2014	World Steel Association (2015)

Country code	Country name	Sector code	Activity code	Activity amount	Units	Year	Source
GIN	Guinea	BIO	PSB – DR	107612.9589	TJ	2015	IEA (2017)#
		BIO	PSB – IND	1959.167785	TJ	2015	IEA (2017)#
		BIO	PSB – PP	700.9027893	TJ	2015	IEA (2017)#
		CEM	CEM	500	kt	2014	USGS (2017a)
		NFMP-AU	GP-L	17000	kg	2015	USGS (2017b)
		SC-DR-coal	HC-DR	3.18557701	kt	2015	IEA (2017)#
		SC-DR-oil	CO-LF-DR	106.868524	kt	2015	IEA (2017)#
		SC-IND-coal	HC-IND-OTH	3.299347618	kt	2015	IEA (2017)#
		SC-IND-gas	NG-IND	1.061859003	TJ	2015	IEA (2017)#
		SC-IND-oil	CO-HF-IND	19.45477388	kt	2015	IEA (2017)#
		SC-IND-oil	CO-IND	5.347218553	kt	2015	IEA (2017)#
		SC-IND-oil	CO-LF-IND	18.6204561	kt	2015	IEA (2017)#
		SC-PP-coal	HC-B-PP	27.91172237	kt	2015	IEA (2017)#
		SC-PP-gas	NG-PP	734.7685068	TJ	2015	IEA (2017)#
		SC-PP-oil	CO-HF-PP	25.2949984	kt	2015	IEA (2017)#
		SC-PP-oil	CO-LF-PP	52.33447945	kt	2015	IEA (2017)#
GNB	Guinea-Bissau	BIO	PSB – DR	15768.73571	TJ	2015	IEA (2017)#
		BIO	PSB – IND	358.8508222	TJ	2015	IEA (2017)#
		BIO	PSB – PP	128.3808075	TJ	2015	IEA (2017)#
		SC-DR-coal	HC-DR	0.583485977	kt	2015	IEA (2017)#
		SC-DR-oil	CO-LF-DR	19.57456528	kt	2015	IEA (2017)#
		SC-IND-coal	HC-IND-OTH	0.604324762	kt	2015	IEA (2017)#
		SC-IND-gas	NG-IND	0.194495326	TJ	2015	IEA (2017)#
		SC-IND-oil	CO-HF-IND	3.563432217	kt	2015	IEA (2017)#
		SC-IND-oil	CO-IND	0.97942289	kt	2015	IEA (2017)#
		SC-IND-oil	CO-LF-IND	3.410614461	kt	2015	IEA (2017)#
		SC-PP-coal	HC-B-PP	5.112448561	kt	2015	IEA (2017)#
		SC-PP-gas	NG-PP	134.5838191	TJ	2015	IEA (2017)#
		SC-PP-oil	CO-HF-PP	4.633156508	kt	2015	IEA (2017)#
		SC-PP-oil	CO-LF-PP	9.585841052	kt	2015	IEA (2017)#
GUY	Guyana	BIO	PSB – DR	764.4453441	TJ	2015	IEA (2017)#
		BIO	PSB – IND	977.4916149	TJ	2015	IEA (2017)#
		BIO	PSB – PP	320.7836731	TJ	2015	IEA (2017)#
		CEM	CEM	2	kt	2014	USGS (2017a)
		NFMP-AU	GP-L	14029	kg	2015	USGS (2017b)
		OR	CO-OR	119.1552554	kt	2015	IEA (2017)#
		SC-DR-coal	HC-DR	24.98813724	kt	2015	IEA (2017)#
		SC-DR-gas	NG-DR	59.33143916	TJ	2015	IEA (2017)#
		SC-DR-oil	CO-HF-DR	5.293053701	kt	2015	IEA (2017)#
		SC-DR-oil	CO-LF-DR	126.9101946	kt	2015	IEA (2017)#
		SC-IND-gas	NG-IND	2.708073987	TJ	2015	IEA (2017)#
		SC-IND-oil	CO-HF-IND	16.00225537	kt	2015	IEA (2017)#
		SC-IND-oil	CO-LF-IND	9.108976137	kt	2015	IEA (2017)#
		SC-PP-gas	NG-PP	3788.472413	TJ	2015	IEA (2017)#
		SC-PP-oil	CO-HF-PP	193.3811015	kt	2015	IEA (2017)#
		SC-PP-oil	CO-LF-PP	142.2969786	kt	2015	IEA (2017)#
HTI	Haiti	BIO	PSB – DR	61824	TJ	2015	IEA (2017)
		BIO	PSB – IND	3369	TJ	2015	IEA (2017)
		CEM	CEM	300	kt	2014	USGS (2017a)
		SC-DR-oil	CO-LF-DR	232	kt	2015	IEA (2017)
		SC-IND-oil	CO-HF-IND	10	kt	2015	IEA (2017)
		SC-IND-oil	CO-LF-IND	175	kt	2015	IEA (2017)
		SC-PP-oil	CO-HF-PP	109	kt	2015	IEA (2017)
		SC-PP-oil	CO-LF-PP	189	kt	2015	IEA (2017)

Country code	Country name	Sector code	Activity code	Activity amount	Units	Year	Source
HND	Honduras	BIO	PSB – DR	84987	TJ	2015	IEA (2017)
		BIO	PSB – IND	5383	TJ	2015	IEA (2017)
		BIO	PSB – PP	11304	TJ	2015	IEA (2017)
		CEM	CEM	1700	kt	2014	USGS (2017a)
		NFMP-AU	GP-L	2598	kg	2015	USGS (2017b)
		SC-DR-oil	CO-HF-DR	37	kt	2015	IEA (2017)
		SC-DR-oil	CO-LF-DR	617	kt	2015	IEA (2017)
		SC-IND-coal	HC-IND-OTH	77	kt	2015	IEA (2017)
		SC-IND-oil	CO-HF-IND	86	kt	2015	IEA (2017)
		SC-IND-oil	CO-LF-IND	259	kt	2015	IEA (2017)
		SC-PP-coal	HC-B-PP	36	kt	2015	IEA (2017)
		SC-PP-oil	CO-HF-PP	1048	kt	2015	IEA (2017)
		SC-PP-oil	CO-LF-PP	35	kt	2015	IEA (2017)
HKG	Hong Kong (if separately reported)	BIO	PSB – DR	2284	TJ	2015	IEA (2017)
		CEM	CEM	1900	kt	2014	USGS (2017a)
		SC-DR-gas	NG-DR	26754	TJ	2015	IEA (2017)
		SC-DR-oil	CO-LF-DR	1552	kt	2015	IEA (2017)
		SC-IND-coal	HC-IND-OTH	2042	kt	2015	IEA (2017)
		SC-IND-gas	NG-IND	1649	TJ	2015	IEA (2017)
		SC-IND-oil	CO-LF-IND	623	kt	2015	IEA (2017)
		SC-PP-coal	HC-B-PP	9142	kt	2015	IEA (2017)
		SC-PP-gas	NG-PP	107828	TJ	2015	IEA (2017)
		SC-PP-oil	CO-HF-PP	43	kt	2015	IEA (2017)
		SC-PP-oil	CO-LF-PP	12	kt	2015	IEA (2017)
HUN	Hungary	BIO	PSB – DR	75550	TJ	2015	IEA (2017)
		BIO	PSB – IND	4826	TJ	2015	IEA (2017)
		BIO	PSB – PP	23494	TJ	2015	IEA (2017)
		CEM	CEM	2100	kt	2014	USGS (2017a)
		CEM	PC-CEM	94	kt	2015	IEA (2017)
		CSP	CSP-C	131	kt	2015	UNEP (2013)
		NFMP	AL-P	50	kt	2015	USGS (2017b)
		OR	CO-OR	6477	kt	2015	IEA (2017)
		PISP	PIP	801	kt	2014	USGS (2017a)
		SC-DR-coal	BC-DR	380	kt	2015	IEA (2017)
		SC-DR-coal	HC-DR	24	kt	2015	IEA (2017)
		SC-DR-gas	NG-DR	187417	TJ	2015	IEA (2017)
		SC-DR-oil	CO-HF-DR	6	kt	2015	IEA (2017)
		SC-DR-oil	CO-LF-DR	2892	kt	2015	IEA (2017)
		SC-IND-coal	BC-IND-CEM	40	kt	2015	IEA (2017)
		SC-IND-coal	BC-IND-OTH	12	kt	2015	IEA (2017)
		SC-IND-coal	HC-IND-CEM	18	kt	2015	IEA (2017)
		SC-IND-gas	NG-IND	58161	TJ	2015	IEA (2017)
		SC-IND-oil	CO-HF-IND	3	kt	2015	IEA (2017)
		SC-IND-oil	CO-LF-IND	159	kt	2015	IEA (2017)
		SC-PP-coal	BC-L-PP	8822	kt	2015	IEA (2017)
		SC-PP-coal	BC-S-PP	69	kt	2015	IEA (2017)
		SC-PP-coal	HC-B-PP	14	kt	2015	IEA (2017)
		SC-PP-gas	NG-PP	80319	TJ	2015	IEA (2017)
		SC-PP-oil	CO-HF-PP	38	kt	2015	IEA (2017)
		SC-PP-oil	CO-LF-PP	12	kt	2015	IEA (2017)
		SSC	SP-S	178	kt	2014	World Steel Association (2015)

Country code	Country name	Sector code	Activity code	Activity amount	Units	Year	Source
ISL	Iceland	NFMP	AL-P	800	kt	2015	USGS (2017b)
		SC-DR-oil	CO-HF-DR	61	kt	2015	IEA (2017)
		SC-DR-oil	CO-LF-DR	289	kt	2015	IEA (2017)
		SC-IND-coal	HC-IND-PIP	116	kt	2015	IEA (2017)
		SC-IND-oil	CO-HF-IND	3	kt	2015	IEA (2017)
		SC-IND-oil	CO-LF-IND	30	kt	2015	IEA (2017)
		SC-PP-oil	CO-LF-PP	1	kt	2015	IEA (2017)
IND	India	BIO	PSB – DR	5993873	TJ	2015	IEA (2017)
		BIO	PSB – IND	1309246	TJ	2015	IEA (2017)
		BIO	PSB – PP	573072	TJ	2015	IEA (2017)
		CEM	CEM	275000	kt	2014	USGS (2017a)
		CEM	PC-CEM	19297	kt	2015	IEA (2017)
		NFMP	AL-P	2355	kt	2015	USGS (2017b)
		NFMP	CU-P	790000	t	2015	USGS (2017b)
		NFMP	PB-P	143000	t	2015	USGS (2017b)
		NFMP	ZN-T	821617	t	2015	USGS (2017b)
		NFMP-AU	GP-L	1400	kg	2015	USGS (2017b)
		OR	CO-OR	232865	kt	2015	IEA (2017)
		PISP	PIP	55166	kt	2014	USGS (2017a)
		SC-DR-coal	HC-DR	28528	kt	2015	IEA (2017)
		SC-DR-gas	NG-DR	181509	TJ	2015	IEA (2017)
		SC-DR-oil	CO-HF-DR	2068	kt	2015	IEA (2017)
		SC-DR-oil	CO-LF-DR	63375	kt	2015	IEA (2017)
		SC-IND-coal	BC-IND-CEM	617	kt	2015	IEA (2017)
		SC-IND-coal	BC-IND-NFM	1020	kt	2015	IEA (2017)
		SC-IND-coal	BC-IND-OTH	2385	kt	2015	IEA (2017)
		SC-IND-coal	BC-IND-PIP	12	kt	2015	IEA (2017)
		SC-IND-coal	HC-IND-CEM	33953	kt	2015	IEA (2017)
		SC-IND-coal	HC-IND-NFM	440	kt	2015	IEA (2017)
		SC-IND-coal	HC-IND-OTH	44358	kt	2015	IEA (2017)
		SC-IND-coal	HC-IND-PIP	67204	kt	2015	IEA (2017)
		SC-IND-gas	NG-IND	216952	TJ	2015	IEA (2017)
		SC-IND-oil	CO-HF-IND	3604	kt	2015	IEA (2017)
		SC-IND-oil	CO-LF-IND	3968	kt	2015	IEA (2017)
		SC-PP-coal	BC-L-PP	37574	kt	2015	IEA (2017)
		SC-PP-coal	BC-S-PP	79441	kt	2015	IEA (2017)
		SC-PP-coal	HC-B-PP	489196	kt	2015	IEA (2017)
		SC-PP-gas	NG-PP	664259	TJ	2015	IEA (2017)
		SC-PP-oil	CO-HF-PP	481	kt	2015	IEA (2017)
		SC-PP-oil	CO-LF-PP	7079	kt	2015	IEA (2017)
		SSC	SP-S	50211	kt	2014	World Steel Association (2015)
		VCM	VCM-P	5000	kg	2015	National information
		VCM	VCM-R	2500	kg	2015	Lin et al. (2016)

Country code	Country name	Sector code	Activity code	Activity amount	Units	Year	Source
IDN	Indonesia	BIO	PSB – DR	1996913	TJ	2015	IEA (2017)
		BIO	PSB – IND	274252	TJ	2015	IEA (2017)
		BIO	PSB – PP	8298	TJ	2015	IEA (2017)
		CEM	CEM	58000	kt	2014	USGS (2017a)
		CSP	CSP-C	25	kt	2010	UNEP (2011e)
		NFMP	AL-P	250	kt	2015	USGS (2017b)
		NFMP	CU-P	199700	t	2015	USGS (2017b)
		NFMP-AU	GP-L	61500	kg	2015	USGS (2017b)
		NFMP-HG	HG-P	450	t	2015	UN Environment (2017a)
		OR	CO-OR	40551	kt	2015	IEA (2017)
		SC-DR-gas	NG-DR	11504	TJ	2015	IEA (2017)
		SC-DR-oil	CO-HF-DR	104	kt	2015	IEA (2017)
		SC-DR-oil	CO-LF-DR	16840	kt	2015	IEA (2017)
		SC-IND-coal	BC-IND-CEM	7180	kt	2015	IEA (2017)
		SC-IND-coal	BC-IND-OTH	9142	kt	2015	IEA (2017)
		SC-IND-coal	HC-IND-PIP	399	kt	2015	IEA (2017)
		SC-IND-gas	NG-IND	589875	TJ	2015	IEA (2017)
		SC-IND-oil	CO-HF-IND	576	kt	2015	IEA (2017)
		SC-IND-oil	CO-LF-IND	2897	kt	2015	IEA (2017)
		SC-PP-coal	BC-S-PP	70080	kt	2015	IEA (2017)
		SC-PP-gas	NG-PP	940498	TJ	2015	IEA (2017)
		SC-PP-oil	CO-HF-PP	2277	kt	2015	IEA (2017)
		SC-PP-oil	CO-LF-PP	3883	kt	2015	IEA (2017)
		SSC	SP-S	4428	kt	2014	World Steel Association (2015)
IRN	Iran	BIO	PSB – DR	20933	TJ	2015	IEA (2017)
		CEM	CEM	66000	kt	2014	USGS (2017a)
		CSP	CSP-C	332	kt	2010	UNEP (2011e)
		NFMP	AL-P	350	kt	2015	USGS (2017b)
		NFMP	CU-P	155000	t	2015	USGS (2017b)
		NFMP	PB-P	16000	t	2015	USGS (2017b)
		NFMP	ZN-P	140000	t	2015	USGS (2017b)
		NFMP-AU	GP-L	3000	kg	2015	USGS (2017b)
		OR	CO-OR	83034	kt	2015	IEA (2017)
		PISP	PIP	2782	kt	2014	USGS (2017a)
		SC-DR-coal	HC-DR	14	kt	2015	IEA (2017)
		SC-DR-gas	NG-DR	2480773	TJ	2015	IEA (2017)
		SC-DR-oil	CO-HF-DR	4679	kt	2015	IEA (2017)
		SC-DR-oil	CO-LF-DR	18753	kt	2015	IEA (2017)
		SC-IND-coal	HC-IND-OTH	242	kt	2015	IEA (2017)
		SC-IND-gas	NG-IND	1493841	TJ	2015	IEA (2017)
		SC-IND-oil	CO-HF-IND	1409	kt	2015	IEA (2017)
		SC-IND-oil	CO-LF-IND	1992	kt	2015	IEA (2017)
		SC-PP-gas	NG-PP	2809650	TJ	2015	IEA (2017)
		SC-PP-oil	CO-HF-PP	6837	kt	2015	IEA (2017)
		SC-PP-oil	CO-LF-PP	5252	kt	2015	IEA (2017)
		SSC	SP-S	13607	kt	2014	World Steel Association (2015)

Country code	Country name	Sector code	Activity code	Activity amount	Units	Year	Source
IRQ	Iraq	BIO	PSB – DR	285	TJ	2015	IEA (2017)
		CEM	CEM	13000	kt	2014	USGS (2017a)
		CSP	CSP-C	68	kt	2010	UNEP (2011e)
		OR	CO-OR	20330	kt	2015	IEA (2017)
		SC-DR-oil	CO-LF-DR	3543	kt	2015	IEA (2017)
		SC-IND-gas	NG-IND	46348	TJ	2015	IEA (2017)
		SC-IND-oil	CO-HF-IND	212	kt	2015	IEA (2017)
		SC-IND-oil	CO-LF-IND	1771	kt	2015	IEA (2017)
		SC-PP-gas	NG-PP	207313	TJ	2015	IEA (2017)
		SC-PP-oil	CO-HF-PP	5861	kt	2015	IEA (2017)
		SC-PP-oil	CO-LF-PP	8366	kt	2015	IEA (2017)
		SC-PP-oil	CO-PP	10797	kt	2015	IEA (2017)
IRL	Ireland	BIO	PSB – DR	2054	TJ	2015	IEA (2017)
		BIO	PSB – IND	6031	TJ	2015	IEA (2017)
		BIO	PSB – PP	1804	TJ	2015	IEA (2017)
		CEM	CEM	2000	kt	2014	USGS (2017a)
		CEM	PC-CEM	163	kt	2015	IEA (2017)
		NFMP	AL-P	1983	kt	2015	USGS (2017b)
		OR	CO-OR	3366	kt	2015	IEA (2017)
		SC-DR-coal	HC-DR	267	kt	2015	IEA (2017)
		SC-DR-gas	NG-DR	44305	TJ	2015	IEA (2017)
		SC-DR-oil	CO-LF-DR	3138	kt	2015	IEA (2017)
		SC-IND-coal	HC-IND-CEM	126	kt	2015	IEA (2017)
		SC-IND-coal	HC-IND-OTH	33	kt	2015	IEA (2017)
		SC-IND-gas	NG-IND	35622	TJ	2015	IEA (2017)
		SC-IND-oil	CO-HF-IND	50	kt	2015	IEA (2017)
		SC-IND-oil	CO-LF-IND	139	kt	2015	IEA (2017)
		SC-PP-coal	HC-B-PP	1886	kt	2015	IEA (2017)
		SC-PP-gas	NG-PP	88178	TJ	2015	IEA (2017)
		SC-PP-oil	CO-HF-PP	60	kt	2015	IEA (2017)
		SC-PP-oil	CO-LF-PP	18	kt	2015	IEA (2017)
ISR	Israel	BIO	PSB – DR	183	TJ	2015	IEA (2017)
		CEM	CEM	6603	kt	2014	USGS (2017a)
		CSP	CSP-C	33	kt	2010	UNEP (2011e)
		OR	CO-OR	11546	kt	2015	IEA (2017)
		SC-DR-gas	NG-DR	3112	TJ	2015	IEA (2017)
		SC-DR-oil	CO-HF-DR	9	kt	2015	IEA (2017)
		SC-DR-oil	CO-LF-DR	2528	kt	2015	IEA (2017)
		SC-IND-gas	NG-IND	23105	TJ	2015	IEA (2017)
		SC-IND-oil	CO-HF-IND	261	kt	2015	IEA (2017)
		SC-PP-coal	HC-B-PP	10665	kt	2015	IEA (2017)
		SC-PP-gas	NG-PP	306331	TJ	2015	IEA (2017)
		SC-PP-oil	CO-HF-PP	20	kt	2015	IEA (2017)
		SC-PP-oil	CO-LF-PP	94	kt	2015	IEA (2017)
		SSC	SP-S	300	kt	2014	World Steel Association (2015)

Country code	Country name	Sector code	Activity code	Activity amount	Units	Year	Source
ITA	Italy	BIO	PSB – DR	269476	TJ	2015	IEA (2017)
		BIO	PSB – IND	15235	TJ	2015	IEA (2017)
		BIO	PSB – PP	73818	TJ	2015	IEA (2017)
		CEM	CEM	21400	kt	2014	USGS (2017a)
		CEM	PC-CEM	1808	kt	2015	IEA (2017)
		NFMP	PB-P	50000	t	2015	USGS (2017b)
		NFMP	ZN-P	139200	t	2015	USGS (2017b)
		OR	CO-OR	67092	kt	2015	IEA (2017)
		PISP	PIP	6371	kt	2014	USGS (2017a)
		SC-DR-gas	NG-DR	1149535	TJ	2015	IEA (2017)
		SC-DR-oil	CO-HF-DR	410	kt	2015	IEA (2017)
		SC-DR-oil	CO-LF-DR	25166	kt	2015	IEA (2017)
		SC-IND-coal	BC-IND-CEM	3	kt	2015	IEA (2017)
		SC-IND-coal	HC-IND-CEM	224	kt	2015	IEA (2017)
		SC-IND-coal	HC-IND-PIP	159	kt	2015	IEA (2017)
		SC-IND-gas	NG-IND	384873	TJ	2015	IEA (2017)
		SC-IND-oil	CO-HF-IND	796	kt	2015	IEA (2017)
		SC-IND-oil	CO-LF-IND	401	kt	2015	IEA (2017)
		SC-PP-coal	BC-S-PP	445	kt	2015	IEA (2017)
		SC-PP-coal	HC-B-PP	15869	kt	2015	IEA (2017)
		SC-PP-gas	NG-PP	999353	TJ	2015	IEA (2017)
		SC-PP-oil	CO-HF-PP	1154	kt	2015	IEA (2017)
		SC-PP-oil	CO-LF-PP	105	kt	2015	IEA (2017)
		SSC	SP-S	17200	kt	2014	World Steel Association (2015)
CIV	Ivory Coast	BIO	PSB – DR	132382	TJ	2015	IEA (2017)
		BIO	PSB – PP	1885	TJ	2015	IEA (2017)
		CEM	CEM	2600	kt	2014	USGS (2017a)
		NFMP-AU	GP-L	26000	kg	2015	USGS (2017b)
		OR	CO-OR	3186	kt	2015	IEA (2017)
		SC-DR-oil	CO-LF-DR	787	kt	2015	IEA (2017)
		SC-IND-gas	NG-IND	11633	TJ	2015	IEA (2017)
		SC-IND-oil	CO-HF-IND	29	kt	2015	IEA (2017)
		SC-IND-oil	CO-LF-IND	196	kt	2015	IEA (2017)
		SC-PP-gas	NG-PP	67526	TJ	2015	IEA (2017)
		SC-PP-oil	CO-HF-PP	152	kt	2015	IEA (2017)
		SC-PP-oil	CO-LF-PP	3	kt	2015	IEA (2017)
JAM	Jamaica	BIO	PSB – DR	1849	TJ	2015	IEA (2017)
		BIO	PSB – IND	3608	TJ	2015	IEA (2017)
		BIO	PSB – PP	3377	TJ	2015	IEA (2017)
		CEM	CEM	830	kt	2014	USGS (2017a)
		NFMP	AL-P	1865	kt	2015	USGS (2017b)
		OR	CO-OR	1218	kt	2015	IEA (2017)
		SC-DR-oil	CO-HF-DR	7	kt	2015	IEA (2017)
		SC-DR-oil	CO-LF-DR	172	kt	2015	IEA (2017)
		SC-IND-coal	HC-IND-CEM	97	kt	2015	IEA (2017)
		SC-IND-oil	CO-HF-IND	586	kt	2015	IEA (2017)
		SC-IND-oil	CO-LF-IND	33	kt	2015	IEA (2017)
		SC-PP-oil	CO-HF-PP	667	kt	2015	IEA (2017)
		SC-PP-oil	CO-LF-PP	181	kt	2015	IEA (2017)

Country code	Country name	Sector code	Activity code	Activity amount	Units	Year	Source
JPN	Japan	BIO	PSB – DR	472	TJ	2015	IEA (2017)
		BIO	PSB – IND	96748	TJ	2015	IEA (2017)
		BIO	PSB – PP	276103	TJ	2015	IEA (2017)
		CEM	CEM	57913	kt	2014	USGS (2017a)
		CEM	PC-CEM	700	kt	2015	IEA (2017)
		NFMP	AL-P	30	kt	2015	USGS (2017b)
		NFMP	CU-P	1176600	t	2015	USGS (2017b)
		NFMP	PB-P	85000	t	2015	USGS (2017b)
		NFMP	ZN-T	566619	t	2015	USGS (2017b)
		NFMP-AU	GP-L	7700	kg	2015	USGS (2017b)
		OR	CO-OR	154011	kt	2015	IEA (2017)
		PISP	PIP	83872	kt	2014	USGS (2017a)
		SC-DR-coal	HC-DR	2	kt	2015	IEA (2017)
		SC-DR-gas	NG-DR	838834	TJ	2015	IEA (2017)
		SC-DR-oil	CO-HF-DR	2188	kt	2015	IEA (2017)
		SC-DR-oil	CO-LF-DR	29456	kt	2015	IEA (2017)
		SC-IND-coal	HC-IND-CEM	5904	kt	2015	IEA (2017)
		SC-IND-coal	HC-IND-NFM	57	kt	2015	IEA (2017)
		SC-IND-coal	HC-IND-OTH	6810	kt	2015	IEA (2017)
		SC-IND-coal	HC-IND-PIP	3037	kt	2015	IEA (2017)
		SC-IND-gas	NG-IND	517970	TJ	2015	IEA (2017)
		SC-IND-oil	CO-HF-IND	2016	kt	2015	IEA (2017)
		SC-IND-oil	CO-IND	23	kt	2015	IEA (2017)
		SC-IND-oil	CO-LF-IND	6695	kt	2015	IEA (2017)
		SC-PP-coal	HC-B-PP	105420	kt	2015	IEA (2017)
		SC-PP-gas	NG-PP	3540529	TJ	2015	IEA (2017)
		SC-PP-oil	CO-HF-PP	10744	kt	2015	IEA (2017)
		SC-PP-oil	CO-LF-PP	1371	kt	2015	IEA (2017)
		SC-PP-oil	CO-PP	4875	kt	2015	IEA (2017)
		SSC	SP-S	25679	kt	2014	World Steel Association (2015)
JOR	Jordan	BIO	PSB – DR	154	TJ	2015	IEA (2017)
		CEM	CEM	4500	kt	2014	USGS (2017a)
		CEM	PC-CEM	199	kt	2015	IEA (2017)
		OR	CO-OR	3314	kt	2015	IEA (2017)
		SC-DR-oil	CO-HF-DR	1	kt	2015	IEA (2017)
		SC-DR-oil	CO-LF-DR	1465	kt	2015	IEA (2017)
		SC-IND-coal	HC-IND-CEM	253	kt	2015	IEA (2017)
		SC-IND-oil	CO-LF-IND	148	kt	2015	IEA (2017)
		SC-PP-gas	NG-PP	90441	TJ	2015	IEA (2017)
		SC-PP-oil	CO-HF-PP	1735	kt	2015	IEA (2017)
		SC-PP-oil	CO-LF-PP	564	kt	2015	IEA (2017)
		SSC	SP-S	150	kt	2014	World Steel Association (2015)

Country code	Country name	Sector code	Activity code	Activity amount	Units	Year	Source
KAZ	Kazakhstan	BIO	PSB – DR	2935	TJ	2015	IEA (2017)
		CEM	CEM	7977	kt	2014	USGS (2017a)
		NFMP	AL-P	200	kt	2015	USGS (2017b)
		NFMP	CU-P	307400	t	2015	USGS (2017b)
		NFMP	PB-T	126000	t	2015	USGS (2017b)
		NFMP	ZN-T	324340	t	2015	USGS (2017b)
		NFMP-AU	GP-L	63614	kg	2015	USGS (2017b)
		OR	CO-OR	14610	kt	2015	IEA (2017)
		PISP	PIP	3185	kt	2014	USGS (2017a)
		SC-DR-coal	BC-DR	506	kt	2015	IEA (2017)
		SC-DR-coal	HC-DR	6003	kt	2015	IEA (2017)
		SC-DR-gas	NG-DR	51397	TJ	2015	IEA (2017)
		SC-DR-oil	CO-HF-DR	490	kt	2015	IEA (2017)
		SC-DR-oil	CO-LF-DR	2774	kt	2015	IEA (2017)
		SC-IND-coal	BC-IND-CEM	36	kt	2015	IEA (2017)
		SC-IND-coal	BC-IND-OTH	2089	kt	2015	IEA (2017)
		SC-IND-coal	HC-IND-NFM	2258	kt	2015	IEA (2017)
		SC-IND-coal	HC-IND-OTH	1306	kt	2015	IEA (2017)
		SC-IND-coal	HC-IND-PIP	2317	kt	2015	IEA (2017)
		SC-IND-gas	NG-IND	83101	TJ	2015	IEA (2017)
		SC-IND-oil	CO-HF-IND	1085	kt	2015	IEA (2017)
		SC-IND-oil	CO-IND	488	kt	2015	IEA (2017)
		SC-IND-oil	CO-LF-IND	1737	kt	2015	IEA (2017)
		SC-PP-coal	BC-L-PP	42	kt	2015	IEA (2017)
		SC-PP-coal	HC-B-PP	42421	kt	2015	IEA (2017)
		SC-PP-gas	NG-PP	1092543	TJ	2015	IEA (2017)
		SC-PP-oil	CO-HF-PP	457	kt	2015	IEA (2017)
		SC-PP-oil	CO-LF-PP	225	kt	2015	IEA (2017)
		SC-PP-oil	CO-PP	888	kt	2015	IEA (2017)
		SSC	SP-S	155	kt	2014	World Steel Association (2015)
KEN	Kenya	BIO	PSB – DR	339597	TJ	2015	IEA (2017)
		BIO	PSB – PP	1464	TJ	2015	IEA (2017)
		CEM	CEM	5583	kt	2014	USGS (2017a)
		NFMP-AU	GP-L	300	kg	2015	USGS (2017b)
		OR	CO-OR	698	kt	2015	IEA (2017)
		SC-DR-oil	CO-HF-DR	14	kt	2015	IEA (2017)
		SC-DR-oil	CO-LF-DR	1467	kt	2015	IEA (2017)
		SC-IND-coal	HC-IND-CEM	566	kt	2015	IEA (2017)
		SC-IND-oil	CO-HF-IND	75	kt	2015	IEA (2017)
		SC-IND-oil	CO-LF-IND	448	kt	2015	IEA (2017)
		SC-PP-oil	CO-HF-PP	186	kt	2015	IEA (2017)
		SC-PP-oil	CO-LF-PP	167	kt	2015	IEA (2017)
		SSC	SP-S	20	kt	2014	World Steel Association (2015)
KIR	Kiribati	BIO	PSB – DR	344.3808131	TJ	2015	IEA (2017)[#]
		BIO	PSB – IND	14.20268976	TJ	2015	IEA (2017)[#]
		OR	CO-OR	1.44153565	kt	2015	IEA (2017)[#]
		SC-DR-gas	NG-DR	7.24676295	TJ	2015	IEA (2017)[#]
		SC-DR-oil	CO-HF-DR	8.97E-02	kt	2015	IEA (2017)[#]
		SC-DR-oil	CO-LF-DR	2.295651271	kt	2015	IEA (2017)[#]
		SC-IND-coal	BC-IND-OTH	2.76E-02	kt	2015	IEA (2017)[#]
		SC-IND-coal	HC-IND-OTH	1.939290783	kt	2015	IEA (2017)[#]

Country code	Country name	Sector code	Activity code	Activity amount	Units	Year	Source
		SC-IND-oil	CO-HF-IND	0.196573043	kt	2015	IEA (2017)[#]
		SC-IND-oil	CO-LF-IND	0.214965843	kt	2015	IEA (2017)[#]
		SC-PP-coal	HC-B-PP	0.510400182	kt	2015	IEA (2017)[#]
		SC-PP-gas	NG-PP	7.911202827	TJ	2015	IEA (2017)[#]
		SC-PP-oil	CO-HF-PP	1.012753515	kt	2015	IEA (2017)[#]
		SC-PP-oil	CO-LF-PP	1.324281554	kt	2015	IEA (2017)[#]
PRK	Korea – Dem. Rep.	BIO	PSB – DR	32670	TJ	2015	IEA (2017)
		CEM	CEM	7200	kt	2014	USGS (2017a)
		CSP	CSP-C	25	kt	2010	UNEP (2011e)
		NFMP	CU-T	12000	t	2015	USGS (2017b)
		NFMP	PB-T	3000	t	2015	USGS (2017b)
		NFMP	ZN-T	20000	t	2015	USGS (2017b)
		OR	CO-OR	532	kt	2015	IEA (2017)
		PISP	PIP	900	kt	2014	USGS (2017a)
		SC-DR-coal	BC-DR	851	kt	2015	IEA (2017)
		SC-DR-coal	HC-DR	1068	kt	2015	IEA (2017)
		SC-DR-oil	CO-LF-DR	252	kt	2015	IEA (2017)
		SC-IND-coal	BC-IND-OTH	1442	kt	2015	IEA (2017)
		SC-IND-coal	HC-IND-OTH	4132	kt	2015	IEA (2017)
		SC-IND-oil	CO-HF-IND	93	kt	2015	IEA (2017)
		SC-PP-coal	BC-S-PP	237	kt	2015	IEA (2017)
		SC-PP-coal	HC-B-PP	850	kt	2015	IEA (2017)
		SC-PP-oil	CO-HF-PP	380	kt	2015	IEA (2017)
KOR	Korea – Rep. of	BIO	PSB – DR	43038	TJ	2015	IEA (2017)
		BIO	PSB – IND	24414	TJ	2015	IEA (2017)
		BIO	PSB – PP	11243	TJ	2015	IEA (2017)
		CEM	CEM	44815934	t	2015	National information
		CEM	PC-CEM	57	kt	2015	IEA (2017)
		NFMP	CU-P	510000	t	2015	USGS (2017b)
		NFMP	PB-P	291000	t	2015	USGS (2017b)
		NFMP	ZN-P	930180	t	2015	National information
		NFMP-AU	GP-L	300	kg	2015	USGS (2017b)
		OR	CO-OR	130945	kt	2015	National information
		PISP	PIP	47345000	t	2015	National information
		SC-DR-gas	NG-DR	608957	TJ	2015	IEA (2017)
		SC-DR-oil	CO-HF-DR	459	kt	2015	IEA (2017)
		SC-DR-oil	CO-LF-DR	20050	kt	2015	IEA (2017)
		SC-IND-coal	HC-IND-CEM	4650	kt	2015	IEA (2017)
		SC-IND-coal	HC-IND-OTH	955	kt	2015	IEA (2017)
		SC-IND-coal	HC-IND-PIP	1431	kt	2015	IEA (2017)
		SC-IND-gas	NG-IND	344869	TJ	2015	IEA (2017)
		SC-IND-oil	CO-HF-IND	1261	kt	2015	IEA (2017)
		SC-IND-oil	CO-LF-IND	1264	kt	2015	IEA (2017)
		SC-PP-coal	BC-S-PP	6824	kt	2015	IEA (2017)
		SC-PP-coal	HC-A-PP	2273	kt	2015	IEA (2017)
		SC-PP-coal	HC-B-PP	80653	kt	2015	IEA (2017)
		SC-PP-gas	NG-PP	895074	TJ	2015	IEA (2017)
		SC-PP-oil	CO-HF-PP	3299	kt	2015	IEA (2017)
		SC-PP-oil	CO-LF-PP	111	kt	2015	IEA (2017)
		SC-PP-oil	CO-PP	1	kt	2015	IEA (2017)
		SSC	SP-S	24197	kt	2014	World Steel Association (2015)

Country code	Country name	Sector code	Activity code	Activity amount	Units	Year	Source
XKX	Kosovo	BIO	PSB – DR	10527	TJ	2015	IEA (2017)
		BIO	PSB – IND	502	TJ	2015	IEA (2017)
		CEM	CEM	630	kt	2014	USGS (2017a)
		CEM	PC-CEM	79	kt	2015	IEA (2017)
		SC-DR-coal	BC-DR	156	kt	2015	IEA (2017)
		SC-DR-oil	CO-HF-DR	9	kt	2015	IEA (2017)
		SC-DR-oil	CO-LF-DR	344	kt	2015	IEA (2017)
		SC-IND-coal	BC-IND-OTH	12	kt	2015	IEA (2017)
		SC-IND-coal	BC-IND-PIP	54	kt	2015	IEA (2017)
		SC-IND-coal	HC-IND-PIP	12	kt	2015	IEA (2017)
		SC-IND-oil	CO-HF-IND	20	kt	2015	IEA (2017)
		SC-IND-oil	CO-LF-IND	39	kt	2015	IEA (2017)
		SC-PP-coal	BC-L-PP	8143	kt	2015	IEA (2017)
		SC-PP-oil	CO-HF-PP	4	kt	2015	IEA (2017)
		SC-PP-oil	CO-LF-PP	2	kt	2015	IEA (2017)
KWT	Kuwait	CEM	CEM	3800	kt	2014	USGS (2017a)
		OR	CO-OR	43661	kt	2015	IEA (2017)
		SC-DR-oil	CO-LF-DR	1256	kt	2015	IEA (2017)
		SC-IND-gas	NG-IND	261902	TJ	2015	IEA (2017)
		SC-IND-oil	CO-LF-IND	837	kt	2015	IEA (2017)
		SC-PP-gas	NG-PP	532640	TJ	2015	IEA (2017)
		SC-PP-oil	CO-HF-PP	5862	kt	2015	IEA (2017)
		SC-PP-oil	CO-LF-PP	1450	kt	2015	IEA (2017)
		SC-PP-oil	CO-PP	1693	kt	2015	IEA (2017)
KGZ	Kyrgystan	BIO	PSB – DR	121	TJ	2015	IEA (2017)
		CEM	CEM	1727	kt	2014	USGS (2017a)
		NFMP-AU	GP-L	17000	kg	2015	USGS (2017b)
		NFMP-HG	HG-P	40	t	2015	USGS (2017b)
		OR	CO-OR	323	kt	2015	IEA (2017)
		SC-DR-coal	BC-DR	543	kt	2015	IEA (2017)
		SC-DR-coal	HC-DR	167	kt	2015	IEA (2017)
		SC-DR-gas	NG-DR	4579	TJ	2015	IEA (2017)
		SC-DR-oil	CO-HF-DR	13	kt	2015	IEA (2017)
		SC-DR-oil	CO-LF-DR	481	kt	2015	IEA (2017)
		SC-IND-coal	BC-IND-CEM	99	kt	2015	IEA (2017)
		SC-IND-coal	BC-IND-OTH	4	kt	2015	IEA (2017)
		SC-IND-coal	HC-IND-CEM	364	kt	2015	IEA (2017)
		SC-IND-coal	HC-IND-OTH	8	kt	2015	IEA (2017)
		SC-IND-gas	NG-IND	909	TJ	2015	IEA (2017)
		SC-IND-oil	CO-HF-IND	242	kt	2015	IEA (2017)
		SC-IND-oil	CO-LF-IND	39	kt	2015	IEA (2017)
		SC-PP-coal	BC-L-PP	452	kt	2015	IEA (2017)
		SC-PP-coal	HC-B-PP	973	kt	2015	IEA (2017)
		SC-PP-gas	NG-PP	4510	TJ	2015	IEA (2017)
		SC-PP-oil	CO-HF-PP	28	kt	2015	IEA (2017)
		SC-PP-oil	CO-LF-PP	16	kt	2015	IEA (2017)

Country code	Country name	Sector code	Activity code	Activity amount	Units	Year	Source
LAO	Lao Peoples Dem. Rep.	BIO	PSB – DR	22516.13496	TJ	2015	IEA (2017)
		BIO	PSB – IND	2734.191073	TJ	2015	IEA (2017)
		CEM	CEM	2400	kt	2014	USGS (2017a)
		NFMP-AU	GP-L	6893	kg	2015	USGS (2017b)
		OR	CO-OR	277.5132016	kt	2015	IEA (2017)
		SC-DR-gas	NG-DR	1395.090289	TJ	2015	IEA (2017)
		SC-DR-oil	CO-HF-DR	17.2615867	kt	2015	IEA (2017)
		SC-DR-oil	CO-LF-DR	441.94088	kt	2015	IEA (2017)
		SC-IND-coal	BC-IND-OTH	5.311257446	kt	2015	IEA (2017)
		SC-IND-coal	HC-IND-OTH	373.337138	kt	2015	IEA (2017)
		SC-IND-oil	CO-HF-IND	37.84270931	kt	2015	IEA (2017)
		SC-IND-oil	CO-LF-IND	41.3835476	kt	2015	IEA (2017)
		SC-PP-coal	HC-B-PP	98.25826276	kt	2015	IEA (2017)
		SC-PP-gas	NG-PP	1523.003073	TJ	2015	IEA (2017)
		SC-PP-oil	CO-HF-PP	194.9674088	kt	2015	IEA (2017)
		SC-PP-oil	CO-LF-PP	254.9403574	kt	2015	IEA (2017)
LVA	Latvia	BIO	PSB – DR	22947	TJ	2015	IEA (2017)
		BIO	PSB – IND	14992	TJ	2015	IEA (2017)
		BIO	PSB – PP	14053	TJ	2015	IEA (2017)
		CEM	CEM	1200	kt	2014	USGS (2017a)
		SC-DR-coal	HC-DR	32	kt	2015	IEA (2017)
		SC-DR-gas	NG-DR	9115	TJ	2015	IEA (2017)
		SC-DR-oil	CO-LF-DR	904	kt	2015	IEA (2017)
		SC-IND-coal	HC-IND-CEM	40	kt	2015	IEA (2017)
		SC-IND-coal	HC-IND-OTH	2	kt	2015	IEA (2017)
		SC-IND-gas	NG-IND	5610	TJ	2015	IEA (2017)
		SC-IND-oil	CO-LF-IND	36	kt	2015	IEA (2017)
		SC-PP-coal	HC-B-PP	7	kt	2015	IEA (2017)
		SC-PP-gas	NG-PP	35997	TJ	2015	IEA (2017)
		SC-PP-oil	CO-LF-PP	7	kt	2015	IEA (2017)
LBN	Lebanon	BIO	PSB – DR	4091	TJ	2015	IEA (2017)
		CEM	CEM	5517	kt	2014	USGS (2017a)
		SC-DR-oil	CO-LF-DR	748	kt	2015	IEA (2017)
		SC-IND-coal	HC-IND-CEM	253	kt	2015	IEA (2017)
		SC-IND-oil	CO-HF-IND	141	kt	2015	IEA (2017)
		SC-PP-oil	CO-HF-PP	1334	kt	2015	IEA (2017)
		SC-PP-oil	CO-LF-PP	2617	kt	2015	IEA (2017)
LSO	Lesotho	BIO	PSB – DR	17792.44357	TJ	2015	IEA (2017)
		BIO	PSB – IND	809.809121	TJ	2015	IEA (2017)
		BIO	PSB – PP	289.713559	TJ	2015	IEA (2017)
		SC-DR-coal	HC-DR	1.31673731	kt	2015	IEA (2017)
		SC-DR-oil	CO-LF-DR	44.17340165	kt	2015	IEA (2017)
		SC-IND-coal	HC-IND-OTH	1.363763642	kt	2015	IEA (2017)
		SC-IND-gas	NG-IND	0.438912437	TJ	2015	IEA (2017)
		SC-IND-oil	CO-HF-IND	8.041502856	kt	2015	IEA (2017)
		SC-IND-oil	CO-IND	2.210237627	kt	2015	IEA (2017)
		SC-IND-oil	CO-LF-IND	7.696643085	kt	2015	IEA (2017)
		SC-PP-coal	HC-B-PP	11.5371269	kt	2015	IEA (2017)
		SC-PP-gas	NG-PP	303.7117307	TJ	2015	IEA (2017)
		SC-PP-oil	CO-HF-PP	10.45552126	kt	2015	IEA (2017)
		SC-PP-oil	CO-LF-PP	21.63211295	kt	2015	IEA (2017)

Country code	Country name	Sector code	Activity code	Activity amount	Units	Year	Source
LBR	Liberia	BIO	PSB – DR	38327.82882	TJ	2015	IEA (2017)
		BIO	PSB – IND	523.3383248	TJ	2015	IEA (2017)
		BIO	PSB – PP	187.2270943	TJ	2015	IEA (2017)
		CEM	CEM	295	kt	2014	USGS (2017a)
		NFMP-AU	GP-L	883	kg	2015	USGS (2017b)
		SC-DR-coal	HC-DR	0.850940154	kt	2015	IEA (2017)
		SC-DR-oil	CO-LF-DR	28.54701611	kt	2015	IEA (2017)
		SC-IND-coal	HC-IND-OTH	0.881330874	kt	2015	IEA (2017)
		SC-IND-gas	NG-IND	0.283646718	TJ	2015	IEA (2017)
		SC-IND-oil	CO-HF-IND	5.196813082	kt	2015	IEA (2017)
		SC-IND-oil	CO-IND	1.42836383	kt	2015	IEA (2017)
		SC-IND-oil	CO-LF-IND	4.973947804	kt	2015	IEA (2017)
		SC-PP-coal	HC-B-PP	7.455856586	kt	2015	IEA (2017)
		SC-PP-gas	NG-PP	196.2733986	TJ	2015	IEA (2017)
		SC-PP-oil	CO-HF-PP	6.756870031	kt	2015	IEA (2017)
		SC-PP-oil	CO-LF-PP	13.9797311	kt	2015	IEA (2017)
LBY	Libyan Arab Jamah	BIO	PSB – DR	6352	TJ	2015	IEA (2017)
		CEM	CEM	2000	kt	2014	USGS (2017a)
		CSP	CSP-C	45	kt	2010	UNEP (2011e)
		OR	CO-OR	4368	kt	2015	IEA (2017)
		SC-DR-oil	CO-LF-DR	1947	kt	2015	IEA (2017)
		SC-IND-gas	NG-IND	2130	TJ	2015	IEA (2017)
		SC-IND-oil	CO-HF-IND	253	kt	2015	IEA (2017)
		SC-PP-gas	NG-PP	218638	TJ	2015	IEA (2017)
		SC-PP-oil	CO-HF-PP	1113	kt	2015	IEA (2017)
		SC-PP-oil	CO-LF-PP	3327	kt	2015	IEA (2017)
		SSC	SP-S	712	kt	2014	World Steel Association (2015)
LTU	Lithuania	BIO	PSB – DR	22351	TJ	2015	IEA (2017)
		BIO	PSB – IND	3598	TJ	2015	IEA (2017)
		BIO	PSB – PP	24402	TJ	2015	IEA (2017)
		CEM	CEM	903	kt	2014	USGS (2017a)
		OR	CO-OR	8486	kt	2015	IEA (2017)
		SC-DR-coal	HC-DR	104	kt	2015	IEA (2017)
		SC-DR-gas	NG-DR	10926	TJ	2015	IEA (2017)
		SC-DR-oil	CO-LF-DR	1336	kt	2015	IEA (2017)
		SC-IND-coal	HC-IND-CEM	141	kt	2015	IEA (2017)
		SC-IND-coal	HC-IND-OTH	3	kt	2015	IEA (2017)
		SC-IND-gas	NG-IND	13215	TJ	2015	IEA (2017)
		SC-IND-oil	CO-HF-IND	10	kt	2015	IEA (2017)
		SC-IND-oil	CO-LF-IND	20	kt	2015	IEA (2017)
		SC-PP-coal	HC-B-PP	4	kt	2015	IEA (2017)
		SC-PP-gas	NG-PP	28225	TJ	2015	IEA (2017)
		SC-PP-oil	CO-HF-PP	116	kt	2015	IEA (2017)
		SC-PP-oil	CO-LF-PP	5	kt	2015	IEA (2017)
LUX	Luxembourg	BIO	PSB – DR	866	TJ	2015	IEA (2017)
		BIO	PSB – IND	1025	TJ	2015	IEA (2017)
		BIO	PSB – PP	785	TJ	2015	IEA (2017)
		CEM	CEM	1100	kt	2014	USGS (2017a)
		SC-DR-gas	NG-DR	15034	TJ	2015	IEA (2017)
		SC-DR-oil	CO-LF-DR	1803	kt	2015	IEA (2017)
		SC-IND-coal	HC-IND-CEM	62	kt	2015	IEA (2017)
		SC-IND-coal	HC-IND-PIP	11	kt	2015	IEA (2017)
		SC-IND-gas	NG-IND	13024	TJ	2015	IEA (2017)
		SC-IND-oil	CO-LF-IND	13	kt	2015	IEA (2017)
		SC-PP-gas	NG-PP	7936	TJ	2015	IEA (2017)

Country code	Country name	Sector code	Activity code	Activity amount	Units	Year	Source
		SC-PP-oil	CO-LF-PP	1	kt	2015	IEA (2017)
		SSC	SP-S	2193	kt	2014	World Steel Association (2015)
MKD	Macedonia	BIO	PSB – DR	9762	TJ	2015	IEA (2017)
		BIO	PSB – IND	241	TJ	2015	IEA (2017)
		BIO	PSB – PP	2	TJ	2015	IEA (2017)
		CEM	CEM	687	kt	2014	USGS (2017a)
		CEM	PC-CEM	57	kt	2015	IEA (2017)
		SC-DR-coal	BC-DR	10	kt	2015	IEA (2017)
		SC-DR-gas	NG-DR	261	TJ	2015	IEA (2017)
		SC-DR-oil	CO-HF-DR	13	kt	2015	IEA (2017)
		SC-DR-oil	CO-LF-DR	498	kt	2015	IEA (2017)
		SC-IND-coal	BC-IND-CEM	1	kt	2015	IEA (2017)
		SC-IND-coal	BC-IND-OTH	7	kt	2015	IEA (2017)
		SC-IND-coal	BC-IND-PIP	190	kt	2015	IEA (2017)
		SC-IND-coal	HC-IND-PIP	12	kt	2015	IEA (2017)
		SC-IND-gas	NG-IND	1195	TJ	2015	IEA (2017)
		SC-IND-oil	CO-HF-IND	53	kt	2015	IEA (2017)
		SC-IND-oil	CO-LF-IND	44	kt	2015	IEA (2017)
		SC-PP-coal	BC-L-PP	5833	kt	2015	IEA (2017)
		SC-PP-gas	NG-PP	3720	TJ	2015	IEA (2017)
		SC-PP-oil	CO-HF-PP	39	kt	2015	IEA (2017)
		SC-PP-oil	CO-LF-PP	2	kt	2015	IEA (2017)
		SSC	SP-S	188	kt	2014	World Steel Association (2015)
MDG	Madagascar	BIO	PSB – DR	217531.2242	TJ	2015	IEA (2017)[#]
		BIO	PSB – IND	4950.38157	TJ	2015	IEA (2017)[#]
		BIO	PSB – PP	1771.025574	TJ	2015	IEA (2017)[#]
		CEM	CEM	240	kt	2014	USGS (2017a)
		SC-DR-coal	HC-DR	8.049245115	kt	2015	IEA (2017)[#]
		SC-DR-oil	CO-LF-DR	270.0330087	kt	2015	IEA (2017)[#]
		SC-IND-coal	HC-IND-OTH	8.336718155	kt	2015	IEA (2017)[#]
		SC-IND-gas	NG-IND	2.683081705	TJ	2015	IEA (2017)[#]
		SC-IND-oil	CO-HF-IND	49.15788981	kt	2015	IEA (2017)[#]
		SC-IND-oil	CO-IND	13.51123287	kt	2015	IEA (2017)[#]
		SC-IND-oil	CO-LF-IND	47.04975418	kt	2015	IEA (2017)[#]
		SC-PP-coal	HC-B-PP	70.5267191	kt	2015	IEA (2017)[#]
		SC-PP-gas	NG-PP	1856.596715	TJ	2015	IEA (2017)[#]
		SC-PP-oil	CO-HF-PP	63.91483919	kt	2015	IEA (2017)[#]
		SC-PP-oil	CO-LF-PP	132.2375983	kt	2015	IEA (2017)[#]
MWI	Malawi	BIO	PSB – DR	164109.3051	TJ	2015	IEA (2017)[#]
		BIO	PSB – IND	2738.745669	TJ	2015	IEA (2017)[#]
		BIO	PSB – PP	979.8009611	TJ	2015	IEA (2017)[#]
		CEM	CEM	450	kt	2014	USGS (2017a)
		SC-DR-coal	HC-DR	4.453158789	kt	2015	IEA (2017)[#]
		SC-DR-oil	CO-LF-DR	149.3928746	kt	2015	IEA (2017)[#]
		SC-IND-coal	HC-IND-OTH	4.612200174	kt	2015	IEA (2017)[#]
		SC-IND-gas	NG-IND	1.484386263	TJ	2015	IEA (2017)[#]
		SC-IND-oil	CO-HF-IND	27.19607689	kt	2015	IEA (2017)[#]
		SC-IND-oil	CO-IND	7.47494511	kt	2015	IEA (2017)[#]
		SC-IND-oil	CO-LF-IND	26.0297734	kt	2015	IEA (2017)[#]
		SC-PP-coal	HC-B-PP	39.0181532	kt	2015	IEA (2017)[#]
		SC-PP-gas	NG-PP	1027.14228	TJ	2015	IEA (2017)[#]
		SC-PP-oil	CO-HF-PP	35.36020134	kt	2015	IEA (2017)[#]
		SC-PP-oil	CO-LF-PP	73.15903725	kt	2015	IEA (2017)[#]

Country code	Country name	Sector code	Activity code	Activity amount	Units	Year	Source
MYS	Malaysia	BIO	PSB – DR	25374	TJ	2015	IEA (2017)
		BIO	PSB – PP	9878	TJ	2015	IEA (2017)
		CEM	CEM	22000	kt	2014	USGS (2017a)
		NFMP	AL-P	440	kt	2015	USGS (2017b)
		NFMP-AU	GP-L	4732	kg	2015	USGS (2017b)
		OR	CO-OR	23745	kt	2015	IEA (2017)
		SC-DR-gas	NG-DR	13398	TJ	2015	IEA (2017)
		SC-DR-oil	CO-HF-DR	208	kt	2015	IEA (2017)
		SC-DR-oil	CO-LF-DR	7873	kt	2015	IEA (2017)
		SC-IND-coal	HC-IND-OTH	2821	kt	2015	IEA (2017)
		SC-IND-gas	NG-IND	223653	TJ	2015	IEA (2017)
		SC-IND-oil	CO-HF-IND	495	kt	2015	IEA (2017)
		SC-IND-oil	CO-LF-IND	1366	kt	2015	IEA (2017)
		SC-PP-coal	HC-B-PP	24789	kt	2015	IEA (2017)
		SC-PP-gas	NG-PP	1160350	TJ	2015	IEA (2017)
		SC-PP-oil	CO-HF-PP	119	kt	2015	IEA (2017)
		SC-PP-oil	CO-LF-PP	325	kt	2015	IEA (2017)
		SC-PP-oil	CO-PP	383	kt	2015	IEA (2017)
		SSC	SP-S	4316	kt	2014	World Steel Association (2015)
MDV	Maldives	BIO	PSB – DR	1281.122948	TJ	2015	IEA (2017)[#]
		BIO	PSB – IND	437.3571462	TJ	2015	IEA (2017)[#]
		OR	CO-OR	44.39059986	kt	2015	IEA (2017)[#]
		SC-DR-gas	NG-DR	223.1565722	TJ	2015	IEA (2017)[#]
		SC-DR-oil	CO-HF-DR	2.761137791	kt	2015	IEA (2017)[#]
		SC-DR-oil	CO-LF-DR	70.69220728	kt	2015	IEA (2017)[#]
		SC-IND-coal	BC-IND-OTH	0.849580859	kt	2015	IEA (2017)[#]
		SC-IND-coal	HC-IND-OTH	59.71845452	kt	2015	IEA (2017)[#]
		SC-IND-oil	CO-HF-IND	6.053263618	kt	2015	IEA (2017)[#]
		SC-IND-oil	CO-LF-IND	6.619650857	kt	2015	IEA (2017)[#]
		SC-PP-coal	HC-B-PP	15.71724589	kt	2015	IEA (2017)[#]
		SC-PP-gas	NG-PP	243.6173112	TJ	2015	IEA (2017)[#]
		SC-PP-oil	CO-HF-PP	31.18669735	kt	2015	IEA (2017)[#]
		SC-PP-oil	CO-LF-PP	40.77988122	kt	2015	IEA (2017)[#]
MLI	Mali	BIO	PSB – DR	154890.5183	TJ	2015	IEA (2017)[#]
		BIO	PSB – IND	5169.795047	TJ	2015	IEA (2017)[#]
		BIO	PSB – PP	1849.521923	TJ	2015	IEA (2017)[#]
		NFMP-AU	GP-L	41186	kg	2015	USGS (2017b)
		SC-DR-coal	HC-DR	8.40600809	kt	2015	IEA (2017)[#]
		SC-DR-oil	CO-LF-DR	282.0015571	kt	2015	IEA (2017)[#]
		SC-IND-coal	HC-IND-OTH	8.706222665	kt	2015	IEA (2017)[#]
		SC-IND-gas	NG-IND	2.802002697	TJ	2015	IEA (2017)[#]
		SC-IND-oil	CO-HF-IND	51.33669226	kt	2015	IEA (2017)[#]
		SC-IND-oil	CO-IND	14.11008501	kt	2015	IEA (2017)[#]
		SC-IND-oil	CO-LF-IND	49.13511872	kt	2015	IEA (2017)[#]
		SC-PP-coal	HC-B-PP	73.65264231	kt	2015	IEA (2017)[#]
		SC-PP-gas	NG-PP	1938.885795	TJ	2015	IEA (2017)[#]
		SC-PP-oil	CO-HF-PP	66.7477071	kt	2015	IEA (2017)[#]
		SC-PP-oil	CO-LF-PP	138.0987043	kt	2015	IEA (2017)[#]

Country code	Country name	Sector code	Activity code	Activity amount	Units	Year	Source
MLT	Malta	BIO	PSB – DR	48	TJ	2015	IEA (2017)
		SC-DR-oil	CO-HF-DR	6	kt	2015	IEA (2017)
		SC-DR-oil	CO-LF-DR	142	kt	2015	IEA (2017)
		SC-IND-oil	CO-HF-IND	4	kt	2015	IEA (2017)
		SC-IND-oil	CO-LF-IND	4	kt	2015	IEA (2017)
		SC-PP-oil	CO-HF-PP	254	kt	2015	IEA (2017)
		SC-PP-oil	CO-LF-PP	20	kt	2015	IEA (2017)
MTQ	Martinique	BIO	PSB – DR	400.8757448	TJ	2015	IEA (2017)#
		CEM	CEM	150	kt	2014	USGS (2017a)
MRT	Mauritania	BIO	PSB – DR	32856.23274	TJ	2015	IEA (2017)#
		BIO	PSB – IND	2193.290992	TJ	2015	IEA (2017)#
		BIO	PSB – PP	784.6616231	TJ	2015	IEA (2017)#
		CEM	CEM	770	kt	2014	USGS (2017a)
		NFMP-AU	GP-L	8800	kg	2015	USGS (2017b)
		SC-DR-coal	HC-DR	3.566257783	kt	2015	IEA (2017)#
		SC-DR-oil	CO-LF-DR	119.6394575	kt	2015	IEA (2017)#
		SC-IND-coal	HC-IND-OTH	3.693624132	kt	2015	IEA (2017)#
		SC-IND-gas	NG-IND	1.188752594	TJ	2015	IEA (2017)#
		SC-IND-oil	CO-HF-IND	21.77964574	kt	2015	IEA (2017)#
		SC-IND-oil	CO-IND	5.986218421	kt	2015	IEA (2017)#
		SC-IND-oil	CO-LF-IND	20.84562585	kt	2015	IEA (2017)#
		SC-PP-coal	HC-B-PP	31.24721105	kt	2015	IEA (2017)#
		SC-PP-gas	NG-PP	822.5743397	TJ	2015	IEA (2017)#
		SC-PP-oil	CO-HF-PP	28.31778501	kt	2015	IEA (2017)#
		SC-PP-oil	CO-LF-PP	58.58852071	kt	2015	IEA (2017)#
MUS	Mauritius	BIO	PSB – DR	217	TJ	2015	IEA (2017)
		BIO	PSB – IND	1345	TJ	2015	IEA (2017)
		BIO	PSB – PP	8309	TJ	2015	IEA (2017)
		SC-DR-oil	CO-HF-DR	3	kt	2015	IEA (2017)
		SC-DR-oil	CO-LF-DR	171	kt	2015	IEA (2017)
		SC-IND-coal	HC-IND-OTH	36	kt	2015	IEA (2017)
		SC-IND-oil	CO-HF-IND	37	kt	2015	IEA (2017)
		SC-IND-oil	CO-LF-IND	37	kt	2015	IEA (2017)
		SC-PP-coal	HC-B-PP	684	kt	2015	IEA (2017)
		SC-PP-oil	CO-HF-PP	230	kt	2015	IEA (2017)
		SC-PP-oil	CO-LF-PP	1	kt	2015	IEA (2017)
MEX	Mexico	BIO	PSB – DR	252840	TJ	2015	IEA (2017)
		BIO	PSB – IND	37150	TJ	2015	IEA (2017)
		BIO	PSB – PP	68740	TJ	2015	IEA (2017)
		CEM	CEM	35000	kt	2014	USGS (2017a)
		CEM	PC-CEM	3789	kt	2015	IEA (2017)
		CSP	CSP-C	120	kt	2015	UNEP (2013)
		NFMP	CU-P	256000	t	2015	USGS (2017b)
		NFMP	PB-P	116000	t	2015	USGS (2017b)
		NFMP	ZN-P	326642	t	2015	USGS (2017b)
		NFMP-AU	GP-L	134759	kg	2015	USGS (2017b)
		NFMP-HG	HG-P	300	t	2015	USGS (2017b)
		OR	CO-OR	59485	kt	2015	IEA (2017)
		PISP	PIP	5116	kt	2014	USGS (2017a)
		SC-DR-gas	NG-DR	49021	TJ	2015	IEA (2017)
		SC-DR-oil	CO-HF-DR	25	kt	2015	IEA (2017)

Country code	Country name	Sector code	Activity code	Activity amount	Units	Year	Source
		SC-DR-oil	CO-LF-DR	17054	kt	2015	IEA (2017)
		SC-IND-coal	BC-IND-CEM	330	kt	2015	IEA (2017)
		SC-IND-coal	BC-IND-OTH	2535	kt	2015	IEA (2017)
		SC-IND-coal	HC-IND-OTH	89	kt	2015	IEA (2017)
		SC-IND-gas	NG-IND	576685	TJ	2015	IEA (2017)
		SC-IND-oil	CO-HF-IND	536	kt	2015	IEA (2017)
		SC-IND-oil	CO-LF-IND	1601	kt	2015	IEA (2017)
		SC-PP-coal	BC-S-PP	10386	kt	2015	IEA (2017)
		SC-PP-coal	HC-B-PP	5328	kt	2015	IEA (2017)
		SC-PP-gas	NG-PP	2231293	TJ	2015	IEA (2017)
		SC-PP-oil	CO-HF-PP	7572	kt	2015	IEA (2017)
		SC-PP-oil	CO-LF-PP	1219	kt	2015	IEA (2017)
		SSC	SP-S	13311	kt	2014	World Steel Association (2015)
MNG	Mongolia	BIO	PSB – DR	3169	TJ	2015	IEA (2017)
		CEM	CEM	411	kt	2014	USGS (2017a)
		NFMP-AU	GP-L	14556	kg	2015	USGS (2017b)
		SC-DR-coal	BC-DR	493	kt	2015	IEA (2017)
		SC-DR-coal	HC-DR	409	kt	2015	IEA (2017)
		SC-DR-oil	CO-LF-DR	232	kt	2015	IEA (2017)
		SC-IND-coal	BC-IND-OTH	35	kt	2015	IEA (2017)
		SC-IND-coal	HC-IND-OTH	23	kt	2015	IEA (2017)
		SC-IND-oil	CO-LF-IND	349	kt	2015	IEA (2017)
		SC-PP-coal	BC-L-PP	5259	kt	2015	IEA (2017)
		SC-PP-coal	HC-B-PP	1429	kt	2015	IEA (2017)
		SC-PP-oil	CO-HF-PP	3	kt	2015	IEA (2017)
		SC-PP-oil	CO-LF-PP	74	kt	2015	IEA (2017)
		SSC	SP-S	45	kt	2014	World Steel Association (2015)
MSR	Monserrat	BIO	PSB – DR	5.449317415	TJ	2015	IEA (2017)#
		BIO	PSB – IND	7.897076929	TJ	2015	IEA (2017)#
		BIO	PSB – PP	2.591585755	TJ	2015	IEA (2017)#
		OR	CO-OR	0.962645821	kt	2015	IEA (2017)#
		SC-DR-coal	HC-DR	0.201877171	kt	2015	IEA (2017)#
		SC-DR-gas	NG-DR	0.479333973	TJ	2015	IEA (2017)#
		SC-DR-oil	CO-HF-DR	4.28E-02	kt	2015	IEA (2017)#
		SC-DR-oil	CO-LF-DR	1.025297357	kt	2015	IEA (2017)#
		SC-IND-gas	NG-IND	2.19E-02	TJ	2015	IEA (2017)#
		SC-IND-oil	CO-HF-IND	0.129280947	kt	2015	IEA (2017)#
		SC-IND-oil	CO-LF-IND	7.36E-02	kt	2015	IEA (2017)#
		SC-PP-gas	NG-PP	30.60676699	TJ	2015	IEA (2017)#
		SC-PP-oil	CO-HF-PP	1.562310522	kt	2015	IEA (2017)#
		SC-PP-oil	CO-LF-PP	1.14960596	kt	2015	IEA (2017)#
MNE	Montenegro	BIO	PSB – DR	6688	TJ	2015	IEA (2017)
		BIO	PSB – IND	396	TJ	2015	IEA (2017)
		NFMP	AL-P	40	kt	2015	USGS (2017b)
		SC-DR-coal	BC-DR	22	kt	2015	IEA (2017)
		SC-DR-oil	CO-HF-DR	2	kt	2015	IEA (2017)
		SC-DR-oil	CO-LF-DR	148	kt	2015	IEA (2017)
		SC-IND-coal	BC-IND-OTH	6	kt	2015	IEA (2017)
		SC-IND-coal	BC-IND-PIP	24	kt	2015	IEA (2017)
		SC-IND-oil	CO-HF-IND	3	kt	2015	IEA (2017)
		SC-IND-oil	CO-LF-IND	36	kt	2015	IEA (2017)
		SC-PP-coal	BC-L-PP	1668	kt	2015	IEA (2017)
		SSC	SP-S	140	kt	2014	World Steel Association (2015)

Country code	Country name	Sector code	Activity code	Activity amount	Units	Year	Source
MAR	Morocco	BIO	PSB – DR	51091	TJ	2015	IEA (2017)
		BIO	PSB – IND	1269	TJ	2015	IEA (2017)
		CEM	CEM	15710	kt	2014	USGS (2017a)
		CEM	PC-CEM	1222	kt	2015	IEA (2017)
		CSP	CSP-C	8	kt	2010	UNEP (2011e)
		NFMP-AU	GP-L	500	kg	2015	USGS (2017b)
		NFMP-HG	HG-P	5	t	2015	USGS (2017b)
		OR	CO-OR	2623	kt	2015	IEA (2017)
		PISP	PIP	15	kt	2014	USGS (2017a)
		SC-DR-oil	CO-HF-DR	1	kt	2015	IEA (2017)
		SC-DR-oil	CO-LF-DR	5054	kt	2015	IEA (2017)
		SC-IND-coal	HC-IND-CEM	2	kt	2015	IEA (2017)
		SC-IND-coal	HC-IND-NFM	15	kt	2015	IEA (2017)
		SC-IND-coal	HC-IND-OTH	10	kt	2015	IEA (2017)
		SC-IND-gas	NG-IND	3097	TJ	2015	IEA (2017)
		SC-IND-oil	CO-HF-IND	693	kt	2015	IEA (2017)
		SC-IND-oil	CO-LF-IND	222	kt	2015	IEA (2017)
		SC-PP-coal	HC-B-PP	6707	kt	2015	IEA (2017)
		SC-PP-gas	NG-PP	43985	TJ	2015	IEA (2017)
		SC-PP-oil	CO-HF-PP	714	kt	2015	IEA (2017)
		SC-PP-oil	CO-LF-PP	10	kt	2015	IEA (2017)
		SSC	SP-S	501	kt	2014	World Steel Association (2015)
MOZ	Mozambique	BIO	PSB – DR	268809	TJ	2015	IEA (2017)
		BIO	PSB – IND	37888	TJ	2015	IEA (2017)
		CEM	CEM	1502	kt	2014	USGS (2017a)
		NFMP	AL-P	558	kt	2015	USGS (2017b)
		NFMP-AU	GP-L	250	kg	2015	USGS (2017b)
		SC-DR-gas	NG-DR	146	TJ	2015	IEA (2017)
		SC-DR-oil	CO-LF-DR	599	kt	2015	IEA (2017)
		SC-IND-gas	NG-IND	6252	TJ	2015	IEA (2017)
		SC-IND-oil	CO-LF-IND	136	kt	2015	IEA (2017)
		SC-PP-coal	HC-B-PP	14	kt	2015	IEA (2017)
		SC-PP-gas	NG-PP	23936	TJ	2015	IEA (2017)
		SC-PP-oil	CO-LF-PP	25	kt	2015	IEA (2017)
MMR	Myanmar	BIO	PSB – DR	407625	TJ	2015	IEA (2017)
		BIO	PSB – IND	13197	TJ	2015	IEA (2017)
		CEM	CEM	1317	kt	2014	USGS (2017a)
		CSP	CSP-C	7	kt	2010	UNEP (2011e)
		NFMP	PB-P	2000	t	2015	USGS (2017b)
		NFMP-AU	GP-L	1692	kg	2015	USGS (2017b)
		OR	CO-OR	637	kt	2015	IEA (2017)
		PISP	PIP	1.5	kt	2014	USGS (2017a)
		SC-DR-coal	BC-DR	54	kt	2015	IEA (2017)
		SC-DR-gas	NG-DR	9028	TJ	2015	IEA (2017)
		SC-DR-oil	CO-HF-DR	34	kt	2015	IEA (2017)
		SC-DR-oil	CO-LF-DR	1337	kt	2015	IEA (2017)
		SC-IND-coal	HC-IND-CEM	517	kt	2015	IEA (2017)
		SC-IND-coal	HC-IND-OTH	67	kt	2015	IEA (2017)
		SC-IND-gas	NG-IND	17584	TJ	2015	IEA (2017)
		SC-IND-oil	CO-HF-IND	31	kt	2015	IEA (2017)
		SC-IND-oil	CO-LF-IND	775	kt	2015	IEA (2017)
		SC-PP-coal	HC-B-PP	113	kt	2015	IEA (2017)
		SC-PP-gas	NG-PP	103754	TJ	2015	IEA (2017)
		SC-PP-oil	CO-LF-PP	34	kt	2015	IEA (2017)
		SSC	SP-S	35	kt	2014	World Steel Association (2015)

Country code	Country name	Sector code	Activity code	Activity amount	Units	Year	Source
NAM	Namibia	BIO	PSB – DR	4030	TJ	2015	IEA (2017)
		BIO	PSB – IND	1173	TJ	2015	IEA (2017)
		CEM	CEM	731	kt	2014	USGS (2017a)
		NFMP	CU-P	49000	t	2015	USGS (2017b)
		NFMP	ZN-P	72000	t	2015	USGS (2017b)
		NFMP-AU	GP-L	6105	kg	2015	USGS (2017b)
		SC-DR-oil	CO-HF-DR	16	kt	2015	IEA (2017)
		SC-DR-oil	CO-LF-DR	676	kt	2015	IEA (2017)
		SC-IND-oil	CO-HF-IND	2	kt	2015	IEA (2017)
		SC-IND-oil	CO-LF-IND	88	kt	2015	IEA (2017)
		SC-PP-coal	HC-B-PP	4	kt	2015	IEA (2017)
		SC-PP-oil	CO-LF-PP	9	kt	2015	IEA (2017)
NPL	Nepal	BIO	PSB – DR	383914	TJ	2015	IEA (2017)
		BIO	PSB – IND	2447	TJ	2015	IEA (2017)
		CEM	CEM	3100	kt	2014	USGS (2017a)
		SC-DR-coal	HC-DR	4	kt	2015	IEA (2017)
		SC-DR-oil	CO-LF-DR	610	kt	2015	IEA (2017)
		SC-IND-coal	HC-IND-OTH	925	kt	2015	IEA (2017)
		SC-IND-oil	CO-LF-IND	9	kt	2015	IEA (2017)
NLD	Netherlands	BIO	PSB – DR	21963	TJ	2015	IEA (2017)
		BIO	PSB – IND	5384	TJ	2015	IEA (2017)
		BIO	PSB – PP	22006	TJ	2015	IEA (2017)
		CEM	CEM	2000	kt	2014	USGS (2017a)
		NFMP	AL-P	75	kt	2015	USGS (2017b)
		NFMP	ZN-P	291000	t	2015	USGS (2017b)
		OR	CO-OR	52787	kt	2015	IEA (2017)
		PISP	PIP	5868	kt	2014	USGS (2017a)
		SC-DR-gas	NG-DR	560230	TJ	2015	IEA (2017)
		SC-DR-oil	CO-HF-DR	24	kt	2015	IEA (2017)
		SC-DR-oil	CO-LF-DR	6455	kt	2015	IEA (2017)
		SC-IND-coal	BC-IND-CEM	27	kt	2015	IEA (2017)
		SC-IND-coal	BC-IND-OTH	14	kt	2015	IEA (2017)
		SC-IND-coal	HC-IND-OTH	33	kt	2015	IEA (2017)
		SC-IND-gas	NG-IND	217366	TJ	2015	IEA (2017)
		SC-IND-oil	CO-HF-IND	5	kt	2015	IEA (2017)
		SC-IND-oil	CO-LF-IND	414	kt	2015	IEA (2017)
		SC-PP-coal	HC-B-PP	13476	kt	2015	IEA (2017)
		SC-PP-gas	NG-PP	454342	TJ	2015	IEA (2017)
		SC-PP-oil	CO-HF-PP	7	kt	2015	IEA (2017)
		SC-PP-oil	CO-LF-PP	22	kt	2015	IEA (2017)
		SSC	SP-S	125	kt	2014	World Steel Association (2015)
NCL	New Caledonia	BIO	PSB – DR	884.8558592	TJ	2015	IEA (2017)[#]
		BIO	PSB – IND	786.6171126	TJ	2015	IEA (2017)[#]
		CEM	CEM	106	kt	2014	USGS (2017a)
		OR	CO-OR	79.83956773	kt	2015	IEA (2017)[#]
		SC-DR-gas	NG-DR	401.3625478	TJ	2015	IEA (2017)[#]
		SC-DR-oil	CO-HF-DR	4.966097514	kt	2015	IEA (2017)[#]
		SC-DR-oil	CO-LF-DR	127.1448299	kt	2015	IEA (2017)[#]
		SC-IND-coal	BC-IND-OTH	1.528030004	kt	2015	IEA (2017)[#]
		SC-IND-coal	HC-IND-OTH	107.4077757	kt	2015	IEA (2017)[#]

Country code	Country name	Sector code	Activity code	Activity amount	Units	Year	Source
		SC-IND-oil	CO-HF-IND	10.88721378	kt	2015	IEA (2017)[#]
		SC-IND-oil	CO-LF-IND	11.90590045	kt	2015	IEA (2017)[#]
		SC-PP-coal	HC-B-PP	28.26855508	kt	2015	IEA (2017)[#]
		SC-PP-gas	NG-PP	438.1626037	TJ	2015	IEA (2017)[#]
		SC-PP-oil	CO-HF-PP	56.09143474	kt	2015	IEA (2017)[#]
		SC-PP-oil	CO-LF-PP	73.34544021	kt	2015	IEA (2017)[#]
NZL	New Zealand	BIO	PSB – DR	6517	TJ	2015	IEA (2017)
		BIO	PSB – IND	35973	TJ	2015	IEA (2017)
		BIO	PSB – PP	3787	TJ	2015	IEA (2017)
		CEM	CEM	1100	kt	2014	USGS (2017a)
		NFMP	AL-P	333	kt	2015	USGS (2017b)
		NFMP-AU	GP-L	11600	kg	2015	USGS (2017b)
		OR	CO-OR	5428	kt	2015	IEA (2017)
		PISP	PIP	670	kt	2014	USGS (2017a)
		SC-DR-coal	BC-DR	169	kt	2015	IEA (2017)
		SC-DR-gas	NG-DR	17295	TJ	2015	IEA (2017)
		SC-DR-oil	CO-HF-DR	67	kt	2015	IEA (2017)
		SC-DR-oil	CO-LF-DR	2480	kt	2015	IEA (2017)
		SC-IND-coal	BC-IND-NFM	3	kt	2015	IEA (2017)
		SC-IND-coal	BC-IND-OTH	895	kt	2015	IEA (2017)
		SC-IND-coal	HC-IND-CEM	116	kt	2015	IEA (2017)
		SC-IND-coal	HC-IND-OTH	9	kt	2015	IEA (2017)
		SC-IND-gas	NG-IND	57745	TJ	2015	IEA (2017)
		SC-IND-oil	CO-LF-IND	332	kt	2015	IEA (2017)
		SC-PP-coal	BC-L-PP	16	kt	2015	IEA (2017)
		SC-PP-coal	BC-S-PP	600	kt	2015	IEA (2017)
		SC-PP-gas	NG-PP	66138	TJ	2015	IEA (2017)
		SSC	SP-S	264	kt	2014	World Steel Association (2015)
NIC	Nicaragua	BIO	PSB – DR	40531	TJ	2015	IEA (2017)
		BIO	PSB – IND	2781	TJ	2015	IEA (2017)
		BIO	PSB – PP	19779	TJ	2015	IEA (2017)
		CEM	CEM	700	kt	2014	USGS (2017a)
		NFMP-AU	GP-L	8200	kg	2015	USGS (2017b)
		OR	CO-OR	729	kt	2015	IEA (2017)
		SC-DR-oil	CO-LF-DR	481	kt	2015	IEA (2017)
		SC-IND-oil	CO-HF-IND	27	kt	2015	IEA (2017)
		SC-IND-oil	CO-LF-IND	91	kt	2015	IEA (2017)
		SC-PP-oil	CO-HF-PP	498	kt	2015	IEA (2017)
		SC-PP-oil	CO-LF-PP	15	kt	2015	IEA (2017)
NER	Niger	BIO	PSB – DR	88279	TJ	2015	IEA (2017)
		CEM	CEM	21	kt	2014	USGS (2017a)
		NFMP-AU	GP-L	1209	kg	2015	USGS (2017b)
		OR	CO-OR	742	kt	2015	IEA (2017)
		SC-DR-oil	CO-LF-DR	168	kt	2015	IEA (2017)
		SC-IND-oil	CO-HF-IND	2	kt	2015	IEA (2017)
		SC-IND-oil	CO-LF-IND	61	kt	2015	IEA (2017)
		SC-PP-coal	BC-L-PP	221	kt	2015	IEA (2017)
		SC-PP-oil	CO-HF-PP	16	kt	2015	IEA (2017)
		SC-PP-oil	CO-LF-PP	53	kt	2015	IEA (2017)

Country code	Country name	Sector code	Activity code	Activity amount	Units	Year	Source
NGA	Nigeria	BIO	PSB – DR	4009489	TJ	2015	IEA (2017)
		BIO	PSB – IND	173369	TJ	2015	IEA (2017)
		CEM	CEM	20000	kt	2014	USGS (2017a)
		NFMP-AU	GP-L	7700	kg	2015	USGS (2017b)
		OR	CO-OR	1335	kt	2015	IEA (2017)
		SC-DR-oil	CO-LF-DR	527	kt	2015	IEA (2017)
		SC-IND-coal	HC-IND-CEM	47	kt	2015	IEA (2017)
		SC-IND-gas	NG-IND	119044	TJ	2015	IEA (2017)
		SC-IND-oil	CO-HF-IND	451	kt	2015	IEA (2017)
		SC-PP-gas	NG-PP	469517	TJ	2015	IEA (2017)
		SC-PP-oil	CO-HF-PP	123	kt	2015	IEA (2017)
		SC-PP-oil	CO-LF-PP	14	kt	2015	IEA (2017)
		SSC	SP-S	100	kt	2014	World Steel Association (2015)
NOR	Norway	BIO	PSB – DR	22158	TJ	2015	IEA (2017)
		BIO	PSB – IND	10315	TJ	2015	IEA (2017)
		BIO	PSB – PP	6364	TJ	2015	IEA (2017)
		CEM	CEM	1700	kt	2014	USGS (2017a)
		CEM	PC-CEM	13	kt	2015	IEA (2017)
		NFMP	AL-P	1225	kt	2015	USGS (2017b)
		NFMP	ZN-P	162878	t	2015	USGS (2017b)
		OR	CO-OR	13430	kt	2015	IEA (2017)
		PISP	PIP	102	kt	2014	USGS (2017a)
		SC-DR-gas	NG-DR	7444	TJ	2015	IEA (2017)
		SC-DR-oil	CO-HF-DR	9	kt	2015	IEA (2017)
		SC-DR-oil	CO-LF-DR	3909	kt	2015	IEA (2017)
		SC-IND-coal	HC-IND-CEM	93	kt	2015	IEA (2017)
		SC-IND-coal	HC-IND-OTH	262	kt	2015	IEA (2017)
		SC-IND-coal	HC-IND-PIP	212	kt	2015	IEA (2017)
		SC-IND-gas	NG-IND	11965	TJ	2015	IEA (2017)
		SC-IND-oil	CO-HF-IND	6	kt	2015	IEA (2017)
		SC-IND-oil	CO-LF-IND	306	kt	2015	IEA (2017)
		SC-PP-coal	HC-B-PP	26	kt	2015	IEA (2017)
		SC-PP-gas	NG-PP	202999	TJ	2015	IEA (2017)
		SC-PP-oil	CO-LF-PP	213	kt	2015	IEA (2017)
		SSC	SP-S	600	kt	2014	World Steel Association (2015)
OMN	Oman	CEM	CEM	5000	kt	2014	USGS (2017a)
		NFMP	AL-P	377	kt	2015	USGS (2017b)
		NFMP	CU-P	12000	t	2015	USGS (2017b)
		OR	CO-OR	9212	kt	2015	IEA (2017)
		SC-DR-gas	NG-DR	7492	TJ	2015	IEA (2017)
		SC-DR-oil	CO-LF-DR	1908	kt	2015	IEA (2017)
		SC-IND-gas	NG-IND	447010	TJ	2015	IEA (2017)
		SC-IND-oil	CO-LF-IND	417	kt	2015	IEA (2017)
		SC-PP-gas	NG-PP	454854	TJ	2015	IEA (2017)
		SC-PP-oil	CO-LF-PP	202	kt	2015	IEA (2017)
		SSC	SP-S	1500	kt	2014	World Steel Association (2015)
PAK	Pakistan	BIO	PSB – DR	1187378	TJ	2015	IEA (2017)
		BIO	PSB – IND	149375	TJ	2015	IEA (2017)
		CEM	CEM	32000	kt	2014	USGS (2017a)
		CSP	CSP-C	33	kt	2010	UNEP (2011e)
		NFMP	CU-P	13000	t	2015	USGS (2017b)
		OR	CO-OR	12999	kt	2015	IEA (2017)
		PISP	PIP	216.5	kt	2014	USGS (2017a)

Country code	Country name	Sector code	Activity code	Activity amount	Units	Year	Source
		SC-DR-gas	NG-DR	395135	TJ	2015	IEA (2017)
		SC-DR-oil	CO-HF-DR	7	kt	2015	IEA (2017)
		SC-DR-oil	CO-LF-DR	6769	kt	2015	IEA (2017)
		SC-IND-coal	BC-IND-CEM	1082	kt	2015	IEA (2017)
		SC-IND-coal	HC-IND-CEM	7390	kt	2015	IEA (2017)
		SC-IND-gas	NG-IND	305417	TJ	2015	IEA (2017)
		SC-IND-oil	CO-HF-IND	773	kt	2015	IEA (2017)
		SC-IND-oil	CO-LF-IND	471	kt	2015	IEA (2017)
		SC-PP-coal	HC-B-PP	158	kt	2015	IEA (2017)
		SC-PP-gas	NG-PP	310856	TJ	2015	IEA (2017)
		SC-PP-oil	CO-HF-PP	9045	kt	2015	IEA (2017)
		SC-PP-oil	CO-LF-PP	563	kt	2015	IEA (2017)
		SSC	SP-S	2280	kt	2014	World Steel Association (2015)
PLW	Palau	BIO	PSB – DR	69.27621526	TJ	2015	IEA (2017)[#]
		BIO	PSB – IND	23.96736273	TJ	2015	IEA (2017)[#]
		OR	CO-OR	2.43262427	kt	2015	IEA (2017)[#]
		SC-DR-gas	NG-DR	12.22907767	TJ	2015	IEA (2017)[#]
		SC-DR-oil	CO-HF-DR	0.151311557	kt	2015	IEA (2017)[#]
		SC-DR-oil	CO-LF-DR	3.87396385	kt	2015	IEA (2017)[#]
		SC-IND-coal	BC-IND-OTH	4.66E-02	kt	2015	IEA (2017)[#]
		SC-IND-coal	HC-IND-OTH	3.272597403	kt	2015	IEA (2017)[#]
		SC-IND-oil	CO-HF-IND	0.331721491	kt	2015	IEA (2017)[#]
		SC-IND-oil	CO-LF-IND	0.36275976	kt	2015	IEA (2017)[#]
		SC-PP-coal	HC-B-PP	0.861311943	kt	2015	IEA (2017)[#]
		SC-PP-gas	NG-PP	13.35033511	TJ	2015	IEA (2017)[#]
		SC-PP-oil	CO-HF-PP	1.709044643	kt	2015	IEA (2017)[#]
		SC-PP-oil	CO-LF-PP	2.23475531	kt	2015	IEA (2017)[#]
PAN	Panama	BIO	PSB – DR	7053	TJ	2015	IEA (2017)
		BIO	PSB – IND	3557	TJ	2015	IEA (2017)
		BIO	PSB – PP	2862	TJ	2015	IEA (2017)
		CEM	CEM	2188	kt	2014	USGS (2017a)
		SC-DR-oil	CO-LF-DR	670	kt	2015	IEA (2017)
		SC-IND-oil	CO-HF-IND	31	kt	2015	IEA (2017)
		SC-IND-oil	CO-LF-IND	433	kt	2015	IEA (2017)
		SC-PP-coal	HC-B-PP	339	kt	2015	IEA (2017)
		SC-PP-oil	CO-HF-PP	708	kt	2015	IEA (2017)
		SC-PP-oil	CO-LF-PP	60	kt	2015	IEA (2017)
PNG	Papua New Guinea	BIO	PSB – DR	21737.15625	TJ	2015	IEA (2017)[#]
		BIO	PSB – IND	1344.700727	TJ	2015	IEA (2017)[#]
		CEM	CEM	200	kt	2014	USGS (2017a)
		NFMP-AU	GP-L	60046	kg	2015	USGS (2017b)
		OR	CO-OR	136.4835865	kt	2015	IEA (2017)[#]
		SC-DR-gas	NG-DR	686.1184446	TJ	2015	IEA (2017)[#]
		SC-DR-oil	CO-HF-DR	8.489409689	kt	2015	IEA (2017)[#]
		SC-DR-oil	CO-LF-DR	217.3506557	kt	2015	IEA (2017)[#]
		SC-IND-coal	BC-IND-OTH	2.612126058	kt	2015	IEA (2017)[#]
		SC-IND-coal	HC-IND-OTH	183.6106942	kt	2015	IEA (2017)[#]
		SC-IND-oil	CO-HF-IND	18.61139816	kt	2015	IEA (2017)[#]
		SC-IND-oil	CO-LF-IND	20.35281554	kt	2015	IEA (2017)[#]
		SC-PP-coal	HC-B-PP	48.32433207	kt	2015	IEA (2017)[#]
		SC-PP-gas	NG-PP	749.0271471	TJ	2015	IEA (2017)[#]
		SC-PP-oil	CO-HF-PP	95.88679405	kt	2015	IEA (2017)[#]
		SC-PP-oil	CO-LF-PP	125.3820508	kt	2015	IEA (2017)[#]

Country code	Country name	Sector code	Activity code	Activity amount	Units	Year	Source
PRY	Paraguay	BIO	PSB – DR	28526	TJ	2015	IEA (2017)
		BIO	PSB – IND	45055	TJ	2015	IEA (2017)
		CEM	CEM	1000	kt	2014	USGS (2017a)
		PISP	PIP	71	kt	2014	USGS (2017a)
		SC-DR-oil	CO-LF-DR	1202	kt	2015	IEA (2017)
		SC-IND-oil	CO-HF-IND	46	kt	2015	IEA (2017)
		SC-PP-oil	CO-LF-PP	1	kt	2015	IEA (2017)
PER	Peru	BIO	PSB – DR	88672	TJ	2015	IEA (2017)
		BIO	PSB – IND	3	TJ	2015	IEA (2017)
		BIO	PSB – PP	11677	TJ	2015	IEA (2017)
		CEM	CEM	10676	kt	2014	USGS (2017a)
		CSP	CSP-C	76	kt	2010	UNEP (2011e)
		NFMP	CU-P	327900	t	2015	USGS (2017b)
		NFMP	ZN-P	335422	t	2015	USGS (2017b)
		NFMP-AU	GP-L	121431	kg	2015	USGS (2017b)
		OR	CO-OR	8802	kt	2015	IEA (2017)
		SC-DR-coal	HC-DR	4	kt	2015	IEA (2017)
		SC-DR-gas	NG-DR	39546	TJ	2015	IEA (2017)
		SC-DR-oil	CO-HF-DR	177	kt	2015	IEA (2017)
		SC-DR-oil	CO-LF-DR	4164	kt	2015	IEA (2017)
		SC-IND-coal	HC-IND-OTH	857	kt	2015	IEA (2017)
		SC-IND-coal	HC-IND-PIP	138	kt	2015	IEA (2017)
		SC-IND-gas	NG-IND	49901	TJ	2015	IEA (2017)
		SC-IND-oil	CO-HF-IND	65	kt	2015	IEA (2017)
		SC-IND-oil	CO-LF-IND	720	kt	2015	IEA (2017)
		SC-PP-coal	HC-B-PP	236	kt	2015	IEA (2017)
		SC-PP-gas	NG-PP	266090	TJ	2015	IEA (2017)
		SC-PP-oil	CO-HF-PP	236	kt	2015	IEA (2017)
		SC-PP-oil	CO-LF-PP	120	kt	2015	IEA (2017)
		SSC	SP-S	1078	kt	2014	World Steel Association (2015)
PHL	Philippines	BIO	PSB – DR	126895	TJ	2015	IEA (2017)
		BIO	PSB – IND	73847	TJ	2015	IEA (2017)
		BIO	PSB – PP	5390	TJ	2015	IEA (2017)
		CEM	CEM	22000	kt	2014	USGS (2017a)
		CSP	CSP-C	14	kt	2010	UNEP (2011e)
		NFMP	CU-P	189000	t	2015	USGS (2017b)
		NFMP-AU	GP-L	20643	kg	2015	USGS (2017b)
		OR	CO-OR	10278	kt	2015	IEA (2017)
		SC-DR-oil	CO-HF-DR	330	kt	2015	IEA (2017)
		SC-DR-oil	CO-LF-DR	6833	kt	2015	IEA (2017)
		SC-IND-coal	BC-IND-CEM	3356	kt	2015	IEA (2017)
		SC-IND-coal	BC-IND-OTH	447	kt	2015	IEA (2017)
		SC-IND-coal	BC-IND-PIP	412	kt	2015	IEA (2017)
		SC-IND-gas	NG-IND	2334	TJ	2015	IEA (2017)
		SC-IND-oil	CO-HF-IND	648	kt	2015	IEA (2017)
		SC-IND-oil	CO-LF-IND	585	kt	2015	IEA (2017)
		SC-PP-coal	BC-S-PP	3961	kt	2015	IEA (2017)
		SC-PP-coal	HC-B-PP	13593	kt	2015	IEA (2017)
		SC-PP-gas	NG-PP	131431	TJ	2015	IEA (2017)
		SC-PP-oil	CO-HF-PP	1146	kt	2015	IEA (2017)
		SC-PP-oil	CO-LF-PP	286	kt	2015	IEA (2017)
		SC-PP-oil	CO-PP	234	kt	2015	IEA (2017)
		SSC	SP-S	1196	kt	2014	World Steel Association (2015)

Country code	Country name	Sector code	Activity code	Activity amount	Units	Year	Source
POL	Poland	BIO	PSB – DR	131096	TJ	2015	IEA (2017)
		BIO	PSB – IND	56853	TJ	2015	IEA (2017)
		BIO	PSB – PP	95657	TJ	2015	IEA (2017)
		CEM	CEM	15358	kt	2014	USGS (2017a)
		NFMP	CU-P	515000	t	2015	USGS (2017b)
		NFMP	PB-P	39000	t	2015	USGS (2017b)
		NFMP	ZN-P	140000	t	2015	USGS (2017b)
		NFMP-AU	GP-L	2703	kg	2015	USGS (2017b)
		OR	CO-OR	26140	kt	2015	IEA (2017)
		PISP	PIP	4637	kt	2014	USGS (2017a)
		SC-DR-coal	BC-DR	560	kt	2015	IEA (2017)
		SC-DR-coal	HC-DR	12151	kt	2015	IEA (2017)
		SC-DR-gas	NG-DR	244684	TJ	2015	IEA (2017)
		SC-DR-oil	CO-HF-DR	10	kt	2015	IEA (2017)
		SC-DR-oil	CO-LF-DR	11589	kt	2015	IEA (2017)
		SC-IND-coal	BC-IND-CEM	48	kt	2015	IEA (2017)
		SC-IND-coal	BC-IND-OTH	16	kt	2015	IEA (2017)
		SC-IND-coal	HC-IND-CEM	897	kt	2015	IEA (2017)
		SC-IND-coal	HC-IND-NFM	1	kt	2015	IEA (2017)
		SC-IND-coal	HC-IND-OTH	3629	kt	2015	IEA (2017)
		SC-IND-coal	HC-IND-PIP	32	kt	2015	IEA (2017)
		SC-IND-gas	NG-IND	150250	TJ	2015	IEA (2017)
		SC-IND-oil	CO-HF-IND	81	kt	2015	IEA (2017)
		SC-IND-oil	CO-LF-IND	265	kt	2015	IEA (2017)
		SC-PP-coal	BC-L-PP	62421	kt	2015	IEA (2017)
		SC-PP-coal	HC-B-PP	42465	kt	2015	IEA (2017)
		SC-PP-gas	NG-PP	122747	TJ	2015	IEA (2017)
		SC-PP-oil	CO-HF-PP	962	kt	2015	IEA (2017)
		SC-PP-oil	CO-LF-PP	76	kt	2015	IEA (2017)
		SSC	SP-S	3492	kt	2014	World Steel Association (2015)
PRT	Portugal	BIO	PSB – DR	32212	TJ	2015	IEA (2017)
		BIO	PSB – IND	39761	TJ	2015	IEA (2017)
		BIO	PSB – PP	25376	TJ	2015	IEA (2017)
		CEM	CEM	5500	kt	2014	USGS (2017a)
		CEM	PC-CEM	456	kt	2015	IEA (2017)
		OR	CO-OR	13847	kt	2015	IEA (2017)
		PISP	PIP	100	kt	2014	USGS (2017a)
		SC-DR-gas	NG-DR	23514	TJ	2015	IEA (2017)
		SC-DR-oil	CO-HF-DR	86	kt	2015	IEA (2017)
		SC-DR-oil	CO-LF-DR	4221	kt	2015	IEA (2017)
		SC-IND-coal	HC-IND-OTH	5	kt	2015	IEA (2017)
		SC-IND-coal	HC-IND-PIP	5	kt	2015	IEA (2017)
		SC-IND-gas	NG-IND	52913	TJ	2015	IEA (2017)
		SC-IND-oil	CO-HF-IND	123	kt	2015	IEA (2017)
		SC-IND-oil	CO-LF-IND	188	kt	2015	IEA (2017)
		SC-PP-coal	HC-B-PP	5494	kt	2015	IEA (2017)
		SC-PP-gas	NG-PP	103112	TJ	2015	IEA (2017)
		SC-PP-oil	CO-HF-PP	365	kt	2015	IEA (2017)
		SC-PP-oil	CO-LF-PP	21	kt	2015	IEA (2017)
		SSC	SP-S	2070	kt	2014	World Steel Association (2015)

Country code	Country name	Sector code	Activity code	Activity amount	Units	Year	Source
QAT	Qatar	CEM	CEM	6000	kt	2014	USGS (2017a)
		NFMP	AL-P	610	kt	2015	USGS (2017b)
		OR	CO-OR	3699	kt	2015	IEA (2017)
		SC-DR-oil	CO-LF-DR	3294	kt	2015	IEA (2017)
		SC-IND-gas	NG-IND	239306	TJ	2015	IEA (2017)
		SC-PP-gas	NG-PP	1004423	TJ	2015	IEA (2017)
		SSC	SP-S	3019	kt	2014	World Steel Association (2015)
MDA	Republic of Moldova	BIO	PSB – DR	12510	TJ	2015	IEA (2017)
		BIO	PSB – IND	62	TJ	2015	IEA (2017)
		BIO	PSB – PP	389	TJ	2015	IEA (2017)
		CEM	CEM	1300	kt	2014	USGS (2017a)
		OR	CO-OR	7	kt	2015	IEA (2017)
		SC-DR-coal	HC-DR	96	kt	2015	IEA (2017)
		SC-DR-gas	NG-DR	13947	TJ	2015	IEA (2017)
		SC-DR-oil	CO-LF-DR	487	kt	2015	IEA (2017)
		SC-IND-coal	HC-IND-CEM	70	kt	2015	IEA (2017)
		SC-IND-coal	HC-IND-OTH	2	kt	2015	IEA (2017)
		SC-IND-gas	NG-IND	11497	TJ	2015	IEA (2017)
		SC-IND-oil	CO-HF-IND	2	kt	2015	IEA (2017)
		SC-IND-oil	CO-LF-IND	9	kt	2015	IEA (2017)
		SC-PP-coal	HC-A-PP	3	kt	2015	IEA (2017)
		SC-PP-gas	NG-PP	71214	TJ	2015	IEA (2017)
		SC-PP-oil	CO-HF-PP	7	kt	2015	IEA (2017)
		SSC	SP-S	351	kt	2014	World Steel Association (2015)
REU	Reunion	BIO	PSB – DR	6796.340895	TJ	2015	IEA (2017)#
		BIO	PSB – IND	494.9282048	TJ	2015	IEA (2017)#
		BIO	PSB – PP	177.0632214	TJ	2015	IEA (2017)#
		CEM	CEM	400	kt	2014	USGS (2017a)
		SC-DR-coal	HC-DR	0.804745731	kt	2015	IEA (2017)#
		SC-DR-oil	CO-LF-DR	26.99730321	kt	2015	IEA (2017)#
		SC-IND-coal	HC-IND-OTH	0.83348665	kt	2015	IEA (2017)#
		SC-IND-gas	NG-IND	0.268248577	TJ	2015	IEA (2017)#
		SC-IND-oil	CO-HF-IND	4.914697142	kt	2015	IEA (2017)#
		SC-IND-oil	CO-IND	1.350823191	kt	2015	IEA (2017)#
		SC-IND-oil	CO-LF-IND	4.703930403	kt	2015	IEA (2017)#
		SC-PP-coal	HC-B-PP	7.051105451	kt	2015	IEA (2017)#
		SC-PP-gas	NG-PP	185.6184349	TJ	2015	IEA (2017)#
		SC-PP-oil	CO-HF-PP	6.390064315	kt	2015	IEA (2017)#
		SC-PP-oil	CO-LF-PP	13.22082272	kt	2015	IEA (2017)#
ROU	Romania	BIO	PSB – DR	128301	TJ	2015	IEA (2017)
		BIO	PSB – IND	10172	TJ	2015	IEA (2017)
		BIO	PSB – PP	7862	TJ	2015	IEA (2017)
		CEM	CEM	7900	kt	2014	USGS (2017a)
		CEM	PC-CEM	376	kt	2015	IEA (2017)
		NFMP	AL-P	271	kt	2015	USGS (2017b)
		OR	CO-OR	10352	kt	2015	IEA (2017)
		PISP	PIP	1631	kt	2014	USGS (2017a)
		SC-DR-coal	BC-DR	286	kt	2015	IEA (2017)
		SC-DR-gas	NG-DR	142444	TJ	2015	IEA (2017)

Country code	Country name	Sector code	Activity code	Activity amount	Units	Year	Source
		SC-DR-oil	CO-LF-DR	4045	kt	2015	IEA (2017)
		SC-IND-coal	BC-IND-CEM	239	kt	2015	IEA (2017)
		SC-IND-coal	BC-IND-OTH	248	kt	2015	IEA (2017)
		SC-IND-coal	BC-IND-PIP	364	kt	2015	IEA (2017)
		SC-IND-coal	HC-IND-OTH	2	kt	2015	IEA (2017)
		SC-IND-coal	HC-IND-PIP	108	kt	2015	IEA (2017)
		SC-IND-gas	NG-IND	104079	TJ	2015	IEA (2017)
		SC-IND-oil	CO-HF-IND	7	kt	2015	IEA (2017)
		SC-IND-oil	CO-LF-IND	311	kt	2015	IEA (2017)
		SC-PP-coal	BC-L-PP	26065	kt	2015	IEA (2017)
		SC-PP-coal	BC-S-PP	197	kt	2015	IEA (2017)
		SC-PP-gas	NG-PP	146307	TJ	2015	IEA (2017)
		SC-PP-oil	CO-HF-PP	49	kt	2015	IEA (2017)
		SC-PP-oil	CO-LF-PP	72	kt	2015	IEA (2017)
		SSC	SP-S	1314	kt	2014	World Steel Association (2015)
RUS	Russia	BIO	PSB – DR	82843	TJ	2015	IEA (2017)
		BIO	PSB – IND	2877	TJ	2015	IEA (2017)
		BIO	PSB – PP	30719	TJ	2015	IEA (2017)
		CEM	CEM	68545	kt	2014	USGS (2017a)
		CSP	CSP-C	379	kt	2015	UNEP (2013)
		NFMP	AL-P	3530	kt	2015	USGS (2017b)
		NFMP	CU-P	660000	t	2015	USGS (2017b)
		NFMP	PB-T	114000	t	2015	USGS (2017b)
		NFMP	ZN-T	229602	t	2015	USGS (2017b)
		NFMP-AU	GP-L	252000	kg	2015	USGS (2017b)
		OR	CO-OR	259786	kt	2015	IEA (2017)
		PISP	PIP	51474	kt	2014	USGS (2017a)
		SC-DR-coal	BC-DR	1126	kt	2015	IEA (2017)
		SC-DR-coal	HC-DR	5482	kt	2015	IEA (2017)
		SC-DR-gas	NG-DR	3387745	TJ	2015	IEA (2017)
		SC-DR-oil	CO-DR	68	kt	2015	IEA (2017)
		SC-DR-oil	CO-HF-DR	613	kt	2015	IEA (2017)
		SC-DR-oil	CO-LF-DR	23591	kt	2015	IEA (2017)
		SC-IND-coal	BC-IND-CEM	14	kt	2015	IEA (2017)
		SC-IND-coal	BC-IND-OTH	114	kt	2015	IEA (2017)
		SC-IND-coal	HC-IND-CEM	1562	kt	2015	IEA (2017)
		SC-IND-coal	HC-IND-OTH	494	kt	2015	IEA (2017)
		SC-IND-gas	NG-IND	1651484	TJ	2015	IEA (2017)
		SC-IND-oil	CO-HF-IND	397	kt	2015	IEA (2017)
		SC-IND-oil	CO-IND	23	kt	2015	IEA (2017)
		SC-IND-oil	CO-LF-IND	3437	kt	2015	IEA (2017)
		SC-PP-coal	BC-L-PP	70970	kt	2015	IEA (2017)
		SC-PP-coal	HC-B-PP	72817	kt	2015	IEA (2017)
		SC-PP-gas	NG-PP	10120992	TJ	2015	IEA (2017)
		SC-PP-oil	CO-HF-PP	7718	kt	2015	IEA (2017)
		SC-PP-oil	CO-LF-PP	5190	kt	2015	IEA (2017)
		SC-PP-oil	CO-PP	674	kt	2015	IEA (2017)
		SSC	SP-S	21852	kt	2014	World Steel Association (2015)
		VCM	VCM-P	6196.515	kg	2016	National information
		VCM	VCM-R	3717.909	kg	2016	Lin et al. (2016)

Country code	Country name	Sector code	Activity code	Activity amount	Units	Year	Source
RWA	Rwanda	BIO	PSB – DR	115666.1982	TJ	2015	IEA (2017)#
		BIO	PSB – IND	3158.673802	TJ	2015	IEA (2017)#
		BIO	PSB – PP	1130.032504	TJ	2015	IEA (2017)#
		CEM	CEM	140	kt	2014	USGS (2017a)
		NFMP-AU	GP-L	319	kg	2015	USGS (2017b)
		SC-DR-coal	HC-DR	5.135955544	kt	2015	IEA (2017)#
		SC-DR-oil	CO-LF-DR	172.29908	kt	2015	IEA (2017)#
		SC-IND-coal	HC-IND-OTH	5.319382527	kt	2015	IEA (2017)#
		SC-IND-gas	NG-IND	1.711985181	TJ	2015	IEA (2017)#
		SC-IND-oil	CO-HF-IND	31.36601421	kt	2015	IEA (2017)#
		SC-IND-oil	CO-IND	8.621068234	kt	2015	IEA (2017)#
		SC-IND-oil	CO-LF-IND	30.020883	kt	2015	IEA (2017)#
		SC-PP-coal	HC-B-PP	45.00075334	kt	2015	IEA (2017)#
		SC-PP-gas	NG-PP	1184.632603	TJ	2015	IEA (2017)#
		SC-PP-oil	CO-HF-PP	40.78193271	kt	2015	IEA (2017)#
		SC-PP-oil	CO-LF-PP	84.37641251	kt	2015	IEA (2017)#
KNA	Saint Kitts	BIO	PSB – DR	54.00033377	TJ	2015	IEA (2017)#
		BIO	PSB – IND	226.4836672	TJ	2015	IEA (2017)#
		BIO	PSB – PP	74.32520297	TJ	2015	IEA (2017)#
		OR	CO-OR	27.60813372	kt	2015	IEA (2017)#
		SC-DR-coal	HC-DR	5.789722258	kt	2015	IEA (2017)#
		SC-DR-gas	NG-DR	13.74702526	TJ	2015	IEA (2017)#
		SC-DR-oil	CO-HF-DR	1.22639437	kt	2015	IEA (2017)#
		SC-DR-oil	CO-LF-DR	29.40494408	kt	2015	IEA (2017)#
		SC-IND-gas	NG-IND	0.627457585	TJ	2015	IEA (2017)#
		SC-IND-oil	CO-HF-IND	3.707703909	kt	2015	IEA (2017)#
		SC-IND-oil	CO-LF-IND	2.110539148	kt	2015	IEA (2017)#
		SC-PP-gas	NG-PP	877.78464	TJ	2015	IEA (2017)#
		SC-PP-oil	CO-HF-PP	44.8061757	kt	2015	IEA (2017)#
		SC-PP-oil	CO-LF-PP	32.97004399	kt	2015	IEA (2017)#
LCA	Saint Lucia	BIO	PSB – DR	170.4375137	TJ	2015	IEA (2017)#
		BIO	PSB – IND	339.9823639	TJ	2015	IEA (2017)#
		BIO	PSB – PP	111.5720993	TJ	2015	IEA (2017)#
		OR	CO-OR	41.44351194	kt	2015	IEA (2017)#
		SC-DR-coal	HC-DR	8.691149714	kt	2015	IEA (2017)#
		SC-DR-gas	NG-DR	20.63612888	TJ	2015	IEA (2017)#
		SC-DR-oil	CO-HF-DR	1.840982452	kt	2015	IEA (2017)#
		SC-DR-oil	CO-LF-DR	44.14076529	kt	2015	IEA (2017)#
		SC-IND-gas	NG-IND	0.941897999	TJ	2015	IEA (2017)#
		SC-IND-oil	CO-HF-IND	5.5657609	kt	2015	IEA (2017)#
		SC-IND-oil	CO-LF-IND	3.168202359	kt	2015	IEA (2017)#
		SC-PP-gas	NG-PP	1317.672486	TJ	2015	IEA (2017)#
		SC-PP-oil	CO-HF-PP	67.2600798	kt	2015	IEA (2017)#
		SC-PP-oil	CO-LF-PP	49.49245847	kt	2015	IEA (2017)#
VCT	Saint Vincent and the Grenadines	BIO	PSB – DR	106.7061817	TJ	2015	IEA (2017)#
		BIO	PSB – IND	200.1186674	TJ	2015	IEA (2017)#
		BIO	PSB – PP	65.67299423	TJ	2015	IEA (2017)#
		OR	CO-OR	24.39426647	kt	2015	IEA (2017)#
		SC-DR-coal	HC-DR	5.115739766	kt	2015	IEA (2017)#
		SC-DR-gas	NG-DR	12.14673186	TJ	2015	IEA (2017)#
		SC-DR-oil	CO-HF-DR	1.083629606	kt	2015	IEA (2017)#

Country code	Country name	Sector code	Activity code	Activity amount	Units	Year	Source
		SC-DR-oil	CO-LF-DR	25.98190984	kt	2015	IEA (2017)#
		SC-IND-gas	NG-IND	0.554415147	TJ	2015	IEA (2017)#
		SC-IND-oil	CO-HF-IND	3.276089505	kt	2015	IEA (2017)#
		SC-IND-oil	CO-LF-IND	1.864850949	kt	2015	IEA (2017)#
		SC-PP-gas	NG-PP	775.60159	TJ	2015	IEA (2017)#
		SC-PP-oil	CO-HF-PP	39.59028164	kt	2015	IEA (2017)#
		SC-PP-oil	CO-LF-PP	29.13199591	kt	2015	IEA (2017)#
WSM	Samoa	BIO	PSB – DR	644.2964929	TJ	2015	IEA (2017)#
		BIO	PSB – IND	76.76234956	TJ	2015	IEA (2017)#
		OR	CO-OR	7.791176556	kt	2015	IEA (2017)#
		SC-DR-gas	NG-DR	39.1671268	TJ	2015	IEA (2017)#
		SC-DR-oil	CO-HF-DR	0.484618637	kt	2015	IEA (2017)#
		SC-DR-oil	CO-LF-DR	12.40747973	kt	2015	IEA (2017)#
		SC-IND-coal	BC-IND-OTH	0.149113427	kt	2015	IEA (2017)#
		SC-IND-coal	HC-IND-OTH	10.4814313	kt	2015	IEA (2017)#
		SC-IND-oil	CO-HF-IND	1.062433167	kt	2015	IEA (2017)#
		SC-IND-oil	CO-LF-IND	1.161842118	kt	2015	IEA (2017)#
		SC-PP-coal	HC-B-PP	2.758598398	kt	2015	IEA (2017)#
		SC-PP-gas	NG-PP	42.75827517	TJ	2015	IEA (2017)#
		SC-PP-oil	CO-HF-PP	5.473705379	kt	2015	IEA (2017)#
		SC-PP-oil	CO-LF-PP	7.157444491	kt	2015	IEA (2017)#
STP	Sao Tome and Principe	BIO	PSB – DR	1772.264227	TJ	2015	IEA (2017)#
		BIO	PSB – IND	86.04076475	TJ	2015	IEA (2017)#
		BIO	PSB – PP	30.78154535	TJ	2015	IEA (2017)#
		SC-DR-coal	HC-DR	0.139900974	kt	2015	IEA (2017)#
		SC-DR-oil	CO-LF-DR	4.693344594	kt	2015	IEA (2017)#
		SC-IND-coal	HC-IND-OTH	0.144897438	kt	2015	IEA (2017)#
		SC-IND-gas	NG-IND	4.66E-02	TJ	2015	IEA (2017)#
		SC-IND-oil	CO-HF-IND	0.854395237	kt	2015	IEA (2017)#
		SC-IND-oil	CO-IND	0.234833778	kt	2015	IEA (2017)#
		SC-IND-oil	CO-LF-IND	0.817754505	kt	2015	IEA (2017)#
		SC-PP-coal	HC-B-PP	1.225799014	kt	2015	IEA (2017)#
		SC-PP-gas	NG-PP	32.26882594	TJ	2015	IEA (2017)#
		SC-PP-oil	CO-HF-PP	1.110880356	kt	2015	IEA (2017)#
		SC-PP-oil	CO-LF-PP	2.298373151	kt	2015	IEA (2017)#
SAU	Saudi Arabia	BIO	PSB – DR	5	TJ	2015	IEA (2017)
		CEM	CEM	57223	kt	2014	USGS (2017a)
		NFMP	AL-P	682	kt	2015	USGS (2017b)
		NFMP-AU	GP-L	5100	kg	2015	USGS (2017b)
		OR	CO-OR	112225	kt	2015	IEA (2017)
		SC-DR-oil	CO-LF-DR	20294	kt	2015	IEA (2017)
		SC-IND-gas	NG-IND	770165	TJ	2015	IEA (2017)
		SC-IND-oil	CO-HF-IND	13907	kt	2015	IEA (2017)
		SC-IND-oil	CO-IND	5345	kt	2015	IEA (2017)
		SC-IND-oil	CO-LF-IND	4160	kt	2015	IEA (2017)
		SC-PP-gas	NG-PP	2327141	TJ	2015	IEA (2017)
		SC-PP-oil	CO-HF-PP	7900	kt	2015	IEA (2017)
		SC-PP-oil	CO-LF-PP	13631	kt	2015	IEA (2017)
		SC-PP-oil	CO-PP	23260	kt	2015	IEA (2017)
		SSC	SP-S	6291	kt	2014	World Steel Association (2015)

Country code	Country name	Sector code	Activity code	Activity amount	Units	Year	Source
SEN	Senegal	BIO	PSB – DR	30980	TJ	2015	IEA (2017)
		BIO	PSB – IND	1749	TJ	2015	IEA (2017)
		BIO	PSB – PP	1522	TJ	2015	IEA (2017)
		CEM	CEM	4899	kt	2014	USGS (2017a)
		NFMP-AU	GP-L	5670	kg	2015	USGS (2017b)
		OR	CO-OR	894	kt	2015	IEA (2017)
		SC-DR-oil	CO-LF-DR	666	kt	2015	IEA (2017)
		SC-IND-coal	HC-IND-CEM	389	kt	2015	IEA (2017)
		SC-IND-oil	CO-HF-IND	59	kt	2015	IEA (2017)
		SC-IND-oil	CO-LF-IND	22	kt	2015	IEA (2017)
		SC-PP-gas	NG-PP	1688	TJ	2015	IEA (2017)
		SC-PP-oil	CO-HF-PP	599	kt	2015	IEA (2017)
		SC-PP-oil	CO-LF-PP	152	kt	2015	IEA (2017)
SRB	Serbia	BIO	PSB – DR	37651	TJ	2015	IEA (2017)
		BIO	PSB – IND	5484	TJ	2015	IEA (2017)
		BIO	PSB – PP	191	TJ	2015	IEA (2017)
		CEM	CEM	1605	kt	2014	USGS (2017a)
		CEM	PC-CEM	104	kt	2015	IEA (2017)
		NFMP	CU-P	43000	t	2015	USGS (2017b)
		NFMP-AU	GP-L	628	kg	2015	USGS (2017b)
		OR	CO-OR	2933	kt	2015	IEA (2017)
		PISP	PIP	550	kt	2014	USGS (2017a)
		SC-DR-coal	BC-DR	556	kt	2015	IEA (2017)
		SC-DR-gas	NG-DR	14489	TJ	2015	IEA (2017)
		SC-DR-oil	CO-HF-DR	44	kt	2015	IEA (2017)
		SC-DR-oil	CO-LF-DR	1416	kt	2015	IEA (2017)
		SC-IND-coal	BC-IND-CEM	103	kt	2015	IEA (2017)
		SC-IND-coal	BC-IND-NFM	6	kt	2015	IEA (2017)
		SC-IND-coal	BC-IND-OTH	203	kt	2015	IEA (2017)
		SC-IND-coal	HC-IND-CEM	84	kt	2015	IEA (2017)
		SC-IND-coal	HC-IND-NFM	11	kt	2015	IEA (2017)
		SC-IND-coal	HC-IND-OTH	11	kt	2015	IEA (2017)
		SC-IND-coal	HC-IND-PIP	14	kt	2015	IEA (2017)
		SC-IND-gas	NG-IND	20117	TJ	2015	IEA (2017)
		SC-IND-oil	CO-HF-IND	82	kt	2015	IEA (2017)
		SC-IND-oil	CO-LF-IND	131	kt	2015	IEA (2017)
		SC-PP-coal	BC-L-PP	36969	kt	2015	IEA (2017)
		SC-PP-gas	NG-PP	35494	TJ	2015	IEA (2017)
		SC-PP-oil	CO-HF-PP	202	kt	2015	IEA (2017)
		SC-PP-oil	CO-LF-PP	29	kt	2015	IEA (2017)
SCG	Serbia and Montenegro	CSP	CSP-C	10	kt	2010	UNEP (2011e)
SYC	Seychelles	BIO	PSB – DR	844.3573007	TJ	2015	IEA (2017)#
		BIO	PSB – IND	336.9052848	TJ	2015	IEA (2017)#
		BIO	PSB – PP	120.5296737	TJ	2015	IEA (2017)#
		SC-DR-coal	HC-DR	0.547802867	kt	2015	IEA (2017)#
		SC-DR-oil	CO-LF-DR	18.3774819	kt	2015	IEA (2017)#
		SC-IND-coal	HC-IND-OTH	0.567367255	kt	2015	IEA (2017)#
		SC-IND-gas	NG-IND	0.182600956	TJ	2015	IEA (2017)#
		SC-IND-oil	CO-HF-IND	3.345510368	kt	2015	IEA (2017)#
		SC-IND-oil	CO-IND	0.919526241	kt	2015	IEA (2017)#
		SC-IND-oil	CO-LF-IND	3.202038188	kt	2015	IEA (2017)#
		SC-PP-coal	HC-B-PP	4.799796551	kt	2015	IEA (2017)#
		SC-PP-gas	NG-PP	126.3533399	TJ	2015	IEA (2017)#
		SC-PP-oil	CO-HF-PP	4.349815624	kt	2015	IEA (2017)#
		SC-PP-oil	CO-LF-PP	8.999618533	kt	2015	IEA (2017)#

Country code	Country name	Sector code	Activity code	Activity amount	Units	Year	Source
SLE	Sierra Leone	BIO	PSB – DR	53706.14863	TJ	2015	IEA (2017)[#]
		BIO	PSB – IND	1303.676402	TJ	2015	IEA (2017)[#]
		BIO	PSB – PP	466.3972292	TJ	2015	IEA (2017)[#]
		CEM	CEM	336	kt	2014	USGS (2017a)
		NFMP-AU	GP-L	40	kg	2015	USGS (2017b)
		SC-DR-coal	HC-DR	2.119757994	kt	2015	IEA (2017)[#]
		SC-DR-oil	CO-LF-DR	71.11283366	kt	2015	IEA (2017)[#]
		SC-IND-coal	HC-IND-OTH	2.195463637	kt	2015	IEA (2017)[#]
		SC-IND-gas	NG-IND	0.706585998	TJ	2015	IEA (2017)[#]
		SC-IND-oil	CO-HF-IND	12.94566489	kt	2015	IEA (2017)[#]
		SC-IND-oil	CO-IND	3.558165205	kt	2015	IEA (2017)[#]
		SC-IND-oil	CO-LF-IND	12.39049018	kt	2015	IEA (2017)[#]
		SC-PP-coal	HC-B-PP	18.57311766	kt	2015	IEA (2017)[#]
		SC-PP-gas	NG-PP	488.9322754	TJ	2015	IEA (2017)[#]
		SC-PP-oil	CO-HF-PP	16.83188788	kt	2015	IEA (2017)[#]
		SC-PP-oil	CO-LF-PP	34.82459562	kt	2015	IEA (2017)[#]
SGP	Singapore	BIO	PSB – PP	2654	TJ	2015	IEA (2017)
		OR	CO-OR	38275	kt	2015	IEA (2017)
		SC-DR-gas	NG-DR	7092	TJ	2015	IEA (2017)
		SC-DR-oil	CO-LF-DR	1255	kt	2015	IEA (2017)
		SC-IND-coal	HC-IND-OTH	233	kt	2015	IEA (2017)
		SC-IND-gas	NG-IND	50656	TJ	2015	IEA (2017)
		SC-IND-oil	CO-HF-IND	886	kt	2015	IEA (2017)
		SC-IND-oil	CO-LF-IND	216	kt	2015	IEA (2017)
		SC-PP-coal	HC-B-PP	415	kt	2015	IEA (2017)
		SC-PP-gas	NG-PP	380065	TJ	2015	IEA (2017)
		SC-PP-oil	CO-HF-PP	481	kt	2015	IEA (2017)
		SSC	SP-S	540	kt	2014	World Steel Association (2015)
SVK	Slovakia	BIO	PSB – DR	1587	TJ	2015	IEA (2017)
		BIO	PSB – IND	17055	TJ	2015	IEA (2017)
		BIO	PSB – PP	18144	TJ	2015	IEA (2017)
		CEM	CEM	3319	kt	2014	USGS (2017a)
		CEM	PC-CEM	49	kt	2015	IEA (2017)
		NFMP	AL-P	171	kt	2015	USGS (2017b)
		NFMP-AU	GP-L	600	kg	2015	USGS (2017b)
		OR	CO-OR	5930	kt	2015	IEA (2017)
		PISP	PIP	3838	kt	2014	USGS (2017a)
		SC-DR-coal	BC-DR	89	kt	2015	IEA (2017)
		SC-DR-coal	HC-DR	103	kt	2015	IEA (2017)
		SC-DR-gas	NG-DR	78693	TJ	2015	IEA (2017)
		SC-DR-oil	CO-LF-DR	1331	kt	2015	IEA (2017)
		SC-IND-coal	BC-IND-CEM	11	kt	2015	IEA (2017)
		SC-IND-coal	BC-IND-OTH	45	kt	2015	IEA (2017)
		SC-IND-coal	HC-IND-CEM	54	kt	2015	IEA (2017)
		SC-IND-coal	HC-IND-PIP	349	kt	2015	IEA (2017)
		SC-IND-gas	NG-IND	36689	TJ	2015	IEA (2017)
		SC-IND-oil	CO-HF-IND	2	kt	2015	IEA (2017)
		SC-IND-oil	CO-LF-IND	12	kt	2015	IEA (2017)
		SC-PP-coal	BC-L-PP	2451	kt	2015	IEA (2017)
		SC-PP-coal	HC-A-PP	40	kt	2015	IEA (2017)
		SC-PP-coal	HC-B-PP	454	kt	2015	IEA (2017)
		SC-PP-gas	NG-PP	35237	TJ	2015	IEA (2017)
		SC-PP-oil	CO-HF-PP	203	kt	2015	IEA (2017)
		SSC	SP-S	362	kt	2014	World Steel Association (2015)

Country code	Country name	Sector code	Activity code	Activity amount	Units	Year	Source
SVN	Slovenia	BIO	PSB – DR	19396	TJ	2015	IEA (2017)
		BIO	PSB – IND	3126	TJ	2015	IEA (2017)
		BIO	PSB – PP	2187	TJ	2015	IEA (2017)
		CEM	CEM	1326	kt	2014	USGS (2017a)
		CEM	PC-CEM	30	kt	2015	IEA (2017)
		NFMP	AL-P	85	kt	2015	USGS (2017b)
		SC-DR-gas	NG-DR	7244	TJ	2015	IEA (2017)
		SC-DR-oil	CO-LF-DR	1510	kt	2015	IEA (2017)
		SC-IND-coal	BC-IND-OTH	57	kt	2015	IEA (2017)
		SC-IND-coal	HC-IND-CEM	1	kt	2015	IEA (2017)
		SC-IND-coal	HC-IND-NFM	2	kt	2015	IEA (2017)
		SC-IND-gas	NG-IND	18712	TJ	2015	IEA (2017)
		SC-IND-oil	CO-HF-IND	3	kt	2015	IEA (2017)
		SC-IND-oil	CO-LF-IND	45	kt	2015	IEA (2017)
		SC-PP-coal	BC-L-PP	3190	kt	2015	IEA (2017)
		SC-PP-coal	BC-S-PP	340	kt	2015	IEA (2017)
		SC-PP-coal	HC-B-PP	5	kt	2015	IEA (2017)
		SC-PP-gas	NG-PP	4714	TJ	2015	IEA (2017)
		SC-PP-oil	CO-LF-PP	8	kt	2015	IEA (2017)
		SSC	SP-S	615	kt	2014	World Steel Association (2015)
SLB	Solomon Islands	BIO	PSB – DR	2027.853112	TJ	2015	IEA (2017)#
		BIO	PSB – IND	88.27734092	TJ	2015	IEA (2017)#
		OR	CO-OR	8.959917889	kt	2015	IEA (2017)#
		SC-DR-gas	NG-DR	45.04252183	TJ	2015	IEA (2017)#
		SC-DR-oil	CO-HF-DR	0.557315467	kt	2015	IEA (2017)#
		SC-DR-oil	CO-LF-DR	14.26870496	kt	2015	IEA (2017)#
		SC-IND-coal	BC-IND-OTH	0.171481682	kt	2015	IEA (2017)#
		SC-IND-coal	HC-IND-OTH	12.05373324	kt	2015	IEA (2017)#
		SC-IND-oil	CO-HF-IND	1.221806985	kt	2015	IEA (2017)#
		SC-IND-oil	CO-LF-IND	1.336128106	kt	2015	IEA (2017)#
		SC-PP-coal	HC-B-PP	3.172411118	kt	2015	IEA (2017)#
		SC-PP-gas	NG-PP	49.17237234	TJ	2015	IEA (2017)#
		SC-PP-oil	CO-HF-PP	6.294806746	kt	2015	IEA (2017)#
		SC-PP-oil	CO-LF-PP	8.23112074	kt	2015	IEA (2017)#
SOM	Somalia	BIO	PSB – DR	96981.69382	TJ	2015	IEA (2017)#
		BIO	PSB – IND	588.5394357	TJ	2015	IEA (2017)#
		BIO	PSB – PP	210.5531416	TJ	2015	IEA (2017)#
		SC-DR-coal	HC-DR	0.956956168	kt	2015	IEA (2017)#
		SC-DR-oil	CO-LF-DR	32.10360097	kt	2015	IEA (2017)#
		SC-IND-coal	HC-IND-OTH	0.991133174	kt	2015	IEA (2017)#
		SC-IND-gas	NG-IND	0.318985389	TJ	2015	IEA (2017)#
		SC-IND-oil	CO-HF-IND	5.844268026	kt	2015	IEA (2017)#
		SC-IND-oil	CO-IND	1.606319282	kt	2015	IEA (2017)#
		SC-IND-oil	CO-LF-IND	5.593636649	kt	2015	IEA (2017)#
		SC-PP-coal	HC-B-PP	8.384758806	kt	2015	IEA (2017)#
		SC-PP-gas	NG-PP	220.7264971	TJ	2015	IEA (2017)#
		SC-PP-oil	CO-HF-PP	7.598687668	kt	2015	IEA (2017)#
		SC-PP-oil	CO-LF-PP	15.72142276	kt	2015	IEA (2017)#
ZAF	South Africa	BIO	PSB – DR	355953	TJ	2015	IEA (2017)
		BIO	PSB – IND	83833	TJ	2015	IEA (2017)
		BIO	PSB – PP	4464	TJ	2015	IEA (2017)
		CEM	CEM	12070	kt	2014	USGS (2017a)
		NFMP	AL-P	695	kt	2015	USGS (2017b)

Country code	Country name	Sector code	Activity code	Activity amount	Units	Year	Source
		NFMP	CU-P	71800	t	2015	USGS (2017b)
		NFMP-AU	GP-L	144515	kg	2015	USGS (2017b)
		OR	CO-OR	20577	kt	2015	IEA (2017)
		PISP	PIP	4690	kt	2014	USGS (2017a)
		SC-DR-coal	HC-DR	8684	kt	2015	IEA (2017)
		SC-DR-gas	NG-DR	79	TJ	2015	IEA (2017)
		SC-DR-oil	CO-HF-DR	34	kt	2015	IEA (2017)
		SC-DR-oil	CO-LF-DR	9366	kt	2015	IEA (2017)
		SC-IND-coal	HC-IND-CEM	1519	kt	2015	IEA (2017)
		SC-IND-coal	HC-IND-NFM	2290	kt	2015	IEA (2017)
		SC-IND-coal	HC-IND-OTH	7629	kt	2015	IEA (2017)
		SC-IND-coal	HC-IND-PIP	2380	kt	2015	IEA (2017)
		SC-IND-gas	NG-IND	80993	TJ	2015	IEA (2017)
		SC-IND-oil	CO-HF-IND	572	kt	2015	IEA (2017)
		SC-IND-oil	CO-LF-IND	1682	kt	2015	IEA (2017)
		SC-PP-coal	HC-B-PP	147899	kt	2015	IEA (2017)
		SC-PP-oil	CO-LF-PP	44	kt	2015	IEA (2017)
		SSC	SP-S	2819	kt	2014	World Steel Association (2015)
SSD	South Sudan	BIO	PSB – DR	6682	TJ	2015	IEA (2017)
		BIO	PSB – PP	16	TJ	2015	IEA (2017)
		SC-DR-oil	CO-LF-DR	180	kt	2015	IEA (2017)
		SC-IND-oil	CO-LF-IND	2	kt	2015	IEA (2017)
		SC-PP-oil	CO-LF-PP	88	kt	2015	IEA (2017)
		SC-PP-oil	CO-PP	23	kt	2015	IEA (2017)
ESP	Spain	BIO	PSB – DR	110460	TJ	2015	IEA (2017)
		BIO	PSB – IND	53916	TJ	2015	IEA (2017)
		BIO	PSB – PP	50350	TJ	2015	IEA (2017)
		CEM	CEM	14587	kt	2014	USGS (2017a)
		CEM	PC-CEM	1440	kt	2015	IEA (2017)
		CSP	CSP-C	574.882	kt	2015	OSPAR (2016)
		NFMP	AL-P	230	kt	2015	USGS (2017b)
		NFMP	CU-P	283000	t	2015	USGS (2017b)
		NFMP	ZN-P	491000	t	2015	USGS (2017b)
		NFMP-AU	GP-L	1800	kg	2015	USGS (2017b)
		OR	CO-OR	64933	kt	2015	IEA (2017)
		PISP	PIP	3958	kt	2014	USGS (2017a)
		SC-DR-coal	HC-DR	175	kt	2015	IEA (2017)
		SC-DR-gas	NG-DR	294115	TJ	2015	IEA (2017)
		SC-DR-oil	CO-HF-DR	161	kt	2015	IEA (2017)
		SC-DR-oil	CO-LF-DR	25301	kt	2015	IEA (2017)
		SC-IND-coal	HC-IND-CEM	12	kt	2015	IEA (2017)
		SC-IND-coal	HC-IND-OTH	223	kt	2015	IEA (2017)
		SC-IND-coal	HC-IND-PIP	80	kt	2015	IEA (2017)
		SC-IND-gas	NG-IND	320912	TJ	2015	IEA (2017)
		SC-IND-oil	CO-HF-IND	373	kt	2015	IEA (2017)
		SC-IND-oil	CO-LF-IND	1092	kt	2015	IEA (2017)
		SC-PP-coal	BC-S-PP	2298	kt	2015	IEA (2017)
		SC-PP-coal	HC-A-PP	2176	kt	2015	IEA (2017)
		SC-PP-coal	HC-B-PP	18214	kt	2015	IEA (2017)
		SC-PP-gas	NG-PP	501668	TJ	2015	IEA (2017)
		SC-PP-oil	CO-HF-PP	1873	kt	2015	IEA (2017)
		SC-PP-oil	CO-LF-PP	842	kt	2015	IEA (2017)
		SSC	SP-S	10042	kt	2014	World Steel Association (2015)

Country code	Country name	Sector code	Activity code	Activity amount	Units	Year	Source
LKA	Sri Lanka	BIO	PSB – DR	125215	TJ	2015	IEA (2017)
		BIO	PSB – IND	72725	TJ	2015	IEA (2017)
		BIO	PSB – PP	1574	TJ	2015	IEA (2017)
		CEM	CEM	1885	kt	2014	USGS (2017a)
		OR	CO-OR	1692	kt	2015	IEA (2017)
		SC-DR-oil	CO-HF-DR	40	kt	2015	IEA (2017)
		SC-DR-oil	CO-LF-DR	1812	kt	2015	IEA (2017)
		SC-IND-coal	HC-IND-CEM	87	kt	2015	IEA (2017)
		SC-IND-oil	CO-HF-IND	684	kt	2015	IEA (2017)
		SC-IND-oil	CO-LF-IND	109	kt	2015	IEA (2017)
		SC-PP-coal	HC-B-PP	1880	kt	2015	IEA (2017)
		SC-PP-oil	CO-HF-PP	290	kt	2015	IEA (2017)
		SC-PP-oil	CO-LF-PP	86	kt	2015	IEA (2017)
		SSC	SP-S	30	kt	2014	World Steel Association (2015)
SPM	St. Pierre-Miquelon	BIO	PSB – DR	5.881852436	TJ	2015	IEA (2017)[#]
		BIO	PSB – IND	34.99813395	TJ	2015	IEA (2017)[#]
		BIO	PSB – PP	11.48534656	TJ	2015	IEA (2017)[#]
		OR	CO-OR	4.266237711	kt	2015	IEA (2017)[#]
		SC-DR-coal	HC-DR	0.894675884	kt	2015	IEA (2017)[#]
		SC-DR-gas	NG-DR	2.124304315	TJ	2015	IEA (2017)[#]
		SC-DR-oil	CO-HF-DR	0.189512626	kt	2015	IEA (2017)[#]
		SC-DR-oil	CO-LF-DR	4.543895744	kt	2015	IEA (2017)[#]
		SC-IND-gas	NG-IND	9.70E-02	TJ	2015	IEA (2017)[#]
		SC-IND-oil	CO-HF-IND	0.572945147	kt	2015	IEA (2017)[#]
		SC-IND-oil	CO-LF-IND	0.326138007	kt	2015	IEA (2017)[#]
		SC-PP-gas	NG-PP	135.6425599	TJ	2015	IEA (2017)[#]
		SC-PP-oil	CO-HF-PP	6.923821739	kt	2015	IEA (2017)[#]
		SC-PP-oil	CO-LF-PP	5.094804539	kt	2015	IEA (2017)[#]
SDN	Sudan	BIO	PSB – DR	160650	TJ	2015	IEA (2017)
		BIO	PSB – IND	34217	TJ	2015	IEA (2017)
		CEM	CEM	3478	kt	2014	USGS (2017a)
		NFMP-AU	GP-L	8240	kg	2015	USGS (2017b)
		OR	CO-OR	4273	kt	2015	IEA (2017)
		SC-DR-oil	CO-LF-DR	1713	kt	2015	IEA (2017)
		SC-IND-oil	CO-HF-IND	70	kt	2015	IEA (2017)
		SC-IND-oil	CO-LF-IND	113	kt	2015	IEA (2017)
		SC-PP-oil	CO-HF-PP	427	kt	2015	IEA (2017)
		SC-PP-oil	CO-LF-PP	393	kt	2015	IEA (2017)
		SC-PP-oil	CO-PP	472	kt	2015	IEA (2017)
SUR	Suriname	BIO	PSB – DR	1028	TJ	2015	IEA (2017)
		BIO	PSB – IND	192	TJ	2015	IEA (2017)
		CEM	CEM	130	kt	2014	USGS (2017a)
		NFMP	AL-P	748	kt	2015	USGS (2017b)
		NFMP-AU	GP-L	30000	kg	2015	USGS (2017b)
		OR	CO-OR	431	kt	2015	IEA (2017)
		SC-DR-oil	CO-HF-DR	17	kt	2015	IEA (2017)
		SC-DR-oil	CO-LF-DR	162	kt	2015	IEA (2017)
		SC-IND-oil	CO-LF-IND	17	kt	2015	IEA (2017)
		SC-PP-oil	CO-HF-PP	274	kt	2015	IEA (2017)
		SC-PP-oil	CO-LF-PP	17	kt	2015	IEA (2017)
		SC-PP-oil	CO-PP	3	kt	2015	IEA (2017)

Country code	Country name	Sector code	Activity code	Activity amount	Units	Year	Source
SWZ	Swaziland	BIO	PSB – DR	13114.46844	TJ	2015	IEA (2017)#
		BIO	PSB – IND	1691.201792	TJ	2015	IEA (2017)#
		BIO	PSB – PP	605.0365172	TJ	2015	IEA (2017)#
		SC-DR-coal	HC-DR	2.749868383	kt	2015	IEA (2017)#
		SC-DR-oil	CO-LF-DR	92.25153693	kt	2015	IEA (2017)#
		SC-IND-coal	HC-IND-OTH	2.848077968	kt	2015	IEA (2017)#
		SC-IND-gas	NG-IND	0.916622794	TJ	2015	IEA (2017)#
		SC-IND-oil	CO-HF-IND	16.79383905	kt	2015	IEA (2017)#
		SC-IND-oil	CO-IND	4.615850499	kt	2015	IEA (2017)#
		SC-IND-oil	CO-LF-IND	16.07363543	kt	2015	IEA (2017)#
		SC-PP-coal	HC-B-PP	24.09408488	kt	2015	IEA (2017)#
		SC-PP-gas	NG-PP	634.2702371	TJ	2015	IEA (2017)#
		SC-PP-oil	CO-HF-PP	21.83526442	kt	2015	IEA (2017)#
		SC-PP-oil	CO-LF-PP	45.17640914	kt	2015	IEA (2017)#
SWE	Sweden	BIO	PSB – DR	45624	TJ	2015	IEA (2017)
		BIO	PSB – IND	179234	TJ	2015	IEA (2017)
		BIO	PSB – PP	157338	TJ	2015	IEA (2017)
		CEM	CEM	2500	kt	2014	USGS (2017a)
		CSP	CSP-C	120	kt	2015	OSPAR (2016)
		NFMP	AL-P	115	kt	2015	USGS (2017b)
		NFMP	CU-P	150000	t	2015	USGS (2017b)
		NFMP	PB-P	26000	t	2015	USGS (2017b)
		OR	CO-OR	19981	kt	2015	IEA (2017)
		PISP	PIP	3078	kt	2014	USGS (2017a)
		SC-DR-gas	NG-DR	7675	TJ	2015	IEA (2017)
		SC-DR-oil	CO-HF-DR	43	kt	2015	IEA (2017)
		SC-DR-oil	CO-LF-DR	4101	kt	2015	IEA (2017)
		SC-IND-coal	HC-IND-CEM	250	kt	2015	IEA (2017)
		SC-IND-coal	HC-IND-NFM	50	kt	2015	IEA (2017)
		SC-IND-coal	HC-IND-OTH	160	kt	2015	IEA (2017)
		SC-IND-coal	HC-IND-PIP	61	kt	2015	IEA (2017)
		SC-IND-gas	NG-IND	18768	TJ	2015	IEA (2017)
		SC-IND-oil	CO-HF-IND	220	kt	2015	IEA (2017)
		SC-IND-oil	CO-LF-IND	249	kt	2015	IEA (2017)
		SC-PP-coal	HC-B-PP	286	kt	2015	IEA (2017)
		SC-PP-gas	NG-PP	8677	TJ	2015	IEA (2017)
		SC-PP-oil	CO-HF-PP	71	kt	2015	IEA (2017)
		SC-PP-oil	CO-LF-PP	49	kt	2015	IEA (2017)
		SSC	SP-S	1443	kt	2014	World Steel Association (2015)
CHE	Switzerland	BIO	PSB – DR	25822	TJ	2015	IEA (2017)
		BIO	PSB – IND	9284	TJ	2015	IEA (2017)
		BIO	PSB – PP	4944	TJ	2015	IEA (2017)
		CEM	CEM	4290	kt	2014	USGS (2017a)
		CEM	PC-CEM	25	kt	2015	IEA (2017)
		CSP	CSP-C	26.5	kt	2015	OSPAR (2016)
		OR	CO-OR	2804	kt	2015	IEA (2017)
		SC-DR-coal	HC-DR	16	kt	2015	IEA (2017)
		SC-DR-gas	NG-DR	81031	TJ	2015	IEA (2017)
		SC-DR-oil	CO-HF-DR	1	kt	2015	IEA (2017)
		SC-DR-oil	CO-LF-DR	5358	kt	2015	IEA (2017)
		SC-IND-coal	BC-IND-CEM	130	kt	2015	IEA (2017)

Country code	Country name	Sector code	Activity code	Activity amount	Units	Year	Source
		SC-IND-coal	HC-IND-CEM	46	kt	2015	IEA (2017)
		SC-IND-coal	HC-IND-OTH	1	kt	2015	IEA (2017)
		SC-IND-coal	HC-IND-PIP	14	kt	2015	IEA (2017)
		SC-IND-gas	NG-IND	43367	TJ	2015	IEA (2017)
		SC-IND-oil	CO-HF-IND	6	kt	2015	IEA (2017)
		SC-IND-oil	CO-LF-IND	299	kt	2015	IEA (2017)
		SC-PP-gas	NG-PP	8937	TJ	2015	IEA (2017)
		SC-PP-oil	CO-HF-PP	13	kt	2015	IEA (2017)
		SC-PP-oil	CO-LF-PP	11	kt	2015	IEA (2017)
		SSC	SP-S	1475	kt	2014	World Steel Association (2015)
SYR	Syrian Arab Rep.	BIO	PSB – DR	190	TJ	2015	IEA (2017)
		CEM	CEM	3800	kt	2014	USGS (2017a)
		CSP	CSP-C	14	kt	2010	UNEP (2011e)
		OR	CO-OR	5457	kt	2015	IEA (2017)
		SC-DR-oil	CO-HF-DR	282	kt	2015	IEA (2017)
		SC-DR-oil	CO-LF-DR	1773	kt	2015	IEA (2017)
		SC-IND-gas	NG-IND	9556	TJ	2015	IEA (2017)
		SC-IND-oil	CO-HF-IND	642	kt	2015	IEA (2017)
		SC-IND-oil	CO-LF-IND	338	kt	2015	IEA (2017)
		SC-PP-gas	NG-PP	135089	TJ	2015	IEA (2017)
		SC-PP-oil	CO-HF-PP	1298	kt	2015	IEA (2017)
		SC-PP-oil	CO-LF-PP	209	kt	2015	IEA (2017)
		SSC	SP-S	5	kt	2014	World Steel Association (2015)
TWN	Taiwan (China)	BIO	PSB – IND	4597	TJ	2015	IEA (2017)
		BIO	PSB – PP	12028	TJ	2015	IEA (2017)
		CEM	CEM	14592	kt	2014	USGS (2017a)
		OR	CO-OR	43753	kt	2015	IEA (2017)
		PISP	PIP	14440	kt	2014	USGS (2017a)
		SC-DR-gas	NG-DR	57422	TJ	2015	IEA (2017)
		SC-DR-oil	CO-HF-DR	418	kt	2015	IEA (2017)
		SC-DR-oil	CO-LF-DR	4612	kt	2015	IEA (2017)
		SC-IND-coal	HC-IND-CEM	2121	kt	2015	IEA (2017)
		SC-IND-coal	HC-IND-OTH	7220	kt	2015	IEA (2017)
		SC-IND-coal	HC-IND-PIP	253	kt	2015	IEA (2017)
		SC-IND-gas	NG-IND	74130	TJ	2015	IEA (2017)
		SC-IND-oil	CO-HF-IND	1516	kt	2015	IEA (2017)
		SC-IND-oil	CO-LF-IND	97	kt	2015	IEA (2017)
		SC-PP-coal	BC-S-PP	11418	kt	2015	IEA (2017)
		SC-PP-coal	HC-B-PP	31281	kt	2015	IEA (2017)
		SC-PP-gas	NG-PP	592732	TJ	2015	IEA (2017)
		SC-PP-oil	CO-HF-PP	2644	kt	2015	IEA (2017)
		SC-PP-oil	CO-LF-PP	143	kt	2015	IEA (2017)
		SSC	SP-S	9677	kt	2014	World Steel Association (2015)
TJK	Tajikistan	CEM	CEM	1150	kt	2014	USGS (2017a)
		NFMP	AL-P	100	kt	2015	USGS (2017b)
		NFMP-AU	GP-L	3500	kg	2015	USGS (2017b)
		NFMP-HG	HG-P	30	t	2015	USGS (2017b)
		OR	CO-OR	25	kt	2015	IEA (2017)
		SC-DR-coal	BC-DR	57	kt	2015	IEA (2017)
		SC-DR-coal	HC-DR	834	kt	2015	IEA (2017)

Country code	Country name	Sector code	Activity code	Activity amount	Units	Year	Source
		SC-DR-gas	NG-DR	156	TJ	2015	IEA (2017)
		SC-DR-oil	CO-HF-DR	12	kt	2015	IEA (2017)
		SC-DR-oil	CO-LF-DR	229	kt	2015	IEA (2017)
		SC-PP-coal	HC-B-PP	164	kt	2015	IEA (2017)
		SC-PP-oil	CO-HF-PP	7	kt	2015	IEA (2017)
THA	Thailand	BIO	PSB – DR	133363	TJ	2015	IEA (2017)
		BIO	PSB – IND	308439	TJ	2015	IEA (2017)
		BIO	PSB – PP	153538	TJ	2015	IEA (2017)
		CEM	CEM	34980	kt	2014	USGS (2017a)
		NFMP	ZN-P	74121	t	2015	USGS (2017b)
		NFMP-AU	GP-L	3305	kg	2015	USGS (2017b)
		OR	CO-OR	61539	kt	2015	IEA (2017)
		SC-DR-gas	NG-DR	114394	TJ	2015	IEA (2017)
		SC-DR-oil	CO-LF-DR	14340	kt	2015	IEA (2017)
		SC-IND-coal	BC-IND-CEM	814	kt	2015	IEA (2017)
		SC-IND-coal	BC-IND-OTH	109	kt	2015	IEA (2017)
		SC-IND-coal	HC-IND-CEM	10304	kt	2015	IEA (2017)
		SC-IND-coal	HC-IND-NFM	54	kt	2015	IEA (2017)
		SC-IND-coal	HC-IND-OTH	1864	kt	2015	IEA (2017)
		SC-IND-gas	NG-IND	141536	TJ	2015	IEA (2017)
		SC-IND-oil	CO-HF-IND	603	kt	2015	IEA (2017)
		SC-IND-oil	CO-LF-IND	3418	kt	2015	IEA (2017)
		SC-PP-coal	BC-L-PP	14484	kt	2015	IEA (2017)
		SC-PP-coal	HC-B-PP	8209	kt	2015	IEA (2017)
		SC-PP-gas	NG-PP	1422743	TJ	2015	IEA (2017)
		SC-PP-oil	CO-HF-PP	184	kt	2015	IEA (2017)
		SC-PP-oil	CO-LF-PP	47	kt	2015	IEA (2017)
		SSC	SP-S	4095	kt	2014	World Steel Association (2015)
TLS	Timor-Leste	BIO	PSB – DR	4010.677499	TJ	2015	IEA (2017)[#]
		BIO	PSB – IND	514.5942354	TJ	2015	IEA (2017)[#]
		OR	CO-OR	52.22996125	kt	2015	IEA (2017)[#]
		SC-DR-gas	NG-DR	262.5659296	TJ	2015	IEA (2017)[#]
		SC-DR-oil	CO-HF-DR	3.24875357	kt	2015	IEA (2017)[#]
		SC-DR-oil	CO-LF-DR	83.17642154	kt	2015	IEA (2017)[#]
		SC-IND-coal	BC-IND-OTH	0.999616483	kt	2015	IEA (2017)[#]
		SC-IND-coal	HC-IND-OTH	70.26470863	kt	2015	IEA (2017)[#]
		SC-IND-oil	CO-HF-IND	7.122267443	kt	2015	IEA (2017)[#]
		SC-IND-oil	CO-LF-IND	7.788678432	kt	2015	IEA (2017)[#]
		SC-PP-coal	HC-B-PP	18.49290494	kt	2015	IEA (2017)[#]
		SC-PP-gas	NG-PP	286.6400266	TJ	2015	IEA (2017)[#]
		SC-PP-oil	CO-HF-PP	36.69425507	kt	2015	IEA (2017)[#]
		SC-PP-oil	CO-LF-PP	47.98159119	kt	2015	IEA (2017)[#]
TGO	Togo	BIO	PSB – DR	41305	TJ	2015	IEA (2017)
		BIO	PSB – IND	133	TJ	2015	IEA (2017)
		BIO	PSB – PP	83	TJ	2015	IEA (2017)
		CEM	CEM	1677	kt	2014	USGS (2017a)
		SC-DR-oil	CO-LF-DR	293	kt	2015	IEA (2017)
		SC-IND-oil	CO-HF-IND	53	kt	2015	IEA (2017)
		SC-IND-oil	CO-LF-IND	2	kt	2015	IEA (2017)
		SC-PP-oil	CO-LF-PP	4	kt	2015	IEA (2017)

Country code	Country name	Sector code	Activity code	Activity amount	Units	Year	Source
TON	Tonga	BIO	PSB – DR	346.9544416	TJ	2015	IEA (2017)#
		BIO	PSB – IND	40.54168323	TJ	2015	IEA (2017)#
		OR	CO-OR	4.114874202	kt	2015	IEA (2017)#
		SC-DR-gas	NG-DR	20.68593857	TJ	2015	IEA (2017)#
		SC-DR-oil	CO-HF-DR	0.255949113	kt	2015	IEA (2017)#
		SC-DR-oil	CO-LF-DR	6.552953574	kt	2015	IEA (2017)#
		SC-IND-coal	BC-IND-OTH	7.88E-02	kt	2015	IEA (2017)#
		SC-IND-coal	HC-IND-OTH	5.53571992	kt	2015	IEA (2017)#
		SC-IND-oil	CO-HF-IND	0.561119209	kt	2015	IEA (2017)#
		SC-IND-oil	CO-LF-IND	0.613621592	kt	2015	IEA (2017)#
		SC-PP-coal	HC-B-PP	1.456941105	kt	2015	IEA (2017)#
		SC-PP-gas	NG-PP	22.58258713	TJ	2015	IEA (2017)#
		SC-PP-oil	CO-HF-PP	2.890912418	kt	2015	IEA (2017)#
		SC-PP-oil	CO-LF-PP	3.780171516	kt	2015	IEA (2017)#
TTO	Trinidad and Tobago	BIO	PSB – DR	427	TJ	2015	IEA (2017)
		CEM	CEM	837	kt	2014	USGS (2017a)
		OR	CO-OR	6464	kt	2015	IEA (2017)
		SC-DR-gas	NG-DR	3622	TJ	2015	IEA (2017)
		SC-DR-oil	CO-LF-DR	422	kt	2015	IEA (2017)
		SC-IND-gas	NG-IND	83796	TJ	2015	IEA (2017)
		SC-IND-oil	CO-LF-IND	122	kt	2015	IEA (2017)
		SC-PP-gas	NG-PP	270001	TJ	2015	IEA (2017)
		SC-PP-oil	CO-LF-PP	28	kt	2015	IEA (2017)
		SSC	SP-S	487	kt	2014	World Steel Association (2015)
TUN	Tunisia	BIO	PSB – DR	29903	TJ	2015	IEA (2017)
		CEM	CEM	9127	kt	2014	USGS (2017a)
		CEM	PC-CEM	815	kt	2015	IEA (2017)
		OR	CO-OR	1315	kt	2015	IEA (2017)
		SC-DR-gas	NG-DR	22863	TJ	2015	IEA (2017)
		SC-DR-oil	CO-HF-DR	24	kt	2015	IEA (2017)
		SC-DR-oil	CO-LF-DR	1857	kt	2015	IEA (2017)
		SC-IND-gas	NG-IND	37099	TJ	2015	IEA (2017)
		SC-IND-oil	CO-HF-IND	216	kt	2015	IEA (2017)
		SC-IND-oil	CO-LF-IND	57	kt	2015	IEA (2017)
		SC-PP-gas	NG-PP	174159	TJ	2015	IEA (2017)
		SC-PP-oil	CO-HF-PP	266	kt	2015	IEA (2017)
		SC-PP-oil	CO-LF-PP	21	kt	2015	IEA (2017)
		SSC	SP-S	150	kt	2014	World Steel Association (2015)
TUR	Turkey	BIO	PSB – DR	117640	TJ	2015	IEA (2017)
		BIO	PSB – PP	1545	TJ	2015	IEA (2017)
		CEM	CEM	71329	kt	2014	USGS (2017a)
		NFMP	AL-P	50	kt	2015	USGS (2017b)
		NFMP	CU-T	35000	t	2015	USGS (2017b)
		NFMP-AU	GP-L	25000	kg	2015	USGS (2017b)
		OR	CO-OR	26168	kt	2015	IEA (2017)
		PISP	PIP	9364	kt	2014	USGS (2017a)
		SC-DR-coal	BC-DR	3136	kt	2015	IEA (2017)
		SC-DR-coal	HC-DR	6739	kt	2015	IEA (2017)
		SC-DR-gas	NG-DR	563684	TJ	2015	IEA (2017)
		SC-DR-oil	CO-HF-DR	248	kt	2015	IEA (2017)
		SC-DR-oil	CO-LF-DR	19278	kt	2015	IEA (2017)
		SC-IND-coal	BC-IND-CEM	1406	kt	2015	IEA (2017)
		SC-IND-coal	BC-IND-OTH	2617	kt	2015	IEA (2017)

Country code	Country name	Sector code	Activity code	Activity amount	Units	Year	Source
		SC-IND-coal	HC-IND-CEM	3307	kt	2015	IEA (2017)
		SC-IND-coal	HC-IND-NFM	9	kt	2015	IEA (2017)
		SC-IND-coal	HC-IND-OTH	1060	kt	2015	IEA (2017)
		SC-IND-coal	HC-IND-PIP	406	kt	2015	IEA (2017)
		SC-IND-gas	NG-IND	392838	TJ	2015	IEA (2017)
		SC-IND-oil	CO-HF-IND	259	kt	2015	IEA (2017)
		SC-IND-oil	CO-LF-IND	611	kt	2015	IEA (2017)
		SC-PP-coal	BC-L-PP	49987	kt	2015	IEA (2017)
		SC-PP-coal	BC-S-PP	492	kt	2015	IEA (2017)
		SC-PP-coal	HC-B-PP	15774	kt	2015	IEA (2017)
		SC-PP-gas	NG-PP	854936	TJ	2015	IEA (2017)
		SC-PP-oil	CO-HF-PP	601	kt	2015	IEA (2017)
		SC-PP-oil	CO-LF-PP	225	kt	2015	IEA (2017)
		SSC	SP-S	23752	kt	2014	World Steel Association (2015)
TKM	Turkmenistan	CEM	CEM	2900	kt	2014	USGS (2017a)
		OR	CO-OR	8600	kt	2015	IEA (2017)
		SC-DR-gas	NG-DR	439444	TJ	2015	IEA (2017)
		SC-DR-oil	CO-HF-DR	931	kt	2015	IEA (2017)
		SC-DR-oil	CO-LF-DR	2080	kt	2015	IEA (2017)
		SC-IND-gas	NG-IND	46570	TJ	2015	IEA (2017)
		SC-PP-gas	NG-PP	507202	TJ	2015	IEA (2017)
TCA	Turks and Caicos Islands	BIO	PSB – DR	52.27851166	TJ	2015	IEA (2017)[#]
		BIO	PSB – IND	259.3710746	TJ	2015	IEA (2017)[#]
		BIO	PSB – PP	85.11787184	TJ	2015	IEA (2017)[#]
		OR	CO-OR	31.61707596	kt	2015	IEA (2017)[#]
		SC-DR-coal	HC-DR	6.630440516	kt	2015	IEA (2017)[#]
		SC-DR-gas	NG-DR	15.74321344	TJ	2015	IEA (2017)[#]
		SC-DR-oil	CO-HF-DR	1.404477548	kt	2015	IEA (2017)[#]
		SC-DR-oil	CO-LF-DR	33.67479887	kt	2015	IEA (2017)[#]
		SC-IND-gas	NG-IND	0.718569908	TJ	2015	IEA (2017)[#]
		SC-IND-oil	CO-HF-IND	4.246094911	kt	2015	IEA (2017)[#]
		SC-IND-oil	CO-LF-IND	2.417007873	kt	2015	IEA (2017)[#]
		SC-PP-gas	NG-PP	1005.246639	TJ	2015	IEA (2017)[#]
		SC-PP-oil	CO-HF-PP	51.31242389	kt	2015	IEA (2017)[#]
		SC-PP-oil	CO-LF-PP	37.75758244	kt	2015	IEA (2017)[#]
UGA	Uganda	BIO	PSB – DR	338928.1538	TJ	2015	IEA (2017)[#]
		BIO	PSB – IND	10284.03282	TJ	2015	IEA (2017)[#]
		BIO	PSB – PP	3679.167932	TJ	2015	IEA (2017)[#]
		CEM	CEM	2141	kt	2014	USGS (2017a)
		SC-DR-coal	HC-DR	16.72168089	kt	2015	IEA (2017)[#]
		SC-DR-oil	CO-LF-DR	560.9725805	kt	2015	IEA (2017)[#]
		SC-IND-coal	HC-IND-OTH	17.31888378	kt	2015	IEA (2017)[#]
		SC-IND-gas	NG-IND	5.573893631	TJ	2015	IEA (2017)[#]
		SC-IND-oil	CO-HF-IND	102.121694	kt	2015	IEA (2017)[#]
		SC-IND-oil	CO-IND	28.06853579	kt	2015	IEA (2017)[#]
		SC-IND-oil	CO-LF-IND	97.74220618	kt	2015	IEA (2017)[#]
		SC-PP-coal	HC-B-PP	146.5137755	kt	2015	IEA (2017)[#]
		SC-PP-gas	NG-PP	3856.935325	TJ	2015	IEA (2017)[#]
		SC-PP-oil	CO-HF-PP	132.778109	kt	2015	IEA (2017)[#]
		SC-PP-oil	CO-LF-PP	274.713329	kt	2015	IEA (2017)[#]
		SSC	SP-S	30	kt	2014	World Steel Association (2015)

Country code	Country name	Sector code	Activity code	Activity amount	Units	Year	Source
UKR	Ukraine	BIO	PSB – DR	47358	TJ	2015	IEA (2017)
		BIO	PSB – IND	3621	TJ	2015	IEA (2017)
		BIO	PSB – PP	23507	TJ	2015	IEA (2017)
		CEM	CEM	9636	kt	2014	USGS (2017a)
		OR	CO-OR	2104	kt	2015	IEA (2017)
		PISP	PIP	24787	kt	2014	USGS (2017a)
		SC-DR-coal	HC-DR	596	kt	2015	IEA (2017)
		SC-DR-gas	NG-DR	510854	TJ	2015	IEA (2017)
		SC-DR-oil	CO-HF-DR	15	kt	2015	IEA (2017)
		SC-DR-oil	CO-LF-DR	4426	kt	2015	IEA (2017)
		SC-IND-coal	HC-IND-CEM	931	kt	2015	IEA (2017)
		SC-IND-coal	HC-IND-NFM	192	kt	2015	IEA (2017)
		SC-IND-coal	HC-IND-OTH	54	kt	2015	IEA (2017)
		SC-IND-coal	HC-IND-PIP	1922	kt	2015	IEA (2017)
		SC-IND-gas	NG-IND	128539	TJ	2015	IEA (2017)
		SC-IND-oil	CO-HF-IND	10	kt	2015	IEA (2017)
		SC-IND-oil	CO-LF-IND	768	kt	2015	IEA (2017)
		SC-PP-coal	HC-A-PP	1939	kt	2015	IEA (2017)
		SC-PP-coal	HC-B-PP	27535	kt	2015	IEA (2017)
		SC-PP-gas	NG-PP	443274	TJ	2015	IEA (2017)
		SC-PP-oil	CO-HF-PP	358	kt	2015	IEA (2017)
		SC-PP-oil	CO-LF-PP	77	kt	2015	IEA (2017)
		SC-PP-oil	CO-PP	3	kt	2015	IEA (2017)
		SSC	SP-S	1678	kt	2014	World Steel Association (2015)
ARE	United Arab Emirates	CEM	CEM	16000	kt	2014	USGS (2017a)
		CSP	CSP-C	9	kt	2010	UNEP (2011e)
		NFMP	AL-P	2400	kt	2015	USGS (2017b)
		OR	CO-OR	29062	kt	2015	IEA (2017)
		SC-DR-oil	CO-LF-DR	2783	kt	2015	IEA (2017)
		SC-IND-coal	HC-IND-CEM	405	kt	2015	IEA (2017)
		SC-IND-gas	NG-IND	1235488	TJ	2015	IEA (2017)
		SC-IND-oil	CO-HF-IND	1339	kt	2015	IEA (2017)
		SC-PP-gas	NG-PP	1423864	TJ	2015	IEA (2017)
		SC-PP-oil	CO-HF-PP	50	kt	2015	IEA (2017)
		SC-PP-oil	CO-LF-PP	547	kt	2015	IEA (2017)
		SSC	SP-S	2390	kt	2014	World Steel Association (2015)
GBR	United Kingdom	BIO	PSB – DR	74666	TJ	2015	IEA (2017)
		BIO	PSB – IND	33806	TJ	2015	IEA (2017)
		BIO	PSB – PP	146795	TJ	2015	IEA (2017)
		CEM	CEM	8958	kt	2014	USGS (2017a)
		CSP	CSP-C	277	kt	2015	OSPAR (2016)
		NFMP	AL-P	47	kt	2015	USGS (2017b)
		NFMP	PB-P	150000	t	2015	USGS (2017b)
		OR	CO-OR	55376	kt	2015	IEA (2017)
		PISP	PIP	9705	kt	2014	USGS (2017a)
		SC-DR-coal	HC-DR	584	kt	2015	IEA (2017)
		SC-DR-gas	NG-DR	1406088	TJ	2015	IEA (2017)
		SC-DR-oil	CO-HF-DR	106	kt	2015	IEA (2017)
		SC-DR-oil	CO-LF-DR	26083	kt	2015	IEA (2017)
		SC-IND-coal	HC-IND-CEM	1010	kt	2015	IEA (2017)
		SC-IND-coal	HC-IND-NFM	21	kt	2015	IEA (2017)
		SC-IND-coal	HC-IND-OTH	937	kt	2015	IEA (2017)
		SC-IND-coal	HC-IND-PIP	44	kt	2015	IEA (2017)

Country code	Country name	Sector code	Activity code	Activity amount	Units	Year	Source
		SC-IND-gas	NG-IND	340103	TJ	2015	IEA (2017)
		SC-IND-oil	CO-HF-IND	160	kt	2015	IEA (2017)
		SC-IND-oil	CO-LF-IND	1647	kt	2015	IEA (2017)
		SC-PP-coal	HC-B-PP	29410	kt	2015	IEA (2017)
		SC-PP-gas	NG-PP	1065975	TJ	2015	IEA (2017)
		SC-PP-oil	CO-HF-PP	553	kt	2015	IEA (2017)
		SC-PP-oil	CO-LF-PP	740	kt	2015	IEA (2017)
		SSC	SP-S	1955	kt	2014	World Steel Association (2015)
TZA	United Republic of Tanzania	BIO	PSB – DR	619657	TJ	2015	IEA (2017)
		BIO	PSB – IND	116991	TJ	2015	IEA (2017)
		BIO	PSB – PP	378	TJ	2015	IEA (2017)
		CEM	CEM	2809	kt	2014	USGS (2017a)
		NFMP-AU	GP-L	45777	kg	2015	USGS (2017b)
		SC-DR-oil	CO-LF-DR	1415	kt	2015	IEA (2017)
		SC-IND-coal	HC-IND-OTH	257	kt	2015	IEA (2017)
		SC-IND-gas	NG-IND	6412	TJ	2015	IEA (2017)
		SC-IND-oil	CO-HF-IND	158	kt	2015	IEA (2017)
		SC-PP-gas	NG-PP	27590	TJ	2015	IEA (2017)
		SC-PP-oil	CO-HF-PP	236	kt	2015	IEA (2017)
		SC-PP-oil	CO-LF-PP	200	kt	2015	IEA (2017)
USA	United States	BIO	PSB – DR	543962	TJ	2015	IEA (2017)
		BIO	PSB – IND	1187436	TJ	2015	IEA (2017)
		BIO	PSB – PP	461853	TJ	2015	IEA (2017)
		CEM	CEM	83188	kt	2014	USGS (2017a)
		CEM	PC-CEM	514	kt	2015	IEA (2017)
		CSP	CSP-C	73	kt	2015	UNEP (2013)
		NFMP	AL-P	1586.512	kt	2015	USGS (2017b)
		NFMP	CU-P	527000	t	2015	USGS (2017b)
		NFMP	ZN-P	124000	t	2015	USGS (2017b)
		NFMP-AU	GP-L	214000	kg	2015	USGS (2017b)
		OR	CO-OR	798452	kt	2015	IEA (2017)
		PISP	PIP	29400	kt	2014	USGS (2017a)
		SC-DR-coal	BC-DR	540	kt	2015	IEA (2017)
		SC-DR-coal	HC-DR	676	kt	2015	IEA (2017)
		SC-DR-gas	NG-DR	9302671	TJ	2015	IEA (2017)
		SC-DR-oil	CO-HF-DR	1386	kt	2015	IEA (2017)
		SC-DR-oil	CO-LF-DR	169690	kt	2015	IEA (2017)
		SC-IND-coal	BC-IND-CEM	445	kt	2015	IEA (2017)
		SC-IND-coal	BC-IND-OTH	5734	kt	2015	IEA (2017)
		SC-IND-coal	HC-IND-CEM	8336	kt	2015	IEA (2017)
		SC-IND-coal	HC-IND-OTH	10361	kt	2015	IEA (2017)
		SC-IND-coal	HC-IND-PIP	163	kt	2015	IEA (2017)
		SC-IND-gas	NG-IND	5485063	TJ	2015	IEA (2017)
		SC-IND-oil	CO-HF-IND	1047	kt	2015	IEA (2017)
		SC-IND-oil	CO-LF-IND	13514	kt	2015	IEA (2017)
		SC-PP-coal	BC-L-PP	60366	kt	2015	IEA (2017)
		SC-PP-coal	BC-S-PP	353114	kt	2015	IEA (2017)
		SC-PP-coal	HC-A-PP	1035	kt	2015	IEA (2017)
		SC-PP-coal	HC-B-PP	258269	kt	2015	IEA (2017)
		SC-PP-gas	NG-PP	13937704	TJ	2015	IEA (2017)
		SC-PP-oil	CO-HF-PP	2550	kt	2015	IEA (2017)
		SC-PP-oil	CO-LF-PP	7984	kt	2015	IEA (2017)
		SSC	SP-S	55174	kt	2014	World Steel Association (2015)

Country code	Country name	Sector code	Activity code	Activity amount	Units	Year	Source
URY	Uruguay	BIO	PSB – DR	14578	TJ	2015	IEA (2017)
		BIO	PSB – IND	55554	TJ	2015	IEA (2017)
		BIO	PSB – PP	12083	TJ	2015	IEA (2017)
		CEM	CEM	820	kt	2014	USGS (2017a)
		CSP	CSP-C	15	kt	2015	UNEP (2013)
		NFMP-AU	GP-L	1664	kg	2015	USGS (2017b)
		OR	CO-OR	1892	kt	2015	IEA (2017)
		SC-DR-gas	NG-DR	1488	TJ	2015	IEA (2017)
		SC-DR-oil	CO-HF-DR	21	kt	2015	IEA (2017)
		SC-DR-oil	CO-LF-DR	724	kt	2015	IEA (2017)
		SC-IND-gas	NG-IND	544	TJ	2015	IEA (2017)
		SC-IND-oil	CO-HF-IND	156	kt	2015	IEA (2017)
		SC-IND-oil	CO-LF-IND	13	kt	2015	IEA (2017)
		SC-PP-gas	NG-PP	93	TJ	2015	IEA (2017)
		SC-PP-oil	CO-HF-PP	88	kt	2015	IEA (2017)
		SC-PP-oil	CO-LF-PP	181	kt	2015	IEA (2017)
		SSC	SP-S	94	kt	2014	World Steel Association (2015)
UZB	Uzbekistan	BIO	PSB – DR	169	TJ	2015	IEA (2017)
		CEM	CEM	7350	kt	2014	USGS (2017a)
		NFMP	CU-P	100000	t	2015	USGS (2017b)
		NFMP	ZN-P	73000	t	2015	USGS (2017b)
		NFMP-AU	GP-L	102000	kg	2015	USGS (2017b)
		OR	CO-OR	2655	kt	2015	IEA (2017)
		SC-DR-coal	BC-DR	429	kt	2015	IEA (2017)
		SC-DR-gas	NG-DR	657978	TJ	2015	IEA (2017)
		SC-DR-oil	CO-HF-DR	140	kt	2015	IEA (2017)
		SC-DR-oil	CO-LF-DR	773	kt	2015	IEA (2017)
		SC-IND-coal	BC-IND-OTH	173	kt	2015	IEA (2017)
		SC-IND-coal	HC-IND-OTH	367	kt	2015	IEA (2017)
		SC-IND-gas	NG-IND	222272	TJ	2015	IEA (2017)
		SC-IND-oil	CO-HF-IND	1	kt	2015	IEA (2017)
		SC-IND-oil	CO-LF-IND	82	kt	2015	IEA (2017)
		SC-PP-coal	BC-L-PP	2916	kt	2015	IEA (2017)
		SC-PP-gas	NG-PP	755004	TJ	2015	IEA (2017)
		SC-PP-oil	CO-HF-PP	51	kt	2015	IEA (2017)
		SC-PP-oil	CO-PP	5	kt	2015	IEA (2017)
		SSC	SP-S	723	kt	2014	World Steel Association (2015)
VUT	Vanuatu	BIO	PSB – DR	886.9701139	TJ	2015	IEA (2017)#
		BIO	PSB – IND	50.80519746	TJ	2015	IEA (2017)#
		OR	CO-OR	5.156593899	kt	2015	IEA (2017)#
		SC-DR-gas	NG-DR	25.92278145	TJ	2015	IEA (2017)#
		SC-DR-oil	CO-HF-DR	0.320745075	kt	2015	IEA (2017)#
		SC-DR-oil	CO-LF-DR	8.211896344	kt	2015	IEA (2017)#
		SC-IND-coal	BC-IND-OTH	0.098690792	kt	2015	IEA (2017)#
		SC-IND-coal	HC-IND-OTH	6.937140277	kt	2015	IEA (2017)#
		SC-IND-oil	CO-HF-IND	0.703171895	kt	2015	IEA (2017)#
		SC-IND-oil	CO-LF-IND	0.768965757	kt	2015	IEA (2017)#
		SC-PP-coal	HC-B-PP	1.825779658	kt	2015	IEA (2017)#
		SC-PP-gas	NG-PP	28.2995847	TJ	2015	IEA (2017)#
		SC-PP-oil	CO-HF-PP	3.622774501	kt	2015	IEA (2017)#
		SC-PP-oil	CO-LF-PP	4.737158031	kt	2015	IEA (2017)#

Country code	Country name	Sector code	Activity code	Activity amount	Units	Year	Source
VEN	Venezuela	BIO	PSB – DR	11266	TJ	2015	IEA (2017)
		BIO	PSB – IND	19411	TJ	2015	IEA (2017)
		CEM	CEM	8000	kt	2014	USGS (2017a)
		NFMP	AL-P	110	kt	2015	USGS (2017b)
		NFMP-AU	GP-L	1500	kg	2015	USGS (2017b)
		OR	CO-OR	41053	kt	2015	IEA (2017)
		SC-DR-gas	NG-DR	54769	TJ	2015	IEA (2017)
		SC-DR-oil	CO-LF-DR	2750	kt	2015	IEA (2017)
		SC-IND-coal	HC-IND-CEM	187	kt	2015	IEA (2017)
		SC-IND-gas	NG-IND	311889	TJ	2015	IEA (2017)
		SC-IND-oil	CO-HF-IND	977	kt	2015	IEA (2017)
		SC-IND-oil	CO-LF-IND	1569	kt	2015	IEA (2017)
		SC-PP-gas	NG-PP	548677	TJ	2015	IEA (2017)
		SC-PP-oil	CO-HF-PP	665	kt	2015	IEA (2017)
		SC-PP-oil	CO-LF-PP	5799	kt	2015	IEA (2017)
		SSC	SP-S	1485	kt	2014	World Steel Association (2015)
VNM	Vietnam	BIO	PSB – DR	477483	TJ	2015	IEA (2017)
		BIO	PSB – IND	114125	TJ	2015	IEA (2017)
		BIO	PSB – PP	672	TJ	2015	IEA (2017)
		CEM	CEM	60507	kt	2014	USGS (2017a)
		NFMP	AL-P	484	kt	2015	USGS (2017b)
		NFMP	CU-P	8000	t	2015	USGS (2017b)
		NFMP	ZN-P	10000	t	2015	USGS (2017b)
		OR	CO-OR	7249	kt	2015	IEA (2017)
		SC-DR-coal	HC-DR	2677	kt	2015	IEA (2017)
		SC-DR-oil	CO-HF-DR	41	kt	2015	IEA (2017)
		SC-DR-oil	CO-LF-DR	5856	kt	2015	IEA (2017)
		SC-IND-coal	BC-IND-OTH	1160	kt	2015	IEA (2017)
		SC-IND-coal	HC-IND-CEM	9651	kt	2015	IEA (2017)
		SC-IND-coal	HC-IND-OTH	6934	kt	2015	IEA (2017)
		SC-IND-coal	HC-IND-PIP	770	kt	2015	IEA (2017)
		SC-IND-gas	NG-IND	69371	TJ	2015	IEA (2017)
		SC-IND-oil	CO-HF-IND	298	kt	2015	IEA (2017)
		SC-IND-oil	CO-LF-IND	1128	kt	2015	IEA (2017)
		SC-PP-coal	HC-A-PP	22345	kt	2015	IEA (2017)
		SC-PP-coal	HC-B-PP	1226	kt	2015	IEA (2017)
		SC-PP-gas	NG-PP	366899	TJ	2015	IEA (2017)
		SC-PP-oil	CO-HF-PP	216	kt	2015	IEA (2017)
		SC-PP-oil	CO-LF-PP	40	kt	2015	IEA (2017)
		SSC	SP-S	4385	kt	2014	World Steel Association (2015)
YEM	Yemen	CEM	CEM	2800	kt	2014	USGS (2017a)
		OR	CO-OR	942	kt	2015	IEA (2017)
		SC-DR-oil	CO-LF-DR	290	kt	2015	IEA (2017)
		SC-IND-coal	HC-IND-CEM	133	kt	2015	IEA (2017)
		SC-IND-oil	CO-HF-IND	138	kt	2015	IEA (2017)
		SC-IND-oil	CO-LF-IND	124	kt	2015	IEA (2017)
		SC-PP-gas	NG-PP	38085	TJ	2015	IEA (2017)
		SC-PP-oil	CO-HF-PP	426	kt	2015	IEA (2017)
		SC-PP-oil	CO-LF-PP	400	kt	2015	IEA (2017)
		SC-PP-oil	CO-PP	41	kt	2015	IEA (2017)

Country code	Country name	Sector code	Activity code	Activity amount	Units	Year	Source
ZMB	Zambia	BIO	PSB – DR	161121	TJ	2015	IEA (2017)
		BIO	PSB – IND	64500	TJ	2015	IEA (2017)
		CEM	CEM	2200	kt	2014	USGS (2017a)
		NFMP	CU-P	649000	t	2015	USGS (2017b)
		NFMP-AU	GP-L	4500	kg	2015	USGS (2017b)
		OR	CO-OR	643	kt	2015	IEA (2017)
		SC-DR-oil	CO-LF-DR	143	kt	2015	IEA (2017)
		SC-IND-coal	HC-IND-OTH	159	kt	2015	IEA (2017)
		SC-IND-oil	CO-HF-IND	48	kt	2015	IEA (2017)
		SC-IND-oil	CO-LF-IND	319	kt	2015	IEA (2017)
		SC-PP-oil	CO-HF-PP	81	kt	2015	IEA (2017)
		SC-PP-oil	CO-LF-PP	10	kt	2015	IEA (2017)
ZWE	Zimbabwe	BIO	PSB – DR	304237	TJ	2015	IEA (2017)
		BIO	PSB – IND	5762	TJ	2015	IEA (2017)
		BIO	PSB – PP	1841	TJ	2015	IEA (2017)
		CEM	CEM	1300	kt	2014	USGS (2017a)
		NFMP-AU	GP-L	20000	kg	2015	USGS (2017b)
		SC-DR-coal	HC-DR	47	kt	2015	IEA (2017)
		SC-DR-oil	CO-LF-DR	659	kt	2015	IEA (2017)
		SC-IND-coal	HC-IND-CEM	82	kt	2015	IEA (2017)
		SC-IND-coal	HC-IND-OTH	158	kt	2015	IEA (2017)
		SC-IND-coal	HC-IND-PIP	1	kt	2015	IEA (2017)
		SC-IND-oil	CO-LF-IND	31	kt	2015	IEA (2017)
		SC-PP-coal	HC-B-PP	2751	kt	2015	IEA (2017)
		SC-PP-oil	CO-LF-PP	32	kt	2015	IEA (2017)

#activity amount derived from regionally aggregated data for small nations.

A3.9 Estimates of 2015 mercury emissions to air

Country code	Country name	Region	Sector Code	Activity Code	Emission estimate, kg	Low range estimate, kg	High range estimate, kg	Technology group	Waste group
AFG	Afghanistan	South Asia	BIO	PSB – DR	132.608	23.206	301.684	5	
			BIO	PSB – IND	5.701	0.998	12.969	5	
			CEM	CEM	11.118	3.927	58.609	5	
			CREM	CREM	0.136	0.113	0.156		4
			NFMP-AU	GP-L	2.200	0.770	4.290	5	
			OR	CO-OR	12.949	4.532	25.250	5	
			SC-DR-gas	NG-DR	0.012	0.002	0.027	5	
			SC-DR-oil	CO-HF-DR	0.583	0.102	1.327	5	
			SC-DR-oil	CO-LF-DR	1.493	0.261	3.396	5	
			SC-IND-coal	BC-IND-OTH	1.329	0.558	3.743	5	
			SC-IND-coal	HC-IND-OTH	88.677	37.244	249.772	5	
			SC-IND-oil	CO-HF-IND	1.278	0.224	2.908	5	
			SC-IND-oil	CO-LF-IND	0.140	0.024	0.318	5	
			SC-PP-coal	HC-B-PP	18.671	7.842	52.590	5	
			SC-PP-gas	NG-PP	0.013	0.002	0.029	5	
			SC-PP-oil	CO-HF-PP	6.586	1.153	14.984	5	
			SC-PP-oil	CO-LF-PP	0.861	0.151	1.959	5	
			WASOTH	WASOTH	225.101	67.530	675.303		4
			WI	WI	0.704	0.211	2.113		4
ALB	Albania	CIS & other European countries	BIO	PSB – DR	10.170	2.288	19.577	4	
			BIO	PSB – IND	0.511	0.115	0.983	4	
			CEM	CEM	215.600	76.134	1093.593	4	
			CEM	PC-CEM	1.645	0.925	9.274	4	
			CREM	CREM	0.781	0.572	1.041		4
			OR	CO-OR	0.312	0.140	0.515	4	
			SC-DR-coal	HC-DR	0.750	0.405	1.788	4	
			SC-DR-oil	CO-LF-DR	1.474	0.332	2.837	4	
			SC-IND-coal	HC-IND-CEM	25.725	13.892	61.311	4	
			SC-IND-gas	NG-IND	0.003	0.001	0.005	4	
			SC-IND-oil	CO-HF-IND	0.020	0.005	0.039	4	
			SC-IND-oil	CO-LF-IND	0.014	0.003	0.027	4	
			SC-PP-gas	NG-PP	0.004	0.001	0.007	4	
			SSC	SP-S	16.338	6.081	77.960	4	
			WASOTH	WASOTH	94.512	28.354	283.536		4
			WI	WI	0.296	0.089	0.887		4
DZA	Algeria	North Africa	BIO	PSB – DR	0.105	0.024	0.202	5	
			BIO	PSB – IND	0.206	0.046	0.397	5	
			CEM	CEM	2079.000	735.000	10742.550	5	
			CREM	CREM	0.173	0.130	0.216		4
			CSP	CSP-C	280.000	98.000	546.000	5	
			NFMP	ZN-P	568.980	201.579	1563.042	5	

Country code	Country name	Region	Sector Code	Activity Code	Emission estimate, kg	Low range estimate, kg	High range estimate, kg	Technology group	Waste group
			NFMP-AU	GP-L	11.000	3.850	21.450	5	
			OR	CO-OR	83.477	37.565	137.738	5	
			PISP	PIP	22.680	7.951	120.042	5	
			SC-DR-gas	NG-DR	1.904	0.428	3.666	5	
			SC-DR-oil	CO-DR	0.060	0.014	0.116	5	
			SC-DR-oil	CO-LF-DR	19.050	4.286	36.671	5	
			SC-IND-gas	NG-IND	0.798	0.180	1.537	5	
			SC-IND-oil	CO-LF-IND	1.344	0.302	2.587	5	
			SC-PP-gas	NG-PP	4.488	1.010	8.639	5	
			SC-PP-oil	CO-LF-PP	0.842	0.189	1.621	5	
			SC-PP-oil	CO-PP	6.080	1.368	11.704	5	
			WASOTH	WASOTH	1600.841	480.252	4802.524		4
			WI	WI	5.009	1.503	15.028		4
AND	Andorra	CIS & other European countries	CREM	CREM	0.051	0.038	0.068		2
			WASOTH	WASOTH	6.248	1.875	18.745		2
			WI	WI	0.182	0.055	0.546		2
AGO	Angola	Sub-Saharan Africa	ASGM	GP-A	225.000	56.250	393.750		
			BIO	PSB – DR	232.196	52.244	446.978	4	
			BIO	PSB – IND	6.575	1.479	12.657	4	
			CEM	CEM	229.688	81.156	1191.531	4	
			CREM	CREM	0.447	0.322	0.644		4
			CSP	CSP-C	100.000	35.000	195.000	4	
			OR	CO-OR	1.059	0.476	1.747	4	
			SC-DR-oil	CO-LF-DR	5.650	1.271	10.876	4	
			SC-IND-gas	NG-IND	0.146	0.033	0.282	4	
			SC-IND-oil	CO-HF-IND	0.780	0.176	1.502	4	
			SC-IND-oil	CO-LF-IND	0.272	0.061	0.524	4	
			SC-PP-oil	CO-HF-PP	0.840	0.189	1.617	4	
			SC-PP-oil	CO-LF-PP	2.272	0.511	4.374	4	
			WASOTH	WASOTH	912.787	394.719	1406.185		4
			WI	WI	0.175	0.076	0.269		4
AIA	Anguilla	Central America and the Caribbean	CREM	CREM	0.003	0.003	0.004		4
			WASOTH	WASOTH	0.461	0.138	1.384		4
			WI	WI	0.001	0.000	0.004		4
ATG	Antigua	Central America and the Caribbean	BIO	PSB – DR	0.120	0.021	0.273	3	
			BIO	PSB – IND	0.411	0.072	0.935	3	
			BIO	PSB – PP	0.146	0.026	0.332	3	
			CREM	CREM	0.018	0.014	0.021		4
			OR	CO-OR	0.039	0.014	0.077	3	
			SC-DR-coal	HC-DR	1.483	0.623	4.177	3	
			SC-DR-gas	NG-DR	0.000	0.000	0.000	3	
			SC-DR-oil	CO-HF-DR	0.042	0.007	0.095	3	
			SC-DR-oil	CO-LF-DR	0.100	0.018	0.228	3	
			SC-IND-gas	NG-IND	0.000	0.000	0.000	3	
			SC-IND-oil	CO-HF-IND	0.120	0.021	0.274	3	
			SC-IND-oil	CO-LF-IND	0.007	0.001	0.016	3	
			SC-PP-gas	NG-PP	0.007	0.001	0.017	3	

Country code	Country name	Region	Sector Code	Activity Code	Emission estimate, kg	Low range estimate, kg	High range estimate, kg	Technology group	Waste group
			SC-PP-oil	CO-HF-PP	1.148	0.201	2.611	3	
			SC-PP-oil	CO-LF-PP	0.084	0.015	0.192	3	
			WASOTH	WASOTH	5.627	1.688	16.880		4
			WI	WI	0.018	0.005	0.053		4
ARG	Argentina	South America	BIO	PSB – DR	13.201	2.970	25.412	3	
			BIO	PSB – IND	37.111	8.350	71.439	3	
			BIO	PSB – PP	34.639	7.794	66.680	3	
			CEM	CEM	839.629	297.064	4455.052	3	
			CREM	CREM	10.598	7.419	14.838		3
			CSP	CSP-P	500.000	175.000	975.000	3	
			NFMP	AL-P	11.000	3.729	20.773	3	
			NFMP	PB-P	10.268	5.593	16.221	3	
			NFMP	ZN-P	333.540	118.167	916.266	3	
			NFMP-AU	GP-L	2534.400	887.040	4942.080	3	
			NFMP-HG	HG-P	168.750	59.063	329.063	3	
			OR	CO-OR	107.447	48.351	177.288	3	
			PISP	PIP	152.476	53.451	807.032	3	
			SC-DR-gas	NG-DR	3.075	0.692	5.920	3	
			SC-DR-oil	CO-HF-DR	4.820	1.085	9.279	3	
			SC-DR-oil	CO-LF-DR	20.018	4.504	38.535	3	
			SC-IND-coal	HC-IND-OTH	0.788	0.425	1.877	3	
			SC-IND-gas	NG-IND	1.681	0.378	3.236	3	
			SC-IND-oil	CO-HF-IND	3.363	0.757	6.474	3	
			SC-IND-oil	CO-LF-IND	0.211	0.047	0.406	3	
			SC-PP-coal	HC-B-PP	91.935	49.645	219.112	3	
			SC-PP-gas	NG-PP	4.932	1.110	9.494	3	
			SC-PP-oil	CO-HF-PP	51.525	11.593	99.186	3	
			SC-PP-oil	CO-LF-PP	2.928	0.659	5.636	3	
			SC-PP-oil	CO-PP	0.683	0.154	1.314	3	
			SSC	SP-S	69.137	25.732	329.899	3	
			WASOTH	WASOTH	1374.550	412.365	4123.650		3
			WI	WI	8.942	2.682	26.825		3
ARM	Armenia	CIS & other European countries	BIO	PSB – DR	9.956	2.240	19.166	4	
			BIO	PSB – IND	0.001	0.000	0.002	4	
			CEM	CEM	41.846	14.777	212.256	4	
			CREM	CREM	0.261	0.192	0.348		4
			NFMP	CU-P	133.771	47.746	763.742	4	
			NFMP-AU	GP-L	272.250	95.288	530.888	4	
			SC-DR-gas	NG-DR	0.217	0.049	0.418	4	
			SC-DR-oil	CO-LF-DR	0.256	0.058	0.493	4	
			SC-IND-gas	NG-IND	0.040	0.009	0.077	4	
			SC-IND-oil	CO-LF-IND	0.002	0.000	0.004	4	
			SC-PP-gas	NG-PP	0.126	0.028	0.243	4	
			WASOTH	WASOTH	72.450	21.735	217.349		4
			WI	WI	0.227	0.068	0.680		4

Country code	Country name	Region	Sector Code	Activity Code	Emission estimate, kg	Low range estimate, kg	High range estimate, kg	Technology group	Waste group
ABW	Aruba	Central America and the Caribbean	BIO	PSB – DR	0.146	0.026	0.332	3	
			BIO	PSB – IND	0.534	0.094	1.216	3	
			BIO	PSB – PP	0.190	0.033	0.432	3	
			CREM	CREM	0.021	0.017	0.026		4
			OR	CO-OR	0.051	0.018	0.100	3	
			SC-DR-coal	HC-DR	1.929	0.810	5.433	3	
			SC-DR-gas	NG-DR	0.000	0.000	0.000	3	
			SC-DR-oil	CO-HF-DR	0.054	0.010	0.124	3	
			SC-DR-oil	CO-LF-DR	0.131	0.023	0.297	3	
			SC-IND-gas	NG-IND	0.000	0.000	0.000	3	
			SC-IND-oil	CO-HF-IND	0.156	0.027	0.356	3	
			SC-IND-oil	CO-LF-IND	0.009	0.002	0.020	3	
			SC-PP-gas	NG-PP	0.010	0.002	0.022	3	
			SC-PP-oil	CO-HF-PP	1.493	0.261	3.396	3	
			SC-PP-oil	CO-LF-PP	0.110	0.019	0.250	3	
			WASOTH	WASOTH	6.615	1.985	19.846		4
			WI	WI	0.021	0.006	0.062		4
AUS	Australia (and Christmas Is.)	Australia, New Zealand & Oceania	BIO	PSB – DR	61.080	14.507	112.235	2	
			BIO	PSB – IND	95.498	22.681	175.477	2	
			BIO	PSB – PP	21.840	5.187	40.130	2	
			CEM	CEM	795.960	281.119	4200.136	2	
			CREM	CREM	70.336	63.176	84.235		1
			NFMP	AL-P	41.125	25.909	58.809	2	
			NFMP	CU-P	63.294	22.772	299.137	2	
			NFMP	PB-P	16.256	8.867	25.662	2	
			NFMP	ZN-P	722.974	401.128	1414.967	2	
			NFMP-AU	GP-L	1833.480	641.718	3575.286	2	
			OR	CO-OR	27.208	12.924	42.852	2	
			PISP	PIP	5.317	1.964	19.648	2	
			SC-DR-coal	BC-DR	0.437	0.290	0.596	2	
			SC-DR-coal	HC-DR	0.298	0.198	0.406	2	
			SC-DR-gas	NG-DR	1.163	0.276	2.136	2	
			SC-DR-oil	CO-HF-DR	1.160	0.276	2.132	2	
			SC-DR-oil	CO-LF-DR	30.756	7.305	56.514	2	
			SC-IND-coal	BC-IND-CEM	22.634	15.052	30.896	2	
			SC-IND-coal	BC-IND-NFM	72.756	48.383	99.312	2	
			SC-IND-coal	BC-IND-OTH	9.100	6.052	12.422	2	
			SC-IND-coal	HC-IND-CEM	11.380	7.568	15.533	2	
			SC-IND-coal	HC-IND-NFM	10.206	6.787	13.931	2	
			SC-IND-coal	HC-IND-OTH	14.057	9.348	19.188	2	
			SC-IND-coal	HC-IND-PIP	1.205	0.801	1.645	2	
			SC-IND-gas	NG-IND	1.793	0.426	3.295	2	
			SC-IND-oil	CO-HF-IND	4.598	1.092	8.449	2	
			SC-IND-oil	CO-IND	0.143	0.034	0.262	2	
			SC-IND-oil	CO-LF-IND	5.596	1.329	10.282	2	

Country code	Country name	Region	Sector Code	Activity Code	Emission estimate, kg	Low range estimate, kg	High range estimate, kg	Technology group	Waste group
			SC-PP-coal	BC-L-PP	2002.475	1331.646	2733.379	2	
			SC-PP-coal	BC-S-PP	351.491	233.741	479.785	2	
			SC-PP-coal	HC-B-PP	524.329	348.679	715.710	2	
			SC-PP-gas	NG-PP	4.440	1.054	8.158	2	
			SC-PP-oil	CO-HF-PP	2.240	0.532	4.116	2	
			SC-PP-oil	CO-LF-PP	5.081	1.207	9.335	2	
			SC-PP-oil	CO-PP	0.265	0.063	0.487	2	
			SSC	SP-S	24.134	8.982	115.158	2	
			WASOTH	WASOTH	581.179	174.354	1743.538		1
			WI	WI	235.113	70.534	705.339		1
AUT	Austria	EU28	BIO	PSB – DR	93.143	22.121	171.150	1	
			BIO	PSB – IND	41.537	9.865	76.324	1	
			BIO	PSB – PP	71.637	17.014	131.633	1	
			CEM	CEM	252.305	89.081	1858.645	1	
			CEM	PC-CEM	0.966	0.573	5.197	1	
			CREM	CREM	16.191	12.722	19.372		1
			OR	CO-OR	16.043	7.620	25.267	1	
			PISP	PIP	194.851	68.306	1031.320	1	
			SC-DR-coal	BC-DR	0.293	0.167	0.665	1	
			SC-DR-coal	HC-DR	0.919	0.524	2.090	1	
			SC-DR-gas	NG-DR	0.429	0.102	0.789	1	
			SC-DR-oil	CO-HF-DR	0.600	0.143	1.103	1	
			SC-DR-oil	CO-LF-DR	13.594	3.229	24.979	1	
			SC-IND-coal	BC-IND-CEM	6.866	3.914	15.620	1	
			SC-IND-coal	HC-IND-CEM	2.188	1.247	4.978	1	
			SC-IND-coal	HC-IND-OTH	9.019	5.141	20.518	1	
			SC-IND-gas	NG-IND	0.582	0.138	1.070	1	
			SC-IND-oil	CO-HF-IND	2.337	0.555	4.294	1	
			SC-IND-oil	CO-LF-IND	0.680	0.162	1.250	1	
			SC-PP-coal	HC-B-PP	49.991	28.495	113.728	1	
			SC-PP-gas	NG-PP	0.504	0.120	0.927	1	
			SC-PP-oil	CO-HF-PP	2.880	0.684	5.292	1	
			SC-PP-oil	CO-LF-PP	0.006	0.001	0.011	1	
			SSC	SP-S	16.128	6.003	76.957	1	
			WASOTH	WASOTH	90.475	27.143	271.426		1
			WI	WI	34.581	10.374	103.742		1
AZE	Azerbaijan	CIS & other European countries	ASGM	GP-A	225.000	56.250	393.750		
			BIO	PSB – DR	3.775	0.849	7.267	4	
			BIO	PSB – IND	0.013	0.003	0.026	4	
			CEM	CEM	280.966	99.216	1425.150	4	
			CREM	CREM	0.558	0.409	0.744		4
			CSP	CSP-C	1450.000	507.500	2827.500	4	
			NFMP	AL-P	2.500	0.847	4.721	4	
			NFMP-AU	GP-L	110.336	38.617	215.154	4	
			OR	CO-OR	1.554	0.699	2.564	4	

Country code	Country name	Region	Sector Code	Activity Code	Emission estimate, kg	Low range estimate, kg	High range estimate, kg	Technology group	Waste group
			SC-DR-gas	NG-DR	0.592	0.133	1.139	4	
			SC-DR-oil	CO-HF-DR	0.060	0.014	0.116	4	
			SC-DR-oil	CO-LF-DR	2.164	0.487	4.166	4	
			SC-IND-gas	NG-IND	0.211	0.047	0.406	4	
			SC-IND-oil	CO-HF-IND	0.260	0.059	0.501	4	
			SC-IND-oil	CO-LF-IND	0.100	0.023	0.193	4	
			SC-PP-gas	NG-PP	1.198	0.270	2.307	4	
			SC-PP-oil	CO-HF-PP	7.780	1.751	14.977	4	
			SC-PP-oil	CO-LF-PP	0.010	0.002	0.019	4	
			SSC	SP-S	5.252	1.955	25.058	4	
			WASOTH	WASOTH	489.255	146.776	1467.764		4
			WI	WI	1.531	0.459	4.593		4
BHS	Bahamas	Central America and the Caribbean	BIO	PSB – DR	0.422	0.074	0.960	3	
			BIO	PSB – IND	1.541	0.270	3.505	3	
			BIO	PSB – PP	0.547	0.096	1.245	3	
			CREM	CREM	0.062	0.049	0.074		4
			OR	CO-OR	0.148	0.052	0.288	3	
			SC-DR-coal	HC-DR	5.560	2.335	15.661	3	
			SC-DR-gas	NG-DR	0.000	0.000	0.001	3	
			SC-DR-oil	CO-HF-DR	0.157	0.027	0.357	3	
			SC-DR-oil	CO-LF-DR	0.377	0.066	0.857	3	
			SC-IND-gas	NG-IND	0.000	0.000	0.000	3	
			SC-IND-oil	CO-HF-IND	0.451	0.079	1.026	3	
			SC-IND-oil	CO-LF-IND	0.026	0.004	0.058	3	
			SC-PP-gas	NG-PP	0.028	0.005	0.064	3	
			SC-PP-oil	CO-HF-PP	4.303	0.753	9.789	3	
			SC-PP-oil	CO-LF-PP	0.317	0.055	0.720	3	
			WASOTH	WASOTH	23.468	7.040	70.403		4
			WI	WI	0.073	0.022	0.220		4
BHR	Bahrain	Middle Eastern States	CEM	CEM	114.921	40.578	595.606	1	
			CREM	CREM	0.042	0.031	0.049		2
			NFMP	AL-P	12.008	4.070	22.677	1	
			OR	CO-OR	4.917	2.213	8.114	1	
			SC-DR-oil	CO-LF-DR	0.644	0.145	1.240	1	
			SC-IND-gas	NG-IND	0.207	0.047	0.399	1	
			SC-PP-gas	NG-PP	2.336	0.526	4.497	1	
			SC-PP-oil	CO-HF-PP	0.040	0.009	0.077	1	
			WASOTH	WASOTH	72.079	21.624	216.236		2
			WI	WI	2.100	0.630	6.300		2
BGD	Bangladesh	South Asia	BIO	PSB – DR	475.170	106.913	914.702	5	
			CEM	CEM	1853.000	654.500	9768.200	5	
			CREM	CREM	7.030	5.825	8.034		4
			OR	CO-OR	2.184	0.983	3.604	5	
			SC-DR-gas	NG-DR	0.936	0.211	1.802	5	
			SC-DR-oil	CO-LF-DR	5.518	1.242	10.622	5	

Country code	Country name	Region	Sector Code	Activity Code	Emission estimate, kg	Low range estimate, kg	High range estimate, kg	Technology group	Waste group
			SC-IND-coal	BC-IND-OTH	4.740	2.560	11.297	5	
			SC-IND-coal	HC-IND-CEM	596.700	322.218	1422.135	5	
			SC-IND-gas	NG-IND	0.813	0.183	1.565	5	
			SC-IND-oil	CO-HF-IND	0.260	0.059	0.501	5	
			SC-IND-oil	CO-LF-IND	0.398	0.090	0.766	5	
			SC-PP-coal	HC-B-PP	61.425	33.170	146.396	5	
			SC-PP-gas	NG-PP	2.784	0.626	5.359	5	
			SC-PP-oil	CO-HF-PP	18.460	4.154	35.536	5	
			SC-PP-oil	CO-LF-PP	0.940	0.212	1.810	5	
			SSC	SP-S	2.697	1.004	12.868	5	
			WASOTH	WASOTH	1927.565	578.270	5782.695		4
			WI	WI	6.032	1.810	18.095		4
BRB	Barbados	Central America and the Caribbean	BIO	PSB – DR	0.378	0.066	0.859	3	
			BIO	PSB – IND	0.909	0.159	2.067	3	
			BIO	PSB – PP	0.323	0.056	0.734	3	
			CEM	CEM	9.088	3.270	73.549	3	
			CREM	CREM	0.055	0.044	0.066		4
			OR	CO-OR	0.087	0.030	0.170	3	
			SC-DR-coal	HC-DR	3.279	1.377	9.236	3	
			SC-DR-gas	NG-DR	0.000	0.000	0.001	3	
			SC-DR-oil	CO-HF-DR	0.093	0.016	0.211	3	
			SC-DR-oil	CO-LF-DR	0.222	0.039	0.505	3	
			SC-IND-gas	NG-IND	0.000	0.000	0.000	3	
			SC-IND-oil	CO-HF-IND	0.266	0.047	0.605	3	
			SC-IND-oil	CO-LF-IND	0.015	0.003	0.034	3	
			SC-PP-gas	NG-PP	0.017	0.003	0.038	3	
			SC-PP-oil	CO-HF-PP	2.538	0.444	5.773	3	
			SC-PP-oil	CO-LF-PP	0.187	0.033	0.425	3	
			WASOTH	WASOTH	12.246	3.674	36.737		4
			WI	WI	0.038	0.011	0.115		4
BLR	Belarus	CIS & other European countries	BIO	PSB – DR	29.411	6.618	56.617	4	
			BIO	PSB – IND	2.603	0.586	5.011	4	
			BIO	PSB – PP	37.480	8.433	72.149	4	
			CEM	CEM	535.817	197.859	1258.924	4	
			CREM	CREM	4.917	3.606	6.556		2
			OR	CO-OR	26.013	11.706	42.921	4	
			SC-DR-coal	HC-DR	1.650	0.891	3.933	4	
			SC-DR-gas	NG-DR	0.477	0.107	0.919	4	
			SC-DR-oil	CO-HF-DR	0.200	0.045	0.385	4	
			SC-DR-oil	CO-LF-DR	5.168	1.163	9.948	4	
			SC-IND-coal	HC-IND-CEM	83.081	44.864	198.010	4	
			SC-IND-gas	NG-IND	0.216	0.049	0.417	4	
			SC-IND-oil	CO-HF-IND	0.440	0.099	0.847	4	
			SC-IND-oil	CO-LF-IND	0.236	0.053	0.454	4	
			SC-PP-coal	HC-B-PP	0.225	0.122	0.536	4	

Country code	Country name	Region	Sector Code	Activity Code	Emission estimate, kg	Low range estimate, kg	High range estimate, kg	Technology group	Waste group
			SC-PP-gas	NG-PP	2.655	0.597	5.110	4	
			SC-PP-oil	CO-HF-PP	9.800	2.205	18.865	4	
			SC-PP-oil	CO-LF-PP	0.034	0.008	0.065	4	
			SSC	SP-S	73.317	27.288	349.844	4	
			WASOTH	WASOTH	326.950	98.085	980.849		2
			WI	WI	9.526	2.858	28.578		2
BEL	Belgium	EU28	BIO	PSB – DR	27.929	6.633	51.319	1	
			BIO	PSB – IND	24.588	5.840	45.181	1	
			BIO	PSB – PP	32.501	7.719	59.720	1	
			CEM	CEM	343.650	121.351	2195.829	1	
			CEM	PC-CEM	0.503	0.299	2.707	1	
			CREM	CREM	26.505	20.826	31.712		1
			CSP	CSP-C	138.600	48.510	270.270	1	
			NFMP	ZN-P	68.016	24.097	186.846	1	
			OR	CO-OR	57.898	27.501	91.189	1	
			PISP	PIP	141.816	49.714	750.611	1	
			SC-DR-coal	HC-DR	15.750	8.978	35.831	1	
			SC-DR-gas	NG-DR	1.195	0.284	2.196	1	
			SC-DR-oil	CO-HF-DR	0.020	0.005	0.037	1	
			SC-DR-oil	CO-LF-DR	21.276	5.053	39.095	1	
			SC-IND-coal	HC-IND-CEM	17.731	10.107	40.337	1	
			SC-IND-coal	HC-IND-OTH	4.856	2.768	11.048	1	
			SC-IND-coal	HC-IND-PIP	5.342	3.045	12.153	1	
			SC-IND-gas	NG-IND	0.869	0.206	1.597	1	
			SC-IND-oil	CO-HF-IND	1.064	0.253	1.955	1	
			SC-IND-oil	CO-LF-IND	0.458	0.109	0.841	1	
			SC-PP-coal	HC-B-PP	40.106	22.861	91.242	1	
			SC-PP-gas	NG-PP	0.933	0.221	1.714	1	
			SC-PP-oil	CO-HF-PP	0.320	0.076	0.588	1	
			SC-PP-oil	CO-LF-PP	0.009	0.002	0.017	1	
			SSC	SP-S	55.526	20.666	264.952	1	
			WASOTH	WASOTH	109.042	32.713	327.126		1
			WI	WI	41.677	12.503	125.031		1
BLZ	Belize	Central America and the Caribbean	BIO	PSB – DR	0.451	0.079	1.027	3	
			BIO	PSB – IND	0.550	0.096	1.250	3	
			BIO	PSB – PP	0.195	0.034	0.444	3	
			CREM	CREM	0.067	0.053	0.080		4
			OR	CO-OR	0.053	0.018	0.103	3	
			SC-DR-coal	HC-DR	1.983	0.833	5.587	3	
			SC-DR-gas	NG-DR	0.000	0.000	0.000	3	
			SC-DR-oil	CO-HF-DR	0.056	0.010	0.127	3	
			SC-DR-oil	CO-LF-DR	0.134	0.024	0.306	3	
			SC-IND-gas	NG-IND	0.000	0.000	0.000	3	
			SC-IND-oil	CO-HF-IND	0.161	0.028	0.366	3	
			SC-IND-oil	CO-LF-IND	0.009	0.002	0.021	3	

Country code	Country name	Region	Sector Code	Activity Code	Emission estimate, kg	Low range estimate, kg	High range estimate, kg	Technology group	Waste group
			SC-PP-gas	NG-PP	0.010	0.002	0.023	3	
			SC-PP-oil	CO-HF-PP	1.535	0.269	3.492	3	
			SC-PP-oil	CO-LF-PP	0.113	0.020	0.257	3	
			WASOTH	WASOTH	8.108	2.432	24.325		4
			WI	WI	0.025	0.008	0.076		4
BEN	Benin	Sub-Saharan Africa	ASGM	GP-A	225.000	56.250	393.750		
			BIO	PSB – DR	75.259	16.933	144.873	5	
			BIO	PSB – IND	0.465	0.105	0.896	5	
			CEM	CEM	146.580	51.792	760.401	5	
			CREM	CREM	0.238	0.171	0.343		4
			SC-DR-oil	CO-LF-DR	1.338	0.301	2.576	5	
			SC-IND-coal	HC-IND-OTH	5.766	3.113	13.741	5	
			SC-IND-oil	CO-HF-IND	0.500	0.113	0.963	5	
			SC-IND-oil	CO-LF-IND	0.082	0.018	0.158	5	
			SC-PP-oil	CO-LF-PP	0.144	0.032	0.277	5	
			WASOTH	WASOTH	110.507	47.787	170.241		4
			WI	WI	0.021	0.009	0.033		4
BMU	Bermuda	Central America and the Caribbean	BIO	PSB – DR	0.091	0.016	0.208	3	
			BIO	PSB – IND	1.133	0.198	2.578	3	
			BIO	PSB – PP	0.402	0.070	0.916	3	
			CREM	CREM	0.013	0.011	0.016		4
			OR	CO-OR	0.109	0.038	0.212	3	
			SC-DR-coal	HC-DR	4.089	1.717	11.518	3	
			SC-DR-gas	NG-DR	0.000	0.000	0.001	3	
			SC-DR-oil	CO-HF-DR	0.115	0.020	0.263	3	
			SC-DR-oil	CO-LF-DR	0.277	0.048	0.630	3	
			SC-IND-gas	NG-IND	0.000	0.000	0.000	3	
			SC-IND-oil	CO-HF-IND	0.332	0.058	0.755	3	
			SC-IND-oil	CO-LF-IND	0.019	0.003	0.043	3	
			SC-PP-gas	NG-PP	0.021	0.004	0.047	3	
			SC-PP-oil	CO-HF-PP	3.165	0.554	7.199	3	
			SC-PP-oil	CO-LF-PP	0.233	0.041	0.530	3	
			WASOTH	WASOTH	13.667	4.100	41.002		4
			WI	WI	0.043	0.013	0.128		4
BTN	Bhutan	South Asia	BIO	PSB – DR	3.021	0.529	6.873	5	
			BIO	PSB – IND	0.561	0.098	1.275	5	
			CEM	CEM	75.210	26.565	396.474	5	
			CREM	CREM	0.430	0.356	0.491		4
			OR	CO-OR	1.273	0.446	2.483	5	
			SC-DR-gas	NG-DR	0.001	0.000	0.003	5	
			SC-DR-oil	CO-HF-DR	0.057	0.010	0.130	5	
			SC-DR-oil	CO-LF-DR	0.147	0.026	0.334	5	
			SC-IND-coal	BC-IND-OTH	0.131	0.055	0.368	5	
			SC-IND-coal	HC-IND-OTH	8.719	3.662	24.559	5	
			SC-IND-oil	CO-HF-IND	0.126	0.022	0.286	5	

Country code	Country name	Region	Sector Code	Activity Code	Emission estimate, kg	Low range estimate, kg	High range estimate, kg	Technology group	Waste group
			SC-IND-oil	CO-LF-IND	0.014	0.002	0.031	5	
			SC-PP-coal	HC-B-PP	1.836	0.771	5.171	5	
			SC-PP-gas	NG-PP	0.001	0.000	0.003	5	
			SC-PP-oil	CO-HF-PP	0.648	0.113	1.473	5	
			SC-PP-oil	CO-LF-PP	0.085	0.015	0.193	5	
			WASOTH	WASOTH	23.250	6.975	69.750		4
			WI	WI	0.073	0.022	0.218		4
BOL	Bolivia	South America	ASGM	GP-A	40500.000	28350.000	52650.000		
			BIO	PSB – DR	23.309	5.244	44.869	3	
			BIO	PSB – IND	21.852	4.917	42.066	3	
			BIO	PSB – PP	5.303	1.193	10.208	3	
			CEM	CEM	257.600	91.140	1366.820	3	
			CREM	CREM	4.239	2.967	5.934		4
			NFMP-AU	GP-L	481.932	168.676	939.767	3	
			OR	CO-OR	2.843	1.279	4.691	3	
			SC-DR-gas	NG-DR	0.150	0.034	0.290	3	
			SC-DR-oil	CO-LF-DR	2.850	0.641	5.486	3	
			SC-IND-gas	NG-IND	0.159	0.036	0.306	3	
			SC-IND-oil	CO-LF-IND	0.167	0.038	0.322	3	
			SC-PP-gas	NG-PP	0.371	0.083	0.714	3	
			SC-PP-oil	CO-LF-PP	0.086	0.019	0.165	3	
			WASOTH	WASOTH	168.370	50.511	505.109		4
			WI	WI	0.566	0.170	1.699		4
BIH	Bosnia-Herzegovina	CIS & other European countries	BIO	PSB – DR	70.508	15.864	135.727	4	
			BIO	PSB – IND	1.867	0.420	3.594	4	
			BIO	PSB – PP	0.160	0.036	0.308	4	
			CEM	CEM	82.320	29.069	417.554	4	
			CEM	PC-CEM	0.105	0.059	0.592	4	
			CREM	CREM	1.984	1.455	2.645		2
			NFMP	AL-P	31.000	10.850	60.450	4	
			OR	CO-OR	1.047	0.471	1.728	4	
			PISP	PIP	52.013	18.233	275.296	4	
			SC-DR-coal	BC-DR	96.150	51.921	229.158	4	
			SC-DR-gas	NG-DR	0.014	0.003	0.027	4	
			SC-DR-oil	CO-HF-DR	0.060	0.014	0.116	4	
			SC-DR-oil	CO-LF-DR	1.746	0.393	3.361	4	
			SC-IND-coal	BC-IND-CEM	8.925	4.820	21.271	4	
			SC-IND-coal	BC-IND-NFM	23.839	12.873	56.816	4	
			SC-IND-coal	BC-IND-OTH	5.265	2.843	12.548	4	
			SC-IND-gas	NG-IND	0.017	0.004	0.033	4	
			SC-IND-oil	CO-HF-IND	0.400	0.090	0.770	4	
			SC-IND-oil	CO-LF-IND	0.130	0.029	0.250	4	
			SC-PP-coal	BC-L-PP	504.798	295.307	1665.833	4	
			SC-PP-coal	BC-S-PP	777.465	419.831	1852.958	4	
			SC-PP-gas	NG-PP	0.010	0.002	0.020	4	

Country code	Country name	Region	Sector Code	Activity Code	Emission estimate, kg	Low range estimate, kg	High range estimate, kg	Technology group	Waste group
			SC-PP-oil	CO-HF-PP	2.280	0.513	4.389	4	
			SC-PP-oil	CO-LF-PP	0.096	0.022	0.185	4	
			WASOTH	WASOTH	77.613	23.284	232.838		2
			WI	WI	2.261	0.678	6.784		2
BWA	Botswana	Sub-Saharan Africa	ASGM	GP-A	380.000	95.000	665.000		
			BIO	PSB – DR	28.945	6.513	55.719	4	
			CEM	CEM	33.994	12.011	176.347	4	
			CREM	CREM	0.049	0.035	0.071		4
			NFMP	CU-P	1202.211	429.093	6863.799	4	
			NFMP-AU	GP-L	37.422	13.098	72.973	4	
			SC-DR-coal	HC-DR	1.050	0.567	2.503	4	
			SC-DR-oil	CO-LF-DR	0.734	0.165	1.413	4	
			SC-IND-coal	HC-IND-OTH	9.844	5.316	23.461	4	
			SC-IND-oil	CO-HF-IND	0.220	0.050	0.424	4	
			SC-IND-oil	CO-LF-IND	0.316	0.071	0.608	4	
			SC-PP-coal	HC-B-PP	186.413	100.663	444.283	4	
			SC-PP-oil	CO-LF-PP	0.072	0.016	0.139	4	
			WASOTH	WASOTH	178.387	77.140	274.812		4
			WI	WI	0.034	0.015	0.053		4
BRA	Brazil	South America	ASGM	GP-A	49875.000	24937.500	74812.500		
			BIO	PSB – DR	483.654	108.822	931.033	3	
			BIO	PSB – IND	1319.782	296.951	2540.581	3	
			BIO	PSB – PP	1050.293	236.316	2021.813	3	
			CEM	CEM	1549.775	1047.434	4654.668	3	
			CEM	PC-CEM	130.980	73.676	738.400	3	
			CREM	CREM	9.941	6.959	13.917		3
			CSP	CSP-P	1106.500	387.275	2157.675	3	
			NFMP	AL-P	119.691	41.892	233.397	3	
			NFMP	CU-P	1274.286	454.818	7275.298	3	
			NFMP	ZN-P	2866.030	1018.848	6183.469	3	
			NFMP-AU	GP-L	2894.364	1013.027	5644.010	3	
			OR	CO-OR	95.140	33.299	185.523	3	
			PISP	PIP	1275.421	471.197	4713.153	3	
			SC-DR-gas	NG-DR	0.615	0.138	1.185	3	
			SC-DR-oil	CO-HF-DR	16.180	3.641	31.147	3	
			SC-DR-oil	CO-LF-DR	83.666	18.825	161.057	3	
			SC-IND-coal	BC-IND-CEM	17.550	9.477	41.828	3	
			SC-IND-coal	BC-IND-OTH	189.083	102.105	450.647	3	
			SC-IND-coal	HC-IND-CEM	12.825	6.926	30.566	3	
			SC-IND-coal	HC-IND-NFM	136.013	73.447	324.163	3	
			SC-IND-coal	HC-IND-OTH	44.775	24.179	106.714	3	
			SC-IND-coal	HC-IND-PIP	419.288	226.415	999.302	3	
			SC-IND-gas	NG-IND	2.190	0.493	4.216	3	
			SC-IND-oil	CO-HF-IND	43.776	9.850	84.269	3	
			SC-IND-oil	CO-LF-IND	2.105	0.474	4.053	3	

Country code	Country name	Region	Sector Code	Activity Code	Emission estimate, kg	Low range estimate, kg	High range estimate, kg	Technology group	Waste group
			SC-PP-coal	BC-L-PP	264.600	154.791	873.180	3	
			SC-PP-coal	BC-S-PP	415.935	224.605	991.312	3	
			SC-PP-coal	HC-B-PP	464.738	250.958	1107.624	3	
			SC-PP-gas	NG-PP	4.790	1.078	9.220	3	
			SC-PP-oil	CO-HF-PP	55.740	12.542	107.300	3	
			SC-PP-oil	CO-LF-PP	5.600	1.260	10.779	3	
			SSC	SP-S	198.757	73.976	948.400	3	
			WASOTH	WASOTH	5006.449	1501.935	15019.346		3
			WI	WI	32.568	9.770	97.703		3
VGB	British Virgin Islands	Central America and the Caribbean	BIO	PSB – DR	0.043	0.008	0.099	3	
			BIO	PSB – IND	0.267	0.047	0.606	3	
			BIO	PSB – PP	0.095	0.017	0.215	3	
			CREM	CREM	0.006	0.005	0.008		4
			OR	CO-OR	0.026	0.009	0.050	3	
			SC-DR-coal	HC-DR	0.962	0.404	2.709	3	
			SC-DR-gas	NG-DR	0.000	0.000	0.000	3	
			SC-DR-oil	CO-HF-DR	0.027	0.005	0.062	3	
			SC-DR-oil	CO-LF-DR	0.065	0.011	0.148	3	
			SC-IND-gas	NG-IND	0.000	0.000	0.000	3	
			SC-IND-oil	CO-HF-IND	0.078	0.014	0.178	3	
			SC-IND-oil	CO-LF-IND	0.004	0.001	0.010	3	
			SC-PP-gas	NG-PP	0.005	0.001	0.011	3	
			SC-PP-oil	CO-HF-PP	0.744	0.130	1.694	3	
			SC-PP-oil	CO-LF-PP	0.055	0.010	0.125	3	
			WASOTH	WASOTH	1.315	0.394	3.944		4
			WI	WI	0.004	0.001	0.012		4
BRN	Brunei Darussalam	East and Southeast Asia	CEM	CEM	30.520	10.780	160.888	3	
			CREM	CREM	0.063	0.057	0.070		2
			OR	CO-OR	0.226	0.102	0.373	3	
			SC-DR-gas	NG-DR	0.004	0.001	0.007	3	
			SC-DR-oil	CO-LF-DR	0.328	0.074	0.631	3	
			SC-IND-oil	CO-LF-IND	0.226	0.051	0.435	3	
			SC-PP-gas	NG-PP	0.398	0.090	0.767	3	
			SC-PP-oil	CO-LF-PP	0.017	0.004	0.032	3	
			WASOTH	WASOTH	68.715	20.614	206.145		2
			WI	WI	2.002	0.601	6.006		2
BGR	Bulgaria	EU28	BIO	PSB – DR	38.701	8.708	74.500	4	
			BIO	PSB – IND	12.885	2.899	24.803	4	
			BIO	PSB – PP	2.004	0.451	3.857	4	
			CEM	CEM	178.063	62.888	1084.805	4	
			CEM	PC-CEM	3.920	2.205	22.099	4	
			CREM	CREM	1.224	0.897	1.631		2
			NFMP	CU-P	3482.664	1243.032	19883.620	4	
			NFMP	PB-T	789.480	286.524	2029.482	4	

Country code	Country name	Region	Sector Code	Activity Code	Emission estimate, kg	Low range estimate, kg	High range estimate, kg	Technology group	Waste group
			NFMP	ZN-P	1178.770	417.616	3238.192	4	
			NFMP-AU	GP-L	361.350	126.473	704.633	4	
			OR	CO-OR	10.905	4.907	17.994	4	
			SC-DR-coal	BC-DR	13.950	7.533	33.248	4	
			SC-DR-coal	HC-DR	23.250	12.555	55.413	4	
			SC-DR-gas	NG-DR	0.092	0.021	0.177	4	
			SC-DR-oil	CO-HF-DR	0.400	0.090	0.770	4	
			SC-DR-oil	CO-LF-DR	3.874	0.872	7.457	4	
			SC-IND-coal	BC-IND-CEM	1.575	0.851	3.754	4	
			SC-IND-coal	BC-IND-OTH	0.439	0.237	1.046	4	
			SC-IND-coal	HC-IND-CEM	13.519	7.300	32.220	4	
			SC-IND-coal	HC-IND-OTH	19.688	10.631	46.922	4	
			SC-IND-gas	NG-IND	0.214	0.048	0.411	4	
			SC-IND-oil	CO-HF-IND	0.580	0.131	1.117	4	
			SC-IND-oil	CO-LF-IND	0.090	0.020	0.173	4	
			SC-PP-coal	BC-L-PP	3274.180	1915.395	10804.794	4	
			SC-PP-coal	HC-A-PP	5.625	3.038	23.719	4	
			SC-PP-coal	HC-B-PP	66.938	36.146	159.534	4	
			SC-PP-gas	NG-PP	0.203	0.046	0.391	4	
			SC-PP-oil	CO-HF-PP	0.780	0.176	1.502	4	
			SC-PP-oil	CO-LF-PP	0.004	0.001	0.008	4	
			SSC	SP-S	17.855	6.646	85.199	4	
			WASOTH	WASOTH	109.095	32.729	327.286		2
			WI	WI	3.179	0.954	9.536		2
BFA	Burkina Faso	Sub-Saharan Africa	ASGM	GP-A	26325.000	13162.500	39487.500		
			BIO	PSB – DR	216.179	37.831	491.806	5	
			BIO	PSB – IND	5.506	0.964	12.526	5	
			BIO	PSB – PP	1.995	0.349	4.538	5	
			CEM	CEM	42.315	14.951	219.514	5	
			CREM	CREM	0.432	0.312	0.623		4
			NFMP-AU	GP-L	1991.550	697.043	3883.523	5	
			SC-DR-coal	HC-DR	1.088	0.457	3.064	5	
			SC-DR-oil	CO-LF-DR	0.487	0.085	1.107	5	
			SC-IND-coal	HC-IND-OTH	1.056	0.444	2.975	5	
			SC-IND-gas	NG-IND	0.000	0.000	0.000	5	
			SC-IND-oil	CO-HF-IND	0.886	0.155	2.015	5	
			SC-IND-oil	CO-IND	0.122	0.021	0.277	5	
			SC-IND-oil	CO-LF-IND	0.085	0.015	0.193	5	
			SC-PP-coal	HC-B-PP	7.149	3.003	20.136	5	
			SC-PP-gas	NG-PP	0.008	0.001	0.019	5	
			SC-PP-oil	CO-HF-PP	1.152	0.202	2.620	5	
			SC-PP-oil	CO-LF-PP	0.238	0.042	0.542	5	
			WASOTH	WASOTH	147.686	63.864	227.516		4
			WI	WI	0.028	0.012	0.044		4

Country code	Country name	Region	Sector Code	Activity Code	Emission estimate, kg	Low range estimate, kg	High range estimate, kg	Technology group	Waste group
BDI	Burundi	Sub-Saharan Africa	ASGM	GP-A	225.000	56.250	393.750		
			BIO	PSB – DR	122.665	21.466	279.062	5	
			BIO	PSB – IND	1.470	0.257	3.345	5	
			BIO	PSB – PP	0.533	0.093	1.212	5	
			CEM	CEM	7.350	2.597	38.129	5	
			CREM	CREM	0.246	0.177	0.354		4
			NFMP-AU	GP-L	27.500	9.625	53.625	5	
			SC-DR-coal	HC-DR	0.290	0.122	0.818	5	
			SC-DR-oil	CO-LF-DR	0.130	0.023	0.296	5	
			SC-IND-coal	HC-IND-OTH	0.282	0.118	0.794	5	
			SC-IND-gas	NG-IND	0.000	0.000	0.000	5	
			SC-IND-oil	CO-HF-IND	0.237	0.041	0.538	5	
			SC-IND-oil	CO-IND	0.033	0.006	0.074	5	
			SC-IND-oil	CO-LF-IND	0.023	0.004	0.052	5	
			SC-PP-coal	HC-B-PP	1.909	0.802	5.377	5	
			SC-PP-gas	NG-PP	0.002	0.000	0.005	5	
			SC-PP-oil	CO-HF-PP	0.308	0.054	0.700	5	
			SC-PP-oil	CO-LF-PP	0.064	0.011	0.145	5	
			WASOTH	WASOTH	40.144	17.360	61.844		4
			WI	WI	0.008	0.003	0.012		4
KHM	Cambodia	East and Southeast Asia	ASGM	GP-A	3562.500	1781.250	5343.750		
			BIO	PSB – DR	110.154	24.785	212.046	4	
			BIO	PSB – IND	45.202	10.170	87.014	4	
			BIO	PSB – PP	0.681	0.153	1.311	4	
			CEM	CEM	133.525	47.163	703.885	4	
			CREM	CREM	10.180	9.264	11.297		4
			SC-DR-oil	CO-LF-DR	2.058	0.463	3.962	4	
			SC-IND-coal	BC-IND-CEM	3.544	1.914	8.446	4	
			SC-IND-oil	CO-HF-IND	0.520	0.117	1.001	4	
			SC-IND-oil	CO-LF-IND	0.058	0.013	0.112	4	
			SC-PP-coal	BC-S-PP	163.080	88.063	388.674	4	
			SC-PP-oil	CO-HF-PP	0.900	0.203	1.733	4	
			SC-PP-oil	CO-LF-PP	0.030	0.007	0.058	4	
			WASOTH	WASOTH	171.061	51.318	513.183		4
			WI	WI	0.535	0.161	1.606		4
CMR	Cameroon	Sub-Saharan Africa	ASGM	GP-A	1125.000	281.250	1968.750		
			BIO	PSB – DR	247.050	55.586	475.571	5	
			BIO	PSB – PP	0.896	0.202	1.725	5	
			CEM	CEM	136.500	48.230	708.110	5	
			CREM	CREM	0.540	0.389	0.778		4
			NFMP	AL-P	11.700	7.245	19.305	5	
			NFMP-AU	GP-L	82.500	28.875	160.875	5	
			OR	CO-OR	1.511	0.680	2.494	5	
			SC-DR-oil	CO-LF-DR	1.260	0.284	2.426	5	
			SC-IND-oil	CO-HF-IND	2.260	0.509	4.351	5	

Country code	Country name	Region	Sector Code	Activity Code	Emission estimate, kg	Low range estimate, kg	High range estimate, kg	Technology group	Waste group
			SC-IND-oil	CO-LF-IND	0.016	0.004	0.031	5	
			SC-PP-gas	NG-PP	0.055	0.012	0.106	5	
			SC-PP-oil	CO-HF-PP	1.880	0.423	3.619	5	
			SC-PP-oil	CO-LF-PP	0.420	0.095	0.809	5	
			WASOTH	WASOTH	359.147	155.307	553.281		4
			WI	WI	0.069	0.030	0.106		4
CAN	Canada	North America	BIO	PSB – DR	153.173	36.378	281.454	1	
			BIO	PSB – IND	218.397	51.869	401.304	1	
			BIO	PSB – PP	113.547	26.968	208.643	1	
			CEM	CEM	120.215	43.905	2456.316	1	
			CEM	PC-CEM	7.955	4.723	42.809	1	
			CREM	CREM	88.810	74.383	101.932		1
			NFMP	AL-P	36.000	12.203	67.986	1	
			NFMP	CU-P	4.760	2.548	9.355	1	
			NFMP	PB-P	1.690	0.923	2.662	1	
			NFMP	ZN-P	37.708	21.375	337.993	1	
			NFMP-AU	GP-L	352.846	123.496	688.049	1	
			OR	CO-OR	71.225	33.832	112.180	1	
			PISP	PIP	200.185	70.186	1139.673	1	
			SC-DR-coal	BC-DR	2.779	1.584	6.322	1	
			SC-DR-gas	NG-DR	7.016	1.666	12.892	1	
			SC-DR-oil	CO-HF-DR	20.020	4.755	36.787	1	
			SC-DR-oil	CO-LF-DR	46.674	11.085	85.763	1	
			SC-IND-coal	BC-IND-CEM	27.258	15.537	62.012	1	
			SC-IND-coal	BC-IND-OTH	24.006	13.683	54.613	1	
			SC-IND-coal	HC-IND-CEM	27.258	15.537	62.012	1	
			SC-IND-coal	HC-IND-NFM	20.674	11.784	47.033	1	
			SC-IND-coal	HC-IND-OTH	19.356	11.033	44.034	1	
			SC-IND-gas	NG-IND	3.308	0.786	6.079	1	
			SC-IND-oil	CO-HF-IND	11.666	2.771	21.436	1	
			SC-IND-oil	CO-LF-IND	5.341	1.268	9.814	1	
			SC-PP-coal	BC-L-PP	516.488	343.464	705.006	1	
			SC-PP-coal	BC-S-PP	1246.593	828.984	1701.600	1	
			SC-PP-coal	HC-B-PP	73.359	48.784	100.135	1	
			SC-PP-gas	NG-PP	10.680	2.537	19.625	1	
			SC-PP-oil	CO-HF-PP	8.000	1.900	14.700	1	
			SC-PP-oil	CO-LF-PP	2.922	0.694	5.369	1	
			SSC	SP-S	116.864	43.496	557.635	1	
			WASOTH	WASOTH	306.852	92.056	920.557		1
			WI	WI	117.282	35.185	351.846		1
CPV	Cape Verde	Sub-Saharan Africa	BIO	PSB – DR	6.235	1.091	14.184	5	
			BIO	PSB – IND	0.607	0.106	1.381	5	
			BIO	PSB – PP	0.220	0.038	0.500	5	
			CREM	CREM	0.012	0.009	0.018		4
			SC-DR-coal	HC-DR	0.120	0.050	0.338	5	

Country code	Country name	Region	Sector Code	Activity Code	Emission estimate, kg	Low range estimate, kg	High range estimate, kg	Technology group	Waste group
			SC-DR-oil	CO-LF-DR	0.054	0.009	0.122	5	
			SC-IND-coal	HC-IND-OTH	0.116	0.049	0.328	5	
			SC-IND-gas	NG-IND	0.000	0.000	0.000	5	
			SC-IND-oil	CO-HF-IND	0.098	0.017	0.222	5	
			SC-IND-oil	CO-IND	0.013	0.002	0.031	5	
			SC-IND-oil	CO-LF-IND	0.009	0.002	0.021	5	
			SC-PP-coal	HC-B-PP	0.788	0.331	2.220	5	
			SC-PP-gas	NG-PP	0.001	0.000	0.002	5	
			SC-PP-oil	CO-HF-PP	0.127	0.022	0.289	5	
			SC-PP-oil	CO-LF-PP	0.026	0.005	0.060	5	
			WASOTH	WASOTH	16.585	7.172	25.550		4
			WI	WI	0.003	0.001	0.005		4
CYM	Cayman Islands	Central America and the Caribbean	BIO	PSB – DR	0.073	0.013	0.166	3	
			BIO	PSB – IND	0.463	0.081	1.053	3	
			BIO	PSB – PP	0.164	0.029	0.374	3	
			CREM	CREM	0.011	0.009	0.013		4
			OR	CO-OR	0.044	0.016	0.086	3	
			SC-DR-coal	HC-DR	1.670	0.701	4.704	3	
			SC-DR-gas	NG-DR	0.000	0.000	0.000	3	
			SC-DR-oil	CO-HF-DR	0.047	0.008	0.107	3	
			SC-DR-oil	CO-LF-DR	0.113	0.020	0.257	3	
			SC-IND-gas	NG-IND	0.000	0.000	0.000	3	
			SC-IND-oil	CO-HF-IND	0.135	0.024	0.308	3	
			SC-IND-oil	CO-LF-IND	0.008	0.001	0.018	3	
			SC-PP-gas	NG-PP	0.008	0.001	0.019	3	
			SC-PP-oil	CO-HF-PP	1.292	0.226	2.940	3	
			SC-PP-oil	CO-LF-PP	0.095	0.017	0.216	3	
			WASOTH	WASOTH	6.592	1.978	19.775		4
			WI	WI	0.021	0.006	0.062		4
CAF	Central African Republic	Sub-Saharan Africa	ASGM	GP-A	6000.000	1500.000	10500.000		
			BIO	PSB – DR	61.565	10.774	140.061	5	
			BIO	PSB – IND	0.553	0.097	1.259	5	
			BIO	PSB – PP	0.200	0.035	0.456	5	
			CREM	CREM	0.122	0.088	0.176		4
			SC-DR-coal	HC-DR	0.109	0.046	0.308	5	
			SC-DR-oil	CO-LF-DR	0.049	0.009	0.111	5	
			SC-IND-coal	HC-IND-OTH	0.106	0.045	0.299	5	
			SC-IND-gas	NG-IND	0.000	0.000	0.000	5	
			SC-IND-oil	CO-HF-IND	0.089	0.016	0.203	5	
			SC-IND-oil	CO-IND	0.012	0.002	0.028	5	
			SC-IND-oil	CO-LF-IND	0.009	0.001	0.019	5	
			SC-PP-coal	HC-B-PP	0.719	0.302	2.024	5	
			SC-PP-gas	NG-PP	0.001	0.000	0.002	5	
			SC-PP-oil	CO-HF-PP	0.116	0.020	0.263	5	
			SC-PP-oil	CO-LF-PP	0.024	0.004	0.054	5	
			WASOTH	WASOTH	14.974	6.475	23.068		4
			WI	WI	0.003	0.001	0.004		4

Country code	Country name	Region	Sector Code	Activity Code	Emission estimate, kg	Low range estimate, kg	High range estimate, kg	Technology group	Waste group
TCD	Chad	Sub-Saharan Africa	ASGM	GP-A	225.000	56.250	393.750		
			BIO	PSB – DR	132.818	23.243	302.161	5	
			BIO	PSB – IND	5.174	0.905	11.770	5	
			BIO	PSB – PP	1.874	0.328	4.264	5	
			CEM	CEM	21.000	7.420	108.940	5	
			CREM	CREM	0.263	0.189	0.378		4
			SC-DR-coal	HC-DR	1.022	0.429	2.879	5	
			SC-DR-oil	CO-LF-DR	0.457	0.080	1.040	5	
			SC-IND-coal	HC-IND-OTH	0.993	0.417	2.796	5	
			SC-IND-gas	NG-IND	0.000	0.000	0.000	5	
			SC-IND-oil	CO-HF-IND	0.832	0.146	1.894	5	
			SC-IND-oil	CO-IND	0.114	0.020	0.260	5	
			SC-IND-oil	CO-LF-IND	0.080	0.014	0.181	5	
			SC-PP-coal	HC-B-PP	6.718	2.821	18.921	5	
			SC-PP-gas	NG-PP	0.008	0.001	0.018	5	
			SC-PP-oil	CO-HF-PP	1.082	0.189	2.462	5	
			SC-PP-oil	CO-LF-PP	0.224	0.039	0.509	5	
			WASOTH	WASOTH	150.838	65.227	232.371		4
			WI	WI	0.029	0.012	0.045		4
CHL	Chile	South America	ASGM	GP-A	1900.000	475.000	3325.000		
			BIO	PSB – DR	86.745	20.602	159.394	3	
			BIO	PSB – IND	86.429	20.527	158.813	3	
			BIO	PSB – PP	171.865	40.818	315.802	3	
			CEM	CEM	368.000	130.200	1952.600	3	
			CEM	PC-CEM	9.216	5.472	49.594	3	
			CREM	CREM	6.820	4.774	9.548		4
			NFMP	CU-P	12221.710	4362.171	69777.569	3	
			NFMP-AU	GP-L	1683.040	589.064	3281.927	3	
			OR	CO-OR	8.214	3.901	12.936	3	
			PISP	PIP	268.275	102.839	506.529	3	
			SC-DR-coal	HC-DR	0.750	0.428	1.706	3	
			SC-DR-gas	NG-DR	0.141	0.033	0.259	3	
			SC-DR-oil	CO-HF-DR	5.500	1.306	10.106	3	
			SC-DR-oil	CO-LF-DR	9.072	2.155	16.670	3	
			SC-IND-coal	HC-IND-CEM	0.120	0.068	0.273	3	
			SC-IND-coal	HC-IND-OTH	44.213	25.201	100.583	3	
			SC-IND-gas	NG-IND	0.179	0.043	0.329	3	
			SC-IND-oil	CO-HF-IND	9.234	2.193	16.967	3	
			SC-IND-oil	CO-LF-IND	5.267	1.251	9.678	3	
			SC-PP-coal	HC-B-PP	1131.874	645.168	2575.013	3	
			SC-PP-gas	NG-PP	0.501	0.119	0.921	3	
			SC-PP-oil	CO-HF-PP	2.295	0.545	4.217	3	
			SC-PP-oil	CO-LF-PP	0.753	0.179	1.384	3	
			SSC	SP-S	9.639	3.588	45.993	3	
			WASOTH	WASOTH	945.512	283.654	2836.537		4
			WI	WI	3.181	0.954	9.543		4

Country code	Country name	Region	Sector Code	Activity Code	Emission estimate, kg	Low range estimate, kg	High range estimate, kg	Technology group	Waste group
CHN	China (and Hong Kong if not separately estimated)	East and Southeast Asia	ASGM	GP-A	33750.000	8437.500	59062.500		
			BIO	PSB – DR	4221.320	949.797	8126.041	3	
			BIO	PSB – PP	894.667	201.300	1722.233	3	
			CEM	CEM	106159.200	43958.880	929117.280	3	
			CREM	CREM	547.921	498.574	608.017		2
			CSP	CSP-C	405.000	141.750	789.750	3	
			NFMP	AL-P	3121.160	1209.450	7825.194	3	
			NFMP	CU-P	1755.504	858.670	18505.299	3	
			NFMP	PB-P	28164.839	11704.621	60459.038	3	
			NFMP	ZN-T	96299.627	33704.869	187784.273	3	
			NFMP-AU	GP-L	202.410	70.843	394.700	3	
			NFMP-HG	HG-P	8100.000	2835.000	15795.000	3	
			OR	CO-OR	2694.977	1212.740	4446.712	3	
			PISP	PIP	8565.677	3007.349	387020.955	3	
			SC-DR-coal	HC-DR	37803.160	23815.991	54058.519	3	
			SC-DR-gas	NG-DR	13.247	2.980	25.500	3	
			SC-DR-oil	CO-HF-DR	119.560	26.901	230.153	3	
			SC-DR-oil	CO-LF-DR	304.310	68.470	585.797	3	
			SC-IND-coal	HC-IND-CEM	26599.808	16757.879	38037.725	3	
			SC-IND-coal	HC-IND-NFM	2201.587	1387.000	3148.269	3	
			SC-IND-coal	HC-IND-OTH	24718.064	15572.380	35346.832	3	
			SC-IND-coal	HC-IND-PIP	9613.705	6056.634	13747.599	3	
			SC-IND-gas	NG-IND	8.959	2.016	17.246	3	
			SC-IND-oil	CO-HF-IND	72.352	16.279	139.278	3	
			SC-IND-oil	CO-IND	19.627	4.416	37.782	3	
			SC-IND-oil	CO-LF-IND	32.754	7.370	63.052	3	
			SC-PP-coal	HC-B-PP	81280.508	51206.720	116231.126	3	
			SC-PP-gas	NG-PP	12.343	2.777	23.761	3	
			SC-PP-oil	CO-HF-PP	49.770	11.198	95.807	3	
			SC-PP-oil	CO-LF-PP	4.451	1.001	8.567	3	
			SC-PP-oil	CO-PP	34.470	7.756	66.355	3	
			SSC	SP-S	1022.730	357.956	1994.324	3	
			VCM	VCM-P	12170.000	4259.500	23731.500	3	
			VCM	VCM-R	45637.500	15973.125	88993.125	3	
			WASOTH	WASOTH	18708.389	5612.517	56125.167		2
			WI	WI	8471.520	2541.456	25414.559		2
CCK	Cocos Islands	Australia, New Zealand & Oceania	CREM	CREM	0.000	0.000	0.000		4
			WASOTH	WASOTH	0.000	0.000	0.000		4
			WI	WI	0.000	0.000	0.000		4
COL	Colombia	South America	ASGM	GP-A	51041.667	25520.833	76562.500		
			BIO	PSB – DR	105.563	23.752	203.208	3	
			BIO	PSB – IND	32.804	7.381	63.147	3	
			BIO	PSB – PP	26.656	5.998	51.313	3	
			CEM	CEM	911.462	322.479	4836.200	3	
			CREM	CREM	13.684	9.579	19.158		3
			CSP	CSP-C	110.000	38.500	214.500	3	
			NFMP-AU	GP-L	2344.399	820.540	4571.578	3	

Country code	Country name	Region	Sector Code	Activity Code	Emission estimate, kg	Low range estimate, kg	High range estimate, kg	Technology group	Waste group
			OR	CO-OR	11.932	5.370	19.688	3	
			PISP	PIP	12.899	4.522	68.274	3	
			SC-DR-coal	HC-DR	17.100	9.234	40.755	3	
			SC-DR-gas	NG-DR	0.432	0.097	0.831	3	
			SC-DR-oil	CO-HF-DR	0.360	0.081	0.693	3	
			SC-DR-oil	CO-LF-DR	11.934	2.685	22.973	3	
			SC-IND-coal	HC-IND-CEM	67.560	36.482	161.018	3	
			SC-IND-coal	HC-IND-OTH	68.400	36.936	163.020	3	
			SC-IND-coal	HC-IND-PIP	29.138	15.734	69.444	3	
			SC-IND-gas	NG-IND	0.567	0.128	1.092	3	
			SC-IND-oil	CO-HF-IND	1.197	0.269	2.304	3	
			SC-IND-oil	CO-LF-IND	0.429	0.097	0.827	3	
			SC-PP-coal	HC-B-PP	303.143	163.697	722.490	3	
			SC-PP-gas	NG-PP	0.903	0.203	1.738	3	
			SC-PP-oil	CO-HF-PP	0.660	0.149	1.271	3	
			SC-PP-oil	CO-LF-PP	0.101	0.023	0.193	3	
			SC-PP-oil	CO-PP	1.710	0.385	3.292	3	
			SSC	SP-S	22.962	8.546	109.565	3	
			WASOTH	WASOTH	1037.984	311.395	3113.951		3
			WI	WI	6.752	2.026	20.257		3
COM	Comoros	Sub-Saharan Africa	BIO	PSB – DR	8.918	1.561	20.288	5	
			BIO	PSB – IND	0.200	0.035	0.456	5	
			BIO	PSB – PP	0.073	0.013	0.165	5	
			CREM	CREM	0.001	0.001	0.001		4
			SC-DR-coal	HC-DR	0.040	0.017	0.112	5	
			SC-DR-oil	CO-LF-DR	0.018	0.003	0.040	5	
			SC-IND-coal	HC-IND-OTH	0.038	0.016	0.108	5	
			SC-IND-gas	NG-IND	0.000	0.000	0.000	5	
			SC-IND-oil	CO-HF-IND	0.032	0.006	0.073	5	
			SC-IND-oil	CO-IND	0.004	0.001	0.010	5	
			SC-IND-oil	CO-LF-IND	0.003	0.001	0.007	5	
			SC-PP-coal	HC-B-PP	0.260	0.109	0.733	5	
			SC-PP-gas	NG-PP	0.000	0.000	0.001	5	
			SC-PP-oil	CO-HF-PP	0.042	0.007	0.095	5	
			SC-PP-oil	CO-LF-PP	0.009	0.002	0.020	5	
			WASOTH	WASOTH	5.776	2.498	8.899		4
			WI	WI	0.001	0.000	0.002		4
COG	Congo	Sub-Saharan Africa	ASGM	GP-A	1125.000	281.250	1968.750		
			BIO	PSB – DR	56.408	12.692	108.584	5	
			CEM	CEM	48.300	17.066	250.562	5	
			CREM	CREM	0.107	0.077	0.155		4
			NFMP-AU	GP-L	8.250	2.888	16.088	5	
			OR	CO-OR	0.678	0.305	1.118	5	
			SC-DR-oil	CO-LF-DR	0.908	0.204	1.748	5	
			SC-IND-oil	CO-LF-IND	0.048	0.011	0.092	5	
			SC-PP-gas	NG-PP	0.047	0.011	0.091	5	
			WASOTH	WASOTH	145.601	62.963	224.305		4
			WI	WI	0.028	0.012	0.043		4

Country code	Country name	Region	Sector Code	Activity Code	Emission estimate, kg	Low range estimate, kg	High range estimate, kg	Technology group	Waste group
COK	Cook Islands	Australia, New Zealand & Oceania	BIO	PSB – DR	0.040	0.007	0.091	4	
			BIO	PSB – IND	0.011	0.002	0.025	4	
			CREM	CREM	0.029	0.026	0.035		4
			OR	CO-OR	0.000	0.000	0.001	4	
			SC-DR-gas	NG-DR	0.000	0.000	0.000	4	
			SC-DR-oil	CO-HF-DR	0.001	0.000	0.003	4	
			SC-DR-oil	CO-LF-DR	0.003	0.001	0.007	4	
			SC-IND-coal	BC-IND-OTH	0.003	0.001	0.007	4	
			SC-IND-coal	HC-IND-OTH	0.162	0.068	0.456	4	
			SC-IND-oil	CO-HF-IND	0.003	0.000	0.006	4	
			SC-IND-oil	CO-LF-IND	0.000	0.000	0.001	4	
			SC-PP-coal	HC-B-PP	0.037	0.015	0.103	4	
			SC-PP-gas	NG-PP	0.000	0.000	0.000	4	
			SC-PP-oil	CO-HF-PP	0.013	0.002	0.029	4	
			SC-PP-oil	CO-LF-PP	0.002	0.000	0.004	4	
			WASOTH	WASOTH	0.810	0.243	2.430		4
			WI	WI	0.003	0.001	0.008		4
CRI	Costa Rica	Central America and the Caribbean	ASGM	GP-A	142.500	35.625	249.375		
			BIO	PSB – DR	7.791	1.753	14.998	3	
			BIO	PSB – IND	20.049	4.511	38.595	3	
			BIO	PSB – PP	1.511	0.340	2.909	3	
			CEM	CEM	127.200	44.940	698.100	3	
			CREM	CREM	0.919	0.736	1.103		4
			NFMP-AU	GP-L	15.840	5.544	30.888	3	
			SC-DR-oil	CO-HF-DR	0.100	0.023	0.193	3	
			SC-DR-oil	CO-LF-DR	1.792	0.403	3.450	3	
			SC-IND-coal	HC-IND-CEM	0.120	0.065	0.286	3	
			SC-IND-oil	CO-HF-IND	1.881	0.423	3.621	3	
			SC-IND-oil	CO-LF-IND	0.112	0.025	0.216	3	
			SC-PP-oil	CO-HF-PP	0.480	0.108	0.924	3	
			SC-PP-oil	CO-LF-PP	0.002	0.000	0.003	3	
			WASOTH	WASOTH	200.740	60.222	602.219		4
			WI	WI	0.628	0.188	1.884		4
HRV	Croatia	EU28	BIO	PSB – DR	60.805	13.681	117.050	4	
			BIO	PSB – IND	1.550	0.349	2.984	4	
			BIO	PSB – PP	2.736	0.616	5.267	4	
			CEM	CEM	225.706	79.715	1375.064	4	
			CEM	PC-CEM	5.845	3.288	32.951	4	
			CREM	CREM	2.216	1.625	2.955		2
			OR	CO-OR	3.238	1.457	5.342	4	
			SC-DR-coal	BC-DR	1.200	0.648	2.860	4	
			SC-DR-gas	NG-DR	0.148	0.033	0.285	4	
			SC-DR-oil	CO-HF-DR	0.180	0.041	0.347	4	
			SC-DR-oil	CO-LF-DR	3.180	0.716	6.122	4	
			SC-IND-coal	BC-IND-CEM	0.394	0.213	0.938	4	

Country code	Country name	Region	Sector Code	Activity Code	Emission estimate, kg	Low range estimate, kg	High range estimate, kg	Technology group	Waste group
			SC-IND-coal	BC-IND-OTH	3.803	2.053	9.063	4	
			SC-IND-coal	HC-IND-CEM	9.844	5.316	23.461	4	
			SC-IND-coal	HC-IND-PIP	0.394	0.213	0.938	4	
			SC-IND-gas	NG-IND	0.079	0.018	0.153	4	
			SC-IND-oil	CO-HF-IND	0.460	0.104	0.886	4	
			SC-IND-oil	CO-LF-IND	0.226	0.051	0.435	4	
			SC-PP-coal	BC-L-PP	0.784	0.459	2.587	4	
			SC-PP-coal	HC-B-PP	98.213	53.035	234.073	4	
			SC-PP-gas	NG-PP	0.139	0.031	0.267	4	
			SC-PP-oil	CO-HF-PP	3.700	0.833	7.123	4	
			SC-PP-oil	CO-LF-PP	0.012	0.003	0.023	4	
			SSC	SP-S	4.872	1.813	23.249	4	
			WASOTH	WASOTH	78.733	23.620	236.198		2
			WI	WI	2.294	0.688	6.882		2
CUB	Cuba	Central America and the Caribbean	BIO	PSB – DR	3.033	0.682	5.838	3	
			BIO	PSB – IND	44.713	10.060	86.073	3	
			BIO	PSB – PP	15.009	3.377	28.892	3	
			CEM	CEM	133.984	47.337	735.332	3	
			CREM	CREM	1.055	0.844	1.266		4
			CSP	CSP-C	35.000	12.250	68.250	3	
			OR	CO-OR	4.376	1.969	7.220	3	
			SC-DR-gas	NG-DR	0.012	0.003	0.023	3	
			SC-DR-oil	CO-HF-DR	11.240	2.529	21.637	3	
			SC-DR-oil	CO-LF-DR	1.264	0.284	2.433	3	
			SC-IND-coal	HC-IND-OTH	0.338	0.182	0.804	3	
			SC-IND-gas	NG-IND	0.074	0.017	0.142	3	
			SC-IND-oil	CO-HF-IND	22.781	5.126	43.853	3	
			SC-IND-oil	CO-IND	8.085	1.819	15.563	3	
			SC-IND-oil	CO-LF-IND	0.762	0.171	1.467	3	
			SC-PP-gas	NG-PP	0.148	0.033	0.284	3	
			SC-PP-oil	CO-HF-PP	24.120	5.427	46.431	3	
			SC-PP-oil	CO-LF-PP	0.695	0.156	1.337	3	
			SC-PP-oil	CO-PP	18.300	4.118	35.228	3	
			SSC	SP-S	6.460	2.404	30.823	3	
			WASOTH	WASOTH	349.436	104.831	1048.308		4
			WI	WI	1.093	0.328	3.280		4
CUW	Curaçao	Central America and the Caribbean	CREM	CREM	0.036	0.029	0.043		
			OR	CO-OR	7.709	3.469	12.719	3	
			SC-DR-oil	CO-LF-DR	0.544	0.122	1.047	3	
			SC-IND-oil	CO-HF-IND	2.413	0.543	4.645	3	
			SC-PP-oil	CO-HF-PP	4.155	0.935	7.998	3	
			SC-PP-oil	CO-LF-PP	0.024	0.005	0.046	3	
			WASOTH	WASOTH	8.225	2.467	24.674		
			WI	WI	0.026	0.008	0.077		

Country code	Country name	Region	Sector Code	Activity Code	Emission estimate, kg	Low range estimate, kg	High range estimate, kg	Technology group	Waste group
CYP	Cyprus	EU28	BIO	PSB – DR	0.196	0.044	0.378	1	
			BIO	PSB – IND	0.142	0.032	0.273	1	
			CEM	CEM	35.381	12.558	217.994	1	
			CEM	PC-CEM	3.471	1.953	19.570	1	
			CREM	CREM	2.801	2.201	3.351		1
			SC-DR-oil	CO-HF-DR	0.060	0.014	0.116	1	
			SC-DR-oil	CO-LF-DR	0.710	0.160	1.367	1	
			SC-IND-coal	HC-IND-CEM	0.610	0.330	1.454	1	
			SC-IND-oil	CO-HF-IND	0.418	0.094	0.805	1	
			SC-IND-oil	CO-LF-IND	0.019	0.004	0.037	1	
			SC-PP-oil	CO-HF-PP	8.580	1.931	16.517	1	
			SC-PP-oil	CO-LF-PP	0.137	0.031	0.263	1	
			WASOTH	WASOTH	5.669	1.701	17.008		1
			WI	WI	2.167	0.650	6.501		1
CZE	Czech Republic	EU28	BIO	PSB – DR	90.703	21.542	166.667	1	
			BIO	PSB – IND	18.282	4.342	33.593	1	
			BIO	PSB – PP	26.717	6.345	49.092	1	
			CEM	CEM	217.219	76.676	1421.578	1	
			CREM	CREM	39.568	31.089	47.340		1
			OR	CO-OR	13.048	6.198	20.550	1	
			PISP	PIP	134.188	47.041	710.240	1	
			SC-DR-coal	BC-DR	216.889	123.627	493.422	1	
			SC-DR-coal	HC-DR	45.806	26.110	104.209	1	
			SC-DR-gas	NG-DR	0.685	0.163	1.259	1	
			SC-DR-oil	CO-HF-DR	0.240	0.057	0.441	1	
			SC-DR-oil	CO-LF-DR	8.444	2.005	15.516	1	
			SC-IND-coal	BC-IND-CEM	1.056	0.602	2.403	1	
			SC-IND-coal	BC-IND-OTH	82.526	47.040	187.747	1	
			SC-IND-coal	BC-IND-PIP	1.770	1.009	4.027	1	
			SC-IND-coal	HC-IND-CEM	12.374	7.053	28.150	1	
			SC-IND-coal	HC-IND-OTH	4.787	2.729	10.890	1	
			SC-IND-coal	HC-IND-PIP	4.163	2.373	9.470	1	
			SC-IND-gas	NG-IND	0.483	0.115	0.888	1	
			SC-IND-oil	CO-HF-IND	0.323	0.077	0.594	1	
			SC-IND-oil	CO-LF-IND	0.110	0.026	0.202	1	
			SC-PP-coal	BC-L-PP	2853.781	1762.210	8989.411	1	
			SC-PP-coal	HC-B-PP	186.921	106.545	425.245	1	
			SC-PP-gas	NG-PP	0.290	0.069	0.533	1	
			SC-PP-oil	CO-HF-PP	0.230	0.055	0.423	1	
			SC-PP-oil	CO-LF-PP	0.030	0.007	0.055	1	
			SSC	SP-S	8.262	3.075	39.425	1	
			WASOTH	WASOTH	75.464	22.639	226.392		1
			WI	WI	28.843	8.653	86.529		1

Country code	Country name	Region	Sector Code	Activity Code	Emission estimate, kg	Low range estimate, kg	High range estimate, kg	Technology group	Waste group
COD	Dem. Rep. of Congo (Zaire)	Sub-Saharan Africa	ASGM	GP-A	11250.000	2812.500	19687.500		
			BIO	PSB – DR	733.868	165.120	1412.695	5	
			BIO	PSB – IND	158.263	35.609	304.656	5	
			BIO	PSB – PP	3.768	0.848	7.252	5	
			CEM	CEM	34.650	12.243	179.751	5	
			CREM	CREM	1.802	1.298	2.597		4
			NFMP-AU	GP-L	2035.000	712.250	3968.250	5	
			SC-DR-oil	CO-LF-DR	1.076	0.242	2.071	5	
			SC-IND-oil	CO-HF-IND	0.320	0.072	0.616	5	
			SC-PP-gas	NG-PP	0.000	0.000	0.000	5	
			SC-PP-oil	CO-LF-PP	0.006	0.001	0.012	5	
			SSC	SP-S	0.899	0.335	4.289	5	
			WASOTH	WASOTH	300.692	130.029	463.228		4
			WI	WI	0.058	0.025	0.089		4
DNK	Denmark	EU28	BIO	PSB – DR	53.075	12.605	97.526	1	
			BIO	PSB – IND	4.197	0.997	7.713	1	
			BIO	PSB – PP	59.351	14.096	109.057	1	
			CEM	CEM	22.647	11.559	271.718	1	
			CEM	PC-CEM	4.205	2.497	22.629	1	
			CREM	CREM	20.793	16.337	24.877		1
			OR	CO-OR	3.208	1.524	5.053	1	
			SC-DR-coal	HC-DR	4.069	2.319	9.256	1	
			SC-DR-gas	NG-DR	0.187	0.044	0.343	1	
			SC-DR-oil	CO-HF-DR	0.100	0.024	0.184	1	
			SC-DR-oil	CO-LF-DR	6.152	1.461	11.304	1	
			SC-IND-coal	HC-IND-CEM	6.111	3.484	13.904	1	
			SC-IND-coal	HC-IND-OTH	4.787	2.729	10.890	1	
			SC-IND-gas	NG-IND	0.151	0.036	0.278	1	
			SC-IND-oil	CO-HF-IND	0.817	0.194	1.501	1	
			SC-IND-oil	CO-LF-IND	0.321	0.076	0.590	1	
			SC-PP-coal	HC-B-PP	153.491	87.490	349.191	1	
			SC-PP-gas	NG-PP	0.325	0.077	0.597	1	
			SC-PP-oil	CO-HF-PP	0.560	0.133	1.029	1	
			SC-PP-oil	CO-LF-PP	0.035	0.008	0.063	1	
			WASOTH	WASOTH	59.034	17.710	177.102		1
			WI	WI	22.563	6.769	67.690		1
DJI	Djibouti	Sub-Saharan Africa	BIO	PSB – DR	9.459	1.655	21.518	5	
			BIO	PSB – IND	0.453	0.079	1.032	5	
			BIO	PSB – PP	0.164	0.029	0.374	5	
			CEM	CEM	36.750	12.985	190.645	5	
			CREM	CREM	0.019	0.014	0.027		4
			SC-DR-coal	HC-DR	0.090	0.038	0.252	5	
			SC-DR-oil	CO-LF-DR	0.040	0.007	0.091	5	
			SC-IND-coal	HC-IND-OTH	0.087	0.037	0.245	5	
			SC-IND-gas	NG-IND	0.000	0.000	0.000	5	
			SC-IND-oil	CO-HF-IND	0.073	0.013	0.166	5	

Country code	Country name	Region	Sector Code	Activity Code	Emission estimate, kg	Low range estimate, kg	High range estimate, kg	Technology group	Waste group
			SC-IND-oil	CO-IND	0.010	0.002	0.023	5	
			SC-IND-oil	CO-LF-IND	0.007	0.001	0.016	5	
			SC-PP-coal	HC-B-PP	0.589	0.247	1.658	5	
			SC-PP-gas	NG-PP	0.001	0.000	0.002	5	
			SC-PP-oil	CO-HF-PP	0.095	0.017	0.216	5	
			SC-PP-oil	CO-LF-PP	0.020	0.003	0.045	5	
			WASOTH	WASOTH	15.309	6.620	23.584		4
			WI	WI	0.003	0.001	0.005		4
DMA	Dominica	Central America and the Caribbean	BIO	PSB – DR	0.096	0.017	0.218	3	
			BIO	PSB – IND	0.148	0.026	0.337	3	
			BIO	PSB – PP	0.053	0.009	0.120	3	
			CREM	CREM	0.014	0.011	0.017		4
			OR	CO-OR	0.014	0.005	0.028	3	
			SC-DR-coal	HC-DR	0.535	0.225	1.508	3	
			SC-DR-gas	NG-DR	0.000	0.000	0.000	3	
			SC-DR-oil	CO-HF-DR	0.015	0.003	0.034	3	
			SC-DR-oil	CO-LF-DR	0.036	0.006	0.082	3	
			SC-IND-gas	NG-IND	0.000	0.000	0.000	3	
			SC-IND-oil	CO-HF-IND	0.043	0.008	0.099	3	
			SC-IND-oil	CO-LF-IND	0.002	0.000	0.006	3	
			SC-PP-gas	NG-PP	0.003	0.000	0.006	3	
			SC-PP-oil	CO-HF-PP	0.414	0.073	0.943	3	
			SC-PP-oil	CO-LF-PP	0.030	0.005	0.069	3	
			WASOTH	WASOTH	2.076	0.623	6.229		4
			WI	WI	0.006	0.002	0.019		4
DOM	Dominican Republic	Central America and the Caribbean	ASGM	GP-A	225.000	56.250	393.750		
			BIO	PSB – DR	21.959	4.941	42.271	3	
			BIO	PSB – IND	10.335	2.325	19.895	3	
			BIO	PSB – PP	0.748	0.168	1.439	3	
			CEM	CEM	407.040	143.808	2233.920	3	
			CREM	CREM	2.001	1.601	2.402		4
			NFMP-AU	GP-L	1220.314	427.110	2379.612	3	
			OR	CO-OR	0.702	0.316	1.159	3	
			SC-DR-gas	NG-DR	0.005	0.001	0.009	3	
			SC-DR-oil	CO-LF-DR	1.254	0.282	2.414	3	
			SC-IND-coal	HC-IND-CEM	12.960	6.998	30.888	3	
			SC-IND-coal	HC-IND-OTH	0.338	0.182	0.804	3	
			SC-IND-gas	NG-IND	0.019	0.004	0.037	3	
			SC-IND-oil	CO-HF-IND	2.033	0.457	3.914	3	
			SC-IND-oil	CO-LF-IND	0.188	0.042	0.362	3	
			SC-PP-coal	HC-B-PP	95.783	51.723	228.282	3	
			SC-PP-gas	NG-PP	0.183	0.041	0.352	3	
			SC-PP-oil	CO-HF-PP	23.775	5.349	45.767	3	
			SC-PP-oil	CO-LF-PP	0.936	0.211	1.802	3	
			WASOTH	WASOTH	394.117	118.235	1182.351		4
			WI	WI	1.233	0.370	3.700		4

Country code	Country name	Region	Sector Code	Activity Code	Emission estimate, kg	Low range estimate, kg	High range estimate, kg	Technology group	Waste group
ECU	Ecuador	South America	ASGM	GP-A	26350.000	13175.000	39525.000		
			BIO	PSB – DR	11.141	2.507	21.447	3	
			BIO	PSB – IND	16.256	3.658	31.293	3	
			BIO	PSB – PP	13.184	2.966	25.378	3	
			CEM	CEM	485.760	171.864	2577.432	3	
			CREM	CREM	6.213	4.349	8.699		4
			NFMP-AU	GP-L	281.635	98.572	549.189	3	
			OR	CO-OR	6.513	2.931	10.747	3	
			SC-DR-gas	NG-DR	0.000	0.000	0.000	3	
			SC-DR-oil	CO-HF-DR	0.600	0.135	1.155	3	
			SC-DR-oil	CO-LF-DR	6.294	1.416	12.116	3	
			SC-IND-gas	NG-IND	0.003	0.001	0.006	3	
			SC-IND-oil	CO-HF-IND	5.073	1.141	9.766	3	
			SC-IND-oil	CO-LF-IND	1.742	0.392	3.354	3	
			SC-PP-gas	NG-PP	0.127	0.028	0.244	3	
			SC-PP-oil	CO-HF-PP	23.685	5.329	45.594	3	
			SC-PP-oil	CO-LF-PP	1.239	0.279	2.385	3	
			SC-PP-oil	CO-PP	2.648	0.596	5.096	3	
			SSC	SP-S	16.830	6.264	80.308	3	
			WASOTH	WASOTH	418.182	125.455	1254.547		4
			WI	WI	1.407	0.422	4.221		4
EGY	Egypt	North Africa	BIO	PSB – DR	91.574	20.604	176.279	5	
			CEM	CEM	5978.000	2109.450	30894.500	5	
			CREM	CREM	1.626	1.220	2.033		4
			NFMP	AL-P	15.000	5.084	28.327	5	
			NFMP-AU	GP-L	753.500	263.725	1469.325	5	
			OR	CO-OR	50.294	22.632	82.985	5	
			PISP	PIP	34.650	12.147	183.398	5	
			SC-DR-gas	NG-DR	0.432	0.097	0.832	5	
			SC-DR-oil	CO-HF-DR	6.800	1.530	13.090	5	
			SC-DR-oil	CO-LF-DR	19.878	4.473	38.265	5	
			SC-IND-gas	NG-IND	0.993	0.223	1.911	5	
			SC-IND-oil	CO-HF-IND	42.000	9.450	80.850	5	
			SC-IND-oil	CO-LF-IND	5.168	1.163	9.948	5	
			SC-PP-gas	NG-PP	6.219	1.399	11.972	5	
			SC-PP-oil	CO-HF-PP	181.580	40.856	349.542	5	
			SC-PP-oil	CO-LF-PP	3.636	0.818	6.999	5	
			SSC	SP-S	178.883	66.579	853.569	5	
			WASOTH	WASOTH	2576.230	772.869	7728.691		4
			WI	WI	8.667	2.600	26.001		4
SLV	El Salvador	Central America and the Caribbean	ASGM	GP-A	225.000	56.250	393.750		
			BIO	PSB – DR	13.916	3.131	26.789	3	
			BIO	PSB – IND	0.991	0.223	1.908	3	
			BIO	PSB – PP	13.250	2.981	25.507	3	
			CEM	CEM	84.800	29.960	465.400	3	

Country code	Country name	Region	Sector Code	Activity Code	Emission estimate, kg	Low range estimate, kg	High range estimate, kg	Technology group	Waste group
			CREM	CREM	1.162	0.929	1.394		4
			SC-DR-oil	CO-HF-DR	0.560	0.126	1.078	3	
			SC-DR-oil	CO-LF-DR	1.016	0.229	1.956	3	
			SC-IND-oil	CO-HF-IND	0.418	0.094	0.805	3	
			SC-IND-oil	CO-LF-IND	0.296	0.067	0.571	3	
			SC-PP-oil	CO-HF-PP	7.665	1.725	14.755	3	
			SSC	SP-S	3.053	1.136	14.569	3	
			WASOTH	WASOTH	138.638	41.592	415.915		4
			WI	WI	0.434	0.130	1.301		4
GNQ	Equatorial Guinea	Sub-Saharan Africa	ASGM	GP-A	225.000	56.250	393.750		
			BIO	PSB – DR	8.458	1.480	19.243	5	
			BIO	PSB – IND	4.030	0.705	9.168	5	
			BIO	PSB – PP	1.460	0.255	3.321	5	
			CREM	CREM	0.017	0.012	0.024		4
			SC-DR-coal	HC-DR	0.796	0.334	2.243	5	
			SC-DR-oil	CO-LF-DR	0.356	0.062	0.810	5	
			SC-IND-coal	HC-IND-OTH	0.773	0.325	2.178	5	
			SC-IND-gas	NG-IND	0.000	0.000	0.000	5	
			SC-IND-oil	CO-HF-IND	0.648	0.113	1.475	5	
			SC-IND-oil	CO-IND	0.089	0.016	0.203	5	
			SC-IND-oil	CO-LF-IND	0.062	0.011	0.141	5	
			SC-PP-coal	HC-B-PP	5.232	2.198	14.738	5	
			SC-PP-gas	NG-PP	0.006	0.001	0.014	5	
			SC-PP-oil	CO-HF-PP	0.843	0.148	1.918	5	
			SC-PP-oil	CO-LF-PP	0.174	0.031	0.397	5	
			WASOTH	WASOTH	168.341	72.796	259.337		4
			WI	WI	0.032	0.014	0.050		4
ERI	Eritrea	Sub-Saharan Africa	ASGM	GP-A	225.000	56.250	393.750		
			BIO	PSB – DR	17.614	3.963	33.906	5	
			CEM	CEM	31.500	11.130	163.410	5	
			CREM	CREM	0.130	0.094	0.187		4
			NFMP-AU	GP-L	76.450	26.758	149.078	5	
			SC-DR-oil	CO-HF-DR	0.020	0.005	0.039	5	
			SC-DR-oil	CO-LF-DR	0.094	0.021	0.181	5	
			SC-IND-oil	CO-HF-IND	0.100	0.023	0.193	5	
			SC-IND-oil	CO-LF-IND	0.002	0.000	0.004	5	
			SC-PP-oil	CO-HF-PP	1.460	0.329	2.811	5	
			SC-PP-oil	CO-LF-PP	0.076	0.017	0.146	5	
			WASOTH	WASOTH	45.281	19.581	69.758		4
			WI	WI	0.009	0.004	0.013		4
EST	Estonia	EU28	BIO	PSB – DR	19.138	4.545	35.166	1	
			BIO	PSB – IND	3.927	0.933	7.216	1	
			BIO	PSB – PP	14.959	3.553	27.487	1	
			CEM	CEM	24.957	8.814	155.792	1	
			CREM	CREM	2.924	2.297	3.498		1
			SC-DR-coal	HC-DR	0.525	0.299	1.194	1	

Country code	Country name	Region	Sector Code	Activity Code	Emission estimate, kg	Low range estimate, kg	High range estimate, kg	Technology group	Waste group
			SC-DR-gas	NG-DR	0.030	0.007	0.055	1	
			SC-DR-oil	CO-HF-DR	0.140	0.033	0.257	1	
			SC-DR-oil	CO-LF-DR	1.264	0.300	2.323	1	
			SC-IND-coal	HC-IND-CEM	1.660	0.946	3.776	1	
			SC-IND-gas	NG-IND	0.022	0.005	0.040	1	
			SC-IND-oil	CO-HF-IND	0.247	0.059	0.454	1	
			SC-IND-oil	CO-LF-IND	0.095	0.023	0.175	1	
			SC-PP-coal	HC-B-PP	0.155	0.088	0.353	1	
			SC-PP-gas	NG-PP	0.039	0.009	0.072	1	
			SC-PP-oil	CO-HF-PP	0.410	0.097	0.753	1	
			SC-PP-oil	CO-LF-PP	0.023	0.005	0.041	1	
			WASOTH	WASOTH	8.075	2.422	24.224		1
			WI	WI	3.086	0.926	9.259		1
ETH	Ethiopia	Sub-Saharan Africa	ASGM	GP-A	225.000	56.250	393.750		
			BIO	PSB – DR	1689.720	380.187	3252.711	5	
			CEM	CEM	567.000	200.340	2941.380	5	
			CEM	PC-CEM	8.440	4.748	47.581	5	
			CREM	CREM	2.268	1.634	3.269		4
			NFMP-AU	GP-L	506.000	177.100	986.700	5	
			SC-DR-oil	CO-LF-DR	2.932	0.660	5.644	5	
			SC-IND-coal	HC-IND-CEM	61.650	33.291	146.933	5	
			SC-IND-oil	CO-HF-IND	1.340	0.302	2.580	5	
			SC-IND-oil	CO-LF-IND	0.908	0.204	1.748	5	
			SC-PP-oil	CO-LF-PP	0.002	0.000	0.004	5	
			WASOTH	WASOTH	805.114	348.157	1240.311		4
			WI	WI	0.154	0.067	0.238		4
FRO	Faeroe Islands	CIS & other European countries	CREM	CREM	0.022	0.016	0.029		1
			WASOTH	WASOTH	0.957	0.287	2.871		1
			WI	WI	0.366	0.110	1.097		1
FLK	Falkland Is. (Malvinas)	South America	BIO	PSB – DR	0.004	0.001	0.010	3	
			BIO	PSB – IND	0.035	0.006	0.080	3	
			BIO	PSB – PP	0.012	0.002	0.028	3	
			CREM	CREM	0.001	0.001	0.002		4
			OR	CO-OR	0.004	0.001	0.008	3	
			SC-DR-coal	HC-DR	0.127	0.053	0.356	3	
			SC-DR-gas	NG-DR	0.000	0.000	0.000	3	
			SC-DR-oil	CO-HF-DR	0.004	0.001	0.008	3	
			SC-DR-oil	CO-LF-DR	0.009	0.001	0.019	3	
			SC-IND-gas	NG-IND	0.000	0.000	0.000	3	
			SC-IND-oil	CO-HF-IND	0.010	0.002	0.023	3	
			SC-IND-oil	CO-LF-IND	0.001	0.000	0.001	3	
			SC-PP-gas	NG-PP	0.001	0.000	0.001	3	
			SC-PP-oil	CO-HF-PP	0.098	0.017	0.223	3	
			SC-PP-oil	CO-LF-PP	0.007	0.001	0.016	3	
			WASOTH	WASOTH	0.636	0.191	1.908		4
			WI	WI	0.002	0.001	0.006		4

Country code	Country name	Region	Sector Code	Activity Code	Emission estimate, kg	Low range estimate, kg	High range estimate, kg	Technology group	Waste group
FSM	Federated States of Micronesia	Australia, New Zealand & Oceania	CREM	CREM	0.320	0.288	0.384		4
			WASOTH	WASOTH	1.212	0.364	3.636		4
			WI	WI	0.004	0.001	0.011		4
FJI	Fiji	Australia, New Zealand & Oceania	BIO	PSB – DR	3.703	0.648	8.425	4	
			BIO	PSB – IND	0.745	0.130	1.694	4	
			CEM	CEM	18.121	6.401	95.527	4	
			CREM	CREM	2.800	2.515	3.353		4
			NFMP-AU	GP-L	67.320	23.562	131.274	4	
			OR	CO-OR	0.032	0.011	0.063	4	
			SC-DR-gas	NG-DR	0.002	0.000	0.004	4	
			SC-DR-oil	CO-HF-DR	0.077	0.013	0.175	4	
			SC-DR-oil	CO-LF-DR	0.197	0.035	0.449	4	
			SC-IND-coal	BC-IND-OTH	0.174	0.073	0.489	4	
			SC-IND-coal	HC-IND-OTH	10.948	4.598	30.837	4	
			SC-IND-oil	CO-HF-IND	0.169	0.030	0.385	4	
			SC-IND-oil	CO-LF-IND	0.018	0.003	0.042	4	
			SC-PP-coal	HC-B-PP	2.470	1.037	6.957	4	
			SC-PP-gas	NG-PP	0.002	0.000	0.004	4	
			SC-PP-oil	CO-HF-PP	0.871	0.152	1.982	4	
			SC-PP-oil	CO-LF-PP	0.114	0.020	0.259	4	
			WASOTH	WASOTH	27.597	8.279	82.791		4
			WI	WI	0.086	0.026	0.259		4
FIN	Finland	EU28	BIO	PSB – DR	72.209	17.150	132.683	1	
			BIO	PSB – IND	131.667	31.271	241.938	1	
			BIO	PSB – PP	133.051	31.600	244.481	1	
			CEM	CEM	72.306	25.527	493.695	1	
			CEM	PC-CEM	1.046	0.621	5.630	1	
			CREM	CREM	12.773	10.036	15.282		1
			NFMP	CU-P	33.635	12.005	192.033	1	
			NFMP	ZN-P	79.976	28.334	219.700	1	
			NFMP-AU	GP-L	21.483	7.519	41.892	1	
			OR	CO-OR	17.719	8.417	27.908	1	
			PISP	PIP	387.828	135.955	2052.718	1	
			SC-DR-coal	HC-DR	0.525	0.299	1.194	1	
			SC-DR-gas	NG-DR	0.014	0.003	0.026	1	
			SC-DR-oil	CO-HF-DR	1.200	0.285	2.205	1	
			SC-DR-oil	CO-LF-DR	6.116	1.453	11.238	1	
			SC-IND-coal	HC-IND-CEM	3.923	2.236	8.926	1	
			SC-IND-coal	HC-IND-OTH	4.718	2.689	10.732	1	
			SC-IND-coal	HC-IND-PIP	0.416	0.237	0.947	1	
			SC-IND-gas	NG-IND	0.129	0.031	0.236	1	
			SC-IND-oil	CO-HF-IND	3.477	0.826	6.389	1	
			SC-IND-oil	CO-LF-IND	0.876	0.208	1.609	1	
			SC-PP-coal	HC-B-PP	123.890	70.617	281.849	1	
			SC-PP-gas	NG-PP	0.316	0.075	0.581	1	

Country code	Country name	Region	Sector Code	Activity Code	Emission estimate, kg	Low range estimate, kg	High range estimate, kg	Technology group	Waste group
			SC-PP-oil	CO-HF-PP	2.540	0.603	4.667	1	
			SC-PP-oil	CO-LF-PP	0.035	0.008	0.063	1	
			SSC	SP-S	29.525	10.989	140.884	1	
			WASOTH	WASOTH	49.124	14.737	147.371		1
			WI	WI	18.776	5.633	56.327		1
FRA	France	EU28	BIO	PSB – DR	352.369	83.688	647.477	1	
			BIO	PSB – IND	50.504	11.995	92.801	1	
			BIO	PSB – PP	62.100	14.749	114.108	1	
			CEM	CEM	932.059	329.214	5552.592	1	
			CEM	PC-CEM	12.052	7.156	64.854	1	
			CREM	CREM	108.691	85.400	130.041		1
			CSP	CSP-C	350.960	122.836	684.373	1	
			NFMP	AL-P	5.250	1.780	9.915	1	
			NFMP	ZN-P	44.210	15.663	121.450	1	
			OR	CO-OR	103.584	49.202	163.144	1	
			PISP	PIP	351.178	123.107	1858.736	1	
			SC-DR-coal	HC-DR	12.075	6.883	27.471	1	
			SC-DR-gas	NG-DR	3.870	0.919	7.111	1	
			SC-DR-oil	CO-HF-DR	1.600	0.380	2.940	1	
			SC-DR-oil	CO-LF-DR	83.846	19.913	154.067	1	
			SC-IND-coal	BC-IND-CEM	1.962	1.118	4.463	1	
			SC-IND-coal	BC-IND-OTH	10.509	5.990	23.909	1	
			SC-IND-coal	BC-IND-PIP	0.221	0.126	0.503	1	
			SC-IND-coal	HC-IND-CEM	25.351	14.450	57.674	1	
			SC-IND-coal	HC-IND-OTH	61.466	35.036	139.836	1	
			SC-IND-coal	HC-IND-PIP	61.674	35.154	140.309	1	
			SC-IND-gas	NG-IND	2.393	0.568	4.397	1	
			SC-IND-oil	CO-HF-IND	9.766	2.319	17.945	1	
			SC-IND-oil	CO-LF-IND	1.744	0.414	3.205	1	
			SC-PP-coal	HC-B-PP	204.206	116.397	464.568	1	
			SC-PP-gas	NG-PP	1.442	0.343	2.650	1	
			SC-PP-oil	CO-HF-PP	3.900	0.926	7.166	1	
			SC-PP-oil	CO-LF-PP	0.135	0.032	0.248	1	
			SSC	SP-S	128.324	47.761	612.318	1	
			WASOTH	WASOTH	581.782	174.535	1745.347		1
			WI	WI	222.363	66.709	667.090		1
GUF	French Guiana	Central America and the Caribbean	ASGM	GP-A	5625.000	2812.500	8437.500		
			BIO	PSB – DR	0.325	0.057	0.740	3	
			CEM	CEM	7.293	2.577	40.024	3	
			CREM	CREM	0.047	0.038	0.057		4
			NFMP-AU	GP-L	47.520	16.632	92.664	3	
			WASOTH	WASOTH	0.000	0.000	0.000		4
			WI	WI	0.000	0.000	0.000		4

Country code	Country name	Region	Sector Code	Activity Code	Emission estimate, kg	Low range estimate, kg	High range estimate, kg	Technology group	Waste group
PYF	French Polynesia	Australia, New Zealand & Oceania	BIO	PSB – DR	1.151	0.201	2.619	4	
			BIO	PSB – IND	0.671	0.117	1.527	4	
			CREM	CREM	0.873	0.784	1.045		4
			OR	CO-OR	0.029	0.010	0.057	4	
			SC-DR-gas	NG-DR	0.001	0.000	0.003	4	
			SC-DR-oil	CO-HF-DR	0.070	0.012	0.158	4	
			SC-DR-oil	CO-LF-DR	0.178	0.031	0.405	4	
			SC-IND-coal	BC-IND-OTH	0.156	0.066	0.441	4	
			SC-IND-coal	HC-IND-OTH	9.870	4.145	27.801	4	
			SC-IND-oil	CO-HF-IND	0.152	0.027	0.347	4	
			SC-IND-oil	CO-LF-IND	0.017	0.003	0.038	4	
			SC-PP-coal	HC-B-PP	2.227	0.935	6.272	4	
			SC-PP-gas	NG-PP	0.002	0.000	0.003	4	
			SC-PP-oil	CO-HF-PP	0.785	0.137	1.787	4	
			SC-PP-oil	CO-LF-PP	0.103	0.018	0.234	4	
			WASOTH	WASOTH	18.215	5.465	54.646		4
			WI	WI	0.057	0.017	0.171		4
GAB	Gabon	Sub-Saharan Africa	ASGM	GP-A	225.000	56.250	393.750		
			BIO	PSB – DR	54.335	12.225	104.595	5	
			BIO	PSB – IND	142.967	32.167	275.211	5	
			BIO	PSB – PP	0.383	0.086	0.736	5	
			CEM	CEM	17.850	6.307	92.599	5	
			CREM	CREM	0.039	0.028	0.056		4
			OR	CO-OR	0.201	0.090	0.331	5	
			SC-DR-oil	CO-LF-DR	0.456	0.103	0.878	5	
			SC-IND-gas	NG-IND	0.001	0.000	0.001	5	
			SC-IND-oil	CO-HF-IND	1.340	0.302	2.580	5	
			SC-IND-oil	CO-LF-IND	0.568	0.128	1.093	5	
			SC-PP-gas	NG-PP	0.071	0.016	0.136	5	
			SC-PP-oil	CO-LF-PP	0.128	0.029	0.246	5	
			WASOTH	WASOTH	170.879	73.893	263.245		4
			WI	WI	0.033	0.014	0.050		4
GMB	Gambia	Sub-Saharan Africa	ASGM	GP-A	225.000	56.250	393.750		
			BIO	PSB – DR	22.469	3.932	51.117	5	
			BIO	PSB – IND	0.539	0.094	1.225	5	
			BIO	PSB – PP	0.195	0.034	0.444	5	
			CREM	CREM	0.011	0.008	0.016		4
			SC-DR-coal	HC-DR	0.106	0.045	0.300	5	
			SC-DR-oil	CO-LF-DR	0.048	0.008	0.108	5	
			SC-IND-coal	HC-IND-OTH	0.103	0.043	0.291	5	
			SC-IND-gas	NG-IND	0.000	0.000	0.000	5	
			SC-IND-oil	CO-HF-IND	0.087	0.015	0.197	5	
			SC-IND-oil	CO-IND	0.012	0.002	0.027	5	
			SC-IND-oil	CO-LF-IND	0.008	0.001	0.019	5	
			SC-PP-coal	HC-B-PP	0.699	0.294	1.970	5	

Country code	Country name	Region	Sector Code	Activity Code	Emission estimate, kg	Low range estimate, kg	High range estimate, kg	Technology group	Waste group
			SC-PP-gas	NG-PP	0.001	0.000	0.002	5	
			SC-PP-oil	CO-HF-PP	0.113	0.020	0.256	5	
			SC-PP-oil	CO-LF-PP	0.023	0.004	0.053	5	
			WASOTH	WASOTH	16.515	7.142	25.442		4
			WI	WI	0.003	0.001	0.005		4
GEO	Georgia	CIS & other European countries	BIO	PSB – DR	20.796	4.679	40.033	4	
			BIO	PSB – IND	0.043	0.010	0.082	4	
			CEM	CEM	159.348	56.270	808.264	4	
			CREM	CREM	1.688	1.238	2.251		4
			NFMP-AU	GP-L	178.200	62.370	347.490	4	
			OR	CO-OR	0.016	0.007	0.026	4	
			SC-DR-coal	BC-DR	0.450	0.243	1.073	4	
			SC-DR-coal	HC-DR	0.150	0.081	0.358	4	
			SC-DR-gas	NG-DR	0.242	0.054	0.466	4	
			SC-DR-oil	CO-HF-DR	0.020	0.005	0.039	4	
			SC-DR-oil	CO-LF-DR	1.052	0.237	2.025	4	
			SC-IND-coal	BC-IND-CEM	39.375	21.263	93.844	4	
			SC-IND-coal	HC-IND-CEM	15.356	8.292	36.599	4	
			SC-IND-coal	HC-IND-OTH	0.394	0.213	0.938	4	
			SC-IND-gas	NG-IND	0.022	0.005	0.043	4	
			SC-IND-oil	CO-LF-IND	0.158	0.036	0.304	4	
			SC-PP-coal	BC-L-PP	0.098	0.057	0.323	4	
			SC-PP-gas	NG-PP	0.126	0.028	0.243	4	
			WASOTH	WASOTH	101.861	30.558	305.583		4
			WI	WI	0.319	0.096	0.956		4
DEU	Germany	EU28	BIO	PSB – DR	332.312	78.924	610.623	1	
			BIO	PSB – IND	83.326	19.790	153.112	1	
			BIO	PSB – PP	145.487	34.553	267.333	1	
			CEM	CEM	625.931	244.354	2143.812	1	
			CEM	PC-CEM	1.530	0.908	8.233	1	
			CREM	CREM	206.287	162.083	246.808		1
			CSP	CSP-C	225.312	78.859	439.359	1	
			NFMP	AL-P	6.625	2.246	12.511	1	
			NFMP	CU-P	65.021	23.207	371.227	1	
			NFMP	PB-P	3.172	1.729	5.002	1	
			NFMP	ZN-T	909.862	328.353	1425.831	1	
			OR	CO-OR	168.618	80.094	265.574	1	
			PISP	PIP	856.771	300.853	3697.459	1	
			SC-DR-coal	HC-DR	61.950	35.312	140.936	1	
			SC-DR-gas	NG-DR	7.118	1.691	13.079	1	
			SC-DR-oil	CO-LF-DR	98.928	23.495	181.780	1	
			SC-IND-coal	BC-IND-OTH	58.189	33.168	132.379	1	
			SC-IND-coal	HC-IND-CEM	24.581	14.011	55.922	1	
			SC-IND-coal	HC-IND-NFM	1.873	1.068	4.261	1	
			SC-IND-coal	HC-IND-OTH	100.663	57.378	229.009	1	

Country code	Country name	Region	Sector Code	Activity Code	Emission estimate, kg	Low range estimate, kg	High range estimate, kg	Technology group	Waste group
			SC-IND-coal	HC-IND-PIP	75.133	42.826	170.928	1	
			SC-IND-gas	NG-IND	4.350	1.033	7.993	1	
			SC-IND-oil	CO-HF-IND	27.949	6.638	51.356	1	
			SC-IND-oil	CO-LF-IND	1.395	0.331	2.563	1	
			SC-PP-coal	BC-L-PP	8544.538	5682.118	11663.294	1	
			SC-PP-coal	HC-A-PP	151.457	86.330	609.613	1	
			SC-PP-coal	HC-B-PP	2026.892	1155.329	4611.180	1	
			SC-PP-gas	NG-PP	3.604	0.856	6.622	1	
			SC-PP-oil	CO-HF-PP	10.200	2.423	18.743	1	
			SC-PP-oil	CO-LF-PP	0.461	0.109	0.846	1	
			SSC	SP-S	304.869	113.470	1454.729	1	
			WASOTH	WASOTH	831.466	249.440	2494.398		1
			WI	WI	317.795	95.338	953.385		1
GHA	Ghana	Sub-Saharan Africa	ASGM	GP-A	41250.000	20625.000	61875.000		
			BIO	PSB – DR	61.244	13.780	117.894	5	
			BIO	PSB – IND	20.919	4.707	40.269	5	
			CEM	CEM	315.000	111.300	1634.100	5	
			CREM	CREM	0.596	0.430	0.859		4
			NFMP	AL-P	12.400	4.340	24.180	5	
			NFMP-AU	GP-L	4840.000	1694.000	9438.000	5	
			OR	CO-OR	0.093	0.042	0.153	5	
			SC-DR-oil	CO-LF-DR	2.794	0.629	5.378	5	
			SC-IND-oil	CO-HF-IND	0.260	0.059	0.501	5	
			SC-IND-oil	CO-LF-IND	1.012	0.228	1.948	5	
			SC-PP-gas	NG-PP	0.247	0.056	0.476	5	
			SC-PP-oil	CO-HF-PP	0.040	0.009	0.077	5	
			SC-PP-oil	CO-PP	2.490	0.560	4.793	5	
			SSC	SP-S	0.749	0.279	3.574	5	
			WASOTH	WASOTH	569.944	246.462	878.023		4
			WI	WI	0.109	0.047	0.168		4
GIB	Gibraltar	CIS & other European countries	CREM	CREM	0.035	0.026	0.047		1
			SC-DR-oil	CO-LF-DR	0.198	0.045	0.381	1	
			SC-PP-oil	CO-HF-PP	0.510	0.115	0.982	1	
			WASOTH	WASOTH	0.977	0.293	2.932		1
			WI	WI	0.374	0.112	1.121		1
GRC	Greece	EU28	BIO	PSB – DR	42.353	10.059	77.823	1	
			BIO	PSB – IND	6.961	1.653	12.791	1	
			BIO	PSB – PP	0.004	0.001	0.008	1	
			CEM	CEM	265.677	93.890	1369.782	1	
			CEM	PC-CEM	14.708	8.733	79.146	1	
			CREM	CREM	0.000	0.000	0.000		1
			NFMP	AL-P	13.175	4.611	25.691	1	
			NFMP-AU	GP-L	1.155	0.404	2.252	1	
			OR	CO-OR	39.190	18.615	61.725	1	
			SC-DR-coal	BC-DR	7.459	4.251	16.969	1	

Country code	Country name	Region	Sector Code	Activity Code	Emission estimate, kg	Low range estimate, kg	High range estimate, kg	Technology group	Waste group
			SC-DR-gas	NG-DR	0.125	0.030	0.230	1	
			SC-DR-oil	CO-HF-DR	6.620	1.572	12.164	1	
			SC-DR-oil	CO-LF-DR	7.490	1.779	13.763	1	
			SC-IND-coal	BC-IND-NFM	21.351	12.170	48.573	1	
			SC-IND-coal	HC-IND-CEM	6.111	3.484	13.904	1	
			SC-IND-coal	HC-IND-NFM	13.875	7.909	31.566	1	
			SC-IND-gas	NG-IND	0.100	0.024	0.184	1	
			SC-IND-oil	CO-HF-IND	3.667	0.871	6.738	1	
			SC-IND-oil	CO-LF-IND	0.393	0.093	0.723	1	
			SC-PP-coal	BC-L-PP	3671.518	2267.162	11565.282	1	
			SC-PP-gas	NG-PP	0.309	0.073	0.568	1	
			SC-PP-oil	CO-HF-PP	14.050	3.337	25.817	1	
			SC-PP-oil	CO-LF-PP	0.389	0.092	0.714	1	
			SSC	SP-S	23.854	8.878	113.821	1	
			WASOTH	WASOTH	60.483	18.145	181.450		1
			WI	WI	23.117	6.935	69.352		1
GRL	Greenland	North America	CREM	CREM	0.145	0.121	0.166		4
			WASOTH	WASOTH	2.509	0.753	7.528		4
			WI	WI	0.008	0.002	0.024		4
GRD	Grenada	Central America and the Caribbean	BIO	PSB – DR	0.144	0.025	0.327	3	
			BIO	PSB – IND	0.273	0.048	0.621	3	
			BIO	PSB – PP	0.097	0.017	0.221	3	
			CREM	CREM	0.021	0.017	0.025		4
			OR	CO-OR	0.026	0.009	0.051	3	
			SC-DR-coal	HC-DR	0.986	0.414	2.776	3	
			SC-DR-gas	NG-DR	0.000	0.000	0.000	3	
			SC-DR-oil	CO-HF-DR	0.028	0.005	0.063	3	
			SC-DR-oil	CO-LF-DR	0.067	0.012	0.152	3	
			SC-IND-gas	NG-IND	0.000	0.000	0.000	3	
			SC-IND-oil	CO-HF-IND	0.080	0.014	0.182	3	
			SC-IND-oil	CO-LF-IND	0.005	0.001	0.010	3	
			SC-PP-gas	NG-PP	0.005	0.001	0.011	3	
			SC-PP-oil	CO-HF-PP	0.763	0.133	1.735	3	
			SC-PP-oil	CO-LF-PP	0.056	0.010	0.128	3	
			WASOTH	WASOTH	3.808	1.142	11.425		4
			WI	WI	0.012	0.004	0.036		4
GLP	Guadeloupe	Central America and the Caribbean	BIO	PSB – DR	0.523	0.091	1.189	3	
			CEM	CEM	25.440	8.988	139.620	3	
			CREM	CREM	0.076	0.061	0.091		4
			WASOTH	WASOTH	0.000	0.000	0.000		4
			WI	WI	0.000	0.000	0.000		4
GTM	Guatemala	Central America and the Caribbean	ASGM	GP-A	712.500	178.125	1246.875		
			BIO	PSB – DR	314.376	70.735	605.174	3	
			BIO	PSB – PP	63.523	14.293	122.281	3	
			CEM	CEM	296.800	104.860	1628.900	3	

Country code	Country name	Region	Sector Code	Activity Code	Emission estimate, kg	Low range estimate, kg	High range estimate, kg	Technology group	Waste group
			CREM	CREM	2.866	2.293	3.439		4
			NFMP-AU	GP-L	221.760	77.616	432.432	3	
			OR	CO-OR	0.053	0.024	0.087	3	
			SC-DR-oil	CO-LF-DR	2.112	0.475	4.066	3	
			SC-IND-oil	CO-HF-IND	4.332	0.975	8.339	3	
			SC-IND-oil	CO-LF-IND	0.230	0.052	0.443	3	
			SC-PP-coal	HC-B-PP	154.710	83.543	368.726	3	
			SC-PP-oil	CO-HF-PP	4.665	1.050	8.980	3	
			SC-PP-oil	CO-LF-PP	0.062	0.014	0.118	3	
			SSC	SP-S	9.967	3.710	47.558	3	
			WASOTH	WASOTH	331.810	99.543	995.431		4
			WI	WI	1.038	0.311	3.115		4
GIN	Guinea	Sub-Saharan Africa	ASGM	GP-A	14325.000	10027.500	18622.500		
			BIO	PSB – DR	134.516	23.540	306.024	5	
			BIO	PSB – IND	2.418	0.423	5.502	5	
			BIO	PSB – PP	0.876	0.153	1.993	5	
			CEM	CEM	52.500	18.550	272.350	5	
			CREM	CREM	0.201	0.145	0.290		4
			NFMP-AU	GP-L	935.000	327.250	1823.250	5	
			SC-DR-coal	HC-DR	0.478	0.201	1.346	5	
			SC-DR-oil	CO-LF-DR	0.214	0.037	0.486	5	
			SC-IND-coal	HC-IND-OTH	0.464	0.195	1.307	5	
			SC-IND-gas	NG-IND	0.000	0.000	0.000	5	
			SC-IND-oil	CO-HF-IND	0.389	0.068	0.885	5	
			SC-IND-oil	CO-IND	0.053	0.009	0.122	5	
			SC-IND-oil	CO-LF-IND	0.037	0.007	0.085	5	
			SC-PP-coal	HC-B-PP	3.140	1.319	8.845	5	
			SC-PP-gas	NG-PP	0.004	0.001	0.008	5	
			SC-PP-oil	CO-HF-PP	0.506	0.089	1.151	5	
			SC-PP-oil	CO-LF-PP	0.105	0.018	0.238	5	
			WASOTH	WASOTH	75.281	32.554	115.973		4
			WI	WI	0.014	0.006	0.022		4
GNB	Guinea-Bissau	Sub-Saharan Africa	ASGM	GP-A	225.000	56.250	393.750		
			BIO	PSB – DR	19.711	3.449	44.842	5	
			BIO	PSB – IND	0.443	0.078	1.008	5	
			BIO	PSB – PP	0.160	0.028	0.365	5	
			CREM	CREM	0.039	0.028	0.056		4
			SC-DR-coal	HC-DR	0.088	0.037	0.247	5	
			SC-DR-oil	CO-LF-DR	0.039	0.007	0.089	5	
			SC-IND-coal	HC-IND-OTH	0.085	0.036	0.239	5	
			SC-IND-gas	NG-IND	0.000	0.000	0.000	5	
			SC-IND-oil	CO-HF-IND	0.071	0.012	0.162	5	
			SC-IND-oil	CO-IND	0.010	0.002	0.022	5	
			SC-IND-oil	CO-LF-IND	0.007	0.001	0.016	5	
			SC-PP-coal	HC-B-PP	0.575	0.242	1.620	5	

Country code	Country name	Region	Sector Code	Activity Code	Emission estimate, kg	Low range estimate, kg	High range estimate, kg	Technology group	Waste group
			SC-PP-gas	NG-PP	0.001	0.000	0.002	5	
			SC-PP-oil	CO-HF-PP	0.093	0.016	0.211	5	
			SC-PP-oil	CO-LF-PP	0.019	0.003	0.044	5	
			WASOTH	WASOTH	13.260	5.734	20.427		4
			WI	WI	0.003	0.001	0.004		4
GUY	Guyana	South America	ASGM	GP-A	11250.000	5625.000	16875.000		
			BIO	PSB – DR	0.956	0.167	2.174	3	
			BIO	PSB – IND	1.039	0.182	2.363	3	
			BIO	PSB – PP	0.369	0.065	0.839	3	
			CEM	CEM	0.147	0.052	0.781	3	
			CREM	CREM	0.139	0.111	0.167		4
			NFMP-AU	GP-L	555.548	194.442	1083.319	3	
			OR	CO-OR	0.115	0.040	0.224	3	
			SC-DR-coal	HC-DR	3.748	1.574	10.557	3	
			SC-DR-gas	NG-DR	0.000	0.000	0.001	3	
			SC-DR-oil	CO-HF-DR	0.106	0.019	0.241	3	
			SC-DR-oil	CO-LF-DR	0.254	0.044	0.577	3	
			SC-IND-gas	NG-IND	0.000	0.000	0.000	3	
			SC-IND-oil	CO-HF-IND	0.304	0.053	0.692	3	
			SC-IND-oil	CO-LF-IND	0.017	0.003	0.039	3	
			SC-PP-gas	NG-PP	0.019	0.003	0.043	3	
			SC-PP-oil	CO-HF-PP	2.901	0.508	6.599	3	
			SC-PP-oil	CO-LF-PP	0.213	0.037	0.486	3	
			WASOTH	WASOTH	13.047	3.914	39.140		4
			WI	WI	0.044	0.013	0.132		4
HTI	Haiti	Central America and the Caribbean	BIO	PSB – DR	77.280	17.388	148.764	4	
			BIO	PSB – IND	4.106	0.924	7.904	4	
			CEM	CEM	27.825	9.831	152.709	4	
			CREM	CREM	1.979	1.583	2.374		4
			SC-DR-oil	CO-LF-DR	0.464	0.104	0.893	4	
			SC-IND-oil	CO-HF-IND	0.200	0.045	0.385	4	
			SC-IND-oil	CO-LF-IND	0.350	0.079	0.674	4	
			SC-PP-oil	CO-HF-PP	2.180	0.491	4.197	4	
			SC-PP-oil	CO-LF-PP	0.378	0.085	0.728	4	
			WASOTH	WASOTH	49.513	14.854	148.540		4
			WI	WI	0.155	0.046	0.465		4
HND	Honduras	Central America and the Caribbean	ASGM	GP-A	2375.000	1187.500	3562.500		
			BIO	PSB – DR	106.234	23.903	204.500	3	
			BIO	PSB – IND	5.719	1.287	11.010	3	
			BIO	PSB – PP	13.000	2.925	25.024	3	
			CEM	CEM	144.160	50.932	791.180	3	
			CREM	CREM	1.678	1.342	2.014		4
			NFMP-AU	GP-L	102.881	36.008	200.618	3	
			SC-DR-oil	CO-HF-DR	0.740	0.167	1.425	3	
			SC-DR-oil	CO-LF-DR	1.234	0.278	2.375	3	

Country code	Country name	Region	Sector Code	Activity Code	Emission estimate, kg	Low range estimate, kg	High range estimate, kg	Technology group	Waste group
			SC-IND-coal	HC-IND-OTH	8.663	4.678	20.646	3	
			SC-IND-oil	CO-HF-IND	1.634	0.368	3.145	3	
			SC-IND-oil	CO-LF-IND	0.492	0.111	0.947	3	
			SC-PP-coal	HC-B-PP	3.645	1.968	8.687	3	
			SC-PP-oil	CO-HF-PP	15.720	3.537	30.261	3	
			SC-PP-oil	CO-LF-PP	0.053	0.012	0.101	3	
			WASOTH	WASOTH	108.150	32.445	324.450		4
			WI	WI	0.338	0.102	1.015		4
HKG	Hong Kong (if separately estimated)	East and Southeast Asia	BIO	PSB – DR	2.855	0.642	5.496	3	
			CEM	CEM	124.260	43.890	655.044	3	
			CREM	CREM	5.144	4.681	5.708		2
			SC-DR-gas	NG-DR	0.134	0.030	0.258	3	
			SC-DR-oil	CO-LF-DR	3.104	0.698	5.975	3	
			SC-IND-coal	HC-IND-OTH	229.725	124.052	547.511	3	
			SC-IND-gas	NG-IND	0.008	0.002	0.016	3	
			SC-IND-oil	CO-LF-IND	1.184	0.266	2.279	3	
			SC-PP-coal	HC-B-PP	524.111	283.020	1249.131	3	
			SC-PP-gas	NG-PP	0.539	0.121	1.038	3	
			SC-PP-oil	CO-HF-PP	0.645	0.145	1.242	3	
			SC-PP-oil	CO-LF-PP	0.018	0.004	0.035	3	
			WASOTH	WASOTH	392.902	117.871	1178.706		2
			WI	WI	177.914	53.374	533.741		2
HUN	Hungary	EU28	BIO	PSB – DR	92.077	21.868	169.191	1	
			BIO	PSB – IND	4.449	1.057	8.175	1	
			BIO	PSB – PP	24.081	5.719	44.249	1	
			CEM	CEM	117.249	41.407	731.910	1	
			CEM	PC-CEM	1.891	1.123	10.177	1	
			CREM	CREM	22.941	18.025	27.447		1
			CSP	CSP-C	327.500	114.625	638.625	1	
			NFMP	AL-P	3.875	1.356	7.556	1	
			OR	CO-OR	11.700	5.558	18.428	1	
			PISP	PIP	25.888	9.075	137.019	1	
			SC-DR-coal	BC-DR	55.575	31.678	126.433	1	
			SC-DR-coal	HC-DR	3.150	1.796	7.166	1	
			SC-DR-gas	NG-DR	0.937	0.223	1.722	1	
			SC-DR-oil	CO-HF-DR	0.120	0.029	0.221	1	
			SC-DR-oil	CO-LF-DR	5.784	1.374	10.628	1	
			SC-IND-coal	BC-IND-CEM	3.018	1.720	6.866	1	
			SC-IND-coal	BC-IND-OTH	1.328	0.757	3.020	1	
			SC-IND-coal	HC-IND-CEM	1.358	0.774	3.090	1	
			SC-IND-gas	NG-IND	0.291	0.069	0.534	1	
			SC-IND-oil	CO-HF-IND	0.057	0.014	0.105	1	
			SC-IND-oil	CO-LF-IND	0.302	0.072	0.555	1	
			SC-PP-coal	BC-L-PP	735.755	454.329	2317.628	1	
			SC-PP-coal	BC-S-PP	7.530	4.292	17.130	1	

Country code	Country name	Region	Sector Code	Activity Code	Emission estimate, kg	Low range estimate, kg	High range estimate, kg	Technology group	Waste group
			SC-PP-coal	HC-B-PP	0.725	0.413	1.648	1	
			SC-PP-gas	NG-PP	0.402	0.095	0.738	1	
			SC-PP-oil	CO-HF-PP	0.380	0.090	0.698	1	
			SC-PP-oil	CO-LF-PP	0.018	0.004	0.033	1	
			SSC	SP-S	4.155	1.546	19.824	1	
			WASOTH	WASOTH	55.181	16.554	165.543		1
			WI	WI	21.091	6.327	63.272		1
ISL	Iceland	CIS & other European countries	CREM	CREM	0.144	0.105	0.192		1
			NFMP	AL-P	10.000	3.390	18.885	1	
			SC-DR-oil	CO-HF-DR	1.220	0.290	2.242	1	
			SC-DR-oil	CO-LF-DR	0.578	0.137	1.062	1	
			SC-IND-coal	HC-IND-PIP	8.048	4.587	18.308	1	
			SC-IND-oil	CO-HF-IND	0.057	0.014	0.105	1	
			SC-IND-oil	CO-LF-IND	0.057	0.014	0.105	1	
			SC-PP-oil	CO-LF-PP	0.002	0.000	0.003	1	
			WASOTH	WASOTH	7.544	2.263	22.633		1
			WI	WI	2.884	0.865	8.651		1
IND	India	South Asia	ASGM	GP-A	4500.000	2250.000	6750.000		
			BIO	PSB – DR	7492.341	1685.777	14422.757	5	
			BIO	PSB – IND	1616.101	363.623	3110.994	5	
			BIO	PSB – PP	716.340	161.177	1378.955	5	
			CEM	CEM	25660.250	12457.638	43581.038	5	
			CEM	PC-CEM	580.840	326.722	3274.484	5	
			CREM	CREM	725.706	601.300	829.379		4
			NFMP	AL-P	730.050	255.518	1423.598	5	
			NFMP	CU-P	973.675	521.203	1913.558	5	
			NFMP	PB-P	223.938	97.973	436.679	5	
			NFMP	ZN-T	15582.788	5520.691	42807.396	5	
			NFMP-AU	GP-L	77.000	26.950	150.150	5	
			OR	CO-OR	3426.774	1542.048	5654.177	5	
			PISP	PIP	4011.341	1481.202	9312.799	5	
			SC-DR-coal	HC-DR	8330.176	5248.011	11912.152	5	
			SC-DR-gas	NG-DR	0.908	0.204	1.747	5	
			SC-DR-oil	CO-HF-DR	41.360	9.306	79.618	5	
			SC-DR-oil	CO-LF-DR	126.750	28.519	243.994	5	
			SC-IND-coal	BC-IND-CEM	135.573	85.411	193.870	5	
			SC-IND-coal	BC-IND-NFM	294.117	185.294	420.587	5	
			SC-IND-coal	BC-IND-OTH	687.715	433.260	983.432	5	
			SC-IND-coal	BC-IND-PIP	3.460	2.180	4.948	5	
			SC-IND-coal	HC-IND-CEM	7460.493	4700.110	10668.505	5	
			SC-IND-coal	HC-IND-NFM	120.450	75.884	172.244	5	
			SC-IND-coal	HC-IND-OTH	12143.003	7650.092	17364.494	5	
			SC-IND-coal	HC-IND-PIP	18397.095	11590.170	26307.846	5	
			SC-IND-gas	NG-IND	1.085	0.244	2.088	5	
			SC-IND-oil	CO-HF-IND	72.080	16.218	138.754	5	

Country code	Country name	Region	Sector Code	Activity Code	Emission estimate, kg	Low range estimate, kg	High range estimate, kg	Technology group	Waste group
			SC-IND-oil	CO-LF-IND	7.936	1.786	15.277	5	
			SC-PP-coal	BC-L-PP	10752.176	6773.871	15375.611	5	
			SC-PP-coal	BC-S-PP	10724.535	5791.249	25560.142	5	
			SC-PP-coal	HC-B-PP	39722.715	25025.311	56803.483	5	
			SC-PP-gas	NG-PP	3.321	0.747	6.393	5	
			SC-PP-oil	CO-HF-PP	9.620	2.165	18.519	5	
			SC-PP-oil	CO-LF-PP	14.158	3.186	27.254	5	
			SSC	SP-S	1504.506	559.968	7178.988	5	
			VCM	VCM-P	25.000	8.750	48.750	5	
			VCM	VCM-R	125.000	43.750	243.750	5	
			WASOTH	WASOTH	28752.358	8625.707	86257.073		4
			WI	WI	89.973	26.992	269.919		4
IDN	Indonesia	East and Southeast Asia	ASGM	GP-A	124541.667	62270.833	186812.500		
			BIO	PSB – DR	2496.141	561.632	4805.072	3	
			BIO	PSB – IND	291.393	65.563	560.931	3	
			BIO	PSB – PP	9.543	2.147	18.370	3	
			CEM	CEM	5057.600	1786.400	26661.440	3	
			CREM	CREM	13.184	11.997	14.630		2
			CSP	CSP-C	125.000	43.750	243.750	3	
			NFMP	AL-P	38.750	13.563	75.563	3	
			NFMP	CU-P	1631.249	582.225	9313.314	3	
			NFMP-AU	GP-L	2435.400	852.390	4749.030	3	
			NFMP-HG	HG-P	3037.500	1063.125	5923.125	3	
			OR	CO-OR	526.087	236.739	868.043	3	
			SC-DR-gas	NG-DR	0.058	0.013	0.111	3	
			SC-DR-oil	CO-HF-DR	2.080	0.468	4.004	3	
			SC-DR-oil	CO-LF-DR	33.680	7.578	64.834	3	
			SC-IND-coal	BC-IND-CEM	861.600	465.264	2053.480	3	
			SC-IND-coal	BC-IND-OTH	1165.605	629.427	2778.025	3	
			SC-IND-coal	HC-IND-PIP	44.888	24.239	106.982	3	
			SC-IND-gas	NG-IND	2.949	0.664	5.678	3	
			SC-IND-oil	CO-HF-IND	10.944	2.462	21.067	3	
			SC-IND-oil	CO-LF-IND	5.504	1.238	10.596	3	
			SC-PP-coal	BC-S-PP	8199.360	4427.654	19541.808	3	
			SC-PP-gas	NG-PP	4.702	1.058	9.052	3	
			SC-PP-oil	CO-HF-PP	34.155	7.685	65.748	3	
			SC-PP-oil	CO-LF-PP	5.825	1.311	11.212	3	
			SSC	SP-S	111.730	41.585	533.136	3	
			WASOTH	WASOTH	5904.542	1771.363	17713.625		2
			WI	WI	172.034	51.610	516.103		2
IRN	Iran	Middle Eastern States	ASGM	GP-A	225.000	56.250	393.750		
			BIO	PSB – DR	26.166	5.887	50.370	3	
			CEM	CEM	5966.400	2106.720	30922.320	3	
			CREM	CREM	1.255	0.941	1.464		4
			CSP	CSP-C	1660.000	581.000	3237.000	3	

Country code	Country name	Region	Sector Code	Activity Code	Emission estimate, kg	Low range estimate, kg	High range estimate, kg	Technology group	Waste group
			NFMP	AL-P	54.250	18.988	105.788	3	
			NFMP	CU-P	1266.118	451.903	7228.661	3	
			NFMP	PB-P	20.536	11.186	32.443	3	
			NFMP	ZN-P	1556.520	551.446	4275.908	3	
			NFMP-AU	GP-L	118.800	41.580	231.660	3	
			OR	CO-OR	43.593	19.617	71.928	3	
			PISP	PIP	153.358	53.760	811.701	3	
			SC-DR-coal	HC-DR	2.100	1.134	5.005	3	
			SC-DR-gas	NG-DR	12.404	2.791	23.877	3	
			SC-DR-oil	CO-HF-DR	93.580	21.056	180.142	3	
			SC-DR-oil	CO-LF-DR	37.506	8.439	72.199	3	
			SC-IND-coal	HC-IND-OTH	27.225	14.702	64.886	3	
			SC-IND-gas	NG-IND	7.469	1.681	14.378	3	
			SC-IND-oil	CO-HF-IND	26.771	6.023	51.534	3	
			SC-IND-oil	CO-LF-IND	3.785	0.852	7.286	3	
			SC-PP-gas	NG-PP	14.048	3.161	27.043	3	
			SC-PP-oil	CO-HF-PP	102.555	23.075	197.418	3	
			SC-PP-oil	CO-LF-PP	7.878	1.773	15.165	3	
			SSC	SP-S	343.340	127.789	1638.299	3	
			WASOTH	WASOTH	2280.120	684.036	6840.359		4
			WI	WI	7.135	2.141	21.405		4
IRQ	Iraq	Middle Eastern States	BIO	PSB – DR	0.356	0.080	0.686	3	
			CEM	CEM	1175.200	414.960	6090.760	3	
			CREM	CREM	0.867	0.650	1.012		4
			CSP	CSP-C	340.000	119.000	663.000	3	
			OR	CO-OR	3.558	1.601	5.870	3	
			SC-DR-oil	CO-LF-DR	7.086	1.594	13.641	3	
			SC-IND-gas	NG-IND	0.232	0.052	0.446	3	
			SC-IND-oil	CO-HF-IND	4.028	0.906	7.754	3	
			SC-IND-oil	CO-LF-IND	3.365	0.757	6.477	3	
			SC-PP-gas	NG-PP	1.037	0.233	1.995	3	
			SC-PP-oil	CO-HF-PP	87.915	19.781	169.236	3	
			SC-PP-oil	CO-LF-PP	12.549	2.824	24.157	3	
			SC-PP-oil	CO-PP	80.978	18.220	155.882	3	
			WASOTH	WASOTH	967.569	290.271	2902.706		4
			WI	WI	3.028	0.908	9.083		4
IRL	Ireland	EU28	BIO	PSB – DR	2.503	0.595	4.600	1	
			BIO	PSB – IND	5.560	1.320	10.216	1	
			BIO	PSB – PP	1.849	0.439	3.398	1	
			CEM	CEM	115.690	40.844	789.911	1	
			CEM	PC-CEM	3.280	1.947	17.648	1	
			CREM	CREM	3.452	2.712	4.130		1
			NFMP	AL-P	24.788	8.402	46.811	1	
			OR	CO-OR	6.080	2.888	9.577	1	
			SC-DR-coal	HC-DR	35.044	19.975	79.725	1	

Country code	Country name	Region	Sector Code	Activity Code	Emission estimate, kg	Low range estimate, kg	High range estimate, kg	Technology group	Waste group
			SC-DR-gas	NG-DR	0.222	0.053	0.407	1	
			SC-DR-oil	CO-LF-DR	6.276	1.491	11.532	1	
			SC-IND-coal	HC-IND-CEM	9.507	5.419	21.628	1	
			SC-IND-coal	HC-IND-OTH	2.289	1.305	5.208	1	
			SC-IND-gas	NG-IND	0.178	0.042	0.327	1	
			SC-IND-oil	CO-HF-IND	0.950	0.226	1.746	1	
			SC-IND-oil	CO-LF-IND	0.264	0.063	0.485	1	
			SC-PP-coal	HC-B-PP	97.601	55.632	222.041	1	
			SC-PP-gas	NG-PP	0.441	0.105	0.810	1	
			SC-PP-oil	CO-HF-PP	0.600	0.143	1.103	1	
			SC-PP-oil	CO-LF-PP	0.027	0.006	0.050	1	
			WASOTH	WASOTH	67.415	20.225	202.246		1
			WI	WI	25.767	7.730	77.301		1
ISR	Israel	Middle Eastern States	BIO	PSB – DR	0.223	0.053	0.410	1	
			CEM	CEM	505.882	178.626	2621.858	1	
			CREM	CREM	0.000	0.000	0.000		2
			CSP	CSP-C	82.500	28.875	160.875	1	
			OR	CO-OR	4.251	2.019	6.695	1	
			SC-DR-gas	NG-DR	0.016	0.004	0.029	1	
			SC-DR-oil	CO-HF-DR	0.180	0.043	0.331	1	
			SC-DR-oil	CO-LF-DR	5.056	1.201	9.290	1	
			SC-IND-gas	NG-IND	0.116	0.027	0.212	1	
			SC-IND-oil	CO-HF-IND	4.959	1.178	9.112	1	
			SC-PP-coal	HC-B-PP	578.310	329.636	1315.654	1	
			SC-PP-gas	NG-PP	1.532	0.364	2.814	1	
			SC-PP-oil	CO-HF-PP	0.200	0.048	0.368	1	
			SC-PP-oil	CO-LF-PP	0.141	0.033	0.259	1	
			SSC	SP-S	7.002	2.606	33.411	1	
			WASOTH	WASOTH	339.948	101.984	1019.845		2
			WI	WI	9.905	2.971	29.714		2
ITA	Italy	EU28	BIO	PSB – DR	328.424	78.001	603.479	1	
			BIO	PSB – IND	14.045	3.336	25.807	1	
			BIO	PSB – PP	75.663	17.970	139.032	1	
			CEM	CEM	1162.534	410.654	6471.975	1	
			CEM	PC-CEM	36.377	21.599	195.754	1	
			CREM	CREM	43.216	33.956	51.705		1
			NFMP	PB-P	1.220	0.665	1.924	1	
			NFMP	ZN-P	36.415	12.901	100.035	1	
			OR	CO-OR	121.196	57.568	190.884	1	
			PISP	PIP	205.904	72.181	1089.822	1	
			SC-DR-gas	NG-DR	5.748	1.365	10.561	1	
			SC-DR-oil	CO-HF-DR	8.200	1.948	15.068	1	
			SC-DR-oil	CO-LF-DR	50.332	11.954	92.485	1	
			SC-IND-coal	BC-IND-CEM	0.226	0.129	0.515	1	
			SC-IND-coal	HC-IND-CEM	16.901	9.633	38.449	1	

Country code	Country name	Region	Sector Code	Activity Code	Emission estimate, kg	Low range estimate, kg	High range estimate, kg	Technology group	Waste group
			SC-IND-coal	HC-IND-PIP	11.031	6.287	25.095	1	
			SC-IND-gas	NG-IND	1.924	0.457	3.536	1	
			SC-IND-oil	CO-HF-IND	15.124	3.592	27.790	1	
			SC-IND-oil	CO-LF-IND	0.762	0.181	1.400	1	
			SC-PP-coal	BC-S-PP	48.561	27.680	110.475	1	
			SC-PP-coal	HC-B-PP	821.221	468.096	1868.277	1	
			SC-PP-gas	NG-PP	4.997	1.187	9.182	1	
			SC-PP-oil	CO-HF-PP	11.540	2.741	21.205	1	
			SC-PP-oil	CO-LF-PP	0.158	0.037	0.289	1	
			SSC	SP-S	401.450	149.417	1915.583	1	
			WASOTH	WASOTH	479.796	143.939	1439.388		1
			WI	WI	183.383	55.015	550.149		1
CIV	Ivory Coast	Sub-Saharan Africa	ASGM	GP-A	225.000	56.250	393.750		
			BIO	PSB – DR	165.478	37.232	318.544	5	
			BIO	PSB – PP	2.356	0.530	4.536	5	
			CEM	CEM	273.000	96.460	1416.220	5	
			CREM	CREM	0.526	0.379	0.758		4
			NFMP-AU	GP-L	1430.000	500.500	2788.500	5	
			OR	CO-OR	0.239	0.108	0.394	5	
			SC-DR-oil	CO-LF-DR	1.574	0.354	3.030	5	
			SC-IND-gas	NG-IND	0.058	0.013	0.112	5	
			SC-IND-oil	CO-HF-IND	0.580	0.131	1.117	5	
			SC-IND-oil	CO-LF-IND	0.392	0.088	0.755	5	
			SC-PP-gas	NG-PP	0.338	0.076	0.650	5	
			SC-PP-oil	CO-HF-PP	3.040	0.684	5.852	5	
			SC-PP-oil	CO-LF-PP	0.006	0.001	0.012	5	
			WASOTH	WASOTH	395.044	170.830	608.582		4
			WI	WI	0.076	0.033	0.117		4
JAM	Jamaica	Central America and the Caribbean	BIO	PSB – DR	2.311	0.520	4.449	3	
			BIO	PSB – IND	3.834	0.863	7.379	3	
			BIO	PSB – PP	3.884	0.874	7.476	3	
			CEM	CEM	70.384	24.867	386.282	3	
			CREM	CREM	0.560	0.448	0.673		4
			NFMP	AL-P	289.075	101.176	563.696	3	
			OR	CO-OR	1.017	0.458	1.678	3	
			SC-DR-oil	CO-HF-DR	0.140	0.032	0.270	3	
			SC-DR-oil	CO-LF-DR	0.344	0.077	0.662	3	
			SC-IND-coal	HC-IND-CEM	11.640	6.286	27.742	3	
			SC-IND-oil	CO-HF-IND	11.134	2.505	21.433	3	
			SC-IND-oil	CO-LF-IND	0.063	0.014	0.121	3	
			SC-PP-oil	CO-HF-PP	10.005	2.251	19.260	3	
			SC-PP-oil	CO-LF-PP	0.272	0.061	0.523	3	
			WASOTH	WASOTH	65.168	19.550	195.503		4
			WI	WI	0.204	0.061	0.612		4

Country code	Country name	Region	Sector Code	Activity Code	Emission estimate, kg	Low range estimate, kg	High range estimate, kg	Technology group	Waste group
JPN	Japan	East and Southeast Asia	BIO	PSB – DR	0.575	0.137	1.057	1	
			BIO	PSB – IND	89.190	21.183	163.886	1	
			BIO	PSB – PP	283.006	67.214	520.023	1	
			CEM	CEM	3455.321	1209.362	6737.876	1	
			CEM	PC-CEM	18.984	11.272	102.158	1	
			CREM	CREM	100.941	91.850	112.012		1
			NFMP	AL-P	0.375	0.127	0.708	1	
			NFMP	CU-P	226.143	80.715	1291.118	1	
			NFMP	PB-P	2.074	1.130	3.271	1	
			NFMP	ZN-T	1334.048	472.628	3664.756	1	
			NFMP-AU	GP-L	17.787	6.225	34.685	1	
			OR	CO-OR	1138.132	540.613	1792.558	1	
			PISP	PIP	2218.834	1510.824	4405.394	1	
			SC-DR-coal	HC-DR	0.079	0.053	0.108	1	
			SC-DR-gas	NG-DR	4.194	0.996	7.707	1	
			SC-DR-oil	CO-HF-DR	43.760	10.393	80.409	1	
			SC-DR-oil	CO-LF-DR	58.912	13.992	108.251	1	
			SC-IND-coal	HC-IND-CEM	181.732	120.852	248.064	1	
			SC-IND-coal	HC-IND-NFM	1.197	0.796	1.634	1	
			SC-IND-coal	HC-IND-OTH	83.786	55.718	114.368	1	
			SC-IND-coal	HC-IND-PIP	37.365	24.848	51.004	1	
			SC-IND-gas	NG-IND	2.590	0.615	4.759	1	
			SC-IND-oil	CO-HF-IND	38.304	9.097	70.384	1	
			SC-IND-oil	CO-IND	0.219	0.052	0.401	1	
			SC-IND-oil	CO-LF-IND	12.721	3.021	23.374	1	
			SC-PP-coal	HC-B-PP	1297.024	862.521	1770.438	1	
			SC-PP-gas	NG-PP	17.703	4.204	32.529	1	
			SC-PP-oil	CO-HF-PP	107.440	25.517	197.421	1	
			SC-PP-oil	CO-LF-PP	2.057	0.488	3.779	1	
			SC-PP-oil	CO-PP	24.375	5.789	44.789	1	
			SSC	SP-S	599.351	223.075	2859.898	1	
			WASOTH	WASOTH	2398.913	719.674	7196.738		1
			WI	WI	1209.410	362.823	3628.231		1
JOR	Jordan	Middle Eastern States	BIO	PSB – DR	0.193	0.043	0.371	3	
			CEM	CEM	406.800	143.640	2108.340	3	
			CEM	PC-CEM	6.368	3.582	35.900	3	
			CREM	CREM	0.248	0.186	0.289		4
			OR	CO-OR	1.220	0.549	2.013	3	
			SC-DR-oil	CO-HF-DR	0.020	0.005	0.039	3	
			SC-DR-oil	CO-LF-DR	2.930	0.659	5.640	3	
			SC-IND-coal	HC-IND-CEM	30.360	16.394	72.358	3	
			SC-IND-oil	CO-LF-IND	0.281	0.063	0.541	3	
			SC-PP-gas	NG-PP	0.452	0.102	0.870	3	
			SC-PP-oil	CO-HF-PP	26.025	5.856	50.098	3	
			SC-PP-oil	CO-LF-PP	0.846	0.190	1.629	3	

Country code	Country name	Region	Sector Code	Activity Code	Emission estimate, kg	Low range estimate, kg	High range estimate, kg	Technology group	Waste group
			SSC	SP-S	3.785	1.409	18.060	3	
			WASOTH	WASOTH	139.567	41.870	418.700		4
			WI	WI	0.437	0.131	1.310		4
KAZ	Kazakhstan	CIS & other European countries	ASGM	GP-A	225.000	56.250	393.750		
			BIO	PSB – DR	3.669	0.825	7.062	4	
			CEM	CEM	781.746	276.054	3965.267	4	
			CREM	CREM	8.332	6.110	11.110		4
			NFMP	AL-P	62.000	21.700	120.900	4	
			NFMP	CU-P	3544.937	1265.258	20239.155	4	
			NFMP	PB-T	1105.272	401.134	2841.275	4	
			NFMP	ZN-T	5090.841	1803.590	13985.022	4	
			NFMP-AU	GP-L	3148.893	1102.113	6140.341	4	
			OR	CO-OR	16.522	7.435	27.261	4	
			PISP	PIP	192.629	67.527	1019.557	4	
			SC-DR-coal	BC-DR	75.900	40.986	180.895	4	
			SC-DR-coal	HC-DR	900.450	486.243	2146.073	4	
			SC-DR-gas	NG-DR	0.257	0.058	0.495	4	
			SC-DR-oil	CO-HF-DR	9.800	2.205	18.865	4	
			SC-DR-oil	CO-LF-DR	5.548	1.248	10.680	4	
			SC-IND-coal	BC-IND-CEM	4.725	2.552	11.261	4	
			SC-IND-coal	BC-IND-OTH	305.516	164.979	728.147	4	
			SC-IND-coal	HC-IND-NFM	296.363	160.036	706.331	4	
			SC-IND-coal	HC-IND-OTH	171.413	92.563	408.533	4	
			SC-IND-coal	HC-IND-PIP	304.106	164.217	724.787	4	
			SC-IND-gas	NG-IND	0.416	0.093	0.800	4	
			SC-IND-oil	CO-HF-IND	21.700	4.883	41.773	4	
			SC-IND-oil	CO-IND	4.880	1.098	9.394	4	
			SC-IND-oil	CO-LF-IND	3.474	0.782	6.687	4	
			SC-PP-coal	BC-L-PP	4.116	2.408	13.583	4	
			SC-PP-coal	HC-B-PP	4772.363	2577.076	11374.131	4	
			SC-PP-gas	NG-PP	5.463	1.229	10.516	4	
			SC-PP-oil	CO-HF-PP	9.140	2.057	17.595	4	
			SC-PP-oil	CO-LF-PP	0.450	0.101	0.866	4	
			SC-PP-oil	CO-PP	8.880	1.998	17.094	4	
			SSC	SP-S	4.522	1.683	21.578	4	
			WASOTH	WASOTH	1253.031	375.909	3759.093		4
			WI	WI	3.921	1.176	11.763		4
KEN	Kenya	Sub-Saharan Africa	ASGM	GP-A	2625.000	656.250	4593.750		
			BIO	PSB – DR	424.496	95.512	817.155	5	
			BIO	PSB – PP	1.830	0.412	3.523	5	
			CEM	CEM	586.215	207.129	3041.060	5	
			CREM	CREM	1.036	0.747	1.494		4
			NFMP-AU	GP-L	16.500	5.775	32.175	5	
			OR	CO-OR	0.588	0.265	0.971	5	
			SC-DR-oil	CO-HF-DR	0.280	0.063	0.539	5	

Country code	Country name	Region	Sector Code	Activity Code	Emission estimate, kg	Low range estimate, kg	High range estimate, kg	Technology group	Waste group
			SC-DR-oil	CO-LF-DR	2.934	0.660	5.648	5	
			SC-IND-coal	HC-IND-CEM	84.900	45.846	202.345	5	
			SC-IND-oil	CO-HF-IND	1.500	0.338	2.888	5	
			SC-IND-oil	CO-LF-IND	0.896	0.202	1.725	5	
			SC-PP-oil	CO-HF-PP	3.720	0.837	7.161	5	
			SC-PP-oil	CO-LF-PP	0.334	0.075	0.643	5	
			SSC	SP-S	0.599	0.223	2.860	5	
			WASOTH	WASOTH	704.310	304.566	1085.018		4
			WI	WI	0.135	0.058	0.208		4
KIR	Kiribati	Australia, New Zealand & Oceania	BIO	PSB – DR	0.430	0.075	0.979	4	
			BIO	PSB – IND	0.017	0.003	0.039	4	
			CREM	CREM	0.327	0.294	0.392		4
			OR	CO-OR	0.001	0.000	0.001	4	
			SC-DR-gas	NG-DR	0.000	0.000	0.000	4	
			SC-DR-oil	CO-HF-DR	0.002	0.000	0.004	4	
			SC-DR-oil	CO-LF-DR	0.005	0.001	0.010	4	
			SC-IND-coal	BC-IND-OTH	0.004	0.002	0.011	4	
			SC-IND-coal	HC-IND-OTH	0.255	0.107	0.717	4	
			SC-IND-oil	CO-HF-IND	0.004	0.001	0.009	4	
			SC-IND-oil	CO-LF-IND	0.000	0.000	0.001	4	
			SC-PP-coal	HC-B-PP	0.057	0.024	0.162	4	
			SC-PP-gas	NG-PP	0.000	0.000	0.000	4	
			SC-PP-oil	CO-HF-PP	0.020	0.004	0.046	4	
			SC-PP-oil	CO-LF-PP	0.003	0.000	0.006	4	
			WASOTH	WASOTH	0.744	0.223	2.232		4
			WI	WI	0.002	0.001	0.007		4
PRK	Korea – Dem. Rep.	East and Southeast Asia	BIO	PSB – DR	40.838	9.188	78.612	4	
			CEM	CEM	686.700	242.550	3619.980	4	
			CREM	CREM	16.023	14.580	17.780		4
			CSP	CSP-C	250.000	87.500	487.500	4	
			NFMP	CU-T	138.384	49.392	790.078	4	
			NFMP	PB-T	26.316	9.551	67.649	4	
			NFMP	ZN-T	313.920	111.216	862.368	4	
			OR	CO-OR	6.902	3.106	11.388	4	
			PISP	PIP	54.432	19.081	288.101	4	
			SC-DR-coal	BC-DR	127.650	68.931	304.233	4	
			SC-DR-coal	HC-DR	160.200	86.508	381.810	4	
			SC-DR-oil	CO-LF-DR	0.504	0.113	0.970	4	
			SC-IND-coal	BC-IND-OTH	210.893	113.882	502.627	4	
			SC-IND-coal	HC-IND-OTH	542.325	292.856	1292.541	4	
			SC-IND-oil	CO-HF-IND	1.860	0.419	3.581	4	
			SC-PP-coal	BC-S-PP	31.995	17.277	76.255	4	
			SC-PP-coal	HC-B-PP	95.625	51.638	227.906	4	
			SC-PP-oil	CO-HF-PP	7.600	1.710	14.630	4	
			WASOTH	WASOTH	141.477	42.443	424.430		4
			WI	WI	0.443	0.133	1.328		4

Country code	Country name	Region	Sector Code	Activity Code	Emission estimate, kg	Low range estimate, kg	High range estimate, kg	Technology group	Waste group
KOR	Korea – Rep. of	East and Southeast Asia	BIO	PSB – DR	52.453	12.457	96.382	1	
			BIO	PSB – IND	22.507	5.345	41.356	1	
			BIO	PSB – PP	11.524	2.737	21.175	1	
			CEM	CEM	1256.863	477.077	2059.662	1	
			CEM	PC-CEM	0.901	0.535	4.846	1	
			CREM	CREM	40.570	36.916	45.020		1
			NFMP	CU-P	49.011	17.493	279.819	1	
			NFMP	PB-P	3.550	1.935	5.599	1	
			NFMP	ZN-P	243.335	86.209	668.465	1	
			NFMP-AU	GP-L	0.693	0.243	1.351	1	
			OR	CO-OR	967.676	338.686	1886.968	1	
			PISP	PIP	686.503	472.266	907.840	1	
			SC-DR-gas	NG-DR	3.045	0.723	5.595	1	
			SC-DR-oil	CO-HF-DR	9.180	2.180	16.868	1	
			SC-DR-oil	CO-LF-DR	40.100	9.524	73.684	1	
			SC-IND-coal	HC-IND-CEM	126.736	84.279	172.994	1	
			SC-IND-coal	HC-IND-OTH	30.476	20.267	41.600	1	
			SC-IND-coal	HC-IND-PIP	45.667	30.368	62.335	1	
			SC-IND-gas	NG-IND	1.724	0.410	3.168	1	
			SC-IND-oil	CO-HF-IND	23.959	5.690	44.025	1	
			SC-IND-oil	CO-LF-IND	2.402	0.570	4.413	1	
			SC-PP-coal	BC-S-PP	744.669	424.461	1694.122	1	
			SC-PP-coal	HC-A-PP	38.097	25.335	52.003	1	
			SC-PP-coal	HC-B-PP	927.510	616.794	1266.050	1	
			SC-PP-gas	NG-PP	4.475	1.063	8.223	1	
			SC-PP-oil	CO-HF-PP	32.990	7.835	60.619	1	
			SC-PP-oil	CO-LF-PP	0.167	0.040	0.306	1	
			SC-PP-oil	CO-PP	0.014	0.003	0.025	1	
			SSC	SP-S	340.210	128.161	509.428	1	
			WASOTH	WASOTH	670.657	201.197	2011.971		1
			WI	WI	570.215	171.064	1710.645		1
XKX	Kosovo	CIS & other European countries	BIO	PSB – DR	13.159	2.961	25.331	5	
			BIO	PSB – IND	0.620	0.139	1.193	5	
			CEM	CEM	70.560	24.917	357.903	5	
			CEM	PC-CEM	3.160	1.778	17.815	5	
			CREM	CREM	0.464	0.340	0.618		
			SC-DR-coal	BC-DR	23.400	12.636	55.770	5	
			SC-DR-oil	CO-HF-DR	0.180	0.041	0.347	5	
			SC-DR-oil	CO-LF-DR	0.688	0.155	1.324	5	
			SC-IND-coal	BC-IND-OTH	1.778	0.960	4.236	5	
			SC-IND-coal	BC-IND-PIP	7.999	4.319	19.064	5	
			SC-IND-coal	HC-IND-PIP	1.688	0.911	4.022	5	
			SC-IND-oil	CO-HF-IND	0.400	0.090	0.770	5	
			SC-IND-oil	CO-LF-IND	0.078	0.018	0.150	5	
			SC-PP-coal	BC-L-PP	798.014	466.838	2633.446	5	

Country code	Country name	Region	Sector Code	Activity Code	Emission estimate, kg	Low range estimate, kg	High range estimate, kg	Technology group	Waste group
			SC-PP-oil	CO-HF-PP	0.080	0.018	0.154	5	
			SC-PP-oil	CO-LF-PP	0.004	0.001	0.008	5	
			WASOTH	WASOTH	32.777	9.833	98.331		
			WI	WI	0.955	0.286	2.865		
KWT	Kuwait	Middle Eastern States	CEM	CEM	291.133	102.798	1508.869	1	
			CREM	CREM	0.086	0.064	0.100		2
			OR	CO-OR	10.915	4.912	18.010	1	
			SC-DR-oil	CO-LF-DR	2.512	0.565	4.836	1	
			SC-IND-gas	NG-IND	1.310	0.295	2.521	1	
			SC-IND-oil	CO-LF-IND	1.590	0.358	3.061	1	
			SC-PP-gas	NG-PP	2.663	0.599	5.127	1	
			SC-PP-oil	CO-HF-PP	58.620	13.190	112.844	1	
			SC-PP-oil	CO-LF-PP	2.175	0.489	4.187	1	
			SC-PP-oil	CO-PP	8.465	1.905	16.295	1	
			WASOTH	WASOTH	322.490	96.747	967.471		2
			WI	WI	9.396	2.819	28.188		2
KGZ	Kyrgystan	CIS & other European countries	ASGM	GP-A	3562.500	890.625	6234.375		
			BIO	PSB – DR	0.151	0.034	0.291	4	
			CEM	CEM	169.246	59.765	858.470	4	
			CREM	CREM	0.981	0.719	1.308		4
			NFMP-AU	GP-L	841.500	294.525	1640.925	4	
			NFMP-HG	HG-P	270.000	94.500	526.500	4	
			OR	CO-OR	0.365	0.164	0.603	4	
			SC-DR-coal	BC-DR	81.450	43.983	194.123	4	
			SC-DR-coal	HC-DR	25.050	13.527	59.703	4	
			SC-DR-gas	NG-DR	0.023	0.005	0.044	4	
			SC-DR-oil	CO-HF-DR	0.260	0.059	0.501	4	
			SC-DR-oil	CO-LF-DR	0.962	0.216	1.852	4	
			SC-IND-coal	BC-IND-CEM	12.994	7.017	30.968	4	
			SC-IND-coal	BC-IND-OTH	0.585	0.316	1.394	4	
			SC-IND-coal	HC-IND-CEM	47.775	25.799	113.864	4	
			SC-IND-coal	HC-IND-OTH	1.050	0.567	2.503	4	
			SC-IND-gas	NG-IND	0.005	0.001	0.009	4	
			SC-IND-oil	CO-HF-IND	4.840	1.089	9.317	4	
			SC-IND-oil	CO-LF-IND	0.078	0.018	0.150	4	
			SC-PP-coal	BC-L-PP	44.296	25.913	146.177	4	
			SC-PP-coal	HC-B-PP	109.463	59.110	260.886	4	
			SC-PP-gas	NG-PP	0.023	0.005	0.043	4	
			SC-PP-oil	CO-HF-PP	0.560	0.126	1.078	4	
			SC-PP-oil	CO-LF-PP	0.032	0.007	0.062	4	
			WASOTH	WASOTH	58.559	17.568	175.677		4
			WI	WI	0.183	0.055	0.550		4
LAO	Lao Peoples Dem. Rep.	East and Southeast Asia	ASGM	GP-A	2250.000	1125.000	3375.000		
			BIO	PSB – DR	28.145	4.925	64.030	4	
			BIO	PSB – IND	3.332	0.583	7.581	4	

Country code	Country name	Region	Sector Code	Activity Code	Emission estimate, kg	Low range estimate, kg	High range estimate, kg	Technology group	Waste group
			CEM	CEM	228.900	80.850	1206.660	4	
			CREM	CREM	4.478	4.075	4.969		4
			NFMP-AU	GP-L	341.204	119.421	665.347	4	
			OR	CO-OR	3.600	1.260	7.020	4	
			SC-DR-gas	NG-DR	0.007	0.001	0.016	4	
			SC-DR-oil	CO-HF-DR	0.345	0.060	0.785	4	
			SC-DR-oil	CO-LF-DR	0.884	0.155	2.011	4	
			SC-IND-coal	BC-IND-OTH	0.777	0.326	2.188	4	
			SC-IND-coal	HC-IND-OTH	49.000	20.580	138.018	4	
			SC-IND-oil	CO-HF-IND	0.757	0.132	1.722	4	
			SC-IND-oil	CO-LF-IND	0.083	0.014	0.188	4	
			SC-PP-coal	HC-B-PP	11.054	4.643	31.136	4	
			SC-PP-gas	NG-PP	0.008	0.001	0.017	4	
			SC-PP-oil	CO-HF-PP	3.899	0.682	8.871	4	
			SC-PP-oil	CO-LF-PP	0.510	0.089	1.160	4	
			WASOTH	WASOTH	121.303	36.391	363.908		4
			WI	WI	0.380	0.114	1.139		4
LVA	Latvia	EU28	BIO	PSB – DR	27.967	6.292	53.836	2	
			BIO	PSB – IND	12.415	2.793	23.899	2	
			BIO	PSB – PP	14.931	3.360	28.743	2	
			CEM	CEM	67.000	23.450	130.649	2	
			CREM	CREM	4.567	3.588	5.464		1
			SC-DR-coal	HC-DR	4.200	2.268	10.010	2	
			SC-DR-gas	NG-DR	0.046	0.010	0.088	2	
			SC-DR-oil	CO-LF-DR	1.808	0.407	3.480	2	
			SC-IND-coal	HC-IND-CEM	3.018	1.630	7.193	2	
			SC-IND-coal	HC-IND-OTH	0.169	0.091	0.402	2	
			SC-IND-gas	NG-IND	0.028	0.006	0.054	2	
			SC-IND-oil	CO-LF-IND	0.068	0.015	0.132	2	
			SC-PP-coal	HC-B-PP	0.362	0.196	0.863	2	
			SC-PP-gas	NG-PP	0.180	0.040	0.346	2	
			SC-PP-oil	CO-LF-PP	0.011	0.002	0.020	2	
			WASOTH	WASOTH	10.450	3.135	31.351		1
			WI	WI	3.994	1.198	11.983		1
LBN	Lebanon	Middle Eastern States	BIO	PSB – DR	5.114	1.151	9.844	3	
			CEM	CEM	498.737	176.103	2584.825	3	
			CREM	CREM	1.418	1.063	1.654		4
			SC-DR-oil	CO-LF-DR	1.496	0.337	2.880	3	
			SC-IND-coal	HC-IND-CEM	30.360	16.394	72.358	3	
			SC-IND-oil	CO-HF-IND	2.679	0.603	5.157	3	
			SC-PP-oil	CO-HF-PP	20.010	4.502	38.519	3	
			SC-PP-oil	CO-LF-PP	3.926	0.883	7.557	3	
			WASOTH	WASOTH	137.429	41.229	412.286		4
			WI	WI	0.430	0.129	1.290		4

Country code	Country name	Region	Sector Code	Activity Code	Emission estimate, kg	Low range estimate, kg	High range estimate, kg	Technology group	Waste group
LSO	Lesotho	Sub-Saharan Africa	ASGM	GP-A	225.000	75.000	375.000		
			BIO	PSB – DR	22.241	3.892	50.597	4	
			BIO	PSB – IND	0.987	0.173	2.245	4	
			BIO	PSB – PP	0.362	0.063	0.824	4	
			CREM	CREM	0.043	0.031	0.062		4
			SC-DR-coal	HC-DR	0.198	0.083	0.556	4	
			SC-DR-oil	CO-LF-DR	0.088	0.015	0.201	4	
			SC-IND-coal	HC-IND-OTH	0.179	0.075	0.504	4	
			SC-IND-gas	NG-IND	0.000	0.000	0.000	4	
			SC-IND-oil	CO-HF-IND	0.161	0.028	0.366	4	
			SC-IND-oil	CO-IND	0.022	0.004	0.050	4	
			SC-IND-oil	CO-LF-IND	0.015	0.003	0.035	4	
			SC-PP-coal	HC-B-PP	1.298	0.545	3.656	4	
			SC-PP-gas	NG-PP	0.002	0.000	0.003	4	
			SC-PP-oil	CO-HF-PP	0.209	0.037	0.476	4	
			SC-PP-oil	CO-LF-PP	0.043	0.008	0.098	4	
			WASOTH	WASOTH	31.748	13.729	48.910		4
			WI	WI	0.006	0.003	0.009		4
LBR	Liberia	Sub-Saharan Africa	ASGM	GP-A	225.000	56.250	393.750		
			BIO	PSB – DR	47.910	8.384	108.995	5	
			BIO	PSB – IND	0.646	0.113	1.470	5	
			BIO	PSB – PP	0.234	0.041	0.532	5	
			CEM	CEM	30.975	10.945	160.687	5	
			CREM	CREM	0.095	0.069	0.137		4
			NFMP-AU	GP-L	48.565	16.998	94.702	5	
			SC-DR-coal	HC-DR	0.128	0.054	0.360	5	
			SC-DR-oil	CO-LF-DR	0.057	0.010	0.130	5	
			SC-IND-coal	HC-IND-OTH	0.124	0.052	0.349	5	
			SC-IND-gas	NG-IND	0.000	0.000	0.000	5	
			SC-IND-oil	CO-HF-IND	0.104	0.018	0.236	5	
			SC-IND-oil	CO-IND	0.014	0.002	0.032	5	
			SC-IND-oil	CO-LF-IND	0.010	0.002	0.023	5	
			SC-PP-coal	HC-B-PP	0.839	0.352	2.363	5	
			SC-PP-gas	NG-PP	0.001	0.000	0.002	5	
			SC-PP-oil	CO-HF-PP	0.135	0.024	0.307	5	
			SC-PP-oil	CO-LF-PP	0.028	0.005	0.064	5	
			WASOTH	WASOTH	18.579	8.034	28.621		4
			WI	WI	0.004	0.002	0.005		4
LBY	Libyan Arab Jamah	North Africa	BIO	PSB – DR	7.940	1.787	15.285	5	
			CEM	CEM	210.000	74.200	1089.400	5	
			CREM	CREM	0.084	0.063	0.105		4
			CSP	CSP-C	900.000	315.000	1755.000	5	
			OR	CO-OR	8.421	3.790	13.895	5	
			SC-DR-oil	CO-LF-DR	3.894	0.876	7.496	5	
			SC-IND-gas	NG-IND	0.011	0.002	0.021	5	

Country code	Country name	Region	Sector Code	Activity Code	Emission estimate, kg	Low range estimate, kg	High range estimate, kg	Technology group	Waste group
			SC-IND-oil	CO-HF-IND	5.060	1.139	9.741	5	
			SC-PP-gas	NG-PP	1.093	0.246	2.104	5	
			SC-PP-oil	CO-HF-PP	22.260	5.009	42.851	5	
			SC-PP-oil	CO-LF-PP	6.654	1.497	12.809	5	
			SSC	SP-S	21.334	7.940	101.799	5	
			WASOTH	WASOTH	265.938	79.781	797.814		4
			WI	WI	0.051	0.015	0.153		4
LTU	Lithuania	EU28	BIO	PSB – DR	27.240	6.129	52.438	2	
			BIO	PSB – IND	2.980	0.670	5.736	2	
			BIO	PSB – PP	25.927	5.834	49.910	2	
			CEM	CEM	49.963	17.646	304.388	2	
			CREM	CREM	6.631	5.210	7.933		1
			OR	CO-OR	15.329	6.898	25.293	2	
			SC-DR-coal	HC-DR	13.650	7.371	32.533	2	
			SC-DR-gas	NG-DR	0.055	0.012	0.105	2	
			SC-DR-oil	CO-LF-DR	2.672	0.601	5.144	2	
			SC-IND-coal	HC-IND-CEM	10.638	5.745	25.355	2	
			SC-IND-coal	HC-IND-OTH	0.253	0.137	0.603	2	
			SC-IND-gas	NG-IND	0.066	0.015	0.127	2	
			SC-IND-oil	CO-HF-IND	0.190	0.043	0.366	2	
			SC-IND-oil	CO-LF-IND	0.038	0.009	0.073	2	
			SC-PP-coal	HC-B-PP	0.207	0.112	0.493	2	
			SC-PP-gas	NG-PP	0.141	0.032	0.272	2	
			SC-PP-oil	CO-HF-PP	1.160	0.261	2.233	2	
			SC-PP-oil	CO-LF-PP	0.008	0.002	0.014	2	
			WASOTH	WASOTH	17.825	5.348	53.476		1
			WI	WI	6.813	2.044	20.439		1
LUX	Luxembourg	EU28	BIO	PSB – DR	1.055	0.251	1.939	1	
			BIO	PSB – IND	0.945	0.224	1.736	1	
			BIO	PSB – PP	0.805	0.191	1.478	1	
			CEM	CEM	61.970	21.883	395.969	1	
			CREM	CREM	1.623	1.275	1.942		1
			SC-DR-gas	NG-DR	0.075	0.018	0.138	1	
			SC-DR-oil	CO-LF-DR	3.606	0.856	6.626	1	
			SC-IND-coal	HC-IND-CEM	4.678	2.666	10.642	1	
			SC-IND-coal	HC-IND-PIP	0.763	0.435	1.736	1	
			SC-IND-gas	NG-IND	0.065	0.015	0.120	1	
			SC-IND-oil	CO-LF-IND	0.025	0.006	0.045	1	
			SC-PP-gas	NG-PP	0.040	0.009	0.073	1	
			SC-PP-oil	CO-LF-PP	0.002	0.000	0.003	1	
			SSC	SP-S	51.185	19.051	244.237	1	
			WASOTH	WASOTH	12.587	3.776	37.762		1
			WI	WI	4.811	1.443	14.433		1

Country code	Country name	Region	Sector Code	Activity Code	Emission estimate, kg	Low range estimate, kg	High range estimate, kg	Technology group	Waste group
MKD	Macedonia	CIS & other European countries	BIO	PSB – DR	12.203	2.746	23.490	4	
			BIO	PSB – IND	0.294	0.066	0.565	4	
			BIO	PSB – PP	0.003	0.001	0.005	4	
			CEM	CEM	67.326	23.774	341.499	4	
			CEM	PC-CEM	1.995	1.122	11.247	4	
			CREM	CREM	0.000	0.000	0.000		2
			SC-DR-coal	BC-DR	1.500	0.810	3.575	4	
			SC-DR-gas	NG-DR	0.001	0.000	0.003	4	
			SC-DR-oil	CO-HF-DR	0.260	0.059	0.501	4	
			SC-DR-oil	CO-LF-DR	0.996	0.224	1.917	4	
			SC-IND-coal	BC-IND-CEM	0.131	0.071	0.313	4	
			SC-IND-coal	BC-IND-OTH	1.024	0.553	2.440	4	
			SC-IND-coal	BC-IND-PIP	27.788	15.005	66.227	4	
			SC-IND-coal	HC-IND-PIP	1.575	0.851	3.754	4	
			SC-IND-gas	NG-IND	0.006	0.001	0.012	4	
			SC-IND-oil	CO-HF-IND	1.060	0.239	2.041	4	
			SC-IND-oil	CO-LF-IND	0.088	0.020	0.169	4	
			SC-PP-coal	BC-L-PP	571.634	334.406	1886.392	4	
			SC-PP-gas	NG-PP	0.019	0.004	0.036	4	
			SC-PP-oil	CO-HF-PP	0.780	0.176	1.502	4	
			SC-PP-oil	CO-LF-PP	0.004	0.001	0.008	4	
			SSC	SP-S	5.485	2.041	26.172	4	
			WASOTH	WASOTH	54.761	16.428	164.283		2
			WI	WI	1.596	0.479	4.787		2
MDG	Madagascar	Sub-Saharan Africa	ASGM	GP-A	1125.000	281.250	1968.750		
			BIO	PSB – DR	271.914	47.585	618.604	5	
			BIO	PSB – IND	6.111	1.069	13.902	5	
			BIO	PSB – PP	2.214	0.387	5.036	5	
			CEM	CEM	25.200	8.904	130.728	5	
			CREM	CREM	0.541	0.390	0.780		4
			SC-DR-coal	HC-DR	1.207	0.507	3.401	5	
			SC-DR-oil	CO-LF-DR	0.540	0.095	1.229	5	
			SC-IND-coal	HC-IND-OTH	1.172	0.492	3.302	5	
			SC-IND-gas	NG-IND	0.000	0.000	0.000	5	
			SC-IND-oil	CO-HF-IND	0.983	0.172	2.237	5	
			SC-IND-oil	CO-IND	0.135	0.024	0.307	5	
			SC-IND-oil	CO-LF-IND	0.094	0.016	0.214	5	
			SC-PP-coal	HC-B-PP	7.934	3.332	22.348	5	
			SC-PP-gas	NG-PP	0.009	0.002	0.021	5	
			SC-PP-oil	CO-HF-PP	1.278	0.224	2.908	5	
			SC-PP-oil	CO-LF-PP	0.264	0.046	0.602	5	
			WASOTH	WASOTH	175.383	75.841	270.184		4
			WI	WI	0.034	0.015	0.052		4

Country code	Country name	Region	Sector Code	Activity Code	Emission estimate, kg	Low range estimate, kg	High range estimate, kg	Technology group	Waste group
MWI	Malawi	Sub-Saharan Africa	ASGM	GP-A	225.000	56.250	393.750		
			BIO	PSB – DR	205.137	35.899	466.686	4	
			BIO	PSB – IND	3.338	0.584	7.594	4	
			BIO	PSB – PP	1.225	0.214	2.786	4	
			CEM	CEM	41.344	14.608	214.476	4	
			CREM	CREM	0.411	0.296	0.593		4
			SC-DR-coal	HC-DR	0.668	0.281	1.881	4	
			SC-DR-oil	CO-LF-DR	0.299	0.052	0.680	4	
			SC-IND-coal	HC-IND-OTH	0.605	0.254	1.705	4	
			SC-IND-gas	NG-IND	0.000	0.000	0.000	4	
			SC-IND-oil	CO-HF-IND	0.544	0.095	1.237	4	
			SC-IND-oil	CO-IND	0.075	0.013	0.170	4	
			SC-IND-oil	CO-LF-IND	0.052	0.009	0.118	4	
			SC-PP-coal	HC-B-PP	4.390	1.844	12.364	4	
			SC-PP-gas	NG-PP	0.005	0.001	0.012	4	
			SC-PP-oil	CO-HF-PP	0.707	0.124	1.609	4	
			SC-PP-oil	CO-LF-PP	0.146	0.026	0.333	4	
			WASOTH	WASOTH	100.602	43.504	154.981		4
			WI	WI	0.019	0.008	0.030		4
MYS	Malaysia	East and Southeast Asia	ASGM	GP-A	1662.500	415.625	2909.375		
			BIO	PSB – DR	30.925	6.958	59.530	2	
			BIO	PSB – PP	10.495	2.361	20.204	2	
			CEM	CEM	1654.620	584.430	8722.428	2	
			CREM	CREM	4.936	4.492	5.478		2
			NFMP	AL-P	68.200	23.870	132.990	2	
			NFMP-AU	GP-L	127.527	44.635	248.678	2	
			OR	CO-OR	223.797	100.708	369.264	2	
			SC-DR-gas	NG-DR	0.067	0.015	0.129	2	
			SC-DR-oil	CO-HF-DR	4.160	0.936	8.008	2	
			SC-DR-oil	CO-LF-DR	15.746	3.543	30.311	2	
			SC-IND-coal	HC-IND-OTH	238.022	128.532	567.285	2	
			SC-IND-gas	NG-IND	1.118	0.252	2.153	2	
			SC-IND-oil	CO-HF-IND	9.405	2.116	18.105	2	
			SC-IND-oil	CO-LF-IND	2.595	0.584	4.996	2	
			SC-PP-coal	HC-B-PP	2389.040	1290.082	5693.878	2	
			SC-PP-gas	NG-PP	5.802	1.305	11.168	2	
			SC-PP-oil	CO-HF-PP	1.190	0.268	2.291	2	
			SC-PP-oil	CO-LF-PP	0.488	0.110	0.938	2	
			SC-PP-oil	CO-PP	1.915	0.431	3.686	2	
			SSC	SP-S	100.736	37.493	480.678	2	
			WASOTH	WASOTH	1693.648	508.094	5080.944		2
			WI	WI	49.346	14.804	148.038		2

Country code	Country name	Region	Sector Code	Activity Code	Emission estimate, kg	Low range estimate, kg	High range estimate, kg	Technology group	Waste group
MDV	Maldives	South Asia	BIO	PSB – DR	1.601	0.280	3.643	5	
			BIO	PSB – IND	0.540	0.094	1.228	5	
			CREM	CREM	0.001	0.001	0.001		4
			OR	CO-OR	1.226	0.429	2.391	5	
			SC-DR-gas	NG-DR	0.001	0.000	0.003	5	
			SC-DR-oil	CO-HF-DR	0.055	0.010	0.126	5	
			SC-DR-oil	CO-LF-DR	0.141	0.025	0.322	5	
			SC-IND-coal	BC-IND-OTH	0.126	0.053	0.354	5	
			SC-IND-coal	HC-IND-OTH	8.398	3.527	23.654	5	
			SC-IND-oil	CO-HF-IND	0.121	0.021	0.275	5	
			SC-IND-oil	CO-LF-IND	0.013	0.002	0.030	5	
			SC-PP-coal	HC-B-PP	1.768	0.743	4.980	5	
			SC-PP-gas	NG-PP	0.001	0.000	0.003	5	
			SC-PP-oil	CO-HF-PP	0.624	0.109	1.419	5	
			SC-PP-oil	CO-LF-PP	0.082	0.014	0.186	5	
			WASOTH	WASOTH	18.733	5.620	56.198		4
			WI	WI	0.059	0.018	0.176		4
MLI	Mali	Sub-Saharan Africa	ASGM	GP-A	9375.000	4687.500	14062.500		
			BIO	PSB – DR	193.613	33.882	440.470	5	
			BIO	PSB – IND	6.381	1.117	14.518	5	
			BIO	PSB – PP	2.312	0.405	5.260	5	
			CREM	CREM	0.193	0.139	0.279		4
			NFMP-AU	GP-L	2265.230	792.831	4417.199	5	
			SC-DR-coal	HC-DR	1.261	0.530	3.552	5	
			SC-DR-oil	CO-LF-DR	0.564	0.099	1.283	5	
			SC-IND-coal	HC-IND-OTH	1.224	0.514	3.448	5	
			SC-IND-gas	NG-IND	0.000	0.000	0.000	5	
			SC-IND-oil	CO-HF-IND	1.027	0.180	2.336	5	
			SC-IND-oil	CO-IND	0.141	0.025	0.321	5	
			SC-IND-oil	CO-LF-IND	0.098	0.017	0.224	5	
			SC-PP-coal	HC-B-PP	8.286	3.480	23.339	5	
			SC-PP-gas	NG-PP	0.010	0.002	0.022	5	
			SC-PP-oil	CO-HF-PP	1.335	0.234	3.037	5	
			SC-PP-oil	CO-LF-PP	0.276	0.048	0.628	5	
			WASOTH	WASOTH	176.280	76.229	271.567		4
			WI	WI	0.034	0.015	0.052		4
MLT	Malta	EU28	BIO	PSB – DR	0.059	0.013	0.113	1	
			CREM	CREM	0.965	0.758	1.154		1
			SC-DR-oil	CO-HF-DR	0.120	0.027	0.231	1	
			SC-DR-oil	CO-LF-DR	0.284	0.064	0.547	1	
			SC-IND-oil	CO-HF-IND	0.076	0.017	0.146	1	
			SC-IND-oil	CO-LF-IND	0.008	0.002	0.015	1	
			SC-PP-oil	CO-HF-PP	2.540	0.572	4.890	1	
			SC-PP-oil	CO-LF-PP	0.030	0.007	0.058	1	
			WASOTH	WASOTH	3.286	0.986	9.858		1
			WI	WI	1.256	0.377	3.768		1

Country code	Country name	Region	Sector Code	Activity Code	Emission estimate, kg	Low range estimate, kg	High range estimate, kg	Technology group	Waste group
MHL	Marshall Islands	Australia, New Zealand & Oceania	CREM	CREM	0.224	0.202	0.269		4
			WASOTH	WASOTH	0.688	0.206	2.063		4
			WI	WI	0.002	0.001	0.006		4
MTQ	Martinique	Central America and the Caribbean	BIO	PSB – DR	0.501	0.088	1.140	3	
			CEM	CEM	12.720	4.494	69.810	3	
			CREM	CREM	0.073	0.058	0.088		4
			WASOTH	WASOTH	0.000	0.000	0.000		4
			WI	WI	0.000	0.000	0.000		4
MRT	Mauritania	Sub-Saharan Africa	ASGM	GP-A	225.000	56.250	393.750		
			BIO	PSB – DR	41.070	7.187	93.435	5	
			BIO	PSB – IND	2.707	0.474	6.159	5	
			BIO	PSB – PP	0.981	0.172	2.231	5	
			CEM	CEM	80.850	28.567	419.419	5	
			CREM	CREM	0.000	0.000	0.001		4
			NFMP-AU	GP-L	484.000	169.400	943.800	5	
			SC-DR-coal	HC-DR	0.535	0.225	1.507	5	
			SC-DR-oil	CO-LF-DR	0.239	0.042	0.544	5	
			SC-IND-coal	HC-IND-OTH	0.519	0.218	1.463	5	
			SC-IND-gas	NG-IND	0.000	0.000	0.000	5	
			SC-IND-oil	CO-HF-IND	0.436	0.076	0.991	5	
			SC-IND-oil	CO-IND	0.060	0.010	0.136	5	
			SC-IND-oil	CO-LF-IND	0.042	0.007	0.095	5	
			SC-PP-coal	HC-B-PP	3.515	1.476	9.901	5	
			SC-PP-gas	NG-PP	0.004	0.001	0.009	5	
			SC-PP-oil	CO-HF-PP	0.566	0.099	1.288	5	
			SC-PP-oil	CO-LF-PP	0.117	0.021	0.267	5	
			WASOTH	WASOTH	79.205	34.251	122.019		4
			WI	WI	0.015	0.007	0.023		4
MUS	Mauritius	Sub-Saharan Africa	BIO	PSB – DR	0.271	0.061	0.522	5	
			BIO	PSB – IND	1.660	0.374	3.196	5	
			BIO	PSB – PP	10.386	2.337	19.994	5	
			CREM	CREM	0.030	0.022	0.043		4
			SC-DR-oil	CO-HF-DR	0.060	0.014	0.116	5	
			SC-DR-oil	CO-LF-DR	0.342	0.077	0.658	5	
			SC-IND-coal	HC-IND-OTH	5.063	2.734	12.066	5	
			SC-IND-oil	CO-HF-IND	0.740	0.167	1.425	5	
			SC-IND-oil	CO-LF-IND	0.074	0.017	0.142	5	
			SC-PP-coal	HC-B-PP	76.950	41.553	183.398	5	
			SC-PP-oil	CO-HF-PP	4.600	1.035	8.855	5	
			SC-PP-oil	CO-LF-PP	0.002	0.000	0.004	5	
			WASOTH	WASOTH	75.729	32.748	116.664		4
			WI	WI	2.206	0.954	3.399		4

Country code	Country name	Region	Sector Code	Activity Code	Emission estimate, kg	Low range estimate, kg	High range estimate, kg	Technology group	Waste group
MEX	Mexico	Central America and the Caribbean	ASGM	GP-A	3562.500	890.625	6234.375		
			BIO	PSB – DR	316.050	75.062	580.742	3	
			BIO	PSB – IND	39.472	9.375	72.530	3	
			BIO	PSB – PP	79.051	18.775	145.256	3	
			CEM	CEM	1120.000	401.800	8736.000	3	
			CEM	PC-CEM	121.248	71.991	652.466	3	
			CREM	CREM	34.861	27.889	41.833		3
			CSP	CSP-C	600.000	210.000	1170.000	3	
			NFMP	CU-P	2091.136	746.368	11938.950	3	
			NFMP	PB-P	148.886	81.099	235.210	3	
			NFMP	ZN-P	3631.606	1286.610	9976.365	3	
			NFMP-AU	GP-L	5336.456	1867.760	10406.090	3	
			NFMP-HG	HG-P	2025.000	708.750	3948.750	3	
			OR	CO-OR	53.537	25.430	84.320	3	
			PISP	PIP	284.598	99.767	1506.336	3	
			SC-DR-gas	NG-DR	0.245	0.058	0.450	3	
			SC-DR-oil	CO-HF-DR	0.500	0.119	0.919	3	
			SC-DR-oil	CO-LF-DR	34.108	8.101	62.673	3	
			SC-IND-coal	BC-IND-CEM	77.352	51.439	105.585	3	
			SC-IND-coal	BC-IND-OTH	631.342	419.842	861.781	3	
			SC-IND-coal	HC-IND-OTH	10.013	5.707	22.778	3	
			SC-IND-gas	NG-IND	2.883	0.685	5.298	3	
			SC-IND-oil	CO-HF-IND	10.184	2.419	18.713	3	
			SC-IND-oil	CO-LF-IND	3.042	0.722	5.589	3	
			SC-PP-coal	BC-S-PP	2373.616	1578.455	3239.986	3	
			SC-PP-coal	HC-B-PP	539.460	307.492	1227.272	3	
			SC-PP-gas	NG-PP	11.156	2.650	20.500	3	
			SC-PP-oil	CO-HF-PP	113.580	26.975	208.703	3	
			SC-PP-oil	CO-LF-PP	1.829	0.434	3.360	3	
			SSC	SP-S	335.871	125.009	1602.660	3	
			WASOTH	WASOTH	3461.718	1038.515	10385.153		3
			WI	WI	23.816	7.145	71.447		3
MCO	Monaco	CIS & other European countries	CREM	CREM	0.071	0.056	0.085		1
			WASOTH	WASOTH	3.669	1.101	11.006		1
			WI	WI	1.402	0.421	4.207		1
MNG	Mongolia	East and Southeast Asia	ASGM	GP-A	5462.500	2731.250	8193.750		
			BIO	PSB – DR	3.961	0.891	7.625	3	
			CEM	CEM	35.839	12.659	188.928	3	
			CREM	CREM	0.725	0.660	0.805		4
			NFMP-AU	GP-L	576.418	201.746	1124.014	3	
			SC-DR-coal	BC-DR	73.950	39.933	176.248	3	
			SC-DR-coal	HC-DR	61.350	33.129	146.218	3	
			SC-DR-oil	CO-LF-DR	0.464	0.104	0.893	3	
			SC-IND-coal	BC-IND-OTH	4.463	2.410	10.636	3	
			SC-IND-coal	HC-IND-OTH	2.588	1.397	6.167	3	

Country code	Country name	Region	Sector Code	Activity Code	Emission estimate, kg	Low range estimate, kg	High range estimate, kg	Technology group	Waste group
			SC-IND-oil	CO-LF-IND	0.663	0.149	1.276	3	
			SC-PP-coal	BC-L-PP	510.649	298.730	1685.141	3	
			SC-PP-coal	HC-B-PP	144.686	78.131	344.836	3	
			SC-PP-oil	CO-HF-PP	0.045	0.010	0.087	3	
			SC-PP-oil	CO-LF-PP	0.111	0.025	0.214	3	
			SSC	SP-S	1.135	0.423	5.418	3	
			WASOTH	WASOTH	113.770	34.131	341.310		4
			WI	WI	0.356	0.107	1.068		4
MSR	Monserrat	Central America and the Caribbean	BIO	PSB – DR	0.007	0.001	0.015	3	
			BIO	PSB – IND	0.008	0.001	0.019	3	
			BIO	PSB – PP	0.003	0.001	0.007	3	
			CREM	CREM	0.001	0.001	0.001		4
			OR	CO-OR	0.001	0.000	0.002	3	
			SC-DR-coal	HC-DR	0.030	0.013	0.085	3	
			SC-DR-gas	NG-DR	0.000	0.000	0.000	3	
			SC-DR-oil	CO-HF-DR	0.001	0.000	0.002	3	
			SC-DR-oil	CO-LF-DR	0.002	0.000	0.005	3	
			SC-IND-gas	NG-IND	0.000	0.000	0.000	3	
			SC-IND-oil	CO-HF-IND	0.002	0.000	0.006	3	
			SC-IND-oil	CO-LF-IND	0.000	0.000	0.000	3	
			SC-PP-gas	NG-PP	0.000	0.000	0.000	3	
			SC-PP-oil	CO-HF-PP	0.023	0.004	0.053	3	
			SC-PP-oil	CO-LF-PP	0.002	0.000	0.004	3	
			WASOTH	WASOTH	0.115	0.035	0.345		4
			WI	WI	0.000	0.000	0.001		4
MNE	Montenegro	CIS & other European countries	BIO	PSB – DR	8.360	1.881	16.093	4	
			BIO	PSB – IND	0.483	0.109	0.929	4	
			CREM	CREM	0.265	0.194	0.353		
			NFMP	AL-P	12.400	4.340	24.180	4	
			SC-DR-coal	BC-DR	3.300	1.782	7.865	4	
			SC-DR-oil	CO-HF-DR	0.040	0.009	0.077	4	
			SC-DR-oil	CO-LF-DR	0.296	0.067	0.570	4	
			SC-IND-coal	BC-IND-OTH	0.878	0.474	2.091	4	
			SC-IND-coal	BC-IND-PIP	3.510	1.895	8.366	4	
			SC-IND-oil	CO-HF-IND	0.060	0.014	0.116	4	
			SC-IND-oil	CO-LF-IND	0.072	0.016	0.139	4	
			SC-PP-coal	BC-L-PP	163.464	95.626	539.431	4	
			SSC	SP-S	4.085	1.520	19.490	4	
			WASOTH	WASOTH	18.910	5.673	56.729		
			WI	WI	0.551	0.165	1.653		
MAR	Morocco	North Africa	BIO	PSB – DR	63.864	14.369	122.938	5	
			BIO	PSB – IND	1.566	0.352	3.015	5	
			CEM	CEM	1555.290	549.850	8036.451	5	
			CEM	PC-CEM	48.880	27.495	275.561	5	
			CREM	CREM	0.058	0.043	0.072		4

Country code	Country name	Region	Sector Code	Activity Code	Emission estimate, kg	Low range estimate, kg	High range estimate, kg	Technology group	Waste group
			CSP	CSP-C	160.000	56.000	312.000	5	
			NFMP-AU	GP-L	27.500	9.625	53.625	5	
			NFMP-HG	HG-P	33.750	11.813	65.813	5	
			OR	CO-OR	5.057	2.276	8.344	5	
			PISP	PIP	0.945	0.331	5.002	5	
			SC-DR-oil	CO-HF-DR	0.020	0.005	0.039	5	
			SC-DR-oil	CO-LF-DR	10.108	2.274	19.458	5	
			SC-IND-coal	HC-IND-CEM	0.300	0.162	0.715	5	
			SC-IND-coal	HC-IND-NFM	2.109	1.139	5.027	5	
			SC-IND-coal	HC-IND-OTH	1.406	0.759	3.352	5	
			SC-IND-gas	NG-IND	0.015	0.003	0.030	5	
			SC-IND-oil	CO-HF-IND	13.860	3.119	26.681	5	
			SC-IND-oil	CO-LF-IND	0.444	0.100	0.855	5	
			SC-PP-coal	HC-B-PP	754.538	407.450	1798.314	5	
			SC-PP-gas	NG-PP	0.220	0.049	0.423	5	
			SC-PP-oil	CO-HF-PP	14.280	3.213	27.489	5	
			SC-PP-oil	CO-LF-PP	0.020	0.005	0.039	5	
			SSC	SP-S	15.012	5.587	71.631	5	
			WASOTH	WASOTH	753.011	225.903	2259.034		4
			WI	WI	2.356	0.707	7.069		4
MOZ	Mozambique	Sub-Saharan Africa	ASGM	GP-A	3000.000	1500.000	4500.000		
			BIO	PSB – DR	336.011	75.603	646.822	4	
			BIO	PSB – IND	46.176	10.390	88.889	4	
			CEM	CEM	137.996	48.759	715.872	4	
			CREM	CREM	0.574	0.414	0.828		4
			NFMP	AL-P	172.980	60.543	337.311	4	
			NFMP-AU	GP-L	12.375	4.331	24.131	4	
			SC-DR-gas	NG-DR	0.001	0.000	0.001	4	
			SC-DR-oil	CO-LF-DR	1.198	0.270	2.306	4	
			SC-IND-gas	NG-IND	0.031	0.007	0.060	4	
			SC-IND-oil	CO-LF-IND	0.272	0.061	0.524	4	
			SC-PP-coal	HC-B-PP	1.575	0.851	3.754	4	
			SC-PP-gas	NG-PP	0.120	0.027	0.230	4	
			SC-PP-oil	CO-LF-PP	0.050	0.011	0.096	4	
			WASOTH	WASOTH	164.698	71.221	253.723		4
			WI	WI	0.032	0.014	0.049		4
MMR	Myanmar	East and Southeast Asia	ASGM	GP-A	11250.000	2812.500	19687.500		
			BIO	PSB – DR	509.531	114.645	980.848	5	
			BIO	PSB – IND	16.290	3.665	31.358	5	
			CEM	CEM	143.553	50.705	756.748	5	
			CREM	CREM	36.295	33.026	40.276		4
			CSP	CSP-C	140.000	49.000	273.000	5	
			NFMP	PB-P	5.307	2.883	8.369	5	
			NFMP-AU	GP-L	93.060	32.571	181.467	5	
			OR	CO-OR	8.264	3.719	13.636	5	

Country code	Country name	Region	Sector Code	Activity Code	Emission estimate, kg	Low range estimate, kg	High range estimate, kg	Technology group	Waste group
			PISP	PIP	0.095	0.033	0.500	5	
			SC-DR-coal	BC-DR	8.100	4.374	19.305	5	
			SC-DR-gas	NG-DR	0.045	0.010	0.087	5	
			SC-DR-oil	CO-HF-DR	0.680	0.153	1.309	5	
			SC-DR-oil	CO-LF-DR	2.674	0.602	5.147	5	
			SC-IND-coal	HC-IND-CEM	77.550	41.877	184.828	5	
			SC-IND-coal	HC-IND-OTH	9.422	5.088	22.455	5	
			SC-IND-gas	NG-IND	0.088	0.020	0.169	5	
			SC-IND-oil	CO-HF-IND	0.620	0.140	1.194	5	
			SC-IND-oil	CO-LF-IND	1.550	0.349	2.984	5	
			SC-PP-coal	HC-B-PP	12.713	6.865	30.298	5	
			SC-PP-gas	NG-PP	0.519	0.117	0.999	5	
			SC-PP-oil	CO-LF-PP	0.068	0.015	0.131	5	
			SSC	SP-S	1.049	0.390	5.004	5	
			WASOTH	WASOTH	890.161	267.048	2670.482		4
			WI	WI	2.786	0.836	8.357		4
NAM	Namibia	Sub-Saharan Africa	BIO	PSB – DR	5.038	1.133	9.697	3	
			BIO	PSB – IND	1.246	0.280	2.399	3	
			CEM	CEM	61.404	21.696	318.541	3	
			CREM	CREM	0.054	0.039	0.078		2
			NFMP	CU-P	1365.581	487.403	7796.530	3	
			NFMP	ZN-P	2300.976	817.765	4929.350	3	
			NFMP-AU	GP-L	241.758	84.615	471.428	3	
			SC-DR-oil	CO-HF-DR	0.320	0.072	0.616	3	
			SC-DR-oil	CO-LF-DR	1.352	0.304	2.603	3	
			SC-IND-oil	CO-HF-IND	0.038	0.009	0.073	3	
			SC-IND-oil	CO-LF-IND	0.167	0.038	0.322	3	
			SC-PP-coal	HC-B-PP	0.405	0.219	0.965	3	
			SC-PP-oil	CO-LF-PP	0.014	0.003	0.026	3	
			WASOTH	WASOTH	126.425	54.670	194.763		2
			WI	WI	0.024	0.010	0.037		2
NRU	Nauru	Australia, New Zealand & Oceania	CREM	CREM	0.029	0.026	0.035		4
			WASOTH	WASOTH	0.541	0.162	1.622		4
			WI	WI	0.002	0.001	0.005		4
NPL	Nepal	South Asia	BIO	PSB – DR	479.893	107.976	923.793	5	
			BIO	PSB – IND	3.021	0.680	5.814	5	
			CEM	CEM	337.900	119.350	1781.260	5	
			CREM	CREM	16.631	13.780	19.007		4
			SC-DR-coal	HC-DR	0.600	0.324	1.430	5	
			SC-DR-oil	CO-LF-DR	1.220	0.275	2.349	5	
			SC-IND-coal	HC-IND-OTH	130.078	70.242	310.020	5	
			SC-IND-oil	CO-LF-IND	0.018	0.004	0.035	5	
			WASOTH	WASOTH	251.685	75.505	755.054		4
			WI	WI	0.788	0.236	2.363		4

Country code	Country name	Region	Sector Code	Activity Code	Emission estimate, kg	Low range estimate, kg	High range estimate, kg	Technology group	Waste group
NLD	Netherlands	EU28	BIO	PSB – DR	26.767	6.357	49.185	1	
			BIO	PSB – IND	4.963	1.179	9.120	1	
			BIO	PSB – PP	22.556	5.357	41.447	1	
			CEM	CEM	112.672	39.787	719.944	1	
			CREM	CREM	47.440	37.274	56.759		1
			NFMP	AL-P	0.938	0.318	1.770	1	
			NFMP	ZN-P	76.126	26.970	209.124	1	
			OR	CO-OR	95.355	45.294	150.185	1	
			PISP	PIP	189.648	66.482	1003.779	1	
			SC-DR-gas	NG-DR	2.801	0.665	5.147	1	
			SC-DR-oil	CO-HF-DR	0.480	0.114	0.882	1	
			SC-DR-oil	CO-LF-DR	12.910	3.066	23.722	1	
			SC-IND-coal	BC-IND-CEM	2.037	1.161	4.635	1	
			SC-IND-coal	BC-IND-OTH	1.549	0.883	3.523	1	
			SC-IND-coal	HC-IND-OTH	2.289	1.305	5.208	1	
			SC-IND-gas	NG-IND	1.087	0.258	1.997	1	
			SC-IND-oil	CO-HF-IND	0.095	0.023	0.175	1	
			SC-IND-oil	CO-LF-IND	0.787	0.187	1.445	1	
			SC-PP-coal	HC-B-PP	697.383	397.508	1586.546	1	
			SC-PP-gas	NG-PP	2.272	0.540	4.174	1	
			SC-PP-oil	CO-HF-PP	0.070	0.017	0.129	1	
			SC-PP-oil	CO-LF-PP	0.033	0.008	0.061	1	
			SSC	SP-S	2.918	1.086	13.921	1	
			WASOTH	WASOTH	177.988	53.396	533.964		1
			WI	WI	68.029	20.409	204.087		1
NCL	New Caledonia	Australia, New Zealand & Oceania	BIO	PSB – DR	1.106	0.194	2.516	4	
			BIO	PSB – IND	0.959	0.168	2.181	4	
			CEM	CEM	10.110	3.571	53.294	4	
			CREM	CREM	0.842	0.757	1.009		4
			OR	CO-OR	0.042	0.015	0.081	4	
			SC-DR-gas	NG-DR	0.002	0.000	0.005	4	
			SC-DR-oil	CO-HF-DR	0.099	0.017	0.226	4	
			SC-DR-oil	CO-LF-DR	0.254	0.045	0.579	4	
			SC-IND-coal	BC-IND-OTH	0.223	0.094	0.629	4	
			SC-IND-coal	HC-IND-OTH	14.097	5.921	39.707	4	
			SC-IND-oil	CO-HF-IND	0.218	0.038	0.495	4	
			SC-IND-oil	CO-LF-IND	0.024	0.004	0.054	4	
			SC-PP-coal	HC-B-PP	3.180	1.336	8.958	4	
			SC-PP-gas	NG-PP	0.002	0.000	0.005	4	
			SC-PP-oil	CO-HF-PP	1.122	0.196	2.552	4	
			SC-PP-oil	CO-LF-PP	0.147	0.026	0.334	4	
			WASOTH	WASOTH	35.734	10.720	107.201		4
			WI	WI	0.112	0.034	0.335		4

Country code	Country name	Region	Sector Code	Activity Code	Emission estimate, kg	Low range estimate, kg	High range estimate, kg	Technology group	Waste group
NZL	New Zealand	Australia, New Zealand & Oceania	BIO	PSB – DR	7.943	1.886	14.595	2	
			BIO	PSB – IND	29.790	7.075	54.739	2	
			BIO	PSB – PP	4.024	0.956	7.394	2	
			CEM	CEM	82.731	29.222	436.121	2	
			CREM	CREM	13.687	12.293	16.391		1
			NFMP	AL-P	8.325	2.822	15.722	2	
			NFMP-AU	GP-L	312.620	109.417	609.609	2	
			OR	CO-OR	2.826	1.342	4.450	2	
			PISP	PIP	35.034	12.281	185.432	2	
			SC-DR-coal	BC-DR	24.716	14.088	56.229	2	
			SC-DR-gas	NG-DR	0.086	0.021	0.159	2	
			SC-DR-oil	CO-HF-DR	1.340	0.318	2.462	2	
			SC-DR-oil	CO-LF-DR	4.960	1.178	9.114	2	
			SC-IND-coal	BC-IND-NFM	0.298	0.170	0.678	2	
			SC-IND-coal	BC-IND-OTH	88.941	50.696	202.340	2	
			SC-IND-coal	HC-IND-CEM	12.006	6.843	27.314	2	
			SC-IND-coal	HC-IND-OTH	0.759	0.433	1.728	2	
			SC-IND-gas	NG-IND	0.289	0.069	0.531	2	
			SC-IND-oil	CO-LF-IND	0.631	0.150	1.159	2	
			SC-PP-coal	BC-L-PP	1.539	0.950	4.848	2	
			SC-PP-coal	BC-S-PP	69.525	39.629	158.169	2	
			SC-PP-gas	NG-PP	0.331	0.079	0.608	2	
			SSC	SP-S	6.162	2.293	29.402	2	
			WASOTH	WASOTH	97.032	29.110	291.096		1
			WI	WI	37.087	11.126	111.260		1
NIC	Nicaragua	Central America and the Caribbean	ASGM	GP-A	700.000	490.000	910.000		
			BIO	PSB – DR	50.664	11.399	97.528	3	
			BIO	PSB – IND	2.955	0.665	5.688	3	
			BIO	PSB – PP	22.746	5.118	43.786	3	
			CEM	CEM	59.360	20.972	325.780	3	
			CREM	CREM	1.126	0.901	1.351		4
			NFMP-AU	GP-L	324.720	113.652	633.204	3	
			OR	CO-OR	0.609	0.274	1.005	3	
			SC-DR-oil	CO-LF-DR	0.962	0.216	1.852	3	
			SC-IND-oil	CO-HF-IND	0.513	0.115	0.988	3	
			SC-IND-oil	CO-LF-IND	0.173	0.039	0.333	3	
			SC-PP-oil	CO-HF-PP	7.470	1.681	14.380	3	
			SC-PP-oil	CO-LF-PP	0.023	0.005	0.043	3	
			WASOTH	WASOTH	84.468	25.340	253.404		4
			WI	WI	0.264	0.079	0.793		4
NER	Niger	Sub-Saharan Africa	ASGM	GP-A	225.000	56.250	393.750		
			BIO	PSB – DR	110.349	24.828	212.421	5	
			CEM	CEM	2.205	0.779	11.439	5	
			CREM	CREM	0.103	0.074	0.149		4
			NFMP-AU	GP-L	66.495	23.273	129.665	5	

Country code	Country name	Region	Sector Code	Activity Code	Emission estimate, kg	Low range estimate, kg	High range estimate, kg	Technology group	Waste group
			OR	CO-OR	0.626	0.281	1.032	5	
			SC-DR-oil	CO-LF-DR	0.336	0.076	0.647	5	
			SC-IND-oil	CO-HF-IND	0.040	0.009	0.077	5	
			SC-IND-oil	CO-LF-IND	0.122	0.027	0.235	5	
			SC-PP-coal	BC-L-PP	21.658	12.670	71.471	5	
			SC-PP-oil	CO-HF-PP	0.320	0.072	0.616	5	
			SC-PP-oil	CO-LF-PP	0.106	0.024	0.204	5	
			WASOTH	WASOTH	93.898	40.604	144.653		4
			WI	WI	0.018	0.008	0.028		4
NGA	Nigeria	Sub-Saharan Africa	ASGM	GP-A	15000.000	7500.000	22500.000		
			BIO	PSB – DR	5011.861	1127.669	9647.833	5	
			BIO	PSB – IND	214.002	48.151	411.955	5	
			CEM	CEM	2100.000	742.000	10894.000	5	
			CREM	CREM	4.121	2.970	5.941		4
			NFMP-AU	GP-L	423.500	148.225	825.825	5	
			OR	CO-OR	1.001	0.451	1.652	5	
			SC-DR-oil	CO-LF-DR	1.054	0.237	2.029	5	
			SC-IND-coal	HC-IND-CEM	7.050	3.807	16.803	5	
			SC-IND-gas	NG-IND	0.595	0.134	1.146	5	
			SC-IND-oil	CO-HF-IND	9.020	2.030	17.364	5	
			SC-PP-gas	NG-PP	2.348	0.528	4.519	5	
			SC-PP-oil	CO-HF-PP	2.460	0.554	4.736	5	
			SC-PP-oil	CO-LF-PP	0.028	0.006	0.054	5	
			SSC	SP-S	2.996	1.115	14.298	5	
			WASOTH	WASOTH	5402.354	2336.153	8322.545		4
			WI	WI	1.035	0.447	1.594		4
NIU	Niue	Australia, New Zealand & Oceania	CREM	CREM	0.004	0.003	0.004		4
			WASOTH	WASOTH	0.033	0.010	0.100		4
			WI	WI	0.000	0.000	0.000		4
NFK	Norfolk Islands	Australia, New Zealand & Oceania	CREM	CREM	0.007	0.006	0.008		4
			WASOTH	WASOTH	0.000	0.000	0.000		4
			WI	WI	0.000	0.000	0.000		4
MNP	North Mariana Islands	Australia, New Zealand & Oceania	CREM	CREM	0.164	0.147	0.196		4
			WASOTH	WASOTH	2.263	0.679	6.788		4
			WI	WI	0.007	0.002	0.021		4
NOR	Norway	CIS & other European countries	BIO	PSB – DR	27.005	6.414	49.622	1	
			BIO	PSB – IND	9.509	2.258	17.473	1	
			BIO	PSB – PP	6.523	1.549	11.986	1	
			CEM	CEM	98.337	34.717	671.425	1	
			CEM	PC-CEM	0.262	0.155	1.408	1	
			CREM	CREM	3.607	2.645	4.809		1
			NFMP	AL-P	15.313	5.190	28.917	1	
			NFMP	ZN-P	39.938	14.161	115.314	1	
			OR	CO-OR	65.471	31.099	103.117	1	
			PISP	PIP	3.297	1.156	17.448	1	

Country code	Country name	Region	Sector Code	Activity Code	Emission estimate, kg	Low range estimate, kg	High range estimate, kg	Technology group	Waste group
			SC-DR-gas	NG-DR	0.037	0.009	0.068	1	
			SC-DR-oil	CO-HF-DR	0.180	0.043	0.331	1	
			SC-DR-oil	CO-LF-DR	7.818	1.857	14.366	1	
			SC-IND-coal	HC-IND-CEM	7.017	4.000	15.963	1	
			SC-IND-coal	HC-IND-OTH	18.176	10.360	41.351	1	
			SC-IND-coal	HC-IND-PIP	14.708	8.383	33.460	1	
			SC-IND-gas	NG-IND	0.060	0.014	0.110	1	
			SC-IND-oil	CO-HF-IND	0.114	0.027	0.209	1	
			SC-IND-oil	CO-LF-IND	0.581	0.138	1.068	1	
			SC-PP-coal	HC-B-PP	1.346	0.767	3.061	1	
			SC-PP-gas	NG-PP	1.015	0.241	1.865	1	
			SC-PP-oil	CO-LF-PP	0.320	0.076	0.587	1	
			SSC	SP-S	14.004	5.212	66.823	1	
			WASOTH	WASOTH	153.967	46.190	461.901		1
			WI	WI	58.848	17.654	176.543		1
PSE	Occupied Palestinian Territories	Middle Eastern States	CREM	CREM	0.135	0.101	0.157		4
			WASOTH	WASOTH	0.000	0.000	0.000		4
			WI	WI	0.000	0.000	0.000		4
OMN	Oman	Middle Eastern States	CEM	CEM	383.070	135.261	1985.354	1	
			CREM	CREM	0.102	0.076	0.119		2
			NFMP	AL-P	4.713	1.597	8.899	1	
			NFMP	CU-P	2.306	0.823	13.168	1	
			OR	CO-OR	3.455	1.555	5.700	1	
			SC-DR-gas	NG-DR	0.037	0.008	0.072	1	
			SC-DR-oil	CO-LF-DR	3.816	0.859	7.346	1	
			SC-IND-gas	NG-IND	2.235	0.503	4.302	1	
			SC-IND-oil	CO-LF-IND	0.792	0.178	1.525	1	
			SC-PP-gas	NG-PP	2.274	0.512	4.378	1	
			SC-PP-oil	CO-LF-PP	0.303	0.068	0.583	1	
			SSC	SP-S	35.010	13.031	167.057	1	
			WASOTH	WASOTH	199.233	59.770	597.700		2
			WI	WI	5.805	1.741	17.415		2
PAK	Pakistan	South Asia	BIO	PSB – DR	1484.223	333.950	2857.128	5	
			BIO	PSB – IND	184.385	41.487	354.941	5	
			CEM	CEM	3488.000	1232.000	18387.200	5	
			CREM	CREM	2.479	2.054	2.834		4
			CSP	CSP-C	660.000	231.000	1287.000	5	
			NFMP	CU-P	181.149	64.656	1034.234	5	
			OR	CO-OR	23.482	10.567	38.745	5	
			PISP	PIP	13.640	4.781	72.192	5	
			SC-DR-gas	NG-DR	1.976	0.445	3.803	5	
			SC-DR-oil	CO-HF-DR	0.140	0.032	0.270	5	
			SC-DR-oil	CO-LF-DR	13.538	3.046	26.061	5	
			SC-IND-coal	BC-IND-CEM	162.300	87.642	386.815	5	
			SC-IND-coal	HC-IND-CEM	1108.500	598.590	2641.925	5	

Country code	Country name	Region	Sector Code	Activity Code	Emission estimate, kg	Low range estimate, kg	High range estimate, kg	Technology group	Waste group
			SC-IND-gas	NG-IND	1.527	0.344	2.940	5	
			SC-IND-oil	CO-HF-IND	15.460	3.479	29.761	5	
			SC-IND-oil	CO-LF-IND	0.942	0.212	1.813	5	
			SC-PP-coal	HC-B-PP	17.775	9.599	42.364	5	
			SC-PP-gas	NG-PP	1.554	0.350	2.992	5	
			SC-PP-oil	CO-HF-PP	180.900	40.703	348.233	5	
			SC-PP-oil	CO-LF-PP	1.126	0.253	2.168	5	
			SSC	SP-S	68.317	25.427	325.986	5	
			WASOTH	WASOTH	3393.902	1018.171	10181.706		4
			WI	WI	10.620	3.186	31.861		4
PLW	Palau	Australia, New Zealand & Oceania	BIO	PSB – DR	0.087	0.015	0.197	4	
			BIO	PSB – IND	0.029	0.005	0.066	4	
			CREM	CREM	0.065	0.059	0.078		4
			OR	CO-OR	0.001	0.000	0.002	4	
			SC-DR-gas	NG-DR	0.000	0.000	0.000	4	
			SC-DR-oil	CO-HF-DR	0.003	0.001	0.007	4	
			SC-DR-oil	CO-LF-DR	0.008	0.001	0.018	4	
			SC-IND-coal	BC-IND-OTH	0.007	0.003	0.019	4	
			SC-IND-coal	HC-IND-OTH	0.430	0.180	1.210	4	
			SC-IND-oil	CO-HF-IND	0.007	0.001	0.015	4	
			SC-IND-oil	CO-LF-IND	0.001	0.000	0.002	4	
			SC-PP-coal	HC-B-PP	0.097	0.041	0.273	4	
			SC-PP-gas	NG-PP	0.000	0.000	0.000	4	
			SC-PP-oil	CO-HF-PP	0.034	0.006	0.078	4	
			SC-PP-oil	CO-LF-PP	0.004	0.001	0.010	4	
			WASOTH	WASOTH	1.082	0.325	3.246		4
			WI	WI	0.003	0.001	0.010		4
PAN	Panama	Central America and the Caribbean	ASGM	GP-A	712.500	178.125	1246.875		
			BIO	PSB – DR	8.816	1.984	16.971	3	
			BIO	PSB – IND	3.779	0.850	7.275	3	
			BIO	PSB – PP	3.291	0.741	6.336	3	
			CEM	CEM	185.542	65.552	1018.295	3	
			CREM	CREM	0.699	0.559	0.839		4
			SC-DR-oil	CO-LF-DR	1.340	0.302	2.580	3	
			SC-IND-oil	CO-HF-IND	0.589	0.133	1.134	3	
			SC-IND-oil	CO-LF-IND	0.823	0.185	1.584	3	
			SC-PP-coal	HC-B-PP	34.324	18.535	81.805	3	
			SC-PP-oil	CO-HF-PP	10.620	2.390	20.444	3	
			SC-PP-oil	CO-LF-PP	0.090	0.020	0.173	3	
			WASOTH	WASOTH	229.732	68.920	689.196		4
			WI	WI	0.719	0.216	2.157		4
PNG	Papua New Guinea	East and Southeast Asia	ASGM	GP-A	3325.000	831.250	5818.750		
			BIO	PSB – DR	27.171	4.755	61.815	3	
			BIO	PSB – IND	1.429	0.250	3.250	3	
			CEM	CEM	17.440	6.160	91.936	3	

Country code	Country name	Region	Sector Code	Activity Code	Emission estimate, kg	Low range estimate, kg	High range estimate, kg	Technology group	Waste group
			CREM	CREM	4.333	3.943	4.808		4
			NFMP-AU	GP-L	2377.822	832.238	4636.752	3	
			OR	CO-OR	1.771	0.620	3.453	3	
			SC-DR-gas	NG-DR	0.003	0.001	0.008	3	
			SC-DR-oil	CO-HF-DR	0.170	0.030	0.386	3	
			SC-DR-oil	CO-LF-DR	0.435	0.076	0.989	3	
			SC-IND-coal	BC-IND-OTH	0.333	0.140	0.938	3	
			SC-IND-coal	HC-IND-OTH	20.656	8.676	58.182	3	
			SC-IND-oil	CO-HF-IND	0.354	0.062	0.804	3	
			SC-IND-oil	CO-LF-IND	0.039	0.007	0.088	3	
			SC-PP-coal	HC-B-PP	4.893	2.055	13.781	3	
			SC-PP-gas	NG-PP	0.004	0.001	0.009	3	
			SC-PP-oil	CO-HF-PP	1.438	0.252	3.272	3	
			SC-PP-oil	CO-LF-PP	0.188	0.033	0.428	3	
			WASOTH	WASOTH	67.276	20.183	201.829		4
			WI	WI	0.211	0.063	0.632		4
PRY	Paraguay	South America	ASGM	GP-A	225.000	56.250	393.750		
			BIO	PSB – DR	35.658	8.023	68.641	3	
			BIO	PSB – IND	47.871	10.771	92.152	3	
			CEM	CEM	73.600	26.040	390.520	3	
			CREM	CREM	2.652	1.856	3.712		4
			PISP	PIP	3.914	1.372	20.716	3	
			SC-DR-oil	CO-LF-DR	2.404	0.541	4.628	3	
			SC-IND-oil	CO-HF-IND	0.874	0.197	1.682	3	
			SC-PP-oil	CO-LF-PP	0.002	0.000	0.003	3	
			WASOTH	WASOTH	137.864	41.359	413.593		4
			WI	WI	0.464	0.139	1.391		4
PER	Peru	South America	ASGM	GP-A	110362.500	55181.250	165543.750		
			BIO	PSB – DR	110.840	24.939	213.367	3	
			BIO	PSB – IND	0.003	0.001	0.006	3	
			BIO	PSB – PP	13.429	3.021	25.850	3	
			CEM	CEM	785.754	278.003	4169.192	3	
			CREM	CREM	17.817	12.472	24.944		4
			CSP	CSP-C	380.000	133.000	741.000	3	
			NFMP	CU-P	2678.451	955.992	15292.117	3	
			NFMP	ZN-P	2132.613	762.381	9206.730	3	
			NFMP-AU	GP-L	4808.668	1683.034	9376.902	3	
			OR	CO-OR	8.503	3.827	14.031	3	
			SC-DR-coal	HC-DR	0.600	0.324	1.430	3	
			SC-DR-gas	NG-DR	0.198	0.044	0.381	3	
			SC-DR-oil	CO-HF-DR	3.540	0.797	6.815	3	
			SC-DR-oil	CO-LF-DR	8.328	1.874	16.031	3	
			SC-IND-coal	HC-IND-OTH	96.413	52.063	229.783	3	
			SC-IND-coal	HC-IND-PIP	15.525	8.384	37.001	3	
			SC-IND-gas	NG-IND	0.250	0.056	0.480	3	

Country code	Country name	Region	Sector Code	Activity Code	Emission estimate, kg	Low range estimate, kg	High range estimate, kg	Technology group	Waste group
			SC-IND-oil	CO-HF-IND	1.235	0.278	2.377	3	
			SC-IND-oil	CO-LF-IND	1.368	0.308	2.633	3	
			SC-PP-coal	HC-B-PP	23.895	12.903	56.950	3	
			SC-PP-gas	NG-PP	1.330	0.299	2.561	3	
			SC-PP-oil	CO-HF-PP	3.540	0.797	6.815	3	
			SC-PP-oil	CO-LF-PP	0.180	0.041	0.347	3	
			SSC	SP-S	27.201	10.124	129.792	3	
			WASOTH	WASOTH	887.475	266.242	2662.424		4
			WI	WI	2.986	0.896	8.957		4
PHL	Philippines	East and Southeast Asia	ASGM	GP-A	23625.000	11812.500	35437.500		
			BIO	PSB – DR	158.619	35.689	305.341	3	
			BIO	PSB – IND	78.462	17.654	151.040	3	
			BIO	PSB – PP	6.199	1.395	11.932	3	
			CEM	CEM	1971.200	696.080	10822.240	3	
			CREM	CREM	65.472	59.576	72.653		2
			CSP	CSP-C	70.000	24.500	136.500	3	
			NFMP	CU-P	1543.847	551.030	8814.303	3	
			NFMP-AU	GP-L	817.463	286.112	1594.052	3	
			OR	CO-OR	133.341	60.004	220.013	3	
			SC-DR-oil	CO-HF-DR	6.600	1.485	12.705	3	
			SC-DR-oil	CO-LF-DR	13.666	3.075	26.307	3	
			SC-IND-coal	BC-IND-CEM	402.720	217.469	959.816	3	
			SC-IND-coal	BC-IND-OTH	56.993	30.776	135.832	3	
			SC-IND-coal	BC-IND-PIP	52.530	28.366	125.197	3	
			SC-IND-gas	NG-IND	0.012	0.003	0.022	3	
			SC-IND-oil	CO-HF-IND	12.312	2.770	23.701	3	
			SC-IND-oil	CO-LF-IND	1.112	0.250	2.140	3	
			SC-PP-coal	BC-S-PP	463.437	250.256	1104.525	3	
			SC-PP-coal	HC-B-PP	1376.291	743.197	3280.161	3	
			SC-PP-gas	NG-PP	0.657	0.148	1.265	3	
			SC-PP-oil	CO-HF-PP	17.190	3.868	33.091	3	
			SC-PP-oil	CO-LF-PP	0.429	0.097	0.826	3	
			SC-PP-oil	CO-PP	1.755	0.395	3.378	3	
			SSC	SP-S	30.178	11.232	144.000	3	
			WASOTH	WASOTH	1542.583	462.775	4627.750		2
			WI	WI	44.945	13.483	134.834		2
PCN	Pitcairn	Australia, New Zealand & Oceania	CREM	CREM	0.000	0.000	0.000		4
			WASOTH	WASOTH	0.000	0.000	0.000		4
			WI	WI	0.000	0.000	0.000		4
POL	Poland	EU28	BIO	PSB – DR	159.773	37.946	293.583	1	
			BIO	PSB – IND	52.411	12.448	96.306	1	
			BIO	PSB – PP	98.048	23.287	180.164	1	
			CEM	CEM	880.658	310.934	5608.790	1	
			CREM	CREM	26.849	21.096	32.123		1
			NFMP	CU-P	98.983	35.329	565.125	1	

Country code	Country name	Region	Sector Code	Activity Code	Emission estimate, kg	Low range estimate, kg	High range estimate, kg	Technology group	Waste group
			NFMP	PB-P	0.952	0.519	1.501	1	
			NFMP	ZN-P	36.624	12.975	100.610	1	
			NFMP-AU	GP-L	6.244	2.185	12.176	1	
			OR	CO-OR	47.220	22.429	74.371	1	
			PISP	PIP	149.863	52.535	793.205	1	
			SC-DR-coal	BC-DR	81.900	46.683	186.323	1	
			SC-DR-coal	HC-DR	1594.819	909.047	3628.213	1	
			SC-DR-gas	NG-DR	1.223	0.291	2.248	1	
			SC-DR-oil	CO-HF-DR	0.200	0.048	0.368	1	
			SC-DR-oil	CO-LF-DR	23.178	5.505	42.590	1	
			SC-IND-coal	BC-IND-CEM	3.622	2.064	8.239	1	
			SC-IND-coal	BC-IND-OTH	1.770	1.009	4.027	1	
			SC-IND-coal	HC-IND-CEM	67.679	38.577	153.969	1	
			SC-IND-coal	HC-IND-NFM	0.069	0.040	0.158	1	
			SC-IND-coal	HC-IND-OTH	251.762	143.504	572.758	1	
			SC-IND-coal	HC-IND-PIP	2.220	1.265	5.051	1	
			SC-IND-gas	NG-IND	0.751	0.178	1.380	1	
			SC-IND-oil	CO-HF-IND	1.539	0.366	2.828	1	
			SC-IND-oil	CO-LF-IND	0.504	0.120	0.925	1	
			SC-PP-coal	BC-L-PP	5205.911	3214.650	16398.621	1	
			SC-PP-coal	HC-B-PP	2197.564	1252.611	4999.458	1	
			SC-PP-gas	NG-PP	0.614	0.146	1.128	1	
			SC-PP-oil	CO-HF-PP	9.620	2.285	17.677	1	
			SC-PP-oil	CO-LF-PP	0.114	0.027	0.209	1	
			SSC	SP-S	81.504	30.335	388.908	1	
			WASOTH	WASOTH	216.336	64.901	649.008		1
			WI	WI	82.686	24.806	248.058		1
PRT	Portugal	EU28	BIO	PSB – DR	39.258	9.324	72.137	1	
			BIO	PSB – IND	36.655	8.705	67.353	1	
			BIO	PSB – PP	26.010	6.177	47.794	1	
			CEM	CEM	284.950	100.701	1469.150	1	
			CEM	PC-CEM	9.175	5.447	49.371	1	
			CREM	CREM	25.169	19.776	30.113		1
			OR	CO-OR	25.013	11.881	39.396	1	
			PISP	PIP	3.232	1.133	17.106	1	
			SC-DR-gas	NG-DR	0.118	0.028	0.216	1	
			SC-DR-oil	CO-HF-DR	1.720	0.409	3.161	1	
			SC-DR-oil	CO-LF-DR	8.442	2.005	15.512	1	
			SC-IND-coal	HC-IND-OTH	0.347	0.198	0.789	1	
			SC-IND-coal	HC-IND-PIP	0.347	0.198	0.789	1	
			SC-IND-gas	NG-IND	0.265	0.063	0.486	1	
			SC-IND-oil	CO-HF-IND	2.337	0.555	4.294	1	
			SC-IND-oil	CO-LF-IND	0.357	0.085	0.656	1	
			SC-PP-coal	HC-B-PP	284.315	162.059	646.815	1	
			SC-PP-gas	NG-PP	0.516	0.122	0.947	1	

Country code	Country name	Region	Sector Code	Activity Code	Emission estimate, kg	Low range estimate, kg	High range estimate, kg	Technology group	Waste group
			SC-PP-oil	CO-HF-PP	3.650	0.867	6.707	1	
			SC-PP-oil	CO-LF-PP	0.032	0.007	0.058	1	
			SSC	SP-S	48.314	17.982	230.538	1	
			WASOTH	WASOTH	65.211	19.563	195.632		1
			WI	WI	24.924	7.477	74.773		1
PRI	Puerto Rico	Central America and the Caribbean	CREM	CREM	0.675	0.540	0.810		4
			WASOTH	WASOTH	344.440	103.332	1033.321		4
			WI	WI	1.078	0.323	3.234		4
QAT	Qatar	Middle Eastern States	CEM	CEM	459.684	162.313	2382.424	1	
			CREM	CREM	0.068	0.051	0.080		2
			NFMP	AL-P	7.625	2.585	14.400	1	
			OR	CO-OR	1.850	0.832	3.052	1	
			SC-DR-oil	CO-LF-DR	6.588	1.482	12.682	1	
			SC-IND-gas	NG-IND	1.197	0.269	2.303	1	
			SC-PP-gas	NG-PP	5.022	1.130	9.668	1	
			SSC	SP-S	70.464	26.226	336.229	1	
			WASOTH	WASOTH	351.205	105.362	1053.616		2
			WI	WI	10.233	3.070	30.698		2
MDA	Republic of Moldova	CIS & other European countries	BIO	PSB – DR	15.638	3.518	30.102	4	
			BIO	PSB – IND	0.076	0.017	0.145	4	
			BIO	PSB – PP	0.486	0.109	0.936	4	
			CEM	CEM	127.400	44.988	646.214	4	
			CREM	CREM	0.601	0.441	0.802		4
			OR	CO-OR	0.008	0.004	0.013	4	
			SC-DR-coal	HC-DR	14.400	7.776	34.320	4	
			SC-DR-gas	NG-DR	0.070	0.016	0.134	4	
			SC-DR-oil	CO-LF-DR	0.974	0.219	1.875	4	
			SC-IND-coal	HC-IND-CEM	9.188	4.961	21.897	4	
			SC-IND-coal	HC-IND-OTH	0.263	0.142	0.626	4	
			SC-IND-gas	NG-IND	0.057	0.013	0.111	4	
			SC-IND-oil	CO-HF-IND	0.040	0.009	0.077	4	
			SC-IND-oil	CO-LF-IND	0.018	0.004	0.035	4	
			SC-PP-coal	HC-A-PP	0.338	0.182	1.423	4	
			SC-PP-gas	NG-PP	0.356	0.080	0.685	4	
			SC-PP-oil	CO-HF-PP	0.140	0.032	0.270	4	
			SSC	SP-S	10.240	3.811	48.864	4	
			WASOTH	WASOTH	51.225	15.367	153.675		4
			WI	WI	0.160	0.048	0.481		4
REU	Reunion	Sub-Saharan Africa	BIO	PSB – DR	8.495	1.487	19.327	5	
			BIO	PSB – IND	0.611	0.107	1.390	5	
			BIO	PSB – PP	0.221	0.039	0.504	5	
			CEM	CEM	42.000	14.840	217.880	5	
			CREM	CREM	0.019	0.013	0.027		4
			SC-DR-coal	HC-DR	0.121	0.051	0.340	5	
			SC-DR-oil	CO-LF-DR	0.054	0.009	0.123	5	

Country code	Country name	Region	Sector Code	Activity Code	Emission estimate, kg	Low range estimate, kg	High range estimate, kg	Technology group	Waste group
			SC-IND-coal	HC-IND-OTH	0.117	0.049	0.330	5	
			SC-IND-gas	NG-IND	0.000	0.000	0.000	5	
			SC-IND-oil	CO-HF-IND	0.098	0.017	0.224	5	
			SC-IND-oil	CO-IND	0.014	0.002	0.031	5	
			SC-IND-oil	CO-LF-IND	0.009	0.002	0.021	5	
			SC-PP-coal	HC-B-PP	0.793	0.333	2.234	5	
			SC-PP-gas	NG-PP	0.001	0.000	0.002	5	
			SC-PP-oil	CO-HF-PP	0.128	0.022	0.291	5	
			SC-PP-oil	CO-LF-PP	0.026	0.005	0.060	5	
			WASOTH	WASOTH	17.636	7.626	27.169		4
			WI	WI	0.003	0.001	0.005		4
ROU	Romania	EU28	BIO	PSB – DR	160.376	36.085	308.724	4	
			BIO	PSB – IND	12.397	2.789	23.864	4	
			BIO	PSB – PP	9.828	2.211	18.918	4	
			CEM	CEM	711.988	251.615	3670.883	4	
			CEM	PC-CEM	13.160	7.403	74.190	4	
			CREM	CREM	3.699	2.713	4.932		2
			NFMP	AL-P	13.550	4.593	25.589	4	
			OR	CO-OR	18.700	8.415	30.855	4	
			PISP	PIP	98.643	34.580	522.103	4	
			SC-DR-coal	BC-DR	42.900	23.166	102.245	4	
			SC-DR-gas	NG-DR	0.712	0.160	1.371	4	
			SC-DR-oil	CO-LF-DR	8.090	1.820	15.573	4	
			SC-IND-coal	BC-IND-CEM	31.369	16.939	74.762	4	
			SC-IND-coal	BC-IND-OTH	36.270	19.586	86.444	4	
			SC-IND-coal	BC-IND-PIP	53.235	28.747	126.877	4	
			SC-IND-coal	HC-IND-OTH	0.263	0.142	0.626	4	
			SC-IND-coal	HC-IND-PIP	14.175	7.655	33.784	4	
			SC-IND-gas	NG-IND	0.520	0.117	1.002	4	
			SC-IND-oil	CO-HF-IND	0.140	0.032	0.270	4	
			SC-IND-oil	CO-LF-IND	0.622	0.140	1.197	4	
			SC-PP-coal	BC-L-PP	2554.370	1494.306	8429.421	4	
			SC-PP-coal	BC-S-PP	26.595	14.361	63.385	4	
			SC-PP-gas	NG-PP	0.732	0.165	1.408	4	
			SC-PP-oil	CO-HF-PP	0.980	0.221	1.887	4	
			SC-PP-oil	CO-LF-PP	0.144	0.032	0.277	4	
			SSC	SP-S	38.336	14.268	182.927	4	
			WASOTH	WASOTH	364.239	109.272	1092.716		2
			WI	WI	10.612	3.184	31.837		2
RUS	Russia	CIS & other European countries	ASGM	GP-A	5225.000	1306.250	9143.750		
			BIO	PSB – DR	103.554	23.300	199.341	4	
			BIO	PSB – IND	3.506	0.789	6.750	4	
			BIO	PSB – PP	38.399	8.640	73.918	4	
			CEM	CEM	2339.098	1616.377	3742.557	4	
			CREM	CREM	121.894	89.389	162.526		4

Country code	Country name	Region	Sector Code	Activity Code	Emission estimate, kg	Low range estimate, kg	High range estimate, kg	Technology group	Waste group
			CSP	CSP-C	3790.000	1326.500	7390.500	4	
			NFMP	AL-P	1094.300	383.005	2133.885	4	
			NFMP	CU-P	7611.120	2716.560	43454.268	4	
			NFMP	PB-T	1000.008	362.930	2570.677	4	
			NFMP	ZN-T	4278.863	1497.602	8343.783	4	
			NFMP-AU	GP-L	12474.000	4365.900	24324.300	4	
			OR	CO-OR	201.334	90.600	332.201	4	
			PISP	PIP	4842.674	1833.298	9635.933	4	
			SC-DR-coal	BC-DR	112.600	70.938	161.018	4	
			SC-DR-coal	HC-DR	548.200	345.366	783.926	4	
			SC-DR-gas	NG-DR	16.939	3.811	32.607	4	
			SC-DR-oil	CO-DR	0.680	0.153	1.309	4	
			SC-DR-oil	CO-HF-DR	12.260	2.759	23.601	4	
			SC-DR-oil	CO-LF-DR	47.182	10.616	90.825	4	
			SC-IND-coal	BC-IND-CEM	1.225	0.772	1.752	4	
			SC-IND-coal	BC-IND-OTH	10.830	6.823	15.487	4	
			SC-IND-coal	HC-IND-CEM	136.675	86.105	195.445	4	
			SC-IND-coal	HC-IND-OTH	37.050	23.342	52.982	4	
			SC-IND-gas	NG-IND	8.257	1.858	15.896	4	
			SC-IND-oil	CO-HF-IND	7.940	1.787	15.285	4	
			SC-IND-oil	CO-IND	0.230	0.052	0.443	4	
			SC-IND-oil	CO-LF-IND	6.874	1.547	13.232	4	
			SC-PP-coal	BC-L-PP	3022.470	1904.156	4322.133	4	
			SC-PP-coal	HC-B-PP	2759.364	1738.399	3945.890	4	
			SC-PP-gas	NG-PP	50.605	11.386	97.415	4	
			SC-PP-oil	CO-HF-PP	154.360	34.731	297.143	4	
			SC-PP-oil	CO-LF-PP	10.380	2.336	19.982	4	
			SC-PP-oil	CO-PP	6.740	1.517	12.975	4	
			SSC	SP-S	637.536	237.287	3042.101	4	
			VCM	VCM-P	123.930	43.376	241.664	4	
			VCM	VCM-R	185.895	65.063	362.496	4	
			WASOTH	WASOTH	9896.247	2968.874	29688.741		4
			WI	WI	30.968	9.290	92.903		4
RWA	Rwanda	Sub-Saharan Africa	ASGM	GP-A	225.000	56.250	393.750		
			BIO	PSB – DR	144.583	25.302	328.926	5	
			BIO	PSB – IND	3.899	0.682	8.870	5	
			BIO	PSB – PP	1.413	0.247	3.214	5	
			CEM	CEM	14.700	5.194	76.258	5	
			CREM	CREM	0.288	0.207	0.415		4
			NFMP-AU	GP-L	17.545	6.141	34.213	5	
			SC-DR-coal	HC-DR	0.770	0.324	2.170	5	
			SC-DR-oil	CO-LF-DR	0.345	0.060	0.784	5	
			SC-IND-coal	HC-IND-OTH	0.748	0.314	2.107	5	
			SC-IND-gas	NG-IND	0.000	0.000	0.000	5	
			SC-IND-oil	CO-HF-IND	0.627	0.110	1.427	5	

Country code	Country name	Region	Sector Code	Activity Code	Emission estimate, kg	Low range estimate, kg	High range estimate, kg	Technology group	Waste group
			SC-IND-oil	CO-IND	0.086	0.015	0.196	5	
			SC-IND-oil	CO-LF-IND	0.060	0.011	0.137	5	
			SC-PP-coal	HC-B-PP	5.063	2.126	14.260	5	
			SC-PP-gas	NG-PP	0.006	0.001	0.013	5	
			SC-PP-oil	CO-HF-PP	0.816	0.143	1.856	5	
			SC-PP-oil	CO-LF-PP	0.169	0.030	0.384	5	
			WASOTH	WASOTH	63.447	27.436	97.742		4
			WI	WI	1.849	0.799	2.848		4
SHN	Saint Helena	Sub-Saharan Africa	CREM	CREM	0.000	0.000	0.000		4
			WASOTH	WASOTH	0.154	0.066	0.237		4
			WI	WI	0.000	0.000	0.000		4
KNA	Saint Kitts	Central America and the Caribbean	BIO	PSB – DR	0.068	0.012	0.154	3	
			BIO	PSB – IND	0.241	0.042	0.547	3	
			BIO	PSB – PP	0.085	0.015	0.194	3	
			CREM	CREM	0.010	0.008	0.012		4
			OR	CO-OR	0.023	0.008	0.045	3	
			SC-DR-coal	HC-DR	0.868	0.365	2.446	3	
			SC-DR-gas	NG-DR	0.000	0.000	0.000	3	
			SC-DR-oil	CO-HF-DR	0.025	0.004	0.056	3	
			SC-DR-oil	CO-LF-DR	0.059	0.010	0.134	3	
			SC-IND-gas	NG-IND	0.000	0.000	0.000	3	
			SC-IND-oil	CO-HF-IND	0.070	0.012	0.160	3	
			SC-IND-oil	CO-LF-IND	0.004	0.001	0.009	3	
			SC-PP-gas	NG-PP	0.004	0.001	0.010	3	
			SC-PP-oil	CO-HF-PP	0.672	0.118	1.529	3	
			SC-PP-oil	CO-LF-PP	0.049	0.009	0.113	3	
			WASOTH	WASOTH	3.666	1.100	10.997		4
			WI	WI	0.011	0.003	0.034		4
LCA	Saint Lucia	Central America and the Caribbean	BIO	PSB – DR	0.213	0.037	0.485	3	
			BIO	PSB – IND	0.361	0.063	0.822	3	
			BIO	PSB – PP	0.128	0.022	0.292	3	
			CREM	CREM	0.031	0.025	0.037		4
			OR	CO-OR	0.035	0.012	0.067	3	
			SC-DR-coal	HC-DR	1.304	0.548	3.672	3	
			SC-DR-gas	NG-DR	0.000	0.000	0.000	3	
			SC-DR-oil	CO-HF-DR	0.037	0.006	0.084	3	
			SC-DR-oil	CO-LF-DR	0.088	0.015	0.201	3	
			SC-IND-gas	NG-IND	0.000	0.000	0.000	3	
			SC-IND-oil	CO-HF-IND	0.106	0.019	0.241	3	
			SC-IND-oil	CO-LF-IND	0.006	0.001	0.014	3	
			SC-PP-gas	NG-PP	0.007	0.001	0.015	3	
			SC-PP-oil	CO-HF-PP	1.009	0.177	2.295	3	
			SC-PP-oil	CO-LF-PP	0.074	0.013	0.169	3	
			WASOTH	WASOTH	5.297	1.589	15.891		4
			WI	WI	0.017	0.005	0.050		4

Country code	Country name	Region	Sector Code	Activity Code	Emission estimate, kg	Low range estimate, kg	High range estimate, kg	Technology group	Waste group
VCT	Saint Vincent and the Grenadines	Central America and the Caribbean	BIO	PSB – DR	0.133	0.023	0.303	3	
			BIO	PSB – IND	0.213	0.037	0.484	3	
			BIO	PSB – PP	0.076	0.013	0.172	3	
			CREM	CREM	0.019	0.015	0.023		4
			OR	CO-OR	0.020	0.007	0.040	3	
			SC-DR-coal	HC-DR	0.767	0.322	2.161	3	
			SC-DR-gas	NG-DR	0.000	0.000	0.000	3	
			SC-DR-oil	CO-HF-DR	0.022	0.004	0.049	3	
			SC-DR-oil	CO-LF-DR	0.052	0.009	0.118	3	
			SC-IND-gas	NG-IND	0.000	0.000	0.000	3	
			SC-IND-oil	CO-HF-IND	0.062	0.011	0.142	3	
			SC-IND-oil	CO-LF-IND	0.004	0.001	0.008	3	
			SC-PP-gas	NG-PP	0.004	0.001	0.009	3	
			SC-PP-oil	CO-HF-PP	0.594	0.104	1.351	3	
			SC-PP-oil	CO-LF-PP	0.044	0.008	0.099	3	
			WASOTH	WASOTH	3.206	0.962	9.618		4
			WI	WI	0.010	0.003	0.030		4
WSM	Samoa	Australia, New Zealand & Oceania	BIO	PSB – DR	0.805	0.141	1.832	4	
			BIO	PSB – IND	0.094	0.016	0.213	4	
			CREM	CREM	0.608	0.547	0.729		4
			OR	CO-OR	0.004	0.001	0.008	4	
			SC-DR-gas	NG-DR	0.000	0.000	0.000	4	
			SC-DR-oil	CO-HF-DR	0.010	0.002	0.022	4	
			SC-DR-oil	CO-LF-DR	0.025	0.004	0.056	4	
			SC-IND-coal	BC-IND-OTH	0.022	0.009	0.061	4	
			SC-IND-coal	HC-IND-OTH	1.376	0.578	3.875	4	
			SC-IND-oil	CO-HF-IND	0.021	0.004	0.048	4	
			SC-IND-oil	CO-LF-IND	0.002	0.000	0.005	4	
			SC-PP-coal	HC-B-PP	0.310	0.130	0.874	4	
			SC-PP-gas	NG-PP	0.000	0.000	0.000	4	
			SC-PP-oil	CO-HF-PP	0.109	0.019	0.249	4	
			SC-PP-oil	CO-LF-PP	0.014	0.003	0.033	4	
			WASOTH	WASOTH	3.805	1.141	11.415		4
			WI	WI	0.012	0.004	0.036		4
STP	Sao Tome and Principe	Sub-Saharan Africa	BIO	PSB – DR	2.215	0.388	5.040	5	
			BIO	PSB – IND	0.106	0.019	0.242	5	
			BIO	PSB – PP	0.038	0.007	0.088	5	
			CREM	CREM	0.004	0.003	0.006		4
			SC-DR-coal	HC-DR	0.021	0.009	0.059	5	
			SC-DR-oil	CO-LF-DR	0.009	0.002	0.021	5	
			SC-IND-coal	HC-IND-OTH	0.020	0.009	0.057	5	
			SC-IND-gas	NG-IND	0.000	0.000	0.000	5	
			SC-IND-oil	CO-HF-IND	0.017	0.003	0.039	5	
			SC-IND-oil	CO-IND	0.002	0.000	0.005	5	
			SC-IND-oil	CO-LF-IND	0.002	0.000	0.004	5	

Country code	Country name	Region	Sector Code	Activity Code	Emission estimate, kg	Low range estimate, kg	High range estimate, kg	Technology group	Waste group
			SC-PP-coal	HC-B-PP	0.138	0.058	0.388	5	
			SC-PP-gas	NG-PP	0.000	0.000	0.000	5	
			SC-PP-oil	CO-HF-PP	0.022	0.004	0.051	5	
			SC-PP-oil	CO-LF-PP	0.005	0.001	0.010	5	
			WASOTH	WASOTH	3.026	1.308	4.661		4
			WI	WI	0.001	0.000	0.001		4
SAU	Saudi Arabia	Middle Eastern States	BIO	PSB – DR	0.006	0.001	0.012	1	
			CEM	CEM	4384.083	1548.008	22721.577	1	
			CREM	CREM	0.853	0.640	0.996		2
			NFMP	AL-P	52.855	18.499	103.067	1	
			NFMP-AU	GP-L	11.781	4.123	22.973	1	
			OR	CO-OR	42.084	18.938	69.439	1	
			SC-DR-oil	CO-LF-DR	40.588	9.132	78.132	1	
			SC-IND-gas	NG-IND	3.851	0.866	7.413	1	
			SC-IND-oil	CO-HF-IND	264.233	59.452	508.649	1	
			SC-IND-oil	CO-IND	50.778	11.425	97.747	1	
			SC-IND-oil	CO-LF-IND	7.904	1.778	15.215	1	
			SC-PP-gas	NG-PP	11.636	2.618	22.399	1	
			SC-PP-oil	CO-HF-PP	79.000	17.775	152.075	1	
			SC-PP-oil	CO-LF-PP	20.447	4.600	39.360	1	
			SC-PP-oil	CO-PP	116.300	26.168	223.878	1	
			SSC	SP-S	146.833	54.650	700.635	1	
			WASOTH	WASOTH	1891.801	567.540	5675.403		2
			WI	WI	55.119	16.536	165.358		2
SEN	Senegal	Sub-Saharan Africa	ASGM	GP-A	2250.000	1575.000	2925.000		
			BIO	PSB – DR	38.725	8.713	74.546	5	
			BIO	PSB – IND	2.159	0.486	4.156	5	
			BIO	PSB – PP	1.903	0.428	3.662	5	
			CEM	CEM	514.395	181.753	2668.485	5	
			CREM	CREM	0.079	0.057	0.114		4
			NFMP-AU	GP-L	311.850	109.148	608.108	5	
			OR	CO-OR	0.753	0.339	1.243	5	
			SC-DR-oil	CO-LF-DR	1.332	0.300	2.564	5	
			SC-IND-coal	HC-IND-CEM	58.350	31.509	139.068	5	
			SC-IND-oil	CO-HF-IND	1.180	0.266	2.272	5	
			SC-IND-oil	CO-LF-IND	0.044	0.010	0.085	5	
			SC-PP-gas	NG-PP	0.008	0.002	0.016	5	
			SC-PP-oil	CO-HF-PP	11.980	2.696	23.062	5	
			SC-PP-oil	CO-LF-PP	0.304	0.068	0.585	5	
			WASOTH	WASOTH	180.873	78.215	278.642		4
			WI	WI	0.035	0.015	0.053		4
SRB	Serbia	CIS & other European countries	BIO	PSB – DR	47.064	10.589	90.598	4	
			BIO	PSB – IND	6.684	1.504	12.866	4	
			BIO	PSB – PP	0.239	0.054	0.460	4	
			CEM	CEM	157.290	55.543	797.825	4	

Country code	Country name	Region	Sector Code	Activity Code	Emission estimate, kg	Low range estimate, kg	High range estimate, kg	Technology group	Waste group
			CEM	PC-CEM	3.640	2.048	20.521	4	
			CREM	CREM	2.584	1.895	3.445		
			NFMP	CU-P	495.876	176.988	2831.111	4	
			NFMP-AU	GP-L	31.086	10.880	60.618	4	
			OR	CO-OR	3.317	1.493	5.473	4	
			PISP	PIP	33.264	11.661	176.062	4	
			SC-DR-coal	BC-DR	83.400	45.036	198.770	4	
			SC-DR-gas	NG-DR	0.072	0.016	0.139	4	
			SC-DR-oil	CO-HF-DR	0.880	0.198	1.694	4	
			SC-DR-oil	CO-LF-DR	2.832	0.637	5.452	4	
			SC-IND-coal	BC-IND-CEM	13.519	7.300	32.220	4	
			SC-IND-coal	BC-IND-NFM	0.878	0.474	2.091	4	
			SC-IND-coal	BC-IND-OTH	29.689	16.032	70.758	4	
			SC-IND-coal	HC-IND-CEM	11.025	5.954	26.276	4	
			SC-IND-coal	HC-IND-NFM	1.444	0.780	3.441	4	
			SC-IND-coal	HC-IND-OTH	1.444	0.780	3.441	4	
			SC-IND-coal	HC-IND-PIP	1.838	0.992	4.379	4	
			SC-IND-gas	NG-IND	0.101	0.023	0.194	4	
			SC-IND-oil	CO-HF-IND	1.640	0.369	3.157	4	
			SC-IND-oil	CO-LF-IND	0.262	0.059	0.504	4	
			SC-PP-coal	BC-L-PP	3622.962	2119.433	11955.775	4	
			SC-PP-gas	NG-PP	0.177	0.040	0.342	4	
			SC-PP-oil	CO-HF-PP	4.040	0.909	7.777	4	
			SC-PP-oil	CO-LF-PP	0.058	0.013	0.112	4	
			WASOTH	WASOTH	188.054	56.416	564.161		
			WI	WI	5.479	1.644	16.437		
SCG	Serbia and Montenegro	CIS & other European countries	CSP	CSP-C	100.000	35.000	195.000	4	
SYC	Seychelles	Sub-Saharan Africa	BIO	PSB – DR	1.055	0.185	2.401	5	
			BIO	PSB – IND	0.416	0.073	0.946	5	
			BIO	PSB – PP	0.151	0.026	0.343	5	
			CREM	CREM	0.002	0.001	0.003		4
			SC-DR-coal	HC-DR	0.082	0.035	0.231	5	
			SC-DR-oil	CO-LF-DR	0.037	0.006	0.084	5	
			SC-IND-coal	HC-IND-OTH	0.080	0.034	0.225	5	
			SC-IND-gas	NG-IND	0.000	0.000	0.000	5	
			SC-IND-oil	CO-HF-IND	0.067	0.012	0.152	5	
			SC-IND-oil	CO-IND	0.009	0.002	0.021	5	
			SC-IND-oil	CO-LF-IND	0.006	0.001	0.015	5	
			SC-PP-coal	HC-B-PP	0.540	0.227	1.521	5	
			SC-PP-gas	NG-PP	0.001	0.000	0.001	5	
			SC-PP-oil	CO-HF-PP	0.087	0.015	0.198	5	
			SC-PP-oil	CO-LF-PP	0.018	0.003	0.041	5	
			WASOTH	WASOTH	7.582	3.279	11.680		4
			WI	WI	0.221	0.096	0.340		4

Country code	Country name	Region	Sector Code	Activity Code	Emission estimate, kg	Low range estimate, kg	High range estimate, kg	Technology group	Waste group
SLE	Sierra Leone	Sub-Saharan Africa	ASGM	GP-A	8250.000	4125.000	12375.000		
			BIO	PSB – DR	67.133	11.748	152.727	5	
			BIO	PSB – IND	1.609	0.282	3.661	5	
			BIO	PSB – PP	0.583	0.102	1.326	5	
			CEM	CEM	35.280	12.466	183.019	5	
			CREM	CREM	0.133	0.096	0.192		4
			NFMP-AU	GP-L	2.200	0.770	4.290	5	
			SC-DR-coal	HC-DR	0.318	0.134	0.896	5	
			SC-DR-oil	CO-LF-DR	0.142	0.025	0.324	5	
			SC-IND-coal	HC-IND-OTH	0.309	0.130	0.870	5	
			SC-IND-gas	NG-IND	0.000	0.000	0.000	5	
			SC-IND-oil	CO-HF-IND	0.259	0.045	0.589	5	
			SC-IND-oil	CO-IND	0.036	0.006	0.081	5	
			SC-IND-oil	CO-LF-IND	0.025	0.004	0.056	5	
			SC-PP-coal	HC-B-PP	2.089	0.878	5.885	5	
			SC-PP-gas	NG-PP	0.002	0.000	0.006	5	
			SC-PP-oil	CO-HF-PP	0.337	0.059	0.766	5	
			SC-PP-oil	CO-LF-PP	0.070	0.012	0.158	5	
			WASOTH	WASOTH	50.081	21.657	77.152		4
			WI	WI	0.010	0.004	0.015		4
SGP	Singapore	East and Southeast Asia	BIO	PSB – PP	2.820	0.634	5.428	2	
			CREM	CREM	3.458	3.147	3.837		2
			OR	CO-OR	496.559	223.452	819.323	2	
			SC-DR-gas	NG-DR	0.035	0.008	0.068	2	
			SC-DR-oil	CO-LF-DR	2.510	0.565	4.832	2	
			SC-IND-coal	HC-IND-OTH	19.659	10.616	46.855	2	
			SC-IND-gas	NG-IND	0.253	0.057	0.488	2	
			SC-IND-oil	CO-HF-IND	16.834	3.788	32.405	2	
			SC-IND-oil	CO-LF-IND	0.410	0.092	0.790	2	
			SC-PP-coal	HC-B-PP	39.996	21.598	95.323	2	
			SC-PP-gas	NG-PP	1.900	0.428	3.658	2	
			SC-PP-oil	CO-HF-PP	4.810	1.082	9.259	2	
			SSC	SP-S	12.604	4.691	60.140	2	
			WASOTH	WASOTH	987.723	296.317	2963.169		2
			WI	WI	28.778	8.633	86.335		2
SVK	Slovakia	EU28	BIO	PSB – DR	1.934	0.459	3.554	1	
			BIO	PSB – IND	15.723	3.734	28.890	1	
			BIO	PSB – PP	18.598	4.417	34.173	1	
			CEM	CEM	183.640	64.858	1118.787	1	
			CEM	PC-CEM	0.986	0.585	5.305	1	
			CREM	CREM	12.652	9.941	15.137		1
			NFMP	AL-P	2.138	0.725	4.037	1	
			NFMP-AU	GP-L	1.386	0.485	2.703	1	
			OR	CO-OR	10.712	5.088	16.871	1	
			PISP	PIP	124.040	43.483	656.528	1	

Country code	Country name	Region	Sector Code	Activity Code	Emission estimate, kg	Low range estimate, kg	High range estimate, kg	Technology group	Waste group
			SC-DR-coal	BC-DR	13.016	7.419	29.612	1	
			SC-DR-coal	HC-DR	13.519	7.706	30.755	1	
			SC-DR-gas	NG-DR	0.393	0.093	0.723	1	
			SC-DR-oil	CO-LF-DR	2.662	0.632	4.891	1	
			SC-IND-coal	BC-IND-CEM	0.830	0.473	1.888	1	
			SC-IND-coal	BC-IND-OTH	4.978	2.838	11.325	1	
			SC-IND-coal	HC-IND-CEM	4.074	2.322	9.269	1	
			SC-IND-coal	HC-IND-PIP	24.212	13.801	55.082	1	
			SC-IND-gas	NG-IND	0.183	0.044	0.337	1	
			SC-IND-oil	CO-HF-IND	0.038	0.009	0.070	1	
			SC-IND-oil	CO-LF-IND	0.023	0.005	0.042	1	
			SC-PP-coal	BC-L-PP	204.413	126.225	643.902	1	
			SC-PP-coal	HC-A-PP	2.649	1.510	10.662	1	
			SC-PP-coal	HC-B-PP	23.495	13.392	53.450	1	
			SC-PP-gas	NG-PP	0.176	0.042	0.324	1	
			SC-PP-oil	CO-HF-PP	2.030	0.482	3.730	1	
			SSC	SP-S	8.449	3.145	40.316	1	
			WASOTH	WASOTH	34.399	10.320	103.196		1
			WI	WI	13.147	3.944	39.442		1
SVN	Slovenia	EU28	BIO	PSB – DR	23.639	5.614	43.436	1	
			BIO	PSB – IND	2.882	0.684	5.295	1	
			BIO	PSB – PP	2.242	0.532	4.119	1	
			CEM	CEM	14.674	9.338	28.180	1	
			CEM	PC-CEM	3.229	1.950	4.627	1	
			CREM	CREM	7.353	5.777	8.797		1
			NFMP	AL-P	1.063	0.360	2.007	1	
			SC-DR-gas	NG-DR	0.036	0.009	0.067	1	
			SC-DR-oil	CO-LF-DR	3.020	0.717	5.549	1	
			SC-IND-coal	BC-IND-OTH	6.306	3.594	14.345	1	
			SC-IND-coal	HC-IND-CEM	0.075	0.043	0.172	1	
			SC-IND-coal	HC-IND-NFM	0.139	0.079	0.316	1	
			SC-IND-gas	NG-IND	0.094	0.022	0.172	1	
			SC-IND-oil	CO-HF-IND	0.057	0.014	0.105	1	
			SC-IND-oil	CO-LF-IND	0.086	0.020	0.157	1	
			SC-PP-coal	BC-L-PP	266.046	164.283	838.045	1	
			SC-PP-coal	BC-S-PP	37.103	21.148	84.408	1	
			SC-PP-coal	HC-B-PP	0.271	0.155	0.617	1	
			SC-PP-gas	NG-PP	0.024	0.006	0.043	1	
			SC-PP-oil	CO-LF-PP	0.012	0.003	0.022	1	
			SSC	SP-S	14.354	5.343	68.493	1	
			WASOTH	WASOTH	13.988	4.196	41.963		1
			WI	WI	5.346	1.604	16.039		1
SLB	Solomon Islands	Australia, New Zealand & Oceania	BIO	PSB – DR	2.535	0.444	5.767	4	
			BIO	PSB – IND	0.108	0.019	0.245	4	
			CREM	CREM	1.942	1.745	2.326		4

Country code	Country name	Region	Sector Code	Activity Code	Emission estimate, kg	Low range estimate, kg	High range estimate, kg	Technology group	Waste group
			OR	CO-OR	0.005	0.002	0.009	4	
			SC-DR-gas	NG-DR	0.000	0.000	0.001	4	
			SC-DR-oil	CO-HF-DR	0.011	0.002	0.025	4	
			SC-DR-oil	CO-LF-DR	0.029	0.005	0.065	4	
			SC-IND-coal	BC-IND-OTH	0.025	0.011	0.071	4	
			SC-IND-coal	HC-IND-OTH	1.582	0.664	4.456	4	
			SC-IND-oil	CO-HF-IND	0.024	0.004	0.056	4	
			SC-IND-oil	CO-LF-IND	0.003	0.000	0.006	4	
			SC-PP-coal	HC-B-PP	0.357	0.150	1.005	4	
			SC-PP-gas	NG-PP	0.000	0.000	0.001	4	
			SC-PP-oil	CO-HF-PP	0.126	0.022	0.286	4	
			SC-PP-oil	CO-LF-PP	0.016	0.003	0.037	4	
			WASOTH	WASOTH	4.262	1.278	12.785		4
			WI	WI	0.013	0.004	0.040		4
SOM	Somalia	Sub-Saharan Africa	BIO	PSB – DR	121.227	21.215	275.792	5	
			BIO	PSB – IND	0.726	0.127	1.653	5	
			BIO	PSB – PP	0.263	0.046	0.599	5	
			CREM	CREM	0.001	0.001	0.002		4
			SC-DR-coal	HC-DR	0.144	0.060	0.404	5	
			SC-DR-oil	CO-LF-DR	0.064	0.011	0.146	5	
			SC-IND-coal	HC-IND-OTH	0.139	0.059	0.393	5	
			SC-IND-gas	NG-IND	0.000	0.000	0.000	5	
			SC-IND-oil	CO-HF-IND	0.117	0.020	0.266	5	
			SC-IND-oil	CO-IND	0.016	0.003	0.037	5	
			SC-IND-oil	CO-LF-IND	0.011	0.002	0.025	5	
			SC-PP-coal	HC-B-PP	0.943	0.396	2.657	5	
			SC-PP-gas	NG-PP	0.001	0.000	0.003	5	
			SC-PP-oil	CO-HF-PP	0.152	0.027	0.346	5	
			SC-PP-oil	CO-LF-PP	0.031	0.006	0.072	5	
			WASOTH	WASOTH	23.305	10.078	35.902		4
			WI	WI	0.004	0.002	0.007		4
ZAF	South Africa	Sub-Saharan Africa	ASGM	GP-A	1662.500	415.625	2909.375		
			BIO	PSB – DR	444.941	100.112	856.512	3	
			BIO	PSB – IND	89.073	20.041	171.465	3	
			BIO	PSB – PP	5.134	1.155	9.882	3	
			CEM	CEM	887.145	313.458	4602.170	3	
			CREM	CREM	6.014	4.335	8.669		2
			NFMP	AL-P	45.175	27.974	74.539	3	
			NFMP	CU-P	2000.994	714.195	11424.303	3	
			NFMP-AU	GP-L	5722.794	2002.978	11159.448	3	
			OR	CO-OR	17.346	7.806	28.622	3	
			PISP	PIP	258.536	90.631	1368.395	3	
			SC-DR-coal	HC-DR	2431.520	1531.858	3477.074	3	
			SC-DR-gas	NG-DR	0.000	0.000	0.001	3	
			SC-DR-oil	CO-HF-DR	0.680	0.153	1.309	3	

Country code	Country name	Region	Sector Code	Activity Code	Emission estimate, kg	Low range estimate, kg	High range estimate, kg	Technology group	Waste group
			SC-DR-oil	CO-LF-DR	18.732	4.215	36.059	3	
			SC-IND-coal	HC-IND-CEM	297.724	187.566	425.745	3	
			SC-IND-coal	HC-IND-NFM	480.900	302.967	687.687	3	
			SC-IND-coal	HC-IND-OTH	1602.090	1009.317	2290.989	3	
			SC-IND-coal	HC-IND-PIP	499.800	314.874	714.714	3	
			SC-IND-gas	NG-IND	0.405	0.091	0.780	3	
			SC-IND-oil	CO-HF-IND	10.868	2.445	20.921	3	
			SC-IND-oil	CO-LF-IND	3.196	0.719	6.152	3	
			SC-PP-coal	HC-B-PP	27642.323	17414.664	39528.522	3	
			SC-PP-oil	CO-LF-PP	0.066	0.015	0.127	3	
			SSC	SP-S	71.131	26.474	339.411	3	
			WASOTH	WASOTH	2173.320	939.814	3348.088		2
			WI	WI	63.322	27.382	97.550		2
SSD	South Sudan	Sub-Saharan Africa	BIO	PSB – DR	8.353	1.879	16.079	5	
			BIO	PSB – PP	0.020	0.005	0.039	5	
			SC-DR-oil	CO-LF-DR	0.360	0.081	0.693	5	
			SC-IND-oil	CO-LF-IND	0.004	0.001	0.008	5	
			SC-PP-oil	CO-LF-PP	0.176	0.040	0.339	5	
			SC-PP-oil	CO-PP	0.230	0.052	0.443	5	
			WASOTH	WASOTH	112.971	48.852	174.037		
			WI	WI	0.022	0.009	0.033		
ESP	Spain	EU28	BIO	PSB – DR	134.623	31.973	247.370	1	
			BIO	PSB – IND	49.704	11.805	91.331	1	
			BIO	PSB – PP	51.609	12.257	94.831	1	
			CEM	CEM	807.099	285.053	4587.989	1	
			CEM	PC-CEM	28.973	17.203	155.910	1	
			CREM	CREM	56.411	44.323	67.492		1
			CSP	CSP-C	215.581	75.453	420.382	1	
			NFMP	AL-P	2.875	0.975	5.429	1	
			NFMP	CU-P	54.393	19.414	310.544	1	
			NFMP	ZN-P	159.477	78.742	373.023	1	
			NFMP-AU	GP-L	4.158	1.455	8.108	1	
			OR	CO-OR	117.296	55.716	184.741	1	
			PISP	PIP	127.919	44.843	677.055	1	
			SC-DR-coal	HC-DR	22.969	13.092	52.254	1	
			SC-DR-gas	NG-DR	1.471	0.349	2.702	1	
			SC-DR-oil	CO-HF-DR	3.220	0.765	5.917	1	
			SC-DR-oil	CO-LF-DR	50.602	12.018	92.981	1	
			SC-IND-coal	HC-IND-CEM	0.905	0.516	2.060	1	
			SC-IND-coal	HC-IND-OTH	15.471	8.818	35.196	1	
			SC-IND-coal	HC-IND-PIP	5.550	3.164	12.626	1	
			SC-IND-gas	NG-IND	1.605	0.381	2.948	1	
			SC-IND-oil	CO-HF-IND	7.087	1.683	13.022	1	
			SC-IND-oil	CO-LF-IND	2.075	0.493	3.812	1	
			SC-PP-coal	BC-S-PP	250.769	142.938	570.500	1	

Country code	Country name	Region	Sector Code	Activity Code	Emission estimate, kg	Low range estimate, kg	High range estimate, kg	Technology group	Waste group
			SC-PP-coal	HC-A-PP	144.106	82.140	580.025	1	
			SC-PP-coal	HC-B-PP	942.575	537.267	2144.357	1	
			SC-PP-gas	NG-PP	2.508	0.596	4.609	1	
			SC-PP-oil	CO-HF-PP	18.730	4.448	34.416	1	
			SC-PP-oil	CO-LF-PP	1.263	0.300	2.321	1	
			SSC	SP-S	234.382	87.235	1118.388	1	
			WASOTH	WASOTH	341.752	102.525	1025.255		1
			WI	WI	130.621	39.186	391.863		1
LKA	Sri Lanka	South Asia	BIO	PSB – DR	156.519	35.217	301.299	5	
			BIO	PSB – IND	89.770	20.198	172.807	5	
			BIO	PSB – PP	1.968	0.443	3.787	5	
			CEM	CEM	205.465	72.573	1083.121	5	
			CREM	CREM	12.737	10.553	14.556		4
			OR	CO-OR	3.056	1.375	5.043	5	
			SC-DR-oil	CO-HF-DR	0.800	0.180	1.540	5	
			SC-DR-oil	CO-LF-DR	3.624	0.815	6.976	5	
			SC-IND-coal	HC-IND-CEM	13.050	7.047	31.103	5	
			SC-IND-oil	CO-HF-IND	13.680	3.078	26.334	5	
			SC-IND-oil	CO-LF-IND	0.218	0.049	0.420	5	
			SC-PP-coal	HC-B-PP	211.500	114.210	504.075	5	
			SC-PP-oil	CO-HF-PP	5.800	1.305	11.165	5	
			SC-PP-oil	CO-LF-PP	0.172	0.039	0.331	5	
			SSC	SP-S	0.899	0.335	4.289	5	
			WASOTH	WASOTH	885.287	265.586	2655.862		4
			WI	WI	2.770	0.831	8.311		4
SPM	St. Pierre-Miquelon	Central America and the Caribbean	BIO	PSB – DR	0.007	0.001	0.017	3	
			BIO	PSB – IND	0.037	0.007	0.085	3	
			BIO	PSB – PP	0.013	0.002	0.030	3	
			CREM	CREM	0.001	0.001	0.001		4
			OR	CO-OR	0.004	0.001	0.007	3	
			SC-DR-coal	HC-DR	0.134	0.056	0.378	3	
			SC-DR-gas	NG-DR	0.000	0.000	0.000	3	
			SC-DR-oil	CO-HF-DR	0.004	0.001	0.009	3	
			SC-DR-oil	CO-LF-DR	0.009	0.002	0.021	3	
			SC-IND-gas	NG-IND	0.000	0.000	0.000	3	
			SC-IND-oil	CO-HF-IND	0.011	0.002	0.025	3	
			SC-IND-oil	CO-LF-IND	0.001	0.000	0.001	3	
			SC-PP-gas	NG-PP	0.001	0.000	0.002	3	
			SC-PP-oil	CO-HF-PP	0.104	0.018	0.236	3	
			SC-PP-oil	CO-LF-PP	0.008	0.001	0.017	3	
			WASOTH	WASOTH	0.566	0.170	1.698		4
			WI	WI	0.002	0.001	0.005		4
SDN	Sudan	Sub-Saharan Africa	ASGM	GP-A	62250.000	15562.500	108937.500		
			BIO	PSB – DR	200.813	45.183	386.564	5	
			BIO	PSB – IND	42.237	9.503	81.305	5	

Country code	Country name	Region	Sector Code	Activity Code	Emission estimate, kg	Low range estimate, kg	High range estimate, kg	Technology group	Waste group
			CEM	CEM	365.190	129.034	1894.467	5	
			CREM	CREM	1.091	0.786	1.573		4
			NFMP-AU	GP-L	453.200	158.620	883.740	5	
			OR	CO-OR	36.321	16.344	59.929	5	
			SC-DR-oil	CO-LF-DR	3.426	0.771	6.595	5	
			SC-IND-oil	CO-HF-IND	1.400	0.315	2.695	5	
			SC-IND-oil	CO-LF-IND	0.226	0.051	0.435	5	
			SC-PP-oil	CO-HF-PP	8.540	1.922	16.440	5	
			SC-PP-oil	CO-LF-PP	0.786	0.177	1.513	5	
			SC-PP-oil	CO-PP	4.720	1.062	9.086	5	
			WASOTH	WASOTH	871.879	377.029	1343.165		4
			WI	WI	0.167	0.072	0.257		4
SUR	Suriname	South America	ASGM	GP-A	14332.500	10032.750	18632.250		
			BIO	PSB – DR	1.285	0.289	2.474	3	
			BIO	PSB – IND	0.204	0.046	0.393	3	
			CEM	CEM	9.568	3.385	50.768	3	
			CREM	CREM	0.226	0.158	0.317		4
			NFMP	AL-P	115.940	40.579	226.083	3	
			NFMP-AU	GP-L	1188.000	415.800	2316.600	3	
			OR	CO-OR	0.416	0.187	0.687	3	
			SC-DR-oil	CO-HF-DR	0.340	0.077	0.655	3	
			SC-DR-oil	CO-LF-DR	0.324	0.073	0.624	3	
			SC-IND-oil	CO-LF-IND	0.032	0.007	0.062	3	
			SC-PP-oil	CO-HF-PP	4.110	0.925	7.912	3	
			SC-PP-oil	CO-LF-PP	0.026	0.006	0.049	3	
			SC-PP-oil	CO-PP	0.023	0.005	0.043	3	
			WASOTH	WASOTH	19.635	5.891	58.906		4
			WI	WI	0.066	0.020	0.198		4
SWZ	Swaziland	Sub-Saharan Africa	ASGM	GP-A	225.000	56.250	393.750		
			BIO	PSB – DR	16.393	2.869	37.294	4	
			BIO	PSB – IND	2.061	0.361	4.689	4	
			BIO	PSB – PP	0.756	0.132	1.721	4	
			CREM	CREM	0.032	0.023	0.046		4
			SC-DR-coal	HC-DR	0.412	0.173	1.162	4	
			SC-DR-oil	CO-LF-DR	0.185	0.032	0.420	4	
			SC-IND-coal	HC-IND-OTH	0.374	0.157	1.053	4	
			SC-IND-gas	NG-IND	0.000	0.000	0.000	4	
			SC-IND-oil	CO-HF-IND	0.336	0.059	0.764	4	
			SC-IND-oil	CO-IND	0.046	0.008	0.105	4	
			SC-IND-oil	CO-LF-IND	0.032	0.006	0.073	4	
			SC-PP-coal	HC-B-PP	2.711	1.138	7.635	4	
			SC-PP-gas	NG-PP	0.003	0.001	0.007	4	
			SC-PP-oil	CO-HF-PP	0.437	0.076	0.994	4	
			SC-PP-oil	CO-LF-PP	0.090	0.016	0.206	4	
			WASOTH	WASOTH	55.858	24.155	86.051		4
			WI	WI	0.011	0.005	0.016		4

Country code	Country name	Region	Sector Code	Activity Code	Emission estimate, kg	Low range estimate, kg	High range estimate, kg	Technology group	Waste group
SWE	Sweden	EU28	BIO	PSB – DR	55.604	13.206	102.173	1	
			BIO	PSB – IND	165.231	39.242	303.613	1	
			BIO	PSB – PP	161.271	38.302	296.336	1	
			CEM	CEM	39.780	14.459	73.593	1	
			CREM	CREM	36.727	28.857	43.941		1
			CSP	CSP-C	15.600	5.460	30.420	1	
			NFMP	AL-P	1.438	0.487	2.715	1	
			NFMP	CU-P	52.560	19.105	165.496	1	
			NFMP	PB-P	0.952	0.519	1.501	1	
			OR	CO-OR	36.094	17.145	56.848	1	
			PISP	PIP	75.793	27.080	199.114	1	
			SC-DR-gas	NG-DR	0.038	0.009	0.071	1	
			SC-DR-oil	CO-HF-DR	0.860	0.204	1.580	1	
			SC-DR-oil	CO-LF-DR	8.202	1.948	15.071	1	
			SC-IND-coal	HC-IND-CEM	11.475	6.541	26.106	1	
			SC-IND-coal	HC-IND-NFM	3.469	1.977	7.891	1	
			SC-IND-coal	HC-IND-OTH	11.100	6.327	25.253	1	
			SC-IND-coal	HC-IND-PIP	4.232	2.412	9.628	1	
			SC-IND-gas	NG-IND	0.094	0.022	0.172	1	
			SC-IND-oil	CO-HF-IND	4.180	0.993	7.681	1	
			SC-IND-oil	CO-LF-IND	0.473	0.112	0.869	1	
			SC-PP-coal	HC-B-PP	7.722	4.402	17.568	1	
			SC-PP-gas	NG-PP	0.043	0.010	0.080	1	
			SC-PP-oil	CO-HF-PP	0.710	0.169	1.305	1	
			SC-PP-oil	CO-LF-PP	0.074	0.017	0.135	1	
			SSC	SP-S	33.680	12.535	160.708	1	
			WASOTH	WASOTH	99.378	29.814	298.135		1
			WI	WI	37.983	11.395	113.950		1
CHE	Switzerland	CIS & other European countries	BIO	PSB – DR	31.471	7.474	57.827	1	
			BIO	PSB – IND	8.559	2.033	15.727	1	
			BIO	PSB – PP	5.068	1.204	9.312	1	
			CEM	CEM	88.473	48.336	697.100	1	
			CEM	PC-CEM	0.503	0.299	2.707	1	
			CREM	CREM	12.607	9.245	16.809		1
			CSP	CSP-C	29.680	10.388	57.876	1	
			OR	CO-OR	3.171	1.506	4.994	1	
			SC-DR-coal	HC-DR	2.100	1.197	4.778	1	
			SC-DR-gas	NG-DR	0.405	0.096	0.744	1	
			SC-DR-oil	CO-HF-DR	0.020	0.005	0.037	1	
			SC-DR-oil	CO-LF-DR	10.716	2.545	19.691	1	
			SC-IND-coal	BC-IND-CEM	9.809	5.591	22.314	1	
			SC-IND-coal	HC-IND-CEM	3.471	1.978	7.896	1	
			SC-IND-coal	HC-IND-OTH	0.069	0.040	0.158	1	
			SC-IND-coal	HC-IND-PIP	0.971	0.554	2.210	1	
			SC-IND-gas	NG-IND	0.217	0.051	0.398	1	

Country code	Country name	Region	Sector Code	Activity Code	Emission estimate, kg	Low range estimate, kg	High range estimate, kg	Technology group	Waste group
			SC-IND-oil	CO-HF-IND	0.114	0.027	0.209	1	
			SC-IND-oil	CO-LF-IND	0.568	0.135	1.044	1	
			SC-PP-gas	NG-PP	0.045	0.011	0.082	1	
			SC-PP-oil	CO-HF-PP	0.130	0.031	0.239	1	
			SC-PP-oil	CO-LF-PP	0.017	0.004	0.030	1	
			SSC	SP-S	34.427	12.813	164.272	1	
			WASOTH	WASOTH	247.541	74.262	742.622		1
			WI	WI	94.613	28.384	283.838		1
SYR	Syrian Arab Rep.	Middle Eastern States	BIO	PSB – DR	0.238	0.053	0.457	3	
			CEM	CEM	343.520	121.296	1780.376	3	
			CREM	CREM	0.521	0.391	0.608		4
			CSP	CSP-C	70.000	24.500	136.500	3	
			OR	CO-OR	2.009	0.904	3.315	3	
			SC-DR-oil	CO-HF-DR	5.640	1.269	10.857	3	
			SC-DR-oil	CO-LF-DR	3.546	0.798	6.826	3	
			SC-IND-gas	NG-IND	0.048	0.011	0.092	3	
			SC-IND-oil	CO-HF-IND	12.198	2.745	23.481	3	
			SC-IND-oil	CO-LF-IND	0.642	0.144	1.236	3	
			SC-PP-gas	NG-PP	0.675	0.152	1.300	3	
			SC-PP-oil	CO-HF-PP	19.470	4.381	37.480	3	
			SC-PP-oil	CO-LF-PP	0.314	0.071	0.603	3	
			SSC	SP-S	0.126	0.047	0.602	3	
			WASOTH	WASOTH	84.745	25.424	254.235		4
			WI	WI	0.265	0.080	0.796		4
TWN	Taiwan (China)	East and Southeast Asia	BIO	PSB – IND	4.238	0.954	8.158	1	
			BIO	PSB – PP	12.329	2.774	23.733	1	
			CEM	CEM	1078.378	380.895	5684.734	1	
			CREM	CREM	17.216	15.665	19.104		1
			OR	CO-OR	567.628	255.433	936.586	1	
			PISP	PIP	466.686	163.599	2470.104	1	
			SC-DR-gas	NG-DR	0.287	0.065	0.553	1	
			SC-DR-oil	CO-HF-DR	8.360	1.881	16.093	1	
			SC-DR-oil	CO-LF-DR	9.224	2.075	17.756	1	
			SC-IND-coal	HC-IND-CEM	215.706	116.481	514.099	1	
			SC-IND-coal	HC-IND-OTH	500.888	270.479	1193.782	1	
			SC-IND-coal	HC-IND-PIP	17.552	9.478	41.832	1	
			SC-IND-gas	NG-IND	0.371	0.083	0.714	1	
			SC-IND-oil	CO-HF-IND	28.804	6.481	55.448	1	
			SC-IND-oil	CO-LF-IND	0.184	0.041	0.355	1	
			SC-PP-coal	BC-S-PP	1245.989	672.834	2969.608	1	
			SC-PP-coal	HC-B-PP	1696.212	915.955	4042.639	1	
			SC-PP-gas	NG-PP	2.964	0.667	5.705	1	
			SC-PP-oil	CO-HF-PP	26.440	5.949	50.897	1	
			SC-PP-oil	CO-LF-PP	0.215	0.048	0.413	1	
			SSC	SP-S	225.862	84.065	1077.738	1	

Country code	Country name	Region	Sector Code	Activity Code	Emission estimate, kg	Low range estimate, kg	High range estimate, kg	Technology group	Waste group
			WASOTH	WASOTH	597.190	179.157	1791.570		1
			WI	WI	228.252	68.476	684.757		1
TJK	Tajikistan	CIS & other European countries	ASGM	GP-A	3000.000	750.000	5250.000		
			CEM	CEM	112.700	39.797	571.651	4	
			CREM	CREM	0.357	0.262	0.476		4
			NFMP	AL-P	5.000	1.695	9.442	4	
			NFMP-AU	GP-L	173.250	60.638	337.838	4	
			NFMP-HG	HG-P	202.500	70.875	394.875	4	
			OR	CO-OR	0.028	0.013	0.047	4	
			SC-DR-coal	BC-DR	8.550	4.617	20.378	4	
			SC-DR-coal	HC-DR	125.100	67.554	298.155	4	
			SC-DR-gas	NG-DR	0.001	0.000	0.002	4	
			SC-DR-oil	CO-HF-DR	0.240	0.054	0.462	4	
			SC-DR-oil	CO-LF-DR	0.458	0.103	0.882	4	
			SC-PP-coal	HC-B-PP	18.450	9.963	43.973	4	
			SC-PP-oil	CO-HF-PP	0.140	0.032	0.270	4	
			WASOTH	WASOTH	68.541	20.562	205.622		4
			WI	WI	0.214	0.064	0.643		4
THA	Thailand	East and Southeast Asia	ASGM	GP-A	1125.000	281.250	1968.750		
			BIO	PSB – DR	162.536	36.571	312.882	2	
			BIO	PSB – IND	255.426	57.471	491.695	2	
			BIO	PSB – PP	163.134	36.705	314.033	2	
			CEM	CEM	2775.663	979.930	14511.890	2	
			CREM	CREM	43.511	39.592	48.283		2
			NFMP	ZN-P	112.462	39.843	308.945	2	
			NFMP-AU	GP-L	89.070	31.174	173.686	2	
			OR	CO-OR	798.374	359.268	1317.317	2	
			SC-DR-gas	NG-DR	0.572	0.129	1.101	2	
			SC-DR-oil	CO-LF-DR	28.680	6.453	55.209	2	
			SC-IND-coal	BC-IND-CEM	84.249	45.494	200.793	2	
			SC-IND-coal	BC-IND-OTH	10.832	5.849	25.816	2	
			SC-IND-coal	HC-IND-CEM	1066.464	575.891	2541.739	2	
			SC-IND-coal	HC-IND-NFM	4.556	2.460	10.859	2	
			SC-IND-coal	HC-IND-OTH	157.275	84.929	374.839	2	
			SC-IND-gas	NG-IND	0.708	0.159	1.362	2	
			SC-IND-oil	CO-HF-IND	11.457	2.578	22.055	2	
			SC-IND-oil	CO-LF-IND	6.494	1.461	12.501	2	
			SC-PP-coal	BC-L-PP	1393.361	815.116	4598.091	2	
			SC-PP-coal	HC-B-PP	791.142	427.217	1885.556	2	
			SC-PP-gas	NG-PP	7.114	1.601	13.694	2	
			SC-PP-oil	CO-HF-PP	1.840	0.414	3.542	2	
			SC-PP-oil	CO-LF-PP	0.071	0.016	0.136	2	
			SSC	SP-S	95.578	35.573	456.065	2	
			WASOTH	WASOTH	2307.763	692.329	6923.289		2
			WI	WI	67.239	20.172	201.716		2

Country code	Country name	Region	Sector Code	Activity Code	Emission estimate, kg	Low range estimate, kg	High range estimate, kg	Technology group	Waste group
TLS	Timor-Leste	East and Southeast Asia	BIO	PSB – DR	5.013	0.877	11.405	4	
			BIO	PSB – IND	0.627	0.110	1.427	4	
			CREM	CREM	0.805	0.732	0.893		4
			OR	CO-OR	0.678	0.237	1.321	4	
			SC-DR-gas	NG-DR	0.001	0.000	0.003	4	
			SC-DR-oil	CO-HF-DR	0.065	0.011	0.148	4	
			SC-DR-oil	CO-LF-DR	0.166	0.029	0.378	4	
			SC-IND-coal	BC-IND-OTH	0.146	0.061	0.412	4	
			SC-IND-coal	HC-IND-OTH	9.222	3.873	25.976	4	
			SC-IND-oil	CO-HF-IND	0.142	0.025	0.324	4	
			SC-IND-oil	CO-LF-IND	0.016	0.003	0.035	4	
			SC-PP-coal	HC-B-PP	2.080	0.874	5.860	4	
			SC-PP-gas	NG-PP	0.001	0.000	0.003	4	
			SC-PP-oil	CO-HF-PP	0.734	0.128	1.670	4	
			SC-PP-oil	CO-LF-PP	0.096	0.017	0.218	4	
			WASOTH	WASOTH	8.942	2.683	26.826		4
			WI	WI	0.028	0.008	0.084		4
TGO	Togo	Sub-Saharan Africa	ASGM	GP-A	3000.000	750.000	5250.000		
			BIO	PSB – DR	51.631	11.617	99.390	5	
			BIO	PSB – IND	0.164	0.037	0.316	5	
			BIO	PSB – PP	0.104	0.023	0.200	5	
			CEM	CEM	176.085	62.217	913.462	5	
			CREM	CREM	0.172	0.124	0.248		4
			SC-DR-oil	CO-LF-DR	0.586	0.132	1.128	5	
			SC-IND-oil	CO-HF-IND	1.060	0.239	2.041	5	
			SC-IND-oil	CO-LF-IND	0.004	0.001	0.008	5	
			SC-PP-oil	CO-LF-PP	0.008	0.002	0.015	5	
			WASOTH	WASOTH	52.680	22.781	81.156		4
			WI	WI	0.010	0.004	0.016		4
TKL	Tokelau	Australia, New Zealand & Oceania	CREM	CREM	0.004	0.004	0.005		4
			WASOTH	WASOTH	0.005	0.001	0.015		4
			WI	WI	0.000	0.000	0.000		4
TON	Tonga	Australia, New Zealand & Oceania	BIO	PSB – DR	0.434	0.076	0.987	4	
			BIO	PSB – IND	0.049	0.009	0.112	4	
			CREM	CREM	0.326	0.293	0.390		4
			OR	CO-OR	0.002	0.001	0.004	4	
			SC-DR-gas	NG-DR	0.000	0.000	0.000	4	
			SC-DR-oil	CO-HF-DR	0.005	0.001	0.012	4	
			SC-DR-oil	CO-LF-DR	0.013	0.002	0.030	4	
			SC-IND-coal	BC-IND-OTH	0.012	0.005	0.032	4	
			SC-IND-coal	HC-IND-OTH	0.727	0.305	2.046	4	
			SC-IND-oil	CO-HF-IND	0.011	0.002	0.026	4	
			SC-IND-oil	CO-LF-IND	0.001	0.000	0.003	4	
			SC-PP-coal	HC-B-PP	0.164	0.069	0.462	4	
			SC-PP-gas	NG-PP	0.000	0.000	0.000	4	

Country code	Country name	Region	Sector Code	Activity Code	Emission estimate, kg	Low range estimate, kg	High range estimate, kg	Technology group	Waste group
			SC-PP-oil	CO-HF-PP	0.058	0.010	0.132	4	
			SC-PP-oil	CO-LF-PP	0.008	0.001	0.017	4	
			WASOTH	WASOTH	1.950	0.585	5.849		4
			WI	WI	0.006	0.002	0.018		4
TTO	Trinidad and Tobago	Central America and the Caribbean	BIO	PSB – DR	0.534	0.120	1.027	3	
			CEM	CEM	70.978	25.077	389.540	3	
			CREM	CREM	0.115	0.092	0.138		4
			OR	CO-OR	5.399	2.429	8.908	3	
			SC-DR-gas	NG-DR	0.018	0.004	0.035	3	
			SC-DR-oil	CO-LF-DR	0.844	0.190	1.625	3	
			SC-IND-gas	NG-IND	0.419	0.094	0.807	3	
			SC-IND-oil	CO-LF-IND	0.232	0.052	0.446	3	
			SC-PP-gas	NG-PP	1.350	0.304	2.599	3	
			SC-PP-oil	CO-LF-PP	0.042	0.009	0.081	3	
			SSC	SP-S	12.288	4.574	58.635	3	
			WASOTH	WASOTH	119.115	35.734	357.344		4
			WI	WI	0.373	0.112	1.118		4
TUN	Tunisia	North Africa	BIO	PSB – DR	37.379	8.410	71.954	5	
			CEM	CEM	903.573	319.445	4668.917	5	
			CEM	PC-CEM	32.600	18.338	183.783	5	
			CREM	CREM	0.096	0.072	0.120		4
			OR	CO-OR	2.535	1.141	4.183	5	
			SC-DR-gas	NG-DR	0.114	0.026	0.220	5	
			SC-DR-oil	CO-HF-DR	0.480	0.108	0.924	5	
			SC-DR-oil	CO-LF-DR	3.714	0.836	7.149	5	
			SC-IND-gas	NG-IND	0.185	0.042	0.357	5	
			SC-IND-oil	CO-HF-IND	4.320	0.972	8.316	5	
			SC-IND-oil	CO-LF-IND	0.114	0.026	0.219	5	
			SC-PP-gas	NG-PP	0.871	0.196	1.676	5	
			SC-PP-oil	CO-HF-PP	5.320	1.197	10.241	5	
			SC-PP-oil	CO-LF-PP	0.042	0.009	0.081	5	
			SSC	SP-S	4.495	1.673	21.446	5	
			WASOTH	WASOTH	329.775	98.933	989.326		4
			WI	WI	1.109	0.333	3.328		4
TUR	Turkey	Middle Eastern States	BIO	PSB – DR	147.050	34.924	270.204	3	
			BIO	PSB – PP	1.777	0.422	3.265	3	
			CEM	CEM	6790.521	2396.654	35162.344	3	
			CREM	CREM	0.304	0.228	0.355		2
			NFMP	AL-P	7.750	2.713	15.113	3	
			NFMP	CU-T	285.898	102.043	1632.278	3	
			NFMP-AU	GP-L	990.000	346.500	1930.500	3	
			OR	CO-OR	9.634	4.576	15.174	3	
			PISP	PIP	516.191	180.953	2732.123	3	
			SC-DR-coal	BC-DR	470.400	268.128	1070.160	3	
			SC-DR-coal	HC-DR	1010.850	576.185	2299.684	3	

Country code	Country name	Region	Sector Code	Activity Code	Emission estimate, kg	Low range estimate, kg	High range estimate, kg	Technology group	Waste group
			SC-DR-gas	NG-DR	2.818	0.669	5.179	3	
			SC-DR-oil	CO-HF-DR	4.960	1.178	9.114	3	
			SC-DR-oil	CO-LF-DR	38.556	9.157	70.847	3	
			SC-IND-coal	BC-IND-CEM	168.720	96.170	383.838	3	
			SC-IND-coal	BC-IND-OTH	333.668	190.190	759.094	3	
			SC-IND-coal	HC-IND-CEM	396.840	226.199	902.811	3	
			SC-IND-coal	HC-IND-NFM	1.013	0.577	2.303	3	
			SC-IND-coal	HC-IND-OTH	119.250	67.973	271.294	3	
			SC-IND-coal	HC-IND-PIP	45.675	26.035	103.911	3	
			SC-IND-gas	NG-IND	1.964	0.466	3.609	3	
			SC-IND-oil	CO-HF-IND	4.921	1.169	9.042	3	
			SC-IND-oil	CO-LF-IND	1.161	0.276	2.133	3	
			SC-PP-coal	BC-L-PP	4853.738	2997.183	15289.274	3	
			SC-PP-coal	BC-S-PP	57.564	32.811	130.958	3	
			SC-PP-coal	HC-B-PP	1597.118	910.357	3633.442	3	
			SC-PP-gas	NG-PP	4.275	1.015	7.855	3	
			SC-PP-oil	CO-HF-PP	9.015	2.141	16.565	3	
			SC-PP-oil	CO-LF-PP	0.338	0.080	0.620	3	
			SSC	SP-S	323.027	113.060	629.903	3	
			WASOTH	WASOTH	2089.880	626.964	6269.641		2
			WI	WI	60.891	18.267	182.672		2
TKM	Turkmenistan	CIS & other European countries	CEM	CEM	284.200	100.358	1441.554	4	
			CREM	CREM	0.498	0.365	0.665		4
			OR	CO-OR	9.725	4.376	16.047	4	
			SC-DR-gas	NG-DR	2.197	0.494	4.230	4	
			SC-DR-oil	CO-HF-DR	18.620	4.190	35.844	4	
			SC-DR-oil	CO-LF-DR	4.160	0.936	8.008	4	
			SC-IND-gas	NG-IND	0.233	0.052	0.448	4	
			SC-PP-gas	NG-PP	2.536	0.571	4.882	4	
			WASOTH	WASOTH	253.342	76.003	760.025		4
			WI	WI	0.793	0.238	2.378		4
TCA	Turks and Caicos Islands	Central America and the Caribbean	BIO	PSB – DR	0.065	0.011	0.149	3	
			BIO	PSB – IND	0.276	0.048	0.627	3	
			BIO	PSB – PP	0.098	0.017	0.223	3	
			CREM	CREM	0.010	0.008	0.012		4
			OR	CO-OR	0.026	0.009	0.051	3	
			SC-DR-coal	HC-DR	0.995	0.418	2.801	3	
			SC-DR-gas	NG-DR	0.000	0.000	0.000	3	
			SC-DR-oil	CO-HF-DR	0.028	0.005	0.064	3	
			SC-DR-oil	CO-LF-DR	0.067	0.012	0.153	3	
			SC-IND-gas	NG-IND	0.000	0.000	0.000	3	
			SC-IND-oil	CO-HF-IND	0.081	0.014	0.184	3	
			SC-IND-oil	CO-LF-IND	0.005	0.001	0.010	3	
			SC-PP-gas	NG-PP	0.005	0.001	0.011	3	
			SC-PP-oil	CO-HF-PP	0.770	0.135	1.751	3	

Country code	Country name	Region	Sector Code	Activity Code	Emission estimate, kg	Low range estimate, kg	High range estimate, kg	Technology group	Waste group
			SC-PP-oil	CO-LF-PP	0.057	0.010	0.129	3	
			WASOTH	WASOTH	1.662	0.499	4.985		4
			WI	WI	0.005	0.002	0.016		4
TUV	Tuvalu	Australia, New Zealand & Oceania	CREM	CREM	0.034	0.030	0.040		4
			WASOTH	WASOTH	0.129	0.039	0.388		4
			WI	WI	0.000	0.000	0.001		4
UGA	Uganda	Sub-Saharan Africa	ASGM	GP-A	3000.000	750.000	5250.000		
			BIO	PSB – DR	423.660	74.141	963.827	5	
			BIO	PSB – IND	12.694	2.222	28.880	5	
			BIO	PSB – PP	4.599	0.805	10.463	5	
			CEM	CEM	224.805	79.431	1166.203	5	
			CREM	CREM	0.849	0.612	1.224		4
			SC-DR-coal	HC-DR	2.508	1.053	7.065	5	
			SC-DR-oil	CO-LF-DR	1.122	0.196	2.552	5	
			SC-IND-coal	HC-IND-OTH	2.435	1.023	6.860	5	
			SC-IND-gas	NG-IND	0.000	0.000	0.000	5	
			SC-IND-oil	CO-HF-IND	2.042	0.357	4.647	5	
			SC-IND-oil	CO-IND	0.281	0.049	0.639	5	
			SC-IND-oil	CO-LF-IND	0.195	0.034	0.445	5	
			SC-PP-coal	HC-B-PP	16.483	6.923	46.427	5	
			SC-PP-gas	NG-PP	0.019	0.003	0.044	5	
			SC-PP-oil	CO-HF-PP	2.656	0.465	6.041	5	
			SC-PP-oil	CO-LF-PP	0.549	0.096	1.250	5	
			SSC	SP-S	0.899	0.335	4.289	5	
			WASOTH	WASOTH	357.275	154.497	550.397		4
			WI	WI	0.068	0.030	0.105		4
UKR	Ukraine	CIS & other European countries	ASGM	GP-A	225.000	56.250	393.750		
			BIO	PSB – DR	59.198	13.319	113.955	4	
			BIO	PSB – IND	4.413	0.993	8.495	4	
			BIO	PSB – PP	29.384	6.611	56.564	4	
			CEM	CEM	944.328	333.466	4789.935	4	
			CREM	CREM	22.713	16.656	30.284		2
			OR	CO-OR	2.379	1.071	3.926	4	
			PISP	PIP	1499.118	525.524	7934.616	4	
			SC-DR-coal	HC-DR	89.400	48.276	213.070	4	
			SC-DR-gas	NG-DR	2.554	0.575	4.917	4	
			SC-DR-oil	CO-HF-DR	0.300	0.068	0.578	4	
			SC-DR-oil	CO-LF-DR	8.852	1.992	17.040	4	
			SC-IND-coal	HC-IND-CEM	122.194	65.985	291.228	4	
			SC-IND-coal	HC-IND-NFM	25.200	13.608	60.060	4	
			SC-IND-coal	HC-IND-OTH	7.088	3.827	16.892	4	
			SC-IND-coal	HC-IND-PIP	252.263	136.222	601.226	4	
			SC-IND-gas	NG-IND	0.643	0.145	1.237	4	
			SC-IND-oil	CO-HF-IND	0.200	0.045	0.385	4	
			SC-IND-oil	CO-LF-IND	1.536	0.346	2.957	4	

Country code	Country name	Region	Sector Code	Activity Code	Emission estimate, kg	Low range estimate, kg	High range estimate, kg	Technology group	Waste group
			SC-PP-coal	HC-A-PP	218.138	117.794	919.813	4	
			SC-PP-coal	HC-B-PP	3097.688	1672.751	7382.822	4	
			SC-PP-gas	NG-PP	2.216	0.499	4.267	4	
			SC-PP-oil	CO-HF-PP	7.160	1.611	13.783	4	
			SC-PP-oil	CO-LF-PP	0.154	0.035	0.296	4	
			SC-PP-oil	CO-PP	0.030	0.007	0.058	4	
			SSC	SP-S	48.956	18.221	233.601	4	
			WASOTH	WASOTH	639.563	191.869	1918.690		2
			WI	WI	18.634	5.590	55.903		2
ARE	United Arab Emirates	Middle Eastern States	CEM	CEM	1225.824	432.835	6353.131	1	
			CREM	CREM	0.180	0.135	0.210		2
			CSP	CSP-C	22.500	7.875	43.875	1	
			NFMP	AL-P	30.000	10.169	56.655	1	
			OR	CO-OR	12.351	5.558	20.380	1	
			SC-DR-oil	CO-LF-DR	5.566	1.252	10.715	1	
			SC-IND-coal	HC-IND-CEM	41.189	22.242	98.166	1	
			SC-IND-gas	NG-IND	6.177	1.390	11.892	1	
			SC-IND-oil	CO-HF-IND	25.441	5.724	48.974	1	
			SC-PP-gas	NG-PP	7.119	1.602	13.705	1	
			SC-PP-oil	CO-HF-PP	0.500	0.113	0.963	1	
			SC-PP-oil	CO-LF-PP	0.821	0.185	1.579	1	
			SSC	SP-S	55.783	20.762	266.177	1	
			WASOTH	WASOTH	713.795	214.139	2141.386		2
			WI	WI	20.797	6.239	62.391		2
GBR	United Kingdom	EU28	BIO	PSB – DR	90.999	21.612	167.211	1	
			BIO	PSB – IND	31.165	7.402	57.266	1	
			BIO	PSB – PP	150.465	35.735	276.479	1	
			CEM	CEM	443.300	156.633	2697.586	1	
			CREM	CREM	224.833	176.654	268.996		1
			CSP	CSP-C	249.300	87.255	486.135	1	
			NFMP	AL-P	0.588	0.199	1.109	1	
			NFMP	PB-P	3.660	1.995	5.772	1	
			OR	CO-OR	100.032	47.515	157.551	1	
			PISP	PIP	313.656	109.954	1660.136	1	
			SC-DR-coal	HC-DR	76.650	43.691	174.379	1	
			SC-DR-gas	NG-DR	7.030	1.670	12.918	1	
			SC-DR-oil	CO-HF-DR	2.120	0.504	3.896	1	
			SC-DR-oil	CO-LF-DR	52.166	12.389	95.855	1	
			SC-IND-coal	HC-IND-CEM	71.402	40.699	162.439	1	
			SC-IND-coal	HC-IND-NFM	1.457	0.830	3.314	1	
			SC-IND-coal	HC-IND-OTH	65.004	37.052	147.885	1	
			SC-IND-coal	HC-IND-PIP	3.053	1.740	6.944	1	
			SC-IND-gas	NG-IND	1.701	0.404	3.125	1	
			SC-IND-oil	CO-HF-IND	3.040	0.722	5.586	1	
			SC-IND-oil	CO-LF-IND	3.129	0.743	5.750	1	

Country code	Country name	Region	Sector Code	Activity Code	Emission estimate, kg	Low range estimate, kg	High range estimate, kg	Technology group	Waste group
			SC-PP-coal	HC-B-PP	1521.968	867.521	3462.476	1	
			SC-PP-gas	NG-PP	5.330	1.266	9.794	1	
			SC-PP-oil	CO-HF-PP	5.530	1.313	10.161	1	
			SC-PP-oil	CO-LF-PP	1.110	0.264	2.040	1	
			SSC	SP-S	45.630	16.983	217.730	1	
			WASOTH	WASOTH	576.863	173.059	1730.588		1
			WI	WI	220.483	66.145	661.449		1
TZA	United Republic of Tanzania	Sub-Saharan Africa	ASGM	GP-A	26250.000	6562.500	45937.500		
			BIO	PSB – DR	774.571	174.279	1491.050	4	
			BIO	PSB – IND	142.583	32.081	274.472	4	
			BIO	PSB – PP	0.473	0.106	0.910	4	
			CEM	CEM	258.077	91.187	1338.805	4	
			CREM	CREM	1.163	0.838	1.676		4
			NFMP-AU	GP-L	2265.962	793.087	4418.625	4	
			SC-DR-oil	CO-LF-DR	2.830	0.637	5.448	4	
			SC-IND-coal	HC-IND-OTH	33.731	18.215	80.393	4	
			SC-IND-gas	NG-IND	0.032	0.007	0.062	4	
			SC-IND-oil	CO-HF-IND	3.160	0.711	6.083	4	
			SC-PP-gas	NG-PP	0.138	0.031	0.266	4	
			SC-PP-oil	CO-HF-PP	4.720	1.062	9.086	4	
			SC-PP-oil	CO-LF-PP	0.400	0.090	0.770	4	
			WASOTH	WASOTH	685.131	296.273	1055.472		4
			WI	WI	0.131	0.057	0.202		4
USA	United States	North America	BIO	PSB – DR	662.954	157.452	1218.177	1	
			BIO	PSB – IND	1094.668	259.984	2011.452	1	
			BIO	PSB – PP	473.399	112.432	869.871	1	
			CEM	CEM	3102.081	1105.469	22693.129	1	
			CEM	PC-CEM	17.425	9.932	54.887	1	
			CREM	CREM	523.081	438.104	600.365		1
			CSP	CSP-C	182.500	63.875	355.875	1	
			NFMP	AL-P	122.955	43.034	239.762	1	
			NFMP	CU-P	101.289	36.152	578.293	1	
			NFMP	ZN-P	8.407	3.081	15.185	1	
			NFMP-AU	GP-L	494.340	173.019	963.963	1	
			OR	CO-OR	1033.537	490.930	1627.820	1	
			PISP	PIP	512.795	180.006	2852.798	1	
			SC-DR-coal	BC-DR	78.975	45.016	179.668	1	
			SC-DR-coal	HC-DR	88.725	50.573	201.849	1	
			SC-DR-gas	NG-DR	46.513	11.047	85.468	1	
			SC-DR-oil	CO-HF-DR	27.720	6.584	50.936	1	
			SC-DR-oil	CO-LF-DR	339.380	80.603	623.611	1	
			SC-IND-coal	BC-IND-CEM	45.257	25.796	102.959	1	
			SC-IND-coal	BC-IND-OTH	634.324	361.565	1443.087	1	
			SC-IND-coal	HC-IND-CEM	847.771	483.230	1928.679	1	
			SC-IND-coal	HC-IND-OTH	718.794	409.713	1635.257	1	

Country code	Country name	Region	Sector Code	Activity Code	Emission estimate, kg	Low range estimate, kg	High range estimate, kg	Technology group	Waste group
			SC-IND-coal	HC-IND-PIP	11.308	6.446	25.726	1	
			SC-IND-gas	NG-IND	27.425	6.514	50.394	1	
			SC-IND-oil	CO-HF-IND	19.893	4.725	36.553	1	
			SC-IND-oil	CO-LF-IND	25.677	6.098	47.181	1	
			SC-PP-coal	BC-L-PP	2616.806	1615.878	8242.938	1	
			SC-PP-coal	BC-S-PP	9931.688	6604.572	13556.754	1	
			SC-PP-coal	HC-A-PP	68.543	39.069	275.885	1	
			SC-PP-coal	HC-B-PP	6528.007	4341.125	8910.730	1	
			SC-PP-gas	NG-PP	69.689	16.551	128.053	1	
			SC-PP-oil	CO-HF-PP	25.500	6.056	46.856	1	
			SC-PP-oil	CO-LF-PP	11.976	2.844	22.006	1	
			SSC	SP-S	1287.768	479.299	6144.788	1	
			WASOTH	WASOTH	3297.817	989.345	9893.451		1
			WI	WI	1252.992	375.898	3758.976		1
URY	Uruguay	South America	BIO	PSB – DR	18.223	4.100	35.078	3	
			BIO	PSB – IND	59.026	13.281	113.625	3	
			BIO	PSB – PP	13.895	3.126	26.749	3	
			CEM	CEM	60.352	21.353	320.226	3	
			CREM	CREM	1.295	0.906	1.813		4
			CSP	CSP-C	75.000	26.250	146.250	3	
			NFMP-AU	GP-L	65.894	23.063	128.494	3	
			OR	CO-OR	1.828	0.823	3.016	3	
			SC-DR-gas	NG-DR	0.007	0.002	0.014	3	
			SC-DR-oil	CO-HF-DR	0.420	0.095	0.809	3	
			SC-DR-oil	CO-LF-DR	1.448	0.326	2.787	3	
			SC-IND-gas	NG-IND	0.003	0.001	0.005	3	
			SC-IND-oil	CO-HF-IND	2.964	0.667	5.706	3	
			SC-IND-oil	CO-LF-IND	0.025	0.006	0.048	3	
			SC-PP-gas	NG-PP	0.000	0.000	0.001	3	
			SC-PP-oil	CO-HF-PP	1.320	0.297	2.541	3	
			SC-PP-oil	CO-LF-PP	0.272	0.061	0.523	3	
			SSC	SP-S	2.372	0.883	11.318	3	
			WASOTH	WASOTH	163.572	49.072	490.716		4
			WI	WI	0.550	0.165	1.651		4
VIR	US Virgin Islands	Central America and the Caribbean	CREM	CREM	0.019	0.016	0.023		4
			WASOTH	WASOTH	9.970	2.991	29.911		4
			WI	WI	0.031	0.009	0.094		4
UZB	Uzbekistan	CIS & other European countries	ASGM	GP-A	225.000	56.250	393.750		
			BIO	PSB – DR	0.211	0.048	0.407	4	
			CEM	CEM	720.300	254.356	3653.593	4	
			CREM	CREM	4.038	2.961	5.384		4
			NFMP	CU-P	1153.200	411.600	6583.980	4	
			NFMP	ZN-P	1145.808	405.938	3147.643	4	
			NFMP-AU	GP-L	5049.000	1767.150	9845.550	4	
			OR	CO-OR	3.002	1.351	4.954	4	

Country code	Country name	Region	Sector Code	Activity Code	Emission estimate, kg	Low range estimate, kg	High range estimate, kg	Technology group	Waste group
			SC-DR-coal	BC-DR	64.350	34.749	153.368	4	
			SC-DR-gas	NG-DR	3.290	0.740	6.333	4	
			SC-DR-oil	CO-HF-DR	2.800	0.630	5.390	4	
			SC-DR-oil	CO-LF-DR	1.546	0.348	2.976	4	
			SC-IND-coal	BC-IND-OTH	25.301	13.663	60.301	4	
			SC-IND-coal	HC-IND-OTH	48.169	26.011	114.802	4	
			SC-IND-gas	NG-IND	1.111	0.250	2.139	4	
			SC-IND-oil	CO-HF-IND	0.020	0.005	0.039	4	
			SC-IND-oil	CO-LF-IND	0.164	0.037	0.316	4	
			SC-PP-coal	BC-L-PP	285.768	167.174	943.034	4	
			SC-PP-gas	NG-PP	3.775	0.849	7.267	4	
			SC-PP-oil	CO-HF-PP	1.020	0.230	1.964	4	
			SC-PP-oil	CO-PP	0.050	0.011	0.096	4	
			SSC	SP-S	21.094	7.851	100.652	4	
			WASOTH	WASOTH	541.717	162.515	1625.151		4
			WI	WI	1.695	0.509	5.085		4
VUT	Vanuatu	Australia, New Zealand & Oceania	BIO	PSB – DR	1.109	0.194	2.522	4	
			BIO	PSB – IND	0.062	0.011	0.141	4	
			CREM	CREM	0.849	0.763	1.017		4
			OR	CO-OR	0.003	0.001	0.005	4	
			SC-DR-gas	NG-DR	0.000	0.000	0.000	4	
			SC-DR-oil	CO-HF-DR	0.006	0.001	0.015	4	
			SC-DR-oil	CO-LF-DR	0.016	0.003	0.037	4	
			SC-IND-coal	BC-IND-OTH	0.014	0.006	0.041	4	
			SC-IND-coal	HC-IND-OTH	0.910	0.382	2.565	4	
			SC-IND-oil	CO-HF-IND	0.014	0.002	0.032	4	
			SC-IND-oil	CO-LF-IND	0.002	0.000	0.003	4	
			SC-PP-coal	HC-B-PP	0.205	0.086	0.579	4	
			SC-PP-gas	NG-PP	0.000	0.000	0.000	4	
			SC-PP-oil	CO-HF-PP	0.072	0.013	0.165	4	
			SC-PP-oil	CO-LF-PP	0.009	0.002	0.022	4	
			WASOTH	WASOTH	2.624	0.787	7.871		4
			WI	WI	0.008	0.002	0.025		4
VEN	Venezuela	South America	ASGM	GP-A	34425.000	17212.500	51637.500		
			BIO	PSB – DR	14.083	3.169	27.109	3	
			BIO	PSB – IND	20.624	4.640	39.702	3	
			CEM	CEM	588.800	208.320	3124.160	3	
			CREM	CREM	11.944	8.361	16.722		4
			NFMP	AL-P	17.050	5.968	33.248	3	
			NFMP-AU	GP-L	59.400	20.790	115.830	3	
			OR	CO-OR	43.106	19.398	71.124	3	
			SC-DR-gas	NG-DR	0.274	0.062	0.527	3	
			SC-DR-oil	CO-LF-DR	5.500	1.238	10.588	3	
			SC-IND-coal	HC-IND-CEM	22.440	12.118	53.482	3	

Country code	Country name	Region	Sector Code	Activity Code	Emission estimate, kg	Low range estimate, kg	High range estimate, kg	Technology group	Waste group
			SC-IND-gas	NG-IND	1.559	0.351	3.002	3	
			SC-IND-oil	CO-HF-IND	18.563	4.177	35.734	3	
			SC-IND-oil	CO-LF-IND	2.981	0.671	5.739	3	
			SC-PP-gas	NG-PP	2.743	0.617	5.281	3	
			SC-PP-oil	CO-HF-PP	9.975	2.244	19.202	3	
			SC-PP-oil	CO-LF-PP	8.699	1.957	16.745	3	
			SSC	SP-S	37.470	13.946	178.796	3	
			WASOTH	WASOTH	963.946	289.184	2891.837		4
			WI	WI	3.243	0.973	9.729		4
VNM	Vietnam	East and Southeast Asia	ASGM	GP-A	3562.500	890.625	6234.375		
			BIO	PSB – DR	596.854	134.292	1148.943	4	
			BIO	PSB – IND	139.090	31.295	267.748	4	
			BIO	PSB – PP	0.840	0.189	1.617	4	
			CEM	CEM	5770.855	2038.330	30421.407	4	
			CREM	CREM	60.775	55.301	67.440		4
			NFMP	AL-P	150.040	52.514	292.578	4	
			NFMP	CU-P	92.256	32.928	526.718	4	
			NFMP	ZN-P	156.960	55.608	431.184	4	
			OR	CO-OR	120.515	54.232	198.849	4	
			SC-DR-coal	HC-DR	401.550	216.837	957.028	4	
			SC-DR-oil	CO-HF-DR	0.820	0.185	1.579	4	
			SC-DR-oil	CO-LF-DR	11.712	2.635	22.546	4	
			SC-IND-coal	BC-IND-OTH	169.650	91.611	404.333	4	
			SC-IND-coal	HC-IND-CEM	1266.694	684.015	3018.953	4	
			SC-IND-coal	HC-IND-OTH	910.088	491.447	2169.042	4	
			SC-IND-coal	HC-IND-PIP	101.063	54.574	240.866	4	
			SC-IND-gas	NG-IND	0.347	0.078	0.668	4	
			SC-IND-oil	CO-HF-IND	5.960	1.341	11.473	4	
			SC-IND-oil	CO-LF-IND	2.256	0.508	4.343	4	
			SC-PP-coal	HC-A-PP	2513.813	1357.459	10599.909	4	
			SC-PP-coal	HC-B-PP	137.925	74.480	328.721	4	
			SC-PP-gas	NG-PP	1.834	0.413	3.531	4	
			SC-PP-oil	CO-HF-PP	4.320	0.972	8.316	4	
			SC-PP-oil	CO-LF-PP	0.080	0.018	0.154	4	
			SSC	SP-S	127.933	47.616	610.453	4	
			WASOTH	WASOTH	1741.088	522.326	5223.265		4
			WI	WI	5.448	1.634	16.345		4
WLF	Wallis and Futuna Islands	Australia, New Zealand & Oceania	CREM	CREM	0.048	0.043	0.057		4
			WASOTH	WASOTH	0.199	0.060	0.597		4
			WI	WI	0.001	0.000	0.002		4
ESH	Western Sahara	Sub-Saharan Africa	CREM	CREM	0.000	0.000	0.000		4
			WASOTH	WASOTH	4.477	1.936	6.897		4
			WI	WI	0.001	0.000	0.001		4

Country code	Country name	Region	Sector Code	Activity Code	Emission estimate, kg	Low range estimate, kg	High range estimate, kg	Technology group	Waste group
YEM	Yemen	Middle Eastern States	CEM	CEM	276.850	97.755	1434.843	4	
			CREM	CREM	0.208	0.156	0.242		4
			OR	CO-OR	0.347	0.156	0.572	4	
			SC-DR-oil	CO-LF-DR	0.580	0.131	1.117	4	
			SC-IND-coal	HC-IND-CEM	17.456	9.426	41.604	4	
			SC-IND-oil	CO-HF-IND	2.760	0.621	5.313	4	
			SC-IND-oil	CO-LF-IND	0.248	0.056	0.477	4	
			SC-PP-gas	NG-PP	0.190	0.043	0.367	4	
			SC-PP-oil	CO-HF-PP	8.520	1.917	16.401	4	
			SC-PP-oil	CO-LF-PP	0.800	0.180	1.540	4	
			SC-PP-oil	CO-PP	0.410	0.092	0.789	4	
			WASOTH	WASOTH	127.570	38.271	382.710		4
			WI	WI	0.399	0.120	1.198		4
ZMB	Zambia	Sub-Saharan Africa	ASGM	GP-A	225.000	56.250	393.750		
			BIO	PSB – DR	201.401	45.315	387.697	4	
			BIO	PSB – IND	78.609	17.687	151.323	4	
			CEM	CEM	202.125	71.418	1048.548	4	
			CREM	CREM	0.344	0.248	0.495		4
			NFMP	CU-P	978.692	638.973	1394.636	4	
			NFMP-AU	GP-L	222.750	77.963	434.363	4	
			OR	CO-OR	0.542	0.244	0.894	4	
			SC-DR-oil	CO-LF-DR	0.286	0.064	0.551	4	
			SC-IND-coal	HC-IND-OTH	20.869	11.269	49.737	4	
			SC-IND-oil	CO-HF-IND	0.960	0.216	1.848	4	
			SC-IND-oil	CO-LF-IND	0.638	0.144	1.228	4	
			SC-PP-oil	CO-HF-PP	1.620	0.365	3.119	4	
			SC-PP-oil	CO-LF-PP	0.020	0.005	0.039	4	
			WASOTH	WASOTH	307.079	132.791	473.068		4
			WI	WI	0.059	0.025	0.091		4
ZWE	Zimbabwe	Sub-Saharan Africa	ASGM	GP-A	7750.000	3875.000	11625.000		
			BIO	PSB – DR	380.296	85.567	732.070	4	
			BIO	PSB – IND	7.022	1.580	13.518	4	
			BIO	PSB – PP	2.301	0.518	4.430	4	
			CEM	CEM	119.438	42.201	619.596	4	
			CREM	CREM	0.322	0.232	0.464		4
			NFMP-AU	GP-L	990.000	346.500	1930.500	4	
			SC-DR-coal	HC-DR	7.050	3.807	16.803	4	
			SC-DR-oil	CO-LF-DR	1.318	0.297	2.537	4	
			SC-IND-coal	HC-IND-CEM	10.763	5.812	25.651	4	
			SC-IND-coal	HC-IND-OTH	20.738	11.198	49.424	4	
			SC-IND-coal	HC-IND-PIP	0.131	0.071	0.313	4	
			SC-IND-oil	CO-LF-IND	0.062	0.014	0.119	4	
			SC-PP-coal	HC-B-PP	309.488	167.123	737.612	4	
			SC-PP-oil	CO-LF-PP	0.064	0.014	0.123	4	
			WASOTH	WASOTH	156.861	67.832	241.650		4
			WI	WI	0.030	0.013	0.046		4

4. Levels of mercury in air

Lead author: Nicola Pirrone

Co-authors: Hélène Angot, Mariantonia Bencardino, Sergio Cinnirella, Amanda Cole, Aurélien Dommergue, Joseph Timothy Dvonch, Ralf Ebinghaus, Xinbin Feng, Alessandra Fino, Xuewu Fu, Katarina Gårdfeldt, David Gay, Milena Horvat, Dan Jaffe, Jože Kotnik, Antonella Macagnano, David Schmeltz, Henrik Skov, Francesca Sprovieri, Alexandra Steffen, Elsie Sunderland, Kjetil Tørseth, Simon Wilson (Members of the UNEP Fate & Transport Partnership Group, Air Subgroup Technical Expert Team)

Key messages

- *Data from existing air mercury (Hg) monitoring networks show a clear gradient in Hg concentration between the northern and southern hemispheres.*

- *There are insufficient data to assess the global temporal trend in atmospheric Hg concentration and deposition. Data from Europe, Canada, and the United States show a general decrease in the level of Hg in air.*

- *Existing networks and their spatial distribution, however, show large gaps in geographical coverage (i.e., Africa, Latin America and the Caribbean, Russia) and filling these gaps will be key for determining future regional changes in Hg deposition transport patterns and identifying regional source-receptor relationships.*

- *Close cooperation among existing monitoring networks is needed to support global action to reduce Hg emissions.*

4.1 Introduction

The aim of this chapter is to update the information presented in the 2013 Global Mercury Assessment on mercury (Hg) levels in air (AMAP/UNEP, 2013). It focuses in particular on atmospheric Hg measurements and regional/worldwide spatial and temporal trends. The information presented here includes an overview of measurements currently collected in regional monitoring networks around the world. The chapter also includes an overview of high altitude and vertical profile measurements and Hg exchange fluxes at the air/water/soil/vegetation/snow-ice interfaces. A summary of new non-standard/conventional methods available (or under development) for monitoring Hg in air is also given. The chapter concludes with an overall assessment of the state of atmospheric Hg measurements and current understanding of the state of the science.

The chapter specifically highlights recent key findings on:

- Atmospheric Hg measurements and trends worldwide and at the regional/continental scale with a focus on the spatial and temporal variability in concentrations of Hg and its compounds at ground-based sites, and at different altitudes and latitudes in the southern and northern hemispheres.

- Atmospheric Hg in the polar environment (Arctic, Antarctic) and specific aspects related to these regions, namely impacts caused by long-range transport and *in situ* formation and transformation processes.

- Recent studies on vertical profile measurements over background regions and impacted (industrial, urban) regions, with a view to helping reduce modelling uncertainty

and advance understanding of long-range transport and patterns of deposition/re-emission.

- Temporal and spatial variability in Hg exchange fluxes between air and soil/vegetation/snow-ice interfaces, including at contaminated sites (industrial, mining areas).

- Advances in monitoring using new/non-standard methods for measuring Hg species in the atmosphere.

4.2 Atmospheric Hg measurements and trends worldwide

4.2.1 Background

Atmospheric Hg is monitored in national programs driven by national legislation or international agreements and conventions. Extensive monitoring is also conducted as a part of long-term research programs. Appendix Table A4.1 provides a global review of Hg monitoring programs at national, regional and local scales, based on a global review of Hg monitoring networks (United Nations Environment, 2016), produced within the framework of the Global Environmental Facility (GEF)-funded project *Development of a Plan for Global Monitoring of Human Exposure to and Environmental Concentrations of Mercury*, with supplementary information collected through negotiations under the Minamata Convention and reported by countries and experts. Many national networks operate in order to support environmental policy within international conventions or agreements and this cooperation includes development of joint procedures both for measurements and reporting of data and for regular evaluation of trends and patterns. For example, in Europe, air monitoring data on Hg are reported to the European Monitoring and Evaluation Programme (EMEP) under the Convention on Long-range Transboundary Air Pollution (CLRTAP). Arctic countries report data to the Arctic Monitoring and Assessment Programme (AMAP) under the Arctic Council. Several countries in the Asian/Pacific region participate in the Asia Pacific Mercury Monitoring Network (APMMN). National networks differ in terms of ambition level, for example concerning sampling frequency and whether speciation of airborne Hg is included.

National monitoring can provide the basis and infrastructure for research programs where routine monitoring can be expanded to include more advanced methodologies (e.g., speciation of airborne Hg), as well as new sites in locations where measurement data were previously not available. Examples of programs generating data used in this chapter are the Global Mercury Observation System (GMOS) program and several other research projects focused on polar regions. The GMOS network continues to operate many of the sites in coordination with national programs and regional agreements. Monitoring stations are mostly located at background sites in

order to intercept major intercontinental and continental air mass movements. GMOS monitoring sites are classified as 'master' or 'secondary' sites. Master stations are those where gaseous elemental mercury (GEM; i.e., gas phase Hg in its ground electronic state), gaseous oxidized mercury (GOM; i.e., oxidized gas phase Hg compounds), Hg associated with suspended particulate matter (i.e., particle-bound mercury; $PBM_{2.5}$) and Hg in precipitation are continuously measured. Secondary stations are those where only total gaseous mercury (TGM; i.e., the sum of gas phase Hg species, including ground state and reactive forms) and Hg in precipitation are continuously measured.

The 2016 UN Environment Global Review lists the main information on existing national and regional/global monitoring networks but does not include data on Hg concentrations and deposition (UN Environment, 2016).

Figure 4.1 shows the major Hg monitoring networks contributing to the global and regional networks mentioned in this chapter. It shows that although monitoring sites are located in both hemispheres there are regions (even large regions) for which monitoring data/sites are totally lacking, which makes a full evaluation of the current geospatial distribution (gradients and variability) of Hg concentration in ambient air impossible.

4.2.2 Spatial and temporal variability at the hemispheric scale

This section presents atmospheric Hg concentrations recorded worldwide within the GMOS network, analyzing measurement results in terms of temporal and spatial variability. Major findings are presented in the following section which includes a clear gradient in Hg concentration between the northern and southern hemispheres, confirming that the gradient observed is mostly driven by local and regional sources, which can be anthropogenic, natural or a combination of both. Appendix Tables A4.2 and A4.3 show annual values for speciated Hg concentrations at all sites from 2012 to 2014. In both tables, the stations are ordered by latitude, thus describing the spatial atmospheric Hg variations moving from the northern to southern hemisphere. Mean GEM values for most of the northern hemisphere sites were between 1.3 and 1.6 ng/m³, which is comparable to concentrations measured at the long-term monitoring stations at Mace Head, Ireland (Ebinghaus et al., 2011; Slemr et al., 2011; Cole et al., 2014; Weigelt et al., 2015) and Zingst, Germany (Kock et al., 2005). In contrast, GEM concentrations from the Ev-K2 site, located 5050 m above sea level in the Eastern Himalaya of

International networks
- AMAP
- EMEP
- GMOS
- MDN (Canada and United States)
- Long-term air monitoring (>10-year time-series)

National networks
- Australia
- China
- Republic of Korea
- Canada
- Japan
- Mexico
- Antarctic
- Other

Figure 4.1 Global map of Hg monitoring networks (www.gos4m.org and metadata description therein for each regional network).

Nepal, reported mean values below 1.3 ng/m³. This value is comparable to free tropospheric concentrations measured in August 2013 over Europe (Weigelt et al., 2016a,b). GEM concentration means observed at the northern hemisphere stations are also in good agreement with the overall mean concentrations observed at many sites in Canada (ranging from 1.23±0.37 to 3.75±2.22 ng/m³ overall, measurements collected over the period 1994–2011; Cole et al., 2014) and those reported from two Arctic stations (Villum Research Station and Pallas; Sprovieri et al., 2016). Seasonal variations in GEM concentration have also been observed at all European sites in the northern hemisphere, with most showing higher concentrations during winter and spring and lower concentrations in summer and autumn. For the southern hemisphere sites included in the GMOS network (see Table 4.2), mean GEM concentrations (~1.0 ng/m³) are lower than those reported in the northern hemisphere (~1.5 ng/m³) but are in good agreement with previously reported southern hemispheric background levels (Sprovieri et al., 2010; Angot et al., 2014; Slemr et al., 2015) and the expected range for remote sites in this region. A small (within ~0.1 ng/m³) seasonal variability in GEM concentrations was observed at Cape Point and Amsterdam Island with the highest values during winter and the lowest in summer (Slemr et al., 2015), and with the variability in concentration much lower than in the northern hemisphere. GEM concentrations are comparable at all southern hemisphere monitoring sites, whereas the lower concentrations of GEM observed (<1 ng/m³) were associated with air masses arriving from the southern Indian Ocean and the Antarctic continent (Angot et al., 2014).

Appendix Table A4.4 summarizes annual wet deposition fluxes and the weighted total mercury (THg) concentrations observed at the 17 GMOS sites from the northern hemisphere, tropics, and southern hemisphere between 2011 and 2015 (Sprovieri et al., 2017). Seasonal trend analysis of THg in precipitation showed increasing Hg concentrations and Hg deposition during spring and summer. However, the patterns of THg concentration and precipitation amount reveal that at most sites the seasonal THg wet deposition maximum corresponds to the maximum in precipitation amount collected (Sprovieri et al., 2017). The main factor determining the Hg wet deposition loading recorded at all European sites was generally the amount of precipitation collected (Sprovieri et al., 2017).

There are few Hg deposition measurements in tropical latitudes; hence there have been few scientific reports within the past decade for this region (Shanley et al., 2015 and references therein). The tropics are a particularly important region in terms of global atmospheric chemistry and 49% of total GOM deposition occurs in the tropical oceans (Horowitz et al., 2017a). Due to intense ultraviolet radiation and high water-vapor concentrations, high OH concentrations oxidize inorganic and organic gases, and drive efficient removal from the atmosphere of the oxidized products. To help address the regional gap in information, the GMOS program initiated Hg deposition measurements in Mexico at the Sisal station (see Table 4.3). A high wet Hg deposition flux at this site suggests that other tropical areas may also be hotspots for Hg deposition. Some studies suggest that this could be due to higher precipitation and the scavenging ratios from the global pool in the subtropical free troposphere where high concentrations of oxidized Hg species occur (Selin et al.,

2008). Such findings were also highlighted in previous studies in southern Florida and Gulf of Mexico coastal areas, confirming that local and regional Hg emissions play only a minor role in wet Hg deposition (Sillman et al., 2013) and suggesting that the main source of scavenged oxidized Hg could be the global pool. In remote areas, especially in the southern hemisphere and far from any local sources, atmospheric deposition is recognized as the main source of Hg to the ocean (Lindberg et al., 2007; Sunderland and Mason, 2007; Pirrone et al., 2008). THg exhibited annual and seasonal patterns in Hg wet deposition. Interannual differences in total wet deposition are mostly linked with precipitation volume, with the greatest deposition flux occurring in the wettest years (see Table 4.4) (Sprovieri et al., 2017).

4.2.3 Hemispheric temporal gradients

Descriptive statistics for GEM, GOM and PBM from all GMOS sites distributed from the northern to southern hemisphere are summarized in Tables 4.2 and 4.3, while Figure 4.2 illustrates the annual GEM data for these stations for 2013 and 2014. The sites have been organized by latitude in both plots. The GEM data show a clear north-south difference, with higher median concentrations at the 13 northern sites than at the southern sites, confirming findings at long-term monitoring sites such as Mace Head (Ireland) (Ebinghaus et al., 2011; Weigelt et al., 2015) and Cape Point (South Africa) (Slemr et al., 2015). At Mace Head, the annual baseline mean GEM concentrations observed by Ebinghaus et al. (2011) decreased from 1.82 ng/m³ in 1996 to 1.4 ng/m³ in 2011, showing a decline of 1.4–1.8% per year. Across the GMOS network, a decrease of 1.6% was observed at Mace Head between 2013 and 2014 and a slight increase in Hg concentrations was observed at Cape Point from 2007 to 2014 (Slemr et al., 2015). The clear north–south gradient, which is in line with previous studies (Lindberg et al., 2007; Soerensen et al., 2010a,b, 2012; Sommar et al., 2010; Sprovieri et al., 2010), has also been confirmed by the probability density functions calculated on the data (Sprovieri et al., 2016).

4.2.4 Spatial and temporal variability in North America

4.2.4.1 NADP MDN

The National Atmospheric Deposition Program (NADP) Mercury Deposition Network (MDN) undertakes long-term measurements of Hg in precipitation (wet deposition) across North America. Monitoring began in 1996. The MDN sites follow standard procedures, and use uniform precipitation collectors and rain gauges to generate weekly-integrated measurements of THg in precipitation (wet-only deposition) from Tuesday to Tuesday. All MDN samples are analyzed for THg concentration using cold vapor atomic florescence spectroscopy (CVAFS). Invalid samples are identified using standard protocols. Subsamples for some sites are analyzed for methylmercury (MeHg). Valid and invalid results are provided for use by the scientific community (http://nadp.isws.illinois.edu/mdn/).

All observations are used to determine THg concentration and deposition over North America in annual maps of precipitation weighted-mean concentration and flux
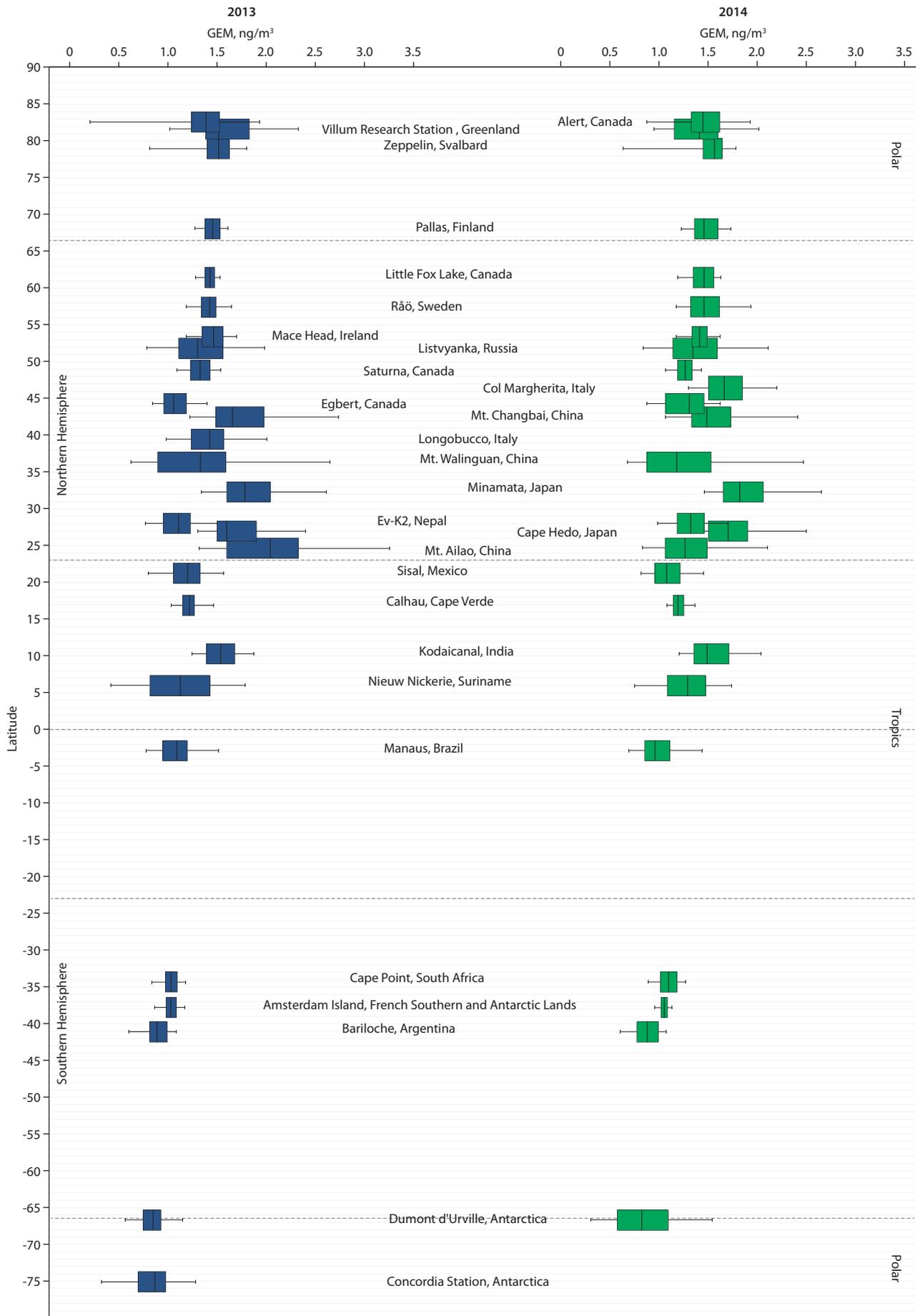
Figure 4.2 Hemispheric gradient in GEM concentration for GMOS data in 2013 and 2014. Sites are organized by latitude. For each box the midline indicates the median, the box indicates the 25th and 75th percentiles, and the whiskers indicate the 5th and 95th percentiles (Sprovieri et al., 2016).
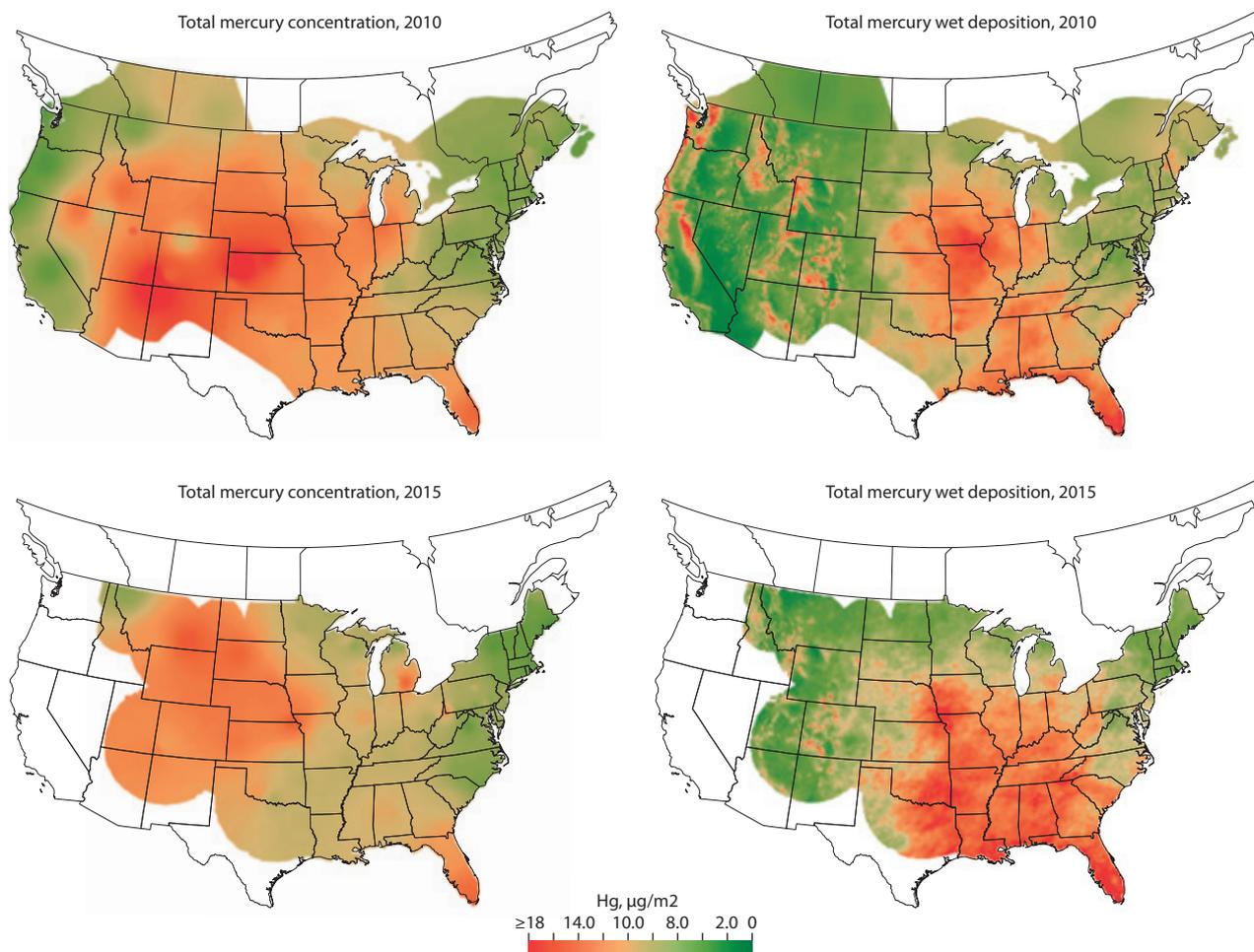
Figure 4.3 Total mercury concentration and wet deposition flux as measured across North America for 2010 and 2015 (http://nadp.isws.illinois.edu).

(Figure 4.3). Precipitation-weighted average concentrations from earlier years are shown for comparison (Table 4.1). Significant wet deposition is found along the Gulf Coast, and somewhat inland. Wet Hg deposition in these areas strongly correlates with areas of higher precipitation (>1000 cm/y). This pattern is repeated annually. The highest concentrations of Hg in precipitation samples are found in the western areas where precipitation is lowest, and dominated by winter snowfall.

Temporal trends in MDN data have been studied by several research groups (Butler et al., 2008; Prestbo and Gay, 2009; Risch et al., 2012; Weiss-Penzias et al., 2016). Evaluating data

Table 4.1 Annual precipitation-weighted Hg concentrations for all MDN sites in North America (http://nadp.isws.illinois.edu).

Year	Valid observations	Precipitation-weighted mean, ng/L	Precipitation-weighted median, ng/L
2010	4495	8.51	6.33
2011	4286	9.01	6.99
2012	4357	9.15	7.03
2013	4391	9.02	7.17
2014	4848	8.83	6.98
2015	4798	8.04	6.40

through the mid-2000s, Butler et al. (2008) found a general decreases in concentration at eastern U.S. sites, with significant decreases at about half the sites. Fewer significant trends were seen at sites in the southeast, but the general tendency was also for decreasing concentrations. Prestbo and Gay (2009) found significant decreasing concentrations at about half the sites (mostly eastern sites), especially across Pennsylvania and extending northeastward, and fully consistent with the findings of Butler et al. (2008). Two western sites (Colorado, Washington) showed the same decreases. No significant increases in concentration were noted, with little change in concentration or deposition at upper midwestern sites. Risch et al. (2012), focusing on the Great Lakes region, found only small localized decreases in Hg concentration. Deposition trends were present, but not at the same sites. Overall, Hg deposition in the Great Lakes area was unchanged between 2002 and 2008. Weiss-Penzias et al. (2016) reported wet deposition fluxes to be almost exclusively decreasing between 1997 and 2013, with over 50% of MDN sites showing significant decreases (of 19 sites). However, for the period 2007–2013 (with 71 sites), increasing concentrations were just as numerous as decreasing concentrations, and this tendency increased with a shorter data series (2008–2013), with positive tendencies widespread. Regional trend analyses revealed significant positive trends in Hg concentration in the Rocky Mountains, Plains, and Upper Midwest regions for the more recent periods.

Figure 4.4 AMNet sites as of the end of 2015 (http://nadp.isws.illinois.edu).

4.2.4.2 **NADP AMNet**

The NADP Atmospheric Mercury Network (AMNet) measures atmospheric Hg concentrations that contribute to Hg deposition using automated, continuous measurement systems, and standardized methodology. The network has 22 active AMNet sites (Figure 4.4); AMNet data are available on the NADP website (http://nadp.isws.illinois.edu/amn). Observations have been made continuously since 2009, generating five-minute and two-hour averages. Data are qualified and averaged to one-hour (GEM) and two-hour (GOM and PBM$_{2.5}$) values.

Valid data are released for use by the scientific community, and as annual data for Hg variability at sites meeting certain criteria. Annual average statistics for the network are shown in Table 4.2, with annual GEM values by site and year in Appendix Table A4.5. The median GEM concentration for the network is 1.38 ng/m³. However, larger differences occurred between sites for GOM and PBM in AMNet. GOM concentrations are generally higher in the urban environment, with lowest concentrations along the Pacific Ocean and other coastal sites. Measured PBM$_{2.5}$ concentrations were generally the same as for GOM. Very high outlier concentrations were noted at almost all sites (Appendix Table A4.5 and Figure 4.5). Investigations of AMNet trends over time are currently ongoing. Data are also being used to estimate speciated and total Hg dry deposition at certain locations in North America (Zhang et al., 2016c).

Figure 4.5 Hourly GEM concentrations (upper) and 2-hour GOM and PBM$_{2.5}$ concentrations (lower) for each AMNet site in 2015. For each plot, boxes indicate 25th, 50th and 75th percentile; whiskers 5th and 95th percentile. Numbers in italics are numbers of valid observations for GEM ≥8 ng/m³, and GOM and PBM$_{2.5}$ ≥40 pg/m³. Horizontal lines in each graph represent the respective 2015 median values (NADP, 2016).

Table 4.2 Number of valid observations and annual GEM, GOM, and PBM concentrations for all AMNet stations from 2010 to 2015 (http://nadp.isws.illinois.edu).

	GEM, ng/m³			GOM, pg/m³			PBM, pg/m³		
	n	Mean	Median	n	Mean	Median	n	Mean	Median
2010	51 289	1.57	1.43	38 744	6.5	1.39	38 099	6.67	3.78
2011	54 541	1.59	1.44	44 864	15.92	1.35	44 817	8.23	4.09
2012	42 924	1.47	1.42	36 226	19.74	1.22	37 386	13.13	4.18
2013	39 078	1.49	1.44	30 806	14.35	1.29	30 919	10.33	4.45
2014	49 348	1.47	1.4	35 390	12.64	1.52	35 238	10.99	4.96
2015	52 938	1.58	1.38	44 179	12.47	1.59	43 022	8.62	4.11

Figure 4.6 Atmospheric mercury measurements made at monitoring sites currently operational in Canada, as of December 2017 (Steffen et al., 2008, 2014):

- orange – total gaseous mercury (TGM);
- green – speciated mercury (gaseous elemental mercury, reactive gaseous mercury and total particulate mercury);
- yellow – precipitation (total mercury, THg_{wet}).

4.2.5 Environment and Climate Change Canada – Atmospheric monitoring

Since 1994, much atmospheric Hg monitoring has taken place across Canada as well as many focused Hg research projects. The parameters measured have evolved over time and the breadth and volume of data collected are significant. Atmospheric monitoring in Canada is undertaken to serve three main goals: to measure atmospheric input/deposition into vulnerable Canadian ecosystems; to measure ambient levels of Hg resulting from domestic and regional emission sources; and to assess transboundary transport of Hg into and around Canada. The Canadian Mercury Science Assessment – Summary of Key Results – describes which sites address these goals (ECCC, 2016a). Ongoing continuous monitoring of Hg in Canada has been rationalized, in part, because Canada has been shown to be a net recipient of Hg, by means of atmospheric transport and deposition (ECCC, 2016a).

Most monitoring in Canada began as independent research programs to measure TGM in the early 1990s. The number and location of measurement sites has since changed and, as of 2017, the current sites for atmospheric Hg monitoring have been consolidated and fall under the Environment and Climate Change Canada – Atmospheric Mercury Monitoring (ECCC–AMM) network. Appendix Table A4.6 shows all atmospheric Hg measurements that have been taken across Canada. In 1996, Canada joined the United States-led Mercury Deposition Network (MDN) and began to collect wet deposition samples for THg and, at some sites, MeHg. Sites where these precipitation measurements have been made over time are listed in Appendix Table A4.6. In the early 2000s, to meet increasing research needs, many advancements were made in instrument capabilities to collect and analyze Hg species in the air. From 2002 onward, some sites began continuous measurements that could distinguish between GEM, GOM and PBM (collectively termed speciated atmospheric Hg). Such sites are also listed in Appendix Table A4.6. As of December 2017, the ECCC-AMM

monitors TGM at 11 sites, atmospheric speciated Hg at four sites and wet deposition at six sites; Figure 4.6 indicates the active ECCC-AMM sites.

From the measurements collected over the past 20+ years, concentrations of TGM in Canada are broadly within the ranges reported by other northern hemispheric countries, with some exceptions. One difference being the annual concentrations reported from Alert (in the High Arctic) which are, in general, lower than the national average, with low GEM concentrations and high speciated mercury concentrations (Steffen et al., 2008, 2014). This difference is seen at many coastal Arctic sites and is primarily explained by the springtime chemistry associated with atmospheric mercury depletion events (AMDEs). The other Canadian location that deviates from the norm is Flin Flon (Manitoba), which shows higher concentrations than the national average. Flin Flon was the site of Canada's largest copper and zinc smelter from 1927 to its closure in 2010. While Hg levels have decreased since the closure, atmospheric Hg levels around this site remain the highest in Canada. This is attributed to the re-emission of previously deposited Hg in the vicinity of the smelter (ECCC, 2016b). The remaining Canadian sites have distinct seasonal and diurnal patterns reflective of the surrounding environment (be it rural or urban) (Cole et al., 2014).

Trends in Hg over time, including TGM, speciated mercury and THg in precipitation (Cole et al., 2014), have been investigated for several Canadian measurement sites. Updated trends of monthly median TGM and monthly volume-weighted mean concentrations of Hg in precipitation (total mercury or THg) are listed in Appendix Table A4.7. The most recent data were used in the analysis, where monthly values were deemed valid with at least 75% data coverage, and a minimum of five years of data were required to perform trend analysis. Trends were calculated using the seasonal Kendall test for trend and the related Sen's slope calculation (van Belle and Hughes, 1984; Gilbert, 1987). This method is an extension of the non-parametric Mann-Kendall test for trend, which is

Trend in TGM and THg$_{wet}$, annual change, %
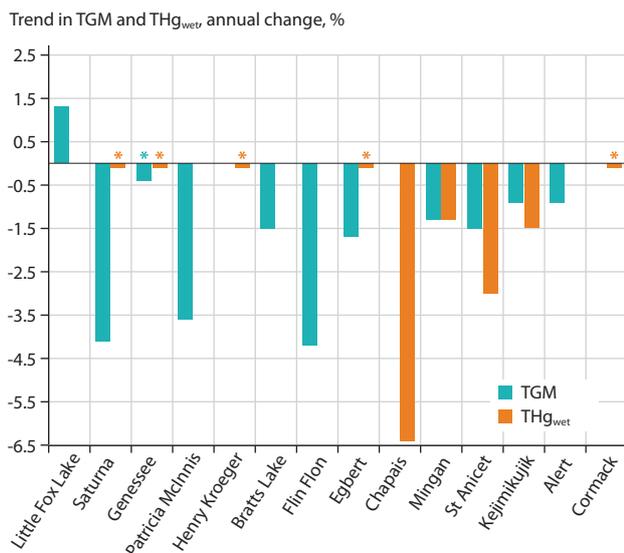
Figure 4.7 Trend in mercury concentrations as expressed as a percentage per year for total gaseous mercury and total mercury from wet deposition in Canada from most current data including data ending in 2010 for some sites. Bars with an asterisk indicate trends that are not statistically significant.

recommended when there are missing values and when the data are not normally distributed; both conditions apply to these datasets.[4] Monthly long-term trends for speciated Hg have been made for some sites in Canada (Cole et al., 2014); but these vary greatly by season and are not easily summarized by an overall annual trend. As a result, only the annually averaged trends are included in Appendix Table A4.7.

The TGM data show decreasing Hg concentrations at most sites in Canada. Figure 4.7 shows trends for both TGM and THg based on the more recent data. Stations in Figure 4.7 are oriented from west to east across Canada. Where the bar is above zero, the trend is increasing, and where it is below zero the trend is decreasing. The only site reporting an increasing trend in TGM is Little Fox Lake (Yukon). All other sites indicate decreasing trends. The THg wet deposition data show decreasing trends at three eastern locations (Chapais, St Anicet, Kejimikujik). No statistically significant increases or decreases were observed at the other sites. This is consistent with other reports of THg in wet deposition in North America (Weiss-Penzias et al., 2016). The majority of the TGM decreasing trends in Canada shown in Figure 4.7 reflect typical northern hemispheric declines (Cole et al., 2014; Zhang et al., 2016c; Zhou et al., 2017) or declines indicative of changes in local emissions (e.g., Flin Flon). Such decreases primarily result from decreases in Hg emissions within the region. The decrease at Alert is less than that at other sites, probably reflecting a decrease in northern hemispheric background levels as well as the Arctic atmospheric chemistry processes occurring at this site (Cole et al., 2013). In the recent trend analysis, it is interesting to note that Kejimikujik shows the same low percentage decrease as Alert. This shift to a lower decreasing trend could result from both decreases in emissions

in the area (Zhou et al., 2017) and potential increases in the release of Hg from the nearby ocean (Amos et al., 2013).

4.2.6 Atmospheric concentrations in Asia

Before the GMOS network was established, independent programs and networks for monitoring atmospheric Hg species and deposition had been developed in Asia, including those in Korea, Japan and China supported by the National Science Foundation in each of the Asian countries and region. Since 2010, some of these Asian sites have been incorporated into the global network (Sprovieri et al., 2016), including Mt. Waliguan, Mt. Ailao, Shangri-La and Mt. Changbai in mainland China, Lulin in Taiwan, Cape Hedo, Okinawa and Minamata, Kyushu islands in Japan, Kanghwa Island in Korea, and Kodaikanal in India. A statistical summary of speciated atmospheric Hg concentrations and associated site information (urban and remote areas) in Asia is shown in Appendix Table A4.8, while Appendix Table A4.9 reports Hg concentrations and deposition fluxes in precipitation, throughfall, and litterfall. GEM and PBM concentrations at remote Chinese sites are elevated compared to those observed at background/remote areas in Europe and North America, and at other sites in the northern hemisphere (Fu et al., 2015; Sprovieri et al., 2016). In Chinese urban areas, the highly elevated GEM, GOM and PBM were mainly derived from local anthropogenic Hg emissions, whereas regional anthropogenic emissions and long-range transport from domestic source regions are the primary causes of elevated GEM and PBM concentrations at remote sites (Fu et al., 2015). Mean GOM concentrations at remote sites in China ranged from 2.2 to 10.1 pg/m^3, significantly below those observed in Chinese urban areas but comparable to values in Europe and North America (Fu et al., 2015; see Appendix Table A4.4). Wet-only deposition fluxes of THg and MeHg ranged between 1.8–7.0 and 0.01–0.06 μg/m^2/y, respectively, at remote sites and 13.4–56.5 and 0.05–0.28 μg/m^2/y at urban sites, respectively. Wet deposition fluxes of THg and MeHg at urban sites in China were higher than those in North America and Europe, whereas wet deposition fluxes of THg at remote sites in China were in the lower range of those observed in North America and Europe. Details of THg recorded from 2011 to 2015 at Chinese GMOS sites are reported in Appendix Table A4.9.

4.2.7 Concentrations and trends in Europe

Heavy metals were first considered by CLRTAP in the 1980s. At that time, Hg was only of secondary priority, because measurements of the relevant chemical forms and understanding of the chemistry involved were not considered mature enough to allow regional-scale harmonized monitoring (EMEP, 1985). The first EMEP data report on heavy metals (EMEP, 1986) does not therefore include Hg data, even though the first measurements were already available at that time. By 1990, the number of sites measuring Hg in air had increased to seven, with sites located in Norway, Sweden, Denmark, Germany and the UK. Mercury was included in the first priority list of measurements for the late 1990s, and the

---

[4] In the seasonal Kendall method, data from the 12 months are treated as 12 separate datasets. For each month, the presence of a trend is confirmed or rejected by the Mann-Kendall test, and a slope is estimated using Sen's nonparametric estimator of slope. An overall annual trend is estimated from the monthly trend statistics; however, this estimate may be questionable if the monthly trends are not homogeneous. Thus, to ensure reliability of the data, a test for seasonal homogeneity was also performed. If seasonal trends were homogeneous, the results were used to determine an overall trend for the entire period. The disadvantage of this technique is that it produces a linear trend over the entire period and can miss complex patterns such as a decrease followed by an increase.

Figure 4.8 Mercury observation network for the European Monitoring and Evaluation Programme (EMEP).

uncertain data from Portugal and Ireland), followed by sites in the Czech Republic and Sweden with concentrations of 8 µg/L, while the lowest levels (<5 µg/L) are seen in Great Britain. Annual average Hg concentrations in air and precipitation for 2014 are shown in Figure 4.9. There is an indication of elevated levels in central Europe as could be expected due to the influence of anthropogenic sources such as coal combustion. An interesting observation is that the coastal Arctic site in Norway has slightly higher levels than those observed on Greenland and inland in Finland and Sweden, which may be due to the summertime evasion of Hg from the ocean or due to Svalbard receiving several direct transport episodes from the continent, especially in winter and spring. PL05 (Diabla Gora, Poland) and SI08 (Iskrba, Slovenia) show unexpectedly low concentrations; 1.2 and 0.8 ng/m^3, respectively. The latter is even lower than observed in Antarctica (Pfaffhuber et al., 2012). Given the locations of these stations and their proximity to emission sources, it seems likely that there may be a bias in the concentrations measured at these two sites.

Mercury concentrations in precipitation are highest in Eastern Europe (Czech Republic, Poland, Slovenia), as may be expected because anthropogenic emissions are highest in this region. On the basis that Hg precipitation measurements are more complex than for air and that the expected measurement uncertainty is 42% (Umweltbundesamt, 2006), the concentrations and spatial pattern observed seem reasonable. Because most of the data reported by Poland are below the detection limit it is difficult to fully assess the spatial concentration pattern. Most of the data reported by Ireland and Portugal are also below the detection limit. Two recent reports consider the spatial and temporal trends of Hg in EMEP: Tørseth et al. (2012) provides a broad introductory overview to the full dataset available but did not go into detail at site level and individual time series, while Colette et al. (2016) focused mainly on the period 1990–2012 and relied heavily on results from the EMEP-MSC-E model, using official emissions data.

number of sites has since increased gradually. The CLRTAP Aarhus Protocol on heavy metals was adopted in 1998, and countries agreed to reduce their emissions compared to 1990 levels. Monitoring efforts currently include about 37 sites across 17 countries (Figure 4.8). For all years, the total numbers are 64 sites and 23 countries.

Compared to other heavy metals, relatively few stations measure Hg in precipitation in Europe, and of those that do many are related to the OSPAR Commission program. There are several sites with high detection limits (in Ireland, Latvia, Portugal) and these can only give an indication of upper concentration limit. There is no clear regional distribution of Hg in precipitation; the highest concentration is seen in the Netherlands (10 µg/L at NL0091, when excluding

Figure 4.9 Mercury concentrations in air and precipitation at EMEP sites in 2014.

Hg in precipitation, ng/L   Hg in air, ng/m³

Air
- ····· Rörvik (SE02)/Råö (SE14)
- ····· Zingst (DE09)
- ····· Pallas-Matorova (FI36)
- ····· Mace Head (IE31)
- ····· Zeppelin Mountain, Ny-Ålesund (NO42)

Precipitation
- —— Pallas-Matorova (FI36)
- —— De Zilk (NL91)
- —— Westerland (DE01)
- —— Rörvik (SE02)/Råö (SE14)
- —— Zingst (DE09)
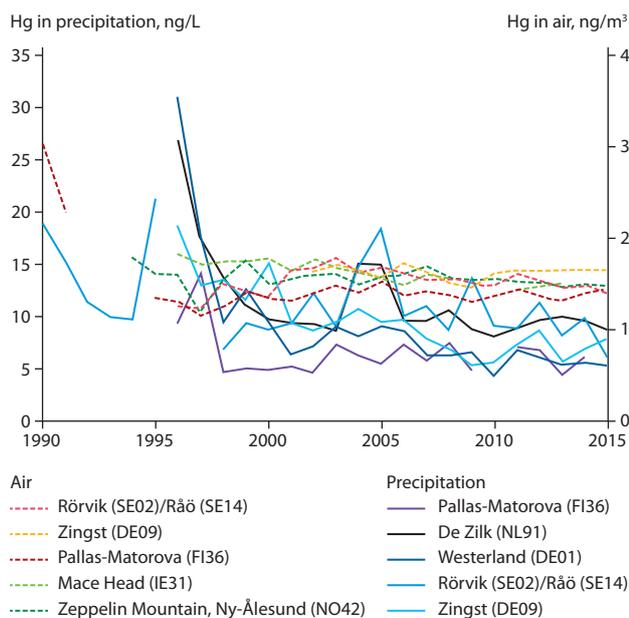
Figure 4.10 Time series of Hg in air and precipitation at selected EMEP stations, 1990–2015 (Tørseth et al., 2012).

Figure 4.10 presents annual time series of Hg in air and precipitation at sites with long-term data series across Europe. It is clear that most sites are located in northern Europe and that there are gaps in the time series in the early 1990s. Interannual variability is large, but a significant reduction in concentration is apparent. Trend analysis suggests reductions of the order of 5–10% since the late 1990s. More recent work by Zhang et al. (2016c) suggests declines of more than 2% per year since the mid-1990s in western Europe and a total reduction of more than 30% due to declines in primary anthropogenic source releases.

As well as describing the full EMEP dataset, Tørseth et al. (2012) also referred to studies on trends in emissions and observations, to determine Hg levels before the late 1980s. They concluded that there had been a major decline in European Hg emissions at the end of the 1980s. Also, that measurements of TGM for the period 1980 to about 1993 show a decrease of about 60% in ambient concentrations. Concentration changes reflect emission changes in Europe. Reduced emissions in Europe and the long lifetime of Hg have resulted in an increased focus on non-European sources to ambient levels (Pirrone and Keating, 2010). Monitoring efforts within Europe have gradually improved in northern Europe, while other regions still have few data available.

4.2.8 Concentrations and pattern analysis in polar areas

The Arctic Monitoring and Assessment Programme (AMAP) established in 1991, is a coordinated air monitoring program covering the circum-Arctic of North America and Eurasia. It has an active ambient air Hg monitoring component with sites in Canada, Greenland (Denmark), Norway, Russia and the USA. The Global Atmospheric Watch (GAW) site at Alert operated by Environment and Climate Change Canada – and funded through the Northern Contaminants Program (NCP)

of Indigenous and Northern Affairs Canada (INAC) – has the longest continuous record of GEM (22 years) and Hg speciation (15 years) in the Arctic (Cole et al., 2013; Steffen et al., 2014). Continuous monitoring for long periods has also occurred at Amderma (Russia) (Steffen et al., 2005), GAW Ny-Ålesund 'Zeppelin' site (Svalbard, Norway) (Berg et al., 2013), AMAP Villum Research Station at Station Nord (hereafter named Station Nord, Greenland-Denmark) (Skov et al., 2004) and Andøya (northern Norway) (Berg et al., 2001). Four multi-year records over the period 2011–2015 from High Arctic sites (Alert, Station Nord, Zeppelin) and European subarctic sites (Andøya) were recently analyzed (Angot et al., 2016a). In addition, summer measurements were undertaken in 2004 over the North Atlantic Ocean (Aspmo et al., 2004) and in 2005, 2010 and 2012 in the marine boundary layer over the Arctic Ocean (Sommar et al., 2010; Yu et al., 2014). Table 4.3 gives annual GEM concentrations at ground-based sites for the period 2011–2015 in the Arctic region. While the Arctic has been extensively monitored, measurements are more sporadic in the Antarctic. Several short ambient air measurement campaigns were undertaken in summer in the 2000s at Terra Nova Bay, McMurdo, South Pole and Concordia stations (Sprovieri et al., 2002; Brooks et al., 2008a,b; Dommergue et al., 2012). A year-round record (January 2000 to February 2001) was reported for Neumayer (Ebinghaus et al., 2002; Temme et al., 2003) while multi-year GEM records were initiated at the Norwegian Antarctic Research Station, Troll in 2007 (Pfaffhuber et al., 2012). In 2012, GMOS (2011–2015) supported the implementation of two other monitoring stations: Dumont d'Urville on the East Antarctic coast and Concordia on the East Antarctic ice sheet (Angot et al., 2016b,c). Monitoring at Concordia is now supported by the French Polar Institute IPEV. Plus, short-term field campaigns dedicated to atmospheric Hg (Nerentorp Mastromonaco et al., 2016a; Wang et al., 2016c) and Hg deposition (Han et al., 2011, 2014a, 2017) were recently undertaken over the Southern Ocean and the East Antarctic ice sheet, producing supplementary data. Nerentorp Mastromonaco et al. (2016b) suggested a seasonal increase of total Hg in seawater due to a contribution of Hg^{II} deposition combined with contributions from melting sea ice and snow.

First discovered in 1995 (Schroeder et al., 1998), atmospheric mercury depletion events (AMDEs) take place in spring throughout the Arctic (Lindberg et al., 2001; Berg et al., 2003; Poissant and Pilote, 2003; Skov et al., 2004; Steffen et al., 2005) through the oxidation of GEM by reactive bromine species (Lu et al., 2001; Brooks et al., 2006; Sommar et al., 2007). AMDEs can lead to the deposition of ~100 t of Hg per year to the Arctic (Ariya et al., 2004; Skov et al., 2004; Dastoor et al., 2015). The proportion retained in the snowpack during AMDEs is still under debate in the scientific community.

Several studies have reported significant re-emission (e.g., Ferrari et al., 2005; Brooks et al., 2006; Kirk et al., 2006; Sommar et al., 2007; Dommergue et al., 2010; Steffen et al., 2008; Soerensen et al., 2016a), reducing the amount of Hg that accumulates within the snowpack (Douglas and Blum, 2019; Hirdman et al., 2009; Kamp et al., 2018; Larose et al., 2010). Net accumulation based on flux measurements of wet deposition, dry deposition and re-emission has not yet been determined. During AMDEs, dramatically higher levels of GOM and/or PBM$_{2.5}$ are observed (Lu et al., 2001; Lindberg et al., 2002; Lu

Table 4.3 Annually based statistics: number of hourly-averaged data (n), mean, median and standard deviation (SD) of GEM concentrations (ng/m^3) at ground-based polar sites for the period 2011–2015 (Sprovieri et al., 2002; Brooks et al., 2008a,b; Dommergue et al., 2012; Angot et al., 2016a).

		Alert	Villum Research Station at Station Nord	Zeppelin station at Ny-Ålesund	Andøya	Troll	Concordia Station at Dome C	Dumont d'Urville
2011	mean	1.39	1.26	1.51	1.61	0.95	NA	NA
	median	1.35	1.34	1.59	1.61	0.99	NA	NA
	SD	0.45	0.32	1.61	0.15	0.20	NA	NA
	n	8040	4712	8173	7444	5978	NA	NA
2012	mean	1.21	1.44	1.51	1.61	0.98	0.76	0.91
	median	1.21	1.44	1.54	1.61	0.97	0.70	0.92
	SD	0.35	0.26	0.21	0.13	0.15	0.24	0.20
	n	8447	7932	8181	8428	7808	3761	5949
2013	mean	1.31	1.57	1.47	1.53	0.90	0.84	0.85
	median	1.39	1.49	1.52	1.56	0.93	0.87	0.85
	SD	0.46	0.44	0.30	0.15	0.15	0.27	0.19
	n	8048	6605	6980	7862	8197	2900	5121
2014	mean	1.45	1.36	1.48	1.50	0.95	NA	0.85
	median	1.45	1.36	1.57	1.51	1.00	NA	0.82
	SD	0.33	0.35	0.33	0.16	0.21	NA	0.38
	n	8358	4991	6730	8146	7421	NA	1958
2015	mean	NA	1.11	1.49	1.50	0.94	1.06	0.86
	median	NA	1.11	1.49	1.50	0.93	1.12	0.87
	SD	NA	0.32	0.21	0.10	0.31	0.41	0.19
	n	NA	1059	8342	7146	3670	8383	3114

and Schroeder, 2004; Sprovieri et al., 2005a,b; Steffen et al., 2008). For example, Lindberg et al. (2002) reported GOM concentrations of up to 900 pg/m^3 during an AMDE at Barrow (Alaska) and showed a strong positive correlation between GOM production and both UV-B radiation and surface snow Hg concentration. Preliminary multi-year trends of GOM and PBM$_{2.5}$ concentration at Alert were analyzed by Cole et al. (2013) and showed increases from 2002 to 2009 in both GOM and PBM$_{2.5}$ in spring when concentrations are highest. Steffen et al. (2014) studied the behavior of GOM and PBM$_{2.5}$ over 10 years at Alert and showed that there is a transition from high PBM$_{2.5}$ levels in March and April to high GOM levels in May. The transition was found to be driven by air temperature and the presence of springtime particles (sea salts and Arctic haze). They also reported that the highest deposition of Hg to the snow occurs when GOM levels peak and not when PBM$_{2.5}$ levels are highest. They concluded that, from this information, it is possible to predict when the most Hg will be deposited to the snow and ice surfaces in the High Arctic.

Despite significant challenges in the measurements, the behavior of Hg over the Arctic sea ice has been studied. Nghiem et al. (2012) showed that declining perennial sea ice in the Arctic Ocean affects the amount of active bromine in this area. Because bromine photochemistry drives GEM depletion, a decrease in perennial sea ice will certainly affect the amount of Hg depleted in the atmosphere over Arctic sea ice. Moore et al. (2014) showed that a shift from perennial to annual sea ice drives changes in sea-ice dynamics. Annual sea ice creates more dynamic sea ice, enabling it to provide more turbulence within the ice and to produce more open leads. These open leads cause convective forcing of the overlying atmosphere to pull down air masses that contain more Hg than those which are depleted at the surface, which replenishes the pool of Hg available for conversion and eventual deposition. It has also been shown that some of the Hg deposited to the surfaces is re-emitted to the atmosphere (see references above); however, several studies have shown that photo-reduction of the Hg in snow is dependent on the amount of chlorine in the surface snow (Poulain et al., 2004; Lehnherr and St Louis, 2009). Thus, the more chlorine in the snow, the less Hg is re-emitted. Steffen et al. (2013) demonstrated that there is significantly more GEM re-emitted to the atmosphere from inland snow than from snow over sea ice. Taken together, these studies demonstrate that Hg chemistry in the Arctic is very dependent on sea ice and its overlying atmosphere. With major changes underway in the Arctic and the dynamics of the sea ice, the spring Hg cycle will clearly be impacted including the amount of Hg deposited and retained in the Arctic ecosystem.
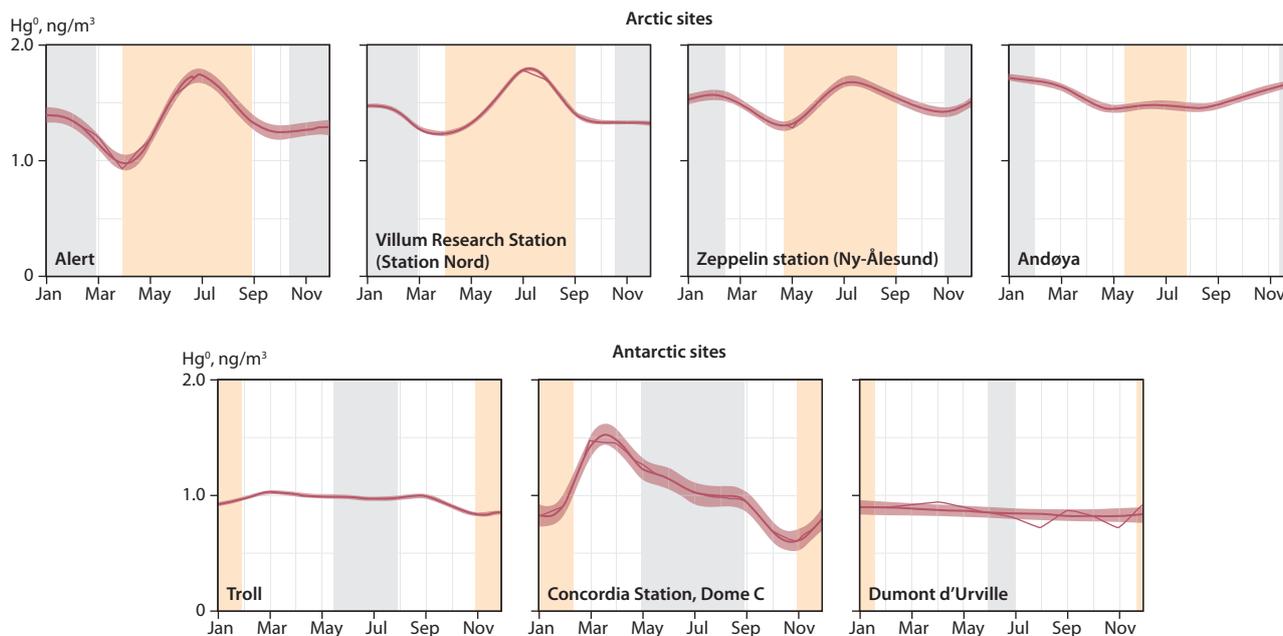
Figure 4.11 Seasonal variation in GEM (Hg⁰) (monthly mean and 95% confidence interval) at four Arctic sites and three Antarctic sites for the period 2011–2015 (Angot et al., 2016a). Coloured bars indicate periods of 24h sunlight (orange) and 24h darkness (grey).

As Figure 4.11 shows, a different seasonal pattern is evident in the High Arctic (Alert, Villum Research Station at Station Nord, and Zeppelin station at Ny-Ålesund – ranging from 78° to 82°N) compared to lower latitudes (Andøya, northern Norway – 69°N). The variability at High Arctic sites in spring is due to the occurrence of AMDEs (Angot et al., 2016a). Summer measurements (June–August) also differ from what is seen at lower latitudes and this is probably due to the re-emission of GEM by the Arctic Ocean and/or by snow surfaces (Angot et al., 2016a and references therein). Yu et al. (2014) reported highly variable GEM concentrations (0.15–4.58 ng/m³) over the central Arctic Ocean in summer, highlighting the need for additional oceanographic campaigns to better understand and constrain oceanic fluxes of GEM.

The analysis of ten-year trends in TGM (GEM+GOM) concentration (Cole et al., 2013) revealed discrepancies among Arctic sites. While no trend was observed at Zeppelin, a slight decreasing trend (-0.9% per year) was reported at Alert. The difference in trends may be due to several factors including differences in the origin of air masses and local-scale processes (e.g., oceanic evasion).

Similar to the Arctic, AMDEs can occur at coastal Antarctic sites after polar sunrise (e.g., Ebinghaus et al., 2002). However, recent studies indicate major differences between Arctic and Antarctic atmospheric Hg cycles, primarily owing to their different geography; while the Arctic is a semi-enclosed ocean almost totally surrounded by land, Antarctica is a land mass – covered by an immense ice shelf – surrounded by ocean. In summer (November to mid-February, permanent sunlight), GEM concentrations exhibit a distinct diurnal cycle on the East Antarctic ice sheet, peaking at noon, attributed to a dynamic daily cycle of GEM oxidation, deposition to the snowpack, and re-emission from the snowpack (Dommergue et al., 2010; Angot et al., 2016c; Wang et al., 2016c). In addition, GEM depletion events can be seen on the ice sheet in summer, with GEM concentrations remaining low (~0.4 ng/m³) for several

weeks (Angot et al., 2016c). These depletion events do not resemble those observed in spring in the Arctic since they are not associated with ozone depletion. They occur when air masses stagnate over the East Antarctic ice sheet, which is likely to favor an accumulation of oxidants within the shallow (few hundred meters) atmospheric boundary layer. These observations, as well as GOM/PBM$_{2.5}$ concentrations up to 1000 pg/m³ recorded at the South Pole (Brooks et al., 2008a), suggest that the inland atmospheric reservoir is depleted in GEM and enriched in GOM in summer. Observations at coastal Antarctic stations suggest that divalent Hg species produced inland can be transported – due to the large-scale airflow pattern flowing from the East Antarctic ice sheet towards the coast (katabatic winds) – leading to Hg deposition and accumulation in coastal ecosystems (Angot et al., 2016b; Bargagli, 2016). Atmospheric models are currently unable to reproduce this complex reactivity (Angot et al., 2016a). Field studies also show that the sea ice environment is a significant interphase between the polar ocean and the atmosphere and should be accounted for in studies of how climate change may affect the Hg cycle in polar regions (Nerentorp Mastromonaco et al., 2016b).

4.3 Vertical profile and UTLS (upper troposphere-lower stratosphere) measurements

4.3.1 Vertical profiles

Vertical profiling of GEM from inside the boundary layer to the free troposphere was undertaken during European Tropospheric Mercury Experiment (ETMEP) flights in 2013 (Weigelt et al., 2015). Several flights were performed with a CASA-212 research aircraft equipped with scientific instruments to measure GEM, GOM, and TGM as well as trace gases (carbon monoxide, CO; ozone, O₃; sulfur dioxide, SO₂; nitric oxide, NO; nitrogen dioxide,
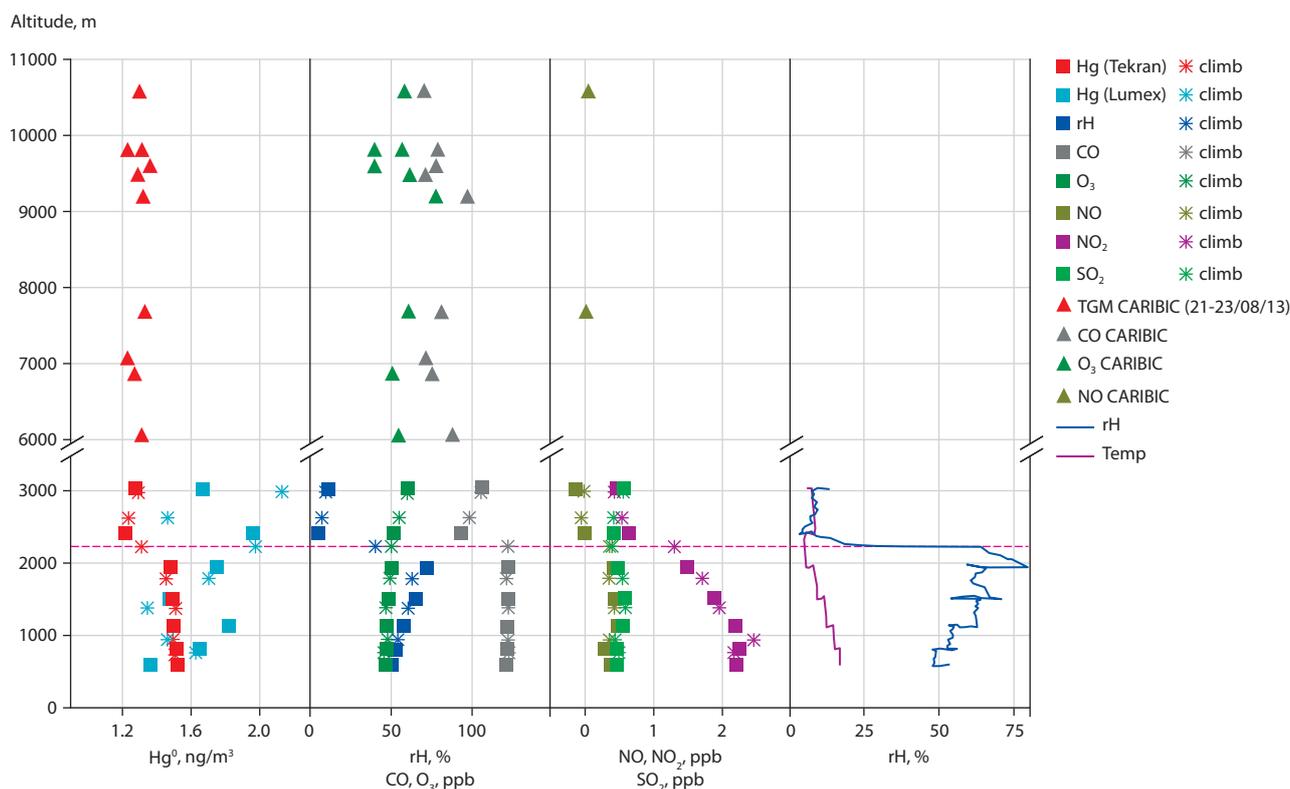
Figure 4.12 Vertical profiles for GEM, carbon monoxide (CO), ozone (O_3), sulfur dioxide (SO_2), nitric oxide (NO), nitrogen dioxide (NO_2), temperature (T), and relative humidity (RH) over Leipzig, Germany during ETMEP and CARIBIC flights in 2013.

NO_2) and meteorological parameters (temperature, pressure, relative humidity). A specially designed gas inlet system was installed on the aircraft fuselage. Five vertical profiles were flown over flat and mountainous rural- and industrialized sites in Slovenia and Germany. In contrast to previously measured vertical profiles, a significant difference was detected between boundary layer air and free tropospheric air. While the free tropospheric overall GEM background concentration over central Europe is ~1.3 ng/m³, inside the boundary layer the GEM background concentration was 10–30% higher (~1.6 ng/m³). At all measurement locations, a clear vertical gradient was not apparent in either the boundary layer or the free troposphere. This indicates that GEM is homogeneously distributed within the particular layers of the atmosphere. Combining ETMEP measurements over Leipzig with CARIBIC measurements (see Section 4.3.3) over western Europe (Figure 4.12) revealed for the first time a complete vertical profile from 0.5 km (lower boundary layer) to 10.5 km (upper free troposphere). From above the boundary layer to the top of the free troposphere, the GEM background concentration was on average 1.3 ng/m³. All concentrations are given at STP (0°C, 1013.25 hPa).

4.3.2 Aircraft-based emission estimates for point and area sources

Large Hg point sources were sampled on several NOMADSS (Nitrogen, Oxidants, Mercury and Aerosol Distributions, Sources and Sinks) project flights, mainly coal-fired power plants in the southeastern USA. Ambrose et al. (2015) developed a unique method for using the NOMADSS data to evaluate Hg point source emissions. This relies on the simultaneous C-130 observations of nitrogen oxides (NO_X), SO_2, CO and carbon

dioxide (CO_2). A key conclusion is that for some coal-fired power plants, including some of the largest Hg emitters in the USA, observations suggest substantially higher Hg emissions than do the emission inventories.

During ETMEP flights over central Europe significant Hg emissions were measured from a modern coal-fired power plant south of Leipzig, Germany. Sampling was undertaken using a denuder – an air sampling device designed to distinguish between the gaseous and particle-bound phase of a compound. GEM peaked at 10 ng/m³. The denuder sample inside the plume indicated that modern coal-fired power plants may be an overestimated source of GOM. The measured fraction of GOM inside the plume was between 0.5% and 2%. This contrasts with the 40%, given by the 'AMAP/UNEP geospatially distributed mercury emissions dataset 2010v1' (AMAP/UNEP, 2013). The emission of gaseous Hg from that power plant was estimated at 268–283 kg/y for GEM and 2–12 kg/y for GOM (Weigelt et al., 2015).

The Chicago-Gary area is highly industrialized with significant emissions of Hg and other pollutants. Using data from NOMADSS flight RF-15, Gratz et al. (2016) developed a new method to evaluate the Hg emission inventory for this region. Observations showed an area of enhanced Hg, CO, SO_2 and NO_X. Combining the observations with the Flexpart model allowed for the characterization of the 'footprint' of the observations and thus a good comparison between the observations and expectations based on the emission inventory. Gratz' analysis indicated that there are many small emission sources that are not fully accounted for within the inventory, and/or that the re-emission of legacy Hg is a significant source of THg to the atmosphere in this region (Gratz et al., 2016).

4.3.3 Large-scale tropospheric distribution and plumes

During the CARIBIC (Civil Aircraft for the Regular Investigation of the atmosphere Based on an Instrument Container) project more than 100 large-scale pollution plumes have been detected in the global upper troposphere. The largest with an extension of 1000 km was detected on a flight from Frankfurt to Osaka between the Korean peninsula and the Yellow Sea. This mixed plume could be attributed to large forest fires in southern Siberia as well as industrial sources in the Chinese provinces of Shandong, Henan, Shanxi and Hebei.

Most of the plumes were found over East Asia during the flights from Frankfurt to Guangzhou, Osaka, Seoul and Manila, in the African equatorial region during the flights to South Africa, over South America during the flights to Sao Paulo and Santiago de Chile, and over Pakistan and India during the flights to Chennai. The plumes encountered over the African equatorial region and over South America originate from biomass burning as evidenced by low Hg/CO emission ratios and elevated mixing ratios of acetonitrile, CH_3Cl and CH_3Br. Backward trajectories point to the region around the Rift Valley and Amazon basin and its outskirts as the source areas. The plumes encountered over East Asia and over Pakistan and India are predominantly of urban/industrial origin, sometimes mixed with products of biomass/biofuel burning. Many plumes with elevated Hg concentrations were encountered during the tropospheric sections of the CARIBIC flights since May 2005. Mercury correlated significantly with CO in more than 50% of the observed plumes and with CO_2 in about 30% of plumes for which CO_2 data were available. Extensive ancillary data on chemical fingerprint of the air in these plumes and backward trajectories provide additional means for identifying the origin and type of source (Slemr et al., 2014).

Large plumes over equatorial Africa were observed during all flights between Frankfurt and South Africa. These plumes which extend over thousands of kilometers are embedded within a north-south gradient of Hg, CO, and CO_2, and comprise a number of overlapping smaller plumes. Due to the changing regional background levels, the inhomogeneity of the plumes and low precision of the Hg measurements, only a few of the plume encounters gave significant Hg vs. CO correlations. Most plumes were observed over Far East Asia and relative to the number of flights to Far East destinations the yield of plumes with significant Hg vs. CO correlations was the second highest after the African flights. Lower yields of plume occurrence were found for flights to South America and to South Asia. Only one plume was encountered over North America and one over Europe (Slemr et al., 2009a, 2013, 2014).

The Hg:CO emission ratios derived from these correlations are consistent with the previous data and tend to smaller values of ~1 pg/m³/ppb for plumes from biomass burning and larger values of ~6 pg/m³/ppb for urban/industrial emissions. Most of the plumes observed over South America and Africa originate from biomass burning and one observed over the mid-Atlantic could be attributed to forest fires in the southeastern USA. Plumes observed over Far East Asia are mostly of urban/industrial or mixed origin. Only a few Hg:CO_2 emission ratios have been reported to date. The range in Hg:CO_2 emission ratios from CARIBIC flights is comparable to that observed at Cape Point (Ebinghaus and Slemr, 2000; Slemr et al., 2016b). The

Hg:CO_2 emission ratios of 107–964 pg/m³/ppm observed in the plumes over Far East Asia, however, are substantially higher than 2–30 pg/m³/ppm calculated by Brunke et al. (2012) for coal burning. If confirmed by further measurements, the higher observed than calculated Hg:CO_2 emission ratios would imply substantial other Hg emissions additional to those from coal burning. Generally, it can be concluded from the CARIBIC data that the major industrial sources of atmospheric Hg are located in East Asia, Pakistan and India, while major contributions to Hg emissions from biomass burning originate from Equatorial Africa (Rift-Valley) and the Amazon region.

An El Niño Southern Oscillation signal could be detected in the tropospheric CARIBIC data (Slemr et al., 2016a). The highest Hg concentrations are always associated with the most negative Southern Oscillation Index (SOI) values, i.e., are related to El Niño events. Cross-correlation reveals that peak Hg concentrations are delayed by 6 to 12 months against SOI values. This lag is similar to that for CO which has been shown to originate from biomass burning following El Niño events. Slemr et al. (2016a,b) suggested that the ENSO signal in the global Hg concentration data is also due to Hg emissions from biomass burning (Slemr et al., 2009a,b, 2013, 2014).

4.3.4 Airborne observations of speciated Hg

Mercury observations on the aircraft NCAR C-130 were made by the University of Washington in summer 2013 with a specially developed Detector for Oxidized Hg Species (DOHGS) (Ambrose et al., 2015), which measures GEM, GOM and a fraction of particle-bound oxidized Hg. GOM is believed to comprise Hg^{II} compounds, such as $HgCl_2$, $HgBr_2$, etc. Measurements were routinely calibrated in-flight with a high precision source of Hg^0, and in the laboratory with sources of gaseous $HgBr_2$ and $HgCl_2$. The dual channel difference method avoids problems with earlier measurements based on KCl denuders, which are known to have significant interferences. It is considered that these are the most carefully calibrated and accurate measurements of speciated Hg to date on an aircraft platform. Details of methodology and further information on calibration, accuracy, and precision are given by Ambrose et al. (2015). Substantial concentrations of Hg^{II} were identified on several flights. Although the location and timing of these events were corrected in the GEOS-Chem Hg model, the concentrations were much higher (two- to four-fold higher). Figure 4.13 shows an example from RF-06 (research flight 6), as well as the base simulations from the GEOS-Chem model (Gratz et al., 2015). This flight was also one of the few with detectable concentrations of BrO. It was concluded that the likely source of Hg^{II} on this flight was oxidation of GEM by Br radicals. This was supported by a detailed chemical mechanism and box-model calculation. This is a major finding and has implications for both Hg and halogens. Note that the halogen chemistry and Hg oxidation mechanism in the GEOS-Chem model were recently updated, as reported in Horowitz et al. (2017a).

Shah et al. (2016) further analyzed the origins of oxidized Hg using a range of sensitivity studies with the GEOS-Chem model. For observations above the detection limit it was found that modelled Hg^{II} concentrations are a factor of 3 too low (observations: 212±112 ng/m³, model: 67±44 ng/m³). The highest Hg^{II} concentrations (300–680 pg/m³) were observed in dry (RH <35%) and clean air masses during two flights over

Hg^{II}, ng/m^3
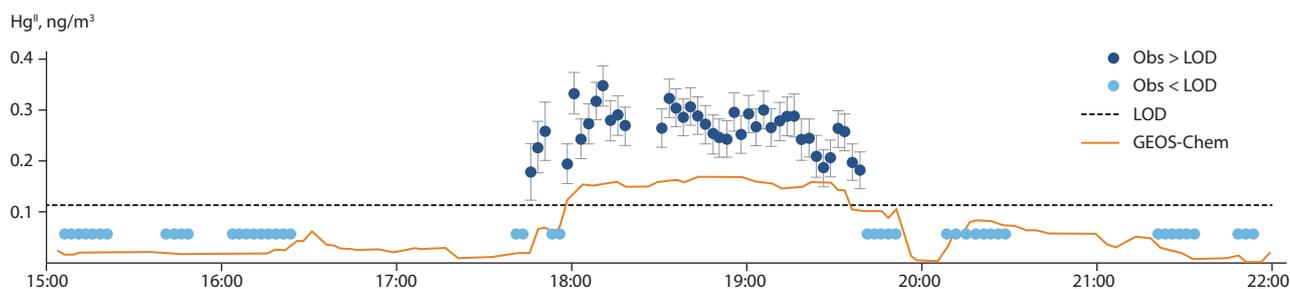
Figure 4.13 Oxidized Hg (Hg^{II}) concentrations measured during a research flight (Ambrose et al., 2015) on 19 June 2013 and base simulations from the GEOS-Chem model.

Texas at 5–7 km altitude and off the North Carolina coast at 1–3 km. The GEOS-Chem model, back trajectories and observed chemical tracers for these air masses indicate subsidence and transport from the upper and middle troposphere of the subtropical anticyclones, where fast oxidation of elemental Hg (Hg^0) to Hg^{II} and lack of Hg^{II} removal lead to efficient accumulation of Hg^{II}. Shah et al. (2016) suggested that the most likely explanation for the model bias is a systematic underestimate of the Hg^0 +Br reaction rate, which has now been updated by Horowitz et al. (2017a). It was shown that sensitivity simulations with tripled bromine radical concentrations or a faster oxidation rate constant for Hg^0 +Br, result in 1.5–2 times higher modelled Hg^{II} concentrations and improved agreement with observations. The modelled tropospheric lifetime of Hg^0 against oxidation to Hg^{II} decreases from five months in the base simulation to 2.8–1.2 months in the sensitivity simulations. In order to maintain the modelled global burden of THg, the in-cloud reduction of Hg^{II} was increased, thus leading to faster chemical cycling between Hg^0 and Hg^{II}. Observations and model results for the NOMADSS campaign suggest subtropical anticyclones are significant global sources of Hg^{II}.

In the lower stratosphere, TGM concentrations (Figure 4.14) always decrease with increasing PV (potential vorticity) and O$_3$. This behavior is similar to that for all trace species with ground sources and stratospheric sinks such as CO and methane (CH$_4$). In contrast, elemental Hg (Hg^0) can only be transformed to other Hg species such as GOM or PBM. The transformation rate of TGM to PBM can be
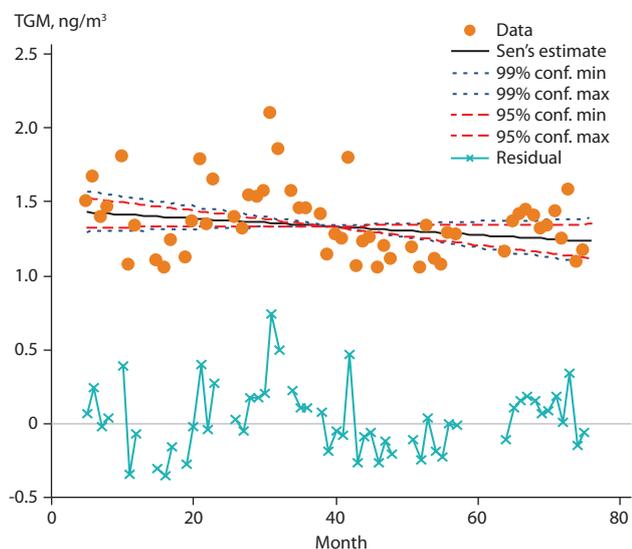
calculated using SF$_6$ concentration annual change rate as a timer. SF$_6$ is a very long-lived tracer whose concentration increases by about 0.230 ppt/y. Correlations of TGM with SF$_6$ suggest a seasonally dependent TGM conversion rate of about 0.43 ng/m^3/y resulting in a stratospheric TGM lifetime of about 2 y. This is longer than the several weeks claimed recently by Lyman and Jaffe (2012) but closer to the one year estimated by Holmes et al. (2010) using the GEOS-Chem model with included bromine oxidation chemistry.

4.4 Temporal and spatial variability in exchange fluxes between air and soil/vegetation/snow-ice

Air–soil (or vegetation covered) exchange fluxes are an important part of the global and regional Hg biogeochemical cycles (Lindberg et al., 2007; Pierce et al., 2015). Much of the Hg^{II} deposited in precipitation or taken up by plants is reduced to Hg^0 and may be evaded back to the atmosphere. Recent vegetation and soil Hg stable isotope studies suggest that vegetation Hg^0 uptake dominates (50-80%) Hg net deposition at terrestrial sites (Jiskra et al., 2018; Obrist et al. 2017). Based on a global terrestrial Hg model, Smith-Downey et al. (2010) estimated that evasion of Hg linked to the decomposition of soil organic carbon pools and subsequent liberation of Hg^{II} sorbed to soil organic matter is over 700 t/y, reflecting the large pool of Hg stored in terrestrial ecosystems globally (over 240,000 t). In total, this study estimated that 56% of Hg deposited to terrestrial ecosystems is reemitted. Similarly, Graydon et al. (2012) found that 45–70% of isotopically labelled Hg^{II} wet deposited to a forested watershed had been reemitted to the atmosphere after a year. Recent observations suggest the evasion flux of Hg from global soils may be slightly lower and the reservoir even higher (e.g., Hararuk et al., 2013).

Mercury exchange flux between soil (vegetation) and the air depends on several environmental factors (soil moisture, soil porosity, substrate temperature), chemical factors (Hg species and their concentrations in soil, organic matter, atmospheric oxidants), meteorological factors (atmospheric pressure, air temperature, wind speed and turbulence, solar radiation, snow cover) and surface characteristics (vegetation type, substrate type, surface roughness) (Gustin et al., 2004; Schroeder et al., 2005). Such factors lead to highly variable Hg fluxes for different landscapes and determine spatial and temporal variability in deposition or evasion of GEM (Schroeder et al., 2005). All forms of atmospheric Hg can be deposited to soils or vegetated surfaces by wet or dry deposition processes (Gustin, 2011) and can then remain within the terrestrial system and undergo

TGM, ng/m^3

Figure 4.14 Monthly median TGM concentrations in the troposphere (PV <1.5 PVU) north of 15°N from May 2005 to April 2011 with Sen's slope estimate (Shah et al., 2016).

further biogeochemical cycling or be emitted back to the atmosphere according to the relative importance of different controlling factors (Gustin, 2011). Changes in flux direction were observed for several soil types covered by different types of vegetation (Poissant et al., 2005; Gustin and Jaffe, 2010), and this can occur quickly, within a few hours (Bash and Miller, 2008; Converse et al., 2010).

Soil type, moisture, and the Hg content and speciation in soil are important factors influencing the GEM flux between soil and air (Kocman and Horvat, 2010; Lin et al., 2010a). Soil porosity and disturbance promote Hg^{II} reduction and GEM transport from soil (Bash and Miller, 2007; Fu et al., 2012a). Soils characterized by small grain size, silt and clay with higher surface area showed higher GEM fluxes to air (Gustin et al., 2002). Rainfall and soil moisture promote GEM emission by an order of magnitude (Lindberg et al., 1999). Soil irrigation enhances Hg^{II} reduction and the added water replaces GEM binding sites and thus promotes GEM emission. Organic matter in soil is reported to be one of the main factors affecting GEM emission, because organic matter forms stable complexes with Hg^{II} and thus reduces the GEM flux (Grigal, 2003; Skyllberg et al., 2006; Yang et al., 2007). Microbial activity in soil and increasing soil pH may promote GEM flux by Hg^{II} reduction (Yang et al., 2007; Fritsche et al., 2008; Choi and Holsen, 2009). High ambient air GEM concentrations were reported to reduce the flux between soil and air by reducing the Hg^0 concentration gradient and thus deposition dominates despite the influence of other factors promoting Hg emission (Bash and Miller, 2007; Wang et al., 2007a; Xin and Gustin, 2007; Zhu et al., 2016). Flux measured from background soils was between -51.7 and 97.8 ng/m²/h with a mean of 2.1 ng/m²/h (Zhu et al., 2016 and references therein).

Vegetation affects environmental factors at the ground surface by reducing solar radiation, temperature, and wind velocity (Gustin et al., 2004) and serves as a surface for Hg uptake (Zhu et al., 2016). Deforestation can increase GEM emission due to higher solar radiation and increased temperature at the soil surface (Carpi et al., 2014; Mazur et al., 2014; Zhu et al., 2016). Recent measurements showed that the GEM exchange flux between plants and air is bidirectional and that growing plants act as a net sink (Ericksen et al., 2003; Stamenkovic et al., 2008; Hartman et al., 2009; Zhu et al., 2016). Most fluxes measured in forest foliage and grasslands were between -9.6 and 37 ng/m²/h (mean 6.3 ng/m²/h) and -19 to 41 ng/m²/h (mean 5.5 ng/m²/h), respectively (Zhu et al., 2016 and references therein).

Air-snow exchange fluxes have mostly been studied in polar regions. During AMDEs, air GEM is oxidized and deposited in snow as GOM and PBM which can be rapidly volatilized back to the atmosphere by photochemical reduction on snow or in melted snow (Dommergue et al., 2003; Kirk et al., 2006; Faïn et al., 2007). Photo-reduction is a major factor for re-emission from snow and is linearly correlated to UV radiation intensity (Lalonde et al., 2002; Mann et al., 2015). An important factor controlling snow-air fluxes is temperature, which also affects the solid-liquid water ratio (Mann et al., 2015). Similar factors control snow-air Hg exchange in temperate regions (Maxwell et al., 2013). Measured fluxes from the snowpack are within the same range reported for vegetation cover and were between -10.8 and 40 ng/m²/h (mean 5.7 ng/m²/h) (Zhu et al., 2016 and references therein).

Polar air-sea water exchange of Hg^0 was for the first time measured continuously in the remote seas of western Antarctica. The measurements were performed during winter and spring (2013) in the Weddell Sea and during summer (2010/2011) in the Bellingshausen, Amundsen and Ross seas, and show spatial and seasonal variations. The average dissolved gaseous mercury DGM) concentration in surface water in open sea areas was highest in spring (12±7 pg/L) and lowest in summer (7±6.8 pg/L), resulting in a net evasion of Hg in spring (1.1±1.6 ng/m²/h) and a net deposition in summer (-0.2±1.3 ng/m²/h). In the open sea, higher average concentrations of GEM (or TGM) and DGM were found near Drake Passage than in the Bellingshausen and Weddell seas. Emission sources in South America, identified with back trajectories, were suggested to explain the spatial variation observed. Annual Hg evasion from open sea surfaces in the Southern Ocean was estimated at 30 t (-450–1700 t), using the average (and minimum and maximum) flux rates obtained in this study. Higher DGM was measured under sea ice (19–62 pg/L) than in open sea areas due to a capsuling effect, resulting in a theoretical prevented evasion of 520 t/y (0–3400 t/y). Diminishing sea ice and higher water temperatures in polar regions could result in increased Hg evasion to the atmosphere. However, the contribution of the Southern Ocean to the global modelled annual Hg emission from sea surfaces is probably only a few percentage points (Nerentorp Mastromonaco et al., 2017).

Mercury evasion from contaminated or naturally enriched soils is recognized as an important input to regional and global budgets (Ferrara et al., 1998; Kotnik et al., 2005). The average evasion flux for urban areas and agricultural fields is 5 to 10 times higher than for background soils (Zhu et al., 2016). Measured Hg exchange fluxes from naturally enriched surfaces were in the range 5.5–239 μg/m²/h, whereas for anthropogenically contaminated sites the flux was in the range 0.001–14 μg/m²/h (Zhu et al., 2016 and references therein).

Fluxes from soils, mines and snow surfaces (Figure 4.15), where GEM can be formed due to photoreduction, are typically higher during the day than at night (Zhu et al., 2016). Higher evasion flux was observed in warm seasons than in cold seasons, from different soils and enriched surfaces (Zhu et al., 2016). Hg flux measurements over soil, vegetation or snow-covered surfaces were consistently higher in East Asia than in Europe, North America, South America, Australia and South Africa. This is explained by higher anthropogenic emissions and re-emissions of deposited Hg (Zhu et al., 2016 and references therein).

4.5 Advances in monitoring using new/ non-standard methodology

Complex commercial instruments (Gustin et al., 2015) as well as sensors and sensing systems have been redesigned and improved by introducing innovative technologies. Many sensors have been developed to detect the several forms of Hg making use of nanotechnology. Over the past 20 years, biomolecules, macromolecules, nanostructures (rods, tubes, fibers, particles, dots) and nanocomposite-based systems have been found to be the most intriguing and effective devices for Hg detection in several environmental compartments. Most have exploited the strong affinity between Hg and gold, others the affinity of Hg ions to specific biomolecules. Being able to manipulate and investigate the features of the nanomaterials has made it possible to fabricate selective and more sensitive tools. Table 4.4 lists some of the most recent technologies used to develop sensors and devices for Hg detection.
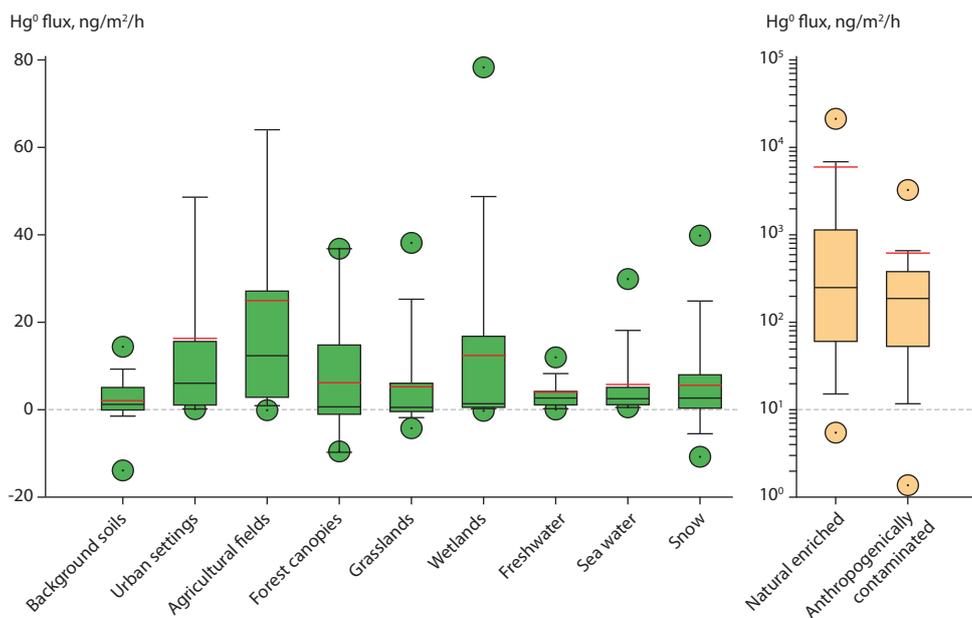
Figure 4.15 Box and whisker plots of global field-observed GEM fluxes for various landscapes (Zhu et al., 2016). For each plot, boxes indicate 25th and 75th percentile; whiskers 10th and 90th percentile and outliers (circles). Red line and black line indicate mean and median flux, respectively.

Table 4.4 Recent technologies used to develop sensors and devices for Hg detection.

Sampling	Materials/device	Linearity range	LOD	Samples	Reference
Hg ions	CV-AAS +SDS-coated chromosorb P + 2-mercaptobenzo xazole	0.05–85.6 µg/L 90 µg/L – 9.6 mg/L	0.1 µg/L	Real samples in liquids	Ghaedi et al., 2006
TGM-continuous emission monitor	Catalysts to oxidize + polymer composites to absorb + chemicals to remove (CVA-AFS)	60 pptv – 228 ppbv	6 pptv	Real samples	Tekran331OXi (www.tekran.com)
Optical sensors: Hg^{II}, FRET bio-sensor (gold nanoparticles-DNA)	Fluorescence quenching		8 µg/L	Water	Miyake et al., 2006
Optical sensors: Hg^{II}, surface energy transfer probe-Rhodamine B-AuNPs	Fluorescence quenching		2 µg/L	Buffer solution, water, river water, contaminated soil	Darbha et al., 2007
Optical sensor: surface-enhanced resonance Raman scattering (SERRS) sensor	Structure-switching double stranded DNAs (dsDNAs)		0.02 µg/L	Aqueous solution	Kang et al., 2011
Electrochemical sensors: Hg^{II}, array of 256 gold microelectrodes	Anodic stripping voltammetry	10 µg/L – 200 µg/L $\times 10^{-8} – 1 \times 10^{-6}$ M	3.2 µg/L (16 nM)	Chloride media	Ordeig et al., 2006
FET sensors: Hg^{II}	Thioglycolic acid (TGA)-functionalized -AuNPs-reduced graphene oxide (rGO)		5 µg/L	Aqueous solution	Chen et al., 2012
Colorimetric sensors: Hg^{II} (naked eye)	Au-nanorods/glass	2.0 µg/L – 0.58 mg/L	1 µg/L	Aqueous solution	Chemnasiri et al., 2012
LSPR (prediction model)	Au-nanorods (shift wavelength)		4.5 attograms (mass)	Hg^0 vapor	James et al., 2013
Conductive sensors	CNT-AuNP		2 ppbv	Hg^0 vapor	McNicholas et al., 2011
Conductive sensors	TiO2NFs-AuNPs (tens of min)		2 pptv	Hg^0 vapor	Macagnano et al., 2017b
Conductive sensors	TiO2NF-AuNPs	20–100 ppbv	1.5 ppbv	Hg^0 vapor	Macagnano et al. 2017b
QCM sensor (AT cut quartz)	Nanostructured gold electrode		2.5 ppbv	Hg^0 vapor	Kabir et al., 2015
Jerome® J405, mercury vapor analyzer	Gold thin film (750 ccmin-1)	60 pptv – 120 ppbv	60 pptv	Hg^0 vapor	www.azi.com

On the other hand, identifying as well monitoring GOM and PBM in the atmosphere, both of which are commonly present at ultra-trace concentrations (pg/m³), seems even more difficult due to their complex physiochemical properties (Gustin et al., 2013). To date, strategies based on ultrasensitive gas chromatography mass spectrometry (GC/MS) systems, soft ionization mass spectrometry coupled with nanostructured preconcentrators (Deeds et al., 2015), detectors for oxidized Hg species (DOHGS) (Ambrose et al., 2013) and proper calibrators and filters associated with a Tekran system (Lyman et al., 2016) appear to be the most advanced technologies to quantify GOM and PBM in quasi-real time from air.

Given the uncertainty and restrictions associated with automated measurements, passive sampling systems are currently a useful alternative for making regional and global estimates of air Hg concentrations. Some passive samplers used for Hg have been biological materials, such as leaves, lichens, tree cores, and mosses (Harmens et al., 2008; Grangeon et al., 2012). Others have been designed using a range of synthetic materials, such as sulfur-impregnated carbon (SIC), chlorine-impregnated carbon (CIC), bromine-impregnated carbon (BIC), gold-coated (GCS) sorbents (Lin et al., 2017) and housings for Hg collection (McLagan et al., 2016). The latter work on the basis of diffusion. In addition, surrogate surfaces have been developed for passive measurement of Hg dry deposition. Most commercially available passive/diffusive samplers are planar or axial in shape and offer lower sampling rates and limited sampling capacity. As a result, sensitivity can suffer during short-term analysis (due to low sampling rates), or long-term sampling (analyte back-diffusion due to low capacity). Alternatively, radial samplers, comprising a columnar sorbent surrounded by a cylindrical diffusive barrier, aim to increase the sampling rate by maximizing the surface area across which diffusion occurs (Radiello®, Król et al., 2010). Passive samplers have also been designed with external shields to protect the sampler components from direct wind, sunlight, and precipitation and to reduce turbulent airflow. Passive samplers more recently developed are listed in Table 4.5.

Table 4.5 Passive samplers developed in recent years to measure TGM and GOM.

Target	Location	TGM, ng/m³ GOM, pg/m³	Material/sampler	Sampling rate, ml/min	Blank	DL, pg/m³	Influences	Reference
TGM	Rural	1–4	Gold coated plate	87 (lab); 51±19 (field); 260 theoretical	80 pg	90 (3 days)		Gustin et al., 2011
		0.8–1.5	Silver wire / radial sampler	20 measured; 33 theoretical	80 pg	430 (3 days)		Gustin et al., 2011
TGM	Industrial	25	Gold solution with LDPE / passive integrative mercury sampler (PIMS)	1.4	0.3 ng	2000 (4 weeks)		Brumbaugh et al., 2000
TGM	Chamber	10	Gold coated tube / laboratory scale	57 measured; 114 theoretical	0.02 ng	50 (2.8 days); 140 (1 day)	Wind speed	Skov et al., 2007
TGM	Chamber indoor, outdoor	2–3.5	Gold-coated silica / axial sampler	0.22 measured; 0.32 theoretical		30% (uncertainty)		Brown et al., 2012
TGM	Industrial, suburban, rural	2–5.5	Sulfur-impregnated carbon/axial sampler	90		80 (30 days)	Wind speed	Zhang et al., 2012c
TGM	Industrial	2	Gold-coated filter-cation exchange membrane / two-bowl sampler	460 measured; 556 theoretical	0.17 ng	10 (3 days)	Wind speed, humidity	Huang et al., 2012a
TGM	Chamber, indoor, outdoor	1.35–2.16 ng/m³ (indoor); d 1.17–3.29 ng/m³ (outdoor)	Sulfur impregnated carbon sampler / radial in a protective shield	0.158–0.121 m³/ day indoor–outdoor		11–12 months		McLagan et al., 2016
GOM	Rural, suburban	DL–65	Cation-exchange membrane / multiple configurations	0.7–3.2 measured; 0.055 theoretical	0.27–0.68 ng	5 (2 weeks)	Wind speed	Lyman et al., 2010a
GOM	Remote	DL–67	Cation-exchange membrane / aerohead configuration		0.56 ng	2.3 (2 weeks)	Wind speed	Wright et al., 2013
GOM	Industrial, suburban, rural	DL–35	Cation-exchange membrane / two-bowl sampler	1042 measured; 486 theoretical	0.02–0.04 ng	3 (3 days)	Wind speed, humidity	Huang et al., 2012a

4.6 **Conclusions**

Data from existing air Hg monitoring networks show a clear gradient in Hg concentration between the northern and southern hemispheres. Existing networks and their spatial distribution, however, show large gaps in geographical coverage (i.e., Africa, Latin America and the Caribbean, Russia) and filling these gaps will be key to determining future regional changes of Hg deposition transport patterns and identifying regional source-receptor relationships.

There are too few data to assess the global temporal trend in atmospheric Hg concentration and deposition. Data from Europe, Canada, and the United States show a general decrease in the level of Hg in air.

Close cooperation among existing monitoring networks is needed to support global actions to reduce Hg emissions: by ensuring sustainability of a long-term monitoring program covering both hemispheres; by assuring comparability among different monitoring data sets by promoting the adoption of common methods and standards; by promoting experiments for testing and validating new methods and technologies for Hg monitoring such as passive air samplers, among others; and by supporting nations as they develop their own monitoring programs by promoting a continuous capacity building and transfer of knowledge program in cooperation with UN Environment.

Acknowledgements

Chapter 4 Appendix

Table A4.1 Global Review of mercury monitoring sites in national or regional/global areas (UN Environment, 2016).

National / regional area	Program/ network/ inventory – dates of Hg measurements	Number of monitoring stations/ sites	Managing institution	Main URLs
National networks				
Andorra	Andorran Air Quality network. 2011 onwards	Not available	Department of Environment and Sustainability	
Australia	Australian National Pollutant inventory (NPI). 1996 onwards	2		https://data.gov.au/dataset/npi
Austria	Network for Mercury impacts in forest foliage. 1983 (as bio-monitoring) onwards	Not available	Austrian Federal Research Centre for Forests controls	www.bioindikatornetz.at
Brazil	Mercury monitoring sites. Dates not available	Not available	CETESB, the environmental agency of the State of São Paulo	www.cetesb.sp.gov.br/2014/10/27/ cetesb-realiza-treinamentos-internacionais-sobre-pops-e-mercurio/
Canada	Environment and Climate Change Canada (ECCC) – Atmospheric Mercury Monitoring (AMM) network or ECCC-AMM. Includes combination of other networks; 1994 onwards	3 for air measurements	ECCC	http://donnees-data.intranet.ec.gc. ca/data/air/monitor/monitoring-of-atmospheric-gases/total-gaseous-mercury-tgm/?lang=en
		+7 for air measurements	Environment and Climate Change Canada	http://donnees-data.intranet.ec.gc. ca/data/air/monitor/monitoring-of-combined-atmospheric-gases-and-particles/speciated-mercury/
		+ 2 remote	Canadian Northern Contaminants Program (NCP) – Environment Canada	http://nadp.sws.uiuc.edu/
China	Mercury monitoring sites (including GMOS sites)	9 for air measurements	Institute of Geochemistry, CAS	
China (Taiwan)	Wet deposition Network. 2009 onwards	11	Environmental Protection Administration	
		+ 1 remote		
Hungary	Hungarian Air Quality Monitoring Network. 2010 onwards	1	Hungarian Meteorological Service	
Republic of Korea	Mercury Monitoring Network in Korean Air Pollution Monitoring Network. 2009 onwards	12 TGM / 1 Hg speciation / 4 Hg precipitation	National Institute of Environmental Research in the Ministry of Environment	https://seoulsolution.kr/en/content/ air-pollution-monitoring-network www.airkorea.or.kr (Korean only)
Japan	Mercury Monitoring Networks. 1998 onwards	5	National Institute for Minamata Disease (NIMD) and the National Institute for Environmental Studies (NIES)/ Ministry of Environment (MOE)	www.env.go.jp/en/chemi/mercury/ bms.htmlhttp://www.env.go.jp/ press/104568.html (Japanese only) www.env.go.jp/air/osen/monitoring/ mon_h27/index.html (Japanese only)
Poland	Polish State Environmental Monitoring program. 2000 onwards	5	Inspection of Environmental Protection	www.gios.gov.pl/en/state-of-the-environment/state-environmental-monitoring
Indonesia	Mercury Monitoring Site	1		http://apmmn.org
Switzerland	Mercury Monitoring Site	1		www.hfsjg.ch
Romania	Mercury Monitoring Network. 2000 onwards		Ministry of Environment, NEPA and the National Environmental Guard	
United Kingdom	National Metals Network and National Atmospheric Emission Inventory. Dates not available	2	Department for Environment, Food and Rural Affairs (DEFRA); Centre for Ecology and Hydrology (CEH)	www.auchencorth.ceh.ac.uk/ node/211 https://uk-air.defra.gov.uk/networks/ network-info?view=metals http://naei.defra.gov.uk/overview/ pollutants?pollutant_id=15
Vietnam	Mercury Monitoring System. 2014 onwards	1	Vietnamese Centre for Environmental Monitoring (CEM) of the Vietnam Environment Administration (VEA)	

Table A4.1 continued

National / regional area	Program/ network/ inventory – dates of Hg measurements	Number of monitoring stations/ sites	Managing institution	Main URLs
Regional/Global networks				
Global network	Global Mercury Observation System (GMOS)	Stations in both hemispheres	CNR-IIA, Division of Rende, Italy	www.gmos.eu
Regional Network	European Union Network under EU Directive 2004/107/EC	Several stations in Europe	European Environment Agency (EEA)	http://cdr.eionet.europa.eu/ https://www.eea.europa.eu/ publications/92-9167-058-8/page010. html
	European Monitoring and Evaluation Programme (EMEP)	Many stations in Europe	EMEP Organization	http://emep.int/index.html
	National Atmospheric Deposition Program (NADP)	Many stations in USA, Canada	NADP Program Office	http://nadp.sws.uiuc.edu/mdn/
	Asia Pacific Mercury Monitoring Network (APMMN)	Several stations in the Asia-Pacific Region	APMMN	http://apmmn.org/
	Arctic Monitoring and Assessment Programme (AMAP)	Several stations across the circum-Arctic region	AMAP	www.amap.no

Table A4.2 Annually-averaged gaseous elemental mercury concentrations from 2012 to 2014 at GMOS stations (Sprovieri et al., 2016).

Code	Site	Type	Elevation, masl	Lat	Lon	Country	GEM mean ± SD, ng/m^3		
							2012	2013	2014
Northern Hemisphere									
VRS	Villum Research Station	Remote	30	81.58033	-16.60961	Greenland	1.44±0.27	1.61±0.41	1.41±0.35
PAL	Pallas	Remote	340	68.00000	24.23972	Finland	-	1.45±0.11	1.47±0.17
RAO*	Råö	Remote	5	57.39384	11.91407	Sweden	1.33±0.20	1.43±0.16	1.48±0.23
MHE	Mace Head	Remote	5	53.32511	-9.90500	Ireland	-	1.46±0.17	1.41±0.14
LIS	Listvyanka	Rural	670	51.84670	104.89300	Russia	-	1.34±0.38	1.39±0.40
CMA	Col Margherita	Rural	2545	46.36711	11.79341	Italy	-	-	1.69±0.29
LON*	Longobucco	Rural	1379	39.39408	16.61348	Italy	-	1.43±0.33	-
MIN	Minamata	Rural	20	32.23056	130.40389	Japan	1.95±0.48	1.86±0.40	1.91±0.40
EVK	Ev-K2	Remote	5050	27.95861	86.81333	Nepal	1.14±0.17	1.11±0.42	1.33±0.22
Tropics									
SIS	Sisal	Rural	7	21.16356	-90.04679	Mexico	-	1.20±0.24	1.11±0.37
CAL	Calhau	Remote	10	16.86402	-24.86730	Cape Verde	-	1.22±0.14	1.20±0.09
KOD	Kodaicanal	Rural	2333	10.23170	77.46524	India	-	1.54±0.20	1.54±0.26
NIK	Nieuw Nickerie	Rural	1	5.95679	-57.03923	Suriname	-	1.13±0.42	1.28±0.46
MAN*	Manaus	Remote	110	-2.89056	-59.96975	Brazil	-	1.08±0.23	0.99±0.23
Southern Hemisphere									
AMS*	Amsterdam Island	Remote	70	-37.79604	77.55095	French Southern and Antarctic Lands	1.03±0.07	1.03±0.09	1.05±0.05
CPT	Cape Point	Remote	230	-34.35348	18.48983	South Africa	1.07±0.10	1.03±0.11	1.09±0.12
BAR	Bariloche	Rural	801	-41.12873	-71.42010	Argentina	1.01±0.11	0.89±0.15	0.87±0.15
DDU	Dumont d'Urville	Remote	40	-66.66281	140.00292	Antarctica	0.91±0.2	0.85±0.19	0.86±0.38
DMC	Concordia Station	Remote	3220	-75.10170	123.34895	Antarctica	0.76±0.24	0.84±0.27	-

*GMOS Master stations with speciation Hg data.

Table A4.3 Annually-averaged particle-bound mercury and gaseous oxidized mercury concentrations from 2012 to 2014 at the GMOS stations (Sprovieri et al., 2016).

Code	Site	Elevation, masl	Lat	Lon	Country	PBM mean ± SD, pg/m³			GOM mean ± SD, pg/m³		
						2012	2013	2014	2012	2013	2014
Northern Hemisphere											
RAO	Råö	5	57.39384	11.91407	Sweden	2.89±3.27	3.96±3.77	4.41±5.87	0.63±1.73	0.54±0.85	1.25±1.87
LON	Longobucco	1379	39.39408	16.61348	Italy	-	3.28±3.82	-	-	11.33±29.90	-
CHE	Cape Hedo	60	26.86430	128.25141	Japan	1.77±2.46	3.70±3.60	4.03±5.25	1.10±1.80	1.46±2.19	2.26±3.71
Tropics											
MAN	Manaus	110	-2.89056	-59.96975	Brazil	-	5.04±4.13	1.45±1.81	-	1.72±0.72	1.61±1.75
Southern Hemisphere											
AMS	Amsterdam Island	70	-37.79604	77.55095	French Southern and Antarctic Lands	1.76±1.20	2.05±1.37	2.22±1.83	1.65±0.82	1.53±0.45	2.03±1.44

Table A4.4 Annual wet deposition fluxes and weighted total mercury concentrations observed at GMOS stations from 2011 to 2015 (Sprovieri et al., 2017).

Code	Station	Elevation, masl	Lat	Lon	Country	Annual wet deposition flux, µg/m²/y					Weighted THg, ng/L				
						2011	2012	2013	2014	2015	2011	2012	2013	2014	2015
Northern Hemisphere															
NYA	Zeppelin	474	78.90806	11.88139	Norway	-	0.9	0.9	1.7	0.8	-	3.8	4.1	5.7	4.4
PAL	Pallas	340	68	24.23972	Finland	2.9	1.9	1.3	2.3	-	7.1	6.8	4.5	6.1	-
RAO	Råö	5	57.393835	11.914066	Sweden	5.8	6.5	4.2	6.3	-	8.9	10.4	8.2	9.9	-
MHE	Mace Head	5	53.325106	-9.905	Ireland	-	0.9	4.8	4.1	-	-	2.2	4.6	6.6	-
LIS	Listvyanka	670	51.8467	104.893	Russia	-	0.2	0.1	-	-	-	9.7	2.6	-	-
CMA	Col Margherita	2545	46.36711	11.79341	Italy	-	-	-	4.4	-	-	-	-	7.8	-
ISK	Iskrba	520	45.561217	14.858047	Slovenia	5.1	8.4	7.2	10.0	3.0	7.5	6.2	5.3	6.1	3.0
MCH	Mt. Changbai	741	42.40028	128.11250	China	2.8	4.8	1.2	1.0	-	10.6	8.4	3.9	5.4	-
LON	Longobucco	1379	39.39408	16.61348	Italy	-	0.3	3.1	-	-	-	3.9	6.6	-	-
MWA	Mt. Walinguan	3816	36.28667	100.89797	China	-	0.3	0.4	2.2	-	-	4.3	6.4	15.0	-
MAL	Mt. Ailao	2503	24.53791	101.03024	China	4.3	3.2	5.5	0.2	-	2.8	3.3	5.3	6.7	-
Tropics															
SIS	Sisal	7	21.16356	-90.04679	Mexico	-	-	7.4	6.5	-	-	-	11.0	9.1	-
CST	Celestun	3	20.85838	-90.38309	Mexico	-	2.4	0.1	-	-	-	8.1	13.5	-	-
Southern Hemisphere															
AMS	Amsterdam Island	70	-37.79604	77.55095	French Southern and Antarctic Lands	-	-	1.95	1.55	-	-	-	2.34	1.80	-
CPT	Cape Point	230	-34.35348	18.48983	South Africa	0.3	3.8	5.2	0.57	0.6	2.1	14.6	19.6	1.84	3.0
CGR	Cape Grim	94	-40.683333	144.689444	Australia	-	-	3.1	3.8	3.1	-	-	4.0	6.7	6.5
BAR	Bariloche	801	-41.12873	-71.42010	Argentina	-	-	-	0.1	0.5	-	-	-	0.4	0.6

Table A4.5 Annual gaseous elemental mercury concentrations observed at AMNet stations from 2009 to 2015. Only average values with greater than 2000 valid two-hourly averages are included (http://nadp.isws.illinois.edu).

Site	Name	State	Lat	Lon	Elevation, masl	Start Date	Stop Date
AK03	Denali NP-Mt. McKinley	AK	63.7232	-148.9676	661	03/10/14	
AL19	Birmingham	AL	33.5530	-86.8148	200	01/01/09	06/30/16
CA48	Elkhorn Slough	CA	36.8100	-121.7800	15	01/01/10	01/01/11
FL96	Pensacola	FL	30.5499	-87.3750	45	01/01/09	10/01/16
GA40	Yorkville	GA	33.9282	-85.0451	395	01/01/09	10/01/16
HI00	Mauna Loa	HI	19.5392	-155.5792	3399	12/30/10	
MD08	Piney Reservoir	MD	39.7053	-79.0122	769	01/01/08	
MD98	Beltsville #2	MD	39.0280	-76.8171	46	01/26/07	
MD99	Beltsville	MD	39.0280	-76.8171	46	11/07/06	
ME97	Presque Isle	ME	46.6964	-68.0332	165	12/06/13	
MS12	Grand Bay NERR	MS	30.4294	-88.4277	2	09/29/06	
MS99	Grand Bay NERR #2	MS	30.4294	-88.4277	2	10/18/07	11/12/12
NH06	Thompson Farm	NH	43.1100	-70.9500		01/01/09	11/29/11
NJ05	Brigantine	NJ	39.4649	-74.4488	1	06/01/09	10/01/15
NJ30	New Brunswick	NJ	40.4728	-74.4226	21	10/01/15	
NJ54	Elizabeth Lab	NJ	40.6414	-74.2084	11	10/01/15	
NS01	Kejimkujik NP, Canada	NS	44.4328	-65.2056	155	01/26/09	
NY06	Bronx	NY	40.8680	-73.8782	68	08/27/08	
NY20	Huntington Wildlife	NY	43.9731	-74.2231	500	11/21/07	
NY43	Rochester	NY	43.1463	-77.5482	136	09/26/08	
NY95	Rochester_B	NY	43.1463	-77.5481	136	11/21/07	11/13/09
OH02	Athens Super Site	OH	39.3078	-82.1182	275	01/01/07	
OH52	South Bass Island	OH	41.6582	-82.8270	177	12/31/11	
OK99	Stilwell	OK	35.7508	-94.6700	299	10/20/08	
TW01	Mt. Lulin	TW	23.5100	120.9200	2862	01/01/10	
UT96	Antelope Island	UT	41.0467	-112.0248	1287	06/18/09	06/30/11
UT97	Salt Lake City	UT	40.7118	-111.9609	1297	11/23/08	
VT99	Underhill	VT	44.5283	-72.8684	399	01/01/08	01/04/16
WI07	Horicon Marsh	WI	43.4660	-88.6210	287	01/02/11	

GEM (ng/m3)						
2009	2010	2011	2012	2013	2014	2015
					1.34±0.16	1.35±0.14
2.06±4.70	2.16±1.28	2.23±1.28	1.95±1.39	1.85±2.08	1.80±0.70	1.67±1.11
	1.48±0.17	1.48±0.15				
1.36±0.15	1.42±0.14	1.38±0.16	1.41±0.14	1.37±0.20	1.35±0.20	1.28±0.13
1.28±0.16	1.31±0.21	1.41±0.30	1.45±0.20	1.42±0.32	1.44±0.24	1.37±0.28
		1.45±0.51	1.33±0.52	1.42±0.42	1.34±0.33	1.37±0.32
1.29±0.21	1.39±0.17	1.43±0.17		1.34±0.19	1.34±0.20	
1.30±0.23	1.45±0.43	1.51±0.23	1.42±0.19	1.40±0.21	1.32±0.20	1.31±0.19
1.33±0.20	1.45±0.43	1.46±0.20	1.43±0.20	1.37±0.20	1.41±0.18	
					1.58±0.28	
1.36±0.18	1.40±0.13	1.44±0.14	1.36±0.17	1.41±0.14	1.41±0.25	1.35±0.24
1.40±0.23	1.39±0.13	1.45±0.16				
1.33±0.25	1.32±0.15	1.36±0.21				
1.37±0.31	1.35±0.20	1.41±0.19	1.28±0.19	1.32±0.20	1.27±0.21	1.24±0.23
1.50±0.34		1.51±0.34	1.60±0.39		2.05±0.74	1.80±0.42
1.25±0.28	1.39±0.55	1.23±0.27	1.32±0.27			1.24±0.25
1.41±0.19	1.43±0.19	1.33±0.16	1.41±0.42		1.73±1.14	1.50±0.75
1.58±0.29						
1.33±0.16	1.43±0.19	1.40±0.24			1.54±0.22	1.49±0.23
				1.72±0.71		
1.32±0.19	1.40±0.18	1.36±0.18				
	1.68±0.93					
2.19±0.98		1.80±0.80	1.81±1.14	1.85±0.94	1.74±0.48	
1.41±0.23	1.51±0.15	1.46±0.19	1.33±0.17	1.08±0.14	1.33±0.19	1.30±0.17
		1.34±0.17	1.49±0.15	1.53±0.20	1.47±0.22	1.52±0.41

Table A4.6 Mean concentrations of mercury in Canada (Steffen et al., 2008, 2014; ECCC, 2016a).

Station	Lon, Lat	Measurement period, TGM	Mean TGM, ng/m^{-3}	Measurement period, speciated Hg	Mean GEM, ng/m^3	Mean GOM, pg/m^3	Mean PBM, pg/m^{-3}	Measurement period, wet deposition	Mean total Hg, ng/L
Little Fox Lake YK [a,g]	135.63, 61.35	Jun 2007–Dec 2016	1.39±0.15	-	-	-	-	-	-
Ucluelet BC[b]	125.54, 48.92	Aug 2013–Dec 2016	1.34±0.13	-	-	-	-	-	-
Reifel Island BC[c, d]	123.17, 49.10	Mar 1999–Feb 2004	1.67±0.19	-	-	-	-	Apr 2000–Feb 2004	5.6
Saturna BC[c, d, e]	123.13, 48.78	Feb 2010–Aug 2016	1.31±0.16	-	-	-	-	Sep 2009–Dec 2015	5.2
Whistler BC[b]	122.93, 50.07	Aug 2008–Dec 2015	1.26±0.20	-	-	-	-	-	-
Fort Vermilion AB[f]	116.02, 58.38	-	-	-	-	-	-	Dec 2006–Jan 2008	4.3
Meadows AB	114.64, 53.53	May 2005–Dec 2008	1.51±0.21	-	-	-	-	-	-
Genesee AB[b,d]	114.20, 53.30	Mar 2004–Dec 2010	1.53±0.25	Jan 2009–Dec 2010	1.38±0.17	5.0±4.6	5.0±4.3	Jul 2006–Dec 2015	11.6
Crossfield AB[f]	114.00, 51.29	-	-	-	-	-	-	May 2006–Dec 2007	9.3
Fort Chipewyan AB[c]	111.12, 58.78	Jun 2000–July 2001	1.36±0.15	-	-	-	-	-	-
Henry Kroeger AB[d]	110.83, 51.42	-	-	-	-	-	-	Oct 2004–Dec 2015	12.3
Esther AB[d, e]	110.20, 51.67	Jun 1998–Apr 2001	1.65±0.15					Apr 2000–May 2001	14.9
Fort McKay South AB[h]	111.64, 57.15	Jan 2016–Dec 2016	1.24±0.38	Aug 2013–Dec 2016	1.18±0.19	0.7±1.5	4.4±8.7	-	-
Patricia McInnis AB[h]	111.48, 56.75	Oct 2010–Dec 2016	1.32±0.22	-	-	-	-	-	-
Pinehouse Lake SK[e]	106.725, 55.5121							May 2015–Dec 2015	8.4
Bratt's Lake SK[d,e]	104.71, 50.20	May 2001–Apr 2013	1.44±0.24	-	-	-	-	Jun 2001–Apr 2013	11.3
Flin Flon MB[b]	101.88, 54.77	Jul 2008–Dec 2016	3.23±1.87	Jul 2010–Mar 2011	2.04±0.58	3.9±8.4	11±16	Sep 2009–Dec 2010	59.9
ELA ON[d,e,]	93.72, 49.66	-	-					Nov 2009–Jan 2011	13.4
Burnt Island ON[c]	82.95, 45.81	May 1998–Dec 2007	1.55±0.22					Dec 2001–Mar 2003	10.1
Egbert ON[c,d,e]	79.78, 44.23	Dec 1996–Dec 2016	1.51±0.31	-	-	-	-	Mar 2000–Dec 2015	8.1
Kuujjuarapik QC[c]	77.73, 55.30	Aug 1999–Sep 2009	1.68±0.46	-	-	-	-	-	-
Point Petre ON[c]	77.15, 43.84	Nov 1996–Dec 2007	1.75±0.33	-	-	-	-	Nov 2001–Mar 2003	8.4
Chapais QC[d,e]	74.98, 49.82	-	-	-	-	-	-	Dec 2009–Dec 2015	5.2
St. Anicet QC[b,c,d]	74.03, 45.20	Aug 1994–Dec 2016	1.53±0.35	Jan 2003–Dec 2015	1.43±0.30	2.7±4.1	17.2±25.8	Apr 1998–Aug 2007	8.0
St. Andrews NB[c,d]	67.08, 45.08	Jan 1996–Jul 2007	1.38±0.24	-	-	-	-	Jul 1996–Dec 2003	6.5

Table A4.6 continued

Station	Lon, Lat	Measurement period, TGM	Mean TGM, ng/m⁻³	Measurement period, speciated Hg	Mean GEM, ng/m³	Mean GOM, pg/m³	Mean PBM, pg/m⁻³	Measurement period, wet deposition	Mean total Hg, ng/L
Keimkujik NS[c,d,e]	65.21, 44.43	Jan 1996–Dec 2016	1.36±0.28	Jan 2009–Dec 2016	1.31±0.20	0.6±1.3	5.4±8.8	Jul 1996–Dec 2015	5.1
Mingan QC[b,c]	64.17, 50.27	Jan 1997–Dec 2015	1.42±0.23	-	-	-	-	Apr 1998–Aug 2007	5.1
Halifax NS[b]	63.67, 44.67			Oct 2009–Dec 2011	1.53±0.42	2.0±2.1	2.1±1.8		
Southampton PE[c]	62.58, 46.39	Jan 2005–Dec 2006	1.23±0.19	-	-	-	-	-	-
Alert NU[a]	62.33, 82.50	Jan 1995–Dec 2016	1.47±0.38	Jan 2002–Dec 2016	1.25±0.40	25±54	42±77	-	-
StephenvilleNL[d,e]	58.57, 48.56	-	-	-	-	-	-	Feb 2010–Dec 2015	5.2
Cormak NL[d,e]	57.38, 49.32	-	-	-	-	-	-	May 2000–Jul 2010	4.3

a-h are the previous network names under which the data were collected: [a]Northern Contaminants Program (NCP); [b]Clean Air Regulatory Agenda Mercury Science Program (CARA) currently Climate Change and Air Pollution program (CCAP); [c]Canadian Atmospheric Mercury Measurement Network (CAMNet); [d]The Mercury Deposition Network (MDN); [e]The Canadian Air and Precipitation Monitoring Network (CAPMoN); [f]Geological Survey of Canada (GSC); [g]Intercontinental Atmospheric Transport of Anthropogenic Pollutants to the Arctic (INCATPA); [h]Joint Oil Sands Monitoring Program (JOSM). Note: Fort McKay south is collecting THg as of October 2017, no results were available at the time of writing.

Table A4.7 Annual trends in mercury data collected in Canada (Steffen et al., 2008, 2014; ECCC, 2016a).

Station	Measurement period, TGM	Trend TGM, %/y	Measurement period, wet deposition	Trend THg in precipitation
Little Fox Lake YK[a]	Jun 2007–Dec 2016	+1.3 (+0.7 to +1.9)	-	-
Reifel Island BC	Mar 1999–Feb 2004	-3.3(-4.2 to -2.4)	-	-
Saturna BC[a]	Feb 2010–Aug 2016	-4.1 (-5.1 to -2.2)	Sep 2009–Dec 2015	Ns (-2.5 to +6.7)
Genesee AB	Mar 2004–Dec 2010	-0.4 (ns) (-1.4 to +0.1)	Jul 2006–Dec 2015	Ns (-6.6 to +0.3)
Patricia McInnis AB[a]	Oct 2010–Dec 2016	-3.6 (-5.4 to -2.1)	-	-
Henry Kroeger AB	-	-	Oct 2004–Dec 2015	Ns (-4.2 to +3.8)
Bratt's Lake SK	Nov 2001–Apr 2013	-1.5 (-2.3 to -0.9)	Jun 2001–Apr 2013	Ns (-2.7 to +4.1)
Flin Flon MB[a]	Jul 2008–Dec 2016	-4.2 (-6.5 to -2.4)	-	-
Burnt Island ON	May 1998–Nov 2007	-2.5 (-3.4 to -1.6)	-	-
Egbert ON[a]	Dec 1996–Dec 2016	-1.7 (-1.9 to -1.5)	Apr 2000–Dec 2015	Ns (-1.2 to +0.6)
Point Petre ON	Nov 1996–Nov 2007	-1.7 (-2.2 to -1.2)	-	-
Chapais QC	-	-	Dec 2009–Dec 2015	-6.4 (-10.8 to -1.8)
Mingan QC[a]	Jan 1997–Dec 2015	-1.1 (-1.4 to -0.9)	Apr 1998–Aug 2007	Ns (-5.1 to +0.5)
St. Anicet QC[a]	Jan 1995–Dec 2016	-1.5 (-1.6 to -1.3)	May 1998–Aug 2007	-3.0 (-5.3 to -1.0)
St. Andrews NB	Jan 1996–Jun 2007	-1.0 (-1.4 to -0.5)	Jul 1996–Dec 2003	Ns (-7.0 to +0.5)
Kejimkujik NS[a]	Jan 1996–Dec 2016	-0.9 (-1.1 to -0.7)	Jul 1996–Dec 2015	-1.5 (-2.3 to -0.8)
Alert NU[a]	Apr 1995–Dec 2016	-0.9 (-1.1 to -0.7)		
Cormak NF			May 2000–Jul 2010	Ns (-3.5 to +0.5)

[a] Sites currently operated in Canada as of December 2017

Table A4.8 Atmospheric Hg concentrations at ground-based stations in Asia.

Site	Country	Elevation, masl	Lat, °N	Lon, °E	Type	Study period	TGM or GEM mean ± SD, ng/m³	PBM/TPM mean ± SD, pg/m³	GOM mean ± SD, pg/m³	Reference
An-myun	Korea	45.7	36.533	126.317	Background	12/2004–04/2006	4.61±2.21	-	-	Nguyen et al., 2007
Beijing	China	48	38.898	116.392	Urban	02&09/1998	10.4±3.25	-	-	Liu et al., 2002
						01–12/2006	-	272	-	Schleicher et al., 2015
							-	573±551*	-	
Cape Hedo	Japan	60	26.864	128.251	Background	04/2009–03/2017	1.86±0.22	2.6±0.9	1.6±0.5	www.env.go.jp/ press/104568.html
Changchun	China	270	43.824	125.319	Urban	-/2001	18.4	276*	-	Fang et al., 2004
Chengshantou	China	30	37.38	122.68	Remote coast	07&10/2007, 01&04/2009	2.31±0.74	-	-	Ci et al., 2011
Chongming Island	China	11	31.522	121.908	Remote coast	2009-09-12	2.5±1.50	-	-	Dou et al., 2013
Chongqing	China	350	29.6	106.5	Urban	08/2006–09/2007	6.74±0.37	-	-	Yang et al., 2009
Chuncheon	Rep. Korea	120	37.999	127.810	Residential town	03–12/2006	1.58±0.62	-	-	Han et al., 2014b
						01–12/2007	2.14±1.56	4.7±4.3	2.7±3.2	
						01/2008–02/2009	2.52±1.8	2.5±3.2	2.8±2.4	
Guangzhou	China	60	23.124	113.355	Urban	11/2010–10/2011	4.6±1.60	-	-	Chen et al., 2013
Guiyang	China	1040	26.57	106.72	Urban	11/2001–11/2002	8.4±4.87	-	-	Feng et al., 2004
						12/2009–11/2010	10.2±7.06	-	-	Fu and Feng, 2015
						08–12/2009	9.72±10.2	368±276	35.7±43.9	Fu et al., 2011
Jeju Island (Go-san)	Rep. Korea	67	33.294	126.163	Remote coast/ Background	2014–2016	0.55±0.88	-	-	www.airkorea.or.kr
Jiaxing	China	10	30.833	120.7	Urban	09/2005	5.4±4.10	-	-	Wang et al., 2007b
Lanzhou	China	1540	36.067	103.79	Urban	-/2004	28.6	-	-	Su et al., 2007
						04&07&10&12/1994	-	955*	-	Duan and Yang, 1995
Lulin	Chinese Taipei	2862	23.51	120.92	Background	04/2006–12/2007	1.73±0.61	2.3±3.9	12.1±20.0	Sheu et al., 2010
Minamata[τ]	Japan	20	32.231	130.403	Rural	04/2011–12/2014	1.89±0.43	-	-	Sprovieri et al., 2016
Miyun	China	220	40.481	116.775	Remote forest	12/2008–11/2009	3.22±1.94	98.2±113	10.1±18.8	Zhang et al., 2013
Mt. Ailao	China	2450	24.533	101.017	Remote forest	05/2011–05/2012	2.09±0.63	31.3±28.0	2.2±2.3	Zhang et al., 2015
Mt. Changbai	China	740	42.402	128.112	Remote forest	10/2008–10/2010	1.6±0.51	-	-	Fu et al., 2012b
						07/2013–07/2014	1.73±0.48	18.9±15.6	5.7±6.8	Fu et al., 2014
Mt. Damei	China	550	29.632	121.565	Remote forest	04/2011–04/2013	3.31±1.44	154±104	6.3±3.9	Yu et al., 2015
Mt. Dinghu	China	700	23.164	112.549	Remote forest	09/2009–04/2010	5.07±2.89	-	-	Chen et al., 2013
Mt. Gongga	China	1640	29.649	102.117	Remote forest	05/2005–07/2007	3.98±1.62	30.7±32.0*	6.2±3.9	Fu et al., 2008a,b
Mt. Jiuxian	China	1700	25.71	118.11	Remote forest	11/2010. 01&04&08/2010	-	24.0±14.6	-	Xu et al., 2013
Mt. Leigong	China	2178	26.39	108.2	Remote forest	05/2008–05/2009	2.8±1.51	-	-	Fu et al., 2010b
Mt. Walinguan	China	3816	36.287	100.898	Remote grassland	09/2007–09/2008	1.98±0.98	19.4±18.0	7.4±4.8	Fu et al., 2012c

Table A4.8 continued

Site	Country	Elevation, masl	Lat, °N	Lon, °E	Type	Study period	TGM or GEM mean ± SD, ng/m³	PBM/TPM mean ± SD, pg/m³	GOM mean ± SD, pg/m³	Reference
Nanjing	China	100	32.05°N	118.78	Urban	01–12/2011	7.9±7.00	-	-	Zhu et al., 2012
						06/2011–02/2012	-	1100±570*	-	Zhu et al., 2014
Ningbo	China	10	29.867	121.544	Urban	10/2007–01/2008	3.79±1.29	-	-	Nguyen et al., 2011
Pohang	Rep. Korea	10	35.992	129.404	Urban/ Industry	08&10/2012, 01&03&04/2013	5.00±4.70	-	-	Seo et al., 2016
Qingdao	China	40	36.16	120.5	Urban	01/2013	2.8±0.90	245±174*	-	Zhang et al., 2014
Seoul	Rep. Korea	77	37.610	126.934	Urban	2014–2016	2.15±1.21	-	-	www.airkorea.or.kr
Seoul	Rep. Korea	17	37.514	127.001	Urban	02/2005–12/2006	3.44±2.13	-	-	Choi et al., 2009
Seoul	Rep. Korea	17	37.514	127.001	Urban	01/2006–12/2008	3.77±2.96	13.4±12.0	11.3±9.5	Han et al., 2014b
Shangai	China	19	31.23	121.54	Urban	08–09/2009	2.7±1.70	-	-	Friedli et al., 2011
						07/2004–04/2006	-	560±220*	-	Xiu et al., 2009
Shangri-La	China	3580	28.017	99.733	Remote forest	11/2009–10/2010	2.55±2.73	37.8±31.0	7.9±7.9	Zhang et al., 2015
Southeastern coastal cities	China	-	-	-	Urban	11/2010, 01&04&08/2011	-	141±128	-	Xu et al., 2013
Tae-An	Rep. Korea	23	36.738	126.133	Rural	2014–2016	2.15±1.29	-	-	www.airkorea.or.kr
Tokai-mura	Japan	15	36.27	140.36	Urban	10/2005–08/2006	3.78±1.62	-	-	Osawa et al., 2007
Wanqingsha	China	3	22.7	113.55	Remote coast	2009–11-12	2.94	-	-	Li et al., 2011
Wuhan	China	20	30.6	114.3	Urban	-/2002	14.8	-	-	Xiang and Liu, 2008
Xiamen	China	7	24.60	118.05	Urban	03/2012–02/2013	3.5	174±280	61.0±69.0	Xu et al., 2015
Yongheung island	Rep. Korea	32	37.279	126.457	Rural / but, coal-fired power plant is located.	01/2013–08/2014	2.8±1.10	10.9±11.2	8.3±9.7	Xu et al., 2015

PBM/TPM: * Indicates TPM, otherwise indicates PBM.

Table A4.9 Mercury concentrations and deposition fluxes in precipitation, throughfall, and litterfall in Asia.

Site	Elevation, masl	Lat	Lon	Type	Study period	Samples	Hg concentration, ng/L or ng/g		Deposition flux, µg/m²/y		Reference
							THg	MeHg	THg	MeHg	
Chuncheon, Korea	120	37.999	127.810	Residential town	08/2006–07/2008	Precipitation	8.8	-	9.4	-	Ahn et al., 2011
Seoul, Korea	77	37.27	127.57	Urban	07/2013–06/2014	Precipitation	16.1	0.04	6.0	0.01	Won et al., 2019
Mt. Ailao, Yunnan	2500	24.53	101.02	Remote	06/2011–05/2012	Precipitation	3.0	-	5.4	-	Zhou et al., 2013
						Litterfall	54.0	-	71.2	-	
Mt. Leigong, Guizhou	2178	26.39	108.20	Remote	05/2008–05/2009	Precipitation	4.0	0.04	6.1	0.06	Fu et al., 2010b
						Throughfall	8.9	0.1	10.5	0.12	
						Litterfall	91.0	0.48	39.5	0.28	
Mt. Damei, Zhejiang	550	29.63	121.57	Remote	08/2012–07/2013	Precipitation	4.1	-	7.0	-	Lang, 2014
						Litterfall	46.6	-	26.0	-	
Nam Co, Tibet	4730	30.77	90.99	Remote	07/2009–07/2011	Precipitation	4.8	0.03	1.8	0.01	Huang et al., 2012b
Mt. Gongga[a], Suchuan	1640	29.65	102.12	Remote	2006-01-12	Precipitation*	9.9	-	9.1	-	Fu et al., 2008b
Mt. Gongga[b], Suchuan	3000	29.58	101.93	Remote	05/2005–04/2007	Precipitation*	14.2	0.16	26.1	0.3	Fu et al., 2010a
						Throughfall	40.2	0.3	57.1	0.43	
						Litterfall	35.7	-	35.5	-	
Mt. Changbai, Jilin	750	42.40	128.47	Remote	08/2005–07/2006	Precipitation*	13.4	-	8.4	-	Wan et al., 2009
Puding, Guizhou	1145	26.37	105.80	Remote	08/2005–07/2006	Precipitation*	20.6	0.18	24.8	0.22	Guo et al., 2008
Hongjiadu, Guizhou	1130	26.88	105.85	Remote	08/2005–07/2006	Precipitation*	39.4	0.18	34.7	0.16	Guo et al., 2008
Yinzidu, Guizhou	1088	26.57	106.12	Remote	08/2005–07/2006	Precipitation*	35.7	0.18	38.1	0.19	Guo et al., 2008
Dongfeng, Guizhou	970	26.85	106.13	Remote	08/2005–07/2006	Precipitation*	37.4	0.2	36.3	0.19	Guo et al., 2008
Wujiangdu, Guizhou		27.32	106.77	Remote	08/2005–07/2006	Precipitation*	57.1	0.25	39.6	0.17	Guo et al., 2008
Guiyang	1040	26.57	106.72	Urban	2008-07-09	Precipitation	13.3	0.05	13.4	0.05	Liu et al., 2011
Xiamen	50	24.60	118.31	Urban	07/2013–02/2014	Precipitation	26.6	-	30.4	-	Wu, 2014
Chongqing				Urban	06/2010–06/2011	Precipitation	30.7	0.31	28.7	0.28	Wang et al., 2012b, 2014b
Tieshanping, Chongqing	500	29.63	104.68	Urban	03/2005–03/2006	Precipitation	32.3	-	29.0	-	Wang et al., 2009
						Throughfall	69.7	-	71.3	-	
						Litterfall	105	-	220	-	
Nanjing	100	32.05	118.78	Urban	06/2011–02/2012	Precipitation	52.9	-	56.5	-	Zhu et al., 2014

Precipitation: * indicates bulk precipitation, otherwise indicates wet-only precipitation. Mt. Gongga: [a]elevation of the sampling site 1600m above sea level; [b]elevation of the sampling site 3000m above sea level.

5. Atmospheric pathways, transport and fate

AUTHORS: OLEG TRAVNIKOV, HÉLÈNE ANGOT, JOHANNES BIESER, MARK COHEN, ASHU DASTOOR, FRANCESCO DE SIMONE, IAN HEDGECOCK, SAE YUN KWON, CHE-JEN LIN, ANDREI RYJKOV, NOELLE SELIN, COLIN P. THACKRAY, XUN WANG

Key messages

- *Significant progress has been made since the last Global Mercury Assessment in 2013 in all key areas of interest regarding the atmospheric mercury (Hg) cycle. Uncertainties remain in quantifying emissions, particularly from certain regions and sectors and in Hg speciation. Emission rates from natural surfaces need to be better constrained. New information has solidified our knowledge of Hg oxidation reactions, including the importance of bromine chemistry.*

- *Both model simulations and natural archives provide evidence for peak atmospheric Hg concentrations during the latter half of the 20th century and declines in more recent decades. Future changes under policy scenarios could reduce Hg deposition in the future, but the influence of climate change and legacy Hg complicates our ability to assess this.*

- *Atmospheric Hg concentrations are highest in the temperate latitudes of the Northern Hemisphere and lowest in the high latitudes of the Southern Hemisphere. Highest concentrations are found in East, South, and Southeast Asia due to high anthropogenic emissions as well as in equatorial Africa and South America because of active artisanal and small-scale gold mining (ASGM). Total Hg deposition is more equally distributed between the Northern and Southern Hemispheres, highest in large industrial regions and lowest in remote unpopulated regions. Regions with active ASGM are also subject to a relatively high total Hg deposition rate.*

- *Atmospheric deposition from direct anthropogenic emissions is the mixture of domestic emissions and atmospherically transported Hg from sources in other regions. The share of domestic sources varies from more than 65% in Asia to less than 5% in the Arctic and Antarctica. In East and South Asia, anthropogenic Hg deposition is dominated by the contribution from domestic sources (77% and 66%,*

respectively). Domestic and foreign anthropogenic sources contribute almost equally to the total anthropogenic Hg deposition in Europe.

- *Mercury removal from the atmosphere occurs via wet and dry deposition. Dry deposition remains more poorly quantified than wet deposition, and there remains disagreement among models on its global magnitude.*

- *In North America, the contribution of domestic sources to regional deposition has declined from 23% to 17%, due to the reduction in North American anthropogenic emissions since 2010. Regions with active ASGM (Africa, South and Central America) also receive a relatively large fraction of anthropogenic deposition from domestic sources (30–38%). The largest foreign contributors to various receptor regions are East Asia, Africa, South America, and Southeast Asia.*

- *East Asia and Africa remain the largest contributors to the global ocean reservoirs, owing to their large anthropogenic emissions (20–50% and 10–27%, respectively). The only exception is the Mediterranean and Black Seas, where the contribution from European anthropogenic emissions (20%) dominates over East Asian and African sources.*

- *Mercury deposition from the power generation sectors is largely restricted to a few industrial regions, with the largest contribution in Europe and South Asia. Deposition from industrial sources covers wider areas in Asia, Europe, North and South America, and Africa. The impact of emissions from intentional use and product waste is insignificant in all regions. Mercury emissions from ASGM are transported globally, but the most significant deposition occurs closer to the sources and largely impacts South America, equatorial Africa, and East and Southeast Asia.*

5.1 Introduction

Mercury (Hg) has a long environmental lifetime and cycles between the atmosphere, ocean, and land. Mercury released to the atmosphere can travel globally: it undergoes atmospheric redox reactions, deposits to the Earth's surface, and can continue to cycle between surface and atmosphere for decades to centuries and longer. Using a combination of models and measurements, work since the 2013 Global Mercury Assessment (GMA 2013) (AMAP/UNEP, 2013) has addressed various aspects of Hg transport and fate, including emissions, atmospheric chemistry, removal processes, modelling, and historical trends. A number of other studies have also provided insights into regional and local Hg cycling.

Emissions and their speciation: The emergence of new regional and global emissions inventories provides alternatives to the UNEP/AMAP inventories for the present day as well as

new historical estimates. Uncertainties remain in quantifying emissions, particularly from certain regions and sectors and in Hg speciation.

Atmospheric chemistry: New information has solidified knowledge about Hg oxidation reactions, including the importance of bromine (Br) chemistry in Hg oxidation. Models including these reactions have shorter Hg lifetimes and can reproduce some free tropospheric observations. It should be noted that use of oxidation reactions with hydroxyl radical (OH) and ozone (O_3) in Hg modelling studies also allows reproducing of spatial and temporal patterns of Hg measurements. However, while oxidation in the presence of OH and O_3 has been observed in laboratory experiments, direct reactions of Hg with OH and O_3 are not supported by the theoretical chemical literature implying the possibility of heterogeneous pathways. Thus, significant uncertainties remain in the understanding of atmospheric Hg oxidation

and reduction. Recent model intercomparison studies have shown that there remain challenges in reproducing observed concentrations and patterns when varying atmospheric redox mechanisms are used in the models. In particular, uncertainty remains in atmospheric speciation (Jaffe et al., 2014), the potential importance of heterogeneous chemistry (Ariya et al., 2015), and the mechanism and rate of atmospheric reduction reactions (de Foy et al., 2016).

Removal processes: Measurement and model comparison studies of wet deposition, especially in convective storms, have provided insight into the vertical distribution of Hg in the troposphere as well as oxidation processes. Dry deposition remains more poorly quantified than wet deposition, and there remains disagreement among models on its global magnitude. New measurement analyses of dry deposition have shown the importance of gaseous elemental mercury (Hg^0) uptake into the terrestrial environment, in addition to deposition of oxidized Hg forms.

Mercury modelling: Recent model development has advanced the ability to simulate Hg transport in the atmosphere between different geographical regions and to account for multi-media cycling of Hg, including the importance of legacy Hg. New modelling results based on the updated global Hg emissions inventory for 2015 provided up-to-date estimates of Hg dispersion on a global scale, source apportionment of Hg deposition to various terrestrial and aquatic regions and the contribution of different emission sectors to Hg atmospheric loads (see Section 5.3).

Historical trends and future scenarios: Recent declines have been observed in both atmospheric Hg concentration and wet deposition, on the order of 1–2% per year, that differ by region. Some modelling studies have reproduced these trends, attributing some regional variations to declines in emissions. The observed trends, however, are small compared with uncertainties in surface-atmosphere fluxes, anthropogenic sources, and their attributable fraction. Future changes in Hg emissions under policy scenarios could reduce Hg deposition in the future; however, the influence of climate change and legacy Hg complicates the ability to identify sources and mechanisms that may lead to future changes in atmospheric Hg.

5.2 Atmospheric processes

In GMA 2013, the atmospheric chemistry section (section 3.2) focused on emission speciation, atmospheric Hg redox chemistry, processes governing the exchange of Hg at environmental interfaces and atmospheric Hg dynamics. Progress has since been made in all key areas of interest regarding atmospheric Hg chemistry as well as in some that were not included, especially progress in the last few years of using Hg isotope fractionation to probe Hg processes and origins. However, it may seem that more questions have been posed than answered. Atmospheric Hg processes have been studied or inferred using theoretical, experimental, monitoring and modelling techniques, and usually a combination of all four. The chemical nature of atmospheric Hg, whether elemental, oxidized or bound (tightly or loosely) to atmospheric particulate matter, and its interconversion between these forms, continues to pose a challenge for the emission inventory, modelling and measurement communities alike.

5.2.1 Emissions and their speciation

As discussed in Chapter 2, there are numerous uncertainties in estimating current and historical anthropogenic Hg emissions as well as natural and legacy emissions. In addition to the AMAP/UNEP emission inventories of 2008 and 2013 (AMAP/UNEP, 2008, 2013) new global Hg emission inventories have been developed. In particular, the EDGAR global inventory of Hg anthropogenic emissions for the period 1970–2008 (Muntean et al., 2014) uses different approaches to determine emissions from anthropogenic activity sectors and differs in both total Hg emissions and their speciation compared to the AMAP/UNEP inventory. The EDGAR inventory total Hg emissions are roughly two-thirds of the AMAP/UNEP totals for 2008 and 2013 (1287 and 1960 Mg, respectively), and the relative contributions of elemental, oxidized, and particulate Hg also differ, 81:14:5 for AMAP/UNEP and 72:22:6 for EDGAR. Geographical distribution is broadly similar in the two emission inventories (see De Simone et al., 2016). All-time emissions to the atmosphere have also been quantified by taking into account estimates of releases (Streets et al., 2011, 2017). Other developments include regional inventories (Rafaj et al., 2014; Wu et al., 2016b), estimates of historical and legacy Hg emissions (Amos et al., 2013, 2015), and the contribution of the past and current use of Hg in commercial products (Horowitz et al., 2014). A model comparison study of the effect of using different global emission inventories (De Simone et al., 2016) showed a consistent geographical pattern across the models, in which anthropogenic emissions contribute less than 15% of total Hg deposition in the Southern Hemisphere, 15–20% in the Tropics and 20–30% in the Northern Hemisphere. Exceptions were observed in industrial 'hotspots', where domestic anthropogenic emissions accounted for the majority of Hg deposition.

The importance of accurate emission inventories and how their uncertainty relates to the effectiveness evaluation of the Minamata Convention was discussed by Kwon and Selin (2016). The observed decrease in atmospheric Hg species concentrations (e.g., Castro and Sherwell, 2015; Ren et al., 2016; Zhou et al., 2017a) in the USA is consistent with significant regional decreases in emissions upwind of measurement sites as shown in global as well as U.S. and Canadian national inventories. In addition, the observed increase in Hg concentrations measured in the Southern Hemisphere at Cape Point (South Africa) over the past decade is consistent with the estimated increase in Hg emissions from artisanal and small-scale gold mining in the Southern Hemisphere over the same period (Martin et al., 2017). However, some authors call into question the accuracy of current global emission inventories, particularly in their estimation of European and North American sources (Zhang et al., 2016c), and suggest that there has been a 20% decrease in global anthropogenic Hg emissions between 1990 and 2010, with a 30% decrease in anthropogenic Hg^0. Some additional factors that could result in underestimated reduction of Hg levels in the atmosphere were discussed by Amos et al. (2015) and include the overestimation of geogenic emissions and oceanic evasion of Hg.

Since GMA 2013, some progress has been made in emission speciation. Regional and global modelling studies have also called into question the speciation in emission inventories for specific areas (Kos et al., 2013; Bieser et al., 2014; Zhang et al.,

2015c). The partitioning of oxidized Hg compounds (Hg^{II}) between the gas and particulate phases is still difficult to determine. This is partly due to the lack of information on the Hg^{II} species present in the atmosphere, but also to the vast range of particulate chemical composition. Ariya et al. (2015) discussed heterogeneous reactions of Hg in some detail as well as interactions between Hg and fly ash generated at coal-fired power plants, which is particularly important during the combustion processes leading to Hg emissions. Uncertainties in the atmospheric measurements of speciated Hg further complicate this issue. The tendency of models to produce oxidized Hg concentrations higher than measured may be at least partly due to the measurements being biased low in some situations, rather than solely because of emissions speciation errors.

While Hg emission and speciation from anthropogenic sources have been quantified and updated with a reasonable consistency, estimates of natural Hg emission from the Earth's surfaces, including re-emission of previously deposited Hg, are poorly constrained and have large uncertainties (±2000 Mg/y). This limits the understanding of global and regional Hg cycling budgets (Pirrone et al., 2010; Song et al., 2015; Zhu et al., 2016). The primary challenge in quantifying Hg^0 release from natural surfaces is the lack of understanding in fundamental processes driving the release from different types of surface. Measurements of Hg stable isotope ratios in soil, biomass and air samples suggests that Hg^0 re-emitted from soil and leaf litter is derived from Hg previously bound in the soils and leaf interior, which is subsequently sequestered and recycled, rather than originating from Hg deposited recently on soil and foliage surfaces (Demers et al., 2013; Yu et al., 2016; Yuan et al., 2018).

5.2.2 Atmospheric chemistry

Atmospheric redox reactions can occur homogeneously in the gas and aqueous phases, and heterogeneously on the surface of fog/cloud droplets and atmospheric particulate matter. It is clear that the heterogeneous reactions are more complex to study than the homogenous reactions due to the very wide range of composition of the surfaces at which reactions may take place. A recent review by Ariya et al. (2015) provides an in-depth overview of Hg reactions and transformations in environmental media.

Perhaps the major obstacle to understanding the processes by which Hg is oxidized, reduced, adsorbed and desorbed in the atmosphere and both in and on atmospheric particles is because the nature of the oxidized Hg compounds in the atmosphere remains uncertain. While it seems clear that O_3, OH, and Br are all implicated in the oxidation of atmospheric Hg, the precise nature of the reactions occurring and the identity (and phase) of the products remains the subject of speculation. Recent theoretical studies have given further insight into the Br-initiated oxidation of Hg; this reaction proceeds via an unstable $HgBr^·$ intermediate which may react further to form oxidized Hg species or decompose back to Hg and Br (Goodsite et al., 2004, 2012). Several theoretical studies have investigated the possibility that $HgBr^·$ may react with a series of small atmospheric compounds (Dibble et al., 2012, 2013, 2014; Jiao and Dibble, 2015, 2017) and volatile organic compounds (Dibble and Schwid, 2016). Based on these studies, it appears likely that the $HgBr^·$ intermediate may react further with the relatively abundant radicals HO_2 and NO_2. Meanwhile the likelihood that elemental Hg is oxidized by molecular halogens has been shown to be improbable and that oxidation to Hg halides requires either halogen atom initiation or the presence of a reactive surface (Auzmendi-Murua et al., 2014).

Discussion of atmospheric Hg oxidation by halogens and their compounds must come with the caveat that while the latitudinal, vertical and seasonal variations in O_3 and OH concentrations have been well studied and documented, those of the halogens have not. Thus the halogen concentration fields used in Hg modelling studies are themselves the subject of not insignificant uncertainty, meaning that it remains difficult to draw firm conclusions on the precise role of individual Hg oxidants in the atmosphere. Nonetheless ever more studies on halogen and halogen compounds are becoming available as their impact on numerous aspects of atmospheric chemistry, beyond their role in stratospheric O_3 depletion becomes clear (see, for example, Hossaini et al., 2015; Simpson et al., 2015; Wang et al., 2015; Jourdain et al., 2016; Sherwen et al., 2016).

Considering only oxidation reactions can lead to atmospheric lifetimes for Hg^0 which cannot be reconciled with its global distribution and relatively uniform background hemispheric concentrations. Experimental and observational evidence (in particular the rapid depletion of Hg^0 concentrations seen during atmospheric mercury depletion events; AMDEs) as well as the results from theoretical kinetics studies, point to an atmospheric lifetime against oxidation shorter than that previously estimated of around 12 months (Schroeder and Munthe, 1998). Two recent model studies (Shah et al., 2016; Horowitz et al., 2017b) suggested that it may be less than three months; however, these studies both use hypothetical reduction mechanisms to constrain the Hg^0 concentration to observed values. There is, therefore, likely to be Hg reduction taking place in the atmosphere, and over the years several mechanisms have been suggested, most of which have involved the atmospheric aqueous phase, cloud and fog droplets and deliquesced aerosols, as the reaction medium. See Ariya et al. (2015) for a thorough discussion of possible reduction pathways. Most recently it has been suggested that atmospheric reduction occurs in cloud droplets via the photo-reduction of organic Hg compounds. This mechanism was tested in a model study using simulated organic aerosol concentrations as an indicator of organic Hg compound concentrations (Horowitz et al., 2017b). However, it should be noted that the rate of reduction in global models is largely tuned to reproduce observed Hg species concentrations. As for the stratosphere, estimates based on long-term aircraft measurements show that the stratospheric lifetime of Hg (72±37 years) is longer than was previously estimated (Slemr et al., 2018).

Further information concerning Hg oxidation at different levels in the atmosphere has been obtained as a result of the increasing availability of observational data available from high-altitude measurement sites and aircraft measurements. Observations combined with modelling can help determine which Hg atmospheric oxidation pathways are more or less likely. Weiss-Penzias et al. (2015) found that, during one high Hg^{II} free tropospheric event, there was almost quantitative oxidation of Hg^0 to Hg^{II}. Interestingly, a better model reproduction of the observations (using the GEOS-Chem model prior to the update

of the Hg chemistry scheme as described by Horowitz et al., 2017b) was found when employing the O_3/OH rather than the HgBr˙ oxidation scheme. Recent model-measurement comparison studies have shown episodes of high oxidized Hg concentrations that can be explained by Br oxidation (Gratz et al., 2015; Coburn et al., 2016) and that this is consistent with constraints from global biogeochemical cycling (Shah et al., 2016). These studies collectively show that measurements in free tropospheric air can significantly aid understanding of the atmospheric chemistry and dynamics of Hg.

Kos et al. (2013) performed a detailed analysis of the uncertainties associated with Hg^{II} measurement and modelling. Several model sensitivity runs were carried out to evaluate different chemical mechanisms and speciation of anthropogenic Hg emissions. In particular, Kos et al. (2013) found evident inconsistencies between the emission speciation in existing emission inventories and the measured Hg^{II} concentration in surface air. Besides, the OH oxidation chemistry provided better agreement with observations at simulation of the seasonal cycle of wet deposition in North America.

A complex analysis of the major Hg oxidation mechanisms was carried out by Travnikov et al. (2017) involving both measured data from ground-based sites and simulation results from four global chemical transport models. It was shown that the Br oxidation mechanism can reproduce successfully the observed seasonal variation of the Hg^{II}:Hg^0 ratio in the near-surface air, but predicts a wet deposition maximum in spring instead of summer as observed at monitoring sites in North America and Europe. Model runs with OH chemistry correctly simulated both the periods of maximum and minimum values and the amplitude of observed seasonal variation but shift the maximum Hg^{II}:Hg^0 ratios from spring to summer. Ozone chemistry did not predict significant seasonal variation in Hg oxidation. Travnikov et al. (2017) suggested the possibility of more complex chemistry and/or multiple Hg oxidation pathways occurring concurrently in various parts of the atmosphere.

Bieser et al. (2017) used the same model ensemble and various aircraft observations to study vertical and hemispheric distributions of atmospheric Hg. They also found that different chemical mechanisms were better at reproducing observed Hg^{II} patterns depending on altitude. Increased Hg^{II} concentrations above the planetary boundary layer in spring and summer could only be reproduced by models using O_3 and OH chemistry. On the other hand, the use of the Br oxidation mechanism generated better agreement with observed intercontinental gradients of total Hg in the upper troposphere.

As shown above, measurements of oxidized Hg are an important tool for assessing Hg chemistry and fate. However, uncertainties in the measurement techniques challenge our ability to further advance model-measurement comparison of Hg species (Gustin et al., 2015). There is growing evidence that oxidized Hg measurements performed using a Tekran speciation technique suffer from significant biases and interferences (Lyman et al., 2010b; Gustin et al., 2013; Jaffe et al., 2014; Maruszak et al., 2016). While modelled results discussed in this report as well as other studies are often evaluated against available measurements, further coordination between measurement and modelling communities to address measurement biases will enhance our understanding of atmospheric Hg processes.

5.2.3 Removal process

Mercury removal from the atmosphere occurs via wet and dry deposition (Risch et al., 2012; Weiss-Penzias et al., 2016). Studies of Hg deposition are providing insights into atmospheric oxidation through the study of Hg in precipitation according to precipitation type (Dvonch et al., 2005; Holmes et al., 2016; Kaulfus et al., 2017). These studies show that precipitation system morphology influences Hg deposition, with convective systems showing enhanced Hg deposition by a factor of 1.6. The magnitude of Hg deposition via precipitation also differs by season and region. The nature of the precipitation system is of particular interest because convective systems scavenge Hg from much higher altitudes than stratiform systems. Thus indirectly these studies provide information regarding the atmospheric oxidation of Hg because the scavenging height of different cloud types differs significantly and combined with information on the vertical distribution of potential Hg oxidants, modelling studies can help to evaluate possible, probable and unlikely oxidation mechanisms at varying levels in the troposphere. This does of course require the models to more or less accurately reproduce precipitation system morphologies. More sites measuring Hg in precipitation would clearly help estimate ecosystem deposition fluxes and so refine models.

Nair et al. (2013) carried out cloud-resolving simulations of Hg wet deposition processes in several case studies in the northeastern and southeastern USA. This study is of particular interest as many modelling simulations have tended to underestimate Hg wet deposition in the southeastern USA. It was found that wet deposition in typical northeastern thunderstorms would generally be less than in comparable storms in the southeast – assuming identical atmospheric concentrations of Hg – due to differences in typical cloud dynamics between the two regions. In addition, it was found that stratiform precipitation typically only scavenges Hg from the lowest ~4 km of the atmosphere, while southeastern thunderstorms can scavenge Hg up to ~10 km.

In another wet deposition process analysis, apparent scavenging ratios based on ground-level measurements of speciated air concentrations of Hg and total Hg in precipitation were studied at four sites in the northeastern USA (Huang et al., 2013). While the use of ground-based measurements introduced inherent uncertainties, the authors suggested that gaseous oxidized mercury (GOM) concentrations may be underestimated by current measurements, because scavenging ratios based on existing GOM measurements appeared anomalously high.

Several studies investigated Hg dry deposition processes. Zhang et al. (2012b) compared CMAQ- and GRAHM-modelled dry deposition against field measurements in the Great Lakes region for 2002 and in some cases, 2005. Dry deposition from the different models varied by as much as a factor of 2 at regional scales, and larger variations were found at local scales. Zhang et al. (2012b) suggested that the model-estimated dry deposition values were upper estimates given the tendency of the models to produce atmospheric concentrations of GOM and particulate-bound mercury (PBM) that are significantly higher than measured concentrations. Following a proposed methodology to estimate bi-directional Hg^0 surface exchange (Wright and Zhang, 2015c), dry deposition of Hg was estimated

at 24 measurement sites in the USA and Canada (Zhang et al., 2016b). In this analysis, the dry deposition flux of Hg^0 was estimated to be significantly larger than that of GOM or PBM at most of the sites.

Foliar uptake of Hg (usually assumed to be Hg^0) and Hg dynamics in forests in general have been studied in a number of locations since GMA 2013. Risch et al. (2012) studied Hg deposition in the eastern USA, while Laacouri et al. (2013) examined Hg in the leaves of deciduous trees. Two recent studies in China have shown that more study is needed. Yu et al. (2017) found that forests can be a source of Hg. In contrast, Fu et al. (2016b) suggested that at a mountain forest site Hg^0 uptake via foliage predominates, which explains the observed Hg depletion events. Fu et al. (2016b) concluded that "such depletion events of GEM are likely to be a widespread phenomenon, suggesting that the forest ecosystem represents one of the largest sinks (~1930 Mg) of atmospheric Hg on a global scale", which is the equivalent of all annual anthropogenic emissions as estimated in GMA 2013. Moreover, it was found that stomatal uptake of Hg^0 is more effective than previously expected and thus is a significant sink for atmospheric mercury (Jiskra et al., 2018). In particular, based on global Hg^0 and carbon dioxide (CO_2) measurements it was estimated that the annual Hg^0 removal through stomatal uptake is on the order of 1000 Mg. While the precise level of Hg^0 uptake via foliage is uncertain, it does seem reasonably certain that deciduous trees are a Hg sink, especially during the growing season.

The importance of Hg^0 dry deposition was also supported by Obrist et al. (2017) who showed that most of the Hg (about 70%) in the interior Arctic tundra is derived from Hg^0 deposition, with only minor contributions from the deposition of Hg^{II} from precipitation or AMDEs. Additional work is required to reconcile these results with those of many fate-and-transport models (e.g., Selin et al., 2007; Holmes et al., 2010; Lei et al., 2013; Song et al., 2015; Cohen et al., 2016) and estimates based on field measurement surveys (e.g., Pirrone et al., 2010; Denkenberger et al., 2012; Eckley et al., 2016) that suggest that the overall net flux of Hg^0 from terrestrial surfaces is upward.

Another aspect of Hg removal from the atmosphere that has been studied by a number of groups is the deposition of Hg via litterfall. Forest canopies seem to be effective sinks for both particulate and oxidized Hg (Fu et al., 2016a; Wang et al., 2016a; Wright et al., 2016).

5.3 Global atmospheric transport and fate modelling

5.3.1 Recent modelling studies

Since GMA 2013 (AMAP/UNEP, 2013) and GMA Update 2015 (AMAP/UNEP, 2015), various modelling studies have addressed the issue of Hg dispersion and fate on a global scale. Global chemical transport models have been used for simulations of Hg atmospheric transport (Lei et al., 2013, 2014; De Simone et al., 2014, 2015, 2016), source apportionment of Hg deposition in various geographic regions (Lei et al., 2013; Chen et al., 2014b, 2015a; Dastoor et al., 2015; Cohen et al., 2016), and study of processes governing Hg cycling in the atmosphere (Song et al., 2015; Angot et al., 2016a; Shah et al., 2016; Bieser et al., 2017; Horowitz et al., 2017b; Travnikov et al., 2017).

Some of the above-mentioned modelling studies were focused on assessing source-receptor relationships, that is, how emissions in one region or country contribute to deposition in others. These assessments are based on emission inventories describing current anthropogenic emissions. All models also include estimates of emissions from natural surfaces. These emissions are a mixture of natural emissions and re-emissions of Hg emitted from anthropogenic activities in previous years. A summary of source-receptor relationship estimates from several recent studies including the GMA Update 2015 and the current assessment is presented in Table 5.1. This contains model estimates of the relative contributions of direct anthropogenic emissions from selected source regions (East Asia, Europe, North America) to total Hg deposition in some receptor region (East Asia, Europe, North America, Arctic). The total deposition here implies contributions from both direct anthropogenic emissions and natural and secondary emissions. It should be noted that the model studies concern different years and, in particular, used essentially different inventories of both Hg anthropogenic emissions and estimates of Hg natural/secondary emissions.

As seen from Table 5.1, the contribution of domestic sources to total Hg deposition in East Asia varies from 37% to 62%. The upper estimates published by Chen et al. (2014b, 2015a) are based on outdated inventories for 2000 (Pacyna et al., 2006) and 2005 (AMAP/UNEP, 2008), respectively, which were characterized by significantly higher emissions in this region compared to more recent inventories for 2010 (AMAP/UNEP, 2013) and 2015 (Chapter 2) used in other studies. Another reason is the higher proportion of

Table 5.1 Summary of source apportionment estimates for selected source and receptor regions. Data show the relative percentage contribution of direct anthropogenic emissions from a source region to total Hg deposition in a receptor region.

Receptor region	Source region		
	East Asia	Europe	North America
East Asia	62[a], 50[b], 37[c], 37[d]	1.0[c], 0.8[d]	0.6[c], 0.3[d]
Europe	3.0[a], 8.2[c], 6.1[d]	19[b], 20[c], 16[d]	0.6[c], 0.5[d]
North America	9[e], 4.8[a], 10[c], 7.4[d]	1.6[c], 1.2[d]	22[e], 9.3[b], 7.1[c], 3.7[d]
Arctic	12[f], 11[c], 9.3[d]	2.5[f], 2.5[c], 2.3[d]	2.2[f], 1.2[c], 0.7[d]

[a] Chen et al. (2015a); Hg emissions for 2000 (Pacyna et al., 2006); [b] Chen et al. (2014b); Hg emissions for 2005 (AMAP/UNEP, 2008); [c] GMA Update 2015; Hg emissions for 2010 (AMAP/UNEP, 2013); [d] Current study; Hg emissions for 2015 (see Chapter 2); [e] Lei et al. (2013); Hg emissions for 2000 (Pacyna et al., 2006); [f] Dastoor et al. (2015); Hg emissions for 2005 (AMAP/UNEP, 2008).

oxidized Hg species in anthropogenic emissions from East Asia accepted in the older inventories that leads to shorter Hg dispersion from emission sources. This effect can also explain discrepancies in simulations of the East Asia contribution to total Hg deposition over Europe and North America, which vary within the ranges 3–8.2% and 4.8–10% respectively. The lower estimates are based on the emissions inventory for 2000 with a significant share of oxidized Hg (Chen et al., 2015a). The studies provide consistent estimates of the contribution of domestic sources to total Hg deposition in Europe (16–20%). In contrast, similar estimates for North America vary over a wide range (3.7–22%). It should be noted that all four available estimates were based on different inventories, with the lower values referring to more recent years. This agrees with the gradual reduction in total emissions of Hg in North America from 145 t/y in 2000 (Pacyna et al., 2006) to 44 t/y in 2015 (Chapter 2). Besides, the upper estimate (22%) obtained by Lei et al. (2013) relates to the USA and, probably, overestimates the contribution of domestic sources to the continent as a whole. Thus, model evaluation of source-receptor relationships is strongly dependent on the availability of reliable emissions inventories. More detailed discussion of multi-model simulations of Hg dispersion on a global scale using updated emissions data for 2015 is presented in Sections 5.3.2 to 5.3.4.

5.3.2 Deposition to terrestrial and aquatic regions

The current state of Hg dispersion in the atmosphere and deposition to various terrestrial and aquatic regions was studied by an ensemble of chemical transport models using the new inventory of Hg anthropogenic emissions discussed in Chapter 2. Four global-scale chemical transport models for Hg were applied in the study – ECHMERIT, GEM-MACH-Hg, GEOS-Chem (v11-02), and GLEMOS. A short summary of major model characteristics is given in the Appendix, Table A5.1. All models cover the global atmosphere (the entire troposphere and at least the lower stratosphere) with somewhat different spatial resolution ranging from 0.5 to 2.8 geographical degrees. Three of the four models (ECHMERIT, GEM-MACH-Hg, GLEMOS) are atmospheric transport models simulating the processes of Hg transport and fate in the atmosphere as well as air-surface exchange leading to Hg input to and removal from the

atmosphere. The fourth model (GEOS-Chem) is a coupled multi-media transport model simulating Hg processes both in the atmosphere and in slab oceanic and terrestrial layers. The models differ in terms of major Hg oxidation mechanisms using chemical schemes based on Hg oxidation by atomic Br (GEOS-Chem), OH initiated reactions (GEM-MACH-Hg) or a combination of OH and O_3 initiated reactions (ECHMERIT and GLEMOS). See Travnikov et al. (2017) for a more detailed description of the models along with a discussion of their differences.

All models used the new global Hg anthropogenic emissions inventory for 2015 described in Chapter 2. The dataset consists of gridded emission data with a spatial resolution of $0.1° × 0.1°$ for three Hg species (Hg^0, GOM, PBM), which were redistributed into the native model grids using mass conservation methods. The total global emission of Hg from anthropogenic sources is estimated at 2220 t/y. The overall proportions of Hg^0, GOM, and PBM emissions are 82%, 14% and 4%, respectively. In contrast to the anthropogenic emissions, total values of natural and secondary emissions differed significantly among the models. Parameterization of these processes is an essential part of the model setup and describes Hg cycling between the Earth's surface and the atmosphere. Particular approaches used by the models vary between empirically prescribed and dynamically simulated air-surface exchange fluxes and are based on different theoretical assumptions. More details on applied parameterizations can be found in the sources provided in the Appendix, Table A5.1. It should be noted that there is a significant gap in understanding of major processes determining Hg cycling within environmental media (soil, vegetation, ocean) and air-surface exchange. Therefore, existing model estimates of natural and secondary emissions contain considerable uncertainties and disparity.

The analysis presented in this section and the next contains information on emissions and deposition fluxes averaged over a number of geographical regions. The definition of source and receptor regions is consistent with the GMA Update 2015 and is shown in Figure 5.1. The regions are divided into six continents (Europe, North, Central, and South America, Africa, and Australia and New Zealand), five large subcontinents (Middle East, countries of the Commonwealth of Independent States (CIS), and South, East, and Southeast Asia), and two polar regions (Arctic and Antarctica). Aquatic regions of the world ocean are defined in accordance with the Major Fishing Areas of the UN Food and Agriculture Organization (FAO, 2018).

Legend:
- Arctic
- North America
- Central America
- South America
- Europe
- CIS countries
- Africa
- South Asia
- East Asia
- Southeast Asia
- Middle East
- Australia and New Zealand
- Antarctica
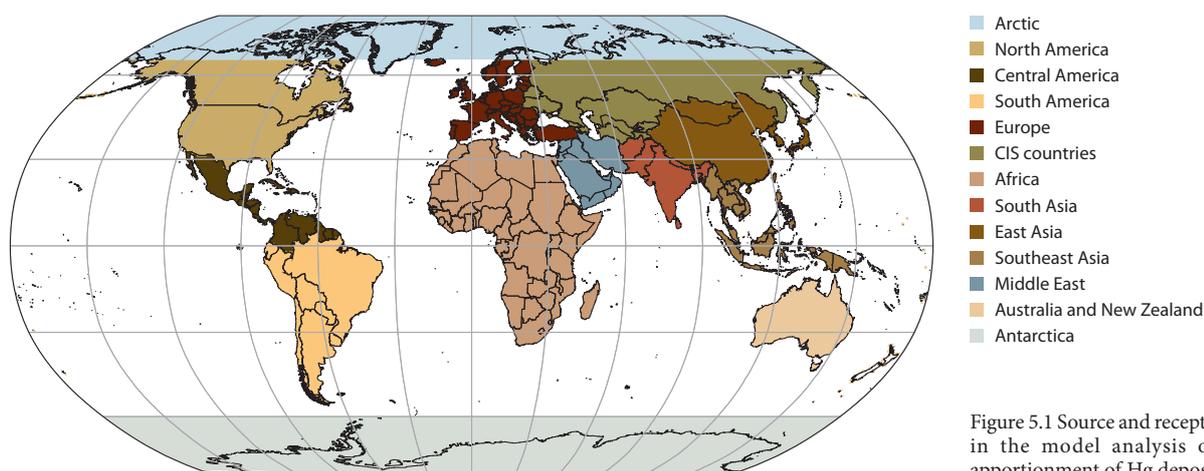
Figure 5.1 Source and receptor regions in the model analysis of source apportionment of Hg deposition.

Modeled H⁰ in air, ng/m³

| 0 | 1.1 | 1.2 | 1.3 | 1.4 | 1.5 | 1.8 | 2.4 |

○ Observed values using the same color scales

Modeled Hg wet deposition, g/km²/y

| 0 | 1 | 2 | 3 | 5 | 8 | 12 | 25 |
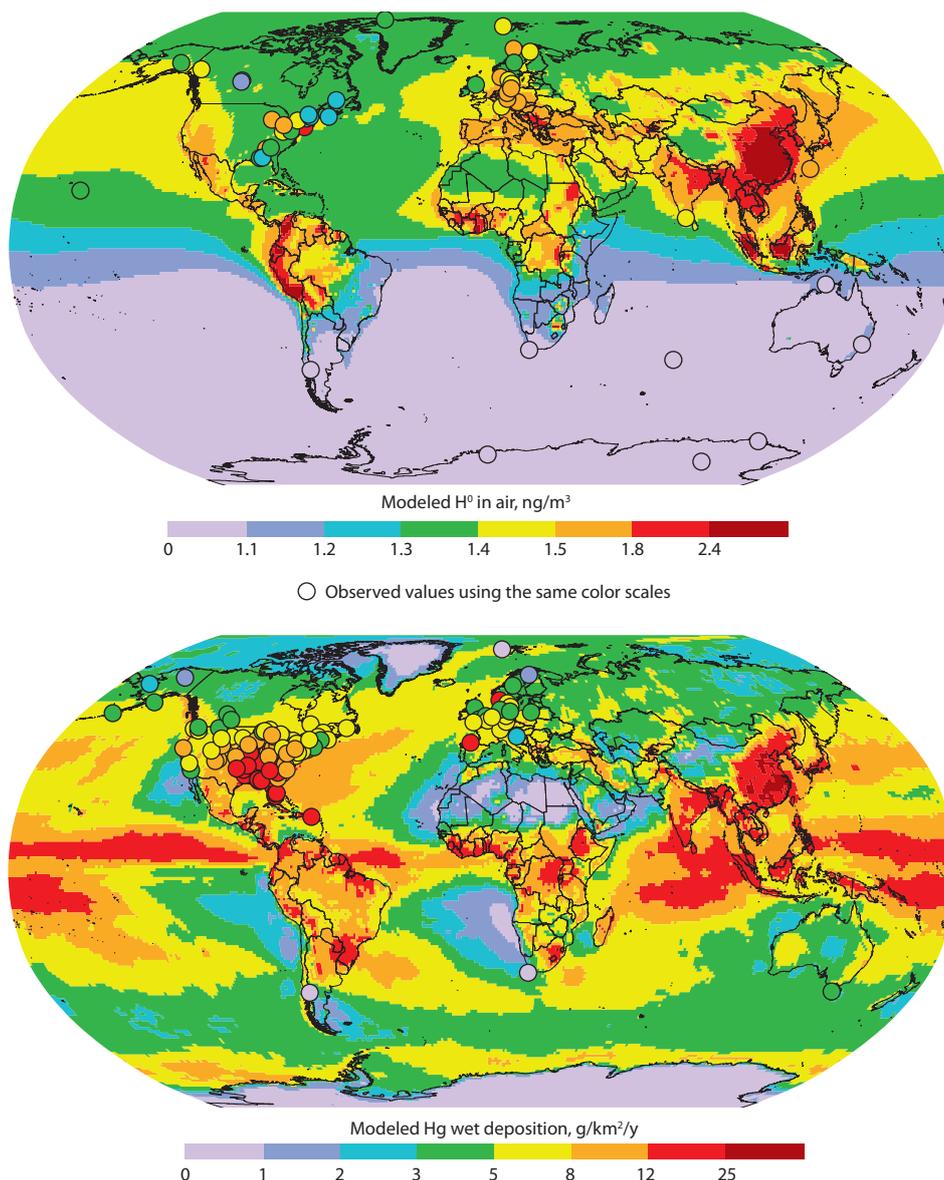
Figure 5.2 Model ensemble median global distributions of Hg⁰ concentration in surface air and Hg wet deposition flux in 2015.

The global distribution of Hg^0 concentration in surface air in 2015 as simulated by the model ensemble is shown in Figure 5.2 in terms of the model ensemble median. The spatial pattern is characterized by the latitudinal gradient with elevated concentrations (above 1.4 ng/m³) in the temperate latitudes of the Northern Hemisphere and the lowest concentrations (below 1 ng/m³) in the southernmost parts of the Southern Hemisphere. The highest concentrations (above 2 ng/m³) are located in East, South and Southeast Asia due to high levels of anthropogenic emissions as well as in equatorial Africa and South America owing to high emission amounts attributed to artisanal and small-scale gold mining (ASGM). The simulated Hg^0 concentration pattern is very similar to previous estimates presented in the GMA Update 2015. The modelling results were evaluated against observations from global and regional monitoring networks (GMOS, EMEP, AMNet and NAtChem). Available measurement data generally confirm large-scale spatial variation of simulated Hg^0 (Figure 5.2) with the interhemispheric gradient and

elevated concentrations in the major industrial regions. There are still some discrepancies between the modelling results and observations in particular locations, which characterize more complicated small-scale spatial patterns in Hg^0 levels that are not captured by the models.

Both simulated and observed levels of Hg wet deposition are shown in Figure 5.2. The measurement data were obtained from the GMOS, NADP/MDN and EMEP networks. Wet deposition is relatively equally distributed between the Northern Hemisphere and Southern Hemisphere and reflects the influence of multiple factors including anthropogenic emissions, oxidation chemistry and precipitation pattern. Elevated fluxes of Hg wet deposition are found in areas inside and downwind of the industrial regions of Asia, North America and Europe as well as over the high precipitation zones in the Tropics. The lowest model-estimated wet deposition levels are in arid areas of Greenland, northern Africa and Antarctica. The simulations reproduce measured levels of wet deposition in North America, Europe and Australia relatively well.
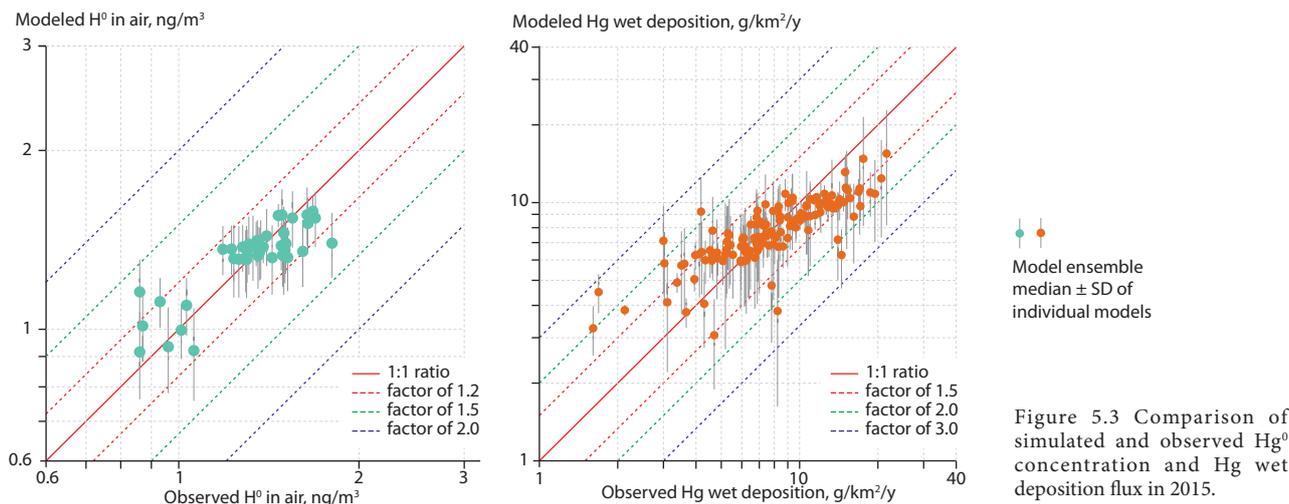
Figure 5.3 Comparison of simulated and observed Hg⁰ concentration and Hg wet deposition flux in 2015.

A detailed comparison between model results and observations is illustrated in Figure 5.3. The model ensemble median of Hg⁰ concentration agrees with observed values within ±20% at most of the measurement sites. The scatter of simulated values among the models presented by the standard deviation is relatively small and does not exceed 20%. The model-to-measurement difference is larger for wet deposition. The model ensemble demonstrates good correlation ($r^2 = 0.7$) with observations but tends to overestimate low and underestimate high deposition fluxes. The deviation between the modelling results and measurements does not exceed a factor of 2 at the majority of measurement sites. However, it should be noted that available measurement data cover limited regions of North America and Europe and cannot provide complete evaluation of the global spatial pattern. The inter-model variance is also larger for wet deposition, which can be explained by the differences in parameterizations of Hg oxidation chemistry, and the scavenging and precipitation amount between the models.

A comprehensive evaluation of the participating models against a variety of ground-based and aircraft measurements as well as their sensitivity to various parameters and processes can be found in a series of recent publications (Angot et al., 2016a; Bieser et al., 2017; Travnikov et al., 2017).

It should be noted that measurements of Hg⁰ air concentration and Hg wet deposition obtained from global and regional networks may not provide a complete evaluation of model performance. Mercury removal from the atmosphere is largely determined by the oxidation/reduction chemistry and air-surface exchange. Therefore, reliable measurements of oxidized Hg forms and air-surface exchange fluxes (including Hg⁰ gaseous exchange, Hg^{II} dry deposition as well as Hg throughfall and litterfall deposition) are critical for understanding the distribution, cycling and fate of Hg in the atmosphere and, ultimately, for improving Hg chemical transport models. Available measurements of reactive Hg concentration in air and air-surface exchange are relatively scarce and uncertain (see discussion in Section 5.2).

Figure 5.4 shows Hg⁰ air concentration and Hg wet and dry deposition (including dry deposition of Hg⁰) averaged over various geographic regions. The regional pattern of deposition fluxes generally follows that of Hg⁰ concentration with the exceptions of relatively low wet and dry deposition in the Middle East and CIS countries and elevated deposition fluxes in
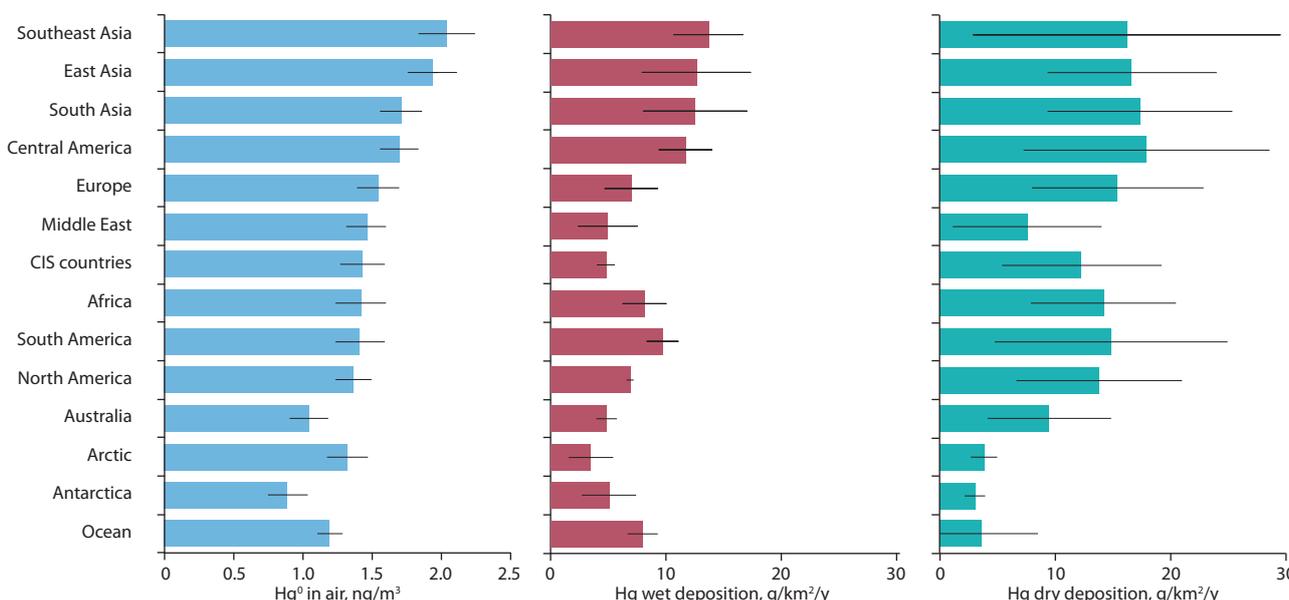
Figure 5.4 Model ensemble median Hg⁰ concentration, Hg wet deposition and Hg dry deposition in 2015 averaged over the various geographic regions defined in Figure 5.1. Whiskers show the standard deviation of the models from the ensemble median.

Hg deposition, g/km²/y

0 1 2 4 7 13 25 60
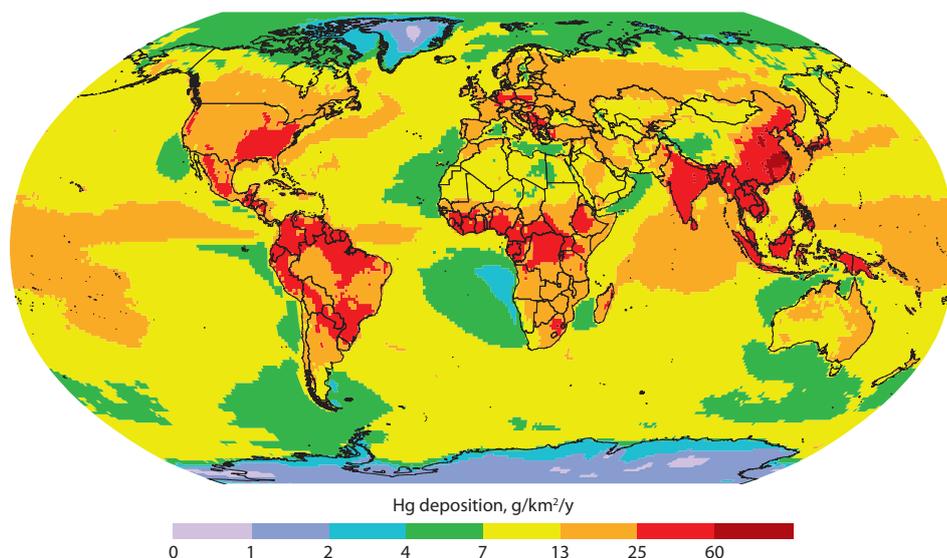
Figure 5.5 Global distribution of the model ensemble median total (wet and dry) Hg deposition in 2015.

Africa and South America relative to Hg⁰ concentration. These exceptions can be explained by the regional precipitation and climatic characteristics. In most receptor regions, the average dry deposition is higher than wet deposition by 20–120%. In contrast to terrestrial regions, wet deposition to the ocean is higher than dry deposition. The inter-model variation also demonstrates significantly higher uncertainty for dry deposition (±28–85%) in comparison to wet deposition (±4–55%) and Hg⁰ concentration (±7–16%). Thus, the uncertainty of total deposition (wet and dry) discussed in this and the two following sections, consists largely of the uncertainty of dry deposition.

The global distribution of Hg deposition in 2015 simulated by the model ensemble is shown in Figure 5.5. The spatial pattern partly follows the spatial distribution of wet deposition with elevated deposition fluxes over the major industrial regions and areas of intensive precipitation. In comparison to wet deposition, however, much higher deposition fluxes are observed over land than the ocean due to the large contribution of dry deposition. The deposition pattern does not reveal any considerable difference in Hg deposition to the ocean in the Northern Hemisphere and Southern Hemisphere. Levels of

Hg deposition to land vary within the continents reflecting the spatial pattern of anthropogenic emissions as well as surface and climatic characteristics. There are increasing north-to-south gradients of Hg deposition in North America and Eurasia with the exception of the desert and mountain regions in Central and East Asia. Most territory in South America is subject to high Hg fluxes determined by both wet and dry deposition, except for the most southern part of the continent, due to the significant contribution of ASGM emissions and oxidized chemistry. In Africa, Hg deposition differs significantly from relatively low fluxes in the desert north to high deposition fluxes in the equatorial and southern parts of the continent.

Figure 5.6 summarizes the total Hg deposition fluxes to terrestrial and aquatic receptor regions as well as the relative contributions of direct anthropogenic and natural/secondary sources simulated by the model ensemble. Total Hg deposition fluxes are highest in large industrial regions such as South, East, and Southeast Asia (25–30 g/km²/y). Regions with active ASGM (Central and South America), which emit Hg in the form of Hg⁰, are also subject to a high total Hg deposition flux of 25 g/km²/y due to intensive *in situ* Hg⁰ oxidation in the atmosphere of
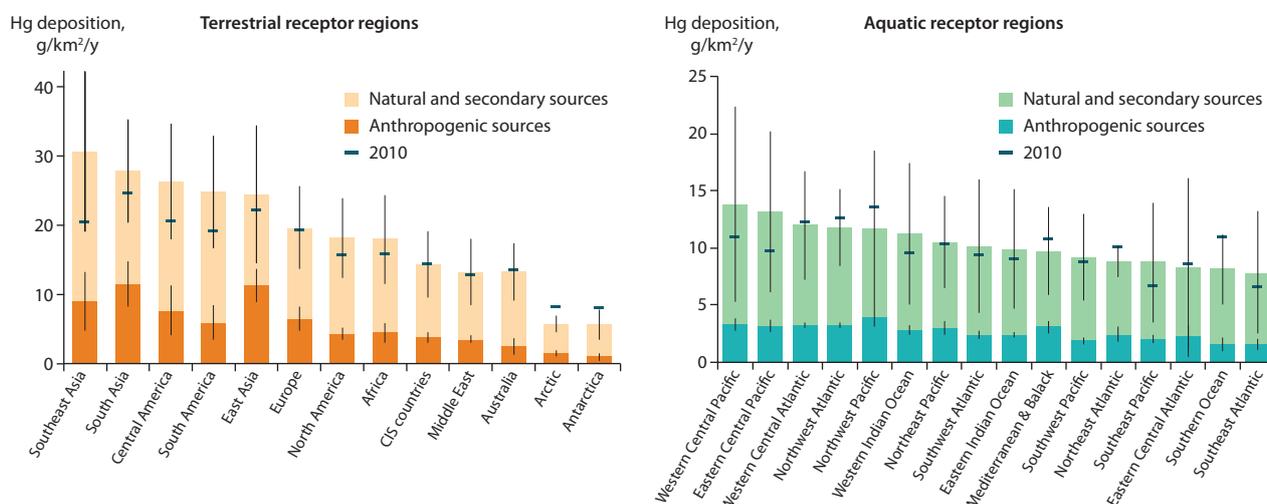
Figure 5.6 Total Hg deposition fluxes and the relative contributions of direct anthropogenic and natural and secondary sources to various terrestrial and aquatic receptor regions in 2015. Whiskers show the standard deviation of the models from the ensemble median for direct anthropogenic and natural/secondary sources, respectively. Results of the GMA Update 2015 (year 2010 anthropogenic Hg emission inventory) are shown for comparison.

the Tropics (Horowitz et al., 2017b). The lowest deposition levels are in remote regions such as the Arctic and Antarctic (below 6 g/km²/y). A comparison between the modelled results here and the GMA Update 2015 (year 2010 anthropogenic Hg emission inventory) shows an average 20% (2–40%) increase in total Hg deposition flux to most receptor regions, except in the polar regions, which show a 30% reduction. This is consistent with the global increase in anthropogenic emissions (~12%) since 2010 (Chapter 2). Southeast Asia, South America and Central America demonstrate the largest increase in total Hg deposition fluxes of 50%, 30% and 27%, respectively. This is explained by the large magnitude change in their domestic anthropogenic emissions in the new emissions inventory and indicates refinement of emissions data rather than a real temporal trend of anthropogenic emissions in these regions. The reduction of Hg deposition in the polar regions is mostly due to refinement of the model parameterizations for polar-specific processes and the interannual variation in meteorological conditions.

Total Hg deposition consists of contributions from direct anthropogenic emissions as well as natural and secondary sources, which account for 53–81% of the total Hg deposition. The contribution of natural and secondary sources evaluated here is very similar to that reported in the GMA Update 2015 (52–79%). As illustrated in Figure 5.6, the relative contributions of direct anthropogenic sources show a regional pattern – decreasing from regions of the highest (South, East and Southeast Asia; 30–47%) to the lowest total Hg deposition flux (the polar regions; 20–25%). The contribution of direct anthropogenic sources to other receptor regions is within 25–35%. The regional pattern can be explained by the level of domestic anthropogenic emissions, which generate a substantial fraction of oxidized Hg that deposits rapidly within the source region. It should be noted that there can be substantial variation in the relative contributions of anthropogenic and natural/secondary sources within a given region.

Mercury deposition to various regions of the world ocean is shown in Figure 5.6. Deposition flux averaged over the regions varies from 8 g/km²/y over the Southeast Atlantic to 14 g/km²/y over the Western Central Pacific. This agrees well with model deposition fluxes to the ocean reported in the GMA Update 2015 (6.5–13.6 g/km²/y). The new estimates show higher deposition fluxes in the Tropics (Western Central Pacific, Eastern Central Pacific, Indian Ocean) due to refinement of Hg oxidation chemistry (Horowitz et al., 2017b). Mercury deposition to the ocean is also influenced by direct anthropogenic emissions as well as by natural and secondary sources. The relative contribution of direct anthropogenic sources to ocean reservoirs evaluated here varies from 19% (Southern Ocean) to 35% (Northwest Pacific) and is slightly lower compared to the direct anthropogenic contribution of terrestrial reservoirs (20–50%).

The inter-model differences in the simulated total Hg deposition fluxes from anthropogenic and natural/secondary sources are shown in Figure 5.6 in terms of the standard deviation. The inter-model difference in deposition from direct anthropogenic sources (±9–52% for terrestrial and ±8–47% for aquatic regions) is mostly determined by the differences in the chemical mechanisms implemented in the models and the parameterizations of removal processes. The inter-model differences in simulated deposition from natural/secondary

sources is much lower compared to those of anthropogenic sources (±28–76% for terrestrial and ±20–130% for aquatic regions), which is also affected by the model parameterizations of natural and secondary emissions. The source apportionment analysis of Hg deposition from direct anthropogenic emissions shown in the two following sections represents the sources that can be most easily regulated by environmental policy.

5.3.3 Source apportionment of anthropogenic Hg deposition

Source apportionment of Hg deposition, illustrating atmospheric transport of Hg between different continents and regions, was evaluated in the GMA 2013 and the GMA Update 2015. This section provides an updated source-receptor analysis of Hg deposition generated from the same four global chemical transport models. It should be noted that the results discussed in this section present shares of source regions to deposition from direct anthropogenic emissions instead of the share of total deposition, which also includes a contribution from natural and secondary sources. The source apportionment of total deposition is briefly discussed in Section 5.3.1 along with a comparison with results of other recent studies.

Figure 5.7 illustrates the source apportionment of Hg deposition from direct anthropogenic sources to various receptor regions. The direct anthropogenic emissions represent the mixture of domestic emissions and atmospherically transported Hg from sources located in other regions (foreign emissions). The share of foreign sources varies from 100% in Antarctica to 23% in East Asia. The largest foreign contributors to various receptor regions are East Asia, Africa, South America, and Southeast Asia, with their contributions ranging between 10–34%, 4–24%, 3–23%, 3–11%, respectively. The largest foreign contributors are characterized by large anthropogenic emissions as well as active ASGM, which contributes to the global Hg burden and thus to long-range transport via Hg⁰ emissions. The smallest foreign contributors are the Middle East (<2%), Australia (<1%), and the polar regions (<1%), which are characterized by the lowest anthropogenic emissions. It should be noted that there are substantial variations in the overall averages within particular regions. In general, the results shown here are in accord with the GMA Update 2015.

As illustrated in Figure 5.7, the share of domestic sources to various receptor regions is ranked in the order of East Asia (77%), South Asia (66%), Europe (48%), Southeast Asia (39%), Africa (38%), South America (34%), Central America (30%), CIS countries (28%), Middle East (18%), North America (15%), Australia and New Zealand (6%), Arctic (3%), and Antarctica (0%). In East and South Asia, anthropogenic Hg deposition is dominated by the contribution from domestic sources. This is due to the significant domestic anthropogenic emissions mainly from the industrial and power sectors, which emit a substantial fraction of oxidized Hg. The domestic shares in East and South Asian anthropogenic deposition show some increase since 2010 (GMA Update 2015; 76% and 58% respectively), which is explained by the increase in Asian anthropogenic emissions since 2010 (Chapter 2). Consistent with the GMA Update 2015, both domestic and foreign anthropogenic sources contribute almost equally to the total anthropogenic Hg deposition in Europe. The largest foreign contributors are ranked in the order of East Asia (18%), Africa (8%), CIS countries (6%), and
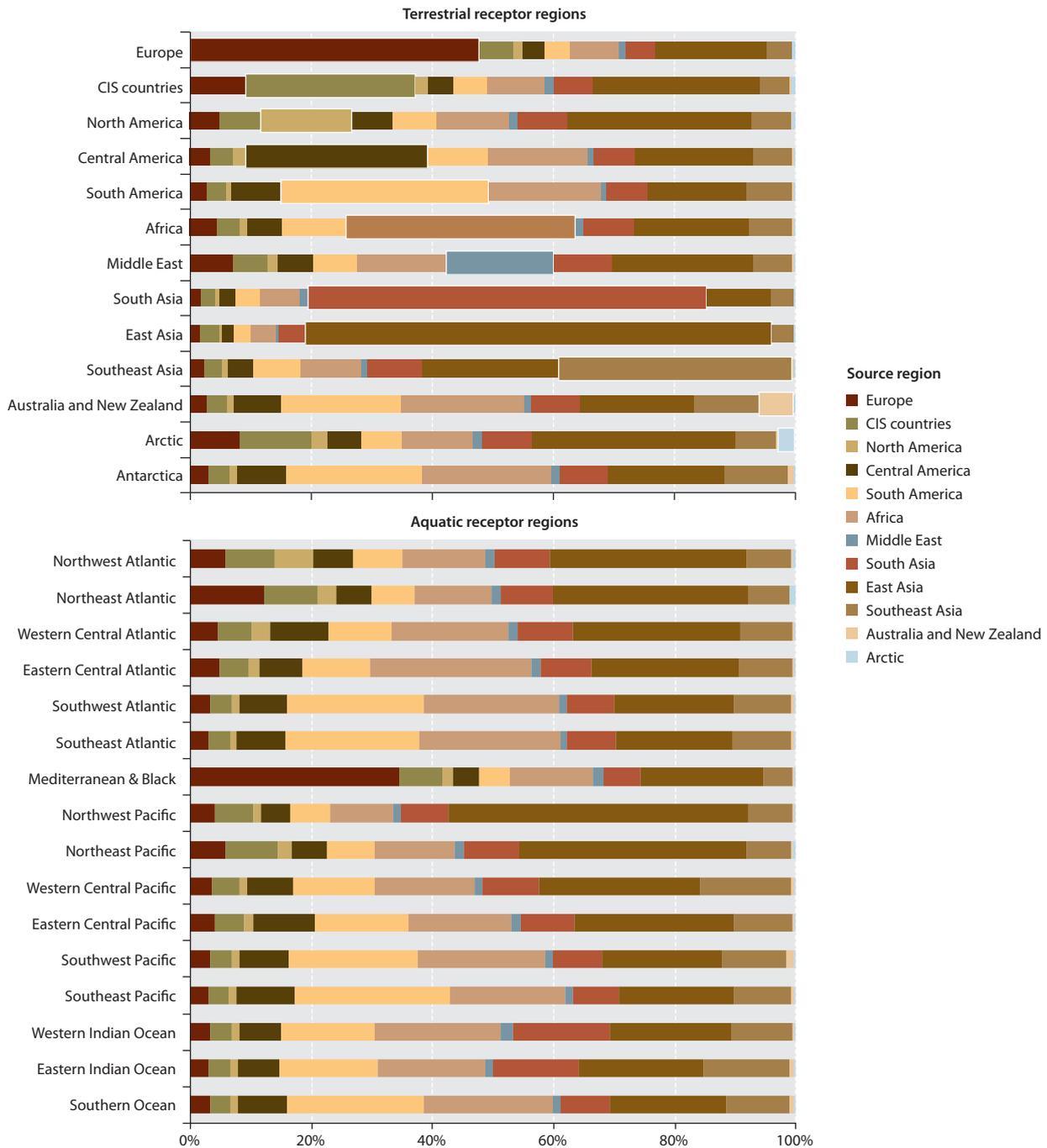
Figure 5.7 Model ensemble median source apportionment of Hg deposition from direct anthropogenic emissions to various terrestrial and aquatic regions in 2015. The colors depict source regions, which are consistent with Figure 5.1. The contribution of domestic sources is shown by wider bars. Source apportionment for individual models are given in the Appendix, Figures A5.1 and A5.2.

South Asia (5%). Regions with active ASGM (Africa, South and Central America) also receive a relatively large fraction of anthropogenic deposition from domestic sources as well as from East Asia. In North America, the share of domestic sources shows a reduction from 23% to 15% (GMA Update 2015). This is consistent with the reduction in North American anthropogenic emissions since 2010 (Chapter 2). Significant foreign contributors to North American anthropogenic deposition are ranked in the order East Asia (31%), Africa (12%), South Asia (8%), and Southeast Asia (7%). Remote regions including the Arctic and Antarctic are predominantly influenced by the long-range transport of atmospheric Hg from East Asia and Africa.

Figure 5.7 also illustrates the source apportionment of Hg deposition from direct anthropogenic sources to various ocean regions. Overall, the results shown here are in accord with the GMA Update 2015. East Asia and Africa remain the largest contributors to the global ocean regions, owing to their large anthropogenic emissions. The contributions from East Asia and Africa to various ocean regions range between 20–50% and 11–27%, respectively. Northwest (50%) and Northeast Pacific (38%) receive the largest contribution from East Asian anthropogenic emissions. Eastern Central (27%), Southeast (23%), and Southwest Atlantic (22%) receive the largest contribution from African anthropogenic emissions. South America also significantly contributes to Hg deposition to the

ocean (5–26%), particularly, over the Southeast Pacific (26%), Southwest Atlantic (23%), and Southeast Atlantic (22%). The only exceptions are the Mediterranean Sea and Black Sea, where the contribution from European anthropogenic emissions (20%) dominates over East Asian, African, and South American anthropogenic emissions. A number of the ocean regions – particularly the Northwest Pacific – receive high anthropogenic Hg deposition and demonstrate a large total capture fisheries production as reported in the GMA Update 2015. The lowest contributors to the global ocean regions are the Arctic (<2%) and Australia (<1%), which are characterized by the lowest anthropogenic emissions.

5.3.4 Contribution of different emission sectors to Hg deposition

The four global chemical transport models were also applied for simulating Hg deposition from different anthropogenic emissions sectors. In this study, all the sectors of anthropogenic emissions discussed in Chapter 2 were aggregated into four general groups: power generation; industrial sources; intentional use and product waste; and ASGM. Total emissions from these four sector groups in 2015 amount to 347 t/y, 874 t/y, 166 t/y and 838 t/y, respectively. Chemical speciation of Hg emissions differs considerably between different sector groups (Figure 5.8). According to the applied inventory (Chapter 2), emissions from power generation roughly comprise equal contributions of elemental mercury (Hg^0) and oxidized forms (GOM, PBM). The proportion of oxidized Hg is much smaller in emissions from industrial sources (20%). A quarter of total Hg emissions from intentional use and product waste is emitted in the oxidized forms. It is expected that all Hg emitted from
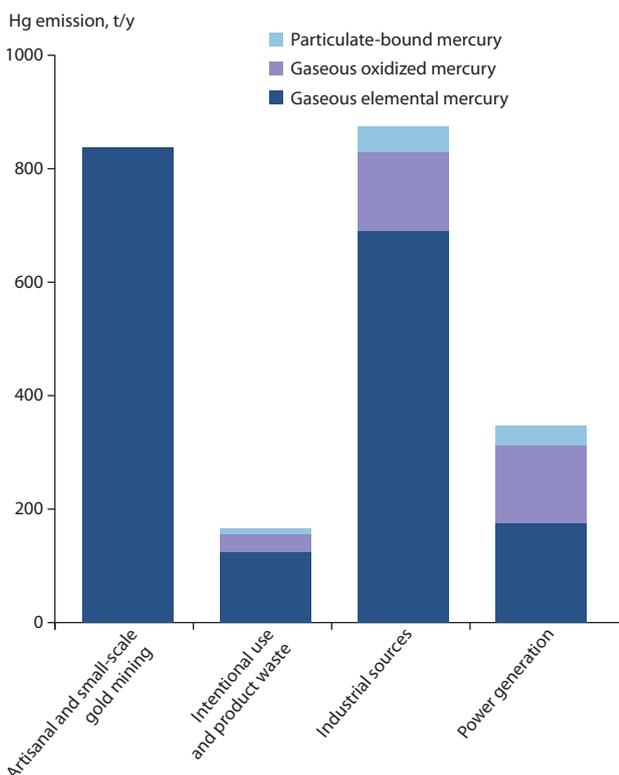
ASGM is in the elemental gaseous form. It should be noted that available estimates of Hg emissions speciation are associated with significant uncertainties (Section 5.2).

The model simulated patterns of Hg deposition from the four emission sectors are shown in Figure 5.9. Mercury deposition from the power generation group is largely restricted to industrial regions in East and South Asia, Europe, North America, and South Africa, where the majority of large stationary combustion sources are located. It results from the large proportion of oxidized Hg in emissions from this sector. Mercury deposition flux from power generation in these regions exceeds 2.5 g/km²/y, whereas in other regions it falls below 1.4 g/km²/y. The relatively short distance of Hg dispersion from this sector group is caused by the substantial proportion of oxidized Hg in the emissions. Emissions from the industrial sectors group are more widely distributed over the world and contain a substantial fraction of Hg^0 (80%). Therefore, significant deposition (above 2.5 g/km²/y) from industrial sources covers wide areas in Asia, Europe, North and South America, and Africa. In South and East Asia, deposition from this sector group exceeds 5 and 10 g/km²/y, respectively. Deposition from the intentional use and product waste group is also mostly related to major industrial regions but its contribution is much lower and generally does not exceed 1.4 g/km²/y except for South and East Asia. The majority of ASGM emission sources are located in the low latitudes of both hemispheres. Being in the elemental form, Hg emissions from this sector are transported globally, however, most significant deposition fluxes (above 2.5 g/km²/y) occur close to emission sources and largely impact South America, equatorial Africa, East and Southeast Asia.

The relative contribution of the emission sectors to Hg deposition from direct anthropogenic emissions varies substantially between different geographic regions (Figure 5.10). Power generation contributes from 11% to 35% of total anthropogenic deposition with the largest contribution in Europe and South Asia, and the smallest contribution in Central and South America and Antarctica. The contribution of industrial sources ranges from 33% (South America) to 60% (East Asia). The share of the intentional use and product waste sector group in Hg anthropogenic deposition is less significant in all regions (6–12%). The relative contribution of ASGM is the largest over the continents of the Southern Hemisphere: South America (50%), Antarctica (49%), Australia and New Zealand (46%); and the smallest in industrial regions of the Northern Hemisphere: Europe (17%), South Asia (15%) and East Asia (12%).

Aquatic regions of the global ocean are also differently affected by the emission sectors (Figure 5.10). Most regions of the Northern Hemisphere are predominantly influenced by industrial sources (43–50%). The contribution of the power generation group commonly does not exceed 20% with the exception of the Mediterranean Sea and Black Sea (30%), which are located close to European emission sources. The relative contribution of ASGM to the aquatic regions of the Northern Hemisphere is below 30%. In contrast, this sector makes up the largest contribution (40–50%) to Hg deposition over the ocean in the Southern Hemisphere. The group of sectors associated with intentional use and product waste contributes less than 10% of Hg anthropogenic deposition to all regions of the global ocean.

Figure 5.8 Chemical speciation of Hg emissions from the four groups of emission sectors in 2015.
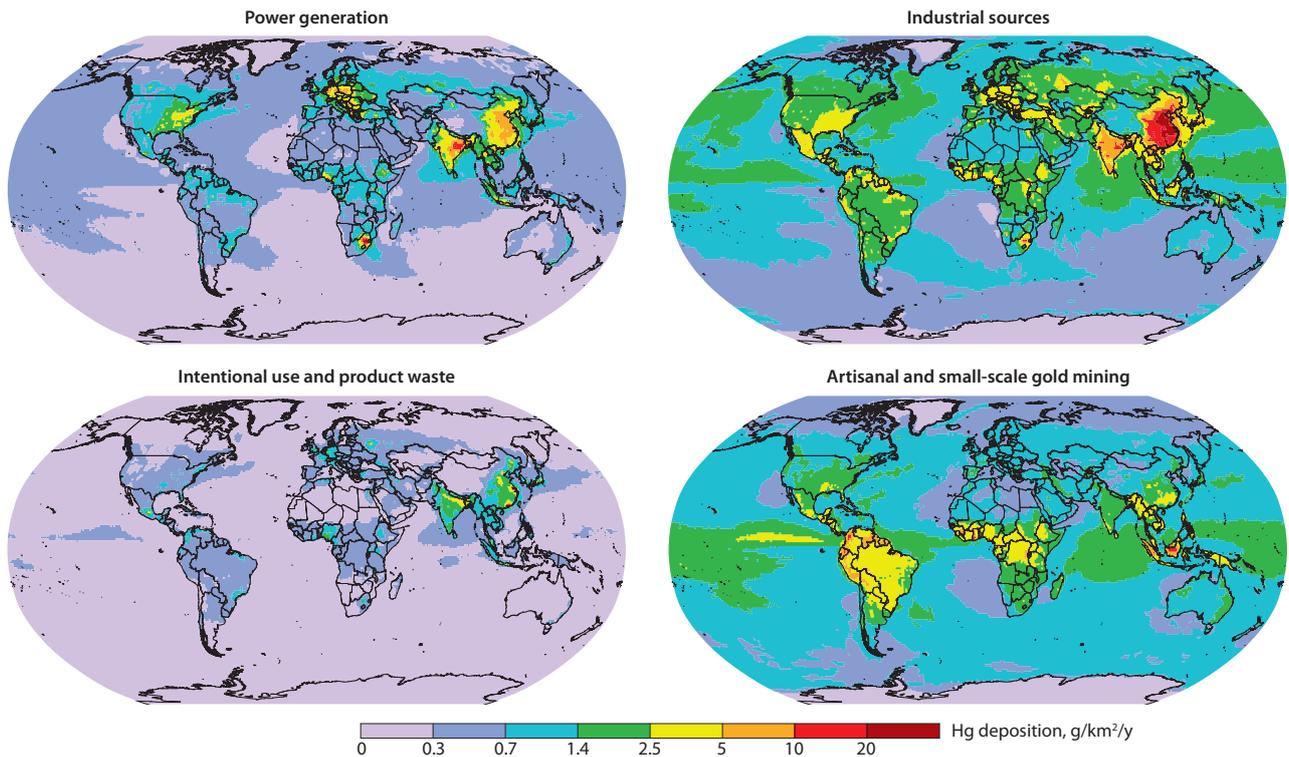
Figure 5.9 Global distribution of Hg deposition (model ensemble median) from the four groups of emission sectors in 2015: power generation, industrial sources, intentional use and product waste, and artisanal and small-scale gold mining.
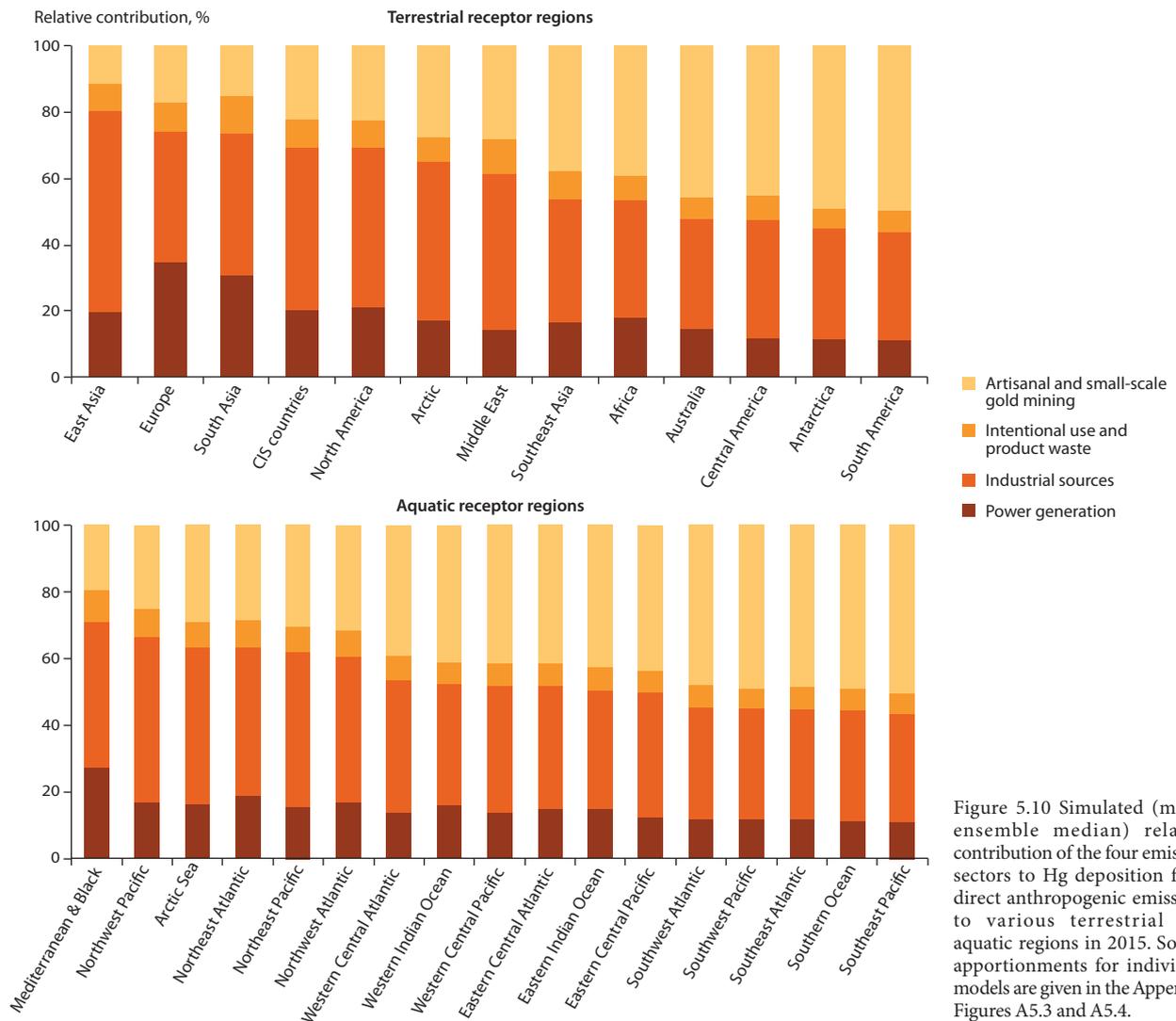
Figure 5.10 Simulated (model ensemble median) relative contribution of the four emission sectors to Hg deposition from direct anthropogenic emissions to various terrestrial and aquatic regions in 2015. Source apportionments for individual models are given in the Appendix, Figures A5.3 and A5.4.

5.4 **Historical trends and future scenarios**

Evaluation of historical changes in Hg atmospheric concentration and deposition to other environmental media is important because it explains how legacy Hg (previously emitted and deposited anthropogenic Hg) affects present-day Hg levels and future environmental responses to expected emission control measures. Human disturbance of natural Hg cycling in the environment by mining and industrial activities has led to significant enrichment of atmospheric Hg since pre-industrial times (e.g., Fitzgerald et al., 1998; Biester et al., 2007; Lindberg et al., 2007). Amos et al. (2013, 2014, 2015) recently applied a multi-media box model coupling the atmosphere, ocean, and terrestrial reservoirs to reconstruct historical Hg cycling among geochemical reservoirs at the millennial scale. They found that present-day atmospheric deposition has increased by a factor of 2.6 relative to the preindustrial period (~1850), which is consistent with sediment archives. Moreover, all-time anthropogenic emissions (since ~2000 BC) have enriched present-day Hg levels in the atmosphere, surface ocean, and deep ocean by factors of 7.5, 5.9, and 2.1, respectively, relative to natural conditions (Amos et al., 2013). Amos et al. (2014) also showed that accounting for the additional loss of Hg to ocean margin sediments showed that the all-time relative enrichment in surface reservoirs was two-fold higher than was previously estimated. Application of a coupled 3D atmospheric and ocean transport model by Zhang et al. (2014b) on 600 years cycling of Hg in the global environment provides lower enrichment factors for Hg levels in the atmosphere, surface ocean and deep ocean (5.5, 4.4 and 1.2, respectively). This difference is attributed to lower estimates of Hg emissions from historical mining and more complex vertical mixing in the ocean by Zhang et al. (2014b). Model simulations and natural archives both provide evidence for peak atmospheric Hg concentrations during the latter half of the 20th century and declines in more recent decades (Amos et al., 2015).

Changes in atmospheric Hg deposition over the past two decades in different geographic regions were evaluated in several recent modelling studies. Long-term trends in Hg deposition in Europe were analyzed by the Task Force on Measurements and Modelling under the Co-operative Programme for Monitoring and Evaluation of the Long-range Transmission of Air Pollutants in Europe (Colette et al., 2016). According to the modelling results presented in the study, total Hg deposition in the EMEP region considered (Europe and Central Asia) decreased on average by 23% during the period 1990–2012 (about -1%/y). However, the deposition trend was essentially non-linear with the rates of deposition reduction being higher at the beginning and lower at the end of the period. The trend broadly agrees with available long-term measurements of Hg in precipitation in this region (Tørseth el al., 2012; Colette et al., 2016). The magnitude of deposition changes differs significantly between individual countries ranging from a 70% decrease to a 10% increase. The decrease in deposition was generally larger in the countries of the European Union (EU28) (35% for the period 1990–2012 or -1.5%/y) than in other parts of the region (Eastern Europe and Central Asia). Similar rates (-1.5±0.7%/y) of Hg wet deposition reduction at monitoring sites in Western Europe were simulated

for the period 1996–2008 (Muntean et al., 2014) and were two-fold lower than the observed trend at these sites. Zhang et al. (2016c) estimated a steeper trend in Hg wet deposition in the same region (-2.0±0.14%/y). Muntean et al. (2014) estimated a Hg wet deposition decline in North America of -2.4±0.7%/y for the period 1996–2008. Zhang et al. (2016c) utilized an updated emissions inventory and obtained a smaller decline of -1.4±0.1%/y for a longer period (1996–2013) in the same region.

Using a global Hg model (GEOS-Chem) that coupled the atmosphere, soil, and surface ocean, Soerensen et al. (2012) found a long-term decline in Hg^0 concentration over the northern Atlantic. They concluded that existing inventories of Hg anthropogenic emissions cannot explain the substantial decrease in observed Hg^0 concentration (-2.5%/y) for the period 1990–2009 since significant emissions reductions in North America and Europe are balanced by the rise in Hg emissions in East Asia. Instead, it was hypothesized that the reduction in riverine and wastewater Hg inputs to ocean margins could lead to a reduction in subsurface seawater Hg concentration as well as lower Hg emissions from the ocean (Soerensen et al., 2012). Amos et al. (2014) later showed that riverine Hg inputs to the North Atlantic did not contribute substantially to these changes. Zhang et al. (2016c) demonstrated that revised anthropogenic emissions can explain the observed decline in atmospheric Hg. Thus, there are multiple plausible explanations for the decline in Hg concentration over the past two decades which cannot be resolved without a better understanding of past Hg emissions.

Despite increases in global anthropogenic emissions since the mid-20th century (Streets et al., 2011), atmospheric Hg levels in the Arctic have decreased or remained constant (Cole and Steffen, 2010; Berg et al., 2013; Cole et al., 2013). The effects of climate change-related factors such as increased air temperatures (particularly in spring) and reduced sea-ice extent and thickness on Hg levels in Arctic ecosystems are complex and multidirectional (Bekryaev et al., 2010; Cavalieri and Parkinson, 2012; Stern et al., 2012).

Fisher et al. (2013) investigated the factors controlling Hg^0 trends in the Arctic between 1979 and 2008 by using the global historical anthropogenic emissions inventory of Streets et al. (2011) in GEOS-Chem. The model simulated a small increasing trend in Hg^0 concentrations over the 30 year-period mainly reflecting the growth in emissions. The authors also suggested that climate warming may lead to decreased fluxes of Hg from the atmosphere to the cryosphere and increased Hg^0 concentrations in the Arctic. Chen et al. (2015b) extended the study of Fisher et al. (2013) to quantitatively determine the contributions of changes in environmental variables and anthropogenic emissions to Hg trends in the Arctic using the anthropogenic emission inventories of AMAP/UNEP for 2000, 2005, and 2010. In addition to confirming the results of Fisher et al. (2013) for spring and summer, the study found that a decrease in Atlantic Ocean evasion of Hg at lower latitudes contributed to the decrease in Hg^0 concentrations in the Arctic from November to March.

Dastoor et al. (2015) assessed the impact of changing anthropogenic emissions and meteorology on Hg^0 concentrations and deposition in the Canadian Arctic from 1990 to 2005 using GEM-MACH-Hg and AMAP anthropogenic emissions (AMAP, 2011). Changes in meteorology and decline in emissions in North America and Europe were found to contribute equally to the decrease in surface air Hg^0 concentrations in the Canadian
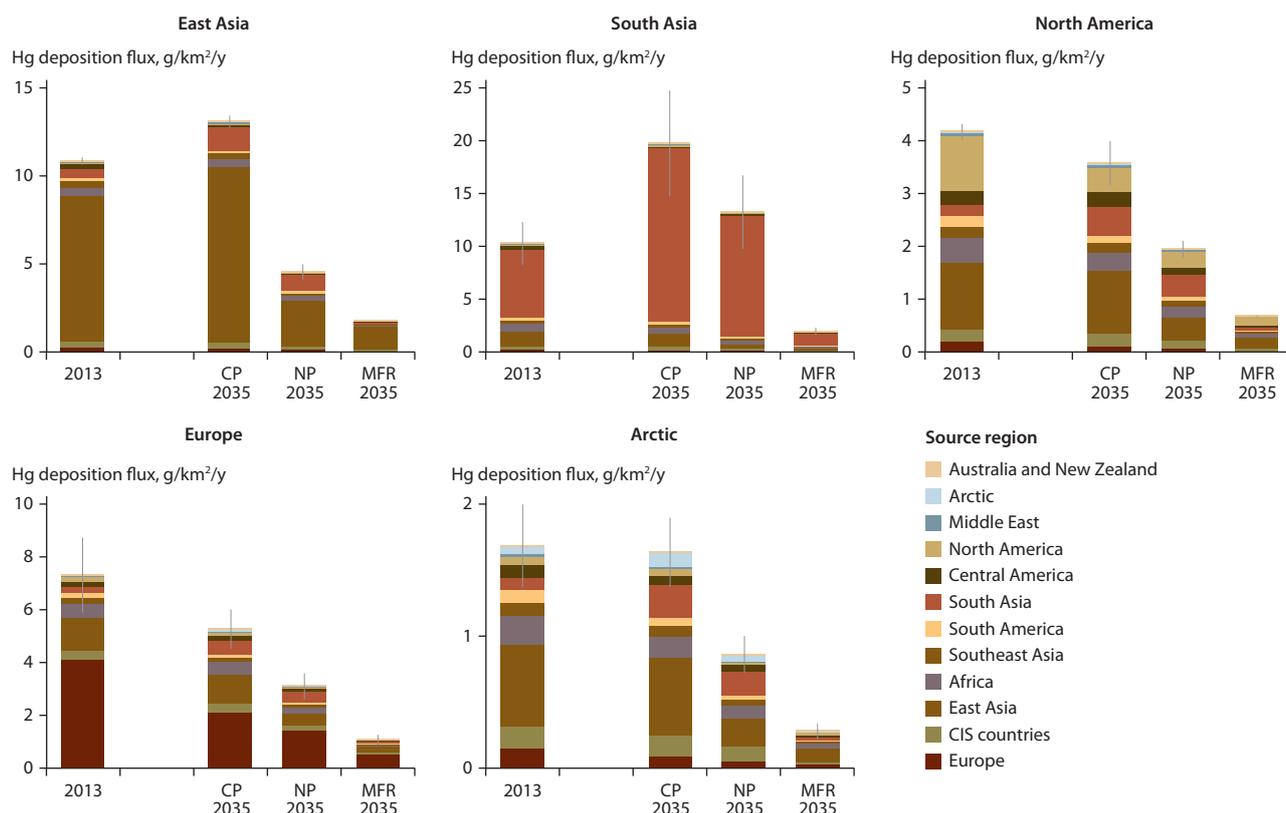
Figure 5.11 Source apportionment of Hg deposition from direct anthropogenic sources (average of two models) in 2013 and 2035 in various regions: East Asia, South Asia, North America, Europe, and the Arctic. Whiskers show deviation between the models. Contributions of natural and secondary emissions are not shown. Source: Pacyna et al. (2016).

Arctic with an overall decline of ~12% from 1990 to 2005, which is in accord with measurements at Alert (Cole and Steffen, 2010; Cole et al., 2013). In contrast, a slow increase (10%) in Hg net deposition is found in the Canadian Arctic in response to combined changes in meteorology and emissions. Changes in snowpack and sea-ice characteristics and an increase in precipitation in the Arctic related to climate change are found to be primary causes for the meteorology-related changes in Hg air concentration and deposition. Increasing precipitation results in some increase in wet deposition, whereas increasing areas of snowpack on first-year sea ice and decreasing snow cover extent both lead to a decline in Hg re-emission and air concentration. Although the link between Hg deposition and lake sediment fluxes is not fully understood, an increase in deposition of Hg in the Arctic appears to be consistent with observed increases in Hg fluxes in some Arctic lake sediments in recent decades (Goodsite et al., 2013).

Despite modelling differences, all studies suggested a dominant role of climate warming-related changes in environmental factors on Hg trends in the Arctic. Current Hg models lack a complete representation of the complexity of climate sensitive Hg processes. Fully interactive atmosphere-land-ocean biogeochemical Hg models including detailed representation of sea-ice dynamics are required to reduce the discrepancy between modelling results. Moreover, field measurements together with model parametrization of climate warming-related environmental factors (temperature, ultraviolet radiation, nutrients etc.) are needed to gain process-based understanding and project future changes in atmospheric Hg trends.

Recently, several modelling studies have investigated future changes in atmospheric Hg concentration and deposition as a result of changes in anthropogenic emissions, land use and land cover as well as climate change. Pacyna et al. (2016) used two chemical transport models (GLEMOS, ECHMERIT) to evaluate future changes in Hg deposition in various geographic regions using three anthropogenic emissions scenarios of 2035 (Figure 5.11). The 'current policy' scenario (CP 2035) predicted a considerable decrease (20–30%) in Hg deposition in Europe and North America and a strong (up to 50%) increase in South and East Asia. According to the 'new policy' scenario (NP 2035) a moderate decrease in Hg deposition (20–30%) was predicted in all regions except South Asia. Model predictions based on the 'maximum feasible reduction' scenario (MFR 2035) showed a consistent Hg deposition reduction on a global scale. It should be noted that the geogenic and legacy sources were assumed to be unchanged in this study.

The combined effect of emissions changes and warming associated with climate change was studied by Lei et al. (2014) with the CAM-Chem model using three emissions scenarios of 2050 (B1, A1B, A1FI) based on projections developed by the Intergovernmental Panel on Climate Change (IPCC). It was found that all three scenarios predict a general increase in total gaseous mercury (TGM) concentration around the globe due to increasing use of fossil fuel energy. The increase in temperature enhances emissions from land and ocean and accelerates oxidation of Hg^0 leading to increased deposition. The effect of climate change as well as change in land use on future Hg levels were studied more thoroughly by Zhang et al. (2016a) by combining a chemical transport model (GEOS-

Chem), a general circulation model (GISS GCM 3), and a dynamic vegetation model (LPJ). Using the IPCC A1B scenario for simulating 2000–2050 climate change they found a global increase in surface Hg^0 concentration with significant changes occurring over most continental and ocean regions due to changes in atmospheric Hg redox chemistry. The study also found that changes in natural vegetation and anthropogenic land use can lead to general increases in Hg^0 dry deposition. The gross Hg deposition flux is expected to increase over most continental regions driven by the combined changes in climate and land use. However, these results do not take into account the possible feedback of the deep ocean and terrestrial reservoirs to the future emissions and climate changes. Besides, current understanding of processes governing Hg cycling in the aquatic and terrestrial environments as well as the air-surface exchange is very limited. Interactions between the Hg cycle and important environmental constituents (e.g. organic carbon, nutrients and biota) and dependence on ambient parameters (e.g. temperature, moisture, radiation) requires further refinement in the model to improve future projections.

Amos et al. (2013) used a fully coupled biogeochemical model and showed that even if anthropogenic emissions remain constant, Hg deposition will continue to increase due to the legacy of anthropogenic production emissions accumulated in the ocean. Generally, the atmosphere responds quickly to a change in emissions but long-term changes are sensitive to various factors, including historical changes in anthropogenic emissions, air-sea exchange, and Hg burial in deep ocean and coastal sediments (Amos et al., 2014, 2015).

5.5 Region-specific modelling studies

5.5.1 Polar regions

Since GMA 2013, three global Hg models have been applied to study Hg cycling in polar regions – GLEMOS (Travnikov and Ilyin, 2009), GEOS-Chem (Holmes et al., 2010; Fisher et al., 2012), and GEM-MACH-Hg (formerly GRAHM; Dastoor et al., 2008; Durnford et al., 2012; Kos et al., 2013). The greatest differences among models in the polar regions concern the representation of Hg^0-Br oxidation rates, Br concentrations, parameterization of photo-reduction and re-emission of Hg^0 from the snowpack, and Hg evasion fluxes from the Arctic Ocean (Angot et al., 2016a). Durnford et al. (2012) developed and implemented a dynamic multi-layer snowpack-meltwater parameterization in GEM-MACH-Hg. Fisher et al. (2012) and Durnford et al. (2012) introduced enhanced evasion of Hg from the Arctic Ocean during summer to explain the observed summer maximum in Hg^0 concentrations (Steffen et al., 2005; Berg et al., 2013). Dastoor and Durnford (2014) found that summer concentrations in the Arctic are characterized by two distinct maxima with the peaks varying in time with location and year. Using GEM-MACH-Hg, the authors demonstrated that an early summer peak in Hg^0 concentrations is supported primarily by re-emission of Hg from melting snowpack and meltwater and a late summer peak is supported by evasion of Hg^0 from the Arctic Ocean. Toyota et al. (2014) developed a detailed one-dimensional air-snowpack model for interactions of Br, O_3, and Hg in the springtime Arctic which provided a physical-chemical mechanism for AMDEs and concurrently occurring ozone depletion events (ODEs). The authors also developed a temperature dependent GOM-
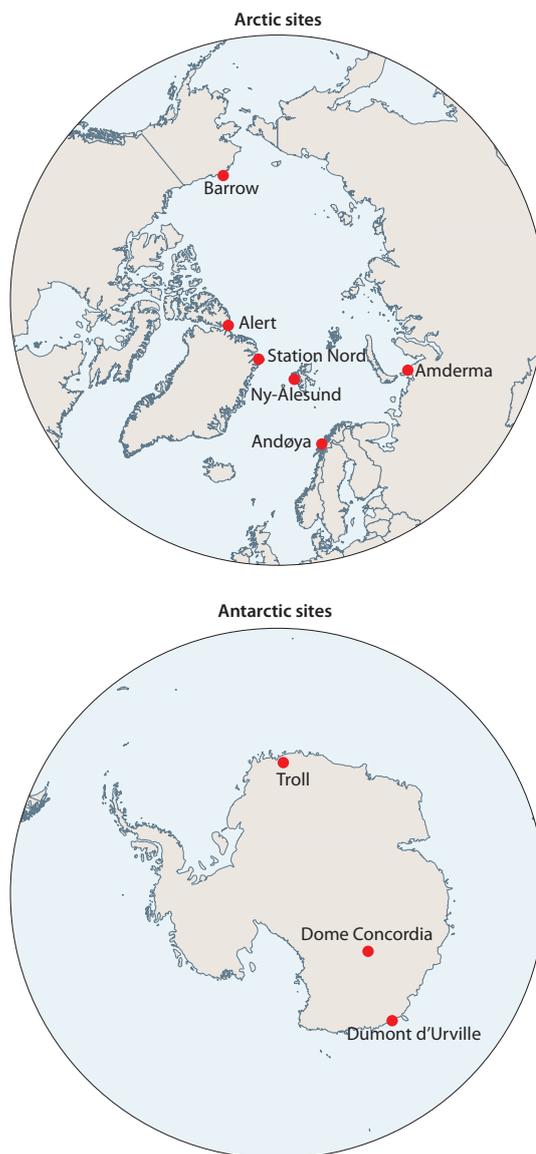
Figure 5.12 Location of Arctic and Antarctic ground-based sites used for model evaluation.

PBM partitioning mechanism explaining the observed seasonal transition between oxidized Hg species (Steffen et al., 2014) and demonstrated that PBM is mainly produced as $HgBr_4^{2-}$ through uptake of GOM into Br-enriched aerosols after O_3 is significantly depleted in the Arctic air masses.

Dastoor and Durnford (2014) conducted a comprehensive evaluation of GEM-MACH-Hg simulated concentrations of Hg^0 and Hg^{II} in air, total Hg concentrations in precipitation and seasonal snowpack, and snow/air Hg fluxes with measurements for 2005–2009 at four Arctic sites – Alert, Ny-Ålesund, Amderma, and Barrow (see Figure 5.12). The model median concentrations of Hg^0 and Hg^{II} were found within the range of observed medians at all locations. Mercury concentrations in snow collected during the springtime (AMDE season) are significantly higher at Barrow than Alert, which was simulated well by the model. Modelled Hg concentrations in seasonal snowpack were also within the measured range.

Angot et al. (2016a) evaluated GEM-MACH-Hg, GEOS-Chem and GLEMOS using atmospheric monitoring data of Hg concentrations for 2013 at four Arctic sites (Alert, Station Nord, Ny-Ålesund, Andøya) and three Antarctic sites (Troll,
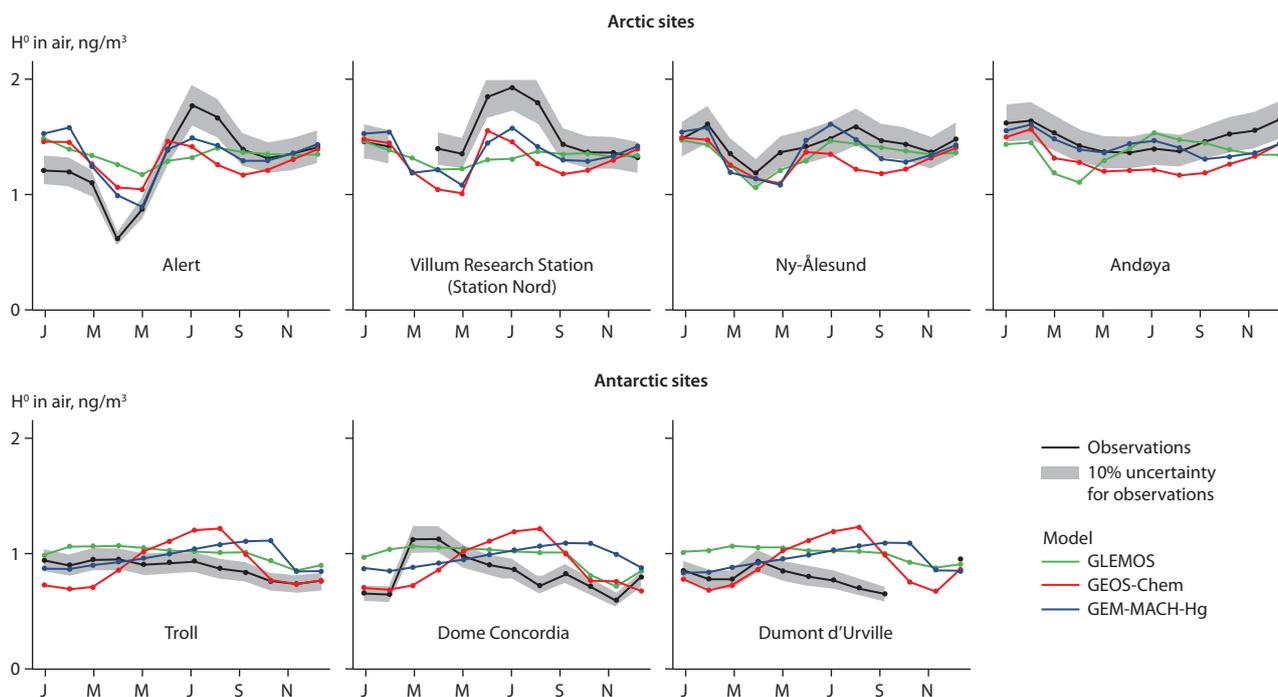
Figure 5.13 Year 2013 monthly-averaged Hg^0 concentrations at Arctic and Antarctic ground-based sites. Adapted from Angot et al. (2016a). Only models that explicitly implement high-latitude specific processes are shown.

Dome Concordia, Dumont d'Urville; see Figure 12). In addition, interannual variability in Hg^0 concentrations was evaluated using GEOS-Chem and GEM-MACH-Hg simulations for 2011–2014. The models captured the broad spatial and seasonal patterns in Hg^0 concentration observed in the Arctic. The decline in Hg^0 concentrations from Andøya (the site closest to European industrialized areas) to Alert (the most northerly site) was reproduced well by the models and suggests transport of anthropogenic Hg from lower latitudes to the Arctic. The more pronounced seasonal cycle observed at Alert and Station Nord than at Ny-Ålesund and Andøya was also captured by the models (Figure 5.13).

All models reproduced the characteristic low Hg^0 concentrations in spring and high Hg^0 concentrations in summer. Consistent with observations, the models simulated enhanced total oxidized Hg concentrations (i.e., oxidized gaseous and particulate Hg) at Alert and Ny-Ålesund during the AMDE season but underestimated the values compared to measurements. At Ny-Ålesund all the models overestimated Hg wet deposition along with overestimation of precipitation amount. The model-measurement discrepancy was attributed to lower collection efficiency for precipitation in polar regions due to frequent strong winds and blowing snow conditions (Lynch et al., 2003; Prestbo and Gay, 2009) and to the uncertainties in gas-particle partitioning of oxidized Hg in the models.

Simulated Hg^0 interannual variability in GEOS-Chem and GEM-MACH-Hg in winter was lower than measured which suggests an impact of interannual variability in anthropogenic emissions; the models used 2010 global anthropogenic Hg emissions (AMAP/UNEP, 2013) for simulations over the 2011–2014 period. Interannual variability in the frequency of AMDEs was fairly well reproduced by GEM-MACH-Hg but not by GEOS-Chem. Real-time modelling of the distribution of Br concentrations and sea-ice dynamics is needed to improve the models (Moore et al., 2014).

In contrast, at Antarctic sites, the models overestimated Hg^0 concentrations and failed to reproduce observed seasonal patterns in Hg^0 concentration (Figure 5.13). GEM-MACH-Hg and GEOS-Chem simulated increasing Hg^0 concentrations at all sites over the course of winter in contrast to the pattern shown by observations; whereas, GLEMOS simulated a lower than observed winter decline in Hg^0 concentrations at Dumont d'Urville and Dome Concordia (Angot et al., 2016a). High summer variability and a strong diurnal cycle in Hg^0 concentrations observed at Dumont d'Urville and Dome Concordia were also not well reproduced by the models. GEM-MACH-Hg did not simulate the infrequent AMDEs observed at Troll and Dumont d'Urville in spring; whereas, GEOS-Chem simulated AMDEs at Dumont d'Urville with somewhat higher frequency than observed. Angot et al. (2016a) attributed poor model simulation of Hg at the Antarctic sites to missing local Hg^0 oxidation pathways involving OH, O$_3$, NO$_X$, organic peroxy radicals and air circulation, and bias in Southern Hemisphere emissions including oceanic evasion in the models.

Modelling estimates of Hg mass fluxes in the Arctic including the Arctic Ocean were provided by Fisher et al. (2012), Durnford et al. (2012) and Dastoor and Durnford (2014). Using GEOS-Chem, Fisher et al. (2012) estimated Hg deposition of 55 Mg/y (25 Mg/y directly to open ocean, 20 Mg/y to ocean via snow melt on sea ice, 10 Mg/y to land via snow melt), evasion from ocean of 90 Mg/y and a net surface loss of 35 Mg/y in the Arctic north of 70°N. In contrast, using GEM-MACH-Hg, Durnford et al. (2012) estimated Hg deposition of 153 Mg/y (58 Mg/y directly to open ocean, 50 Mg/y to ocean via snow melt on sea ice, 29 Mg/y directly to land, 16 Mg/y to land via snow melt), emission of 36 Mg/y (33 Mg/y from ocean, 3 Mg/y from land) and a net surface gain of 117 Mg/y in the Arctic north of 66.5°N. Thus, Fisher et al. (2012) concluded that the Arctic Ocean is a net source of Hg to the atmosphere, i.e., 45 Mg/y; whereas, Durnford et al. (2012) concluded that

the Arctic Ocean is a net sink of atmospheric Hg, i.e., 75 Mg/y. In comparison, GLEMOS estimated the yearly net gain of Hg in the Arctic to be 131 Mg/y (Travnikov and Ilyin, 2009).

Model disagreements in the estimates of atmosphere-ocean-snowpack Hg fluxes indicate sources of uncertainty in the models. Constraining models in the polar regions is challenging due to insufficient measurements (Dastoor and Durnford, 2014; Angot et al., 2016a). Fisher et al. (2012) inferred that a 95 Mg/y input of Hg from circumpolar rivers (and coastal erosion) resulting in a 90 Mg/y evasion of Hg from the Arctic Ocean was required to balance the observed summer peak in Hg^0 concentrations at the Arctic sites. In contrast, Durnford et al. (2012) found that 33 Mg/y Hg evasion from the Arctic Ocean was sufficient to reproduce the summer peak in Hg^0 concentrations in the Arctic. Dastoor and Durnford (2014) estimated riverine Hg export to the Arctic Ocean from North American, Russian and all Arctic watersheds to be in the range 2.8–5.6, 12.7–25.4 and 15.5–31.0 Mg/y, respectively, based on GEM-MACH-Hg simulated Hg in meltwater. Using the MITgcm ocean model and GEOS-Chem, Zhang et al. (2015c) concluded that an input of 63 Mg/y of Hg discharge from rivers and coastal erosion to the Arctic Ocean was needed to reproduce the observed summer maximum in atmospheric Hg^0 concentrations. River discharge to the Arctic Ocean is poorly constrained by observations with estimates ranging from 12.5 to 44 Mg/y (Outridge et al., 2008; Amos et al., 2014). Zhang et al. (2015c) noted that enhanced turbulence associated with sea-ice dynamics facilitates increased evasion of Hg discharged by Arctic rivers in estuaries resulting in a much larger proportion of riverine Hg in the Arctic Ocean subject to evasion than estimated by Fisher et al. (2012). In addition, Fisher et al. (2012) assumed that the Hg input from rivers is uniformly distributed across the entire Arctic Ocean; whereas, latitudinal variation in Hg evasion from the Arctic Ocean was assumed by Durnford et al. (2012) and Zhang et al. (2015c), which is supported by observations (Andersson et al., 2008; Hirdman et al., 2009; Sommar et al., 2010). Other sources of differences between models were related to the parameterizations of Br concentrations and Hg snowpack/meltwater processes (Dastoor and Durnford, 2014).

5.5.2 Europe

In recent years, the development of regional atmospheric Hg models for Europe was supported by the FP7 project GMOS (Global Mercury Observations System). Mercury chemistry was incorporated into the on-line coupled meteorological CTM WRF-Chem model by Gencarelli et al. (2014) and the CCLM-CMAQ model was further developed (Bieser et al., 2014; Zhu et al., 2015). These models have been used to evaluate key processes and identify their impact on Hg dispersion and deposition in Europe (Gencarelli et al., 2016; Bieser et al., 2017).

Historically, Europe has been one of the major emitters of Hg (Streets et al., 2011). A major decline in European Hg emissions occurred at the end of the 1980s (Pacyna et al., 2009). Since 1990 atmospheric Hg emissions have been reduced by 60% (Maas and Grennfelt, 2016). A large proportion of this reduction is due to regulatory and economic changes in the late 20th century. However, based on the recent estimates of Muntean et al. (2014) Hg emissions in Europe continue to decrease, but at different rates for each Hg species. Coal-fired power plants are the main

source of Hg in Europe. Due to technological development, emissions of GOM are declining faster than total Hg emissions, which affects the regional deposition and global transport patterns. This finding was further confirmed by model studies where the models' tendency to overestimate ground-based GOM concentrations could be attributed to the speciation of primary anthropogenic Hg emissions (Bieser et al., 2014, 2017). Moreover, airborne *in situ* measurements at a modern coal-fired power plant did not detect any GOM 1 km downwind from the stack (Weigelt et al., 2016b).

The models have in common that the modelled annual wet deposition fluxes are in good agreement with observations. This was found for regional models (Bieser et al., 2014; Gencarelli et al., 2014) and global models (Muntean et al., 2014). At the same time, models tend to underestimate total gaseous mercury concentrations for Europe; something also seen in the results from global models (Muntean et al., 2014; Chen et al., 2015a). The reason for this is not yet understood. In a global long-term simulation with the GEOS-Chem model, Muntean et al. (2014) showed that modelled total gaseous mercury concentrations were closer to observations in the 1990s but that the model overestimates the decreasing trend of recent decades. This, in turn, can be explained by overestimation of the emissions trend. It is also in line with the fact that new regional emission models lead to higher estimates for European Hg emissions (Rafaj et al., 2014).

A recent study with a newly developed regional multi-media model indicates that an underestimation of air-sea exchange from regional oceans could be a source of model bias for Europe (Bieser and Schrum, 2016). Comparing the impact of air-sea exchange on Hg concentrations at two ground-based stations in Europe (Figure 5.14) shows that air-sea exchange has a larger impact on Hg^0 concentrations near the ocean (Zingst) than 200 km inland (Waldhof).

A first model analysis on the vertical distribution of Hg in Europe was recently published by Bieser et al. (2017). Based on the combination of ground-based observations and aircraft measurements in the troposphere and lower stratosphere a comprehensive Hg vertical profile in Europe was reconstructed up to 12 km in altitude. The measurements were compared with multi-model simulations of Hg vertical distribution in the atmosphere. This showed that models are generally able to reproduce the Hg^0 gradient from the surface to the tropopause (Figure 5.15). Moreover, models were also able to reproduce the GOM gradient inside the planetary boundary layer (not shown), in those cases where a small GOM fraction in the anthropogenic emissions was assumed (Bieser et al., 2017). This is in line with the findings on decreasing GOM fraction in European Hg emissions discussed earlier in this section.

The impact of long-range atmospheric transport on European Hg deposition was investigated in the GMA Update 2015. Since then, there has only been one new study on the global transport of Hg from Asia (Chen et al., 2015a). In this study, the estimated contribution of Chinese emissions to Hg deposition in Europe is 3%, which is less than estimates of 8% by other models (AMAP/UNEP, 2015). It should be noted that most global model results appear to be relatively consistent in terms of estimating the contribution of Asian emissions to European deposition values and so the study by Chen et al. (2015a) seems to be an outlier (see also Section 5.3.1). The impact of long-range transport on
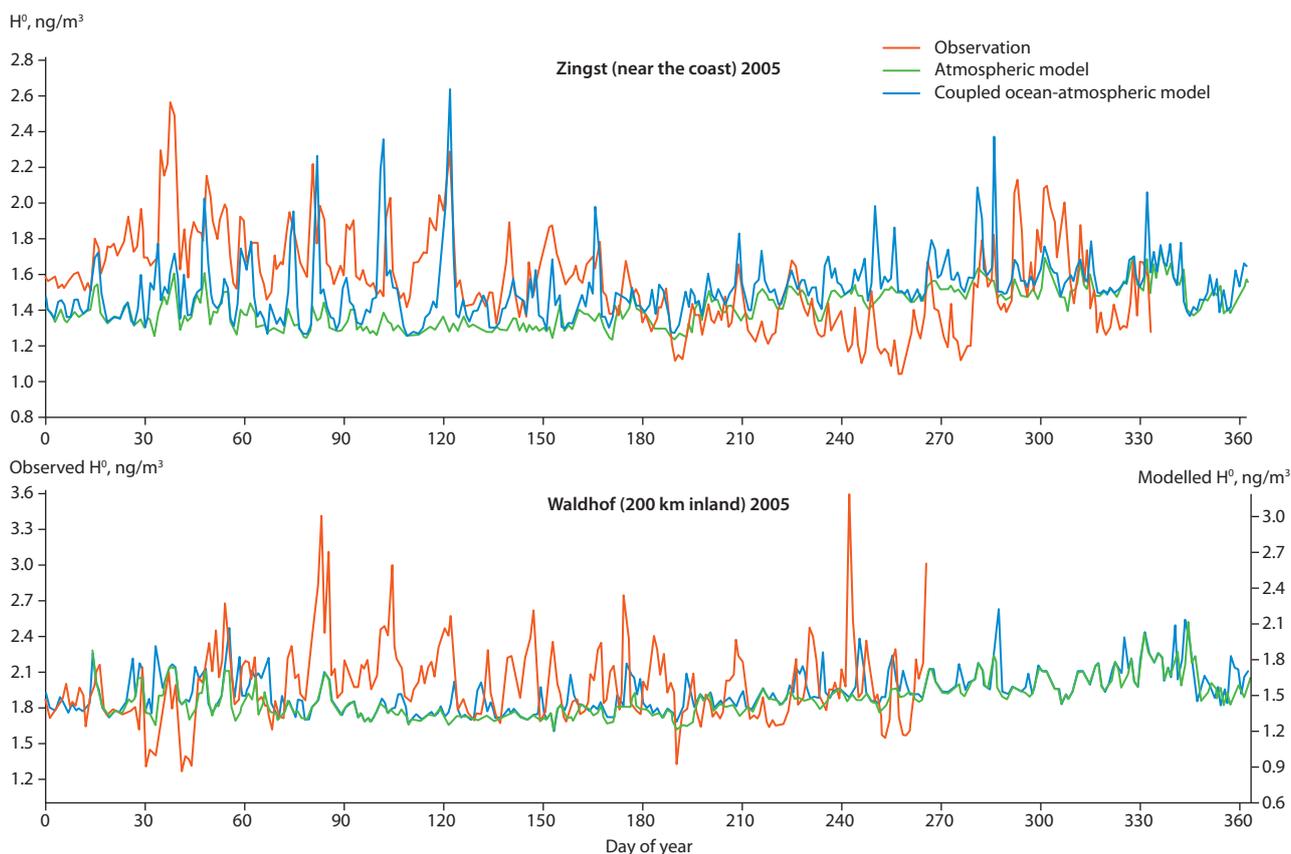
Figure 5.14 Impact of air-sea exchange on atmospheric Hg concentrations at two ground-based observations sites in Germany: Zingst and Waldhof. Source: Bieser and Schrum (2016).
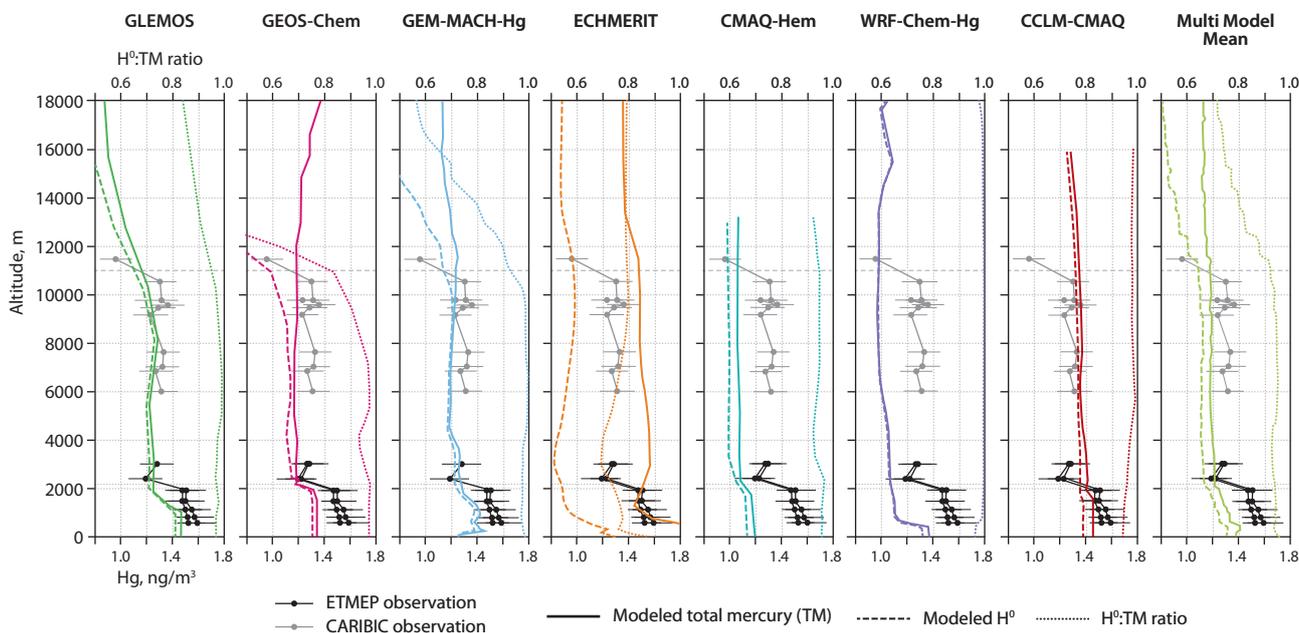
Figure 5.15 Vertical profiles at Leipzig, Germany 23 August 2013 from two aircraft campaigns and simulations with seven atmospheric chemistry transport models. Source: Bieser et al. (2017).

regional Hg deposition in Europe is strongly dependent on the lifetime of Hg in the atmospheric models. An important factor is the speciation of emissions in China, as Hg⁰ and PBM have much longer atmospheric lifetimes than GOM. Thus, if novel technology leads to a similar shift in Hg emission speciation in Asia as recently observed in Europe, a longer lifetime of Hg emitted in Asia could be expected.

De Simone et al. (2015, 2017) investigated the impact of biomass burning on atmospheric Hg concentrations and deposition. Wildfires in the boreal forests can have an especially large impact on regional Hg concentration and deposition. For Europe, De Simone et al. (2015, 2017) estimated the fraction of Hg deposition due to biomass burning at between 5% and 10%.

5.5.3 **North America**

The model CMAQ, with global boundary conditions estimated with the MOZART model, was used to estimate atmospheric Hg deposition to the Great Lakes in 2005 (Grant et al., 2014). Emissions from U.S. power plants had the greatest impact on Lake Erie. The model tended to overestimate wet deposition in the Great Lakes region. In another CMAQ-based investigation, the model was used with boundary conditions from GEOS-Chem, and alternatively GRAHM, to estimate atmospheric Hg deposition in the United States (Myers et al., 2013) in a series of 2001–2005 case studies. Simulation results were significantly influenced by the choice of boundary conditions. CMAQ, with a new aqueous-phase oxidized Hg reduction chemical mechanism (involving dicarboxylic acids) and GEOS-Chem boundary conditions, was used to simulate Hg fate and transport in the USA during the period 2001–2002 (Bash et al., 2014). Results for wet deposition with the new chemical mechanism were found to be more consistent with observations than earlier mechanisms used in CMAQ. Using a weight-of-evidence approach, Sunderland et al. (2016) argued that historical EPA CMAQ-based modelling may have underestimated the impact of local and regional sources on near-field Hg deposition, and consequently underestimated the benefits of Hg emissions reductions.

The GEOS-Chem model was used to estimate the cumulative benefits of domestic and international Hg controls for atmospheric deposition – and subsequent public health impacts – in the USA through 2050 (Giang and Selin, 2016). For the same amount of avoided Hg emissions, domestic reductions were estimated to have nearly an order of magnitude higher public health benefit than international actions. The CAM-Chem-Hg model was used to estimate present day (~2000; Lei et al., 2013) and future (~2050; Lei et al., 2014) atmospheric Hg concentrations and deposition in the USA, as influenced by different scenarios of changes in domestic and global emissions, and different climate change scenarios. Concentrations and deposition in the USA increased significantly in scenarios with higher future emissions and higher air temperatures. Under the scenario of highest impact considered, climate change alone caused an approximate 50–100% increase in atmospheric Hg concentrations in the USA. When increased Hg emissions in this scenario were included, the average Hg^0, GOM, and PBM concentrations in the USA increased by factors of ~2.5, ~5, and ~3, respectively. The GRE-CAPS model – which included a version of the regional CAMx model – was used to investigate the influence of climate change on atmospheric Hg deposition in the eastern USA (Megaritis et al., 2014). Simulations for the present day (~2000s) were compared with climate change-influenced simulations for 2050, assuming constant 2001 Hg emissions. The study found that average deposition in the USA increased by about 5% due to climate-change impacts (e.g., enhanced atmospheric oxidation of Hg^0 at higher temperatures), but regional differences were found (e.g., related to changes in precipitation patterns).

The HYSPLIT-Hg, a special version of the NOAA HYSPLIT model developed to simulate the fate and transport of atmospheric Hg, including chemical transformations, was used to estimate 2005 atmospheric Hg deposition to the Great Lakes (Cohen et al., 2016). Results for a base case and ten alternative model configurations were developed, examining the sensitivity

Hg deposition, µg/m²/y
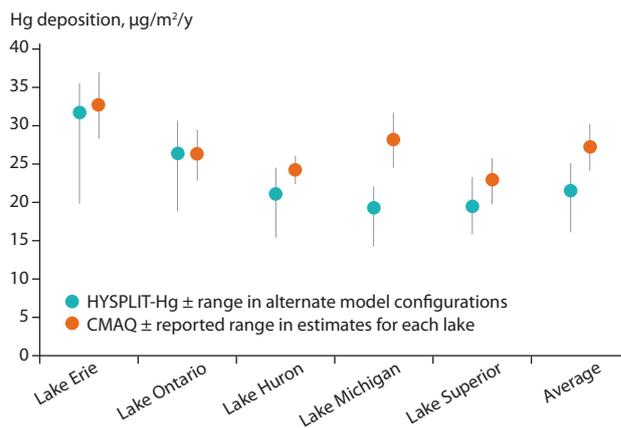
Figure 5.16 Atmospheric Hg deposition flux to the Great Lakes for 2005, estimated by CMAQ (Grant et al., 2014) and HYSPLIT-Hg (Cohen et al., 2016). The Great Lakes summary values shown are based on an area-weighted average of individual-lake results.

of the results to different assumptions regarding atmospheric reaction rates and chemical mechanisms. Model evaluation against measurements in the Great Lakes region showed good agreement between modelled and measured wet deposition and Hg^0 concentrations, but also that the model tended to overestimate reported GOM and PBM concentrations. The total deposition and source-attribution for that deposition was similar to that found by Grant et al. (2014) (see Figure 5.16). Lake Erie, downwind of significant local/regional emissions sources was estimated by the model to be the most impacted by direct anthropogenic emissions (58% of the base-case total deposition), while Lake Superior, with the fewest upwind local/regional sources was the least impacted (27%). On average, the USA was the largest national contributor (25%) for the Great Lakes, followed by China (6%). The contribution of U.S. direct anthropogenic emissions to total Hg deposition varied between 46% for the base case (with a range of 24–51% over all model configurations) for Lake Erie and 11% (range 6–13%) for Lake Superior. The relative contributions of different sources are illustrated in Figure 5.17 for the base-case simulation. These results were used in an International Joint Commission report (IJC, 2015) which called for increased monitoring and modelling of atmospheric Hg in the Great Lakes region.

A number of analyses were conducted in which measurements of atmospheric concentration were combined with back-trajectory and other receptor-based modelling approaches to assess the relative importance of different source regions and other factors to the atmospheric Hg arriving at the measurement site (see Table 5.2 for examples). In most cases, the HYSPLIT model (Stein et al., 2015) was used for simulating back-trajectories. Similar studies were carried out for flight-based measurements of atmospheric Hg concentration above the surface, utilizing back-trajectories and/or other model simulations, above Tullahoma, TN (Brooks et al., 2014), Texas and the southeastern USA (Ambrose et al., 2015; Gratz et al., 2015; Shah et al., 2016), and Lake Michigan (Gratz et al., 2016).

In a hybrid analysis combining fate-and-transport modelling with measurements, GEOS-Chem was used to examine trends in Hg wet deposition over the United States over the 2004–2010 period (Zhang and Jaeglé, 2013). The modelling results were subtracted from the observations to assess the
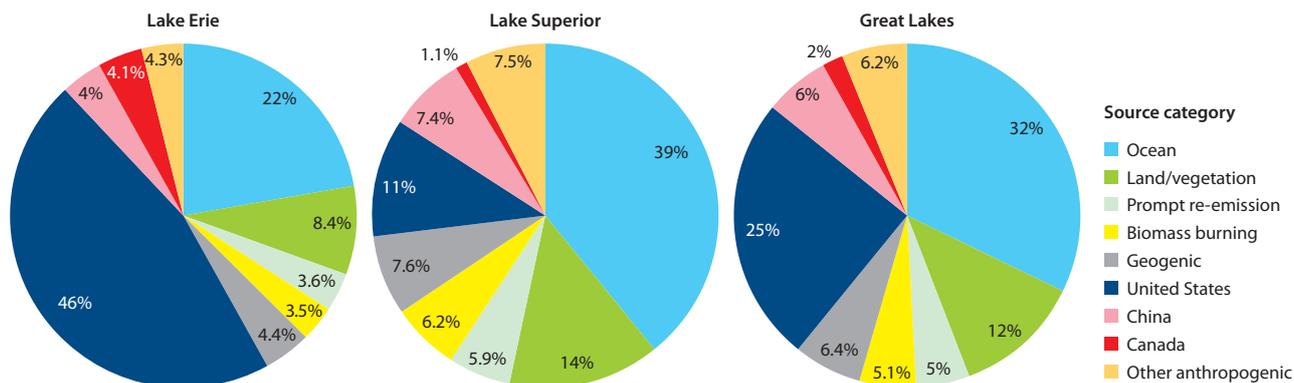
Figure 5.17 Relative contributions of different source categories to the 2005 atmospheric Hg deposition to Lake Erie, Lake Superior, and an area-weighted average for the Great Lakes as a whole, estimated by the HYSPLIT-Hg model (Cohen et al., 2016) (base-case simulation). The values shown for specific countries (United States, China, and Canada) and for all other countries ('Other anthropogenic') include only the contributions from direct, anthropogenic emissions and do not include contributions arising from re-emissions of previously deposited material from terrestrial or oceanic surfaces.

roles of changing meteorology and emissions on observed wet deposition at 47 U.S. sites. In the northeast and midwest USA, approximately half of the decreasing trend in Hg concentrations in precipitation could be explained by decreasing U.S. emissions over the study period. The use of receptor-based analyses to investigate source-receptor relationships for atmospheric Hg has been reviewed by Cheng et al. (2015).

Table 5.2 Measurement sites analyzed with receptor-based modelling.

Measurement site	Back-trajectory study
Canada	
Dartmouth, NS	Cheng et al., 2013a, 2016
Kejimkujik, NS	Cheng et al., 2013a, 2016
Windsor, ON	Xu et al., 2014
USA	
Beltsville, MD	Ren et al., 2016
Chicago, IL	Gratz et al., 2013a
Grand Bay, MS	Rolison et al., 2013; Ren et al., 2014
Holland MI	Gratz et al., 2013a
Huntington Forest, NY	Cheng et al., 2013b; Choi et al., 2013; Zhou et al., 2017a;
Illinois (several sites)	Gratz et al., 2013b; Lynam et al., 2014
Oxford, MS	Jiang et al., 2013
Pensacola, FL	Demers et al., 2015; Huang et al., 2016
Piney Reservoir, MD	Castro and Sherwell, 2015
Reno, NV	Gustin et al., 2016b
Rochester, NY	Choi et al., 2013
Steubenville, OH	White et al., 2013
Underhill, VT	Zhou et al., 2017a
Western U.S. (several sites)	Wright et al., 2014; Huang and Gustin, 2015; Gustin et al., 2016b
Mexico	
Celestun, Yucatan	Velasco et al., 2016

5.5.4 East Asia

East Asia (including Southeast Asia) is the largest source region for atmospheric Hg release worldwide, with China contributing the largest amount of anthropogenic Hg emissions. According to GMA 2013, Hg release in East and Southeast Asia accounted for 40% of global anthropogenic emission in 2010. Mercury outflow from East Asia has been regarded as a global Hg pollution issue (Jaffe et al., 2005; Lin et al., 2010b; Chen et al., 2014b).

Rapid economic growth and improving air emission control in East Asia are causing changes in anthropogenic Hg emission and speciation over a relatively short period. As better emission data become available, reassessment using updated emission data is necessary. For example, Wu et al. (2016b) applied updated industrial activity statistics and emission factors to estimate anthropogenic Hg release in China between 1978 and 2014, and found the emission varied significantly due to increased industrial production, energy use and implementation of emission control measures. Atmospheric Hg emission in China peaked in 2011 at 565 Mg/y and then fell to 531 Mg/y in 2014 (Wu et al., 2017). More importantly, the emission speciation gradually shifted to a larger fraction of oxidized Hg (Wu et al., 2016b). Such a shift implies increased local deposition and reduced emission outflow.

Wang et al. (2016b) re-evaluated the natural release of Hg^0 vapor from soil, vegetation and water surfaces using new soil Hg data in China and updated model schemes with recently reported physical-chemical parameters. They found a different spatial distribution of estimated Hg release compared to the data reported by Shetty et al. (2008), despite a similar net natural release at ~460 Mg/y in China.

Several regional and global modelling studies have simulated atmospheric Hg levels in China and the East Asian region (e.g., Lin et al., 2010b; Pan et al., 2010; Chen et al., 2014b, 2015a; Zhu et al., 2015; Wang et al., 2018). It should be noted that most model results are not directly comparable due to differences in the emission inventory (particularly, natural emissions since many earlier studies did not specify the quantity and spatial distribution), Hg chemistry and model configuration. In general, regional models reproduced Hg concentrations that were more representative of the observed elevated levels in urban and industrial areas. Previous global model results estimated that Asian emissions contributed 16–25% of Hg
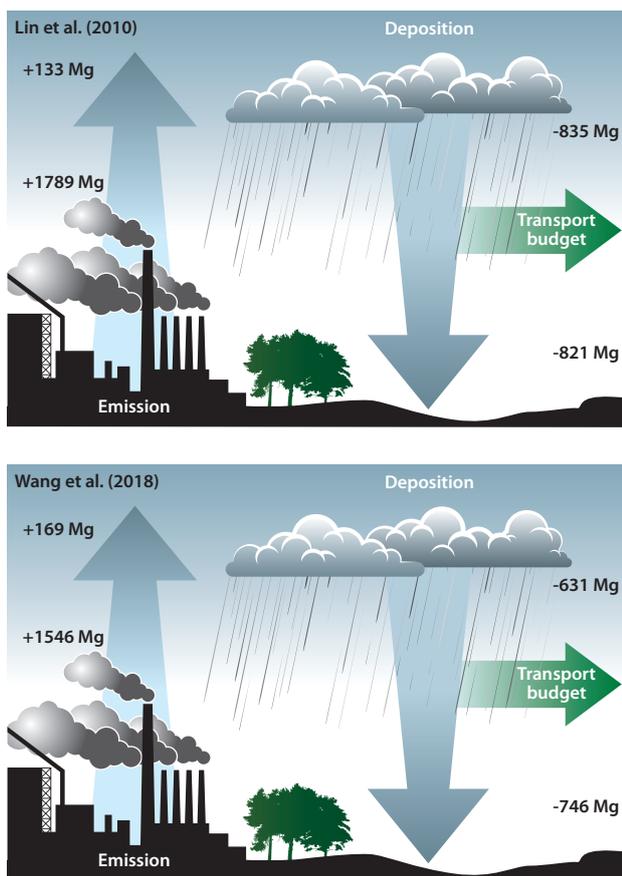
Figure 5.18 Comparison of annual Hg mass budget in East Asia by Lin et al. (2010b) and Wang et al. (2018).

deposition in North America and 10–15% in the European region. More recent modelling studies provide lower values (8–10% for North America and 7–8% for Europe), except for one study (Chen et al., 2014b) which reported a contribution of <5% for both regions (see also Section 5.3.1). Recently, It was estimated that the contribution of foreign countries to the Hg^0 concentration on the Korean Peninsula averaged ~15% (Seo et al., 2016a; Sung et al., 2016).

The results of two regional modelling studies using CMAQ-Hg with identical model specifications are directly comparable (Lin et al., 2010b; Wang et al., 2018). The two studies use the same model configuration of CMAQ-Hg with different emission inventories: from Streets et al. (2005) and Shetty et al. (2008) for the former and Wu et al. (2016b) and Wang et al. (2016b) for the latter. The difference in the annual budgets is mainly caused by the reduced anthropogenic emission in the region, increased fraction of Hg^{II}, and a change in the spatial distribution of natural emissions. Given the changes in emissions, the transport budget from East Asia by Wang et al. (2018) is 25% lower than the earlier estimate by Lin et al. (2010b), as shown in Figure 5.18. In addition, the greater Hg mass accumulated within the regional domain of Wang et al. (2018) also better explains the elevated atmospheric Hg concentrations in China. More modelling studies are still needed in this region. Recent observational data obtained from the ambient monitoring network in China (Fu et al., 2015) provide a unique opportunity to better understand the chemical transport of atmospheric Hg in a region undergoing dynamic emission changes.

5.6 **Conclusions**

A number of regional and global models have been used to simulate the atmospheric transport and fate of Hg, using meteorological data and emissions inventories as inputs and atmospheric measurements to evaluate the results. In particular, the new modelling results based on the updated global Hg emissions inventory for 2015 present up-to-date estimates of Hg transport and fate on a global scale, including source apportionment of Hg deposition in various terrestrial and aquatic regions as well as an evaluation of contributions from different emission sectors. A comparison between the current modelled results and GMA Update 2015 (year 2010 anthropogenic Hg emission inventory) shows an average 20% increase in total Hg deposition flux to most geographic regions, except in the polar regions, which show a 30% reduction. This is consistent with the global increase in anthropogenic Hg emissions (~12%) between 2010 and 2015. Overall, the new analysis of Hg intercontinental transport is consistent with previous results presented in GMA Update 2015. The changes include an increase in deposition from sources in East and South Asia and a reduction in deposition from domestic sources in North America since 2010 due to emission changes in these regions. The contribution of Hg emissions from artisanal and small-scale gold mining to Hg deposition worldwide was estimated for the first time, indicating global dispersion but with the largest effect closer to emission sources in South America, equatorial Africa, and East and Southeast Asia.

Significant uncertainties remain in model physics (e.g., gas-particle partitioning and deposition processes) and chemistry (e.g., elemental Hg oxidation mechanisms, reaction kinetics and oxidation products), as well as in model inputs (e.g., emission amounts and speciation) and measurements used for evaluation. Nevertheless, scientific understanding of atmospheric Hg as represented in the models has progressed to the point where useful policy-relevant information about source-receptor relationships can be derived. This also implies that models can be used to provide first estimates of the effects on Hg deposition of emission reductions, both regionally and globally.

Atmospheric measurements are essential to evaluate and improve models; given the uncertainties noted in Section 5.2, models must continually be tested by comparison against measurements. At the same time, measurements alone cannot provide the depth of source-receptor and trend explanation information that can be obtained by models. Likewise, uncertainties in emissions inventories (e.g., speciation of emissions from power plants and industrial sources, contribution of emissions from ASGM, natural and secondary emissions) have emerged as a critical limitation in atmospheric model analyses. In particular, the quantity of Hg^0 release from natural surfaces needs to be better constrained, and the parameterization of estimating the re-emission of previously deposited Hg in models must be further improved to more realistically determine the source-receptor relationship of global Hg emission and deposition. Improvement in these fundamental model inputs is essential to enhance model accuracy.

Chapter 5 Appendix

Table A5.1 Characteristics of the participating global chemical transport models.

	ECHMERIT	GEM-MACH-Hg	GEOS-Chem (v11-02)	GLEMOS
Institution performing model simulation	CNR-Institute of Atmospheric Pollution Research, Italy	Environment and Climate Change Canada, Canada	Massachusetts Institute of Technology, USA	Meteorological Synthesizing Centre – East of EMEP
Model type	Atmospheric	Atmospheric	Multi-media [a]	Atmospheric
Spatial resolution				
Horizontal	T42 (~ 2.8° × 2.8°)	0.5° × 0.5°	2.5° × 2°	1° × 1°
Vertical (atmosphere)	19 levels, top 10 hPa	58 levels, top 7 hPa	47 levels, top 0.01 hPa	20 levels, top 10 hPa
Atmospheric chemistry				
Gas-phase oxidation (major oxidants)	O_3, OH	OH, Br [b]	Br, NO_2, HO_2 [c]	O_3, OH
Gas-phase reduction	no	no	no	no
Aqueous chemistry (in cloud water)	yes	no	yes [d]	yes
Emissions				
Anthropogenic, t/y	2224	2224	2224	2224
Average speciation GEM:GOM:PBM	82:14:4	87:10:3 [e]	82:18:0 [f]	82:14:4
Natural and secondary, t/y [g]	8600 [h]	5460 [i]	4900 [j]	3730 [k]
Reference	De Simone et al. 2014; Jung et al. 2009	Durnford at al. 2012; Kos et al. 2013; Dastoor et al. 2015	Holmes et al. 2010; Amos et al. 2012; Horowitz et al. 2017b	Travnikov and Ilyin 2009; Travnikov et al. 2009

[a] Off-line land and ocean according to Horowitz et al., (2017b); [b] OH is a main oxidizing agent globally, Br is a main oxidizing agent in the polar regions; [c] Two-step oxidation initiated by Br. The second-stage HgBr oxidation is mainly by the NO_2 and HO_2 radicals; [d] Oxidation of $Hg^0_{(aq)}$ takes place in clouds only. Photo-reduction of $Hg^{2+}_{(aq)}$ takes place in both aqueous aerosols and clouds (Horowitz et al., 2017b); [e] The original speciation of Hg emissions from coal-fired power plants is corrected by converting 80% of GOM and PBM to GEM; [f] Dynamic gas-particle partitioning of reactive Hg in the atmosphere according to Amos et al. (2012); [g] Gross emissions from natural and secondary sources; [h] Prescribed emission from terrestrial surfaces as a function of temperature and solar radiation, dynamically calculated ocean emissions based on prescribed seawater concentrations; [i] Prescribed emission from terrestrial surfaces as a function of temperature and solar radiation, dynamic re-emission from snow and aquatic surfaces; [j] Prescribed emission from terrestrial surfaces as a function of temperature and solar radiation, dynamic fluxes from aquatic surfaces based on multi-media modelling; [k] Prescribed emission from terrestrial and aquatic surfaces as a function of temperature and solar radiation, dynamic re-emission from snow.

Terrestrial receptor regions
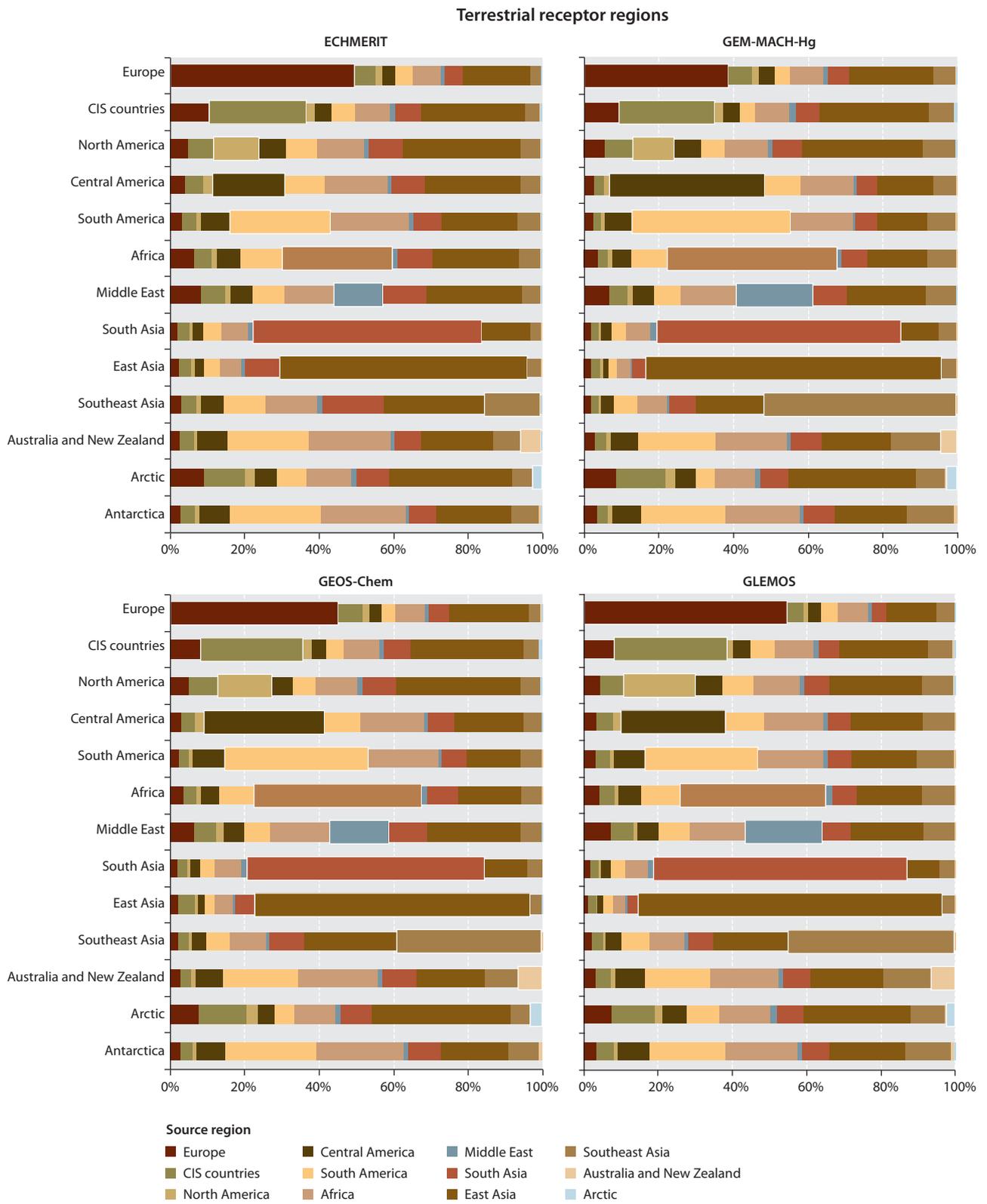
Figure A5.1 Source apportionment of Hg deposition from direct anthropogenic emissions to terrestrial receptor regions in 2015 simulated by four models: ECHMERIT, GEM-MACH-Hg, GEOS-Chem, and GLEMOS. Contribution of domestic sources is shown by wider bars.

Aquatic receptor regions
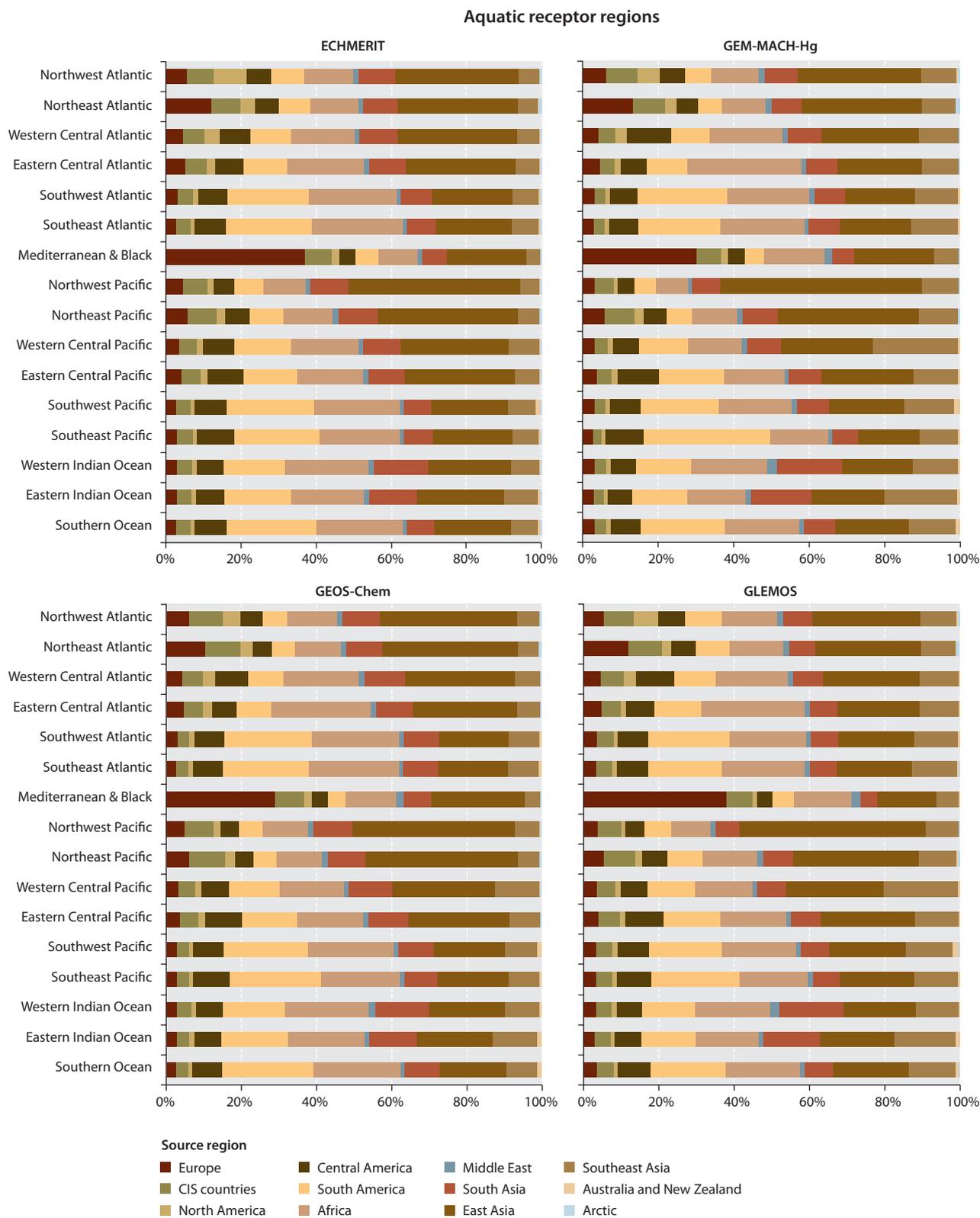
Figure A5.2 Source apportionment of Hg deposition from direct anthropogenic emissions to aquatic receptor regions in 2015 simulated by four models: ECHMERIT, GEM-MACH-Hg, GEOS-Chem, and GLEMOS.

Terrestrial receptor regions
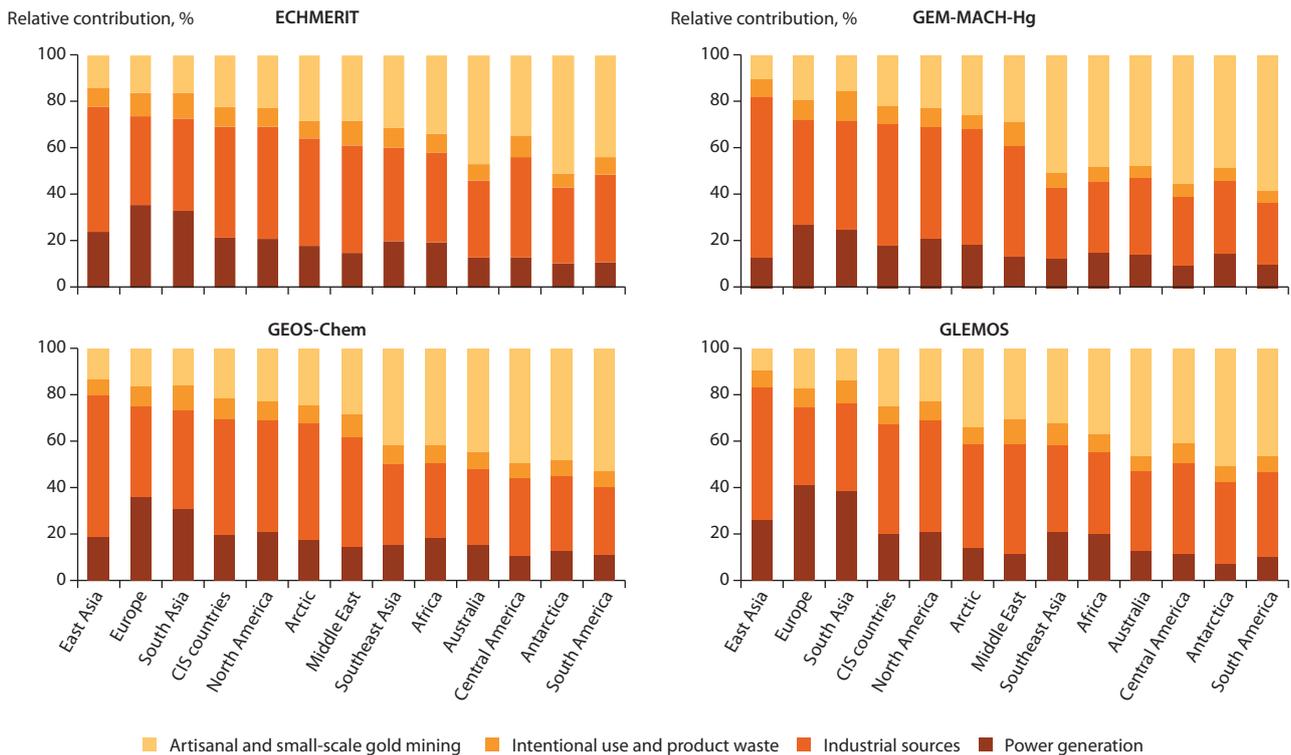
Figure A5.3 Simulated relative contribution of the four emission sectors to Hg deposition from direct anthropogenic emissions to terrestrial receptor regions in 2015 simulated by four models: ECHMERIT, GEM-MACH-Hg, GEOS-Chem, and GLEMOS.

Aquatic receptor regions
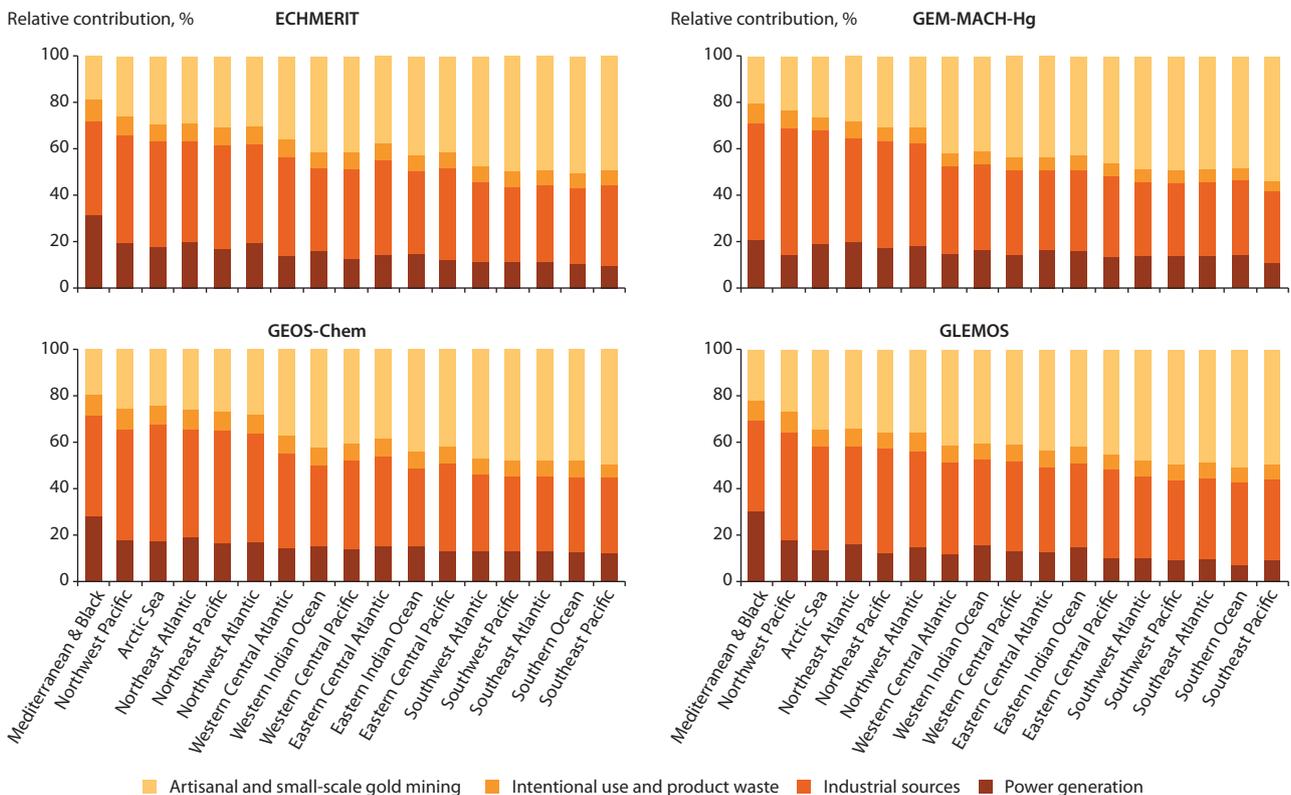
Figure A5.4 Simulated relative contribution of the four emission sectors to Hg deposition from direct anthropogenic emissions to aquatic receptor regions in 2015 simulated by four models: ECHMERIT, GEM-MACH-Hg, GEOS-Chem, and GLEMOS.

6. Releases of mercury to the aquatic environment from anthropogenic sources

Authors: David Kocman, Simon J. Wilson, Katarina Yaramenka, Karin Kindbom, Helen M. Amos, Peter Outridge, Rasmus Parsmo, Kevin Telmer, Milena Horvat

Key messages

- *The 2015 global inventory of mercury (Hg) releases to aquatic environments from anthropogenic sources (excluding artisanal and small scale gold mining, ASGM) currently amounts to ~600 t/y. The new inventory is more complete and reinforces the importance of these sources in the global context.*

- *The current inventory of global anthropogenic Hg releases to aquatic systems is a work in progress, and an important step towards filling a major gap in inventories of anthropogenic Hg releases to the environment.*

- *Quantifiable releases to water from anthropogenic sources comprising ten key sectors are included in the inventory, with some new important sectors added and newly evaluated in 2015 compared to 2010, such as releases associated with municipal wastewater, coal washing and coal-fired power plants. In addition to methodological changes introduced to derive the estimates, these newly added sectors are driving the relatively large difference between the 2010 and 2015 anthropogenic Hg release inventory.*

- *For the first time, the inventory was extended to include primary releases to land and solid waste streams from some of the sources considered. The magnitude of these terrestrial Hg pathways can be substantial. It was established that releases of the order of tens to hundreds of tonnes per year may arise following these pathways, and this Hg initially accumulated in terrestrial systems, if not treated properly, can act as a potential secondary source of Hg for both water and the atmosphere.*

- *Regional and sectoral attribution of the global release inventory indicates both similarities and differences with atmospheric emission patterns. Excluding the artisanal and small-scale gold mining (ASGM) sector for which combined releases to water and land are estimated, the majority of releases to water occur in Asia (55%; primarily East and South-east Asia) followed by Europe and CIS countries (14%), Latin America (11%) and Sub-Saharan Africa (8%).*

- *Sector-wise the majority of the global anthropogenic releases of Hg to aquatic systems are relatively equally distributed between ore mining and processing (41%) and waste treatment sectors (42%), followed by energy sectors (16%). The relative contribution of sectors within individual regions varies widely and depends on the technological and socio-economic status of the region. For example, releases resulting from ASGM, the sector considered the major single current anthropogenic source of Hg to aquatic systems, occur primarily in South America (53%) and East and South East Asia (36%).*

- *In future assessments of aquatic Hg releases, it is reasonable to expect that additional releases may arise from sectors and activities not quantified in the 2015 inventory due to the lack of information that would enable a reliable global quantification, or from smaller anthropogenic sources not currently detailed in the global inventory work.*

- *Uncertainties associated with release estimates for 2015 are still large and are mainly the result of either unavailable or unreliable/inconsistent information on global-scale sector-specific production rates, waste-water generation, treatment practices.*

6.1 Introduction

This chapter is an extension to work on the global inventory of air emissions discussed in Chapter 3. The results presented are an attempt to compile a comprehensive global inventory of releases of mercury (Hg) to water from anthropogenic sources for which sufficient information is available. The work builds on, updates and extends the aquatic Hg release inventory prepared as part of the UNEP global mercury assessment 2013 (GMA2013) (AMAP/UNEP, 2013).

This is the second time only that the GMA has an aquatic release section. The first time was in 2013, and this version is an updated and extended version of that. The general lack of data in the literature on Hg releases to aquatic systems and related information needed to estimate releases (e.g., wastewater quantities) still limits the accuracy and completeness of such estimates. As a result, the methodology is largely driven by the type and amount of information available for the different source categories. Part of this work is directly linked to the air emissions inventory work and applies factors employed in the UNEP Toolkit (UN Environment, 2017b,c) that are used to derive releases to water from sectors responsible for emissions to air. Some newly evaluated releases from sectors not covered by the UNEP Toolkit or in Chapter 3, but which are recognized as relevant with respect to releases to water, are addressed using independent methods and assumptions.

To the extent possible, the estimates presented in this chapter are compared with available national and other estimates/inventories of releases to water. Because information regarding global releases of Hg to aquatic systems is still incomplete, a substantial proportion of this chapter is devoted to discussion on data sources and their availability, data gaps and associated uncertainties, and the different methods for estimating releases (see the electronic E-Annex 6: *Methodology for estimating mercury releases to water* for further details).

The focus of this chapter is on Hg released from current primary anthropogenic sources to adjacent freshwater systems. It should be noted that this inventory does not represent the total global load of Hg to aquatic systems. Thus, in addition to primary anthropogenic sources for which lack of information prevented reliable quantification, releases associated with leaching and runoff of legacy Hg accumulated in terrestrial environments can also be important contributors. Moreover, significant quantities of the Hg that is currently being released to land and waste pathways from primary sources have the potential to end up in nearby aquatic systems. While the magnitude and relative importance of primary Hg releases to land is discussed for some sources for which information exists, the associated secondary aquatic releases are not quantified here. In this chapter, the relative contribution and significance of the sources quantified are assessed by comparing inventory results with the magnitudes of sources and pathways of other components of the global Hg cycle as previously established (see Section 6.3.5).

In contrast to air emission estimates (Chapter 3), the numbers presented here do not necessarily correspond to the year 2015. For example, the underlying assumptions for estimating Hg releases associated with industrial wastewaters are based on information corresponding to the latest available information, while releases from point sources were derived from atmospheric inventory data for 2015 presented in Chapter 3.

Inventory results for individual release sectors are summarized and discussed according to sub-continental regions. The purpose of this regionalization is comparability with the air emissions inventory.

The fate of terrestrial Hg once entering aquatic systems will largely depend on the site-specific environmental conditions governing its transport and the transformation processes taking place within catchments. Climate change can also influence processes controlling the mobility of terrestrial Hg and its delivery to aquatic systems, especially in sensitive ecosystems

such as the Arctic (AMAP, 2016). Nevertheless, these aspects are not addressed in the present inventory as the focus of this chapter is on the quantification of releases only.

6.2 Estimating global anthropogenic Hg releases for 2010–2015: Methodology

A key component of this work to update the GMA2013 (AMAP/ UNEP, 2013) is the production of a new global inventory of primary anthropogenic Hg releases to aquatic systems. This new inventory has the target year of 2015 – but recognizing that the necessary information may not yet be available for all countries and release categories the basis for most of this new inventory is the latest available data, which mostly fall within the 2000–2015 period.

6.2.1 Methodology for estimating releases

Releases of Hg at the plant/facility, national, regional and global level are estimated using various methods. The approaches used and underlying assumptions depend on the data available. Assumptions have been validated to the extent possible. For reasons of transparency, details of the approaches and assumptions made in deriving the estimates are given in E-Annex 6 (the electronic annex assciated with this chapter) and summarized in the following sections. In general, they fall under one of the three main groups shown schematically in Figure 6.1.

Group 1: This group comprises sectors covered by the UNEP Toolkit (chlor-alkali industry, oil refining, large-scale gold production, non-ferrous metal production) and for which the Toolkit (UN Environment, 2017b,c) provides 'distribution factors' (DFs) that proportionally 'distribute' total Hg releases between emissions to air and releases to water and land.
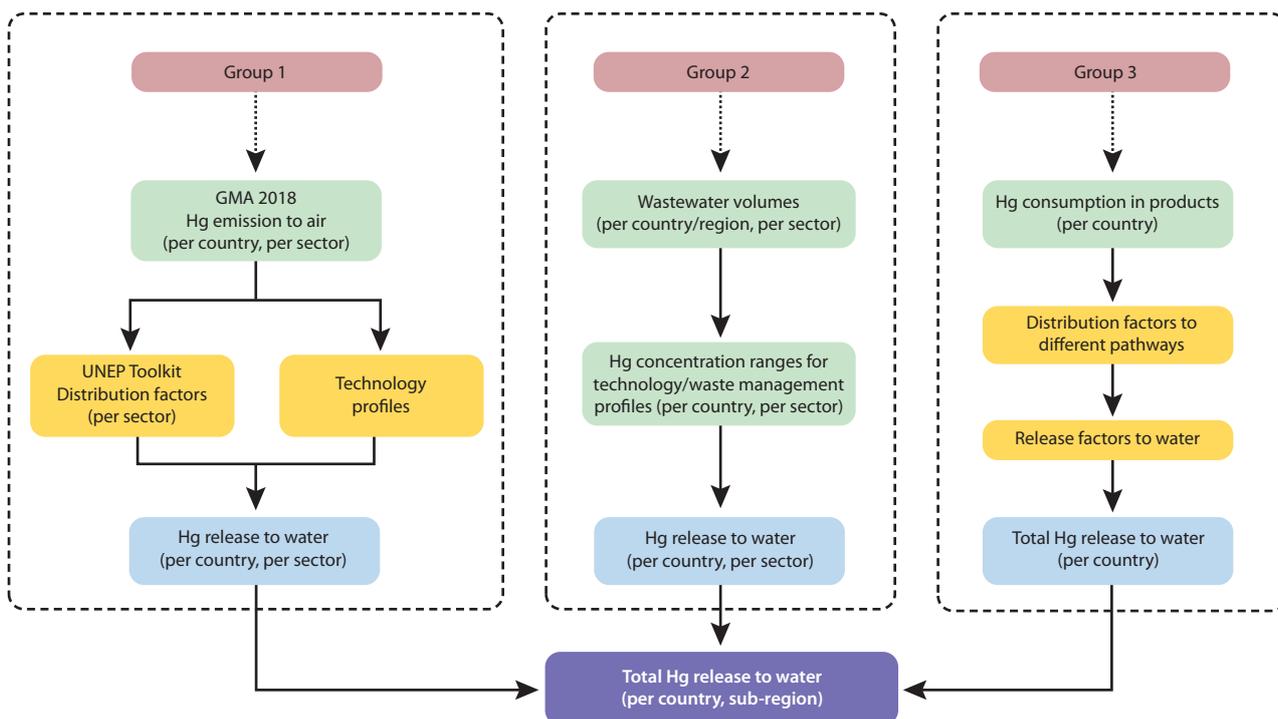
Figure 6.1 Methodology for estimating anthropogenic Hg releases to aquatic systems.

These DFs are used here together with the most recent GMA atmospheric Hg emission inventory (see Chapter 3) to estimate the corresponding releases to water. Sectors in this first group are those included in the 2010 GMA inventory. However, in contrast to the 2010 inventory where DFs were directly adopted from the UNEP Toolkit, in the 2015 GMA inventory country/group-specific abatement profiles used to derive atmospheric emissions were taken into account and the DFs adjusted accordingly (see E-Annex 6 for details).

Group 2: This group comprises sectors for which estimates were derived based on measured Hg concentrations reported in the literature for selected case studies, and associated volumes of wastewater released and other relevant activity data. Following the approach of Liu et al. (2016) to develop an aquatic Hg release inventory for China, sectors considered important in terms of their relative contribution and included in this inventory are: Hg releases associated with produced municipal wastewater, wastewater from coal-fired power plants and coal washing. All sectors listed under Group 2 are new additions to the global inventory and were not addressed in the 2010 GMA inventory.

Group 3: This group covers Hg releases from wastes associated with the use of Hg-added products: batteries, measuring devices, lamps, electrical and electronic devices, and other uses. Releases are estimated using an approach comparable to that applied to calculate emissions to air (see Chapter 3, Section 3.2 and E-Annex 3 for details), adjusted to aquatic Hg fate. The model used considers regional patterns of consumption of Hg and Hg-added products and initially distributes Hg in products to different pathways using DFs. Releases to water are then assumed for breakage during use, waste recycling and from leaching of landfilled waste, using fate-specific release factors (see E-Annex 6, Section A6.5 for details). This is a new methodological approach, as releases from the use of Hg-added products in the 2010 GMA inventory were derived using the UNEP Toolkit distribution factors approach.

Estimates of Hg releases for all sectors were initially made at the country level, because the majority of input data used are country-specific. Technology and waste-management profiles for individual countries were used to select Hg concentration ranges and other related activity data. Based on the country-level information, Hg release estimates were then summarized according to sub-continental regions, using the same regionalization as for the air emission inventory.

6.2.2 Sectors and activities

6.2.2.1 Sectors and activities quantified in the inventory

Selection of the sectors and activities for the aquatic inventory is driven by previously established knowledge and assumptions about their relative importance, while their categorization depends mainly on the data and type of information available for individual sector/activity. To the extent possible, categorization was kept comparable with that used for the air emission sectors. The release estimates in the 2015 inventory correspond to the following ten sectors:

- Production of non-ferrous metals (primary production of aluminum, copper, lead and zinc) (O1)

- Production of mercury metal (O2)

- Production of gold from large-scale mining (O3)

- Mercury releases from oil refining (E1)

- Production of gold from artisanal and small-scale gold mining (O4)

- Mercury releases from the chlor-alkali industry (Hg cell technology) (W1)

- Mercury releases from Hg-added products (batteries, measuring devices, lamps, electrical and electronic devices and other uses), use and waste disposal (W2)

- Mercury releases with municipal wastewater (W3)

- Mercury releases from coal-fired power plants (E2)

- Mercury releases from coal washing (E3)

In broader terms these release sectors can be subdivided into three general categories: ore mining and processing (O), energy (E) and waste treatment and disposal (W). The first seven items on the list were included in the 2010 GMA inventory; of these, the first four (O1, O2, O3, E1) are associated with by-product or unintentional Hg releases and the latter three (O4, W1, W2) with intentional uses of Hg. The last three sectors (W3, E2, E3) are new additions for the 2015 GMA inventory and comprise categories for which Hg releases to aquatic systems is considered to be significant, mostly following the work of Liu et al. (2016) and their release estimates for China.

6.2.2.2 Sectors and activities not quantified in the inventory

Additional sectors and anthropogenic activities not taken into account in this inventory could also be responsible for the delivery of additional Hg to local aquatic systems. For example, the Hg release inventory for anthropogenic sources in China, identified Hg releases from the iron and steel industry, the fabrication of textiles and apparel, and the printing industry, but these accounted for <5% of total releases (Liu et al., 2016). The recent global estimates of Streets et al. (2017) also reported cumulative releases of Hg to land and water for sectors such as iron and steel manufacturing and the dental industry, but again these represent a relatively small proportion of total releases. Taking into account the relatively low importance of these sectors and the poor data availability, these sectors were not included in the 2015 GMA inventory. Other possible sources of Hg to aquatic systems omitted from this inventory include vinyl chloride monomer (VCM) production, aluminum fluoride production, cellulose-production and titanium dioxide production.

On the other hand, there are also processes associated with some of the sectors covered in the inventory that might result in additional quantities of Hg released, but which are not accounted for here due to lack of sufficient information to develop a global inventory. For example, releases during the production stage of Hg-added products (e.g., thermometers, lamps and batteries), because only releases associated with the use, disposal and recycling of these products are considered in this inventory. Similarly, the large quantities of water used during coal mining and transport (other than associated with coal washing), might also be responsible for the release of significant amounts of Hg.

6.2.2.3 Primary releases to land and waste

In addition to direct releases to air and water, releases of Hg from anthropogenic sources can follow other pathways, such as to terrestrial systems and waste disposal sites that can in the long term act as secondary sources of Hg to nearby aquatic systems. Nevertheless, detailed quantification of secondary sources was beyond the scope of this work. This assessment addresses the magnitude and relative importance of primary Hg releases to land and waste for some sectors for which information is available.

For the Group 1 sectors for which water release estimates are based on distribution factors provided by the UNEP Toolkit, primary releases to land and waste are also derived using the same approach (see E-Annex 6, Section A6.1 for details). In addition to the three environmental media that receive Hg directly (air, water, land/soil), the UNEP Toolkit also considers three intermediate output pathways – products, general waste and sector-specific waste treatment. By definition, 'products' as an output pathway are Hg-containing by-products sent back into the market and cannot be directly allocated to environmental releases; the 'general waste' pathway comprises the mass of general waste that undergoes a general treatment (e.g., incineration or deposition) under controlled circumstances; while the 'sector-specific waste treatment' pathway covers waste from industry and consumers that is collected and treated in separate systems, and in some cases recycled (UN Environment, 2017b,c).

Some of the information on Hg releases to terrestrial ecosystems is available as part of independent global and country-level estimates. These estimates use different approaches and assumptions to follow various environmental pathways of Hg, and are broken down into a diverse combination of sectors where Hg is/was intentionally or unintentionally used and/or present in products and processes, which makes comparisons difficult. For example, Streets et al. (2017) estimated combined releases to water and land as part of the estimated all-time total Hg released to the environment by human activities globally up to 2010. For commercially-used Hg, Horowitz et al. (2014) quantified global time-dependent historical releases to different

environmental reservoirs including air, water, soil and landfill. Lin et al. (2016) used a similar method based on a mass-balance material flow-model of Hg with air, water, soil, landfill and Hg reclaimed by recycling as final environmental fates for intentional use of Hg in China. In addition to quantifying Hg releases from municipal sewage to aquatic environments in China, Liu et al. (2018a) also evaluated the associated Hg releases to other sinks including landfill, cropland, urban areas, natural land and the atmosphere.

6.2.3 Sources of data and information used in the inventory

The primary sources of data and information used in the production of the release inventory are shown in Table 6.1. This section briefly summarizes the data and information used to produce the estimates.

Group 1 sources: For release categories using UNEP Toolkit distribution factors (chlor-alkali industry, oil refining, and large-scale gold and non-ferrous metal production), respective air emissions developed in Chapter 3 were used as input data for calculating the corresponding releases to water. For the artisanal and small-scale gold mining (ASGM) category, releases are discussed based on the amounts of Hg used in these activities and practices employed in individual countries (discussed in detail in Chapter 3, E-Annex 3, Section A3.2).

Group 2 sources: Information on amounts of municipal wastewater generated and its treatment practices in individual countries were used for estimating Hg releases associated with municipal sewage. Amounts of municipal wastewater were mostly from AQUASTAT (the FAO's global water information system), while national wastewater treatment practices were from Malik et al. (2015). For countries with no data, general regional averages were adopted based on data from Malik et al. (2015) and the UN (WWAP, 2017). Mercury concentration ranges for treated and untreated wastewater were selected based on ranges typically reported in the

Table 6.1 Primary sources of activity and other related data used to derive Hg release estimates.

Release category	Activity data[a]	Distribution/release factors[a]	Hg content[a]	Other
Non-ferrous metal (Cu, Pb, Zn, Al, Hg, large-scale Au) production	GMA 2015 air emissions[b]	UN Environment, 2017b,c	-	
Chlor-alkali industry	GMA 2015 air emissions[b]	UN Environment, 2017b,c	-	
Oil refining	GMA 2015 air emissions[b]	UN Environment, 2017b,c	-	
Artisanal and small-scale gold mining	Artisanal Gold Council	Artisanal Gold Council / UNEP Partnership on Reducing Mercury in ASGM	Artisanal Gold Council / UNEP Partnership on Reducing Mercury in ASGM	See E-Annex 3, Section A3.2
Municipal sewage	FAO, 2016	-		Malik et al., 2015; WWAP, 2017
Coal-fired power plants	Liu et al., 2016; GCPT, 2017	-	Liu et al., 2016	Biesheuvel et al., 2016
Coal washing	Enerdata, 2016; EIA, 2017	Liu et al., 2016; UN Environment, 2017b	See E-Annex 3, Section A3.6.1 and A3.6.2	ENM, 2016; DTI, 2001
Use of Hg-added products and waste disposal	UN Environment, 2017a	Lin et al., 2016; UN Environment, 2017b	-	

[a]See E-Annex 6, Sections A6 to A6.5; [b]see Chapter 3.

literature, and taking into account the waste management profile of individual countries (see E-Annex 6, Section A6.1 for details).

Releases associated with wastewater from coal-fired power plants were estimated based on the amounts of wastewater generated per MWh of energy produced, as estimated from data presented by Liu et al. (2016). The Hg concentration ranges applied were taken from the same source. Realized total energy outputs from coal-fired power plants in individual countries were estimated from electricity generation capacities obtained from the Global Coal Plant Tracker database (GCPT, 2017) using country-specific capacity factors adopted from Biesheuvel et al. (2016).

Global releases due to coal washing are estimated using information on production rates, Hg coal content, the Hg-removal efficiency of coal washing, and coal washing rates. Activity levels of raw coal production for individual countries were obtained from the global energy statistical yearbook (Enerdata, 2016), and information on the type of coal produced was obtained from international energy statistics (EIA, 2017). The Hg content of various coal types was selected based on ranges reported in the scientific literature (see Chapter 3, E-Annex 3, Section A3.6), coal washing rates in major producing countries were adopted from Energy News Monitor (ENM, 2016) and Hg removal efficiency from UN Environment (2017b) and Liu et al. (2016).

Group 3 sources: Mercury releases associated with the use and disposal of Hg-added products were estimated from Hg consumption in one year for the product groups: batteries, measuring devices, lamps, electrical and electronic devices, dental applications, and other uses (UN Environment, 2017b). The same distribution factors as for air emissions were used to follow the fate of Hg through the major pathways (see Chapter 3, E-Annex 3, Section A3.3 for details). Water-specific release factors were selected and adjusted according to the waste management profiles of individual countries based on distribution factors from the UNEP Toolkit (UN Environment, 2017b) and Lin et al. (2016).

6.2.4 Uncertainties and limitations

It should be noted that, given the global scope of this assessment, there are several limitations to this work and that the estimates presented here are just that – estimates. Numbers discussed in the following sections are derived using several different approaches and various assumptions, which could introduce significant variability. However, it was beyond the scope of the present work to address this in detail.

To provide some quantification of the uncertainties associated with the 2015 GMA inventory, upper and lower range releases were produced for some sectors. For the Group 2 and Group 3 sectors, upper and lower bounds were produced using the respective upper and lower ranges of Hg concentration and associated activity data, respectively. Uncertainties related to the input data selected are further discussed in Section 6.3.2.

The potential for both double counting releases and underestimating releases is an additional limitation of this work. All sectors included in the inventory have distinctive Hg sources and their pathways are clearly identified. The exception is releases associated with municipal wastewater, which might contain a proportion of the releases counted under the Hg-added products sector; specifically releases resulting from breakage during the use pathway. This latter pathway is however a minor share, representing only 5% of releases from the Hg-added products sector. In terms of the potential for underestimation, Section 6.2.2.2 identifies several sectors and activities that are not included in the present inventory, but which might be important contributors to Hg releases at a global level. For example, sectors such as the iron and steel industry and others considered relatively less important in China (Liu et al., 2016) might be more important elsewhere. The current inventory of global anthropogenic Hg releases to aquatic systems is a work in progress, and an important step towards filling a major gap in inventories of anthropogenic Hg releases to the environment.

6.3 Estimating global anthropogenic Hg releases: Results

Given the specific nature of releases associated with ASGM (see Section 6.3.2.6 for details), results for ASGM and non-ASGM sectors are discussed separately. In Section 6.3.1, overall results are discussed on the basis of three source categories (ore mining and processing, energy sector, waste treatment) and sub-regions, while details for selected sectors are given in Section 6.3.2, including discussion of trends where possible and the associated uncertainties.

Using the methodology described above, the total inventory of anthropogenic Hg releases from sources for which there was enough information to provide quantitative estimates, is estimated at 583 t/y (ASGM not included).

6.3.1 Inventory results by region and sector

Table 6.2 and Figure 6.2 summarize the distribution of the estimated global anthropogenic Hg releases to aquatic systems according to sub-continental regions. Table 6.3 presents the same results per region on a per capita and per international dollar ($INT) basis, for ASGM and other sectors.

Table 6.2 Global anthropogenic Hg releases to aquatic systems by region. Release data rounded to three significant figures, ASGM not included.

Sub-continent	Annual release, t	%
Australia, New Zealand & Oceania	7.22	1.2
Central America and the Caribbean	22.4	3.8
CIS & other European countries	48.7	8.3
East and Southeast Asia	266	46
European Union	33.9	5.8
Middle Eastern States	16.7	2.9
North Africa	10.5	1.8
North America	32.4	5.6
South America	42.8	7.3
South Asia	55.3	9.5
Sub-Saharan Africa	47.1	8.1
Total	583	100

Table 6.3 Per capita anthropogenic Hg release to aquatic systems by region.

Sub-continent	Per capita releases from non-ASGM sectors, g	Per capita releases from ASGM[a], g	Per million $INT of GDP at PPP[b] from non-ASGM, g	Per million $INT of GDP at PPP for ASGM, g
Australia, New Zealand & Oceania	0.23	-	5.62	-
Central America and the Caribbean	0.10	0.08	7.13	5.38
CIS & other European countries	0.15	0.03	7.87	1.78
East and Southeast Asia	0.12	0.20	7.68	12.7
European Union[c]	0.07	-	1.77	-
Middle Eastern States	0.05	0.00	2.31	0.01
North Africa	0.06	-	5.08	-
North America	0.09	-	1.66	-
South America	0.10	1.56	6.56	100
South Asia	0.03	0.00	5.60	0.15
Sub-Saharan Africa	0.05	0.10	12.7	27.1

[a]To both land and water, [b]$INT-International dollar, GDP-Gross Domestic Product, PPP-Purchasing Power Parity (UN Environment, 2017a), [c]25 countries.

- Sub-Saharan Africa
- South Asia
- South America
- North America
- North Africa
- Middle Eastern states
- EU28
- East and Southeast Asia
- CIS and other European countries
- Central America and the Caribbean
- Australia and New Zealand
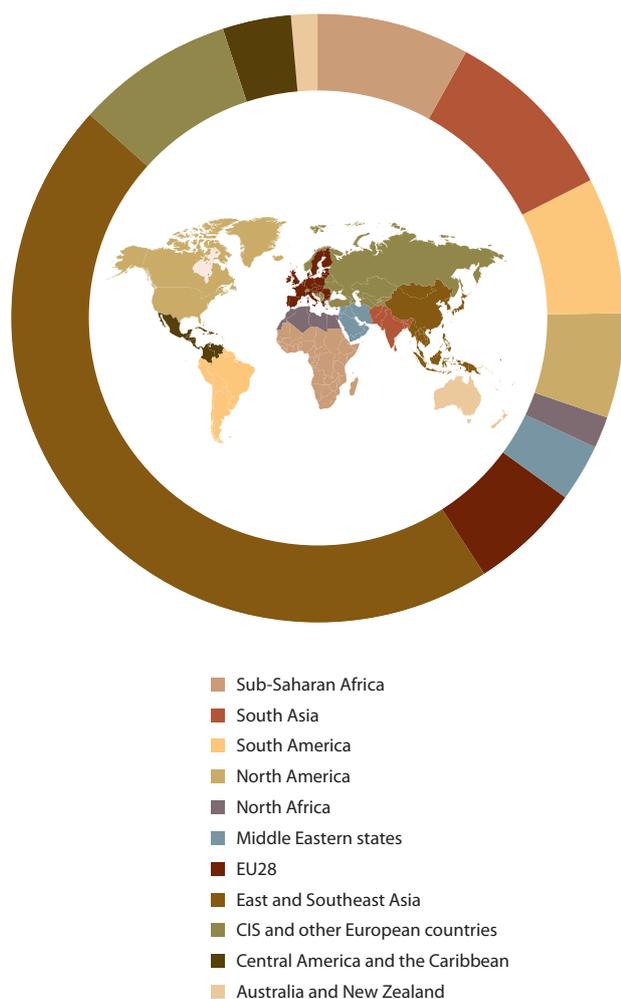
Figure 6.2 Contribution to global Hg releases to water (excluding releases from artisinal and small-scale gold mining) in 2015 from different regions.

Figure 6.3 and Table 6.4 summarize the distribution of the estimated global anthropogenic Hg releases to aquatic systems by sector. Apart from combined releases to water and land resulting from ASGM activities, the majority of the global anthropogenic releases of Hg to aquatic systems are associated with the waste treatment sectors (42%), followed by the ore mining and processing group of sectors (41%) and energy sectors (16%). Overall, the new inventory is dominated by releases from non-ferrous metal production (copper, lead, zinc, aluminum) and both waste-treatment related sectors; namely, releases from the use and disposal of Hg-added products and releases associated with municipal wastewater. These three sectors alone contribute over 70% of the total releases from all sectors included. Other major release sectors include wastewater from coal-fired power plants (10%), coal washing (7%) and production of gold from large-scale mining (10%).

In addition to methodological changes introduced to derive the estimates on releases associated with the Group 1 sectors (see E-Annex, Section A6.1 for details), the three newly added sectors (municipal wastewater, coal-fired power plants, coal washing) are driving the relatively large difference between the 2010 (185 t/y) and 2015 (583 t/y) anthropogenic Hg release inventory. However, it should be noted that compilation of the global aquatic Hg inventory including identification of new sources is an ongoing activity, and as already recognized in the 2010 GMA inventory, global releases are assumed to be underestimated due to the lack of information for some sources. In any case, both inventories cannot be directly compared. It should also be noted that the three newly added sectors have the largest associated uncertainty among all included sectors. Methodological changes and uncertainties are further discussed in Section 6.3.2.

Figure 6.4 presents the 2015 GMA inventory graphically by region and sector. This clearly shows that the relative contribution to the total global anthropogenic Hg releases to water is by far the greatest in East and Southeast Asia. This is driven by the large population and associated industrial and other activities. Because this region is a predominant source
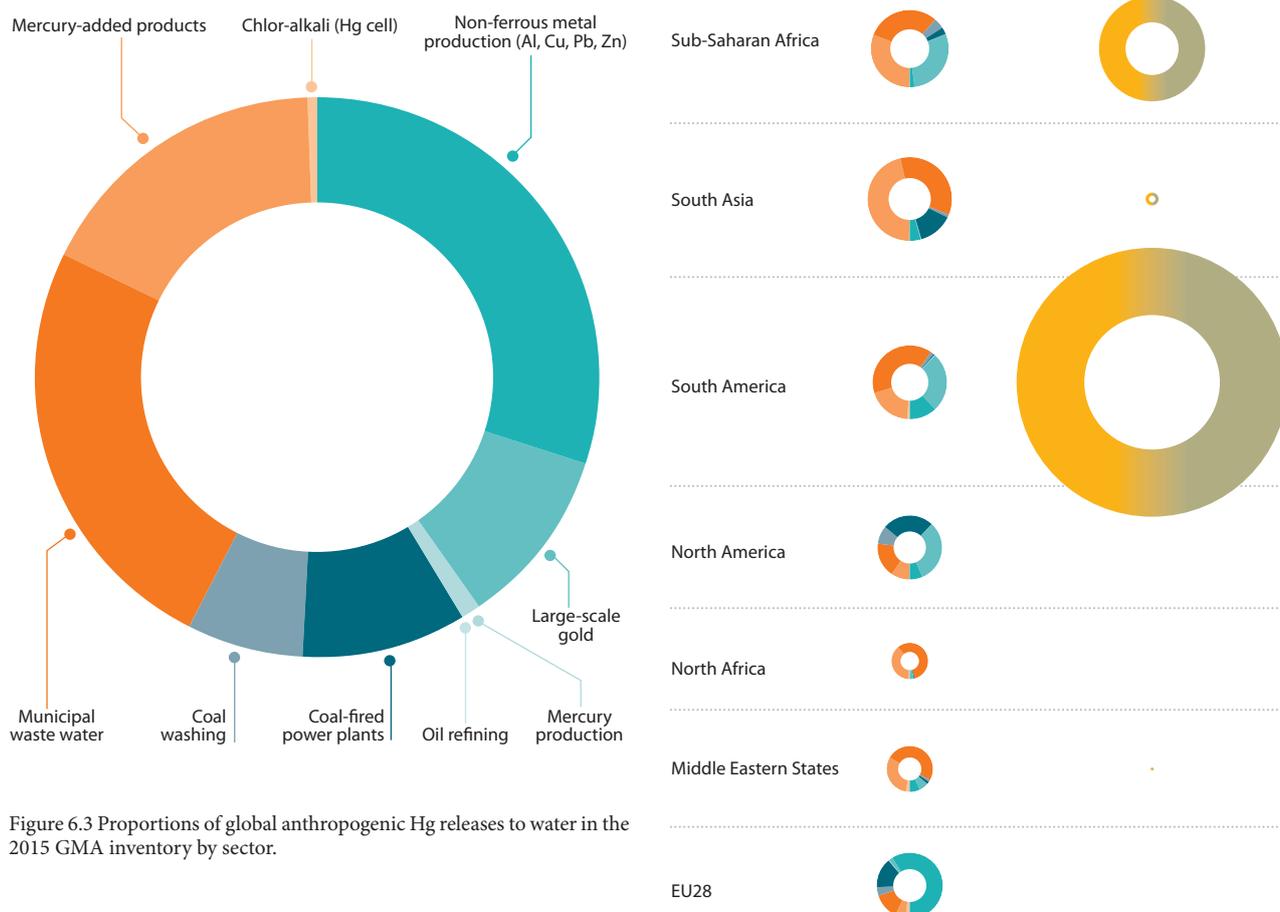
Figure 6.3 Proportions of global anthropogenic Hg releases to water in the 2015 GMA inventory by sector.

Table 6.4 Global anthropogenic Hg releases to aquatic systems by sector. Release data rounded to three significant figures.

Sector	Releases (range), t	%[a]
Production of non-ferrous metals (primary production of copper, lead, zinc and aluminum)	175	30
Production of mercury metal	5.18	0.9
Production of gold from large-scale mining	61.2	10
Mercury releases from oil refining	0.56	0.1
Mercury releases from chlor-alkali industry (Hg-cell technology)	2.70	0.5
Mercury releases with municipal sewage	145 (48.4–242)	25
Mercury releases from coal-fired power plants	55.6 (12.3–123)	10
Mercury releases from coal washing	38.0 (21.3–59.2)	6.5
Mercury releases from Hg-added products use and waste disposal	99.4 (66.5–133)	17
Total (ASGM not included)	583	100
Production of gold from artisanal and small-scale gold mining (releases to both land and water)	1221 (585–1858)	-
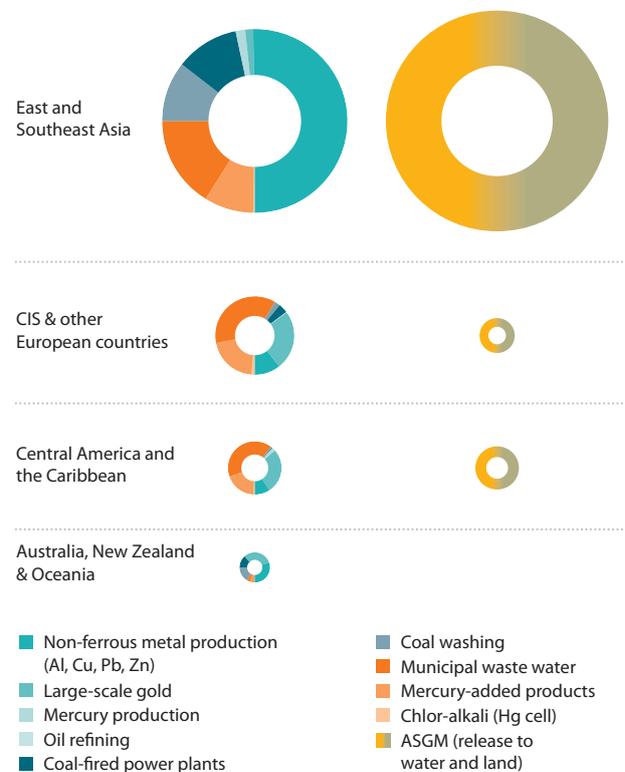
Figure 6.4 Regional pattern of global anthropogenic mercury releases to water in the 2015 inventory from different sector groups (graphs, left column), and contributions from artisinal and small-scale gold mining to releases to both water and land (graphs, right column); releases to water alone from artisinal and small-scale gold mining activities cannot yet be distinguished.

of Hg releases from most sectors, the distribution of releases between sectors reflects the global pattern.

On the other hand, the relative contributions of individual sectors are distributed unevenly between regions. For the ore mining and ore processing sectors, the majority of associated releases occur in East and Southeast Asia (59%), followed by the EU28 region (9%), South America (7%) and CIS and other European countries (7%). The contribution from energy sectors is also by far the largest in East and Southeast Asia (61%), followed by North America (12%) and South Asia (9%). In contrast to these two general groups of sectors, the contribution of releases from waste treatment sectors is more equally distributed with East and South Asia contributing 27%, followed by South Asia (18%), Sub-Saharan Africa (12%), CIS and other European countries (12%) and South America (10%).

Consequently, the relative contribution to total releases from various sectors within individual regions varies widely, reflecting differences in types of industrial activities, and the technological and socio-economic status of the region. For example, non-ferrous metal production dominates releases in East and Southeast Asia, EU28 countries and to a lesser degree in Australia, New Zealand and Oceania. In many regions, releases associated with waste streams, both from municipal wastewater and from the use and disposal of Hg-added products predominate, such as in North Africa, Middle Eastern States and South Asia. Large-scale gold production is an important contributor to releases in Australia, New Zealand and Oceania, Central America and Caribbean, North America, South America and Sub-Saharan Africa. In North America and Australia, New Zealand and Oceania releases associated with coal washing and from coal-fired power plants, respectively, are also important contributors.

6.3.2 Discussion of results for selected sectors

This section discusses Hg releases associated with the major release sectors. For sectors included in both the 2010 and 2015 GMA inventories, differences in release estimates are also addressed, as well as differences in methodology used to derive the estimates.

6.3.2.1 Non-ferrous metal production

The estimates included in the current inventory for releases from copper (Cu), lead (Pb), zinc (Zn), aluminum (Al), Hg and large-scale gold (Au) production were all included in the 2010 GMA inventory. Compared to 2010, the sum of releases from these sectors for 2015 is almost three-fold higher (242 vs. 92.5 t/y). Although there are some differences in the input data between the two inventories (see Chapter 3), the large discrepancy is mostly a result of methodological changes incorporated in the 2015 GMA inventory. Namely, country/group-specific abatement technologies were used to derive the release estimates, resulting in more releases to water when wet gas cleaning technologies dominate technology profiles (see E-Annex 6, Section A6.1 for details). Using the new approach, among the non-ferrous metal production sectors, the vast majority of releases (58%) are associated with Zn production mostly in East and Southeast Asia, followed by large-scale Au (25%), Cu (8%) and Al (5%) production. It should be noted

that some of the non-ferrous metal production installations considered here might use water pollution abatement technologies that would also decrease Hg releases. This is not addressed here and as a result some of the numbers discussed might be overestimated. On the other hand, the non-ferrous metal production sectors have considerable potential for secondary Hg releases to water, because large quantities of Hg from these sectors are distributed to land and waste, respectively (see Section 6.3.4 for details).

6.3.2.2 Municipal sewage

Releases from municipal sewage were not addressed in the 2010 GMA inventory. Estimates suggest that this sector is an important source of Hg (25%) to the global inventory. Given the input data and approach used for estimating Hg releases (details in E-Annex 6, Section A6.2), Hg releases from this sector are closely linked to water-use patterns and wastewater treatment practices in individual countries. A substantial component of municipal wastewater results from domestic water uses, as well as from commercial and industrial effluents and storm water. While developed nations have large per-capita water use and efficient wastewater treatment, developing countries have much lower per-capita water use and poorly developed wastewater collection and treatment systems (Sato et al., 2013). It is expected that population growth in developing nations will be accompanied by increased water demand and associated Hg releases in these regions. On the other hand, the global distribution and consumption of Hg-added products (as one of the most important sources of Hg for this sector) is not uniform, and will largely depend on the economy of individual countries, with more products being consumed in developed nations. Phase-out of products containing Hg under the Minamata Convention is expected to result in lower Hg releases with municipal sewage, as is the anticipated increase in wastewater treatment.

While Hg concentrations in treated and untreated municipal wastewater are relatively well documented in the literature, Hg release estimates for this sector largely depend on global water use patterns; data for which are considered the least reliable and most inconsistent of all water resources information (Gleick et al., 2014). The major limitations are lack of reporting standards, differences in approaches used to derive information on water usage, and large inconsistencies in reporting years (Gleick et al., 2014). Another source of uncertainty is the poor knowledge of country-scale wastewater treatment levels (i.e., primary, secondary, tertiary); practices that significantly influence effluent Hg concentrations. In this inventory, different Hg removal efficiencies for treated water were assigned to individual countries based on their waste management profile.

6.3.2.3 Coal industry

Releases from the coal industry have not been addressed in previous global inventories. In the 2015 GMA inventory two types of release resulting from associated water use are considered: Hg releases with wastewater from coal-fired power plants and Hg releases resulting from coal washing. Together, these are estimated to contribute 16% to the global inventory. The estimates for both types of release are considered preliminary and to have large associated uncertainties. For coal-fired power plants, this reflects the fact that information on actual profiles of installations (water use practices, treatment

and wastewater generation) is missing for most of the world's coal-fired power plants, as is information on Hg concentrations in the respective effluents. In the case of coal washing, the main uncertainties result from assumptions made regarding coal washing rates, removal efficiencies and the share of Hg reaching aquatic systems in individual countries. Estimates are therefore made based on generic assumptions described in E-Annex 6, Sections A6.3 and A6.4.

Coal-fired power plants

Coal-fired power plants are recognized as one of the major anthropogenic Hg emission sources. However, due to the lack of quantitative information, Hg releases to water from this sector were not addressed in previous inventories. Large releases reflect the fact that the coal industry is by far the greatest water-demanding activity worldwide; globally, coal-fired power plants were estimated to consume 19 billion m^3 of freshwater in 2013 (Cheng and Lammi, 2016). While the vast majority of this water is used for cooling, and is not usually contaminated by Hg, additional water uses such as for pollution control can generate large amounts of Hg-contaminated wastewater. Here, an attempt was made to quantify Hg releases associated with the latter non-cooling water-use types.

Despite many uncertainties, there is now a body of evidence based on measured and estimated data about the significance of aquatic Hg releases from coal-fired power plants. Plants using wet scrubbers are known to discharge up to tens of kilograms of Hg to local surface waters per year (EEA, 2014; EIP, 2016). In addition to discharges to surface water, even larger amounts of Hg (up to hundreds of kilograms per year) are dumped into ash ponds which are prone to leaks (EIP, 2016). In a recent aquatic release inventory for China, wastewater discharged from coal-fired power plants, although showing a gradual decline over the past decade, is still recognized as one of the most important anthropogenic sources of Hg (Liu et al., 2016). According to the European Pollutant Release and Transfer Register (EEA, 2017), Hg releases from thermal power stations and other combustion installations are the second largest source – second only to urban wastewater treatment plants. Global Hg releases from this sector, using assumptions described in E-Annex 6 (Section A6.3) and based on information available for China (Liu et al., 2016), are estimated to be in the 12–123 t/y range. An alternative to this approach is an estimate based on simple global upscaling of the ratio of anthropogenic Hg released to water and air for China for this sector, which is approximately 1:4. This would result in a global release of 50–110 t/y, which is a range comparable to the first approach.

Coal washing

Large amounts of water are used during coal mining and washing. The latter is used to remove impurities and ash from the coal and results in the generation of a slurry of toxic material (Cheng and Lammi, 2016). In the absence of detailed information, the approach used here is similar to that of Liu et al. (2016) and results in a preliminary estimate of the likely magnitude of global Hg releases due to coal washing based on global coal production, coal Hg content, assumed Hg removal efficiencies, washing rates and environmental fate in individual countries (see E-Annex 6, Section A6.4 for details). Given that coal washing results in a higher caloric value of coal and consequently a higher economic

value, coal beneficiation is increasing worldwide. Available information suggests that a higher share of the coal produced is treated in more developed countries but is also increasing in developing economies (Budge et al., 2000). Estimates available for China, the major global coal producer, indicate a rapid increase in Hg releases from coal mining and washing with an annual average growth rate of 25% in the 2001–2012 period, making this sector the second largest anthropogenic source of aquatic Hg in China (Liu et al., 2016). Overall releases from this sector are largely dominated by releases from China (>60%), followed by other important coal producing countries such as the USA, South Africa, Australia and Indonesia. In addition to high uncertainty in the approach and sensitivity of all input information used to derive these estimates, these numbers are obtained based on gross assumptions regarding the environmental fate of Hg once washed from coal. It should also be noted that releases can occur during mining operations or later before the actual use of coal, such as at sites where coal-fired power plants are located. Nevertheless, even greater quantities of Hg (up to tens of tonnes per year) are assumed to accumulate in slurry ponds at coal washing sites globally, representing a significant environmental hazard for local aquatic systems since these ponds are often prone to leakage (Cheng and Lammi, 2016). Moreover, coal-washing practices result in millions of tonnes of coal-washing products, and in China for example, a significant share of these by-products is reported to be re-used for various industrial and domestic purposes, and from which secondary emissions and releases can occur (Zhao and Luo, 2017).

6.3.2.4 Oil industry

Mercury releases from oil refining were included in the 2010 GMA inventory. Given that oil refineries processed similar amounts of crude oil in 2015 as in 2010, and that the same method was used to estimate releases, differences between the two inventories are negligible. In addition to oil refining, there are Hg releases associated with the discharge of produced water during crude oil and gas extraction, as well as the transportation of oil and gas. According to a preliminary assessment made by the International Petroleum Industry Environmental Conservation Association (IPIECA, 2016), Hg releases with produced water during oil production are 13.5 t/y globally, with the vast majority (~90%) of releases occurring offshore. It should be noted however, that this estimate is based on very generic assumptions and that additional work is needed to better quantify these releases.

6.3.2.5 Hg-added products – use and waste disposal

The Hg-added products sector comprises releases from the following product groups: batteries, measuring devices, lamps, electrical and electronic devices, and other uses (see E-Annex 6, Section A6.5 for details). In the 2010 GMA inventory, releases for this sector were estimated based on the Hg emission inventory and by using the distribution factors from the UNEP Toolkit to calculate the corresponding releases to water. The 2015 GMA inventory adopts the model used to estimate Hg emission from waste streams associated with intentional use sectors and considers releases for three main pathways of Hg-added products: breakage during use, waste recycling and waste

landfilling (see E-Annex 6, Section A6.6). In addition to the new method used to derive the estimates, there is a change in the model input data. In the 2010 GMA inventory part of the Hg from Hg-added products (~30%) was considered as 'retained in use' and is now included in the waste streams and consequently in emission and release pathways, respectively.

The present estimates suggest significant Hg releases due to usage and disposal of Hg-added products (66–133 t/y), the vast majority (91%) being associated with uncontrolled landfilling of waste which is primarily occurring in developing countries, followed by releases during breakage (5%) and recycling (4%). Due to environmental regulations and the availability of new technologies, use of Hg in products is in decline and so are environmental releases of Hg, especially in developed countries. Substitution of Hg-added products with non-Hg containing alternatives, however, is also becoming evident in developing countries. An exception is products without adequate Hg-free alternatives such as lightning devices, which are also excluded from the Minamata Convention.

It should be noted that these estimates depend largely on estimates of regional consumption of Hg-added products. While this information is available for developed countries, little information is available on the real consumption patterns for Hg-added products in developing countries.

6.3.2.6 Artisanal and small-scale gold mining

Given that there is still not enough information and knowledge to separate terrestrial releases between water and land, releases associated with ASGM remain a 'special' sector in the inventory. The detailed reasoning for this is given in the 2010 GMA inventory (AMAP/UNEP, 2013). In summary, Hg releases are based on amounts of Hg used in ASGM activities and the characteristics of the mining practices applied in individual countries. The methodology used differentiates between emissions to air and releases to both land and water (see Chapter 3, E-Annex 3, Section A3.2 for details and example calculation). At present, it is not possible to directly determine the proportion of Hg associated with this latter pathway that will enter the hydrosphere. In addition to the direct losses occurring during ore amalgamation, large quantities of Hg are continuing to accumulate in the soils and sediments surrounding ASGM sites. This accumulated Hg has the potential to be remobilized and enter aquatic systems, however with a time-lag usually unknown, depending largely on site-specific environmental conditions. It is estimated that ASGM releases to water and land in 2015 were 1221 t/y (range 585–1858 t/y). The vast majority of these releases are occurring in South America (53%), East and Southeast Asia (36%) and Sub-Saharan Africa (8%), while other regions where ASGM activities are undertaken – Central America and the Caribbean, CIS and other European countries, South Asia and Middle East – contribute a minor share to the total.

6.3.3 Comparison of estimates with independent inventories and approaches

Compared to air emission inventories, there are fewer national inventories of Hg releases to water available for comparison with the GMA 2015 estimates. Furthermore, available inventories are typically based on different input data using different assumptions and approaches, and are broken down into various combinations of sectors. As a result, direct comparisons are not usually possible and comparisons must be discussed in a qualitative sense only.

For several European countries, the European Pollutant Release and Transfer Register (E-PRTR) provides a publically available resource that includes nationally reported values for Hg emissions to air and releases to water and soil, as well as off-site transfers of waste. It reports pollutant emissions and releases from over 30,000 industrial facilities in EU Member States, as well as Iceland, Liechtenstein, Norway, Serbia and Switzerland (UN Environment, 2016). It should be noted that the E-PRTR applies a relatively high mandatory reporting requirement for Hg of 1 kg Hg/y (at a given facility). This threshold means that not all industrial facilities with Hg emissions and releases report to the E-PRTR although some with emissions/releases below this threshold report on a voluntary basis. For the EU28 countries, total Hg releases to water reported in the E-PRTR for 2015 are an order of magnitude lower than those estimated here (3.5 vs. 34 t/y). However, the relative contribution of sectors is similar. With the exception of NFMP sector, municipal sewage and thermal power stations dominate the releases in both inventories.

Canada, Mexico and the USA report data on emissions and releases of various pollutants including Hg to the North American Pollutant Release and Transfer Register (NA-PRTR). Data from 2006 to 2013 are available for states, provinces and territories at different levels of detail (www.cec.org). As for the E-PRTR, on-site surface water discharges for North America (USA and Canada) as reported in the NA-PRTR are substantially lower than the estimates for the North America (0.7–1.6 vs. 32 t/yr). Dominant sectors in the NA-PRTR register vary from year to year, and include paper and food manufacturing sectors not included here, while mining and electric power generation are recognized as important contributors in both inventories.

In addition to nationally reported inventories, there are other independent global inventories where releases of Hg to water are considered to some extent. For example, present-day releases from commercial Hg use to water globally, as estimated by Horowitz et al. (2014) are comparable in magnitude with releases in the 2015 GMA inventory from comparable sectors, despite differences in the methodology used to derive the estimates. Similarly, sectors included, and their relative importance as indicated in the 2015 GMA inventory are to a large extent comparable to those considered currently important globally by Streets et al. (2017), although it should be noted that in their work they estimate combined releases to land and water (see section 6.3.4 for details).

More detailed country-level inventories, including estimates for releases to water are becoming available as countries prepare these data as part of their commitments under the Minamata Convention. At the time of preparing the GMA estimates, few Minamata Initial Assessments (MIAs) had been finalized and thus most were not available for comparison.

6.3.4 Potential secondary sources of aquatic Hg releases

In addition to direct emissions/releases to air and water, respectively, for some of the sectors discussed here pathways to other environmental media can be equally if not more important. In this work, primary global releases of Hg to land, waste and

sector-specific storage/treatment are estimated for Group 1 sectors using the UNEP Toolkit distribution factors. Using this approach, sectors contributing directly to land/soil are large-scale Au mining, primary Hg production and the chlor-alkali industry with ~2700, ~60 and ~16 t of annual Hg releases globally. Compared to releases to water, releases to land/soil from these sectors are 45-, 12- and 6-fold higher, respectively, and all this Hg initially released to land/soil acts as a potential secondary source of aquatic as well as atmospheric Hg. Large amounts of Hg being released as a general waste are also associated with Al production (~76 t/y), while even larger quantities are subject to sector-specific waste treatment, with the vast majority associated with Zn production (~4200 t/y), followed by VCM production (~870 t/y), Cu production (~490 t/y), the chlor-alkali industry (~190 t/y), Al production (~12 t/y) and oil refining (~8 t/y). The fate of Hg associated with this latter pathway remains largely unknown, as facility-specific information is usually lacking and so it is not possible to estimate the share of Hg that ultimately reaches particular environmental compartments. In case of the VCM industry for example, the largest user of Hg in China, Lin et al. (2016) estimated that ~75% of all Hg used will end up as sector-specific waste of which 80–90% will be recycled with the rest equally distributed between air, water and landfill.

Large amounts of Hg secondary releases are also expected from wastes associated with the use of Hg-added products. For example, out of ~1200 t/y of Hg consumed on average globally for batteries, measuring devices, lamps, electrical and electronic devices, and other uses, only ~260 t/y are estimated to be emitted/released directly to atmosphere and water, respectively (see Section 6.3.2.5 Chapter 3, E-Annex 3, Section A3.3 for details). Thus ~940 t/y of Hg subsequently end up in the waste stream and can be subject to later remobilization, as it is estimated that only 6% of this amount is collected for safe storage globally and for which no further emissions/releases are expected to occur.

Other sectors can also contribute significant amounts of Hg to terrestrial environments, but are currently not covered in global inventories because the distribution factors that would enable estimates of the releases do not exist for these categories. One such example is releases associated with municipal sludge where it was established by Liu et al. (2018a) that in contrast to some other sectors, terrestrial environments can be the major sink of Hg. According to their material flow analysis for 2015, around 120 t or 77% of all Hg from municipal sewage in China was released to land. Similarly, as discussed in Section 6.3.2.3, large primary releases of Hg to terrestrial systems can result from disposal of Hg-containing waste in the form of ash (coal burning) and slurry ponds (coal washing), and the ultimate environmental fate of which is still unknown.

It should be noted however that in contrast to air emissions, it is extremely difficult if not impossible to fully separate the releases between land and water, either primary or secondary ones. According to Streets et al. (2017), this is mostly because information on how waste is/was disposed of is lacking for most installations. As a result, Streets et al. (2017) reported cumulative releases to land and water as part of their all-time total historic releases and which are now estimated to reach 7000−8000 t/y. Due to differences in sectors covered and methodological approaches to derive the estimates, a direct comparison of the results is not possible, however summing releases to water, land and waste for the sectors discussed above results in a value comparable in magnitude to that of Streets et al. (2017). With

the exception of Zn production which dominates cumulative releases in the UNEP Toolkit approach, the relative contribution of individual sectors is also comparable with releases from large-scale Au mining, ASGM, use and disposal of Hg-added products and NFMP prevailing.

6.3.5 Inventory in the context of the global Hg cycle

Assessing the contribution and significance of aquatic Hg releases quantified in this chapter in the global context is not straightforward for several reasons. As well as the uncertainties emphasized above, it should be noted that the inventory is still incomplete and it is not possible to assess the global relevance of the missing sources with confidence. Moreover, for the largest current global user of Hg – the ASGM sector – terrestrial releases cannot be separated in terms of those to land and to water. Nevertheless, the magnitude of aquatic Hg releases indicate that these could be a substantial contributor to the terrestrial part of the global Hg budget.

When the sum of the non-ASGM water releases is compared with the magnitude of non-ASGM atmospheric emissions from Chapter 3, this generates a ratio between releases to water and air of about 1:2 (~600 vs. 1400 t/y). This is comparable to the water/air ratio assessed for global releases in 2010 associated with the intentional use of Hg in commercial products and processes (Horowitz et al., 2014), and so increases confidence in the present estimates derived with a different methodology.

Primary anthropogenic sources quantified in this chapter may contribute Hg amounts to freshwaters that are similar to or greater than those being delivered via atmospheric deposition. Only a small fraction of the terrestrially-deposited Hg from air (globally estimated at 3600 t/y, see Chapter 3) will reach waterbodies whereas the anthropogenic releases estimated in this chapter may directly enter freshwaters. Moreover, evidence shows that primary releases to land and solid waste from anthropogenic sources can be substantial compared to direct releases to water and, depending on the sector, can contribute hundreds of tonnes of Hg per year to terrestrial ecosystems. Following remobilization and revolatilization, these latter sources have the potential to act as secondary sources of Hg to both air and water (Amos et al., 2013).

Globally, releases of Hg to freshwater and terrestrial systems are becoming increasingly important, as the use of emission abatement technologies has resulted in a shifting trend from primary atmospheric emissions to revolatilization of legacy Hg from land and water (Streets et al., 2017). Based on the recent work of Streets et al. (2017), cumulative global releases to land and water are currently estimated at 7000–8000 t/y.

How much of the Hg released from individual anthropogenic sources directly reaches aquatic systems is usually unknown, because this depends on the waste disposal practices of individual facilities, information which is largely lacking. Similarly, the time-lag between the releases to water/land and later remobilization within catchments, and ultimate discharge to coastal waters, is mostly unknown. Nevertheless, from a global perspective it is clear from the magnitude of the estimated inventory that primary anthropogenic Hg releases to waterbodies are likely to have a significant impact on Hg concentrations in many freshwater systems, upon which a large proportion of the world's population depends.

6.4 **Conclusions**

A new global inventory of aquatic Hg releases has been prepared as an extension to the global inventory of air emissions. This is only the second time that a global inventory of aquatic Hg releases has been included in the Global Mercury Assessment, and as such the current inventory is still a work in progress. Improved approaches have been developed to fill some of the existing gaps in the inventories of anthropogenic Hg releases to the environment, with the intention to better characterize differences between countries and sector-specifics in terms of technologies and practices applied. Moreover, the new inventory includes some new source categories relevant for aquatic releases that were not included in the 2010 GMA inventory. This makes the 2015 GMA inventory more complete. On the other hand, it is recognized that additional releases may arise from sectors and activities not quantified in the current inventory, for which lack of information is preventing a reliable global quantification of associated releases. While some of these non-included sectors are considered less important in terms of their relative global contribution to aquatic systems (e.g., iron and steel manufacturing, dental industry), secondary releases resulting from remobilization of Hg initially released from industrial installations to terrestrial systems might be a significant contributor. The magnitude and potential importance of such releases was evaluated for some sectors by quantifying primary releases to land and solid waste streams from relevant facilities using the distribution factors provided by the UNEP Toolkit.

Global releases of anthropogenic Hg to freshwater, excluding ASGM, based on revised estimates are 583 t/y, compared to 180 t/y in the 2010 GMA inventory. The main sectors identified as sources of anthropogenic Hg releases to water are non-ferrous metals production and releases associated with municipal sewage, followed by the disposal of Hg-added products and releases from the coal industry. However, although not directly comparable – because combined releases to land and water are estimated for this sector – ASGM is still considered the major single anthropogenic source of Hg to aquatic systems. Some other industries also release substantial amounts of Hg – of the order of tens to hundreds of tonnes per year – either directly to soil/land (such as large-scale Au and primary Hg mining) or to various waste streams (such as for Zn production, VCM production, Cu production and the chlor-alkali industry).

Many knowledge gaps were recognized when compiling this new inventory. These need filling to decrease the still large uncertainties associated with these estimates. The knowledge gaps are as follows.

- While levels of Hg associated with individual sectors included in the inventory are relatively well established, all other supporting information (such as production rates, wastewater generation, treatment practices etc.) is more unreliable and inconsistently reported, and drives uncertainty in the estimates. Better information is needed on coal washing practices and the fate of Hg during water uses in coal-fired power plants, in particular.

- Some of the uncertainty concerns a lack of knowledge about the environmental fate of Hg once it has been released from anthropogenic sources. In the current inventory only the air emission abatement technologies were considered. However,

in installations where water abatement technologies are used, these would decrease Hg releases to water and increase the share of Hg following sector-specific waste pathways. In the absence of facility-level information, current releases for relevant sectors might be overestimated. On the other hand, there may be substantial secondary releases resulting from Hg initially released to terrestrial pathways, but without detailed knowledge of processes controlling the time-lag between release and later remobilization into water, quantifying associated releases is not possible. One way to investigate these processes and their importance in the global Hg cycle is to use biogeochemical cycling models.

- Additional sectors and anthropogenic activities, not taken into account in this inventory (see Section 6.2.2.2), should be included in future inventories. Although recognized in this work as less relevant in the global context, some of these sources might be significant contributors of Hg to local aquatic systems.

- Estimates in the 2015 GMA inventory are made based on country-level information. Future work would benefit from inclusion of more detailed facility-level information to improve the spatial component of this work. This should include more detailed knowledge of differences in technologies used, waste treatment practices and Hg consumption patterns in individual countries. Some of the information needed will be available through work under the Minamata Convention, because each Party is required to identify relevant sources of releases and establish inventories of Hg releases from such sources.

- There is a need to harmonize methodological approaches for estimating Hg releases, for example something along the lines of the UNEP Toolkit approach for air emissions but focused on aquatic Hg releases. Similarly, a reduction in uncertainties for all sectors included in the inventory is needed by using more systematic and harmonized approaches in data collection. As well as improving information on Hg content, information on related activity data is also needed to derive the estimates.

- Although beyond the scope of this chapter, a lack of knowledge regarding the fate of Hg once released from the source is recognized as a limiting factor for placing inventory results in the context of the global Hg cycle. Future work should focus on establishing relationships between catchment characteristics, sources within individual catchments, and Hg outflows. Techniques such as isotope tracer experiments and isotope ratio measurements of Hg are now available to address these issues.

Chapter 6 E-Annex:
Methodology for estimating 2015 mercury releases to water

Given the global nature of the inventory and general lack of data/information on aquatic Hg releases and associated information, assumptions had to be made to derive the estimates presented in this work. These assumptions are often difficult to validate. For reasons of transparency, details on data/information and assumptions made within individual release category are given here.

A6.1 Methodology for estimating Hg releases to water, land and waste streams for Group 1 sectors

The following sectors for which the UNEP Toolkit provides 'distribution factors' (DFs) for water are included in Group 1: chlor-alkali industry, oil refining, large scale Au and non-ferrous metals production. Water releases for these sectors are estimated using water/air DF ratios as scaling factors together with the GMA atmospheric Hg emission inventory for which details regarding data compilation and the derivation of emissions are given in Chapter 3 and E-Annex 3, Sections A3.1 to A3.6.

For the sectors where abatement is considered for calculation of atmospheric emissions, country/group specific abatement profiles are considered and the DFs revised accordingly, while for others DFs are directly adopted from the UNEP Toolkit. The former sectors comprise production of various non-ferrous metals (primary production of Cu, Pb, Zn and Al), large-scale Au production and the chlor-alkali industry. The methodology applied to calculate water releases involves the following consecutive steps:

1. Using information on the country-/group-specific technology profiles (reduction efficiency and percentage and application rates), total air emissions are distributed between various types of abatement technologies.

2. Using information on air emissions by abatement technology combined with the information on reduction efficiency of individual technology profiles, unabated/uncontrolled emissions to air are calculated.

3. Depending on the sector, input of Hg that is being directly (i.e., not via abatement) released to pathways other than air (non-air inputs) is calculated (see sector-specific comments below).

4. Total Hg input is calculated as the sum of unabated air emissions and non-air inputs.

5. The actual DF for air is calculated from air emissions and total Hg input.

6. Distribution factors for other pathways are revised depending on whether they are assumed to originate from the abatement technologies or considered as direct releases (see sector-specific comments below).

7. Releases to water are calculated based on reported emissions to air and revised water/air ratios. In the same way by using

appropriate DF ratios, outputs to other pathways considered in the UNEP Toolkit are estimated.

The water releases derived using the general methodological approach outlined above are based on sector-specific knowledge regarding the fate and pathways of Hg as described in more detail in the UNEP Toolkit (UN Environment, 2017b,c). In general, two types of release to water are considered – direct releases and those resulting from the abatement technologies used. Direct releases are those where Hg passes directly to water without first entering the air pathway, while abatement releases are associated with wet cleaning technologies (such as scrubbers etc.). For the latter it is further assumed that Hg is initially re-allocated from the air pathway and then subjected to other pathways including water, with the same proportions as defined in the UNEP Toolkit. Whether dry-only abatement methods or wet-based abatement dominates in each particular country and sector was decided based on technology profiles presented in Chapter 3, E-Annex 3, Section A3.6. For the purpose of these estimates, sector-specific assumptions are made, as follows.

Primary production of copper, lead and zinc: Water releases for these sectors are assumed to originate from the wet gas cleaning technologies used. No direct releases to pathways other than air are considered. The exception is Hg bound in slag which, according to data provided by Hui et al. (2017) varies from 3% to 14%, depending on the metal. The share of slag is considered a part of the sector-specific treatment which does not depend on air abatement and is kept constant in the calculations. It is also assumed that Hg once re-allocated from the air pathway is subject to water, products (including sulfuric acid produced at acid plants considered as part of the abatement) and sector-specific treatment. In cases where only dry abatement technologies are used, no water releases are considered.

Primary production of aluminum: Water releases for this sector are assumed to be the sum of direct releases and the abatement technologies used. Where wet cleaning abatement technologies prevail, Hg re-allocated from the air pathway is subject to three pathways: water, general waste and sector-specific treatment. In cases where dry or no abatement is used, the water pathway is excluded.

Production of gold from large-scale gold mining: Water releases for this sector are assumed to be the sum of direct releases and the abatement technologies used. Where wet cleaning dominates the abatement profile, Hg re-allocated from air is distributed between water and land. In cases where dry or no abatement is used, the water pathway is excluded. The share of product-bound Hg is assumed to be constant.

Chlor-alkali industry: Water releases for this sector are assumed to be direct releases, while releases to land and sector-specific treatment are assumed to be the sum of direct releases and abatement technologies used. Hg re-allocated from the air pathway is distributed between these two pathways. The share of product-bound Hg is assumed to be constant.

Primary mercury production and oil refining: For these two sectors no wet abatement technologies are considered when calculating emissions to air. Therefore, DFs are directly adopted from the UNEP Toolkit. For the primary Hg production, in addition to air emissions, releases to water and land are considered. For the oil-refining sector, releases to water and sector-specific treatment are considered.

Gaps/needs to improve methodological approach

- For the releases associated with abatement technologies used, this approach does not consider that a proportion of the Hg that is being abated by dry methods is not associated with water pathways, which in some cases may result in methodological overestimation of water releases. However, since 'dry-only' abatement technologies are in most countries less common than wet-based abatement, this issue can be neglected.

- For Cu, Pb and Zn production the DFs from the UNEP Toolkit reflect the distribution after abatement and no direct releases (except for slag) are assumed – which makes it relatively easy to calculate unabated DFs. For Al production, large-scale Au mining and the chlor-alkali industry the approach assumes that DFs from the UNEP Toolkit imply unabated emissions. Due to the lack of more detailed information regarding abatement used in DFs given in the Toolkit – those are a combination of direct releases and releases via abatement so it is virtually impossible to derive actual unabated DFs. It is therefore assumed for simplicity that DFs in the UNEP Toolkit imply no abatement.

- The approach does not consider potential further abatement of water releases. Efficient water cleaning would also affect actual DFs resulting in lower water releases and more Hg going to sector-specific treatment; however lack of data does not make such corrections possible.

A6.2 Methodology for estimating Hg releases to water associated with municipal wastewater

The 2015 inventory for Hg releases associated with municipal wastewater is based on information regarding volumes of municipal wastewater produced, wastewater treatment practices used and reported Hg ranges for concentrations measured in wastewater before (influent) and after (effluent) treatment. Municipal wastewater is defined here as water that has been used for municipal use and is afterwards released back to the environment. Treatment of this released water mostly depends on prosperity of the country concerned and thus its capacities and number of wastewater treatment plants. Most of the information for individual countries was obtained from the AQUASTAT database of the UN Food and Agriculture Organization. AQUASTAT reports amounts of municipal wastewater generated within urban areas. Since not all countries are reporting their amounts of municipal wastewater on a regular annual basis, the latest available data for each country was used. For countries with no data available, wastewater was calculated based on assumed water use per person per day. Water use averages for individual

Table A6.1 Ranges in Hg concentration in untreated and treated sewage as used to derive the estimates.

Profile	Hg in untreated wastewater, ng/L	Hg removal efficiency, %	Hg in treated wastewater, ng/L
1	100–500	95	5–25
2	300–1500	80	60–300
3	300–1500	70	90–450
4	300–1500	60	120–600
5	300–1500	50	150–750

continents were assigned to the countries with missing data: 230 for Asia (Kamal et al., 2008), 50 for Africa, 200 for Europe, 100 for Oceania and 100 l/person/day for Caribbean countries. The percentage of treated wastewater was then assigned to each country. The most recent information on treatment practices in individual countries was adopted from the global database compiled by Malik et al. (2015). For countries missing from that database, wastewater treatment data were based on regional averages as discussed by Malik et al. (2015) and a recent UN world water development report (WWAP, 2017), assuming similarities within regions and between neighboring countries. Based on these two sources, the following wastewater treatment rates were selected: 80% for the EU28 and developed countries, 50% for North Africa and the Middle East, 15% for countries in Sub-Saharan Africa, 5% for South Asia and 25% for other regions.

The magnitude of Hg releases from this sector will largely depend on the amount of Hg products used, general waste handling practices and especially the level of wastewater treatment – information lacking for most of the countries. In the absence of such information, a generic waste management profile was used and different ranges of Hg concentration were applied for untreated wastewater and wastewater treated in treatment plants, to estimate releases for an individual country. These estimates are based on the assumption that Hg concentrations in untreated wastewater are lower in more developed countries than in developing nations, as seen from values reported in the scientific literature. Furthermore, the assumption is that Hg removal is more efficient in developed countries due to higher levels of wastewater treatment (Table A6.1).

A6.3 Methodology for estimating Hg releases to water from coal-fired power plants

The 2015 inventory for Hg releases with wastewater from coal-fired power plants uses a very coarse approach for a first preliminary estimate of the global magnitude associated with this sector. In the absence of more detailed country-specific information, the approach largely relies on information available for China and work undertaken by Liu et al. (2016), by upscaling global relationships between the electricity generation capacity of coal-fired power plants, the amounts of wastewater produced and the range in Hg concentration reported in their work.

The method applied is based on an assumption that on average global water use patterns in coal-fired power plants are similar to those in China, the single largest user of coal-derived electricity in the world. Although this is a rough generalization, it is necessary to achieve a harmonized global calculation approach.

Based on wastewater volumes reported by Liu et al. (2016) and the total electricity generation capacity of coal-fired power plants in China, wastewater generation was estimated at 0.25–0.5 m³ per MWh of energy produced. For the purposes of this wastewater generation estimate, the realized energy output from coal-fired power plants was calculated using a capacity factor of 0.55 (Biesheuvel et al., 2016). To estimate wastewater generation from coal-fired power plants in each country of the world, the wastewater generation rate from China was used together with country-specific information on the total capacity of coal-fired power plants based on information from the Global Coal Plant Tracker database (GCPT, 2017). Capacity factors used for calculating the amount of energy produced in individual countries were adopted from Biesheuvel et al. (2016). The final amounts of Hg release per country were estimated using Hg concentrations in the range 5–25 mg/m³ for wastewater generated by coal-fired power plants (Liu et al., 2016 and references therein).

A6.4 Methodology for estimating Hg releases to water associated with coal washing

The 2015 inventory for Hg releases associated with coal washing is based on global coal production, coal Hg content, Hg removal efficiency and coal washing rates, similar to the approach of Liu et al. (2016).

Total coal production in 2015 for individual countries was obtained from the Global Energy Statistical Yearbook 2016 (Enerdata, 2016). In the absence of detailed country-specific information on the amounts of different coal types, regional information on coal type produced (anthracite, metallurgical, bituminous, subbituminous, lignite) was obtained from International Energy Statistics for 2014 (EIA, 2017). Regional ratios were then applied to individual countries. For countries where information on the Hg content in coals was available (as summarized in Chapter 3, E-Annex 3, Section A3.6), a country-specific average Hg content was used, whereas generic values were applied for countries for which such information was not available. Information on coal washing rates in individual countries is available for some of the world's major coal producers only and varies from <5% to 90% (ENM, 2016; DTI, 2001). For the rest of the world, it is assumed that high percentages of coal produced are being washed in developed countries and the following washing rates were assigned using technology profiles (TP) for the country concerned: 80% (TP1), 60% (TP2), 40% (TP3), 20% (TP4) and 10% (TP5). The Hg removal efficiency of coal washing is selected in the 20–30% range (Liu et al., 2016; UN Environment, 2017b). It is further assumed that only part of the Hg released during washing will reach local aquatic systems, the rest being deposited in slurry ponds. Using waste management profiles (WP) of individual countries, the following percentages for Hg reaching water courses were selected: 20% (WP1), 30% (WP2), 40% (WP3), 50% (WP4) and 60% (WP5).

A6.5 Methodology for estimating Hg releases to water from the use of and wastes associated with Hg-added products

The 2015 inventory of Hg releases to water from Hg-added products is generated using methodology comparable to that applied to estimate emissions to air (see Chapter 3, E-Annex 3, Section A3.3 for details). The approach uses regional patterns of consumption of Hg and Hg-added products. Mercury releases at various points in the life-cycle of the products are estimated using assumptions regarding rates of breakage, waste handling, and factors for releases to water. The input data comprise estimated Hg consumption in one year (2015) for the following product groups: batteries, measuring devices, lamps, electrical and electronic devices, dental applications, and other uses. The amounts are then distributed to four initial pathways (safe storage, breakage and release of Hg during use, waste stream, products still in use) using DFs. Waste pathways are further differentiated among waste recycling, waste incineration and waste landfill. The final pathway is further differentiated between two levels of waste management: controlled and uncontrolled waste landfill. All the initial and waste DFs used to determine the amount of Hg distributed to the above-mentioned pathways are the same as those used in the case of atmospheric emissions estimates (see Chapter 3, E-Annex 3, Section A3.3 for details). Within these pathways, releases to water are assumed for breakage/release during use, recycling and from waste landfills (Figure A6.1).

Releases to water are then estimated by applying release factors according to Table A6.2 to the distributed individual amounts of Hg. As in the case of atmospheric emissions for this sector, varying waste management practices were taken into account by using five different profiles of release factors. Each country has been assigned one of these five generic profiles based on assumptions and information available as discussed in E-Annex 3, Section A3.3. For releases resulting from breakage during use, waste recycling and controlled landfills, release factors are the same as for the assigned generic profiles of waste management. A differentiation is introduced for releases from uncontrolled landfills by using different release factors for individual profiles.

Table A6.2 Release factors (fraction released) applied to distributed amounts of Hg in Hg-added products.

Profile	Break/release during use	Waste recycling	Landfill	
			controlled	uncontrolled
1	0.1	0.05	0.0001	0.05
2	0.1	0.05	0.0001	0.10
3	0.1	0.05	0.0001	0.15
4	0.1	0.05	0.0001	0.20
5	0.1	0.05	0.0001	0.25
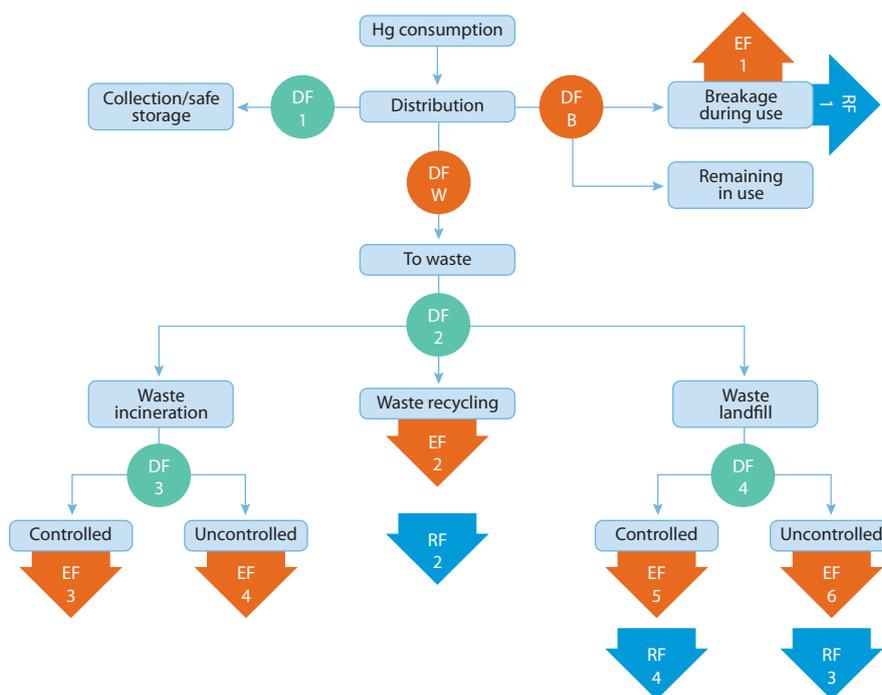
Figure A6.1 Schematic representation of the model used to estimate Hg releases from waste streams associated with Hg-added products and comparison with Hg emission streams.

Example calculation

The following example shows the calculation scheme applied to estimate releases associated with the use and disposal of Hg-added products for Mexico. The distribution of Hg between different distribution pathways, starting with the distribution of regional total amounts of Hg consumed in intentional Hg use products is the same as that for atmospheric emissions and described in detail in Chapter 3, E-Annex 3, Section A3.3.

The flowchart in Figure A6.2 illustrates how, on the basis of this distribution, releases to water totaling about 2.5 t are calculated. Of this, following breakage during use, 0.088 t are released, while other releases are attributed to secondary waste pathways: 0.024 t are estimated to be released during waste recycling and 2.337 t from controlled and uncontrolled waste landfills.
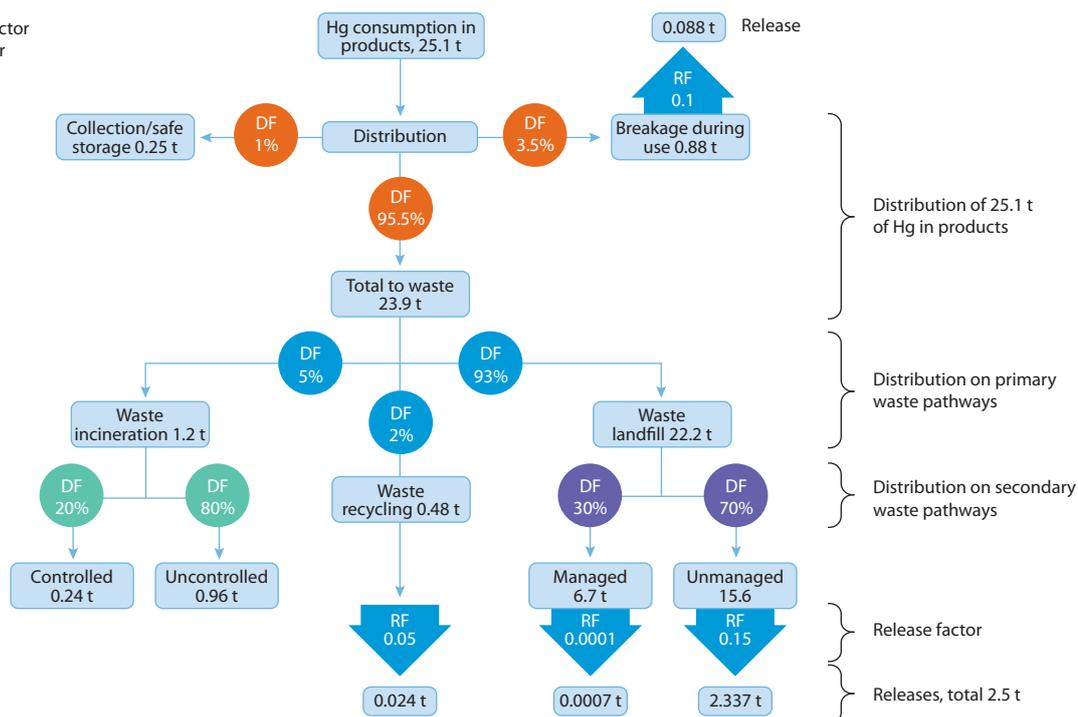
Figure A6.2 Example calculation of Hg releases from waste streams associated with Hg-added products. The example is for Mexico.

7. Mercury concentrations in biota

Authors: David Evers, Josh Ackerman, Staffan Åkerblom, Dominique Bally, Nil Basu, Joel Blum, Nathalie Bodin, David Buck, Paco Bustamante, Celia Chen, John Chetelat, Monica Costa, Rune Dietz, Paul Drevnick, Collin Eagles-Smith, Younghee Kim, José Lailson, Diego Henrique Costa Pereira, Frank Rigét, Carlos Rodriguez Brianza, Elsie Sunderland, Akinori Takeuchi, Eleuterio Umpiérrez, Hans Fredrik Veiteberg Braaten, Simon Wilson, Heleen de Wit

Key messages

- *The main form of mercury that is a concern for biological exposure and effects in wildlife and humans is methylmercury (MeHg). Biotic MeHg exposure varies greatly and is linked to trophic level (which is related to food web structure), ecology, physiology, metabolism, demographics (e.g., lifespan), latitude, and sensitivity of an ecosystem to Hg input.*

- *There is an extensive body of published data on total Hg concentrations in biota. MeHg generally comprises over 95% of the total Hg in tissues commonly sampled from biota. Consequently many biomonitoring programs are in place worldwide that can track local- and regional-scale spatial/temporal patterns of environmentally available MeHg (with an emphasis on fish and birds).*

- *Numerous studies, particularly recent ones, document that food webs in many of the world's biomes and ecosystems have MeHg concentrations at levels of concern for ecological and human health.*

- *Biological MeHg hotspots (areas that have biota with above average MeHg body burdens that are at levels having potential significant human and ecological health impacts) are known throughout the world and can be linked both to contaminated sites and to ecosystems/areas that are especially sensitive to Hg input. Biological MeHg hotspots can be modelled and their identification could be crucial for effective and efficient biomonitoring.*

- *Identifying fish and wildlife species for MeHg biomonitoring is complex because their suitability differs according to geographic area, timescale of interest, conservation concern, and whether the overall goal is for ecological or human health. Tissue choice dictates interpretative power in the biomagnification and bioaccumulation of MeHg and associated impacts.*

- *Temporal trend data for Hg in biota are generally limited, but some key Hg biomonitoring efforts exist in some regions, in particular the Arctic, and the Great Lakes Region/Northeast of the United States and Canada; retrospective studies using museum specimens or samples in specimen banks further provide important insights.*

- *AMAP has established an effective regional template for monitoring MeHg exposure in the Arctic environment that can be used concurrently for ecological and human health. But, overall, there is a general lack of regional initiatives around the world, especially in Central and South America, Africa and Australia. One of the better examples of a national Hg biomonitoring effort is Canada's Northern Contaminants Program.*

- *Biota that best represent biomonitoring needs can generally be identified through current knowledge and reflect key overarching objectives, including linking the source of MeHg exposure to humans, tracking trends of MeHg in the environment, and assessing the health of the environment. In terms of bioindicator selection linked to human health or ecological health, the taxa of greatest interest for the Minamata Convention include fish, sea turtles, birds, and marine mammals.*

- *Careful selection and use of bioindicators that closely match objectives of the interested parties can be a cost-effective and time-efficient way to track human and ecological health from the anthropogenic loading of Hg onto the water and landscape at a global level, especially when incorporating on-going biomonitoring efforts.*

- *Mercury isotopes offer an ever-improving tool that can potentially be used to link Hg source types with MeHg concentrations in fish, wildlife and humans.*

7.1 Introduction

The complex chemical conversions and cycling of mercury (Hg) make it particularly challenging to predict from concentrations in air, water, and sediment the levels of potential concern in upper trophic level fish and wildlife (Gustin et al., 2016a; Sunderland et al., 2016). Inorganic Hg emitted from natural or anthropogenic sources becomes more toxic in the environment when it is converted to methylmercury (MeHg), by sulfur-reducing and iron-reducing bacteria, methanogens, and other microbes (Fleming et al., 2006; Gilmour et al., 2013; Hsu-Kim et al. 2013, Yu et al., 2013). In areas where Hg deposition is low, effects on biota may be disproportionately high if conditions are conducive from MeHg production and biomagnification.

Mercury is a neurotoxic heavy metal that can impair physiology, neurology, behavior, reproduction, and survival in fish, wildlife, and humans (Tan et al., 2009; Scheuhammer et al., 2011; Ackerman et al., 2016; Whitney and Cristol, 2017; Evers, 2018). It readily biomagnifies through ecosystems, resulting in increasing MeHg concentrations as it moves from water and sediment to phytoplankton and plants, zooplankton, aquatic invertebrates, fish, wildlife, and humans. Once MeHg is taken up at the base of the food web it can efficiently biomagnify, even in terrestrial ecosystems where spiders often serve as an important trophic level link for MeHg to terrestrial wildlife (Cristol et al., 2008; Chaves-Ulloa et al., 2016).

Mercury exposure has been well documented in fish and wildlife. Contamination can arise directly from inorganic

Hg point sources, such as those along rivers (Kinghorn et al., 2007; Jackson et al., 2011b; Nguetseng et al., 2015; Santschi et al., 2017; Geyer and Ralston, 2018), around lakes (Anderson et al., 2008; Suchanek et al., 2008) and in estuaries (Eagles-Smith and Ackerman, 2009; Sullivan and Kopec, 2018). Owing to atmospheric transport, inorganic Hg sources may be remote (>100 km) and are well described in most continents, including North America (Evers et al., 2005, 2011a; Kamman et al., 2005; Monson et al., 2011; Ackerman et al., 2016; Eagles-Smith et al., 2016b; Jackson et al., 2016; Scheuhammer et al., 2016), South America (Sebastiano et al., 2016; May Junior et al., 2017), Europe (Åkerblom et al., 2014; Nguetseng et al., 2015; Pacyna et al., 2017), Asia (Kim et al., 2012; Watanuki et al., 2016; Abeysinghe et al., 2017; Noh et al., 2017), Africa (Daso et al., 2015; Hanna et al., 2015; Rajaee et al., 2015), and ocean basins (Carravieri et al., 2014, 2017; Drevnick et al., 2015; Peterson et al., 2015; Lee et al., 2016; Bodin et al., 2017; Drevnick and Brooks, 2017).

Numerous studies, particularly recent ones, document adverse impacts across many fish and wildlife species. In fish, adverse impacts of MeHg exposure include reproductive, behavioral, and immunological impairment (Hammerschmidt et al., 2002; Depew et al., 2012a; Carvan et al., 2017) as well as reduced capacity for predator avoidance (Webber and Haines, 2003). In birds, many studies document reduced reproductive success, behavioral change and neurological problems (Depew et al., 2012a,b; Ackerman et al., 2016; Whitney and Cristol, 2017; Evers 2018). In mammals, elevated MeHg concentrations can result in biochemical changes in the brain, ataxia, and reduced reproductive output (Dietz et al., 2013; Evers, 2018). Based on these and other *in situ* studies, the biomagnification and bioaccumulation of MeHg is shown to adversely affect the reproductive success of many fish and wildlife populations, representing multiple foraging guilds across many habitats and geographic areas of the world. A complicating factor in determining Hg risk to wildlife is that many species vary in their sensitivity to MeHg toxicity (Heinz et al., 2009). For example, embryo survival and hatching success in songbirds (Passeriforms) seems more sensitive to MeHg toxicity than in other orders of birds, such as waterfowl (Anseriformes).

Identifying fish and wildlife species for MeHg biomonitoring is complex because their suitability differs according to geographic area, timescale of interest, conservation concern, and whether the overall goal is for ecological or human health. This chapter reports spatial and temporal global patterns of MeHg exposure in fish and wildlife based on the peer-reviewed literature with an emphasis on bioindicators.

There is an extensive body of published data on total Hg concentrations in biota and many biomonitoring programs are in place worldwide, particularly in high-income countries – such as the USA, Canada, across several European countries, and Japan – that track global-scale spatio-temporal patterns of environmental inorganic Hg (with an emphasis on fish). Existing biomonitoring programs were identified in a recent United Nations Environment review (UN Environment, 2016). Data within the peer-reviewed literature define the many case studies that include MeHg in taxa identified in Article 19 of the Minamata Convention on Mercury. Those published data are summarized here with an emphasis on fish, sea turtles, birds, and marine mammals. The type of Hg in tissues commonly sampled from biota is generally over 95% MeHg.

7.2 Existing biotic Hg data

7.2.1 Literature search

A systematic literature search emphasized long-term, standardized and large-scale monitoring efforts that included, among others, species identified in Article 19 of the Minamata Convention, species for human consumption, taxonomic groups at high risk of MeHg exposure, potential bioindicators, and species from areas of concern due to current Hg sources. Only peer-reviewed publications were used and the references are archived in the Global Biotic Mercury Synthesis (GBMS) database (Evers et al., 2017). Taxonomic groups with comprehensive coverage are shown in boldface in Appendix Table A7.1.

Studies included here are those for which there is reasonable confidence about their validity. For example, with a good description of the characteristics of the organism sampled (species, date, tissue analyzed), an appropriate method of sample collection, and detailed information on sampling location (i.e., market-based fish Hg concentrations are excluded). Terrestrial coverage of biotic Hg levels for North America is limited in in this chapter. However, extensive MeHg datasets synthesized during three regional workshops are available for the northeastern USA and eastern Canada for the period 2000–2004 (Evers and Clair, 2005), the Great Lakes Region of the USA and Canada for the period 2008–2010 (Evers et al., 2011a) and the western USA and Canada for the period 2012–2015 (Eagles-Smith et al., 2016b).

The data collected represent the arithmetic mean, standard deviation, minimum and maximum values, and total number of individuals for each species and tissue type that could be georeferenced within a peer-reviewed publication and were joined by taxa and tissue type to generate a global average and variation (see Appendix Table A7.1). The raw data underlying the averaged statistics presented in Appendix Table A7.1 were not available. Each of the published studies' average Hg concentration was mapped by major taxonomic group (i.e., cartilaginous and bony fish, sea turtles, birds, marine mammals) and tissue type and were placed in three risk categories based on human or ecological health thresholds (i.e., low, medium and high). Available data are summarized in Box 7.1, Figures 7.1 and 7.2.

The risk categories for human health are based on a combination of thresholds generated from standards used in the USA (Great Lakes Fish Advisory Workgroup, 2007), for Arctic communities (AMAP, 2015), and by the World Health Organization (i.e., <0.22 ppm low, 0.22–1.0 ppm moderate, >1.0 ppm high) that generally relate to MeHg exposure level concerns recognized for humans (Višnjevec Miklavčič et al., 2014; see also Chapter 9). For ecological health, risk categories by taxa for various tissue types are summarized by Evers (2018). This approach is conservative since it is the average Hg concentration for published data at the identified site that is ranked within one of the three risk categories.

7.2.2 Preferred tissue types

This review focuses on tissues with well-established methods of measurement and interpretation and for which there is a large body of data. There are many matrices and tissue choice depends on monitoring objectives, interests, and outcomes. Often the most useful tissues can be non-lethally collected in the field. Samples that can be analyzed to assess total Hg

Box 7.1 Overview of available datasets

Biotic Hg concentrations for targeted taxa were collected from nearly 1100 peer-reviewed scientific publications that represent about 515,000 individuals at over 2700 unique locations in 119 countries (Figure 7.1, Appendix Table A7.1). The data are housed in the GBMS database and represent an exhaustive literature review for field Hg concentrations in taxa targeted for this assessment including all elasmobranchs, marine teleosts (particularly tuna and billfish), freshwater teleosts (particularly in South America, Africa, and Asia), sea turtles, birds (especially Procellariformes, Gaviiformes, and Passeriformes), and marine mammals. The literature review is less exhaustive, but still extensive in geographic and taxonomic coverage for freshwater teleosts in North America and birds in Orders other than the three listed above. A large number

of Hg concentrations in biota, especially fish, have been generated by government agencies. Many of these data are not represented here because they are not published in the peer-reviewed literature or in English.

Elasmobranchs (sharks, skates, rays) are represented in 13 Orders by 10,038 individuals at 96 distinct locations. Marine teleosts were represented in 29 Orders by 40,491 individuals at 462 distinct locations, while freshwater teleosts included 31 Orders with 386,908 individuals at 9314 distinct locations. For sea turtles, a total of 38 distinct locations were found with Hg concentrations in one of three tissue types of 1766 individuals. Marine birds were represented in 22 Orders by 67,987 individuals at 845 distinct locations. Marine mammals were placed in four groups and represented 8077 individuals at 328 locations.
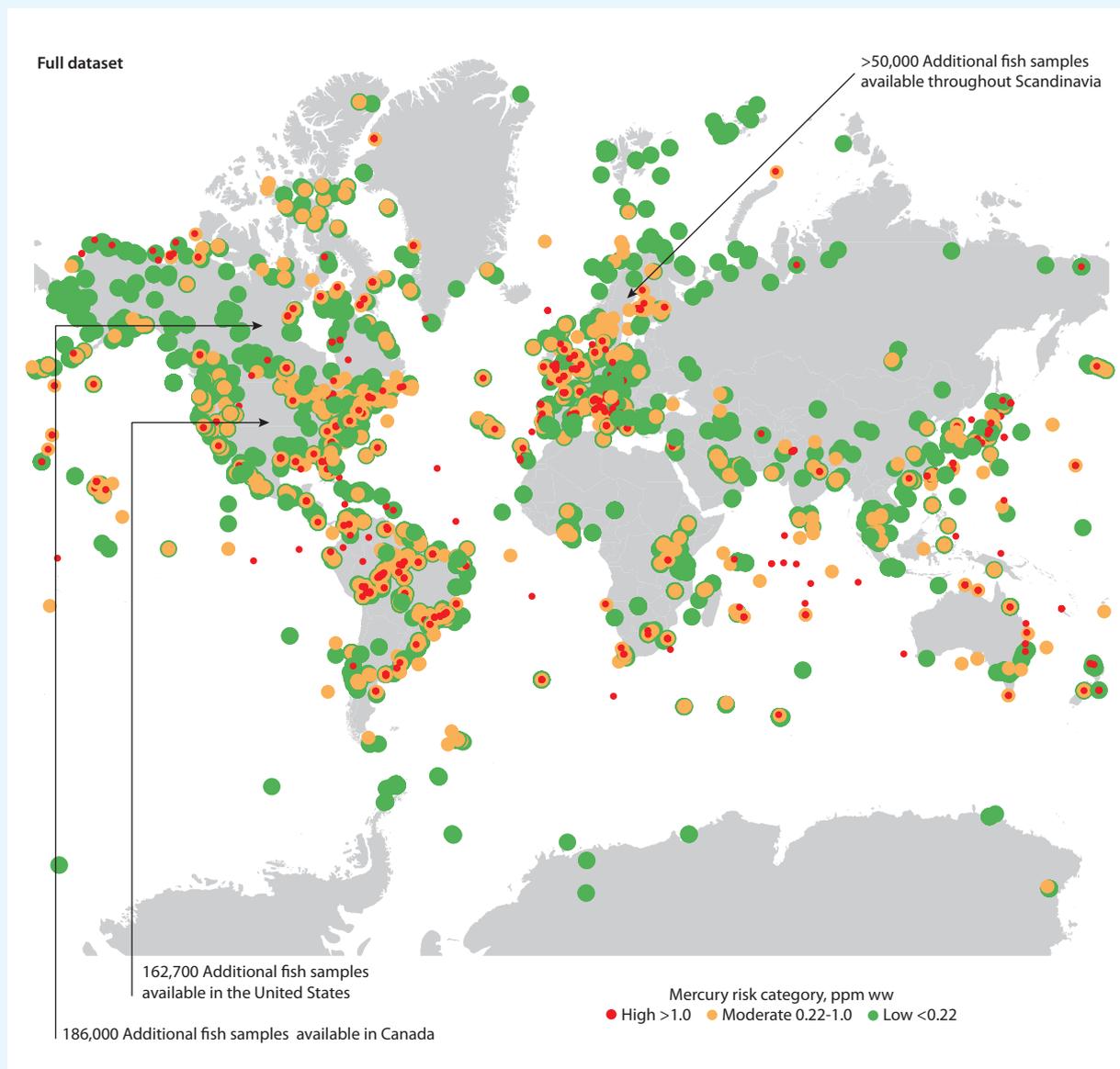
Figure 7.1 Distribution of total Hg concentrations in three risk categories (low, moderate, high) for the full set of mean data derived from a survey of the available peer-reviewed English literature. Additional fish Hg samples that were not mapped are available for Canada, USA and Scandinavia.

Sea turtles

Sharks and Allies, muscle

Marine mammals

Bony fish, muscle

a) 186,000 Additional fish samples available in Canada
b) 162,700 Additional fish samples available in the United States
c) >50,000 Additional fish samples available throughout Scandinavia

Mercury risk category, ppm ww
● High >1.0   ● Moderate 0.22-1.0   ● Low <0.22

Birds
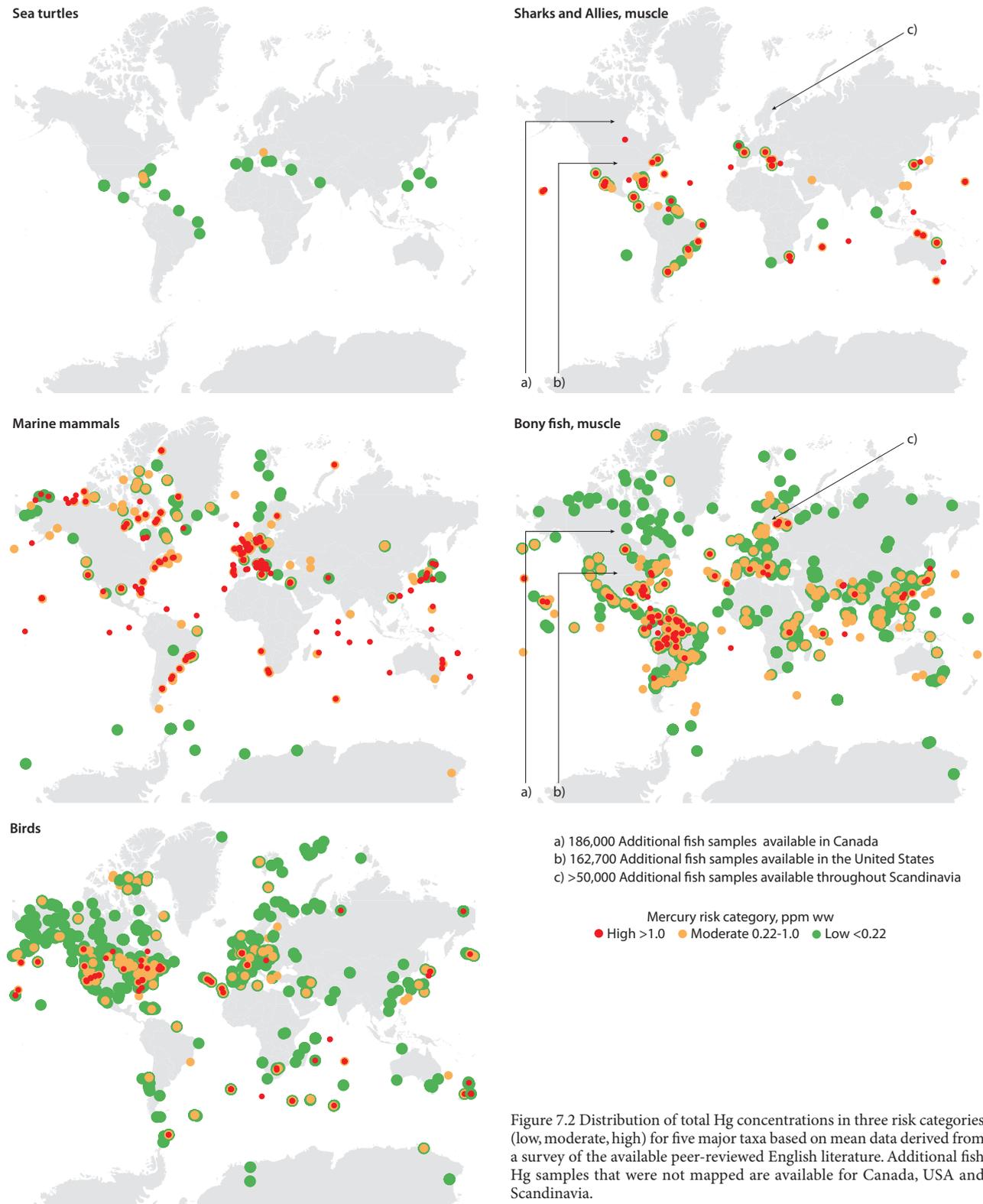
Figure 7.2 Distribution of total Hg concentrations in three risk categories (low, moderate, high) for five major taxa based on mean data derived from a survey of the available peer-reviewed English literature. Additional fish Hg samples that were not mapped are available for Canada, USA and Scandinavia.

or MeHg exposure are often from tissue (i.e., matrix) types for targeted biotic groups (Table 7.1). Composite samples are sometimes used to estimate Hg concentrations at decreased cost (Gandhi et al., 2016), and because most of the Hg in tissues that are commonly tested for biomonitoring purposes is in the MeHg form (generally >95%), analyses of total Hg (which is less expensive to analyze) is also more cost effective. The development of Direct Mercury Analyzers has simplified Hg determination and made analysis more accessible to those without advanced and costly laboratory facilities.

Understanding MeHg concentrations in organisms is important because the organic form of Hg biomagnifies through the food web for Arctic (Ruus et al., 2015), temperate (Arcagni et al., 2018), and tropical (Seixas et al., 2014) ecosystems, and bioaccumulates over time in individual fish (Drevnick and Brooks, 2017), birds (Evers et al., 1998), and marine mammals (Krey et al., 2015). Understanding how the selection of tissue types dictates interpretative power in the biomagnification and bioaccumulation of MeHg and subsequent potential impacts is critical (Eagles-Smith et al., 2016b).

Table 7.1 Major biota groupings and tissues recommended for MeHg monitoring. All tissues can be non-lethally sampled (including biopsies of liver and kidney).

Group	Matrix	MeHg proportion	Sample prep type[a]	Analysis type	Source reference for MeHg %	Comments
Fish	Muscle fillet	>95% (for larger or higher trophic level individuals) >70% (for smaller or lower trophic level individuals)	ww or <u>dw</u>	THg or MeHg	Bloom, 1992, Lescord et al., 2018	Dark muscle is significantly higher than white muscle (Bosch et al., 2016a). New evidence indicates that %MeHg may be lower for small or low trophic level fish species (Lescord et al., 2018) and some cooking approaches (Wang et al., 2013). Small or lower trophic level fish should be analyzed for MeHg content
	Muscle biopsy	>95% (but varies)	dw	THg	Peterson et al., 2004	dw is best owing to moisture loss concerns. Muscle biopsy to muscle fillet has a $r^2 = 0.96$. Biopsy plug depth may impact Hg measured – 5 mm plugs are best below dorsal fin (Cizdziel et al., 2002) and are without skin and adipose tissue
	Fin clips	unknown	dw	THg	Cerveny et al., 2016	There is a significant correlation between fin clips and muscle fillet ($p<0.01$)
	Blood	>95%	ww or dw	THg	-	Assumed to be >95% MeHg based on other vertebrates
Sea turtles	Scutes	>95%	fw (or dw if scutes need washing)	THg	Schneider et al., 2015	Recommended and assumed nearly all MeHg as scutes are composed of keratin
	Blood	>95%	ww or dw	THg	-	Assumed to be >95% MeHg based on other vertebrates
	Muscle	>95%	ww or <u>dw</u>	THg	-	Assumed to be >95% MeHg based on other vertebrates
Birds	Blood	>95%	ww or dw	THg	Rimmer et al., 2005; Edmonds et al., 2010	Elimination of MeHg in blood comprises an initial fast phase, with a half-time of 1 day, and a slow terminal phase with a half-time of 44-65 days. Molt is a crucial factor in determining the rate of MeHg elimination (Monteiro and Furness, 2001)
	Feather	~100%	fw (or dw if feathers are washed due to external contamination)	THg	Burger, 1993	If feathers are not washed, fw = dw because mean feather moisture is <1%, n = 490; R. Taylor, Texas A&M, USA pers. comm.
	Eggs	>96%	ww or dw or <u>fww</u>	THg	Ackerman et al., 2013 (96% for 22 species)	ww and dw can be problematic if eggs are not collected immediately after laying (Dolgova et al., 2018)
	Muscle	>95%	ww or dw	THg		MeHg comprised >99% of total Hg in breast muscle of waterfowl (Sullivan and Kopec, 2018)
	Eggshells and membranes	>95%	dw	THg	Peterson et al., 2017	Membranes are assumed to be primarily MeHg, but shells are entirely inorganic Hg
	Liver and kidney	5–7% in loons and mergansers; 56–90% in egrets; 88% (20–100%) terns and shorebirds	dw	MeHg	Scheuhammer et al., 1998; Spalding et al., 2000; Eagles-Smith et al., 2009b	These tissues are not recommended for monitoring; %MeHg can vary widely
Mammals	Skin	>90%	dw	THg	Wagemann et al., 1998	Muktuk (in marine mammals) includes layers of skin and blubber
	Fur or hair	>90%	fw (or dw if fur needs to be washed)	THg	Evans et al., 2000	Fur/hair may not relate to blood and muscle depending on growth patterns (Peterson et al., 2016a)
	Muscle	>90%	ww or <u>dw</u>	THg	Wagemann et al., 1998	
	Liver and kidney	3–12% in whales/ seals; 57–91% in mink/otter	dw	MeHg	Wagemann et al., 1998; Evans et al., 2000	These tissues are not recommended for monitoring; %MeHg can vary widely

[a] Reported as wet weight (ww), dry weight (dw), fresh weight (fw), or fresh wet weight (fww) analyses, preferred sample type is underlined. Fw denotes keratin-based samples that are not cleaned or dried prior to total Hg analysis.

7.2.3 Other factors related to interpretation of biotic Hg data

Other metadata that are important to improve interpretive power include physiological, demographic, and ecological factors. For example, determining the health and fitness of bioindicators is important for standardized comparisons, as is the identification of size, age, and gender. However, for this data compilation biotic MeHg concentrations were not indexed or standardized according to size because individual or average lengths and/or weights were generally not available. In general, larger and older individuals have higher MeHg concentrations than smaller and younger individuals, and males that are larger in body size than females tend to have higher body burdens in fish (Eagles-Smith et al., 2016a) and birds (Evers et al., 2005; Ackerman et al., 2008, 2015, 2016; Robinson et al., 2012; Hartman et al., 2017), with a few exceptions related to foraging segregation between sexes such as for albatrosses (Carravieri et al., 2014).

Changes in an animal's physiology or ecological life history events can also have a substantial effect on MeHg concentrations, regardless of an animal's actual environmental MeHg exposure. For example, rapid growth of juvenile birds can cause mass dilution of contaminants and substantially reduce MeHg concentrations as juvenile birds age (Ackerman et al., 2011). In contrast, annual life changes in adult body mass such as fasting- and breeding-associated declines in body mass during periods of haul-out on land for marine mammals, can substantially increase MeHg concentrations (Peterson et al., 2018).

Seasonality can have large implications for biotic Hg monitoring programs (Eagles-Smith and Ackerman, 2009). Seasonal changes in MeHg exposure may be related to changing methylation rates and bioavailability in estuaries (e.g., saltmarsh sparrows *Ammodramus caudacutus* increase in blood Hg concentration from early to late summer; Lane et al., 2011), molt strategies (Condon and Cristol, 2009), arrival to overwintering areas for migratory birds (Eagles-Smith et al., 2009a), or lake-specific variation in Hg dynamics (e.g., Clark's and western grebes *Aechmophorus clarkia* and *A. occidentalis* decrease in blood Hg from spring to autumn; Hartman et al., 2017).

7.3 Existing biomonitoring programs

Mercury biomonitoring programs were identified following a formal request to countries globally by the United Nations Environment Interim Secretariat. Responses were compiled (UN Environment, 2016) and provide the most up-to-date record of existing local, regional, and global abiotic and biotic Hg monitoring programs. These include programs underway within many national networks, including initiatives in the EU (Norway, Sweden, Spain, UK, Poland), Canada, USA, Japan, Republic of Korea, Colombia and Brazil, and global or regional networks (UN Environment, 2016). The Arctic is monitored through AMAP (AMAP, 2011) with valuable subsets from Canada's Northern Contaminants Program (Chételat et al., 2015; NCP 2017), the national monitoring program in Greenland and the Faroe Islands (Denmark), and the ARCTOX program based in Europe for tracking MeHg in seabirds. There are many programs in the temperate regions of the USA – such as the U.S. Environmental Protection Agency's seafood Hg monitoring program (Evers et al., 2008) and National Oceanic and Atmospheric Administration's

mussel Hg watch program (Chase et al., 2001) – Europe (e.g., ROCCH, Reseau d'Observation de la Contamination Chimique), and Japan. In developing countries and countries in economic transition, there are fewer national or regional long-term initiatives. In particular, there are very few long-term Hg biomonitoring efforts in tropical biomes. In contrast, there are many oceanic Hg biomonitoring efforts within temperate and Arctic biomes (Evers et al., 2017).

AMAP provides one of the best examples of how to operate a long-term MeHg biomonitoring field program for the benefit of both human and ecological health (AMAP, 2011, 2015). This program uses standardized methodology across a large geographic area, involves multiple taxa (fish, birds, marine mammals), and incorporates other physical and chemical variables. AMAP has established an effective regional template for monitoring MeHg exposure in the environment that can be used concurrently for ecological and human health. The WHO Global Environment Monitoring System – Food Contamination Monitoring and Assessment Programme (commonly known as GEMS/Food) has one of the best global systems for collecting fish Hg data through its network of collaborating centers and recognized national institutions (WHO, 2018).

A review of the geographical coverage of Hg biomonitoring networks reveals a general lack of regional initiatives around the world, especially in Africa and Australia (UN Environment, 2016). Most Asian countries are minimally involved with national initiatives to monitor Hg levels in biota, notable exceptions being Japan and the Republic of Korea where more extensive programs exist. Conversely, Hg biomonitoring is ongoing in many countries within Asia, Europe, Oceana and across the Western Hemisphere. Environmental Specimen Banks can be used as monitoring tools to provide long-term trends for contaminants in the environment, including Hg (Day et al., 2014; Paulus et al., 2015; Qiu et al., 2015; García-Seoane et al., 2017).

One of the better examples for a national Hg biomonitoring effort is Canada's Northern Contaminants Program – an integrated initiative for Hg monitoring throughout Canada's vast Arctic territory (NCP, 2017). Since its establishment in 1991, the program has focused on the measurement of contaminants (including Hg) in fish and wildlife that are traditional foods of northern indigenous peoples (Figure 7.3). One of the strengths of the program is the interdisciplinary approach taken to assess and monitor risk of Hg to ecological and human health through the participation of indigenous organizations, government departments (at federal and territorial level), environmental scientists, and human health professionals. Activities are managed under five subprograms: Human Health; Environmental Monitoring and Research; Community-Based Monitoring and Research; Communications, Capacity and Outreach; and Program Coordination and Indigenous Partnerships. A strategic long-term plan guides the development of subprograms and the links between them. For example, monitoring of Hg in biota is supported by Hg measurements in air as well as focused research on environmental processes that control Hg bioaccumulation. Data generated on Hg in wildlife can be used for human dietary exposure assessments, while community-based projects may focus on species that are local priorities but not covered by routine monitoring.

Monitoring of Hg in fish and wildlife under the Northern Contaminants Program includes terrestrial, freshwater and marine species in focal areas across northern Canada (Figure 7.3).

Trend datasets

Sea-run char

Landlocked char

Lake trout and burbot in Great Slave Lake

Lake trout from two Yukon lakes

Burbot in the Mackenzie River

Ringed seals

Polar bears

Beluga

Seabirds eggs

Caribou (dashed lines indicate herd range)

Figure 7.3 Long-term sampling sites for Arctic fish and wildlife monitored annually under Canada's Northern Contaminants Program in terrestrial, freshwater, and marine ecosystems in five regions of Northern Canada. Biotic monitoring is one of several interdisciplinary subprograms to assess and monitor risks of contaminants (including Hg) to ecological and human health.

Many of the samples are collected by indigenous hunters in nearby communities as part of their subsistence activities. Annual measurements track temporal trends of Hg bioaccumulation, and retrospective analyses of archived tissues from government specimen banks have provided opportunities to extend some time series (e.g., Braune, 2007). Intensive spatial sampling of several species including Arctic char (*Salvelinus alpinus*) (Evans et al., 2015) and ringed seal (*Pusa hispida*) (Brown et al., 2016) have generated complementary information on geographic variation. Another example of an international collaboration, ARCTOX, is a program whereby seabird blood and feather samples have been collected from more than 54 Arctic sites and a total of 14 seabird species (although not every species is sampled at each site); samples are from Arctic countries, including the USA, Canada, Greenland, Scandinavia, and Russia (Fort et al., 2017).

Meanwhile, the hundreds of local studies conducted by the global scientific community that are reflected within the GBMS database provide a relatively comprehensive global data platform containing existing biotic Hg concentrations (Appendix Table A7.1; Evers et al., 2017). Based on the GBMS database, some of the regions with the highest fish consumption are poorly covered by biomonitoring efforts (e.g., Central America and the Caribbean Sea, western and central Africa, the southern Asian mainland, Indo-Pacific Asia and Australia). More efforts are needed to develop and implement projects to fill geographic and ecosystem gaps. Although national efforts are fundamental to regional biomonitoring networks, local scientific studies can make a significant contribution to better identifying where, for which species, and when, to conduct biomonitoring.

To provide sustainable and long-term biomonitoring capacity in key regions – such as the Arctic, tropical areas associated with artisanal and small-scale gold mining (ASGM), and Small Island Developing States – the focus should be on expanding and stabilizing existing national initiatives that use sample sizes that can meet statistical power for confidence in understanding spatial gradients (e.g., biological MeHg hotspots; Evers et al., 2011b) and temporal trends (Bignert et al., 2004). Moreover, it is crucial to foster international collaboration and coordination among national projects to create harmonized regional approaches, and to strive, where possible, to integrate biomonitoring activities into an interdisciplinary framework to assess ecological and human health risk that can be amalgamated to represent regional and eventually global spatio-temporal patterns.

7.4 Selection of bioindicators

A key initial step in bioindicator selection is to decide whether an organism is linked to a human health or ecological health endpoint – which can often be combined for both purposes if carefully considered. Biota that have been identified to best fit these two categories are well described and are categorized within their respective biomes and associated aquatic ecosystems (Table 7.2). The taxa of greatest interest for the Minamata Convention include fish, sea turtles, birds, and marine mammals. The extensive data on Hg in biota found in the published literature provides a selection of species for potential monitoring (Figure 7.2). Careful selection can ensure comparability at regional and global scales.

Organisms that are at risk of developing elevated MeHg body burdens, that represent specific ecological pathways or unique spatial or temporal scales, and that have well-established toxicity benchmarks can be grouped at relevant taxonomic resolutions to aid decisions concerning the selection of bioindicators (Evers et al., 2016; Appendix Table A7.1). The emphasis here is on the selection of biota that may pose concern for (1) human exposure from dietary uptake of MeHg from marine or freshwater ecosystems; (2) temporal timelines of interest, for example short-term timeframes (<6 years) should use young individuals with relatively low trophic level species and long-term timeframes (>12 years) can use market fish; (3) spatial gradients of local to regional to global scales, for example wide-ranging predator species such as swordfish are key bioindicators for regional and global monitoring, while resident species fit better with local scales; (4) conservation purposes, for example wildlife that are rare or are well-established as threatened by Hg exposure, such as albatrosses and loons.

Table 7.2 Potential bioindicator choices for ecological and human health grouped by major terrestrial biomes and their associated aquatic ecosystems (as described and adapted from Evers et al., 2016).

Target Terrestrial Biomes	Arctic Tundra	Boreal Forest and Taiga	Temperate Broadleaf and Mixed Forest	Tropical Rainforest
Associated Aquatic Ecosystems	Arctic Ocean and associated estuaries, lakes, rivers	North Pacific and Atlantic Oceans and associated estuaries, lakes, rivers	North Pacific and Atlantic Oceans, Mediterranean and Caribbean Seas, and associated estuaries, lakes rivers	South Pacific and South Atlantic and Indian Oceans and associated estuaries, lakes, rivers
Ecological Health Bioindicators				
Freshwater and Marine Fish	Sticklebacks[1] (freshwater); Arctic cod[2]; Sculpin[3]; Sticklebacks[1] (marine)	Perch[13] (freshwater); Mummichogs and Silversides[14, 82, 82]; Gobies and Sticklebacks[101, 102] (marine)	Perch[13]; Cyprinnids[78, 83] (freshwater); Mummichogs and Silversides[14, 82, 82]; Rockfish[11]; Sticklebacks[25] (marine)	Catfish[23]; Piranha[34]; Snook[11] (freshwater); Bay snook[11, 34] (marine)
Sea Turtles			Sea turtles[29, 52]	Sea turtles[29]
Freshwater/ Terrestrial Birds	Loons[4, 5]; Shorebirds[100]	Loons[15]; Osprey[17, 98]; Songbirds[18] (blackbirds, flycatchers, warblers)	Eagles[16, 72, 92]; Egrets[27]; Grebes[5, 26, 71, 95]; Gulls[59]; Herons[27]; Loons[4]; Osprey[17, 91, 93, 94, 95]; Shorebirds[104]; Terns[26, 101, 103]; Songbirds[18, 81] (blackbirds, fly-catchers, sparrows, swallows, warblers, wrens)	Cranes[80]; Egrets[27]; Herons[27]; Kingfishers[35]; Songbirds[36] (wrens, thrushes, flycatchers)
Marine Birds	Fulmars[6]; Murres[6]; Gulls[61, 62, 63, 64, 65, 66]	Ducks[107]; Eagles[105]; Osprey[19]; Herring gulls[58, 68]; Petrels[20]	Cormorants[28]; Eagles[72]; Osprey[5, 19]; Pelicans[73]; Shearwaters[76]; Skuas[49]; Terns[26, 28]	Albatrosses[37, 38, 50, 51]; Frigatebirds[4, 74, 75]; Noddy[39, 47]; Penguins[48]; Shearwaters[39, 76]; Skuas[49]; Terns[39, 47]; Tropicbirds[39]
Mammals	Polar bears[7, 99]; Seals[8]	Mink[21, 22]; Otter[21, 22]; Seals[23]	Bats[85, 86, 87, 88]; Otter[21, 22]; Seals[23, 97]; Toothed whales[53, 54, 90, 98]	Jaguar[89]; Otter[40]; Seals[41]; Toothed whales[55, 56]
Human and Ecological Health Bioindicators				
Freshwater Fish	Arctic char[9, 60]; Arctic burbot[67]; Grayling[10]	Catfish[11]; Lake trout[69, 70]; Pike[10, 70]; Sauger[10]; Walleye[10, 70]	Bass[10, 30, 31]; Bream[11]; Lake trout[70]; Mullet[11]; Pike[70]; Walleye[31, 70]	Catfish[11]; Nile perch[79]; Snakehead[11]; Tigerfish[84]
Marine Fish	Halibut[11]; Cod[11]	Flounder[11]; Snapper[11]; Tuna[11]	Barracuda[11]; Mackerel[11]; Mullet[11]; Scabbard-fish[11]; Sharks[11, 32]; Swordfish[11, 45]; Tuna[11, 32]	Barracuda[11]; Grouper[42]; Mahi mahi[108]; Sharks[43, 44, 46]; Snapper[11]; Swordfish[46]; Tuna[46, 77, 106]
Marine Mammals	Beluga[2, 12, 99]; Narwhal[2, 12]; Ringed seal[57, 99]; Hooded seal[8]	Pilot whale[24]		

[1]Kenney et al. 2014, [2]AMAP 2011, [3]Rigét et al. 2007, [4]Evers et al. 2014, [5]Jackson et al. 2016, [6]Braune 2007, [7]Routti et al. 2011, [8]Dietz et al. 2013, [9]Gantner et al. 2010, [10]Eagles-Smith et al. 2016a, [11]Evers et al. 2016, [12]Wagemann and Kozlowska 2005, [13]Wiener et al. 2012, [14]Weis and Kahn 1990, [15]Evers et al. 2011b, [16]Bowerman et al. 1994, [17]Odsjö et al. 2004, [18]Jackson et al. 2015, [19]Wiemeyer et al. 1988, [20]Goodale et al. 2008, [21]Yates et al. 2005, [22]Klenavic et al. 2008, [23]Brookens et al. 2008, [24]Dam and Bloch 2000, [25]Eagles-Smith and Ackerman 2009, [26]Ackerman et al. 2016, [27]Frederick et al. 2002, [28]Braune 1987, [29]Day et al. 2005, [30]Kamman et al. 2005, [31]Monson et al. 2011, [32]Cai et al. 2007, [33]Bastos et al. 2015, [34]Mol et al. 2001, [35]Lane et al. 2011, [36]Townsend et al. 2013, [37]Finkelstein et al. 2006, [38]Burger and Gochfeld 2000, [39]Kojadinovic et al. 2007, [40]Fonseca et al. 2005, [41]Marcovecchio et al. 1994, [42]Evers et al. 2009, [43]Kiszka et al. 2015, [44]Maz-Courrau et al. 2012, [45]Storelli and Marcotrigiano 2001, [46]Bodin et al. 2017, [47]Sebastiano et al. 2017, [48]Carravieri et al. 2016, [49]Carravieri et al. 2017, [50]Bustamante et al. 2016, [51]Anderson et al. 2010, [52]Maffucci et al. 2005, [53]Correa et al. 2013, [54]Aubail et al. 2013, [55]Bustamante et al. 2003, [56]Garrigue et al. 2016, [57]Brown et al. 2016, [58]Burgess et al. 2013, [59]Weseloh et al. 2011, [60]Evans et al. 2015, [61]Braune et al. 2006, [62]Lucia et al. 2015, [63]Lucia et al. 2016, [64]Braune et al. 2016, [65]Miljeteig et al. 2009, [66]Bond et al. 2015, [67]Pelletier et al. 2017, [68]Blukacz-Richards et al. 2017, [69]Abma et al. 2015, [70]Gandhi et al. 2014, [71]Hartman et al. 2017, [72]DeSorbo et al. 2018, [73]Newtoff and Emslie 2017, [74]Sebastiano et al. 2016, [75]Mott et al. 2017, [76]Watanuki et al. 2016, [77]Bosch et al. 2016b, [78]Cerveny et al. 2016, [79]Hanna et al. 2016, [80]Daso et al. 2015, [81]Pacyna et al. 2017, [82]Chen et al. 2014a, [83]Buckman et al. 2015, [84]Webb et al. 2015, [85]Yates et al. 2014, [86]Little et al. 2015, [87]Åkerblom and de Jong 2017, [88]Korstian et al. 2018, [89]May Junior et al. 2017, [90]Titcomb et al. 2017, [91]Rumbold et al. 2017, [92]Kalisinska et al. 2014, [93]Hughes et al. 1997, [94]Henny et al. 2009b, [95]Anderson et al. 2008, [96]DesGranges et al. 1998, [97]Peterson et al. 2016b, [98]Reif et al. 2015, [99]Krey et al. 2015, [100]Perkins et al. 2016, [101]Eagles-Smith and Ackerman 2009, [102]Eagles-Smith and Ackerman 2014, [103]Ackerman et al. 2008, [104]Ackerman et al. 2007, [105]Burger and Gochfeld 2009, [106]Chouvelon et al. 2017, [107]Savoy et al. 2017, [108]Adams 2009.

7.4.1 Human health bioindicators

Many communities around the world depend in part, and sometimes completely, on wild animals for subsistence, including marine fish, freshwater fish, birds, and marine mammals. Patterns of dietary MeHg uptake in humans are described for all the world's major biomes from the Arctic and subarctic to temperate and tropical aquatic ecosystems, with the mechanisms underlying source-exposure-human biomarker measures detailed in Chapter 9. The following case studies illustrate how biotic Hg exposure can be linked to human health concerns in each of these major biomes for key ecosystems in the world using bioindicators.

7.4.1.1 Case study: Global oceans

Tuna species are one of the most important global sources of seafood. Commercial harvests tracked by the UN Food and Agriculture Organization (FAO) totaled 5 million t in 2014, worth an estimated USD 42.21 billion (Galland, 2017), although this total may not include all fisheries, and harvests could be higher than estimated (Pauly and Zeller, 2016). Muscle Hg concentrations and commercial harvests vary widely by species. The smallest tuna species (e.g., skipjack tuna, *Katsuwonus pelamis*) have average Hg concentrations under the U.S. EPA advisory level of 0.30 ppm (ww), while the largest (e.g., Pacific and Atlantic bluefin tunas, *Thunnus orientalis and T. thynnus*) have the highest average Hg
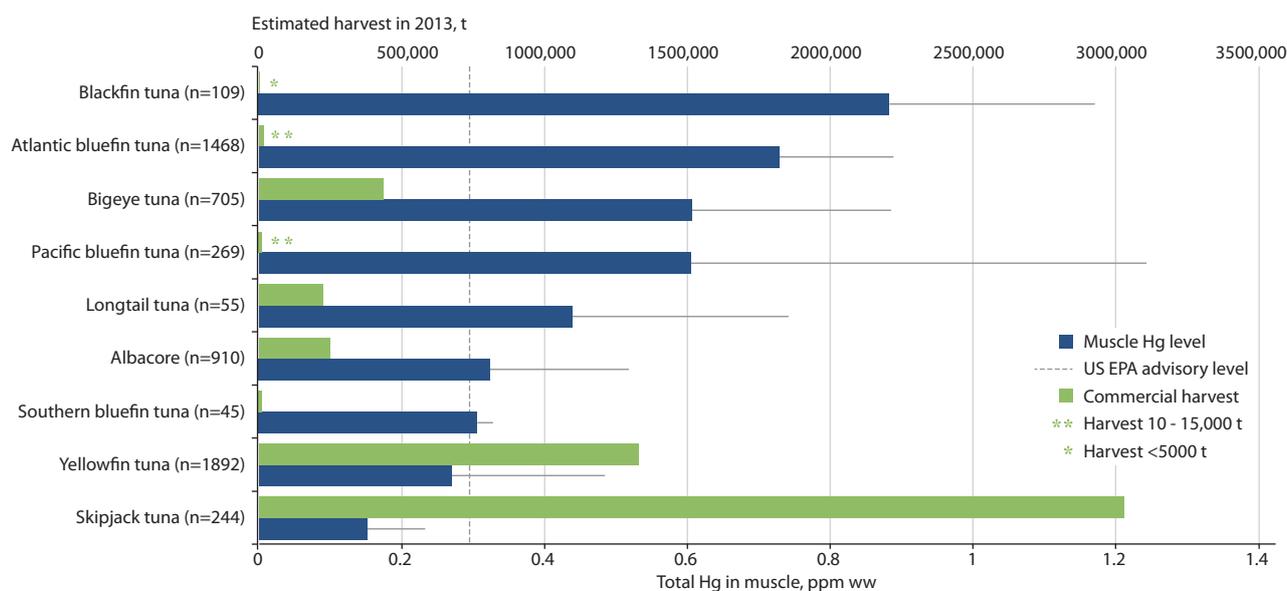
Figure 7.4 Arithmetic mean ± SD of global total Hg concentrations in muscle tissue of nine tuna species from the GBMS database (Evers et al., 2017) compared against FAO harvest data.

concentrations and often exceed advisory levels (Figure 7.4). These patterns vary by size class within species and ocean basin origin. For example, yellowfin tuna (*T. albacares*) tends to have lower average muscle Hg concentrations than seven of the nine tuna species with data (Figure 7.4), however individuals of that species from the south Atlantic Ocean weighing over 70 kg typically have higher Hg concentrations (Bosch et al., 2016a). Yellowfin and bigeye tuna (*T. obesus*) Hg concentrations grouped by major ocean basin indicate that the eastern and northern areas of the Pacific Ocean have significantly higher Hg concentrations than other ocean basins (Ferriss and Essington, 2011; Nicklisch et al., 2017). This is an area where increasing tuna Hg concentrations have been recorded over the past decade (Drevnick et al., 2015; Drevnick and Brooks 2017) and modelled for several decades into the future (Sunderland et al., 2009). As well as size and origin, other factors to consider include whether the tuna is canned or fresh (for the same species, canned tuna tend to have lower Hg concentrations; García et al., 2016) and farmed or wild. Although farmed tuna tend to have lower Hg concentrations (Balshaw et al., 2008), the amount of Hg bioaccumulation in muscle tissue in wild-caught farmed tuna depends on time spent in rearing pens (Srebocan et al., 2007).

7.4.1.2 Case study: Arctic

AMAP regularly fosters international collaboration and compiles measurements of Hg levels in Arctic biota, including shellfish, freshwater and marine fish, seabirds, marine and terrestrial mammals, and humans. Temporal trends from 83 long time-series for Hg in biota monitored at 60 sites around the Arctic establish one of the best standardized, long-term biomonitoring efforts for Hg in the world (AMAP, 2011). There is a need for concerted international effort to reduce Hg levels in the Arctic owing to long-range atmospheric transport of inorganic Hg from distant source regions, warmer and longer ice-free seasons potentially promoting MeHg production, the release of inorganic Hg stored from thawing permafrost, soils, sediments, and glaciers, and the reliance of indigenous communities on biota that are often upper trophic level species with long life spans and elevated MeHg body

burdens (AMAP, 2011; Dietz et al., 2013; Scheuhammer et al., 2015). Studies show a ten-fold increase in Hg levels in birds and marine mammals over the past 150 years with an average annual rate of increase of 1–4% (AMAP, 2011). In contrast, recent temporal trends in Arctic fish and wildlife have been inconsistent, with Hg concentrations over the past 30 years increasing in some cases but declining elsewhere depending on species, location, and period monitored (Rigét et al., 2011). Continued long-term Hg biomonitoring is therefore critical for tracking changes in inorganic Hg emissions, deposition, and bioavailability of MeHg in food webs across the Arctic. This is necessary to protect indigenous communities (AMAP, 2011) and to determine the degree to which global climate change is altering Hg pathways within the Arctic (McKinney et al., 2015; Eagles-Smith et al., 2018a).

7.4.1.3 Case study: Subarctic oceans

In some areas of North America, wildlife remains an important food source among subsistence communities. Baffin Island, located in eastern Arctic Canada, is an ecologically significant area, supporting many species of marine birds and mammals. Many Inuit communities rely upon Baffin Island's marine resources (Chan et al., 1995; Mallory et al., 2004). The presence of MeHg in biota (marine mammals, seabirds) throughout the Canadian Arctic is well established (Muir et al., 1999; Mallory et al., 2004; Campbell et al., 2005; Mallory and Braune, 2012) with increasing trends observed in seabirds over recent decades (Environment and Climate Change Canada, 2016). Generally, MeHg concentrations in seabirds in the Canadian Arctic are below levels associated with health effects in wildlife. However, edible parts (breast muscle, eggs) approach or exceed the action level (0.22 µg/g) set by the Great Lakes Advisory Council (Figure 7.5).

Mercury concentrations in marine bird eggs from the Canadian Arctic have increased significantly over recent decades using kittiwakes (*Rissa* spp.), fulmars (*Fulmarus* spp.) and murres (*Uria* spp.) as bioindicators (Figure 7.5; Campbell et al., 2005; Braune 2007; Braune et al., 2016). In the Aleutian Islands of Alaska there has been an effort to
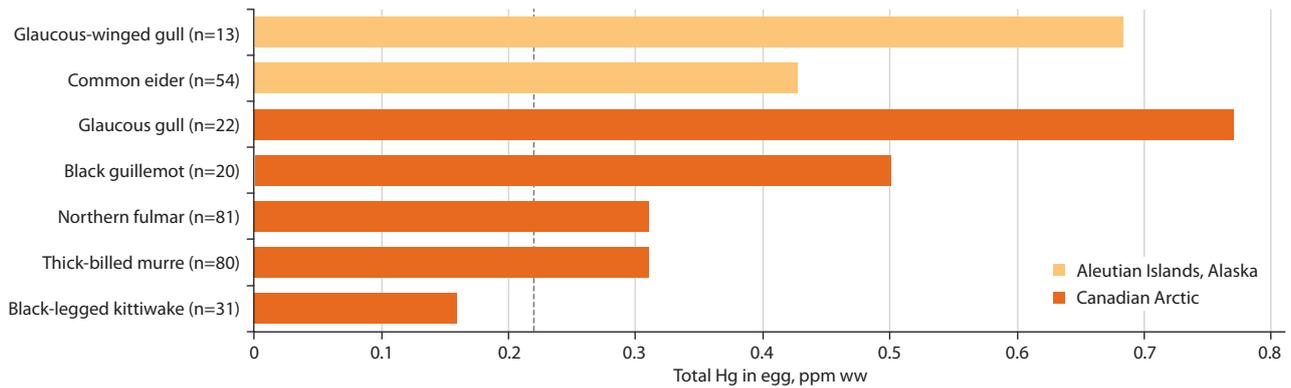
Figure 7.5 Total Hg in marine bird eggs from the Aleutian Islands, Alaska, USA and the Canadian Arctic.

quantify MeHg uptake by local North Pacific fisheries and wildlife due to potential cumulative inputs of Hg from historic military activity (Burger and Gochfeld, 2006; Anthony et al., 2007; Ricca et al., 2008), emissions from local volcanic activity (Ricca et al., 2008), and atmospheric and oceanic transport of Hg from Asia (Rocque and Winker, 2004; Anthony et al., 2007; Driscoll et al., 2013) and Russia (Fisher et al., 2012). Mercury accumulation in marine birds from the Aleutian Islands has been well documented (Burger et al., 2007, 2008, 2009; Burger and Gochfeld, 2009; Savoy et al., 2017).

The Aleuts and subsistence hunters have a history of consuming marine birds (Burger et al., 2007), and especially eggs (Naves, 2009). According to Burger et al. (2007), 90% of households from an Aleutian village consumed birds to some degree each year. Previous studies have shown that some seabird species from the Aleutian Islands contain edible parts (breast meat, eggs) with Hg levels that approach or exceed human consumption advisory levels (0.22 µg/g ww) (Burger et al., 2007, 2009). Abundance and ease of collection mean the eggs of glaucous-winged gull (*Larus glaucescens*) are highly sought, and the number collected each year can exceed 6000 (Naves, 2009). Gulls routinely contain the highest Hg concentrations among seabirds.

7.4.1.4 **Case study: Boreal and temperate lakes (Europe)**

Records of Hg in freshwater fish across Fennoscandia (Norway, Sweden, Finland, Kola Peninsula in Russian Federation) have been collected for over 50 years in almost 3000 lakes and rivers. These data have been collated into a single database by the International Cooperative Programme (or ICP Waters), under the UNECE Air Convention (Figure 7.6, Braaten et al., 2017). Fish Hg concentrations vary widely among lakes in Fennoscandia owing to differences in Hg pollution in the lakes, as well as other factors controlling the rates of methylation and subsequent biomagnification.

Measured Hg concentrations in the south (55°–60°N) are generally higher than in the north (60°–70°N), with over 40% of lakes containing fish muscle Hg concentrations exceeding the WHO/FAO limit of 0.5 ppm widely used as a trigger for human consumption safety (all data are total Hg concentrations in muscle tissue on a wet weight basis). The dataset includes important species for recreational fishing such as pike (*Esox lucius*), Arctic char, perch (*Perca fluviatilis*), and brown trout (*Salmo trutta*) (Figure 7.6).

Long-term patterns of fish Hg concentration in Fennoscandian lakes show a clear decline (Åkerblom et al., 2014; Braaten et al., 2017). However, there is no decline in those lakes for which Hg originates from atmospheric sources only. Closing of local industrial pollution sources over the past 50 years is likely to have led to a reduction in fish Hg concentrations.
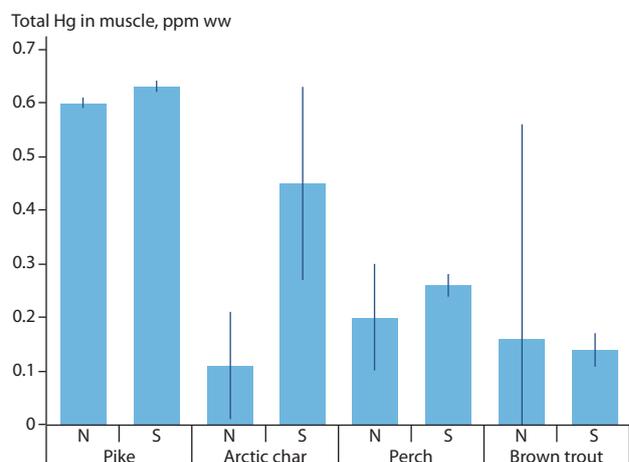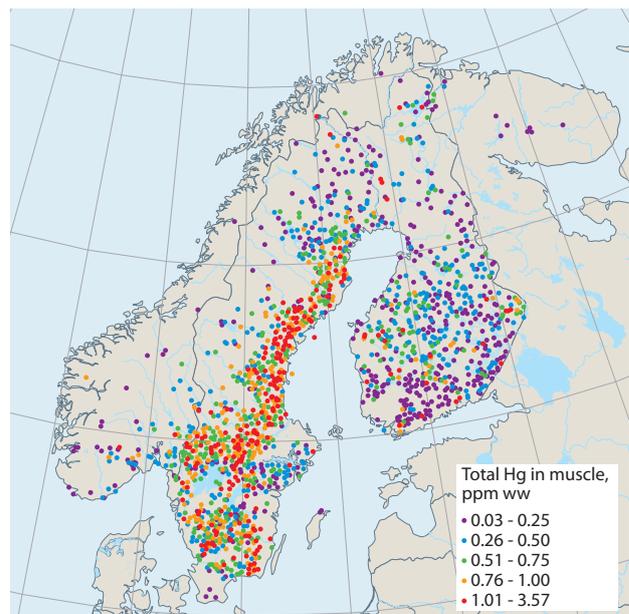
Figure 7.6 Lakes and streams that have been monitored for fish Hg concentrations over more than 50 years in northern Europe and levels observed in four species in northern and southern lakes and streams.

To evaluate spatial and temporal variation of Hg in fish, the fish Hg data are first normalized with regard to size using well-established standard units (e.g., 55 cm and 1 kg for northern pike; Sorensen et al., 1990). Such standards have been applied to robust Hg datasets (i.e., >50,000 data points) in the USA, Canada, and northern Europe for northern pike, bass (*Micropterus* spp.) and walleye (*Sander vitreus*; Johnels et al., 1967; Kamman et al., 2005; Monson 2009; Monson et al., 2011; Gandhi et al., 2015; Eagles-Smith et al., 2016a) for human health assessments and using perch (*Perca* spp.; Scheuhammer et al., 2016) for evaluating concerns for ecological health purposes.

7.4.1.5 Case study: Tropical rivers (Africa)

Mercury sources in Africa are concentrated in West Africa, the East African rift valley, and South Africa. Around 70% of Hg emissions on the African continent are associated with ASGM (UNEP, 2013a). A review of fish Hg levels (407 measures from 166 species) from 31 waterbodies in 12 African countries found that, in general, Hg levels were low but that in fish sampled near ASGM sites (25% of locations) had mean fish Hg levels that exceeded the 0.3 ppm (ww) US EPA guideline value (Hanna et al., 2015). A similar pattern was found in Ghana (1305 measures in 65 species) in which four of 52 sampling sites associated with ASGM had fish Hg levels that exceeded the US EPA guideline value (Rajaee et al., 2015).

In Africa, subsistence and commercial fisheries are important to food and economic security, contributing up to 70% of animal protein consumption (Hanna et al., 2015). Earlier studies documenting Hg concentrations in fish from uncontaminated lakes throughout Africa revealed relatively low concentrations (Black et al., 2011), but only 3.7% of inland water bodies have been studied for Hg contamination in fish (Hanna et al., 2015). Mercury concentrations in Nile perch (*Lates niloticus*) and tilapia (representing multiple genera), the most important commercial species, tend to be <0.5 ppm ww (Hanna et al., 2016). However, local studies within individual countries show aquatic ecosystems that are impacted by Hg. Concentrations in fish from lakes and rivers in Ghana, Tanzania and South Africa have metal contaminants including Hg at levels of concern for human consumption (Hanna et al., 2015; Rajaee et al., 2015; Gbogbo et al., 2017; Walters et al., 2017). A study at a South African gold mine found an extremely high percentage (>90%) of MeHg in water suggesting very high methylation potential in mine watersheds (Lusilao-Makiese et al., 2016). Shellfish from ASGM sites on the Gambia River in Senegal had Hg concentrations above WHO safety guidelines, but fish samples did not (Niane et al., 2015). Although local people consuming fish had elevated Hg levels in hair, the difficulty in measuring Hg in hair from people within ASGM communities is a concern (Chapter 9). Of piscivorous fish in reservoirs in Burkina Faso, 70% have MeHg levels above the threshold for wildlife protection (Ouédraogo and Amyot, 2013). Although, some sites with elevated Hg levels in fish are associated with wetlands, power stations, and dams, associations with ASGM-related Hg contamination highlight the need for further biomonitoring near such sources.

Mercury concentrations in river deltas have been less studied in Africa than in inland waters, but are known for coastal foodwebs in Senegal (Diop and Amara, 2016). Mercury concentrations in terrestrial and freshwater ecosystems of South Africa appear elevated, as observed in some avian species (Daso et al., 2015).

7.4.1.6 Case study: Coast and estuaries (Indo-Pacific)

The world's estuaries represent ecosystems that are sensitive to the input of Hg from contaminated sites and atmospheric deposition into watersheds draining into coastal river deltas (Correia and Guimarães, 2017; Fragoso et al., 2018). Estuaries within the Indo-Pacific area generally comprise mangrove wetlands and associated seasonally-flooded forested areas, habitats which are well known for their ability to capture and methylate Hg (Li et al., 2016a; Haris et al., 2017; Sun et al., 2017).

ASGM activities and emissions from coal-fired power plants are two major contributors to the region's Hg burden. Atmospheric deposition of Hg from these and other sources are being monitored by the Asian-Pacific Mercury Monitoring Network, which helps provide a standard approach for determining temporal trends and spatial gradients (UN Environment, 2016). Recent research using Hg isotope techniques shows Hg in the mangrove wetlands of southeast China to have originated from atmospheric deposition (Sun et al., 2017).

7.4.1.7 Case study: Tropical rivers (South America)

The major river basins of South America, including the Magdalena, Orinoco, Amazon, and La Plata, support a large freshwater fishery, providing livelihoods for small-scale artisanal fishers as well as major commercial enterprises (Barletta et al., 2010). In the remote interior areas of South America, indigenous communities are highly dependent on freshwater resources for subsistence, and for communities with high fish consumption the risk of Hg and MeHg exposure can be high (Uryu et al., 2001; Oliveira et al., 2010). Research over several decades in the Amazon Basin has repeatedly identified a link between a diet high in fish, especially piscivorous and omnivorous species, and elevated Hg concentrations in human biomarkers such as hair (Bidone et al., 1997; Lebel et al., 1997; Castilhos et al., 1998; Boischio and Henshel, 2000; Bastos et al., 2006; Costa et al., 2012; Faial et al., 2015).

The GBMS database for South America contains over 170 peer-reviewed publications on fish Hg concentrations from more than 240 sites across 100 different waterbodies (lakes, rivers, estuaries, bays); more than 27,000 individual fish from more than 240 genera are represented (Evers et al., 2017). Mean Hg concentrations range from below the detection limit to 4.4 ppm ww. The most commonly sampled taxa include species within the *Hoplias* (tigerfishes), *Serrasalmus* (piranhas), *Pseudoplatystoma* (sorubim catfishes), *Cichla* (neotropical cichlids) and *Odontesthes* (silversides) genera. Such data highlight areas of extensive freshwater sampling (e.g., Madeira and Tapajos Rivers of Brazil) as well as areas where extensive data gaps exist (e.g., the countries of Paraguay and Guyana) (Evers et al., 2017).

From these data, 'hotspots' of concern for ecological and human health start to emerge (Figure 7.1). Much of the research on Hg in environmental and human Hg exposure has been conducted in areas impacted by ASGM (Olivero-Verbel et al., 2015; Moreno-Brush et al., 2016; Salazar-Camacho et al., 2017). These and other Hg point sources (such as petroleum extraction; Webb et al., 2015) that are connected with river floodplain habitats, where daily and seasonal water level fluctuations can be extensive, appear to be sensitive to elevated methylation rates (Hsu-Kim et al., 2018).
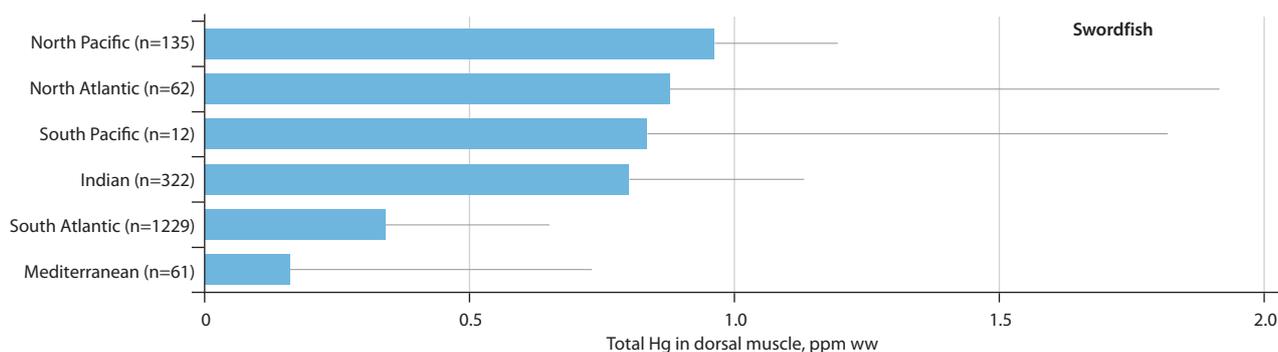
Figure 7.7 Arithmetic mean ± SD of global total Hg concentration in dorsal muscle tissue of swordfish from known ocean basins from the GBMS database (Bodin et al., 2017; Evers et al., 2017).

7.4.1.8 Case study: Small Island Developing States (Seychelles)

Large and relatively long-lived pelagic species such as billfishes are good bioindicators for understanding broad spatial gradients of MeHg contamination in the world's oceans using current commercial resources. Mercury body burdens in billfish, such as marlin (multiple genera; Drevnick and Brooks, 2017; Vega-Sánchez et al., 2017) and swordfish (*Xiphias gladius*, Mendez et al., 2001; Branco et al., 2007), are some of the highest known for marine teleost fish (Table 7.1; Rodrigues and Amorim, 2016). In swordfish, Hg body burdens vary according to major ocean basin with a tendency for more elevated Hg concentrations in the Northern Hemisphere (0.83±0.42 ppm) than the Southern Hemisphere (0.38±0.34 ppm) (Figure 7.7). In addition to their high trophic level and relatively long lifespan (>10 years), swordfish have important commercial value and are an important source of income for many Small Island Developing States.

In the Indian Ocean, 27,000 t of swordfish were harvested annually during the period 2006–2013 (including 270 t caught by local semi-industrial fishing fleets in the Seychelles exclusive economic zone) and were mainly exported as whole fish to the EU (SFA, 2016). The Seychelles Fisheries Authority has recently reported total Hg concentrations of 0.70±0.40 ppm ww (n=226) in Seychelles swordfish edible muscle, with levels increasing with fish size. Similar concentrations were measured in swordfish across the Indian Ocean, except for swordfish caught in east India, Mozambique, and east Rodrigues, with total Hg concentrations of >1.0 ppm (Figure 7.7; Kojadinovic et al., 2006; Esposito et al., 2018).

Islands, such as Sri Lanka (Jinadasa et al., 2014) and the Seychelles, are required to analyse the total Hg concentrations in muscle of swordfish and other large fish species when exporting to the EU – which requires fish imports to have <1.0 ppm ww in tissue for human consumption. Fish with concentrations over this EU advisory level are not permitted (i.e., large specimens with the highest commercial value) and either remain within island communities or are exported to other countries for less value, which can have a significant adverse economic impact. The Seychelles semi-industrial fishing fleet are thus attempting to switch from swordfish to tuna, as Hg concentrations in tuna species within the EEZ are generally <0.5 ppm ww (Bodin et al., 2017). However, this may not be a long-term solution owing to the declining status of tuna populations in the Indian Ocean (e.g., yellowfin tuna: overexploited; bigeye tuna: fully exploited; IOTC, 2016).

7.4.2 Ecological health bioindicators

Many species of fish and wildlife are impacted by the adverse effects of Hg on their physiology, behavior and reproductive success (Dietz et al., 2013; Scheuhammer et al., 2015; Ackerman et al., 2016; Whitney and Cristol, 2017; Evers, 2018). Some are considered high profile species and are included by IUCN on their Red List of Threatened Species, or listed as threatened or endangered by the USA.

Selection of the organism or suite of bioindicators depends on the objective. Taxa suitability may vary according to ecosystem interests (at habitat or biome levels of relevance), spatial resolution (local, regional or global), temporal scale (short- or long-term), human or ecological health interests, endpoints of importance (reproductive impairment), known adverse toxicity thresholds (by tissue and taxa using endpoints of interest), sample availability (simple or challenging), and sampling outcome (non-lethal or lethal). A provisional list of some potential bioindicators for evaluating and monitoring environmental Hg loads for ecological health purposes can be grouped into four target biomes and their associated waterbodies and by major taxa of interest (Table 7.2; Evers et al., 2016).

7.4.2.1 Case study: Sharks

Many elasmobranchs (sharks, skates, rays) have tissue Hg concentrations well above the human health advisory levels set by the World Health Organization (1.0 ppm ww; Table 7.1, Figure 7.8). Species within the mackerel sharks and ground sharks generally have elevated Hg body burdens (de Pinho et al., 2010; de Carvalho et al., 2014; Teffer et al., 2014; McKinney et al., 2016; Matulik et al., 2017), which is of concern because many of these species are already threatened with extinction from overfishing and their meat is also consumed globally. In marine ecosystems, pelagic foraging organisms tend to have higher Hg body burdens than those foraging in benthic habitats (Kim et al., 2012); sharks generally follow this pattern. The potential adverse impacts of MeHg on elasmobranchs are not well understood, although chronic dietary MeHg uptake above 0.2 ppm ww in freshwater fish can affect reproduction and other subclinical endpoints (Depew et al., 2012a). While most sharks have a dietary uptake of MeHg that is well over this benchmark level, it is unclear whether MeHg exposure is causing adverse effects or whether they are actually related to population declines. Of the 14 shark genera with published muscle Hg concentrations, average levels exceed 1.0 ppm ww in 71% of genera.
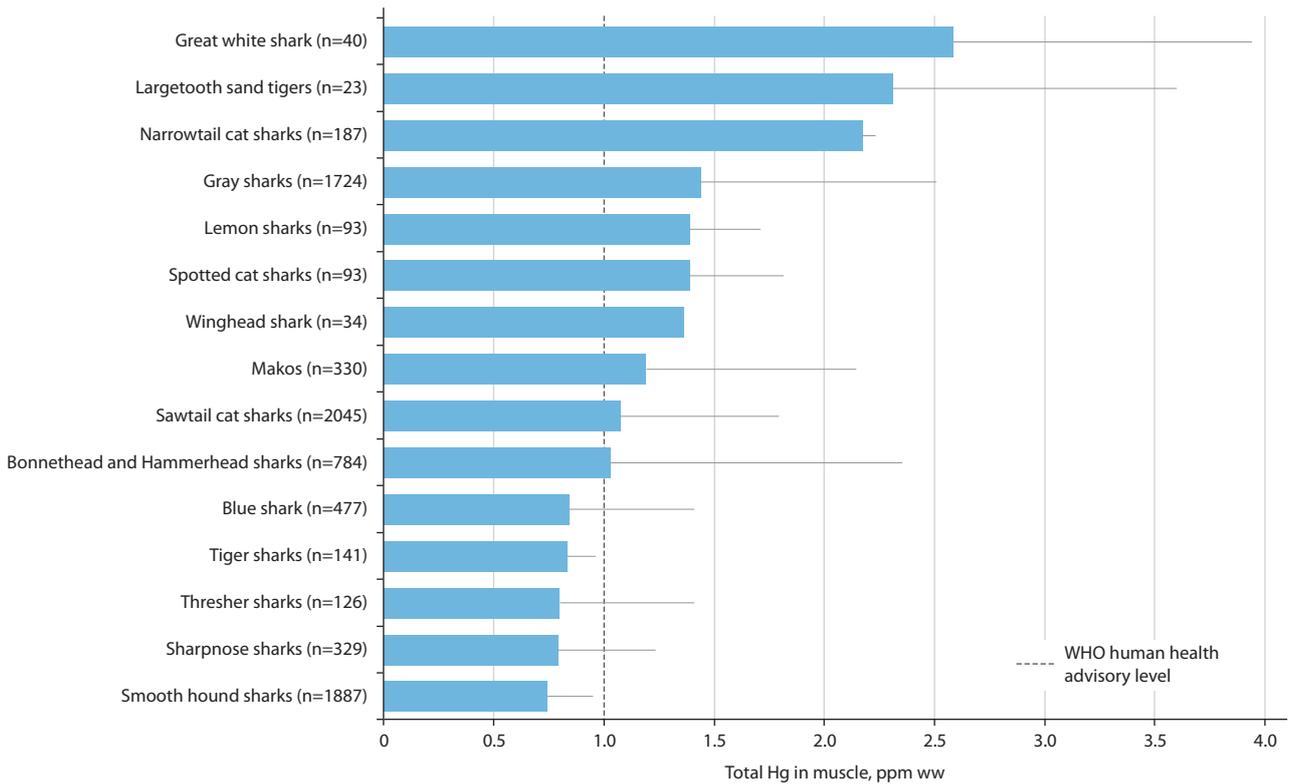
Figure 7.8 Arithmetic mean ± SD of global total Hg concentrations in muscle tissue of sharks by genus from the Orders of Mackerel and Ground Sharks from the GBMS database (Evers et al., 2017).

7.4.2.2 **Case study: Marine birds**

Marine birds occupy a broad range of trophic levels, but most seabirds occur high in the food web and so biomagnify high levels of MeHg (Monteiro and Furness, 1995; Furness and Camphuysen, 1997; Mallory and Braune, 2012; Elliott and Eliott, 2013; Provencher et al., 2014). Due to their foraging strategies, behavioral ecologies, and life-history traits (breeding sequence, molting strategies, foraging ranges, migration patterns), seabirds generally have elevated body burdens of Hg which can ultimately reduce their reproductive capacity and affect their ability to sustain populations over time (Braune et al., 2006; Tartu et al., 2013; Goutte et al., 2014a,b; Bond et al., 2015). Adverse Hg effects on the increasingly rare ivory gull (*Pagophila*

eburnean) are of particular concern (Braune et al., 2006; Bond et al., 2015). Many studies have focused on seabird Hg body burdens from tropical to polar regions and from coastal to oceanic zones, covering most of the world's oceans (Appendix Table A7.1). On a global scale, seabirds exhibit a wide range of Hg concentrations across tissue types (feathers, blood, eggs), driven by spatial differences as well as phylogeny. For example, penguins have the lowest Hg concentrations in eggs, blood, and feathers (except for feathers of tropicbirds), whereas the Procellariiforms (petrels, shearwaters, albatrosses) generally have the highest Hg body burdens (Appendix Table A7.1, Figure 7.9). The Procellariiforms are the best studied group and display a wide range of tissue Hg concentrations which reflect
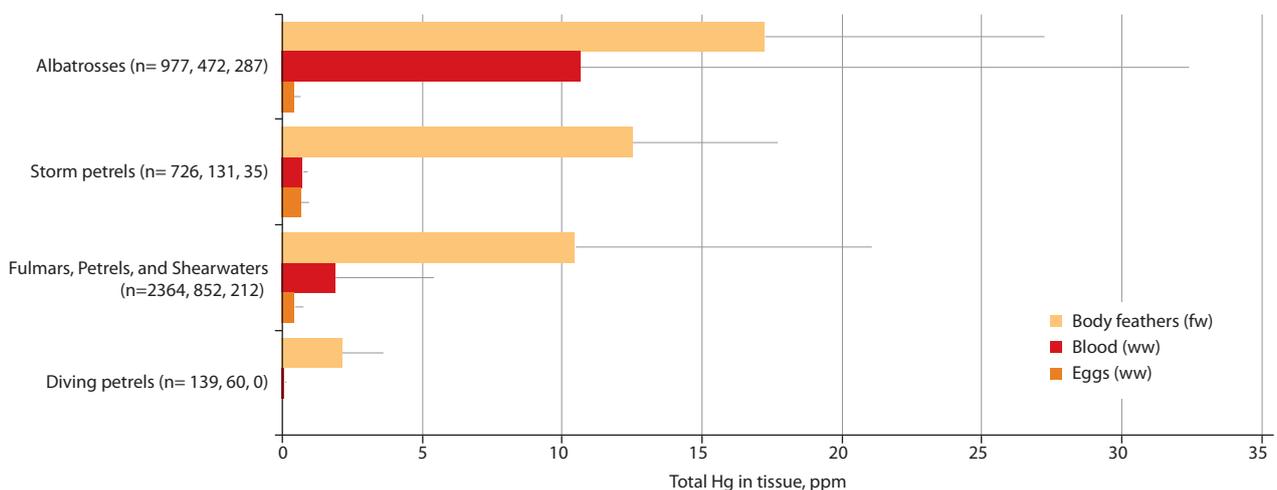
Figure 7.9 Arithmetic mean ± SD of global total Hg concentrations in feathers, blood and eggs of seabird families within the Order Procellariiformes from the GBMS database (Evers et al., 2017).

some phylogenetic differences, with albatrosses exhibiting the highest Hg concentrations (Muirhead and Furness, 1988; Stewart et al., 1999; Anderson et al., 2010; Tavares et al., 2013; Bustamante et al., 2016; Cherel et al., 2018).

The most important factor for predicting seabird Hg exposure is their foraging ecology. Because seabirds use a wide range of habitats, from the littoral zone to the open ocean (benthic and pelagic), different species or individuals with differing foraging behaviors can reflect Hg contamination from different parts of the ecosystems both horizontally (coastal and oceanic food webs) and vertically (benthic, epipelagic, and mesopelagic food webs). Therefore, the study of a group of seabirds with contrasting ecology from the same region allows determination of MeHg availability for multiple marine zones and thus provides a more holistic view (Ochoa-Acuña et al., 2002; Bond and Diamond, 2009; Stenhouse et al., 2018). For example, crustacean-feeding seabirds have lower Hg exposure than cephalopod- and fish-feeders (Carravieri et al., 2014) and epipelagic seabirds have lower Hg exposure than those relying on mesopelagic prey (Ochoa-Acuña et al., 2002). Seabirds of the highest trophic levels with a regular dietary intake of MeHg (such as albatrosses or skuas) are therefore at risk of the effects of MeHg toxicity that are associated with potential long-term population declines (Goutte et al., 2014a,b).

Storm-petrels breeding in the Northern Hemisphere have feather Hg concentrations that are ten times higher (14.1±3.9 ppm) than populations breeding in the Southern Hemisphere (1.6±1.4 ppm) (Figure 7.9). Such a difference is not found for the Procellariidae (8.1±13.1 vs 7.4±13.7 ppm, respectively). Differences between hemispheres should be explored further and should be based on seabirds with similar trophic ecology as well as close phylogeny.

Seabirds permit Hg monitoring across large geographical scales and variations within the same species over longitudinal (e.g., brown noddy, *Anous stolidus*) or latitudinal scales (e.g., skuas). The variation in Hg contamination in seabird tissues can reveal differences in the degree of contamination between major ocean basins, as well as latitudinal gradients of contamination within basins, and trends at a series of spatial and temporal scales.

7.4.2.3 Case study: Loons/Divers

Species within the Order Gaviiformes (loons or divers) are piscivores that breed on freshwater ponds and lakes in temperate and Arctic ecosystems of the Northern Hemisphere. The larger loon species (common loon, *Gavia immer*, and

yellow-billed loon, *G. adamsii*) are obligate piscivores and, as a result, have some of the highest average Hg body burdens of birds in the world (Appendix Table A7.1). In the winter, all loon species migrate to marine ecosystems (with parts of some populations overwintering on freshwater lakes). Loons have been used as bioindicators of MeHg availability in both their breeding and wintering areas for several decades (Evers et al., 1998, 2008, 2011a, 2014; Jackson et al., 2016). In Canada, the common loon and its prey are being studied to evaluate the success of national regulatory standards to reduce Hg emissions (Scheuhammer et al., 2016).

The effects of Hg on loon reproductive success are well established (Burgess and Meyer, 2008; Evers et al., 2011b; Depew et al., 2012b) and are used as benchmarks for evaluating ecological concern. Loons are being used as a standard bioindicator across continents and demonstrate a west to east increasing gradient of MeHg availability in lakes within temperate and boreal forest ecosystems, with Alaskan breeding populations having the lowest Hg concentrations and eastern North American populations the highest (Evers et al., 1998, Figure 7.10). The smaller loon/diver species, while less piscivorous and having lower Hg concentrations (Ackerman et al., 2016), remain potential bioindicators for MeHg availability.

7.4.2.4 Case study: Raptors

Birds of prey, or raptors, comprise a large and varied group of birds generally characterized as predators. Several raptors at the species or genus level have a near global distribution (i.e., ospreys *Pandion haliaetus* and *Haliaeetus* eagles) and so are commonly used in spatial and temporal contaminant monitoring efforts (Bowerman et al., 2002; Weech et al., 2006; Grove et al., 2009; Henny et al., 2009a; DeSorbo et al., 2018). In breeding areas, developing nestlings of many raptor species are often more efficiently captured than resident adults. Adult raptors consistently exhibit higher Hg concentrations than nestlings, largely due to nestlings' ability to depurate Hg into growing feathers (Ackerman et al., 2011). Despite large home range sizes of many raptors, individuals sampled in association with nesting territories generally reflect MeHg exposure in the food web associated with the nesting territory (Bowerman et al., 1994; DeSorbo et al., 2018).

Piscivorous raptors such as ospreys and *Haliaeetus* eagles tend to exhibit the highest adult blood Hg concentrations among raptors (Figure 7.11). Raptor species specializing in bird prey (e.g., many *Accipiter* and *Falco* spp.) generally have higher average Hg concentrations than those predominantly
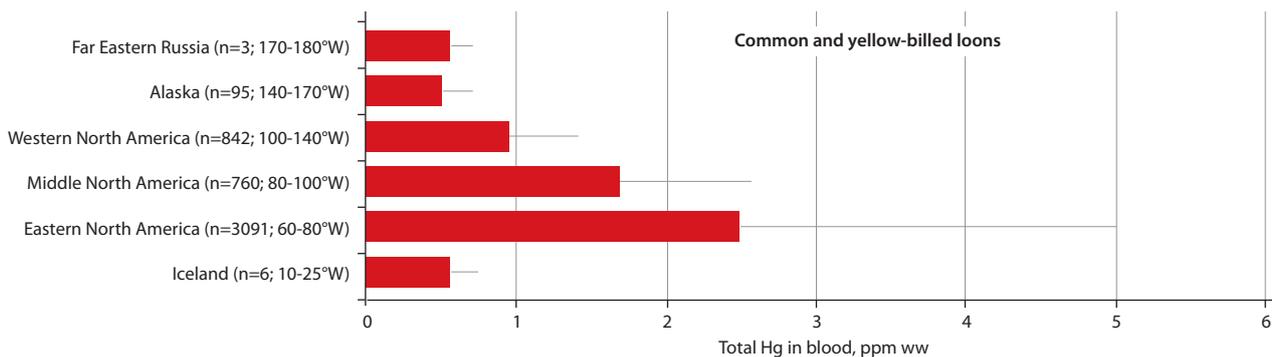
Figure 7.10 Arithmetic mean ± SD of global total Hg concentrations in common and yellow-billed loon indexed blood across parts of the northern hemisphere (10°–180°W) from the GBMS database (Evers et al., 2017).
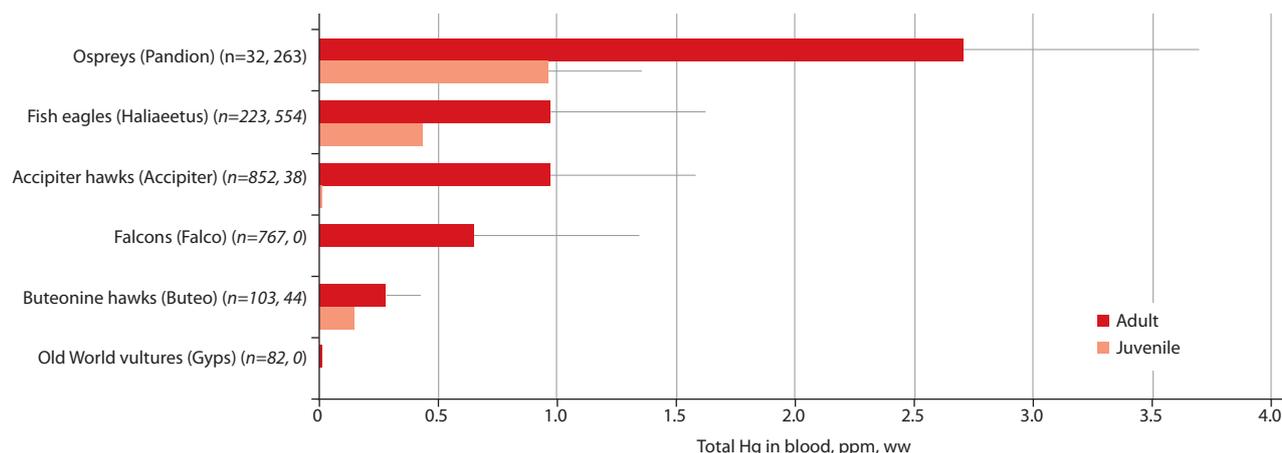
Figure 7.11 Global arithmetic mean ± SD of total Hg concentrations in blood of adult and juvenile age classes of six genera of raptors.

targeting small mammals (e.g., *Buteo* and *Circus* spp.), while obligate scavengers are generally exposed to low levels of Hg.

Piscivorous raptors, namely *Haliaeetus* eagles and ospreys are well-suited for Hg biomonitoring within and across multiple habitat types (marine, estuarine, freshwater river, lake) along the freshwater-marine gradient in ecosystems (Jackson et al., 2016; Rumbold et al., 2017; DeSorbo et al., 2018). *Haliaeetus* eagles are key sentinels in environmental programs used to monitor spatial and temporal Hg exposure patterns in North America, particularly in the U.S. Great Lakes ecosystem (Bowerman et al., 2002). A study of bald eagles (*H. leucocephalus*) in the Great Lakes of the USA found evidence that Hg adversely affects a proportion of this population (Rutkiewicz et al., 2011); in that study, 14–27% of individuals sampled were exposed to Hg at concentrations associated with subclinical neurological damage.

While piscivorous birds were predominantly emphasized in past Hg biomonitoring, recent studies show that MeHg is also prevalent in terrestrial-based food webs, and that invertivorous birds (Passeriformes) can have elevated MeHg concentrations (Jackson et al., 2011a, 2015; Evers, 2018) that result in levels of concern in bird-eating raptors such as Accipiters.

7.4.2.5 Case study: Landbirds

Many species of invertivorous birds (herein landbirds) are also at elevated risk of Hg exposure. In fact, some invertivore-feeding birds have higher tissue Hg concentrations than avian piscivores within the same ecosystem (Evers et al., 2005). They may also be more sensitive to MeHg, resulting in a higher likelihood of adverse impacts on reproductive success (Heinz et al., 2009; Jackson et al., 2011a). An increasing number of studies characterizing Hg exposure in songbirds (Passeriformes) are demonstrating that certain species are at higher risk than

others, based largely on foraging behavior and breeding habitats. Generally, gleaning and flycatching songbirds that breed in wetland habitats (Figure 7.12; Edmonds et al., 2010; Jackson et al., 2011b, 2015; Lane et al., 2011; Hartman et al., 2013; Ackerman et al., 2016; Pacyna et al., 2017), including rice fields (Abeysinghe et al., 2017), are at highest risk of Hg exposure, especially species that forage on predaceous arthropods such as spiders (Cristol et al., 2008). The availability of MeHg to tropical resident songbirds (and other landbird groups) remains relatively unknown, but indications are that some foraging guilds and habitat types are of concern (Lane et al., 2013; Townsend et al., 2013).

Songbird species that spend most of their annual life cycle within wetland-oriented ecosystems and that migrate long-distances (e.g., neotropical migrants or palearctic migrants) may also be at great risk of chronic Hg exposure adversely impacting reproductive success (Jackson et al., 2011a; Varian-Ramos et al., 2014). New findings on elevated Hg exposure and migration physiology/behavior indicate significant adverse impacts are possible, especially for long-distance migrants that may experience decreased flight endurance (Seewagen et al., 2016; Ma et al., 2018) that could also be related to increasing asymmetry in high Hg individuals (Herring et al., 2017).

7.4.2.6 Case study: Marine mammals

Toothed whales and some pinnipeds (or seals) are the marine mammal taxa of greatest concern for human and ecological health, with Hg concentrations regularly recorded in brain tissue that are associated with sub-clinical neurobiochemical changes (Dietz et al., 2013; Krey et al., 2015). Although the effect levels in marine mammals are little understood (Desforges et al., 2016), a study on common bottle-nosed dolphins (*Tursiops truncatus*)
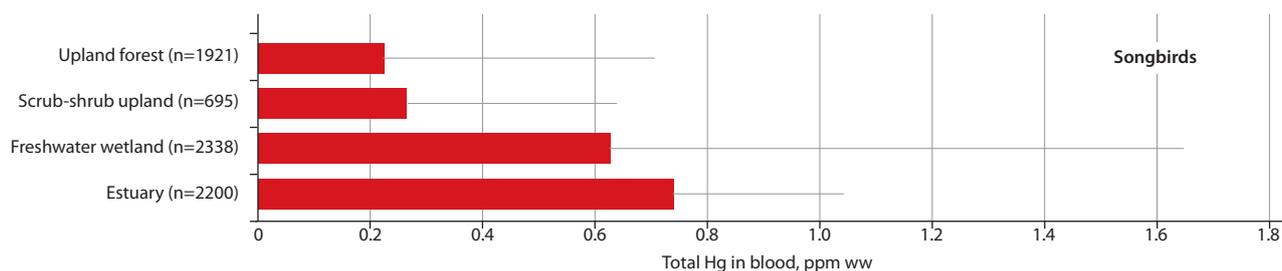
Figure 7.12 Arithmetic mean ± SD of total Hg concentrations in Passeriform (songbird) blood in the United States from the GBMS database (Evers et al., 2017).

found lesions in the liver at 61 ppm ww and is being used by scientists as a benchmark for assessing ecological concern in marine mammals (Dietz et al., 2013). Because liver tissue has a broad percentage of MeHg content and is challenging to relate to muscle tissue (which is a more relevant tissue for human health purposes, Appendix Table A7.1) liver is less useful for rapidly assessing risk for human consumption. Muscle tissue is more useful for assessing the potential exposure of MeHg to humans.

Many subsistence communities, mostly in the Arctic, depend on the harvest of marine mammals such as narwhal (*Monodon monoceros*), beluga (*Delphinapterus leucas*), pilot whale (*Globicephala* spp.), and ringed seal. Ringed seals are potentially important Holarctic bioindicators of MeHg availability to humans because they are common, widely distributed, and regularly harvested (Braune et al., 2015). Based on the GBMS database, over 20 species of toothed whales have average muscle tissue Hg concentrations >1.0 ppm ww. Therefore, toothed whales appear to be one of the more Hg-contaminated groups of marine mammals. Toothed whales have global mean Hg concentrations (2.61 ppm ww; Appendix Table A7.1) well

above general consumption advisory levels recognized by most national standards (and is most relevant for beluga and pilot whales) owing to the dependence of some Arctic human communities on them, and several species have Hg concentrations >4.0 ppm ww (Figure 7.13). Pilot whales are still harvested by some Small Island Developing States, such as the Faroe Islands (Dam and Bloch, 2000; Weihe and Debes Joensen, 2012) and St. Vincent and the Grenadines (Fielding and Evans, 2014) and their elevated body burdens of Hg are of human health concern. Various species of porpoise and dolphin (Aubail et al., 2013; Correa et al., 2013), and beaked whale (which specialize in foraging on deep-water cephalopods), also generally have elevated Hg body burdens (Figure 7.13; Bustamante et al., 2003; Garrigue et al., 2016). Other marine mammals foraging at lower depths in the mesopelagic zone also have elevated MeHg concentrations (Peterson et al., 2015) and are especially vulnerable when MeHg concentrations increase during haul-out periods when body mass declines as they fast and breed on land (Peterson et al., 2018).
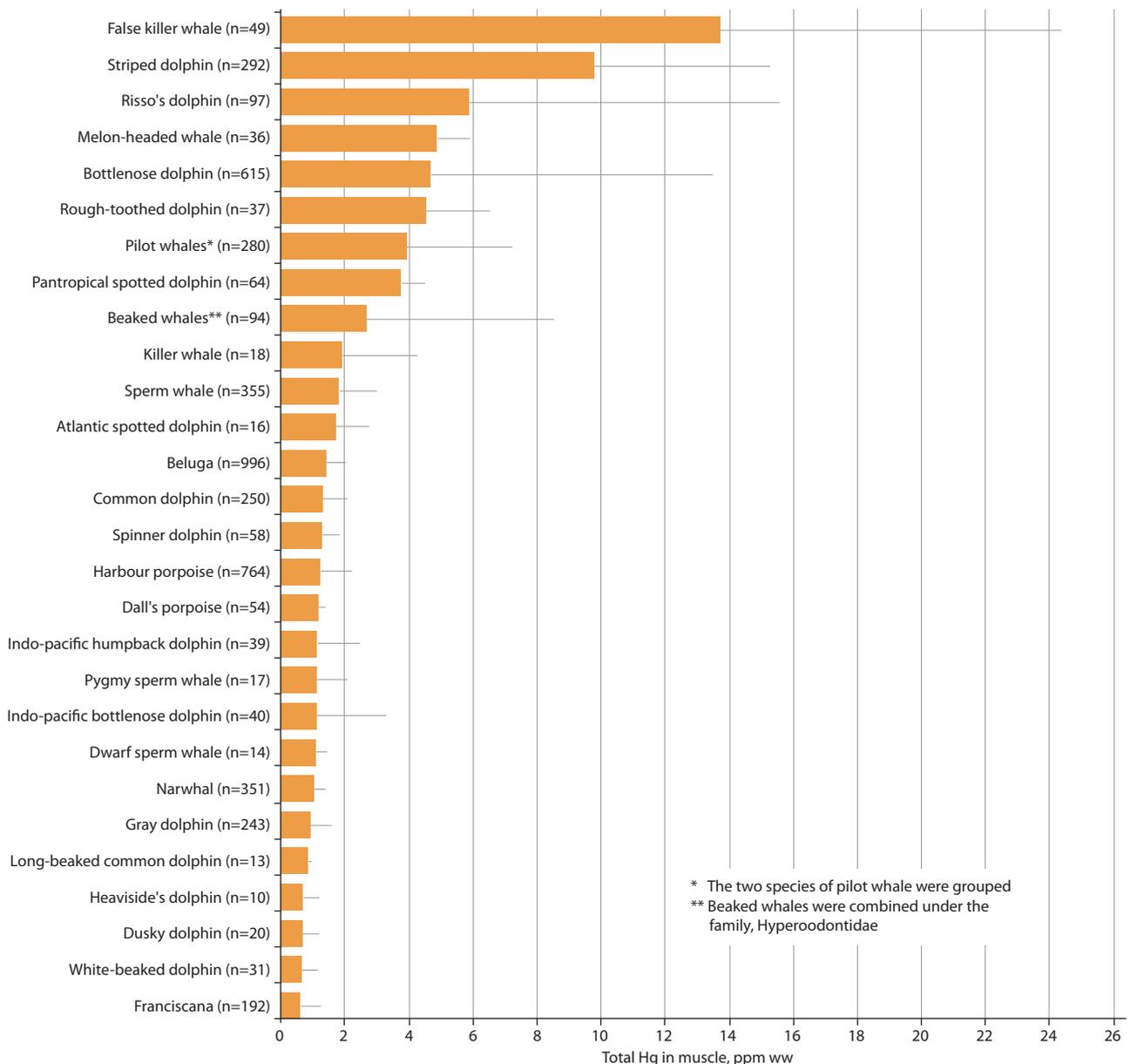
Figure 7.13 Arithmetic mean ± SD of global total Hg concentrations in muscle tissue of toothed whales by species.

7.5 Linkage between Hg source types and biota

Linkage between major Hg source types and Hg found in biota can be evaluated through the use of variations in stable Hg isotope ratios (e.g., Blum et al., 2014; Kwon et al., 2014; Li et al., 2016b). Mercury has seven stable isotopes and undergoes mass fractionation following many different patterns of isotope ratio variation during chemical reactions. The most widely used isotopic 'signals' of sources and chemical processes are mass dependent fractionation (MDF), odd isotope mass independent fractionation (odd-MIF), and even isotope mass independent fractionation (even-MIF). The magnitude of the three 'signals' as well as the ratios between them can be used to distinguish Hg sources and chemical processes in the environment (Blum and Johnson, 2017).

By measuring the isotopic ratios of Hg in environmental samples, certain linkages can be established and others can be eliminated in investigations of Hg sources. The method is often not definitive by itself, but combined with other information based on Hg concentrations and chemical speciation, the evidence considered together can be conclusive. There are many examples in the literature where Hg isotopes have been used to separate the origin of Hg from global gaseous Hg background, global precipitation, coal burning facilities, chlor-alkali facilities, gold mining, and other industrial sources – particularly at local scales.

Several studies have shown that local atmospheric sources of Hg from industrial output can be identified in precipitation and in gaseous Hg because they contrast in isotopic composition with globally well-mixed atmospheric reservoirs (Sherman et al., 2012). Similarly, industrial inputs of Hg to rivers, lakes, and marine coastal areas can often be distinguished from natural background Hg and atmospherically deposited Hg based on isotopic composition (Donovan et al., 2014). Mercury isotopes have also been used as an indicator of Hg methylation and demethylation rates and hotspots within ecosystems, and more broadly as a tool in understanding Hg biogeochemistry (Donovan et al., 2016). In situations where at least two isotopically distinct sources of Hg are present, Hg isotopes have also been used to trace the source of Hg in biota and humans (Sherman et al., 2013).

Using the Hg isotope technique to better track the effects of climate change on Hg dynamics in food webs seems promising. For example, there is evidence that climate change may cause a shift in the depth of Hg methylation in the oceans and that could influence Hg levels in open ocean fisheries (Blum at al., 2014). Separating major Hg sources within existing contaminated sites would increase the potential for identifying how they influence human and ecological health as characterized through bioindicators for purposes related to the Minamata Convention (Evers et al., 2016).

7.6 Overarching global patterns

The compilation of existing biotic Hg data is an important approach to understand broad spatial gradients and temporal patterns. Models based on existing data and scientific findings are useful for extending observations in space and time. Recent global modelling efforts show 49% of global Hg^{II} deposition occurs over the tropical oceans (Horowitz et al., 2017a). The equatorial Pacific region is an essential commercial harvesting location for many large pelagic species such as tunas that are responsible for a large fraction of human exposure to MeHg (Sunderland et al., 2018). Thus, linking elevated Hg deposition to MeHg formation in the ocean and associated biological exposures is an important goal of ongoing research. Similarly, understanding the relationship between enhanced deposition of Hg in India and China and other regions of intense coal use in Europe and the U.S. (Corbitt et al., 2011; Giang et al., 2015) and biological concentrations in inland food webs is essential for linking changes in benefits from future emissions reductions to human and ecological exposures.

In freshwater ecosystems, a global meta-analysis suggests that Hg biomagnification through food webs is highest in cold and low productivity systems (Lavoie et al., 2013), however large contaminated sites (e.g., ASGM areas) are likely to be important drivers of variability in tropical freshwater biota concentrations (Obrist et al., 2018). One recent effort to characterize global aquatic Hg releases to inland ecosystems is therefore especially important for understanding the spatial distribution of these locations (Kocman et al., 2017). Understanding of how Hg released from ASGM and associated conversion to MeHg, exposures, and impacts on human and ecological health is poor (Macdonald et al., 2014; Affum et al., 2016). It is expected that some of the ASGM-derived inorganic Hg into the air, water, and land reaches aquatic food webs and is transferred into higher trophic level organisms but this may vary greatly across these continents. Yet, the associated patterns over time and space are critical to understand for developing biomonitoring activities in a time-efficient and cost-effective manner.

7.6.1 Spatial gradients

The availability of MeHg to high trophic level organisms is not uniform. Some ecosystems are more sensitive to inorganic Hg input than others (Driscoll et al., 2007; Eagles-Smith et al., 2016b) and it is in these areas that biological MeHg hotspots can form and are especially pronounced in higher trophic level organisms (Evers et al., 2007). For terrestrial ecosystems, such areas are generally associated with wetlands and other temporally wetted habitats, and can be particularly pronounced in ecosystems with water chemistry variables such as low pH, moderate to high dissolved organic carbon concentrations, and low to moderate primary productivity. In particular, fluctuating water levels can have a particularly important contribution in generating higher methylation rates and increases in MeHg bioavailability (Willacker et al., 2016); and, may happen at daily (tidal), monthly (artificial reservoirs and pools), or seasonal (river floodplains and dry tropical areas flooded during the wet season) timeframes, as well as under managed areas (rice agriculture).

Therefore, areas that may have elevated MeHg availability are generally not directly related to the deposition or release of inorganic Hg into the environment. For example, compared to the USA, relatively low precipitation-weighted mean concentrations and deposition of total Hg are in Kejimkujik National Park in Nova Scotia, Canada (an average of <5 ng/L and <7.5 µg/m^2 of Hg per year for the past four years of available data; Dastoor and Larocque, 2004; Dastoor et al., 2015; NADP, 2017), yet the biotic MeHg exposure is some of the highest in North America where fish and birds within the

National Park well exceed ecological health thresholds (i.e., 0.30 and 3.0 µg/g ww, respectively; Evers et al., 1998; Burgess and Hobson, 2006; Burgess and Meyer, 2008; Wyn et al., 2009, 2010). This is because most lakes in the area are sensitive to inorganic Hg input and have high methylation potential and MeHg bioavailability owing to a combination of low pH, high dissolved organic carbon, high percentage of shoreline wetlands, and low primary productivity. Ultimately, identification of biological MeHg hotspots can be made through the collection of existing biotic data (Evers et al., 2011b; Ackerman et al., 2016; Eagles-Smith et al., 2016b) and modelling ecosystem sensitivity at regional or global scales.

In marine regions, spatial patterns in biological MeHg concentrations are less resolved but will be facilitated by the development of a global biotic database of Hg concentrations in marine species and modeling efforts to help explain observed spatial patters. Differences in MeHg concentration across ocean basins are apparent in the literature. The highest reported concentrations of MeHg in seawater have been reported in some regions of the Southern Ocean, which also have elevated concentrations of MeHg in some food webs (Cossa et al., 2011). Considerable spatial variability in seawater MeHg concentrations has been reported among other ocean basins, with highest levels in subsurface waters of the most biologically productive areas (Cossa et al., 2009; Sunderland et al., 2009; Bowman et al., 2015, 2016; Munson et al., 2015; Kim et al., 2017). The Arctic appears to have higher concentrations of MeHg in near-surface seawater, which may reflect unique microbial activity resulting from the combination of stratification, freshwater discharges and ice cover (Lehnherr et al., 2011; Heimbürger et al., 2015; Schartup et al., 2015a). Much work remains to link MeHg production regions in the ocean to tissue concentrations in marine biota.

7.6.2 Temporal trends

New models simulating the deposition of Hg from anthropogenic emissions at global scales (using three anthropogenic emissions scenarios) indicate a best case scenario of a decrease of up to 50% in the Northern Hemisphere and up to 35% in the Southern Hemisphere by 2035 (Pacyna et al., 2016). Although tracking Hg emissions, deposition, and releases are important tools for understanding patterns of environmental Hg loads (Sundseth et al., 2017) the relationship between modelled (or measured) deposition and MeHg concentrations in biota is poorly understood. Trends in inorganic Hg concentration are thought to differ among ocean basins because anthropogenic emissions have strongly declined in North America and Europe, leading to large declines in atmospheric concentration, especially in the Atlantic Ocean (Zhang et al., 2016c). Lee and Fisher (2016) postulated that this may also explain observed declines in Atlantic bluefin tuna MeHg concentrations between 2004 and 2012 in the North Atlantic Ocean – which are supported in measured Hg concentrations in blue marlin (*Makaira nigricans*; Barber and Cross, 2015).

The relationship of changing fish MeHg concentrations in different ocean basins is germane to a better understanding of the geographic origins of seafood by country or region. For example, for the USA, 45% of population-wide MeHg exposure originates from open oceans (particularly the Pacific Ocean), 37% from domestic coastal ecosystems, and 18% from aquaculture and freshwater fisheries (Sunderland et al., 2018).

By contrast, both atmospheric emissions and freshwater discharges of Hg have been growing on the Asian continent leading to increased Hg pollution in the North Pacific Ocean (Streets et al., 2009; Sunderland et al., 2009; Amos et al., 2014; Zhang et al., 2015c). Most recent data indicate that the rate of growth in Hg emissions has been slowed by widespread implementation of emissions controls on new coal-fired utilities (Streets et al., 2017). Temporal data on fisheries in the North Pacific are more limited but some researchers have suggested that there is evidence for increases in tuna MeHg concentrations over recent decades (Drevnick et al., 2015), which is further supported by additional analysis of bigeye tuna for the same area (Drevnick and Brooks, 2017).

In North America, long-term biomonitoring in Arctic freshwater (Chételat et al., 2015) and marine (Rigét et al., 2011; Braune et al., 2015) ecosystems provides an important regional platform for examining temporal trends through Canada's Northern Contaminants Program and AMAP. In addition, in the Canadian province of Ontario projected temporal trends in over 200,000 game fish analyzed since 1970 indicate increasing MeHg concentrations in more than 250,000 lakes (which, when including the Great Lakes, represents about a third of the world's freshwater). Using one of the largest consistent Hg biomonitoring efforts in the world, a robust long-term trend in fish Hg concentration can be determined. Using Hg concentrations in the muscle of walleye, northern pike, and lake trout, it is projected that 84–100% of the 250,000+ lakes will have "do not eat" advisories by 2050 for sensitive human populations (Gandhi et al., 2014, 2015). Although inorganic Hg emissions in North America are declining, other factors such as global emissions, climate change, invasive species, and local geochemistry may be impacting the response time and magnitude of biotic MeHg trends for this region (Gandhi et al., 2014). Climate drivers such as higher precipitation rates may be especially important in this area causing increased MeHg concentrations for both cool and warm water gamefish (Chen et al., 2018). Experimental data have suggested that increased discharges of terrestrial natural organic matter, due to climate change, may drive trophic shifts at the base of aquatic food chains that lead to increased biomagnification of MeHg (Jonsson et al., 2017). Recent work on MeHg uptake and trophic transfer for marine food webs in the Northwest Atlantic Ocean suggest that most variability in MeHg concentration in marine plankton can be explained by differences in dissolved organic carbon (Schartup et al., 2018).

The influence of climate change on Hg cycling only increases the importance of generating baseline data for MeHg in bioindicators. An example can be found in Canada where total Hg levels in aquatic birds and fish communities have been monitored across the Canadian Great Lakes by Environment and Climate Change Canada at 22 stations for the past 42 years (1974–2015) (Blukacz-Richards et al., 2017). For the first three decades, Hg levels in gull eggs and fish declined at all stations. In the 2000s, trend reversals were apparent for many stations and in most of the Great Lakes, although the specific taxa responsible varied. While strong trophic interactions among birds and fish are apparent, there also appears to be a high likelihood of trophic decoupling in some ecosystems. This indicates the importance not only of long-term Hg biomonitoring efforts, but also study designs that include other parameters such as food

web structure (Pinkney et al., 2015), watershed disturbances including novel factors such as beaver activity (Brigham et al., 2014), and especially those related to climate change (magnitude and frequency of storm events, increasing wildfire activity, etc.; Sundseth et al., 2015).

7.7 Knowledge gaps

By identifying critical knowledge gaps and adopting quantitative and replicable approaches, a harmonized biomonitoring effort can be developed and made available to countries. A standardized approach that quantifies where, when, how, and what to monitor for tracking environmental inorganic Hg loads, their changes over time, and potential impacts on human and ecological health is now needed. Although there are a few large biological Hg datasets, they do not provide the ability to determine changes in biotic Hg exposure at regional or global scales over decadal periods. Robust statistical approaches are critical for confidently tracking biotic Hg concentrations in the many different biomes around the world, and controlling for the effects of other factors, such as global climate change, altered foraging habitat, changes in primary productivity and changing growth rates that can drive changes in biotic MeHg concentrations with no actual change in inorganic Hg availability (Eagles-Smith et al., 2018a).

One factor in particular, global climate change, will alter future Hg concentrations across the landscape (Sundseth et al., 2017), especially in marine ecosystems (McKinney et al., 2015; Sundseth et al., 2015), subarctic and temperate lakes (Chen et al., 2018), temperate estuarine ecosystems (Willacker et al., 2017), and terrestrial ecosystems (Eagles-Smith et al., 2018a). Specific effects of global climate change include enhanced air-seawater exchange, melting of polar ice caps and glaciers, increased thawing of permafrost, and changes in estuarine sulfur biogeochemistry, but how these landscape processes relate to changes in biotic Hg exposure is relatively unknown.

Iterative efforts to link realistic and applied biomonitoring efforts at local levels with science groups aimed at assisting the Conference of Parties of the Minamata Convention will ultimately help keep pace with the many emerging scientific findings that may fill existing information gaps that are key for global policymaking.

7.8 Conclusions

In summary, the careful selection and use of bioindicators that closely match objectives of the interested parties can be a cost-effective and time-efficient way to track human and ecological health from the anthropogenic loading of Hg onto the water and landscape at a global level (Evers et al., 2016). The methods for biomonitoring and the interpretation of the tissues sampled are generally well-described for many target taxa. The extensive knowledge of Hg exposure in a wide range of fish and wildlife that are available in the peer-reviewed literature, and now available in the GBMS database (Evers et al., 2017), provides a platform for selecting the appropriate taxa within a certain biome or waterbody. Biomonitoring should build from existing programs, which are generally found within developed countries at local, national, and sometimes regional levels. Global pilot projects based on existing networks with local organizations and

governmental agencies have been tested for fish (Buck et al., 2019) and humans (Trasande et al., 2016) and biomonitoring approaches in temperate marine ecosystems are well described (Evers et al., 2008). Generating a more global approach that can amalgamate existing biomonitoring programs and identify the ecosystem, taxa, or geographic gaps is feasible. There are many landscape, ecological, and demographic factors that influence MeHg generation and bioavailability – many of which are known and can be used for scaling models, whereas other factors that affect spatial gradients of biotic MeHg exposure still need further investigation (e.g., climate change). Once country needs and interests of the Minamata Convention are determined by the Conference of Parties, it is feasible to generate cost-efficient and reliable biomonitoring approaches at geographic scales of interest that can be integrated with existing Hg networks.

Chapter 7 Appendix

Table A7.1 Global arithmetic mean ± SD of total Hg (μg/g or ppm) concentrations for selected fish, sea turtle, birds and marine mammals at the taxonomic level of Order (or other groupings for marine mammals). Biota are arranged by major group, then mean Hg concentrations from high to low. Relevant tissue types of target biota vary by major taxonomic classification (i.e., Order) (based on University of Michigan Animal Diversity Web, 2018).

Common Name	Order	Number of locations	Number of individuals	Mean	SD	Min	Max
Sharks, skates, and rays	**Chondrichthyes**			Muscle (ww)			
Chimaeras	Chimaeriformes	6	225	2.81	1.04	0.07	5.16
Cow sharks	Hexanchiformes	6	38	2.51	0.90	0.48	3.43
Electric rays	Torpediniformes	7	47	1.56	1.10	0.02	3.59
Dogfishes	Squaliformes	28	786	1.45	2.11	0.03	10.51
Mackerel sharks	Lamniformes	35	526	1.24	1.02	0.00	10.00
Ground sharks	Carcharhiniformes	205	7806	1.07	0.83	0.00	21.07
Carpet sharks	Orectolobiformes	5	120	0.96	0.29	0.05	3.40
Angel sharks	Squatiniformes	3	98	0.40	0.07	0.03	0.48
Stingrays	Myliobatiformes	33	229	0.33	0.30	0.01	3.50
Guitarfishes	Rhinobatiformes	11	59	0.22	0.28	0.01	2.05
Skates and Rays	Rajiformes	9	88	0.14	0.08	0.01	0.63
Marine fish	**Teleostei**			Muscle (ww)			
Roughy	Beryciformes	18	71	0.53	0.36	0.03	1.91
Tarpons	Elopiformes	15	277	0.46	0.78	0.02	5.78
Perch-like fishes	Perciformes	1430	26231	0.37	0.48	0	24.61
Eels	Anguilliformes	20	349	0.31	0.17	0.01	2.20
Toadfish	Batrachoidiformes	6	117	0.30	0.14	0.03	0.37
Bonefishes	Albuliformes	6	47	0.27	0.19	0.03	1.10
Flatfishes, Flounders, Soles	Pleuronectiformes	112	2713	0.26	0.26	0.00	1.10
Catfishes	Siluriformes	71	1159	0.17	0.14	0.01	1.80
Pipefishes, Sticklebacks	Gasterosteiformes	3	232	0.16	0.13	0.08	0.31
Minnows, Suckers	Cypriniformes	12	312	0.15	0.04	0.00	0.19
Scorpion fishes, Sculpins	Scorpaeniformes	71	1273	0.13	0.11	0.00	1.23
Silversides	Atheriniformes	13	662	0.12	0.07	0.02	0.51
Anglerfishes	Lophiiformes	8	115	0.12	0.10	0.01	0.68
Cods, Hakes, Haddocks	Gadiformes	85	1769	0.12	0.14	0.00	2.35
Mullets	Mugiliformes	91	1048	0.08	0.15	0.00	2.38
Needlefishes	Beloniformes	7	54	0.07	0.03	0.016	0.35
Puffers, Triggerfishes, Leatherjackets	Tetraodontiformes	11	72	0.07	0.06	0.01	0.17
Salmons	Salmoniformes	40	646	0.06	0.03	0.01	0.55
Herrings, Sardinesm Anchovies	Clupeiformes	142	2894	0.06	0.18	0.00	6.48
Aulopiforms, Lizardfishes	Aulopiformes	19	93	0.05	0.08	0.00	0.58
Smelts	Osmeriformes	16	143	0.05	0.09	0.00	0.79
Dragonfishes, Lightfishes	Stomiiformes	5	31	0.05	0.04	0.01	0.19
Lanternfishes	Myctophiformes	11	97	0.04	0.04	0.01	0.32
Freshwater fish	**Teleostei, chondrostei, holostei, dipnoi**			Muscle (ww)			
Bowfins	Amiiformes	544	607	0.97	0.75	0.02	7.00
Needlefishes	Beloniformes	5	116	0.59	0.92	0.02	5.40
Gars	Semionotiformes	164	295	0.45	0.36	0.04	2.41
Bonytongues	Osteoglossiformes	215	1821	0.42	0.84	0.00	20.74

Common Name	Order	Number of locations	Number of individuals	Mean	SD	Min	Max
Perch-like fishes	Perciformes	38981	186940	0.37	0.60	0.00	181.00
Mudminnows, Pikes	Esociformes	7953	31755	0.32	0.23	0.00	9.99
Milkfish	Gonorynchiformes	1	68	0.28		0.11	0.83
Piranhas, Leporins	Characiformes	722	11239	0.26	0.35	0.00	13.44
Catfishes	Siluriformes	6171	21630	0.21	1.24	0.00	175.00
Cods, Hakes, Haddocks	Gadiformes	350	1708	0.20	0.13	0.01	6.40
Eels	Anguilliformes	68	253	0.18	0.12	0.01	0.45
Herrings, Sardinesm Anchovies	Clupeiformes	334	2255	0.16	0.23	0.01	6.64
Knifefishes	Gymnotiformes	16	43	0.16	0.30	0.01	1.92
Sturgeons, Spoonfishes, Paddlefishes	Acipenseriformes	210	614	0.16	0.13	0.00	3.60
Salmons	Salmoniformes	11783	46593	0.14	0.18	0.00	12.30
Minnows, Suckers	Cypriniformes	9420	58094	0.13	0.45	0.00	22.46
Mullets	Mugiliformes	18	67	0.13	0.27	0.00	3.19
Killifishes	Cyprinodontiformes	89	5985	0.13	0.20	0.01	28.50
Scorpion fishes, Sculpins	Scorpaeniformes	1098	4529	0.10	0.14	0.00	2.19
Pipefishes, Sticklebacks	Gasterosteiformes	60	1544	0.08	0.05	0.01	0.46
Silversides	Atheriniformes	1417	6109	0.06	0.05	0.00	0.88
Smelts	Osmeriformes	27	924	0.06	0.07	0.00	2.08
Flatfishes, Flounders, Soles	Pleuronectiformes	1285	3800	0.05	0.21	0.00	5.00
Lungfishes	Lepidosireniformes	15	107	0.01	0.01	0.00	0.04
Reptiles	**Reptilia**	Scutes (fw)					
Sea turtles	Testunides	14	222	0.34	0.57	0.05	2.33
		Blood (ww)					
Sea turtles	Testunides	25	897	0.02	0.02	0.00	0.40
		Muscle (ww)					
Sea turtles	Testunides	41	246	0.06	0.03	0.00	0.66
		Egg Contents (ww)					
Sea turtles	Testunides	15	401	0.07	0.23	0.00	0.13
Birds	**Aves**	Adult Body Feathers (fw)					
Hawks, Eagles, Vultures	Accipitriformes	37	537	18.13	12.46	0.10	193.00
Loons	Gaviiformes	5	637	12.61	1.05	1.72	63.40
Albatrosses, Petrels, Shearwaters	Procellariiformes	183	4206	12.13	10.04	0.08	94.72
Pelecans, Ibises, Herons	Pelecaniformes	6	72	7.24	3.23	0.78	19.07
Rails and Cranes	Gruiformes	4	167	6.88	4.38	0.03	9.04
Grebes	Podicipediformes	3	16	6.16	1.87	4.00	8.00
Kingfishers	Coraciiformes	4	93	6.13	2.28	0.60	46.10
Cormorants	Suliformes	22	252	5.40	2.88	0.25	27.40
Gulls, Terns, Other Shorebirds	Charadriiformes	174	2865	4.20	3.73	0.03	57.00
Tropicbirds	Phaethontiformes	5	79	4.09	3.06	0.80	6.41
Perching Birds	Passeriformes	16	539	2.87	2.04	0.18	10.76
Waterfowl	Anseriformes	26	446	1.92	2.25	0.19	18.00
Penguins	Sphenisciformes	123	1296	1.26	1.28	0.02	9.43
Owls, Goatsuckers	Strigiformes	5	96	1.19	0.36	0.03	12.80
		Adult Blood (ww)					
Pelecans, Ibises, Herons	Pelecaniformes	14	437	5.80	3.72	0.22	20.28
Albatrosses, Petrels, Shearwaters	Procellariiformes	109	1530	4.52	13.11	0.06	209.37
Loons	Gaviiformes	101	4927	2.01	2.14	0.00	20.32

Common Name	Order	Number of locations	Number of individuals	Mean	SD	Min	Max
Grebes	Podicipediformes	10	473	1.67	1.54	0.36	5.37
Cormorants	Suliformes	49	893	1.30	1.75	0.19	17.14
Rails and Cranes	Gruiformes	17	311	1.22	1.18	0.00	3.31
Kingfishers	Coraciiformes	10	275	0.94	0.81	0.04	3.35
Hawks, Eagles, Vultures	Accipitriformes	80	1320	0.90	0.83	0.00	7.40
Woodpeckers	Piciformes	2	18	0.75	0.83	0.09	1.27
Gulls, Terns, Other Shorebirds	Charadriiformes	277	3031	0.65	0.65	0.01	4.26
Falcons	Falconiformes	10	788	0.64	0.69	0.04	2.59
Waterfowl	Anseriformes	248	4230	0.55	1.15	0.00	6.62
Owls, Goatsuckers	Strigiformes	15	147	0.54	0.63	0.02	2.26
Perching Birds	Passeriformes	309	7668	0.50	0.69	0.01	6.72
Penguins	Sphenisciformes	29	330	0.31	0.22	0.04	0.75
Tropicbirds	Phaethontiformes	1	32	0.27		0.27	0.27
Doves, Pigeons	Columbiformes	3	49	0.00	0.00	0.00	0.00
				Eggs (ww)			
Loons	Gaviiformes	25	1941	0.87	0.41	0.00	9.03
Kingfishers	Coraciiformes	1	16	0.56		0.03	3.03
Gulls, Terns, Other Shorebirds	Charadriiformes	433	16413	0.48	0.39	0.00	3.74
Albatrosses, Petrels, Shearwaters	Procellariiformes	26	534	0.44	0.27	0.12	1.74
Falcons	Falconiformes	33	972	0.43	0.20	0.01	1.01
Cormorants	Suliformes	20	586	0.27	0.08	0.00	1.07
Rails and Cranes	Gruiformes	13	761	0.20	0.18	0.03	2.70
Hawks, Eagles, Vultures	Accipitriformes	81	1031	0.17	0.18	0.00	2.48
Pelecans, Ibises, Herons	Pelecaniformes	60	1491	0.17	0.17	0.00	1.90
Waterfowl	Anseriformes	64	1838	0.15	0.21	0.00	3.93
Perching Birds	Passeriformes	68	3856	0.10	0.04	0.00	1.50
Grebes	Podicipediformes	13	639	0.09	0.03	0.04	0.18
Penguins	Sphenisciformes	8	109	0.08	0.05	0.02	0.12
Owls, Goatsuckers	Strigiformes	3	14	0.02	0.01	0.00	0.11
Doves, Pigeons	Columbiformes	2	32	0.01	0.00	0.00	0.06
Marine mammals	**Mammalia**			Muscle (ww)			
Toothed Whales	Cetacea: Odontoceti	526	5068	2.64	4.66	0.00	93.52
Seals and Walruses	Carnivora: Odobenidae, Otariidae, Phocidae	166	2338	0.39	0.38	0.00	3.22
Baleen Whale	Cetacea: Mysticeti	34	594	0.08	0.07	0.02	0.74
Polar Bears	Carnivora: Ursus maritimus	5	77	0.08	0.05	0.06	0.24

8. Relationships between trends in atmospheric mercury and mercury in aquatic biota

Authors: Feiyue Wang, Peter Outridge, Robert Mason, Lars-Eric Heimbürger-Boavida, Xinbin Feng

Key messages

- *There are many transformative steps in the environmental cycle of mercury (Hg), between its emission into air from anthropogenic and natural sources to its eventual bioaccumulation in food chains leading to wildlife and human exposure. Multiple geochemical, climatic, biochemical, ecological and physiological processes and factors influence the environmental fate and bio-uptake of Hg. Therefore, there are good reasons to expect that the biological and atmospheric trends of Hg may not respond coincidentally or proportionately in the future, after regulatory action to reduce anthropogenic emissions. This proposition is tested in this chapter.*

- *Methylation/demethylation, between inorganic Hg and methyl Hg (MeHg), is the key transformative step leading to humans in the environmental Hg cycle, as MeHg is the only Hg species to be biomagnified in food chains and is one of the most neurotoxic forms. Aquatic ecosystems are more favorable for methylation to occur than terrestrial ecosystems, because methylation is favored in anoxic environments. Marine ecosystems are of special concern from the perspective of human exposure to MeHg because of the widespread consumption of marine fish and mammals containing high MeHg by many populations.*

- *The factors controlling methylation and demethylation in aquatic ecosystems (e.g., nutrient and carbon loading, acidity, chemical reduction-oxidation status) are complex and still poorly understood. This knowledge gap adds considerable uncertainty to our understanding of the relationship between atmospheric Hg deposition rates and MeHg concentrations in any given environment or aquatic animal population.*

- *In marine ecosystems, sediments are not the only important source of MeHg to estuarine, coastal and open ocean waters as was once believed. Recent extensive evidence points to in situ water column methylation occurring in coastal and pelagic waters in all ocean basins in the world. It is speculated that methylation occurs within the anoxic micro-environments inside 'marine snow' particles, namely the slowly-sinking, decaying organic remains of phytoplankton, zooplankton and their fecal pellets.*

- *Several regional groupings of case studies were synthesized for this assessment, involving data on atmospheric and aquatic biota Hg trends in the Arctic; Fennoscandia; reservoirs in Europe, North America and China; and North American lakes and coastal waters. Atmospheric Hg levels were either increasing, decreasing or stable, depending on the region in question, thus illustrating a range of possible future scenarios. Our analysis found numerous examples of biotic time-trend datasets that did not agree with the trends in regional atmospheric deposition or concentrations over recent decades; in a minority of cases, the atmosphere and biota trends did agree. In some cases, biota and air trends agreed for the first few decades of the study period but diverged in the most recent decade; in others, multiple species of fish and/or aquatic birds in the same area (and so subject to the same atmospheric Hg deposition trend) displayed significantly different directional patterns that either agreed or disagreed with atmospheric trends. A comparison of fish Hg trends in reservoirs was particularly compelling, with those in China generally exhibiting a quite different trend to North American and European reservoirs, and with biotic trends in both regions being unrelated to atmospheric trends. This finding clearly showed that local terrestrial and/or aquatic processes were more important than atmospheric deposition as drivers of biotic Hg concentrations in those systems.*

- *An over-arching general explanation for these results is that they reflect the dominant effects of other multi-causal factors, such as climate change, biogeochemical changes in aquatic ecosystems, and alterations in terrestrial or catchment soil processes, which masked any impact of changing atmospheric inputs. Further investigation is required to elucidate the specific explanations behind cases of non-concurrent atmospheric and biotic time-trends of Hg.*

- *In terms of implications for the future effects of regulatory action to restrict atmospheric Hg emissions, this assessment refined a general model of biotic responses to atmospheric Hg inputs to propose that a wide range of potential outcomes will be observed as atmospheric Hg declines. Small lakes with small, relatively uncontaminated catchment soils, and coastal marine waters with restricted water exchange with the open ocean, in general may show relatively rapid declines in biotic Hg levels. However, severely contaminated freshwaters, and most ocean basins of the world, may not show early and proportional declines in aquatic biota Hg concentrations. In fact, model predictions suggest that many marine food chains may remain significantly elevated in Hg for many decades to centuries after atmospheric Hg levels have returned to near-natural levels because of the long residence times of anthropogenic Hg in intermediate and deep waters, the revolatilization and redeposition of legacy anthropogenic Hg from global soils and surface waters, and the slow rate of penetration of historical and current anthropogenic emissions into deeper water masses.*

8.1 Introduction

The atmospheric and aquatic chemistry of mercury (Hg) is one of the most complex of all trace metals. The Hg that is emitted from anthropogenic (and natural) sources to air is almost exclusively in an inorganic form, as gaseous elemental mercury (Hg^0) and oxidized species (Hg^{II}) in gaseous and particulate forms (see Chapters 3 and 4). Because of the photo-oxidation of Hg^0 during its residence in the atmosphere, the bulk of the Hg deposited onto the Earth's surface is inorganic Hg, which is also the dominant species in terrestrial soils (Fitzgerald and Lamborg, 2014). Mercury entering the aquatic environment thus occurs mainly as different inorganic Hg species, directly deposited from the atmosphere or released from anthropogenic and natural terrestrial sources in dissolved and particulate forms and transported via surface runoff and groundwater seepage (see Chapter 5).

In aquatic environments, the net transformation of inorganic Hg^{II} through methylation to methylmercury (MeHg) is the key step in the Hg cycle leading to wildlife and human exposure. This chapter uses MeHg as a generic term when referring to methylated Hg species, which may include both monomethylmercury (MMHg) and dimethylmercury (DMHg) but often comprises only MMHg, depending on how MeHg is sampled and analyzed. MMHg is one of the most bioaccumulative and toxic Hg species, as well as being the only form that is biomagnified through food chains, whereas DMHg does not bioaccumulate or biomagnify (Fitzgerald and Lamborg, 2014). Thus, most references to 'methyl Hg' in the context of bio-uptake, and wildlife and human exposure, are in fact referring to MMHg (see Eagles-Smith et al., 2018a). Mercury methylation occurs primarily in the aquatic environment, such that aquatic biota are generally more prone to Hg accumulation than terrestrial biota (see Chapter 7), and consumption of aquatic animals (marine fish, marine mammals and freshwater fish) is the most common Hg exposure pathway to humans (see Chapter 9). This chapter focuses on recent advances in understanding of the aquatic processes that determine MeHg exposure and accumulation by both aquatic biota and humans.

Many environmental and ecological factors (e.g., temperature, light intensity, pH, redox condition, organic carbon and nutrient concentrations, and food web structure and dynamics) have a strong influence on the rates of MeHg production (methylation) and degradation (demethylation), as well as the rate of uptake of inorganic Hg and MeHg by aquatic biota (Eagles-Smith et al., 2018a; Hsu-Kim et al., 2018). The complexity of the Hg cycle through the atmospheric, terrestrial and aquatic environments, the limits of our understanding of Hg methylation/demethylation processes, and the number of factors affecting MeHg bioaccumulation and biomagnification, mean that there is considerable uncertainty about how closely and rapidly changes in the emissions and deposition of Hg into the environment brought about by regulatory action will be tracked by changes of Hg in aquatic food webs.

This chapter describes recent advances in our developing understanding of the aquatic chemistry of Hg, particularly focusing on the connectivity between atmospheric Hg and Hg concentrations in aquatic biota. Rather than provide a comprehensive synopsis of all the aspects that affect Hg dynamics in the aquatic environment, much of which can be found in the overviews by AMAP/UNEP (2013) and Fitzgerald and Lamborg (2014), this chapter focuses on the following major topics: recent advances in understanding of Hg methylation and demethylation in marine systems; and relationships between the trends in atmospheric Hg and in aquatic biota, and the reasons for the match or mis-match between those trends. These topics were chosen because they are of the greatest importance with respect to advances in understanding aquatic Hg processes since the 2013 Global Mercury Assessment (AMAP/UNEP, 2013) and because of their relevance to predicting the efficacy of international regulatory action in ultimately reducing Hg exposure in humans and wildlife.

8.2 New understanding of marine Hg methylation/demethylation

8.2.1 General remarks

The concentration of MeHg in an aquatic water column represents the culminating effect of various processes that influence the methylation of inorganic, divalent Hg^{II} to MeHg, its demethylation, as well as transport from the location of its formation to the water column. Generally, Hg is methylated by bacterial processes in sediments and the water column of large waterbodies, such as the ocean and large lakes, but not in the water column of most freshwater ecosystems. While MeHg can be produced by abiotic processes, its formation is thought to be primarily microbially-mediated (Paranjape and Hall, 2017). A major breakthrough was made recently with the discovery of two key genes, *hgcA* and *hgcB*, that control anaerobic Hg methylation first identified in sulfate-reducing bacteria (Parks et al., 2013). The *hgcA* and *hgcB* genes have since been found in many anaerobic microorganisms. An analysis of publicly available microbial metagenomes found the *hgcAB* genes in nearly all anaerobic environments, but much less abundantly in aerobic systems such as the open ocean water column (Podar et al., 2015). However, laboratory experiments have not found a clear relationship between the expression level of the key genes and net MeHg production (Goni-Urriza et al., 2015), pointing to complex interactions. In contrast, demethylation of MMHg and DMHg is thought to occur by both abiotic and biotic pathways, with DMHg being volatile and less stable in the environment than MMHg. Overall, therefore, the concentration of MeHg in any given aquatic environment is the net result of many competing processes of formation, transport, and destruction.

Methylated Hg compounds constitute a small fraction of the total Hg present in some environments (e.g., <1% in air and typically <5% in marine sediments, but with somewhat higher relative concentrations in freshwater sediments and wetland soils; Paranjape and Hall, 2017). However, these compounds can be a much larger fraction of the total Hg in the water column and can exceed 40% of total Hg in the open ocean. In biota, the fraction as MeHg (specifically MMHg in this case) increases as a function of trophic level, from <20% of total Hg in phytoplankton to >95% in high trophic level biota. As MeHg poses the primary exposure risk to humans and other top predators it is of primary importance to understand the production and fate of this compound.

As discussed in later sections, due to the complexity of methylation and demethylation it is not possible to generalize these processes into either global or regional

MeHg budgets, although some progress is being made in this regard. Furthermore, given the complexities that control the *net* formation of MeHg in the environment, it is clear that while reducing total Hg emissions to the environment can be expected to ultimately reduce MeHg in biota in general and over time, more detailed predictions of the effects of regulatory action on Hg in biota in a specific ecosystem requires further investigation of the methylation/demethylation processes in the ecosystem in focus. The following text focuses on methylation/demethylation in marine systems, owing to the predominance of MeHg from marine food webs as the main exposure route in many human populations around the world (see Chapter 9). Other recent reviews (Lehnherr, 2014; Paranjape and Hall, 2017; Eagles-Smith et al., 2018a; Hsu-Kim et al., 2018) should be consulted for syntheses of recent findings on methylation processes in freshwater ecosystems.

8.2.2 Coastal waters

Much of the earlier work concerning Hg methylation in coastal waters highlighted by AMAP/UNEP (2013) was focused on the factors controlling methylation in the sediments and the flux from sediments to the water column. The generally held view at that time was that in many settings, sediments were the major source of MeHg to coastal waters, although there were indications that inputs from terrestrial watersheds and/or from ocean exchange were important in some ecosystems.

In the last few years, several studies have challenged the predominance of sediments as the main MeHg source in coastal marine biota. First, Chen et al. (2014a) found that the concentrations of MeHg in forage fish across multiple estuaries on the U.S. east coast did not track with the MeHg content of the sediments, but with the water column concentration, even though these fish were considered to forage at the sediment-water interface. Conversely, in the same study MeHg in benthic worms did track the sediment MeHg concentrations. Mercury stable isotope analyses also tended to confirm that the sediment may not have been the most important source of MeHg to the organisms in these ecosystems (Kwon et al., 2014). Li et al. (2016b) used Hg isotope analyses to demonstrate that the source of MeHg in biota in Lake Melville, a large subarctic fjord, was from pelagic production. Similarly, sulfur isotope analyses of plankton from Long Island Sound did not support the idea that the accumulated MeHg had a substantial sediment component (Gosnell et al., 2017).

However, Buckman et al. (2017) showed that within the Delaware River estuary, these patterns were more complex and it was less easy to discern the importance of sediment inputs of MeHg compared to riverine inputs. Gosnell et al. (2016) found that for the Delaware River, sediment could be an important MeHg source at certain times of the year, suggesting that sediment sources should not be ignored, although the sediment resuspension studies of Seelen et al. (2018) further supported the notion that sediments play a minor role. Jonsson et al. (2017) showed that changes in the concentration and type of dissolved organic carbon (DOC) as well as MeHg loading can influence MeHg bioaccumulation (see also Balcom et al., 2015; Schartup et al., 2015b; Gosnell et al., 2016). Comparison of water column and sediment MeHg concentrations indicated that in some ecosystems, such as the Hudson River, there is a reasonably strong relationship between dissolved water

column MeHg and porewater MeHg, and between sediment and suspended particulate MeHg, but there are many ecosystems where there is little correlation.

One important factor that has received less attention is the degree to which the MeHg concentrations are influenced by demethylation of MeHg rather than by its formation. Many studies have assumed that demethylation is not a strong control on MeHg levels in coastal ecosystems but this assumption needs to be tested further. Overall, current literature suggests that there are no clear-cut trends across coastal ecosystems and that both internal and external sources of MeHg are likely to be important contributors of MeHg to the food chain.

Recent studies have reached contrasting conclusions on the effect of the nutrient and oxygen status of waterbodies on Hg methylation rates in sediments. In mesocosm studies using stable Hg isotopes, Liem-Nguyen et al. (2016) showed that the addition of nutrients could increase Hg methylation rates in sediments by increasing the activity of benthic microbial communities, but only for labelled Hg^{II} species with a high availability for methylation (such as labile dissolved forms and Hg-organic complexes). Mercury species with low availability in sediments (such as Hg sulfide) did not show an effect of nutrient loading (see also Jonsson et al., 2014). For oxygen status, the consensus is that increased eutrophication leading to oxygen depletion (hypoxia) in bottom waters results in increased MeHg production by providing ideal conditions for sulfate-reducing bacteria. A recent example of this process was provided by the modelling of Soerensen et al. (2016b), which suggested that increased MeHg in Baltic Sea plankton was associated with increasing eutrophication, although there is little evidence for this phenomenon in some estuaries (e.g., Gosnell et al., 2017). Contrary examples have also been reported recently, with no increase in sediment MeHg levels in some coastal regions with bottom water hypoxia (Liu et al., 2015; Chakraborty et al., 2016). In Long Island Sound, in the more eutrophic regions where bottom waters are seasonally hypoxic, plankton had lower MeHg than those from more oligotrophic regions (Gosnell et al., 2017). Again, these results suggest that the interaction between eutrophication and MeHg levels in biota is complex, and likely to vary between locations.

Organic carbon is an additional important factor influencing both Hg methylation and MeHg retention in sediments. For example, Mazrui et al. (2016) found that the binding of Hg to DOC enhanced methylation compared to Hg bound to particulate organic carbon (POC) and Hg present as cinnabar (the most common source mineral for refining elemental Hg). The origins and geochemical quality of the organic carbon (terrestrial or marine) are at least as important as its quantity in terms of its effect on Hg bioavailability (Jonsson et al., 2012, 2017; Schartup et al., 2015b). Additionally, it has been shown in pure cultures and laboratory sediment studies that nanoparticulate Hg has higher bioavailability for methylation than microparticulate forms (Zhang et al., 2014d; Mazrui et al., 2016). These studies reinforce the conclusions of prior studies (Jonsson et al., 2012; Schartup et al., 2013; 2014) that the factors controlling Hg methylation in sediments are extremely complex given the interactions between Hg (and MeHg) and sediment biogeochemistry (primarily, the levels of organic carbon and reduced sulfur) which impact binding, bioavailability and sediment-water exchange. While speciation of the Hg is an important driver, desorption kinetics and microbial community activity are also important controls over the extent of Hg methylation in sediments.

The weight of evidence for the importance of water column methylation in coastal waters has increased in recent years. A number of studies have followed up on earlier work in the Thau Lagoon, France (Monperrus et al., 2007), examining the potential for methylation of Hg within the water column of coastal environments. Several research groups have now shown that there is potential for methylation in the water column of estuaries and coastal waters, especially in locations of mixing and flocculation of particulate material (Ortiz et al., 2015; Schartup et al., 2015a; Sharif et al., 2014). These studies point to the likely enhancement of methylation within aggregated particles where micro-anoxic conditions could exist, as demonstrated by the laboratory experiments of Ortiz et al. (2015). Overall, these studies do not suggest that Hg methylation is occurring through a different microbial biochemical pathway, but that it is occurring within the anoxic microzones within large particulates. Some of these studies have concluded that there is significant net Hg methylation within the water column (Ortiz et al., 2015; Schartup et al., 2015a) while in other cases, the rate of demethylation leads to a net decrease in MeHg (Sharif et al., 2014).

In summary, there is not one specific source for the MeHg accumulating in biota in coastal systems, and the sources are likely to vary spatially and temporally. In examining, and understanding, the dynamics of MeHg bioaccumulation in coastal environments it is necessary to examine both the potential external inputs (watershed and ocean inputs) and the internal production within the system (water column and sediment net Hg methylation). Furthermore, it is likely that their relative importance will change in the future due to climate and other human-caused alterations within these ecosystems.

8.2.3 Open ocean

Like coastal seas, there is increasing evidence for active Hg methylation in the oxygenated water column of open oceans. Early pioneering work by Mason and Fitzgerald (1990) suggested the potential for high rates of *in situ* production of MeHg in the open ocean, and later studies supported the idea of *in situ* MeHg formation (Monperrus et al., 2007; Cossa et al., 2009, 2011; Sunderland et al., 2009; Heimbürger et al., 2010). However, the prevailing paradigm continued to favor a coastal sediment MeHg source with offshore transport to the open oceans. There is now more recent published evidence for water column methylation from almost all major ocean basins: the Atlantic Ocean (Bowman et al., 2015; Bratkič et al., 2016), Pacific Ocean (Hammerschmidt and Bowman, 2012; Munson et al., 2015; Bowman et al., 2016; Kim et al., 2017), Arctic Ocean (Wang et al., 2012c; Heimbürger et al., 2015), Southern Ocean (Gionfriddo et al., 2016), Mediterranean Sea (Cossa et al., 2012, 2018), Baltic Sea (Soerensen et al., 2016b) and the Black Sea (Rosati et al., 2018). No data have been published for the Indian Ocean thus far. Laboratory experiments confirm that net Hg methylation can occur in 'marine snow' (settling organic particles), with similar rates compared to marine sediments (Ortiz et al., 2015). Furthermore, several papers point out that open ocean methylation is required to balance the oceanic MeHg mass budget (Sunderland et al., 2009; Mason et al., 2012; Soerensen et al., 2016a).

A simplified marine Hg cycle describing *in situ* Hg methylation in the oceanic water column is shown in Figure 8.1. A common feature of the MeHg profiles in all ocean basins is a subsurface peak which coincides with a minimum in oxygen concentrations. At the surface, inorganic Hg adsorbs to organic matter, mostly phytoplankton, and
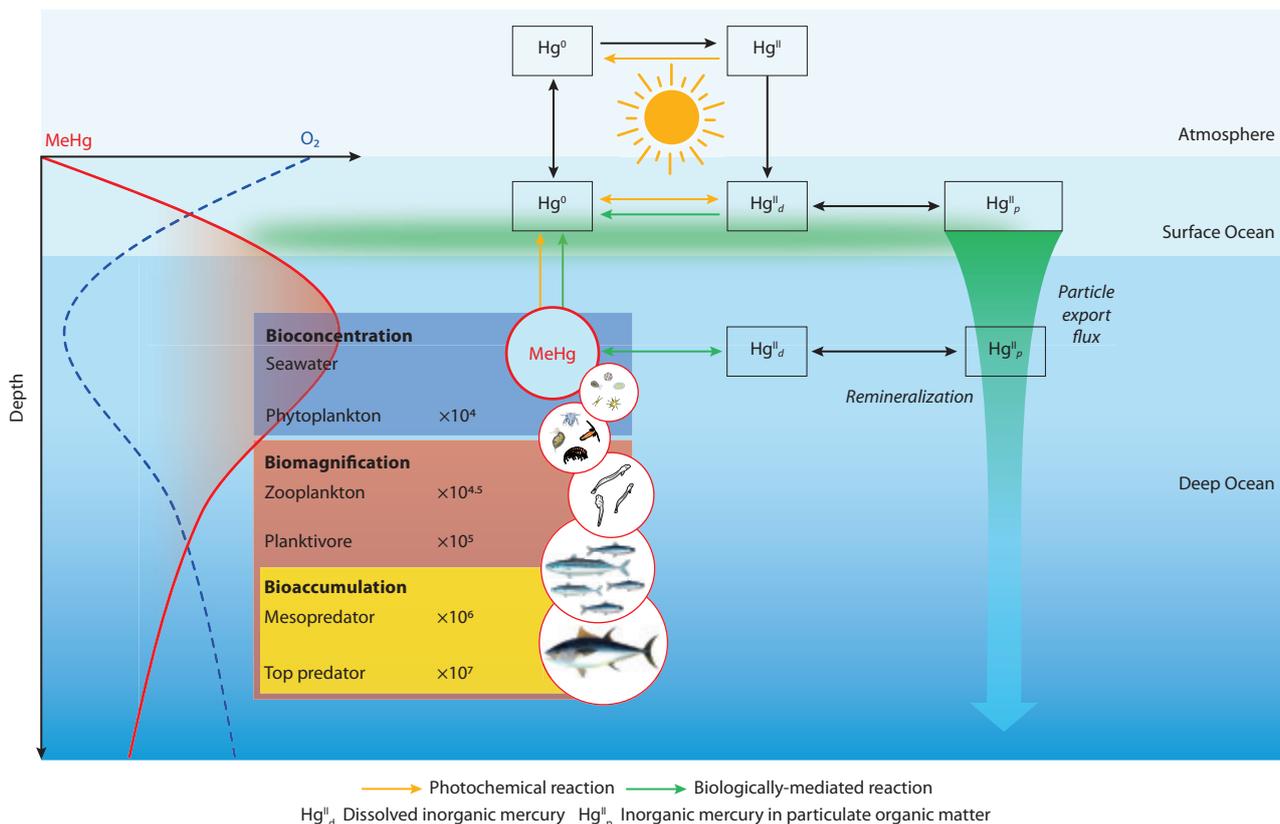
Figure 8.1 Simplified schematic of the marine Hg cycle, showing Hg methylation in the ocean water column.

is then transferred or transported to depth, with particle export flux providing the key ingredients for Hg methylation – organic carbon and Hg. In the subsurface ocean, oxygen is consumed by bacteria that feed on the particulate organic matter, a process known as organic matter remineralization. The correlation of MeHg with oxygen (or apparent oxygen utilization or organic carbon remineralization rates) suggests that organic matter remineralization fuels microbial MeHg production in the water column (Cossa et al., 2009, 2011, 2018; Sunderland et al., 2009; Heimbürger et al., 2010; Kim et al., 2017). The most likely explanation is that particle-attached bacteria generate anoxic micro-niches within marine snow (Sunderland et al., 2009; Ortiz et al., 2015), where anaerobic bacteria can methylate Hg. The MeHg produced at depth is then available for bioconcentration into phytoplankton, which exhibit the largest concentration factor (at least up to 10,000-fold) along marine food chains (Schartup et al., 2018). Bioaccumulation and biomagnification processes in the upper trophic levels control the biotic MeHg concentrations at each trophic step. Different forms of isotopic evidence support this new paradigm. A pioneering study explored the carbon isotope composition of the MMHg compound in tuna and found $\delta^{13}C$ values similar to marine organic matter, suggesting its role as the carbon substrate for Hg methylation (Masbou et al., 2015). Additional evidence comes from Hg isotopic analysis of marine biota. Fish that foraged at different depths in the North Pacific Ocean showed Hg isotope gradients that could only be explained if 60–80% of their MeHg was produced in the water column below the surface mixed layer (Blum et al., 2013).

In general, the depth, shape and importance of the MeHg peak in ocean waters depend on the physical structuring and biological productivity of water columns. Several studies found MeHg hotspots at the density gradients of stratified systems (Wang et al., 2012c; Heimbürger et al., 2015; Schartup et al., 2015a; Soerensen et al., 2016a; Rosati et al., 2018). High MeHg concentrations have also been observed in the oxygen minimum zones of upwelling regions (Conaway et al., 2009; Cossa et al., 2011; Bowman et al., 2016). Two field studies (Baya et al., 2015; St. Pierre et al., 2015) and a modelling study (Soerensen et al., 2016a) suggest the potential for enhanced DMHg evasion from the Arctic Ocean, where MeHg is produced at shallow depths (Wang et al., 2012c; Heimbürger et al., 2015).

Mercury methylation may also take place in the sea ice environment of the polar oceans (Beattie et al., 2014). Marine microaerophilic bacteria have been identified as a potential Hg methylator within sea ice, where the anaerobic bacteria which are known to methylate Hg were absent (Gionfriddo et al., 2016). These bacteria could potentially be responsible for Hg methylation in the open ocean water column (Sunderland and Schartup, 2016).

8.3 How closely do Hg levels in aquatic biota respond to changes in atmospheric Hg, and why?

In addition to methylation and demethylation processes, many other processes and factors affect the uptake of Hg by aquatic biota (Eagles-Smith et al., 2018a; Hsu-Kim et al., 2018).

These include the transport and speciation of Hg between emission sources and terrestrial and aquatic systems (see earlier chapters of this report), biological uptake of Hg (both inorganic Hg and MeHg), and biomagnification of MeHg in the food webs. The complexity of these processes, along with the large inventories of legacy anthropogenic and natural Hg stored in terrestrial and aquatic systems (see Chapter 2), dictate that the biotic Hg trends may or may not follow the same trends as atmospheric Hg. Furthermore, even if they do follow similar trends, there could be a significant time lag between them. This section compares recent trends in atmospheric Hg with those in aquatic biota, and discusses why they may or may not follow each other. This is done by examining major recent studies since GMA 2013 on biotic Hg trends as summarized in four case studies. These case studies are from North America, Europe, China, and the Arctic where Hg concentrations in certain aquatic biota have been monitored continuously or intermittently for several decades. No such long-term, time series data for biotic Hg are available for other regions of the world, especially for the Southern Hemisphere. A more thorough review of biotic Hg concentrations is provided in Chapter 7.

8.3.1 Trends in atmospheric Hg concentration and wet deposition

Before presenting the case studies, this section first reviews the general trends in Hg concentrations in air and in wet deposition, with which the aquatic biotic Hg trends will be compared.

North America and Europe are considered together here because their overall atmospheric Hg concentrations and deposition fluxes have trended similarly over the past few decades (Zhang et al., 2016c). Measured Hg concentrations in the air (Hg^0, or total gaseous Hg) declined by 10–40% between 1990 and 2010 across most of North America and Europe (Slemr et al., 2011; Cole et al., 2014; Weiss-Penzias et al., 2016), a pattern that has been matched by trends in Hg concentrations and fluxes in wet deposition (Prestbo and Gay, 2009; Zhang and Jaeglé, 2013; Brigham et al., 2014; Weiss-Penzias et al., 2016). This general declining trend agrees very well with the declining Hg point-source emissions in North America and Europe over the same period (AMAP, 2010; AMAP/UNEP, 2013) and has been reasonably reproduced by a recent modelling study with revised global Hg emissions inventories (Zhang et al., 2016c; Figure 8.2). This study accounted for the declining emissions from commercial Hg-containing products since 1990, corrected for shifts in the speciation of airborne Hg emissions related to air pollution control technology, and reduced the putative importance of atmospheric Hg emissions from artisanal and small-scale gold mining (ASGM).

However, a closer analysis of the observational data in Figure 8.2 suggests that this systematic declining trend may have become less clear and uniform, and even reversed, over the most recent decade (i.e., since ~2008). This is demonstrated by a recent study in North America (Weiss-Penzias et al., 2016). Gaseous elemental Hg concentrations in the air were found to have stabilized since 2008 with a flat slope over time. While Hg concentrations in wet deposition continued to decline at some sites, an increasing trend has also been observed throughout North America (Weiss-Penzias et al., 2016). Such a diversity in the recent
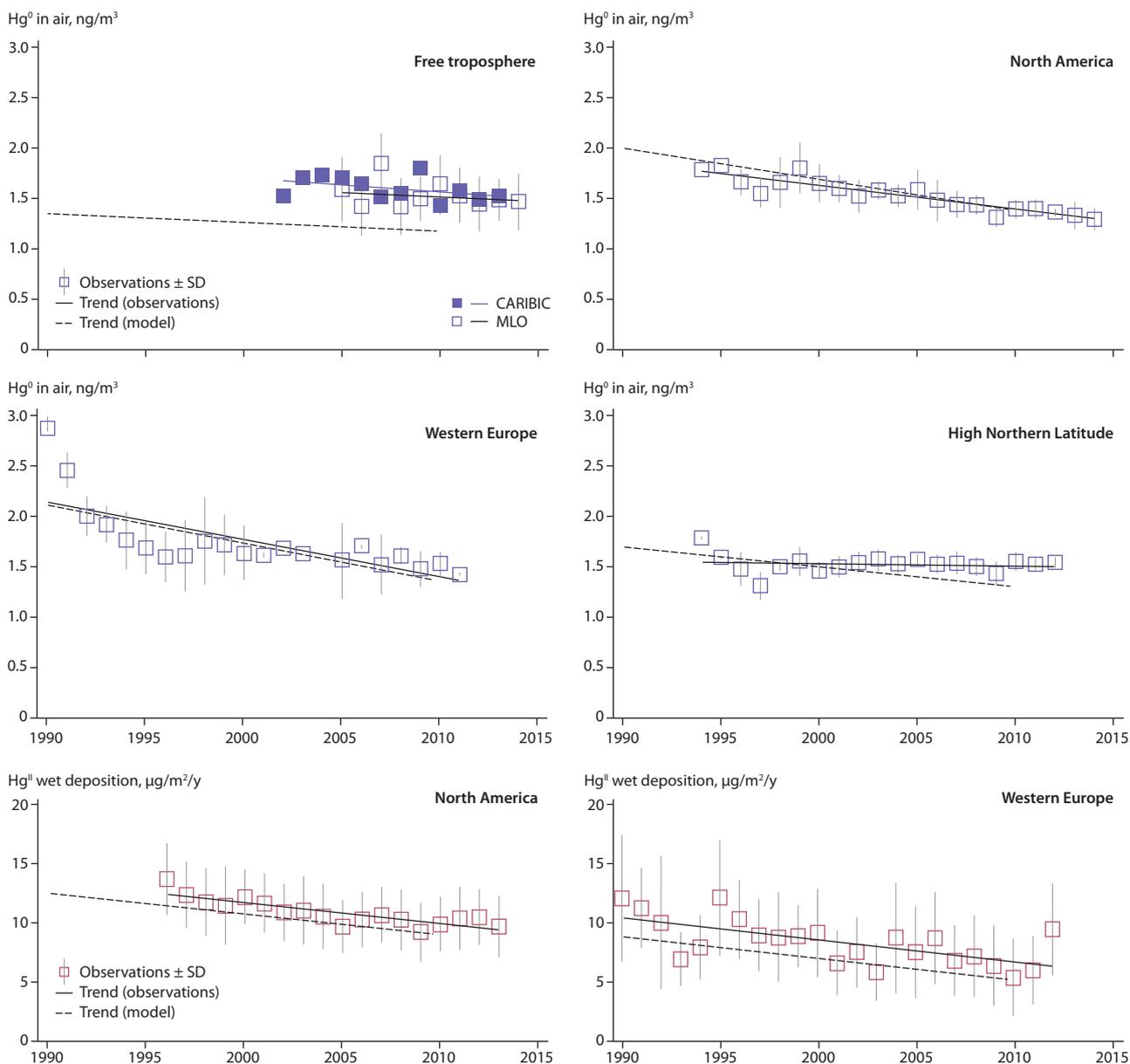
Figure 8.2 Observed and modelled trends for 1990 to 2013 in atmospheric gaseous elemental Hg concentrations (upper four plots) and divalent Hg[II] wet deposition fluxes (lower two plots) in different regions of the Northern Hemisphere. Observations for individual years are shown as squares with linear regression as a solid line. The dashed line is the trend from the GEOS-CHEM simulation using the revised anthropogenic emissions inventory for 1990 and 2010. The data are averaged regionally across the free troposphere, North America, Western Europe, and high northern latitude regions. From Zhang et al. (2016c).

air Hg trends is not reproduced by the model of Zhang et al. (2016c) (see Figure 8.2).

China is the largest national emitter of anthropogenic Hg to the atmosphere (Fu et al., 2015). In contrast to the global trend, anthropogenic Hg emissions in China increased rapidly from 1978 to as recently as 2007 at an average rate of ~5.5% per year, except for the period 1998–2000 when emissions decreased due to the Asian financial crisis, which led to a reduction in fuel consumption (Wu et al., 2016b). Mercury emissions in China are reported to have plateaued around 2007 to 2010, and have shown a declining trend in the past few years (Wu et al., 2016b). Available but limited data on atmospheric Hg concentrations over the past decade in China are in general agreement with this emissions trend. Direct measurements of Hg[0] at Guiyang (an urban site in southwest China) showed that annual mean Hg[0] concentrations increased at a rate of ~2.5% per year between 2002 and 2010 (Fu and Feng, 2015). Hg[0] concentrations also

increased at Mt. Changbai (a remote site in northeastern China) at about the same rate from 2009 to 2013 but have since appeared to stabilize (Fu et al., 2015, 2016; Figure 8.3). Mercury passive sampling and plant biomonitoring on the Tibetan Plateau suggest that atmospheric Hg concentrations were stable during 2006 to 2009 and decreased during 2010 to 2015 (Tong et al., 2016).

In the *Arctic region* (above 60°N) atmospheric Hg[0] concentrations have been generally declining, but at a markedly slower rate than elsewhere (see Figure 8.2). The observed and modelled trends also disagreed more than in other regions, with observed Hg[0] concentrations decreasing by 0.2±0.45% per year since 1994 compared to a modelled decrease of 1.3±0.11% per year. There are no decade-long observational data of Hg deposition flux available for the Arctic or subarctic regions; existing depositional data are limited to one to two years of measurements only (e.g., Sanei et al., 2010).

Hg⁰ in air, ng/m³
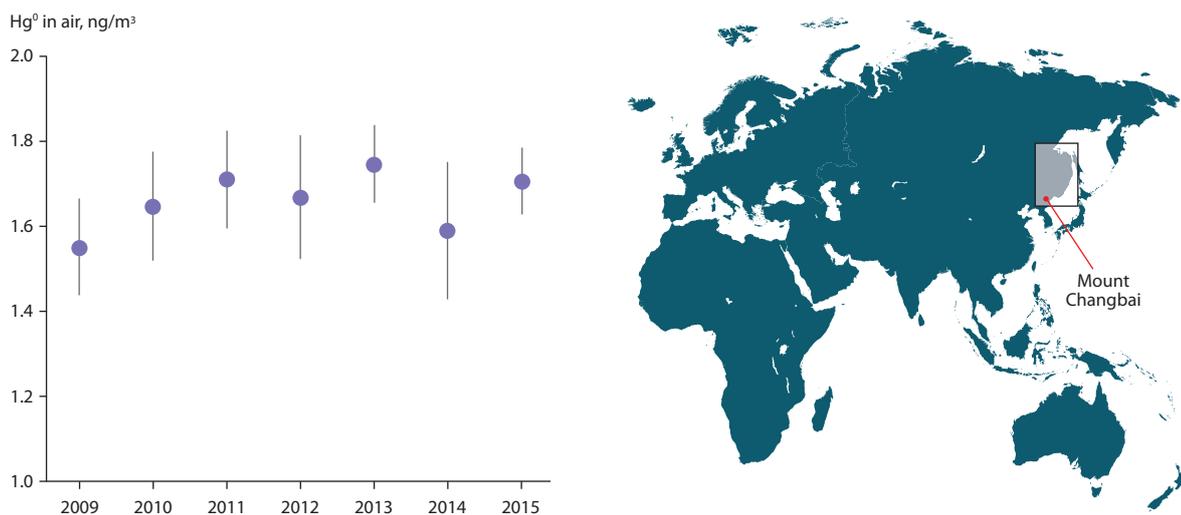
Figure 8.3. Annual mean gaseous elemental Hg concentrations measured at Mt. Changbai, a remote site in northeastern China (Fu et al., 2015). Error bars represent one standard deviation.

8.3.2 Trends in Hg in aquatic biota and possible causes

8.3.2.1 Case Study 1: Fish and birds in lakes and coastal waters of North America

A large number of studies have reported inconsistent, diverging, or mixed temporal trends of Hg in aquatic biota throughout North America. The Great Lakes are an especially interesting study area because of the wide diversity of species monitored within the same general area, and the length of some of the biotic time trend datasets. Also, there is isotopic evidence from two predatory Great Lakes fish (lake trout *Salvelinus namaycush* and burbot *Lota lota*) which establishes that the atmosphere, rather than sediments or watershed soils, was the ultimate source of most of the Hg in fish tissues (Lepak et al., 2015). However, intervening ecological, geochemical or climatic processes may be acting to drive biological time trends along divergent paths. Blukacz-Richards et al. (2017) evaluated the temporal trends since the 1970s of Hg levels in eggs of a piscivorous bird (herring gull *Larus argentatus*), in two piscivorous fish (lake trout and walleye *Sander vitreus*), and in a planktivorous fish (rainbow smelt *Osmerus mordax*) in the Great Lakes. The results presented a mixed temporal pattern (Figure 8.4), with declining biotic Hg trends in all species in the first few decades (up to about 1995–2000), which matched the declining atmospheric Hg trend in North America (see Figure 8.2). After about 2005, however, trend reversals were detected were detected in most species at some locations. Zhou et al. (2017b) also detected a breakpoint in fish Hg trends in the Great Lakes, with a significant decreasing trend before 2010 and no trend or an increasing trend since then.

Similar trend results were reported in fish populations across western Canada and the USA. When examining over 96,000 fish muscle samples from 206 species in over 4200 lakes, Eagles-Smith et al. (2016a) found a significant, rapid decline in length-adjusted tissue Hg concentrations during the 1970s, with no subsequent significant trend up to 2012. In all these studies, the authors attributed the early decline in biotic Hg to regional and local declines in atmospheric Hg concentrations and deposition. They suggested that the subsequent trend reversal, or lack of a significant trend, was caused by factors such as increasing local emissions, food web changes, eutrophication and climate change.

Contrasting biotic Hg trends have also been reported for lakes in the same region. When examining temporal fish Hg trends in hundreds of small Ontario lakes in Canada, Gandhi et al. (2014) found a general decline in length-adjusted fish muscle Hg concentrations from the 1970s to 1990s for northern pike (*Esox lucius*), walleye and lake trout, followed by relatively small increases in some lakes starting about 1995–2000. Both the early declining trends and recent increasing trends were more pronounced in northern Ontario lakes than in southern Ontario lakes and more so in northern pike and walleye than in lake trout. In contrast, when examining changes in fish muscle Hg from 873 Ontario lakes, Tang et al. (2013) reported no significant decreases over the past several decades in any of the seven species (walleye, northern pike, lake trout, burbot, smallmouth bass *Micropterus dolomieu*, whitefish *Coregonus clupeaformis* and white sucker *Catostomus commersonii*). Instead, mean fish Hg concentrations were found to be slightly higher in the period 2005–2010 than in 1974–1981, and were significantly so in northern pike. Divergent trends are also reported in fish Hg in four small lakes within a national park in northern Minnesota (Brigham et al., 2014) and throughout the State of Massachusetts (Hutcheson et al., 2014) in the USA. Whereas the majority of these study lakes showed a decreasing trend in fish Hg between ~2000 and ~2010, a smaller set of lakes showed an increasing or no trend. The variety of trends in fish Hg among lakes from the same region clearly demonstrate the complexity of ecosystem responses to changes in atmospheric Hg concentration and deposition. Along the northeast coast of the USA, substantial reductions in muscle Hg (~30–40%) were reported between 1972–1974 and 2011 in a marine fish species, bluefish (*Pomatomus saltatrix*) (Figure 8.5) (Cross et al., 2015). However, the New York regional data suggest no change in fish Hg levels after ~1994.

Most of these studies did not include stable carbon and nitrogen isotopic data, making it impossible to investigate whether changes in feeding behavior (e.g., prey trophic level and feeding location) influenced the Hg trends. The value of including trophic dynamic information in the
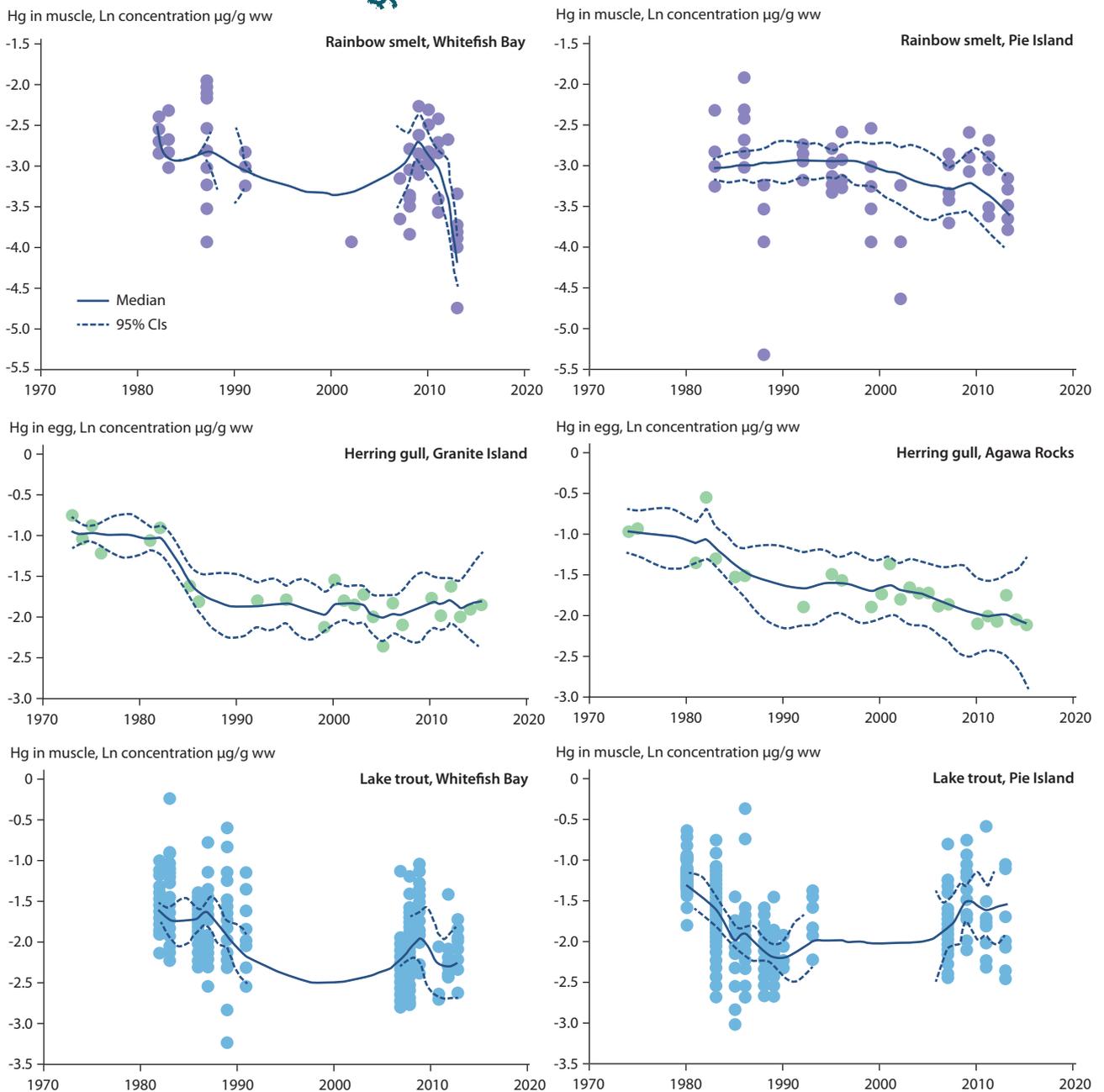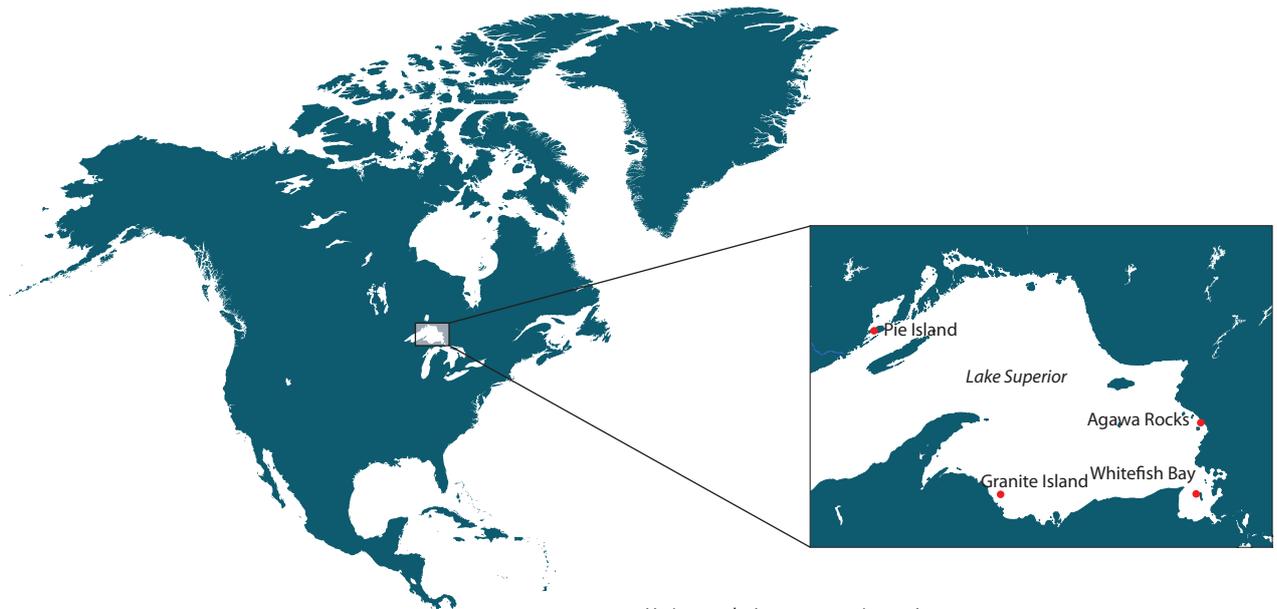
Figure 8.4. Mercury trends in fish and waterfowl of Lake Superior. The plots show Hg concentrations for rainbow smelt (planktivorous), lake trout (piscivorous) and herring gull (piscivorous). (Blukacz-Richards et al., 2017).
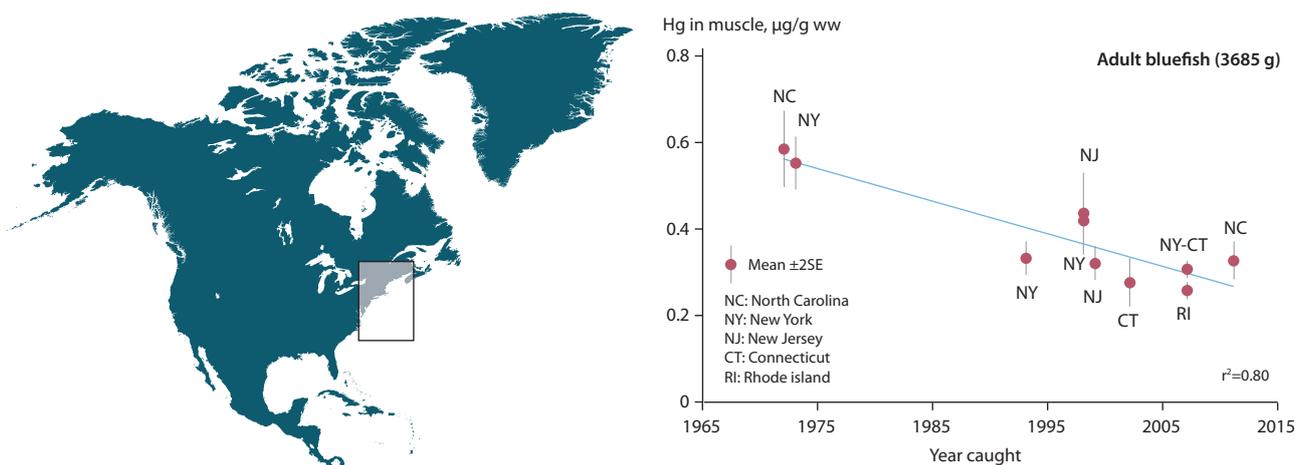
Figure 8.5 Mercury trends in the piscivorous bluefish (*Pomatomus saltatrix*) along the northeast coast of the USA from 1972 to 2011 (Cross et al., 2015).

interpretation of Hg temporal trends was demonstrated by Burgess et al. (2013) in a study of Hg in herring gull eggs on the eastern Canadian seaboard. Between 1972 and 2008, two sites displayed a trend of significantly declining egg Hg, which is consistent with the declining atmospheric Hg deposition occurring at that time (see Figure 8.1). However, when trophic level changes over time were factored into the analysis using $\delta^{15}N$ isotope data, it was found that the Hg declines were due to feeding behavior shifts. $\delta^{15}N$ is a widely-used indictor of the trophic level of species' prey selection and was highly correlated with egg Hg in the birds. These results suggest that Hg in the coastal ecosystem in that region may have remained relatively constant over the past few decades despite the reduction in airborne Hg fluxes.

8.3.2.2 **Case Study 2: Freshwater fish in Fennoscandia**

Braaten et al. (2017) and Åkerblom et al. (2014) assessed the spatial and temporal trends of Hg in various species of freshwater fish (e.g., northern pike, Eurasian perch *Perca fluviatilis*, brown trout *Salmo trutta*, Arctic char *Salvelinus alpinus*, roach *Rutilus rutilus*) over the past 50 years (1965–2015) based on 54,560

observations from 2775 lakes across Fennoscandia (Sweden, Finland, Norway, and the Kola Peninsula in Russia). Some of the lakes were impacted by historical local industrial emissions of Hg directly to surface water, whereas others were impacted primarily by atmospheric Hg deposited onto catchment soils as well as water surfaces.

As expected, lakes that were affected by local pollution sources had higher mean observed fish Hg concentrations than lakes that were predominantly affected by atmospherically deposited Hg. When the fish Hg concentrations are normalized to a standard 1-kg pike, the Hg concentrations in '1-kg pike equivalent fish' showed a consistent and significant decreasing trend for the entire database (Figure 8.6). This declining trend matches well with the general declining atmospheric Hg trend over northern Europe (see Figure 8.2). Of particular interest is the finding that the declining fish Hg trend was much stronger for the entire database than for lakes only impacted by atmospheric Hg deposition. This could suggest that reduced Hg emissions, especially a reduction in local emission sources, lead to lower Hg in fish. However, Braaten et al. (2017) noted that the temporal trends varied with different standardization methods and cautioned that a better understanding of possible confounding environmental processes (such as the impact of
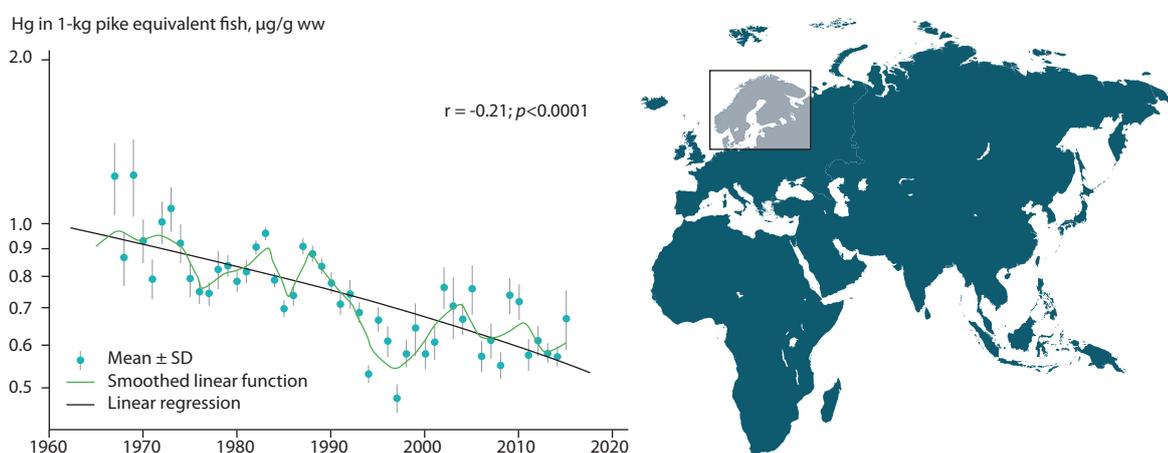
Figure 8.6. Mercury concentrations in five main freshwater fish species (Arctic char, brown trout, perch, pike and roach) over the past 50 years (1965–2015) in lakes across Fennoscandia. The plot shows the temporal trend of fish Hg concentrations after being normalized to 'standard 1-kg pike Hg concentrations'. Data from Braaten et al. (2017).

temperature and dissolved organic matter) is needed prior to concluding that the two declining trends are causally linked.

Also of note is that some of the lakes in Sweden were treated with lime in the 1970s and early 1980s to mitigate the impact of acidification. Fish Hg concentrations in these 'limed' lakes were found to be consistently higher than in lakes that were never limed (Åkerblom et al., 2014), pointing to a significant effect on fish Hg from pH or other indirect ecosystem processes caused by lime treatment. The temporal trends in both limed and non-limed lakes were, however, similar (Åkerblom et al., 2014).

8.3.2.3 Case Study 3: Fish in reservoirs in North America and Europe versus China

Some of the longest time series of aquatic Hg data exist for man-made reservoirs due to concerns about the effects of impoundment on Hg methylation rates and thus on fish Hg levels. Although these reservoirs are not natural habitats for aquatic life they contain abundant fish and invertebrate communities and support important recreational fisheries in some areas and large aquaculture operations in others.

Studies in North America and Europe have shown that following impoundment, the large influx of flooded vegetation and organic matter in submerged soil stimulates microbial methylation of Hg, resulting in a sharp increase in fish Hg due to biomagnification of MeHg (Lucotte et al., 1999; St. Louis et al., 2004; Hall et al., 2005; Bodaly et al., 2007). Mercury methylation rates and fish Hg concentrations typically decrease as the reservoir ages and the organic matter further decomposes (Bodaly et al., 2007). This was demonstrated in a recent analysis of the temporal trends of Hg in a range of fish species from 883 reservoirs across western North America (Willacker et al., 2016). Temporal patterns (normalized for confounding variables such as species and body length) were clearly related to the time elapsed since reservoir impoundment, with maximum fish Hg concentrations being reached on

average three years after the impoundment (Figure 8.7). Fish Hg concentrations thereafter declined relatively rapidly for four to 12 years, followed by a monotonic slow decline over many decades. Because the reservoirs were built at different dates over the past 150 years it may be concluded that the fish Hg trends are not directly related to changing atmospheric Hg deposition. Instead, water storage management is shown to be a key factor influencing this temporal pattern. Fish in reservoirs that experienced maximum drawdown during summer months (May–July) exhibited significantly higher concentrations (up to 11-fold) than fish in reservoirs in which drawdown occurred during other times of the year (Willacker et al., 2016).

Reservoirs in China however present a different story (Feng et al., 2018; Hsu-Kim et al., 2018). Unlike reservoirs in North America and Europe which are typically inhabited by native fish populations, reservoirs in much of China support aquaculture activities with fish harvested for human consumption. The fish in Chinese reservoirs thus tend to grow faster and are harvested younger. Therefore, the fish Hg concentrations from these reservoirs are typically low due to biodilution. Monitoring of fish Hg concentrations in most of the Chinese reservoirs only started recently, making it impossible to deduce long-term temporal trends. One exception is the reservoirs in the Wujiang Basin in southwest China where extensive studies have been carried out in the past decade. Since these reservoirs vary greatly in age (time since their initial impoundment) an interesting evolution scheme in fish Hg concentrations starts to emerge when the data from all reservoirs are pooled (Feng et al., 2018).

The Wujiang River is the largest tributary of the upper Changjiang (Yangtze River). Since the 1960s, numerous large cascade reservoirs have been or are being constructed in the Wujiang Basin, including Wujiangdu (built in 1979), Dongfeng (1994), Puding (1994), Yingzidu (2003), Suofengying (2003), Hongjiadu (2004), and Pengshui (2008) on the main stream, and Aha (1960), Baihua (1966), and Hongfeng (1966) on its
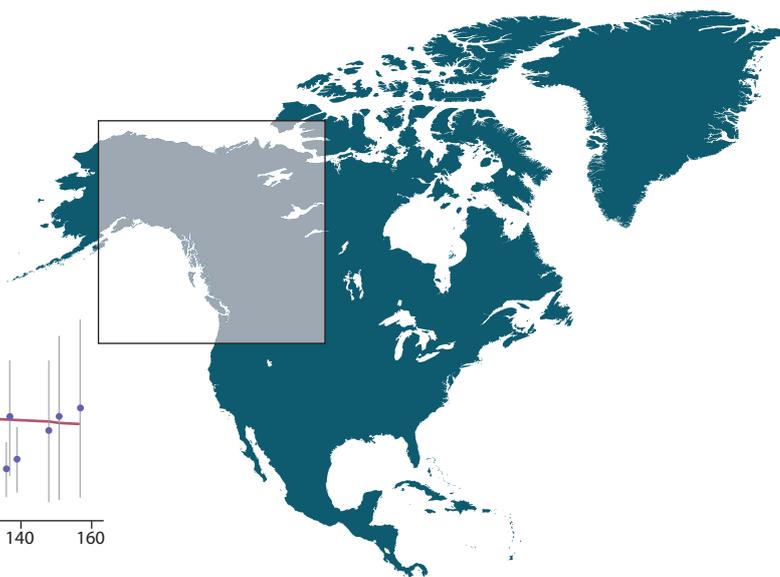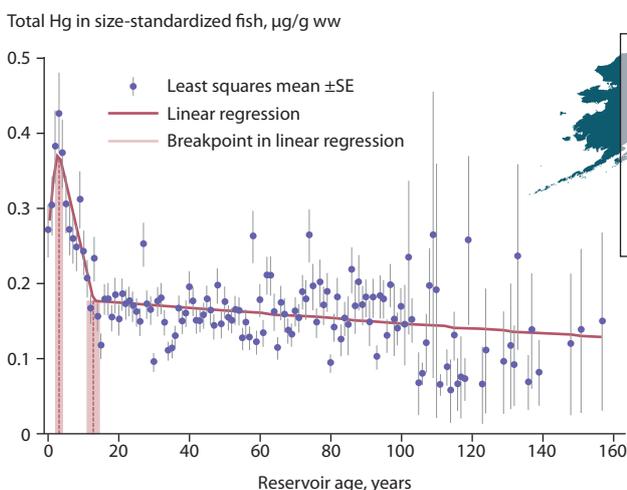
Figure 8.7 Fish tissue Hg trends from reservoirs across western North America. The data show least squares mean total Hg concentrations in size-standardized fish. Least squares means account for the effects of ecoregion, waterbody, species, and sampling year. Vertical red lines and shaded regions indicate estimated breakpoints (±standard error) from segmented linear regression (solid line) on fish Hg concentration when accounting for the effects of ecoregion, waterbody, species, and sampling year. From Willacker et al. (2016).
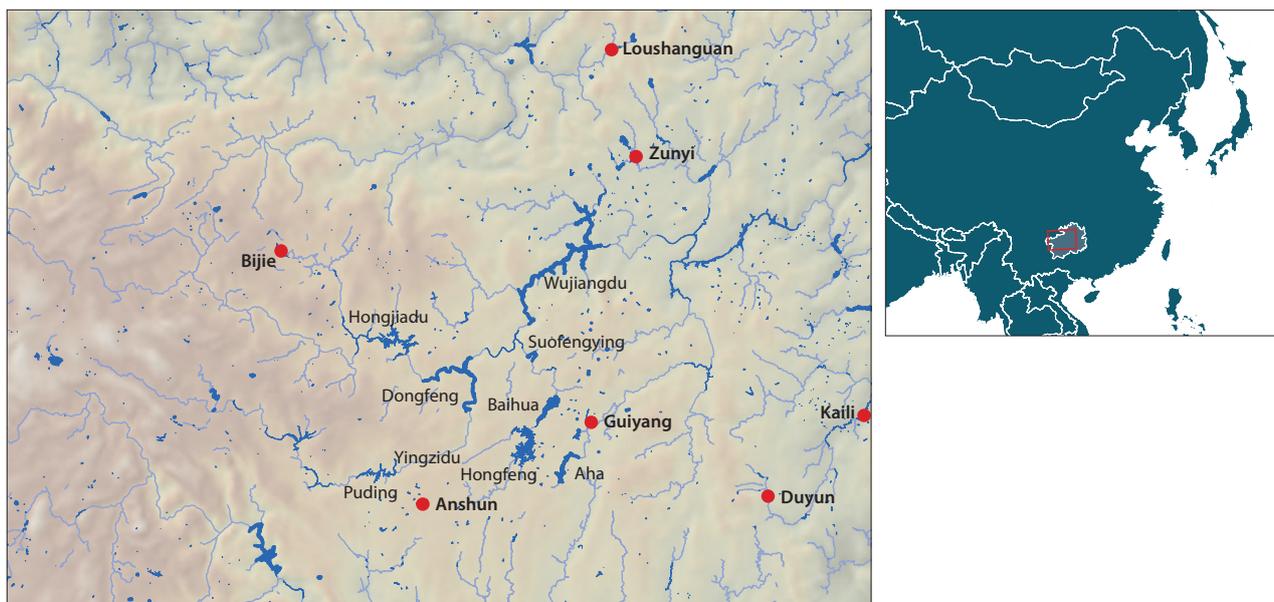
Figure 8.8 Reservoirs in the Wujiang River Basin, southwest China.

tributaries (Figure 8.8). Although impoundment was found to have significantly increased fish Hg concentrations in a newly constructed reservoir (Pengshui) (Li et al., 2013), fish Hg concentrations in this and another newly constructed reservoir (Hongjiadu) (Yao et al., 2011) were much lower than those in newly built reservoirs in North America and Europe (Yao et al., 2011; Li et al., 2013). For the much older Baihua reservoir, no statistically significant differences were observed in Hg concentrations in common carp (Cyprinidae) among the four sampling campaigns from 2003 to 2011, more than 40 years after the impoundment (Liu et al., 2012). In general, Hg concentrations in the various fish species studied, including carnivorous, omnivorous, planktivorous, and herbivorous fish, were remarkably low in all these reservoirs regardless of the age of the reservoir (Li et al., 2009, 2013; Yan et al., 2010; Yao et al., 2011; Liu et al., 2012), often an order of magnitude lower than the Codex guideline levels for MeHg in fish (i.e., predatory fish, 1.0 mg/kg; non-predatory fish, 0.5 mg/kg; wet weight) (FAO/WHO, 2011).

While biodilution and simple (short) food web structures clearly contribute to the generally low fish Hg concentrations (Feng et al., 2009a,b; Larssen, 2010; Meng et al., 2010, 2016; Yan et al., 2010; Yao et al., 2011; Liu et al., 2012), comparisons of fish Hg concentrations in reservoirs of different age in the same basin reveal three distinct stages of evolution due to changes in the source and concentration of organic matter in the submerged soil/sediment as the reservoir ages and cage aquaculture activities increase (Figure 8.9) (Feng et al., 2018). As much of the Wujiang Basin is located in a karst (eroded limestone) environment, the organic matter contents of the soils (typical range: 1.9–4.1%) are much lower than those in submersed soil (typically 30–50%) from the boreal forest or wetlands in North America and Europe (Lucotte et al., 1999; St. Louis et al., 2004; Hall et al., 2005; Yao et al., 2011). In addition, conditions were slightly alkaline in most of the reservoir water, which could restrain Hg methylation (Meng et al., 2010; Yao et al., 2011). Primary productivity in the newly constructed reservoirs in the Wujiang Basin is also low (oligotrophic–mesotrophic) due to the absence of cage

aquaculture fishing (Meng et al., 2010, 2016; Yao et al., 2011) and thus the autochthonous contribution to organic matter is also very limited (Jiang, 2005; Yao et al., 2011). Therefore, in contrast to their counterparts in Europe and North America, the newly constructed reservoirs in the Wujiang Basin are not active sites of net Hg methylation due to the low organic carbon content in the submersed soils and/or low primary productivity (Meng et al., 2010; Yao et al., 2011). Consequently, the newly constructed reservoirs, such as Suofengying, Hongjiadu, and Yingzidu on the Wujiang River, are not a net source of MeHg and instead represent a net sink (Guo, 2008) (Figure 8.9 upper).

As these reservoirs become more productive (mesotrophic to eutrophic) with time, the organic matter content in the sediment increases due to continuous increases in autochthonous productivity due to the cage aquaculture activities. This tends to promote *in situ* Hg methylation, and as such reservoirs at this stage (e.g., Dongfeng and Puding) have transited from a net MeHg sink to a net MeHg source (Guo, 2008; Feng et al., 2009a,b; Zhang et al., 2009) (Figure 8.9 middle). Over the long-term evolution of the reservoir, primary productivity continues to increase and the reservoir will eventually become eutrophic. Phytoplankton-derived organic matter, and fish feed and feces become significant sources of organic matter input to the surface sediments, as shown in Wujiangdu (Feng et al., 2009a; Zhang et al., 2009; Meng et al., 2010, 2016). The increased oxygen consumption during fresh organic matter degradation causes progressively more anoxic conditions at the sediment-water interface (Meng et al., 2010, 2016), which promotes the microbial Hg methylation processes (Figure 8.9 lower), as shown in Wujiangdu (Guo, 2008) where both the surface sediment and the hypolimnetic water were sites of net MeHg production (Feng et al., 2009a; Meng et al., 2010, 2016). Thus, in contrast to fish in North American reservoirs, and despite the relatively high atmospheric Hg loading across much of China, fish Hg levels in Chinese impoundments reflect within-impoundment processes, especially organic matter loadings to sediments, water/soil quality, food web structure, and biodilution, rather than atmospheric inputs (Feng et al., 2018).
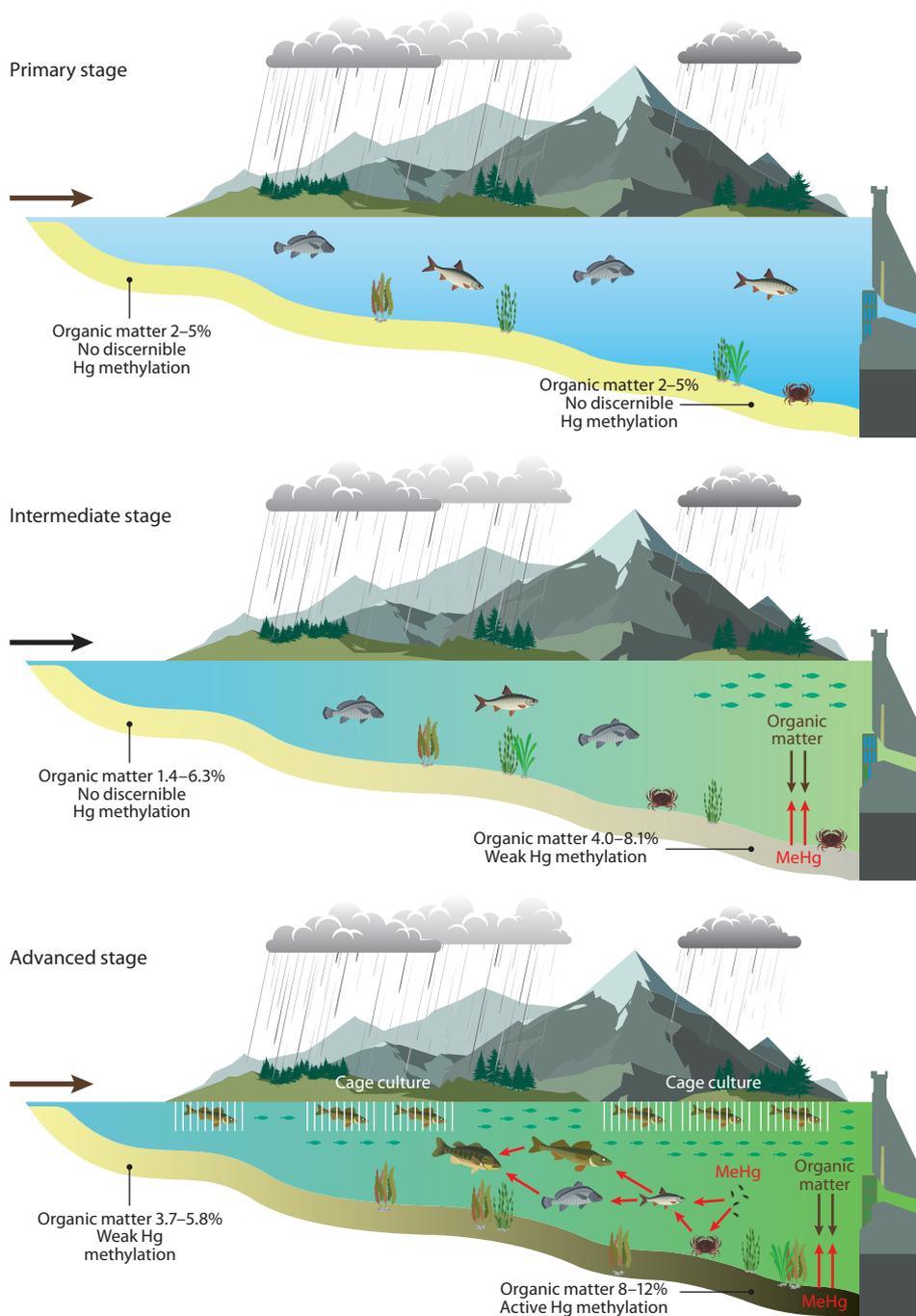
Figure 8.9 Conceptual models of Hg cycling in primary, intermediate, and advanced evolutionary stage reservoirs in the Wujiang River Basin, Southwest China. From Feng et al. (2018).

8.3.2.4 **Case Study 4: The Arctic**

Rigét et al. (2011) summarized all available temporal Hg datasets on Arctic biota up to about 2009 and found that some species in some locations had shown significant increases over recent decades, while others with closely adjacent or overlapping distributions exhibited decreases or non-significant changes. Most of the increasing biotic Hg trends occurred in marine species in the North American and West Greenlandic sector of the Arctic, whereas declining trends were mostly observed in East Greenlandic and European Arctic biota. This regional dichotomy is clearly seen in the hair of polar bears (*Ursus maritimus*) and has been suggested to be due to increased emissions from Asia entering the western Arctic coincident with decreasing emissions from North America and Europe in the eastern Arctic (Dietz et al., 2006).

A few additional studies have since been published. Rigét et al. (2012) analyzed temporal trends of Hg in livers of ringed seals (*Pusa hispida*) collected from the early 1980s to 2010 from Greenland. Increasing levels of Hg were found in ringed seals in two out of three Greenlandic seal populations (Central East and Northwest Greenland), rising at a rate of 10.3% per year and 2% per year, respectively. In addition to age and trophic position, the study showed that the Atlantic Oscillation Index, a parameter related to climate variability, was positively associated with Hg concentrations in seals although the specific mechanism involved was not clear.

By analyzing Hg in the teeth of polar bear from Svalbard in the Norwegian Arctic, Aubail et al. (2012) reported a decreasing trend in Hg concentration over the period 1964–2003 (Figure 8.10). Since no temporal changes were found in tooth $\delta^{15}N$ and $\delta^{13}C$ they concluded that the decrease in Hg was
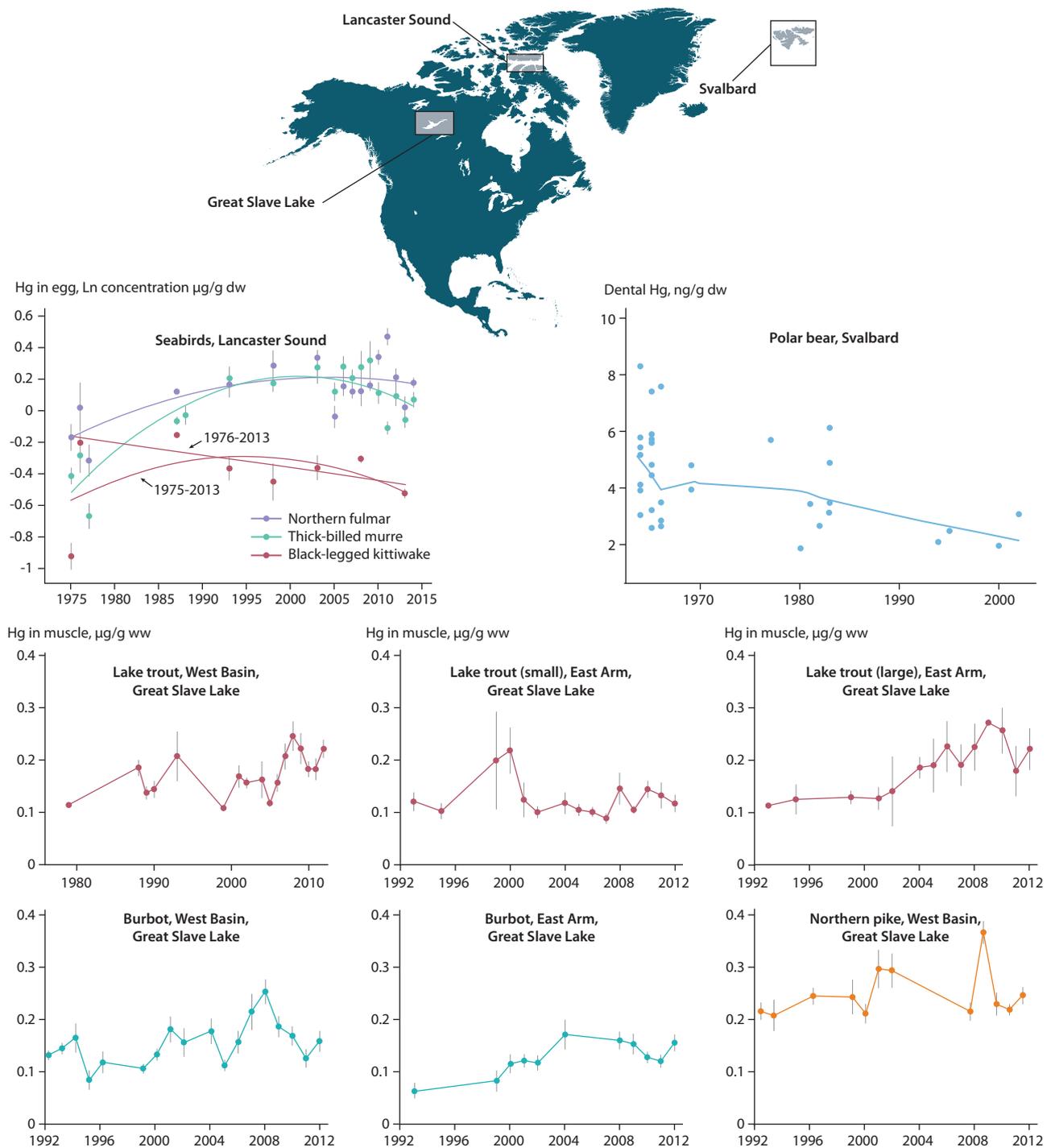
Figure 8.10 Mercury trends in Arctic aquatic biota. The data were derived from several sources: annual mean Hg concentrations adjusted for trophic position in eggs of thick-billed murres, northern fulmars, and black-legged kittiwakes from Lancaster Sound, Nunavut, 1975 to 2014 (Braune et al., 2016); for dental Hg concentrations in polar bears (aged three to 10 years) from Svalbard, smoothing lines (robust, locally weighted scatter plot smoothing system based on the LOWESS algorithm) represent the fitted non-linear trend of the values (Aubail et al., 2012); and Hg concentrations in burbot, lake trout and northern pike collected from the West Basin and East Arm of Great Slave Lake, Northwest Territories, Canada (Evans et al., 2013).

not due to changes in trophic dynamics; instead, it was more likely to be due to a lower environmental Hg exposure in the region. McKinney et al. (2017) also reported a significant declining trend in hair Hg of the southern Beaufort Sea polar bear population, at an average rate of -13% per year between 2004 and 2011. This dataset differs from the general west-east pattern in Arctic biota Hg trends noted above. However, only males in the southern Beaufort Sea area exhibited significant decreases; females from the same area showed no significant trend. Mercury levels in the bears' main prey (ringed seal) also

showed no change up to 2007 (Gaden et al., 2009), which argues against changes in Hg inputs or the biogeochemical Hg cycle as contributing to the decline. Analyses of body condition and diet led to the conclusion that the bears' Hg trend was due to changing foraging patterns over time and not to alteration in environmental Hg levels (McKinney et al., 2017).

Braune et al. (2014) reported the temporal trend of Hg in thick-billed murre (*Uria lomvia*) eggs from Coats Island, northern Hudson Bay, and Prince Leopold Island in Lancaster Sound, Nunvut. Although there was no significant change in

Hg concentrations in murre eggs from Coats Island from 1993 to 2013, δ^{15}N values for the eggs were found to be decreasing significantly, suggesting a decline in trophic position for the bird due to a dietary switch from Arctic cod (*Boreogadus saida*) to capelin (*Mallotus villosus*). After adjusting egg Hg concentrations for the decline in trophic position, time trends in Hg concentration at Coats Island changed from non-significant to significantly increasing. In contrast, at Prince Leopold Island, after adjustment for trophic position the egg Hg time trends changed from non-significant to significantly decreasing over the same period. These results suggest that in addition to trophic change in diet, there may have been other geographic factors at play that influenced Hg concentrations at the base of the marine food web, such as differences in Hg deposition or in Hg bioavailability related to climate change.

Subsequently, Braune et al. (2016) updated the Hg trends in High Arctic seabird eggs at Prince Leopold Island to 2014 for five species: thick-billed murre, northern fulmar (*Fulmarus glacialis*), black-legged kittiwake (*Rissa tridactyla*), black guillemot (*Cepphus grylle*), and glaucous gull (*Larus hyperboreus*). Eggs from the first three species had been collected from the Island as early as 1975, while the guillemots and gulls were sampled from 1993 to 2013. Egg Hg trends were adjusted for possible shifts in trophic position of the birds using δ^{15}N data. Adjusted Hg concentrations in eggs of murres, fulmars and kittiwakes increased from 1975 to the 1990s, followed by a plateauing or slight decline from the 1990s to 2014 (Figure 8.10). However, the kittiwake trend was strongly influenced by the 1975 samples; when these were excluded, kittiwake eggs displayed a significant decreasing trend from 1976 to 2013. Trends in the eggs of murres, fulmars, kittiwakes, and guillemots had negative slopes between 1993 and 2013. The pattern in glaucous gull eggs was different: decreasing by 50% from 1993 to 2003 before increasing again.

Braune et al. (2016) concluded that the general increasing trends in egg Hg during the 1970s and 1980s were consistent with atmospheric Hg increases over the Arctic during that period. They noted that the migratory habits of the five bird species, which overwinter in different southern regions away from Lancaster Sound, complicated interpretation of the reasons for the temporal trends. Environmental Hg changes in their wintering areas could have been different to those in the Arctic. Interpretation is also complicated by significant differences in the findings from glacier archives of atmospheric Hg on the western and eastern edges of the North American Arctic. Greenland glacial snow/firn (Faïn et al., 2009) showed a monotonic decline in atmospheric Hg[0] concentrations during the 1970s and 1980s, following peak levels in the 1950s to 1960s. Glacial snow and ice core reconstructions of atmospheric Hg deposition from Mt. Logan (Yukon) showed increases in deposition through the 1990s, which could be an indication of increasing trans-Pacific contamination from Asia (Beal et al., 2015). Overall, these data, especially the declining Hg[0] trend on Greenland through the 1970s and 1980s, are inconsistent with Braune et al.'s (2016) conclusions. However, the flat or slightly declining egg Hg data from about 1990 onwards is consistent with the recent modelling of atmospheric Hg[0] in the Arctic (see Figure 8.2). Zheng (2015), on the other hand, reported that 20th-century total Hg accumulation in a Greenland ice core was relatively constant until increasing during the 1970s to 2000s, a pattern similar to those in most of the bird species but not in agreement with the Zhang et al. (2016c) modelling. Thus, uncertainty about the actual

trends in Arctic atmospheric Hg deposition is a limiting factor in assessing agreement between environmental and biological Hg trends in this region.

In Great Slave Lake in the western Canadian Arctic, temporal trends of Hg in lake trout, burbot, and northern pike were monitored irregularly between the late 1980s or early 1990s and 2012 (Evans et al., 2013; Figure 8.10). Muscle Hg data were adjusted for fish length, but not for trophic shifts over time. Mercury concentrations generally increased over time in lake trout and burbot but not in northern pike, with considerable interannual variation. These increasing or flat patterns are inconsistent with atmospheric Hg[0] concentrations and wet deposition fluxes that were declining at the time (see Figure 8.2) and with the Mt. Logan atmospheric deposition record of Beal et al. (2015). Statistical analysis of climate factors suggested that varying annual mean air temperatures, and particularly cold season temperatures, were related to the fish Hg patterns although a precise mechanism linking temperature to fish Hg could not be elucidated (Evans et al., 2013).

8.3.3 Causes of the match and mis-match between aquatic biota and atmospheric Hg trends

In contrast to the recent decadal datasets described in the previous section, the available century-scale biotic Hg trends since the pre-industrial era (from the Arctic; Dietz et al., 2009) generally matched remote glacial ice core archives showing increasing atmospheric Hg deposition and Hg[0] concentrations after about 1850 (Beal et al., 2015; Zheng, 2015; Kang et al., 2016; see Chapter 2). In both cases, starting in the mid- to late-19th century, and shortly after major anthropogenic uses and emissions of Hg became more common, Hg concentrations in the atmosphere and in aquatic biota increased steadily up to maxima typically attained at about the 1970s–1980s (Dietz et al., 2009; Rigét et al., 2011). The longer-term datasets thus clearly indicate the effects of anthropogenic contamination of aquatic systems on biotic Hg concentrations and trends over the century or more since about 1850.

As anthropogenic emissions to air began to stabilize after the 1970s, it became increasingly apparent that a mis-match between the aquatic biotic and atmospheric Hg trends was developing in some areas, and in some co-occurring species. In other areas and species, however, the atmospheric and biotic trends continued synchronously. The divergent patterns of match and mis-match between the atmosphere and biota have become more apparent over the past two decades or longer, as atmospheric and biological monitoring became more widespread and frequent.

Fundamentally, the mis-matches may be generally attributed to the large inventories of legacy Hg in soil and ocean reservoirs, and the exceptional sensitivity of Hg biogeochemical cycling to changes in climatic (e.g., temperature, light, hydrology), geochemical (e.g., pH, redox status, complexing ligands), biological (e.g., feeding behavior of an organism) and ecological (e.g., organic carbon flux, microbial processes, food web structure and dynamics) conditions (Table 8.1; see also Hsu-Kim et al., 2018). Some of the major processes that trigger changes in these conditions, and thus cause the decoupling between biotic and environmental Hg, include changes in the soil and terrestrial environment, changes in the aquatic ecosystem, and climate change.

Table 8.1 Unique properties of Hg and implications for its biogeochemistry (Wang and Zhang, 2013)

Property	Implications
Redox between Hg^0 and Hg^{II}	Sensitive to changes in redox and pH conditions; Sensitive to photochemical and microbial processes
High vapor pressure of Hg^0	Sensitive to changes in temperature; Long-range atmospheric transport; A global problem needing global solutions
Hg^{2+} ions being one of the softest Lewis acids	Strong affinity to ligands (e.g., reduced sulfides, halogens); Sensitive to changes in organic carbon
Methylation is primarily microbial, with MeHg being the most bioavailable and toxic	Sensitive to changes in organic carbon, nutrients, redox and microbial processes; Direct source control of MeHg difficult
MeHg biomagnifies in the food chain	Sensitive to changes in food web structure and dynamics

8.3.3.1 Changes in the soil and terrestrial environment

Globally the terrestrial environment represents the largest inventory of Hg (~950 kt), with ~150 kt stored in surface organic soils (Figure 2.3, Chapter 2). Terrestrial biota are much less prone to Hg bioaccumulation as the conversion of inorganic Hg to MeHg is not favored in the terrestrial environment (Fitzgerald and Lamborg, 2014). Also, on a global scale, anthropogenic inputs have altered the Hg inventory in the soils to a lesser degree than in the oceans due to the naturally large mass of Hg that was present in terrestrial systems (see Figure 2.3). However, major changes in landscape and land-use in the watershed (such as urbanization, agricultural activities, flooding, damming, and deforestation) not only affect the net release of soil Hg to downstream aquatic systems (inland and coastal), more importantly they change the organic carbon flux and redox conditions that directly influence Hg methylation processes in the aquatic systems. The importance of such changes is perhaps best demonstrated by reservoir construction in the watershed. As shown in Case Study 3, fish Hg concentrations in reservoirs are primarily controlled by the influx and dynamics of terrestrially-derived organic carbon and Hg, and bear almost no relationship with trends in atmospheric Hg concentrations or deposition, even decades after reservoir impoundment.

8.3.3.2 Changes in the aquatic ecosystem

As MeHg biomagnifies in the food web (i.e., MeHg concentration increases from prey to predator), any changes in ecosystem structure, function and dynamics would result in major changes in Hg concentrations within the ecosystem. Processes such as acidification/liming (Case Study 2) and eutrophication (Case Study 3) affect not only MeHg production (see Section 8.2) by altering Hg speciation and bioavailability, but also Hg food-chain transfer and thus biotic Hg concentrations by altering species composition, biomass and growth rates (e.g., Clayden et al., 2013; Jardine et al., 2013). Aquaculture, overfishing, and invasion of non-native species can change not only the nutrient status of an aquatic ecosystem but also the structure, function, and dynamics of food webs, and thus could result in major changes in biotic Hg.

8.3.3.3 Climate change

On the global scale, climate change is the most prevalent contributor to the mis-match between biotic and environmental Hg. The impact of climate change on biotic Hg is perhaps most profoundly felt in the Arctic, where rapid climate warming has resulted in dramatic changes in many biogeochemical and ecological processes that drive Hg cycling (Wang et al., 2010b; Stern et al., 2012). For instance, the rapid decline in the aerial coverage and thickness of Arctic sea ice and the replacement of multi-year sea ice by first-year ice have been shown to influence Hg distribution and transport across the ocean–ice–atmosphere interface, alter Hg methylation and demethylation rates, promote changes in primary productivity, and shift food web structures (bottom-up processes) (Chaulk et al., 2011; Point et al., 2011; Beattie et al., 2014; Heimbürger et al., 2015; Wang et al., 2017). The very large mass of mainly natural Hg found in northern permafrost deposits, which is projected to be released with further climate warming may profoundly affect biotic Hg levels around the Northern Hemisphere, especially as large amounts of organic carbon that may stimulate Hg methylation rates will be simultaneously released (Schuster et al., 2018).

Changes in animal social behavior associated with changing sea-ice regimes can also potentially affect dietary exposure to Hg (top-down processes) (Stern et al., 2012). As shown in Case Study 4, as sea ice declined in their feeding areas, thick-billed murre from Coats Island in northern Hudson Bay altered their feeding strategy to prey on a lower trophic level, open-water species (capelin) instead of Arctic cod which is an ice-associated species (Braune et al., 2014). This change would have tended to reduce the birds' Hg exposure. However, the population's egg Hg concentrations did not change significantly between 1993 and 2013; thus, to explain this stable trend the availability of MeHg in the environment and efficiency of Hg food web transfer must have increased. It has also been suggested that climate warming may cause a shift in energy flow from benthic to pelagic food webs as aquatic productivity increases in High Arctic lakes. Since zooplankton species such as *Daphnia* contain higher MeHg than benthic organisms, this shift could increase Hg transfer in the food web (Chételat and Amyot, 2009). The impact of climate change on biotic Hg has also been observed in lower latitude regions (e.g., Pinkney et al., 2014).

8.3.4 Implications for the effects on biotic Hg of regulatory action on atmospheric Hg emissions

Reports of biotic Hg trends not following the atmospheric Hg trends in recent decades should not be regarded as discouraging news when considering the efficacy of regulations to reduce atmospheric and other releases of Hg. The fact that the effectiveness of Hg emission control is expected to be followed by long delays before an ensuing reduction is seen in food-web Hg levels makes it all the more pressing to control and reduce Hg emissions as early as possible (Wang et al., 2010b).

Wang et al. (2010b) and Wang and Zhang (2013) proposed that the mis-match between biotic and environmental Hg trends is an indication that an aquatic ecosystem has entered a new paradigm in which the key controls on Hg bioaccumulation have switched from being emissions-driven to processes-driven. This switch occurs because the biotic Hg concentrations in an

aquatic ecosystem are influenced not only by Hg influx (natural or anthropogenic) to the system, but also by the internal processes in the ecosystem that control the recycling, speciation, bioavailability, methylation and biological uptake of Hg. As the accumulated mass of legacy Hg in a waterbody becomes large relative to the loading rate of newly emitted Hg, the internal biogeochemical processes that control its permanent removal (e.g., burial), re-emission, or uptake into the biota, increasingly become the determining steps in bioavailability and bioaccumulation.

The changing relationship over time between atmospheric Hg concentrations (or deposition) and biotic Hg is shown in Figure 8.11. Prior to anthropogenic influences (the exact timeline is subject to debate; see Chapter 2), when Hg emissions were at their natural level, the flux of Hg to the aquatic system was generally low, and so were its biotic concentrations (Phase I – 'Natural background'). At around the mid-19th century, however, as rapid industrialization resulted in a sharp increase in anthropogenic Hg emissions, aquatic biota Hg concentrations responded rapidly due to increasing Hg deposition, exposure and uptake of Hg from a small but growing environmental Hg inventory (Phase II – 'Emissions-driven'). This phase is clearly seen in long-term retrospective studies of Hg levels in Arctic biota (Dietz et al., 2009). Once an aquatic ecosystem has accumulated sufficient Hg, additional increases in Hg influx become secondary to the amount that has been accumulated in the system after decades to centuries of loading (i.e., legacy Hg). Bioaccumulation then draws predominantly on this legacy Hg which is operated on by the internal biogeochemical processes (Phase III – 'Internal Processes-driven'). Throughout these three phases, biogeochemical processes (shown as sine-wave 'noise' in Figure 8.11) determine the transport of Hg from the abiotic part of the ecosystem to biota, but it is in Phase III that these processes emerge to create a variability that is large enough to obscure the external Hg emission trends and hence produces the mis-match between biotic and atmospheric Hg trends (Wang et al., 2010b).

In the context of Hg emission controls mandated by the Minamata Convention, a new phase, Phase IV, can be envisioned (see Figure 8.11), based on observations of biotic Hg trends in the recent past (see Section 8.3.2) and predictions from modelling efforts of seawater Hg concentration trends in the future (see Section 2.4, Chapter 2). As anthropogenic Hg emissions decrease, atmospheric Hg concentrations will decrease and eventually stabilize at a new steady state. However, recycling of the large quantities of legacy anthropogenic Hg presently contained in the world's oceans and soils, and revolatilization between oceans, soils and the atmosphere, means that atmospheric and dissolved Hg concentrations are likely to decrease much more slowly than changes in Hg emissions. While biotic Hg concentrations are also projected to decrease over the long term, the current phase of processes-driven bioaccumulation dictates that it will take much longer to establish a new steady-state in biotic Hg. The biotic Hg concentrations at the new steady-state are also likely to remain above the natural background levels for an extended period after atmospheric Hg levels have returned to natural levels, because of the continued presence of legacy Hg in aquatic and terrestrial systems. In the shorter term, in fact, aquatic biotic Hg concentrations in many instances, especially in some marine ecosystems, are likely to continue to increase despite recent emission controls (Sunderland and Selin, 2013). Biota in smaller waterbodies such as lakes and coastal marine systems with restricted water mass turnover are more likely to respond relatively rapidly to emissions controls.

Examples of this long and uneven recovery in biotic Hg can be found following the impoundment of a river, or following 'de-acidification' of a lake. As shown in Case Study 3, fish Hg in reservoirs decreased a few years after the impoundment but remained above the pre-impoundment level even after more than a century (see Figure 8.7). In the 1970s, liming was applied to many Swedish lakes that were acidified due to atmospheric acid deposition, to help restore the lake ecosystem. Following the liming, fish Hg in those lakes declined by 10–20% by the 1990s (Meili, 1995) and continued to decline to the present day (Åkerblom et al., 2014). Yet, more than 30 years after the liming, fish Hg concentrations in these lakes remained considerably higher (twice as high on average) than those in lakes that were not impacted by acidification (and not subject to liming) (Åkerblom et al., 2014).
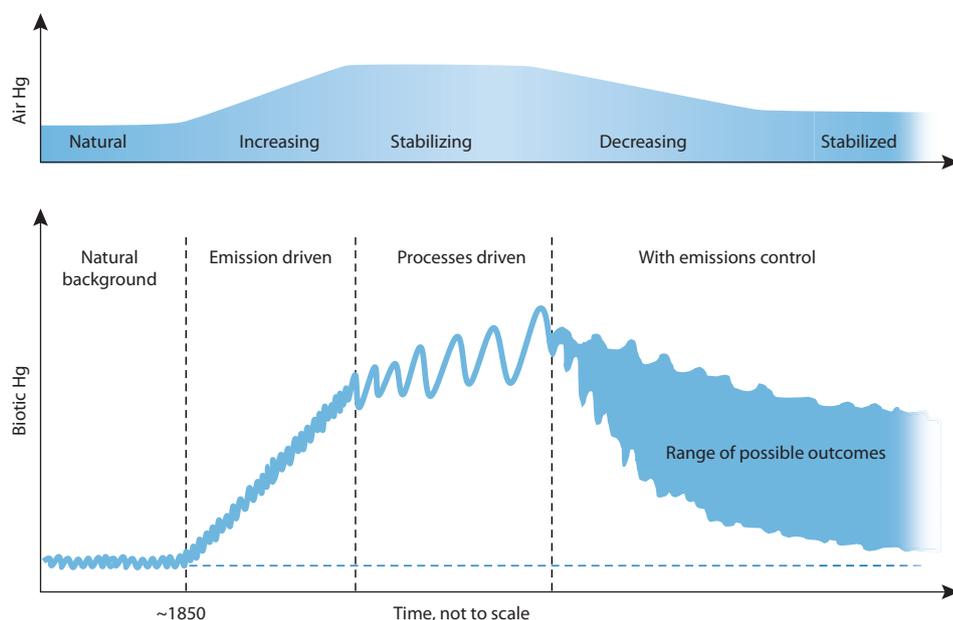
Figure 8.11 A schematic representation of evolution in the Hg concentrations in the air (top panel) and aquatic biota (bottom panel), showing changes over time in the principal drivers of Hg bioaccumulation. Modified from Wang et al. (2010b).

9. Mercury levels and trends in human populations worldwide

Authors: Niladri Basu, Milena Horvat, David C. Evers, Irina Zastenskaya, Pál Weihe, Joanna Tempowski

Key messages

- *All populations are exposed to mercury (Hg) to some extent. For many communities worldwide, dietary consumption of fish, shellfish, marine mammals, and other food items that are contaminated with methylmercury (MeHg), is the most important source of exposure. Exposure to elemental and inorganic Hg mainly occurs in occupational settings via contact with products containing Hg and from environmental contamination.*

- *There is great variability in Hg exposure worldwide. A review of 424,858 biomarker measurements suggests that individuals in background populations (i.e., without significant Hg exposure) have blood Hg levels generally <5 µg/L, hair Hg levels generally <2 µg/g, and urine Hg levels generally <3 µg/L.*

- *Concern remains about Hg exposure in vulnerable groups that are sensitive owing to extrinsic (e.g., high exposures) and intrinsic (e.g., genetic) factors. Elevated Hg exposures in key groups of concern for which there are relatively robust*

datasets include fetuses, Arctic populations (e.g., Inuit) who regularly consume fish and marine mammals, tropical riverine communities (e.g., Amazonian), coastal and/or small-island communities that are high seafood consumers, and individuals who either work or live among artisanal and small-scale gold mining sites, or who otherwise have high occupational exposures.

- *Assessing Hg exposure is relatively straightforward by the use of biomarkers. Mercury can be measured in blood, hair and urine. Measurements in hair and urine samples are particularly suitable because they provide information on the two main forms of Hg, and their collection is relatively non-invasive, requires no specialized training or handling and storage regiment, and is relatively cheap. In addition, the results can be interpreted against guideline values, over different spatial and temporal scales, and following interventions to gauge their effectiveness.*

9.1 Introduction

The aim of this chapter is to provide an overview of worldwide human exposures to Hg as reflected by concentrations in biomarker samples. The specific objectives of this study are to outline: whether exposures have changed over time in specific populations; geographical variations in exposure; exposures in vulnerable groups; exposure biomarker data with respect to guideline values; links between Hg sources and biomarker levels; and key knowledge gaps.

9.2 Background

9.2.1 Sources of human exposure to Hg

Mercury (Hg) is a naturally occurring element that can enter the environment via natural or anthropogenic-mediated processes. There are three major chemical forms relevant to human exposure: elemental Hg (Hg^0), inorganic Hg compounds (Hg^{II}), and organic Hg compounds, of which the most important form is methylmercury (MeHg). The source, environmental fate, exposure, and toxicity of these different Hg forms vary.

Mercury has unique physical and chemical properties that have rendered it attractive for use in a range of industrial and medical applications. Human exposure to Hg^0 and Hg^{II} may occur in occupational settings, for example artisanal and small-scale gold mining (ASGM) and dentistry, through contact with certain products containing Hg, such as dental amalgams, some skin-lightening creams, broken fluorescent lamps, and other waste products, and also from environmental contamination. In addition, thimerosal, which contains ethylmercury, is used as a preservative in some vaccines (WHO, 2017).

Mercury released into the environment may be converted by microorganisms to MeHg which bioaccumulates and biomagnifies through the food chain, particularly in aquatic systems (see Chapters 7 and 8). Seafood is the main source of protein for around one billion people worldwide (FAO, 2014) and some organisms that are widely consumed are likely to be contaminated with MeHg. These include predatory fish such as tuna, swordfish, grouper, and mackerel. Foods, such as rice, grown in heavily contaminated sites may also take up Hg (Rothenberg et al., 2014). For many communities, therefore, dietary consumption of contaminated fish, shellfish, marine mammals, and other food items is arguably the most important source of exposure. Figure 9.1 illustrates some key sources of Hg exposure around the world.

9.2.2 Health effects of Hg

Mercury is a pollutant of global concern principally due to its adverse effects on human health. The current state of knowledge concerning human health impacts has been extensively reviewed by international agencies (IPCS, 1990, 2003; JECFA, 2007a,b, 2011; EFSA CONTAM Panel, 2012) as well as by national agencies and other authors (US EPA, 1997, 2001; ATSDR, 1999; Clarkson and Magos, 2006; Karagas et al., 2012; Ha et al., 2017; Eagles-Smith et al., 2018b).

All populations worldwide are exposed to some amount of Hg, and the possibility of exposure-related adverse health effects is dependent upon a range of factors (e.g., chemical form, concentration, duration of exposure, lifestage). The embryo and fetus are the most vulnerable lifestages with respect to the adverse effects of MeHg (JECFA, 2007a).

Arctic Indigenous Peoples
Marine mammals and seafood drive
dietary MeHg exposures (AMAP, 2015)

Faroese Cohort
Pilot whale consumption
(AMAP, 2015)

European Exposures
Diverse Hg source-exposures
(Višnjevec et al., 2014; Castaño et al., 2015)

Great Lakes Region
Fish consumption advisories
(Knobeloch et al., 2011)

Mediterranean Region
Fish drive dietary MeHg exposures
(Višnjevec et al., 2014)

Dental Professionals and Patients
Amalgams drive Hg⁰ exposure
(Goodrich et al., 2016)

Japan 10 district study
Tuna drives dietary MeHg
exposure (Yasutake et al., 2004)

Amazonian Tapajós River
Fish and mining drive exposures
(Berzas Nevado et al., 2010)

☐ MeHg sources
☐ H⁰ and HgII sources
☐ Mixed Hg sources

Ghana ASGM
Environmental and occupational
factors (Basu et al., 2014)

Seychelles Cohort
Seafood consumption
(Shamlaye et al., 1995)

Contaminated Sites
Contaminated rice in mining
sites (Rothenberg et al., 2014)

Figure 9.1 Selected studies worldwide depicting strong and representative evidence of Hg source-exposure relationships.

All forms of Hg are toxic but the principal target organs differ according to the form. Exposure to Hg^0 may affect the nervous system. Exposure to Hg^{II} compounds may affect the kidneys. Exposure to MeHg is associated with adverse neurodevelopmental outcomes. The latter has received the most attention largely due to notorious MeHg poisoning events in Japan and Iraq following high exposures (IPCS, 1990). Studies on the toxicity of MeHg carried out over recent decades have provided a growing body of evidence that chronic, relatively low-level MeHg exposure can be associated with a range of adverse health outcomes targeting, for example, the cardiovascular and immune systems (Karagas et al., 2012).

9.2.3 Mercury exposure assessment using biomarkers

Detailed reviews of methods for assessing Hg exposure have been undertaken by WHO/UNEP (2008) and the US EPA (1997). Human exposure to Hg can be estimated by measuring Hg in human tissue and other samples (WHO/UNEP, 2008). This chapter focuses on biomarkers of Hg exposure for which there are well-validated methods of measurement and interpretation and for which there is a reasonably large body of knowledge. The most commonly used biomarkers are the concentrations of Hg in hair, urine, blood, and cord blood, and their selection can depend on factors such as the potential source of exposure, chemical form, and exposure lifestage. The logistical requirements and costs differ for each sample type. In all cases it is important that steps are taken to avoid sample contamination during collection, storage, transportation, and analysis, and to be mindful of ethical considerations (WHO Regional Office for Europe, 2015).

Most of the Hg in hair occurs as MeHg and once incorporated the Hg remains in the hair. This biomarker can therefore provide an integrated measurement of Hg exposure given that hair grows at roughly 1 cm per month and thus exposure can be tracked over time by careful sampling. Hair has the advantage that it is easy to collect and transport, although it should be noted that in some communities there may be cultural objections to taking hair samples. On the other hand, in highly contaminated areas such as ASGM sites there is a danger of external contamination of the hair, which can confound interpretation of the results. Studies using stable isotope analysis have, for example, found external contamination of hair in ASGM communities by Hg^0, thus calling for special attention to be paid to the interpretation of hair Hg levels to monitor exposure within ASGM sites (Sherman et al., 2015) and the need to analyze hair for MeHg in such scenarios.

Urine analysis primarily provides information about exposure to Hg^{II} and Hg^0, although MeHg may also contribute to the burden of urinary Hg, particularly among avid seafood consumers (Sherman et al., 2013). The concentration of the analyte may depend on the dilution of the urine, which can vary. It is therefore common for the Hg measurement to be expressed in terms of its concentration per unit of creatinine. Another approach is to relate the Hg concentration to the specific gravity of the urine sample, which is gaining favor given that creatinine measurements may be confounded by factors such as diet and age. Urine is a relatively easy and non-invasive sample to collect.

Mercury is measured in whole blood and this provides information about recent exposure (~1–2 months) to both MeHg and Hg^{II}. In most communities the measurement of blood total Hg is an accepted biomarker for MeHg exposure as it correlates relatively well to seafood consumption (Sheehan et al., 2014). Speciation can provide an indication of potential Hg sources but requires careful sample preparation

and sophisticated instrumentation. The measurement of Hg in cord blood provides information about developmental exposure. Blood collection, storage, and transport pose certain logistical and financial barriers, however.

Each biomarker can provide pertinent exposure information on the type of Hg (organic vs. inorganic) and timeline of exposure (acute vs. chronic). When multiple biomarker measures are taken from a given individual, and also combined with surveys, a deeper exposure assessment can be performed. In general, careful measurement of Hg in hair and urine offers the most convenient and cost-effective scheme to monitor Hg in a given population, particularly those populations situated in resource-limited settings. For a more detailed discussion of Hg biomarkers, including potential challenges in their use, see WHO/UNEP (2008).

To maximize the use of Hg biomarker data, it is sometimes necessary to convert across biomarker types and there are two conventions to be noted for exposure cases that largely involve MeHg (N.B. applicability to Hg^0 and Hg^{II} is not known). First, the Joint Food and Agriculture Organization (FAO) and World Health Organization (WHO) Expert Committee on Food Additives (JECFA) established a MeHg hair-to-blood ratio of 250 (JECFA, 2004) that is now commonly used by the research community. Second, cord blood levels are on average 70% higher than maternal blood levels (range from 10% to over 200%), as discussed by Stern and Smith (2003). While these two biomarker ratios are both used in the current assessment, it is acknowledged that there is ongoing debate in the literature concerning the validity of these approaches particularly in terms of heterogeneity across individuals with respect to influential factors such as sex, age, and ethnicity (Bartell et al., 2000; Stern and Smith, 2003; JECFA, 2007a; EFSA CONTAM Panel, 2012). There is also growing awareness that inter-individual differences in the toxicokinetics of Hg and resulting biomarker measures may be influenced by polymorphisms in certain genes (Basu et al., 2014a), although at this time such information cannot be put into practice. Nonetheless, biomarker conversions facilitate comparability across studies, and have been effective at helping derive large, regional biomonitoring assessments and maps – for example, in Europe by Višnjevec Miklavčič et al. (2014) and in the Arctic by AMAP (2015) – that are effective communication tools. In addition, to make judgements from biomarker measurements it is necessary to have reference values. Proposals by stakeholder organizations are summarized in the Appendix to this chapter (Tables A9.1 and A9.2). The color scale used by Višnjevec Miklavčič et al. (2014) in their European assessment of Hg exposure was adapted for the purposes of this assessment (Appendix, Table A9.3).

9.3 Search strategy and data analyses

An international advisory group of scientific experts on Hg exposure was convened to guide the work. The group (i.e., report authors) decided to focus this initial global assessment on three study population types: A, B and C.

- *A-National human biomonitoring programs.* These programs are usually sponsored and/or operated by official government agencies and provide high quality data on nationally-representative exposures.

- *B-Longitudinal birth cohort studies.* Methylmercury-contaminated seafood poses risk-benefit dilemmas to all populations, especially to pregnant women and young children since there are both health benefits from consumption (such as from the selenium and polyunsaturated fatty acids in seafood) and risks (from the MeHg they contain) (JECFA, 2007a; FAO/WHO, 2010). Concerns over fetal exposure have largely been investigated through birth cohort studies which are usually well designed and the most pertinent for establishing exposure-outcome relationships. They tend to provide high quality exposure data for vulnerable groups (i.e., those with high exposures and/or susceptibility to toxic effects; such as fetuses, newborns, and children) and these data can be used to explore geographic differences and temporal trends, as well as to characterize Hg source-exposure-biomarker relationships.

- *C-Cross-sectional studies.* The focus here is on studies to help better characterize exposures in three pre-determined groups: in background populations, in populations that were vulnerable because of high exposure to MeHg, or to Hg^{II} or Hg^0 sources. For brevity, this review focused on the most illustrative works but it should be noted that this information was extracted from a companion systematic review effort led by the World Health Organization (WHO) that is more comprehensive (Basu et al., 2018).

A bibliographic search of the peer-reviewed scientific literature was performed using three databases: Medline, Biosis, and the Web of Science Core Collection. The search strategy included the following Boolean search phrases: "mercury OR methylmercury OR (methyl AND mercury) OR MeHg"; and "blood OR hair OR urine". Other information sources included grey literature, key researchers identified by report authors, and stakeholders via UN Environment outreach activities. When a study was reported on in multiple articles, the article with the most complete dataset was chosen to serve as a representative piece.

Scientific papers were reviewed through a two-stage process: the title and abstract fields were searched to ascertain relevancy; and the full text was reviewed on papers that were deemed relevant. In brief, national biomonitoring studies (Study Population Type A) were identified through a list compiled by UN Environment (UN Environment, 2016), WHO-Europe (WHO Regional Office for Europe, 2005), and subsequent outreach efforts, an electronic search and authors' knowledge. All of the identified national biomonitoring programs that measured Hg in hair, blood, urine, or cord blood were included. Longitudinal birth cohort studies (Study Population Type B) were identified through the same procedure as the national biomonitoring studies. To be included studies needed to have sampled participants on at least two separate occasions of which one needed to include a biomarker measured during pregnancy or birth. Cross sectional studies of both vulnerable and background population group studies (Study Population Type C) were identified through a review of the bibliographic search results. As previously mentioned, this review focused on the most illustrative cross-sectional studies based on a companion effort led by the WHO (Basu et al., 2018).

For all studies, data were extracted on population characteristics (age, lifestage, sex, city/country/region location),

Hg exposure measurements (sample size, Hg biomarker and speciation information, quality control measures), and measures of central tendencies (geometric mean, median) and high-end (90th or 95th percentile or maximum) biomarkers. In total, 424,858 Hg biomarker measurements were captured from 335,991 individuals represented in 312 articles from 75 countries. To compare across biomarker types, datasets were converted to blood Hg equivalents using the conventions mentioned in Section 9.2.3. To further interpret the results, the values were compared against ranges that were derived based on a scan of existing reference range and guidance resources (Appendix, Table A9.1), and a color scale (Appendix, Table A9.3) was used to visually represent the findings.

9.4 Results

9.4.1 National biomonitoring studies

Data were obtained from nine countries (Belgium, Canada, Czech Republic, France, Germany, Republic of Korea, Slovenia, Sweden, USA) that were identified by those countries as being nationally-representative (Table 9.1). The total sample population of these surveys was 121,413 people from which 192,651 biomarker measurements of Hg exposure were extracted (Table 9.2). The survey data were compared, with a particular focus on country, lifestage, sex, sampling year(s), and biomarker type.

Across the national biomonitoring programs the majority of participants had blood Hg levels that fall below 5 µg/L (Table 9.3 and Figure 9.2). Blood Hg levels were consistently
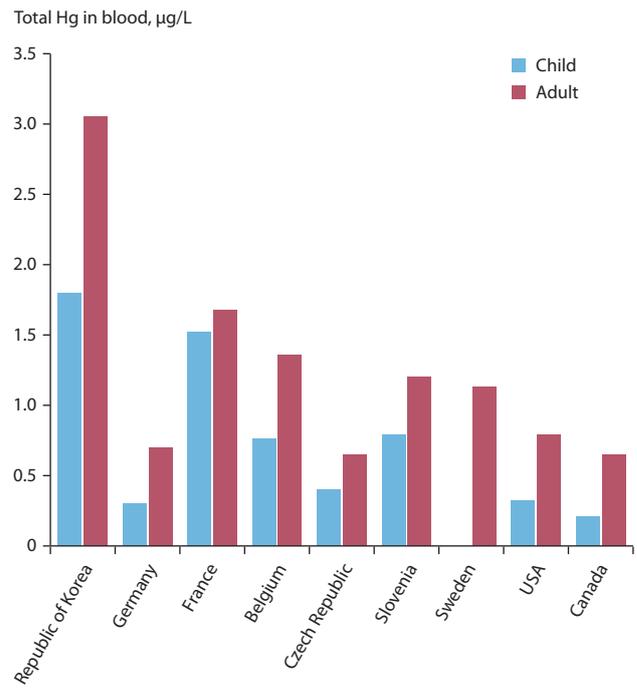
Figure 9.2 Comparison of median blood total Hg measurements across children (<19 years) and adults from national biomonitoring datasets between 2003 and 2014. Note, for Belgium and France that blood Hg values were estimated based on hair Hg levels in women (adults) and children (both sexes).

highest in the Republic of Korea versus the other countries, although the values are similar to those in neighboring countries as gleaned from a comprehensive assessment of

Table 9.1 Summary of national human biomonitoring programs that measure Hg.

Country	Survey	Lead organization	Start date	Frequency	Size/cycle	Age; Sex	Biomarkers	Key reference
Belgium	FLEHS	Vlaanderen Departement Omgeving	2002	2; every 2 years	~5000	1–65; female adults, children both sexes	hair	Croes et al., 2014
Canada	CHMS	Statistics Canada	2007	4; every 2 years	~5000	3–79; both	blood, urine	Health Canada, 2017
Czech Republic	CZ-HBM	National Institute of Public Health	1994	16; ~every year	~400	8–64; both	blood, urine, hair	NIPH, 2016
France	Elfe	Santé publique France	2011	1	~1800	18–47; pregnant women	hair	Dereumeaux et al., 2016
Germany	GerES	German Environment Agency	1985	5; variable	~2000–5000	3–79; both	blood, urine	Schulz et al., 2007; German Federal Environment Agency, 2017
Germany	ESB	German Environment Agency	1981	37; each year	500	20–29; both	blood, urine	German Federal Environment Agency, 2017
Republic of Korea	KoNEHS	Korean Ministry of Environment	2009	3; every 3 years	~6000	3–19+; both	blood, urine	Burm et al., 2016; Choi et al., 2017
Slovenia	SLO-HBM	Jozef Stefan Institute	2008	2; every 2 years	~300–~900	18–49; both	blood, urine, breast milk, hair	Snoj Tratnik et al., 2018
Sweden	Riksmaten	Swedish National Food Agency	1990	2; variable	~300	18–80; both	blood	Bjermo et al., 2013
USA	NHANES	Centers for Disease Control and Prevention	1999	6; every 2 years	~2,500-8000	1–70+; both	blood, urine	US CDC, 2017

Table 9.2 Count of individuals and Hg biomarker measures from the national biomonitoring programs.

Country	Demographics					Number of Hg measurements				
	Total sample size (across years)	Children	Adults	Males	Females	Total	Blood total Hg	Blood MeHg	Urine	Hair
Belgium	465	210	255		255	465				465
Canada	22,805	9,491	13,314	11,227	11,578	41,235	22,425	2,075	16,734	
Czech Republic	7,542	3,623	3,919			13,845	4,700		6,459	2,686
France	1,799		1,799		1,799	1,799				1,799
Germany	25,772	2,602	23,170			41,045	17,056		23,989	
Republic of Korea	14,688	2,346	12,342			14,688	14,688			
Slovenia	1,095		1,095	553	542	3,523	1,085		1,020	947
Sweden	273			128	145	273	273			
USA	46,974	19,086	27,888	23,292	23,682	75,778	46,974	13,016	15,788	
Total	121,413					192,651				

Table 9.3 Cross-sectional comparison of blood total Hg concentrations (μg/L) in adults and children via national biomonitoring data. Males and females are grouped together. Note, for Belgium and France that blood Hg values were estimated based on hair Hg levels in women (adults) and children (both sexes).

	Belgium	Canada	Czech Republic	France	Germany	Republic of Korea	Slovenia	Sweden	USA
Survey Name	FLEHS2	CHMS Cycle 2	CZ-HBM	Elfe (Adults), ENNS (Children)	GerES-III (Adults), GerES-IV (Children)	KoNEHS-2 (Adults), KorEHS-C (Children)	SLO-HBM	Riksmaten	NHANES
Adults									
Year	2007–2011	2009–2011	2015	2011	1998	2014	2008–2012	2010–2011	2011–2012
Age	18–42	20–39	18–64	18–47	18–69	19+	18–49	18–80	20+
Sample size	255	1313	302	1799	3973	6457	1085	273	5030
Median blood Hg	1.36	0.65	0.65	1.68	0.70	3.05	1.20	1.13	0.79
95th% blood Hg	3.44	5.20	2.50	5.56	2.40	9.05	4.78	3.45	5.02
Children									
Year	2007–2011	2009–2011	2008	2006–2007	2003–2006	2012–2014	2008		2011–2012
Age	14–16	6–11	8–10	3–17	3–14	3–18	6–11		6–11
Sample size	210	961	198	1364	1240	2346	174		1048
Median blood Hg	0.76	0.21	0.40	1.52	0.30	1.80	0.79		0.32
95th% blood Hg	1.88	2.00	1.40	4.8	1.00	3.68	2.19		1.40

cross-sectional studies (Basu et al., 2018). Blood Hg levels in adults were approximately 2.1-fold higher than in children, and this varied across lifestage. For example, median blood Hg levels in Canadians from the Canadian Health Measures Survey (CHMS) second cycle (2009–2011) increased with age

as follows: 0.21 μg/L (6–11 years), 0.20 μg/L (12–19 years), 0.65 μg/L (20–39 years), 1.1 μg/L (40–59 years), and 1.2 μg/L (60–79 years) (Health Canada, 2017). Similar trends were observed in the U.S. and Korean datasets (Seo et al., 2015; Burm et al., 2016; US CDC, 2017).

Table 9.4 Cross-sectional comparison of urinary total Hg measurement (μg/L) in adults and children via national biomonitoring data. Males and females are grouped together. When available, creatinine-adjusted values are indicated in parenthesis. Data sources as shown in Table 9.1.

		Canada	Czech Republic	Germany	Slovenia	USA
Adults	Year	2012–2013	2015	1998	2008–2012	2013–2014
	Age	20–39	18–64	18–69	18–49	20+
	Sample size	1048	234	4052	1020	1813 (1812)
	Median urine Hg	0.20 (0.22)	0.91 (0.91)	0.40	0.45 (0.47)	0.24 (0.30)
	Upper (95th%) urine Hg	1.10 (1.20)	6.34 (4.67)	3.00	3.47 (2.48)	1.76 (1.76)
Children	Year	2012–2013	2008	2003–2006	2008	2013–2014
	Age	6–11	8–10	3–14	6–11	6–11
	Sample size	1010	318	1734	164	401
	Median urine Hg	<MDL, i.e. 0.2 (<MDL, i.e. 0.2)	(0.20)	<MDL, i.e. 0.1	0.76 (0.73)	<MDL, i.e. 0.13 (<MDL, i.e. 0.13)
	Upper (95th%) urine Hg	0.93 (1.9)	(1.10)	0.5	4.64 (4.15)	0.89 (1.11)

MDL: Method detection limit.

Urine Hg levels were consistent across the countries from which data were obtained, with the majority of values falling below 3 μg/L (Table 9.4). Like blood, urine Hg levels were higher in adults than in children.

Temporal changes in Hg exposure were evaluated by reviewing national datasets in which there were two or more comparable sampling periods (Figure 9.3). For blood Hg, datasets from four countries (USA, Canada, Czech Republic, Republic of Korea) were reviewed and in general showed declining exposures. For example, combining the data from USA, Canada, and the Czech Republic into a linear regression model showed annual decreases in blood Hg of approximately 0.026 μg/L or 2.25% (i.e., over 10 years this would be a decrease of 0.26 μg/L or ~22.5%) with median blood Hg levels stabilizing around 0.75 μg/L (Figure 9.3 upper plot). For urinary Hg, similar over-time decreases can be observed particularly when examining the US NHANES dataset as the Hg levels in the latest dataset are about 50% lower than they were 10 years earlier (Figure 9.3 lower plot). Urinary Hg values in the US are currently similar to those in Canada and hover around 0.2 μg/L.

9.4.2 Longitudinal birth cohorts

Thirty-two birth cohort studies were found (many of which had multiple sub-cohorts or sites) from 17 countries in which there was at least one Hg exposure measurement during pregnancy or birth, as well as a follow-up period in which at least one outcome measurement was taken (Figure 9.4; Appendix, Table A9.4). The total sample population of these birth cohort studies was 23,374 mother-child pairs, from which 47,699 biomarker measurements were taken. Of these birth cohort studies, 17 (53%) measured Hg in cord blood, 9 (28%) measured Hg in maternal blood during pregnancy, and 19 (59%) measured Hg in maternal hair. In general, the birth cohort studies focused on MeHg exposures.

The overview presented in Figure 9.4 leads to several observations:

- Groups consuming large amounts of seafood (Seychelles, Spain), freshwater fish (Brazil) and/or marine mammals (e.g., Faroe Islands, Inuit communities of the Arctic) have the highest Hg exposures, which often exceed 10 μg/L in cord blood.
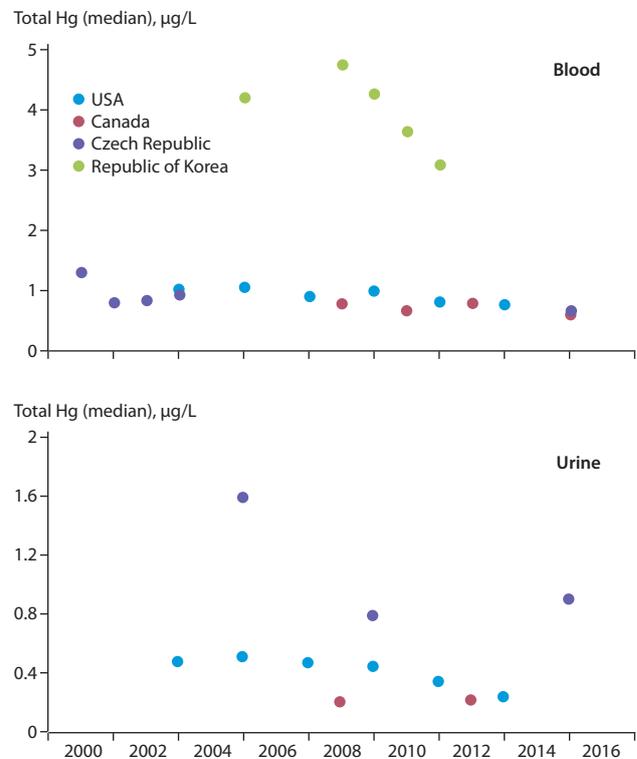
Figure 9.3. Temporal trends of adult blood and urinary total Hg (median values) measurements across the national biomonitoring studies in which data were available from two or more comparable sampling periods.

- Cord blood Hg levels range between 5 and 10 μg/L across several Mediterranean populations, are approximately 5 μg/L in Asia, and generally less than 5 μg/L across communities in North America and Europe (excluding indigenous peoples and the Mediterranean area).

- Exposures in the Faroe Islands show an almost five-fold decline between ~1987 and ~2008 (blood Hg from 22.3 to 4.6 μg/L), and in the Seychelles an approximately two-fold decline between ~1989 and ~2008 (hair Hg from 5.9 to 2.9 μg/g).

In these birth cohort studies, a range of health outcomes were measured in the newborn, infant, toddler, or child, including for example, birth weight, motor function, and intelligence
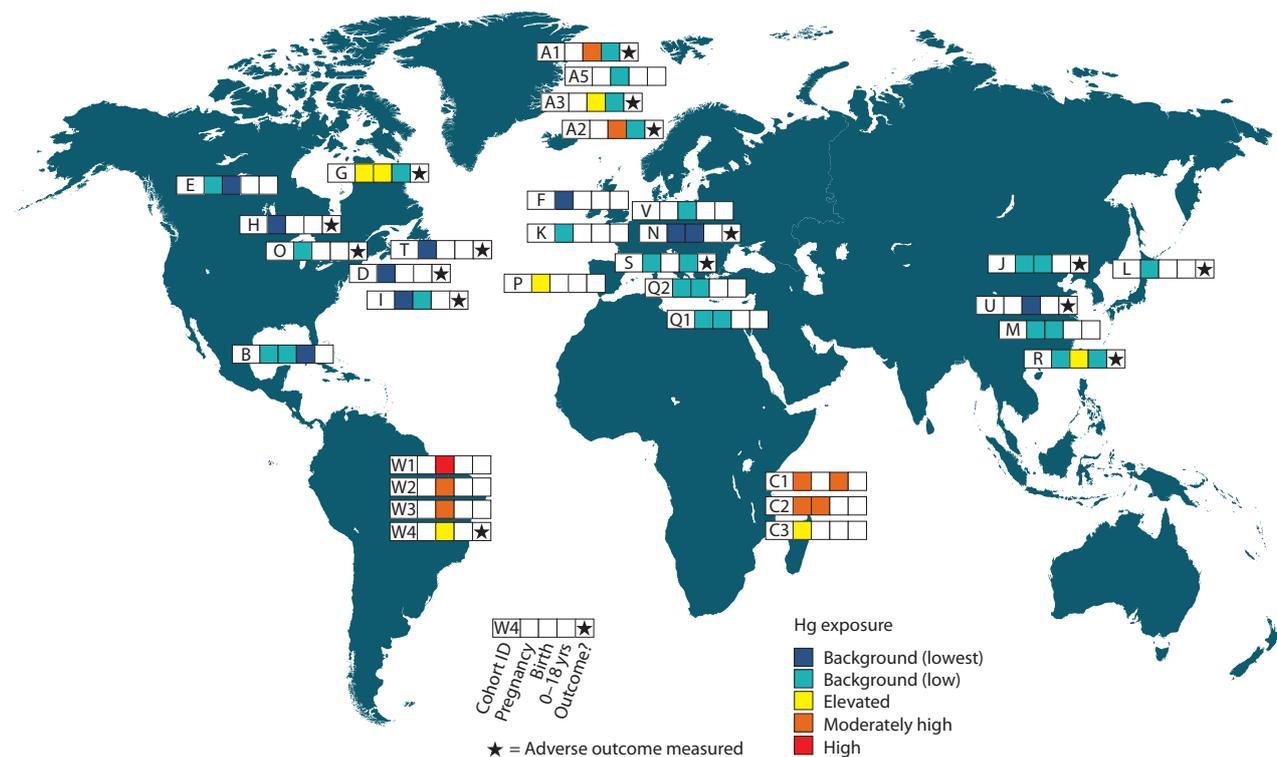
Figure 9.4. Locations of the selected Hg birth cohort studies. Data represent 24 cohort studies and 47,699 Hg biomarker measures. The cohort ID is indicated in the first box as a letter (see Appendix, Table A9.4 for details). The first three boxes refer to group average Hg measures taken during pregnancy, at birth, and up until age 18 years, respectively. Blank cells represent lifestages without a Hg measurement. If the final box has a star, then a Hg-associated adverse outcome was reported in that cohort. Color codes are based on the work by Višnjevec Miklavčič et al. (2014) with minor modifications as detailed in Appendix Table A9.3.

(see reviews by Karagas et al., 2012 and Ha et al., 2017). In flagging cohorts in which a MeHg-associated adverse health outcome was observed (by asterisks in Figure 9.4), such as neurobehavioral effects and motor function, it is apparent that these cohorts span a range of exposures and are not restricted to highly exposed groups or particular regions.

9.4.3 Cross-sectional studies

As detailed in the companion WHO systematic review (Basu et al., 2018), for the cross-sectional studies the initial database search retrieved 9210 non-duplicate articles from which 265 articles were deemed eligible for data extraction. From these articles, the data were organized into 441 sub-populations from which 184,510 Hg biomarker measurements were taken from 167,830 individuals from 73 countries.

This section presents some illustrative findings from the bibliographic search and group discussions, the purpose of which is to showcase the current state of knowledge concerning Hg exposure in background populations and vulnerable groups. In general, conclusions from high-quality review papers and pooled analyses from the systematic review (Basu et al., 2018) were prioritized. Some of these examples were captured in Figure 9.1.

9.4.3.1 Background population groups

For blood Hg, background exposures were characterized from 201 sub-populations from 53 countries that included 52,136 biomarker measures. The pooled central median blood Hg concentration was 2.2 µg/L (inter-quartile range, IQR: 1.0–4.7 µg/L) with the upper bound median value being 9 µg/L. These findings compare well to the national biomonitoring studies in which the majority of participants had blood Hg levels of below 5 µg/L.

For hair Hg, background exposures were characterized from 109 sub-populations that included 39,035 biomarker measures (Figure 9.5). The pooled central median hair Hg concentration was 0.7 µg/g (IQR: 0.3–1.7 µg/g) with the upper bound median value being 4.1 µg/g.
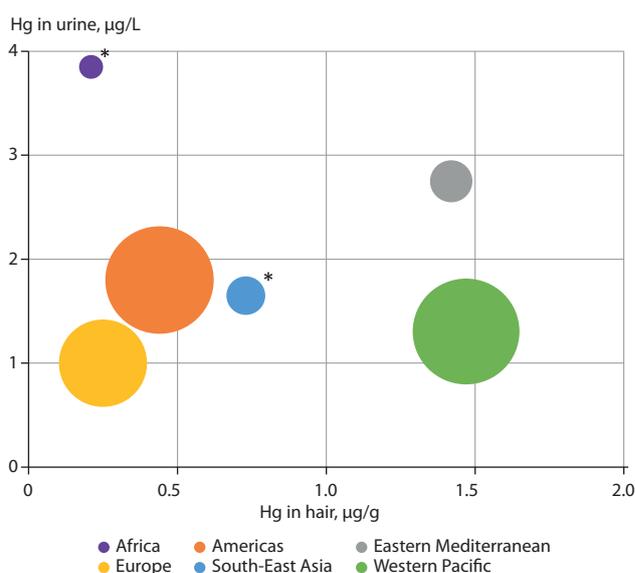
Figure 9.5 Bubble plot of hair and urine Hg levels from cross-sectional studies on background populations according to WHO geographic regions. The size of the bubble reflects the sample size. The asterisk indicates that urinary Hg levels from background populations in Africa and South-East Asia were not available, and thus urinary Hg levels from all populations within these regions was used.

For urine Hg, background exposures were characterized from 35 sub-populations that included 10,435 biomarker measures (Figure 9.5). The pooled central median Hg concentration in the background population was 1.0 µg/L (IQR: 0.6–1.5 µg/L) with the upper bound median value being 6.1 µg/L. These findings compare well to the national biomonitoring studies in which the majority of participants had urine Hg levels of below 3 µg/L.

9.4.3.2 Dietary exposure to MeHg

The systematic review of the cross-sectional studies identified 71 sub-populations from 18 countries that had been specifically studied because of concerns associated with consumption of fish and other aquatic animals. The studies included 29,751 individuals from which 33,814 Hg biomarker measures were taken. The pooled central median blood Hg concentration across these studies was 8.6 µg/L (IQR: 2.9–21.2 µg/L) with the upper bound median value being 38.6 µg/L. Exposures in this group are roughly 4-fold higher than in background populations. This is not surprising given that consumption of fish and other aquatic animals (i.e., high consumption amounts or consumption of relatively highly contaminated items) is widely considered to be the main source of MeHg exposure to most populations worldwide.

Data from the cross-sectional study populations provide strong evidence that indigenous peoples in many areas of the world (but especially Inuit from the Arctic and groups within the Amazonian region) are at increased risk of Hg exposure. Many from these communities are reliant upon traditional and locally-caught foods such as fish and marine mammals for sustenance. For example, Cisneros-Montemayor et al. (2016) compiled data from over 1900 coastal indigenous groups (27 million people from 87 countries) and showed that per capita seafood consumption in these communities is 15-fold higher than in non-indigenous groups. Because traditional foods also form a strong basis for the culture, spirituality, recreation, and economy of many of these communities, contamination of food by Hg presents an issue of environmental justice (Landrigan et al., 2018).

The Inuit in the Arctic are exposed to some of the highest MeHg levels globally largely due to their reliance on fish and marine mammals as culturally important food staples. The systematic review identified 15 Arctic sub-populations from which 8729 individuals were studied with the resulting central median blood Hg concentration being 8.6 µg/L (IQR: 3.6–16.2 µg/L) with an upper bound median concentration of 70.5 µg/L. The findings are in line with the latest AMAP Human Health Assessment (AMAP, 2015) that reviewed several human biomonitoring programs across the circumpolar region. As an example, in Canada as part of the International Polar Year study, the geometric mean of blood Hg across four study regions ranged from 2.8 to 12 µg/L, with individual values ranging from 0.1 to 240 µg/L. In another example, the Greenlandic Inuit Health and Transition Study of 3105 participants from all geographic areas and community sizes (nine towns, 13 villages) reported blood Hg levels ranging from 0.1 to 400 µg/L.

Indigenous peoples living within the Amazon Basin have also been documented to be highly exposed to Hg through both fish consumption and proximity to gold mining (Berzas Nevado et al., 2010), and thus it is not surprising to find elevated Hg levels in both blood and urine. The systematic

review identified 46 sub-populations from which 18,509 individuals were studied with the resulting central median blood Hg concentration being 15.4 µg/L (IQR: 8.7–32.9 µg/L) and an upper bound median concentration of 83.1 µg/L (IQR: 54.3–170.3 µg/L). For urine, the central median urinary Hg concentration was 7.2 µg/L (IQR: 5.5–10.4 µg/L) with an upper bound median concentration of 149.0 µg/L (IQR: 63.8–178.8 µg/L).

9.4.3.3 Point source exposures to inorganic and elemental Hg

The systematic review of the cross-sectional studies identified 79 sub-populations from 28 countries that included 16,673 individuals from which 22,257 Hg biomarker measures were taken. The pooled central median blood Hg concentration was 6.9 µg/L (IQR: 2.8–12.3 µg/L) with the upper bound median value being 42.4 µg/L. For urine, which is the primary biomarker to gauge inorganic and elemental Hg exposures, the pooled central median Hg concentration was 4.2 µg/L (IQR: 1.4–10.9 µg/L) with the upper bound median value being 41.3 µg/L. See summary data in Figure 9.6.

Exposures in this group are driven by the ASGM sector (e.g., pooled central median urine concentration was 5.9 µg/L, IQR: 3.0–14.4 µg/L). Artisanal and small-scale gold mining is rapidly growing worldwide with over 15 million miners estimated to be directly involved in the sector and potentially 100 million people living in ASGM communities (UNEP, 2012; WHO, 2016). There are several public health concerns in ASGM communities (Basu et al., 2015; WHO, 2016) and a growing number of human biomonitoring studies (reviewed by Gibb and O'Leary, 2014).

The values from 3463 individuals from the ASGM sector are comparable with an earlier meta-analysis of data from 1245 miners (many of which data are included here) from across Indonesia, Philippines, Tanzania, Zimbabwe, and Mongolia. This reported median urine Hg value is 3.6 µg/L (95th percentile 119 µg/L) with upward values in excess of 1000 µg/L (Baeuml et al., 2011).
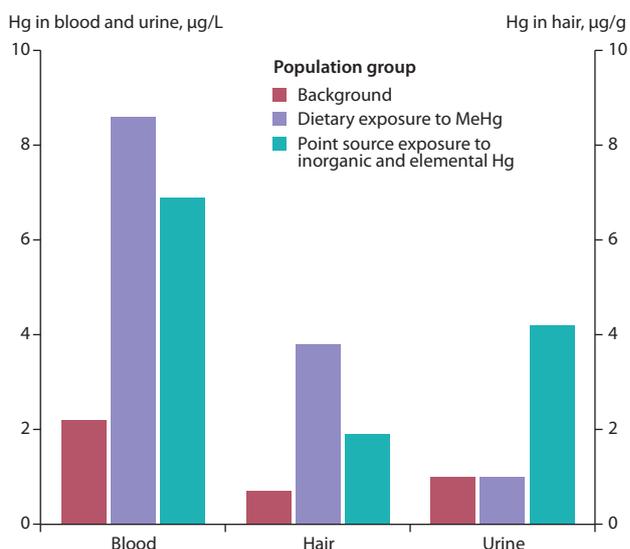
Figure 9.6 Median blood, hair, and urine Hg levels across different population groups following a systematic review of relevant cross-sectional studies.

9.5 **Summary of findings**

This assessment documents great variability in Hg exposures worldwide. All people are exposed to some amount of Hg. Individuals in background populations worldwide with insignificant exposures to Hg sources have blood Hg levels that are generally <5 μg/L, hair Hg levels that are generally <2 μg/g, and urine Hg levels that are generally <3 μg/L (corresponding levels in cord blood may be determined using the ratios outlined in Section 9.2.3; see also the Appendix, Table A9.1). There are a number of notable groups with relatively high Hg exposures. Elevated exposures to Hg in key groups of concern for which there exist a relatively robust dataset include Arctic populations that consume fish and marine mammals as a significant component of their diet (e.g., many indigenous communities), tropical riverine communities (such as those in the Amazon Basin), coastal and/or small-island communities that are high seafood consumers, and individuals who either work or reside at ASGM sites. This type of information is critical in helping understand Hg exposures, particularly in light of certain stipulations within the Minamata Convention on Mercury (e.g., under Article 22, such information can inform effectiveness evaluation especially for vulnerable populations).

Despite a relatively large dataset – this study used 192,651 and 47,699 biomarker measurements from national biomonitoring programs and birth cohort studies, respectively – there remain various outstanding issues.

First, there are several countries and geographic regions for which data are completely lacking. For example, the systematic review described here drew on data from 75 countries, highlighting the lack of data from most countries. Given that the Minamata Convention is motivated by human health concerns (i.e., Article 1), there is a need for Parties to have nationally representative data such that temporal changes in human exposure (and ultimately risk) may be tracked. There is general agreement concerning the methods used to assess Hg exposure. Measures of Hg in hair and urine samples are particularly suitable because they provide information on the two main forms of Hg, and their collection is relatively non-invasive, requires no specialized training, or handling and storage regimen, and is relatively cheap (Evers et al., 2016). Such methods are being scaled across countries to help harmonize Hg biomonitoring. For example, the DEMOnstration of a study to COordinate and Perform Human biomonitoring on a European Scale (DEMOCOPHES) project showed that hair Hg could be measured in 1799 mother-child pairs from 17 European countries to yield comparable values (Castaño et al., 2015).

Exposure to Hg in vulnerable groups that are sensitive owing to extrinsic (e.g., high exposures) and intrinsic (e.g., genetics) factors remain of utmost concern (Eagles-Smith et al., 2018b). There are several highly exposed groups – such as individuals living in Hg-contaminated sites (Trasande et al., 2016), consumers of rice from contaminated sites (Rothenberg et al., 2014), and users of Hg-containing skin-lightening creams (WHO/UNEP, 2008) – for which there is growing awareness but relatively few data from which to draw firm conclusions. There are also certain ecosystems sensitive to Hg loading and methylation (see Chapters 7 and 8), and these may represent hotspots that warrant attention for those who consume local aquatic food items (Evers et al., 2016). In addition to vulnerability based on elevated exposures, there is also concern about Hg susceptibility during certain lifestages (e.g., fetus), the range of physiological systems targeted (Karagas et al., 2012), the complex interactions between Hg and other chemical and non-chemical stressors, particularly in the context of global change drivers (Eagles-Smith et al., 2018b), and the increasing acceptance that genetic differences in sub-populations can influence exposure biomarkers and exposure-outcome relationships (Basu et al., 2014a).

Concerns over Hg pollution and human health risks are firmly established, nevertheless there are success stories to be noted. This review found studies that showed steps to limit Hg exposures – intentional or otherwise – may be effective. For example, the roughly two-fold reduction in urinary Hg levels measured over the past decade across the U.S. population is likely to be due to a combination of the development of encapsulated amalgams, increasing use of composite resins, and overall awareness of the occupational and environmental risks associated with Hg use (Figure 9.3 lower plot). Similar trends have been observed elsewhere such as in German children (Link et al., 2007) and among U.S. dental professionals (Anglen et al., 2015; Goodrich et al., 2016).

A second success story can be gleaned from the Arctic. Although Hg exposures across Arctic circumpolar regions remain elevated, levels have declined over the past two decades, probably owing to local dietary advisories and changing consumption patterns. According to AMAP (2015) these decreases may be a sign that risk management efforts are having a beneficial effect, but there remain concerns about changing consumption patterns and how these may affect indigenous culture, identity and spirituality, recreational opportunities, and human nutrition. In other jurisdictions, there have been cases of decreased Hg exposures as a result of dietary consumption advisories (e.g., Knobeloch et al., 2011; Kirk et al., 2017). Decreases have also been observed in both the Faroe Islands and the Seychelles. However, in other Small Island Developing States the awareness of Hg exposure and its potential health impacts may be lower and thus the decrease observed in the Seychelles is not necessarily representative of other islands.

Acknowledgments

Chapter 9 Appendix

Table A9.1 Reference values for mercury biomarkers. Italicized values are estimated based on biomarker conversions indicated in the text.

	Blood	Hair	Cord blood	Urine
US National Academy of Sciences (NAS) and US National Research Council's Benchmark Dose Lower Limit (BMDL) concerning women of child-bearing age) (US NAS / US NRC, 2000)	*3.5 µg/L*	1 µg/g	5.8 µg/L	
Qualitative conclusions by expert panel on 'High' Levels (Karagas et al., 2012)	>12 µg/L	>4 µg/g	>20 µg/L	
Health Canada, 2004	20 µg/L (general adult population)	6 µg/g		
Proposed guideline values for Canada (Legrand et al., 2010)	8 µg/L (pregnant women); 20 µg/L (non-pregnant adults); 100 µg/L for 'general' men/women	*2 µg/g;* *6 µg/g;* *25 µg/g*	*13.6 µg/L;* *29 µg/L;* *not relevant for the 3rd group*	
German HBM-1 (concentration of a substance in human biological material at which and below which, according to the current knowledge and assessment by the HBM-Commission, there is no risk of adverse health effects) (Schulz et al., 2007)	5 µg/L	*1.25 µg/g*	*8.5 µg/L*	7 µg/L
German HBM-2 (concentration of a substance in human biological material at which and above which adverse health effects are possible and, consequently, an acute need for the reduction of exposure and the provision of biomedical advice is given) (Schulz et al., 2007)	15 µg/L	*3.75 µg/g*	*25.5 µg/L*	25 µg/L
The ACGIH (2007) https://www.osha.gov/dts/osta/otm/ otm_ii/pdfs/otmii_chpt2_appb.pdf				Not exceed 35 µg/g creatinine among occupationally exposed
Florida Health Department (2009)	<10 µg/L (background); >50 µg/L (clinical effects)	*<2.5 µg/g;* *>12.5 µg/g*		<40 µg/L (no clinical effects); 40-60 µg/L (medium); 60+ (high)

Table A9.2 Reference values for mercury intake.

	Inorganic Hg, µg/kg bw/wk	MeHg, µg/kg bw/wk
European Food Safety Authority (ESFA CONTAM Panel, 2012)	4	1.3
Joint FAO/WHO Expert Committee on Food Additives (JECFA, 2011)	4[a]	
Joint FAO/WHO Expert Committee on Food Additives (JECFA, 2007b)		1.6[a]
US EPA Reference Dose (adopted 2001) (US EPA, 2001)		0.7
Canada (adopted 1997) (Health Canada, 2007)		1.4
Japan (adopted 2005) (WHO/UNEP, 2008)		2.0
Netherlands (adopted 2000) (WHO/UNEP, 2008)		0.7

[a]Provisional tolerable weekly intake value.

Table A9.3. Color scale related to mercury biomarker values. Adapted from Višnjevec Miklavčič et al. (2014) with minor modifications.

	Assigned color	Hair, µg/g	Blood, µg/L	Cord blood, µg/L	Urine, µg/L
Background levels (non-seafood consumers)		<0.5	<2	<3.4	<1
Background levels (seafood consumers)		0.5–2	2–8	3.4–13.6	1–3
Elevated levels		2–5	8–20	13.6–34	3–10
Moderately High levels		5–10	20–40	34–68	10–50
High levels		>10	>40	>68	>50

Table A9.4. Summary of birth cohort studies that were reviewed. Color codes are based on the work by Višnjevec Miklavčič et al. (2014) with minor modifications as detailed in Table A9.3. The value in the colored cells represents the median blood Hg measurement.

Cohort-ID	Cohort Name	n	Yr	Pregnancy	Birth	Infant (0–1)	Toddler (1–3)	Child (3–11)	Adolescence (12–17)	Adult (18+)	Health outcome found in relation to Hg exposure	Key reference
H	POUCH (Michigan)	1024	1998	0.92							Yes	Xue et al., 2007
N	Poland	313	2002	0.83	1.09						Yes	Jedrychowski et al., 2006
E	MIREC	1673	2008	2.24	0.80						Yes	Arbuckle et al., 2016
D	VIVA	135	2002	1.80							Yes	Oken et al., 2005
T	Massachusetts	421	1993	1.80							Yes	Sagiv et al., 2012
F	ALSPAC	4131	1991	1.86								Golding et al., 2013
U	Shanghai	1652	2008		1.88						Yes	Yu et al., 2011
O	Oswego	212		2.00							Yes	Stewart et al., 2003
K	EDEN	665	2003	2.08								Drouillet-Pinard et al., 2010
I	World Trade Center	280	2001	1.60	4.44						Yes	Lederman et al., 2008
S	Italy	128	2001	3.20				2.16			Yes	Deroma et al., 2013
B	ELEMENT	348	1994	2.80	4.10			1.37				Basu et al., 2014b
J	MOCEH (Korea)	797	2006	3.10	5.20						Yes	Kim et al., 2011
V	PELAGIE	349	2002		4.24							Chevrier et al., 2013
A5	Faroe Islands	500	2008		4.60							AMAP 2015
Q1	PHIME-Italy	573		4.00	5.60							Llop et al., 2017
M	Zhoushan	406	2004	4.98	5.58							Gao et al., 2007
Q2	PHIME-Greece	281		5.60	7.50							Llop et al., 2017
R	Hong Kong	1057	2000	4.92	8.80			2.62			Yes	Fok et al., 2007
L	Tohoku	498	2001	7.80							Yes	Suzuki et al., 2010
P	INMA	1883	2004		8.20							Ramon et al., 2011
C3	Seychelles		2008	11.68								Strain et al., 2015
A3	Faroe Islands	475	1999		12.40			2.60			Yes	AMAP 2015
G	Nunavik Child Development	130	1994	12.60	15.90			5.90			Yes	Muckle et al., 2001
A2	Faroe Islands	182	1995		21.00			3.20			Yes	AMAP 2015
A1	Faroe Islands	1022	1987		22.30			8.40	4.10	2.53	Yes	AMAP 2015
C1	Seychelles	779	1989	23.60		26.40	19.20	25.20	32.40	27.30		Strain et al., 2015
W4	Madeira R (Tin Mine)	294	2006		30.26						Yes	Marques et al., 2013
C2	Seychelles		2001	22.50	39.30							Davidson et al., 2008
W2	Madeira R (Urban)	676	2006		36.45							Marques et al., 2013
W3	Madeira R (Rural)	67	2006		53.18							Marques et al., 2013
W1	Madeira R (Riverine)	396	2006		82.42							Marques et al., 2013

References

Personal communications

Cox, 2016. R. Cox, International Petroleum Industry Environmental Conservation Association (IPIECA).

Euripidou, 2016/2017. R. Euripidou, 2016-2017, groundWork, South Africa.

Guerrero, 2016/2017. S. Guerrero, Universidad Metropolitana, Caracas, Venezuela.

Hagström, 2016/2017. P. Hagström, Swedish Environmental Protection Agency.

Hoenig, 2016/2017. V. Hoenig, VDZ gGmbH, Germany.

Hylander, 2016/2017. L.D. Hylander, Uppsala University, Sweden.Hylander, 2012. L.D. Hylander, Uppsala University, Sweden.

Maag, 2016/2017. J. Maag, Department of Pollution Prevention, Risk Management and Sustainability, COWI A/S.

Maioli, 2016/2017. O. Maioli, Ministry of Environment, Brasilia, Brazil.

Nelson, 2016/2017. P. Nelson, Macquarie University, New South Wales, Australia.

Seo, 2016/2017. Y.-C. Seo, Yonsei University, Wonju, Republic of Korea.

Solórzano, 2016/2017. G. Solórzano, Ministry of Environment, Mexico.

Suzuki, 2016/2017. N. Suzuki, National Institute for Environmental Studies, Japan.

Telmer and O'Neill, 2017. Telmer, K. and J. O'Neill, Artisanal Gold Council.

Wang, 2016/2017. S. Wang, Tsinghua University, People's Republic of China.

General references

Abeysinghe, K.S., G. Qiu, E. Goodale, C.W. Anderson, K. Bishop, D.C. Evers, M.W. Goodale, H. Hintelmann, S. Liu, C. Mammides and R.C. Quan, 2017. Mercury flow through an Asian rice-based food web. Environmental Pollution, 229:219-228.

Abma, R.A., G. Paterson, A. McLeod and G.D. Haffner, 2015. Cross-basin comparison of mercury bioaccumulation in Lake Huron lake trout emphasizes ecological characteristics. Environmental Toxicology and Chemistry, 34:355-359.

ACGIH, 2007. TLVs and BEIs: Based on the Documentation of the Threshold Limit Values for Chemical Substances and Physical Agents and Biological Exposure Indices. American Conference of Governmental Industrial Hygienists (ACGHI). Signature Publications.

Ackerman, J.T., C.A. Eagles-Smith, J.Y. Takekawa, S.A. Demers, T.L. Adelsbach, J.D. Bluso, A.K. Miles, N. Warnock, T.H. Suchanek and S.E. Schwarzbach, 2007. Mercury concentrations and space use of pre-breeding American avocets and black-necked stilts in San Francisco Bay. Science of the Total Environment, 384:452-466.

Ackerman, J.T., C.A. Eagles-Smith, J.Y. Takekawa, J.D. Bluso and T.L. Adelsbach, 2008. Mercury concentrations in blood and feathers of pre-breeding Forster's terns in relation to space use of San Francisco Bay habitats. Environmental Toxicology and Chemistry, 27:897-908.

Ackerman, J.T., C.A. Eagles-Smith and M.P. Herzog, 2011. Bird mercury concentrations change rapidly as chicks age: toxicological risk is highest at hatching and fledging. Environmental Science and Technology, 45:5418-5425.

Ackerman, J.T., M.P. Herzog and S.E. Schwarzbach, 2013. Methylmercury is the predominant form of mercury in bird eggs: a synthesis. Environmental Science and Technology, 47:2052-2060.

Ackerman, J.T., C.A. Hartman, C.A. Eagles-Smith, M.P. Herzog, J. Davis, G. Ichikawa and A. Bonnema, 2015. Estimating mercury exposure of piscivorous birds and sport fish using prey fish monitoring. Environmental Science and Technology, 49:13596-13604.

Ackerman, J.T., C.A. Eagles-Smith, M.P. Herzog, C.A. Hartman, S.H. Peterson, D.C. Evers, A.K. Jackson, J.E. Elliott, S.S. Vander Pol and C.E. Bryan, 2016. Avian mercury exposure and toxicological risk across western North America: A synthesis. Science of the Total Environment, 568:749-769.

Adams, D.H., 2009. Consistently low mercury concentrations in dolphinfish, *Coryphaena hippurus*, an oceanic pelagic predator. Environmental Research, 109:697-701.

Affum, A.O., S.O. Dede, B.J.B. Nyarko, S.O. Acquaah, E.E. Kwaansa-Ansah, G. Darko, A. Dickson, E.A. Affum and J.R. Fianko, 2016. Influence of small-scale gold mining and toxic element concentrations in Bonsa river, Ghana: a potential risk to water quality and public health. Environmental Earth Sciences, 75:178.

AGC, 2016. Reducing the Use and Release of Mercury by Artisanal and Small-Scale Gold Miners in Nicaragua: Review of the Nicaragua ASGM sector. Artisanal Gold Council (AGC).

Ahn, M.C., S.M. Yi, T.M. Holsen and Y.J. Han, 2011. Mercury wet deposition in rural Korea: concentrations and fluxes. Journal of Environmental Monitoring, 13:2748-2754.

Åkerblom, S. and J. de Jong, 2017. Mercury in fur of Daubenton's bat (*Myotis daubentonii*) in southern Sweden and comparison to ecotoxicological thresholds. Bulletin of Environmental Contamination and Toxicology, 99:561-566.

Åkerblom, S., A. Bignert, M. Meili, L. Sonesten and M. Sundbom, 2014. Half a century of changing mercury levels in Swedish freshwater fish. Ambio, 43 Suppl 1:91-103.

AMAP, 2010. Updating Historical Global Inventories of Anthropogenic Mercury Emissions to Air. By: Wilson, S., J. Munthe, K. Sundseth, K. Kindbom, P. Maxson, J. Pacyna and F. Steenhuisen. AMAP Technical Report No. 3. Arctic Monitoring and Assessment Programme (AMAP), Oslo, Norway.

AMAP, 2011. AMAP Assessment 2011: Mercury in the Arctic. Arctic Monitoring and Assessment Programme (AMAP), Oslo, Norway.

AMAP, 2015. AMAP Assessment 2015: Human Health in the Arctic. Arctic Monitoring and Assessment Programme (AMAP), Oslo.

AMAP, 2016. Influence of Climate Change on Transport, Levels, and Effects of Contaminants in Northern Areas – Part 2. By: P. Carlsson, J.H. Christensen, K. Borgå, R. Kallenborn, K. Aspmo Pfaffhuber, J.Ø. Odland, L.-O. Reiersen, and J.F. Pawlak. Arctic Monitoring and Assessment Programme (AMAP), Oslo, Norway.

AMAP/UNEP, 2008. Technical Background Report to the Global Atmospheric Mercury Assessment. Arctic Monitoring and Assessment Programme, Oslo, Norway / UNEP Chemicals Branch, Geneva, Switzerland.

AMAP/UNEP, 2013. Technical Background Report for the Global Mercury Assessment 2013. Arctic Monitoring and Assessment Programme, Oslo, Norway / UNEP Chemicals Branch, Geneva, Switzerland.

AMAP/UNEP, 2015. Global Mercury Modelling: Update of Modelling Results in the Global Mercury Assessment 2013. Arctic Monitoring and Assessment Programme, Oslo, Norway/UNEP Chemicals Branch, Geneva, Switzerland.

Ambrose, J.L., S.N. Lyman, J. Huang, M.S. Gustin and D.A. Jaffe, 2013. Fast time resolution oxidized mercury measurements during the Reno Atmospheric Mercury Intercomparison Experiment (RAMIX). Environmental Science and Technology, 47:7285-7294.

Ambrose, J.L., L.E. Gratz, D.A. Jaffe, T. Campos, F.M. Flocke, D.J. Knapp, D.M. Stechman, M. Stell, A.J. Weinheimer, C.A. Cantrell and R.L. Mauldin, 2015. Mercury emission ratios from coal-fired power plants in the southeastern United States during NOMADSS. Environmental Science and Technology, 49:10389-10397.

Amos, H.M., D.J. Jacob, C.D. Holmes, J.A. Fisher, Q. Wang, R.M. Yantosca, E.S. Corbitt, E. Galarneau, A.P. Rutter, M.S. Gustin, A. Steffen, J.J. Schauer, J.A. Graydon, V.L. Louis, St., R.W. Talbot, E.S. Edgerton, Y. Zhang and E.M. Sunderland, 2012. Gas-particle partitioning of atmospheric Hg(II) and its effect on global mercury deposition. Atmospheric Chemistry and Physics, 12:591-603.

Amos, H.M., D.J. Jacob, D.G. Streets and E.M. Sunderland, 2013. Legacy impacts of all-time anthropogenic emissions on the global mercury cycle. Global Biogeochemical Cycles, 27:410-421.

Amos, H.M., D.J. Jacob, D. Kocman, H.M. Horowitz, Y. Zhang, S. Dutkiewicz, M. Horvat, E.S. Corbitt, D.P. Krabbenhoft and E.M. Sunderland, 2014. Global biogeochemical implications of mercury discharges from rivers and sediment burial. Environmental Science and Technology, 48:9514-9522.

Amos, H.M., J.E. Sonke, D. Obrist, N. Robins, N. Hagan, H.M. Horowitz, R.P. Mason, M. Witt, I.M. Hedgecock, E.S. Corbitt and E.M. Sunderland, 2015. Observational and modelling constraints on global anthropogenic enrichment of mercury. Environmental Science and Technology, 49:4036-4047.

Anderson, D.W., T.H. Suchanek, C.A. Eagles-Smith and T.M. Cahill, 2008. Mercury residues and productivity in osprey and grebes from a mine-dominated ecosystem. Ecological Applications, 18:A227-A238.

Anderson, O.R.J., R.A. Phillips, R.F. Shore, R.A.R. McGill, R.A. McDonald and S. Bearhop, 2010. Element patterns in albatrosses and petrels: influence of trophic position, foraging range, and prey type. Environmental Pollution, 158:98-107.

Andersson, M., J. Sommar, K. Gårdfeldt and O. Lindqvist, 2008. Enhanced concentrations of dissolved gaseous mercury in the surface waters of the Arctic Ocean. Marine Chemistry, 110:190-194.

Anglen, J., S.E. Gruninger, H.N. Chou, J. Weuve, M.E. Turyk, S. Freels and L.T. Stayner, 2015. Occupational mercury exposure in association with prevalence of multiple sclerosis and tremor among US dentists. Journal of the American Dental Association, 146:659-668.

Angot, H., M. Barret, O. Magand, M. Ramonet and A. Dommergue, 2014. A 2-year record of atmospheric mercury species at a background Southern Hemisphere station on Amsterdam Island. Atmospheric Chemistry and Physics, 14:11461-11473.

Angot, H., A. Dastoor, F. De Simone, K. Gårdfeldt, C.N. Gencarelli, I.M. Hedgecock, S. Langer, O. Magand, M.N. Mastromonaco, C. Nordstrøm, K.A. Pfaffhuber, N. Pirrone, A. Ryjkov, N.E. Selin, H. Skov, S. Song, F. Sprovieri, A. Steffen, K. Toyota, O. Travnikov, X. Yang and A. Dommergue, 2016a. Chemical cycling and deposition of atmospheric mercury in polar regions: review of recent measurements and comparison with models. Atmospheric Chemistry and Physics, 16:10735-10763.

Angot, H., I. Dion, N. Vogel, M. Legrand, O. Magand and A. Dommergue, 2016b. Multi-year record of atmospheric mercury at Dumont d'Urville, East Antarctic coast: continental outflow and oceanic influences. Atmospheric Chemistry and Physics, 16:8265-8279.

Angot, H., O. Magand, D. Helmig, P. Ricaud, B. Quennehen, H. Gallée, M. Del Guasta, F. Sprovieri, N. Pirrone, J. Savarino and A. Dommergue, 2016c. New insights into the atmospheric mercury cycling in central Antarctica and implications on a continental scale. Atmospheric Chemistry and Physics, 16:8249-8264.

Anthony, R.G., A.K. Miles, M.A. Ricca and J.A. Estes, 2007. Environmental contaminants in bald eagle eggs from the Aleutian archipelago. Environmental Toxicology and Chemistry, 26:1843-1855.

Arbuckle, T.E., C.L. Liang, A.S. Morisset, M. Fisher, H. Weiler, C.M. Cirtiu, M. Legrand, K. Davis, A.S. Ettinger, W.D. Fraser and MIREC Study Group, 2016. Maternal and fetal exposure to cadmium, lead, manganese and mercury: The MIREC study. Chemosphere, 163:270-282.

Arcagni, M., R. Juncos, A. Rizzo, M. Pavlin, V. Fajon, M.A. Arribére, M. Horvat and S.R. Guevara, 2018. Species- and habitat-specific bioaccumulation of total mercury and methylmercury in the food web of a deep oligotrophic lake. Science of the Total Environment, 612:1311-1319.

Ariya, P.A., A.P. Dastoor, M. Amyot, W.H. Schroeder, L. Barrie, K. Anlauf, F. Raofie, A. Ryzhkov, D. Davignon, J. Lalonde and A. Steffen, 2004. The Arctic: a sink for mercury. Tellus B. 56. 10.3402/tellusb.v56i5.16458.

Ariya, P.A., M. Amyot, A. Dastoor, D. Deeds, A. Feinberg, G. Kos, A. Poulain, A. Ryjkov, K. Semeniuk, M. Subir and K. Toyota, 2015. Mercury physicochemical and biogeochemical transformation in the atmosphere and at atmospheric interfaces: A review and future directions. Chemical Reviews, 115:3760-3802.

Aspmo, K., C. Temme, T. Berg, C. Ferrari, P.-A. Gauchard, X. Fain and G. Wibetoe, 2004. Mercury in the atmosphere, snow and melt water ponds in the North Atlantic Ocean during Arctic summer. Environmental Science and Technology, 40:4083-4089.

ATSDR, 1999. Toxicological Profile for Mercury. Agency for Toxic Substances and Disease Registry (ATSDR).

Aubail, A., R. Dietz, F. Rigét, C. Sonne, Ø. Wiig and F. Caurant, 2012. Temporal trend of mercury in polar bears (Ursus maritimus) from Svalbard using teeth as a biomonitoring tissue. Journal of Environmental Monitoring, 14:56-63.

Aubail, A., P. Méndez-Fernandez, P. Bustamante, C. Churlaud, M. Ferreira, J.V. Vingada and F. Caurant, 2013. Use of skin and blubber tissues of small cetaceans to assess the trace element content of internal organs. Marine Pollution Bulletin, 76:158-169.

Auzmendi-Murua, I., Ál. Castillo and J.W. Bozzelli, 2014. Mercury oxidation via chlorine, bromine, and iodine under atmospheric conditions: thermochemistry and kinetics. Journal of Physical Chemistry A, 118:2959-2975.

Baeuml, J., S. Bose-O'Reilly, R. Matteucci Gothe, B. Lettmeier, G. Roider, G. Drasch and U. Siebet, 2011. Human biomonitoring data from mercury exposed miners in six artisanal small-scale gold mining areas in Asia and Africa. Minerals, 1:122-143.

Bagnato, E., G. Tamburello, G. Avard, M. Martinez-Cruz, M. Enrico, X. Fu, M.E. Sprovieri and J. Sionke, 2014. Mercury fluxes from volcanic and geothermal sources: an update. In: Zellmer, G.F., M. Edmonds, S.M. Straub (eds.), The Role of Volatiles in the Genesis, Evolution and Eruption of Arc Magmas. Special Publications, 410. Geological Society, London.

Balcom, P.H., A.T. Schartup, R.P. Mason and C.Y. Chen, 2015. Sources of water column methylmercury across multiple estuaries in the Northeast U.S. Marine Chemistry, 177:721-730.

Balshaw, S., J.W. Edwards, K.E. Ross and B.J. Daughtry, 2008. Mercury distribution in the muscular tissue of farmed southern bluefin tuna (Thunnus maccoyii) is inversely related to the lipid content of tissues. Food Chemistry, 111:616-621.

Barber, R.T. and F.A. Cross, 2015. Mercury bioaccumulation response to recent Hg pollution abatement in an oceanic predatory fish, blue marlin, versus the response in a Coastal predatory species, bluefish, in the western North Atlantic Ocean. In: AGU December 2015 Fall Meeting.

Bargagli, R., 2016. Atmospheric chemistry of mercury in Antarctica and the role of cryptogams to assess deposition patterns in coastal ice-free areas. Chemosphere, 163:202-208.

Barletta, M., A.J. Jaureguizar, C. Baigun, N.F. Fontoura, A.A. Agostinho, V.M.F. Almeida-Val, A.L. Val, R.A. Torres, L.F. Jimenes-Segura, T. Giarrizzo, N.N. Fabre, V.S. Batista, C. Lasso, D.C. Taphorn, M.F. Costa, P.T. Chaves, J.P. Vieira and M.F.M. Correa, 2010. Fish and aquatic conservation in South America: a continental overview with emphasis on neotropical systems. Journal of Fish Biology, 76:2118-2176.

Bartell, S.M., R.A. Ponce, R.N. Sanga and E.M. Faustman, 2000. Human variability in mercury toxicokinetics and steady state biomarker ratios. Environmental Research, 84:127-132.

Bash, J.O. and D.R. Miller, 2007. A note on elevated total gaseous mercury concentrations downwind from an agriculture field during tilling. Science of the Total Environment, 388:379-388.

Bash, J.O. and D.R. Miller, 2008. A relaxed eddy accumulation system for measuring surface fluxes of total gaseous mercury. Journal of Atmospheric and Oceanic Technology, 25:244-257.

Bash, J.O., A.G. Carlton, W.T. Hutzell and O.R. Bullock, Jr., 2014. Regional air quality model application of the aqueous-phase photo reduction of atmospheric oxidized mercury by dicarboxylic acids. Atmosphere, 5:1-15.

Bastos, W.R., J.P.O. Gomes, R.C. Oliveira, R. Almeida, E.L. Nascimento, J.V.E. Bernardi, L.D. de Lacerda, E.G. da Silveira and W.C. Pfeiffer, 2006. Mercury in the environment and riverside population in the Madeira River basin, Amazon, Brazil. Science of the Total Environment, 368:344-351.

Bastos, W.R., J.G. Dórea, J.V. Bernardi, L.C. Lauthartte, M.H. Mussy, L.D. Lacerda and O. Malm, 2015. Mercury in fish of the Madeira River (temporal and spatial assessment), Brazilian Amazon. Environmental Research, 140:191-197.

Basu, N., J.M. Goodrich and J. Head, 2014a. Ecogenetics of mercury: from genetic polymorphisms and epigenetics to risk assessment and decision-making. Environmental Toxicology and Chemistry, 33:1248-1258.

Basu, N., R. Tutino, Z. Zhang, D.E. Cantonwine, J.M. Goodrich, E.C. Somers, L. Rodriguez, L. Schnaas, M. Solano, A. Mercado, K. Peterson, B.N. Sánchez, M. Hernández-Avila, H. Hu and M. Maria Téllez-Rojo, 2014b. Mercury levels in pregnant women, children, and seafood from Mexico City. Environmental Research, 135:63-69.

Basu, N., E. Clarke, A. Green, B. Calys-Tagoe, L. Chan, M. Dzodzomenyo, J. Fobil, R.N. Long, R.L. Neitzel, S. Obiri, E. Odei, L. Ovadje, R. Quansah,

M. Rajaee and M.L. Wilson, 2015. Integrated assessment of artisanal and small-scale gold mining in Ghana – part 1: human health review. International Journal of Environmental Research and Public Health, 12:5143-5176.

Basu, N., M. Horvat, D. Evers, I. Zastenskaya, P. Weihe, and. J. Tempowski, 2018. A state-of-the-science review of mercury biomarkers in human populations worldwide between 2000 and 2018. Environmental Health Perspectives, 126. 106001. 10.1289/EHP3904.

BAT/BEP, 2017. Guidance on best available techniques and best environmental practices (BAT/BEP) developed under the Minamata Convention, draft; status of February 2017.

Baya, P.A., M. Gosselin, I. Lehnherr, V.L. St Louis and H. Hintelmann, 2015. Determination of monomethylmercury and dimethylmercury in the arctic marine boundary layer. Environmental Science and Technology, 49: 223-232.

Beal, S.A., E.C. Osterberg, C.M. Zdanowicz and D.A. Fisher, 2015. Ice core perspective on mercury pollution during the past 600 years. Environmental Science and Technology, 49:7641-7647.

Beattie, S.A., D. Armstrong, A. Chaulk, J. Comte, M. Gosselin and F. Wang, 2014. Total and methylated mercury in Arctic multiyear sea ice. Environmental Science and Technology, 48:5575-5582.

Bekryaev, R.V., I.V. Polyakov and V.A. Alexeev, 2010. Role of polar amplification in long-term surface air temperature variations and modern arctic warming. Journal of Climate, 23:3888-3906.

Berg, T., J. Bartnicki, J. Munthe, H. Lattila, J. Hrehoruk and A. Mazur, 2001. Atmospheric mercury species in the European Arctic: measurements and modelling. Atmospheric Environment, 35:5377-5378.

Berg, T., J. Sommar, Wängberg, K. Gardfeldt, J. Munthe and B. Schroeder, 2003. Arctic mercury depletion events at two elevations as observed at the Zeppelin Station and Dirigibile Italia, Ny-Ålesund, spring 2002. Journal de Physique IV, 107:151-154.

Berg, T., K.A. Pfaffhuber, A.S. Cole, O. Engelsen and A. Steffen, 2013. Ten-year trends in atmospheric mercury concentrations, meteorological effects and climate variables at Zeppelin, Ny-Alesund. Atmospheric Chemistry and Physics, 13:6575-6586.

Berzas Nevado, J.J., R.C. Rodríguez Martín-Doimeadios, F.J. Guzmán Bernardo, M. Jiménez Moreno, A.M. Herculano, J.L. do Nascimento and M.E. Crespo-López, 2010. Mercury in the Tapajós River basin, Brazilian Amazon: a review. Environment International, 36:593-608.

Bidone, E.D., Z.C. Casilhos, T.M. Cid de Souza and L.D. Lacerda, 1997. Fish contamination and human exposure to mercury in the Tapajoas River Basin, Para State, Amazon, Brazil: a screening approach. Bulletin of Environmental Contamination and Toxicology, 59:194-201.

Bieser, J. and C. Schrum, 2016. Impact of marine mercury cycling on coastal atmospheric mercury concentrations in the North- and Baltic Sea region. Elementa, 111, 10.12952/journal.elementa.000111.

Bieser, J., F. De Simone, C.N. Gencarelli, I.M. Hedgecock, V. Matthias, O. Travnikov and A. Weigelt, 2014. A diagnostic evaluation of modelled mercury wet deposition in Europe using atmospheric speciated high-resolution observations. Environmental Science and Pollution Research, 21:9995-10012.

Bieser, J., F. Slemr, J. Ambrose, C. Brenninkmeijer, S. Brooks, A. Dastoor, F. DeSimone, R. Ebinghaus, C.N. Gencarelli, B. Geyer, L.E. Gratz, I.M. Hedgecock, D. Jaffe, P. Kelley, C.-J. Lin, L. Jaegle, V. Matthias, A. Ryjkov, N.E. Selin, S. Song, O. Travnikov, A. Weigelt, W. Luke, X. Ren, A. Zahn, X. Yang, Y. Zhu and N. Pirrone, 2017. Multi-model study of mercury dispersion in the atmosphere: vertical and interhemispheric distribution of mercury species. Atmospheric Chemistry and Physics, 17:6925-6955.

Biesheuvel, A., Witteveen+Bos, I. Cheng and X. Liu, 2016. Modelling Global Water Demand for Coal Based Power Generation. Methods and Results Report. Greenpeace. http://policy.nl.go.kr/cmmn/FileDown.do?atchFileId=147482&fileSn=26807

Biester, H., R. Bindler, A. Martinez-Cortizas and D.R. Engstrom, 2007. Modeling the past atmospheric deposition of mercury using natural archives. Environmental Science and Technology, 41:4851-4860.

Bignert, A., F. Riget, B. Braune, P. Outridge and S. Wilson, 2004. Recent temporal trend monitoring of mercury in Arctic biota – how powerful are the existing data sets? Journal of Environmental Monitoring, 6:351-355.

Bjermo, H., S. Sand, C. Nälsén, T. Lundh, H. Enghardt Barbieri, M. Pearson, A.K. Lindroos, B.A. Jönsson, L. Barregård and P.O. Darnerud, 2013. Lead, mercury, and cadmium in blood and their relation to diet among Swedish adults. Food and Chemical Toxicology, 57:161-169.

Black, F.J., A. Paytan, K.L. Knee, N.R. De Sieyes, P.M. Ganguli, E. Gary and A.R. Flegal, 2009. Submarine groundwater discharge of total mercury and monomethylmercury to central California coastal waters. Environmental Science and Technology, 43:5652-5659.

Black, F.J., T. Bokhutlo, A. Somoxa, M. Maethamako, O. Modisaemang, T. Kemosedile, C. Cobb-Adams, K. Mosepele and M. Chimbari, 2011. The tropical African mercury anomaly: lower than expected mercury concentrations in fish and human hair. Science of the Total Environment, 409:1967-1975.

Bloom, N.S., 1992. On the chemical form of mercury in edible fish and marine invertebrate tissue. Canadian Journal of Fisheries and Aquatic Sciences, 49:1010-1017.

Blukacz-Richards, E.A., A. Visha, M.L. Graham, D.L. McGoldrick, S.R. de Solla, D.J. Moore and G.B. Arhonditsis, 2017. Mercury levels in herring gulls and fish: 42 years of spatio-temporal trends in the Great Lakes. Chemosphere, 172:476-487.

Blum, J.D. and M.W. Johnson, 2017. Recent developments in mercury stable isotope analysis. Reviews in Mineralogy and Geochemistry, 82:733-757.

Blum, J.D., B.N. Popp, J.C. Drazen, C. Anela Choy and M.W. Johnson, 2013. Methylmercury production below the mixed layer in the North Pacific Ocean. Nature Geoscience, 6:879-884.

Blum, J.D., L.S. Sherman and M.W. Johnson, 2014. Mercury isotopes in earth and environmental sciences. Annual Review of Earth and Planetary Sciences, 42:249-269.

Bodaly, R.A., W.A. Jansen, A.R. Majewski, R.J.P. Fudge, N.E. Strange, A.J. Derksen and D.J. Green, 2007. Postimpoundment time course of increased mercury concentrations in fish in hydroelectric reservoirs of northern Manitoba, Canada. Archives of Environmental Contamination and Toxicology, 53:379-389.

Bodin, N., D. Lesperance, R. Albert, S. Hollanda, P. Michaud, M. Degroote, C. Churlaud and P. Bustamante, 2017. Trace elements in oceanic pelagic communities in the western Indian Ocean. Chemosphere, 174:354-362.

Boischio, A.A.P. and D. Henshel, 2000. Fish consumption, fish lore, and mercury pollution – risk communication for the Madeira River people. Environmental Research, 84A:108-126.

Boliden, 2015. Environmental Report 2015 of the Boliden Facility in Skelleftehamn, Sweden.

Bond, A.L. and A.W. Diamond, 2009. Mercury concentrations in seabird tissues from Machias Seal Island, New Brunswick, Canada. Science of the Total Environment, 407:4340-4347.

Bond, A.L., K.A. Hobson and B.A. Branfireun, 2015. Rapidly increasing methyl mercury in endangered ivory gull (*Pagophila eburnea*) feathers over a 130 year record. Proceedings of the Royal Society of London B, 282:20150032.

Bone, S.E., M.A. Charette, C.H. Lamborg and M.E. Gonneea, 2007. Has submarine groundwater discharge been overlooked as a source of mercury to coastal waters? Environmental Science and Technology, 41:3090-3095.

Bosch, A.C., B. O'Neill, G.O. Sigge, S.E. Kerwath and L.C. Hoffman, 2016a. Mercury accumulation in yellowfin tuna (*Thunnus albacares*) with regards to muscle type, muscle position and fish size. Food Chemistry, 190:351-356.

Bosch, A.C., B. O'Neill, G.O. Sigge, S.E. Kerwath and L.C. Hoffman, 2016b. Heavy metals in marine fish meat and consumer health: A review. Journal of the Science of Food and Agriculture, 96:32-48.

Bowerman, W.W., E.D. Evans, J.P. Giesy and S. Postupalsky, 1994. Using feathers to assess risk of mercury and selenium to bald eagle reproduction in the Great Lakes region. Archives of Environmental Contamination and Toxicology, 27:294-298.

Bowerman, W.W., A.S. Roe, M.J. Gilbertson, D.A. Best, J.G. Sikarskie, R.S. Mitchell and C.L. Summer, 2002. Using bald eagles to indicate the health of the Great Lakes' environment. Lakes & Reservoirs: Research & Management, 7:183-187.

Bowman, K.L., C.R. Hammerschmidt, C.H. Lamborg and G. Swarr, 2015. Mercury in the North Atlantic Ocean: The U.S. GEOTRACES zonal and meridional sections. Deep-Sea Research II, 116:251-261.

Bowman, K.L., C.R. Hammerschmidt, C.H. Lamborg, G.J. Swarr and A.M. Agather, 2016. Distribution of mercury species across a zonal section of the eastern tropical South Pacific Ocean (U.S. GEOTRACES GP16). Marine Chemistry, 186:156-166.

BP, 2017. BP Statistical Review of World Energy June 2017. 48 pp.

Braaten, H.F.V., S. Åkerblom, H.A. de Wit, G. Skotte, M. Rask, J. Vuorenmaa, K.K. Kahilainen, T. Malinen, S. Rognerud, E. Lydersen and P.A. Amundsen, 2017. Spatial and Temporal Trends of Mercury in Freshwater fish in Fennoscandia (1965-2015). NIVA-Report 7179/2017, ICP Waters Report 132/2017.

Branco, V., C. Vale, J. Canário and M.N. dos Santos, 2007. Mercury and selenium in blue shark (*Prionace glauca*, L. 1758) and swordfish (*Xiphias gladius*, L. 1758) from two areas of the Atlantic Ocean. Environmental Pollution, 150:373-380.

Bratkič, A., M. Vahčič, J. Kotnik, K. Obu Vazner, E. Begu, E.M.S. Woodward and M. Horvat, 2016. Mercury presence and speciation in the South Atlantic Ocean along the 40°S transect. Global Biogeochemical Cycles, 30:105-119.

Braune, B.M., 1987. Comparison of total mercury levels in relation to diet and molt for nine species of marine birds. Archives of Environmental Contamination and Toxicology, 16:217-224.

Braune, B.M., 2007. Temporal trends of organochlorines and mercury in seabird eggs from the Canadian Arctic, 1975–2003. Environmental Pollution, 148:599-613.

Braune, B.M., M.L. Mallory and H.G. Gilchrist, 2006. Elevated mercury levels in a declining population of ivory gulls in the Canadian Arctic. Marine Pollution Bulletin, 52:978-982.

Braune, B.M., A.J. Gaston, K.A. Hobson, H.G. Gilchrist and M.L. Mallory, 2014. Changes in food web structure alter trends of mercury uptake at two seabird colonies in the Canadian Arctic. Environmental Science and Technology, 48:13246-13252.

Braune, B., J. Chételat, M. Amyot, T. Brown, M. Clayden, M. Evans, A. Fisk, A. Gaden, C. Girard, A. Hare and J. Kirk, 2015. Mercury in the marine environment of the Canadian Arctic: Review of recent findings. Science of the Total Environment, 509:67-90.

Braune, B.M., A.J. Gaston and M.L. Mallory, 2016. Temporal trends of mercury in eggs of five sympatrically breeding seabird species in the Canadian Arctic. Environmental Pollution, 214:124-131.

Bravi, M. and R. Basosi, 2014. Environmental impact of electricity from selected geothermal power plants in Italy. Journal of Cleaner Production, 66:301-308.

BREF, 2009. Draft Reference Document on Best Available Techniques for the Non-Ferrous Metals Industries. European Commission, Draft (July 2009).

BREF, 2010. Reference Document on Best Available Techniques in the Cement, Lime and Magnesium Oxide Manufacturing Industries. European Commission, May 2010.

BREF, 2012. (Draft) Best Available Techniques (BAT) Reference Document for the Refining of Mineral Oil and Gas. Industrial Emissions Directive 2010/75/EU. (Integrated Pollution Prevention and Control). European Commission, Draft 2 (March 2012).

Brigham, M.E., M.B. Sandheinrich, D.A. Gay, R.P. Maki, D.P. Krabbenhoft and J.G. Wiener, 2014. Lacustrine responses to decreasing wet mercury deposition rates – Results from a case study in Northern Minnesota. Environmental Science and Technology, 48:6115-6123.

Brookens, T.J., T.M. O'Hara, R.J. Taylor, G.R. Bratton and J.T. Harvey, 2008. Total mercury body burden in Pacific harbor seal, *Phoca vitulina richardii*, pups from central California. Marine Pollution Bulletin, 56:27-41.

Brooks, S., A. Saiz-Lopez, H. Skov, S.E. Lindberg, J.M.C. Plane and M.E. Goodsite, 2006. The mass balance of mercury in the springtime arctic environment. Geophysical Research Letters, 33, L13812. doi:10.1029/2005GL025525.

Brooks, S.B., R. Arimoto, S.E. Lindberg and G. Southworth, 2008a. Antarctic polar plateau snow surface conversion of deposited oxidized mercury to gaseous elemental mercury with fractional long-term burial. Atmospheric Environment, 42:2877-2884.

Brooks, S.B., S.E. Lindberg, G. Southworth and R. Arimoto, 2008b. Springtime atmospheric mercury speciation in the McMurdo, Antarctica coastal region. Atmospheric Environment, 42:2885-2893.

Brooks, S., X. Ren, M. Cohen, W.T. Luke, P. Kelley, R. Artz, A. Hynes, W. Landing and B. Martos, 2014. Airborne vertical profiling of mercury speciation near Tullahoma, TN, USA. Atmosphere, 5:557-574.

Brown, R.J.C., M. Burdon, A.S. Brown and K.-H. Kim, 2012. Assessment of pumped mercury vapour adsorption tubes as passive samplers using a micro-exposure chamber. Journal of Environmental Monitoring, 14:2456-2463.

Brown, T.M., A.T. Fisk, X. Wang, S.H. Ferguson, B.G. Young, K.J. Reimer and D.C. Muir, 2016. Mercury and cadmium in ringed seals in the Canadian Arctic: Influence of location and diet. Science of the Total Environment, 545:503-511.

Brumbaugh, W.G., J.D. Petty and T.W. May, 2000. A passive integrative sampler for mercury vapor in air and neutral mercury species in water. Chemosphere: Global Change Science, 2:1-9.

Buck, D.G., D.C. Evers, E. Adams, J. DiGangi, B. Beeler, J. Samanek, J. Petrlik, M.A. Turnquist, O. Speranskaya, K. Reagan and S. Johnson, 2019. A global-scale assessment of fish mercury concentrations and the identification of biological hotspots. Science of the Total Environment, 687:956-966.

Buckman, K.L., M. Marvin-DiPasquale, V.F. Taylor, A. Chalmers, H.J. Broadley, J. Agee, B.P. Jackson and C.Y. Chen, 2015. Influence of a chlor-alkali superfund site on mercury bioaccumulation in periphyton and low-trophic level fauna. Environmental Toxicology and Chemistry, 34:1649-1658.

Buckman, K., V. Taylor, H. Broadley, D. Hocking, P. Balcom, R.P. Mason, K. Nislow and C. Chen, 2017. Methylmercury bioaccumulation in an urban estuary: Delaware River, USA. Estuaries and Coasts, 40:1358-1370.

Budge, G., J. Brough, J. Knight, D. Woodruff and L. McNamara, 2000. Review of the Worldwide Status of Coal Preparation Technology. http://citeseerx.ist. psu.edu/viewdoc/download?doi=10.1.1.557.9262&rep=rep1&type=pdf

Burger, J., 1993. Metals in avian feathers: bioindicators of environmental pollution. Reviews in Environmental Toxicology, 5:203-311.

Burger, J. and M. Gochfeld, 2000. Metal levels in feathers of 12 species of seabirds from Midway Atoll in the northern Pacific Ocean. Science of the Total Environment, 257:37-52.

Burger, J., and M. Gochfeld, 2006. Locational differences in heavy metals and metalloids in Pacific blue mussels *Mytilus* (*edulis*) *trossulus* from Adak Island in the Aleutian Chain, Alaska. Science of the Total Environment, 368:937-950.

Burger, J. and M. Gochfeld, 2009. Comparison of arsenic, cadmium, chromium, lead, manganese, mercury and selenium in feathers in bald eagle (*Haliaeetus leucocephalus*), and comparison with common eider (*Somateria mollissima*), glaucous-winged gull (*Larus glaucescens*), pigeon guillemot (*Cepphus columba*), and tufted puffin (*Fratercula cirrhata*) from the Aleutian Chain of Alaska. Environmental Monitoring and Assessment, 152:357-367.

Burger, J., M. Gochfeld, C. Jeitner, S. Burke, T. Stamm, R. Snigaroff, D. Snigaroff, R. Patrick and J. Weston, 2007. Mercury levels and potential risk from subsistence foods from the Aleutians. Science of the Total Environment, 384:93-105.

Burger, J., M. Gochfeld, C. Jeitner, D. Snigaroff, R. Snigaroff, T. Stamm and C. Volz, 2008. Assessment of metals in down feathers of female common eiders and their eggs from the Aleutians: arsenic, cadmium, chromium, lead, manganese, mercury, and selenium. Environmental Monitoring and Assessment, 143:247-256.

Burger, J., M. Gochfeld, C. Jeitner, S. Burke, C. Volz, R. Snigaroff, D. Snigaroff, T. Shukla and S. Shukla, 2009. Mercury and other metals in eggs and feathers of glaucous-winged gulls (*Larus glaucescens*) in the Aleutians. Environmental Monitoring and Assessment, 152:179-194.

Burger Chakraborty, L., A. Qureshi, C. Vadenbo and S. Hellweg, 2013. Anthropogenic mercury flows in India and impacts of emission controls. Environmental Science and Technology, 47:8105-8113.

Burgess, N.M. and K.A. Hobson, 2006. Bioaccumulation of mercury in yellow perch (*Perca flavescens*) and common loons (*Gavia immer*) in relation to lake chemistry in Atlantic Canada. Hydrobiologia, 567:275-282.

Burgess, N.M. and M.W. Meyer, 2008. Methylmercury exposure associated with reduced productivity in common loons. Ecotoxicology, 17:83-91.

Burgess, N.M., A.L. Bond, C.E. Hebert, E. Neugebauer and L. Champoux, 2013. Mercury trends in herring gull (*Larus argentatus*) eggs from

Atlantic Canada, 1972-2008: temporal change or dietary shift? Environmental Pollution, 172:216-222.

Burm, E., I. Song, M. Ha, Y.M. Kim, K.J. Lee, H.C. Kim, S. Lim, S.Y. Kim, C.G. Lee, S.Y. Kim, H.K. Cheong, J. Sakong, H.T. Kang, M. Son, G.J. Oh, Y. Kim, J.Y. Yang, S.J. Hong, J.H. Seo, J. Kim, S. Oh, J. Yu, S.S. Chang, H.J. Kwon, Y.H. Choi, W. Choi, S. Kim and S.D. Yu, 2016. Representative levels of blood lead, mercury, and urinary cadmium in youth: Korean Environmental Health Survey in Children and Adolescents (KorEHS-C), 2012-2014. International Journal of Hygiene and Environmental Health, 219:412-418.

Bustamante, P., C. Garrigue, L. Breau, F. Caurant, W. Dabin, J. Greaves and R. Dodémont, 2003. Trace elements in two odontocetes species (*Kogia breviceps* and *Globicephala macrorhynchus*) stranded in New Caledonia (South Pacific). Environmental Pollution, 124:263-271.

Bustamante, P., A. Carravieri, A. Goutte, C. Barbraud, K. Delord, O. Chastel, H. Weimerskirch and Y. Cherel, 2016. High feather mercury concentrations in the wandering albatross are related to sex, breeding status and trophic ecology with no demographic consequences. Environmental Research, 144:1-10.

Butler, T.J., M.D. Cohen, F.M. Vermeylen, G.E. Likens, D. Schmeltz and R.S. Artz, 2008. Regional precipitation mercury trends in the eastern USA, 1998–2005: Declines in the Northeast and Midwest, no trend in the Southeast. Atmospheric Environment, 42:1582-1592.

Cai, Y., J.R. Rooker, G.A. Gill and J.P. Turner, 2007. Bioaccumulation of mercury in pelagic fishes from the northern Gulf of Mexico. Canadian Journal of Fisheries and Aquatic Sciences, 64:458-469.

Campbell, L.M., R.J. Norstrom, K.A. Hobson, D.C. Muir, S. Backus and A.T. Fisk, 2005. Mercury and other trace elements in a pelagic Arctic marine food web (Northwater Polynya, Baffin Bay). Science of the Total Environment, 351:247-263.

Carpi, A., A.H. Fostier, O.R. Orta, J.C. dos Santos and M. Gittings, 2014. Gaseous mercury emissions from soil following forest loss and land use changes: Field experiments in the United States and Brazil. Atmospheric Environment, 96:423-429.

Carravieri, A., Y. Cherel, P. Blévin, M. Brault-Favrou, O. Chastel and P. Bustamante, 2014. Mercury exposure in a large subantarctic avian community. Environmental Pollution, 190C:51-57.

Carravieri, A., Y. Cherel, A. Jaeger, C. Churlaud and P. Bustamante, 2016. Penguins as bioindicators of mercury contamination in the southern Indian Ocean: geographical and temporal trends. Environmental Pollution, 213:195-205.

Carravieri, A., Y. Cherel, M. Brault-Favrou, C. Churlaud, L. Peluhet, P. Labadie, H. Budzinski, O. Chastel and P. Bustamante, 2017. From Antarctica to the subtropics: Contrasted geographical concentrations of selenium, mercury, and persistent organic pollutants in skua chicks (*Catharacta* spp.). Environmental Pollution, 228:464-473.

Carvan, M.J., T.A. Kalluvila, R.H. Klingler, J.K. Larson, M. Pickens, F.X. Mora-Zamorano, V.P. Connaughton, I. Sadler-Riggleman, D. Beck and M.K. Skinner, 2017. Mercury-induced epigenetic transgenerational inheritance of abnormal neurobehavior is correlated with sperm epimutations in zebrafish. PloS ONE, 12:e0176155.

Castaño, A., F. Cutanda, M. Esteban, P. Pärt, C. Navarro, S. Gómez, M. Rosado and 53 others, 2015. Fish consumption patterns and hair mercury levels in children and their mothers in 17 EU countries. Environmental Research, 141:58-68.

Castilhos, Z.C., E.D. Bidone and L.D. Lacerda, 1998. Increase of the background human exposure to mercury through fish consumption due to gold mining at the Tapajos River region, Para State, Amazon. Bulletin of Environmental Contamination and Toxicology, 61:202-209.

Castro, M.S. and J. Sherwell, 2015. Effectiveness of emission controls to reduce the atmospheric concentrations of mercury. Environmental Science and Technology, 49:14000-14007.

Cavalieri, D.J. and C.L. Parkinson, 2012. Arctic sea ice variability and trends, 1979-2010. The Cryosphere, 6:881-889.

CEMBUREAU, 2010. Mercury in the Cement Industry. By: Renzoni, R., C. Ullrich, S. Belboom and A. Germain. The European Cement Association (CEMBUREAU).

Cementa, 2015. Environmental Report 2015 of the Cementa facilities in Slite, Dagerhamn, and Skövde, Sweden.

Cerveny, D., S. Roje, J. Turek and T. Randak, 2016. Fish fin-clips as a non-lethal approach for biomonitoring of mercury contamination in aquatic environments and human health risk assessment. Chemosphere, 163:290-295.

Chakraborty, P., R.P. Mason, S. Jayachandran, K. Vudamala, K. Armoury, A. Sarkar, S. Chakraborty, P. Bardhan and R. Naik, 2016. Effects of bottom water oxygen concentrations on mercury distribution and speciation in sediments below the oxygen minimum zone of the Arabian Sea. Marine Chemistry, 186:24-32.

Chan, H.M., C. Kim, K. Khoday, O. Receveur and H.V. Kuhnlein, 1995. Assessment of dietary exposure to trace-metals in Baffin Inuit food. Environmental Health Perspectives, 103:740-746.

Chase, M.E., S.H. Jones, P. Hennigar, J. Sowles, G.C.H. Harding, K. Freeman, P.G. Wells, C. Krahforst, K. Coombs, R. Crawford and J. Pederson, 2001. Gulfwatch: Monitoring spatial and temporal patterns of trace metal and organic contaminants in the Gulf of Maine (1991–1997) with the blue mussel, *Mytilus edulis* L. Marine Pollution Bulletin, 42:490-504.

Chaulk, A., G.A. Stern, D. Armstrong, D. Barber and F. Wang, 2011. Mercury distribution and transport across the ocean-sea-ice-atmosphere interface in the Arctic Ocean. Environmental Science and Technology, 45:1866-1872.

Chaves-Ulloa, R., B.W. Taylor, H.J. Broadley, K.L. Cottingham, N.A. Baer, K.C. Weathers, H.A. Ewing and C.Y. Chen, 2016. Dissolved organic carbon modulates mercury concentrations in insect subsidies from streams to terrestrial consumers. Ecological Applications, 26:1771-1784.

Chellman, N., J.R. McConnell, M. Arienzo, G.T. Pederson, S.M. Aarons and A. Csank, 2017. Reassessment of the Upper Fremont Glacier ice-core chronologies by synchronizing of ice-core-water isotopes to a nearby tree-ring chronology. Environmental Science and Technology, 51:4230-4238.

Chemnasiri, W. And F.E. Hernandez, 2012. Gold nanorod-based mercury sensor using functionalized glass substrates. Sensors and Actuators B Chemical, 173:322-328.

Chen, K., G. Lu, J. Chang, S. Mao, K. Yu, S. Cui and J. Chen, 2012. Hg(II) ion detection using thermally reduced graphene oxide decorated with functionalized gold nanoparticles. Analytical Chemistry, 84:4057-4062.

Chen, L., L. Ming Liu, F. Ruifang Fan, S. Ma, X. Zhencheng, R. Mingzhong and H. Qiusheng, 2013a. Mercury speciation and emission from municipal solid waste incinerators in the Pearl River Delta, South China. Science of the Total Environment, 447:396-402.

Chen, C., H. Wang, W. Zhang, D. Hu, L. Chen and X. Wang, 2013b. High-resolution inventory of mercury emissions from biomass burning in China for 2000–2010 and a projection for 2020. Journal of Geophysical Research: Atmospheres, 118:12,248-12,256.

Chen, L.G., M. Liu, Z.C. Xu, R.F. Fan, J. Tao, D.H. Chen, D.Q. Zhang, D.H. Xie and J.R. Sun, 2013c. Variation trends and influencing factors of total gaseous mercury in the Pearl River Delta – A highly industrialised region in South China influenced by seasonal monsoons. Atmospheric Environment, 77:757-766.

Chen, C.Y., M.E. Borsuk, D.M. Bugge, T. Hollweg, P.H. Balcom, D.M. Ward, J. Williams and R.P. Mason, 2014a. Benthic and pelagic pathways of methylmercury bioaccumulation in estuarine food webs of the northeast United States. PloS ONE, 9:89305.

Chen, L., H.H. Wang, J.F. Liu, Y.D. Tong, L.B. Ou, W. Zhang, D. Hu, C. Chen and X.J. Wang, 2014b. Intercontinental transport and deposition patterns of atmospheric mercury from anthropogenic emissions. Atmospheric Chemistry and Physics, 14:10163-10176.

Chen, H.S., Z.F. Wang, J. Li, X. Tang, B.Z. Ge, X.L. Wu, O. Wild and G.R. Carmichael, 2015a. GNAQPMS-Hg v1.0, a global nested atmospheric mercury transport model: model description, evaluation and application to trans-boundary transport of Chinese anthropogenic emissions. Geoscientific Model Development, 8:2857-2876.

Chen, L., Y. Zhang, D.J. Jacob, A.L. Soerensen, J.A. Fisher, H.M. Horowitz, E.S. Corbitt and X. Wang, 2015b. A decline in Arctic Ocean mercury suggested by differences in decadal trends of atmospheric mercury between the Arctic and northern midlatitudes. Geophysical Research Letters, 42:6076-6083.

Chen, M.M., L. Lopez, S.P. Bhavsar and S. Sharma, 2018. What's hot about mercury? Examining the influence of climate on mercury levels in Ontario top predator fishes. Environmental Research, 162:63-73.

Cheng, I. and H. Lammi, 2016. The Great Water Grab: How the Coal Industry is Deepening the Global Water Crisis. Greenpeace International.

Cheng, I., L. Zhang, P. Blanchard, J. Dalziel and R. Tordon, 2013a. Concentration-weighted trajectory approach to identifying potential sources of speciated atmospheric mercury at an urban coastal site in Nova Scotia, Canada. Atmospheric Chemistry and Physics, 13:6031-6048.

Cheng, I., l. Zhang, P. Blanchard, J. Dalziel, R. Tordon, J. Huang and T.M. Holsen, 2013b. Comparisons of mercury sources and atmospheric mercury processes between a coastal and inland site. Journal of Geophysical Research Atmospheres, 118:2434-2443.

Cheng, I., X. Xu and L. Zhang, 2015. Overview of receptor-based source apportionment studies for speciated atmospheric mercury. Atmospheric Chemistry and Physics, 15:7877-7895.

Cheng, I., L. Zhang and X. Xu, 2016. Impact of measurement uncertainties on receptor modelling of speciated atmospheric mercury. Scientific Reports, 6: 10.1038/srep20676.

Cherel, Y., C. Barbraud, M. Lahournat, A. Jaeger, S. Jaquemet, R.M. Wanless, R.A. Phillips, D.R. Thompson and P. Bustamante, 2018. Accumulate or eliminate? Seasonal mercury dynamics in albatrosses, the most contaminated family of birds. Environmental Pollution, 241:124-135.

Chételat, J. and M. Amyot, 2009. Elevated methylmercury in High Arctic *Daphnia* and the role of productivity in controlling their distribution. Global Change Biology, 15:706-718.

Chételat, J., B. Braune, J. Stow and S. Tomlinson, 2015. Special issue on mercury in Canada's North: Summary and recommendations for future research. Science of the Total Environment, 509:260-262.

Chevrier, C., C. Warembourg, E. Gaudreau, C. Monfort, A. Le Blanc, L. Guldner and S. Cordier, 2013. Organochlorine pesticides, polychlorinated biphenyls, seafood consumption, and time-to-pregnancy. Epidemiology, 24:251-260.

Choi, H.D. and T.M. Holsen, 2009. Gaseous mercury emissions from unsterilized and sterilized soils: The effect of temperature and UV radiation. Environmental Pollution, 157:1673-1678.

Choi, E.M., S.H. Kim, T.M. Holsen and S.M. Yi, 2009. Total gaseous concentrations in mercury in Seoul, Korea: Local sources compared to long-range transport from China and Japan. Environmental Pollution, 157:816-822.

Choi, H.-D., J. Huang, S. Mondal and T.M. Holsen, 2013. Variation in concentrations of three mercury (Hg) forms at a rural and a suburban site in New York State. Science of the Total Environment, 448:96-106.

Choi, W., S. Kim, Y.-W. Baek, K. Choi, K. Lee, S. Kim, S.D. Yu and K. Choi, 2017. Exposure to environmental chemicals among Korean adults – updates from the second Korean National Environmental Health Survey (20012–2014). International Journal of Hygiene and Environmental Health, 220:29-35.

Chouvelon, T., C. Brach-Papa, D. Auger, N. Bodin, S. Bruzac, S. Crochet, M. Degroote et al. 2017. Chemical contaminants (trace metals, persistent organic pollutants) in albacore tuna from western Indian and south-eastern Atlantic Oceans: Trophic influence and potential as tracers of populations. Science of the Total Environment, 596:481-495.

Ci, Z.J., X.S. Zhang, Z.W. Wang and Z.C. Niu, 2011. Atmospheric gaseous elemental mercury (GEM) over a coastal/rural site downwind of East China: Temporal variation and long-range transport. Atmospheric Environment, 45:2480-2487.

CIA, 2016, 2017. The World Factbook. Country comparison: Population. Central Intelligence Agency www.cia.gov/library/publications/the-world-factbook/rankorder/2119rank.html. Country comparison: GDP – per capita (PPP). www.cia.gov/library/publications/the-world-factbook/rankorder/2004rank.html. Accessed 2016-08-23, updated 2017-12-04.

Cisneros-Montemayor, A.M., D. Pauly, L.V. Weatherdon and Y. Ota, 2016. A global estimate of seafood consumption by coastal Indigenous Peoples. PLoS One, 11(12):e0166681.

Cizdziel, J.V., T.A. Hinners and E.M. Heithmar, 2002. Determination of total mercury in fish tissues using combustion atomic absorption spectrometry with gold amalgamation. Water, Air and Soil Pollution, 135:355-370.

Clarkson, T.W. and L. Magos, 2006. The toxicology of mercury and its chemical compounds. Critical Reviews in Toxicology, 36:609-662.

Clayden, M.G., K.A. Kidd, B. Wyn, J.L. Kirk, D.C.G. Muir and N.J. O'Driscoll, 2013. Mercury biomagnification through food webs is affected by physical and chemical characteristics of lakes. Environmental Science and Technology, 47:12047-12063.

Coburn, S., B. Dix, E. Edgerton, C.D Holmes, D. Kinnison, Q. Liang, A. Ter Schure, S. Wang and R. Volkamer, 2016. Mercury oxidation from bromine chemistry in the free troposphere over the southeastern US. Atmospheric Chemistry and Physics, 16:3743-3760.

Cohen, M.D., R.R. Draxler, R.S. Artz, P. Blanchard, M.S. Gustin, Y.-J. Han, T.M. Holsen, D.A. Jaffe, P. Kelley, H. Lei, C.P. Loughner, W.T. Luke, S.N. Lyman, D. Niemi, J.M. Pacyna, M. Pilote, L. Poissant, D. Ratte, X. Ren, F. Steenhuisen, A. Steffen, R. Tordon and S.J. Wilson, 2016. Modeling the global atmospheric transport and deposition of mercury to the Great Lakes. Elementa, 4:118 doi:10.12952/journal.elementa.000118.

Cole, A.S. and A. Steffen, 2010. Trends in long-term gaseous mercury observations in the Arctic and effects of temperature and other atmospheric conditions. Atmospheric Chemistry and Physics, 10:4661-4672.

Cole, A.S., A. Steffen, K. Aspmo Pfaffhuber, T. Berg, M. Pilote, L. Poissant, R. Tordon and H. Hung, 2013. Ten-year trends of atmospheric mercury in the high Arctic compared to Canadian sub-Arctic and mid-latitude sites. Atmospheric Chemistry and Physics, 13:1535-1545.

Cole, A.S., A. Steffen, C.S. Eckley, J. Narayan, M. Pilote, R. Tordon, J.A. Graydon, V.L. St Louis, X. Xu, and B. Branfireun, 2014. A survey of mercury in air and precipitation across Canada: patterns and trends. Atmosphere, 5:635-668.

Colette, A., W. Aas, L. Banin, C.F. Braban, M. Ferm, A. González Ortiz, I. Ilyin, K. Mar, M. Pandolfi, J.-P. Putaud, V. Shatalov, S. Solberg, G. Spindler, O. Tarasova, M. Vana, M. Adani, P. Almodovar, E. Berton, B. Bessagnet, P. Bohlin-Nizzetto, J. Boruvkova, K. Breivik, G. Briganti, A. Cappelletti, K. Cuvelier, R. Derwent, M. D'Isidoro, H. Fagerli, C. Funk, M. Garcia Vivanco, A. González Ortiz, R. Haeuber, C. Hueglin, S. Jenkins, J. Kerr, F. de Leeuw, J. Lynch, A. Manders, M. Mircea, M.T. Pay, D. Pritula, J.-P. Putaud, X. Querol, V. Raffort, I. Reiss, Y. Roustan, S. Sauvage, K. Scavo, D. Simpson, R.I. Smith, Y.S. Tang, M. Theobald, K. Tørseth, S. Tsyro, A. van Pul, S. Vidic, M. Wallasch and P. Wind, 2016. Air pollution trends in the EMEP region between 1990 and 2012. Joint Report of the EMEP Task Force on Measurements and Modelling (TFMM), Chemical Co-ordinating Centre (CCC), Meteorological Synthesizing Centre-East (MSC-E), Meteorological Synthesizing Centre-West (MSC-W). EMEP/CCC, 01/2016.

Conaway, C.H., F.J. Black, M. Gault-Ringold, J.T. Pennington, F.P. Chavez and A.R. Flegal, 2009. Dimethylmercury in coastal upwelling waters, Monterey Bay, California. Environmental Science and Technology, 43:1305-1309.

Condon, A.M. and D.A. Cristol, 2009. Feather growth influences blood mercury level of young songbirds. Environmental Toxicology and Chemistry, 28:395-401.

Converse, A.D., A.L. Riscassi and T.M. Scanlon, 2010. Seasonal variability in gaseous mercury fluxes measured in a high-elevation meadow. Atmospheric Environment, 44:2176-2185.

Cooke, C.A., H. Hintelmann, J.J. Ague, R. Burger, H. Biester, J.P. Sachs and D.R. Engstrom, 2013. Use and legacy of mercury in the Andes. Environmental Science and Technology, 47:4181-4188.

Copan, L., J. Fowles, T. Barreau and N. McGee, 2015. Mercury toxicity and contamination of households from the use of skin creams adulterated with mercurous chloride (calomel). International Journal of Environmental Research and Public Health, 12:10943-10954.

Corbitt, E.S., D.J. Jacob, C.D. Holmes, D.G. Streets and E.M. Sunderland, 2011. Global source-receptor relationships for mercury deposition under present-day and 2050 emissions scenarios. Environmental Science and Technology, 45:10477-10484.

Cordy, P., M.M. Veiga, I. Salih, S. Al-Saadi, S. Console, O. Garcia and M. Roeser, 2011. Mercury contamination from artisanal gold mining in Antioquia, Colombia: The world's highest per capita mercury pollution. Science of the Total Environment, 410-411:154-160.

Correa, L., J.M. Castellini, R.S. Wells and T. O'Hara, 2013. Distribution of mercury and selenium in blood compartments of bottlenose dolphins (*Tursiops truncatus*) from Sarasota Bay, Florida. Environmental Toxicology and Chemistry, 32:2441-2448.

Correia, R.R.S. and J.R.D. Guimarães, 2017. Mercury methylation and sulfate reduction rates in mangrove sediments, Rio de Janeiro, Brazil: The role of different microorganism consortia. Chemosphere, 167:438-443.

Correla, J.P., B.L. Valero-Garces, F. Wang, A. Martínez-Cortizas, C.A. Cuevas and A. Saiz-Lopez, 2017. 700 years reconstruction of mercury and lead atmospheric deposition in the Pyrenees (NE Spain). Atmospheric Environment, 155:97-107.

Cossa, D., B. Averty and N. Pirrone, 2009. The origin of methylmercury in open Mediterranean waters. Limnology and Oceanography, 54:837-844.

Cossa, D., L.E. Heimbürger, D. Lannuzel, S.R. Rintoul, E.C.V. Butler, A.R. Bowie, B. Averty, R.J. Watson and T. Remenyi, 2011. Mercury in the Southern Ocean. Geochimica Et Cosmochimica Acta, 75:4037-4052.

Cossa, D., M. Harmelin-Vivien, C. Mellon-Duval, V. Loizeau, B. Averty, S. Crochet, L. Chou and J.F. Cadiou, 2012. Influences of bioavailability, trophic position, and growth on methylmercury in hakes (*Merluccius merluccius*) from Northwestern Mediterranean and Northeastern Atlantic. Environmental Science and Technology, 46:4885-4893.

Cossa, D., X. Durrieu de Madron, J. Schäfer, S. Guédron, N. Maruszak, S. Castelle and J.-J. Naudin, 2018. Sources and exchanges of mercury in the waters of the Northwestern Mediterranean margin. Progress in Oceanography, 163:172-183.

Costa, M., W. Landing, H. Kehrig, M. Barletta, C. Holmes, P. Barrocas, D.C. Evers, D. Buck, A. Vasconcellos, S. Hacon, J. Moreia, and O. Malm, 2012. Mercury in tropical and sub-tropical coastal environments. Environmental Research, 119:88-100.

Cristol, D.A., R.L. Brasso, A.M. Condon, R.E. Fovargue, S.L. Friedman, K.K. Hallinger, A.P. Monroe and A.E. White, 2008. The movement of aquatic mercury through terrestrial food webs. Science, 320:335-335.

Croes, K., S. De Coster, S. De Galan, B. Morrens, I. Loots, E. Van de Mieroop, V. Nelen, I. Sioen, L. Bruckers, T. Nawrot, A. Colles, E. Den Hond, G. Schoeters, N. van Larebeke, W. Baeyens and Y. Gao, 2014. Health effects in the Flemish population in relation to low levels of mercury exposure: from organ to transcriptome level. International Journal of Hygiene and Environmental Health, 217:239-247.

Cross, F.A., D.W. Evans and R.T. Barber, 2015. Decadal declines of mercury in adult bluefish (1972–2011) from the Mid-Atlantic Coast of the U.S.A. Environmental Science and Technology, 49:9064-9072.

CSGB, 2017. Cremation Society of Great Britain, https://www.cremation.org.uk/statistics. Accessed May 2017.

CSI, 2005. Guidelines for the Selection and Use of Fuels and Raw Materials in the Cement Manufacturing Process. Cement Sustainability Initiative (CSI).

Dam, M. and D. Bloch, 2000. Screening of mercury and persistent organochlorine pollutants in long-finned pilot whale (*Globicephala melas*) in the Faroe Islands. Marine Pollution Bulletin, 40:1090-1099.

Darbha, G.K., A. Ray and P.C. Ray, 2007. Gold nanoparticle-based miniaturized nanomaterial surface energy transfer probe for rapid and ultrasensitive detection of mercury in soil, water, and fish. ACS Nano, 1:208-214.

Daso, A.P., J.O. Okonkwo, R. Jansen, J.D. Brandao and A. Kotzé, 2015. Mercury concentrations in eggshells of the southern ground-hornbill (*Bucorvus leadbeateri*) and wattled crane (*Bugeranus carunculatus*) in South Africa. Ecotoxicology and Environmental Safety, 114:61-66.

Dastoor, A.P. and D.A. Durnford, 2014. Arctic ocean: is it a sink or a source of atmospheric mercury? Environmental Science and Technology, 48:1707-1717.

Dastoor, A.P. and Y. Larocque, 2004. Global circulation of atmospheric mercury: A modelling study. Atmospheric Environment, 38:147-161.

Dastoor, A.P., D. Davignon, N. Theys, M. Van Roozendael, A. Steffen and P.A. Ariya, 2008. Modelling dynamic exchange of gaseous elemental mercury at polar sunrise. Environmental Science and Technology, 42:5183-5188.

Dastoor, A., A. Ryzhkov, D. Durnford, I. Lehnherr, A. Steffen and H. Morrison, 2015. Atmospheric mercury in the Canadian Arctic. Part II: Insight from modelling. Science of the Total Environment, 509-510:16-27.

Davidson, P.W., J.J. Strain, G.J. Myers, S.W. Thurston, M.P. Bonham, C.F. Shamlaye, A. Stokes-Riner, J.M. Wallace, P.J. Robson, E.M. Duffy, L.A. Georger, J. Sloane-Reeves, E. Cernichiari, R.L. Canfield, C. Cox, L.S. Huang, J. Janciuras and T.W. Clarkson, 2008. Neurodevelopmental effects of maternal nutritional status and exposure to methylmercury from eating fish during pregnancy. Neurotoxicology, 29:767-775.

Day, R.D., S.J. Christopher, P.R. Becker and D.W. Whitaker, 2005. Monitoring mercury in the loggerhead sea turtle, *Caretta caretta*. Environmental Science and Technology, 39:437-446.

Day, R.D., P.R. Becker, O.F. Donard, R.S. Pugh and S.A. Wise, 2014. Environmental specimen banks as a resource for mercury and mercury isotope research in marine ecosystems. Environmental Science: Processes and Impacts, 16:10-27.

de Carvalho, G.G.A., I.A.M. Degaspari, V. Branco, J. Canário, A.F. de Amorim, V.H. Kennedy and J.R. Ferreira, 2014. Assessment of total and organic mercury levels in blue sharks (*Prionace glauca*) from the south and southeastern Brazilian coast. Biological Trace Element Research, 159:128-134.

de Foy, B., Y. Tong, X. Yin, W. Zhang, S. Kang, Q. Zhang, G. Zhang, X. Wang and J.J. Schauer, 2016. First field-based atmospheric observation of the reduction of reactive mercury driven by sunlight. Atmospheric Environment, 134:27-39.

de Pinho, A.P., J.R.D. Guimarães, A.S. Martins, P.A.S. Costa, G. Olavo and J. Valentin, 2010. Total mercury in muscle tissue of five shark species from Brazilian offshore waters: effects of feeding habit, sex, and length. Environmental Research, 89:250-258.

De Simone, F., C.N. Gencarelli, I.M. Hedgecock and N. Pirrone, 2014. Global atmospheric cycle of mercury: a model study on the impact of oxidation mechanisms. Environmental Science and Pollution Research, 21:4110-4123.

De Simone, F., S. Cinnirella, C.N. Gencarelli, X. Yang, I.M. Hedgecock and N. Pirrone, 2015. Model study of global mercury deposition from biomass burning. Environmental Science and Technology, 49:6712-6721.

De Simone, F., C.N. Gencarelli, I.M. Hedgecock and N. Pirrone, 2016. A modelling comparison of mercury deposition from current anthropogenic mercury emission inventories. Environmental Science and Technology, 50:5154-5162.

De Simone, F., P. Artaxo, M. Bencardino, S. Cinnirella, F. Carbone, F. D'Amore, A. Dommergue, X.B. Feng, C.N. Gencarelli, I.M. Hedgecock, M.S. Landis, F. Sprovieri, N. Suzuki, I. Wängberg and N. Pirrone, 2017. Particulate-phase mercury emissions from biomass burning and impact on resulting deposition: a modelling assessment. Atmospheric Chemistry and Physics, 17:1881-1899.

Deeds, D.A., R.F. Ghoshdastidar, E.A. Guerette, A. Tessier and P.A. Ariya, 2015. Development of a particle-trap preconcentration-soft ionization mass spectrometric technique for the quantification of mercury halides in air. Analytical Chemistry, 87:5109-5116.

Demers, J.D., J.D. Blum and D.R. Zak, 2013. Mercury isotopes in a forested ecosystem: Implications for air-surface exchange dynamics and the global mercury cycle. Global Biogeochemical Cycles, 27:222-238.

Demers, J.D., L.S. Sherman, J.D. Blum, F.J. Marsik and J.T. Dvonch, 2015. Coupling atmospheric mercury isotope ratios and meteorology to identify sources of mercury impacting a coastal urban-industrial region near Pensacola, Florida, USA. Global Biogeochemical Cycles, 29:1689-1705.

Denkenberger, J.S., C.T. Driscoll, B.A. Branfireun, C.S. Eckley, M. Cohen and P. Selvendiran, 2012. A synthesis of rates and controls on elemental mercury evasion in the Great Lakes Basin. Environmental Pollution, 161:291-298.

Depew, D.C., N. Basu, N.M. Burgess, L.M. Campbell, E.W. Devlin, P.E. Drevnick, C.R. Hammerschmidt, C.A. Murphy, M.B. Sandheinrich and J.G. Wiener, 2012a. Toxicity of dietary methylmercury to fish: derivation of ecologically meaningful threshold concentrations. Environmental Toxicology and Chemistry, 31:1536-1547.

Depew, D.C., N. Basu, N.M. Burgess, L.M. Campbell, D.C. Evers, K.A. Grasman and A.M. Scheuhammer, 2012b. Derivation of screening benchmarks for dietary methylmercury exposure for the common loon (*Gavia immer*): rationale for use in ecological risk assessment. Environmental Toxicology and Chemistry, 31:2399-2407.

Dereumeaux, C., A. Saoudi, M. Pecheux, B. Berat, P. de Crouy-Chanel, C. Zaros, S. Brunel, C. Delamaire, A. Tertre, A. Lefranc, S. Vandentorren and L. Guldner, 2016. Biomarkers of exposure to environmental contaminants in French pregnant women from the Elfe cohort in 2011. Environment International, 97:56-67.

Deroma, L, M. Parpinel, V. Tognin, L. Channoufi, J. Tratnik, M. Horvat, F. Valent and F. Barbone, 2013. Neuropsychological assessment at school-age and prenatal low-level exposure to mercury through fish consumption in an Italian birth cohort living near a contaminated site. International Journal of Hygiene and Environmental Health, 216:486-493.

Desforges, J.P.W., C. Sonne, M. Levin, U. Siebert, S. De Guise and R. Dietz, 2016. Immunotoxic effects of environmental pollutants in marine mammals. Environment International, 86:126-139.

DesGranges, J.L., J. Rodrigue, B. Tardif and M. Laperle, 1998. Mercury accumulation and biomagnification in ospreys (*Pandion haliaetus*) in the James Bay and Hudson Bay regions of Quebec. Archives of Environmental Contamination and Toxicology, 35:330-341.

DeSorbo, C.R., N.M. Burgess, C.S. Todd, D.C. Evers, R.A. Bodaly, B.H. Massey, S.E. Mierzykowski, C.P. Persico, R.B. Gray, W.E. Hanson, D.E. Meattey and K.J. Regan, 2018. Mercury concentrations in bald eagles across an impacted watershed in Maine, USA. Science of the Total Environment, 627:1515-1527.

Dibble, T.S. and A.C. Schwid, 2016. Thermodynamics limits the reactivity of BrHg• radical with volatile organic compounds. Chemical Physics Letters, 659:289-294.

Dibble, T.S., M.J. Zelie and H. Mao, 2012. Thermodynamics of reactions of ClHg and BrHg radicals with atmospherically abundant free radicals. Atmospheric Chemistry and Physics, 12:10271-10279.

Dibble, T.S., M.J. Zelie and H. Mao, 2013. Corrigendum to "Thermodynamics of reactions of ClHg and BrHg radicals with atmospherically abundant free radicals" published in Atmospheric Chemistry and Physics, 12:10271-10279, 2012. Atmospheric Chemistry and Physics, 13:9211-9212.

Dibble, T.S., M.J. Zelie and Y. Jiao, 2014. Quantum chemistry guide to PTRMS studies of as yet undetected products of the bromine atom initiated oxidation of gaseous elemental mercury. Journal of Physical Chemistry A, 118:7847-7854.

Dietz, R., F. Riget, E.W. Born, C. Sonne, P. Grandjean, M. Kirkegaard, M.T. Olsen, G. Asmund, A. Renzoni, H. Baagoe and C. Andreasen, 2006. Trends in mercury in hair of Greenlandic polar bears (*Ursus maritimus*) during 1892–2001. Environmental Science and Technology, 40:1120-1125.

Dietz, R., P.M. Outridge K.A. and Hobson, 2009. Anthropogenic contributions to mercury levels in present-day Arctic animals – A review. Science of the Total Environment, 407:6120-6131.

Dietz, R., C. Sonne, N. Basu, B. Braune, T. O'Hara, R.J. Letcher, T. Scheuhammer, M. Andersen, C. Andreasen, D. Andriashek and G. Asmund, 2013. What are the toxicological effects of mercury in Arctic biota? Science of the Total Environment, 443:775-790.

Diop, M. and R. Amara, 2016. Mercury concentrations in the coastal marine food web along the Senegalese coast. Environmental Science and Pollution Research, 23:11975-11984.

Dolgova, S., D. Crump, E. Porter, K. Williams and C.E. Hebert. 2018. Stage of development affects dry weight mercury concentrations in bird eggs: Laboratory evidence and adjustment method. Environmental Toxicology and Chemistry 37:1168-1174.

Dommergue, A., C.P. Ferrari, P.-A. Gauchard, C.F. Boutron, L. Poissant, M. Pilote, P. Jitaru and F.C. Adams, 2003. The fate of mercury species in a sub-arctic snowpack during snowmelt. Geophysical Research Letters, 30:10.1029/2003GL017308.

Dommergue, A., F. Sprovieri, N. Pirrone, R. Ebinghaus, S. Brooks, J. Courteaud and C.P. Ferrari, 2010. Overview of mercury measurements in the Antarctic troposphere. Atmospheric Chemistry and Physics, 10:3309-3319.

Dommergue, A., M. Barret, J. Courteaud, P. Cristofanelli, C.P. Ferrari and H. Gallée, 2012. Dynamic recycling of gaseous elemental mercury in the boundary layer of the Antarctic Plateau. Atmospheric Chemistry and Physics, 12:11027-11036.

Donovan, P.M., J.D. Blum, J.D. Demers, B. Gu, S.C. Brooks and J. Peryam, 2014. Identification of multiple mercury sources to stream sediments near Oak Ridge, TN, USA. Environmental Science and Technology, 48:3666-3674.

Donovan, P.M., J.D. Blum, M.B. Singer, M. Marvin-DiPasquale and M.T. Tsui, 2016. Isotopic composition of inorganic mercury and methylmercury downstream of a historical gold mining region. Environmental Science and Technology, 50:1691-1702.

Dou, H.Y., S.X. Wang, L. Wang, L. Zhang and J.M. Hao, 2013. Characteristics of total gaseous mercury concentrations at a rural site of Yangtze Delta, China. Huan Jing Ke Xue, 34:1-7. (In Chinese)

Douglas, T.A. and J.D. Blum, 2019. Mercury isotopes reveal atmospheric gaseous mercury deposition directly to the arctic coastal snowpack. Environmental Science & Technology Letters, 6:235-242.

Drevnick, P.E. and B.A. Brooks, 2017. Mercury in tunas and blue marlin in the North Pacific Ocean. Environmental Toxicology and Chemistry, 36:1365-1374.

Drevnick, P.E., C.H. Lamborg and M.J. Horgan, 2015. Increase in mercury in Pacific yellowfin tuna. Environmental Toxicology and Chemistry, 34:931-934.

Driscoll, C.T., Y.J. Han, C.Y. Chen, D.C. Evers, K.F. Lambert, T.M. Holsen, N.C. Kamman and R. Munson, 2007. Mercury contamination in remote forest and aquatic ecosystems in the northeastern U.S.: Sources, transformations and management options. Bioscience, 57:17-28.

Driscoll, C.T., R.P. Mason, H.M. Chan, D.J. Jacob and N. Pirrone, 2013. Mercury as a global pollutant: sources, pathways, and effects. Environmental Science and Technology, 47:4967-4983.

Drouillet-Pinard, P., G. Huel, R. Slama, A. Forhan, J. Sahuquillo, V. Goua, O. Thiébaugeorges, B. Foliguet, G. Magnin, M. Kaminski, S. Cordier and M.A. Charles, 2010. Prenatal mercury contamination: relationship with maternal seafood consumption during pregnancy and fetal growth in the 'EDEN mother-child' cohort. The British Journal of Nutrition, 104:1096-1100.

DTI, 2001. Coal preparation. Technology Status Report, No. 015. UK Department of Trade and Industry. http://webarchive.nationalarchives. gov.uk/+/http://www.berr.gov.uk/files/file19296.pdf

Duan, X.Q. and H. Yang, 1995. Pollutions of atmospheric particulate mercury in urban Lanzhou. Environmental Monitoring Management and Technology, 7:19-20. (In Chinese).

Durnford, D., A. Dastoor, A. Ryzhkov, L. Poissant, M. Pilote and D. Figueras-Nieto, 2012. How relevant is the deposition of mercury onto snowpacks? Part 2: A modelling study. Atmospheric Chemistry and Physics, 12:9251-9274.

Dvonch, J.T., G.J. Keeler and F.J. Marsik, 2005. The influence of meteorological conditions on the wet deposition of mercury in southern Florida. Journal of Applied Meteorology, 44:1421-1435.

Eagles-Smith, C.A. and J.T. Ackerman, 2009. Rapid changes in small fish mercury concentrations in estuarine wetlands: Implications for wildlife risk and monitoring programs. Environmental Science and Technology, 43:8658-8664.

Eagles-Smith, C.A. and J.T. Ackerman, 2014. Mercury bioaccumulation in estuarine wetland fishes: evaluating habitats and risk to coastal wildlife. Environmental Pollution, 193:147-155.

Eagles-Smith, C.A., J.T. Ackerman, S.E.W. De La Cruz and J.Y. Takekawa, 2009a. Mercury bioaccumulation and risk to three waterbird foraging guilds is influenced by foraging ecology and breeding stage. Environmental Pollution, 157:1993-2002.

Eagles-Smith, C.A., J.T. Ackerman, J. Yee and T.L. Adelsbach, 2009b. Mercury demethylation in waterbird livers: dose-response thresholds and differences among species. Environmental Toxicology and Chemistry, 28:568-577.

Eagles-Smith, C.A., J.T. Ackerman, J.J. Willacker, M.T. Tate, M.A. Lutz, J.A. Fleck, A.R. Stewart, J.G. Wiener, D.C. Evers, J.M. Lepak and J.A. Davis, 2016a. Spatial and temporal patterns of mercury concentrations in freshwater fish across the Western United States and Canada. Science of the Total Environment, 568:1171-1184.

Eagles-Smith, C.A., J.G. Wiener, C.S. Eckley, J.J. Willacker, D.C. Evers, M. Marvin-DiPasquale, D. Obrist, J.A. Fleck, G.R. Aiken, J.M. Lepak and A.K. Jackson, 2016b. Mercury in western North America: A synthesis of environmental contamination, fluxes, bioaccumulation, and risk to fish and wildlife. Science of the Total Environment, 568:1213-1226.

Eagles-Smith, C.A., E.K. Silbergeld, N. Basu, P. Bustamante, F. Diaz-Barriga, W.A. Hopkins, K.A. Kidd and J.F. Nyland, 2018a. Modulators of mercury risk to wildlife and humans in the context of rapid global change. Ambio, 47:170-197.

Eagles-Smith, C., E. Silbergeld, N. Basu, P. Bustamante, F. Diaz-Barriga, W. Hopkins, K. Kidd and J. Nyland, 2018b. A synthesis of how global change drivers modulate mercury exposure, bioaccumulation, and adverse outcomes in wildlife and humans. Ambio, 47:170-197.

Ebinghaus, R. and F. Slemr, 2000. Aircraft measurements of atmospheric mercury over southern and eastern Germany. Atmospheric Environment, 34:895-903.

Ebinghaus, R., H.H. Kock, C. Temme, J.W. Einax, A.G. Lowe, A. Richter, J.P. Burrows and W.H. Schroeder, 2002. Antarctic springtime depletion of atmospheric mercury. Environmental Science and Technology, 36:1238-1244.

Ebinghaus, R., S. Jennings, H. Kock, R. Derwent, A. Manning and T. Spain, 2011. Decreasing trends in total gaseous mercury observations in baseline air at Mace Head, Ireland from 1996 to 2009. Atmospheric Environment, 45:3475-3480.

EC, 2006. Reference Document on Best Available Techniques for Large Combustion Plants. European Commission, July 2006.

ECCC, 2016a. Canadian Mercury Science Assessment, Executive Summary. Environment and Climate Change Canada (ECCC).

ECCC, 2016b. Canadian Mercury Science Assessment, Report. By: Steffen, A. and H. Morrison. Environment and Climate Change Canada (ECCC).

Eckley, C.S., M.T. Tate, C.J. Lin, M. Gustin, S. Dent, C. Eagles-Smith, M.A. Lutz, K.P. Wickland, B. Wang, J.E. Gray, G.C. Edwards, D.P. Krabbenhoft and D.P. Smith, 2016. Surface-air mercury fluxes across Western North America: A synthesis of spatial trends and controlling variables. Science of the Total Environment, 568:651-665.

Edmonds, S.T., D.C. Evers, N.J. O'Driscoll, C. Mettke-Hoffman, L. Powell, D. Cristol, A.J. McGann, J.W. Armiger, O. Lane, D.F. Tessler and P. Newell, 2010. Geographic and seasonal variation in mercury exposure of the declining rusty blackbird. Condor, 112:789-799.

EEA, 2014, The European Pollutant Release and Transfer Register (E-PRTR), 2014. European Environment Agency (EEA). http://prtr.ec.europa.eu

EEB, 2007. Mercury in dental use: Environmental implications for the European Union. Concorde East/West Sprl for the European Environmental Bureau (EEB), Brussels, May 2007.

EFSA CONTAM Panel, 2012. Scientific Opinion on the risk for public health related to the presence of mercury and methylmercury in food. EFSA Journal, 10(12):2985. doi:10.2903/j.efsa.2012.2985.

EIA, 2017, International Energy Statistics, 2017. US Energy Information Administration. https://www.eia.gov/beta/international/data/browser/#/?pa=3g0000000000000000000000000000000000180000000000000g&c=4100000002000060000000000000g000200000000000000001&tl_id=1-A&vs=INTL.7-1-AFRC-TST.A&vo=0&v=H&start=1980&end=2014

EIP, 2016. Toxic Wastewater from Coal Plants. Environmental Integrity Project (EIP). https://www.eenews.net/assets/2016/08/11/document_gw_05.pdf

Elliott, J.E. and K.H. Elliott, 2013. Tracking marine pollution. Science, 340:556-558.

Elvidge, C., M. Zhizhin, K. Baugh, F-C. Hsu, G. Tilottama, 2015. Methods for global survey of natural gas flaring from visible infrared imaging radiometer suite data. Energies. 9:14. 10.3390/en9010014.

EMEP, 1985. Sulphur dioxide and particulate sulphate in ambient air. Monthly mean concentrations January 1978 to December 1982. EMEP/CCC-Report 1/85.

EMEP, 1986. Field intercomparison of measuring methods for sulphur dioxide and particulate sulphate in ambient air. Langenbrügge, Federal Republic of Germany, 7 November 1985 to 24 January 1986. EMEP/CCC-Report 2/86.

EMEP/EEA, 2009. EMEP/EEA Air Pollutant Emission Inventory: Guidebook 2009. Technical guidance to prepare national emission inventories. European Environment Agency (EEA). EEA Technical report No 9/2009.

EMEP/EEA, 2016. EMEP/EEA Air Pollutant Emission Inventory: Guidebook 2016. Technical guidance to prepare national emission inventories. European Environment Agency (EEA). EEA Report No 21/2016.

Enerdata, 2016, Global Energy Statistical Yearbook 2016, https://yearbook.enerdata.net/coal-and-lignite-production.html.

Engineering Toolbox, 2012. Fuels – Higher Calorific Values. www.engineeringtoolbox.com/fuels-higher-calorific-values-d_169.html

Engstrom, D.R., W.F. Fitzgerald, C.A. Cooke, C.H. Lamborg, P.E. Drevnick, E.B. Swain, S.J Balogh and P.H. Balcom, 2014. Atmospheric Hg emissions from preindustrial gold and silver extraction in the Americas: A re-evaluation from lake-sediment archives. Environmental Science and Technology, 48:6533-6543.

ENM, 2016. Energy News Monitor | Volume XII; Issue 30. https://indiaenergyanalysis.wordpress.com/2016/01/08/coal-washing-global-perspective/

Enrico, M., G. Le Roux, N. Marusczak, L.E. Heimburger, A. Claustres, X. Fu, R. Sun and J.E. Sonke, 2016. Atmospheric mercury transfer to peat bogs dominated by gaseous elemental mercury dry deposition. Environmental Science and Technology, 50:2405-2412.

Environment and Climate Change Canada, 2016. Canadian Mercury Science Assessment. Gatineau, QC.

Ericksen, J.A., M.S. Gustin, D.E. Schorran, D.W. Johnson, S.E. Lindberg and J.S. Coleman, 2003. Accumulation of atmospheric mercury in forest foliage. Atmospheric Environment, 37:1613-1622.

Esposito, M., A. De Roma, R. La Nucara, G. Picazio and P. Gallo, 2018. Total mercury content in commercial swordfish (*Xiphias gladius*) from different FAO fishing areas. Chemosphere, 197:14-19.

Euro Chlor, 2017. Chlorine Industry Review 2014-2015. Maintaining Momentum in Uncertain Times. Euro Chlor 17.

Evans, R.D., E.M. Addison, J.Y. Villeneuve, K.S. MacDonald and D.G. Joachim, 2000. Distribution of inorganic and methylmercury among tissues in mink (*Mustela vison*) and otter (*Lutra canadensis*). Environmental Research, 84:133-139.

Evans, M., D. Muir, R.B. Brua, J. Keating and X. Wang, 2013. Mercury trends in predatory fish in Great Slave Lake: The influence of temperature and other climate drivers. Environmental Science and Technology, 47:12793-12801.

Evans, M.S., D.C. Muir, J. Keating and X. Wang, 2015. Anadromous char as an alternate food choice to marine animals: A synthesis of Hg concentrations, population features and other influencing factors. Science of the Total Environment, 509:175-194.

Evers, D.C., 2018. The Effects of Methylmercury on Wildlife: A Comprehensive Review and Approach for Interpretation. Encyclopedia of the Anthropocene. Elsevier.

Evers, D.C. and T.A. Clair, 2005. Mercury in northeastern North America: A synthesis of existing databases. Ecotoxicology, 14:7-14.

Evers, D.C., J.D. Kaplan, M.W. Meyer, P.S. Reaman, A. Major, N. Burgess and W.E. Braselton, 1998. Bioavailability of environmental mercury measured in common loon feathers and blood across North American. Environmental Toxicology and Chemistry, 17:173-183.

Evers, D.C., N. Burgess, L. Champoux, B. Hoskins, A. Major, M.W. Goodale, R. Taylor, R. Poppenga and T. Daigle, 2005. Patterns and interpretation of mercury exposure in freshwater avian communities in northeastern North America. Ecotoxicology 14:193-222.

Evers, D.C., Y.J. Han, C.T. Driscoll, N.C. Kamman, M.W. Goodale, K.F. Lambert, T.M. Holsen, C.Y. Chen, T.A. Clair and T. Butler, 2007. Identification and evaluation of biological hotspots of mercury in the northeastern U.S. and eastern Canada. Bioscience, 57:29-43.

Evers, D.C., R.P. Mason, N.C. Kamman, C.Y. Chen, A.L. Bogomolni, D.H. Taylor, C.R. Hammerschmidt, S.H. Jones, N.M. Burgess, K. Munney and K.C. Parsons, 2008. An integrated mercury monitoring program for temperate estuarine and marine ecosystems on the North American Atlantic Coast. EcoHealth, 5:426-441.

Evers, D.C., R.T. Graham, P. Perkins, R. Michener and T. Divoll, 2009. Mercury concentrations in the goliath grouper of Belize: an anthropogenic stressor of concern. Endangered Species Research, 7:249-256.

Evers D.C., J.G. Wiener, N. Basu, R.A. Bodaly, H.A. Morrison and K.A. Williams, 2011a. Mercury in the Great Lakes region – Bioaccumulation, spatial and temporal patterns, ecological risks, and policy. Ecotoxicology, 20:1487-1499.

Evers, D.C., K.A. Williams, M.W. Meyer, A.M. Scheuhammer, N. Schoch, A.T. Gilbert, L. Siegel, R.J. Taylor, R. Poppenga and C.R. Perkins, 2011b. Spatial gradients of methylmercury for breeding common loons in the Laurentian Great Lakes region. Ecotoxicology, 20:1609-1625.

Evers, D.C., J.A. Schmutz, N. Basu, C.R. DeSorbo, J.S. Fair, C.G. Osborne, J. Paruk, M. Perkin, K. Regan, B.D. Uher-Koch and K.G. Wright, 2014. Mercury exposure and risk in yellow-billed loons breeding in Alaska and Canada. Waterbirds, 37:147-159.

Evers, D.C., S.E. Keane, N. Basu and D. Buck, 2016. Evaluating the effectiveness of the Minamata Convention on Mercury: Principles and recommendations for next steps. Science of the Total Environment, 569:888-903.

Evers, D.C., D.G. Buck, S.M. Johnson and M. Burton, 2017. Mercury in the Global Environment: Understanding spatial patterns for biomonitoring needs of the Minamata Convention on Mercury. Biodiversity Research Institute Science Communications Series 2017-12. Portland, Maine, USA.

Faial, K., R. Deus, S. Deus, R. Neves, I. Jesus, E. Santos, C.N. Alves and D. Brasil, 2015. Mercury levels assessment in hair of riverside inhabitants of the Tapajos River, Para State, Amazon, Brazil: fish consumption as a possible route of exposure. Journal of Trace Elements in Medicine and Biology, 30:66-76.

Faïn, X., S. Grangeon, E. Bahlmann, J. Fritsche, D. Obrist, A. Dommergue, C.P. Ferrari, W. Cairns, R. Ebinghaus and C. Barbante, 2007. Diurnal production of gaseous mercury in the alpine snowpack before snowmelt. Journal of Geophysical Research: Atmospheres, 112:D21311, doi:10.1029/2007JD008520.

Faïn, X., C.P. Ferrari, A. Dommergue, M.R. Albert, M. Battle, J. Severinghaus, L. Arnaud, J.-M. Barnola, W. Cairns, C. Barbante and C. Boutron, 2009. Polar firn air reveals large-scale impact of anthropogenic mercury emissions during the 1970s. Proceedings of the National Academy of Sciences, 106:16114-16119.

Fang, F.M., Q.C. Wang and J.F. Li, 2004. Urban environmental mercury in Changchun, a metropolitan city in northeastern China: source, cycle, and fate. Science of the Total Environment, 330:159-170.

FAO, 2014. The State of World Fisheries and Aquaculture: Opportunities and Challenges. Food and Agriculture Organization (FAO), Rome.

FAO, 2016. AQUASTAT Main Database. Food and Agriculture Organization of the United Nations.

FAO, 2018. Search Geographical Information. FAO Major Fishing Areas. UN Food and Agriculture Organization (www.fao.org/fishery/area/search/en).

FAO/WHO, 2010. Report of the Joint FAO/WHO Expert Consultation on the Risks and Benefits of Fish Consumption. Food and Agriculture Organization (FAO), Fisheries and Aquaculture Report No. 978.

FAO/WHO, 2011. Joint FAO/WHO Food Standards Programme Codex Committee on Contaminants in Foods. Working Document for Information and Use in Discussions Related to Contaminants and Toxins in the GSCTFF. Fifth Session, Hague, Netherlands, 2011.

Feng, X.B., L.H. Shang, S.F. Wang, S.L. Tang and W. Zheng, 2004. Temporal variation of total gaseous mercury in the air of Guiyang, China. Journal of Geophysical Research: Atmospheres, 109:D03303. 10.1029/2003jd004159.

Feng, X.B., H.M. Jiang, G.L. Qiu, H.Y. Yan, G.H. Li and Z.G. Li, 2009a. Geochemical processes of mercury in Wujiangdu and Dongfeng reservoirs, Guizhou, China. Environmental Pollution, 157:2970-2984.

Feng, X.B., H.M. Jiang, G.L. Qiu, H.Y. Yan, G.H. Li and Z.G. Li, 2009b. Mercury mass balance study in Wujiangdu and Dongfeng Reservoirs, Guizhou, China. Environmental Pollution, 157:2594-2603.

Feng, X.B., B. Meng, H.Y. Yan, X.W. Fu, H. Yao and L.H. Shang, 2018. Biogeochemical Cycle of Mercury in Reservoir Systems in Wujiang River Basin, Southwest China. Science Press and Springer Nature.

Ferrara, R., B.E. Maserti, M. Andersson, H. Edner, P. Ragnarson, S. Svanberg and A. Hernandez, 1998. Atmospheric mercury concentrations and fluxes in the Almadén district (Spain). Atmospheric Environment, 32:3897-3904.

Ferrara, R., B. Mazzolai, E. Lanzillotta, E. Nucaro and N. Pirrone, 2000. Volcanoes as emission sources of atmospheric mercury in the Mediterranean basin. Science of the Total Environment, 259:115-121.

Ferrari, C.P., P.-A. Gauchard, K. Aspmo, A. Dommergue, O. Magand, E. Bahlmann, S. Nagorski, C. Temme, R. Ebinghaus, A. Steffen, C. Banic, T. Berg, F. Planchon, C. Barbante, P. Cescon and C.F. Boutron, 2005. Snow-to-air exchanges of mercury in an arctic seasonal snowpack in Ny-Alesund, Svalbard. Atmospheric Environment, 39:7633-7645.

Ferriss, B.E. and T.E. Essington, 2011. Regional patterns in mercury and selenium concentrations of yellowfin tuna (*Thunnus albacares*) and bigeye tuna (*Thunnus obesus*) in the Pacific Ocean. Canadian Journal of Fisheries and Aquatic Sciences, 68:2046-2056.

Fielding, R. and D.W. Evans, 2014. Mercury in Caribbean dolphins (*Stenella longirostris* and *Stenella frontalis*) caught for human consumption off St. Vincent, West Indies. Marine Pollution Bulletin, 89:30-34.

Finkelstein, M., B.S. Keitt, D.A. Croll, B. Tershy, W.M. Jarman, S. Rodriguez-Pastor, D.J. Anderson, P.R. Sievert and D.R. Smith, 2006. Albatross species demonstrate regional differences in North Pacific marine contamination. Ecological Applications, 16:678-686.

Fisher, J.A., D.J. Jacob, A.L. Soerensen, H.M. Amos, A. Steffen and E.M. Sunderland, 2012. Riverine source of Arctic Ocean mercury inferred from atmospheric observations. Natural Geoscience, 5:499-504.

Fisher, J.A., D.J. Jacob, A.L. Soerensen, H.M. Amos, E.S. Corbitt, D.G. Streets, Q. Wang, R.M. Yantosca and E.M. Sunderland, 2013. Factors driving mercury variability in the Arctic atmosphere and ocean over the past 30 years. Global Biogeochemical Cycles, 27:1226-1235.

Fitzgerald, W.F. and C.H. Lamborg, 2014. Geochemistry of Mercury in the Environment. Treatise on Geochemistry, 2nd Edition.

Fitzgerald, W.F., D.R. Engstrom, R.P. Mason and E.A. Nater, 1998. The case for atmospheric mercury contamination in remote areas. Environmental Science and Technology, 32:1-7.

Fleming, E.J., E.E. Mack, P.G. Green and D.C. Nelson, 2006. Mercury methylation from unexpected sources: molybdate-inhibited freshwater sediments and an iron-reducing bacterium. Applied and Environmental Microbiology, 72:457-64.

Florida Health Department, 2009. Guidelines for mercury. Document No. document HG05-2009. www.floridahealth.gov/environmental-health/mercury-spills/mercury-poisoning/_documents/guidelines-for-mercury.pdf

Fok, T.F., H.S. Lam, P.C. Ng, A.S. Yip, N.C. Sin, I.H. Chan, G.J. Gu, H.K. So, E.M. Wong and C.W. Lam, 2007. Fetal methylmercury exposure as measured by cord blood mercury concentrations in a mother-infant cohort in Hong Kong. Environment International, 33:84-92.

Fonseca, F.R.D., O. Malm and H.F. Waldemarin, 2005. Mercury levels in tissues of giant otters (*Pteronura brasiliensis*) from the Rio Negro, Pantanal, Brazil. Environmental Research, 98:368-371.

Fort, J., H. Helgason, F. Amelineau, T. Anker-Nilssen, J.O. Bustnes, J. Danielsen, S. Dechamps, R. Dietz, K. Elliott, K.E. Erikstad and A. Ezhov, 2017. ARCTOX: a pan-Arctic sampling network to track mercury contamination across Arctic marine food webs. In: 13th International Conference on Mercury as a Global Pollutant (ICMGP2017).

Fragoso, C.P., E. Bernini, B.F. Araújo, M.G. de Almeida and C.E. de Rezende, 2018. Mercury in litterfall and sediment using elemental and isotopic composition of carbon and nitrogen in the mangrove of southeastern Brazil. Estuarine, Coastal and Shelf Science, 202:30-39.

Frederick, P.C., M.G. Spalding and R. Dusek, 2002. Wading birds as bioindicators of mercury contamination in Florida, USA: Annual and geographic variation. Environmental Toxicology and Chemistry, 21:163-167.

Frey, C., J. Penman, L. Hanle, S. Monni and S. Ogle, 2006. Chapter 3: Uncertainties. In: 2006 IPCC Guidelines for National Greenhouse Gas Inventories. Intergovernmental Panel on Climate Change.

Friedli, H., A. Arellano, S. Cinnirella and N. Pirrone, 2009. Initial estimates of mercury emissions to the atmosphere from global biomass burning. Environmental Science and Technology, 43:3507-3513.

Friedli, H.R., A.F. Arellano Jr., F. Geng, C. Cai and L. Pan, 2011. Measurements of atmospheric mercury in Shanghai during September 2009. Atmospheric Chemistry and Physics, 11:3781-3788.

Fritsche, J., D. Obrist, M.J. Zeeman, F. Conen, W. Eugster and C. Alewell, 2008. Elemental mercury fluxes over a sub-alpine grassland determined with two micrometeorological methods. Atmospheric Environment, 42:2922-2933.

Fu, X.W. and X.B. Feng, 2015. Variations of atmospheric total gaseous mercury concentrations for the sampling campaigns of 2001/2002 and 2009/2010 and implications of changes in regional emissions of atmospheric mercury. Bulletin of Mineralogy, Petrology and Geochemistry, 34:242-249 (in Chinese, with English abstract).

Fu, X.W., X.B. Feng, W.Z. Zhu, S.F. Wang and J.L. Lu, 2008a. Total gaseous mercury concentrations in ambient air in the eastern slope of Mt. Gongga, South-Eastern fringe of the Tibetan plateau, China. Atmospheric Environment, 42:970-979.

Fu, X.W., X.B. Feng, W.Z. Zhu, W. Zheng, S.F. Wang and J.Y. Lu, 2008b. Total particulate and reactive gaseous mercury in ambient air on the eastern slope of the Mt. Gongga area, China. Applied Geochemistry, 23:408-418.

Fu, X.W., X. Feng, W. Zhu, S. Rothenberg, H. Yao and H. Zhang, 2010a. Elevated atmospheric deposition and dynamics of mercury in a remote upland forest of southwestern China. Environmental Pollution, 158:2324-2333.

Fu, X.W., X. Feng, Z.Q. Dong, R.S. Yin, J.X. Wang, Z.R. Yang and H. Zhang, 2010b. Atmospheric gaseous elemental mercury (GEM) concentrations and mercury depositions at a high-altitude mountain peak in south China. Atmospheric Chemistry and Physics, 10:2425-2437.

Fu, X.W., X.B. Feng, G.L. Qiu, L.H. Shang and H. Zhang, 2011. Speciated atmospheric mercury and its potential source in Guiyang, China. Atmospheric Environment, 45:4205-4212.

Fu, X., X. Feng, H. Zhang, B. Yu and L. Chen, 2012a. Mercury emissions from natural surfaces highly impacted by human activities in Guangzhou province, South China. Atmospheric Environment, 54:185-193.

Fu, X.W., X. Feng, L.H. Shang, S.F. Wang and H. Zhang, 2012b. Two years of measurements of atmospheric total gaseous mercury (TGM) at a remote site in Mt. Changbai area, Northeastern China. Atmospheric Chemistry and Physics, 12:4215-4226.

Fu, X.W., X. Feng, P. Liang, H. Deliger, Zhang, J. Ji and P. Liu, 2012c. Temporal trend and sources of speciated atmospheric mercury at Waliguan GAW station, Northwestern China. Atmospheric Chemistry and Physics, 12:1951-1964.

Fu, X.W., H. Zhang, X.B. Feng and W. Zhu, 2014. Speciated atmospheric mercury in rural Mt. Changbai, northeast China, 17th international conference of heavy metals in the environment, Guiyang, China, 22–25 September.

Fu, X.W., H. Zhang, B. Yu, X. Wang, C.-J. Lin and X.B. Feng, 2015. Observations of atmospheric mercury in China: a critical review. Atmospheric Chemistry and Physics, 15:9455-9476.

Fu, X., X. Yang, X. Lang, J. Zhou, H. Zhang, B. Yum H. Yan, C.-J. Lin and X. Feng, 2016a. Atmospheric wet and litterfall mercury deposition at urban and rural sites in China. Atmospheric Chemistry and Physics, 16:11547-11562.

Fu, X., W. Zhu, H. Zhang, J. Sommar, B. Yu, X. Yang, X. Wang, C.-J. Lin and X. Feng, 2016b. Depletion of atmospheric gaseous elemental mercury by plant uptake at Mt. Changbai, Northeast China. Atmospheric Chemistry and Physics, 16:12861-12873.

Fukuda, N., M. Takaoka, S. Doumoto, K. Oshita, S. Morisawa and T. Mizuno, 2011. Mercury emission and behavior in primary ferrous metal production. Atmospheric Environment, 45:3685-3691.

Furness, R.W. and K.C.J. Camphuysen, 1997. Seabirds as monitors of the marine environment. ICES Journal of Marine Science, 54:726-737.

Gaden, A., S.H. Ferguson, L. Harwood, H. Melling and G. Stern, 2009. Mercury trends in ringed seals (Phoca hispida) from the western Canadian Arctic since 1973: Associations with length of ice-free season. Environmental Science and Technology, 43:3646-3651.

Galland, G.R., 2017. Fishing responsibly and sustainably. Science, 357:558-558.

Gandhi, N., R.W. Tang, S.P. Bhavsar and G.B. Arhonditsis, 2014. Fish mercury levels appear to be increasing lately: a report from 40 years of monitoring in the province of Ontario, Canada. Environmental Science and Technology, 48:5404-5414.

Gandhi, N., S.P. Bhavsar, R.W. Tang and G.B. Arhonditsis, 2015. Projecting fish mercury levels in the province of Ontario, Canada and the implications for fish and human health. Environmental Science and Technology, 49:14494-14502.

Gandhi, N., S.P. Bhavsar, S.B. Gewurtz, K.G. Drouillard, G.B. Arhonditsis and S. Petro, 2016. Is it appropriate to composite fish samples for mercury trend monitoring and consumption advisories? Environment International, 88:80-85.

Ganguli, P.M., C.H. Conaway, P.W. Swarzenski, J.A. Izbicki and A.R. Flegal, 2012. Mercury speciation and transport via submarine groundwater discharge at a southern California coastal lagoon system. Environmental Science and Technology, 46:1480-1488.

Gantner, N., M. Power, D. Iqaluk, M. Meili, H. Borg, M. Sundbom, K.R. Solomon, G. Lawson and D.C. Muir, 2010. Mercury concentrations in landlocked Arctic char (Salvelinus alpinus) from the Canadian Arctic. Part I: insights from trophic relationships in 18 lakes. Environmental Toxicology and Chemistry, 29:621-632.

Gao, Y., C.H. Yan, Y. Tian, Y. Wang, H.F. Xie, X. Zhou, X.D. Yu, X.G. Yu, S. Tong, Q.X. Zhou and X.M. Shen, 2007. Prenatal exposure to mercury and neurobehavioral development of neonates in Zhoushan City, China. Environmental Research, 105:390-399.

García, M.Á., R. Núñez, J. Alonso and M.J. Melgar, 2016. Total mercury in fresh and processed tuna marketed in Galicia (NW Spain) in relation to dietary exposure. Environmental Science and Pollution Research, 23:24960-24969.

García-Seoane, R., Z. Varela, A. Carballeira, J.R. Aboal and J.Á. Fernández, 2017. Temporal trends in mercury concentrations in raptor flight feathers stored in an environmental specimen bank in Galicia (NW Spain) between 2000 and 2013. Ecotoxicology, 26:196-201.

Garnham, B. and K. Langerman, 2016. Mercury emissions from South Africa's coal-fired power stations. Clean Air Journal, 26, No 2. doi. org/10.17159/2410-972X/2016/v26n2a8

Garrigue, C., M. Oremus, R. Dodémont, P. Bustamante, O. Kwiatek, G. Libeau, C. Lockyer, J.C. Vivier and M.L. Dalebout, 2016. A mass stranding of seven Longman's beaked whales (Indopacetus pacificus) in New Caledonia, South Pacific. Marine Mammal Science, 32:884-910.

Gbogbo, F., S.D. Otoo, R.Q. Huago and O. Asomaning, 2017. High levels of mercury in wetland resources from three river basins in Ghana: a concern for public health. Environmental Science and Pollution Research, 24:5619-5627.

GCPT, 2017. Global Coal Plant Tracker. http://endcoal.org/global-coal-plant-tracker/

Gencarelli, C.N., F. De Simone, I.M. Hedgecock, F. Sprovieri and N. Pirrone, 2014. Development and application of a regional-scale atmospheric mercury model based on WRF/Chem: a Mediterranean area investigation. Environmental Science and Pollution Research, 21:4095-4109.

Gencarelli, C.N., J. Bieser, F. Crabone, F. De Simone, I.M. Hedgecock, V. Matthias, O. Travnikov, X. Yang and N. Pirrone, 2016. Sensitivity model study of regional mercury dispersion in the atmosphere. Atmospheric Chemistry and Physics Discussions, doi:10.5194/acp-2016-663.

German, C.R., K.A. Casciotti, J.-C. Dutay, L.E. Heimbürger, W.J. Jenkins, C.I. Measures, R.A. Mills, H. Obata, R. Schlitzer, A. Tagliabue, D.R. Turner and H. Whitby, 2016. Hydrothermal impacts on trace element and isotope ocean biogeochemistry. Philosophical Transactions of the Royal Society A, 374 (2081).

German Federal Environment Agency, 2017. German Environmental Survey. www.umweltbundesamt.de/en/topics/health/assessing-environmentally-related-health-risks/german-environmental-survey-geres (Accessed 30 November 2017)

Geyer, W.R. and D.K. Ralston, 2018. A mobile pool of contaminated sediment in the Penobscot Estuary, Maine, USA. Science of the Total Environment, 612:694-707.

Ghaedi, M., M.R. Fathi, A. Shokrollahi and F. Shajarat, 2006. Highly selective and sensitive preconcentration of mercury ion and determination by cold vapor atomic absorption spectroscopy. Analytical Letters, 39:1171-1185.

Giang, A. and N.E. Selin, 2016. Benefits of mercury controls for the United States. Proceedings of the National Academy of Sciences of the United States of America, 113:286-291.

Giang, A., L.C. Stokes, D.G. Streets, E.S. Corbitt and N.E. Selin, 2015. Impacts of the Minamata Convention on mercury emissions and global deposition from coal-fired power generation in Asia. Environmental Science and Technology, 49:5326-5335.

Gibb, H. and K.G. O'Leary, 2014. Mercury exposure and health impacts among individuals in the artisanal and small-scale gold mining community: a comprehensive review. Environmental Health Perspectives, 122:667-672.

Gilbert, R.O., 1987. Statistical Methods for Environmental Pollution Monitoring. Van Nostrand Reinhold Company, New York.

Gilmour, C.C., M. Podar, A.L. Bullock, A.M. Graham, S.D. Brown, A.C. Somenhally, A. Johs, R.A. Hurt Jr., K.L. Bailey and D.A. Elias, 2013. Mercury methylation by novel microorganisms from new environments. Environmental Science and Technology, 47:11810-11820.

Gionfriddo, C.M., M.T. Tate, R.R. Wick, M.B. Schultz, A. Zemla, M.P. Thelen, R. Schofield, D.P. Krabbenhoft, K.E. Holt and J.W. Moreau, 2016. Microbial mercury methylation in Antarctic sea ice. Nature Microbiology, 1(10):16127.

Giurco, D., T. Prior, G.M. Mudd, L. Mason and J. Behrisch, 2010. Peak Minerals in Australia: A Review of Changing Impacts and Benefits. Institute for Sustainable Futures, University of Technology, Sydney, Australia.

Gleick, P.H. (ed.), 2014. The World's Water Volume 8. The Biennial Report on Freshwater Resources. Island Press.

GNR, 2014. Global Cement Database on CO_2 and Energy Information: Getting the Numbers Right (GNR). Emissions Report 2014. www.wbcsdcement.org/index.php/key-issues/climate-protection/gnr-database

Golding, J., C.D. Steer, J.R. Hibbeln, P.M. Emmett, T. Lowery and R. Jones, 2013. Dietary predictors of maternal prenatal blood mercury levels in the ALSPAC birth cohort study. Environmental Health Perspectives, 121:1214-1218.

Goni-Urriza, M., Y. Corsellis, L. Lanceleur, E. Tessier, J. Gury, M. Monperrus and R. Guyoneaud, 2015. Relationships between bacterial energetic metabolism, mercury methylation potential, and hgcA/hgcB gene expression in Desulfovibrio dechloroacetivorans BerOc1. Environmental Science and Pollution Research, 22 doi: 10.1007/s11356-015-4273-5.

Goodale, M.W., D.C. Evers, S.E. Mierzykowski, A.L. Bond, N.M. Burgess, C.I. Otorowski, L.J. Welch, C.S. Hall, J.C. Ellis, R.B. Allen, A.W. Diamond, S.W. Kress and R.J. Taylor, 2008. Marine foraging birds as bioindicators of mercury in the Gulf of Maine. EcoHealth, 5:409-425.

Goodrich, J.M., H.N. Chou, S.E. Gruninger, A. Franzblau and N. Basu, 2016. Exposures of dental professionals to elemental mercury and methylmercury. Journal of Exposure Science and Environmental Epidemiology, 26:78-85.

Goodsite, M.E., J.M.C. Plane and H. Skov, 2004. A theoretical study of the oxidation of Hg^0 to $HgBr_2$ in the troposphere. Environmental Science and Technology, 38:1772-1776.

Goodsite, M.E., J.M.C. Plane and H. Skov, 2012. Correction to a theoretical study of the oxidation of Hg^0 to $HgBr_2$ in the troposphere. Environmental Science and Technology, 46:5262, doi:10.1021/es301201c.

Goodsite, M.E., P.M. Outridge, J.H. Christensen, A. Dastoor, D. Muir, O. Travnikov and S. Wilson, 2013. How well do environmental archives of atmospheric mercury deposition in the Arctic reproduce rates and trends depicted by atmospheric models and measurements? Science of the Total Environment, 452-453:196-207.

Gosnell, K., P. Balcom, V. Ortiz, B. DiMento, A. Schartup, R. Greene and R. Mason, 2016. Seasonal cycling and transport of mercury and methylmercury in the turbidity maximum of the Delaware Estuary. Aquatic Geochemistry, 22:313-336.

Gosnell, K.J., P.H. Balcom, C.T. Tobias, W.P. Gilhooly III and R.P. Mason, 2017. Spatial and temporal trophic transfer dynamics of mercury and methylmercury into zooplankton and phytoplankton of Long Island Sound. Limnology and Oceanography, 62:1122-1138.

Goutte, A., C. Barbraud, A. Meillère, A. Carravieri, P. Bustamante, P. Labadie, H. Budzinski, K. Delord, Y. Cherel, H. Weimeskirch and O. Chastel, 2014a. Demographic consequences of heavy metals and persistent organic pollutants in a vulnerable long-lived bird, the wandering albatross. Proceedings of the Royal Society B, 281:20133313.

Goutte, A., P. Bustamante, C. Barbraud, K. Delord, H. Weimeskirch and O. Chastel, 2014b. Demographic responses to mercury exposure in two closely-related Antarctic top predators. Ecology, 95:1075-1086.

Grangeon, S., S. Guedron, J. Asta, G. Sarret and L. Charlet, 2012. Lichen and soil as indicators of an atmospheric mercury contamination in the vicinity of a chlor-alkali plant. Ecological Indicators, 13:178-183.

Grant, S.L., M. Kim, P. Lin, K.C. Crist, S. Ghosh and V.R. Kotamarthi, 2014. A simulation study of atmospheric mercury and its deposition in the Great Lakes. Atmospheric Environment, 94:164-172.

Gratz, L.E., G.J. Keeler, F.J. Marsik, J.A. Barres and J.T. Dvonch, 2013a. Atmospheric transport of speciated mercury across southern Lake Michigan: Influence from emission sources in the Chicago/Gary urban area. Science of the Total Environment, 448:84-95.

Gratz, L.E., G.J. Keeler, M. Morishita, J.A. Barres and J.T. Dvonch, 2013b. Assessing the emission sources of atmospheric mercury in wet deposition across Illinois. Science of the Total Environment, 448:120-131.

Gratz, L.E., J. Ambrose, D. Jaffe, V. Shah, L. Jaeglé, J. Stutz, J. Festa, M. Spolaor, C.-C. Tsai, N. Selin, S. Song, X. Zhou, A. Weinheimer, D. Knapp, D. Montzka, F. Flocke, T. Campos, E. Apel, R. Hornbrook and M. Stell, 2015. Oxidation of mercury by bromine in the subtropical Pacific free troposphere. Geophysical Research Letters, 42:10492-10502.

Gratz, L., J.L. Ambrose, D.A. Jaffe, C. Knote, L. Jaeglé, N.E. Selin, T. Campos, F.M. Flocke, M. Reeves, D. Stechman, M. Stell, A.J. Weinheimer, D.J. Knapp, D.D. Montzka, G.S. Tyndall, R.L. Mauldin, C.A. Cantrell, E.C. Apel, R.S. Hornbrook and N.J. Blake, 2016. Airborne observations of mercury emissions from the Chicago/Gary Urban/Industrial Area during the 2013 NOMADSS Campaign. Atmospheric Environment, 145:415-423.

Graydon, J.A., V. St. Louis, S. Lindberg, K.A. Sandilands, J.W.M. Rudd, C.A. Kelly, R. Harris, M. Tate, D.P. Krabbenhoft, C.A. Emmerton, H. Asmath and M. Richardson, 2012. The role of terrestrial vegetation in atmospheric Hg deposition: Pools and fluxes from the METAALICUS experiment. Global Biogeochemical Cycles, 26:1029/2011GB004031.

Great Lakes Fish Advisory Workgroup, 2007. A protocol for mercury-based fish consumption advise. Available from the International Joint Commission. 30pp.

Grigal, D.F., 2003. Mercury sequestration in forests and peatlands: A review. Journal of Environmental Quality, 32:393-405.

Grove, R.A., C.J. Henny and J.L. Kaiser, 2009. Osprey: worldwide sentinel species for assessing and monitoring environmental contamination in rivers, lakes, reservoirs, and estuaries. Journal of Toxicology and Environmental Health B, 12:25-44.

Guerrero, S., 2012. Chemistry as a tool for historical research: Identifying paths of historical mercury pollution in the Hispanic New World. Bulletin for the History of Chemistry, 37:61-70.

Guerrero, S., 2016. The history of silver refining in New Spain, 16C to 18C: back to the basics. History and Technology, 32:2-32.

Guerrero, S., 2017. Silver by Fire, Silver by Mercury: A Chemical History of Silver Refining in New Spain and Mexico, 16th to 19th Centuries. Brill, Leiden.

Guerrero, S., 2018. The environmental history of silver production, and its impact on the United Nations Minamata Convention on mercury. Extended Abstract. Session on Global Production and Distribution of Silver, World Economic History Congress, Boston, USA, July 29–August 3, 2018. Available at: http://wehc2018.org/wp-content/uploads/2018/04/WEHCguerreroMinamata-2.pdf

Gunson, A.J., 2004. Mercury and Artisanal and Small-scale Gold Miners in China. Master's thesis. Retrieved from https://open.library.ubc.ca/cIRcle/collections/ubctheses/

Guo, Y.N., 2008. Input and output fluxes of mercury in different evolutive reservoirs in Wujiang River Basin. Ph.D. Thesis. Graduate School of the Chin. Acad. of Sci., Beijing. (In Chinese, with English abstract)

Guo, Y.N., X.B. Feng, Z.G. Li, T.R. He, H.Y. Yan, B. Meng, J.F. Zhang and G.L. Qiu, 2008. Distribution and wet deposition fluxes of total and methyl mercury in Wujiang River Basin, Guizhou, China. Atmospheric Environment, 42:7096-7103.

Gustin, M.S., 2011. Exchange of mercury between the atmosphere and terrestrial ecosystems. In: Liu, G.L., Y. Cai and N. O'Driscoll (eds.), Environmental Chemistry and Toxicology of Mercury. pp. 423-451.

Gustin, M. and D. Jaffe, 2010. Reducing the uncertainty in measurement and understanding of mercury in the atmosphere. Environmental Science and Technology, 44:2222-2227.

Gustin, M.S., H. Biester and C.S. Kim, 2002. Investigation of the light-enhanced emission of mercury from naturally enriched substrates. Atmospheric Environment, 36:3241-3254.

Gustin, M.S., J.A. Ericksen, D.E. Schorran, D.W. Johnson, S.E. Lindberg and J.S. Coleman, 2004. Application of controlled mesocosms for

understanding mercury air-soil-plant exchange. Environmental Science and Technology, 38:6044-6050.

Gustin, M.S., S.N. Lyman, P. Kilner and E. Prestbo, 2011. Development of a passive sampler for gaseous mercury. Atmospheric Environment, 45:5805-5812.

Gustin, M.S., J. Huang, M.B. Miller, C. Peterson, D.A. Jaffe, J. Ambrose, B.D. Finley, S.N. Lyman, K. Call, R. Talbot, D. Feddersen, H. Mao and S.E. Lindberg, 2013. Do we understand what the mercury speciation instruments are actually measuring? Results of RAMIX. Environmental Science and Technology, 47:7295-7306.

Gustin, M.S., H.M. Amos, J. Huang, M.B. Miller and K. Heidcorn, 2015. Measuring and modeling mercury in the atmosphere: a critical review. Atmospheric Chemistry and Physics, 15:5697-5713.

Gustin, M., D.C. Evers, M. Bank, C.R. Hammerschmidt, A. Pierce, N. Basu, J. Blum, P. Bustamante, C. Chen, C.T. Driscoll, M. Horvat, D. Jaffe, J. Pacyna, N. Pirrone and N. Selin, 2016a. Importance of integration and implementation of emerging and future mercury research into the Minamata Convention. Environmental Science and Technology, 50:2767-2770.

Gustin, M.S., A.M. Pierce, J. Huang, M.B. Miller, H.A. Holmes and S.M. Loria-Salazar, 2016b. Evidence for different reactive Hg sources and chemical compounds at adjacent valley and high elevation locations. Environmental Science and Technology, 50:12225-12231.

Ha, E., N. Basu, S. Bose-O'Reilly, J.G. Dórea, E. McSorley, M. Sakamoto and H.M. Chan, 2017. Current progress on understanding the impact of mercury on human health. Environmental Research, 152:419-433.

Hall, B.D., V.L. St. Louis, K.R. Rolfhus, R.A. Bodaly, K.G. Beaty and M. Paterson, 2005. The impact of reservoir creation on the biogeochemical cycling of methyl and total mercury in boreal upland forests. Ecosystems, 8:248-266.

Hammerschmidt, C.R. and K.L. Bowman, 2012. Vertical methylmercury distribution in the subtropical North Pacific Ocean. Marine Chemistry, 132-133:77-82.

Hammerschmidt, C.R., M.B. Sandheinrich, J.G. Wiener and R.G. Rada, 2002. Effects of dietary methylmercury on reproduction of fathead minnows. Environmental Science and Technology, 36:877-883.

Han, Y., Y. Huh, S. Hong, S.D. Hur, H. Motoyama, S. Fujita, F. Nakazawa and K. Fukui, 2011. Quantification of total mercury in Antarctic surface snow using ICP-SF-MS: spatial variation from the coast to Dome Fuji. Bulletin of the Korean Chemical Society, 32:4258-4264.

Han, Y., Y. Huh, S. Hong, S.D. Hur and H. Motoyama, 2014a. Evidence of air-snow mercury exchange recorded in the snowpack at Dome Fuji, Antarctica. Geosciences Journal, 18:105-113.

Han, Y.J., J.E. Kim, P.R. Kim, W.J. Kim, S.M. Yi, Y.S. Seo and S.H. Kim, 2014b. General trends of atmospheric mercury concentrations in urban and rural areas in Korea and characteristics of high-concentration events. Atmospheric Environment, 94:754-764.

Han, Y., Y. Huh, S.D. Hur, S. Hong, J.W. Chung and H. Motoyama, 2017. Net deposition of mercury to the Antarctic Plateau enhanced by sea salt. Science of the Total Environment, 583:81-87.

Hanna, D.E., C.T. Solomon, A.E. Poste, D.G. Buck and L.J. Chapman, 2015. A review of mercury concentrations in freshwater fishes of Africa: Patterns and predictors. Environmental Toxicology and Chemistry, 34:215-223.

Hanna, D.E., D.G. Buck and L.J. Chapman, 2016. Effects of habitat on mercury concentrations in fish: a case study of Nile perch (Lates niloticus) in Lake Nabugabo, Uganda. Ecotoxicology, 25:178-191.

Hararuk, O., D. Obrist and Y. Luo, 2013. Modeling the sensitivity of soil mercury to climate-induced changes in soil-carbon pools. Biogeosciences, 10:2393-2407.

Haris, H., A.Z. Aris and M. bin Mokhtar, 2017. Mercury and methylmercury distribution in the intertidal surface sediment of a heavily anthropogenically impacted saltwater-mangrove-sediment interplay zone. Chemosphere, 166:323-333.

Harmens, H., D.A. Norris, G.R. Koerber, A. Buse, E. Steinnes and Å. Rühling, 2008. Temporal trends (1990–2000) in the concentration of cadmium, lead and mercury in mosses across Europe. Environmental Pollution, 151:368-376.

Hartman, J.S., P.J. Weisberg, R. Pillai, J.A. Ericksen, T. Kuiken, S.E. Lindberg, H. Zhang, J.J. Rytuba and M.S. Gustin, 2009. Application of a rule-based model to estimate mercury exchange for three background biomes in the Continental United States. Environmental Science and Technology, 43:4989-4994.

Hartman, C.A., J.T. Ackerman, G. Herring, J. Isanhart and M.P. Herzog, 2013. Marsh wrens as bioindicators of mercury in wetlands of Great Salt Lake: Do blood and feathers reflect site-specific exposure risk to bird reproduction? Environmental Science and Technology, 47:6597-6605.

Hartman, C.A., J.T. Ackerman, M.P. Herzog and C.A. Eagles-Smith, 2017. Season, molt, and body size influence mercury concentrations in grebes. Environmental Pollution, 229:29-39.

Health Canada, 2004. Mercury – Your health and the environment. Minister of Health, Ottawa. https://www.canada.ca/en/health-canada/services/environmental-workplace-health/reports-publications/environmental-contaminants/mercury-your-health-environment-resource-tool.html#q-17 (Accessed 20 July 2018).

Health Canada, 2007. Human Health Risk Assessment of Mercury in Fish and Health Benefits of Fish Consumption. Health Canada, Ottawa.

Health Canada, 2017. Fourth Report on Human Biomonitoring of Environmental Chemicals in Canada. Health Canada, Ottawa.

Heimbürger, L.E., D. Cossa, J.-C. Marty, C. Migon, B. Averty, A. Dufour and J. Ras, 2010. Methylmercury distributions in relation to the presence of nano- and picophytoplankton in an oceanic water column (Ligurian Sea, North-western Mediterranean). Geochimica et Cosmochimica Acta, 74:5549-5559.

Heimbürger, L.E., J.E. Sonke, D. Cossa, D. Point, C. Lagane, L. Laffont, B.T. Galfond, M. Nicolaus, B. Rabe and M.R. van der Loeff, 2015. Shallow methylmercury production in the marginal sea ice zone of the central Arctic Ocean. Scientific Reports, 5. doi:10.1038/srep10318.

Heinz, G.H., D.J. Hoffman, J.D. Klimstra, K.R. Stebbins, S.L. Kondrad and C.A. Erwin, 2009. Species differences in the sensitivity of avian embryos to methylmercury. Archives of Environmental Contamination and Toxicology, 56:129-138.

Henny, C.J., M.A. Yates and W.S. Seegar, 2009a. Dramatic declines of DDE and other organochlorines in spring migrant peregrine falcons from Padre Island, Texas, 1978-2004. Journal of Raptor Research, 43:37-42.

Henny, C.J., J.L. Kaiser and R.A. Grove, 2009b. PCDDs, PCDFs, PCBs, OC pesticides and mercury in fish and osprey eggs from Willamette River, Oregon (1993, 2001 and 2006) with calculated biomagnification factors. Ecotoxicology, 18:151-173.

Herring, G., C.A. Eagles-Smith and J.T. Ackerman, 2017. Mercury exposure may influence fluctuating asymmetry in waterbirds. Environmental Toxicology and Chemistry, 36:1599-605.

Hirdman, D., K. Aspmo, J.F. Burkhart, S. Eckhardt, H. Sodemann and A. Stohl, 2009. Transport of mercury in the Arctic atmosphere: Evidence for a spring-time net sink and summer-time source. Geophysical Research Letters, 36:L12814, doi:10.1029/2009GL038345.

Holmes, C.D., D.J. Jacob, E.S. Corbitt, J. Mao, X. Yang, R. Talbot and F. Slemr, 2010. Global atmospheric model for mercury including oxidation by bromine atoms. Atmospheric Chemistry and Physics, 10:12037-12057.

Holmes, C.D., N.P. Krishnamurthy, J.M. Caffrey, W.M. Landing, E.S. Edgerton, K.R. Knapp and U.S. Nair, 2016. Thunderstorms increase mercury wet deposition. Environmental Science and Technology, 50:9343-9350.

Horowitz, H.M., D.J. Jacob, H.M. Amos, D.G. Streets and E.M. Sunderland, 2014. Historical mercury releases from commercial products: global environmental implications. Environmental Science and Technology, 48:10242-10250.

Horowitz, H.M., D.J. Jacob, Y. Zhang, T.S. Dibble, H.M. Amos, J.A. Schmidt, E.S. Corbitt, E.A. Marais and E.M. Sunderland, 2017a. A new mechanism for atmospheric mercury redox chemistry: implications for the global mercury budget. Atmospheric Chemistry and Physics, 17:6353-6371.

Horowitz, H.M., D.J. Jacob, Y. Zhang, T.S. Dibble, F. Slemr, H.M. Amos, J.A. Schmidt, E.S. Corbitt, E.A. Marais and E.M. Sunderland, 2017b. A new mechanism for atmospheric mercury redox chemistry: Implications for the global mercury budget. Atmospheric Chemistry and Physics Discussions, 1-33, 10.5194/acp-2016-1165.

Hossaini, R., M.P. Chipperfield, S.A. Montzka, A. Rap, S. Dhomse and W. Feng, 2015. Efficiency of short-lived halogens at influencing climate through depletion of stratospheric ozone. Nature Geoscience, 8:186-190.

Hsu-Kim, H., K.H. Kucharzyk, T. Zhang and M.A. Deshusses, 2013. Mechanisms regulating mercury bioavailability for methylating

microorganisms in the aquatic environment: a critical review. Environmental Science and Technology, 47:2441-2456.

Hsu-Kim, H., C.S. Eckley, D. Achá, X. Feng, C.C. Gilmour, S. Jonsson and C.P. Mitchell, 2018. Challenges and opportunities for managing aquatic mercury pollution in altered landscapes. Ambio, 47:141-169.

Huang, J. and M.S. Gustin, 2015. Use of passive sampling methods and models to understand sources of mercury deposition to high elevation sites in the western United States. Environmental Science and Technology, 49:432-441.

Huang, X., M. Li, H. Friedli, Y. Song, D. Chang and L. Zhu, 2011. Mercury emissions from biomass burning in China. Environmental Science & Technology, 45:9442-9448.

Huang, J., H.D. Choi, M.S. Landis and T.M. Holsen, 2012a. An application of passive samplers to understand atmospheric mercury concentration and dry deposition spatial distributions. Journal of Environmental Monitoring, 14:2976-2982.

Huang, J., S.C. Kang, Q.G. Zhang, H.Y. Yan, J.M. Guo, M.G. Jenkins, G.S. Zhang and K. Wang, 2012b. Wet deposition of mercury at a remote site in the Tibetan Plateau: Concentrations, speciation, and fluxes. Atmospheric Environment, 62:540-550.

Huang, J., F.-C. Chang, S. Wang, Y.-J. Han, M. Castro, E. Miller and T.M. Holsen, 2013. Mercury wet deposition in the eastern United States: characteristics and scavenging ratios. Environmental Science Processes and Impacts, 15:2321-2328.

Huang, J., M.B. Miller, E. Edgerton and M.S. Gustin, 2016. Deciphering the chemical forms of gaseous oxidized mercury in Florida, USA. Atmospheric Chemistry and Physics Discussions, 1-26, 10.5194/acp-2016-725.

Hughes, K.D., P.J. Ewins and K.E. Clark, 1997. A comparison of mercury levels in feathers and eggs of osprey (*Pandion haliaetus*) in the North American Great Lakes. Archives of Environmental Contamination and Toxicology, 33:441-452.

Hui, M., Q. Wu, S. Wang, S. Liang, L. Zhang, F. Wang, M. Lenzen, Y. Wang, L. Xu, Z. Lin, H. Yang, Y. Lin, T. Larssen, M. Xu and J. Hao, 2017. Mercury flows in China and global drivers. Environmental Science and Technology, 51:222-231.

Hutcheson, M.S., C.M. Smith, J. Rose, C. Batdorf, O. Pancorbo, C.R. West, J. Strube and C. Francis, 2014. Temporal and spatial trends in freshwater fish tissue mercury concentrations associated with mercury emissions reductions. Environmental Science and Technology, 48:2193-2202.

Hylander, L.D. and R.B. Herbert, 2008. Global emissions and production of mercury during the pyrometallurgical extraction of nonferrous sulfide ores. Environmental Science and Technology, 42:5971-5977.

IEA, 2016. World Energy Statistics (2016 edition). International Energy Agency, Paris, France.

IEA, 2017. World Energy Statistics (2017 edition). International Energy Agency, Paris, France.

IJC, 2015. Atmospheric Deposition of Mercury in the Great Lakes Basin. International Joint Commission (IJC), Ottawa.

IKIMP, 2012. Mercury arising from oil and gas production in the United Kingdom and UK continental shelf. By: Lang, D., M. Gardner and J. Holmes. Integrating Knowledge to Inform Mercury Policy (IKIMP). University of Oxford.

IOTC, 2016. Report of the 19th Session of the IOTC Scientific Committee. Indian Ocean Tuna Commission (IOTC), Seychelles, 1-5 December 2016.

IPCS, 1990. Methylmercury. Environmental Health Criteria 101. World Health Organization, International Programme on Chemical Safety (IPCS). www.inchem.org/documents/ehc/ehc/ehc101.htm (Accessed 30 November 2017).

IPCS, 2003. Elemental Mercury and Inorganic Mercury Compounds: Human Health Aspects. World Health Organization, International Programme on Chemical Safety (IPCS). Concise international chemical assessment document No. 50.

IPIECA, 2012. Industry input to the UN global mercury treaty negotiations focus on oil and gas. By: Doll, B.E., B.M. Knickerbocker and E. Nucci. The global oil and gas industry association for environmental and social issues (IPIECA).

IPIECA, 2014. Mercury management in petroleum refining. International Petroleum Industry Environmental Conservation Association (IPIECA) Operations Good Practice Series 2014.

IPIECA, 2016. International Petroleum Industry Environmental Conservation Association, Mercury Emissions in the Oil & Gas industry, November 2016. UNEP Discussions.

Jackson, A.K., D.C. Evers, M.A. Etterson, A.M. Condon, S.B. Folsom, J. Detweiler, J. Schmerfeld and D.A. Cristol, 2011a. Mercury exposure affects the reproductive success of free-living terrestrial songbird, the Carolina wren (*Thryothorus ludovicianus*). Auk, 128:759-769.

Jackson, A.K., D.C. Evers, S.B. Folsom, A.M. Condon, J. Diener, L.F. Goodrick, A.J. McGann, J. Schmerfeld, D.A. Cristol, 2011b. Mercury exposure in terrestrial birds far downstream of an historical point source. Environmental Pollution, 159:3302-3308.

Jackson, A.K., D.C. Evers, E. Adams, C.A. Eagles-Smith, C. Osborne, O. Lane, S. Edmonds, T. Tear, D. Cristol, A. Sauer and N. O'Driscoll, 2015. Mercury exposure in songbirds of eastern North America across habitats and guilds. Ecotoxicology, 24:453-467.

Jackson, A.K., D.C. Evers, C.A. Eagles-Smith, J.T. Ackerman, J.J. Willacker, J.E. Elliot, J.M. Lepak, S.S. Vander Pol and C.E. Bryan, 2016. Mercury risk to avian piscivores across the western United States and Canada. Science of the Total Environment, 568:685-696.

Jaffe, D., E. Prestbo, P. Swartzendruber, P. Weiss-Penzias, S. Kato, A. Takami, S. Hatakeyama and Y. Kajii, 2005. Export of atmospheric mercury from Asia. Atmospheric Environment, 39:3029-3038.

Jaffe D.A., S. Lyman, H. Amos, M.S. Gustin, J. Huang, N. Selin, L. Levin, A. ter Schure, R. Mason, R. Talbot, A. Rutter, B. Finley, L. Jaeglé, V. Shah, C. McClure, J.L. Ambrose, L. Gratz, S. Lindberg, P. Weiss, G. Edwards, 2014. Progress on understanding atmospheric mercury hampered by uncertain measurements. Environmental Science and Technology, 48:7204-7206.

James, J.Z., D. Lucas and C. Koshland, 2013. Elemental mercury vapor interaction with individual gold nanorods. Analyst, 138:2323-2328.

Jardine, T.D., K.A. Kidd and N. O'Driscoll, 2013. Food web analysis reveals effects of pH on mercury bioaccumulation at multiple trophic levels in streams. Aquatic Toxicology, 132-133:46-52.

JECFA, 2004. Evaluation of Certain Food Additives and Contaminants. Sixty-first report of the Joint FAO/WHO Expert Committee on Food Additives (JECFA). World Health Organization (WHO) Technical Report Series 922.

JECFA, 2007a. Methylmercury (addendum). In: Safety Evaluation of Certain Food Additives and Contaminants. Prepared by the sixty-seventh meeting of the Joint FAO/WHO Expert Committee on Food Additives (JECFA). Food Additives Series 58. pp. 269-315.

JECFA, 2007b. Methylmercury. In: Evaluation of Certain Food Additives and Contaminants. Sixty-seventh Report of the Joint FAO/WHO Expert Committee on Food Additives. Geneva: World Health Organization/ Food and Agriculture Organization (JECFA). WHO Technical Report Series 940. pp. 53-59.

JECFA, 2011. Safety Evaluation of Certain Contaminants in Food. Prepared by the seventy-second meeting of the Joint FAO/WHO Expert Committee on Food Additives (JECFA). WHO Food Additives Series 63.

Jedrychowski, W., J. Jankowski, E. Flak, A. Skarupa, E. Mroz, E. Sochacka-Tatara, I. Lisowska-Miszczyk, A. Szpanowska-Wohn, V. Rauh, Z. Skolicki, I. Kaim and F. Perera, 2006. Effects of prenatal exposure to mercury on cognitive and psychomotor function in one-year-old infants: epidemiologic cohort study in Poland. Annals of Epidemiology, 16:439-447.

Jiang, H.M., 2005. Effects of hydroelectric reservoir on the biogeochemical cycle of mercury in the Wujiang River. Ph.D. Thesis. Graduate School of the Chin. Acad. of Sci., Beijing. (In Chinese, with English abstract)

Jiang, Y., J.V. Cizdziel and D. Lu, 2013. Temporal patterns of atmospheric mercury species in northern Mississippi during 2011-2012: Influence of sudden population swings. Chemosphere, 93:1694-1700.

Jiao, Y. and T.S. Dibble, 2015. Quality structures, vibrational frequencies, and thermochemistry of the products of reaction of BrHg• with NO_2, HO_2, ClO, BrO, and IO. Journal of Physical Chemistry A, 119:10502-10510.

Jiao, Y. and T.S. Dibble, 2017. First kinetic study of the atmospherically important reactions BrHg• + NO_2 and BrHg• + HOO. Physical Chemistry Chemical Physics, 19:1826-1838.

Jinadasa, B.K.K.K., E.M.R.K.B. Edirisinghe and I. Wickramasinghe, 2014. Total mercury, cadmium and lead levels in main export fish of Sri Lanka. Food Additives and Contaminants B, 7:309-314.

Jiskra, M., J. Sonke, D. Obrist, J. Bieser, R. Ebinghaus, C. Myhre, K.A. Pfaffhuber, I. Wängberg, K. Kyllönen, D. Worthy, L. Martin, C. Labuschagne, T. Mkololo, M. Ramonet, O. Magand and A. Dommergue, 2018. A vegetation control on seasonal variations in global atmospheric mercury. Nature Geoscience, 11:244-250.

Johnels, A.G., T. Westermark, W. Berg, P.I. Persson and B. Sjöstrand, 1967. Pike (*Esox lucius* L.) and some other aquatic organisms in Sweden as indicators of mercury contamination in the environment. Oikos, 1967:323-333.

Johnson, D.A. and K. Whittle, 1999. The chemistry of the Hispanic-American amalgamation process. Journal of the Chemical Society, Dalton Transactions, 1999:4239-4243.

Joint Research Centre, 2014. Best Available Techniques (BAT) Reference Document for the Non-Ferrous Metal Industries. Final Draft, October 2014. European Commission, Joint Research Centre.

Jonsson, S., U. Skyllberg, M.B. Nilsson, P.-O. Westlund, A. Shchukarev, E. Lundberg and E. Björn, 2012. Mercury methylation rates for geochemically relevant HgII species in sediments. Environmental Science and Technology, 46:11653-11659.

Jonsson, S., U. Skyllberg, M.B. Nilsson, E. Lundberg, A. Andersson and E. Björn, 2014. Differentiated availability of geochemical mercury pools controls methylmercury levels in estuarine sediment and biota. Nature Communications, 5, art. no. 4624.

Jonsson, S., A. Andersson, M.B. Nilsson, U. Skyllberg, E. Lundberg, J.K. Schaefer, S.Å. and E. Björn, 2017. Terrestrial discharges mediate trophic shifts and enhance methylmercury accumulation in estuarine biota. Science Advances, 3:e1601239.

Jourdain, L., T.J. Roberts, M. Pirre and B. Josse, 2016. Modeling the reactive halogen plume from Ambrym and its impact on the troposphere with the CCATT-BRAMS mesoscale model. Atmospheric Chemistry and Physics, 16:12099-12125.

Jung, G., I.M. Hedgecock and N. Pirrone, 2009. ECHMERIT V1.0 – a new global fully coupled mercury-chemistry and transport model. Geoscientific Model Development, 2:175-195.

Kabir, K.M., S.J. Ippolito and G.I. Matthews, 2015. Determining the optimum exposure and recovery periods for efficient operation of a QCM based elemental mercury vapor sensor. Journal of Sensors, 2015:727432.

Kalisinska, E., J. Gorecki, N. Lanocha, A. Okonska, J.B. Melgarejo, H. Budis, I. Rzad and J. Golas, 2014. Total and methylmercury in soft tissues of white-tailed eagle (*Haliaeetus albicilla*) and osprey (*Pandion haliaetus*) collected in Poland. Ambio, 43:858-870.

Kamal, A.S.M., K. Goyer, T. Koottatep, A.T.M.N. Amin, 2008. Domestic wastewater management in South and Southeast Asia: the potential benefits of a decentralised approach. Urban Water Journal, 5:345-354.

Kamman, N.C., N.M. Burgess, C.T. Driscoll, H.A. Simonin, W. Goodale, J. Linehan, R. Estabrook, M. Hutcheson, A. Major, A.M. Scheuhammer and D.A. Scruton, 2005. Mercury in freshwater fish of northeast North America – a geographic perspective based on fish tissue monitoring databases. Ecotoxicology, 14:163-180.

Kamp, J., H. Skov, B. Jensen and L.L. Sørensen, 2018. Fluxes of gaseous elemental mercury (GEM) in the High Arctic during atmospheric mercury depletion events (AMDEs). Atmospheric Chemistry and Physics, 18:6923-6938.

Kang, T.1., S.M. Yoo, I. Yoon, S. Lee, J. Choo, S.Y. Lee and B. Kim, 2011. Au nanowire-on-film SERRS sensor for ultrasensitive Hg2+ detection. Chemistry, 17:2211-2214.

Kang, S., J. Huang, F. Wang, Q. Zhang, Y. Zhang, C. Li, L. Wang, P. Chen, C. Sharma, Q. Li, M. Sillanpää, J. Hou, B. Xu and J. Guo, 2016. Atmospheric mercury depositional chronology reconstructed from lake sediment and ice cores in the Himalayas and Tibetan Plateau. Environmental Science and Technology, 50:2859-2869.

Karagas, M.R., A.L. Choi, E. Oken, M. Horvat, R. Schoeny, E. Kamai, W. Cowell, P. Grandjean and S. Korrick, 2012. Evidence on the human health effects of low-level methylmercury exposure. Environmental Health Perspectives, 120:799-806.

Kaulfus, A.S., U.S. Nair, C.D. Holmes and W.M. Landing, 2017. Mercury wet scavenging and deposition differences by precipitation type. Environmental Science and Technology, 51:2628-2634.

Kenney, L.A., C.A. Eagles-Smith, J.T. Ackerman and F.A. von Hippel, 2014. Temporal variation in fish mercury concentrations within lakes from the western Aleutian archipelago, Alaska. PloS ONE, 9(7):102244.

Kim, J.-H., J-M. Park, S-B. Lee, D.Pudasainee and Y-C. Seo, 2010a. Anthropogenic mercury emission inventory with emission factors and total emission in Korea. Atmospheric Environment, 44:2714-2721.

Kim, J.H., D. Pudasainee, Y.-S. Yoon, S.-U. Son and Y.-C. Seo, 2010b. Studies on speciation changes and mass distribution of mercury in a bituminous coal-fired power plant by combining field data and chemical equilibrium calculation. Industrial and Engineering Chemistry Research, 49:5197-5203.

Kim, B.M., B.E. Lee, Y.C. Hong, H. Park, M. Ha, Y.J. Kim, Y. Kim, N. Chang, B.N. Kim, S.Y. Oh, M. Yoo and E.H. Ha, 2011. Mercury levels in maternal and cord blood and attained weight through the 24 months of life. Science of the Total Environment, 410-411:26-33.

Kim, E., H. Kim, K.H. Shin, M.S. Kim, S.R. Kundu, B.G. Lee and S. Han, 2012. Biomagnification of mercury through the benthic food webs of a temperate estuary: Masan Bay, Korea. Environmental Toxicology and Chemistry, 31:1254-1263.

Kim, H., A.L. Soerensen, J. Hur, L.E. Heimburger, D. Hahm, T.S. Rhee, S. Noh and S. Han, 2017. Methylmercury mass budgets and distribution characteristics in the western Pacific Ocean. Environmental Science and Technology, 51:1186-1194.

Kindbom, K. and J. Munthe, 1998. Hur påverkas kvicksilver i miljön av olika energialternativ? En förstudie fokuserad på biobränslen. IVL B 1299.

Kinghorn, A., P. Solomon and H.M. Chan, 2007. Temporal and spatial trends of mercury in fish collected in the English-Wabigoon river system in Ontario, Canada. Science of the Total Environment, 372:615-623.

Kirk, J.L., V.L. St. Louis and M.J. Sharp, 2006. Rapid reduction and reemission of mercury deposited into snowpacks during atmospheric mercury depletion events at Churchill, Manitoba, Canada. Environmental Science and Technology, 40:7590-7596.

Kirk, L.E., J.S. Jørgensen, F. Nielsen and P. Grandjean, 2017. Public health benefits of hair-mercury analysis and dietary advice in lowering methylmercury exposure in pregnant women. Scandinavian Journal of Public Health, 45:444-451.

Kiszka, J.J., A. Aubail, N.E. Hussey, M.R. Heithaus, F. Caurant and P. Bustamante, 2015. Plasticity of trophic interactions among sharks from the oceanic south-western Indian Ocean revealed by stable isotope and mercury analyses. Deep Sea Research I, 96:49-58.

Klenavic, K., L. Champoux, P.Y. Daoust, R.D. Evans and H.E. Evans, 2008. Mercury concentrations in wild mink (*Mustela vison*) and river otters (*Lontra canadensis*) collected from eastern and Atlantic Canada: relationship to age and parasitism. Environmental Pollution, 156:359-366.

Knobeloch, L., C. Tomasallo and H. Anderson, 2011. Biomonitoring as an intervention against methylmercury exposure. Public Health Reports, 126:568-574.

Kock, H., E. Bieber, R. Ebinghaus, T. Spain and B. Thees, 2005. Comparison of long-term trends and seasonal variations of atmospheric mercury concentrations at the two European coastal monitoring stations Mace Head, Ireland, and Zingst, Germany. Atmospheric Environment, 39:7549-7556.

Kocman, D. and M. Horvat, 2010. A laboratory based experimental study of mercury emission from contaminated soils in the River Idrijca catchment. Atmospheric Chemistry and Physics, 10:1417-1426.

Kocman, D., M. Horvat, N. Pirrone and S. Cinnirella, 2013. Contribution of contaminated sites to the global mercury budget. Environmental Research, 125:160-170.

Kocman, D., S.J. Wilson, H.M. Amos, K.H. Telmer, F. Steenhuisen, E.M. Sunderland, R.P. Mason, P. Outridge and M. Horvat, 2017. Toward an assessment of the global inventory of present-day mercury releases to freshwater environments. International Journal of Environmental Research and Public Health, 14:138. doi:10.3390/ijerph14020138.

Kojadinovic, J., M. Potier, M. Le Corre, R.P. Cosson and P. Bustamante, 2006. Mercury content in commercial pelagic fish and its risk assessment

in the Western Indian Ocean. Science of the Total Environment, 366:688-700.

Kojadinovic, J., P. Bustamante, C. Churlaud, R.P. Cosson and M. Le Corre, 2007. Mercury in seabird feathers: Insight on dietary habits and evidence for exposure levels in the western Indian Ocean. Science of the Total Environment, 384:194-204.

Korstian, J.M., M.M. Chumchal, V.J. Bennett and A.M. Hale, 2018. Mercury contamination in bats from the central United States. Environmental Toxicology and Chemistry, 37:160-165.

Kos, G., A. Ryzhkov, A. Dastoor, J. Narayan, A. Steffen, P.A. Ariya and L. Zhang, 2013. Evaluation of discrepancy between measured and modelled oxidized mercury species. Atmospheric Chemistry and Physics, 13:4839-4863.

Kotnik, J., M. Horvat and T. Dizdarevic, 2005. Current and past mercury distribution in air over the Idrija Hg mine region, Slovenia. Atmospheric Environment, 39:7570-7579.

Krey, A., S.K. Ostertag and H.M. Chan, 2015. Assessment of neurotoxic effects of mercury in beluga whales (*Delphinapterus leucas*), ringed seals (*Pusa hispida*), and polar bears (*Ursus maritimus*) from the Canadian Arctic. Science of the Total Environment, 509:237-247.

Kribek, B., V. Majer, F. Veselovsky and I. Nyambe, 2010, Discrimination of lithogenic and anthropogenic sources of metals and sulphur in soils of the central-northern part of the Zambian Copperbelt Mining District: A topsoil vs. subsurface soil concept. Journal of Geochemical Exploration, 104:69-86.

Król, S., B. Zabiegała and J. Namiesnik, 2010. Monitoring VOCs in atmospheric air II. Sample collection and preparation. TrAC Trends in Analytical Chemistry, 29:1101-1112.

Kumari, R., 2011, Preliminary mercury emission estimates from non-ferrous metal smelting in India. Atmospheric Pollution Research, 2:513-519.

Kwon, S.Y. and N.E. Selin, 2016. Uncertainties in atmospheric mercury modeling for policy evaluation. Current Pollution Reports, 2:103-114.

Kwon, S.Y., J.D. Blum, C.Y. Chen, D.E. Meattey, D.E. and R.P. Mason, 2014. Mercury isotope study of sources and exposure pathways of methylmercury in estuarine food webs in the Northeastern US. Environmental Science and Technology, 48:10089-10097.

Laacouri, A., E.A. Nater and R.K. Kolka, 2013. Distribution and uptake dynamics of mercury in leaves of common deciduous tree species in Minnesota, USA. Environmental Science and Technology, 47:10462-10470.

Lacerda, L.D., 2003. Updating global Hg emissions from small-scale gold mining and assessing its environmental impact. Environmental Geology 43(3):308-314.

Lalonde, J.D., A.J. Poulain and M. Amyot, 2002. The role of mercury redox reactions in snow on snow-to-air mercury transfer. Environmental Science and Technology, 36:174-178.

Lamborg, C.H., W.F. Fitzgerald, J. O'Donnell and T. Torgersen, 2002a. A non-steady-state compartmental model of global-scale mercury biogeochemistry with interhemispheric atmospheric gradients. Geochimica et Cosmochimica Acta, 66:1105-1118.

Lamborg, C.H., W.F. Fitzgerald, A.W.H. Damman, J.M. Benoit, P.H. Balcom and D.R. Engstrom, 2002b. Modern and historic atmospheric mercury fluxes in both hemispheres: Global and regional mercury cycling implications. Global Biogeochemical Cycles, 16:15.1-15.11.

Lamborg, C.H., C.R. Hammerschmidt, G.A. Gill, R.P. Mason and S. Gichuki, 2012. An intercomparison of procedures for the determination of total mercury in seawater and recommendations regarding mercury speciation during GEOTRACES cruises. Limnology and Oceanography-Methods, 10:90-100.

Lamborg, C.H., C.R. Hammerschmidt, K.L. Bowman, G.J. Swarr, K.M. Munson, D.C. Ohnemus, P.J. Lam, L.E. Heimbürger, M.J.A. Rijkenberg and M.A. Saito, 2014. A global ocean inventory of anthropogenic mercury based on water column measurements. Nature, 512:65-68.

Lamborg, C.H., C.R. Hammerschmidt and K.L. Bowman, 2016. An examination of the role of particles in oceanic mercury cycling. Philosophical Transactions of the Royal Society A, 374 (2081), 10.1098/rsta.2015.0297.

Landrigan, P.J., R. Fuller, N.J.R. Acosta, O. Adeyi, R. Arnold, N.N. Basu, A.B. Baldé, R. Bertollini, S. Bose-O'Reilly, J.I. Boufford, P.N. Breysse, T. Chiles, C. Mahidol, A.M. Coll-Seck, M.L. Cropper, J. Fobil, V. Fuster, M.

Greenstone, A. Haines, D. Hanrahan, D. Hunter, M. Khare, A. Krupnick, B. Lanphear, B. Lohani, K. Martin, K.V. Mathiasen, M.A. McTeer, C.J.L. Murray, J.D. Ndahimananjara, F. Perera, J. Potočnik, A.S. Preker, J. Ramesh, J. Rockström, C. Salinas, L.D. Samson, K. Sandilya, P.D. Sly, K.R. Smith, A. Steiner, R.B. Stewart, W.A. Suk, O.C.P. van Schayck, G.N. Yadama, K. Yumkella and M. Zhong, 2018. The Lancet Commission on pollution and health. Lancet, 391:462-512.

Lane, O.P., K.M. O'Brien, D.C. Evers, T.P. Hodgman, A. Major, N. Pau, M.J. Ducey, R. Taylor and D. Perry, 2011. Mercury in breeding saltmarsh sparrows (*Ammodramus caudacutus*). Ecotoxicology, 20:1984-1991.

Lane, O.P., W.J. Arendt, M.A. Tórrez and J.C.G. Castellón, 2013. Pilot assessment of mercury exposure in selected biota from the lowlands of Nicaragua. Mesoamericana, 17:19-28.

Lang, X., 2014. Mercury in atmospheric precipitation and litterfall in Mt.Ailao and Mt.Damei. Master's dissertation. Guizhou University, Guiyang, China. (In Chinese)

Larose, C., A. Dommergue, M. De Angelis, D. Cossa, B. Averty, N. Marusczak, N. Soumis, D. Schneider and C. Ferrari, 2010. Springtime changes in snow chemistry lead to new insights into mercury methylation in the Arctic. Geochimica et Cosmochimica Acta, 74:6263-6275.

Larssen, T., 2010. Mercury in Chinese reservoirs. Environmental Pollution, 158:24-25.

Laurier, F.J.G., D. Cossa, C. Beucher and E. Breviere, 2007. The impact of groundwater discharges on mercury partitioning, speciation and bioavailability to mussels in a coastal zone. Marine Chemistry, 104:143-155.

Lavoie, R.A., T.D. Jardine, M.M. Chumchal, K.A. Kidd and L.M. Campbell, 2013. Biomagnification of mercury in aquatic food webs: a worldwide meta-analysis. Environmental Science and Technology, 47:13385-13394.

Lebel, J., M. Roulet, D. Mergler, M. Lucotte and F. Larribe, 1997. Fish diet and mercury exposure in a riparian Amazonian population. Water, Air and Soil Pollution, 97:31-44.

Lederman, S.A., R.L. Jones, K.L. Caldwell, V. Rauh, S.E. Sheets, D. Tang, S. Viswanathan, M. Becker, J.L. Stein, R.Y. Wang and F.P. Perera, 2008. Relation between cord blood mercury levels and early child development in a World Trade Center cohort. Environmental Health Perspectives, 116:1085-1091.

Lee, C.S. and N.S. Fisher, 2016. Methylmercury uptake by diverse marine phytoplankton. Limnology and Oceanography, 61:1626-1639.

Lee, Y.-G., M.D.M. Rahman, G. Kim and S. Han, 2011. Mass balance of total mercury and monomethylmercury in coastal embayments of a volcanic island: significance of submarine groundwater discharge. Environmental Science and Technology, 45:9891-9900.

Lee, C.S., M.E. Lutcavage, E. Chandler, D.J. Madigan, R.M. Cerrato and N.S. Fisher, 2016. Declining mercury concentrations in bluefin tuna reflect reduced emissions to the North Atlantic Ocean. Environmental Science and Technology, 50:12825-12830.

Legrand, M., M. Feeley, C. Tikhonov, D. Schoen and A. Li-Muller, 2010. Methylmercury blood guidance values for Canada. Canadian Journal of Public Health, 101:28-31.

Lehnherr, I., 2014. Methylmercury biogeochemistry: a review with special reference to Arctic aquatic ecosystems. Environmental Reviews, 22:229-243.

Lehnherr, I. and V. St. Louis, 2009. Importance of ultraviolet radiation in the photodemethylation of methylmercury in freshwater ecosystems. Environmental Science and Technology, 43:5692-5698.

Lehnherr, I., V.L. St. Louis, H. Hintelmann and J.L. Kirk, 2011. Methylation of inorganic mercury in polar marine waters. Nature Geoscience, 4:298-302.

Lei, H., X.Z. Liang, D.J. Wuebbles and Z. Tao, 2013. Model analyses of atmospheric mercury: present air quality and effects of transpacific transport on the United States. Atmospheric Chemistry and Physics, 13:10807-10825.

Lei, H., D.J. Wuebbles, X.-Z. Liang, Z. Tao, S. Olsen, R. Artz, X. Ren and M. Cohen, 2014. Projections of atmospheric mercury levels and their effect on air quality in the United States. Atmospheric Chemistry and Physics, 14:783-795.

Lepak, R.F., R. Yin, D.P. Krabbenhoft, J.M. Ogorek, J.F. DeWild, T.M. Holsen and J.P. Hurley, 2015. Use of stable isotope signatures to determine

mercury sources in the Great Lakes. Environmental Science and Technology Letters, 2:335-341.

Lescord, G.L., T.A. Johnston, B.A. Branfireun and J.M. Gunn, 2018. Percentage of methylmercury in the muscle tissue of freshwater fish varies with body size and age and among species. Environmental Toxicology and Chemistry, 37:2682-2691.

Li, S.X., L.F. Zhou, H.J. Wang, Y.G. Liang, J.X. Hu and J.B. Chang, 2009. Feeding habits and habitats preferences affecting mercury bioaccumulation in 37 subtropical fish species from Wujiang River, China. Ecotoxicology, 18:204-210.

Li, G., X. Feng, Z. Li, G. Qiu, L. Shang, P. Liang, D. Wang and Y. Yang, 2010. Mercury emission to atmosphere from primary Zn production in China. Science of the Total Environment, 408:4607-4612.

Li, Z., C.H. Xia, X.M. Wang, Y.R. Xiang and Z.Q. Xie, 2011. Total gaseous mercury in Pearl River Delta region, China during 2008 winter period. Atmospheric Environment, 45:834-838.

Li, S.X., L.F. Zhou, H.J. Wang, M.H. Xiong, Z. Yang, J.X. Hu, Y.G. Liang and J.B. Chang, 2013. Short-term impact of reservoir impoundment on the patterns of mercury distribution in a subtropical aquatic ecosystem, Wujiang River, southwest China. Environmental Science and Pollution Research, 20:4396-4404.

Li, R., H. Xu, M. Chai and G.Y. Qiu, 2016a. Distribution and accumulation of mercury and copper in mangrove sediments in Shenzhen, the world's most rapid urbanized city. Environmental Monitoring and Assessment, 188:87. doi.org/10.1007/s10661-016-5103-z

Li, M., A.T. Schartup, A.P. Valberg, J.D. Ewald, D.P. Krabbenhoft, R. Yin, P.H. Balcom and E.M. Sunderland, 2016b. Environmental origins of methylmercury accumulated in subarctic estuarine fish indicated by mercury stable isotopes. Environmental Science and Technology, 50:11559-11568.

Liem-Nguyen, V., S. Jonsson, U. Skyllberg, M.B. Nilsson, A. Andersson, E. Lundberg and E. Björn, 2016. Effects of nutrient loading and mercury chemical speciation on the formation and degradation of methylmercury in estuarine sediment. Environmental Science and Technology, 50:6983-6990.

Lin, C.J., M.S. Gustin, P. Singhasuk, C. Eckley and M. Miller, 2010a. Empirical models for estimating mercury flux from soils. Environmental Science and Technology, 44:8522-8528.

Lin, C.J., L. Pan, D.G. Streets, S.K. Shetty, C. Jang, X. Feng, H.W. Chu and T.C. Ho, 2010b. Estimating mercury emission outflow from East Asia using CMAQ-Hg. Atmospheric Chemistry and Physics, 10:1853-1864.

Lin, Y., S. Wang, Q. Wu and T. Larssen, 2016. Material flow for the intentional use of mercury in China. Environmental Science and Technology, 50:2337-2344.

Lin, H., W. Zhang, C. Deng, Y. Tong, Q. Zhang and X. Wang, 2017. Evaluation of passive sampling of gaseous mercury using different sorbing materials. Environmental Science and Pollution Research, 24:14190-14197.

Lindberg, S.E., H. Zhang, M. Gustin, A. Vette, F. Marsik, J. Owens, A. Casimir, R. Ebinghaus, G. Edwards, C. Fitzgerald, J. Kemp, H.H. Kock, J. London, M. Majewski, L. Poissant, M. Pilote, P. Rasmussen, F. Schaedlich, D. Schneeberger, J. Sommar, R. Turner, D. Wallschlager and Z. Xiao, 1999. Increases in mercury emissions from desert soils in response to rainfall and irrigation. Journal of Geophysical Research: Atmospheres, 104:21879-21888.

Lindberg, S.E., S. Brooks, C.-J. Lin, K. Scott, T. Meyers, L. Chambers, M. Landis and R. Stevens, 2001. Formation of reactive gaseous mercury in the Arctic: evidence of oxidation of Hg[0] to gas-phase Hg-II compounds after Arctic sunrise. Water Air and Soil Pollution: Focus, 1:295-302.

Lindberg, S.E., S. Brooks, C.-L. Lin, K.J. Scott, M.S. Landis, R.K. Stevens, M.E. Goodsite and A. Richter, 2002. Dynamic oxidation of gaseous mercury in the arctic troposphere at polar sunrise. Environmental Science and Technology, 36:1245-1256.

Lindberg, S., R. Bullock, R. Ebinghaus, D. Engstrom, X.B. Feng, W. Fitzgerald, N. Pirrone, E. Prestbo and C.A. Seigneur, 2007. A synthesis of progress and uncertainties in attributing the sources of mercury in deposition. Ambio, 36:19-32.

Link, B., T. Gabrio, I. Piechotowski, I. Zöllner and M. Schwenk, 2007. Baden-Wuerttemberg Environmental Health Survey (BW-EHS) from 1996 to 2003: toxic metals in blood and urine of children. International Journal of Hygiene and Environmental Health, 210:357-371.

Little, M.E., N.M. Burgess, H.G. Broders and L.M. Campbell, 2015. Distribution of mercury in archived fur from little brown bats across Atlantic Canada. Environmental Pollution, 207:52-58.

Liu, S.L., F. Nadim, C. Perkins, R.J. Carley, G.E. Hoag, Y.H. Lin and L.T. Chen, 2002. Atmospheric mercury monitoring survey in Beijing, China. Chemosphere, 48:97-107.

Liu, N., G.L. Qiu, X.B. Feng, M. Landis, X.W. Fu and L.H. Shang, 2011. Distribution characteristics of mercury in precipitation of Guiyang, China. Chinese Journal of Ecology, 30:933-938. (In Chinese).

Liu, B., H.Y. Yan, C.P. Wang, Q.H. Li, S. Guedron, J.E. Spangenberg, X.B. Feng and J. Dominik, 2012. Insights into low fish mercury bioaccumulation in a mercury-contaminated reservoir, Guizhou, China. Environmental Pollution, 160:109-117.

Liu, B., L.A. Schaider, R.P. Mason, J.P. Shine, N.N. Rabalais and D.B. Senn, 2015. Controls on methylmercury accumulation in northern Gulf of Mexico sediments. Estuarine, Coastal and Shelf Science, 159:50-59.

Liu, M., W. Zhang, X. Wang, L. Chen, H. Wang, Y. Luo, H. Zhang, H. Shen, Y. Tong, L. Ou, H. Xie, X. Ye and C. Deng, 2016. Mercury release to aquatic environments from anthropogenic sources in China from 2001 to 2012. Environmental Science and Technology, 50:8169-8177.

Liu, M., P. Du, C. Yu, Y. He, H. Zhang, X. Sun, H. Lin, Y. Luo, H. Xie, J. Guo, Y. Tong, Q. Zhang, L. Chen, W. Zhang, X. Li and X. Wang, 2018a. Increases of total mercury and methylmercury releases from municipal sewage into environment in China and implications. Environmental Science and Technology, 52:124-134.

Liu, K., S. Wang, Q. Wu, L. Wang, Q. Ma, L. Zhang, G. Li, H. Tian, L. Duan and J. Hao, 2018b. A highly resolved mercury emission inventory of Chinese coal-fired power plants. Environmental Science and Technology, 52:2400-2408.

LKAB, 2015. Environmental reports 2015 of the LKAB facilities in Malmberget and Kiruna, Sweden.

Llop, S., V. Tran, F. Ballester, F. Barbone, A. Sofianou-Katsoulis, J. Sunyer, K. Engström, A. Alhamdow, T.M. Love, G.E. Watson, M. Bustamante, M. Murcia, C. Iñiguez, C.F. Shamlaye, V. Rosolen, M. Mariuz, M. Horvat, J.S. Tratnik, D. Mazej, E. van Wijngaarden, P.W. Davidson, G.J. Myers, M.D. Rand and K. Broberg, 2017. CYP3A genes and the association between prenatal methylmercury exposure and neurodevelopment. Environment International, 105:34-42.

Lu, J.Y. and W.H. Schroeder, 2004. Annual time-series of total filterable atmospheric mercury concentrations in the Arctic. Tellus, 56B:213-222.

Lu, J.Y., W.H. Schroeder, L.A. Barrie, A. Steffen, H.E. Welch, K. Martin, L. Lockhart, R.V. Hunt, G. Boila and A. Richter, 2001. Magnification of atmospheric mercury deposition to polar regions in springtime: the link to tropospheric ozone depletion chemistry. Geophysical Research Letters, 28:3219-3222.

Lucia, M., N. Verboven, H. Strøm, C. Miljeteig, M.V. Gavrilo, B.M. Braune, D. Boertmann and G.W. Gabrielsen, 2015. Circumpolar contamination in eggs of the high-Arctic ivory gull *Pagophila eburnea*. Environmental Toxicology and Chemistry, 34:1552-1561.

Lucia, M., H. Strøm, P. Bustamante and G.W. Gabrielsen, 2016. Trace element concentrations in relation to the trophic behaviour of endangered ivory gulls (*Pagophila eburnea*) during their stay at a breeding site in Svalbard. Archives of Environmental Contamination and Toxicology, 71:518-529.

Lucotte, M., R. Schetagne, N. Therien, C. Langlois and A. Tremblay, 1999. Mercury in the Biogeochemical Cycle: Natural Environments and Hydroelectric. Springer.

Lusilao-Makiese, J.G., E. Tessier, D. Amouroux, H. Tutu, L. Chimuka, I. Weiersbye and E.M. Cukrowska, 2016. Mercury speciation and dispersion from an active gold mine at the West Wits area, South Africa. Environmental Monitoring and Assessment, 188:47. doi.org/10.1007/s10661-015-5059-4

Lyman, S.N. and D.A. Jaffe, 2012. Formation and fate of oxidized mercury in the upper troposphere and lower stratosphere. Nature Geoscience, 5:114-117.

Lyman, S.N., M.S. Gustin and E.M. Prestbo, 2010a. A passive sampler for ambient gaseous oxidized mercury concentrations, Atmospheric Environment, 44:246-252.

Lyman, S.N., D.A. Jaffe and M.S. Gustin, 2010b. Release of mercury halides from KCl denuders in the presence of ozone. Atmospheric Chemistry and Physics, 10:8197-8204.

Lyman, S., C. Jones, T. O'Neil, T. Allen, M. Miller, M.S. Gustin, A.M. Pierec, L. Winston, X. Ren and P. Kelley, 2016. Automated calibration of atmospheric oxidized mercury measurements. Environmental Science and Technology, 50:12921-12927.

Lynam, M.M., J.T. Dvonch, N.L. Hall, M. Morishita and J.A. Barres, 2014. Spatial patterns in wet and dry deposition of atmospheric mercury and trace elements in central Illinois, USA. Environmental Science and Pollution Research, 21:4032-4043.

Lynch, J.A., K.S. Horner and J.W. Grimm, 2003. Atmospheric deposition: spatial and temporal variations in Pennsylvania 2002, Penn State Institutes of the Environment. The Pennsylvania State University.

Ma, Y., C.R. Perez, B.A. Branfireun and C.G. Guglielmo, 2018. Dietary exposure to methylmercury affects flight endurance in a migratory songbird. Environmental Pollution, 234:894-901.

Maas, R. and P. Grennfelt (eds), 2016. Towards Cleaner Air. Scientific Assessment Report 2016. EMEP Steering Body and Working Group on Effects of the Convention on Long-Range Transboundary Air Pollution, Oslo.

Macagnano, A., V. Perri, E. Zampetti, A.M. Ferretti, F. Sprovieri, N. Pirrone, A. Bearzotti, G. Esposito and F. De Cesare, 2017a. Elemental mercury vapor chemoresistors employing TIO_2 nanofibers photocatalytically decorated with Au-nanoparticles. Sensors and Actuators B, 247:957-967.

Macagnano, A., V. Perri, E. Zampetti, A. Bearzotti, F. De Cesare, F. Sprovieri and N. Pirrone, 2017b. A smart nanofibrous material for adsorbing and detecting elemental mercury in air. Atmospheric Chemistry and Physics, 17:6883-6893.

Macdonald, K.F., M.A. Lund, M.L. Blanchette and C.D. Mccullough, 2014. Regulation of artisanal small scale gold mining (ASGM) in Ghana and Indonesia as currently implemented fails to adequately protect aquatic ecosystems. Proceedings of International Mine Water Association Symposium. pp. 401-405. Xuzhou, China. IMWA. http://ro.ecu.edu.au/ecuworkspost2013/863

Maffucci, F., F. Caurant, P. Bustamante and F. Bentivegna, 2005. Trace element (Cd, Cu, Hg, Se, Zn) accumulation and tissue distribution in loggerhead turtles (Caretta caretta) from the western Mediterranean Sea (southern Italy). Chemosphere, 58:535-542.

Maiz, P., 2008. Informe Final – Inventario Nacional de Liberaciones de Mercurio México 2004 / Final Report – National Inventory of Mercury Releases Mexico 2004. Prepared for: Waste Management Research and Contaminated Sites, Directorate General of the National Environmental Research and Training, National Institute of Ecology, Secretariat of Environment and Natural Resources. Contract INE/ADE-016/2008.

Malik, O.M., A. Hsu and A. Johnson, de Sherbinin, 2015. A global indicator of wastewater treatment to inform the Sustainable Development Goals (SDGs). Environmental Science and Policy, 48:172-185.

Mallory, M.L. and B.M. Braune, 2012. Tracking contaminants in seabirds of Arctic Canada: Temporal and spatial insights. Marine Pollution Bulletin, 64:1475-1484.

Mallory, M.L., M. Wayland, B.M. Braune and K.G. Drouillard, 2004. Trace elements in marine birds, arctic hare and ringed seals breeding near Qikiqtarjuaq, Nunavut, Canada. Marine Pollution Bulletin, 49:136-141.

Mann, E.A., M.L. Mallory, S.E. Ziegler, T.S. Avery, R. Tordon and N.J. O'Driscoll, 2015. Photoreducible mercury loss from Arctic snow is influenced by temperature and snow age. Environmental Science and Technology, 49:12120-12126.

Marcovecchio, J.E., M.S. Gerpe, R.O. Bastida, D.H. Rodríguez and S.G. Morón, 1994. Environmental contamination and marine mammals in coastal waters from Argentina: an overview. Science of the Total Environment, 154:141-151.

Marques, R.C., J.V. Bernardi, J.G. Dórea, K.G. Brandão, L. Bueno, R.S. Leão and O. Malm, 2013. Fish consumption during pregnancy, mercury transfer, and birth weight along the Madeira River Basin in Amazonia. International Journal of Environmental Research and Public Health, 10:2150-2163.

Martin, L.G., C. Labuschagne, E.G. Brunke, A. Weigelt, R. Ebinghaus and F. Slemr, 2017. Trend of atmospheric mercury concentrations at Cape Point for 1995-2004 and since 2007. Atmospheric Chemistry and Physics, 17:2393-2399.

Maruszczak, N., J.E. Sonke, X. Fu and M. Jiskra, 2016. Tropospheric GOM at the Pic du Midi observatory – correcting bias in denuder based observations. Environmental Science and Technology, 51:863-869.

Masbou, J., D. Point, G. Guillou, J.E. Sonke, B. Lebreton and P. Richard, 2015. Carbon stable isotope analysis of methylmercury toxin in biological materials by gas chromatography isotope ratio mass spectrometry. Analytical Chemistry, 87:11732-11738.

Mason, R.P. and W.F. Fitzgerald, 1990. Alkylmercury species in the Equatorial Pacific. Nature, 347: 457-459.

Mason, R.P., W.F. Fitzgerald and F.M.M. Morel, 1994. The biogeochemical cycling of element mercury – anthropogenic influences. Geochimica et Cosmochimica Acta, 58:3191-3198.

Mason, R.P., A.L. Choi, W.F. Fitzgerald, C.R. Hammerschmidt, C.H. Lamborg, A.L. Soerensen and E.M. Sunderland, 2012. Mercury biogeochemical cycling in the ocean and policy implications. Environmental Research, 119:101-117.

Matulik, A.G., D.W. Kerstetter, N. Hammerschlag, T. Divoll, C.R. Hammerschmidt and D.C. Evers, 2017. Bioaccumulation and biomagnification of mercury and methylmercury in four sympatric coastal sharks in a protected subtropical lagoon. Marine Pollution Bulletin, 116:357-364.

Maxson, P., 2009. Mercury Rising: Reducing Global Emissions from Burning Mercury-added Products. Mercury Policy Project. https://www.no-burn.org/mercury-rising-reducing-global-emissions-from-burning-mercury-added-products/

Maxwell, J.A., T.M. Holsen and S. Mondal, 2013. Gaseous elemental mercury (GEM) emissions from snow surfaces in Northern New York. PloS One, 8:e69342.

May Junior, J.A., H. Quigley, R. Hoogesteijn, F.R. Tortao, A. Devlin, R.M. Carvalho Junior, R.G. Mortato, L.R. Sartorello, L.E. Rampim, M. Haberfeld and R.C. Paula, 2017. Mercury content in the fur of jaguars (Panthera onca) from two areas under different levels of gold mining impact in the Brazilian Pantanal. Anais da Academia Brasileira de Ciências, doi.org/10.1590/0001-3765201720170190.

Maz-Courrau, A., C. López-Vera, F. Galvan-Magaña, O. Escobar-Sánchez, R. Rosíles-Martínez and A. Sanjuán-Muñoz, 2012. Bioaccumulation and biomagnification of total mercury in four exploited shark species in the Baja California Peninsula, Mexico. Bulletin of Environmental Contamination and Toxicology, 88:129-134.

Mazrui, N.M., S. Jonsson and R.P. Mason, 2016. Enhanced availability of mercury bound to organic matter for methylation in marine sediments. Geochimica et Cosmochimica Acta, 194:153-162.

Mazur, M., C.P.J. Mitchell, C.S. Eckley, S.L. Eggert, R.K. Kolka, S.D. Sebestyen and E.B. Swain, 2014. Gaseous mercury fluxes from forest soils in response to forest harvesting intensity: A field manipulation experiment. Science of the Total Environment, 496:678-687.

Mazzi, E., S. Glesmann and A. Bell, 2006. Canada Wide Standards Mercury Measurement Methodologies for Coal-fired Power Plants. Paper # 15. EPRI-EPA-DOE-AW&MA Power Plant Air Pollutant Control 'MEGA' Symposium, August 28-31, 2006, Baltimore, Maryland, USA.

McGuire, L., V.J. Hoffman and S. Paulsen, 2009. Bay Area Petroleum Refinery Mercury Air Emissions, Deposition and Fate. Western States Petroleum Association (WSPA), project number 0032209.

McKinney, M.A., S. Pedro, R. Dietz, C. Sonne, A.T. Fisk, D. Roy, B.M. Jenssen and R.J. Letcher, 2015. A review of ecological impacts of global climate change on persistent organic pollutant and mercury pathways and exposures in arctic marine ecosystems. Current Zoology, 61:617-628.

McKinney, M.A., K. Dean, N.E. Hussey, G. Cliff, S.P. Wintner, S.F.J. Dudley, M.P. Zungu and A.T. Fisk, 2016. Global versus local causes and health implications of high mercury concentrations in sharks from the east coast of South Africa. Science of the Total Environment, 541:176-183.

McKinney, M.A., T.C. Atwood, S. Pedro and E. Peacock, 2017. Ecological change drives a decline in mercury concentrations in Southern Beaufort Sea polar bears. Environmental Science and Technology, 51:7814-7822.

McLagan, D.S., M.E.E. Mazur C.P.J. Mitchell and F. Wania, 2016. Passive air sampling of gaseous elemental mercury: a critical review. Atmospheric Chemistry and Physics, 16:3061-3076.

McNicholas, T.P., K. Zhao, C. Yang, S.C. Hernandez, A. Mulchandani, N.V. Myung and M.A. Deshusses, 2011. Sensitive detection of elemental mercury vapor by gold-nanoparticle-decorated carbon nanotube sensors. Journal of Physical Chemistry C, 115:13927-13931.

Megaritis, A.G., B.N. Murphy, P.N. Racherla, P.J. Adams and S.N. Pandis, 2014. Impact of climate change on mercury concentrations and deposition in the eastern United States. Science of the Total Environment, 487:299-312.

Meili, M., 1995. Liming effects on mercury concentrations in fish. In: Henrikson, L. and Y.W. Brodin (eds.), Liming of Acidified Surface Waters – a Swedish Synthesis. pp. 383-398. Springer.

Mendez, E., H. Giudice, A. Pereira, G. Inocente and D. Medina, 2001. Total mercury content – fish weight relationship in swordfish (*Xiphias gladius*) caught in the southwest Atlantic Ocean. Journal of Food Composition and Analysis, 14:453-460.

Meng, B., X.B. Feng, C.X. Chen, G.L. Qiu, J. Sommar, Y.N. Guo and Q. Wan, 2010. Influence of eutrophication on the distribution of total mercury and methylmercury in hydroelectric reservoirs. Journal of Environmental Quality, 39:1624-1635.

Meng, B., X.B. Feng, G.L. Qiu, Z.G. Li, H. Yao, L.H. Shang and H.Y. Yan, 2016. The impacts of organic matter on the distribution and methylation of mercury in a hydroelectric reservoir in Wujiang River, Southwest China. Environmental Toxicology and Chemistry, 35:191-199.

Miljeteig, C., H. Strom, M.V. Gavrilo, A. Volkov, B.M. Jenssen and G.W. Gabrielsen, 2009. High levels of contaminants in ivory gull *Pagophila eburnea* eggs from the Russian and Norwegian Arctic. Environmental Science and Technology, 43:5521-5528.

Miyake, Y., H. Togashi, M. Tashiro, H. Yamaguchi, S. Oda, M. Kudo, Y. Tanaka, Y. Kondo, R. Sawa, T. Fujimoto, T. Machinami and A. Ono, 2006. MercuryII-mediated formation of thymine–HgII–thymine base pairs in DNA duplexes. Journal of American Chemical Society, 128:2172-2173.

Mlakar, T., M. Horvat, T. Vuk, A. Stergarsek, J. Kotnik, J. Tratnik and V. Fajon, 2010. Mercury species, mass flows and processes in a cement plant. Fuel, 89:1936-1945.

Mol, J.H., J.S. Ramlal, C. Lietar and M. Verloo, 2001. Mercury contamination in freshwater, estuarine, and marine fishes in relation to small-scale gold mining in Suriname, South America. Environmental Research, 86:183-197.

Monperrus, M., E. Tessier, D. Amouroux, A. Leynaert, P. Huonnic and O.F.X. Donard, 2007. Mercury methylation, demethylation and reduction rates in coastal and marine surface waters of the Mediterranean Sea. Marine Chemistry, 107:49-63.

Monson, B.A. 2009. Trend reversal of mercury concentrations in piscivorous fish from Minnesota Lakes: 1982–2006. Environmental Science and Technology, 43:1750-1755.

Monson, B.A., D.F. Staples, S.P. Bhavsar, T.M. Holsen, C.S. Schrank, S.K. Moses, D.J. McGoldrick, S.M. Backus and K.A. Williams, 2011. Spatiotemporal trends of mercury in walleye and largemouth bass from the Laurentian Great Lakes region. Ecotoxicology, 20:1555-1567.

Monteiro, L.R. and R.W. Furness, 1995. Seabirds as monitors of mercury in the marine environment. Water, Air and Soil Pollution, 80:851-870.

Monteiro, L.R. and R.W. Furness, 2001. Kinetics, dose-response, and excretion of methylmercury in free-living adult Cory's shearwaters. Environmental Science and Technology, 35:739-746.

Moore, C.W., D. Obrist, A. Steffen, R.M. Staebler, T.A. Douglas, A. Richter and S.V. Nghiem, 2014. Convective forcing of mercury and ozone in the Arctic boundary layer induced by leads in sea ice. Nature, 506:81-84.

Moreno-Brush, M., J. Rydberg, N. Gamboa, I. Storch and H. Biester, 2016. Is mercury from small-scale gold mining prevalent in the southeastern Peruvian Amazon? Environmental Pollution, 218:150-159.

Mott, R., A. Herrod and R.H. Clarke, 2017. Post-breeding dispersal of frigatebirds increases their exposure to mercury. Marine Pollution Bulletin, 119:204-210.

Muckle, G., P. Ayotte, E.E. Dewailly, S.W. Jacobson and J.L. Jacobson, 2001. Prenatal exposure of the northern Québec Inuit infants to environmental contaminants. Environmental Health Perspectives, 109:1291-1299.

Muir, D., B. Braune, B. DeMarch, R. Norstrom, R. Wagemann, L. Lockhart, B. Hargrave, D. Bright, R. Addison, J. Payne and K. Reimer, 1999. Spatial and temporal trends and effects of contaminants in the Canadian Arctic marine ecosystem: A review. Science of the Total Environment, 230:83-144.

Muirhead, S.J. and R.W. Furness, 1988. Heavy metal concentrations in the tissues of seabirds from Gough Island, South Atlantic Ocean. Marine Pollution Bulletin, 19:278-283.

Mukherjee, A.B., P. Bhattacharya, A. Sarkar and R. Zevenhoven, 2008. Mercury emissions from industrial sources in India and its effects in the environment. In: Pirrone, N. and R. Mason (Eds.). Mercury Fate and Transport in the Global Atmosphere, pp. 81-112. Springer.

Munson, K.M., C.H. Lamborg, G.J. Swarr and M.A. Saito, 2015. Mercury species concentrations and fluxes in the Central Tropical Pacific Ocean. Global Biogeochemical Cycles, 29:656-676.

Muntean, M., G. Janssens-Maenhout, S. Song, N.E. Selin, J.G.J. Jos Oliver, D. Guizzardi, R. Maas and F. Dentener, 2014. Trend analysis from 1970 to 2008 and model evaluation of EDGARv4 global gridded anthropogenic mercury emissions. Science of the Total Environment, 494-495:337-350.

Myers, T., R.D. Atkinson, O.R. Bullock Jr. and J.O. Bash, 2013. Investigation of effects of varying model inputs on mercury deposition estimates in the Southwest US. Atmospheric Chemistry and Physics, 13:997-1009.

NADP, 2016. National Atmospheric Deposition Program 2015 Annual Summary. NADP Data Report 2016-02. Illinois State Water Survey, University of Illinois at Urbana-Champaign, IL.

NADP, 2017. National Atmospheric Deposition Program (NADP) Program Office, Illinois State Water Survey, University of Illinois, Champaign, IL 61820. http://nadp.sws.uiuc.edu/maplib/pdf/mdn/hg_Conc_2015.pdf.

Nair, U.S., Y. Wu, C.D. Holmes, A. Ter Schure, G. Kallos and J.T. Walters, 2013. Cloud-resolving simulations of mercury scavenging and deposition in thunderstorms. Atmospheric Chemistry and Physics, 13:10143-10157.

Naves, L.C., 2009. Alaska Migratory Bird Subsistence Harvest Estimates, 2004–2007. Alaska Migratory Bird Co-Management Council. Anchorage.

NCP, 2017. Northern Contaminants Program (NCP). Indigenous and Northern Affairs, Government of Canada. www.science.gc.ca/eic/site/063.nsf/eng/h_7A463DBA.html

Nelson, P.F., H. Nguyen, A.L. Morrison, H. Malfroy, M.E. Cope, M.F. Hibberd, S. Lee, J.L. McGregor and M. Meyer, 2009 (revised April 2011). Mercury Sources, Transportation and Fate in Australia – Final Report to the Department of Environment, Water, Heritage & the Arts. RFT 100/0607.

Nerentorp Mastromonaco, M., K. Gårdfeldt, B. Jourdain, K. Abrahamsson, A. Granfors, M. Anhoff, A. Dommergue, G. Mejan and H.-W. Jacobi, 2016a. Antarctic winter mercury and ozone depletion events over sea ice. Atmospheric Environment, 129:125-132.

Nerentorp Mastromonaco, M., K. Gårdfeldt, S. Langer and A. Dommergue, 2016b. Seasonal study of mercury species in the Antarctic sea ice environment. Environmental Science and Technology, 50:12705-12712.

Nerentorp Mastromonaco, M., K. Gårdfeldt, K.M. Assmann, S. Langerc, T. Delalid, M.Y. Shlyapnikovd, I. Zivkovicd and M. Horvat, 2017. Speciation of mercury in the waters of the Weddell, Amundsen and Ross Seas (Southern Ocean). Marine Chemistry, 193:20-33.

NESHAP, 2010. Summary of Environmental and Cost Impacts of Final Amendments to Portland Cement NESHAP (40 CFR Part 63, subpart LLL). Docket Number EPA-HQ-OAR-2002-0051.

Newtoff, K.N. and S.D. Emslie, 2017. Mercury exposure and diet in brown pelicans (*Pelecanus occidentalis*) in North Carolina, USA. Waterbirds, 40:50-57.

Nghiem, S., I. Rigor, A. Richter, J.P. Burrows, P.B. Shepson, J. Bottenheim, D.G. Barber, A. Steffen, J. Latonas, F. Wang, G. Stern, P. Clemente-Colón, S. Martin, D.K. Hall, L. Kaleschke, P. Tackett, G. Neumann and M.J. Asplin, 2012. Field and satellite observations of the formation and distribution of Arctic atmospheric bromine above a rejuvenated sea ice cover. Journal of Geophysical Research: Atmospheres, 117:D00S05.

Nguetseng, R., A. Fliedner, B. Knopf, B. Lebreton, M. Quack and H. Rüdel, 2015. Retrospective monitoring of mercury in fish from selected European freshwater and estuary sites. Chemosphere, 134:427-434.

Nguyen, H.T., K.H. Kim, K.Y. Kim, S. Hong, Y.H. Youn, Z.H. Shon and J.S. Lee, 2007. Monitoring of atmospheric mercury at a global atmospheric watch (GAW) site on An-Myun Island, Korea. Water, Air and Soil Pollution, 185:149-164.

Nguyen, D.L., J.Y. Kim, S.G. Shim and X.S. Zhang, 2011. Ground and shipboard measurements of atmospheric gaseous elemental mercury over the Yellow Sea region during 2007-2008. Atmospheric Environment, 45:253-260.

Niane, B., S. Guédron, R. Moritz, C. Cosio, P.M. Ngom, N. Deverajan, H.R. Pfeifer and J. Poté, 2015. Human exposure to mercury in artisanal small-scale gold mining areas of Kedougou region, Senegal, as a function of occupational activity and fish consumption. Environmental Science and Pollution Research, 22: 7101-7111.

Nicklisch, S.C., L.T. Bonito, S. Sandin and A. Hamdoun, 2017. Mercury levels of yellowfin tuna (*Thunnus albacares)* are associated with capture location. Environmental Pollution, 229:87-93.

NIPH, 2016. Environmental Health Monitoring Reports. Czech Republic National Institute of Public Health (NIPH). www.szu.cz/topics/environmental-health/environmental-health-monitoring (Accessed 30 Nov 2017)

Noh, S., C.K. Kim, Y. Kim, J.H. Lee and S. Han, 2017. Assessing correlations between monomethylmercury accumulation in fish and trophic states of artificial temperate reservoirs. Science of the Total Environment, 580:912-919.

NPL, 2012. Kaye and Laby: Tables of Physical and Chemical Constants. National Physical Laboratory (NPL).

NPRI, 2016. Canadian National Pollutant Release Inventory (NPRI). https://www.canada.ca/en/services/environment/pollution-waste-management/national-pollutant-release-inventory.html. Accessed September 2016.

Nriagu, J.O., 1989. A global assessment of natural sources of atmospheric trace metals. Nature, 338:47-49.

Nriagu, J.O., 1993. Legacy of mercury pollution. Nature, 363:589.

Nriagu, J.O., 1994. Mercury pollution from the past mining of gold and silver in the Americas. Science of the Total Environment, 149:167-181.

Nriagu, J. and C. Becker, 2003. Volcanic emissions of mercury to the atmosphere: global and regional inventories. Science of the Total Environment, 304:3-12.

O'Neill, J.D. and K. Telmer, 2017. Estimating Mercury Use and Documenting Practices in Artisanal and Small-scale Gold Mining (ASGM). UN Environment, Geneva, Switzerland

Obrist, D., E. Tas, M. Peleg, V. Matveev, X. Faïn, D. Asaf and M. Luria, 2011. Bromine-induced oxidation of mercury in the mid-latitude atmosphere. Nature Geoscience, 4:22-26.

Obrist, D., Y. Agnan, M. Jiskra, C.L. Olson, D.P. Colegrove, J. Hueber, C.W. Moore, Sonke, J.E. and D. Helmig, 2017. Tundra uptake of atmospheric elemental mercury drives Arctic mercury pollution. Nature, 547:201-204.

Obrist, D., J.L. Kirk, L. Zhang, E.M. Sunderland, M. Jiskra and N.E. Selin, 2018. A review of global environmental mercury processes in response to human and natural perturbations: Changes of emissions, climate, and land use. Ambio, 47:116-140.

Ochoa-Acuña, H., M.S. Sepulveda and T.S. Gross, 2002. Mercury in feathers from Chilean birds: Influence of location, feeding strategy and taxonomic affiliation. Marine Pollution Bulletin, 44:340-349.

Ocio, J.A., H. Bilbao, J.L. Gayo and 13 others, 2012. BAT Guide for electric arc furnace iron & steel installations. Project TR-2008-IB-EN-03. Mission no: 2.1.4.c.3.

Odsjö, T., A. Roos and A.G. Johnels, 2004. The tail feathers of osprey nestlings (*Pandion haliaetus* L.) as indicators of change in mercury load in the environment of southern Sweden (1969-1998): Case study with a note on the simultaneous intake of selenium. Ambio, 33:133-137.

OECD/IEA, 2005. Energy Statistics Manual. International Energy Agency (IEA), Organisation for Economic Co-operation and Development (OECD).

Oken, E., R.O. Wright, K.P. Kleinman, D. Bellinger, C.J. Amarasiriwardena, H. Hu, J.W. Rich-Edwards and M.W. Gillman, 2005. Maternal fish consumption, hair mercury, and infant cognition in a U.S. Cohort. Environmental Health Perspectives, 113:1376-1380.

Oliveira, R.C., J.G. Dorea, J.V.E. Bernardi, W.R. Bastos, R. Almeida and A.G. Manzatto, 2010. Fish consumption by traditional subsistence villagers of the Rio Madeira (Amazon): impact on hair mercury. Annals of Human Biology, 37:629-642.

Olivero-Verbel, J., K. Caballero-Gallardo and A. Turizo-Tapia, 2015. Mercury in the gold mining district of San Martin de Loba, South of Bolivar (Colombia). Environmental Science and Pollution Research, 22:5895-5907.

Ordeig, O., C.E. Banks, J. del Campo, F.X. Munoz and R.G. Compton, 2006. Trace detection of mercury(II) using gold ultra-microelectrode arrays. Electroanalysis, 18:573-578.

Ortiz, V.L., R.P. Mason and J. Evan Ward, 2015. An examination of the factors influencing mercury and methylmercury particulate distributions, methylation and demethylation rates in laboratory-generated marine snow. Marine Chemistry, 177:753-762.

Osawa, T., T. Ueno and F.F. Fu, 2007. Sequential variation of atmospheric mercury in Tokai-mura, seaside area of eastern central Japan. Journal of Geophysical Research-Atmospheres, 112:D19.

OSPAR, 2011. Mercury losses from the chlor-alkali industry in 2009, including an assessment of 2008 and 2009 data and trends. OSPAR Commission, London.

OSPAR, 2015. Mercury Losses from the Chlor-alkali Industry in 2014. OSPAR Commission, London.

OSPAR, 2016. Mercury Losses from the Chlor-alkali Industry in 2015. OSPAR Commission, London.

Ouédraogo, O. and M. Amyot, 2013. Mercury, arsenic and selenium concentrations in water and fish from sub-Saharan semi-arid freshwater reservoirs (Burkina Faso). Science of the Total Environment, 444:243-254.

Outridge, P., R. Macdonald, F. Wang, G. Stern and A. Dastoor, 2008. A mass balance inventory of mercury in the Arctic Ocean. Environmental Chemistry, 5:89-111.

Outridge, P.M., N. Rausch, J.B. Percival, W. Shotyk and R. McNeely, 2011. Comparison of mercury and zinc profiles in peat and lake sediment archives with historical changes in emissions from the Flin Flon metal smelter, Manitoba, Canada. Science of the Total Environment, 409:548-563.

Pacyna, E.G. and J.M. Pacyna, 2002. Global emission of mercury from anthropogenic sources in 1995. Water, Air and Soil Pollution, 137:149-165.

Pacyna, J.M., E.G. Pacyna, F. Steenhuisen and S.J. Wilson, 2003. Mapping 1995 global anthropogenic emissions of mercury. Atmospheric Environment, 37(S1):109-117.

Pacyna, E.G., J.M. Pacyna, F. Steenhuisen and S. Wilson, 2006. Global anthropogenic mercury emission inventory for 2000. Atmospheric Environment, 40:4048-4063.

Pacyna, J.M., E.G. Pacyna and W. Aas, 2009. Changes of emissions and atmospheric deposition of mercury, lead, and cadmium. Atmospheric Environment, 43:117-127.

Pacyna, E.G., J.M. Pacyna, K. Sundseth, J. Munthe, K. Kindbom, S. Wilson, F. Steenhuisen and P. Maxson, 2010. Global emission of mercury to the atmosphere from anthropogenic sources in 2005 and projections to 2020. Atmospheric Environment, 44:2487-2499.

Pacyna, J.M., O. Travnikov, F. De Simone, I.M. Hedgecock, K. Sundseth, E.G. Pacyna, F. Steenhuisen, N. Pirrone, J. Munthe and K. Kindbom, 2016. Current and future levels of mercury atmospheric pollution on a global scale. Atmospheric Chemistry and Physics, 16:12495-12511.

Pacyna, A.D., C.Z. Martínez, D. Miguélez, F. Jiguet, Ż. Polkowska and K. Wojczulanis-Jakubas, 2017. Mercury contamination, a potential threat to the globally endangered aquatic warbler *Acrocephalus paludicola*. Environmental Science and Pollution Research, 24:26478-26484.

Pan, L., C.J. Lin, G.R. Carmichael, D.G. Streets, Y.H. Tang, J.H. Woo, S.K. Shetty, H.W. Chu, T.C. Ho, H.R. Friedli and X.B. Feng, 2010. Study of atmospheric mercury budget in East Asia using STEM-Hg modeling system. Science of the Total Environment, 408:3277-3291.

Paranjape, A.R. and B.D. Hall, 2017. Recent advances in the study of mercury methylation in aquatic systems. FACETS, 2:85-119.

Parks, J.M., A. Johs, M. Podar, R. Bridou, R.A. Hurt, S.D. Smith, S.J. Tomanicek, Y. Qian, S.D. Brown, C.C. Brandt, A.V. Palumbo, J.C. Smith, J.D. Wall, D.A. Elias and L. Liang, 2013. The genetic basis for bacterial mercury methylation. Science, 339:1332-1335.

Parsons, M.B., G.E.M. Hall, J. Dalziel, R. Tordon, S. Winch, K.G. Doe, Đ. Mroz and V.P. Palace, 2011. Environmental impacts of historical

mercury amalgamation at gold mines in Nova Scotia, Canada. The 10th International Conference on Mercury as a Pollutant. Halifax, Nova Scotia, Canada. 25 July 2011.

Paulus, M., D. Teubner, H. Rüdel and R. Klein, 2015. Bioaccumulation and long-term monitoring in freshwater ecosystems – knowledge gained from 20 years of zebra mussel analysis by the German Environmental Specimen Bank. In: Environmental Indicators. pp. 781-803. Springer.

Pauly, D. and D. Zeller, 2016. Catch reconstructions reveal that global marine fisheries catches are higher than reported and declining. Nature Communications, 7:10244.

Pavlish, J.H., L.L. Hamre and Y. Zhuang, 2010. Mercury control technologies for coal combustion and gasification systems. Fuel, 89:838-847.

Pelletier, A.R., L. Castello, A.V. Zhulidov, T.Y. Gurtovaya, R.D. Robarts, R.M. Holmes, D.A. Zhulidov and R.G. Spencer, 2017. Temporal and longitudinal mercury trends in burbot (*Lota lota*) in the Russian Arctic. Environmental Science and Technology, 51:13436-13442.

Pereira Filho et al., 2004 cited in Bose-O'Reilly, S., G. Drasch, C. Beinhoff, S. Rodrigues-Filho, G. Roider, B. Lettmeier, A. Maydl, S. Maydl and U. Siebert, 2010. Health assessment of artisanal gold miners in Indonesia. Science of the Total Environment, 408(4):713-725.

Perkins, M., L. Ferguson, R.G. Lanctot, I.J. Stenhouse, S. Kendall, S. Brown, H.R. Gates, J.O. Hall, K. Regan and D.C. Evers, 2016. Mercury exposure and risk in breeding and staging Alaskan shorebirds. Condor, 118:571-582.

Peterson, S.A., J. Van Sickle, R.M. Hughes, J.A. Schacher and S.F. Echols, 2004. A biopsy procedure for determining filet and predicting whole-fish mercury concentration. Archives of Environmental Contamination and Toxicology, 48:99-107.

Peterson, S.H., J.T. Ackerman and D.P. Costa, 2015. Marine foraging ecology influences mercury bioaccumulation in deep-diving northern elephant seals. Proceedings of the Royal Society B, 282:20150710.

Peterson, S.H., J.T. Ackerman and D.P. Costa, 2016a. Mercury correlations among blood, muscle, and hair of northern elephant seals during the breeding and molting fasts. Environmental Toxicology and Chemistry, 35:2103-2110.

Peterson, S.H., E.A. McHuron, S.N. Kennedy, J.T. Ackerman, L.D. Rea, J.M. Castellini, T.M. O'Hara and D.P. Costa, 2016b. Evaluating hair as a predictor of blood mercury: the influence of ontogenetic phase and life history in pinnipeds. Archives of Environmental Contamination and Toxicology, 70:28-45.

Peterson, S.H., J.T. Ackerman, C.A. Eagles-Smith, C.A. Hartman and M.P. Herzog, 2017. A critical evaluation of the utility of eggshells for estimating mercury concentrations in avian eggs. Environmental Toxicology and Chemistry, 36:2417-2427.

Peterson, S.H., J.T. Ackerman, D.E. Crocker and D.P. Costa, 2018. Foraging and fasting can influence contaminant concentrations in animals: an example with mercury contamination in a free-ranging marine mammal. Proceedings of the Royal Society B, 285:20172782.

Petro Industry News, 2015. Measurement and Testing (pages 48-49). Unconsidered Mercury Emissions from the Oil and Gas Industry. Qa³ Ltd.

Pfaffhuber, K.A., T. Berg, D. Hirdman and A. Stohl, 2012. Atmospheric mercury observations from Antarctica: seasonal variation and source and sink region calculations. Atmospheric Chemistry and Physics, 12:3241-3251.

Pierce, A.H., C.W. Moore, G. Wohlfahrt, L. Hörtang, N. Kljun and D. Obrist, 2015. Eddy covariance flux measurements of gaseous elemental mercury using cavity ring-down spectroscopy. Environmental Science and Technology, 49:1559-1568.

Pinkney, A.E., C.T. Driscoll, D.C. Evers, M.J. Hooper, J. Horan, J.W. Jones, R.S. Lazarus, H.G. Marshall, A. Milliken, B.A Rattner, J. Schmerfeld and D.W. Sparling, 2014. Interactive effects of climate change with nutrients, mercury, and freshwater acidification on key taxa in the North Atlantic Landscape Conservation Cooperative Region. Integrated Environmental Assessment and Management, 11:355-369.

Pirrone, N. and T. Keating, 2010. Hemispheric Transport of Air Pollution – Part B. United Nations.

Pirrone, N., I. Hedgecock and F. Sprovieri, 2008. Atmospheric mercury, easy to spot and hard to pin down: impasse? Atmospheric Environment, 42:8549-8551.

Pirrone, N., S. Cinnirella, X. Feng, R.B. Finkelman, H.R. Friedli, J. Leaner, R. Mason, A.B. Mukherjee, G.B. Stracher, D.G. Streets and K. Telmer, 2010. Global mercury emissions to the atmosphere from anthropogenic and natural sources. Atmospheric Chemistry and Physics, 10:5951-5964.

Podar, M., C.C. Gilmour, C.C. Brandt, A. Soren, S.D. Brown, B.R. Crable, A.V. Palumbo, A.C. Somenahally and D.A. Elias, 2015. Global prevalence and distribution of genes and microorganisms involved in mercury methylation. Science Advances, 1: e1500675. 10.1126/sciadv.1500675.

Point, D., J.E. Sonke, R.D. Day, D.G. Roseneau, K.A. Hobson, S.S. Vander Pol, A.J. Moors, R.S. Pugh, O.F.X. Donard and P.R. Becker, 2011. Methylmercury photodegradation influenced by sea-ice cover in Arctic marine ecosystems. Nature Geoscience, 4:188-194.

Poissant, L. and M. Pilote, 2003. Time series analysis of atmospheric mercury in Kuujjuarapik/Whapmagoostui (Quebec). Journal de Physique IV, 107:1079-1082.

Poissant, L., M. Pilote, C. Beauvais, P. Constant and H.H. Zhang, 2005. A year of continuous measurements of three atmospheric mercury species (GEM, RGM and Hgp) in southern Quebec, Canada. Atmospheric Environment, 39:1275-1287.

Poulain, A.J., J.D. Lalonde, J.D. Amyot, J.A. Shead, F. Raofie and P.A. Ariya, 2004. Redox transformations of mercury in an Arctic snowpack at springtime. Atmospheric Environment, 38:6763-6774.

Prestbo, E.M. and D.A. Gay, 2009. Wet deposition of mercury in the U.S. and Canada, 1996–2005: Results and analysis of the NADP mercury deposition network (MDN). Atmospheric Environment, 43:4223-4233.

Provencher, J.F., M.L. Mallory, B.M. Braune, M.R. Forbes and H.G. Gilchrist, 2014. Mercury and marine birds in Arctic Canada: effects, current trends, and why we should be paying closer attention. Environmental Reviews, 22:244-255.

Pudasainee, D., J.-H. Kim, S.-H. Lee, S.-J. Cho, G.-J. Song and Y.-C. Seo, 2009a. Hazardous air pollutants emission characteristics from cement kilns co-burning wastes. Environmental Engineering Research, 14:212-219.

Pudasainee, D., J.-H. Kim and Y.-C. Seo, 2009b. Mercury emission trend influenced by stringent air pollutants regulation for coal-fired power plants in Korea. Atmospheric Environment, 43:6254-6259.

Pudasainee, D., S.J. Lee, S.-H. Lee, J.-H. Kim, H.-N. Jang, S.-J. Cho and Y.-C. Seo, 2010. Effect of selective catalytic reactor on oxidation and enhanced removal of mercury in coal-fired power plants. Fuel, 89:804-809.

Pyle, D.M. and T.A. Mather, 2003. The importance of volcanic emissions for the global atmospheric mercury cycle. Atmospheric Environment, 37:5115-5124.

Qiu, F., X.Z. Meng, Y.L. Qiu, Q.H. Huang, Y. Liu, L.L. Wu, Q.F. Xiao, Y.J. Sun, R. Wang, Y.H. Zhou and Z.Y. Yu, 2015. Historical development and future perspectives of Environmental Specimen Bank in China: a mini review. Environmental Science and Pollution Research, 22:1562-1567.

Rafaj, P., J. Cofala, J. Kuenen, A. Wyrwa and J. Zysk, 2014. Benefits of European climate policies for mercury air pollution. Atmosphere, 5:45-59.

Rajaee, M., S. Obiri, A. Green, R. Long, S.J. Cobbina, V. Nartey, D. Buck, E. Antwi and N. Basu, 2015. Integrated assessment of artisanal and small-scale gold mining in Ghana – Part 2: Natural sciences review. International Journal of Environmental Research and Public Health, 12:8971-9011.

Ramon, R., M. Murcia, X. Aguinagalde, A. Amurrio, S. Llop, J. Ibarluzea, A. Lertxundi, M. Alvarez-Pedrerol, M. Casas, J. Vioque, J. Sunyer, A. Tardon, B. Martinez-Arguelles and F. Ballester, 2011. Prenatal mercury exposure in a multicenter cohort study in Spain Environment International, 37:597-604.

Reif, J.S., A.M. Schaefer and G.D. Bossart, 2015. Atlantic bottlenose dolphins (*Tursiops truncatus*) as a sentinel for exposure to mercury in humans: closing the loop. Veterinary Sciences, 2:407-422.

Remus, R., M. Aguado Monsonet, S. Roudier and L. Delgado Sancho, 2013. Best Available Techniques (BAT) Reference Document for Iron and Steel Production.

Ren, X., W.T. Luke, P. Kelley, M. Cohen, F. Ngan, R. Artz, J. Walker, S. Brooks, C. Moore, P. Swartzendruber, D. Bauer, J. Remeika, A. Hynes, J. Dibb, J. Rolison, N. Krishnamurthy, W.M. Landing, A. Hecobian, J. Shook and L.G. Huey, 2014. Mercury speciation at a coastal site in the northern

Gulf of Mexico: Results from the Grand Bay intensive studies in summer 2010 and spring 2011. Atmosphere, 5:230-251.

Ren, X., W.T. Luke, P. Kelley, M.D. Cohen, R. Artz, M.L. Olson, D. Schmeltz, M. Puchalski, D.L. Goldberg, A. Ring, G.M. Mazzuca, K.A. Cummings, L. Wojdan, S. Preaux and J.W. Stehr, 2016. Atmospheric mercury measurements at a suburban site in the Mid-Atlantic United States: Inter-annual, seasonal and diurnal variations and source-receptor relationships. Atmospheric Environment, 146:141-152.

Ricca, M.A., M.A. Keith and R.G. Anthony, 2008. Sources of organochlorine contaminants and mercury in seabirds from the Aleutian archipelago of Alaska: Inferences from spatial and trophic variation. Science of the Total Environment, 406:308-323.

Rigét, F., R. Dietz, E.W. Born, C. Sonne and K.A. Hobson, 2007. Temporal trends of mercury in marine biota of west and northwest Greenland. Marine Pollution Bulletin, 54:72-80.

Rigét, F., B. Braune, A. Bignert, S. Wilson, J. Aars, E. Born, M. Dam, R. Dietz, M. Evans, T. Evans, M. Gamberg, N. Gantner, N. Green, H. Gunnlaugsdóttir, K. Kannan, R. Letcher, D. Muir, P. Roach, C. Sonne, G. Stern and O. Wiig, 2011. Temporal trends of Hg in Arctic biota, an update. Science of the Total Environment, 409:3520-3526.

Rigét, F., R. Dietz and K.A. Hobson, 2012. Temporal trends of mercury in Greenland ringed seal populations in a warming climate. Journal of Environmental Monitoring, 14:3249-3256.

Rimmer, C.C., K.P. McFarland, D.C. Evers, E.K. Miller, Y. Aubry, D. Busby and R.J. Taylor, 2005. Mercury concentrations in Bicknell's thrush and other insectivorous passerines in montane forests of northeastern North America. Ecotoxicology, 14:223-240.

Risch, M.R., D.A. Gay, K.K. Fowler, G.J. Keeler, S.M. Backus, P. Blanchard, J. Barres and J.T. Dvonch, 2012. Spatial patterns and temporal trends in mercury concentrations, precipitation depths, and mercury wet deposition in the North American Great Lakes region, 2002–2008. Environmental Pollution, 161:261-271.

Risch, M.R., J.F. De Wild, D.A. Gay, L. Zhang, E.W. Boyer and D.P. Krabbenhoft, 2017. Atmospheric mercury deposition to forests in the eastern USA. Environmental Pollution, 228:8-18.

Robinson, S.A., M.J. Lajeunesse and M.R. Forbes, 2012. Sex differences in mercury contamination of birds: testing multiple hypotheses with meta-analysis. Environmental Science and Technology, 46:7094-7101.

Rocque, D.A., and K. Winker, 2004. Biomonitoring of contaminants in birds from two trophic levels in the North Pacific. Environmental Toxicology and Chemistry, 23:759-766.

Rodrigues, T. and A.F. Amorim, 2016. Review and analysis of mercury levels in blue marlin (*Makaira nigricans*, Lacepède 1802) and swordfish (*Xiphias gladius*, Linnaeus 1758). bioRxiv, p.043893. doi. org/10.1101/043893.

Rolison, J.M., W.M. Landing, W. Luke, M. Cohen and V.J.M. Salters, 2013. Isotopic composition of species-specific atmospheric Hg in a coastal environment. Chemical Geology, 336:37-49.

Roos-Barraclough, F. and W. Shotyk, 2003. Millennial-scale records of atmospheric mercury deposition obtained from ombrotrophic and minerotrophic peatlands in the Swiss Jura Mountains. Environmental Science and Technology, 37:235-244.

Roos-Barraclough, F., N. Givelet, A.K. Cheburkin, W. Shotyk and S.A. Norton, 2006. Use of Br and Se in peat to reconstruct the natural and anthropogenic fluxes of atmospheric Hg: a 10, 000-year record from Caribou Bog, Maine. Environmental Science and Technology, 40:3188-3194.

Rosati, G., L.E. Heimbürger, D. Melaku Canu, C. Lagane, L. Laffont, M.J.A. Rijkenberg, L.J.A. Gerringa, C. Solidoro, C.N. Gencarelli, I.M. Hedgecock, H.J.W. De Baar and J.E. Sonke, 2018. Mercury in the Black Sea: new insights from measurements and numerical modelling. Global Biogeochemical Cycles, 32:529-550.

Roseborough, D. and B. Lindblad, 2008. Mercury Emissions from Steelmaking: A Review. Jernkontorets Forskning D825.

Rothenberg, S.E., L. Windham-Myers and J.E. Creswell, 2014. Rice methylmercury exposure and mitigation: a comprehensive review. Environmental Research, 133:407-423.

Routti, H., R.J. Letcher, E.W. Born, M. Branigan, R. Dietz, T.J. Evans, A.T. Fisk, E. Peacock and C. Sonne, 2011. Spatial and temporal trends of selected trace elements in liver tissue from polar bears (*Ursus maritimus*) from

Alaska, Canada and Greenland. Journal of Environmental Monitoring, 13:2260-2267.

Rumbold, D.G., K.E. Miller, T.A. Dellinger and N. Haas, 2017. Mercury concentrations in feathers of adult and nestling osprey (*Pandion haliaetus*) from coastal and freshwater environments of Florida. Archives of Environmental Contamination and Toxicology, 72:31-38.

Rutkiewicz, J., D.-H. Nam, T. Cooley, K. Neumann, I.B. Padilla, W. Route, S. Strom and N. Basu, 2011. Mercury exposure and neurochemical impacts in bald eagles across several Great Lakes states. Ecotoxicology, 20:1669-1676.

Ruus, A., I.B. Øverjordet, H.F.V. Braaten, A. Evenset, G. Christensen, E.S. Heimstad, G.W. Gabrielsen and K. Borgå, 2015. Methylmercury biomagnification in an Arctic pelagic food web. Environmental Toxicology and Chemistry, 34:2636-2643.

Sagiv, S.K., S.W. Thurston, D.C. Bellinger, C. Amarasiriwardena and S.A. Korrick, 2012. Prenatal exposure to mercury and fish consumption during pregnancy and attention-deficit/hyperactivity disorder-related behavior in children. Archives of Pediatrics and Adolescent Medicine, 166:1123-1131.

Salazar-Camacho, C., M. Salas-Moreno, S. Marrugo-Madrid, J. Marrugo-Negrete and S. Díez, 2017. Dietary human exposure to mercury in two artisanal small-scale gold mining communities of northwestern Colombia. Environment International, 107:47-54.

Sanei, H., P.M. Outridge, F. Goodarzi, F. Wang, D. Armstrong, K. Warren and L. Fishback, 2010. Wet deposition mercury fluxes in the Canadian sub-Arctic and southern Alberta, measured using an automated precipitation collector adapted to cold regions. Atmospheric Environment, 44:1672-1681.

Santschi, P.H., K.M. Yeager, K.A. Schwehr and K.J. Schindler, 2017. Estimates of recovery of the Penobscot River and estuarine system from mercury contamination in the 1960s. Science of the Total Environment, 596:351-359.

Sato, T., M. Qadir, S. Yamamoto, T. Endo and A. Zahoor, 2013. Global, regional, and country level need for data on wastewater generation, treatment, and use. Agricultural Water Management, 130:1-13.

Savoy, L., P. Flint, D. Zwiefelhofer, H. Brant, C. Perkins, R. Taylor, O. Lane, J. Hall, D. Evans and J. Schamber, 2017. Geographic and temporal patterns of variation in total mercury concentrations in blood of harlequin ducks and blue mussels from Alaska. Marine Pollution Bulletin, 117:178-183.

Schartup, A.T., R.P. Mason, P.H. Balcom, T.A. Hollweg and C.Y. Chen, 2013. Methylmercury production in estuarine sediments: Role of organic matter. Environmental Science and Technology, 47:695-700.

Schartup, A.T., P.H. Balcom and R.P. Mason, 2014. Sediment-porewater partitioning, total sulfur, and methylmercury production in estuaries. Environmental Science and Technology, 48:954-960.

Schartup, A.T., P.H. Balcom, A.L. Soerensen, K.J. Gosnell, R.S.D. Calder, R.P. Mason and E.M. Sunderland, 2015a. Freshwater discharges drive high levels of methylmercury in Arctic marine biota. Proceedings of the National Academy of Sciences of the United States of America, 112:11789-11794.

Schartup, A.T., U. Ndu, R.P. Mason and E.M. Sunderland, 2015b. Contrasting effects of marine and terrestrially derived dissolved organic matter on mercury speciation and bioavailability in seawater. Environmental Science and Technology, 49:5965-5972.

Schartup, A.T., A. Qureshi, C. Dassuncao, C.P. Thackray, G. Harding and E.M. Sunderland, 2018. A model for methylmercury uptake and trophic transfer by marine plankton. Environmental Science and Technology, 52:654-662.

Scheuhammer, A.M., A.H. Wong and D. Bond, 1998. Mercury and selenium accumulation in common loons (*Gavia immer*) and common mergansers (*Mergus merganser*) from eastern Canada. Environmental Toxicology and Chemistry, 17:197-201.

Scheuhammer, A.M., N. Basu, D.C. Evers, G.H. Heinz, M.B. Sandheinrich and M.S. Bank, 2011. Ecotoxicology of mercury in fish and wildlife: Recent advances. In: M. Bank (ed.). Mercury in the Environment: Pattern and Process. pp. 223-238. University of California Press.

Scheuhammer, A., B. Braune, H.M. Chan, H. Frouin, A. Krey, R. Letcher, L. Loseto, M. Noël, S. Ostertag, P. Ross and M. Wayland, 2015. Recent progress on our understanding of the biological effects of mercury

in fish and wildlife in the Canadian Arctic. Science of the Total Environment, 509:91-103.

Scheuhammer, A.M., S.I. Lord, M. Wayland, N.M. Burgess, L. Champoux and J.E. Elliott, 2016. Major correlates of mercury in small fish and common loons (*Gavia immer*) across four large study areas in Canada. Environmental Pollution, 210:361-370.

Schleicher, N.J., J. Schafer, G. Blanc, Y. Chen, F. Chai, K. Cen and S. Norra, 2015. Atmospheric particulate mercury in the megacity Beijing: Spatiotemporal variations and source apportionment. Atmospheric Environment, 109:251-261.

Schneider, L., S. Eggins, W. Maher, R.C. Vogt, F. Krikowa, L. Kinsley, S.M. Eggins and R. Da Silveira, 2015. An evaluation of the use of reptile dermal scutes as a non-invasive method to monitor mercury concentrations in the environment. Chemosphere, 119:163-170.

Schorcht, F., I. Kourti, B.M. Scalet, S. Roudier and L. Delgado Sancho, 2013. Best Available Techniques (BAT) Reference Document for the Production of Cement, Lime and Magnesium Oxide.

Schroeder, W.H. and J. Munthe, 1998. Atmospheric mercury – An overview. Atmospheric Environment, 32:809-822.

Schroeder, W.H., K.G. Anlauf, L.A. Barrie, J.Y. Lu, A. Steffen, D.R. Schneeberger and T. Berg, 1998. Arctic springtime depletion of mercury. Nature, 394:331-332.

Schroeder, W.H., S. Beauchamp, G. Edwards, L. Poissant, P. Rasmussen, R. Tordon, G. Dias, J. Kemp, B. Van Heyst and C.M. Banic, 2005. Gaseous mercury emissions from natural sources in Canadian landscapes. Journal of Geophysical Research: Atmospheres, 110:D18302.

Schulz, C., J. Angerer, U. Ewers and M. Kolossa-Gehring, 2007. The German Human Biomonitoring Commission. International Journal of Hygiene and Environmental Health, 210:373-382.

Schuster, P.F., K.M. Schaefer, G.R. Aiken, R.C. Antweiler, J.F. Dewild, J.D. Gryziec, A. Gusmeroli, G. Hugelius, E. Jafarov, D.P. Krabbenhoft, L. Liu, N. Herman-Mercer, C. Mu, D.A. Roth, T. Schaefer, R.G. Striegl, K.P. Wickland and T. Zhang, 2018. Permafrost stores a globally significant amount of mercury. Geophysical Research Letters, 45:1463-1471.

Sebastiano, M., P. Bustamante, D. Costantini, I. Eulaers, G. Malarvannan, P. Mendez-Fernandez, C. Churlaud, P. Blévin, A. Hauselmann, G. Dell'Omo and A. Covaci, 2016. High levels of mercury and low levels of persistent organic pollutants in a tropical seabird in French Guiana, the magnificent frigatebird, *Fregata magnificens*. Environmental Pollution, 214:384-393.

Sebastiano, M., P. Bustamante, I. Eulaers, G. Malarvannan, P. Mendez-Fernandez, C. Churlaud, P. Blévin, A. Hauselmann, A. Covaci, M. Eens, D. Costantini and O. Chastel, 2017. Trophic ecology drives contaminant concentrations within a tropical seabird community. Environmental Pollution, 227:183-193.

Seelen, E.A., G.M. Massey and R.P. Mason, 2018. Role of sediment resuspension on estuarine suspended particulate mercury dynamics. Environmental Science and Technology, 52:7736-7744.

Seewagen, C.L., D.A. Cristol and A.R. Gerson, 2016. Mobilization of mercury from lean tissues during simulated migratory fasting in a model songbird. Scientific Reports, 6: 10.1038/srep25762.

Seixas, T.G., I. Moreira, S. Siciliano, O. Malm and H.A. Kehrig, 2014. Differences in methylmercury and inorganic mercury biomagnification in a tropical marine food web. Bulletin of Environmental Contamination and Toxicology, 92:274-278.

Selin, N.E., 2014. Global change and mercury cycling: Challenges for implementing a global mercury treaty. Environmental Toxicology and Chemistry, 33:1202-1210.

Selin, N.E., D.J. Jacob, R.J. Park, R.M. Yantosca, S. Strode, L. Jaegle and D. Jaffe, 2007. Chemical cycling and deposition of atmospheric mercury: Global constraints from observations. Journal of Geophysical Research Atmospheres, 112:D02308, 10.1029/2006JD007450.

Selin, N.E., D.J. Jacob, R.M. Yantosca, S. Strode, L. Jaeglé and E.M. Sunderland, 2008. Global 3-D land-ocean-atmosphere model for mercury: present day versus preindustrial cycles and anthropogenic enrichment factors for deposition. Global Biogeochemical Cycles, 22, GB2011. doi:10.1029/2007GB003040.

Senior, C., 2010. Mercury Emissions Reduction from Portland Cement Kilns using Wet Scrubbers. Paper-2010-A-1419. Presented at the Air & Waste Management Association Annual Meeting and Exhibition, Calgary, Alberta, Canada, June 22-25, 2010.

Seo, J.W., B.G. Kim, Y.M. Kim, R.B. Kim, J.Y. Chung, K.M. Lee and Y.S. Hong, 2015. Trend of blood lead, mercury, and cadmium levels in Korean population: data analysis of the Korea National Health and Nutrition Examination Survey. Environmental Monitoring and Assessment, 187:146. doi:10.1007/s10661-015-4348-2.

Seo, Y.C., S.H. Kim, S.K. Back and J.H. Sung, 2016a. Movement of transboundary mercury with emission inventory from anthropogenic sources in northeast Asian countries. In: 5th Annual International Conference on Sustainable Energy and Environmental Sciences.

Seo, Y.S., S.P. Jeong, T.M. Holsen, Y.J. Han, E. Choi, E.H. Park, T.Y. Kim, H.S. Eum, D.G. Park, E. Kim, S. Kim, J.H. Kim, J. Choi and S.M. Yi, 2016b. Characteristics of total gaseous mercury (TGM) concentrations in an industrial complex in South Korea: impacts from local sources. Atmospheric Chemistry and Physics, 16:10215-10228.

SFA, 2016. Fisheries Statistical Report, 2015. Seychelles Fishing Authority (SFA), Victoria, Seychelles.

Shah, V., L. Jaegle, L.E. Gratz, J.L. Ambrose, D.A. Jaffe, N.E. Selin, S. Song, T.L. Campos, F.M. Flocke, M. Reeves, D. Stechman, M. Stell, J. Festa, J. Stutz, A.J. Weinheimer, D.J. Knapp, D.D. Montzka, G.S. Tyndall, E.C. Apel, R.S. Hornbrook, A.J. Hills, D.D. Riemer, N.J. Blake, C.A. Cantrell and R.L. Mauldin, 2016. Origin of oxidized mercury in the summertime free troposphere over the southeastern US. Atmospheric Chemistry and Physics, 16:1511-1530.

Shamlaye, C.F., D.O. Marsh, G.J. Myers, C. Cox, P.W. Davidson, O. Choisy, E. Cernichiari, A. Choi, M.A. Tanner and T.W. Clarkson, 1995. The Seychelles child development study on neurodevelopmental outcomes in children following in utero exposure to methylmercury from a maternal fish diet: background and demographics. Neurotoxicology, 16:597-612.

Shanley, J.B., M.A. Engle, M. Scholl, D.P. Krabbenhoft, R. Brunette, M.L. Olson and M.E. Conroy, 2015. High mercury wet deposition at a "clean air" site in Puerto Rico. Environmental Science and Technology, 49:12474-12482.

Sharif, A., M. Monperrus, E. Tessier, S. Bouchet, H. Pinaly, P. Rodriguez-Gonzalez, P. Maron and D. Amouroux, 2014. Fate of mercury species in the coastal plume of the Adour River estuary (Bay of Biscay, SW France). Science of the Total Environment, 496:701-713.

Sheehan, M.C., T.A. Burke, A. Navas-Acien, P.N. Breysse, J. McGready and M.A. Fox, 2014. Global methylmercury exposure from seafood consumption and risk of developmental neurotoxicity: a systematic review. Bulletin of the World Health Organization, 92:254-269F.

Sherman, L.S., J.D. Blum, T.A. Douglas and A. Steffen, 2012. Frost flowers growing in the Arctic ocean-atmosphere – sea ice–snow interface: 2. Mercury exchange between the atmosphere, snow, and frost flowers. Journal of Geophysical Research, 117, D00R10, doi:10.1029/2011JD016186.

Sherman, L.S., J.D. Blum, A. Franzblau and N. Basu, 2013. New insight into biomarkers of human mercury exposure using naturally occurring mercury stable isotopes. Environmental Science and Technology, 47:3403-3409.

Sherman, L.S., J.D. Blum, N. Basu, M. Rajaee, D.C. Evers, D.G. Buck, J. Petrlik and J. DiGangi, 2015. Assessment of mercury exposure amongst small-scale gold miners using mercury stable isotopes. Environmental Research, 137:226-234.

Sherwen, T., J.A. Schmidt, M.J. Evans, L.J. Carpenter, K. Grossmann, S.D. Eastham, D.J. Jacob, B. Dix, T.K. Koenig, R. Sinreich, I. Ortega, R. Volkamer, A. Saiz-Lopez, C. Prados-Roman, A.S. Mahajan and C. Ordonez, 2016. Global impacts of tropospheric halogens (Cl, Br, I) on oxidants and composition in GEOS-Chem. Atmospheric Chemistry and Physics, 16:12239-12271.

Shetty, S.K., C.J. Lin, D.G. Streets and C. Jang, 2008. Model estimate of mercury emission from natural sources in East Asia. Atmospheric Environment, 42:8674-8685.

Sheu, G.R., N.H. Lin, J.L. Wang, C.T. Lee, C.F.O. Yang and S.H. Wang, 2010. Temporal distribution and potential sources of atmospheric mercury measured at a high-elevation background station in Taiwan. Atmospheric Environment, 44:2393-2400.

Shotyk, W., M.E. Goodsite, F. Roos-Baraclough, N. Givelet, G. Le Roux, D. Weiss, A.K. Cherbukin, K. Knudsen, J. Heinemeier, W.O. van der Knapp,

S.A. Norton and C. Lohse, 2005. Accumulation rates and predominant atmospheric sources of natural and anthropogenic Hg and Pb on the Faroe Islands. Geochimica et Cosmochimica Acta, 69:1-17.

Sillman, S., F. Marsik, J.T. Dvonch and G.J. Keeler, 2013. Assessing atmospheric deposition of mercury in Florida, USA: Local versus global sources and models versus measurements. E3S Web of Conferences. 1. 07008. 10.1051/e3sconf/20130107008.

Simpson, W.R., S.S. Brown, A. Saiz-Lopez, J.A. Thornton and R. von Glasow, 2015. Tropospheric halogen chemistry: sources, cycling, and impacts. Chemical Reviews, 115:4035-4062.

Skov, H., J. Christensen, M.E. Goodsite, N.Z. Heidam, B. Jensen, P. Wåhlin and G. Geernaert, 2004. Fate of elemental mercury in Arctic during atmospheric mercury depletion episodes and the load of atmospheric mercury to Arctic. Environmental Science and Technology, 38:2373-2382.

Skov, H. B.T. Sørensen, M.E. Landis, M.S. Johnson, C. Lohse, M.E. Goodsite and P. Sacco, 2007. Performance of a new diffusive sampler for Hg0 determination in the troposphere. Environmental Chemistry, 4:75-80.

Skyllberg, U., P.R. Bloom, J. Qian, C.M. Lin and W.F. Bleam, 2006. Complexation of mercury(II) in soil organic matter: EXAFS evidence for linear two-coordination with reduced sulfur groups. Environmental Science and Technology, 40:4174-4180.

Slemr, F., R. Ebinghaus, C.A.M. Brenninkmeijer, M. Hermann, H.H. Kock, B.G. Martinsson, T. Schuck, D. Sprung, P. van Velthoven, A. Zahn and H. Ziereis, 2009a. Gaseous mercury distribution in the upper troposphere and lower stratosphere observed onboard the CARIBIC passenger aircraft. Atmospheric Chemistry and Physics, 9:1957-1969.

Slemr, F., R. Ebinghaus, C.A.M. Brenninkmeijer, M. Hermann, H.H. Kock, I. Levine, B. Martinsson, T. Schuck, D. Sprung, P. van Velthoven, A. Zahn and H. Ziereis, 2009b. Gaseous mercury distribution in the upper troposphere and lower stratosphere observed during the CARIBIC flights from Frankfurt to southern China and to South America. Atmospheric Chemistry and Physics, 9:1957-1969.

Slemr, F., E.-G. Brunke, R. Ebinghaus and J. Kuss, 2011. Worldwide trend of atmospheric mercury since 1995. Atmospheric Chemistry and Physics, 11:4779-4787.

Slemr, F., R. Ebinghaus, A. Weigelt, H.H. Kock, C.A.M. Brenninkmeijer, T. Schuck, M. Hermann, A. Zahn, P. van Veltyhoven and H. Ziereis, 2013. CARIBIC observations of gaseous mercury in the upper troposphere and lower stratosphere. E3S Web of Conferences. 1. 1-4. 10.1051/e3sconf/20130117001.

Slemr, F., A. Weigelt, R. Ebinghaus, C. Brenninkmeijer, A. Baker, T. Schuck, A. Rauthe-Schöch, H. Riede, E. Leedham, M. Hermann, P. van Velthoven, D. Oram, D. O'Sullivan, C. Dyroff, A. Zahn and H. Ziereis, 2014. Mercury plumes in the global upper troposphere observed during flights with the CARIBIC observatory from May 2005 until June 2013. Atmosphere, 5:342-369.

Slemr, F., H. Angot, A. Dommergue, O. Magand, M. Barret, A. Weigelt, R. Ebinghaus, E.-G. Brunke, K.A. Pfaffhuber, G. Edwards, D. Howard, J. Powell, M. Keywood and F. Wang, 2015. Comparison of mercury concentrations measured at several sites in the Southern Hemisphere. Atmospheric Chemistry and Physics, 15:3125-3133.

Slemr, F., C.A. Brenninkmeijer, A. Rauthe-Schöch, A. Weigelt, R. Ebinghaus, E.-G. Brunke, L. Martin, T.G. Spain and S. O'Doherty, 2016a. El Niño – Southern Oscillation influence on tropospheric mercury concentrations. Geophysical Research Letters, 43:1766-1771.

Slemr, F., A. Weigelt, R. Ebinghaus, H.H. Kock, J. Bödewadt, C.A.M. Brenninkmeijer, A. Rauthe-Schöch, S. Weber, M. Hermann, J. Becker, A. Zahn and B. Martinsson, 2016b. Atmospheric mercury measurements onboard the CARIBIC passenger aircraft. Atmospheric Measurement Techniques, 9:2291-2302.

Slemr, F., A. Weigelt, R. Ebinghaus, J. Bieser, C.A.M. Brenninkmeijer, A. Rauthe-Schöch, M. Hermann, B.G. Martinsson, P. van Velthoven, H. Bönisch, M. Neumaier, A. Zahn and H. Ziereis, 2018. Mercury distribution in the upper troposphere and lowermost stratosphere according to measurements by the IAGOS-CARIBIC observatory, 2014–2016. Atmospheric Chemistry and Physics, 18:12329-12343.

Sloss, L.L., 2008. Economics of Mercury Control. CCC/134, IEA Clean Coal Center.

Smith-Downey, N.V., E.M. Sunderland and D.J. Jacob, 2010. Anthropogenic impacts on global storage and emissions of mercury from terrestrial

soils: Insights from a new global model. Journal of Geophysical Research: Biogeosciences, 115:G03008.

Snoj Tratnik, J., I. Falnoga, D. Mazej, D. Kocman, V. Fajon, M. Jagodic, A. Stajnko, A. Trdin, Z. Šlejkovec, Z. Jeran, J. Osredkar, A. Sešek-Briški, M. Krsnik, A.B. Kobal, L. Kononenko and M. Horvat, 2018. Results of the first national human biomonitoring in Slovenia: Trace elements in men and lactating women, predictors of exposure and reference values. International Journal of Hygiene and Environmental Health, 222:563-582.

Soerensen, A., H. Skov, D.J.B. Soerensen and M. Johnson, 2010a. Global concentrations of gaseous elemental mercury and reactive gaseous mercury in the marine boundary layer. Environmental Science and Technology, 44:7425-7430.

Soerensen, A., E. Sunderland, C. Holmes, D. Jacob, R. Yantosca, H. Skov, J. Christensen, S. Strode and R. Mason, 2010b. An improved global model for air-sea exchange of mercury: high concentrations over the North Atlantic. Environmental Science and Technology, 44:8574-8580.

Soerensen, A.L., D.J. Jacob, D.G. Streets, M.L.I. Witt, R. Ebinghaus, R.P. Mason, M. Andersson and E.M. Sunderland, 2012. Multi-decadal decline of mercury in the North Atlantic atmosphere explained by changing subsurface seawater concentrations. Geophysical Research Letters, 39:L21810 10.1029/2012GL053736.

Soerensen, A.L., D.J. Jacob, A.T. Schartup, J.A. Fisher, I. Lehnherr, V.L. St. Louis, L.E. Heimbürger, J.E. Sonke, D.P. Krabbenhoft and E.M. Sunderland, 2016a. A mass budget for mercury and methylmercury in the Arctic Ocean. Global Biogeochemical Cycles, 30: doi:10.1002/2015GB005280.

Soerensen, A.L., A.T. Schartup, E. Gustafsson, B.G. Gustafsson, E. Undeman and E. Björn, 2016b. Eutrophication increases phytoplankton methylmercury concentrations in a coastal sea – A Baltic Sea case study. Environmental Science and Technology, 50:11787-11796.

Sommar, J., I. Wängberg, T. Berg, K. Gårdfeldt, J. Munthe, A. Richter, A. Urba, F. Wittrock and W.H. Schroeder, 2007. A circumpolar transport and air-surface exchange of atmospheric mercury at Ny-Ålesund (79°), Svalbard, spring 2002. Atmospheric Chemistry and Physics, 7:151-166.

Sommar, J., M.E. Andersson and H.-W. Jacobi, 2010. Circumpolar measurements of speciated mercury, ozone and carbon monoxide in the boundary layer of the Arctic Ocean. Atmospheric Chemistry and Physics, 10:5031-5045.

Song, S., N.E. Selin, A.L. Soerensen, H. Angot, R. Artz, S. Brooks, E. Brunke, G. Conley, A. Dommergue, R. Ebinghaus, T. Holsen, S. Kang, P. Kelley, W. Luke, O. Magand, K. Marumoto, K.A. Pfaffhuber, X. Ren and Q. Zhang, 2015. Top-down constraints on atmospheric mercury emissions and implications for global biogeochemical cycling. Atmospheric Chemistry and Physics, 15:7103-7125.

Sorensen, J.A., G.E. Glass, K.W. Schmidt, J.K. Huber and G.R. Rapp Jr, 1990. Airborne mercury deposition and watershed characteristics in relation to mercury concentrations in water, sediments, plankton, and fish of eighty northern Minnesota lakes. Environmental Science and Technology, 24:1716-1727.

Spalding, M.G., P.C. Frederick, H.C. McGill, S.N. Bouton and L.R. McDowell, 2000. Methylmercury accumulation in tissues and its effects on growth and appetite in captive great egrets. Journal of Wildlife Diseases, 36:411-422.

Sprovieri, F., N. Pirrone, I.M. Hedgecock, M.S. Landis and R.K. Stevens, 2002. Intensive atmospheric mercury measurements at Terra Nova Bay in Antarctica during November and December 2000. Journal of Geophysical Research: Atmospheres, 107:4722. doi:10.1029/2002JD002057.

Sprovieri, F., N. Pirrone, M.S. Landis and R.K. Stevens, 2005a. Oxidation of gaseous elemental mercury to gaseous divalent mercury during 2003 polar sunrise at Ny-Alesund. Environmental Science and Technology, 39:9156-9165.

Sprovieri, F., N. Pirrone, M.S. Landis and R.K. Stevens, 2005b. Atmospheric mercury behavior at different altitudes at Ny Alesund during Spring 2003. Atmospheric Environment, 39:7646-7656.

Sprovieri, F., N. Pirrone, R. Ebinghaus, H. Kock and A. Dommergue, 2010. A review of worldwide atmospheric mercury measurements. Atmospheric Chemistry and Physics, 10:8245-8265.

Sprovieri, F., N. Pirrone, M. Bencardino, F. D'Amore, F. Carbone, S. Cinnirella, V. Mannarino, M. Landis, R. Ebinghaus, A. Weigelt, E.-G. Brunke, C. Labuschagne, L. Martin, J. Munthe, I. Wängberg, P. Artaxo,

F. Morais, H. de Melo Jorge Barbosa, J. Brito, W. Cairns, C. Barbante, M. del Carmen Diéguez, P.E. Garcia, A. Dommergue, H. Angot, O. Magand, H. Skov, M. Horvat, J. Kotnik, K.A. Read, L.M. Neves, B.M. Gawlik, F. Sena, N. Mashyanov, W. Obolkin, D. Wip, X.B. Feng, H. Zhang, X. Fu, R. Ramachandran, D. Cossa, J. Knoery, N. Maruszcak, M. Nerentorp and C. Norstrom, 2016. Atmospheric mercury concentrations observed at ground-based monitoring sites globally distributed in the framework of the GMOS network. Atmospheric Chemistry and Physics, 16:11915-11935.

Sprovieri, F., N. Pirrone, M. Bencardino, F. D'Amore, H. Angot, C. Barbante, E.-G. Brunke, F. Arcega-Cabrera, W. Cairns, S. Comero, M.D.C. Diéguez, A. Dommergue, R. Ebinghaus, X.B. Feng, X. Fu, P.E. Garcia, B.M. Gawlik, U. Hageström, K. Hansson, M. Horvat, J. Kotnik, C. Labuschagne, O. Magand, L. Martin, N. Mashyanov, T. Mkololo, J. Munthe, V. Obolkin, M. Ramirez Islas, F. Sena, V. Somerset, P. Spandow, M. Vardè, C. Walters, I. Wängberg, A. Weigelt, X. Yang and H. Zhang, 2017. Five-year records of mercury wet deposition flux at GMOS sites in the Northern and Southern hemispheres. Atmospheric Chemistry and Physics, 17:2689-2708.

Srebocan, E., J. Pompe-Gotal, A. Prevendar-Crnic and E. Ofner, 2007. Mercury concentrations of captive Atlantic bluefin tuna (*Thunnus thynnus*) farmed in the Adriatic Sea. Veterinarni Medicina, 52:175-177.

Srivastava, R.K, N. Hutson, B. Martin and F. Princiotta, 2006. Control of mercury emissions from coal-fired electricity utility boilers. Environmental Science and Technology, 40:1385-1393.

SSAB, 2015. Environmental reports 2015 of the SSAB facilities in Luleå and Oxelösund, Sweden.

St. Louis, V.L., J.W.M. Rudd, C.A. Kelly, R.A.D. Bodaly, M.J. Paterson, K.G. Beaty, R.H. Hesslein, A. Heyes and A.R. Majewsk, 2004. The rise and fall of mercury methylation in an experimental reservoir. Environmental Science and Technology, 38:1348-1358.

St. Pierre, K., V.L. St. Louis, J. Kirk, I. Lehnherr, S. Wang and C. La Farge, 2015. Importance of open marine waters to the enrichment of total mercury and monomethylmercury in lichens in the Canadian High Arctic. Environmental Science and Technology, 49:5930-5938.

Stamenkovic, J., M.S. Gustin, J.A. Arnone, D.W. Johnson, J.D. Larsen and P.S.J. Verburg, 2008. Atmospheric mercury exchange with a tallgrass prairie ecosystem housed in mesocosms. Science of the Total Environment, 406:227-238.

Steenhuisen, F. and S. Wilson, 2015. Identifying and characterizing major emission point sources as a basis for geospatial distribution of mercury emissions inventories. Atmospheric Environment, 112:167-177.

Steenhuisen, F. and S. Wilson, 2019. Development and application of an updated geospatial distribution model for gridding 2015 global mercury emissions. Atmospheric Environment, 211:138-150.

Steffen, A., W. Schroeder, R. Macdonald, L. Poissant and A. Konoplev, 2005. Mercury in the Arctic atmosphere: An analysis of eight years of measurements of GEM at Alert (Canada) and a comparison with observations at Amderma (Russia) and Kuujjuarapik (Canada). Science of the Total Environment, 342:185-198.

Steffen, A., T. Douglas, M. Amyot, P. Ariya, K. Aspmo, T. Berg, J. Bottenheim, S. Brooks, F.D. Cobbett, A. Dastoor, A. Dommergue, R. Ebinghaus, C. Ferrari, K. Gardfeldt, M.E. Goodsite, D. Lean, A.J. Poulain, C. Scherz, H. Skov, J. Sommar and C. Temme, 2008. A synthesis of atmospheric mercury depletion event chemistry in the atmosphere and snow. Atmospheric Chemistry and Physics, 8:1445-1482.

Steffen, A., J. Bottenheim, A. Cole, T.A. Douglas, R. Ebinghaus, U. Friess, S. Netcheva, S. Nghiem, H. Sihler and R. Staebler, 2013. Atmospheric mercury over sea ice during the OASIS-2009 campaign. Atmospheric Chemistry and Physics, 13:7007-7021.

Steffen, A., J. Bottenheim, A. Cole, R. Ebinghaus, G. Lawson and W.R. Leaitch, 2014. Atmospheric mercury speciation and mercury in snow over time at Alert, Canada. Atmospheric Chemistry and Physics, 14:2219-2231.

Stein, A.F., R.R. Draxler, G.D. Rolph, B.J.B. Stunder, M.D. Cohen and F. Ngan, 2015. NOAA's HYSPLIT atmospheric transport and dispersion modelling system. Bulletin of the American Meteorological Society, 96:2059-2077.

Stenhouse, I.J., E.M. Adams, J.L. Goyette, K.J. Regan, M.W. Goodale and D.C. Evers, 2018. Changes in mercury exposure of marine birds breeding in the Gulf of Maine, 2008-2013. Marine Pollution Bulletin, 128:156-161.

Stern, A.H. and A.E. Smith, 2003. An assessment of the cord blood:maternal blood methylmercury ratio: implications for risk assessment. Environmental Health Perspectives, 111:1465-1670.

Stern, G.A., R.W. Macdonald, P.M. Outridge, S. Wilson, J. Chételat, A. Cole, H. Hintelmann, L.I. Loseto, A. Steffen, F. Wang and C. Zdanowicz, 2012. How does climate change influence Arctic mercury? Science of the Total Environment, 414:22-42.

Stewart, F.M., R.A. Phillips, J.A. Bartle, J. Craig and D. Shooter, 1999. Influence of phylogeny, diet, moult schedule and sex on heavy metal concentrations in New Zealand Procellariiformes. Marine Ecology Progress Series, 1999:295-305.

Stewart, P.W., J. Reihman, E.I. Lonky, T.J. Darvill and J. Pagano, 2003. Cognitive development in preschool children prenatally exposed to PCBs and MeHg. Neurotoxicology and Teratology, 25:11-22.

Storelli, M.M. and G.O. Marcotrigiano, 2001. Total mercury levels in muscle tissue of swordfish (*Xiphias gladius*) and bluefin tuna (*Thunnus thynnus*) from the Mediterranean Sea (Italy). Journal of Food Protection, 64:1058-1061.

Strain, J.J., A.J. Yeates, E. van Wijngaarden, S.W. Thurston, M.S. Mulhern, E.M. McSorley, G.E. Watson, T.M. Love, T.H. Smith, K. Yost, D. Harrington, C.F. Shamlaye, J. Henderson, G.J. Myers and P.W. Davidson, 2015. Prenatal exposure to methyl mercury from fish consumption and polyunsaturated fatty acids: associations with child development at 20 mo of age in an observational study in the Republic of Seychelles. American Journal of Clinical Nutrition, 101:530-537.

Streets, D.G., J.M. Hao, Y. Wu, J.K. Jiang, M. Chan, H.Z. Tian and X.B. Feng, 2005. Anthropogenic mercury emissions in china. Atmospheric Environment, 39:7789-7806.

Streets, D.G., Q. Zhang and Y. Wu, 2009. Projections of global mercury emissions in 2050. Environmental Science and Technology, 43:2983-2988.

Streets, D.G., M.K. Devane, Z.F. Lu, T.C. Bond, E.M. Sunderland and D.J. Jacob, 2011. All-time releases of mercury to the atmosphere from human activities. Environmental Science and Technology, 45:10485-10491.

Streets, D.G., H.M. Horowitz, D.J. Jacob, Z. Lu, L. Levin, A.F.H. ter Schure and E.M. Sunderland, 2017. Total mercury released to the environment by human activities. Environmental Science and Technology, 51:5969-5977.

Streets, D.G., Z. Lu, L. Levin, A.F.H. ter Schure and E.M. Sunderland, 2018. Historical releases of mercury to air, land, and water from coal combustion. Science of the Total Environment, 615:131-140.

Strode, S., L. Jaeglé and N.E. Selin, 2009. Impact of mercury emissions from historic gold and silver mining: Global modelling. Atmospheric Environment, 43:2012-2017.

Strode, S., L. Jaegle and S. Emerson, 2010. Vertical transport of anthropogenic mercury in the ocean. Global Biogeochemical Cycles, 24, GB4014 doi:10.1029/2009GB003728.

Su, J., J.P. Cheng, X.F. Ye, T. Yuan, W.H. Wang and L.J. Mi, 2007. Preliminary study on mercury distribution in multimedia environment in Lanzhou. Journal of Agro-environment Science, 26:381-385. (In Chinese)

Suchanek, T.H., C.A. Eagles-Smith, D.G. Slotton, E.J. Harner, A.E. Colwell, N.L. Anderson, L.H. Mullen, J.R. Flanders, D.P. Adam and K.J. McElroy, 2008. Spatiotemporal trends in fish mercury from a mine-dominated ecosystem: Clear Lake, California. Ecological Applications, 18(8) Supplement. A177-A195.

Sullivan, K.M. and A.D. Kopec, 2018. Mercury in wintering American black ducks (*Anas rubripes*) downstream from a point-source on the lower Penobscot River, Maine, USA. Science of the Total Environment, 612:1187-1199.

Sun, L., B. Lu, D. Yuan, W. Hao and Y. Zheng, 2017. Variations in the isotopic composition of stable mercury isotopes in typical mangrove plants of the Jiulong estuary, SE China. Environmental Science and Pollution Research, 24:1459-1468.

Sunderland, E.M. and R.P. Mason, 2007. Human impacts on open ocean mercury concentrations. Global Biogeochemical Cycles, 21:GB4022. doi:10.1029/2006GB002876.

Sunderland, E.M. and A.T. Schartup, 2016. Biogeochemistry: mercury methylation on ice. Nature Microbiology, 1:16165.

Sunderland, E.M. and N.E Selin, 2013. Future trends in environmental mercury concentrations: implications for prevention strategies. Environmental Health 12:2, 10.1186/1476-069X-12-2.

Sunderland, E.M., D.P. Krabbenhoft, J.W. Moreau, S.A. Strode and W.M. Landing, 2009. Mercury sources, distribution, and bioavailability in the North Pacific Ocean: Insights from data and models. Global Biogeochemical Cycles, 23:GB2010, doi:10.1029/2008GB003425.

Sunderland, E.M., C.T. Driscoll Jr, J.K. Hammitt, P. Grandjean, J.S. Evans, J.D. Blum, C.Y. Chen, D.C. Evers, D.A. Jaffe, R.P. Mason, S. Goho and W. Jacobs, 2016. Benefits of regulating hazardous air pollutants from coal and oil-fired utilities in the United States. Environmental Science and Technology, 50:2117-2120.

Sunderland, E.M., M. Li and K. Bullard, 2018. Decadal changes in the edible supply of seafood and methylmercury exposure in the United States. Environmental Health Perspectives, 126:017006-1-017006-6.

Sundseth, K., J.M. Pacyna, A. Banel, E.G. Pacyna and A. Rautio, 2015. Climate change impacts on environmental and human exposure to mercury in the Arctic. International journal of Environmental Research and Public Health, 12:3579-3599.

Sundseth, K., J.M. Pacyna, E.G. Pacyna, N. Pirrone and R.J. Thorne, 2017. Global sources and pathways of mercury in the context of human health. International journal of Environmental Research and Public Health, 14:105. 10.3390/ijerph14010105.

Sung, J.H., J.S. Oh, S.K. Back, A.H.M. Mojammal, E.S. Lee, H.N. Jang, S.H. Kim, Y.C. Seo, C.H. Bae and S.T. Kim, 2016. Mercury emission from major source facilities and modelling of atmospheric movement in Korea and neighbor countries. In: 17th IUAPPA World Clean Air Congress and 9th CAA Better Air Quality Conference.

Suzuki, K., K. Nakai, T. Sugawara, T. Nakamura, T. Ohba, M. Shimada, T. Hosokawa, K. Okamura, T. Sakai, N. Kurokawa, K. Murata, C. Satoh and H. Satoh, 2010. Neurobehavioral effects of prenatal exposure to methylmercury and PCBs, and seafood intake: neonatal behavioral assessment scale results of Tohoku study of child development. Environmental Research, 110:699-704.

Tan, S.W., J.C. Meiller and K.R. Mahaffey, 2009. The endocrine effects of mercury in humans and wildlife. Critical Reviews in Toxicology, 39:228-269.

Tang, R.W.K., T.A. Johnston, J.M. Gunn and S.P. Bhavsar, 2013. Temporal changes in mercury concentrations of large-bodied fishes in the boreal shield ecoregion of northern Ontario, Canada. Science of the Total Environment, 444:409-416.

Tartu, S., A. Goutte, P. Bustamante, F. Angelier, B. Moe, C. Clément-Chastel, C. Bech, G.W. Gabrielsen, J.O. Bustness and O. Chastel, 2013. To breed or not to breed: endocrine response to mercury contamination by an arctic seabird. Biology Letters, 9:20130317. 10.1098/rsbl.2013.0317.

Tavares, S., J.C. Xavier, R.A. Phillips, M.E. Pereira and M.A. Pardal, 2013. Influence of age, sex and breeding status on mercury accumulation patterns in the wandering albatross Diomedea exulans. Environmental Pollution. 181:315-320.

Teffer, A.K., M.D. Staudinger, D.L. Taylor and F. Juanes, 2014. Trophic influences on mercury accumulation in top pelagic predators from offshore New England waters of the northwest Atlantic Ocean. Marine Environmental Research, 101:124-134.

Telmer, K.H. and M.M. Veiga, 2009. World emissions of mercury from artisanal and small scale gold mining. In: Mason, R. and N. Pirrone (Eds.), Mercury Fate and Transport in the Global Atmosphere. pp. 131-172. Springer.

Temme, C., J.W. Einax, R. Ebinghaus and W.H. Schroeder, 2003. Measurements of atmospheric mercury species at a coastal site in the Antarctic and over the Atlantic ocean during polar summer. Environmental Science and Technology, 37:22-31.

TePaske, J.J. and K.W. Brown, 2010. A New World of Gold and Silver. Brill, Leiden.

Theloke, J., U. Kummer, S. Nitter, T. Geftler, R. Friedrich, H. Denier van der Gon and A. Visschedijk, 2008. Überarbeitung der Schwermetallkapitel in CORINAIR Guidebook zur verbesserung der Emissionsinventare und der Berichterstattung im Rahmen der Genfer Luftreinhaltekonvention. Umwelt Bundes Amt.

Titcomb, E.M., J.S. Reif, P.A. Fair, H.C.W. Stavros, M. Mazzoil, G.D. Bossart and A.M. Schaefer, 2017. Blood mercury concentrations in common bottlenose dolphins from the Indian River Lagoon, Florida: Patterns of social distribution. Marine Mammal Science, 33:771-784.

Tong, Y.D., X.F. Yin, H.M. Lin, D. Buduo, H.H. Wang, C.Y. Deng, L. Chen, J.L. Li, W. Zhang, J.J. Schauer, S.C. Kang, G.S. Zhang, X.G. Bu, X.J. Wang and Q.G. Zhang, 2016. Recent decline of atmospheric mercury recorded by Androsace tapete on the Tibetan Plateau. Environmental Science and Technology, 50:13224-13231.

Tørseth, K., W. Aas, K. Breivik, A.M. Fjæraa, M. Fiebig, A.G. Hjellbrekke, C. Lund Myhre, S. Solberg and K.E. Yttri, 2012. Introduction to the European Monitoring and Evaluation Programme (EMEP) and observed atmospheric composition change during 1972-2009. Atmospheric Chemistry and Physics, 12:5447-5481.

Townsend, J.M., C.C. Rimmer, C.T. Driscoll, K.P. McFarland and E. Inigo-Elias, 2013. Mercury concentrations in tropical resident and migrant songbirds on Hispaniola. Ecotoxicology, 22:86-93.

Toyota, K., A.P. Dastoor and A. Ryzhkov, 2014. Air-snowpack exchange of bromine, ozone and mercury in the springtime Arctic simulated by the 1-D model PHANTAS – Part 2: Mercury and its speciation. Atmospheric Chemistry and Physics, 14:4135-4167.

Trasande, L., J. DiGangi, D.C. Evers, P. Jindrich, D.G. Buck, J. Samanek, B. Beeler, M.A. Turnquist and K. Regan, 2016. Economic implications of mercury exposure in the context of the global mercury treaty: hair mercury levels and estimated lost economic productivity in selected developing countries. Journal of Environmental Management, 183:229-235.

Travnikov, O. and I. Ilyin, 2009. The EMEP/MSC-E mercury modelling system. In: Pirrone, N. and R.P. Mason (eds.), Mercury Fate and Transport in the Global Atmosphere. pp. 571-587. Springer.

Travnikov, O., J.E. Jonson, A.S. Andersen, M. Gauss, A. Gusev, O. Rozovskaya, D. Simpson, V. Sokovyh, S. Valiyaveetil and P. Wind, 2009. Development of the EMEP global modeling framework: Progress report. EMEP/MSC-E Technical Report 7/2009, Meteorological Synthesizing Centre – East.

Travnikov, O., H. Angot, P. Artaxo, M. Bencardino, J. Bieser, F. D'Amore, A. Dastoor, F. De Simone, M.D.C. Diéguez, A. Dommergue, R. Ebinghaus, X.B. Feng, C.N. Gencarelli, I.M. Hedgecock, O. Magand, L. Martin, V. Matthias, N. Mashyanov, N. Pirrone, R. Ramachandran, K.A. Read, A. Ryjkov, N.E. Selin, F. Sena, S. Song, F. Sprovieri, D. Wip, I. Wängberg and X. Yang, 2017. Multi-model study of mercury dispersion in the atmosphere: atmospheric processes and model evaluation. Atmospheric Chemistry and Physics, 17:5271-5295.

Tsui, M.T., J.D. Blum, J.C. Finlay, S.J. Balogh, Y.H. Nollet, W.J. Palen and M.E. Power, 2014. Variation in terrestrial and aquatic sources of methylmercury in stream predators as revealed by stable mercury isotopes. Environmental Science and Technology, 48:10128-10135.

Umweltbundesamt, 2006. Annual Report, Federal Environmental Agency, Germany.

UN Environment, 2016. Global Review of Mercury Monitoring Networks. United Nations Environment Programme.

UN Environment, 2017a. Global Mercury Supply, Trade and Demand. United Nations Environment Programme, Chemicals and Health Branch. Geneva, Switzerland.

UN Environment, 2017b. Toolkit for Identification and Quantification of Mercury Releases. Reference Report and Guideline for Inventory Level 2. Version 1.4. January 2017.

UN Environment, 2017c. Toolkit for Identification and Quantification of Mercury Releases. Guideline for Inventory Level 1. Version 2.0. January 2017.

UN Environment, 2017d. Minamata Convention on Mercury – Text and Annexes. United Nations Environment Programme.

UN Environment, 2019. Global Mercury Assessment 2018. UN Environment Programme, Chemicals and Health Branch, Geneva Switzerland.

UNEP, 2002. Global Mercury Assessment. United Nations Environment Programme (UNEP), Chemicals, Geneva, Switzerland.

UNEP, 2008. UNEP Chemicals Branch, 2008. The Global Atmospheric Mercury Assessment: Sources, Emissions and Transport. UNEP Chemicals, Geneva, Switzerland.

UNEP, 2010a. Study on Mercury Sources and Emissions and Analysis of the Cost and Effectiveness of Control Measures: 'Paragraph 29 Study'. (The report plus the associated data compilations.) UNEP-Chemicals, Geneva.

UNEP, 2010b. Process Optimization Guidance for Reducing Mercury Emissions from Coal Combustion in Power Plants.

UNEP, 2011b. Toolkit for Identification and Quantification of Mercury Releases. Revised Inventory Level 2 Report including Description of Mercury Source Characteristics. Version 1.1. January 2011.

UNEP, 2011c. Reducing Mercury Emissions from Coal Combustion in the Energy Sector of China. Prepared for the Ministry of Environment Protection of China and UNEP Chemicals. Tsinghua University, Beijing, China. February 2011.

UNEP, 2011d. Reducing Mercury Emissions from Coal Combustion in the Energy Sector of the Russian Federation. Prepared by the Scientific Research Institute for Atmospheric Air Protection (SRI Atmosphere, JSC), Saint-Petersburg, Russia. November 2011.

UNEP, 2011e. Global Estimate of Global Mercury Cell Chlorine Capacity. United Nations Environment Programme, Geneva.

UNEP, 2012. Reducing Mercury Use in Artisanal and Small-Scale Gold Mining: A Practical Guide. United Nations Environment Programme (UNEP). Available at http://wedocs.unep.org/handle/20.500.11822/11524.

UNEP, 2013a. Global Mercury Assessment 2013: Sources, Emissions, Releases and Environmental Transport. United Nations Environment Programme (UNEP), Chemicals Branch, Geneva, Switzerland.

UNEP, 2013b. UNEP Global Inventories of Chlor Alkali Facilities: Global Estimate of Global Mercury Cell Chlorine Capacity. https://web.unep.org/globalmercurypartnership/our-work/mercury-reduction-chlor-alkali-sector/reports-and-publications

UNEP, 2014. Assessment of the Mercury Content in Coal fed to Power Plants and study of Mercury Emissions from the Sector in India. Central Institute of Mining & Fuel Research (CIMFR). Council of Scientific & Industrial Research. Department of Science & Technology Dhanbad, India.

UNEP, 2015. Toolkit for Identification and Quantification of Mercury Releases: Reference Report and Guideline for Inventory Level 2, Version 1.3. UN Environment Division of Technology, Industry and Economics (Chemicals and Wastes Branch), April 2015.

UNEP, 2016. Guidance on best available techniques and best environmental practices (BAT/BEP) developed under the Minimata Convention. UN Environment. http://www.mercuryconvention.org/Convention/Formsandguidance/tabid/5527/language/en-US/Default.aspx

UNEP/CIMFR-CSIR, 2012. Characterization of the coal fired power sector in India, assessment of the mercury contents in coal fed to power plants and calculation of mercury emissions from the sector. Central Institute of Mining & Fuel Research (CIMFR), Council of Scientific & Industrial Research (CSIR), Department of Science & Technology.

UNIDO, 2016. UNIDO presentation to USEPA (Sept. 2016). UNIDO Activities in the Field of Mercury, Part 3: Introduction on UNIDO/China VCM project "Demonstration of Mercury Reduction and Minimization in the Production of Vinyl Chloride Monomer in China".

University of Michigan Animal Diversity Web, 2018. University of Michigan Museum of Zoology Animal Diversity Web. University of Michigan, Ann Arbor, Michigan. http://animaldiversity.org/.

Uryu, Y., O. Malm, I. Thornton, I. Payne and D. Cleary. 2001. Mercury contamination of fish and its implications for other wildlife of the Tapajós Basin, Brazilian Amazon. Conservation Biology, 15:438-446.

US CDC, 2017. Fourth National Report on Human Exposure to Environmental Chemicals, Updated Tables, January 2017. Centers for Disease Control and Prevention, Atlanta GA.

US EPA, 1997. Mercury Study Report to Congress. United States Environmental Protection Agency (US EPA). www.epa.gov/mercury/mercury-study-report-congress

US EPA, 2001. Risk assessment for methylmercury. In: Water Quality Criterion for the Protection of Human Health: Methylmercury. Chapter 4. United States Environmental Protection Agency (US EPA), Office of Science and Technology.

US EPA, 2008. Meeting Minutes, April 9, 2008 Meeting between the Portland Cement Association and the USEPA 008.

US NAS / US NRC, 2000. Toxicological Effects of Methylmercury. US National Academy of Sciences (US NAS) / US National Research Council (US NRC). National Academy Press.

USGS, 2016. Minerals Yearbook. Volume I: Metals & Minerals. U.S. Geological Survey.

USGS, 2017a. Data for 2014 from the Mineral Resources Data System: U.S. Geological Survey database available online. https://minerals.usgs.gov/minerals/pubs/commodity .

USGS, 2017b. Data for 2015 from the Mineral Resources Data System: U.S. Geological Survey database available online. https://minerals.usgs.gov/minerals/pubs/commodity

van Belle, G. and J.P. Hughes, 1984. Nonparametric tests for trend in water quality. Water Resources Research, 20:127-136.

Varian-Ramos, C.W., J.P. Swaddle and D.A. Cristol, 2014. Mercury reduces avian reproductive success and imposes selection: an experimental study with adult- or lifetime-exposure in zebra finch. PLoS ONE 9:e95674. doi.org/10.1371/journal.pone.0095674.

VDZ, 2015. The German Cement Works Association, 2015. Environmental Data of the German Cement Industry 2014.

Vega-Sánchez, B., S. Ortega-García, J. Ruelas-Inzunza, M. Frías-Espericueta, O. Escobar-Sánchez and J. Guzmán-Rendón, 2017. Mercury in the blue marlin (*Makaira nigricans*) from the southern Gulf of California: Tissue distribution and inter-annual variation (2005–2012). Bulletin of Environmental Contamination and Toxicology, 98:156-161.

Velasco, A., F. Arcega-Cabrera, I. Oceguera-Vargas, M. Ramirez, A. Ortinez, G. Umlauf and F. Sena, 2016. Global Mercury Observatory System (GMOS): measurements of atmospheric mercury in Celestun, Yucatan, Mexico during 2012. Environmental Science and Pollution Research, 23:17474-17483.

Velasquez-Lopez, P., M. Veiga and K. Hall, 2010. Mercury balance in amalgamation in artisanal and small-scale gold mining: identifying strategies for reducing environmental pollution in Portovelo-Zaruma, Ecuador. Journal of Cleaner Production, 18:226-232.

Višnjevec Miklavčič, A.M., D. Kocman and M. Horvat, 2014. Human mercury exposure and effects in Europe. Environmental Toxicology and Chemistry, 33:1259-1270.

Wagemann, R. and H. Kozlowska, 2005. Mercury distribution in the skin of beluga (*Delphinapterus leucas*) and narwhal (*Monodon monoceros*) from the Canadian Arctic and mercury burdens and excretion by moulting. Science of the Total Environment, 351:333-343.

Wagemann, R., E. Trebacz, G. Boila and W.L. Lockhart, 1998. Methylmercury and total mercury in tissues of arctic marine mammals. Science of the Total Environment, 218:19-31.

Walters, C., M. Couto, N. McClurg, B. Silwana and V. Somerset, 2017. Baseline monitoring of mercury levels in environmental matrices in the Limpopo Province. Water, Air, and Soil Pollution, 228:57. doi.org/10.1007/s11270-016-3230-3

Wan, Q., X.B. Feng, J. Lu, W. Zheng, X.J. Song, P. Li, S.J. Han and H. Xu, 2009. Atmospheric mercury in Changbai Mountain area, northeastern China II. The distribution of reactive gaseous mercury and particulate mercury and mercury deposition fluxes. Environmental Research, 109:721-727.

Wang, F. and J. Zhang, 2013. Mercury contamination in aquatic ecosystems under a changing environment: Implications for the Three Gorges Reservoir. Chinese Science Bulletin, 58:141-149.

Wang, S.F., X.B. Feng, G.L. Qiu, X.W. Fu and Z.Q. Wei, 2007a. Characteristics of mercury exchange flux between soil and air in the heavily air-polluted area, eastern Guizhou, China. Atmospheric Environment, 41:5584-5594.

Wang, Z.W., Z.S. Chen, N. Duan and X.S. Zhang, 2007b. Gaseous elemental mercury concentration in atmosphere at urban and remote sites in China. Journal of Environmental Sciences (China), 19:176-180.

Wang, Z., X. Zhang, J. Xiao, C. Zhijia and P. Yu, 2009. Mercury fluxes and pools in three subtropical forested catchments, southwest China. Environmental Pollution, 157:801-808.

Wang, S.X., J.X. Song, G.H. Li, Y. Wu, L. Zhang, Q. Wan, D.G. Streets, C.K. Chin and J.M. Hao, 2010a. Estimating mercury emissions from a zinc smelter in relation to China's mercury control policies. Environmental Pollution, 158:3347-3353.

Wang, F., R.W. Macdonald, G.A. Stern and P.M. Outridge, 2010b. When noise becomes the signal: Chemical contamination of aquatic ecosystems under a changing climate. Marine Pollution Bulletin, 60:1633-1635.

Wang, S., L. Zhang, B. Zhao, Y. Meng and J. Hao, 2012a. Mitigation potential of mercury emissions from coal-fired power plants in China. Energy Fuels, 26:4635-4642.

Wang, Y.M., D.Y. Wang, B. Meng, Y.L. Peng, L. Zhao and J.S. Zhu, 2012b. Spatial and temporal distributions of total and methyl mercury in precipitation in core urban areas, Chongqing, China. Atmospheric Chemistry and Physics, 12:9417-9426.

Wang, F., R.W. Macdonald, D.A. Armstrong and G.A. Stern, 2012c. Total and methylated mercury in the Beaufort Sea: The role of local and recent organic remineralization. Environmental Science and Technology, 46:11821-11828.

Wang, H., W. Xu, Z. Chen, Z. Cheng, L. Ge, Y. Man, J.P. Giesy, J.Du, C.K.C. Wong and M. Wong, 2013. In vitro estimation of exposure of Hong Kong residents to mercury and methylmercury via consumption of market fishes. Journal of Hazardous Materials, 248:387-393.

Wang, S., F. Wang, L. Zhang, H. Yang, Q. Wu and J. Hao, 2014a. Mercury enrichment and its effects on atmospheric emissions in cement plants in China. Atmospheric Environment, 92:421-428.

Wang, Y.M., Y.L. Peng, D.Y. Wang and C. Zhang, 2014b. Wet deposition fluxes of total mercury and methylmercury in core urban areas, Chongqing, China. Atmospheric Environment, 92:87-96.

Wang, S., J.A. Schmidt, S. Baidar, S. Coburn, B. Dix, T.K. Koenig, E. Apel, D. Bowdalo, T.L. Campos, E. Eloranta, M.J. Evans, J.P. DiGangi, M.A. Zondlo, R.-S. Gao, J.A. Haggerty, S.R. Hall, R.S. Hornbrook, D. Jacob, B. Morley, B. Pierce, M. Reeves, P. Romashkin, A. ter Schure and R. Volkamer, 2015. Active and widespread halogen chemistry in the tropical and subtropical free troposphere. Proceedings of the National Academy of Sciences, 112:9281-9286.

Wang, X., Z. Bao, C.J. Lin, W. Yuan and X. Feng, 2016a. Assessment of global mercury deposition through litterfall. Environmental Science and Technology, 50:8548-8557.

Wang, X., C.J. Lin, W. Yuan, J. Sommar, W. Zhu and X. Feng, 2016b. Emission-dominated gas exchange of elemental mercury vapor over natural surfaces in China. Atmospheric Chemistry and Physics, 16:11125-11143.

Wang, J., L. Zhang and Z. Xie, 2016c. Total gaseous mercury along a transect from coastal to central Antarctic: Spatial and diurnal variations. Journal of Hazardous Materials, 317:362-372.

Wang, S., F. Wang, L. Zhang, H. Yang, Q. Wu and J. Hao, 2016d. Mercury mass flow in iron and steel production process and its implications for mercury emission control. Journal of Environmental Sciences, 43:293-301.

Wang, F., M. Pućko and G. Stern, 2017. Transport and transformation of contaminants in sea ice. In: Thomas, D.N. (Ed.), Sea Ice. 3rd ed. Wiley-Blackwell, pp. 472-491.

Wang, X., C.J. Lin and X. Feng, 2018. Assessment of natural mercury emission and atmospheric mercury mass balance in China. Journal of Geophysical Research – Atmosphere, submitted.

Watanuki, Y., A. Yamashita, M. Ishizuka, Y. Ikenaka, S.M. Nakayama, C. Ishii, T. Yamamoto, M. Ito, T. Kuwae and P.N. Trathan, 2016. Feather mercury concentration in streaked shearwaters wintering in separate areas of southeast Asia. Marine Ecology Progress Series, 546:263-269.

Webb, J., O.T. Coomes, N. Mainville and D. Mergler, 2015. Mercury contamination in an indicator fish species from Andean Amazonian rivers affected by petroleum extraction. Bulletin of Environmental Contamination and Toxicology, 95:279-285.

Webber, H.M. and T.A. Haines, 2003. Mercury effects on predator avoidance behavior of a forage fish, golden shiner (Notemigonus crysoleucas). Environmental Toxicology and Chemistry, 22:1556-1561.

Weech, S.A., A.M. Scheuhammer and J.E. Elliott, 2006. Mercury exposure and reproduction in fish-eating birds breeding in the Pinchi Lake region, British Columbia, Canada. Environmental Toxicology and Chemistry, 25:1433-1440.

Weigelt, A., R. Ebinghaus, A. Manning, R. Derwent, P. Simmonds, T. Spain, S. Jennings and F. Slemr, 2015. Analysis and interpretation of 18 years of mercury observations since 1996 at Mace Head, Ireland. Atmospheric Environment, 100:85-93.

Weigelt, A., R. Ebinghaus, N. Pirrone, J. Bieser, J. Bödewadt, G. Esposito, F. Slemr, P.F.J. van Velthoven, A. Zahn and H. Ziereis, 2016a. Tropospheric mercury vertical profiles between 500 and 10 000 m in central Europe. Atmospheric Chemistry and Physics, 16:4135-4146.

Weigelt, A., F. Slemr, R. Ebinghaus, N. Pirrone, J. Bieser, J. Bödewadt, G. Esposito and P.F. J. van Velthoven, 2016b. Mercury emissions of a coal-fired power plant in Germany. Atmospheric Chemistry and Physics, 16:13653-13668.

Weihe, P. and H. Debes Joensen, 2012. Dietary recommendations regarding pilot whale meat and blubber in the Faroe Islands. International Journal of Circumpolar Health, 71:18594.

Weis, J.S. and A.A. Khan, 1990. Effects of mercury on the feeding behavior of the mummichog, Fundulus heteroclitus from a polluted habitat. Marine Environmental Research, 30:243-249.

Weiss-Penzias, P., H.M. Amos, N.E. Selin, M.S. Gustin, D.A. Jaffe, D. Obrist, G.R. Sheu and A. Giang, 2015. Use of a global model to understand speciated atmospheric mercury observations at five high-elevation sites. Atmospheric Chemistry and Physics, 15:1161-1173.

Weiss-Penzias, P.S., D.A. Gay, M.E. Brigham, M.T. Parsons, M.S. Gustin and A. ter Schure, 2016. Trends in mercury wet deposition and mercury air concentrations across the U.S. and Canada. Science of the Total Environment, 568:546-556.

Weseloh, D.C., D.J. Moore, C.E. Hebert, S.R. de Solla, B.M. Braune and D.J. McGoldrick, 2011. Current concentrations and spatial and temporal trends in mercury in Great Lakes Herring Gull eggs, 1974–2009. Ecotoxicology, 20:1644-1658.

White, E.M., M.S. Landis, G.J. Keeler and J.A. Barres, 2013. Investigation of mercury wet deposition physicochemistry in the Ohio River Valley through automated sequential sampling. Science of the Total Environment, 448:107-119.

Whitney, M.C. and D.A. Cristol, 2017. Impacts of sublethal mercury exposure on birds: A detailed review. Reviews of Environmental Contamination and Toxicology, 244:113-163.

WHO, 2016. Environmental and Occupational Health Hazards Associated with Artisanal and Small-scale Gold Mining. World Health Organization (WHO).

WHO, 2017. Mercury and Health. Fact sheet. World Health Organization (WHO). www.who.int/mediacentre/factsheets/fs361/en/ (Accessed 10 November 2017)

WHO, 2018. International Programme on Chemical Safety. World Health Organization (WHO). http://www.who.int/ipcs/assessment/public_health/mercury/en/

WHO Regional Office for Europe, 2015. Human Biomonitoring: Facts and Figures. World Health Organization (WHO).

WHO/UNEP, 2008. Guidance for Identifying Populations at Risk from Mercury Exposure. World Health Organization (WHO) / United Nations Environment Programme (UNEP).

Wiedinmyer, C., J. Robert, R.J. Yokelson and B.K. Gullett, 2014. Global emissions of trace gases, particulate matter, and hazardous air pollutants from open burning of domestic waste. Environmental Science and Technology, 48:9523-9530.

Wiemeyer, S.N., C.M. Bunck and A.J. Krynitsky, 1988. Organochlorine pesticides, polychlorinated biphenyls, and mercury in osprey eggs – 1970–79 – and their relationships to shell thinning and productivity. Archives of Environmental Contamination and Toxicology, 17:767-787.

Wiener, J.G., M.B. Sandheinrich, S.P. Bhavsar, J.R. Bohr, D.C. Evers, B.A. Monson and C.S. Schrank, 2012. Toxicological significance of mercury in yellow perch in the Laurentian Great Lakes region. Environmental Pollution, 161:350-357.

Wilhelm, S., 2001. Mercury in petroleum and natural gas: Estimation of emissions from production, processing and combustion. US EPA, Technical Report prepared by National Risk Management Research Laboratory. EPA/600/R-01/066.

Wilhelm, S.M., L. Liang, D. Cussen and D.A. Kirchgessner, 2007. Mercury in crude oil processed in the United States (2004). Environmental Science and Technology, 41:134509-134514.

Willacker, J.J., C.A. Eagles-Smith, M.A. Lutz, M.T. Tate, J.M. Lepak and J.T. Ackerman, 2016. Reservoirs and water management influence fish mercury concentrations in the western United States and Canada. Science of the Total Environment, 568:739-748.

Willacker, J.J., C.A. Eagles-Smith and J.T. Ackerman, 2017. Mercury bioaccumulation in estuarine fishes: Novel insights from sulfur stable isotopes. Environmental Science and Technology, 51:2131-2139.

Wilson, S.J., F. Steenhuisen, J.M. Pacyna and E.G. Pacyna, 2006. Mapping the spatial distribution of global anthropogenic mercury atmospheric emission inventories. Atmospheric Environment, 40:4621-4632.

Winch, S., D. Fortin, D. Lean and M. Parsons, 2008. Factors affecting methylmercury levels in surficial tailings from historical Nova Scotia gold mines. Geomicrobiology Journal, 25:112-129.

Won, J. and T. Lee, 2012. Estimation of total annual mercury emissions from cement manufacturing facilities in Korea. Atmospheric Environment, 62:265-271.

Won, A.Y., M.K. Kim and K.D. Zoh, 2019. Characteristics of total and methyl mercury in precipitation in Seoul, Korea. Atmospheric Pollution Research, 10:493-500.

World Bank, 2016, 2017. Data Bank, World Development Indicators. Gross domestic product ranking table based on purchasing power parity (PPP). http://data.worldbank.org/data-catalog/GDP-PPP-based-table. Accessed 2016-08-23, updated 2017-12-04.

World Steel Association, 2015. Steel Statistical Yearbook 2015. Worldsteel Committee on Economic Studies, Brussels.

Wright, L.P. and L. Zhang, 2015. An approach estimating bidirectional air-surface exchange for gaseous elemental mercury at AMNet sites. Journal of Advances in Modelling Earth Systems, 7:35-49.

Wright, G., M.S. Gustin, P. Weiss-Penzia and M.B. Miller, 2013. Investigation of mercury deposition and potential sources at six sites from the Pacific Coast to the Great Basin, USA. Science of The Total Environment, 470-471:1099-1113.

Wright, G., M.S. Gustin, P. Weiss-Penzias and M.B. Miller, 2014. Investigation of mercury deposition and potential sources at six sites from the Pacific Coast to the Great Basin, USA. Science of the Total Environment, 470:1099-1113.

Wright, L.P., L. Zhang and F.J. Marsik, 2016. Overview of mercury dry deposition, litterfall, and throughfall studies. Atmospheric Chemistry and Physics, 16:13399-13416.

WSPA, 2009. Bay area petroleum refinery mercury air emissions, deposition and fate. Western States Petroleum Association. Environmental Resource Management, 2009.

Wu, P.P., 2014. Studies on temporal and spatial distributions of atmospheric mercury in Taiwan Strait inshore areas. Master's dissertation. Xiamen University, Xiamen, China. (In Chinese)

Wu, Y., D.G. Streets, S.X. Wang and J.M. Hao, 2010. Uncertainties in estimating mercury emissions from coal-fired power plants in China. Atmospheric Chemistry and Physics, 10:2937-2947.

Wu, Q., S. Wang, L. Zhang, J. Song, H. Yang and Y. Meng, 2012. Update of mercury emissions from China's primary zinc, lead and copper smelters, 2000-2010. Atmospheric Chemistry and Physics, 12:11153-11163.

Wu, Q., S. Wang, L. Zhang, M. Hui, F. Wang and J. Hao, 2016a. Flow analysis of the mercury associated with nonferrous ore concentrates: implications on mercury emissions and recovery in China. Environmental Science and Technology, 50:1796-1803.

Wu, Q., S. Wang, G. Li, S. Liang, C.-L. Lin, Y. Wang, S. Cai, K. Liu and J. Hao, 2016b. Temporal trend and spatial distribution of speciated atmospheric mercury emissions in China during 1978-2014. Environmental Science and Technology, 50:13428-13435.

Wu, Q.R., W. Gao, S.X. Wang and J.M. Hao, 2017. Updated atmospheric speciated mercury emissions from iron and steel production in China during 2000-2015. Atmospheric Chemistry and Physics, 17:10423-10433.

WWAP, 2017. The United Nations World Water Development Report 2017. Wastewater: The Untapped Resource. United Nations World Water Assessment Programme (WWAP). UNESCO, Paris.

Wyn, B., K.A. Kidd, N.M. Burgess and R.A. Curry, 2009. Mercury biomagnification in the food webs of acidic lakes in Kejimkujik National Park and National Historic Site, Nova Scotia. Canadian Journal of Fisheries and Aquatic Sciences, 66:1532-1545.

Wyn, B., K.A. Kidd, N.M. Burgess, R.A. Curry and K.R. Munkittrick, 2010. Increasing mercury in yellow perch at a hotspot in Atlantic Canada, Kejimkujik National Park. Environmental Science and Technology, 44:9176-9181.

Xiang, J.Q. and G.J. Liu, 2008. Distribution and sources of atmospheric mercury in urban areas of Wuhan. Res. Environ. Eng., 22:27-30. (In Chinese)

Xin, M. and M.S. Gustin, 2007. Gaseous elemental mercury exchange with low mercury containing soils: Investigation of controlling factors. Applied Geochemistry, 22:1451-1466.

Xiu, G.L., J. Cai, W.Y. Zhang, D.N. Zhang, A. Bueler, S.C. Lee, Y. Shen, L.H. Xu, X.J. Huang and P. Zhang, 2009. Speciated mercury in size-fractionated particles in Shanghai ambient air. Atmospheric Environment, 43:3145-3154.

Xu, L.L., J.S. Chen, Z.C. Niu, L.Q. Yin and Y.T. Chen, 2013. Characterization of mercury in atmospheric particulate matter in the southeast coastal cities of China. Atmospheric Pollution Research, 4:454-461.

Xu, X.H., U. Akhtar, K. Clark and X.B. Wang, 2014. Temporal variability of atmospheric total gaseous mercury in Windsor, ON, Canada. Atmosphere, 5:536-556.

Xu, L.L., J.S. Chen, L.M. Yang, Z.C. Niu, L. Tong, Q. Yin and Y.T. Chen, 2015. Characteristics and sources of atmospheric mercury speciation in a coastal city, Xiamen, China. Chemosphere, 119:530-539.

Xue, F., C. Holzman, M.H. Rahbar, K. Trosko and L. Fischer, 2007. Maternal fish consumption, mercury levels, and risk of preterm delivery. Environmental Health Perspectives, 115:42-47.

Yan, H.Y., A. Rustadbakken, H. Yao, T. Larssen, X.B. Feng, B. Liu, L.H. Shang and T.O. Haugen, 2010. Total mercury in wild fish in Guizhou reservoirs, China. Journal of Environmental Sciences, 22:1129-1136.

Yang, Y.K., C. Zhang, X.J. Shi, T. Lin and D.Y. Wang, 2007. Effect of organic matter and pH on mercury release from soils. Journal of Environmental Sciences, 19:1349-1354.

Yang, Y.K., H. Chen and D.Y. Wang, 2009. Spatial and temporal distribution of gaseous elemental mercury in Chongqing, China. Environmental Monitoring and Assessment, 156:479-489.

Yang, M., S. Wang, L. Zhang, Q. Wu, F. Wang, M. Hui, H. Yang and J. Hao, 2016. Mercury emission and speciation from industrial gold production using roasting process. Journal of Geochemical Exploration, 170:72-77.

Yao, H., X.B. Feng, Y.N. Guo, H.Y. Yan, X.W. Fu, Z.G. Li and B. Meng, 2011. Mercury and methylmercury concentrations in two newly constructed reservoirs in the Wujiang River, Guizhou, China. Environmental Toxicology and Chemistry, 30:530-537.

Yasutake, A., M. Matsumoto, M. Yamaguchi and N. Hachiya, 2004. Current hair mercury levels in Japanese for estimation of methylmercury exposure. Journal of Health Science, 50:120-125.

Yates, D.E., D.T. Mayack, K. Munney, D.C. Evers, A. Major, T. Kaur and R.J. Taylor, 2005. Mercury levels in mink (*Mustela vison*) and river otter (*Lontra canadensis*) from northeastern North America. Ecotoxicology, 14:263-274.

Yates, D.E., E.M. Adams, S.E. Angelo, D.C. Evers, J. Schmerfeld, M.S. Moore, T.H. Kunz, T. Divoll, S.T. Edmonds, C. Perkins and R. Taylor, 2014. Mercury in bats from the northeastern United States. Ecotoxicology, 23:45-55.

Yu, X.D., C.H. Yan, X.M. Shen, Y. Tian, L.L. Cao, X.G. Yu, L. Zhao and J.X. Liu, 2011. Prenatal exposure to multiple toxic heavy metals and neonatal neurobehavioral development in Shanghai, China. Neurotoxicology and Teratology, 33:437-443.

Yu, R.Q., J.R. Reinfelder, M.E. Hines and T. Barkay, 2013. Mercury methylation by the methanogen *Methanospirillum hungatei*. Applied and Environmental Microbiology, 79:6325-6330.

Yu, J., Z. Xie, H. Kang, Z. Li, C. Sun, L. Bian and P. Zhang, 2014. High variability of atmospheric mercury in the summertime boundary layer through the central Arctic Ocean. Scientific Reports, 4:6091. doi:10.1038/srep06091.

Yu, B., X. Wang, C.-J. Lin, X. Fu, H. Zhang, L. Shang and X. Feng, 2015. Characteristics and potential sources of atmospheric mercury at a subtropical near-coastal site in East China. Journal of Geophysical Research: Atmospheres, 120, 8563-8574.

Yu, B., X.W. Fu, R.S. Yin, H. Zhang, X. Wang, C.J. Lin, C.S. Wu, Y.P. Zhang, N.N. He, P.Q. Fu, Z.F. Wang, L.H. Shang, J. Sommar, J.E. Sonke, L. Maurice, B. Guinot and X.B. Feng, 2016. Isotopic composition of atmospheric mercury in China: new evidence for sources and transformation processes in air and in vegetation. Environmental Science and Technology, 50:9262-9269.

Yu, Q., Y. Luo, S. Wang, Z. Wang, J. Hao and L. Duan, 2017. Gaseous elemental mercury (GEM) fluxes over canopy of two typical subtropical forests in south China. Atmospheric Chemistry and Physics Discussions, 2017, 1-27.

Yuan, W., J. Sommar, C.J. Lin, X. Wang, K. Li., Y. Liu, H. Zhang, C. Wu, Z. Lu and X.B. Feng, 2018. Stable isotope evidence shows reemission of elemental mercury vapor occurring after reductive loss from foliage. Environmental Science and Technology, 53:651-660.

Zhang, Y. and L. Jaeglé, 2013. Decreases in mercury wet deposition over the United States during 2004–2010: Roles of domestic and global background emission reductions. Atmosphere, 4:113-131.

Zhang, L., Z. Yuqun, C. Lei, X. Xu and C. Changhe, 2008. Mercury emissions from six coal-fired power plants in China. Fuel Processing Technology, 89:1033-1040.

Zhang, J.F., X.B. Feng, H.Y. Yan, Y.N. Guo, H. Yao, B. Meng and K. Liu, 2009. Seasonal distributions of mercury species and their relationship to some physicochemical factors in Puding Reservoir, Guizhou, China. Science of the Total Environment, 408:122-129.

Zhang, L., S. Wang, Q. Wu, Y. Meng, H. Yang, F. Wang and J. Hao, 2012a. Were mercury emission factors for Chinese non-ferrous metal smelters overestimated? Evidence from onsite measurements in six smelters. Environmental Pollution, 171:109-117.

Zhang, L., P. Blanchard, D. Johnson, A. Dastoor, A. Ryzhkov, C.J. Lin, K. Vijayaraghavan, D. Gay, T.M. Holsen, J. Huang, J.A. Graydon, V.L. St Louis, M.S. Castro, E.K. Miller, F. Marsik, J. Lu, L. Poissant, M. Pilote and K.M. Zhang, 2012b. Assessment of modelled mercury dry deposition over the Great Lakes region. Environmental Pollution, 161:272-283.

Zhang, W., Y. Tong, D. Hu, L. Ou and X. Wang, 2012c. Characterization of atmospheric mercury concentrations along an urban-rural gradient using a newly developed passive sampler. Atmospheric Environment, 47:26-32.

Zhang, W., W. Wei, D. Hu, Y. Zhu and X. Wang, 2013a. Emission of speciated mercury from residential biomass fuel combustion in China. Energy and Fuels, 27:6792-6800.

Zhang, L., S.X. Wang, L. Wang and J.M. Hao, 2013b. Atmospheric mercury concentration and chemical speciation at a rural site in Beijing, China: implications of mercury emission sources. Atmospheric Chemistry and Physics, 13:10505-10516.

Zhang, Y., L. Jaeglé and L. Thompson, 2014a. Natural biogeochemical cycle of mercury in a global three-dimensional ocean tracer model. Global Biogeochemical Cycles, 28:553-570.

Zhang, Y., L. Jaeglé, L. Thompson and D. Streets, 2014b. Six centuries of changing oceanic mercury. Global Biogeochemical Cycles, 28. 10.1002/2014GB004939.

Zhang, Y.Q., R.H. Liu, Y.Q. Cui, J.P. Zhou and Y. Wang, 2014c. The characteristic analysis of atmospheric mercury during haze days in Qingdao. China Environmental Science, 34:1905-1911. (In Chinese)

Zhang, T., K.H. Kucharzyk, B. Kim, M.A. Deshusses and H. Hsu-Kim, 2014d. Net methylation of mercury in estuarine sediment mesocosms amended with dissolved, nanoparticulate and microparticulate mercuric sulfide. Environmental Science and Technology, 48:9133-9141.

Zhang, H., X.W. Fu, C.-J. Lin, X. Wang and X.B. Feng, 2015a. Observation and analysis of speciated atmospheric mercury in Shangri-La, Tibetan Plateau, China. Atmospheric Chemistry and Physics, 15:653-665.

Zhang, L., S. Wang, L. Wang, Y. Wu, L. Duan, Q. Wu, F. Wang, M. Yang, H. Yang, J. Hao and X. Liu, 2015b. Updated emission inventories for speciated atmospheric mercury from anthropogenic sources in China. Environmental Science and Technology, 49:3185-3194.

Zhang, Y., D.J. Jacob, S. Dutkiewicz, H.M. Amos, M.S. Long and E.M. Sunderland, 2015c. Biogeochemical drivers of the fate of riverine mercury discharged to the global and Arctic oceans. Global Biogeochemical Cycles, 29:854-864.

Zhang, H., C.D. Holmes and S. Wu, 2016a. Impacts of changes in climate, land use and land cover on atmospheric mercury. Atmospheric Environment, 141:230-244.

Zhang, L., Z. Wu, I. Cheng, L.P. Wright, M.L. Olson, D.A. Gay, M.R. Risch, S. Brooks, M.S. Castro, G.D. Conley, E.S. Edgerton, T.M. Holsen, W. Luke, R. Tordon and P. Weiss-Penzias, 2016b. The estimated six-year mercury dry deposition across North America. Environmental Science and Technology, 50:12864-12873.

Zhang, Y., D.J. Jacob, H.M. Horowitz, L. Chen, H.M. Amos, D.P. Krabbenhoft, F. Slemr, V.L. St Louis and E.M. Sunderland, 2016c. Observed decrease in atmospheric mercury explained by global decline in anthropogenic emissions. Proceedings of the National Academy of Sciences of the USA, 113:526-531.

Zhang, L., S. Wang, Q. Wu, F. Wang, C.-J. Lin, L. Zhang, M. Hui, M. Yang, H. Su and J. Hao, 2016d. Mercury transformation and speciation in flue gases from anthropogenic emission sources: a critical review. Atmospheric Chemistry and Physics, 16:2417-2433.

Zhao, C. and K. Luo, 2017. Sulfur, arsenic, fluorine and mercury emissions resulting from coal-washing byproducts: A critical component of China's emission inventory. Atmospheric Environment, 152:270-278.

Zheng, J., 2015. Archives of total mercury reconstructed with ice and snow from Greenland and the Canadian High Arctic. Science of the Total Environment, 509-510:133-144.

Zhou, J., X.B. Feng, H.Y. Liu, H. Zhang, X.W. Fu, Z.D. Bao, X. Wang and Y.P. Zhang, 2013. Examination of total mercury inputs by precipitation and litterfall in a remote upland forest of Southwestern China. Atmospheric Environment, 81:364-372.

Zhou, H., C. Zhou, M.M. Lynman, J.T. Dvonch, J.A. Barres, P.K. Hopke, M. Cohen and T.M. Holsen, 2017a. Atmospheric mercury temporal trends in the northeastern United States from 1992 to 2014: Are measured concentrations responding to decreasing regional emissions? Environmental Science and Technology Letters, 4:91-97.

Zhou, C., M.D. Cohen, B.A. Crimmins, H. Zhou, T.A. Johnson, P.K. Hopke and T.M. Holsen, 2017b. Mercury temporal trends in top predator fish of the Laurentian Great Lakes from 2004 to 2015: Are concentrations still decreasing? Environmental Science and Technology, 51:7386-7394.

Zhu, J., T. Wang, R. Talbot, H. Mao, C.B. Hall, X. Yang, C. Fu, B. Zhuang, S. Li, Y. Han and X. Huang, 2012. Characteristics of atmospheric Total Gaseous Mercury (TGM) observed in urban Nanjing, China. Atmospheric Chemistry and Physics, 12:12103-12118.

Zhu, J., T. Wang, R. Talbot, H. Mao, X. Yang, C. Fu, J. Sun, B. Zhuang, S. Li, Y. Han and M. Xie, 2014. Characteristics of atmospheric mercury deposition and size-fractionated particulate mercury in urban Nanjing, China. Atmospheric Chemistry and Physics, 14:2233-2244.

Zhu, J., T. Wang, J. Bieser and V. Matthias, 2015. Source attribution and process analysis for atmospheric mercury in eastern China simulated by CMAQ-Hg. Atmospheric Chemistry and Physics, 15:8767-8779.

Zhu, W., C.J. Lin, X. Wang, J. Sommar, X. Fu and X. Feng, 2016. Global observations and modeling of atmosphere–surface exchange of elemental mercury: a critical review. Atmospheric Chemistry and Physics, 16:4451-4480.

Acronyms and Abbreviations

AEF	Abated emission factor
Ag	Silver
AMAP	Arctic Monitoring and Assessment Programme
AMDE	Atmospheric mercury depletion event
AMNet	NADP Atmospheric Mercury Network
APC	Air pollution control
APCD	Air pollution control device
ASGM	Artisanal and small-scale gold mining
Au	Gold
Br	Bromine
CARIBIC	Civil Aircraft for the Regular Investigation of the atmosphere Based on an Instrument Container
CHMS	Canadian Health Measures Survey
CLRTAP	Convention on Long-range Transboundary Air Pollution
CO	Carbon monoxide
CO_2	Carbon dioxide
CVAFS	Cold vapor atomic florescence spectroscopy
DF	Distribution factor
DMHg	Dimethylmercury
DOC	Dissolved organic carbon
E-PRTR	European Pollutant Release and Transfer Register
ECCCAMM	Environment and Climate Change Canada – Atmospheric Mercury Monitoring
EF	Emission factor
EMEP	European Monitoring and Evaluation Programme
ENSO	El Niño Southern Oscillation
ETMEP	European Tropospheric Mercury Experiment
FAO	Food and Agriculture Organization
GAW	Global Atmospheric Watch
GBMS	Global Biotic Mercury Synthesis
GEF	Global Environmental Facility
GEM	Gaseous elemental mercury (also known as Hg^0)
GMA	Global Mercury Assessment
GMOS	Global Mercury Observation System
GOM	Gaseous oxidized mercury
Hg	Mercury
Hg^0	Gaseous elemental mercury (also known as GEM)
Hg^{II}	Oxidized mercury compounds
IEA	International Energy Agency
INAC	Indigenous and Northern Affairs Canada
IPCC	Intergovernmental Panel on Climate Change
IPIECA	International Petroleum Industry Environmental Conservation Association
IQR	Interquartile range
kt	Kilotonne (thousand tonnes)
MDN	Mercury Deposition Network
MeHg	Methylmercury

MIA	Minamata Initial Assessment
MMHg	Monomethylmercury
MMSD	Mining, Minerals and Sustainable Development
NA-PRTR	North American Pollutant Release and Transfer Register
NADP	National Atmospheric Deposition Program
NAP	National Action Plan
NCP	Northern Contaminants Program
NEEM	North Greenland Eemian Ice Drilling site
O_3	Ozone
ODE	Ozone depletion event
o.e.	Oil equivalent
OH	Hydroxyl radical
PBM	Particulate-bound mercury
POC	Particulate organic carbon
PVC	Polymer polyvinyl chloride
SO_2	Sulfur dioxide
TGM	Total gaseous mercury
THg	Total mercury
UEF	Unabated emission factor
UN Environment	United Nations Environment Programme
UNECE	United Nations Economic Commission for Europe
UNEP	United Nations Environment Programme
USD	United States dollar
USGS	United States Geological Survey
VCM	Vinyl chloride monomer
WHO	World Health Organization

UN environment

United Nations Environment Programme
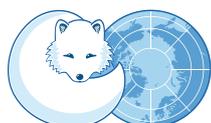
ARCTIC COUNCIL

AMAP
Arctic Monitoring and
Assessment Programme